

**Selected Papers
HISWA Symposium
on
Yacht Architecture**

1969 - 1994

REPORT 1067

**Delft University of Technology
Ship Hydromechanics Laboratory**

**Selected Papers
HISWA Symposium
on
Yacht Architecture**

1969 - 1994

Edited by

**J. Gerritsma
P.W. de Heer
J.A. Keuning**

**Published by: Delft University of Technology
Ship Hydromechanics Laboratory
Delft, The Netherlands**

Gerritsma, J., P.W. de Heer and J.A. Keuning

Selected Papers HISWA Symposium on Yacht Architecture edited by J. Gerritsma, P.W. de Heer and J.A. Keuning - Delft : Faculty of Mechanical Engineering and Marine Technology, Delft University of Technology.

With ref.

ISBN 90-370-0146-7

Subject headings: Yacht, Hydromechanics, Design, Construction, Research, Loads

**Delft University of Technology,
Faculty of Mechanical Engineering and Marine Technology,
Library WBMT,
Mekelweg 2, 2628 CD Delft,
The Netherlands**

**Deze CIP-gegevens ongewijzigd afdrucken op de copyright-
pagina van het boek, incl. het kopje
'CIPGEGEVENS KONINKL@ BIBLIOTHEEK, DEN HAAG'.
Voor informatie: tel.: 070-3140414.**

CIP-DATA KONINKLIJKE BIBLIOTHEEK. DEN HAAG

Contents

	page
Introduction	
1971	
'Systematic model series in the design of the sailing yacht hull' by Pierre DeSaix	1
'Prediction of the power performance of the series 62 parent hull' by J.B. Hadler and Nadine Hubble	27
'Jointdesign in the construction of fibre-glass reinforced yachts' by R.J. Schliekelmann	51
1973	
'The influence of wedges on the performance of planing hulls' by A.J. Cole and A. Millward	65
'The seakeeping performance and steering properties of sailing yachts' by J. Gerritsma and G. Moeyes	91
'Sailing yacht keels' by Justin E. Kerwin and Halsey C. Herreshoff	119
1975	
'The influence of fin keel sweep-back on the performance of sailing yachts' by W. Beukelman and J.A. Keuning.	137
'On noise reduction aboard motoryachts' by J. Buiten and M.J.A.M. de Regt	163
'Sail plans and deck layouts for ocean going cruising yachts' by G. Dijkstra jr	183
1977	
'Noise reduction aboard small yachts' by J. Buiten and H. Hendriks	225
'Test results of a systematic yacht hull series' by J. Gerritsma, G. Moeyes and R. Onnink	237
'Sail plans, spars, rigging and sails' by Roderick Stephens Jr	269

	page
1979	
'The use of a wood-resin composite for marine construction' by Meade A. Gougeon	293
'Considerations relative to a trimaran design for myself' by Richard C. Newick	311
'Balance of helm of sailing yachts' by K. Nomoto and H. Tatano	321
'A philosophy of yacht design' by Olin J. Stephens II	343
1983	
'Some applications of aeronautical engineering in the construction of yachts' by F.A. Jacobs	349
'The design of offshore cruising yachts' by D. Koopmans	373
'Planing craft design performance' by Renato Levi	387
1986	
'Advanced materials for yacht construction' by A. Cocquyt	405
'Sail design and panel calculation' by J.A. Keuning and A. Versluis	425
1988	
'Strength and stiffness of rigs' by T.F. van der Werff and P.J. Keuning	443
1990	
'Multi-stage waterjets for over 40 knot craft' by G.H. Davison	477
'The V.O.C. ship 'AMSTERDAM" - A velocity prediction' by A.H. Hubregtse	487
'Rig load measurements and comparison with calculations' by P.J. Keuning and T.F. van der Werff	509
'Amsterdam is building a Dutch-East Indiaman' by H.J. Wimmers	531

1992

'Carbon fibre reinforced spars and masts'
by A.H.J. Nijhof

543

'Design and construction of the America's Cup Yacht "Challenge Australia"
by Peter van Oossanen

561

1994

'Another new approach to cruising sailboats, safe, long-distance cruisers'
by Lars Bergstrom

595

'Load measurements on the 9.4 m sailing yacht SAIL LAB'
by Markku Hentinen and Gunnar Holm

601

Introduction

This volume contains a reprint of a selection of papers on yacht research, which were presented on the bi-annual HISWA Symposia in the period 1969-1994.

The idea to organize these Symposia was generated in the Working Group Yacht Research, which was founded in 1966, consisting of the main Dutch yacht designers and some researchers of the Delft Ship hydromechanics Laboratory.

The Working Group supports and discusses yacht research in the Laboratory as carried out and suggests new subjects to investigate. In particular the work in Delft on sailing yachts has been focussed to some extent on systematic model experiments to provide the yacht designer with tools to predict yacht performance in the design stage.

However it was felt that the results of yacht research in general and the discussion of the various aspects of yacht design, yacht construction and related subjects could be the subjects for presentator and discussion on a wider basis.

As a consequence the first HISWA Symposium was organized and held in 1969 in Amsterdam: a joint effort of the Ship hydromechanics Laboratory of the Delft University and the HISWA Association (the National Association of Watersport Industries in the Netherlands).

This first Symposium used the Dutch language, but the bi-annual follow up used the English language to reach a larger international audience. The 14th HISWA Symposium will be held this year.

The 122 papers presented and published so far, contain a wealth of information for the yacht designer, the yachtbuilder and those who are interested in the many aspects of yachts and yachting.

For many years it appeared that there is a continuous demand for copies of the printed transactions of the last 25 years.

Therefore it was decided to reprint a large number of the presented papers in one volume. It should be understood that the size of such a volume is restricted due to financial and practical limitations. Consequently a selection of the 122 papers had to be made, rather than a complete reprint of the total material.

The selection of the papers to be reprinted is not an easy task, but hopefully the present selection will be a satisfactory choice for those who are interested in the many aspects and the progress in yacht research.

Prof. ir. J. Gerritsma

Systematic model series in the design of the sailing yacht hull

by Pierre DeSaix

Ship & Yacht Division
Davidson Laboratory

Introduction

The design of the sailing yacht hull is principally influenced by rating rules. For over a century the designer's effort in developing a new yacht hull has been directed towards creating a design which will sail fast but also rate well under a particular rule. Unfortunately, those who write rules have little or no knowledge of the exact effect on speed the parameters they choose to rate actually have. A clever designer is one who will find the proverbial loophole and can design a hull which rates low and sails fast as well.

The towing tank for many years has proved an invaluable tool to those fortunate designers having the use of one and the background of several "tank tested" designs. Through the use of model tests, a designer can evaluate the effect of hull changes on sailing performance on a proposed design within the framework of an existing rule. Figure 1 illustrates the effect of rules on the design of two similarly sized craft, each recently developed through the use of a model testing tank. The slack bilges and narrow ends of the "One Tonner" are in sharp contrast to the craft designed for the Cruising Club of America Rule, yet each hull is considered successful in its class. It is not obvious that the individual design features of these two craft contribute to high speed through the water or low rating. The particular rule itself may limit development. For instance, the 5.5-meter class for many years could not have a separate spade rudder.

The improvement in performance in the sailing yacht as a result of individual development model tests has been painfully slow. Due to cost and available time, a designer must direct his effort towards producing the best design for his client. He cannot explore systematically the effect of any one parameter on yacht performance. It took nearly 10 years for the keel profile of the 5.5-meter yacht to evolve (see Figure 2). The performance of the 12-meter class has improved since VIM was first developed in a towing tank in 1937. The changes in the major parameters affecting speed, sail area, waterline length and displacement are shown in Table 1.

To simplify the task of starting a new design, certain limits of general form characteristics have been set down by design offices. Henry and Miller [1] thoroughly define the form characteristics for a wide variety of craft ranging from small-day sailers to heavy cruisers. Their paper represents the state-of-the-art of yacht design. Rhodes [2] states that both the Universal and International yacht racing measurement rules require the same minimum displacement for a given length, that is, $(0.2 LWL + 0.5)^3$ and admits using this as a yardstick in assaying the relative displacement of a proposed yacht. Rhodes further gives a graph showing optimum values of prismatic coefficient against speed and length. Unfortunately, neither Reference [1] or [2], nor any other literature on yacht design provides the designer with the effect on speed changing any of these parameters.

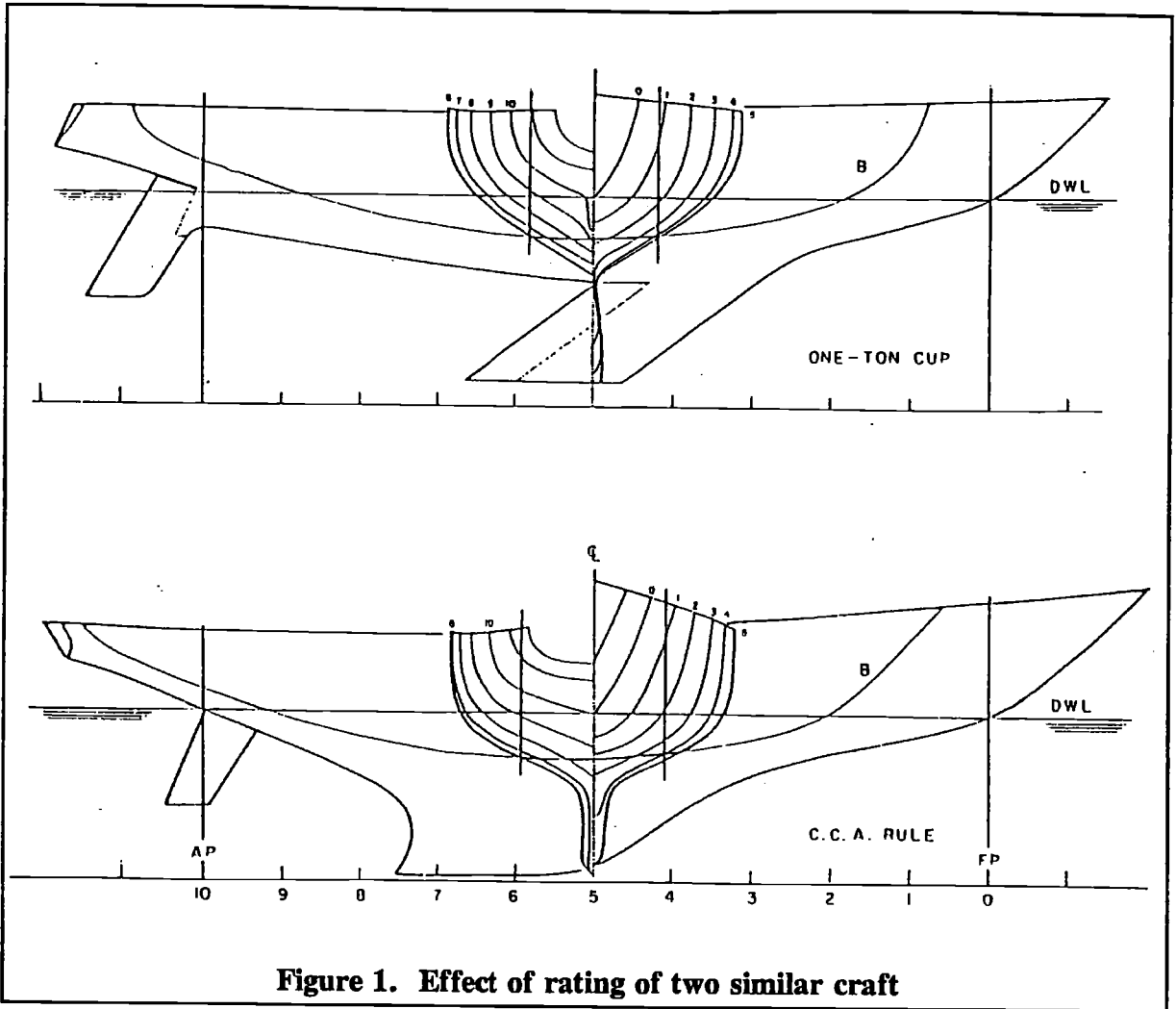


Figure 1. Effect of rating of two similar craft

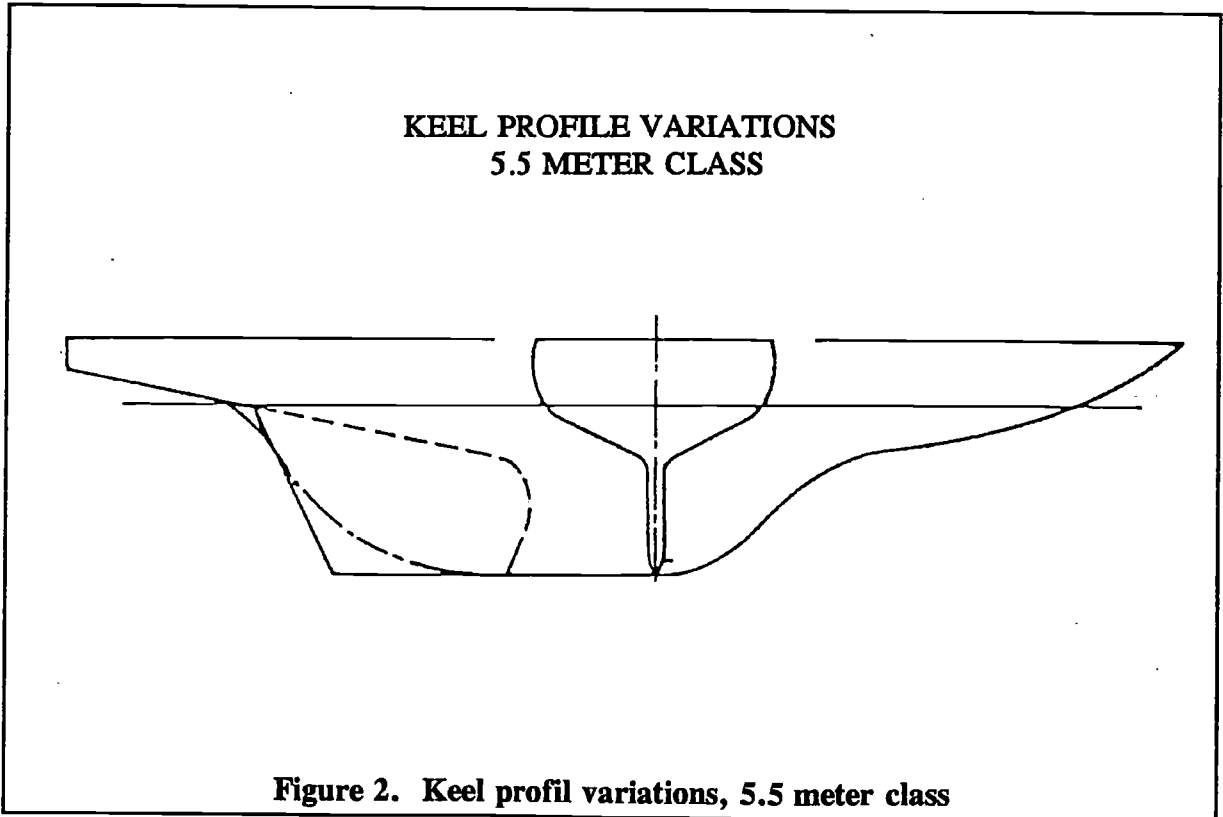


Figure 2. Keel profil variations, 5.5 meter class

Table 1. Development of 12-meter class

	Gleam Early 1930's	Vim 1938	Columbia Weatherly Gretel 1958-62	Constel- lation American Eagle 1964	Intrepid 1967	Intrepid 1970
Waterline Length,	45.0	45.5	46.3	47.0	47.5	48.6
Displacement, lb	60.0	60.4	46.3	64.0	66.0	70.0
Sail Area, ft ²	1890	1880	1820	1800	1750	1725
Heeling Force for 30°						
Heel Angle, lb	3100	3300	3600	3750	3832	4700
Speed-made-good, knots						
Light Wind	5.0	5.0	5.0	4.9	5.0	5.0
Moderate Wind	6.3	6.4	6.5	6.6	6.7	6.8
Strong Wind	6.5	6.7	6.9	7.0	7.1	7.5

The designer must rely on limited model tests or attempt to intuitively modify an already successful design. This paper is directed towards the serious yacht designer and also perhaps to those involved with the creation of rating rules. The author wishes to demonstrate the value of systematic model series in evaluating the effect of certain form parameters on yacht performance regardless of the "rules of the day".

The two series presented here by no means guarantee a "breakthrough" in yacht design. While these data will no doubt be extremely useful to the designer, it is however only a small beginning. The results have answered some serious questions. It is hoped the work will encourage others in the same position as the author to contribute *systematic* data for the use of the individual yacht designer.

Model tests and results of the sailing yacht

General

The techniques of testing yacht models have long been established. It is true that the methods of actual force measurements, turbulence stimulation, use of sail coefficients vary with particular towing tanks. However, the basic principles are essentially those of Davidson [3]. Crago [4] summarizes the methods of yacht performance predictions from model tests. Crewe [5] illustrates the effect of sail performance on windward behaviour and discusses the methods of deriving wind-ward performance from tank tests essential for a proper evaluation of the series results presented here. It is not the purpose of this paper to detail the methods of testing and prediction of performance; the references listed above should provide the reader with a good background.

Briefly, the yacht test yields the following:

1. upright resistance
2. heeled resistance without sideforce
3. heeled resistance with sideforce
4. sideforce with leeway
5. righting moment
6. yawing moment

Results are presented as curves of upright and heeled resistance (at zero sideforce). The

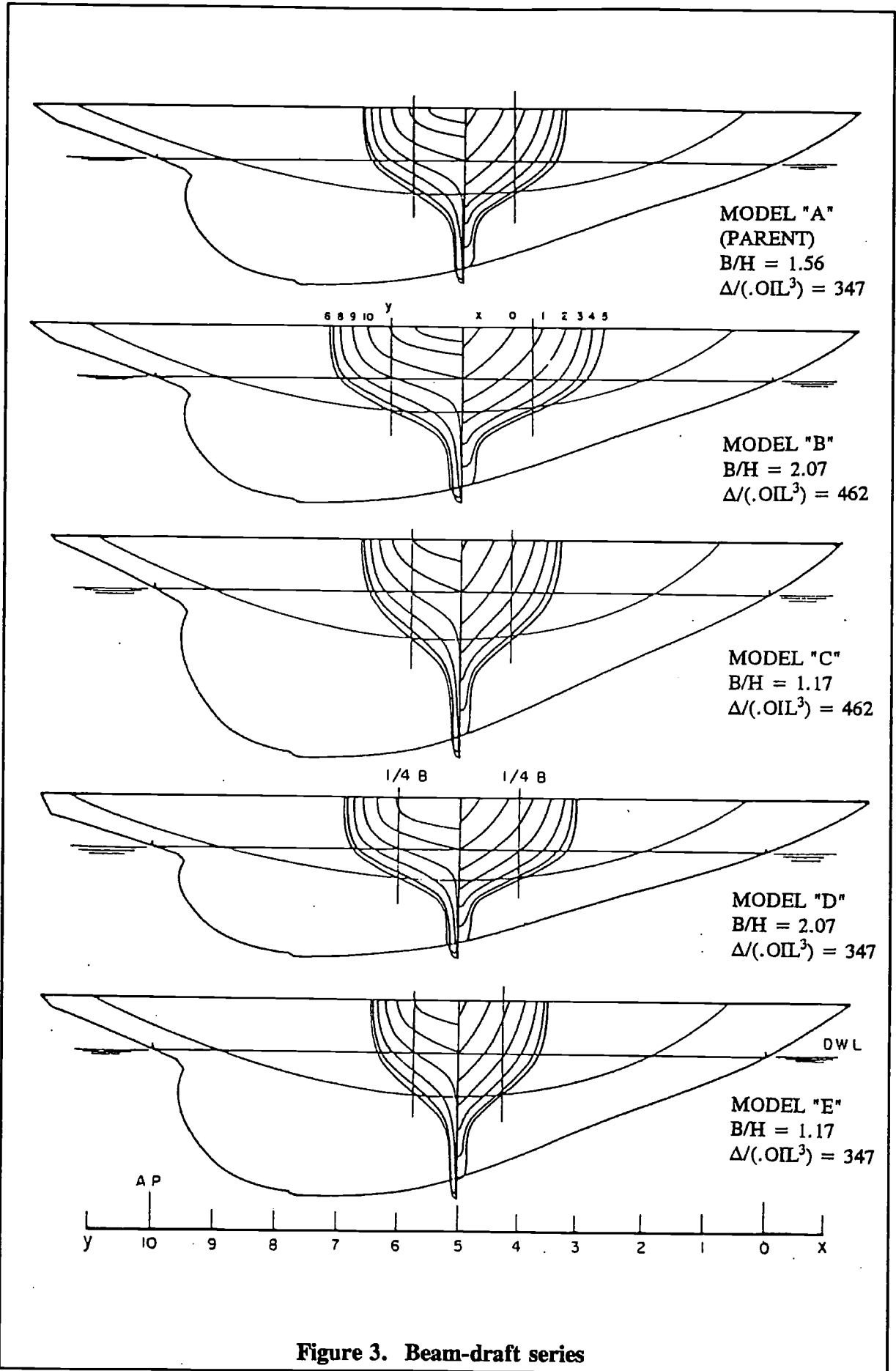


Figure 3. Beam-draft series

heeled resistance with yaw and sideforce, and righting moment, are most conveniently presented in terms of actual sailing performance: speed-made-good to windward and/or speed through the water at various headings to the wind-all against true wind speed.

Beam-draft series

Tests of systematically varied models have been successful in the past. The Taylor Series has even served as a guide for the choice of prismatic coefficient for the sailing yacht! It was logical to embark on a systematic series for the sailing yacht.

Conceived in 1947, the beam-draft series was based on Olin Stephen's N.Y. 32 as a parent form (Model A in Figure 3). Two variations were made; Model B is simply Model A with all half-breadths increased by a factor of 4/3.

For Model C the heights of the buttocks were increased by 4/3. This variation results in a 4/3 increase in displacement as well. The author added Models D and E which have geometrically similar sections as B and C but reduced to size to give the same displacement as the parent. Unfortunately, the depth of the keel varied in proportion to the draft. In the final analysis, it would have been better to maintain the same keel profile while varying the beam-draft series. Extensive tests were run on the parent. However, it wasn't until Models D and E were added to the series that all testing was completed and finally reported for the first time in this paper. Complete data are presented in Reference [6].

Prismatic, series

All previous model series of displacement craft demonstrated the importance of prismatic coefficient on hull resistance. A review of 64 fixed keel cruising yachts developed in the tanks at Davidson Laboratory revealed that 59 models had a prismatic coefficient in the range 0.50-0.58; thirty-four models had a prismatic coefficient in the range 0.52-0.54: One model had a $C_p = 0.40$ and one a prismatic, $C_p = 0.70$. It was decided to test a series of three models of equal displacement and the same lateral plane. The parent was a N.Y. 32 (Model A) modified to give a higher displacement and a smaller, more modern lateral plane. The parent Model 1 (Figure 4) had a $C_p = 0.53$, Model 2 a $C_p = 0.43$ and Model 3 a $C_p = 0.61$.

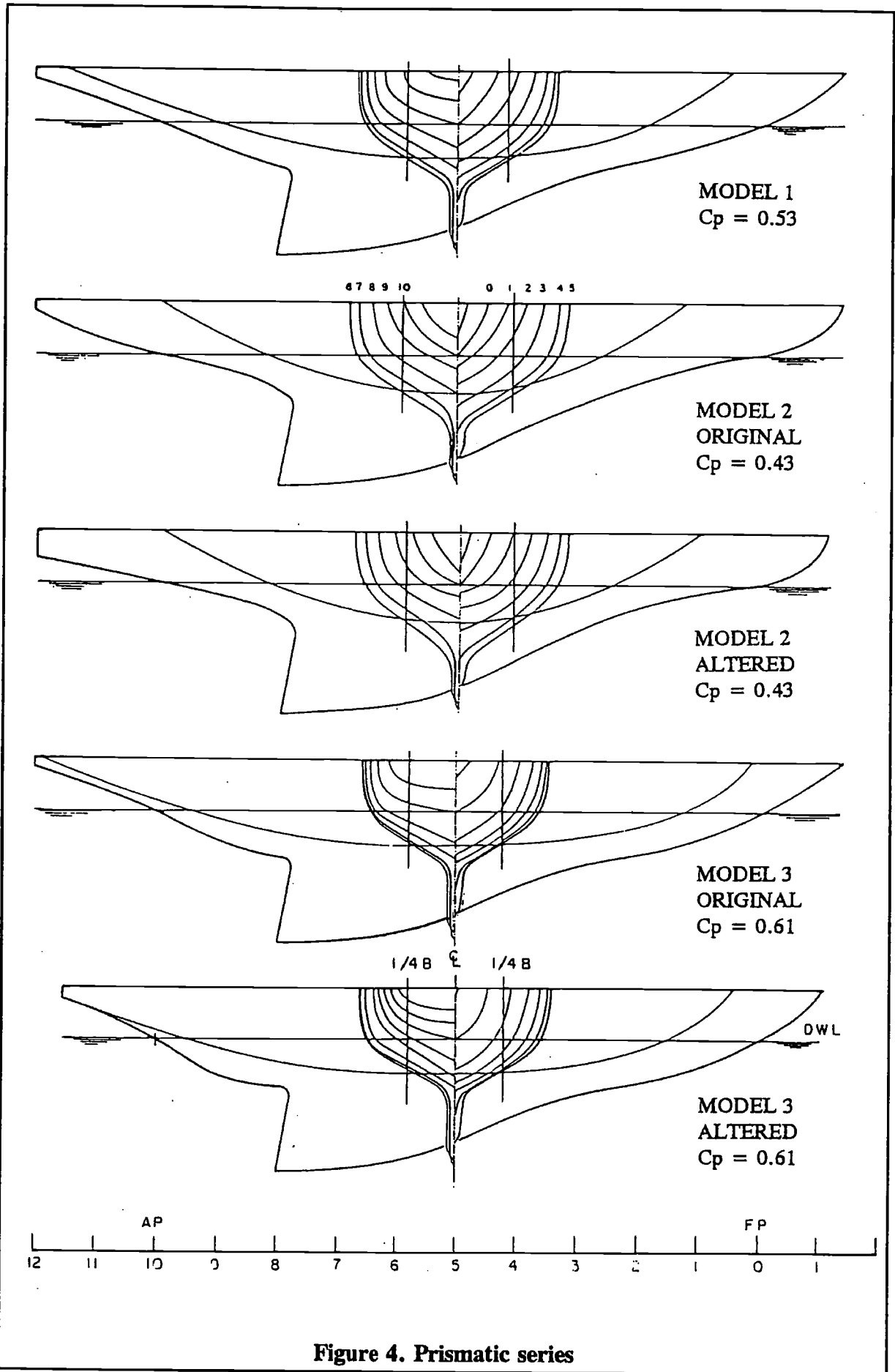
The area curves of the series appear on Figure 5. The sections for the low and high prismatics were reduced or enlarged from the parent to give the required section area. The lines were then faired, keeping the lateral plane and displacement equal to the parent. This resulted in models having extreme hollows in the waterlines or extreme fullness. The models were modified at a later date by straightening the waterlines as much as possible forcing more shape into the buttock lines, thereby keeping the curve of areas the same.

Model test data

Data for the beam-draft series were obtained on the original Davidson Yacht Balance. The data were restricted to upright resistance and heeled testing over the narrow range of speeds and of forces to predict windward performance. The results are presented as curves of upright resistance and predicted speed-made-good to windward.

The new yacht dynamometer now in use at Davidson Laboratory permits testing in the heeled condition over a wider range of speeds and yaw angles. Data for the prismatic series are presented as curves of upright resistance and heeled resistance at zero sideforce.

Curves of heeled resistance and sideforce squared, yawing moment, sideforce and yaw angle are also presented. Data over a wider range of conditions permit prediction of not only windward performance but hull speed for all points of sailing over a range of true wind speeds.



Emphasis is placed on resistance. The effects of stability and sail area can readily be calculated; however, to really improve a yacht's performance, one must be able to reduce resistance. The effects on resistance of the form parameters investigated here will be discussed in detail. All data were expanded to a full-size waterline length 32.0 ft. Rig heights and vertical center of gravity were constant for all models. Gimcrack sail coefficients were used to predict windward performance. Offwind performance was predicted using data available from Spens [8]. Particulars for models of both series are found in Table 2.

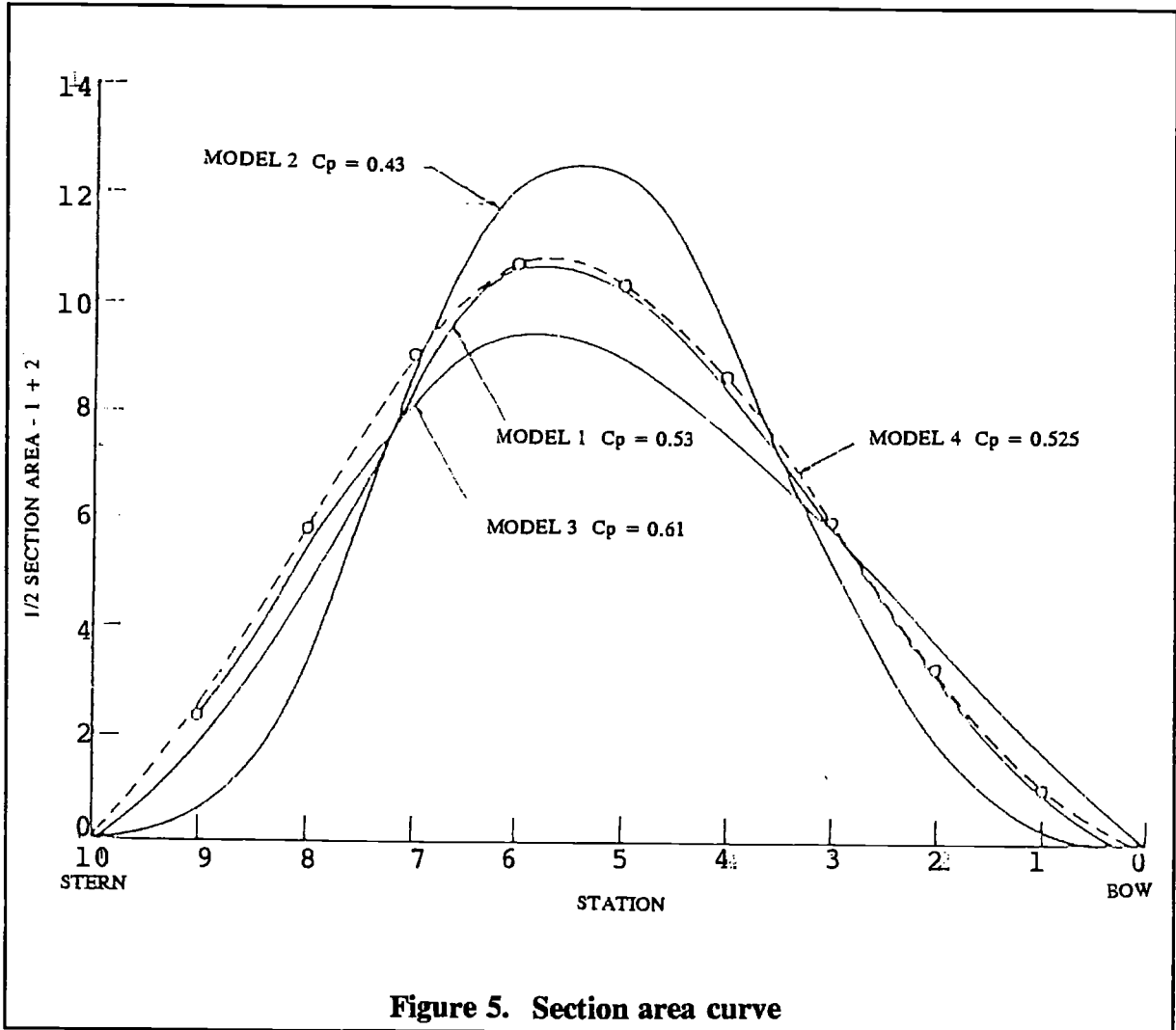


Figure 5. Section area curve

Table 2. Particulars - full size

Model	A	B	C	D	E	1	2	3
Length, L , ft	32.0	32.0	32.0	32.0	32.0	32.0	32.0	32.0
Displ., Δ lb	25.45	33.93	33.93	25.45	25.45	21.65	21.65	21.65
Wetted surface, WS , ft^2	344	438	445	379	385	295	281	299
Vert. Cent. of Grav., ft below L	1.20	1.20	1.20	1.20	1.20	1.20	1.20	1.20
Sail Area, SA , ft^2	865	1048	1048	865	865	780	780	780
CEH, ft	22.50	22.50	22.50	22.50	22.50	22.50	22.50	22.50
CEAO, ft	11.80	11.80	11.80	11.80	11.80	11.80	11.80	11.80
Beam-draft ratio, B/H	1.56	2.07	1.17	2.07	1.17	1.49	1.38	1.62
Displ.-length ratio, $\Delta/(.01 L)^3$	347	462	462	347	347	297	297	297
Sail Area-vol. ratio, $SA^{2/3}/(Vol)^{1/3}$	4.0	4.0	4.0	4.0	4.0	4.0	4.0	4.0
Prismatic coefficient, C_p	0.53	0.53	0.53	0.53	0.53	0.53	0.43	0.61

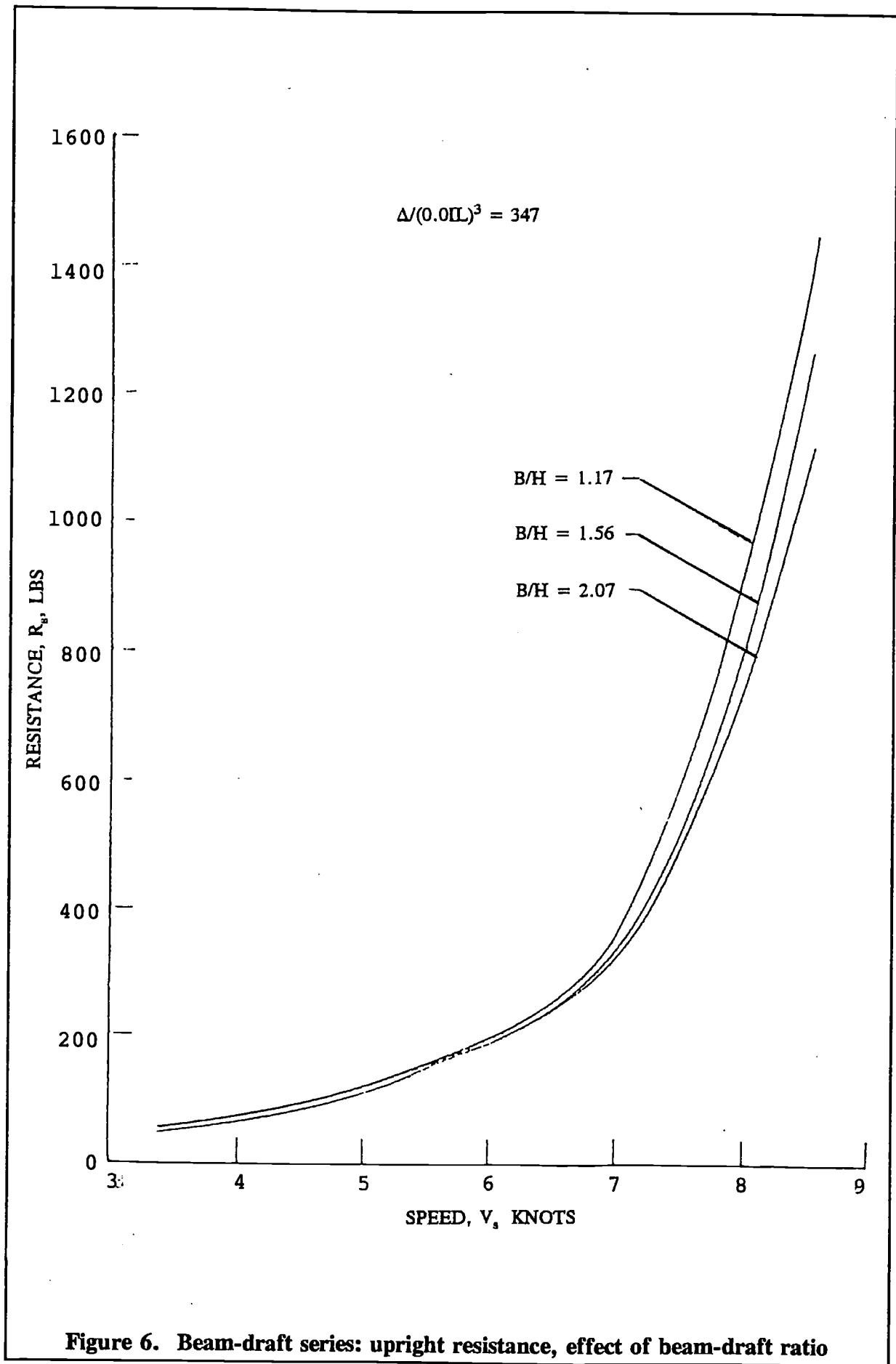


Figure 6. Beam-draft series: upright resistance, effect of beam-draft ratio

Scale Ratios	
Length	10
Area	100
Volume	1000
Displacement	1027
Speed	3.16

Results Beam-Draft Series

Upright resistance data showing the effect of beam-draft ratio at constant displacement appears on Figure 6. The wider hull has lower resistance above 6 knots. The narrow beam is burdened with high resistance over the entire speed range. The effect of displacement on upright resistance appears on Figures 7 and 8. While having generally lower resistance, the wider model suffers a higher percentage increase in resistance due to added displacement. The effect of beam-draft ratio on the rate of increase of heeled resistance with (sideforce)² (Figure 9) varies with keel depth. The widest model (D) has a disproportionately higher rate of added drag, however. Added displacement appears to make a minor difference in the rate of increase of induced drag. There is some advantage to increased displacement at 20° and 30° heel (Figure 10). The windward performance (Figure 11) favours Model D, $B/H = 2.07$, with a distinct advantage above 11 knots wind speed. The narrow hull ($B/H = 1.17$) is the poorest over the entire wind speed range. Added displacement improves the windward performance of the narrow boat while it has no effect on performance of the wider models of the series (Figure 12). One of the major effects of beam-draft and displacement changes is on the form stability of the series. The wind required to heel 30° is 15 knots for Model E (narrow and light) while it is over 28 knots for Model C (wide and heavy).

For the results presented, the rig height and vertical center of gravity were held constant. The sail area was proportioned to the rate of sail area to volume, $SA^{1/2}/Vol^{1/3} = 4$. This appears to be the value used by most designers submitting lines for testing at Davidson Laboratory. These are admittedly simplifying assumptions. The narrow, deep yacht would surely have a lower *V.C.G.* while increased displacement generally allows a higher ballast ratio and lower *L.C.G.* The stiffer vessel could theoretically carry more sail. As a first approximation, the above assumptions appear reasonable. Table 3 has been included to provide the effects on windward performance of changes in sail area and stability.

Results Prismatic Series

Figures 13, 14, and 15 present the resistance at zero sideforce for 0, 10, 20, 30° heel. For prismatic coefficients 0.43 and 0.53, resistance generally increases with heel angle. High prismatic coefficient $C_p = 0.61$ shows a definite reduction in resistance with heel angle in the speed range 6 to 8 knots where most windward sailing is done. Heeled data are presented for Model 1 ($C_p = 0.53$). The resistance is seen to vary linearly with sideforce squared (Figure 16). The rate of change of resistance with sideforce squared is a measure of the effectiveness of the hull and keel as a lifting surface. The higher the rate, the less effective the hull is as a lifting surface. The author is reluctant to use the term "aspect ratio" since all yacht hulls are of very low geometric aspect ratio. The rate of increase is seen in Figure 17 not to vary much with speed until above 7 knots, when the resistance increases at a much more rapid rate. There is also some loss in hull efficiency with heel angle. Since the keels were the same for each model in the prismatic series one would expect little difference in the rate of resistance increase. There is some small advantage to high prismatic, $C_p = 0.61$. Unfortunately, the speed range of the beam-draft series was not as high as the prismatic, and a comparison of the resistance rate increases between series cannot be readily made.

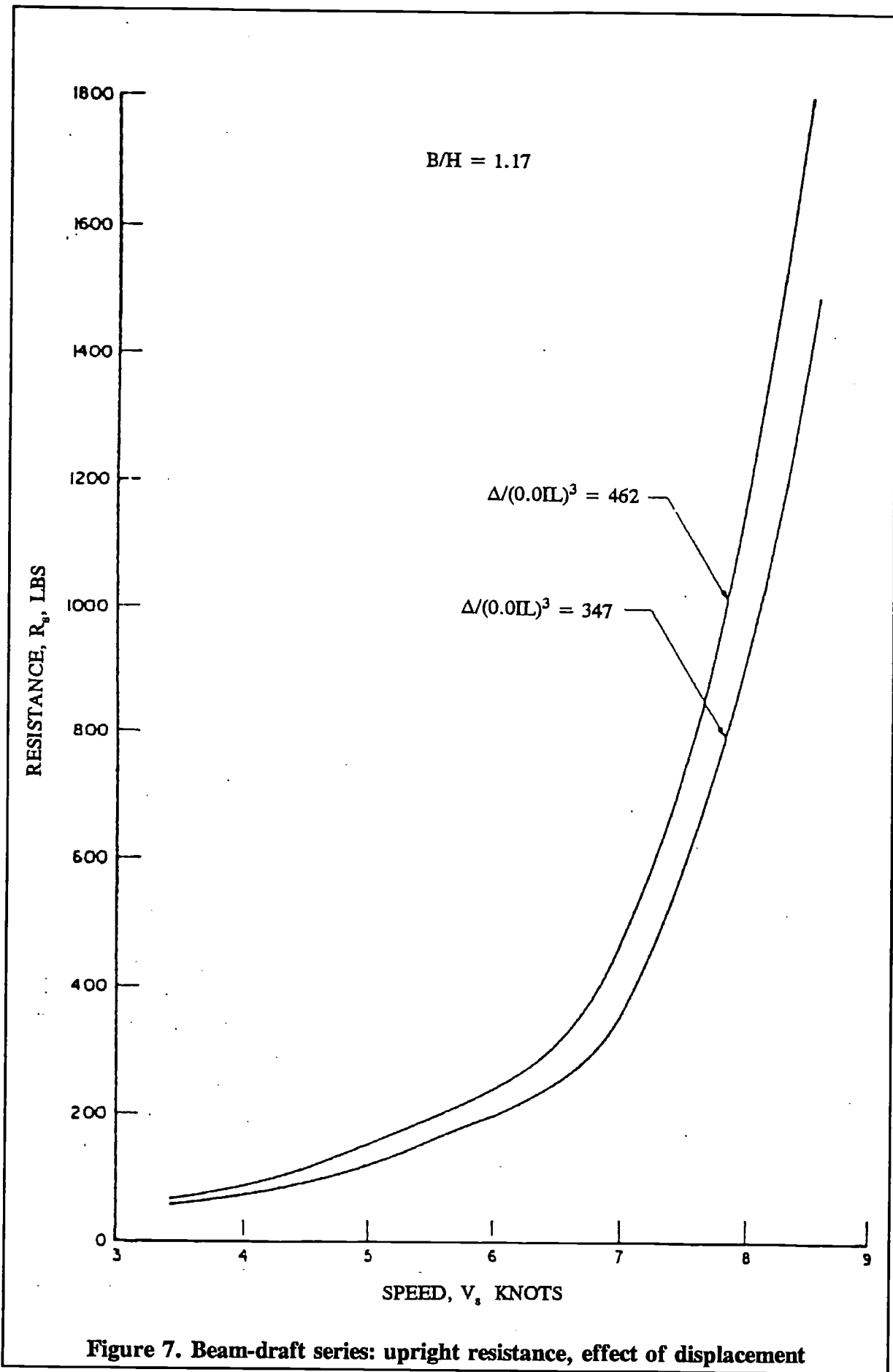
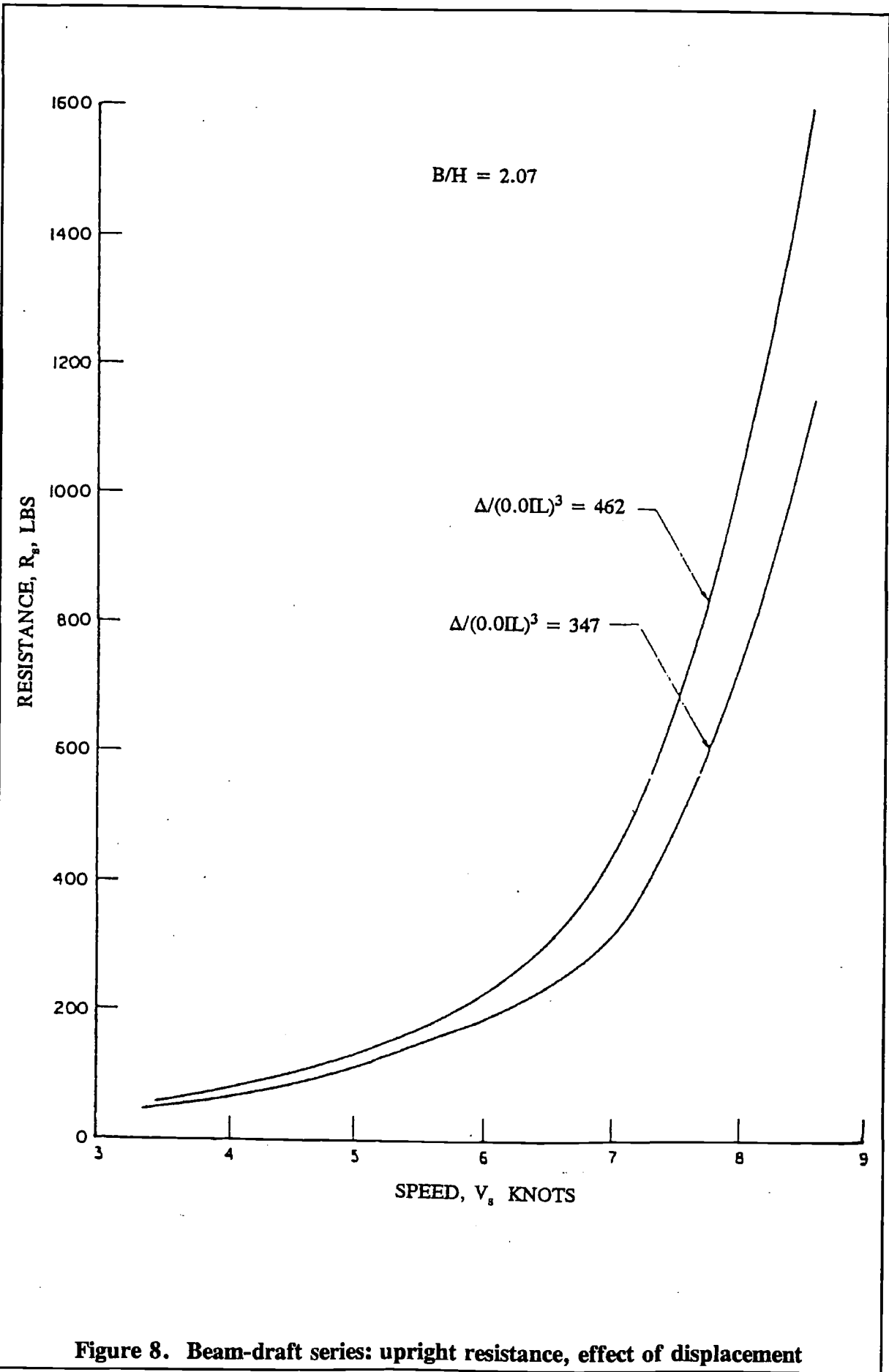


Figure 7. Beam-draft series: upright resistance, effect of displacement



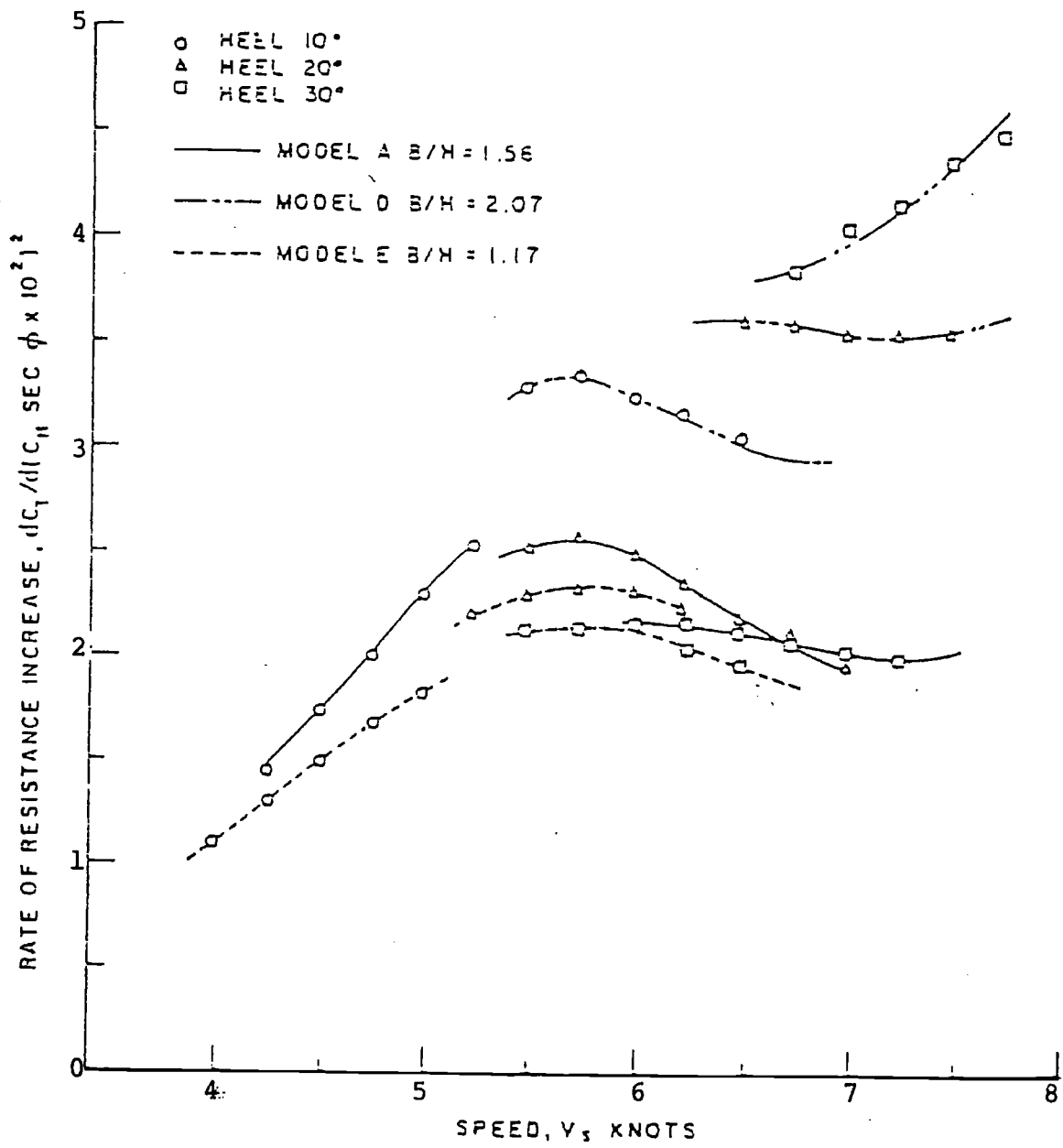


Figure 9. Beam-draft series: resistance increase, constant displacement

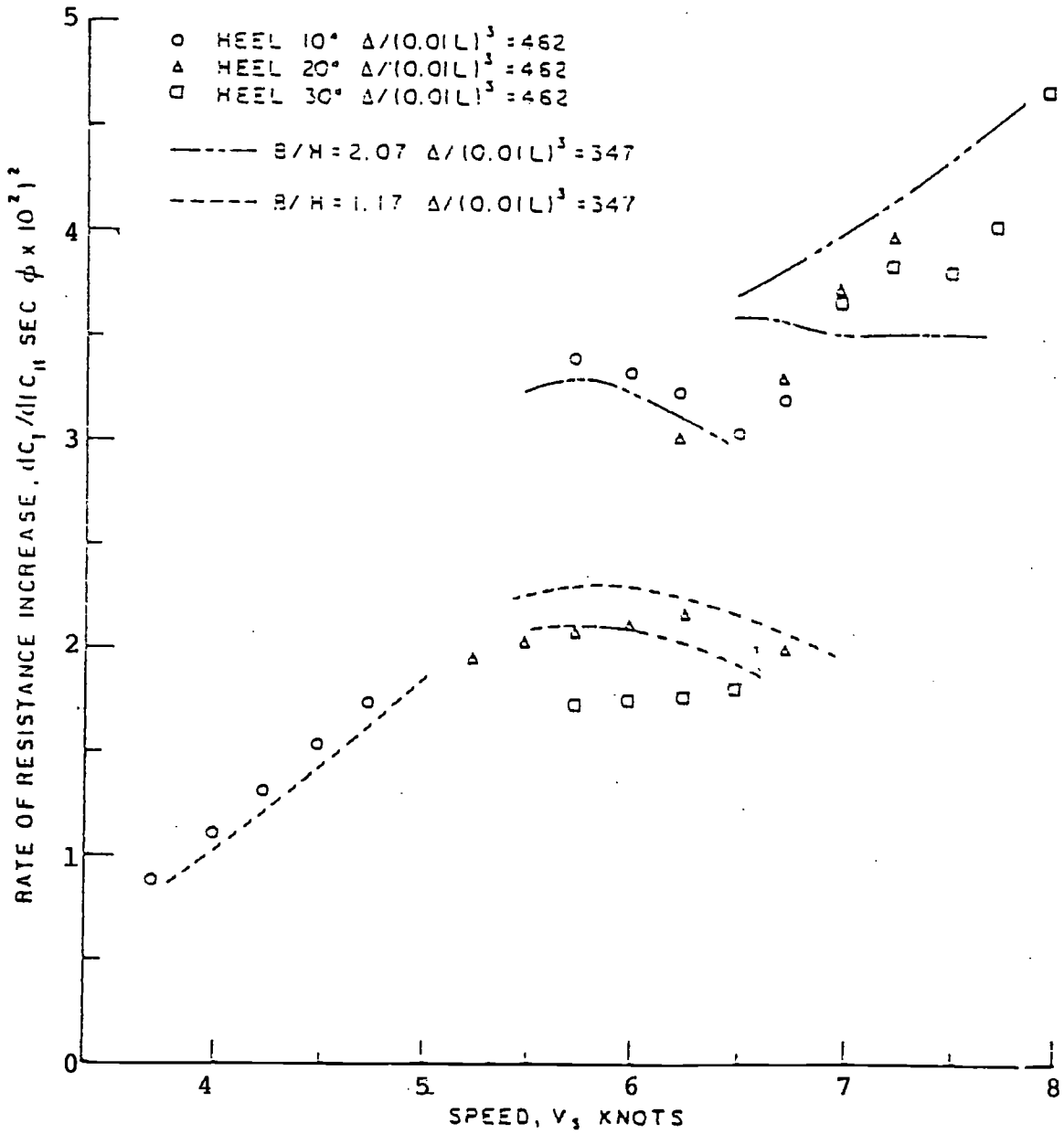


Figure 10. Beam-draft series: resistance increase, effect of displacement

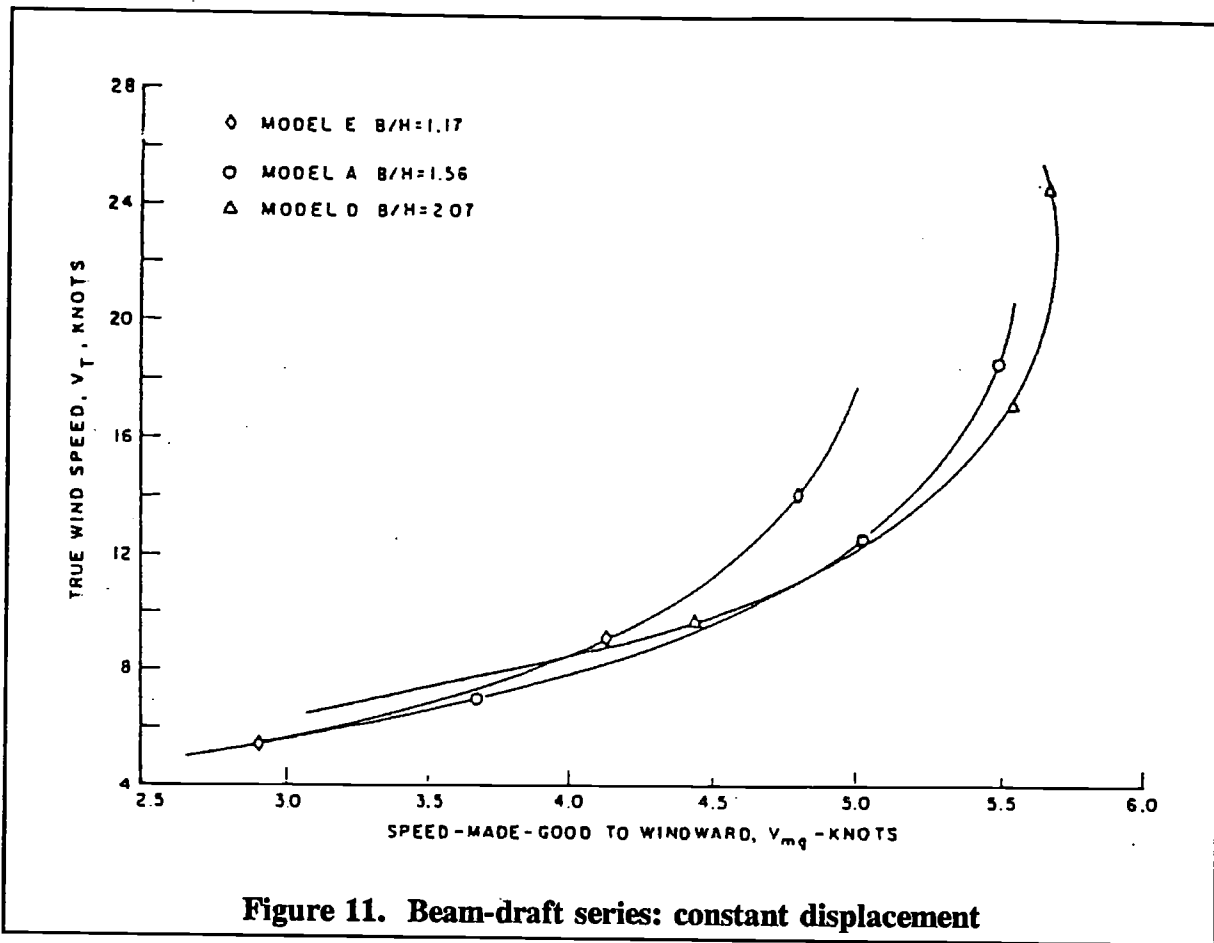


Figure 11. Beam-draft series: constant displacement

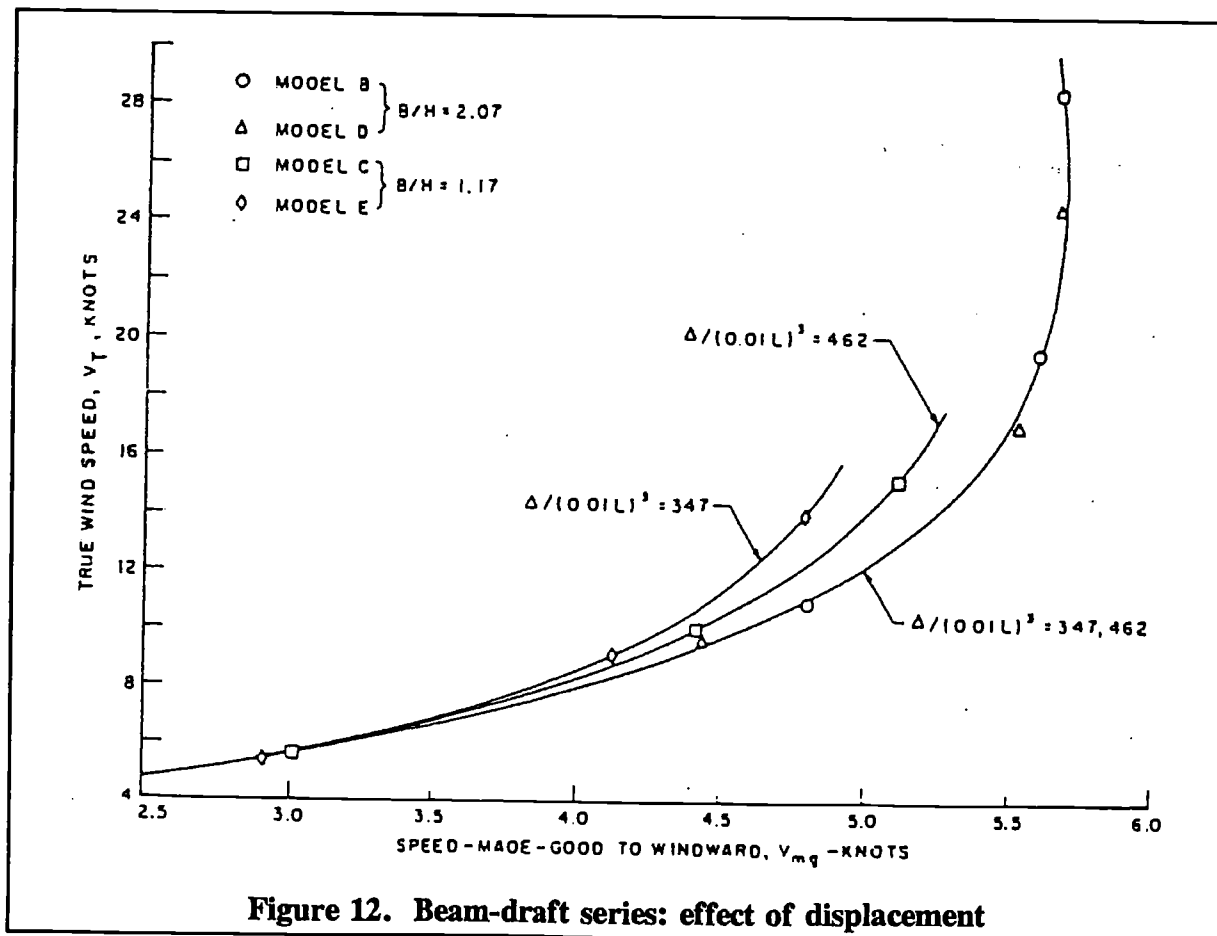


Figure 12. Beam-draft series: effect of displacement

Table 3. Percentage changes in best V_{mg} at constant V_r for changes in sail area and stability

Model	V_r knots	V_{mg} knots	Percentage change in best V_{mg}			
			-10% SA	+10% SA	-10% Stab	+10% Stab
A	7.5	3.87	-3.36	+2.07	-1.03	-.26
	13.0	5.10	-1.37	+ .59	-1.18	+1.18
	19.5	5.51	+ .36	- .91	-2.36	+1.64
B	7.5	4.18	-.96	+1.43	-.72	+1.68
	13.0	5.11	-.78	+ .59	-.98	+ .98
	19.5	5.60	-.36	.00	-.71	+ .36
C	26.0	5.70	+ .70	-1.05	-1.23	+ .88
	7.5	3.73	-2.95	+2.95	+ .80	+1.07
	13.0	4.90	-.82	+ .82	-1.43	+1.22
D	19.5	5.34	-.37	+ .37	-2.62	+ .94
	7.5	3.92	-2.04	+1.79	-1.02	+ .25
	13.0	5.05	-.99	+1.39	-.20	+ .20
E	19.5	5.66	-.35	-.35	-1.06	+ .18
	26.0	5.62	+1.60	-1.78	-2.85	+1.60
	7.5	3.68	-3.26	+1.90	-1.63	.00
	13.0	4.70	-.64	+ .64	-2.13	-1.06
	19.5	5.04	+ .40	-.20	-4.77	+4.37

The slope of the resistance line for $C_p = .53$ (Prismatic Series) is less than that for Model A parent Model (beam-draft series) however indicating some improvement in hull efficiency with the newer keel profile. The sideforce coefficient-yaw angle relationship appears to be independent of speed, the curves can be collapsed for heel angle as well (Figure 18). Yaw moment and sideforce coefficients (Figure 19) show a less definite trend with speed and heel angle. (Sideforce in this case only is measured at right angle to the hull centerline).

Prismatic coefficient has a pronounced effect on the upright resistance of the series. The high prismatic, $C_p = 0.61$, has the lowest resistance above a speed of 7.4 knots. There appears to be no advantage to the lowest prismatic, $C_p = 0.43$ (Figure 20).

Again, as in the beam-draft series, the heeled data are best presented as actual sailing performance. Speed-made-good to windward for the series are presented on Figure 21. The performance of Model 1, $C_p = 0.53$, is appreciably better to wind-ward over a wide range of wind speeds. The low prismatic is better to windward below a wind speed of 8 knots. In high winds above 24 knots, high prismatic, $C_p = 0.61$ may be better.

The sailing performance of the three models for all points of sailing is given on Figure 22. The reaching results using sail coefficients from Spens [8] have been faired into the windward results calculated using Gimcrack to give a complete polar plot. Low prismatic shows a small advantage in light winds, off the wind while in strong wind there is a distinct advantage to the high prismatic form off the wind.

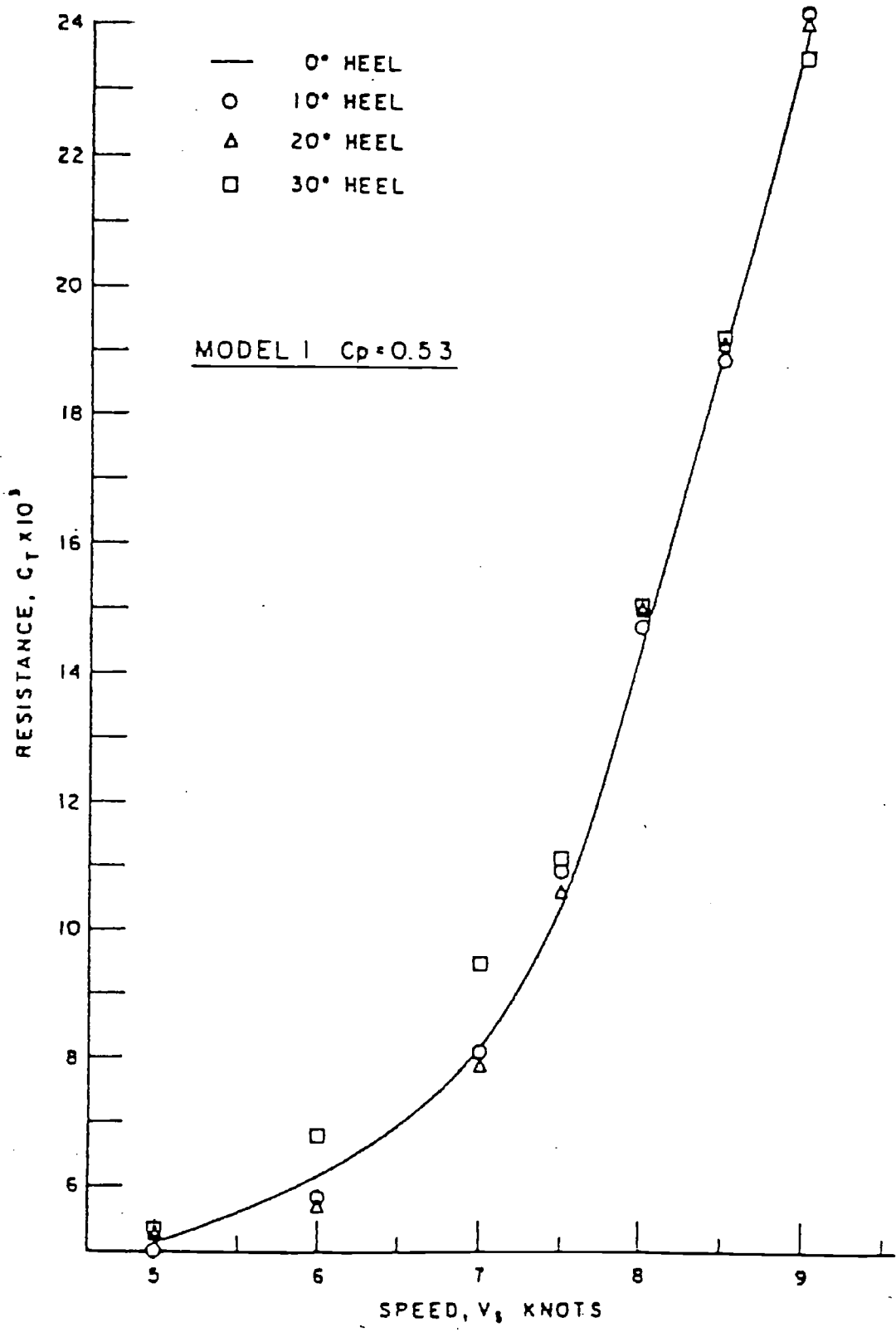


Figure 13. Prismatic series: resistance at zero side force

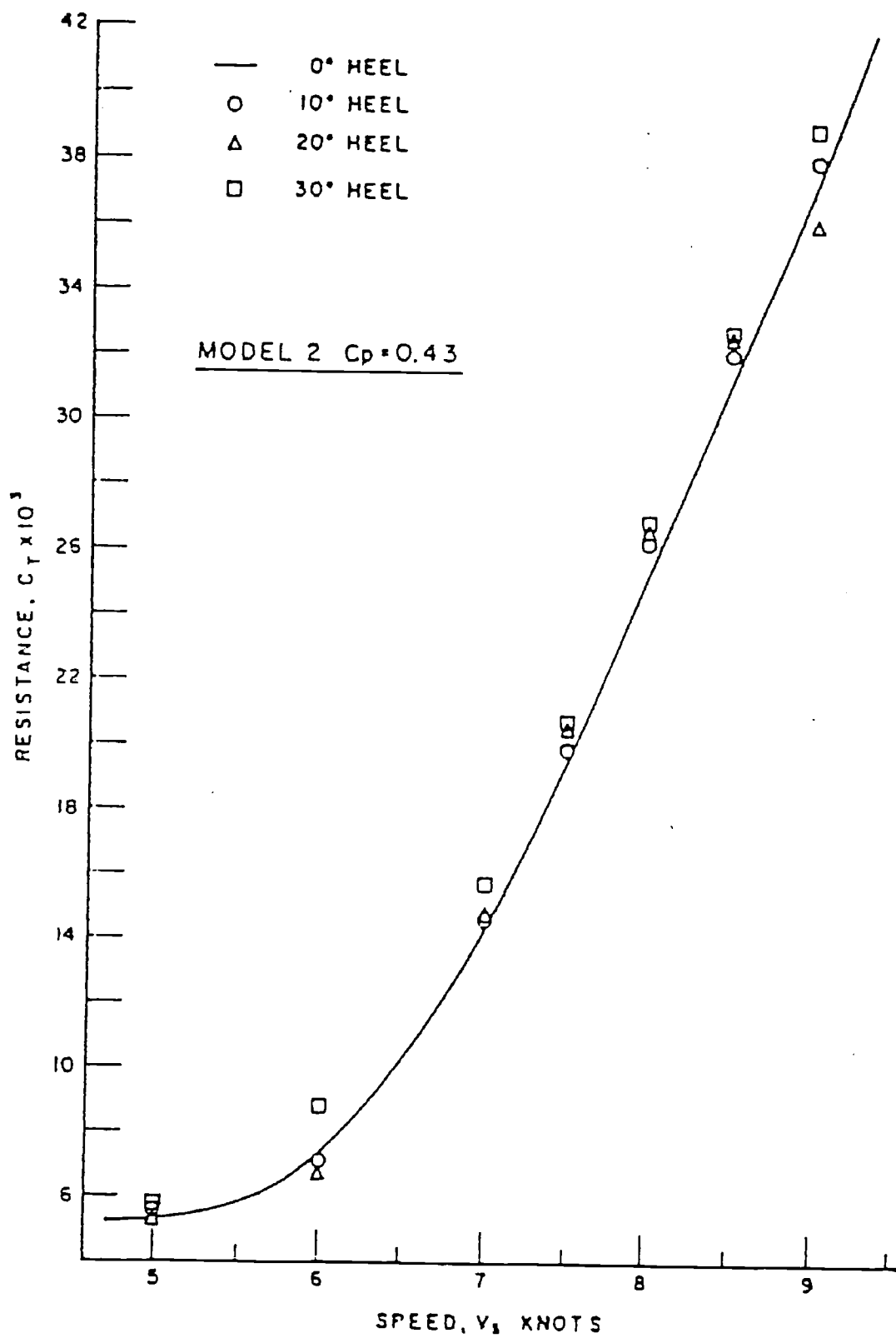


Figure 14. Prismatic series: resistance at zero side force

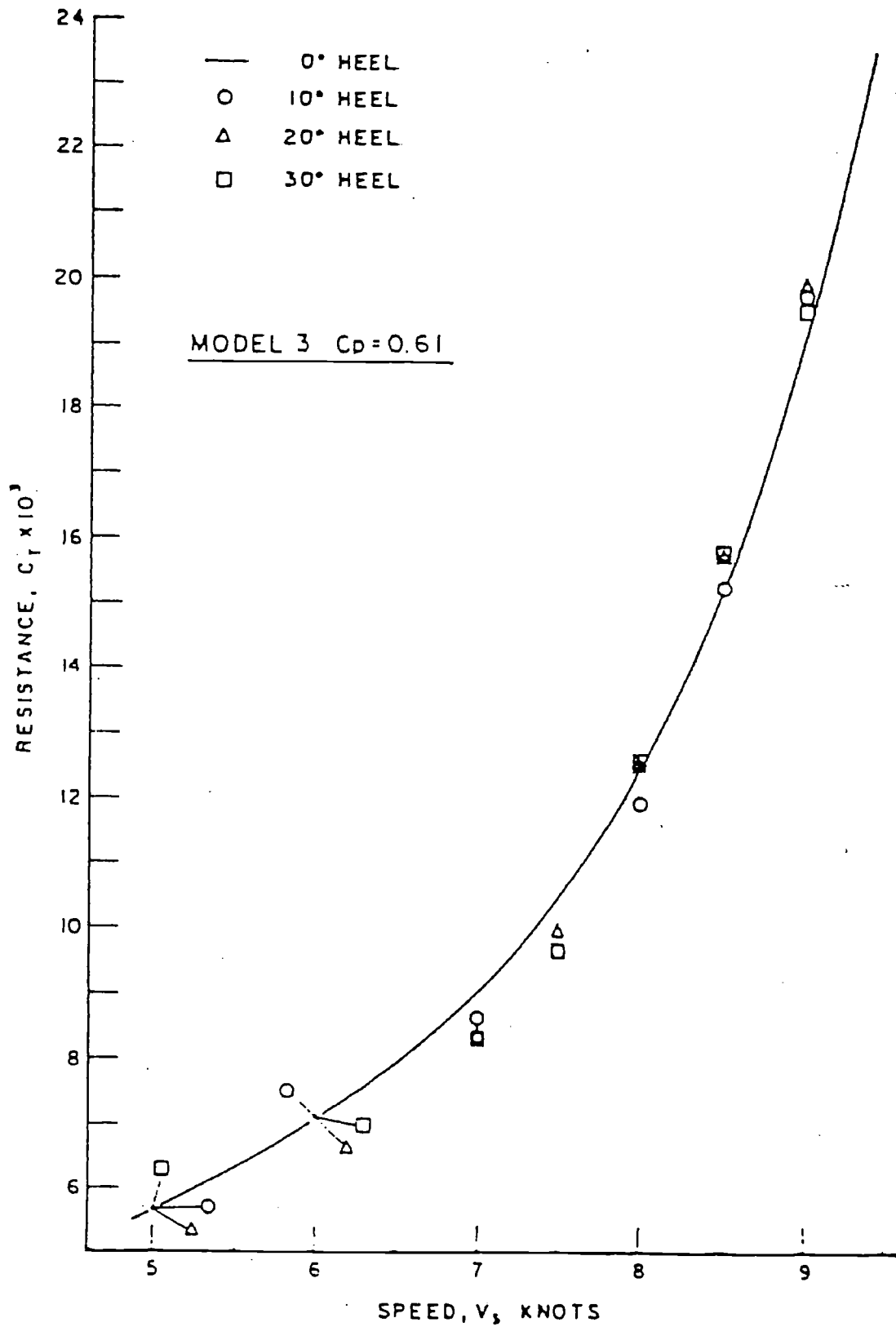


Figure 15. Prismatic series: resistance at zero side force

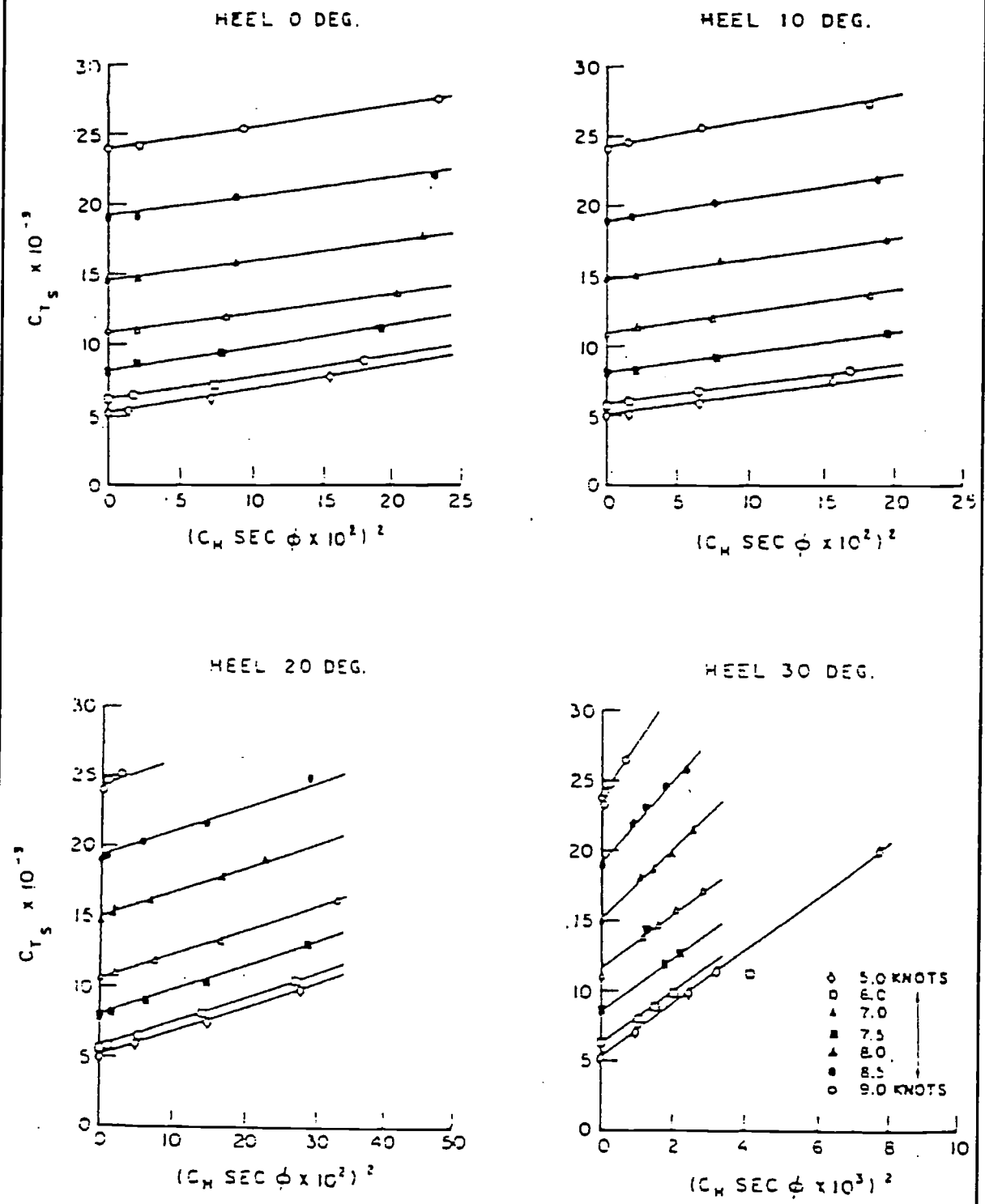


Figure 16. Prismatic series: model I, $C_p = 0.53$, test data scaled to full size, resistance versus side force

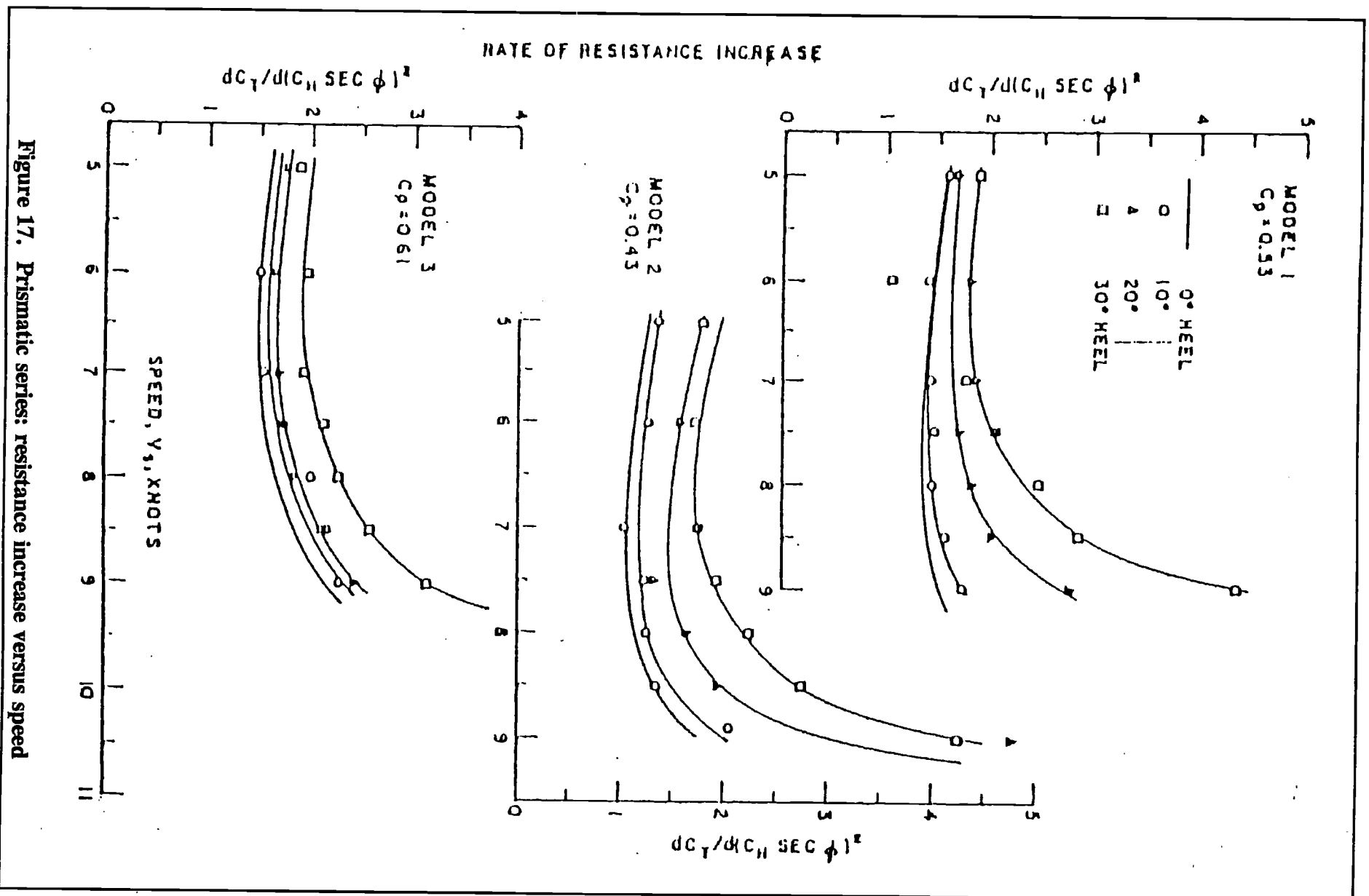


Figure 17. Prismatic series: resistance increase versus speed

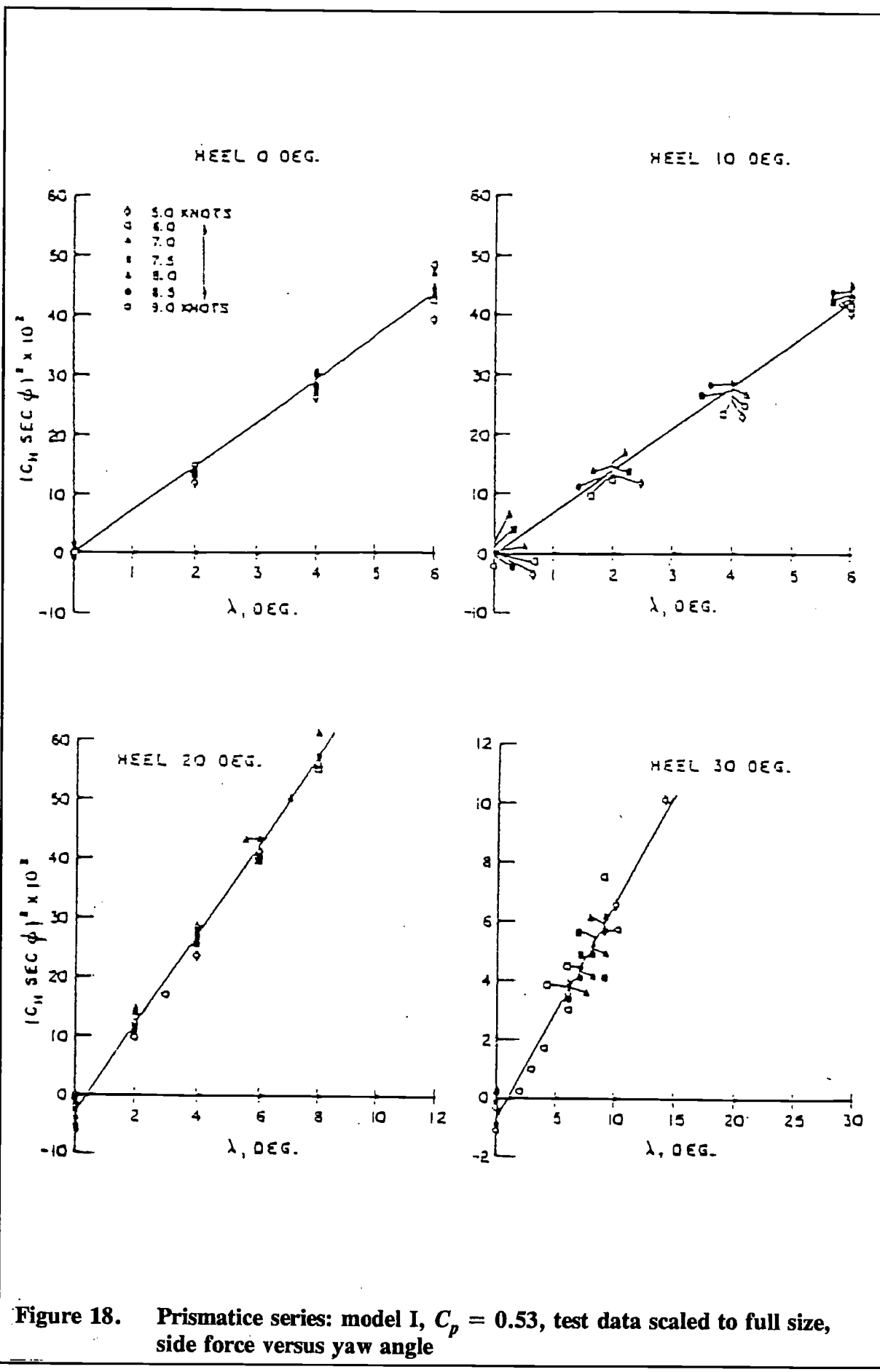


Figure 18. Prismatic series: model I, $C_p = 0.53$, test data scaled to full size, side force versus yaw angle

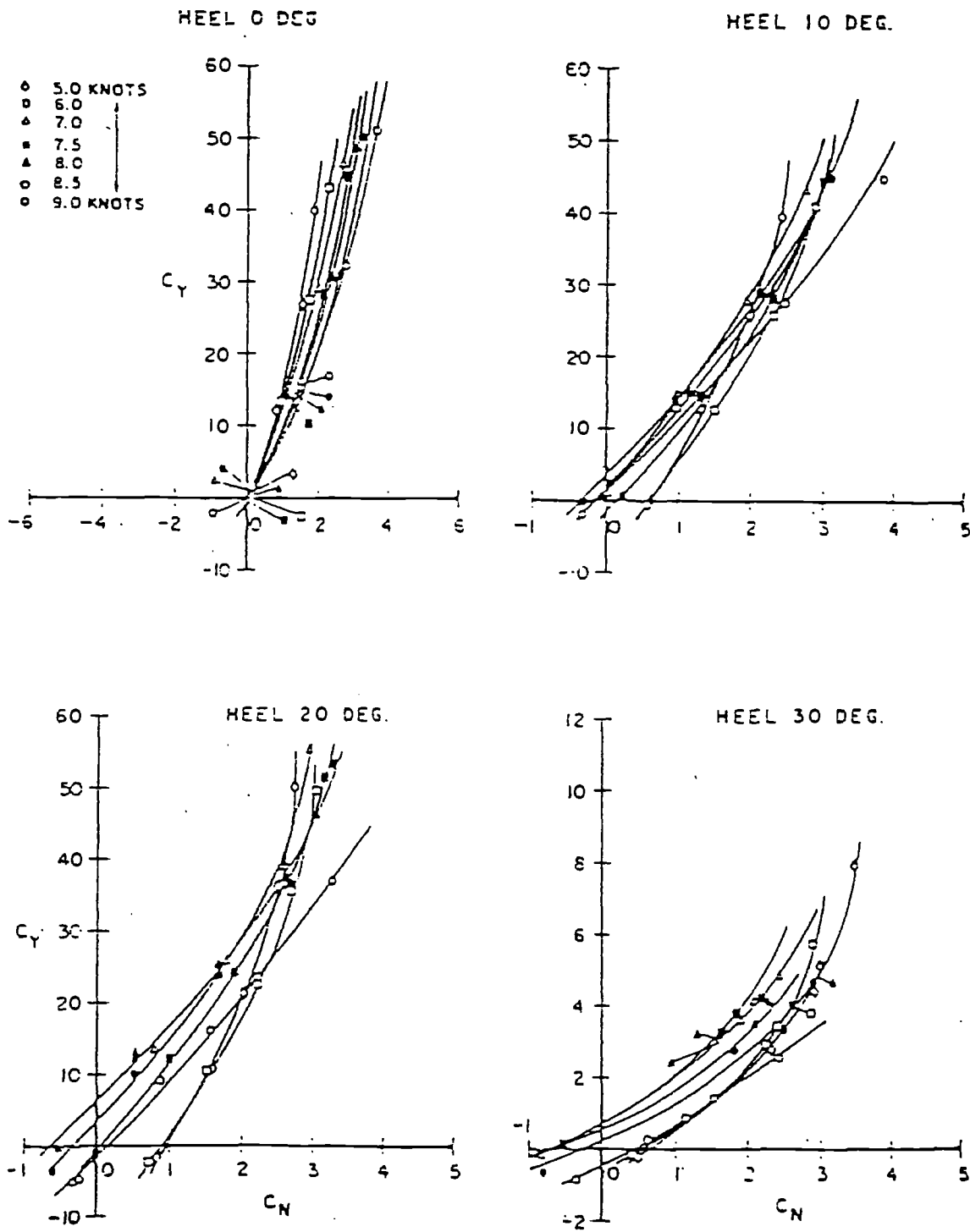


Figure 19. Prismatic series: model I, $C_p = 0.53$, test data scaled to full size, side force versus yaw moment

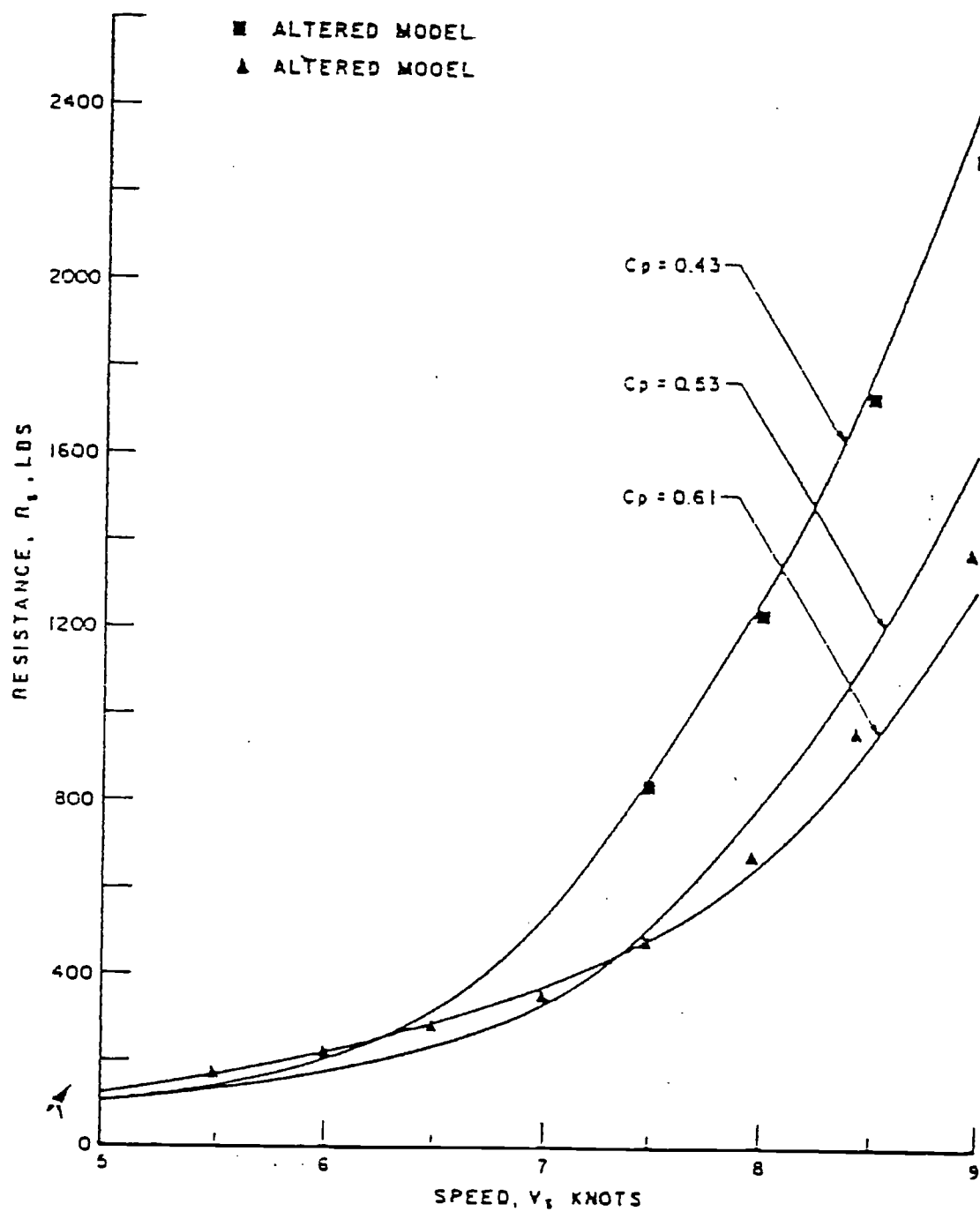


Figure 20. Prismatic series: upright resistance

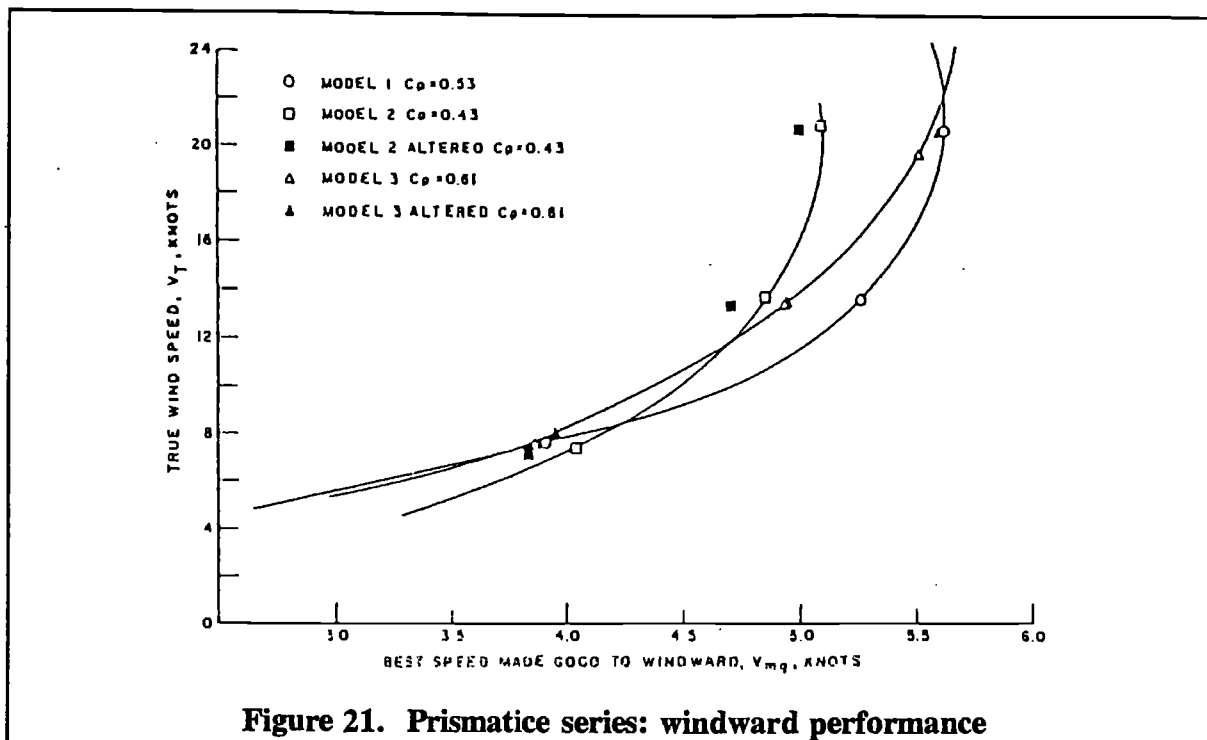


Figure 21. Prismatic series: windward performance

Conclusions

The two series presented in this paper are not intended by any means to provide all necessary information for a designer in creating a winning boat to a given rule. The testing of a systematic model series as reported here does illustrate a relatively rapid means of obtaining the effect of a given parameter on sailing performance. Both series should be extended to light displacement ($\Delta/(\cdot 01L)^3 = 250$). The keel profile should have been the same for all models. The keel profile could also have been reduced in area and a more efficient keel section used for the beam-draft series.

In spite of certain limitations the beam-draft series provided valuable data on the following:

1. effect of displacement for two beam-draft ratios
2. effect of beam-draft ratio on form stability
3. effect of beam-draft on upright resistance
4. effect of beam-draft on windward performance

It appears advantageous to keep the wider yacht light, and the narrow one heavy. The beam-draft ratio of 2.07 at a $\Delta/(\cdot 01L)^3 = 347$ seems to have the best all-around performance. If the lateral plane were the same for Model D ($B/H = 2.07$) as the parent Model A, the windward performance of D would have been further enhanced.

The prismatic series illustrates the dramatic effect this parameter has on sailing performance. The magnitude of the variation was greater than any designer would attempt and perhaps now some intermediate values of prismatic should be added to the series.

The lowest prismatic gave generally the best performance in light air while the high prismatic gave the best performance in strong wind reaching and running. The "normal" prismatic had by far the best windward performance over the usual wind speeds encountered. The advantage of a high prismatic was clearly shown on the upright resistance of the series. A major refairing of the waterlines of the two extremes of the prismatic series did not materially alter the upright resistance or the windward performance. This substantiates the major effect prismatic coefficient has on performance.

Further remarks

The series presented in this paper deals with a particular craft, a moderate to heavy displacement vessel with the keel faired into the hull in such a manner as to give no sharp definition between keel and hull in contrast to the light displacement fin-keel yacht. The designer must also concern himself with other types of sailing craft. The fin-keel yacht and shoal draft centerboarder are two examples. The systematic model series approach is applicable here as well. Barkla [9] presented the results of a beam-draft series based on a fin-keel 5.5 meter as a parent form. For this series, the keel profile and sections were kept the same for all models. DeSaix [10] demonstrated the fin-hull interaction for a 5.5-meter hull. It is possible with some limitations to predict the effects of keel changes on performance.

Evaluations of keel profile changes are available in separate works by K. MacLavery [11] and in less detail by DeSaix [12].

Tanner [13] presents the results of tank tests of a 1/12-scale model of a 50-ft waterline shallow draft ketch with three alternative keel appendages: a centerboard, leeboards and bilge keels. The effects of the fore and aft positions of a fin keel are available in References 14 and 15. The control of the sailing yacht is of equal importance as the potential speed. Millward [16] presents a design procedure for a spade rudder. The control problem is briefly discussed in Reference 17.

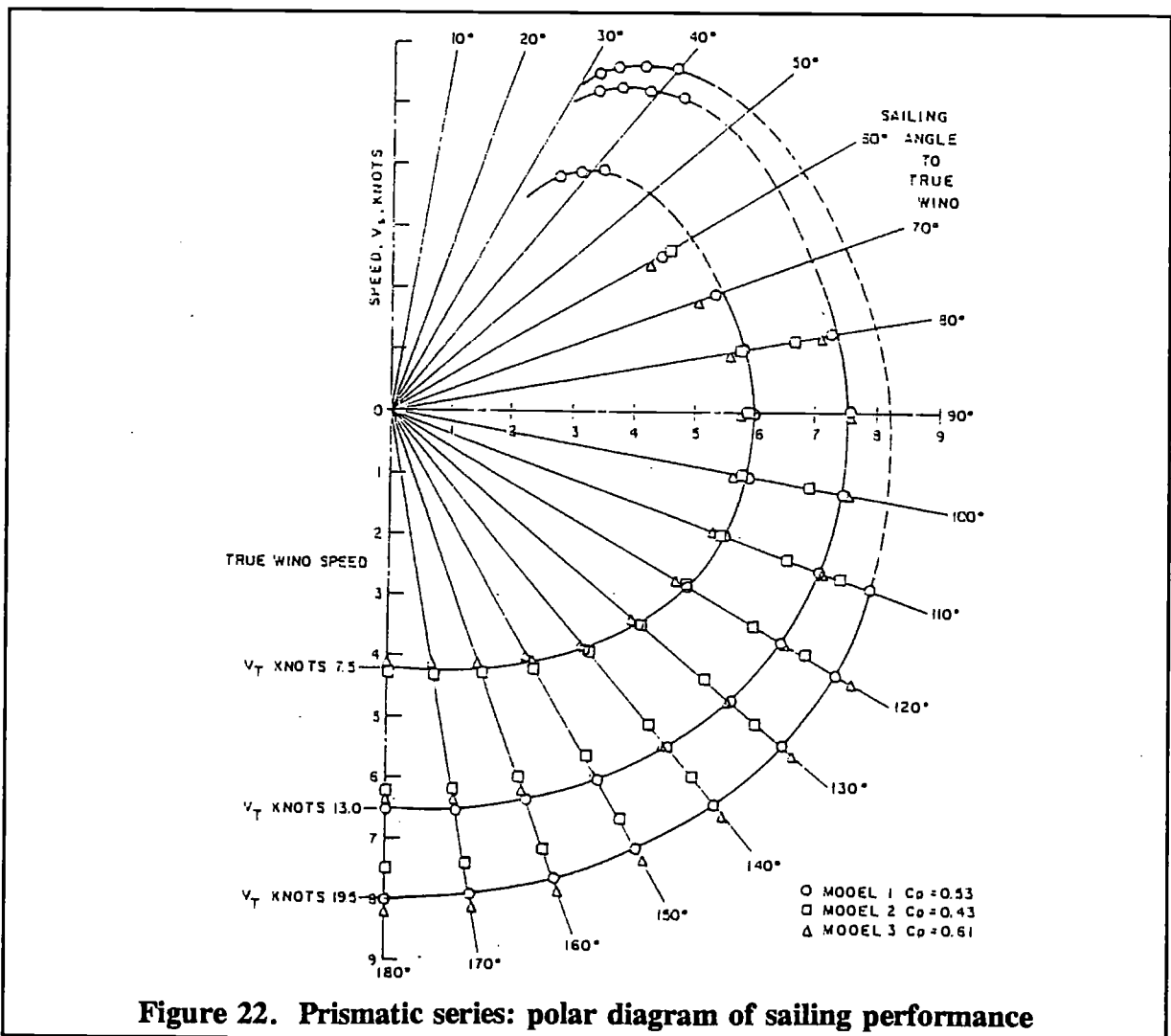
It is hoped the results of the two series presented will encourage others towards the same type of experimentations. Rules change and new yachts must be developed to rate well against them. Identification of the important form parameters affecting performance and a true evaluation of their effects on speed can be achieved through the use of systematic model test series and should lead to a more rapid development of successful sailing craft than has been achieved through the development work on individual yachts.

The bibliography included with this paper should provide the designer with additional information of a more or less systematic nature with which to evaluate his proposed design.

Bibliography

- [1] Henry, R. G. and Miller, R. T., "Sailing Yacht Design ~ An Appreciation of a Fine Art", Paper No. 9 Presented at Annual Meeting, The Society of Naval Architects and Marine Engineers, November 1963.
- [2] Rhodes, Philip L., "Modern Yacht Design", The Experts' Book of boating, Prentice-Hall, Inc., Englewood Cliffs, N. J. 1958.
- [3] Davidson, K., "Experimental Studies of the Sailing Yacht," SNAME, 1937.
- [4] Crago, W. A., "The Prediction of Yacht Performance From Tank Tests," Paper Read in Southampton at a Meeting of the Southern Joint Branch of The Royal Institution of Naval Architects and The Institute of Marine Engineers, March 1962.
- [5] Crewe, P. R., "Estimation of Effect of Sail Performance on Yacht Close-Hauled Behaviour," Paper No. 3 Read at the joint Meeting of the RINA and the Institution of Engineers and Shipbuilders in Scotland in Glasgow, February 1964.
- [6] Yonkers, W. F., "Model Tests of Five Related Sailing Yacht Forms", Prepared for Stevens Institute of Technology, Department of Ocean Engineering, Special Problem OE-400, September 1970.
- [7] DeSaix, P., "Statistical Evaluations of the Effect of Form Variations on the Resistance of Sailing Yachts," Stevens Institute of Technology, Davidson Laboratory Letter Report 906, January 1965.
- [8] Spens, P., "Methods of Predicting Sailing Performance Off the Wind," Davidson Laboratory, Unpublished.

- [9] Barkla, H. M., "Tests of Four Related Yacht Forms," SIT, DL Technical Memorandum 132, October 1962.
- [10] DeSaix, P., "Fin-Hull Interaction of a Sailing Yacht Model," SIT, DL, Technical Memorandum 129, March 1962.
- [11] MacLavery, K., "Tests of a 5.5 Meter Yacht Form With Various Fin Sweep-back Angles," University of Southampton, Report No. 17, February 1966.
- [12] DeSaix, P., "Experiments with End Plate and Keel Profile Shape Variations on a 5.5 Meter Yacht," SIT, DL, Technical Note 589, May 1960.
- [13] Tanner, T., "Tank Tests of a 50-ft W.L. Ketch with a Number of Alternative Keel Appendages," University of Southampton, Tech. Note 506, Feb., 1970.
- [14] "Model Tests to Determine the Effect on Sailing Yacht Resistance of Varying the Fin Location Fore and Aft," University of Southampton Technical Note No. 505, October 1969.
- [15] DeSaix, P., "The Effect of Keel Position on the Upright Resistance of Two Sailing Yachts," SIT DL, Technical Note No. 686, March 1963.
- [16] Millward, A., "The Design of Spade Rudders for Yachts, University of Southampton, Report 28, December 1969.
- [17] Spens, P. G., DeSaix, P. and Brown, P. W., "Some Further Experimental Studies of the Sailing Yacht," Transactions, The Society of Naval Architects and Marine Engineers, Vol. 75, 1967.



Prediction of the power performance of the series 62 parent hull

by J. B. Hadler and Nadine Hubble

Naval Ship Research and
Development Center Washington D.C., U.S.A

Abstract

Results are presented of the first systematic study of the propulsion of planing craft, utilizing propellers driven by inclined shafts with a rudder located behind each of the propellers. The study is focused on the resistance characteristics of the parent model of DTMB Series 62, Model 4667-1. The propellers are derived from the extensive three-bladed Gawn-Burrill series, tested over a wide range of cavitation numbers. The performance predictions are based upon the method recently developed by Hadler. Single-, twin-, and quadruple-screw configurations have been studied for the Series 62 parent prototype hull over a wide range of sizes and speeds. The results have been synthesized into design charts which provide (1) the optimum diameter-rpm for a given design displacement and speed, (2) the value of the maximum propulsive coefficient, (3) the effect on propulsive efficiency of deviations from the optimum diameter and (4) the propeller P/D ratio associated with the desired diameter-rpm chosen. These charts may be easily used by the planing craft designer in making preliminary design and trade-off studies on planing craft propulsion systems with a hull L/B ratio of about four.

Introduction

Very little systematic series information exists about planing craft that will assist the designer in making design choices quantitatively so that well balanced designs can be achieved. The information that does exist is confined to hull resistance. The most comprehensive information published to date is that on the resistance tests of Series 62; see reference 1. The series is composed of five hulls each tested over a wide speed range at each of four LCG positions and three different loadings. There is no comparable systematic propulsion work on planing craft; thus, the designer is limited in his attempts to minimize power requirements by experience gained from working with similar prototypes.

To fill this vacuum, a systematic study has been initiated by the authors concerning the propulsion of Series 62, utilizing propellers driven by inclined shafts and steered with rudders located behind each of the propellers. Since any comprehensive series would involve extensive model tests which would take more time and money than is available for small boat research, this study is being accomplished by synthesis of a wide variety of data on a digital computer. The basic ingredients for the calculations are the resistance information of Series 62 [1]; the Gawn-Burrill Series [2] of threebladed propellers which have been tested over a wide range of cavitation numbers; and the recently published method of Hadler [3] for determining appendage drag, hull-propeller interaction, and performance of a propeller inclined to the flow. These basic data are combined through the equilibrium equations to determine the propulsion performance of the Series 62 hulls under a great variety of practical design

conditions. This paper reports the first step in this systematic study and is limited to the investigation of numerous propulsion system design parameters on the parent model of series 62, DTMB Model 4667-1, which has a length-beam ratio of 4.09; see Figure 1.

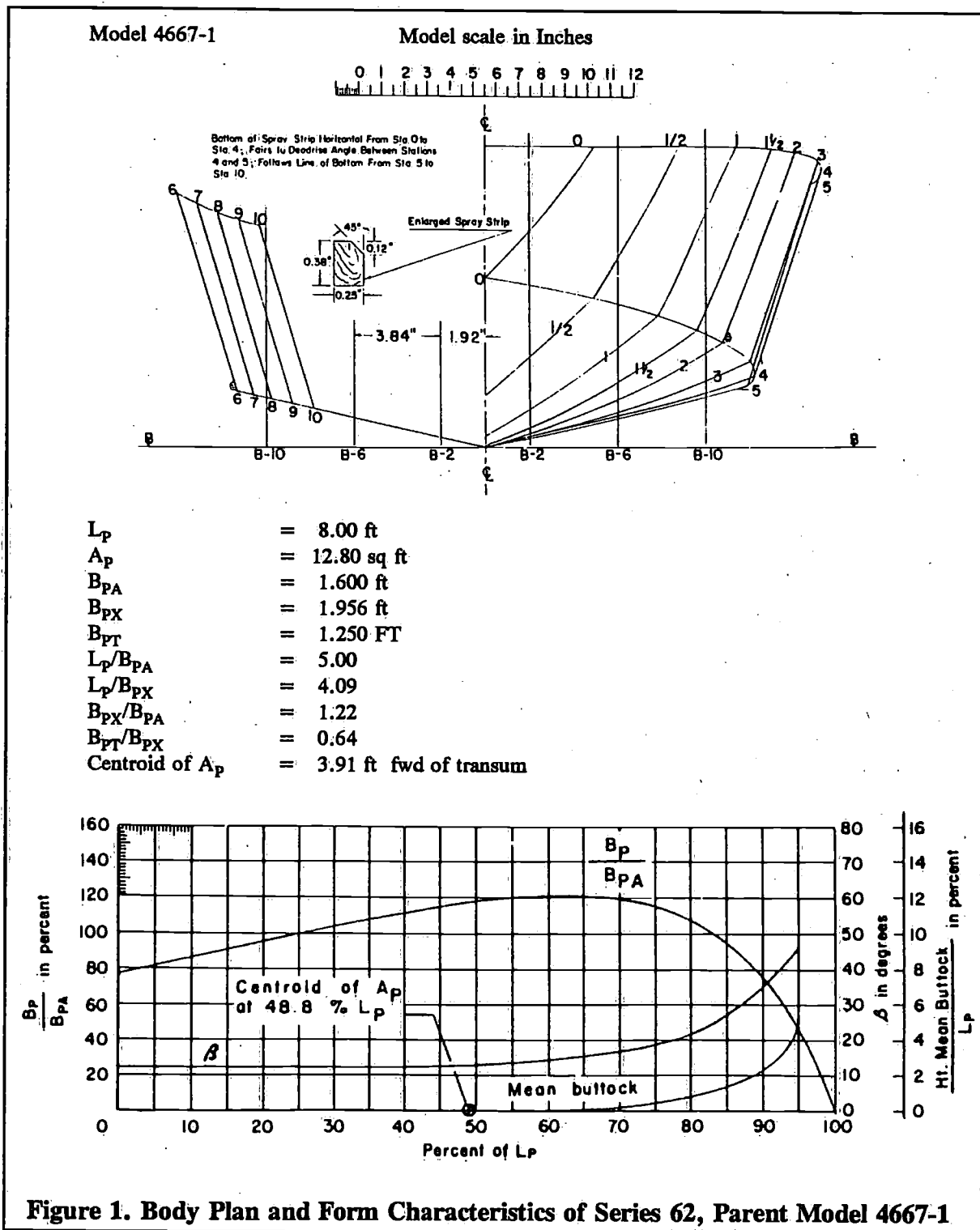


Figure 1. Body Plan and Form Characteristics of Series 62, Parent Model 4667-1

The primary objective of the investigation is to provide the planing craft designer with information about the propeller and propeller shaft-strut-rudder system variables which have the greatest impact upon the power performance. The results of the study are presented in such a form that the small boat designer, without having an extensive knowledge of planing

craft hydrodynamics, can readily choose an optimum propeller diameter, rpm, and pitch for any size of craft having from 1.000 to 2.000.000 lb displacement and operating at speeds up to 38 knots.

Since the approach used in this paper is based upon a mathematical representation of the planing craft, the first section of the report briefly describes the sources of information and how they were adapted for use in the computer. The second section describes the criteria used in the rudder and propeller shaft and strut design. The third section delineates the propeller, hull, and propeller shaft-strut-rudder system parameters that may affect performance and presents results of some preliminary studies. The last section analyzes the results of the single-, twin-, and quadruple-screw configuration studies and describes the synthesis of these results into design charts for use in preliminary design or trade-off studies.

Notation

A_p	=	projected planing bottom area, excluding area of external spray strips, square feet
<i>B.A.R.</i>	=	propeller blade area ratio
B_p	=	breadth or beam over chines, excluding external spray strips, feet
B_{pA}	=	mean breadth over chines, A_p/L_p , feet
B_{PT}	=	breadth over chines at transom, feet
B_{PX}	=	maximum breadth over chines, feet
C_{D33}	=	shafting system drag coefficient, $D_{33}/(1/2\rho V^2)$
<i>CG</i>	=	Center of Gravity
C_{L33}	=	shafting system lift coefficient, $L_{33}/(1/2\rho V^2)$
C_T	=	propeller thrust coefficient, $T/(1/2\rho V_A^2\pi R^2)$
D	=	propeller diameter, feet
D_{33}	=	drag of each shaft-strut configuration, pounds
<i>E.A.R.</i>	=	propeller expanded area ratio
F_z	=	propeller force normal to shaft and in propeller vertical centerplane, pounds
F_{∇}	=	Froude number based on volume, $V/(g\nabla^{1/3})^{1/2}$
g	=	acceleration due to gravity, 32.174 feet/second ²
J	=	advance coefficient of propeller, $V_A/(nD)$
J_v	=	apparent or ship speed advance coefficient, $V/(nD)$
K_{Fz}	=	propeller normal force coefficient, $F_z/(\rho n^2 D^4)$
K_Q	=	torque coefficient, $Q/(\rho n^2 D^5)$
K_T	=	thrust coefficient, $T/(\rho n^2 D^4)$
L_p	=	hull projected chine length, feet
L/B	=	length-beam ratio, L_p/B_{PX}
L_{33}	=	lift of each shaft-strut configuration, pounds
<i>LCG</i>	=	Longitudinal distance of the <i>CG</i> from intersection of chine and transom, feet
n	=	rate of propeller revolution, revolutions/second
N_{pr}	=	number of propellers
p	=	static pressure at shaft axis, pounds/square foot
P_O	=	water vapour pressure, pounds/square foot
P_E	=	effective horsepower, bare hull, $R_h V$
P_D	=	delivered power at propeller, $2\pi Qn$
Q	=	propeller torque, foot-pounds
R	=	radius of propeller, $D/2$, feet
R_h	=	resistance of bare hull, force opposing motion, pounds

S	=	wetted surface area underway, including area of sides wetted at low speeds and wetted bottom of spray strips, but excluding area wetted by spray, square feet
T	=	propeller thrust, pounds
V	=	speed of boat, feet/second (unless otherwise specified)
V_A	=	speed of advance of propeller, feet/second
w	=	water density, pounds/cubic feet
∇	=	volume of water displaced at rest, Δ/w cubic feet
Δ	=	gross weight of boat, or displacement at rest, pounds
ϵ	=	angle of inclination of propeller to direction of flow, degrees
η_D	=	propulsive efficiency, or propulsive coefficient, P_E/P_D
η_O	=	open-water propeller efficiency
ν	=	kinematic viscosity of water, square feet/second
ρ	=	mass density of water, w/g , slugs/cubic feet
σ	=	cavitation number, $(p-p_o)/(\frac{1}{2}\rho V^2)$

Computerization of basic data

To consummate this study it was essential that adequate means be developed for representing the comprehensive quantities of experimental data available in simple, yet accurate, mathematical forms. This section is devoted to a brief description of the methods employed by computer routines for representing the basic source material that is the core of this study.

Series 62, resistance data

The Series 62 planing craft were designed to explore in a systematic way the effects of a wide variation in the length-beam ratio (L/B), the relationship between hull size and gross weight, and the longitudinal location of the Center of Gravity (LCG). Since the latter two may be explored on a single model, only the effect of L/B requires different models. Thus the series was developed around five models in which the L/B varied from 2 to 7. The parent model used for this study has a L/B of 4.09. The configuration was a hard chine hull with a low constant deadrise of $12\frac{1}{2}$ degrees in the afterbody and known to possess low drag in the planing regime. Thus, it served as an ideal series around which to study the effects of the afore mentioned parameters upon propulsive performance.

The resistance experiments have been carefully conducted on each model at several systematic load - LCG conditions, each at speeds up to $F_{\nabla} = 6$ whenever possible, and the results are well documented in reference 1. Since the forces and moments arising from the propeller(s) and appendages vary the hull loading and LCG position for different propulsion conditions, it is essential to estimate the hull resistance for any number of load - LCG conditions throughout the operating speed range. Owing to the nature of the resistance curves, it would be difficult to represent the resistance of any given hull as a function of the three independent variables (load, LCG , and speed) by any simple equation(s). Therefore, a three-way interpolation routine has been developed which considers only the experimental data in the immediate vicinity of the required independent variables. The method uses the Lagrange interpolation formula, applied to one variable at a time.

The experimental data for the hull to be considered (in this case, Model 4667 - 1) are stored in the computer in matrix form. Only three of the four test load conditions are used - $A_p/\nabla^{2/3}$ of 5.5, 7.0, and 8.5. The number of LCG locations used for a particular load varies from three to five. Only the conditions tested over a full speed range are used, except for a few cases where the range of data could be easily extrapolated manually. The input data are not faired but are the actual model test data tabulated in reference 1, with any obvious erroneous

point corrected or deleted. Before the data are used elsewhere, the computer routine is designed to scale the basic data to the size of boat being investigated. Resistance is expanded by standard procedures using the Schoenherr friction line, zero correlation allowance, and the density and viscosity of sea water at 59 deg Fahrenheit. (Other options are available in the computer program, and will be specified whenever there is a deviation from the preceding conditions.) The actual wetted surface area for each condition is used in the friction calculations, and the length used for Reynolds number is the mean of the wetted keel length and the wetted chine length.

The first step in the procedure for deriving resistance for a particular load - *LCG* - speed combination is a third degree interpolation at each experimental load - *LCG* condition to obtain the resistance for the required speed. At each condition, the effect is that of passing a cubic curve through the four test spots closest to the desired speed and of reading from the curve the value of resistance for that speed. With speed as a constant factor, the next step is interpolation of the preceding results at each experimental load for the resistance associated with the prescribed *LCG* location. Finally, with both speed and *LCG* constant, the resistance from the second step is interpolated for the required load. Second degree (three-point) interpolation is used for both *LCG* and loading variation. This method has proven quite accurate within the range of experimental data; however, extrapolation capability is limited.

Other experimental data, namely, trim, wetted keel and chine lengths, wetted surface area, and *CG* rise are interpolated in exactly the same manner as resistance.

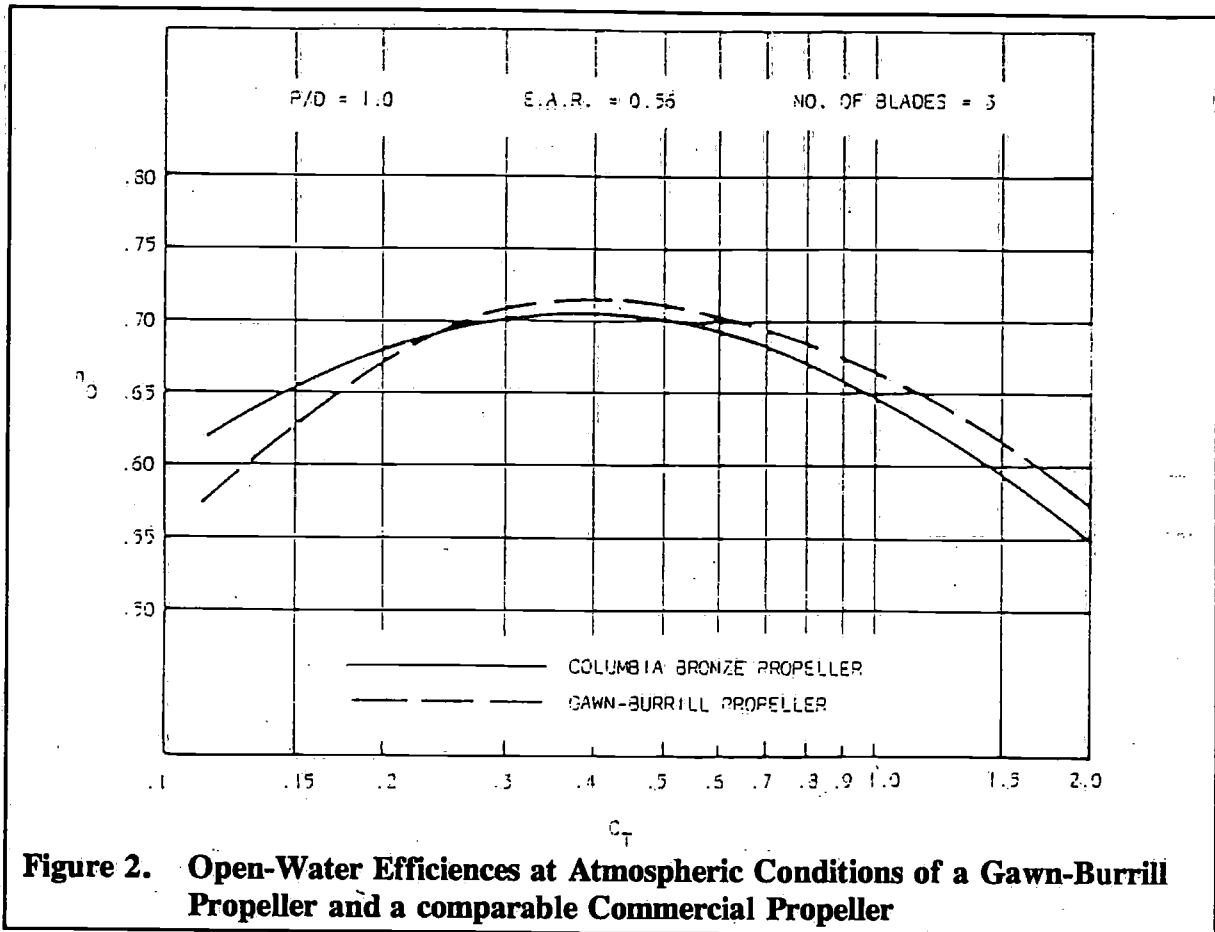
Gawn-Burrill series propeller characteristics

The so-called Gawn-Burrill series of propellers were used in this study. This propeller series was developed in the United Kingdom at the Admiralty Experimental Works and Kings College, Newcastle, in the early 1950's as a basic cavitation and propulsion series and covers a wide range of pitch ratios (*P/D*) and blade area ratios (*B.A.R.*). The propellers were three-bladed with constant face pitch, elliptical blade outline, and segmental blade sections over the outer half of the blade. The series consists of 30 propellers with *B.A.R.*'s ranging from 0.5 to 1.1 and *P/D*'s ranging from 0.6 to 2.0. Each propeller was tested at six cavitation conditions from $\sigma = 0.5$ to atmospheric, a range sufficient for investigating boat speeds to approximately 38 knots. The results are presented in reference 2 as curves of K_T and K_Q versus *J* for each *B.A.R.* - *P/D* - σ combination tested. The series was tested in the variable pressure water tunnel at Kings College, and it was fortunate that the original experimental data were still available, thus making the computerization of these results both easier and more accurate.

The open water test results of some commercially available small craft propellers have been compared with open water test results of corresponding propellers from this series. The comparison has been made of propeller efficiency (η_D) versus thrust coefficient (C_T). From Figure 2 we can see that they are comparable in performance in the non-cavitating domain; hence, the propeller results from this study can be assumed to be achievable with commercially available propellers of comparable geometric properties (excluding number of blades) at least until extensive cavitation sets in.

Since K_T and K_Q are functions of *J*, *B.A.R.*, σ , and *P/D*, it was decided to try fitting curves of the polynomial form to the experimental data by the least-squares method in order to minimize the quantity of information that had to be stored in the digital computer as well as to assure that faired data were available for the propulsion performance calculations. From experience with the data, it was found that a fourth-degree polynomial provided the best fit for the K_T (and K_Q) versus *J* curves for any given σ , *P/D*, and *B.A.R.* The greatest deviation was noted at the low advance ratios for the low cavitation numbers, a regime not frequently used. It was found that a third degree polynomial provided the best fit for K_T (and K_Q) versus

B.A.R. These were combined to form a series of surface equations for K_T (and K_Q) as $f(J, B.A.R.)$ for each P/D and σ tested. At any given J , the K_T and K_Q vary rapidly at low a 's but become constant at atmospheric conditions. Consequently, it was found that a fourth-degree equation with the inverse cavitation number (l/σ) gave a good approximation. Linear interpolation between the test P/D conditions proved adequate for the variation in P/D . This approach resulted in quite accurate fitting to and fairing of the experimental results from the model tests. The resulting 840 coefficient each for K_T and K_Q have been developed into a computer routine for ready use in the performance calculations.



Propeller forces

The forces which arise from the propeller can be attributed to two separate effects: the forces generated by the propeller which are transmitted to the hull through the shaft and struts, and the pressure forces induced on the planing surface from the propeller loading. The first effect results in the thrust force along the shaft which drives the planing craft and a force normal to the thrust when there is a flow component across the propeller disk arising from the shaft inclination. The second effect results in a suction force on the bottom of the hull on the upstream side of the propeller and a pressure force on the downstream side of the propeller. The method for determining the magnitude of these forces was developed in reference 3. The method for determining the shaft forces in inclined flow is a quasi-steady calculation based upon the work of Gutsche [4], which utilizes the open-water characteristics of the propeller when tested in flow normal to the propeller. This procedure includes estimation of the force (F_{zo}) normal to the propeller axis as well as the torque (Q_z) and the thrust (T_z) in the shaft line. The method has been extended to propeller cavitation performance in inclined flow as shown by Taniguchi [5]. In this instance, however, the non-inclined K_T and K_Q must

each be considered as a function of σ as well as J since the section cavitation number varies in non-uniform flow with angular position. The method involves the use of an empirical constant. Based upon experimental results to date, a value of 2.0 gives the best correlation for conventional-type non-cavitating propellers, whereas Taniguchi's work indicated a value of 1.0 for supercavitating propellers. However, no experimental data are available at present for conventional propellers operating at low cavitation numbers, such as the Gawn-Burrill series used in this work. Therefore, a compromise was made to use an empirical constant of 2.0 throughout the procedure, except that in deriving the cavitation number for various angular positions (σ_T) a constant of 1.0 is used. The method for determining the hydrodynamically induced suction and pressure forces essentially involves an integration of the induced axial velocities over the planing bottom area forward of the propeller to obtain the net suction force and its centroid and a similar integration over the area aft of the propeller for the pressure force and its centroid. The pressures in coefficient form have already been integrated longitudinally for any relative position, fore or aft of the propeller (x/R) at selected radial positions (r/R) and are presented in Figure 9 of reference 3; similar contours of the associated centroids are given in Figure 10 of reference 3. To simplify reconstruction of the longitudinal integration by a computer, the contours from these figures have been approximated by polynomials of the form where a_{ji} , b_{ji} , and c_{ji} are coefficients derived by a least-squares method. The contours of longitudinally integrated pressure coefficients had to be represented by two separate equations (1) and (2) to reproduce them accurately enough, whereas, the contours of the centroids were represented quite accurately by a single equation (3). For the transverse interpolation, the relative distance from the propeller centerline to the planing bottom (r/R) is calculated, taking into account the deadrise angle, at 9 equally spaced positions across the underwater surface in the plane of the propeller. At each of these r/R values the associated x/R (i.e., either distance from the propeller centerline to the transom, if pressure is being derived, or distance from propeller to the forward water surface, if suction is being derived) is approximated from the hull geometry. The longitudinal integration at each r/R is then simulated by either Equation (1) or (2), depending on the value of r/R , and Equation (3) using values of a , b , and c previously determined and the estimated value of x/R . The values obtained from the longitudinal integration are then integrated across the hull.

$$\int_0^{x/R} \frac{2u\bar{V}}{C_T} d\frac{x}{R} = \sum_{i=1}^5 \sum_{j=1}^5 a_{ji} \left(\frac{1}{r/R}\right)^{j-1} \left(\frac{1}{1+x/R}\right)^{i-1} \text{ for } r/R < 5.5 \quad (1)$$

$$\int_0^{x/R} \frac{2u\bar{V}}{C_T} d\frac{x}{R} = \sum_{i=1}^5 \sum_{j=1}^5 b_{ji} \left(\frac{1}{r/R}\right)^{j-1} \left(\frac{x}{R}\right)^{i-1} \text{ for } r/R > 5.5 \quad (2)$$

$$\frac{\int_0^{x/R} \frac{x}{R} \frac{2u\bar{V}}{C_T} d\frac{x}{R}}{\int_0^{x/R} \frac{2u\bar{V}}{C_T} d\frac{x}{R}} = \sum_{i=1}^5 \sum_{j=1}^5 c_{ji} \left(\frac{1}{r/R}\right)^{j-1} \left(\frac{x}{R}\right)^{i-1} \text{ for all } r/R \quad (3)$$

The integrated pressure coefficients are multiplied by the constant ($\pm 2R^2 \sigma/2 V^2 C_T$) to obtain the net induced suction and pressure forces on the hull. The integrated centroids are in the form x/R , where x is the distance of the center of force forward or aft of the propeller center-plane. These centroids are transformed to distances from the CG location in order to be consistent With the moment arms of the other forces on the hull for use in the equilibrium equations.

Design criteria for propulsion system

To execute this study effectively it was necessary to establish design criteria for the propeller shaft-strut-rudder systems that were sufficiently flexible to cover a wide range of conditions and yet could be computerized for easy calculation of drag and lift and their centers of application.

Rudder

For the purposes of this study the following assumptions were made in determining the rudder size and location.

1. There are the same number of rudders as there are propellers.
2. The rudders are of the spade type with streamlined section similar in style to those commercially available in the small boat industry.
3. The rudder is assumed to be completely under the hull so that there is no spray drag, and the top of the rudder is assumed to have sufficient clearance from the hull so that the rudder pressure field will have a negligible effect upon the trim of the hull; see page 587 of reference 3.
4. Since there is no general formula for determining the rudder area for planing craft, the rudder data of a number of successful planing craft listed in reference 6 were analyzed. It was found that the total rudder area of these craft could be expressed as Rudder Area = $0.0016 L_p^2$ hence this equation was used in determining the rudder area for this study. An aspect ratio of 4 : 3 was also assumed.
5. The leading edge of the rudder is assumed to be $0.75 D$ behind the propeller centerplane.

Using the preceding dimensional information, the drag equations were developed and computerized utilizing the methods outlined in reference 3. The additional propeller slipstream induced drag was also readily calculated once the propeller tip clearance was established, again based upon the methods developed in reference 3.

Shaft and strut

The criteria used for designing the propeller shaft size and strut bearing location were based upon the standard promulgated by the American Boat and Yachting Council; see ref. 8. The basic formula for determining shaft diameter was as follows:

$$d = \sqrt{\frac{321.000 \cdot P \cdot C_d}{S_T \cdot N}}$$

where

- P = horsepower per shaft
 C_d = design coefficient - a value of 2.0 was used

- S_t = yield strength, torsional shear - a value of 22.500 lb/in² for naval brass was used
 N = shaft speed, rpm
 d = shaft diameter, inches

The formula for computing the maximum shaft bearing spacing was as follows:

$$L = \sqrt{\frac{3.21d}{N}} \cdot \sqrt{\frac{E}{w_1}}$$

where

- L = maximum unsupported length, ft
 E = modulus of elasticity of shaft material - a value of 15×10^6 for naval brass was used
 w_1 = weight of one cubic inch of shaft material - a value of 0.304 lb/in² for naval brass was used

The design of the propeller shaft-strut was based upon data available from commercially available products. A single arm strut was assumed with an ogival strut section. The strut pod was assumed to be mounted in the hull so that the upper palm surface was flush with the planing surface. The importance of eliminating strut palm drag was shown in reference 3. The dimensions of the strut and the strut barrel were developed as a function of both propeller shaft diameter and propeller diameter. Once the principal dimensions of the shafting system components are known, the net lift and drag forces and their centers of application can be readily calculated using the method outlined in reference 3.

In principle a new shaft-strut system should be designed for each condition calculated. The effect on performance of varying propellershaft materials should also be examined. To do this would have added further burden to a calculation procedure which was already quite lengthy. Accordingly, a study was made on Model 4667-1 to determine the conditions which had minimal effect on the shaft-strut system lift and drag coefficients. The shaftstrut system was designed for a twin-screw installation for a 10.000 - lb boat at 30 knots, for various propeller diameters. The lift and drag coefficients are plotted in Figure 3 as a function of propeller diameter. The same system was designed for the same boat at design speeds of 20 and 40 knots for 16 and 20-inch diameter propellers, and the results were not significantly different. Similarly, the the shaft-strut system was designed for a 100.000 lb boat, and the results were scaled to those of a 10.000 lb boat. Again there was not a significant difference; thus, it was decided that only one shaft-strut system need be designed for each hull for each number of propellers. The effect of changing the shaft material to a high tensile steel was more marked, and under certain circumstances its use might be warranted; however, for purposes of the study, naval brass was used in all shafting calculations.

Cavitation criteria

Since all the test results of the Gawn-Burrill propeller series had been computerized, it was possible to make performance calculations over a wide range of cavitation conditions. Preliminary calculations quickly showed that the shaft horsepower requirements increased rapidly as the amount of cavitation increased; thus, it became apparent both in the interest of computer economy as well as of good design practice to establish cavitation criteria which would determine the minimum propeller diameter and blade area ratio at any given pitch. The

K_r , breakdown curve that was established by Gawn-Burrill in reference [2] was utilized as the criteria; see Figure 4. This criteria is comparable to that recommended by Lerbs and later by Burrill, based on further cavitation work done at Kings College, and in general results in cavitation on approximately 15 percent of the back of the blade. This amount of cavitation has relatively small effect upon the thrust and torque but could conceivably cause cavitation erosion problems, particularly when the angle of inclination is large.

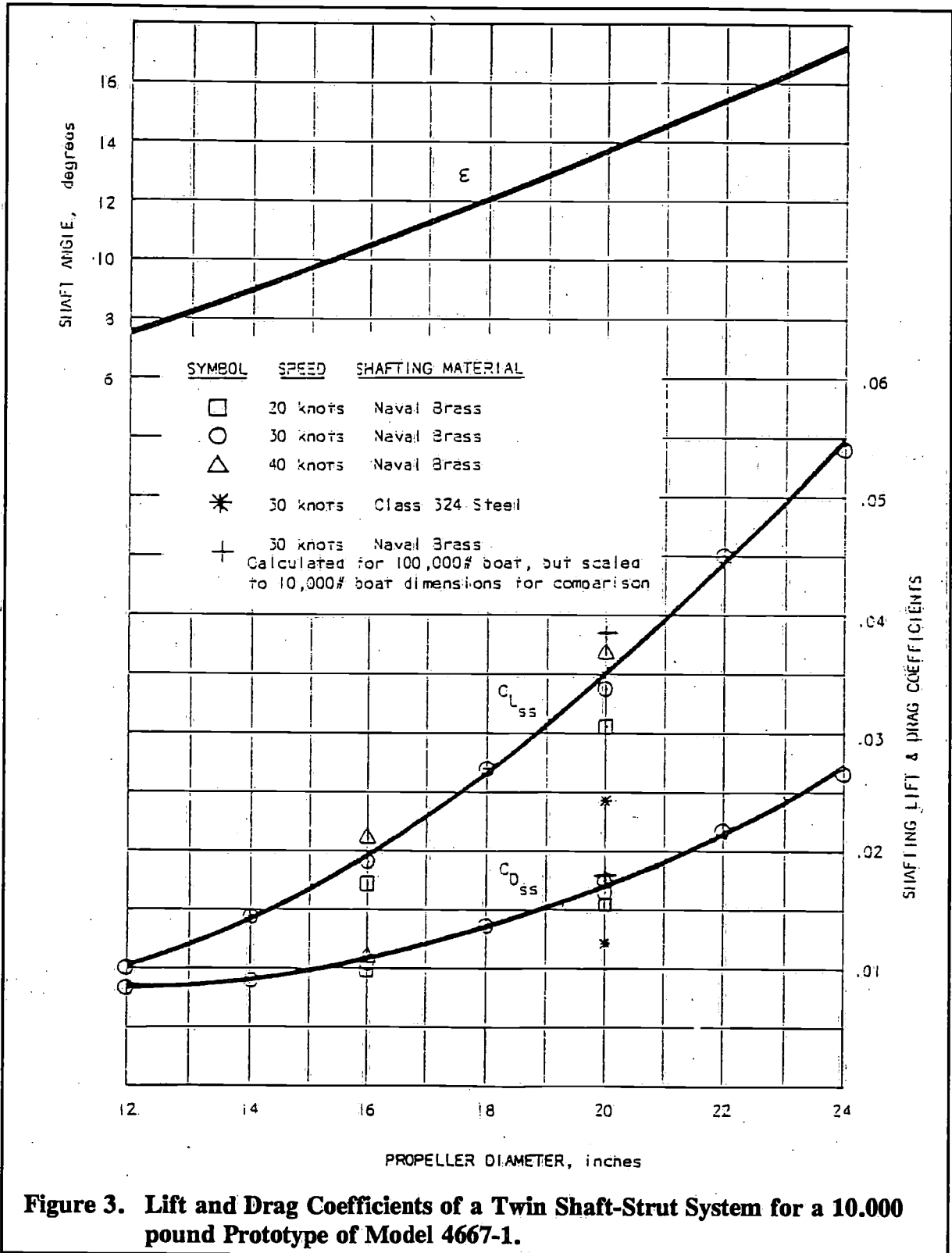


Figure 3. Lift and Drag Coefficients of a Twin Shaft-Strut System for a 10,000 pound Prototype of Model 4667-1.

$$A_{pr} = \text{Exp. Area} \times (1.067 - 0.229P/D)$$

$$v_{R(0.7)} = \sqrt{v^2 \left(1 + \left(\frac{0.7 \pi}{J} \right)^2 \right)}$$

$$\tau_c = \frac{T}{1/2 \rho A_{pr} v_{R(0.7)}^2}$$

$$\sigma_{R(0.7)} = \frac{p - p_0}{1/2 \rho v_{R(0.7)}^2}$$

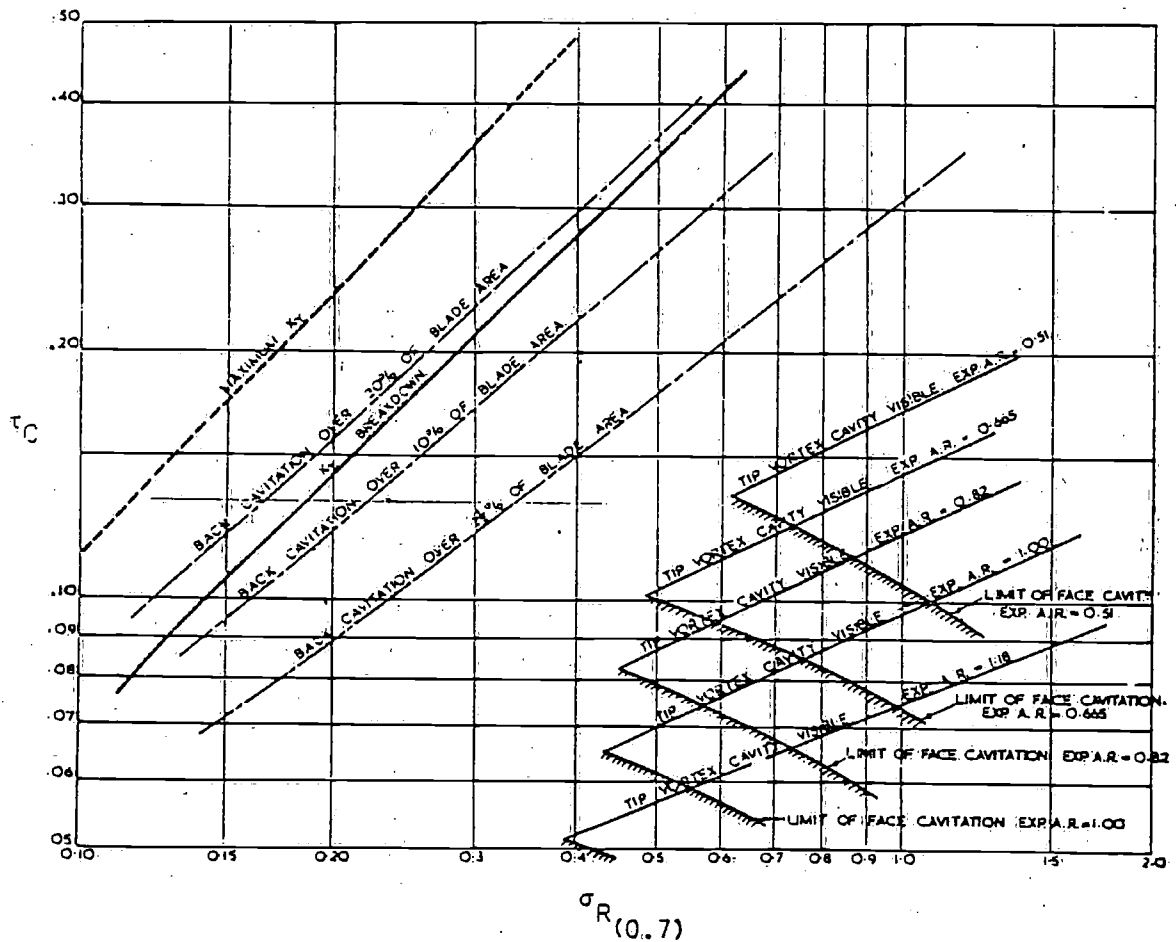


Figure 4. General Trend of Cavitation Phenomena of the Gawn-Burrill Propeller Series

Study plan

Since this is the first systematic study of the propulsion characteristics of planing craft, it was essential to examine a wide variety of design parameters that might affect the propulsion performance and to determine the parameters which are of primary significance and those which have a negligible effect, so that a designer may intelligently make the necessary design compromises. In examining the design parameters of significance, we may treat them as follows: those associated with

1. The propeller(s)
2. The hull
3. The propeller shaft-strut-rudder system

The primary variables of the propeller are:

1. The diameter, D
2. The pitch, generally expressed as a ratio of diameter, P/D
3. The blade area ratio, $B.A.R.$

The first two establish the diameter-rpm relationship, and the last determines the cavitation performance.

The major variables for the hull are:

1. The speed, V
2. The overall size, expressed here as displacement, A
3. The LCG
4. The hull loading coefficient, $A_p/\nabla^{2/3}$
5. The hull roughness, ∇C_f

Clement, in reference 1, has shown the significance of the first four variables upon the resistance characteristics of a planing hull. Hull roughness is added in this study since it represents irregularities which can occur on the planing surface due to manufacturing imperfections, paint roughness, and/or marine fouling. The variation of speed, LCG , and $A_p/\nabla^{2/3}$ for the propulsion studies with Model 4667-1 are, of course, limited by the range of resistance test conditions; see section on Series 62 resistance data. The basic hull condition used throughout the studies, except for the study of $A_p/\nabla^{2/3}$ and LCG variation, was a $A_p/\nabla^{2/3}$ of 7.0 with the LCG at 6 percent of L_p aft of the centroid of A_p . This is the standard condition recommended by Clement for comparison of planing craft power performance. As for the shaft-strut-rudder system there are many combinations and design details possible which can change the configuration and perhaps have some effect upon the hydrodynamic performance. Therefore, some arbitrary conditions had to be established for this study.

1. The shaft-strut system was developed around the work of Clement in reference 1. He assumed a twin-screw arrangement with the shaft emerging from the hull at the one-quarter buttock at Station 8, based on design expedience from a large body of planing craft tested at DTMB.
2. The propeller location is predicated on the assumption that the trailing edge of the rudder is flush with the transom, and that the clearance between the leading edge of the rudder and the propeller centerline is $0.75 D$.
3. The propeller tip clearance from the hull is assumed to be $0.15 D$, predicated on the recommendations in reference 6. Although propeller tip clearance has an effect upon performance, this is secondary to the importance of its effect upon hull-propeller induced vibration. Consequently, the basic configuration used for the studies was a twin-screw arrangement in which the propeller shaft-strut-rudder system was located between the transom and Station 8 on the one-quarter buttocks, and the propeller tip clearance was $0.15 D$, similar to that shown in Figure 5.

The following variations from the basic configuration were studied:

1. a single propeller shaft-strut-rudder system, located on the centerline
2. a quadruple propeller shaft-strut-rudder system, with all four propellers in the same transverse plane
3. the twin propeller shaft-strut-rudder system shifted well inboard and then outboard of the one-quarter buttock
4. the twin propeller shaft-strut-rudder system shifted forward two stations, and
5. the twin propeller shaft-strut-rudder system with propeller tip clearance varied from $0.125 D$ to $0.25 D$.

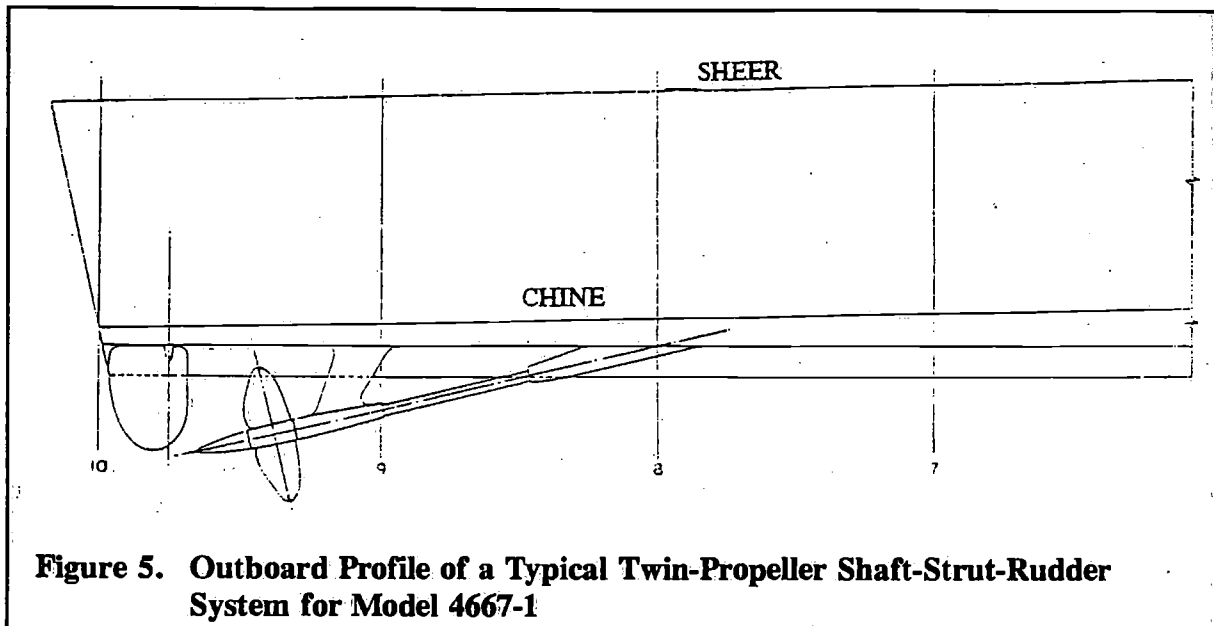
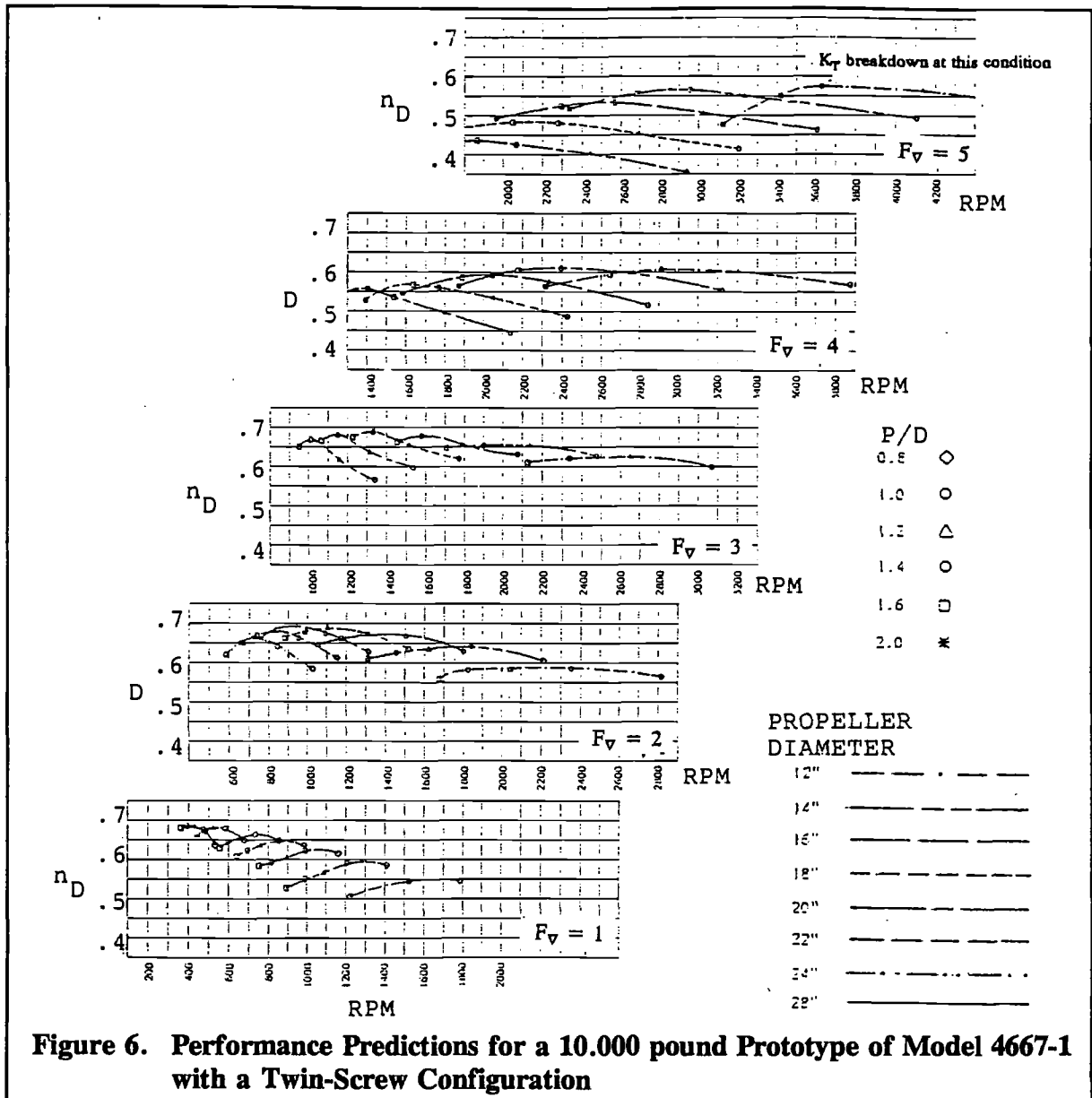


Figure 5. Outboard Profile of a Typical Twin-Propeller Shaft-Strut-Rudder System for Model 4667-1

The one major parameter which has not been included is shaft inclination. For all the configuration studies except Item 4 above, the shafts emerge from the hull at Station 8. This results in a different shaft angle for each propeller diameter in order to keep the $0.15 D$ tip clearance. However, for any given D the angle is constant for all configurations, even Item 4, since the entire system is shifted. Preliminary investigations of the basic twinscrew arrangement with a lengthened shaft showed that a reduced inclination can benefit the power performance, as has already been demonstrated in reference 3. An examination of the stagnation line on the one-quarter buttock of Model 4667-1, when it was planing at high speeds, showed that the shaft should not emerge from the hull forward of Station 5.5 in order to avoid shaft and propeller ventilation in smooth water. Unfortunately, the overall study of shaft inclination has not been completed in time for inclusion in this paper.

Most of the parametric variations were calculated at only one displacement (10,000 lb) and at three speeds (20, 30, and 40 knots) to keep the number of calculations within bounds, inasmuch as the calculations become costly when studying so many variables even when using a high-speed digital computer. The results were then examined for the effect of each variation upon the optimum diameter-rpm relationship and the maximum propulsive efficiency as related to the basic conditions established.

It was found, not unexpectedly, that the variation of the hull roughness, ΔC_f from 0.0 to 0.0004, and the variation of the transverse and longitudinal position of the complete propeller shaft-strut-rudder system had a negligible effect upon the optimum propeller diameter-rpm relationship and upon the propulsive efficiency. It was also found that, for this hull, the variation of LCG within ± 6 percent L_p of the standard location and the variation of $A_p/\nabla^{2/3}$ from 5.5 to 8.5 showed very little effect upon the optimums.



The variation of propeller tip clearance from 12½ percent to 25 percent of the propeller diameter showed a finite effect, although not large. The results are presented in Table I as percentage changes in the maximum propulsive coefficient from the arbitrary tip clearance of 15 percent D used for all other studies.

Table I: Effect of Propeller-Tip Clearance Upon Maximum Propulsive Coefficient for a 10,000 Pound Prototype of Model 4667-1 with a Twin-Screw Arrangement

Percentage Change in η_D from the Arbitrary Tip Clearance of 0.15 D		
F_R	Clearance = 0.125 D	Clearance = 0.25 D
1	+0.1	-0.9
2	+0.4	-1.7
3	+0.4	-2.9
4	+0.5	-1.6
5	+0.3	-1.2

The parameter producing the most significant effect upon the power performance was, of course, the Number of propellers (N_{pr}). The essence of this paper, then, is a study of the single-, twin-, and quadruple-screw configuration over a wide range of displacements and speeds.

Discussion of results of calculations

Performance prediction calculations were made for each N_{pr} configuration at seven displacements from 1.000 to 2.000 000 lb and at speeds corresponding to $F_{\nabla} = 1, 2, 3, 4,$ and 5 . At each of these displacements and speeds, the propeller diameter and P/D were varied over a sufficiently wide range to achieve the maximum propulsive coefficient (minimum P_D). Figure 6 is typical of the results obtained for any N_{pr} configuration and displacement, in this case twin-screw at 10.000 lb. From the results it is apparent for each speed that there is an optimum propulsive coefficient at each diameter, and in turn there is a diameter which gives a maximum propulsive coefficient. The optimum diameter varies with speed, becoming progressively smaller with increasing design speed. Although not shown on the figure, the *B.A.R.* was varied from 0.5 to 1.1 for each diameter and P/D in such a way that sufficient area was obtained to meet the cavitation criteria discussed previously and yet was minimized to achieve maximum propeller efficiency.

The propulsive efficiency (also referred to as propulsive coefficient) utilized throughout this paper is based upon the bare hull effective horsepower, i.e., $\eta_D = P_E/P_D$. This form is used for convenience in comparing the performance between different propulsion systems and in estimating the shaft horsepower requirements when only bare hull resistance is known. It was found that the results of the calculations for any N_{pr} configuration over the range of displacements could be synthesized into the data contained in Figures 7 through 13. These figures are in a form that may be readily used by the planing craft designer for preliminary design or trade-off studies. The results are put in a nondimensional form or are normalized in such a way that they may be used with any consistent set of engineering units. As a consequence the large mass of information obtained was reduced to a few easily used graphs. To assist the designer in using the charts for specific engineering application, Figure 14 is provided, which readily converts F_{∇} to displacements and speeds. Figure 15 converts Δ to $\nabla^{2/3}$ for both sea and fresh water.

Figure 7 contains the basic information to provide the optimum diameter-rpm relationship for any given design displacement and speed. The results are presented as contours of F_{∇} , as a function of $D/\nabla^{1/3}$ and apparent advance ratio (J_{∇}). It was found that this form gave the best synthesis of the computed data. Superimposed is the contour for the $D/\nabla^{1/3}$ associated with the maximum propulsive coefficient.

The shaded area represents the region where the variation from the maximum propulsive coefficient is less than one point; hence, it becomes apparent that the diameter-rpm relationship can vary over a fairly wide region and still maintain high propulsive efficiency.

For the quadruple-screw configuration there is an upper bound on the maximum propeller diameter possible. The calculations were carried to the point where the propeller diameter was slightly less than one-quarter of the beam of the craft in way of the propeller plane. The calculations at this point may be less reliable than for smaller diameters as no account was made for the induced effects of one propeller upon the other. Since the results at the lower design speeds indicate optimum diameters approaching this limit, it is not practical to consider a configuration with four propellers in the same transverse plane, but staggered pairs should be considered with some overlapping of the propeller disks where induced velocities in the propeller slipstream can have a marked effect upon performance. This kind of study is not possible at present.

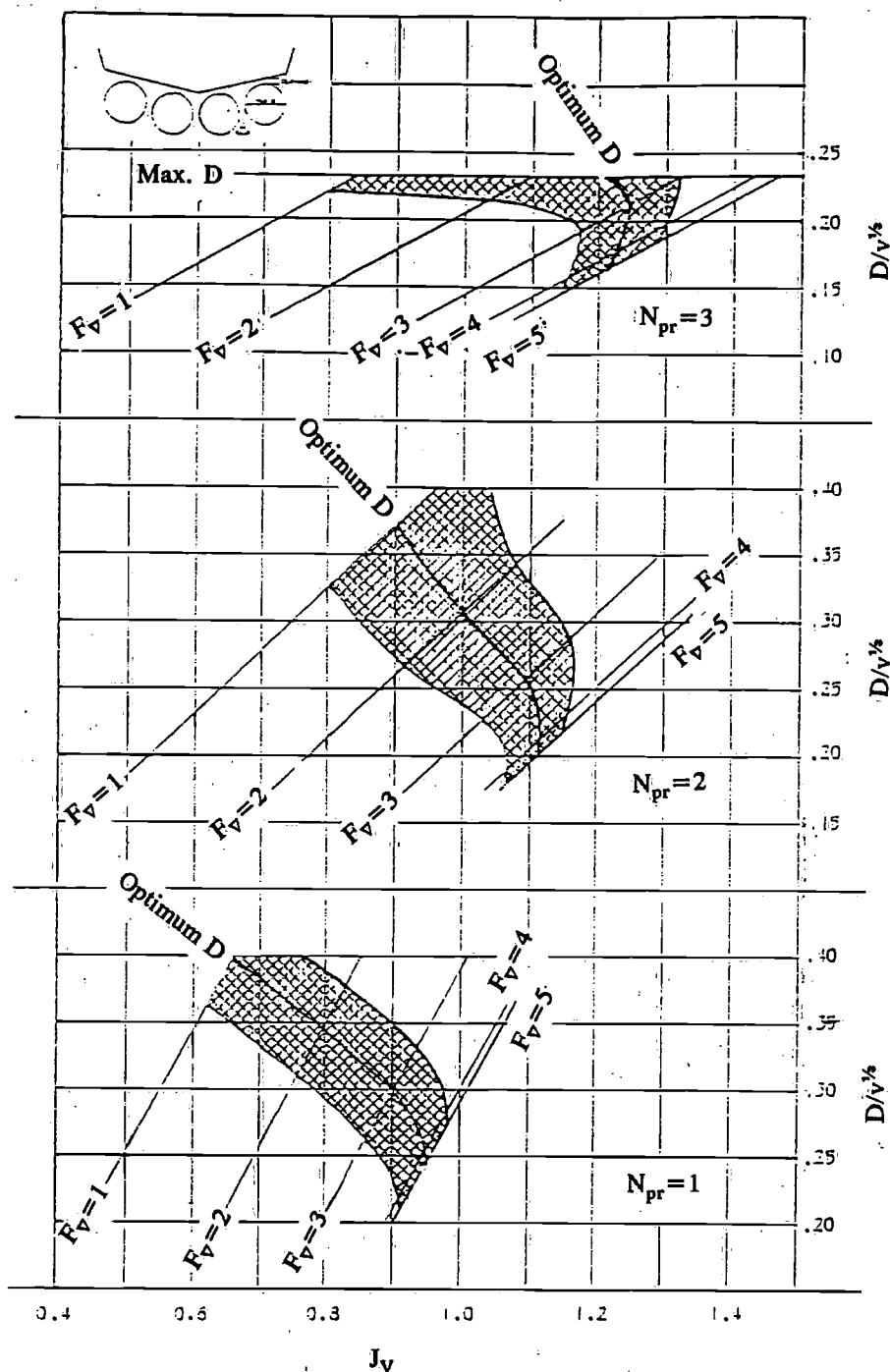
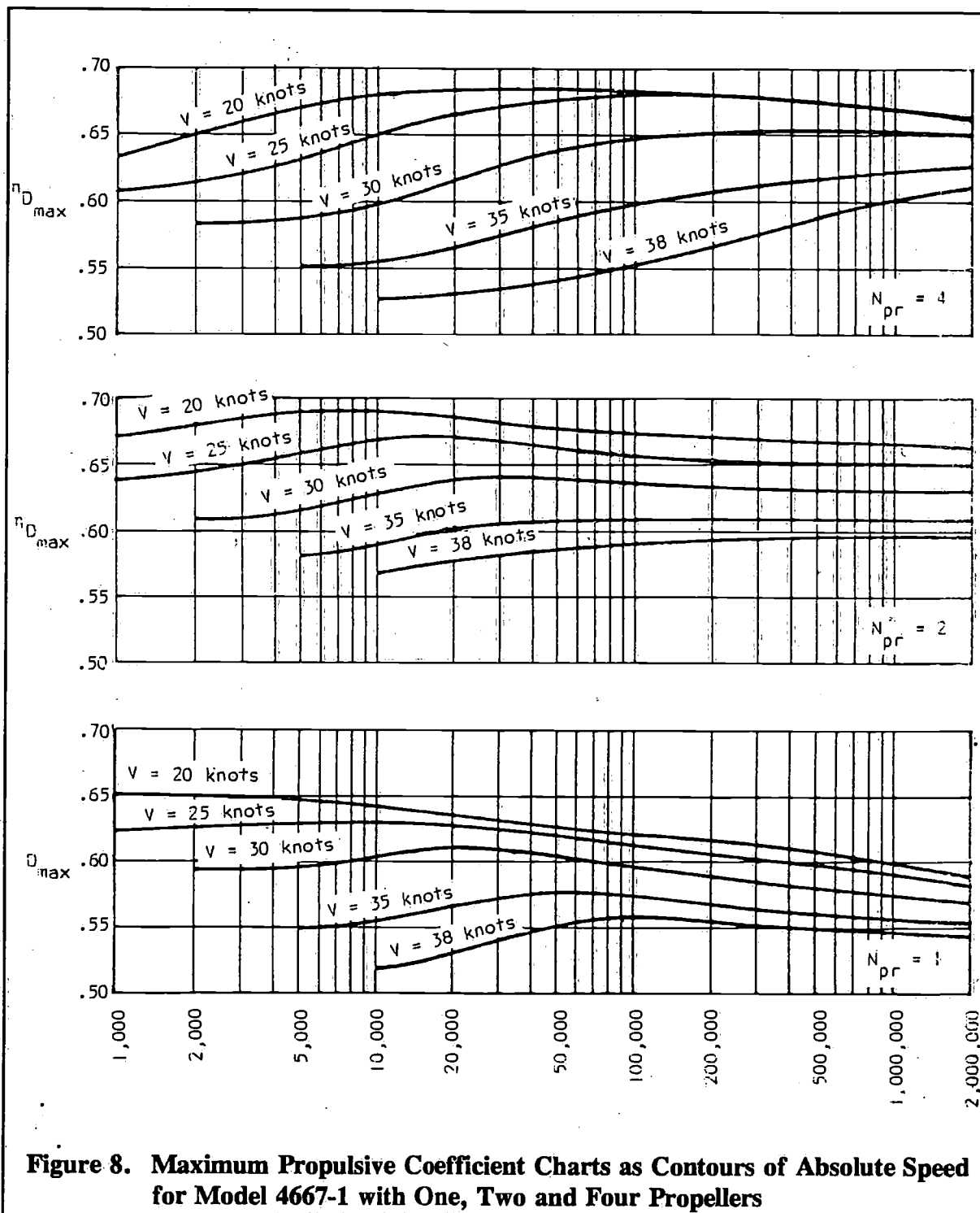


Figure 7. Propeller Diameter-rpm (Charts for Model 4667-1 with Single, Twin, and Quadruple-Screw Configurations)

Figures 8 and 9 show the values of the maximum propulsive coefficient for the single-, twin-, and quadruple-screw configurations. The results are presented as functions of displacement in two forms; as contours of F_v and as contours of speed in knots. The latter form is provided to show how the maximum allowable propulsion efficiency changes with speed and displacement for the three configurations studied. These results clearly indicate the magnitude of the effect of increasing design speed upon the maximum propulsive coefficient. The results also show that absolute size, i.e., displacement, also has an effect which is most pronounced upon the quadruple-screw configuration. The single-screw is clearly less efficient at all speeds

and sizes than is either the twin- or quadruple-screw configuration. Between the twin- and quadruple-screw configurations there are less pronounced differences. The latter is more efficient at the heavier displacements, with the crossover point occurring at increasingly larger displacements as the design speed is increased. The comparison between the twin- and quadruple-screw configurations implies that the triple-screw configuration may be more favorable than either the twin or quadruple at certain displacements and speeds. The triple-screw may also provide a much better arrangement than the quadruple-screw since the optimum diameter indicated for the latter configuration is near the maximum diameter possible for four in-line propellers.



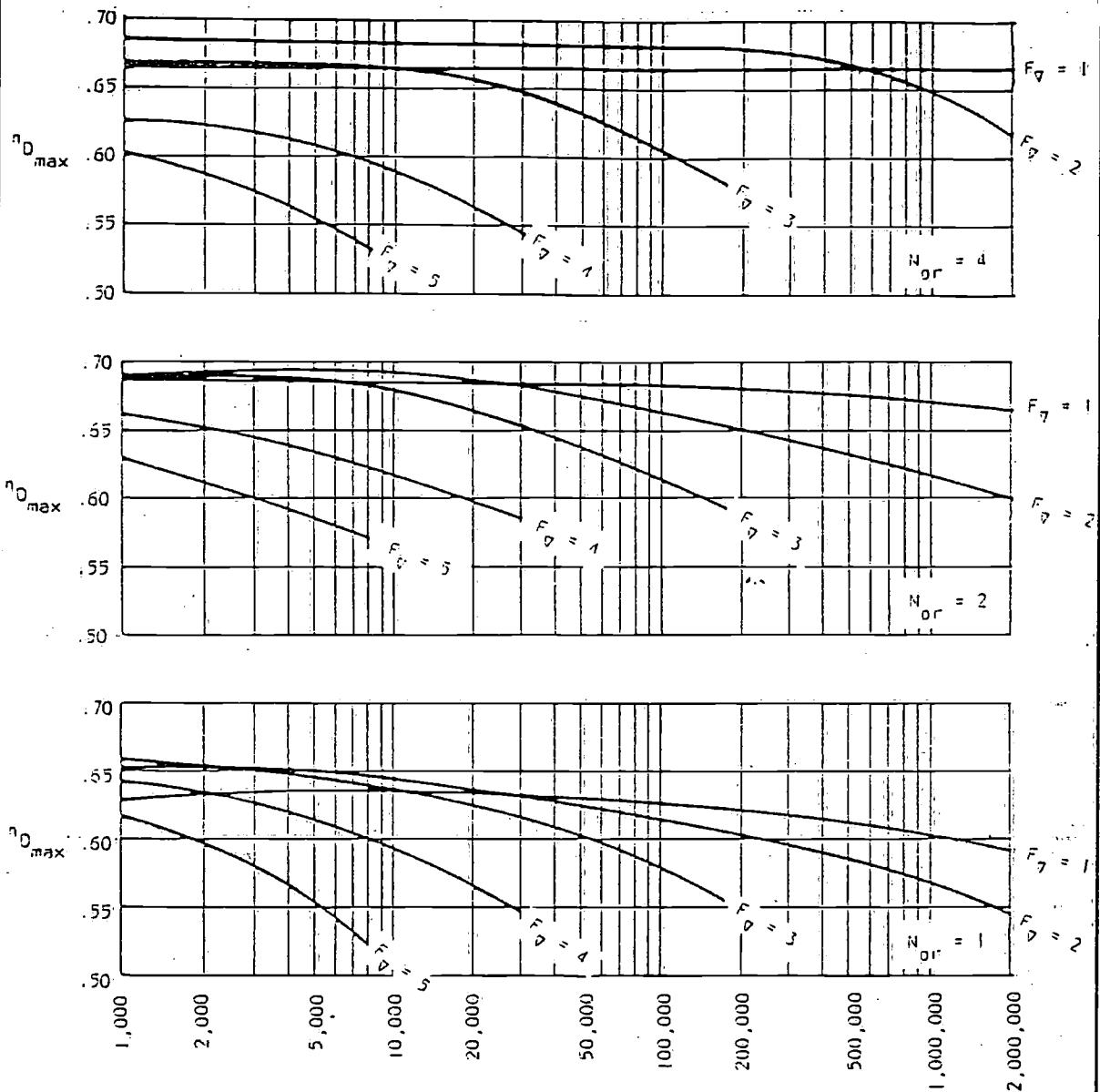


Figure 9. Maximum Propulsive Coefficient Charts as Contours of F_D for Model 4667-1 with One, Two and Four Propellers

Figure 10 is included to provide information about the effect on propulsive efficiency of deviations from the optimum diameter, assuming that at this design point the optimum rpm is chosen consonant with the diameter. This information is particularly useful in tradeoff studies. The results are presented as curves showing the percentage reduction in propulsive coefficient for variations in apparent advance ratio for the five F_D values calculated and the three configurations studied. These results show that the greater the number of propellers, the flatter the curves, i.e., the less the reduction in efficiency for the same deviation from the optimum.

Figures 11 through 13 provide the P/D ratios that are associated with the propeller diameter and propulsive efficiency information provided in the preceding figures. The results are presented as curves of P/D for different displacements for a range of apparent advance coefficients for the five F_V values calculated and the three configurations studied. From these figures it is apparent that, in most cases, the P/D increases as both the apparent advance ratio and displacement increase.

No results are presented for $B.A.R.$ as this is only important in making the final propeller design. If the methods of this paper are used then the $B.A.R.$ will be either 0.5 or that required to meet the cavitation criteria previously described.

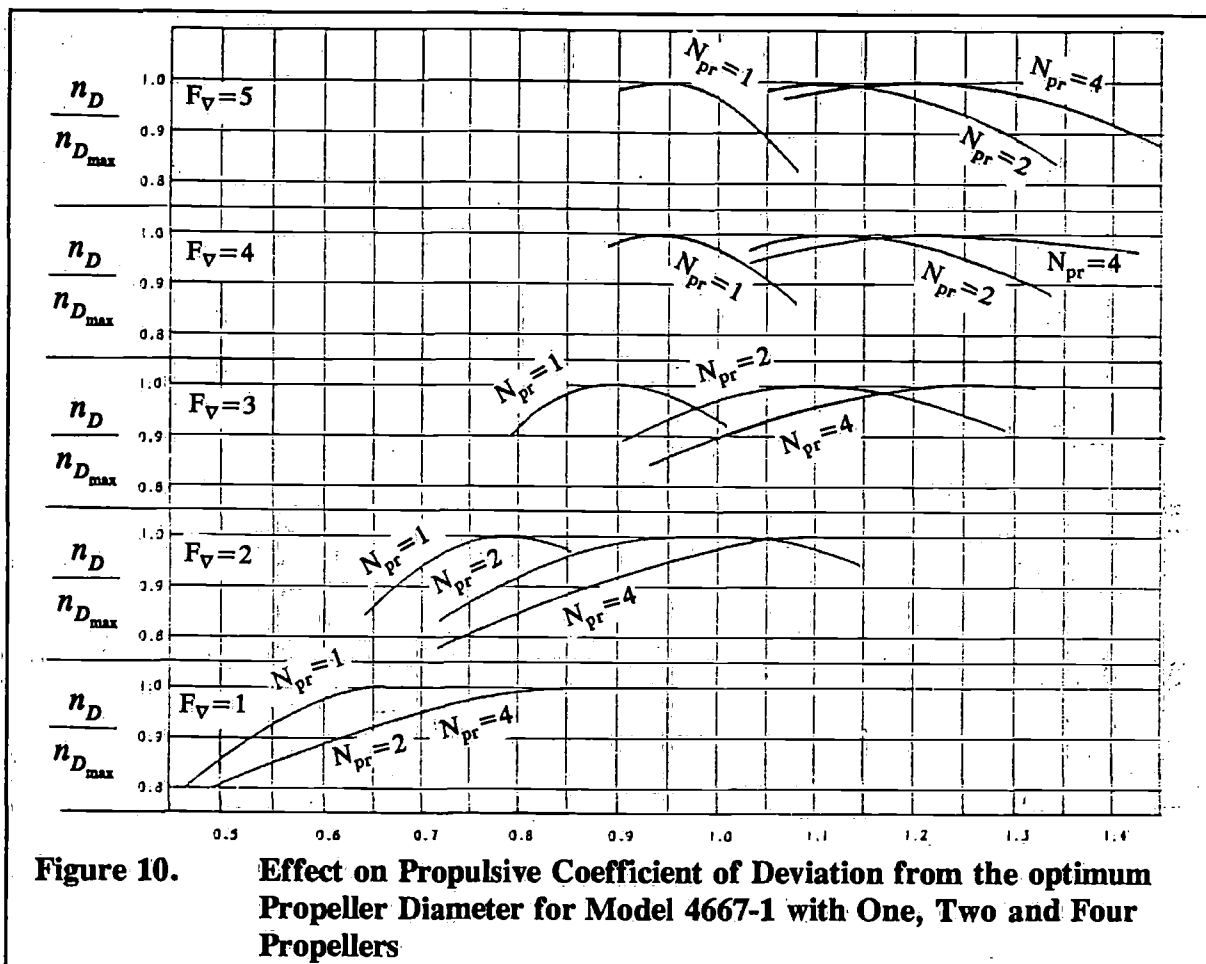


Figure 10. Effect on Propulsive Coefficient of Deviation from the optimum Propeller Diameter for Model 4667-1 with One, Two and Four Propellers

Conclusions

As a result of these studies the following conclusions may be drawn:

1. The non-dimensional propeller shaft-strut lift and drag characteristics do not change significantly with the design speed; thus, it is practical to develop lift and drag coefficients as functions of propeller diameter for any given hull-propeller arrangement which are independent of design speed and size of craft.
2. Propeller tip clearance has a small but finite effect upon the maximum propulsive coefficient, tending to increase the magnitude of η_D with decreased clearance. However, this is not considered to be a primary variable in this study.
3. The results of this study can be assumed to be achievable with commercially available propellers having geometric characteristics, i.e., diameter, pitch and $B.A.R.$, comparable to those of the Gawn-Burrill series.

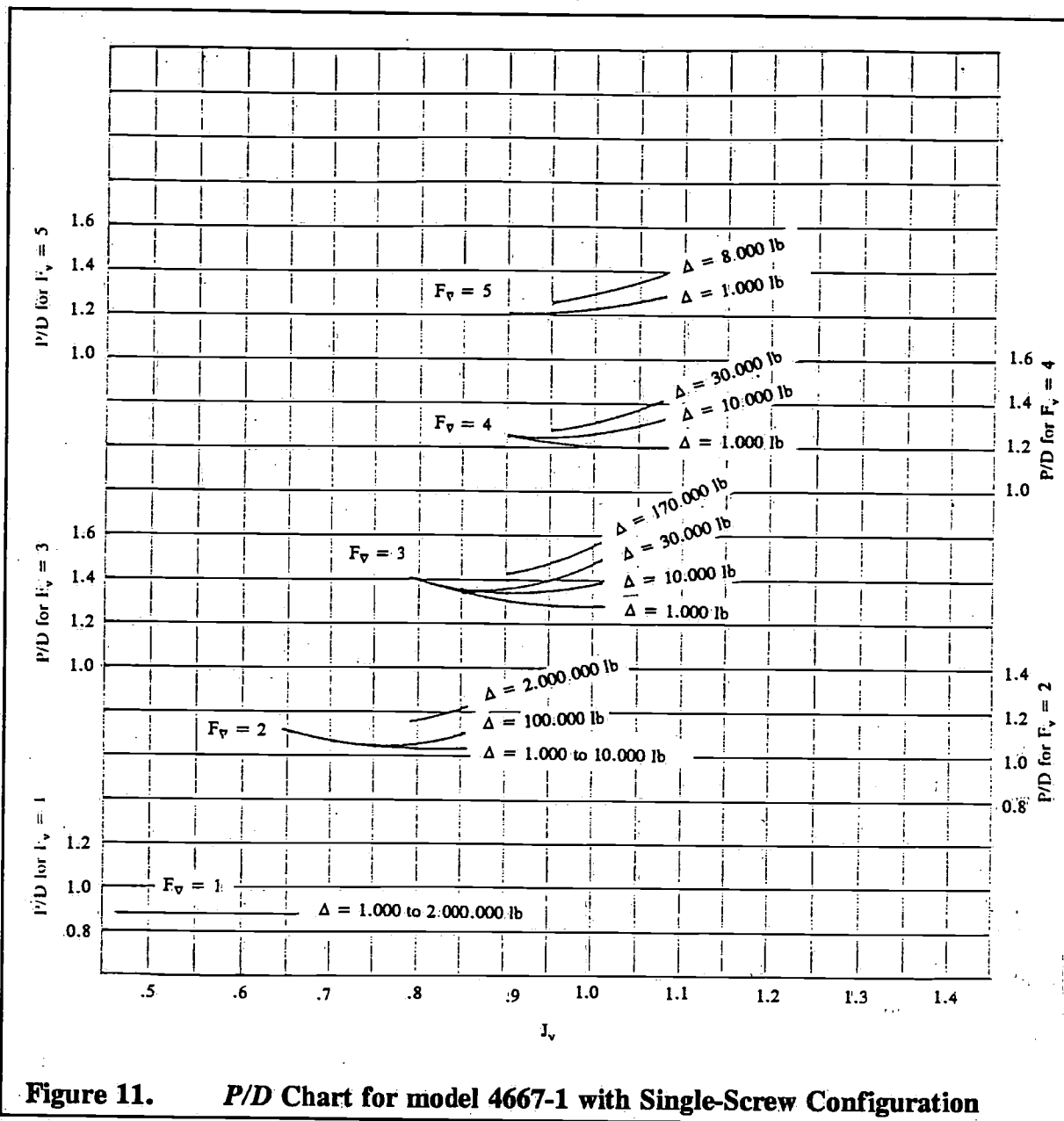


Figure 11. P/D Chart for model 4667-1 with Single-Screw Configuration

4. Hull roughness, within the limits of varying the hull roughness coefficient from 0.0 to 0.0004, did not have a significant effect either upon the propulsive coefficient or upon the choice of principal propeller characteristics, i.e., diameter, pitch and *B.A.R.*, for optimum propulsive efficiency. It should be noted that the shaft horse-power will increase owing to increase in hull resistance.
5. The following design parameters within the limits of the variations made on this hull did not have any significant effect upon the propulsive coefficient or upon the choice of the principal propeller characteristics for optimum propulsive efficiency.
 - a. Hull loading varied ± 21.4 percent
 - b. Longitudinal Center of Gravity, varied ± 6 percent of L_p
 - c. Transverse location of propeller shaft-strut-rudder system of twin-screw configuration
 - d. Longitudinal location of propeller shaft-strut-rudder system of twin-screw configuration, moved forward two stations

6. The diameter-rpm relationship can vary over a fairly wide range and still maintain high propulsive efficiencies. The range of this variation is greater for the multi-screw configurations than for the single-screw configuration.
7. The single-screw configuration is less efficient at all speeds and sizes than are the twin- and quadruple-screw configurations.
8. The twin-screw configuration is most efficient at higher speeds and lighter displacements. The quadruple-screw configuration is most efficient at low speeds and heavier displacements, the crossover point occurring at progressively heavier displacements as the design speed is increased.
9. The maximum achievable propulsive efficiency decreases with increased design speed due largely to the need for greater propeller blade area to minimize the effects of cavitation.
10. Although these results are for a specific hull configuration, it is believed that they would be applicable to any planing hull with comparable L/B proportions and resistance-weight ratios.

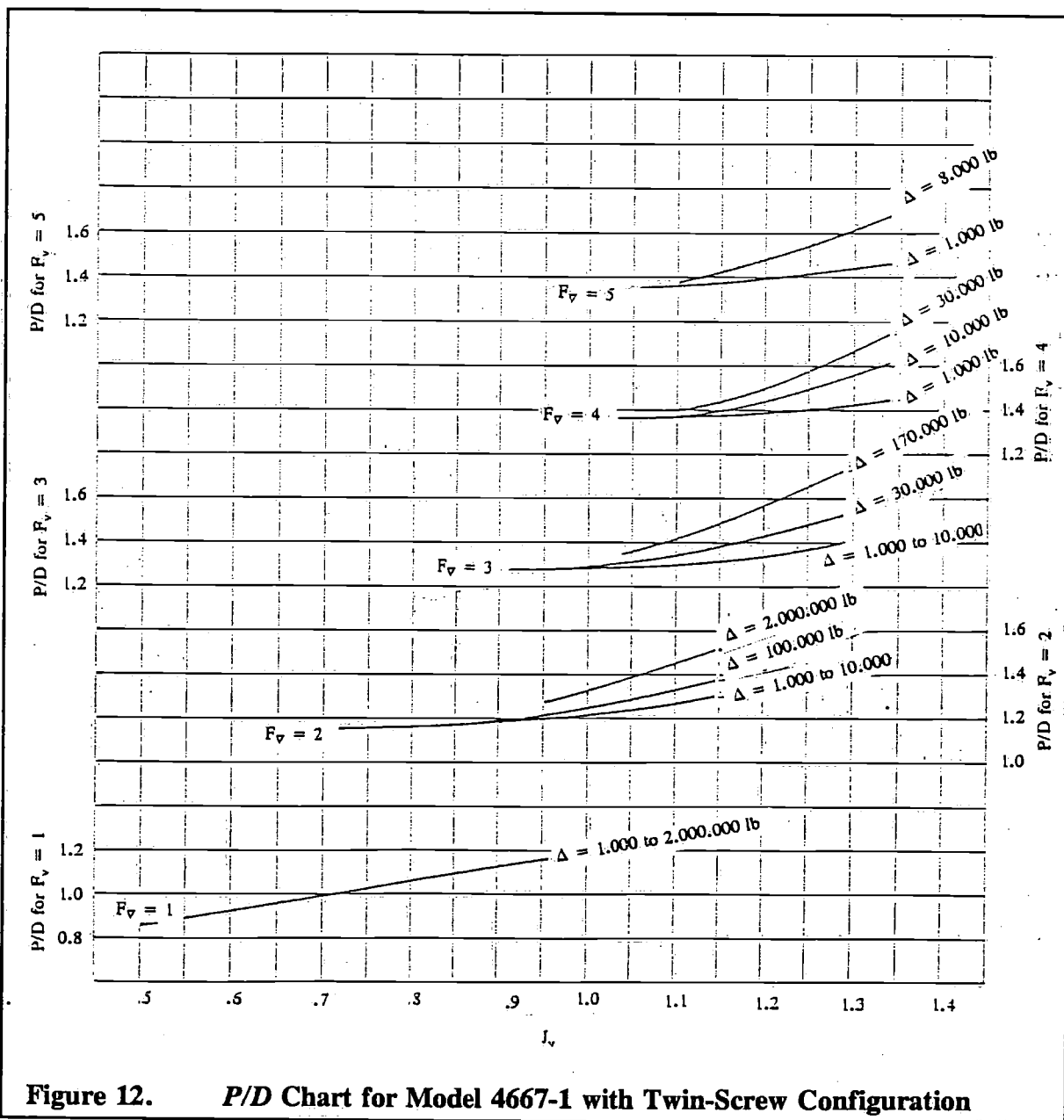


Figure 12. P/D Chart for Model 4667-1 with Twin-Screw Configuration

Recommendations

Since this paper has shown that the performance predictions made for the parent model of Series 62, with $L/B = 4.09$, can be collapsed into useful design charts, it is obviously desirable to extend this research to include the other models of the series and thus to show the effect of L/B variation. It also becomes evident that extensions of this work in several directions would widen the range of its usefulness to the designer. They are as follows:

1. Check the validity of this work on other planform configurations with the same L/B ratio to establish the universality of these results.
2. Extend the work to greater shaft lengths (lower shaft angles).
3. Investigate the triple-screw configuration because it has promise of being the most efficient system over a wide range of speeds and displacements.
4. At the highest speeds, investigate other propeller blade configurations which might have higher propeller efficiencies than those of the Gawn-Burrill series.

Fundamental research investigations are also needed concerning performance of conventional marine propellers operating in inclined flow over a wide range of cavitating conditions so that the assumptions made in predicting K_r , K_Q , and K_{Fz} in inclined flow can be verified.

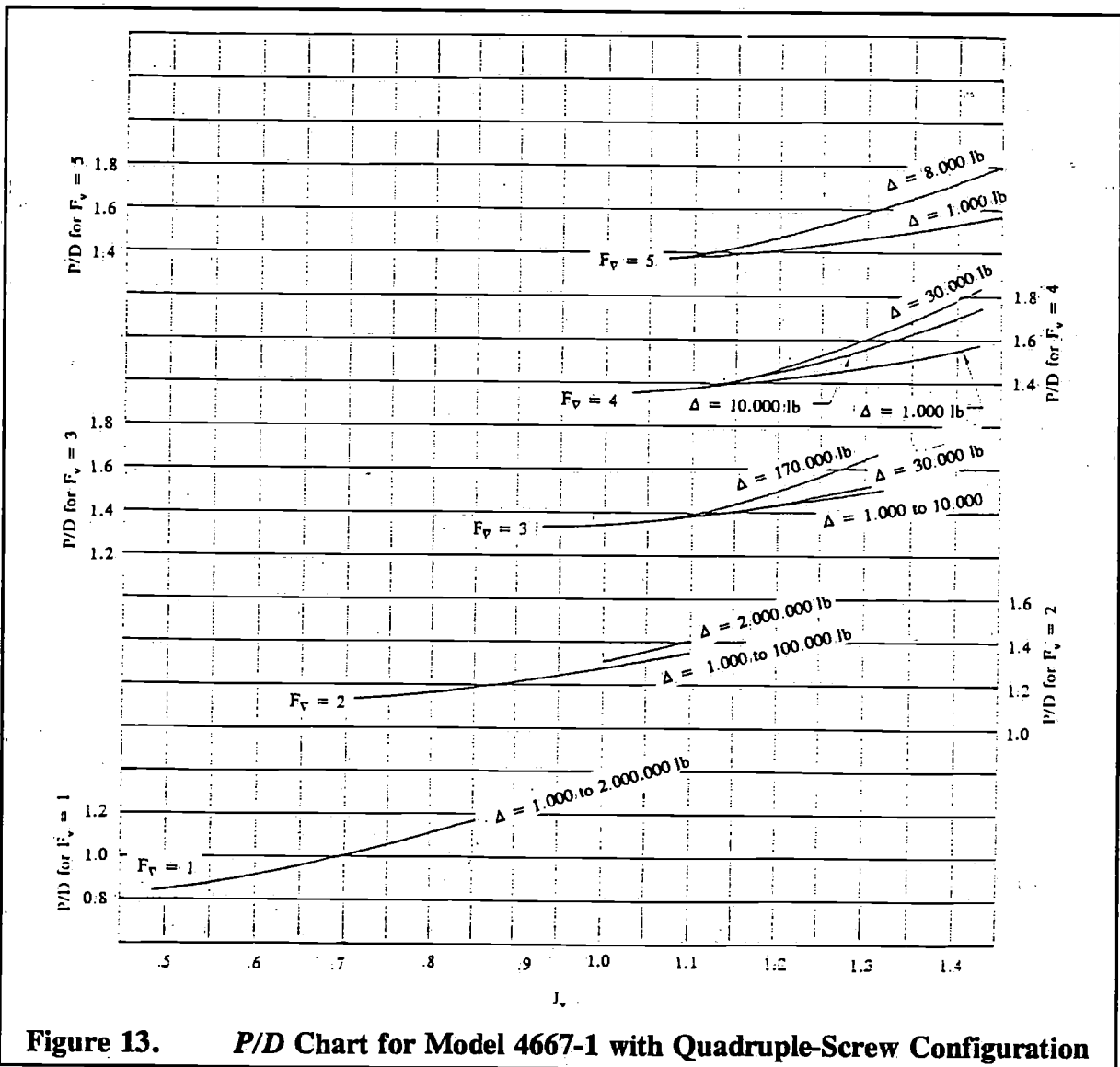
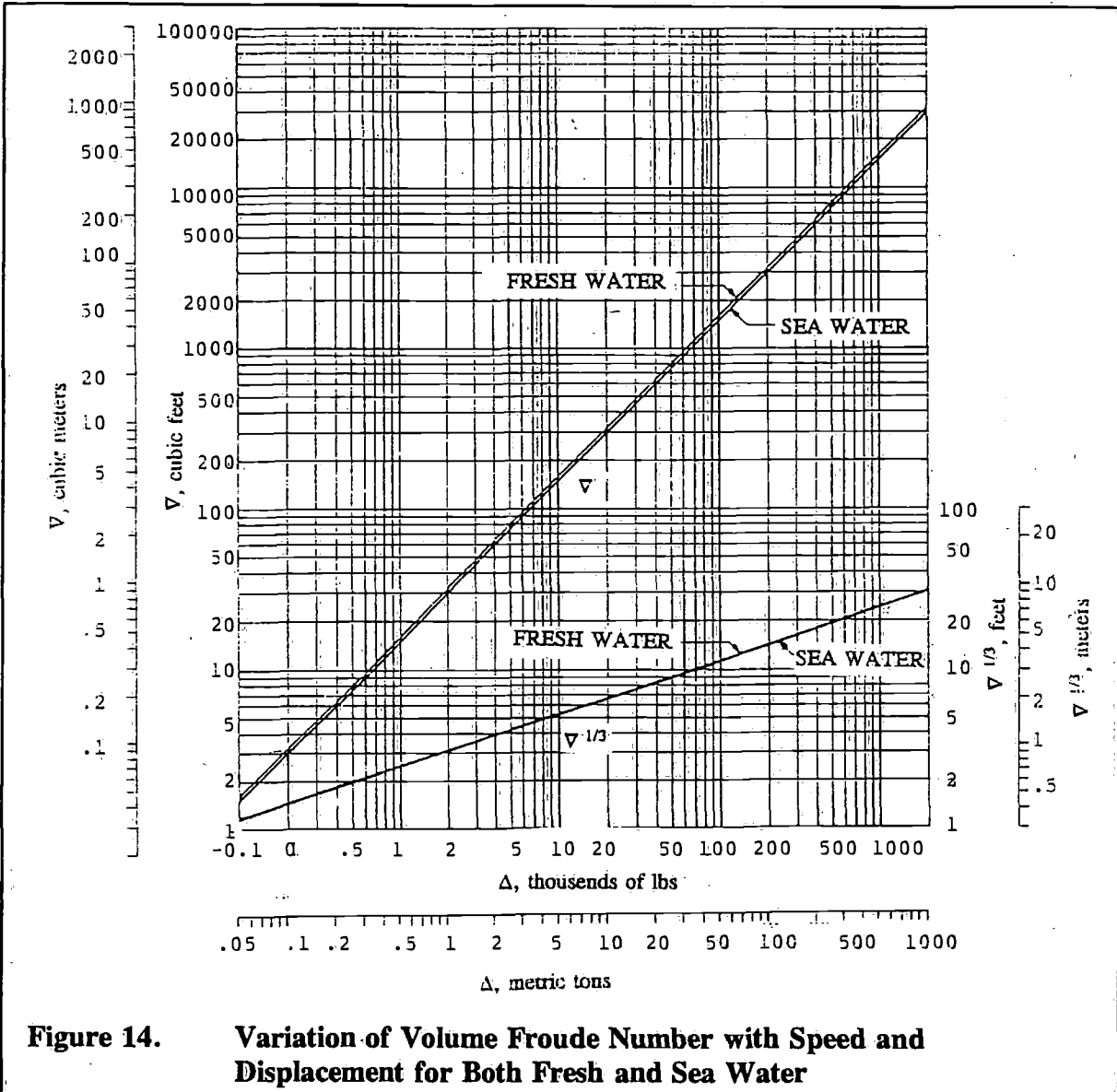


Figure 13. P/D Chart for Model 4667-1 with Quadruple-Screw Configuration

Acknowledgements

Since this project is largely the synthesis of previous work, it is appropriate to acknowledge the authors whose work comprised the essential elements of the study. Special reference is made to the careful documentation of the Series 62 resistance data by Clement and Blount in reference 1. The help provided by Mr. Emerson of Kings College, who did most of the experimental work on the Gawn-Burrill series of propellers, in making available the original test data is also appreciated. The generous support of the General Hydromechanics Research Program, which is under the technical direction of Dr. W.E. Cumunins at the Naval Ship Research and Development Center, is gratefully acknowledged.



References

- [1] Clement, E.P. and Blount, D.L., "Resistance Tests of a Systematic Series of Planing Hull Forms", Volume 71, Society of Naval Architects and Marine Engineers Transactions (1963).
- [2] Gawn, R.W.L. and Burrill, L.C., "Effect of Cavitation on the Performance of a Series of 16. Inch Model Propellers", Volume 99, Transactions of the Institute of Naval Architects, London (1957).

- [3] Hadler, J.B., "The Prediction of Power Performance on Planing Craft", Volume 74, The Society of Naval Architects and Marine Engineers Transactions (1966).
- [4] Gutsche, F., "Untersuchung von Schiffsschrauben in Schräger Anströmung", Schiffbau Forschung (March 1964).
- [5] Taniguchi, K. et al., "Investigation Into the Propeller Cavitation in Oblique Flow, (2nd Report)", Experimental Tank(Nagasaki) Laboratory, Mitsubishi Heavy Industries Ltd., Japan, Report 2221 (May 1966).
- [6] DuCane, P., "High-Speed Small Craft", published by Temple Press Limited London, England, page 159 (1956).
- [7] Ober, G.L., "Characteristic Curves and Blade Measurements of Commercial Small Boat Propeller Series", DTMB Report 966 (May 1955).
- [8] American Boat and Yacht Council Standard P-6 entitled "Recommended Practice and Standards, Size, and Installation of Propeller", published by Boat Construction and Maintenance (February 1966).

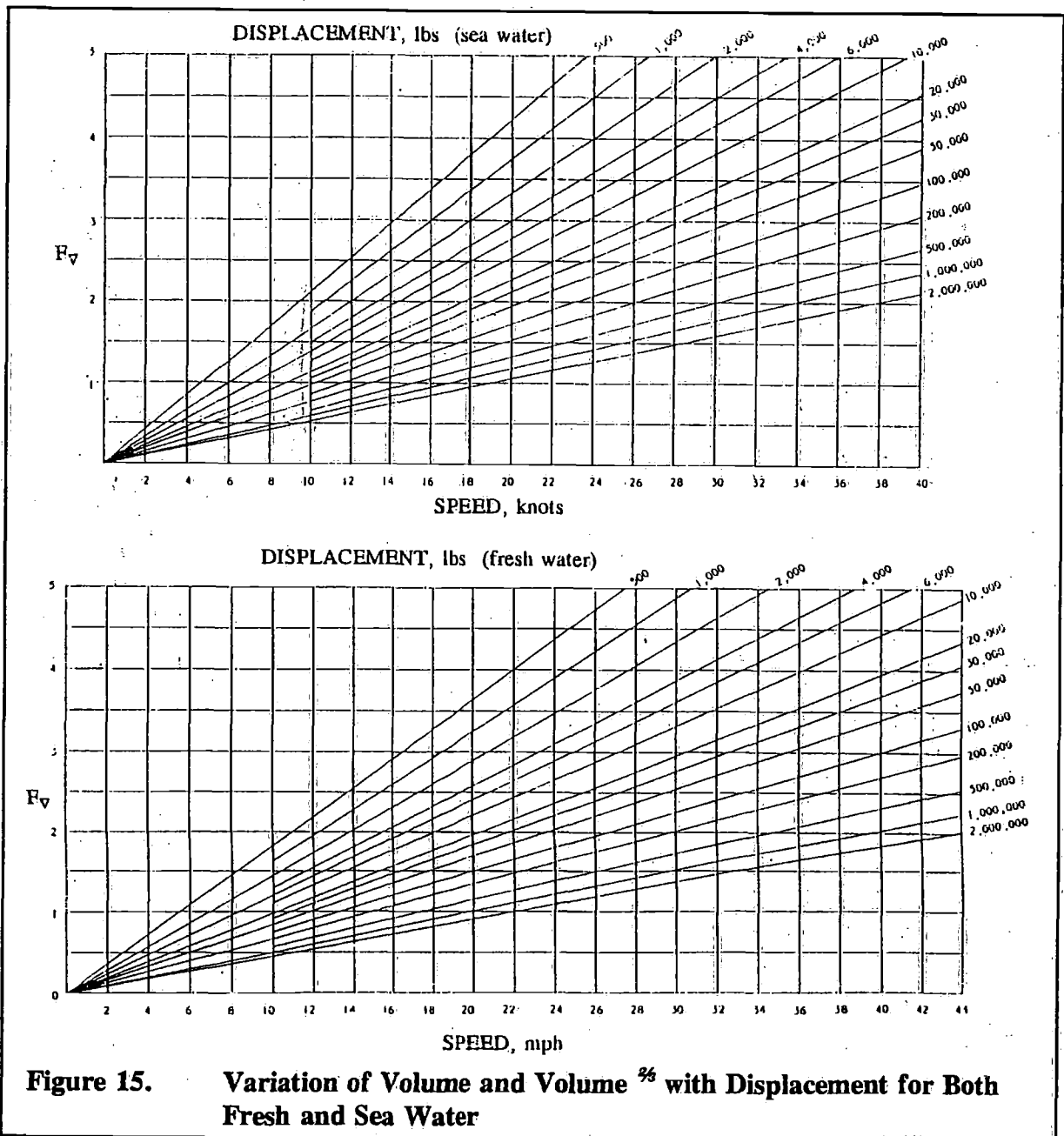


Figure 15. Variation of Volume and Volume % with Displacement for Both Fresh and Sea Water

Jointdesign in the construction of fibre-glass reinforced yachts

by Ir. R. J. Schliekelmann

Fokker-VFW N.V.
Schiphol, The Netherlands.

1 Introduction

Fibreglass Reinforced Plastic (F.R.P.) is in fact a family of materials, similar like the families of "Metal", "Wood" etc. The members of the F.R.P.-family have many common features, but still are individually quite different.

One of the common features of this family is the fact, that they all consist of rather weak, soft, resinous basematerial such as polyester or epoxy resin in which strong and stiff reinforcing fibres are embedded. Differences between the members of the F.R.P.-family are achieved by variations in the glassfibre reinforcement in this resinous matrix. These can be variation of the relative quantity of fibres, but also the form in which they are embedded, such as glassfibre yarn, rovings, stapelfibres, randomfibre mat or woven cloth.

Another typical and very attractive feature of F.R.P.-materials is the fact that structures of quite complicated shape can be produced with rather simple production means. Unfortunately in practical design and production not all structures appear to be feasible and the product has to be split up into various main components, that have to be joined during the final stages of production.

The strength properties of F.R.P. are in many aspects very good. However, metallic components, such as fittings and inserts, still cannot be missed in a yacht. Therefore joints between fibreglass plastic components themselves as well as metallic parts have to be made.

The designer of such joints has, in addition to the normal designfactors, such as nature and magnitude of loads, to consider the fact that many of the components have been made out of this typical material Fibreglass Reinforced Plastic.

History has learned that in several cases the difficulties of jointdesign in yacht-structures have been considerably underrated. Joints between components of further excellent design and quality caused a bad name for both the product and its manufacturer. i.e.: Bad joints were cause of a 'bad ship'. In this paper an effort is made to throw some light on this complicated subject.

2 Principles of jointdesign in F.R.P.-structures




The following aspects shall be taken into account when designing joints in F.R.P.-yacht-structures.

2.1 The material and the type of components to be joined

For the proper transfer of loads from one component into the other the strength- and the stiffness-properties of the F.R.P.-materials used play an important role. It makes all the difference whether the component is made of random fibremat or wovenrovings or combinations of the two.

Table 1 gives data about mechanical properties of various types of F.R.P.-laminates used in ships as given by various literature sources. The typical problem for the average yacht-designer is, that he does not know in detail the strength-properties of the laminate that finally will be incorporated in the yacht concerned.

Table 1

MATERIAL	GLAS S %	FAILINGSTRESS			MODULE	SOURCE
					E _b	
		kgf/mm ²			kgf/mm ²	
POLYESTER EPOXY	0	3-9	9-15	11-18	245	
	0	4-9	6-16	9-25	700-745	
POL/MAT	25	8.5	12.7	-	635	Lloyd's yachts
"	30	10.0	15.5	-	850	"
"	30	10.0	15.0	-	670	Lloyd's fisherb.
"	25-35	8.1	12.6	11.2	595	U.S. Navy
"	35-45	9.8	16.1	11.9	770	"
"	41-51	14.0	21.7	14.7	1015	"
POL/W.R.	50	23	19.0	-	1275	"
"	45-55	22.5	22.4	12.6	1155	"
"	48-58	19.6	25.9	17.5	1400	"
"	57-65	25.9	35.0	23.1	1750	"
4 x MAT 2.8mm	41.7	8.7	18.7	28.0	928	AKU-Silenka
3 x MAT + W.R 3.0 mm	39.3	9.1	39.2	22.5	1110	"
2 x MAT + W.R + 2 mm + 3.9 mm	35.7	9.4	16.0	23.1	-	"
M + W.R + M + W.R + M + 3.8 mm	41.5	12.6	26.5	18.8	946	"
W>R + 3 mm + W.R + 4.0 mm	40.7	13.2	29.4	20.5	1461	"
ALUMINIUM 6061-T3	-	21.0	21.0	20.0	7000	
STAAL QMC 42	-	42.0	42.0	40.0	21500	

He has experience that a certain combination of resin and glass reinforcements yields satisfactory properties for the type of yacht he designs. He does not know either the exact strength and stiffness of the structure he designs and the exact forces the yachtstructure will be subjected to during use. So, to design a suitable structure for a yacht is today in most cases not yet a matter of skilfull manoeuvring with a sliderule using exact load and strength data. The designer could live with this approach for some time, but as soon as other structural configurations have to be designed and with joints in other areas he will run into trouble. The difficulties will then be found primarily in the areas of the joints between the larger components and loose fittings.

Under these circumstances the best advise to be given is:

- avoid joints as much as possible

If it will be impossible to avoid joints, then another important rule to be followed is:

- design the joint such that the components to be joined are not weakened by that joint in the joint area.

It has been overlooked very often, that structural components easily may be weakened by the presence of joints due to insufficient consideration of the load transfer from one component into the other and the resultant stress concentrations. In the following data will be presented about rules for ensuring that no weak spots in the components will be created due to the presence of unavoidable joints.

2.2 Types of joints and their application.

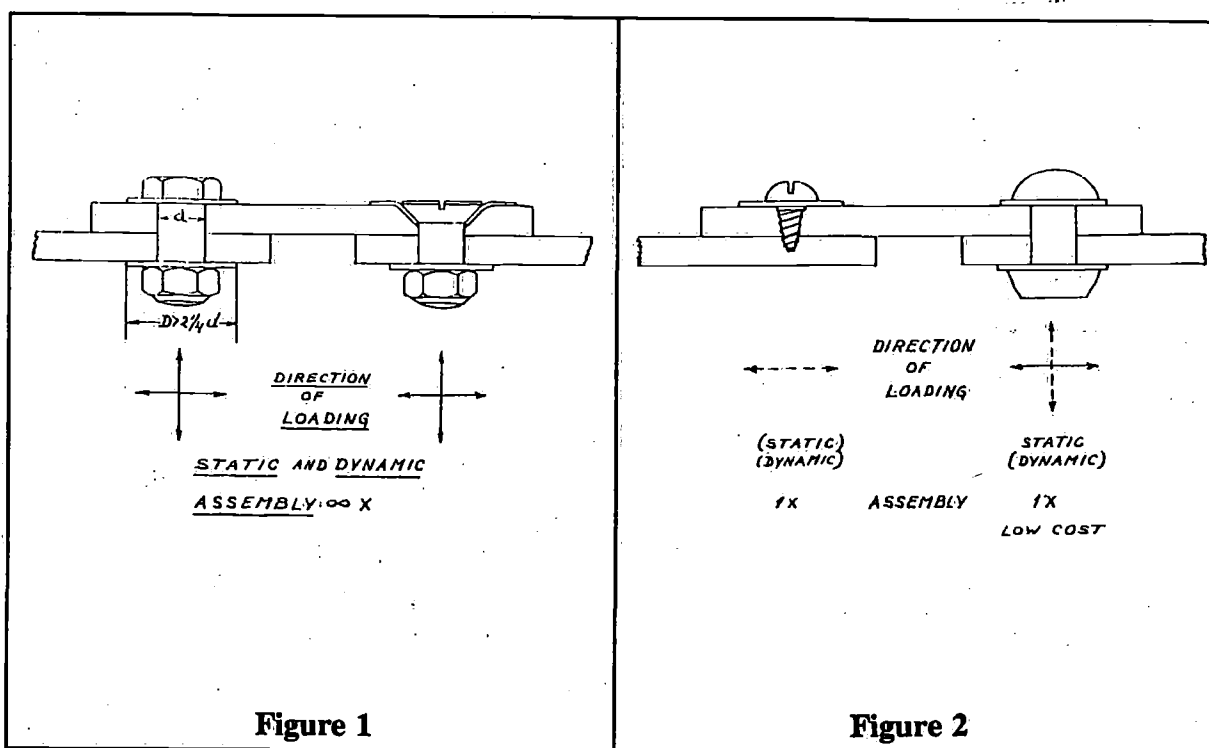
The following main types of joint can be used for attaching fibreglass reinforced components to each other or to metal parts:

a) Bolted joints

Bolted joints are used to transfer both static and dynamic loads. The joints may be disassembled and reassembled several times without harm to the components concerned. They can be used where the holes are allowed to penetrate both components concerned (Figure 1). Bolted joints are the only joints, that are able to guarantee a reliable transfer of tensile loads. With the limitation however that always adequate washers shall be used under bolthead and nut. The washer shall have a minimum diameter of $2\frac{1}{4}$ x the bolt diameter. Countersunk bolts can be used only with countersunk or dimpled washers.

b) Screwed joints

Screwed joints do not take as well as bolted joints dynamic and static loads. They are limited in their application as they may not be reassembled. They find their application where throughfasteners for some reason cannot be permitted. Tensile loads in the direction of the shaft of the screw must be allowed with considerable safety margins only. They generally will be limited to secondary joints only (Figure 2).



c) Riveted joints

Riveted joints are permanent joints that can take dynamic loads but with certain limitations. They generally are used for secondary joints where low cost has to be achieved. The special blind variety does not only allow mechanical fastening in areas where access from only one side of the structure is possible, but also it allows for rivetting in areas where normal percussion or squeeze riveting cannot be tolerated. In more important riveted joints washers shall be used always under both rivetheads. In all cases squeeze-riveting is preferred over percussion-rivetting in view of the possible damage to the adjacent laminate.

d) Adhesive bonded joints

Adhesive bonded joints are permanent joints that are preferably used where a liquidtight joint is required or in areas where the continuous nature of the bond is preferred for reason of avoiding stressraisers or for providing a high degree of stability to the joined components. The adhesive bonded joint is based on a rather weak joining material, but used over a large area. Stress concentrations however may easily lead to failures in the weak gluelayers.

Bolted, screwed and rivetted joints share the feature of requiring holes to be drilled in one or both components to be joined so that the fasteners can be placed. These holes are the main causes for weakening the components to be joined.

In the following paragraphs rules for compensating the strength loss due to the holes are given. Before doing so the F.R.P.-laminate will be discussed more in detail as well as the types of loading the constructions will be subjected to.

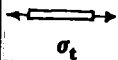
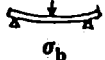
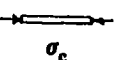
3. Some aspects of the F.R.P.-laminate material

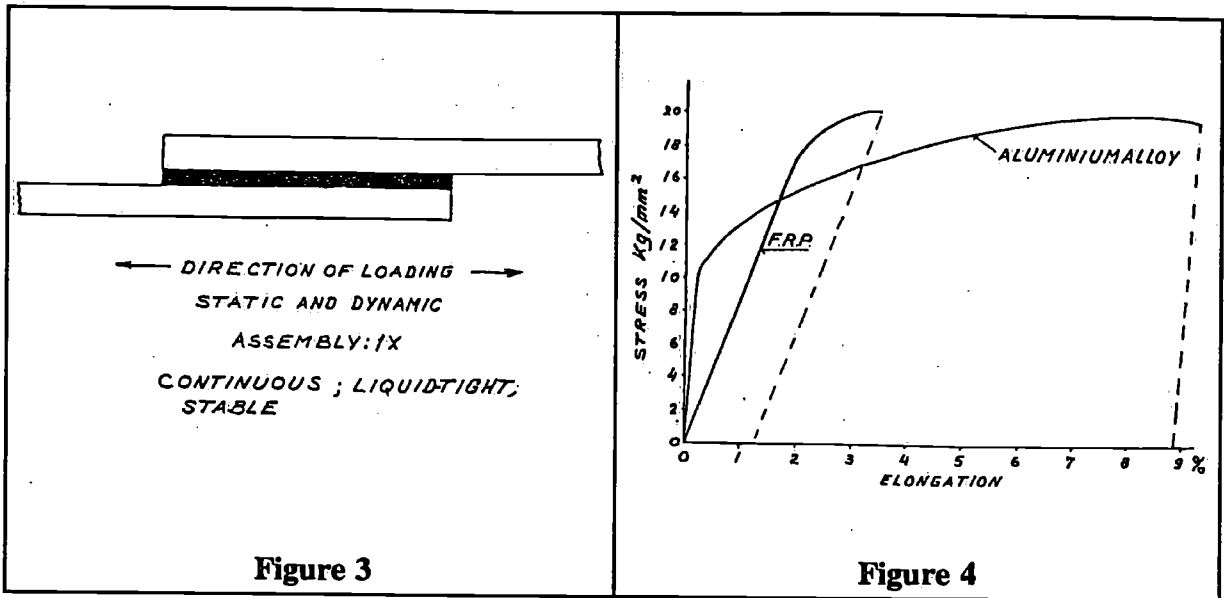
From Table 1 it appears that there is an important influence from the glasscontent on the strength-and stiffness characteristics of the laminate. In composite laminates out of randomfibremat and wovenrovings, the position of the latter layers relative to the direction of the neutral axis of flexure has a distinct influence on the flexural characteristics of the laminate but not on the tensile or compressive properties. Comparing the data of the laminate materials with those of the conventional metals, it appears that the laminates have somewhat lower strength figures but still of the same order of magnitude. The Moduli of elasticity, however, of the aluminium and steel products are respectively still a factor 7 and 20 higher than those of the laminates. (Figure 3)

At a certain stresslevel the laminate deforms considerably more than the metal-structures. The figures for the unreinforced resins are very low indeed. They must be kept in mind, however, when studying adhesivebonded joints that contain un-reinforced resinlayers. It should not be forgotten also, that the laminate materials themselves consist of reinforced layers with in between unreinforced resinlayers. The interlaminar strength is entirely dictated by the resinproperties.

Within each layer the strengthproperties may vary directionally due to variation of the amount of glassfibres in each direction. Table 2 shows the strength retention found when laminates are loaded under 45° to the main fibre direction as compared with strength-figures found in Table 1. The randomfibremat structures do not show much influence on the direction of force; the woven roving laminates, however, show strengthreductions to as low as 25%, when loaded under an angle of 45° with the main direction. When designing joints and their reinforcements this aspect must be kept in mind.

Table 2

STRENGTH RETENTION UNDER 45°				
MATERIAL	GLASS %	 σ_t	 σ_b	 σ_c
POL/MAT	25-35	95	95	100
„	35-45	95	95	100
„	41-51	95	95	100
POL/W.R	45-55	35	35	65
„	48-58	40	40	55
„	57-65	25	45	60
		% σ_{t90°	% σ_{b90°	% σ_{c90°

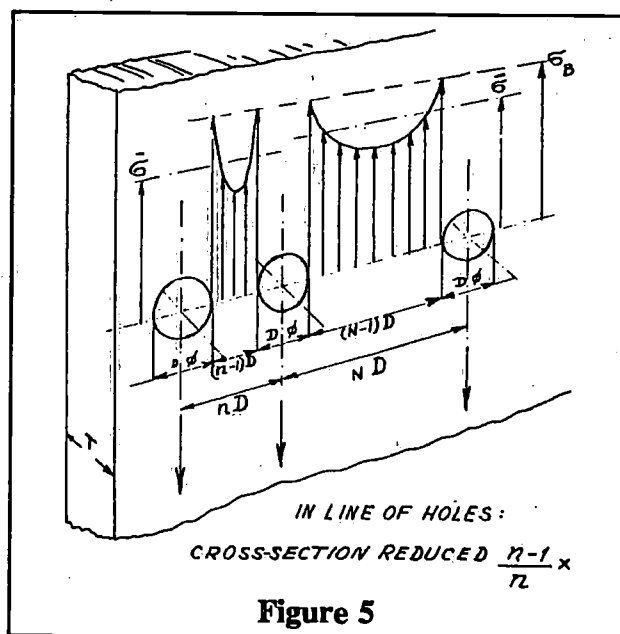


The F.R.P.-materials may show a much higher elastic deformation than the metals, their plastic deformation before failure is only a few percent as compared to 15 tot 40%, of aluminium and steel. In mixed metal-plastic joints this may be a source of problems. At a certain stresslevel the deformation of the F.R.P.- part will be considerably higher than that of the joining metal part; at a higher stresslevel, however the situation may entirely change due to the high plastic elongation before failure of the metals. The metals have a considerably higher ductility after passing their yieldpoint. (Figure 4)

Materials with little plastic deformation before failure are called "brittle". The F.R.P.-materials certainly behave like brittle materials in spite of their plastic origin.

Summarizing can be said about the F.R.P.-materials:

- Their stiffness is much smaller than that of metals.
- They have a typical brittle type of failure.
- With the woven varieties the direction of force relative to the direction of warp and weft should be watched closely.



4 Special kinds of loading

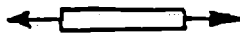

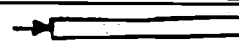
4.1 Shock loading

The properties as listed in Table 1 and discussed in the previous paragraphs, refer all to the situation when the load on the material is gradually increased until failure occurs. In practical operation of yachts that kind of loading will certainly not be the only one. Frequently the loads of the highest order may hit the ship suddenly like the heavy shock of a wave or an obstacle.

The mechanism of failure of F.R.P. in case of shockloading can be completely different as a result of the brittle nature of the base resin. In those cases the resin base-or matrix material will crack, leaving the loadcarrying glassfibres unsupported and unable to transfer loads: leading to complete failure of the F.R.P.-laminate.

According to the U.S.Navy an F.R.P.-laminate will fail at as low as 15% of the normal failing stress, when the load is applied as impact- or shockload. Consequently in all cases where shockloads are introduced into joints, these very low failing stresses must be taken into account. This means that in case the type of loading is such, that the shock will create tension- or compressive stresses in the laminate, the thickness thereof must be increased with a factor of about 7 relative to the thickness required in case of static loading (Table 3).

Table 3

	 $\% \sigma_t$ F_1		 $\% \sigma_b$ F_1		 $\% \sigma_c$ F_1	
IMPACT	15	6.7	15	6.7	15	6.7
FATIGUE	$\% \sigma_t$	F_a	$\% \sigma_b$	F_a	$\% \sigma_c$	F_a
alternating						
$n = 10^3$	60	1.66	-	-	-	-
$n = 10^4$	50	2.00	30	3.33	-	-
$n = 10^5$	35	2.86	25	4.00	-	-
$n = 10^6$	25	4.00	25	4.00	-	-
$n = 10^7$	20	5.00	25	4.00	-	-
fluctuating						
$n = 10^3$	-	F_t	75	1.33	-	F_t
$n = 10^4$	-	-	60	1.66	-	-
$n = 10^5$	-	-	60	1.66	-	-
$n = 10^6$	-	-	55	1.82	-	-
$n = 10^7$	-	-	50	2.00	25	4.0
F_1 = Reinforcement-factor Impact F_a = Reinforcement-factor Alternating Load F_f = Reinforcement-factor Fluctuating Load						

4.2. Fatigue loading

When the loading of the component is not applied statically, but is repeated at a rather high frequency, a considerable reduction of the failing load must be expected. There is a difference between the case when the load alternates between no load and a certain level or that the load fluctuates from a tensile to a compressive load of the same level.

The number of loading cycles during the operational life of the component determines the fatigue failing load level relative to the static failing load.

In the case such a fluctuating or alternating load is introduced via a joint, reinforcement factors have to be applied.

Table 3 gives both the failing load level in of the static failing load as well as reinforcement factors for the two types of fatigueloading and at various required lifes. These reinforcement factors must be applied on the laminate structure that is just suitable for carrying the required static load. In many practical cases the structure will already be overdesigned relative to the static maximum load. The full reinforcement factors shall then not be applied. It will be usefull however to keep their order of magnitude in mind when designing critical cases.

From these rather low shock-and fatiguestrengths of F.R.P.-laminates it can be seen that extreme care should be given to joints, that may weaken the structure locally, and that have to be located in shock-or fatigueloaded areas of the structure.

5 Holes in F.R.P.-laminates for mechanical fasteners

When designing a bolted, screwed or riveted joint much attention must be payed to the requiremments to prevent weakening the components by the unavoidable holes.

5.1 Cross section reduction

When drilling a line of holes with a diameter D at a pitch of nD there is a loss of cross section of D at each pitch distance of nD . This results in a loss of strength in the line of holes of:

$$\frac{(n - 1)}{n} \cdot 100\%$$

Compensation must be given for this by increasing the thickness of the laminate first of all to:

$$\frac{n}{(n - 1)} \cdot (\text{the original thickness } \tau)$$

(Figure 5)

Column 3 of Table 4 gives these factors for 2, 3 and 4D holepitch (Figure 6).

Table 4

1	2	3	4	5
MATERIAL	HOLE PITCH nD	CROSS-SECTION COMP. n/n^{-1}	NOTCH-COMP. FACTOR	TOTAL HOLE-REINF. FACT.
POL/MAT	2 D	2	1.18	2.36
„	3 D	1.5	1.11	1.65
„	4 D	1.33	1.05	1.40
POL/W.R	2 D	2	1.66	3.32
„	3 D	1.5	1.42	2.84
„	4 D	1.33	1.25	2.50

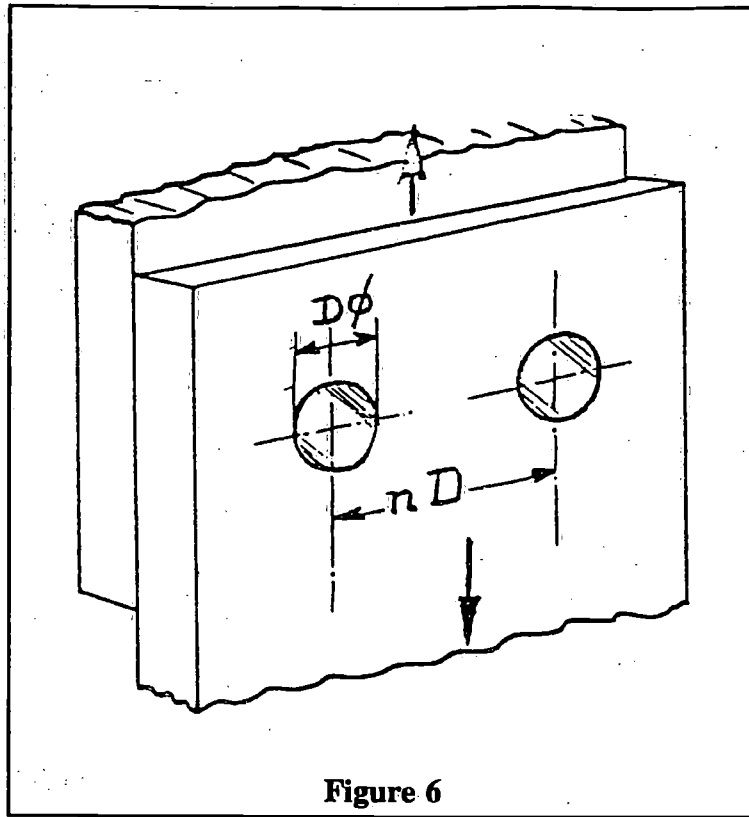


Figure 6

5.2 Notch sensitivity

Unfortunately the stresses in the remaining material between the holes will not be equally distributed.

At the edges of the holes the stresses will be higher than in the middle. As a result of this the remaining material between the holes will fail at an average stress below the normal failing load of the material. How much lower depends on the relative distance between the holes (nD) and the type of laminate: random fibremat, woven roving or cloth. The F.R.P.-laminates with their low plastic elongation before failure do not show a levelling effect of the plastic flow on the stresspeaks as occurs with steel and aluminium (Figure 6). Table 4 column 4 shows the reinforcing factors required to restore the original strength without the notch effect. The compensation for cross section reduction must be applied on top of this. The last column of table 4 gives therefore the complete compensation factor for both cross section reduction and notch sensitivity.

So, in order to cope with static load in a hole line of p.e. $4D$ pitch a reinforcement of 40% is required for a mat laminate and of 150% for a woven roving laminate. Reinforcement of a mat structure by means of woven roving layers is not as effective as sometimes is assumed, not even speaking about the higher sensitivity for the direction of loading (see table 2). A woven roving laminate loaded under 45° with its warp direction is certainly not stronger than a mat laminate and has a higher notch sensitivity.

5.3 Edge effects

In addition to the weakening of the cross section in the holelines, there is the possibility that the material between hole and edge shears. Therefore sufficient distance between holes and edges of components must be maintained. Table 5 shows the reinforcement factors required in case the edge distance is $3D$ or smaller. These factors are lower than the hole reinforcement factors from Table 5, which means that also the edges must be designed according the latter Table 5 (Figure 7).

Table 5

1	2	3
MATERIAL	EDGE-DISTANCE nD	EDGE-REINF. FACTOR
POL/MAT	1 D	1.88
„	2 D	1.44
„	3 D	1.00
POL/W.R	1 D	1.44
„	2 D	1.25
„	3 D	1.00

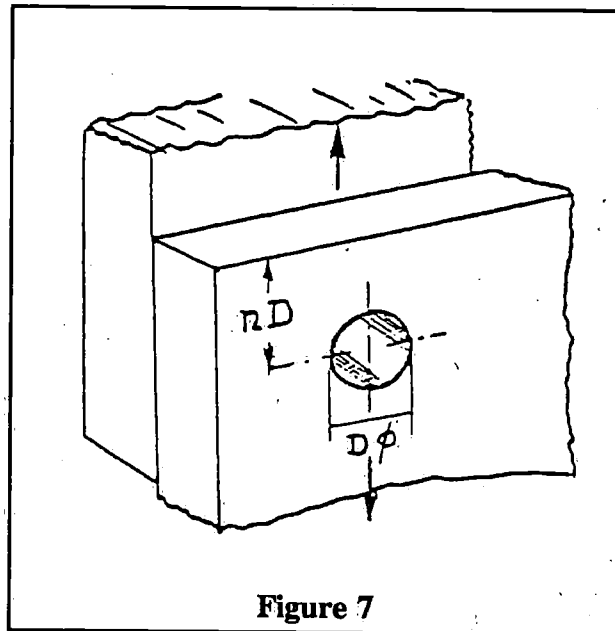


Figure 7

5.4 Bearing strength

Bolts, screws and rivets share the fact, that the shearloads between the components to be joined, have to be transferred via their shafts resting in the holes of the components. in a well balanced joint the shearstrength of the fastenershaft must be of the same order as the bearingstrength of the hole.

For a given boltload to be introduced into the component via the hole the bearingstrength is closely related to the allowable compression strength of the laminate. The latter being considerably less than those of aluminium or steel a proportionally larger bearing area is required. As seen in the previous paragraphs a rather important thickness compensation has to be made in order to cope with the strength loss of the laminate due to the presence of the fastener holes. The diameter of the holes and the pitchdistance dictate for the greater part the amount of this compensation. In this way simultaneously more bearing area for the fasteners is provided. In addition to that it is still good practise to choose the bolt- or rivet diameters at least one diametersize larger than the usual ones in metal structures for the same task. By taking instead of 1/4 inch 5/16 inch bolt diameter the bearing area is considerably increased. Another solution for this problem is to use tubular bushings or sleeves around bolts or rivets having the minimum required diameter for fulfilling the requested task in a metal structure; the bearing area is than provided by the ample diameter of the sleeve (Figure 8).

Another method is to laminate a metal plate in the joint area of the F.R.P.-component. The bolts then rest in the metal plate. The loads will then be transferred from the plate via the metal-resin bond into the F.R.P.-laminate. This method gives a smooth introduction of the load into the F.R.P., but only as long as the resin-metal bond stays intact. This will be the case only when all necessary steps have been taken to ensure a good adhesion of the resin onto the metal surface. A surface preparation of the metal similar as for adhesive bonding of metals is then required. Only when this can be carried out, this method can be used with a reliable result.

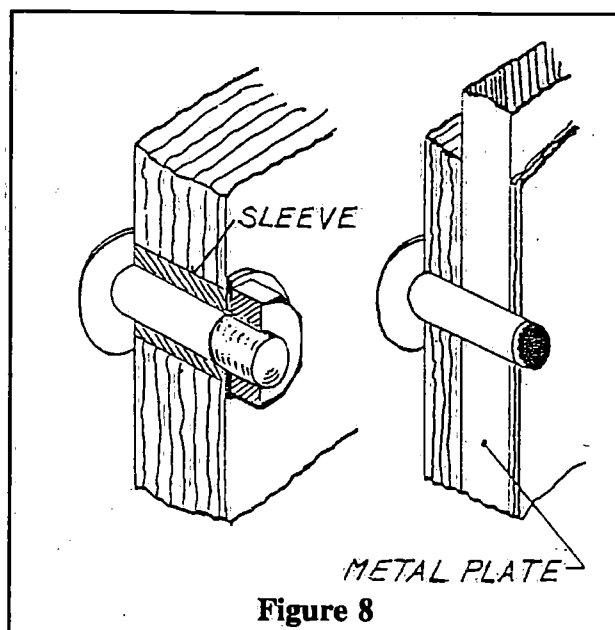


Figure 8

6 Adhesivebonded joints (including wet laminated joints)

6.1 General aspects

Adhesive bonded joints are characterized by the fact that the joining medium has a much lower strength than the F.P.R.-laminates to be joined. The joining medium is an unreinforced resinlayer. Reasonable jointstrength may be obtained only when the load is equally distributed over the whole jointsurface area.

6.2 Tensile loads

In a butt-type joint loaded in pure tension the of failing stress in equal to the tensile strength the adhesive-resin, under the condition that the stresses are equally distributed. In the case the joint is not loaded by a centric tensile force but by an eccentric load the pure tensile stresses must be added to the stresses resulting from the bending moment.

Failure of the bonded joint will occur as soon as locally the adhesive resin reaches its failing stress. In case of eccentric loading, p.e. at the edge of the butt joint, the adhesive failing stress is reached at a moment when the average stress is still much lower: in the example only 25% of the centric case (Figure 9).

In this respect it should not be forgotten, that when the lamination planes of the F.R.P.-material lay perpendicular to the direction of loading the same effect plays. In that direction the laminate strength is not higher than the strength of the laminating resin in between the fibreglasslayers. The interlaminar tensile strength is much lower than that of the laminate as a whole. This means that in the case of tensile loaded bonded joints the jointstrength never will be better than the strength of the laminating resin used (Figure 10).

When the loading eccentricity is that much, that the force works outside the joint and a certain lever effect takes place, the stress concentration will rise sharply. The joint will fail then at a very low load level. This can be easily understood as the resins have tensile failing-stress figures of not more than 4 to 8 kgf/mm². This explains what in practical terminology is indicated with "the low peel strength" of bonded joints between laminates.

This is not only the result of the low adhesive strength but also of the rather low strength of the laminating resin. The effect of shock- and fatigue loading not even taken into account, the best advise to be given is:

be extremely careful with adhesive or resin bonded joints when peel- or tensile loads on the joints cannot be avoided.

This rule is equally valid for adhesive bonded as well as wet- in wet laminated joints loaded in peel or tension.

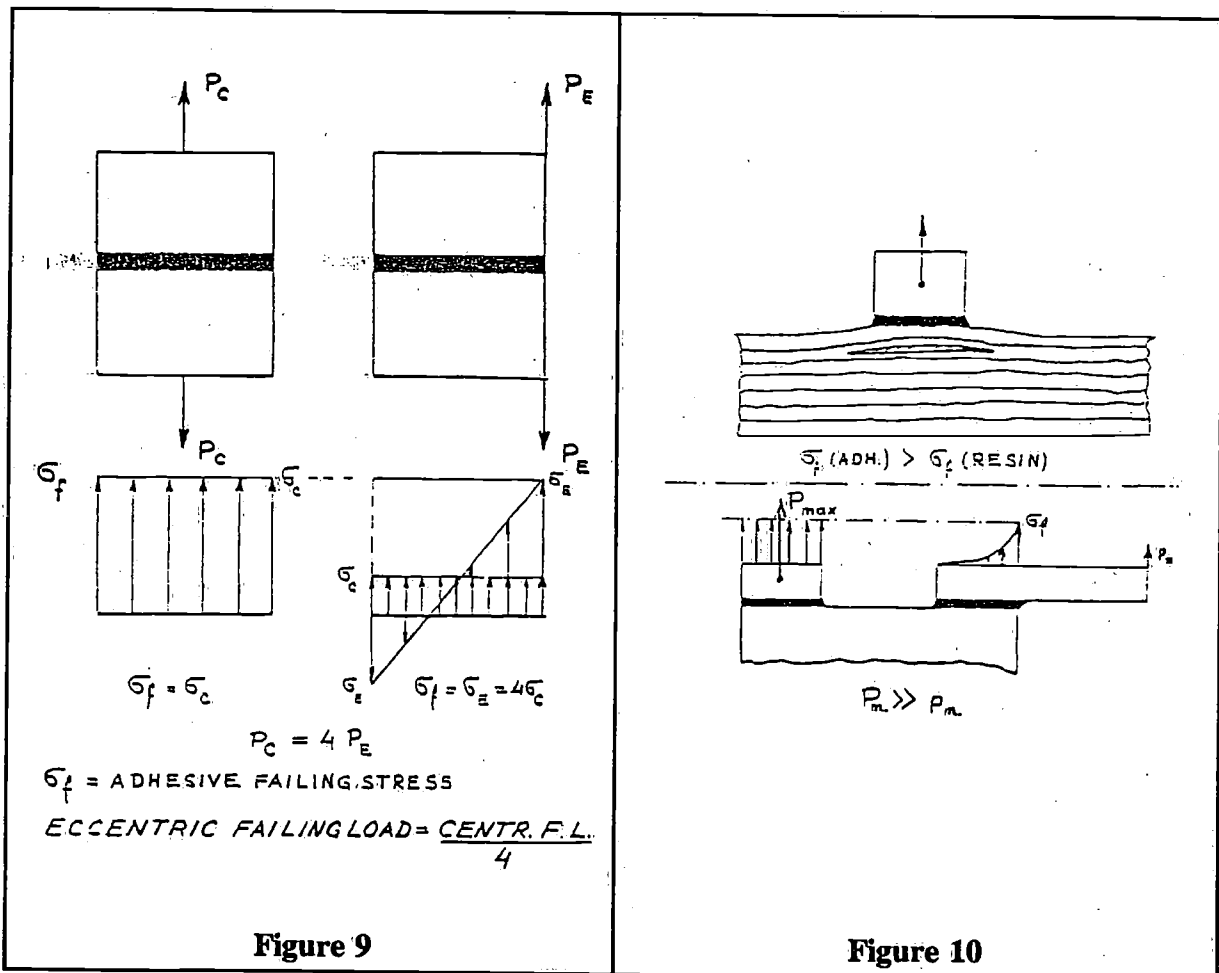


Figure 9

Figure 10

6.3 Shear loads

Shear loading is the most favourable kind of loading for bonded joints. The compensation of the limited adhesive resin strength is possible by allowing for sufficiently large bond area's. Unfortunately pure shear loading seldomly occurs. Tensile stresses at the overlap ends resulting from eccentricities frequently cause untimely failures of the bonded joints. Another source of trouble is differential deformation of the bonded parts, causing irregular stress distribution-concentrations in the joints. However, mechanical joints are as well bothered by this phenomena, that will be discussed in paragraph 7 (Figure 11).

7 Influence of component stiffness on joint strength

It has been mentioned before that F.R.P.-materials have in comparison with metals a rather low modulus of elasticity. This means that at a given stress level the F.R.P.-material deforms much more than aluminium or steel. This low stiffness of F.R.P. relative to metals is in many cases decisive for the joint strength. On the other hand F.R.P. hardly shows plastic deformation prior to failure, while metals show a considerable ductility when reaching the failing stress.

When a load is transferred from one component into the other, the components must in the joint-area be strong enough to carry that load (see par. 4 and 5). However, also the stiffness of the components in that joint area must be taken into account. The best load transfer takes place when in the contact areas the components have a deformation that is as close as possible equal.

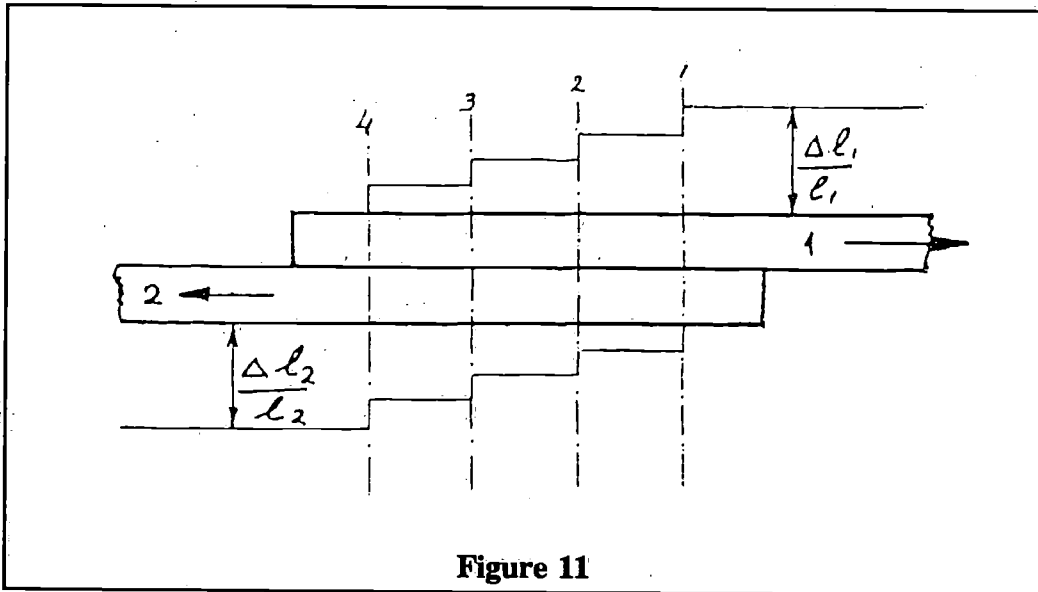


Figure 11

7.1 Mechanical joints (Figure 11)

When two strips are attached to each other by means of 4 mechanical fasteners, rivets or bolts, and loaded in shear by a load P the following situation exists. When approaching the joint area through strip 1 each unit of length of the strip is stretched an amount:

$$\Delta l = \frac{P \cdot l}{E \cdot F}$$

in which E is the modulus of elasticity and F the cross-section of the strips. This elongation remains constant until the first fastener will be reached. At that point a certain amount of load is transferred into strip 2 via the first fastener. In the space between fastener 1 and 2 the elongation of the strip 1 will be proportionally lower. So the load is taken out of strip 1 and transferred via fastener 1 and the following ones into strip 2. However, the deformation pattern in strip 2 will be just opposite. In that strip with each following fastener the load and the resulting elongation will grow step by step. The result of these opposite deformation patterns in the strips is that the fasteners at the ends of the overlap have to bridge a part of strip 1 having a large elongation and of strip 2 having a small elongation. This means that these fasteners at the overlap ends are more heavily stressed than from the transfer of the portion of load P alone.

The fasteners in the middle of the overlap are less affected by this differential elongation of

the adjacent parts of the components in this example; where the strip thicknesses have been chosen equal as well as the moduli of the materials.

In the case the components have different thicknesses or are made out off different materials with different moduli the situation may be more complicated. Then also the middle fasteners may be loaded considerably more than just by the transfer of the external load on the joint. This must be taken into account when designing joints in yachts. The deformation under load is ruled by the stiffness factor, $E \cdot F$, being the product of modulus and crossection of the component. A situation of equal deformation at both sides of the joint can be reached by keeping the factor:

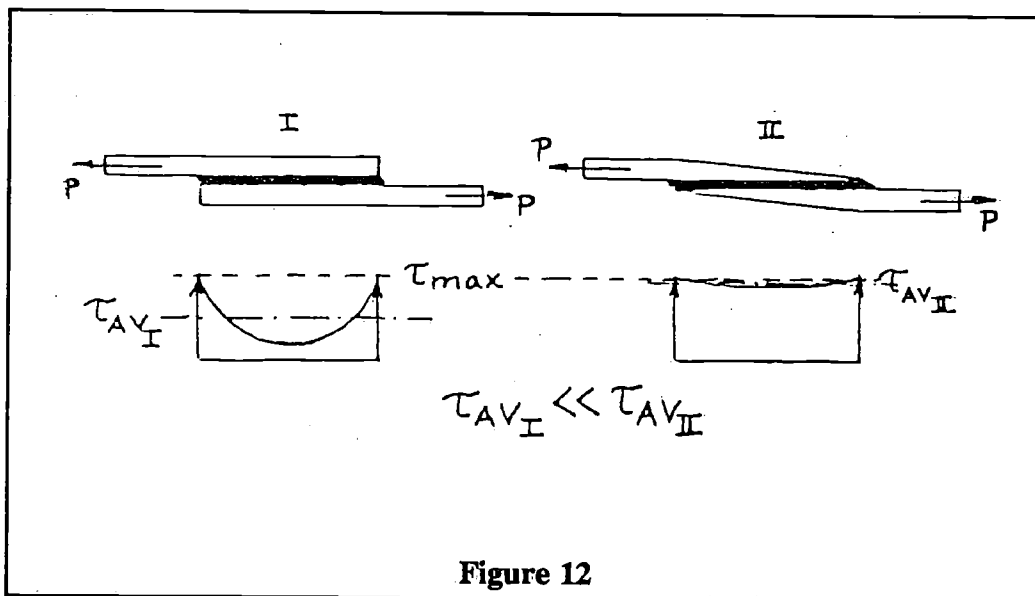
$$\frac{P}{E \cdot F}$$

equal for all joining elements on both sides of the joint.

When dissimilar metals are used in one same joint, then disregarding the load diminution along the joint, the thicknesses should be chosen with the ratio:

$$\frac{F_1}{F_2} = \frac{E_2}{E_1}$$

When per example an aluminium sheet is used to transfer a given load into a Woven Roving Laminate, having an E -modulus of 1000 kgf/mm² against 7000 kgf/mm² of aluminium, the thickness of the aluminium in the jointarea should be only 1/7 of that of the adjacent W.R.-Laminate.



7.2 Bonded joints

The before mentioned differential deformation problem plays also an important role when adhesive -or resinbonded joints are used (Figure 12).

In a loaded lapjoint, based on adhesive bonding, the stresspeaks at the overlap edges easily reach the failingstress of the resin at a moment when the average stress in the glue layer still has a rather low value. This can be corrected considerably by taking into account the loadtransfer over the length of the joint. By chamfering the components in the areas, where the loadlevel is already low, the stressdistribution in the joint can be considerably improved.

Consequently the loadcarrying capacity of the bonded or laminated joint is increased.

In case of bonding dissimilar materials the thicknesses should be chosen taken into account the differences in E -moduli.

When loading bonded joints in tension, the degree of deformation of the adjacent components play also an important role. When a force perpendicular to the main structure is working on an L -profile having a large corner radius, it will deform considerably under this load due to bending in the corner. The resulting high stress peak in the gluelayer will lead to jointfailure at a very low average tensile stress (figure 13).

When a very stiff L -profile is bonded in the same way and loaded, the tensile stresses in the bond will be distributed more equally and failure will be reached at a much higher average stress. In a similar way the local stiffness of \square -profiles influence the loadcarrying capacity in tension of the bonded flange joints.

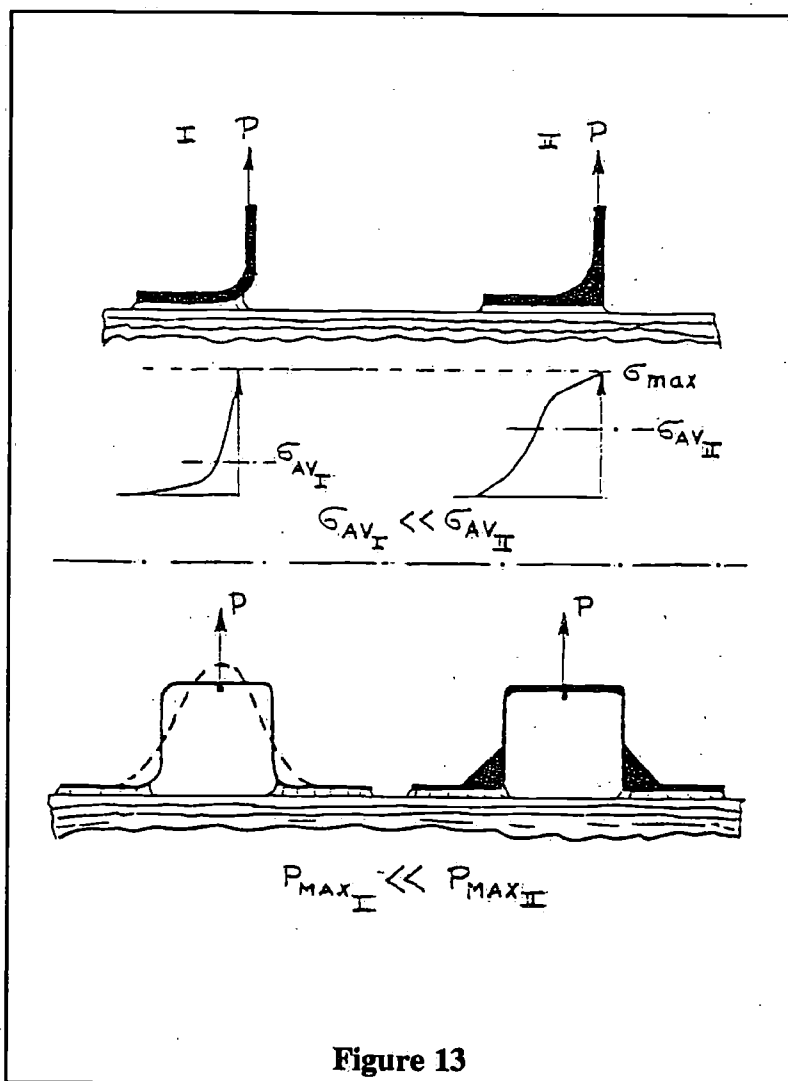


Figure 13

8 Conclusion

In this lecture some observations were made concerning the problems with joining components of yachts, made out off F.R.P.-material.

When the designer takes into account the typical strength- and stiffness properties of the F.R.P.-material family and their relation to the type of loading, the correct choice of the joining means as well as the adaptation of the thicknesses of the adjacent components, he will be able to design good bonds and by doing so a *good ship*.

"The influence of wedges on the performance of planing hulls"

by A. J. Cole and A. Millward

Abstract

The paper describes a series of experiments which investigate the effects of fixed trailing edge wedges on the resistance characteristics of a planing hull. The hull design used was the DTMB Series 62 Revised Parent Model No. 4667-1. Two series of results are presented, the effect of a single wedge under varying hull loading conditions, and the effects of different wedges under one of these loading conditions.

Whether the wedges increased or decreased resistance was seen to be dependent on the loading conditions, the shape and size of the wedge itself, and the speed of the craft. It was found that a wedge became more effective in reducing the resistance as the displacement was increased, and also as the longitudinal centre of gravity of the craft moved aft. Under a given loading condition, there was an optimum for both the length and angle of the wedge, above and below which either its advantageous effect decreased, or its detrimental effect increased.

Introduction

It was Froude who first resolved the resistance of a ship into components as a basis for model testing. He divided the total into the frictional resistance, due to the shear forces at the hull surface, and the residual resistance, due to all the remaining forces acting on the craft. This division remains a useful basis from which to consider the minimisation of the resistance of a planing hull. Figure 1 (taken from ref. 1) shows the total, frictional, and residual resistances for a planing craft at a fixed speed, with a varying angle of trim. It can be seen that to reduce the residual resistance, the craft should be run at the flattest angle that will afford the necessary lift. On the other hand, to reduce frictional resistance it should be run at the steepest angle that will leave sufficient surface for the lift. The most suitable compromise will therefore depend on the relative importance of the two resistance components, which will be a function of, among other things, the speed of the craft. This suggests that it may be advantageous to be able to alter the trim of a craft at its cruising speed from its normal attitude. The first mention of any form of conscious trim control seems to appear in ref. 2. During the last war, German E-boats were fitted with twin auxiliary rudders, level with, and on either side of the propellers. As the boat gained speed, these were each turned outward at an angle of 10 or 15 degrees which had the effect of reducing the resistance appreciably. The author of ref. 2 suggests that their purpose was to delay squatting by the stern, thus reducing the wavemaking resistance. In the written discussion following ref. 3, Du Cane mentions a boat competing in the 1966 Rouen 24 hour race which had a moveable transom flap to adjust her trim. In the same discussion, Clement suggests a pair of independently adjustable transom flaps to correct both trim and undesirable heel angle.

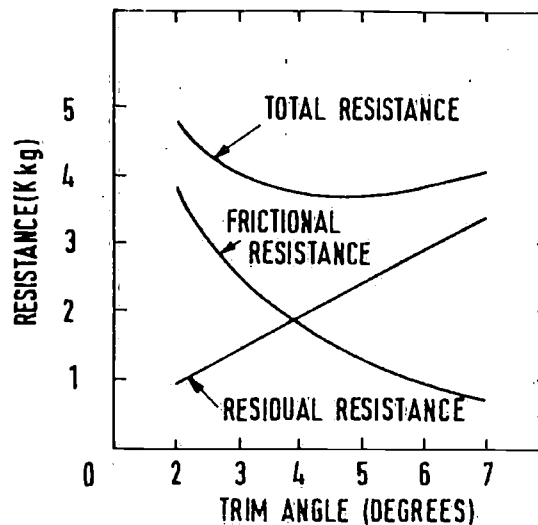


Figure 1. Resistance characteristics of a planing boat; 18.9 m. long weighing 27.200 kg., travelling at 40 knots (taken from ref. [1])

Since these first stirrings, stern flaps have been optimised for individual boats, but no basic investigation of their properties appears to have been carried out. Both stern flaps and trailing edge wedges have been tested on planing craft in the towing tank at the University of Southampton, but this again on an individual optimisation basis for commercial use. The aim of the present work was to investigate the value of adding fixed wedges to a standard planing hull, under a systematic series of conditions.

Wedges were chosen rather than adjustable flaps as they are a simpler and more basic design feature. If a wedge can be found to improve the performance of a given hull, then once it is fitted no more control is necessary. With adjustable flaps another variable (i.e. the inclination of the flap) is introduced into the control of the boat, making operation more complex.

Notation

- A_P = projected planing bottom area (m^2)
- B_{PA} = mean breadth over chines A_P/L_P (m)
- B_{PT} = breadth over chines at transom (m)
- B_{PX} = maximum breadth over chines (m)
- F_{∇} = Froude Number based on the cube root of the volume of water displaced at rest ($F_{\nabla} = V / \sqrt[3]{g(\nabla^{1/3})}$)
- L_P = projected chine length (m)
- LCG = Longitudinal Centre of Gravity
- R = total resistance (kg)
- R_e = Reynolds Number, based on arithmetic mean of wetted keel and chine lengths
- S = wetted surface area, including area of sides wetted at low speeds but excluding area wetted by spray (m^2)

- V = velocity of water in working section of channel (m/s)
 W = displacement at rest (kg)
 h = vertical displacement of centre of gravity from rest position (mm); positive values signify upward displacement
 l = length of wedge in direction parallel to keel (mm)
 ∇ = volume of water displaced at rest (m^3)
 α = trim angle (degrees)
 β = angle between planing surface of wedge and planing surface of hull, measured in direction parallel to keel (degrees)
 λ = length of wedge as a fraction of projected chine length ($\lambda = l/L_p$)

The model

The DTMB Series 62 Revised Parent (ref. 4) design was chosen for the hull and a glass reinforced plastic (GRP) model was made one half* of the size of the original DTMB model, i.e. 1.22 m (4.00 ft.) projected chine length**. The body plan and form characteristics of the model are shown in Figure 2. The reasons for choosing this particular design of hull were twofold. Firstly, it is the basic design for the most comprehensive set of resistance tests ever carried out on planing craft (ref. 4), and so the hull is becoming accepted as a standard form. Secondly, time limits the scope of the present work, both in the number of variables which can be considered, and in the range over which those chosen can be observed. Should it be possible to extend the tests sometime in the future, to investigate for instance the effect of changing the length/beam ratio of the hull on the usefulness of the wedges, the DTMB series would provide an ideal basis for such work.

For a given hull size and design, the two variable factors which affect the planing characteristics are the displacement (W) and the longitudinal position of the centre of gravity (LCG). In this paper these two variables are defined using the parameters described by Clement and Blount (ref. 4). The displacement is expressed as the dimensionless ratio $A_p/\nabla^{2/3}$ where A_p is the projected planing bottom area and ∇ the volume of water displaced at rest. The longitudinal centre of gravity position is defined as the distance of the LCG from the centroid of A_p , expressed as a percentage of the projected chine length L_p . Both these parameters were varied in the tests by moving ballast weights in the hull.

The larger wedges were made from wood and the smaller ones of GRP. They were attached to the hull using waterproof adhesive. As may be seen in Figure 3, when the hull has deadrise there are actually two wedges, one on each planing surface, joining at the keel. The wedge may be adequately described using two parameters; its length, measured in a direction parallel to the keel of the hull and conveniently expressed as a fraction of the projected chine length (λ), and the angle (β) which the surface of the wedge makes with the bottom planing surface

* This was the largest model which could be used in the channel before width effects became appreciable.

** The authors express their gratitude to Commander Dalla Mura of the U.S. Office of Naval Research for help in obtaining the lines of the model.

of the hull, again measured in a direction parallel to the keel. The leading edge of the wedge is perpendicular to the keel, and the trailing edge and sides made flush with the transom and upper hull surfaces respectively.

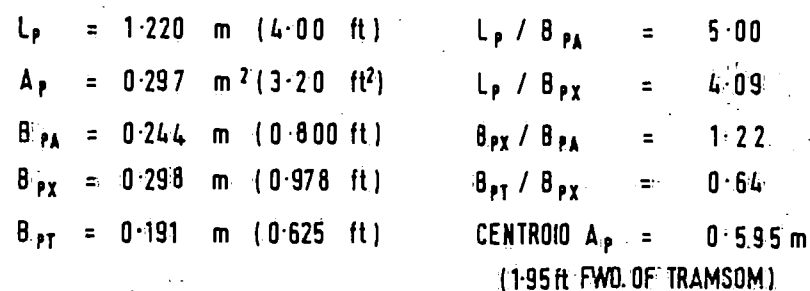
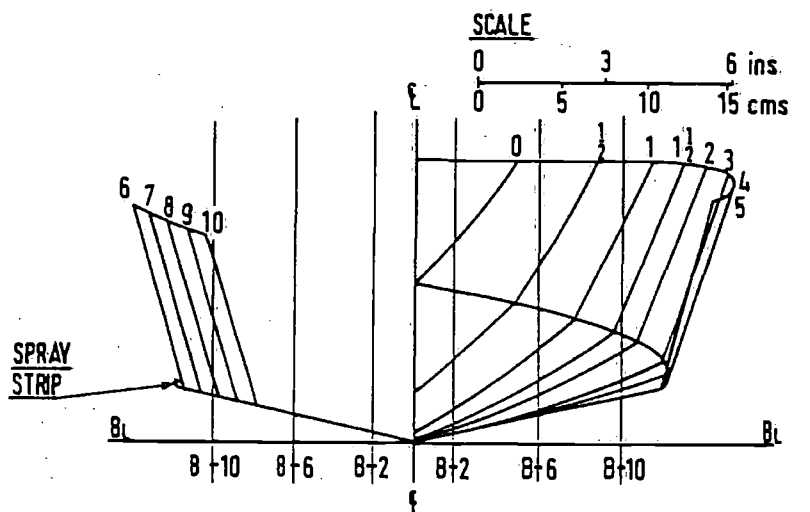


Figure 2. Body plan and form characteristics of DTMB Series 62 Parent Model No. 4667-1

The recirculating water channel

The test programme was carried out in the Recirculating Water Channel ("Flume") at the University of Liverpool, and since the use of such a facility as opposed to a towing tank is unusual in quantitative ship model testing, a brief description seems appropriate. A more detailed account of the design and operation of the flume is given by Preston (ref. 5).

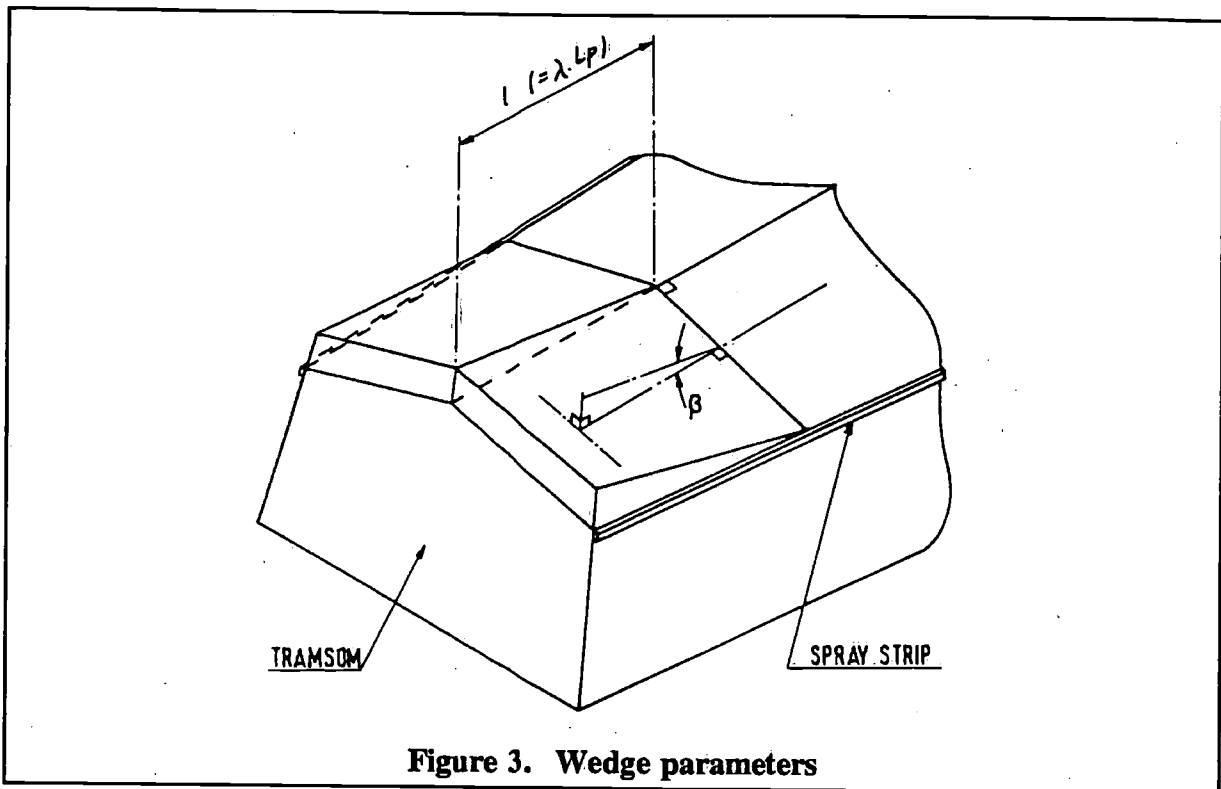


Figure 3. Wedge parameters

The channel (Figure 4) has a capacity of nearly 90.800 litres (20.000 gallons) of water, circulated by a 100 h.p. motor driving an axial flow impeller. On leaving the impeller, the water passes through a long, circular section diffuser, after which the cross-section of the channel becomes rectangular. Two sets of vanes and a honey-comb minimise the swirl, and the flow is accelerated through a contraction into the working section. This has a moveable false floor, which is adjustable in height and inclination to give a flat, level free surface at the required operating speed. After the working section, the topmost layer of water is separated from the flow by the first adjustable flap, or "splitter plate". This narrow layer, travelling at a super-critical speed, contains nearly all the air bubbles caused by the presence of a model in the working section. The water in the layer is slowed to sub-critical speed by a deepening after the splitter plate, and the slower movement of this portion of the flow allows the air time to escape to the surface before the water is re-introduced to the main flow at the second adjustable flap.

The flow velocity in the working section can be set and measured an accuracy of $\pm 1\%$, the maximum speed being in the region of 6.1 m/s (20 ft./s). Due to the adjustable floor in the working section, any speed in this range can be maintained without the presence of either standing waves or a hydraulic jump. If the floor is left fixed at its lowest position the critical speed is in the region of 2.7 m/s (9 ft./s).

Early work on the flume showed that the wake at the free surface, caused by the boundary layer on the upper surface of the contraction, was appreciable, the velocity defect being large enough to render any work on shallow draft surface craft useless, so to correct this, a jetbleed was introduced. Water is bled off from the lowest point of the system and pumped back into the main flow through a 1 mm wide slot, running the whole breadth of the channel, at the beginning of the working section (Figure 5). By adjusting the pump speed, a velocity profile can be obtained which deviates less than $\pm \frac{1}{2}\%$ from stream velocity to within 1 cm of the free surface.

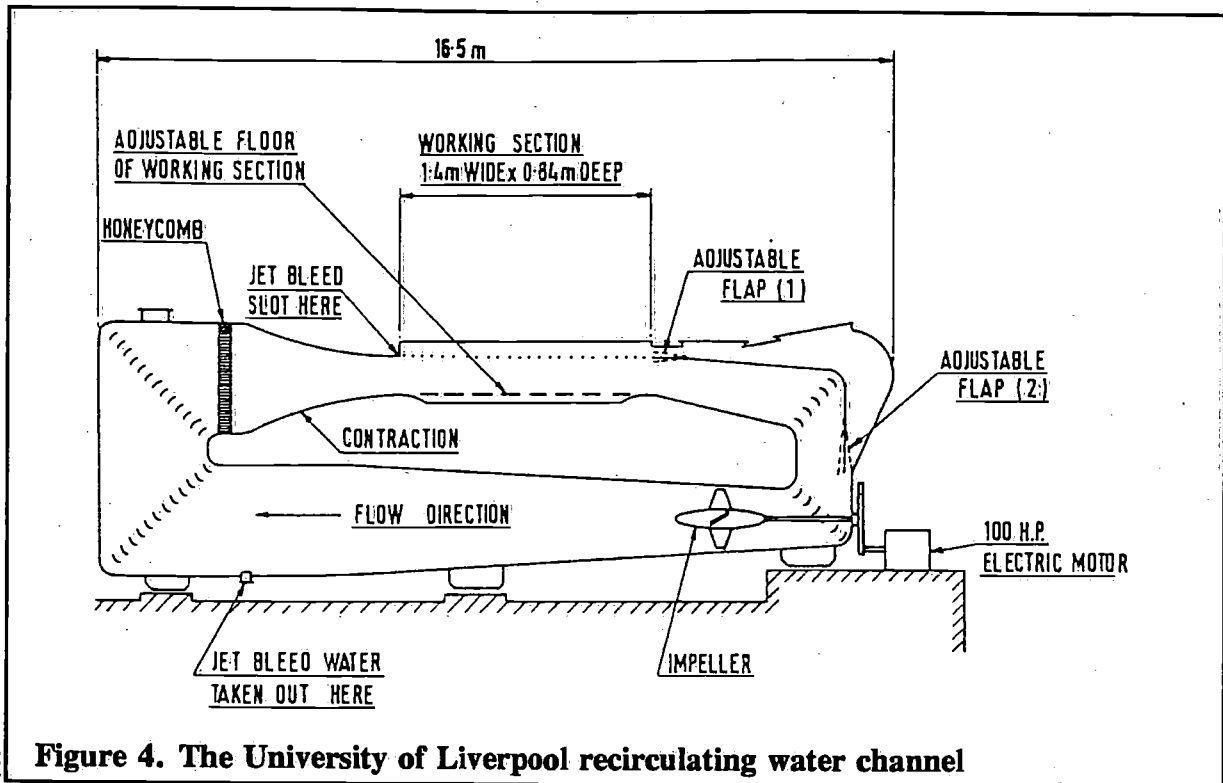


Figure 4. The University of Liverpool recirculating water channel

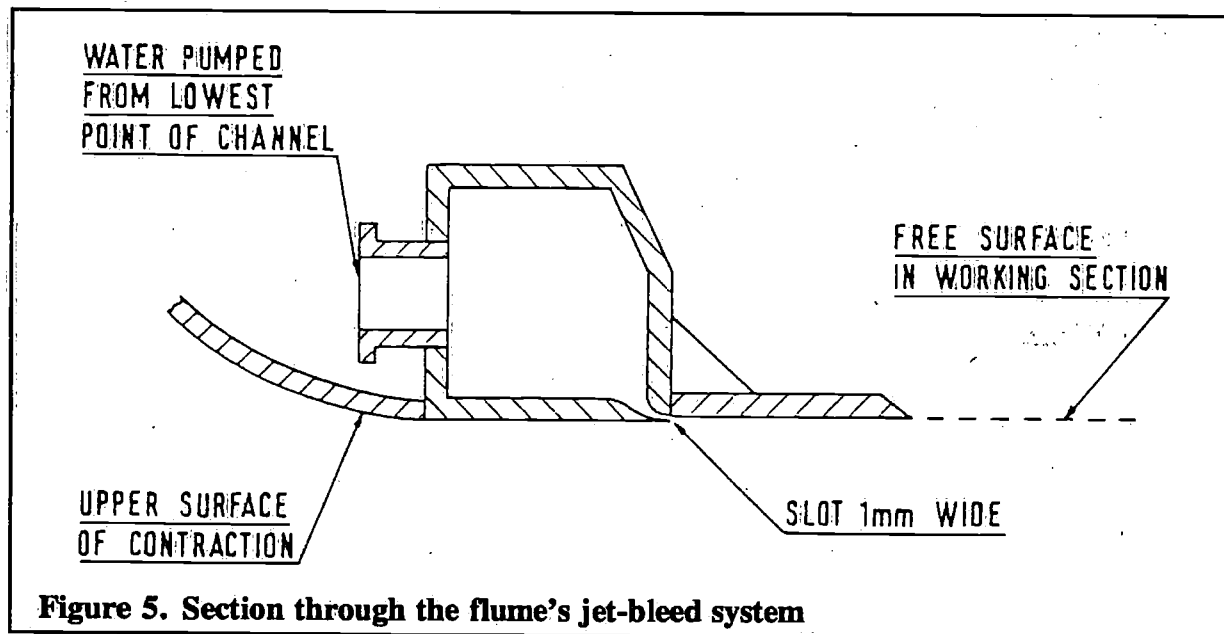


Figure 5. Section through the flume's jet-bleed system

Experimental arrangements and test programme

The model was mounted over the flume on a balance which allowed it to pitch and heave, while measuring its resistance and vertical displacement from rest. An indicator mounted at the bow recorded the trim as well as providing a restraint against a sudden unstable yawing force (see Figure 6). Scales along the keel, chine, and transom of the model allowed the respective wetted lengths and heights to be measured. Earlier work has shown that no turbulence stimulation is necessary when working with planing models in the flume at speeds upwards of 1.2 m/s (4 ft./s).

Preliminary tests showed that under most conditions the maximum possible water speed was in the region of 4.3 m/s (14 ft./s). Above this speed an excessive amount of water from the

wake of the model was thrown clear of the working section into the laboratory. Apart from the more obvious disadvantages, this has the effect of reducing the total volume of water in the flume, thus disturbing the free surface. This maximum speed typifies a military-style planing craft travelling at about 21 m/s (35 knots), and while far from ideal, was considered an acceptable maximum. Moreover it was subsequently found that the pattern of behaviour produced by most wedges was adequately described by the time the model reached this maximum speed. Work is now in hand on modification of the flume to permit higher maximum speeds to be used on this type of work in the future.

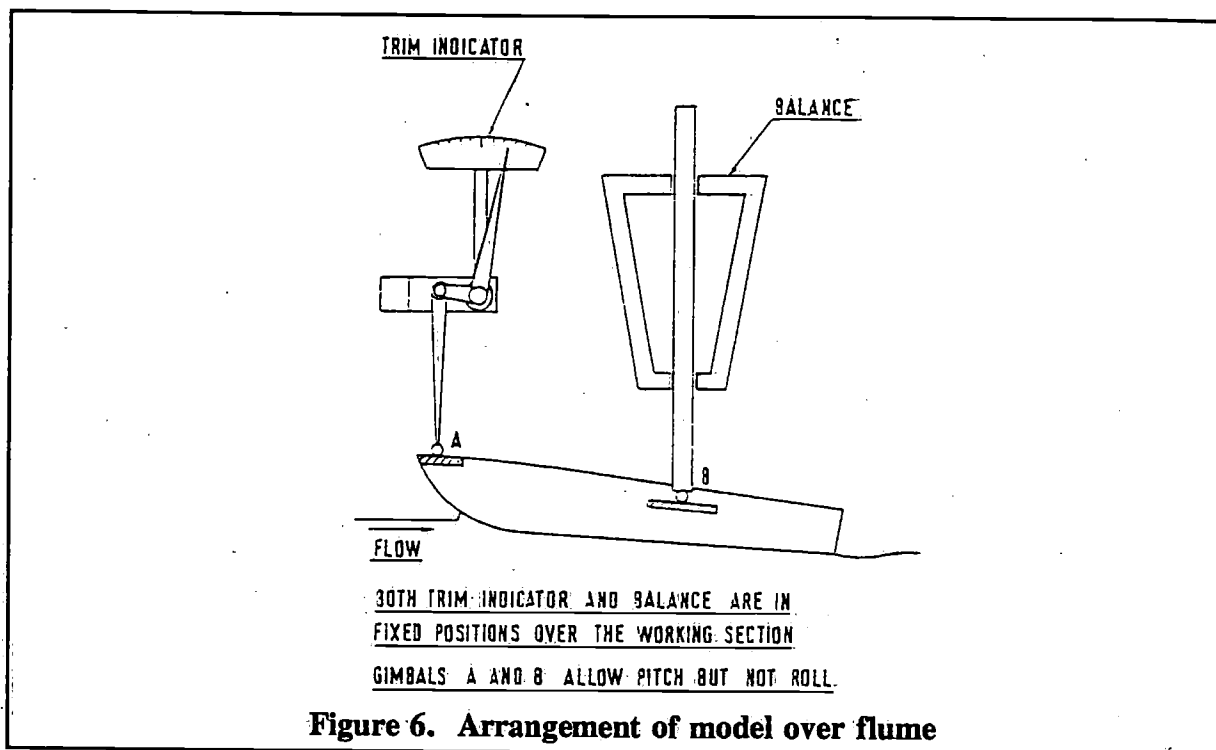


Figure 6. Arrangement of model over flume

The test programme was in two parts. Firstly, using a single small wedge, $A_p/V^{3/2}$ and the LCG position were varied, to discover the broad limits of the effectiveness of wedges in general. Secondly, at fixed values of $A_p/V^{3/2}$ and LCG position, the length and angle of the wedge was varied to see if an optimum wedge shape could be found. The wedges used were as follows:

Wedge Length Chine Length	Wedge Angle
λ	β°
0.05	2, 5 and 10
0.10	2, 5 and 10
0.15	2, 5 and 10

The smallest wedge (i.e. $\lambda = 0.5$, $\beta = 2^\circ$) only was used of the test programme.

Accuracy

The quantities measured are believed to be accurate within the limits shown below. The first column indicates the division to which the measuring device may be read, and the second, the overall accuracy of the readings when fluctuations in the flow are considered.

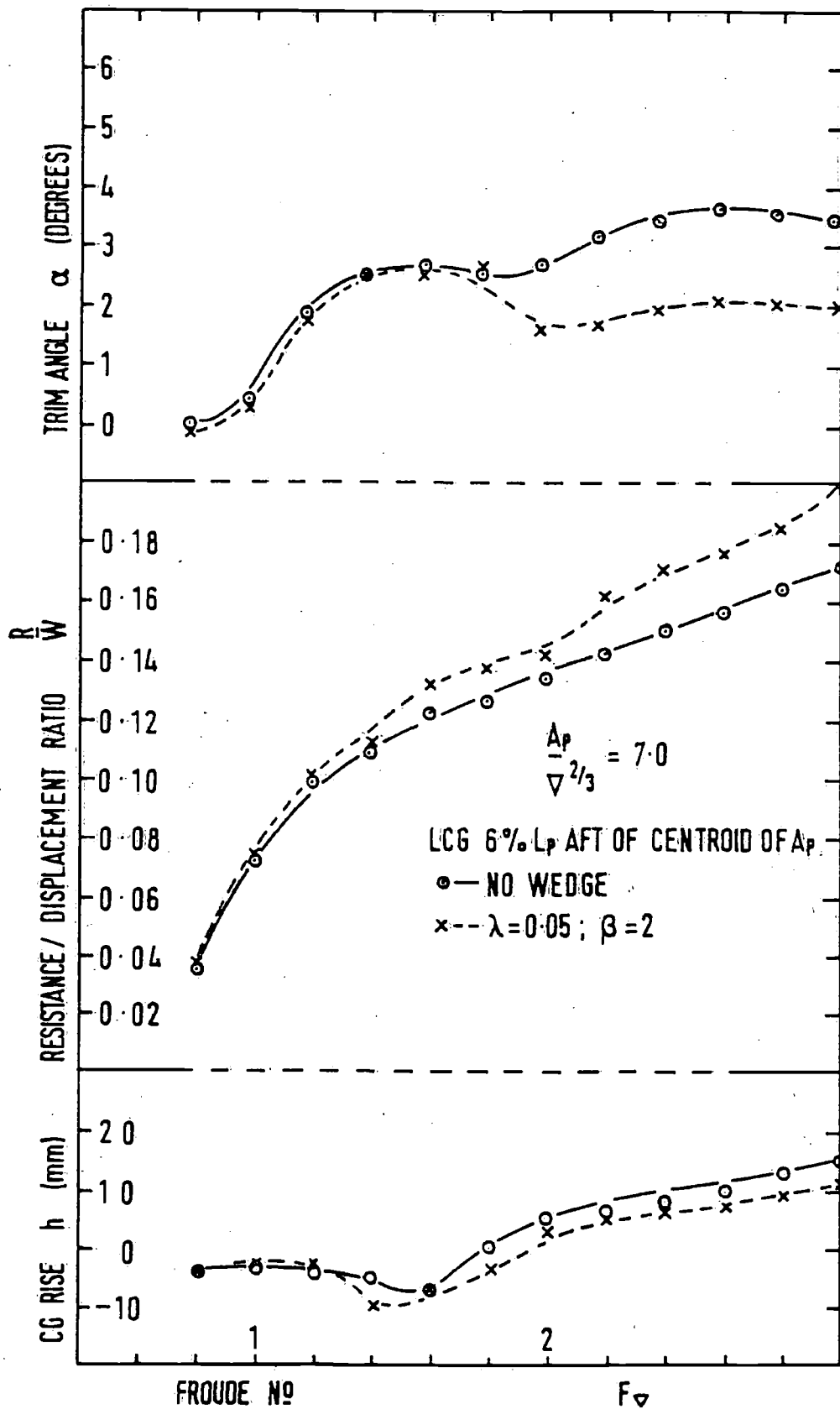


Figure 7. Effects of a single small wedge on the planing characteristics of the model under a range of loading conditions

Resistance (kg)	0.001	± 0.005
Trim (deg)	0.01	± 0.05
Height Change of <i>C</i> of <i>G</i> (mm)	0.2	± 0.5
Wetted Lengths of Keel and Chines (mm)	10	± 10
Wetted Height of Side at Transom (mm)	1	± 2

As mentioned before, the speed of the flow can be set to ± 1%. The speed control mechanism is more sensitive than this, but the overall accuracy is limited by its pitot-tube calibration.

Discussion of results

The results presented apply directly to the model used, but the wetted surface area and Reynolds Number under each set of operating conditions have been calculated and included in the accompanying tables. Thus the figures may be scaled to any size of model or boat if required. The representative length used in calculating the Reynolds Number is the arithmetic mean of the wetted keel and wetted chine lengths.

First under consideration is the effect of a single wedge on the planing characteristics of the model under varying loading conditions (figures 7 - 12). Figure 7 shows the DTMB standard condition for planing craft (discussed in ref. 6). This is included mainly for incidental interest but does show that the wedge is ineffective under these loading conditions over the whole speed range.

The effect of the wedge on resistance, trim, and vertical displacement of the centre of gravity when $A_p/\nabla^{2/3}$ is held constant can be seen in Figures 8 - 10. These show a heavy displacement condition. At the furthest forward *LCG* position (figure 8) the addition of the wedge actually increases the resistance, but as the *LCG* moves aft the wedge becomes more useful both increasing the amount of drag reduction and increasing the range over which it is effective. The amount which trim is reduced is very nearly constant for all *LCG* positions. The wedge appears to decrease the slope of the h/F_{∇} curve (once the initial period of negative *h* has been passed), an effect which becomes more noticeable as the *LCG* is moved forward. In general, the upwards vertical displacement, and therefore the dynamic lift, is decreased by the presence of the wedge.

With the *LCG* position held constant (figures 10 - 12), the wedge becomes more effective as displacement increases (i.e. as $A_p/\nabla^{2/3}$ diminishes). Again both the reduction in resistance and the speed range over which it takes place are improved. The change in trim seems independent of the displacement. The slope of the h/F_{∇} curve and the dynamic lift are once more both decreased by the presence of the wedge, the effect becoming more marked as the displacement decreases. From Figures 7 - 12 overall it seems that a wedge has a better chance of reducing the resistance of the hull if its presence has but a small effect on the dynamic lift.

It is interesting to note that the resistance curve of Figure 10 with the wedge attached approaches closely that of Figure 8 with no wedge present, suggesting that the wedge is cancelling the detrimental effect of moving the *LCG* rearwards. Similarly the resistance curve of Figure 11 with the wedge attached approaches that of Figure 12 with no wedge present, particularly in the upper half of the speed range, showing that in this case the wedge is neutralising the detrimental effect that increasing the displacement has on the resistance to displacement ratio.

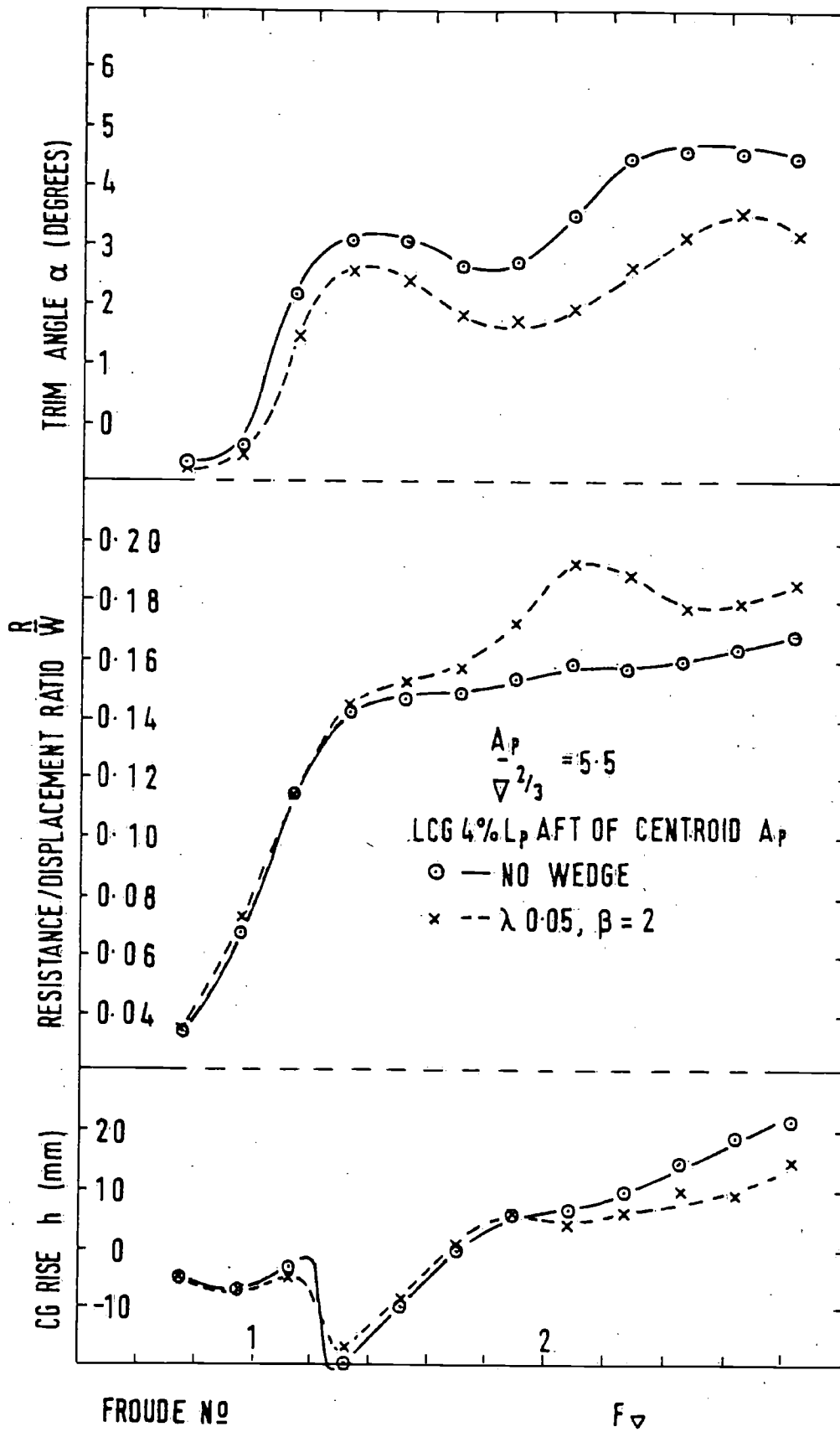


Figure 8. Effects of a single small wedge on the planing characteristics of the model under a range of loading conditions

The effect of using different wedges under a fixed loading condition can be seen in Figures 13 - 15. Each figure presents wedges of the same length but different angles, Figure 13 showing the shortest set of wedges and Figure 15 the longest. In all cases wedge length is expressed as a fraction of the projected chine length. It will be seen that the curves showing the performance of the 10° wedges terminate before the maximum testing speed is reached. This is because these wedges thrust the bow of the hull so far into the water that an unacceptable amount of spray was produced. This was thrown both into the hull and out of the channel, making further increases in speed impracticable.

For all wedge lengths, the resistance curves for the 2 and 5° wedges are very close together, suggesting that there is an optimum wedge angle for these conditions, above and below which the wedge becomes less effective. For all lengths the 10° wedge greatly increased the resistance. Varying the angle of the wedge seems to have a far greater effect than varying its length, both on trim and lift. The only noticeable effect wedge length has on either of these quantities was that the shorter wedges decreased the lift rather more than the longer ones in the upper third of the speed range. Resistance is however, only reduced by the shortest wedges, suggesting that the optimum wedge length is in the region $0 < \lambda < 0.10$.

Overall, it can be seen that wedges do more than merely control the trim; the dynamic lift is also affected. It was more often reduced than increased, especially when the overall resistance was reduced, showing that for this hull at least the suggestion that the wedges help to reduce the drag by increasing the lift is unfounded. Previous work (as yet unpublished) on rectangular section hulls has however shown that this is not always the case. The overall effect of a wedge is undoubtedly complex.

Conclusions

It can be seen from the results that the addition of wedges to the hull proved the most useful when the loading conditions tended towards the abnormal. The DTMB series 62 models were particularly efficient hull forms, as observed by the authors of reference 4, who also collected together data from several other designs - "At low speeds (below a F_{∇} of 1.5) the hull forms of the series have slightly more drag than the other designs. At values of F_{∇} of 2.0 and 2.5 the forms of the series have less drag than most of the other designs, and at values of F_{∇} of 3.0 and above, the hull forms of the series have less drag than any of the other designs". It would seem, therefore, that the addition of a wedge is unlikely to improve the performance of a well designed, correctly loaded hull. On the other hand, the performance of a craft which due to uncontrollable circumstances must be unfavourably loaded, or used in a speed range for which it was not designed, can be improved by a carefully chosen wedge. Such conditions may be brought about by abnormal power requirements, or the conversion of a craft from one use to a completely different one. Having decided that a wedge would be beneficial, it is then of more importance to select the optimum angle than the optimum length of wedge.

Even when limiting the work to one series of hull forms, it will be seen that the present tests have only scratched the surface of the investigation of the effects of trailing edge wedges on planing craft. The programme needs to be expanded in many directions before a true insight into the mechanics involved may be obtained. Two investigations which would be immediately useful are those of the effect of different sizes of wedge on loading conditions other than the one used for the present work, and the effect of the wedges on models of differing length/beam ratios. The latter could easily be carried out by using again the DTMB Series 62 hulls as the basic designs.

References

- [1] Murray, A.B., "The hydrodynamics of planing hulls", SNAME Trans., Vol.58 (1950).
- [2] DU Cane, P., "Small sea-going high speed craft" from "Shipbuilding and Ships", Worshipful Company of Shipwrights (1947).
- [3] Hadler, J.B., "The prediction of power performance on planing craft", SNAME Transactions, Volume 74 (1966).
- [4] Clement, E.P., and Blount, D.L., "Resistance tests on a systematic series of planing hull forms", SNAME Transactions, Volume 71 (1963).
- [5] Preston, J.H., "The design of high speed, free surface water channels", NATO Advanced Study Institute on "Surface Hydrodynamics", (1966).
- [6] Clement, E.P., "How to use the SNAME Small Craft Data Sheets for Design and for Resistance Prediction", SNAME Technical and Research Bulletin No. 1-23.

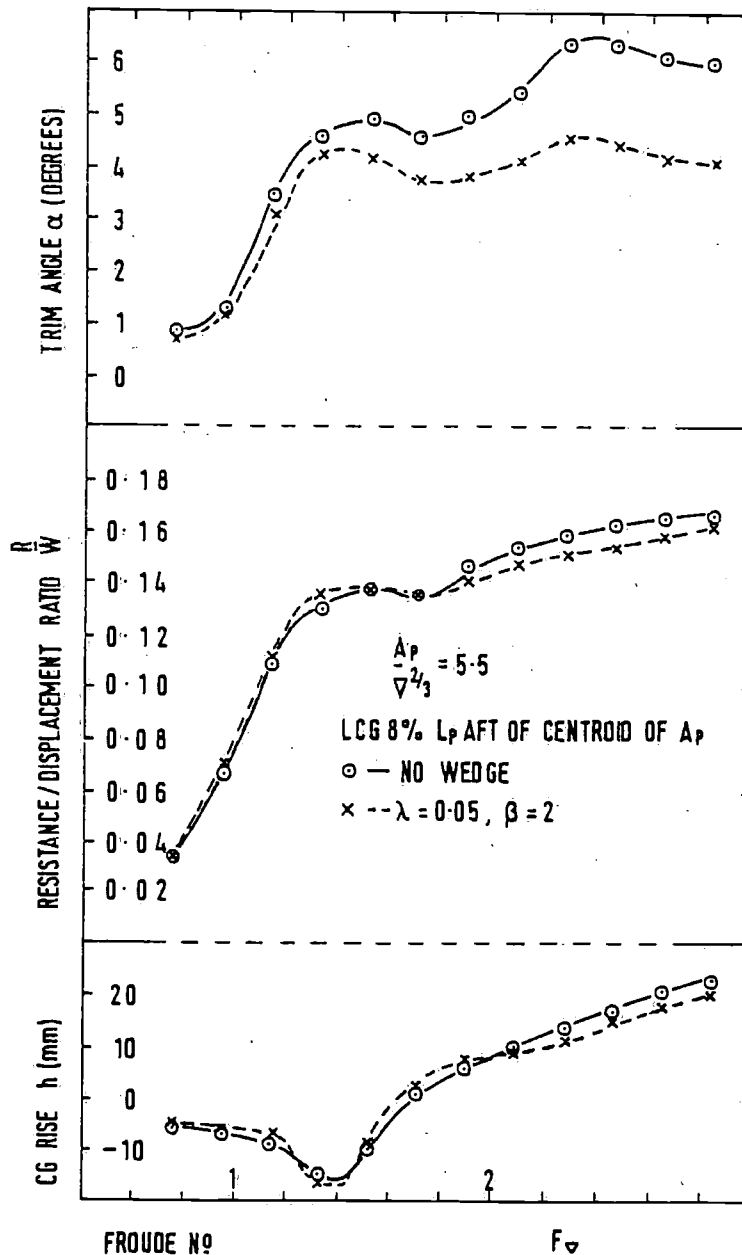


Figure 9. Effects of a single small wedge on the planing characteristics of the model under a range of loading conditions

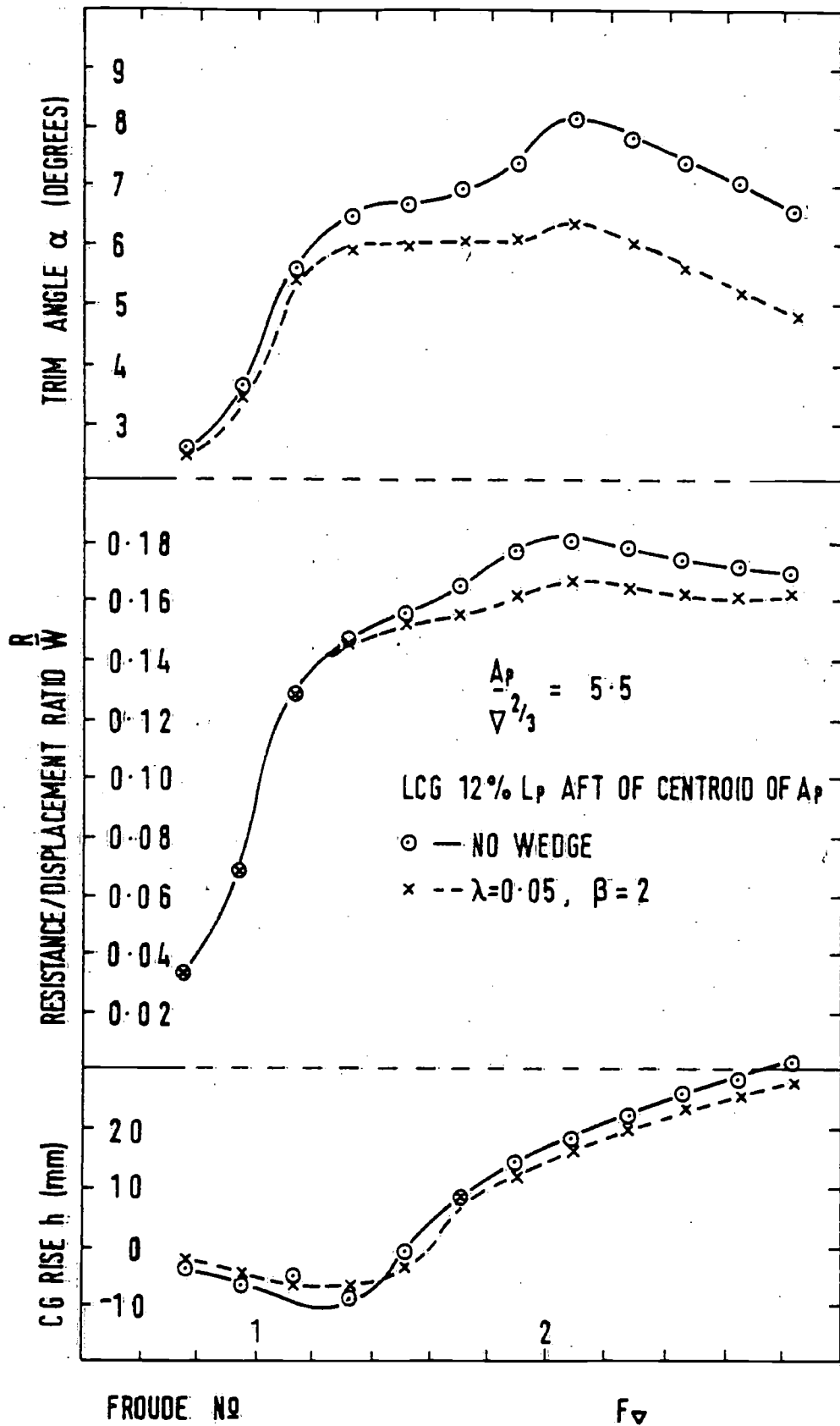


Figure 10. Effects of a single small wedge on the planing characteristics of the model under a range of loading conditions

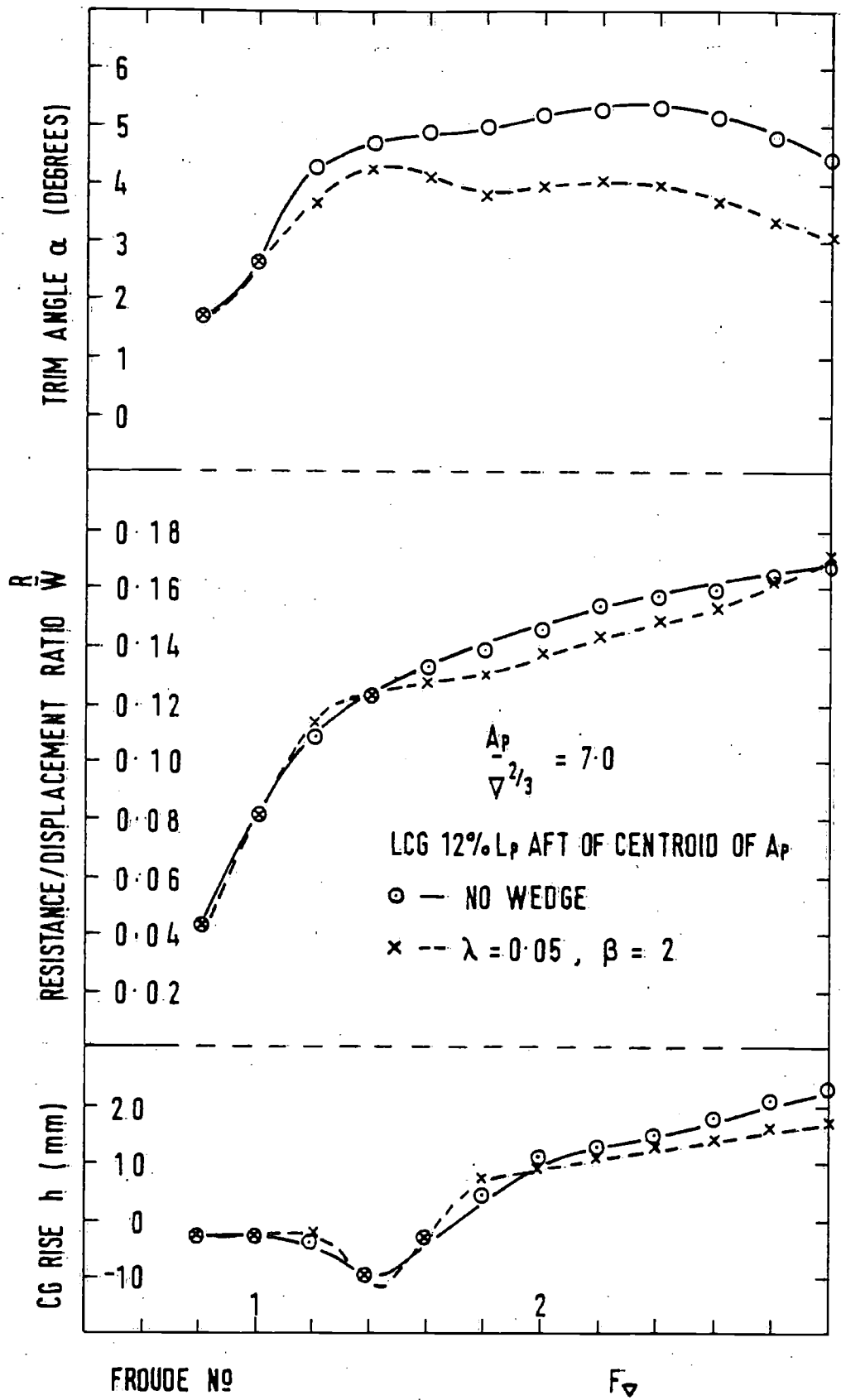


Figure 11. Effects of a single small wedge on the planing characteristics of the model under a range of loading conditions

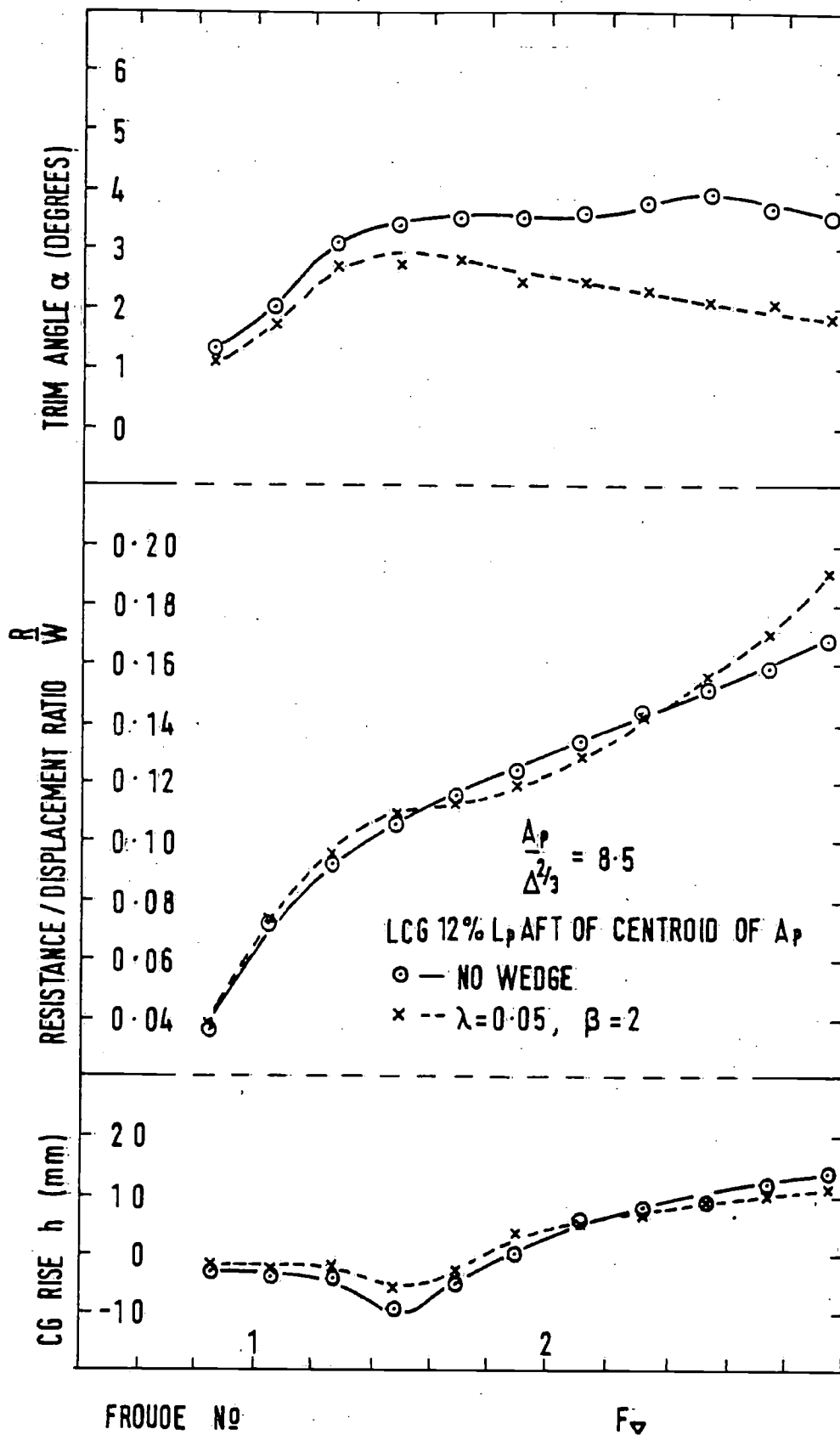


Figure 12. Effects of a single small wedge on the planing characteristics of the model under a range of loading conditions

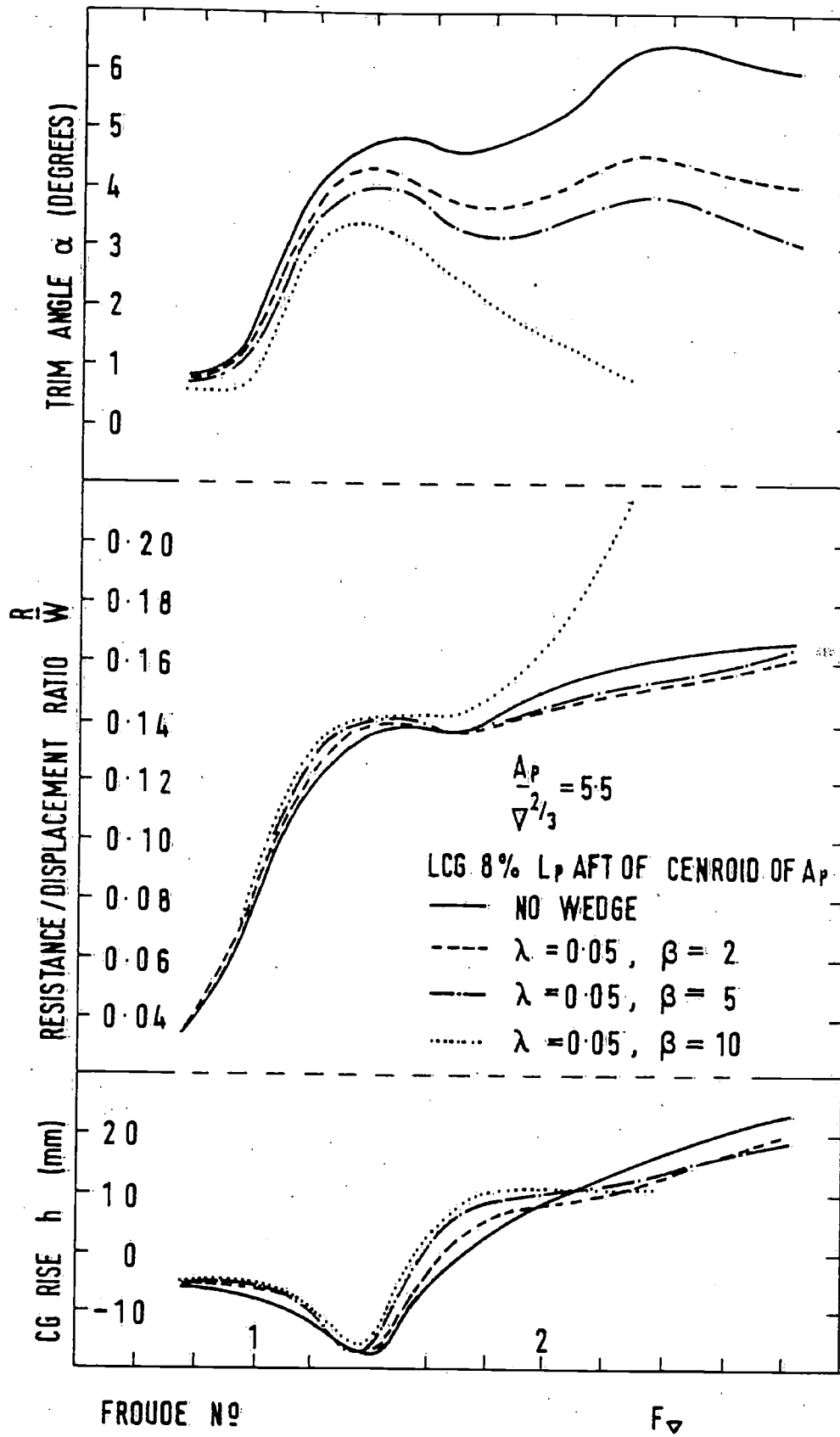


Figure 13. Effects of various wedge shapes on the planing characteristics of the model under constant loading conditions

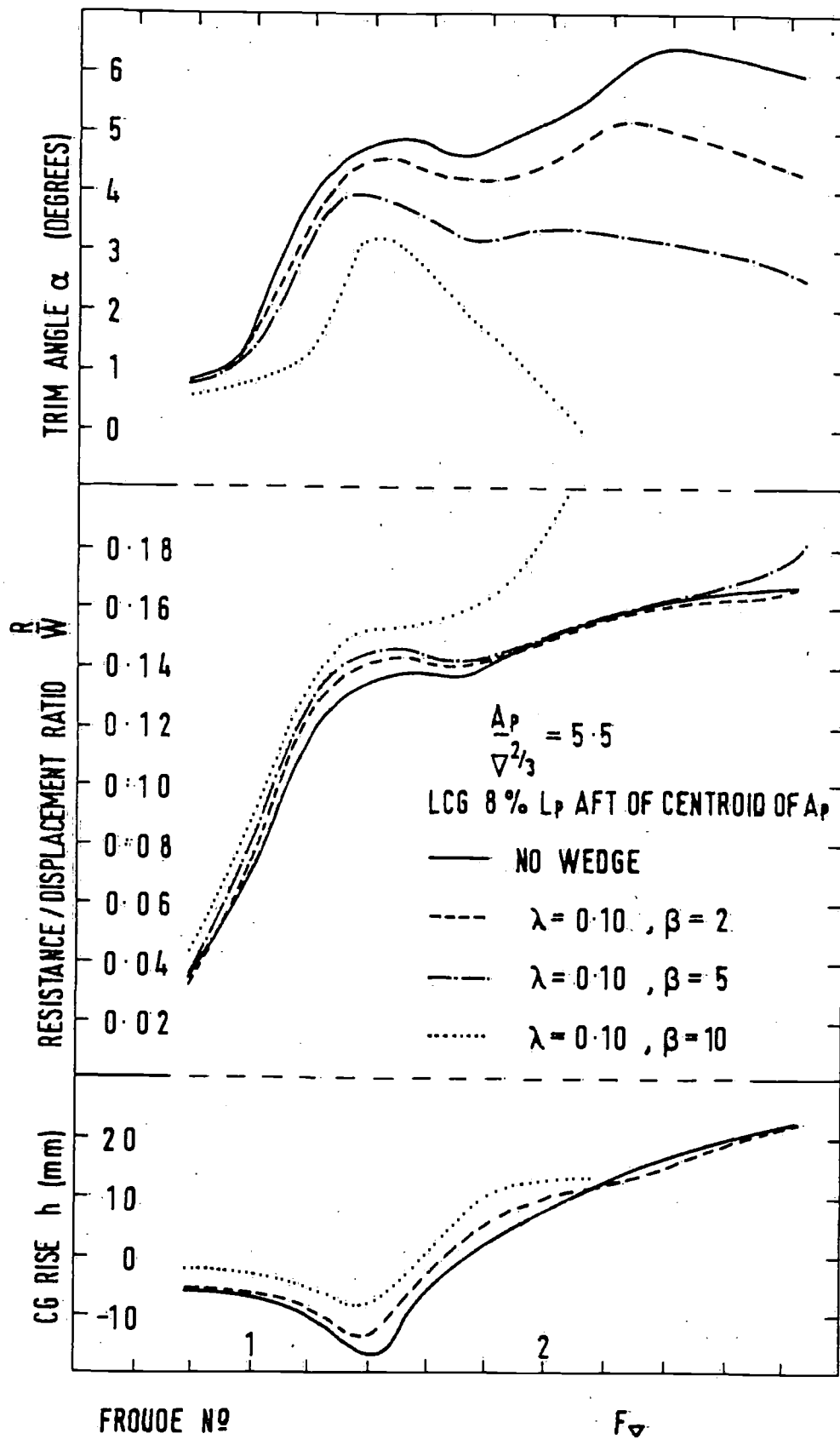


Figure 14. Effects of various wedge shapes on the planing characteristics of the model under constant loading conditions

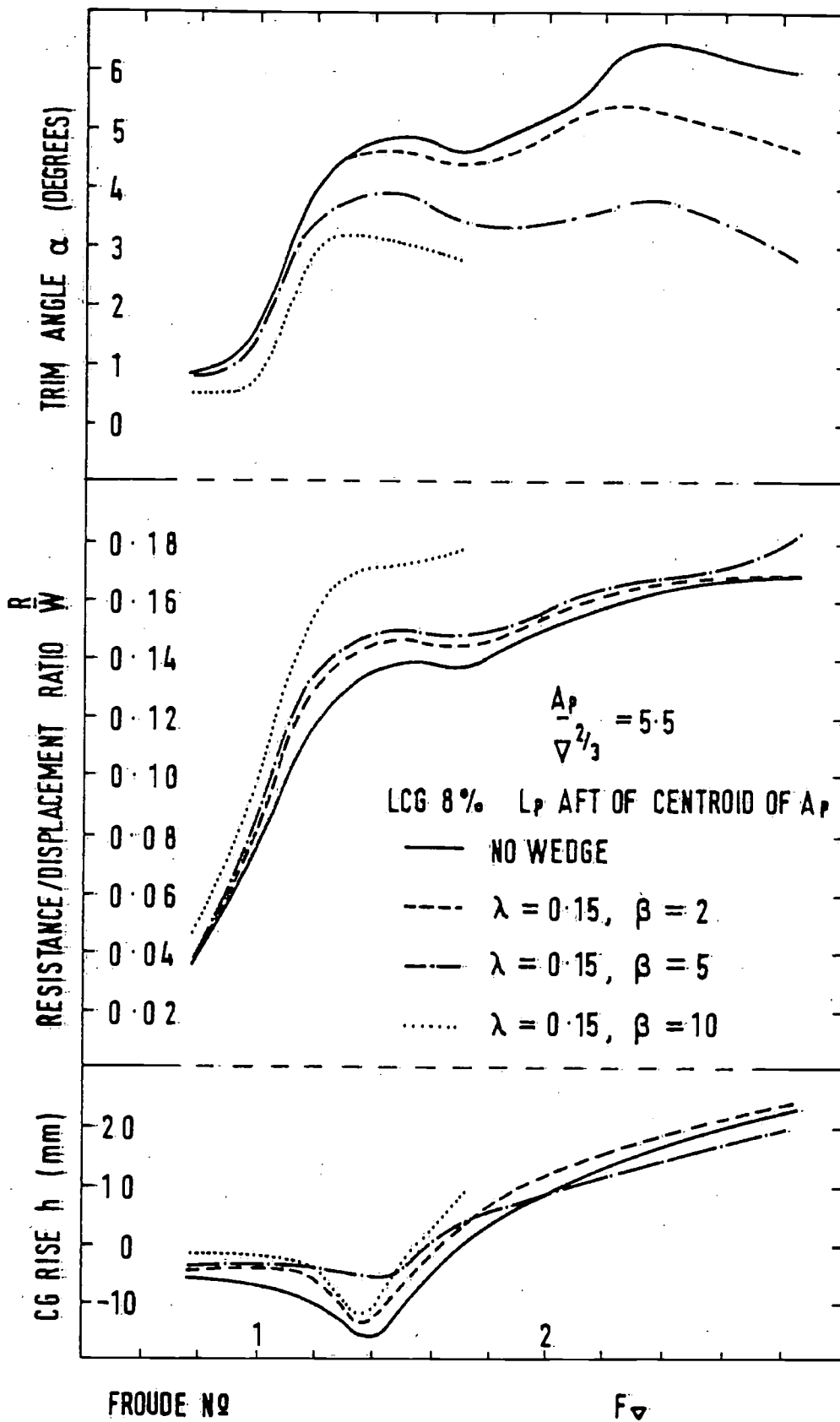


Figure 15. Effects of various wedge shapes on the planing characteristics of the model under constant loading conditions

TEST CONDITIONS

Test no.	Model weight (kg)	$A_p - \nabla^*$	Static trim (deg)	LCG Fwd of station 10 (mm)	LCG aft of centroid of A_p , % L_p	water temp (deg C)	Wedge angle β (deg)	Wedge Length Chine Length λ
1	8.75	7.0	0.10	522	6	21.0	0	0
2	8.75	7.0	0.10	522	6	21.0	2	0.05
3	8.75	7.0	0.10	522	6	21.1	2	0.15
4	6.52	8.5	1.00	449	12	20.1	0	0
5	6.52	8.5	1.00	449	12	20.1	2	0.05
6	8.75	7.0	1.50	449	12	20.1	0	0
7	8.75	7.0	1.50	449	12	20.1	2	0.05
8	12.53	5.5	-0.32	546	4	20.4	0	0
9	12.53	5.5	-0.32	546	4	20.4	2	0.05
10	12.53	5.5	0.85	498	8	20.9	0	0
11	12.53	5.5	0.85	498	8	20.9	2	0.05
12	12.53	5.5	2.16	449	12	20.9	0	0
13	12.53	5.5	2.16	449	12	20.9	2	0.05
14	12.53	5.5	0.85	498	8	20.9	5	0.05
15	12.53	5.5	0.85	498	8	20.9	10	0.05
16	12.53	5.5	0.85	498	8	20.6	2	0.10
17	12.53	5.5	0.85	498	8	20.6	2	0.10
18	12.53	5.5	0.85	498	8	20.7	5	0.10
19	12.53	5.5	0.85	498	8	20.6	2	0.15
20	12.53	5.5	0.85	498	8	20.8	5	0.15
21	12.53	5.5	0.85	498	8	20.5	10	0.15

TEST No. 1

V (m/s)	V (knots)	R (kg)	Wetted length of keel (cm)	Wetted length of chine (cm)	Rex 10^{-6}	S (m ²)	Trim (deg)	CG rise (mm)	F_v
0	0						0.10		0
1.13	2.20	0.31	120	110	1.318	0.320	0.02	-4	0.80
1.42	2.75	0.63	120	110	1.651	0.324	0.44	-3	1.00
1.70	3.30	0.85	118	105	1.925	0.320	1.93	-4	1.20
1.99	3.85	0.94	116	95	2.129	0.302	2.55	-5	1.40
2.27	4.40	1.06	115	95	2.406	0.299	2.72	-7	1.60
2.56	4.95	1.10	114	91	2.633	0.296	2.55	0	1.80
2.84	5.50	1.16	113	87	2.871	0.292	2.72	5	2.00
3.12	6.05	1.24	111	82	3.028	0.279	3.23	6	2.20
3.41	6.60	1.31	107	76	3.134	0.255	3.48	8	2.40
3.70	7.15	1.36	105	73	3.322	0.238	3.65	10	2.60
3.98	7.70	1.43	103	70	3.459	0.229	3.57	13	2.80
4.26	8.25	1.50	101	67	3.617	0.221	3.48	15	3.00
4.55	8.80	1.57	100	64	3.768	0.215	3.31	17	3.20

TEST No. 2

V (m/s)	V (knots)	R (kg)	Wetted length of keel (cm)	Wetted length of chine (cm)	Rex 10 ⁻⁶	S (m ²)	Trim (deg)	CG rise (mm)	F _v
0	0						0.10		
1.13	2.20	0.33	120	110	1.318	0.319	-0.07	-3	0.80
1.42	2.75	0.64	120	110	1.651	0.324	0.27	-3	1.00
1.70	3.30	0.87	118	108	1.925	0.321	1.79	-3	1.20
1.99	3.85	0.98	116	100	2.169	0.307	2.55	-10	1.40
2.27	4.40	1.15	116	98	2.452	0.301	2.55	-7	1.60
2.55	4.95	1.20	116	96	2.736	0.304	2.72	-4	1.80
2.84	5.50	1.23	116	93	2.985	0.298	1.62	3	2.00
3.12	6.05	1.41	116	90	3.249	0.297	1.71	5	2.20
3.41	6.60	1.48	114	85	3.443	0.281	1.96	6	2.40
3.70	7.15	1.54	114	83	3.658	0.275	2.13	7	2.60
3.98	7.70	1.61	113	81	3.902	0.263	2.05	9	2.80
4.26	8.25	1.75	113	79	4.134	0.259	1.96	11	3.00

TEST No. 3

V (m/s)	V (knots)	R (kg)	Wetted length of keel (cm)	Wetted length of chine (cm)	Rex 10 ⁻⁶	S (m ²)	Trim (deg)	CG rise (mm)	F _v
0	0						0.10		0
1.13	2.20	0.34	120	110	1.321	0.320	0.02	-3	0.80
1.42	2.75	0.65	120	110	1.654	0.324	0.02	-3	1.00
1.70	3.30	0.86	118	105	1.912	0.319	1.87	-4	1.20
1.99	3.85	1.01	116	97	2.194	0.299	2.30	-3	1.40
2.27	4.40	1.13	115	95	2.412	0.298	2.64	-6	1.60
2.55	4.95	1.16	115	91	2.665	0.294	2.21	7	1.80
2.84	5.50	1.21	114	90	2.935	0.290	2.04	9	2.00
3.12	6.05	1.29	113	85	3.129	0.284	2.38	8	2.20
3.41	6.60	1.34	112	80	3.313	0.267	2.72	9	2.40
3.70	7.15	1.41	111	77	3.517	0.253	2.72	11	2.60
3.98	7.70	1.49	110	74	3.709	0.247	2.64	13	2.80
4.26	8.25	1.60	110	72	3.927	0.242	2.55	15	3.00

TEST No. 4

V (m/s)	V (knots)	R (kg)	Wetted length of keel (cm)	Wetted length of chine (cm)	Rex 10 ⁻⁶	S (m ²)	Trim (deg)	CG rise (mm)	F _v
0	0						1.00		0
1.13	2.20	0.24	116	60	0.990	0.242	1.34	-3	0.84
1.42	2.75	0.47	116	85	1.410	0.286	2.01	-4	1.05
1.70	3.30	0.60	112	84	1.655	0.278	3.11	-4	1.26
1.99	3.85	0.68	110	81	1.874	0.258	3.37	-10	1.47
2.27	4.40	0.75	109	77	2.094	0.250	3.54	-5	1.68
2.55	4.95	0.81	106	74	2.282	0.241	3.54	0	1.89
2.84	5.50	0.87	102	69	2.397	0.223	3.62	6	2.10
3.12	6.05	0.93	95	65	2.479	0.209	3.79	8	2.31
3.41	6.60	0.99	93	61	2.605	0.200	3.88	9	2.52
3.70	7.15	1.04	92	59	2.751	0.195	3.71	12	2.73
3.98	7.70	1.10	90	57	2.885	0.188	3.54	14	2.94
4.26	8.25	1.16	90	55	3.046	0.185	3.54	14	3.15

TEST No. 5

V (m/s)	V (knots)	R (kg)	Wetted length of keel (cm)	Wetted length of chine (cm)	Rex 10 ⁻⁶	S (m ²)	Trim (deg)	CG rise (mm)	F _v
0	0								0
1.13	2.20	0.25	116	70	1.047	0.258	1.00		0.84
1.42	2.75	0.49	116	90	1.452	0.295	1.08	-2	1.05
1.70	3.30	0.62	113	85	1.672	0.267	1.68	-3	1.26
1.99	3.85	0.70	112	83	1.914	0.264	2.69	-2	1.47
2.27	4.40	0.74	111	79	2.139	0.257	2.69	-6	1.68
2.55	4.95	0.78	111	76	2.358	0.252	2.77	-3	1.68
2.84	5.50	0.84	110	74	2.595	0.247	2.44	3	1.89
3.12	6.05	0.93	110	71	2.789	0.242	2.44	5	2.10
3.41	6.60	1.03	110	71	2.789	0.242	2.27	7	2.31
3.70	7.15	1.11	110	69	3.011	0.238	2.10	9	2.52
3.98	7.70	1.24	110	68	3.264	0.236	2.01	10	2.73
4.26	8.25	1.38	111	67	3.478	0.235	1.85	11	2.94
				65	3.723	0.230	1.68	11	3.15

TEST No. 6

V (m/s)	V (knots)	R (kg)	Wetted length of keel (cm)	Wetted length of chine (cm)	Rex 10 ⁻⁶	S (m ²)	Trim (deg)	CG rise (mm)	F _v
0	0								0
1.13	2.20	0.37	118	78	1.103	0.281	1.50		0.80
1.42	2.75	0.70	117	90	1.452	0.302	1.67	-3	1.00
1.70	3.30	0.92	110	85	1.638	0.284	2.60	-3	1.20
1.99	3.85	1.05	108	81	1.855	0.270	4.29	-4	1.40
2.27	4.40	1.14	104	77	2.026	0.264	4.71	-10	1.40
2.55	4.95	1.20	98	72	2.155	0.247	4.88	-3	1.60
2.84	5.50	1.25	90	67	2.200	0.218	4.97	4	1.80
3.12	6.05	1.32	85	64	2.293	0.193	5.22	11	2.00
3.41	6.60	1.34	83	61	2.436	0.185	5.31	13	2.20
3.70	7.15	1.37	81	59	2.567	0.179	5.31	15	2.40
3.98	7.70	1.40	80	56	2.687	0.172	5.14	18	2.60
4.26	8.25	1.44	79	56	2.687	0.172	4.80	21	2.80
				55	2.834	0.169	4.46	23	3.00

TEST No. 7

V (m/s)	V (knots)	R (kg)	Wetted length of keel (cm)	Wetted length of chine (cm)	Rex 10 ⁻⁶	S (m ²)	Trim (deg)	CG rise (mm)	F _v
0	0								0
1.13	2.20	0.370	117	80	1.108	0.285	1.50		0.80
1.42	2.75	.71	115	95	1.401	0.284	1.67	-3	1.00
1.70	3.30	0.97	112	87	1.672	0.290	2.60	-3	1.20
1.99	3.85	1.05	110	84	1.914	0.279	3.70	-2	1.40
2.27	4.40	1.10	109	82	2.139	0.275	4.29	-10	1.40
2.55	4.95	1.11	105	79	2.333	0.270	4.12	-3	1.60
2.84	5.50	1.18	103	75	2.510	0.260	3.78	7	1.80
3.12	6.05	1.23	100	71	2.634	0.226	3.95	9	2.00
3.41	6.60	1.27	98	68	2.808	0.218	4.04	11	2.20
3.70	7.15	1.32	98	65	2.871	0.214	3.95	13	2.40
3.98	7.70	1.39	100	65	3.241	0.217	3.70	14	2.60
4.26	8.25	1.47	102	63	3.469	0.217	3.36	16	2.80
							3.11	17	3.00

TEST No. 8

V (m/s)	V (knots)	R (kg)	Wetted length of keel (cm)	Wetted length of chine (cm)	Rex 10 ⁻⁶	S (m ²)	Trim (deg)	CG rise (mm)	F _v
0	0						-0.32		0
1.13	2.20	0.41	120	110	1.302	0.325	-0.66	-5	0.75
1.42	2.75	0.84	120	110	1.631	0.332	-0.40	-7	0.94
1.70	3.30	1.43	120	110	1.953	0.336	2.13	-3	1.13
1.99	3.85	1.78	119	110	2.263	0.334	3.06	-21	1.32
2.27	4.40	1.84	118	108	2.559	0.328	3.06	-10	1.51
2.55	4.95	1.85	117	105	2.831	0.326	2.64	0	1.70
2.84	5.50	1.93	116	101	3.064	0.322	2.73	6	1.89
3.12	6.05	1.98	114	94	3.242	0.319	3.49	7	2.08
3.41	6.60	1.96	109	85	3.301	0.286	4.50	10	2.27
3.70	7.15	2.00	106	81	3.431	0.250	4.58	15	2.45
3.98	7.70	2.04	103	77	3.578	0.241	4.58	19	2.64
4.26	8.25	2.09	101	74	3.702	0.233	4.50	22	2.83

TEST No. 9

V (m/s)	V (knots)	R (kg)	Wetted length of keel (cm)	Wetted length of chine (cm)	Rex 10 ⁻⁶	S (m ²)	Trim (deg)	CG rise (mm)	F _v
0	0						-0.32		0
1.13	2.20	0.43	120	110	1.315	0.324	-0.74	-5	0.75
1.42	2.75	0.91	120	110	1.648	0.330	-0.57	-7	0.94
1.70	3.30	1.43	120	110	1.973	0.333	1.45	-5	1.13
1.99	3.85	1.79	119	110	2.285	0.332	2.55	-17	1.32
2.27	4.40	1.91	119	110	2.608	0.329	2.30	-9	1.51
2.55	4.95	1.97	119	110	2.938	0.329	1.79	1	1.70
2.84	5.50	2.16	118	109	3.238	0.329	1.71	6	1.89
3.12	6.05	2.42	118	108	3.558	0.334	1.88	4	2.00
3.41	6.60	2.35	115	97	3.644	0.321	2.64	6	2.27
3.70	7.15	2.22	113	90	3.764	0.275	3.15	10	2.45
3.98	7.70	2.24	112	86	3.976	0.267	3.57	9	2.64
4.26	8.25	2.32	111	83	4.170	0.263	3.15	15	2.83

TEST No. 10

V (m/s)	V (knots)	R (kg)	Wetted length of keel (cm)	Wetted length of chine (cm)	Rex 10 ⁻⁶	S (m ²)	Trim (deg)	CG rise (mm)	F _v
0	0						0.85		0
1.13	2.20	0.43	120	110	1.315	0.333	0.85	-6	0.75
1.42	2.75	0.84	120	105	1.648	0.332	1.32	-7	0.94
1.70	3.30	1.36	118	105	1.905	0.333	3.47	-9	1.13
1.99	3.85	1.65	115	101	2.165	0.319	4.57	-15	1.32
2.27	4.40	1.73	114	97	2.402	0.312	4.91	-10	1.51
2.55	4.95	1.70	112	92	2.628	0.308	4.57	1	1.70
2.84	5.50	1.83	108	87	2.780	0.301	4.99	6	1.69
3.12	6.05	1.93	103	81	2.897	0.275	5.42	10	2.06
3.41	6.60	2.00	101	76	3.025	0.235	6.35	14	2.27
3.70	7.15	2.04	93	72	3.056	0.217	6.35	17	2.45
3.98	7.70	2.06	91	69	3.213	0.209	6.10	21	2.64
4.26	8.25	2.07	89	66	3.310	0.202	6.01	23	2.86

TEST No. 11

V (m/s)	V (knots)	R (kg)	Wetted length of keel (cm)	Wetted length of chine (cm)	Rex 10 ⁻⁶	S (m ²)	Trim (deg)	CG rise (mm)	F _v
0	0						0.85		0
1.13	2.20	0.43	120	110	1.315	0.322	0.77	-5	0.75
1.42	2.75	0.88	120	110	1.648	0.338	1.19	-6	0.94
1.70	3.30	1.39	119	108	1.939	0.341	3.05	-6	1.13
1.99	3.85	1.69	116	105	2.205	0.326	4.23	-17	1.32
2.27	4.40	1.73	115	101	2.471	0.318	4.15	-9	1.51
2.55	4.95	1.71	114	97	2.706	0.314	3.72	2	1.70
2.84	5.50	1.78	113	93	2.952	0.311	3.81	7	1.89
3.12	6.05	1.86	111	88	3.117	0.308	4.15	9	2.08
3.41	6.60	1.90	108	83	3.266	0.278	4.57	11	2.27
3.70	7.15	1.93	106	80	3.466	0.250	4.39	15	2.45
3.98	7.70	1.98	105	78	3.655	0.245	4.23	18	2.64
4.26	8.25	2.04	105	76	3.869	0.242	4.06	20	2.83

TEST No. 12

V (m/s)	V (knots)	R (kg)	Wetted length of keel (cm)	Wetted length of chine (cm)	Rex 10 ⁻⁶	S (m ²)	Trim (deg)	CG rise (mm)	F _v
0	0						2.16		0
1.13	2.20	0.42	118	107	1.281	0.336	2.50	-4	0.75
1.42	2.75	0.85	117	104	1.576	0.337	3.60	-7	0.94
1.70	3.30	1.61	110	92	1.733	0.309	5.63	-6	1.13
1.99	3.85	1.84	105	87	1.925	0.290	6.47	-9	1.32
2.27	4.40	1.95	99	82	2.059	0.277	6.73	-1	1.51
2.55	4.95	2.07	93	77	2.190	0.263	6.98	8	1.70
2.84	5.50	2.20	85	72	2.235	0.241	7.40	14	1.89
3.12	6.05	2.26	80	66	2.299	0.188	8.16	18	2.08
3.41	6.60	2.23	77	63	2.406	0.179	7.82	22	2.27
3.70	7.15	2.18	76	61	2.534	0.175	7.40	26	2.45
3.98	7.70	2.16	75	57	2.651	0.166	7.07	28	2.64
4.26	8.25	2.12	74	56	2.794	0.163	6.64	31	2.83

TEST No. 13

V (m/s)	V (knots)	R (kg)	Wetted length of keel (cm)	Wetted length of chine (cm)	Rex 10 ⁻⁶	S (m ²)	Trim (deg)	CG rise (mm)	F _v
0	0						2.16		0
1.13	2.20	0.42	118	107	1.281	0.336	2.41	-3	0.75
1.42	2.75	0.86	117	106	1.591	0.338	3.43	-5	0.94
1.70	3.30	1.61	112	99	1.802	0.321	5.46	-6	1.13
1.99	3.85	1.83	106	88	1.965	0.293	5.88	-7	1.32
2.27	4.40	1.89	105	84	2.151	0.286	5.96	-4	1.51
2.55	4.95	1.94	99	79	2.293	0.277	6.04	8	1.70
2.84	5.50	2.02	94	75	2.407	0.253	6.13	11	1.89
3.12	6.05	2.09	88	70	2.488	0.206	6.39	16	2.08
3.41	6.60	2.06	85	67	2.613	0.197	6.04	19	2.27
3.70	7.15	2.03	85	65	2.795	0.194	5.63	23	2.45
3.98	7.70	2.02	85	67	3.052	0.197	5.20	25	2.64
4.26	8.25	2.02	86	61	3.138	0.189	4.78	27	2.83

TEST No. 14

V (m/s)	V (knots)	R (kg)	Wetted length of keel (cm)	Wetted length of chine (cm)	Rex 10 ⁻⁶	S (m ²)	Trim (deg)	CG rise (mm)	F _v
0	0						0.85		0
1.13	2.20	0.46	120	110	1.315	0.332	0.73	-5	0.75
1.42	2.75	0.88	120	110	1.648	0.338	1.10	-6	0.94
1.70	3.30	1.45	118	107	1.922	0.335	3.05	-4	1.13
1.99	3.85	1.701	116	101	2.165	0.320	3.89	-15	1.32
2.27	4.40	.75	115	99	2.448	0.316	3.89	-6	1.51
2.55	4.95	1.70	114	94	2.680	0.309	3.30	6	1.70
2.84	5.50	1.77	113	91	2.923	0.310	3.30	9	1.89
3.12	6.05	1.85	112	88	3.149	0.305	3.55	11	2.06
3.41	6.60	1.89	109	83	3.300	0.280	3.81	12	2.27
3.70	7.15	1.93	108	80	3.503	0.253	3.72	14	2.45
3.98	7.70	1.98	109	78	3.735	0.252	3.39	17	2.64
4.26	8.25	2.07	110	77	3.998	0.252	3.13	19	2.83

TEST No. 15

V (m/s)	V (knots)	R (kg)	Wetted length of keel (cm)	Wetted length of chine (cm)	Rex 10 ⁻⁶	S (m ²)	Trim (deg)	CG rise (mm)	F _v
0	0						0.85		0
1.13	2.20	0.48	120	110	1.315	0.332	0.60	-5	0.75
1.42	2.75	0.93	120	110	1.648	0.338	0.68	-5	0.94
1.70	3.30	1.52	118	109	1.939	0.337	2.62	-3	1.13
1.99	3.85	1.73	117	105	2.225	0.326	3.39	-16	1.32
2.27	4.40	1.79	116	103	2.494	0.324	3.05	-6	1.51
2.55	4.95	1.79	116	101	2.783	0.317	2.32	7	1.70
2.84	5.50	1.94	117	102	3.124	0.320	1.70	11	1.89
3.12	6.05	2.22	118	104	3.495	0.324	1.27	11	2.08
3.41	6.60	2.68	119	106	3.850	0.328	0.77	11	2.27

TEST No. 16

V (m/s)	V (knots)	R (kg)	Wetted length of keel (cm)	Wetted length of chine (cm)	Rex 10 ⁻⁶	S (m ²)	Trim (deg)	CG rise (mm)	F _v
0	0						0.85		0
1.13	2.20	0.44	120	110	1.309	0.333	0.93	-5	0.75
1.42	2.75	0.89	120	110	1.638	0.338	1.27	-7	0.94
1.70	3.30	1.47	117	106	1.893	0.335	3.20	-3	1.13
1.99	3.85	1.71	115	100	2.132	0.318	4.40	-13	1.32
2.27	4.40	1.78	113	96	2.365	0.309	4.40	-6	1.51
2.55	4.95	1.75	112	92	2.612	0.308	4.23	2	1.70
2.84	5.50	1.84	109	87	2.791	0.303	4.31	9	1.89
3.12	6.05	1.93	104	82	2.910	0.283	4.90	10	2.08
3.41	6.60	1.99	99	77	3.007	0.235	5.16	14	2.27
3.70	7.15	2.02	98	74	3.185	0.228	4.90	17	2.45
3.98	7.70	2.04	97	71	3.353	0.221	4.65	20	2.64
4.26	8.25	2.07	97	70	3.546	0.220	4.31	22	2.83

TEST No. 17

V (m/s)	V (knots)	R (kg)	Wetted length of keel (cm)	Wetted length of chine (cm)	Rex 10 ⁻⁶	S (m ²)	Trim (deg)	CG rise (mm)	F _v
0	0						0.85		0
1.13	2.20	0.46	120	110	1.310	0.3320	0.77	-5	0.75
1.42	2.75	0.91	120	110	1.641	.338	1.19	-4	0.94
1.70	3.30	1.51	118	107	1.914	0.335	3.05	-5	1.13
1.99	3.85	1.75	116	103	2.176	0.322	3.00	-14	1.32
2.27	4.40	1.79	114	100	2.438	0.316	3.64	-5	1.51
2.55	4.95	1.76	114	96	2.694	0.313	3.22	4	1.70
2.84	5.50	1.85	114	94	2.968	0.312	3.39	4	1.89
3.12	6.05	1.93	113	90	3.167	0.311	3.22	10	2.08
3.41	6.60	1.98	112	87	3.389	0.292	3.22	12	2.27
3.70	7.15	2.05	111	85	3.637	0.283	3.13	15	2.45
3.98	7.70	2.13	112	83	3.879	0.264	2.88	16	2.64
4.26	8.25	2.27	113	83	4.195	0.266	2.46	18	2.83

TEST No. 18

V (m/s)	V (knots)	R (kg)	Wetted length of keel (cm)	Wetted length of chine (cm)	Rex 10 ⁻⁶	S (m ²)	Trim (deg)	CG rise (mm)	F _v
0	0						0.85		0
1.13	2.20	0.54	120	110	1.312	0.328	0.51	-2	0.75
1.42	2.75	1.04	120	110	1.644	0.335	0.85	-3	0.94
1.70	3.30	1.59	119	108	1.934	0.334	1.02	-5	1.13
1.99	3.85	1.90	118	106	2.240	0.325	2.88	-8	1.32
2.27	4.40	1.94	117	104	2.511	0.320	2.88	-3	1.51
2.55	4.95	1.99	117	104	2.828	0.320	1.78	7	1.70
2.84	5.50	2.19	118	106	3.202	0.324	1.10	12	1.89
3.12	6.05	2.79	120	110	3.613	0.327	0.00	13	2.08

TEST No. 19

V (m/s)	V (knots)	R (kg)	Wetted length of keel (cm)	Wetted length of chine (cm)	Rex 10 ⁻⁶	S (m ²)	Trim (deg)	CG rise (mm)	F _v
0	0						0.85		0
1.13	2.20	0.44	120	110	1.307	0.332	0.93	-5	0.75
1.42	2.75	0.87	120	110	1.638	0.338	1.27	-4	0.94
1.70	3.30	1.46	117	105	1.893	0.332	3.56	-3	1.13
1.99	3.85	1.75	115	98	2.112	0.315	4.57	-15	1.32
2.27	4.40	1.81	113	94	2.342	0.307	4.57	-6	1.51
2.55	4.95	1.79	112	90	2.586	0.305	4.40	3	1.70
2.84	5.50	1.86	108	85	2.734	0.299	4.57	10	1.89
3.12	6.05	1.99	102	79	2.816	0.269	5.24	12	2.08
3.41	6.60	2.03	102	75	3.007	0.236	5.33	16	2.27
3.70	7.15	2.05	100	72	3.185	0.227	5.16	19	2.45
3.98	7.70	2.07	93	70	3.233	0.214	4.90	21	2.64
4.26	8.25	2.08	93	67	3.418	0.209	4.57	24	2.83

TEST No. 20

V (m/s)	V (knots)	R (kg)	Wetted length of keel (cm)	Wetted length of chine (cm)	Rex 10 ⁻⁶	S (m ²)	Trim (deg)	CG rise (mm)	F _v
0	0						0.85		0
1.13	2.20	0.45	120	110	1.313	0.330	0.68	-4	0.75
1.42	2.75	0.92	120	110	1.644	0.342	1.02	-4	0.94
1.70	3.30	1.60	117	108	1.918	0.334	3.22	-4	1.13
1.99	3.85	1.79	116	101	2.161	0.317	3.56	-5	1.32
2.27	4.40	1.87	115	100	2.443	0.315	3.89	-4	1.51
2.55	4.95	1.84	114	95	2.674	0.310	3.39	3	1.70
2.84	5.50	1.91	113	91	2.917	0.308	3.56	6	1.89
3.12	6.05	2.00	112	88	3.142	0.305	3.47	11	2.08
3.41	6.60	2.04	110	84	3.328	0.288	3.81	13	2.27
3.70	7.15	2.09	109	81	3.533	0.256	3.56	16	2.45
3.98	7.70	2.16	110	79	3.767	0.255	3.30	17	2.64
4.26	8.25	2.30	111	80	4.075	0.258	2.71	19	2.83

TEST No. 21

V (m/s)	V (knots)	R (kg)	Wetted length of keel (cm)	Wetted length of chine (cm)	Rex 10 ⁻⁶	S (m ²)	Trim (deg)	CG rise (mm)	F _v
0	0						0.85		0
1.13	2.20	0.59	120	110	1.305	0.326	0.51	-2	0.75
1.42	2.75	1.13	120	110	1.634	0.332	0.61	-3	0.94
1.70	3.30	1.82	119	109	1.940	0.333	2.46	-4	1.13
1.99	3.85	2.12	118	106	2.227	0.321	3.22	-14	1.32
2.27	4.40	2.16	117	103	2.496	0.313	2.95	-3	1.51
2.55	4.95	2.22	116	104	2.837	0.318	1.78	9	1.70

The seakeeping performance and steering properties of sailing yachts

by J. Gerritsma and G. Moeyes

Delft University of Technology
Ship Hydromechanics Laboratory

Contents

- 1 Introduction
- 2 The influence of displacement on the still water performance
- 3 The influence of displacement and longitudinal distribution of weights on the windward performance in a seaway
- 4 The steering performance
 - 4.1 Forces and moments owing to rudder angle
 - 4.2 The fixed controls behaviour
 - 4.3 The behaviour with continuous rudder action
- 5 Conclusion
- 6 Acknowledgement
- 7 References

1 Introduction

To a certain extent the performance of a sailing yacht can be predicted with the aid of ship model tests in a towing tank. To evaluate the experimental model results the procedure as published by Davidson [1] is still used in principle, and tank predictions based on his method have proved to be an efficient tool for the designer of sailing yachts.

Particularly in the case of large seagoing yachts the reduction of the risk of failure is important and certainly for this class of vessels routine tank tests are more or less common practice.

Such tests predict the performance for the windward and the running conditions, assuming that there are no seawaves. This simplification is not realistic in all cases, but it is commonly assumed that the yacht, which is superior in calm water compared with an alternative design, will also be the best one in a seaway. Similar assumptions are usually made in the design of ships with mechanical propulsion. The effect of sea waves is taken into account by using statistical power allowances added to the still water tank prediction. In the last decades model

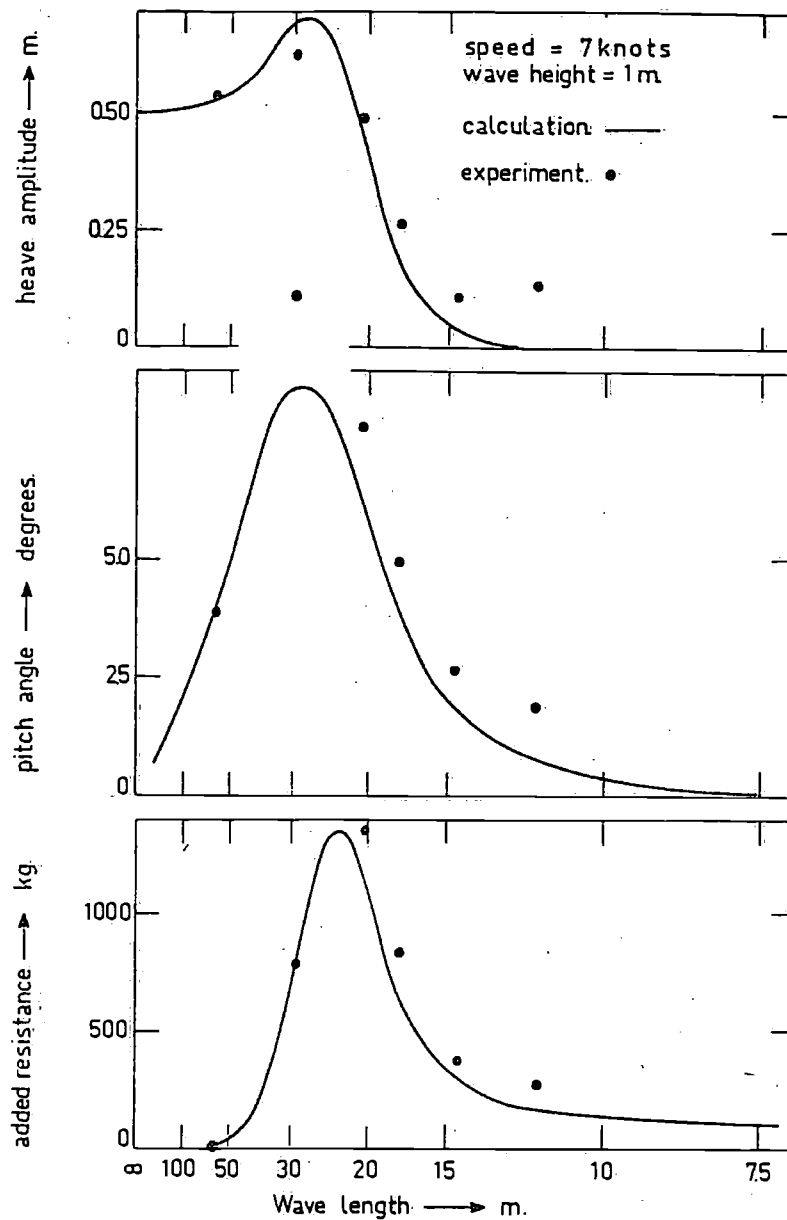


Figure 1. Pitch, heave and added resistance in waves of "Valiant"

tests in waves have become an additional tool to evaluate ship performance in a seaway, in particular for special purpose ships and for designs which are outside of the range for which sufficient empirical knowledge exists. In addition theoretical methods have been developed to calculate with sufficient accuracy the oscillatory motions of a ship in a given irregular seaway and recently a practical method to calculate the added resistance in waves became available.

Up to now very little research on the performance of sailing yachts in waves has been reported. Tank tests in waves are time consuming and expensive; consequently it is not likely that extensive investigations of this sort will be carried out regularly for yacht designs on a commercial basis. One of the very few publications in this field was given by Spens et al [2]. An analysis was made of the motions and the added resistance in waves of the 12 meter "Sovereign", in the heeled condition. Head waves as well as oblique headings were considered and the influence was determined, which the longitudinal distribution of the weight of the

yacht, characterized by the radius of gyration, has on the dynamic behaviour in waves. The model experiments showed the advantage of a small longitudinal radius of gyration with respect to pitching motions and added resistance. For short wave lengths a larger radius of gyration gives slightly better results. As a first approximation it was shown that the added resistance in waves varies as the squared wave height, when wave length and forward speed are constant.

Finally the model experiments indicated that the motions and the added resistance in oblique waves can be estimated from tests in head waves having the same effective wave length and the same frequency of encounter. It was shown that the results are not seriously affected by the increase of the yacht's speed which is necessary to fulfill these conditions.

The agreement is not exact, but the method is useful to compare different designs.

Seakeeping experiments carried out in Delft with a model designed as a half ton cup yacht showed a fair agreement with theoretical predictions of the pitching and heaving motions [3]. In fact the results were better than expected, considering the very "non linear" form of the yacht and the use of a linear strip theory. Differences in amplitudes occur at large wave lengths, but in the region of resonance which is important with regard to added resistance in waves, the agreement is very satisfactory.

The experimental accuracy of the tests in the heeled condition may have suffered from large yawing moments, but the results seem to indicate that motions and resistance for 20 degrees of heel do not differ substantially from the upright condition values.

At the time that these experiments were carried out no suitable method to calculate the added resistance in waves was available, but the test results clearly showed the importance of the added resistance in waves; which can easily double the still water resistance in resonance conditions, even in very moderate sea conditions.

The newly developed method to calculate the added resistance of ships in waves as reported in [4] has proved to give reliable results for a range of ship types, including fast container ships as well as full tankers. This method was also used to analyse the seakeeping characteristics of the 12 meters "Columbia" and "Valiant". The results were compared with corresponding model experiments, carried out in the Delft Shipbuilding Laboratory, showing good agreement for the motions as well as for the added resistance; see Figure 1.

The same methods were used to analyse a small systematic series of yacht designs, which were tank tested to develop the successful racer "Standfast" (Published as "Admiral" in [5]). The three preliminary designs have the same waterline length, breadth and rating, but the displacements vary considerably. The investigation was carried out to analyse the influence of displacement and longitudinal radius of gyration on the windward performance in seawaves.

The performance of a sailing yacht is not only characterized by its speed and behaviour in still water and in waves, but also by the way it steers. This fact has drawn the attention, when with the advent of the modern fast cruiser-racers problems of controllability in running conditions were reported in many cases.

One of the features of these yachts is the short fin keel with separated rudder, which invited many cruising skippers to consider short keel yachts as unmanageable and therefore unsafe. As will be illustrated later in this paper, this opinion is probably not correct.

The improved quality of the modern hull and rig permits the skipper to drive his yacht faster and harder, with more sail in rough wind and sea conditions than before. The larger forces which will be exerted in these conditions can not always be controlled.

The first way to meet the controllability problems is to give the crew devices which can counteract the larger acting forces. As far as it concerns course keeping this method could be called: to increase the "steering power" of the ship. To serve this purpose for example a more effective rudder can be made, by using more rudder area, a better form and by giving it a better location, well aft and without slots between the top of the rudder and the hull. Spens et al [2] included this approach in their paper; they measured the forces and moments on a yacht model as a function of rudder angle.

In the Delft Shipbuilding Laboratory measuring forces and moments owing to rudder angle has been a part of a more extended test program with the half ton cup model and the two 12 meter yachts.

Another approach of the steering problem is to design the yacht and its controls (helm or steering wheel, length of helm, position of kingpost in the ruddert etc.) in such a way that the helmsman, as "operator" of the "system" yacht spends the least amount of energy and attention to things which do not contribute to his only purpose: "optimal steering of the ship". Optimal could then be interpreted as covering in the shortest time a track between two given points. This method can be called improving the "steering compliance" of the ship and its controls. Steering power and compliance together form the steering qualities of a yacht.

Figure 11 shows schematically the control system of a steered yacht.

The input consists of a rudder angle and a disturbance due to wind and waves, both resulting in a turning moment and a side force.

The output is the ships course.

There is no mutual influence between input and output, for which we say that the unsteered yacht is an open loop system.

The open loop system has several times been the subject of investigation. Spens et al [2] determined the dynamic properties of a yawing and swaying yacht hull without sails, partly by experiment, partly by calculation; see Figure 12.

In Delft an extensive oscillation test program has been carried out with the models of the half ton cup yacht [3] and the two 12 meter yachts as well as with the 13 meter waterline yawl "Stormy". The measured forces, proportional to sway, roll and yaw amplitudes, velocities and accelerations determine the linearized equations of motion. In one of the next chapters more attention will be paid to the appearance and characteristics of the equations of motion of the open loop control system.

If a helmsman is asked to steer the ship he will compare the actual course with the desired course and set the helm according to the course deviation. Additional information for his reaction can be the rate of turn or yaw velocity, inclination, helm angle, sail behaviour etc. Whether he uses all sources of information or only the course deviation, and to what degree, depends upon the man and the properties of the system he has to steer. Because of the feedback of the actual course to the helmsman the whole system of yacht and helmsman is called a closed loop system.

It is generally assumed that course deviation and yaw rate have a significant influence upon the helmsmans behaviour. For a first approximate analysis of the helmsmans input and output, however, a linear relation between course deviation and rudder angle may be assumed.

In one of the next chapters the response of a yacht to rudder angle will be considered as a base for further research on the steering performance of the helmsman of a sailing yacht.

2 The influence of displacement on the still water performance

The lines of the three designs, which are the subject of the present analysis are shown in Figure 2 and the corresponding main particulars are given in Table 1.

Table 1. Main particulars of the designs no. I, II and III

			I	II	III
length of design waterline	L_{wl}	m	10.00	10.00	10.00
maximum breadth	B	m	3.66	3.66	3.66
draught		m	2.15	2.15	2.15
displacement	Δ	kg	8207	9759	11443
displacement of hull	Δ_H	kg	7680	9211	10670
centre of buoyancy aft $\frac{1}{2}L_{wl}$		m	0.26	0.26	0.34
centre of gravity under DWL		m	0.25	0.39	0.52
Prismatic coefficient of hull			0.566	0.572	0.566
effective sail area		m ²	66	71	75
length displacement ratio	$L_{wl}/\Delta_H^{1/3}$		5.07	4.77	4.54
rating		ft	33.6	33.6	33.6

With respect to the main dimensions it is important to remark that a larger displacement at constant length, breadth and draught results in a lower aspect ratio fin keel because of the larger depth of the hull.

The windward performance of the three designs in calm water is given in Table 2, as the speed made good V_{mg} versus three standard values of the true wind speed V_{tw} .

Table 2. Speed made good (all speeds in meters per second)

V_{tw}	V_{mg}		
	I	II	III
3.5	1.90	1.87	1.88
7.0	2.73	2.68	2.69
10.0	2.97	2.93	2.94

For running conditions the resistance R for zero angle of heel and no drift is of interest. Figure 3 shows the three resistance curves on a base of forward speed. Design III has the lowest resistance per ton displacement, but the running speeds are almost equal for the three designs, except the lightest version I, which is slightly better for windspeeds exceeding 7 m/s. Based on the stillwater performance the conclusion is that design I is to be preferred. Although the differences between the three designs were measurable, the performances are very close to each other. Considering that the I.O.R. 1970 rating for the three yachts is equal, this means that the rating formula works very well in the considered case.

3 The influence of displacement and longitudinal distribution of weights on the windward performance in a seaway

The added resistance of a yacht in sea waves is mainly caused by the heaving and pitching motions. Heave is defined as the vertical oscillatory motion of the centre of gravity of the vessel, whereas pitching is the rotational oscillatory motion with regard to an athwartship's axis.

The natural periods of heave and pitch are very important for the behaviour of a yacht in waves. If one of these motion periods is equal to the period of wave encounter, violent motions may result. In such resonant conditions a large increase of the resistance is observed and a corresponding loss of speed occurs. Referring to Figure 1, the maximum of the added resistance curve is near to resonance of the heaving and pitching motions. In these conditions the immersion of the bow of the yacht is large due to the unfavourable phase of the bow motion with respect to the wave.

It should be remarked that in resonance conditions the absolute motion amplitudes are not necessarily a maximum. In very long waves the motion amplitudes can be very large, but as the yacht more or less follows the wave contours, the relative motion with respect to the wave and the added resistance are very small.

For the estimation of the natural pitching period the total mass moment of inertia of the yacht has to be known. This consists of the real mass moment of inertia and a hydrodynamic addition, which can be calculated with sufficient accuracy. With the aid of a full scale oscillation experiment the total inertia can be determined and hence the real mass moment of inertia can be estimated.

Full scale oscillation tests with "Standfast", which was forced oscillated in a pitching motion made by hand excitation in calm water, resulted in a natural pitching period $T_{\theta} = 2.4$ sec.

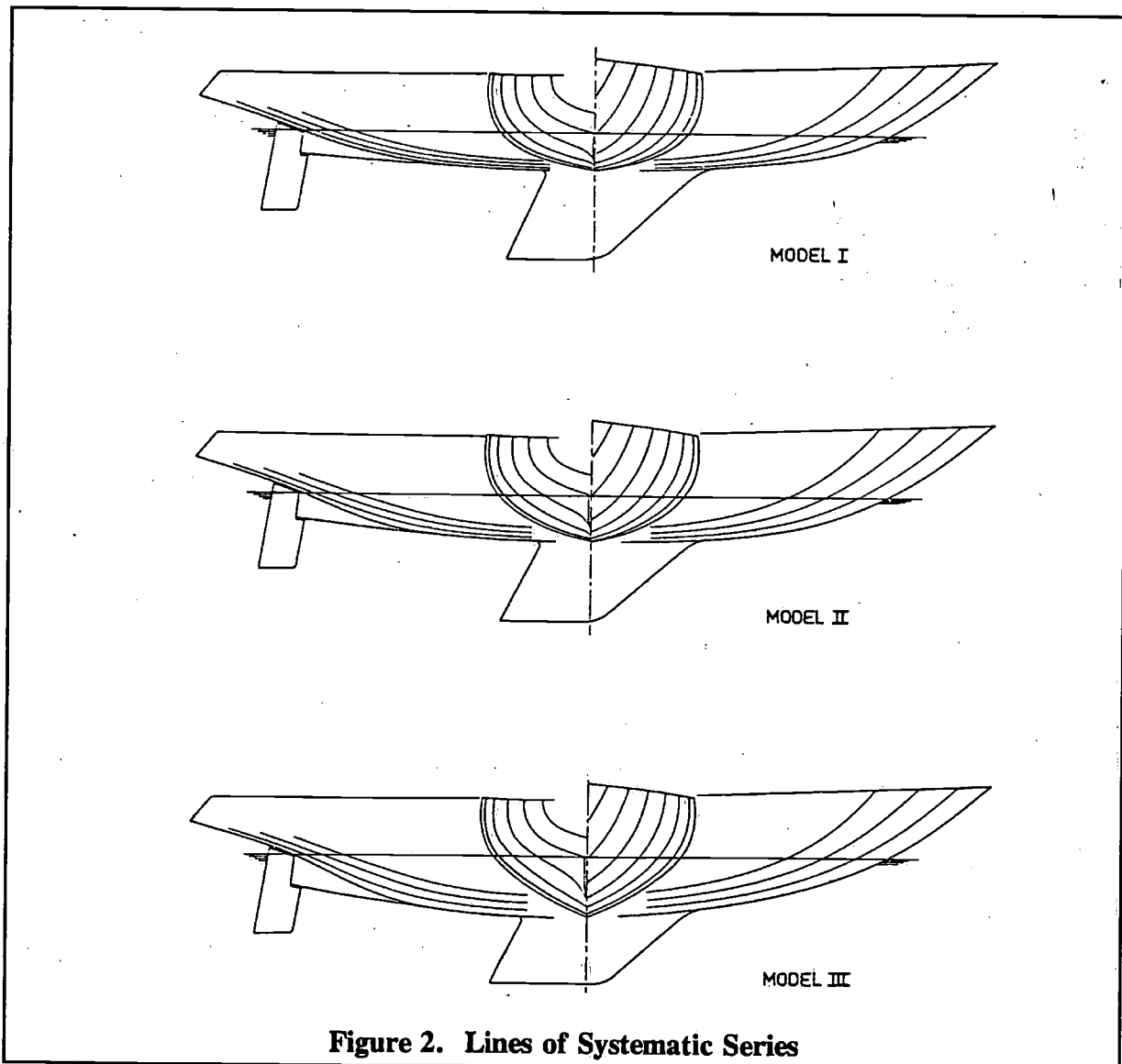


Figure 2. Lines of Systematic Series

With calculated values for the hydrodynamic mass moment of inertia A , the pitch damping coefficient $N_{\theta\theta}$, the real mass moment of inertia of the yacht I_{yy} , could be determined with the measured pitching period:

$$T_{\theta} = 2\pi \sqrt{\frac{I_{yy} + A}{\Delta GM_l}} \quad (3.1)$$

where: Δ = the displacement
 GM_l = the longitudinal metacentric height

The radius of gyration k_{yy} for pitching follows from:

$$k_{yy} = \sqrt{\frac{g I_{yy}}{\Delta}} \quad (3.2)$$

where: g = the acceleration due to gravity

For the "Standfast" the resulting radius of gyration is 25% of the overall length of the yacht. It is assumed that this value may be used for similar yachts of approximately the same dimensions.

The natural period of heaving cannot be determined from full scale experiments, because it is not possible to oscillate a yacht manually in a pure vertical motion. However in this case the calculation of the mass of the yacht is very simple and the hydrodynamic addition to the real mass can be determined with sufficient accuracy.

The natural period for heave T_z follows from:

$$2\pi \sqrt{\frac{\Delta/g + a}{\gamma A_{WL}}} \quad (3.3)$$

where: γ = the specific weight of water
 A_{WL} = the waterplane area
 a = the hydrodynamic mass for vertical motion

For the "Standfast" a natural heaving period $T_z = 2.2$ seconds was found.

In both calculations the influence of the relatively high damping was taken into account. It may be of interest to know that the added mass moment of inertia for the considered yacht is 69% of the real inertia, and the added mass is 185% of the mass of displacement. In comparison with merchant ships the damping of pitch and heave is fairly large, which is probably owing to the relatively high beam/draught ratio of the hull.

Considering the radius of gyration found with the "Standfast" experiment, three values were chosen for the present analysis of the three yacht designs.

The pitching and heaving motions, as well as the added resistance in waves were calculated for: $k_{yy} = 0.23, 0.25$ and 0.27 of the overall lengths of the designs.

When a yacht is progressing in bow or head waves the pitching and heaving motions generate damping waves which are superimposed on the incident wave system. These damping waves carry energy away from the yacht and the added resistance which results can be found by equalizing the work done by the resistant force and the radiated damping wave energy. A practical method following this procedure is given in [4], where the strip theory is used to estimate the energy dissipation of each cross section of the vessel.

The added resistance in waves R_{aw} follows from:

$$R_{aw} = \frac{1}{\lambda} \int_0^L \int_0^{T_e} b' V_z^2 dx_b dt \quad (3.4)$$

- where:
- L = waterline length
 - λ = wave length
 - t = time
 - b' = cross-sectional damping coefficient corrected for the forward speed
 - V_z = relative vertical velocity of the water with respect to a cross-section
 - T_e = period of wave encounter
 - x_b = length ordinate of yacht's hull

The vertical relative motion V_z is calculated by vectorial summation of the heaving motion, the vertical motion due to pitching and the vertical motion of the wave. The strip theory gives reliable results in the case of merchant ship forms, when compared with model experiments [4]. Also for sailing yachts a reasonable correlation with model experiments is found, as already shown in Figure 1.

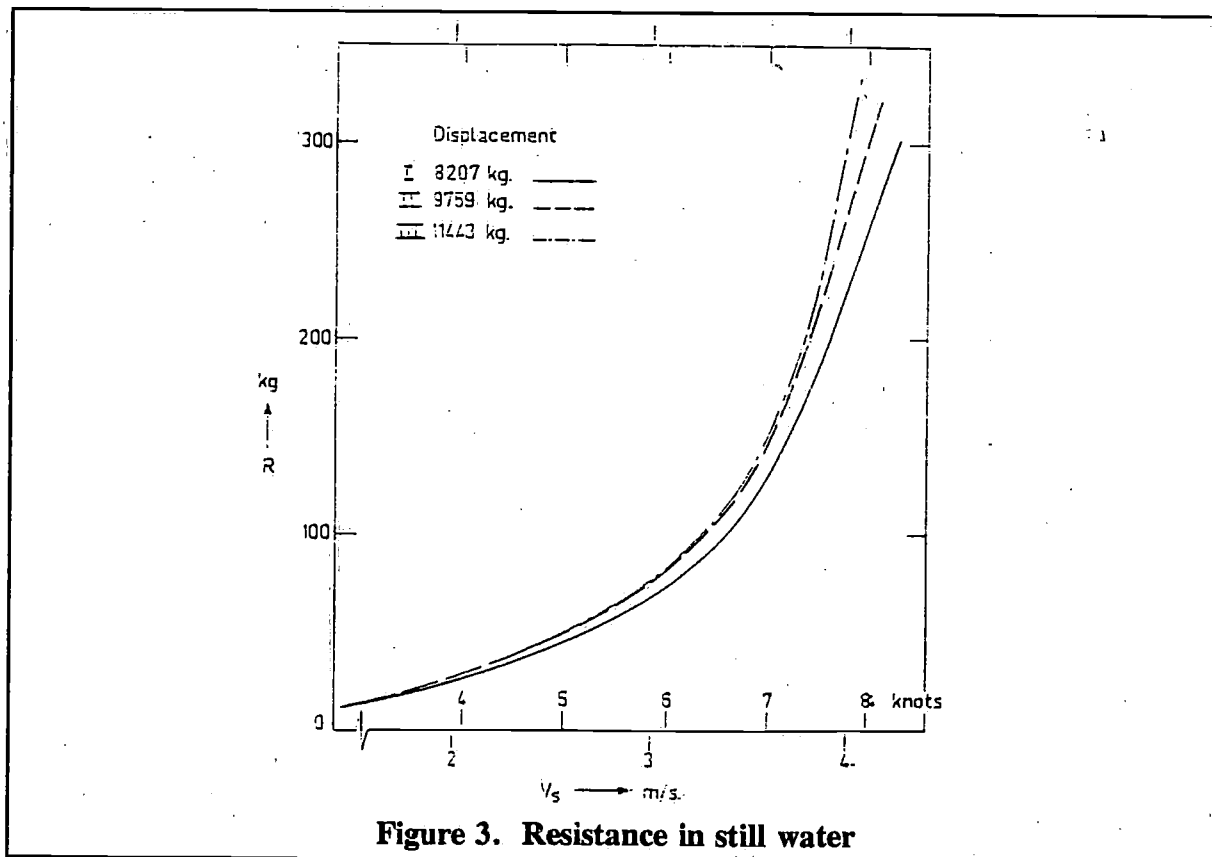


Figure 3. Resistance in still water

For the three yacht designs the motions and the added resistance in a range of wave conditions were calculated for the three values of the radius of gyration already mentioned. The calculations were carried out for zero heeling angle and head waves were assumed. It is admitted that this is a simplification, but not a completely unrealistic one, as shown in the introduction.

Also, it should be mentioned that an extension to oblique headings and the inclusion of a heeling angle offers no difficulties in principle, but for economic reasons the existing computer programs had to be used.

The irregular waves, as used in the analysis, correspond to the spectral density formulation as given by Pierson-Moskovitch, but their relation between wind speed and wave spectrum is not used. The seaway is characterized by the significant wave height only and the wind speeds are chosen independent of the considered moderate sea conditions.

It is possible that sailing yachts operate in sea conditions which differ from those given by the standard sea spectra. However, also in such cases higher energy contents and thus higher wave heights correspond to longer wave lengths, when we consider the high frequency range of the sea spectrum which is important for small vessels. This feature applies to ocean wave spectra as well as to coastal wave spectra, and will prove to be important for the analysis of the three yacht designs.

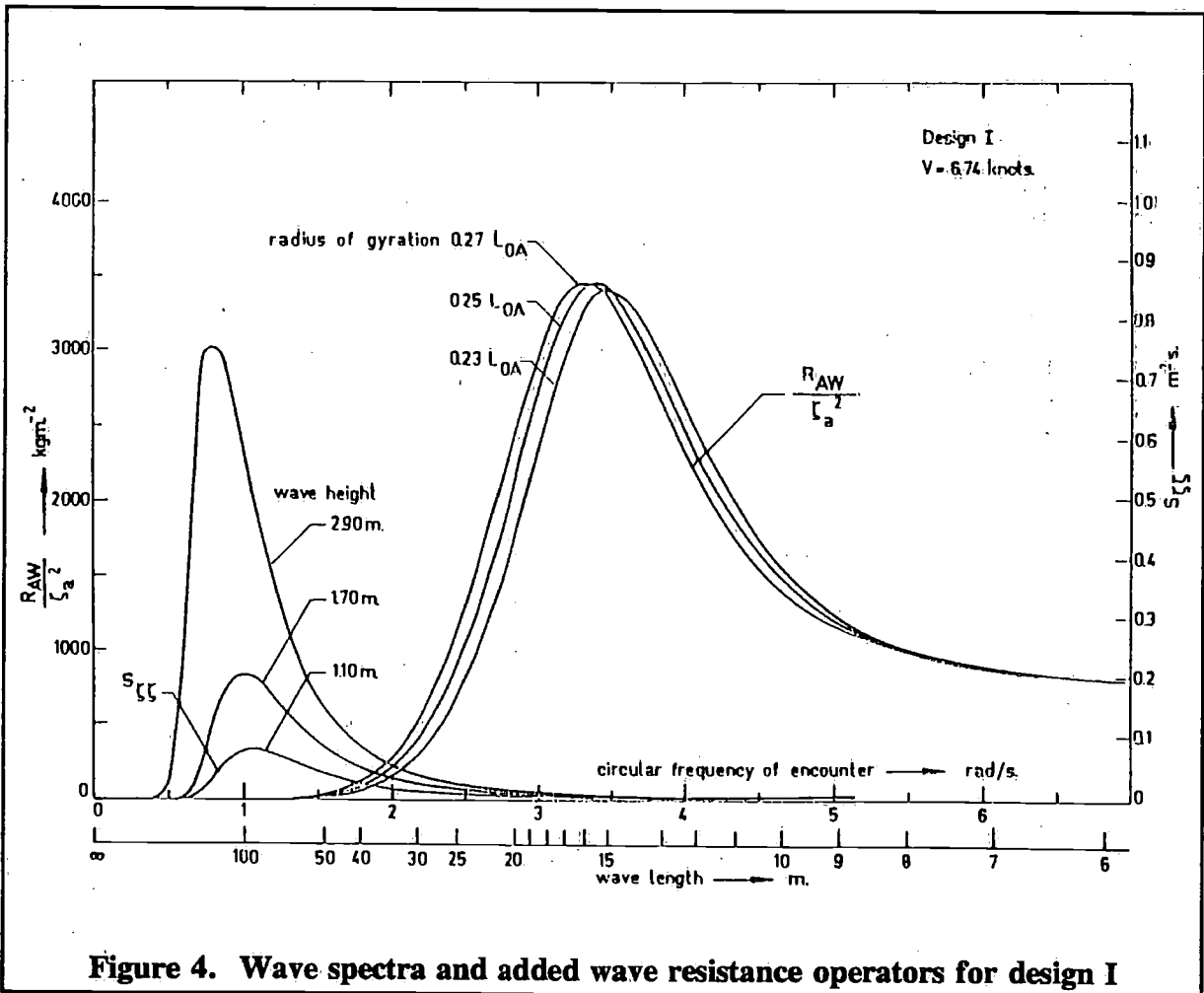


Figure 4. Wave spectra and added wave resistance operators for design I

Figure 4 shows four ocean wave spectra according to the Pierson Moskovich formulation and added wave resistance operators for three radii of gyration for design I, with a forward speed of 6.74 knots in head waves.

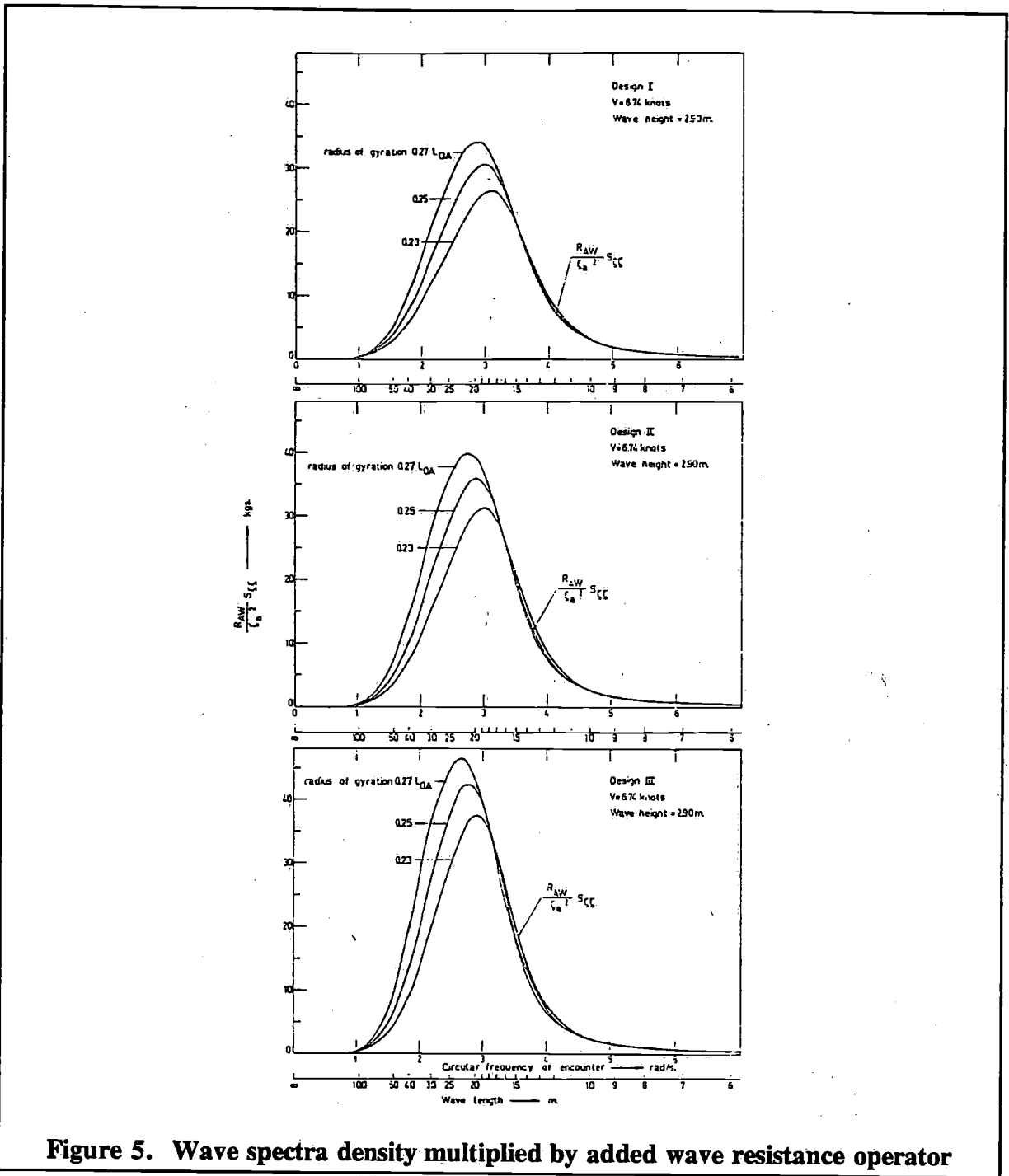


Figure 5. Wave spectra density multiplied by added wave resistance operator

Multiplication of the wave spectral densities with the corresponding added wave resistance operators results in the three curves in Figure 5, where only one sea spectrum is shown as an example. The area under these curves is proportional to the added resistance in waves. Figure 5 shows that an important reason for the differences in added resistance is the shift of the added resistance operators to lower wave frequencies, because in this region of longer wave lengths the wave height and thus the wave spectral densities increase. It is clearly shown that larger displacements and weights distributed more towards the ends of the yacht, both result in higher added resistance. The favourable effect of the larger radius of gyration in small wave lengths is very small and does not counterbalance the former effect. Therefore a small radius of gyration is advisable as the best average solution. A condensed plot of all the added resistance values for the three yacht designs in a range of irregular wave condi-

tions, is shown in Figure 6 again for a speed of 6.74 knots corresponding to a Froude number $F_n = 0.35$.

For comparison purposes the still water resistance is given for each of the three considered hull forms. The irregular seaway is characterized by the significant wave height, which is defined as the average of the one third highest waves and correlates well enough with the estimation from visual observations.

In Table 3 the added resistance is given as a percentage of the corresponding still water values for a speed of 6.74 knots and a radius of gyration $k_{yy} = 0.25 L_{oa}$.

Table 3 Added resistance in waves related to the still water resistance, with $V = 6.74$ kn. and $k_{yy} = 0.25 L_{oa}$

wave height m	I	II	III
2.90	82 %	79 %	76 %
2.15	66 %	64 %	61 %
1.70	52 %	51 %	48 %
1.10	26 %	25 %	24 %

Table 3 shows that the lightest yacht I has the largest resistance increase percentage, when referred to the still water upright condition, although it has the smallest absolute resistance increase. However, the differences between the three designs are relatively small, considering the assumptions having been made in the calculations.

When sailing to windward with a speed of 6.74 knots, the still water resistance is increased due to drift and heeling angle by approximately 59%, 66% and 74% for design I, II and III respectively.

The larger induced resistance of the large displacement yachts is caused by the less efficient fin keels because of the lower aspect ratio. The net result is a better windward performance in waves of the light displacement yacht, provided that the simple addition of induced resistance and added wave resistance is permissible.

Concentration of weights in the mid portion of the yacht's hull is of advantage: in all cases the added resistance is lower for small radii of gyration.

The effect of the added resistance on the speed made good of the three designs is shown in Figure 7 for three standard values of the true windspeed, respectively $V_{tw} = 3.5, 7.0$ and 10.0 meters per second and a range of significant wave heights. Here again the added wave resistance was added to the total still water resistance, now in the heeled condition with a drift angle.

For the speed made good calculation the "Gimcrack" coefficients were used for the sail forces [1]. They were modified by a procedure described in [6] to cope with the larger resistance-side force ratio's due to the waves.

Figure 7 shows that the lightest yacht has the highest speed made good, when the assumptions having been made are excepted. The lowest speed made good values imply some extrapolation of the experimental data and may not be very reliable. As a matter of interest the true wind angle of design I is given in Figure 8 for the same standard windspeeds on a base of wave height.

Finally the significant heave and pitch amplitudes were calculated for the considered sea conditions. The results are summarized in Figures 9 and 10. Apparently there is little influence of the yacht's displacement on heave, but the large displacement hull has the largest pitching motions.

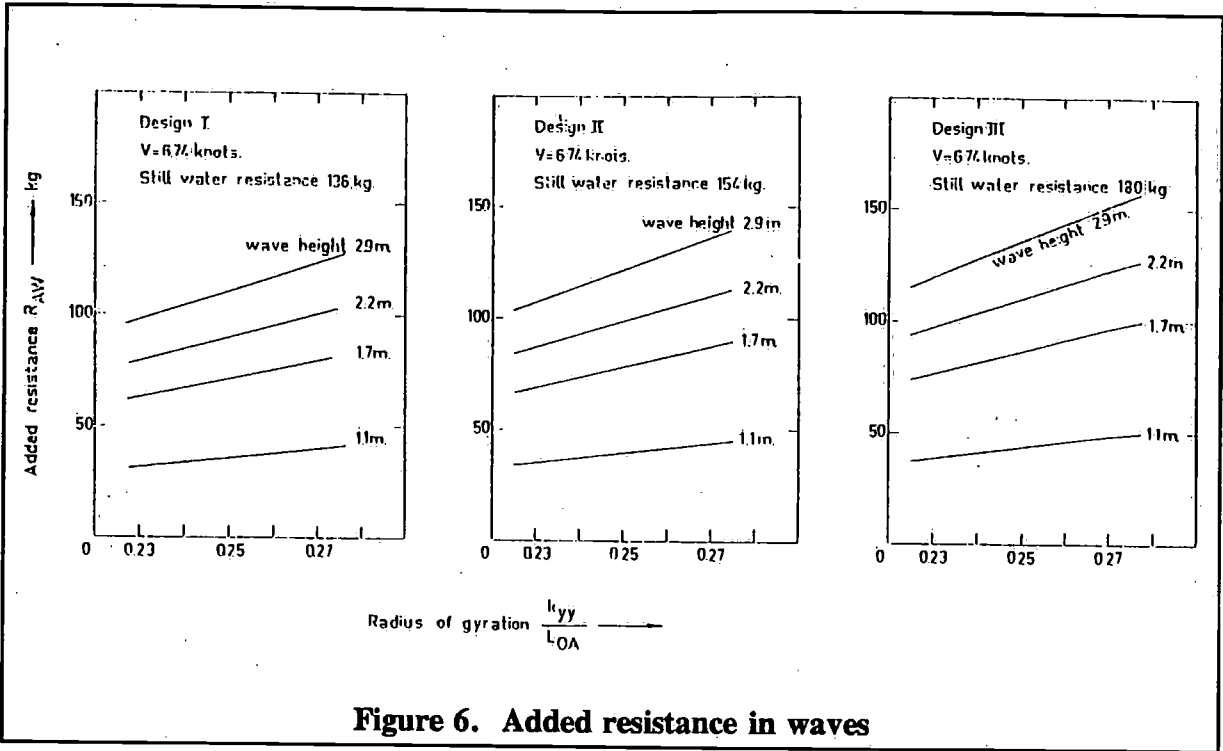


Figure 6. Added resistance in waves

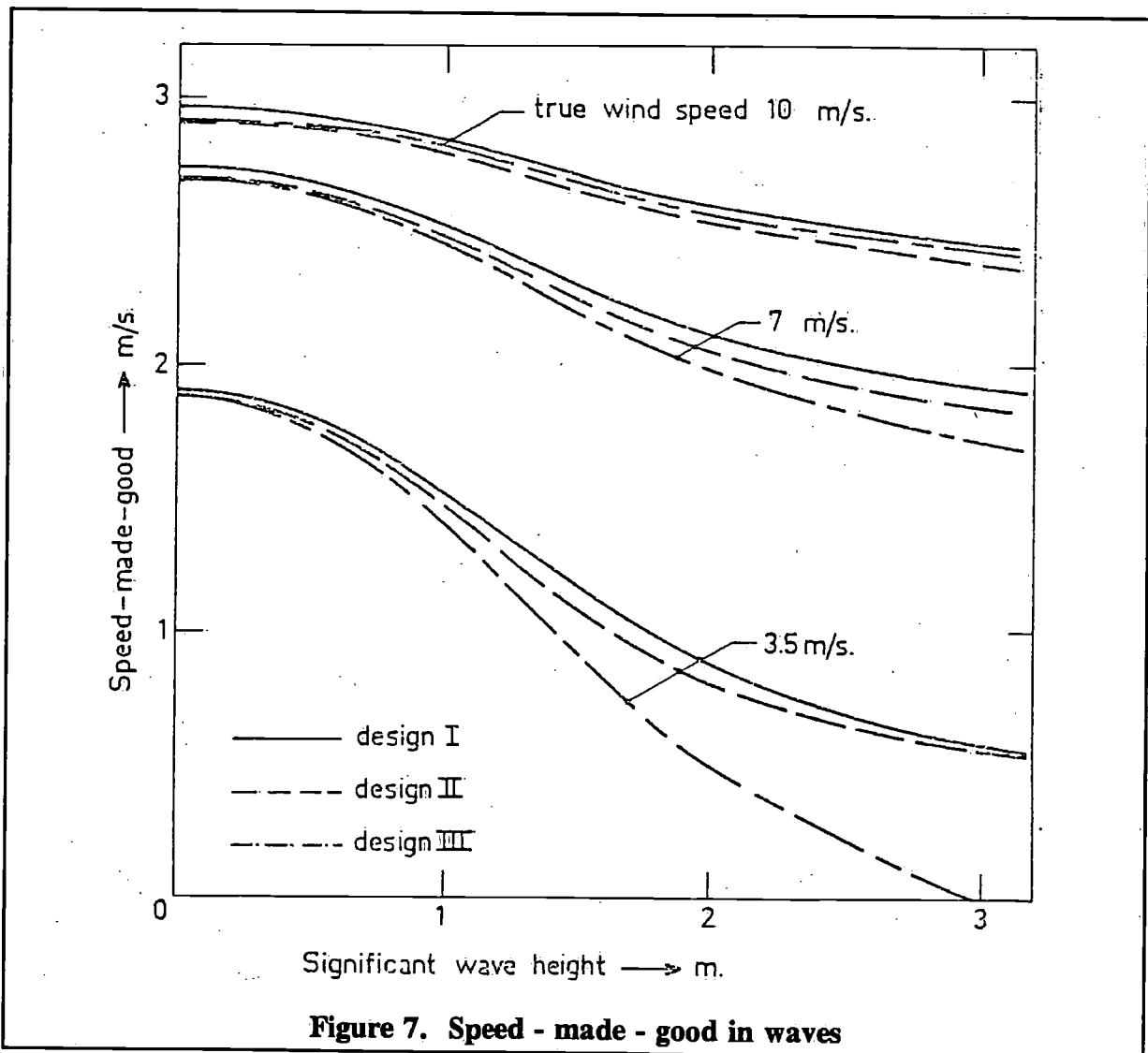


Figure 7. Speed - made - good in waves

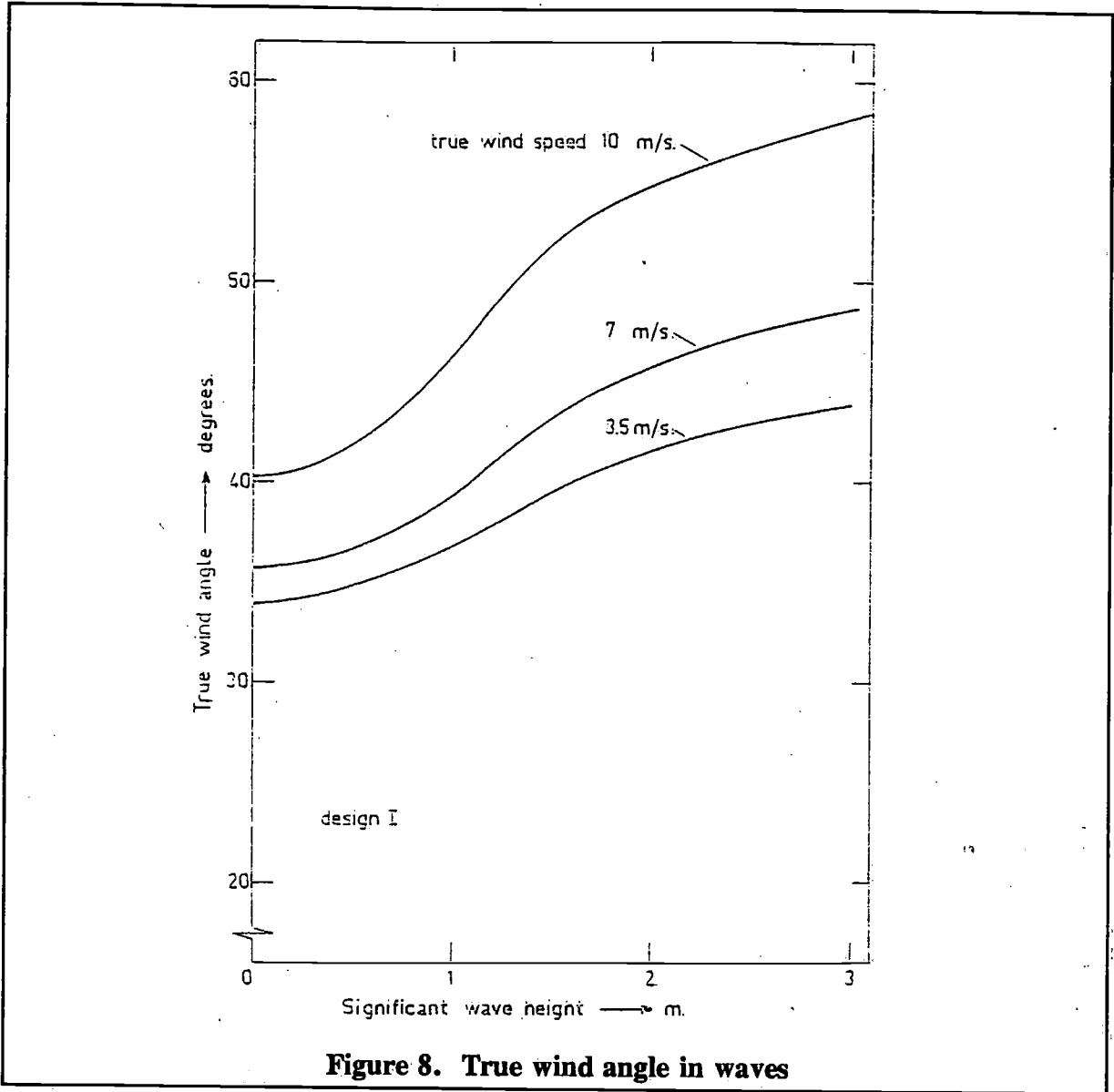


Figure 8. True wind angle in waves

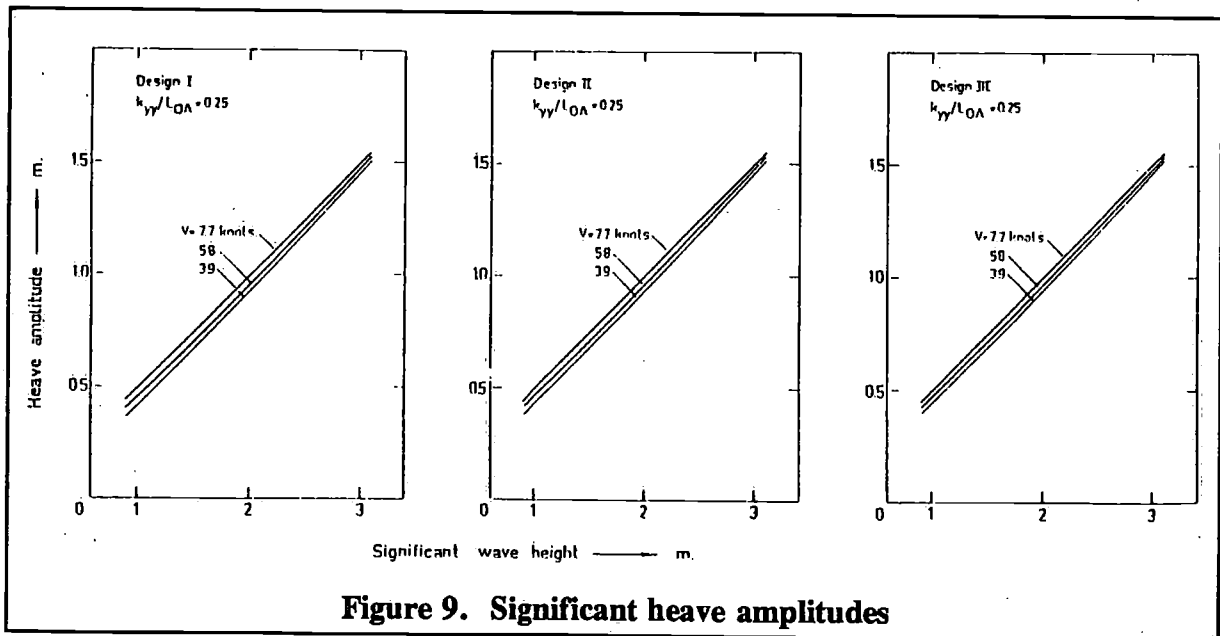


Figure 9. Significant heave amplitudes

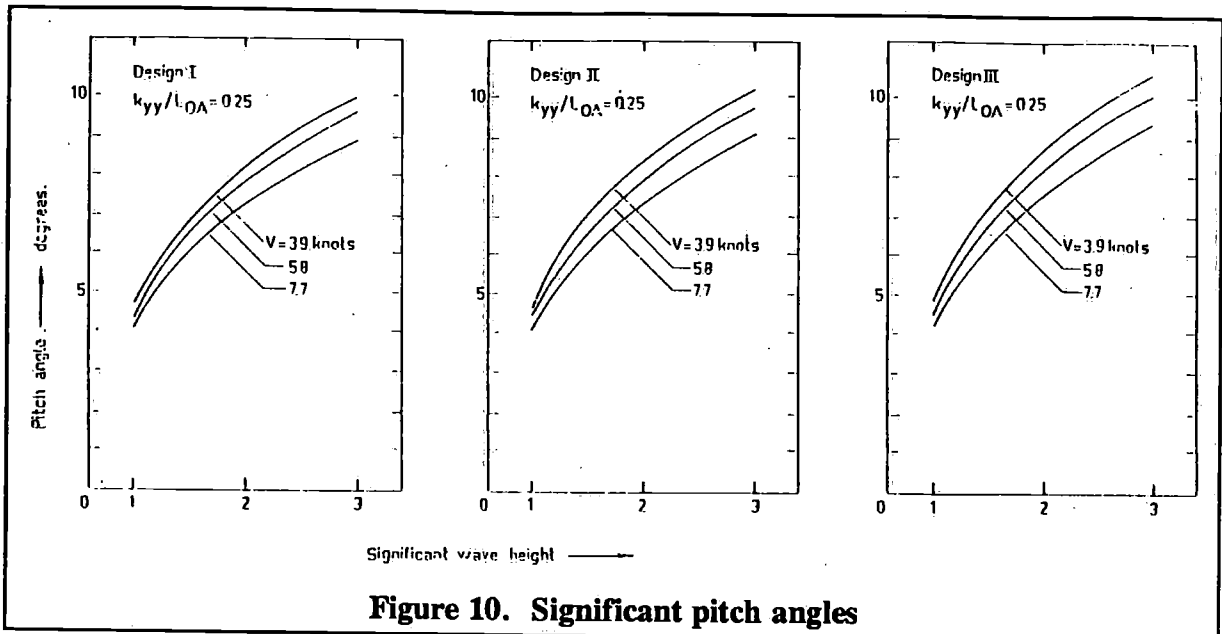


Figure 10. Significant pitch angles

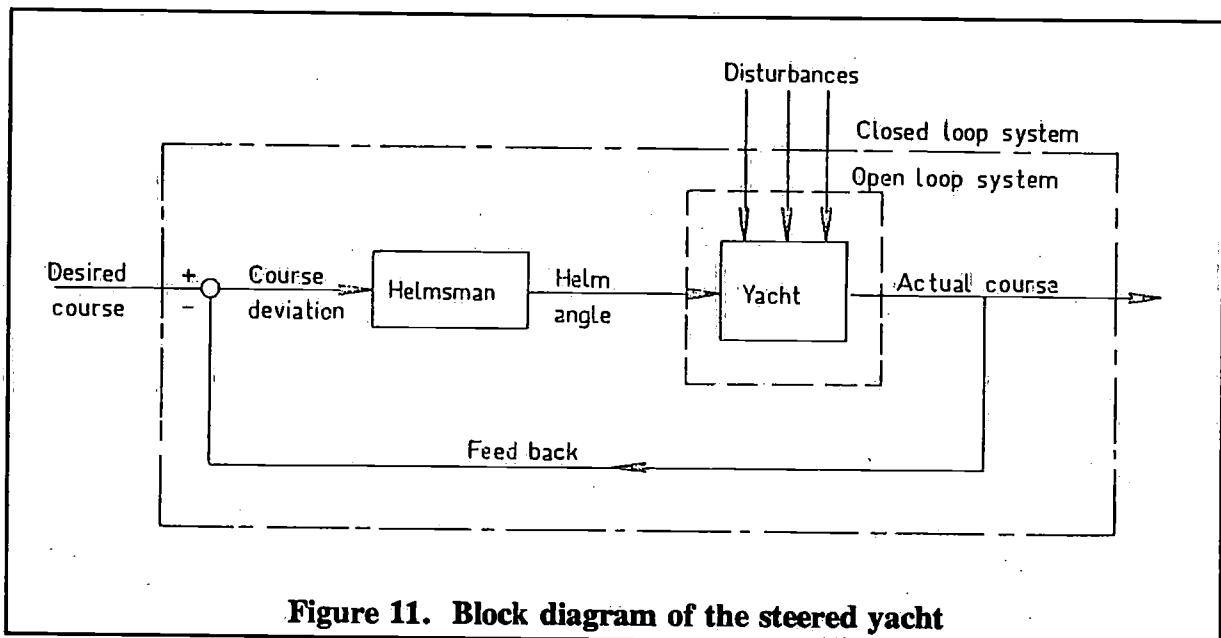


Figure 11. Block diagram of the steered yacht

4 The steering performance

4.1 Forces and moments exerted by the rudder

In Table 4 some experimentally determined forces and moments owing to rudder angle have been collected.

Table 4. Dimensionless side force and turning moment due to rudder angle

ship	$Y_s \cdot 10^5$	$N_s \cdot 10^5$
model 2811-1 (Spens [2])	1344	- 485
model 2811-2 (Spens [2])	1921	- 700
half ton yacht	3079	- 1563
Columbia	3280	- 800

In this table Y_δ is the side force divided by $\frac{1}{2}\rho V^2 L^2$ (ρ is mass density of water, V is ship speed, L is waterline length) N_δ is the turning moment divided by $\rho V^2 L^3$. All values are dimensionless in order to compare yachts of different size at different speed. From the steering point of view the turning moment is the most important. Table 4 shows that the models considered by Spens [2], see Figure 12, have a very poor rudder action, though the rudder separated from the keel (model 2811-2) was an improvement of the original configuration (model 2811-1). This one had the reputation to have bad steering properties. The 12 meter "Columbia", Figure 14, with its combined long keel and rudder, generates a large side force owing to the influence of a rudder angle upon the flow pattern around the whole keel. The rudder acts as a wing-flap.

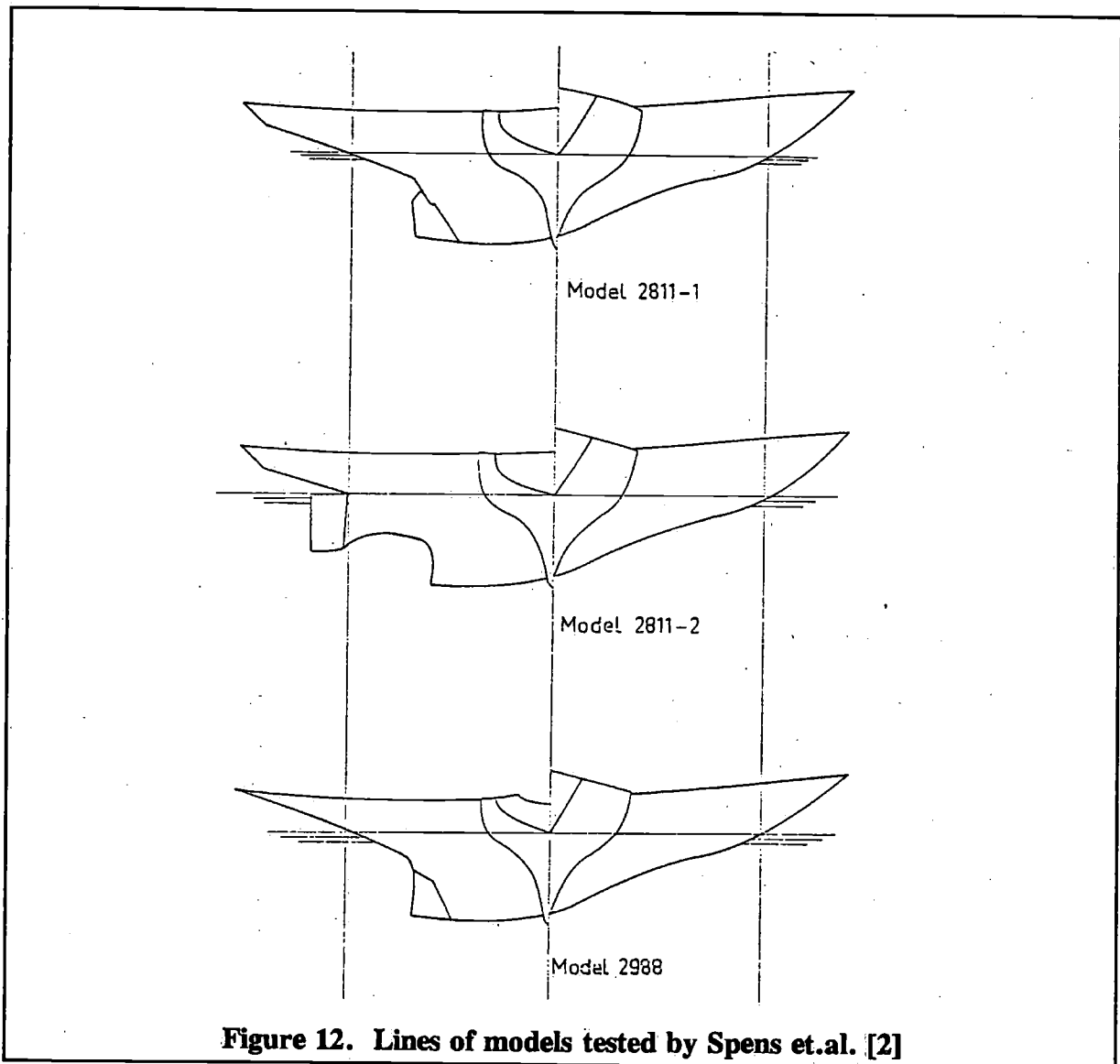


Figure 12. Lines of models tested by Spens et.al. [2]

However, due to the forward position of the rudder and because of the fact that the keel takes part in the additional side force generation, the turning effectiveness is about half that of the half ton model, see Figure 13. The rudder of this last yacht, separated from the keel and located well aft is from all considered cases by far the best steering device. The characteristics of the "Valiant" are of interest. The turning moment versus rudder angle plot of the "Columbia", Figure 15, shows a normal amount of linearity. The turning moment on the "Valiant" however, is not only much smaller but is also strongly non-linear, see Figure 15.

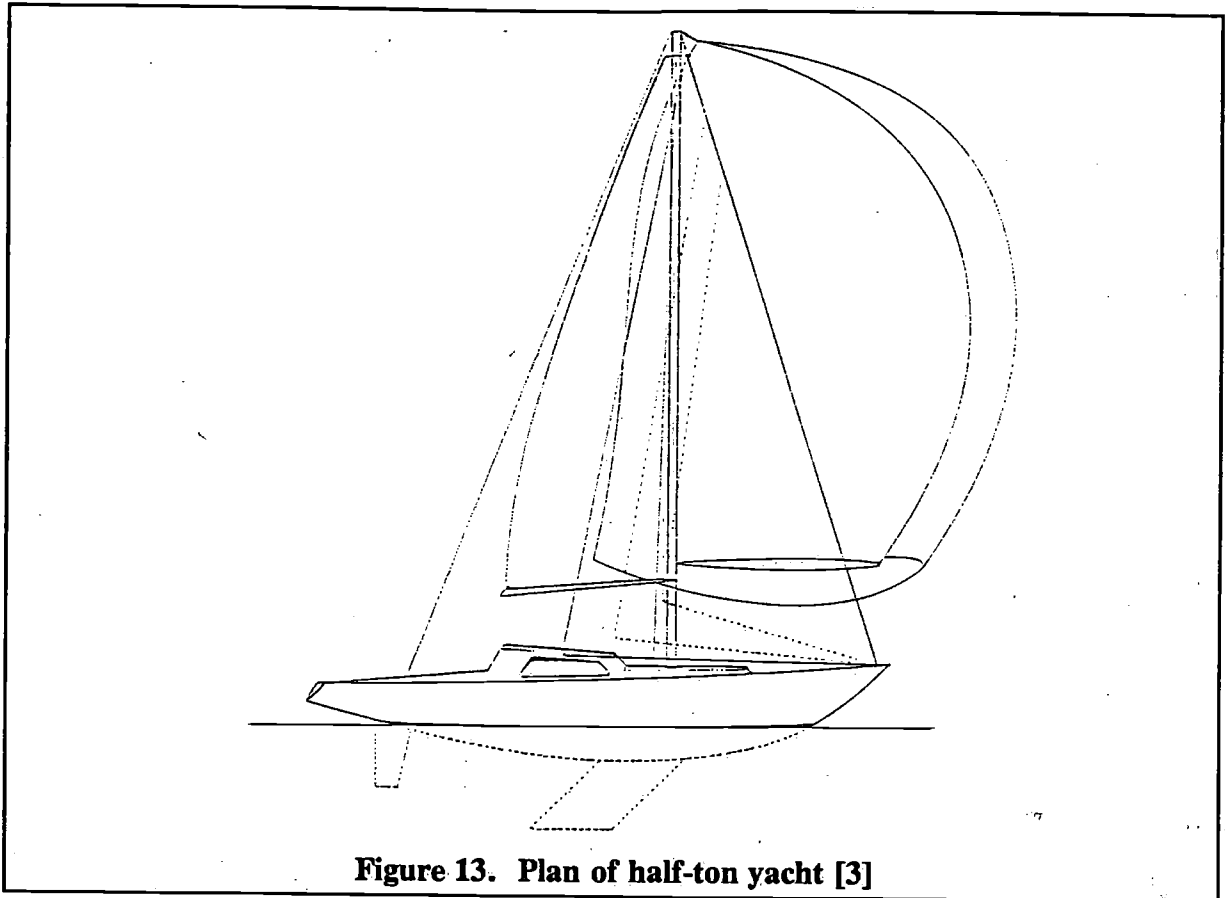


Figure 13. Plan of half-ton yacht [3]

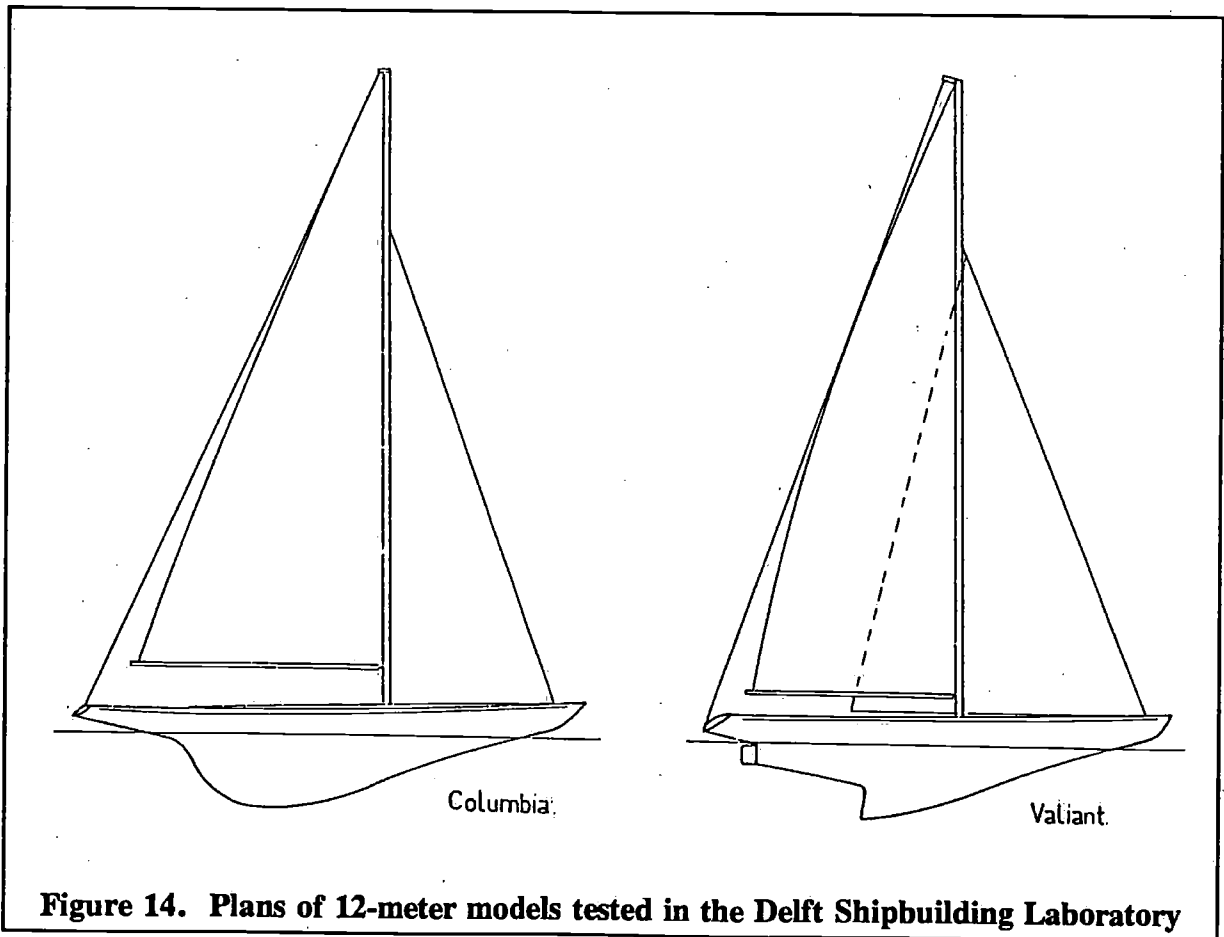


Figure 14. Plans of 12-meter models tested in the Delft Shipbuilding Laboratory

Due to flow separation at the blunt afterbody, the small rudder acts fully in the wake of the ship. At small rudder angles almost no turning moment is produced. Even a turning moment in the wrong direction has been observed, both in the towing tank and in practice. The width of the loop is about 25 degrees. If the helmsman of "Valiant" gives a rudder angle smaller than about 10 degrees, the ship could turn towards the opposite direction than it is supposed to do. During standard yacht performance tests in Delft, the same flow separation phenomena have been observed on several modern ocean racers with very full afterbodies. Both the windward performance and the turning properties could be improved in those cases by fairing the buttock lines. Yacht designers, when increasing the prismatic coefficient and shifting the centre of buoyancy more aft, should be aware of the adverse effects of too steep buttock lines.

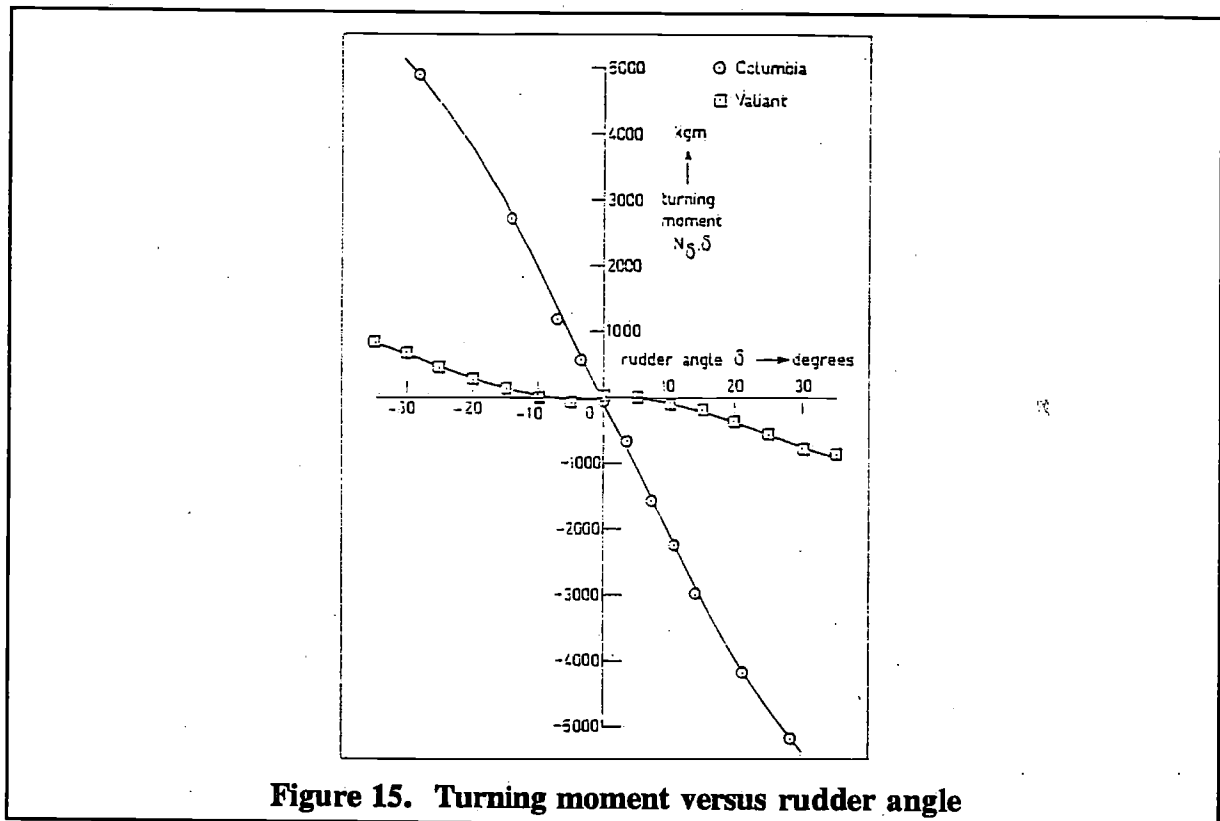


Figure 15. Turning moment versus rudder angle

4.2 The fixed controls behaviour

Static rotating arm and dynamic oscillation tests with ship models are used to determine the equations of motion, from which the fixed controls behaviour can be derived. Following the methods used in the manoeuvrability research of merchant ships Spens and others described the moving yacht with fixed rudder by the linear coupled equations of motion in sway and yaw, neglecting the roll motion:

$$Y_v \cdot v + (Y_{\dot{v}} - m) \cdot \dot{v} + (Y_{\dot{\psi}} - m) \dot{\psi} + Y_{\ddot{\psi}} \cdot \ddot{\psi} = 0$$

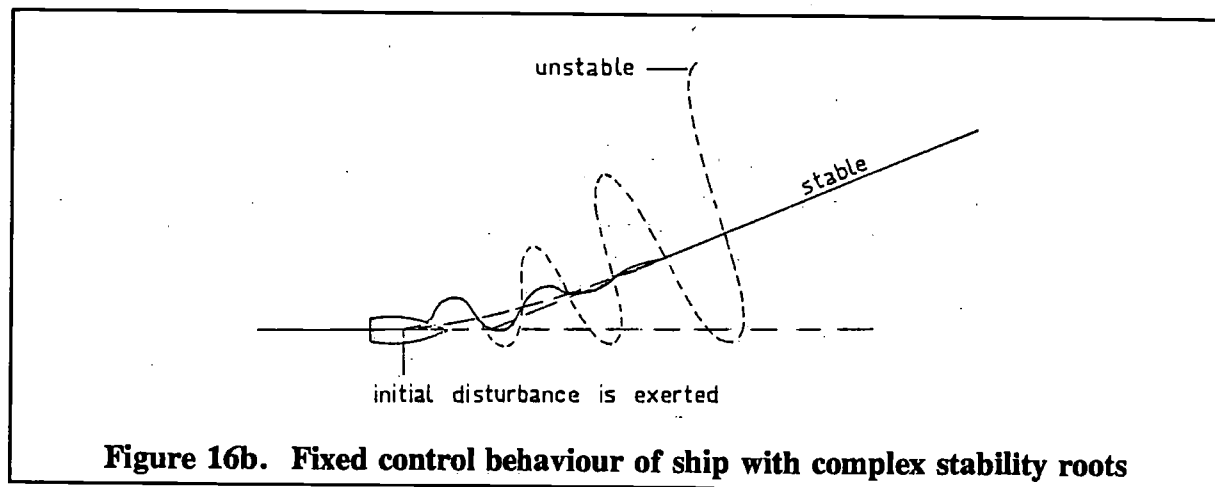
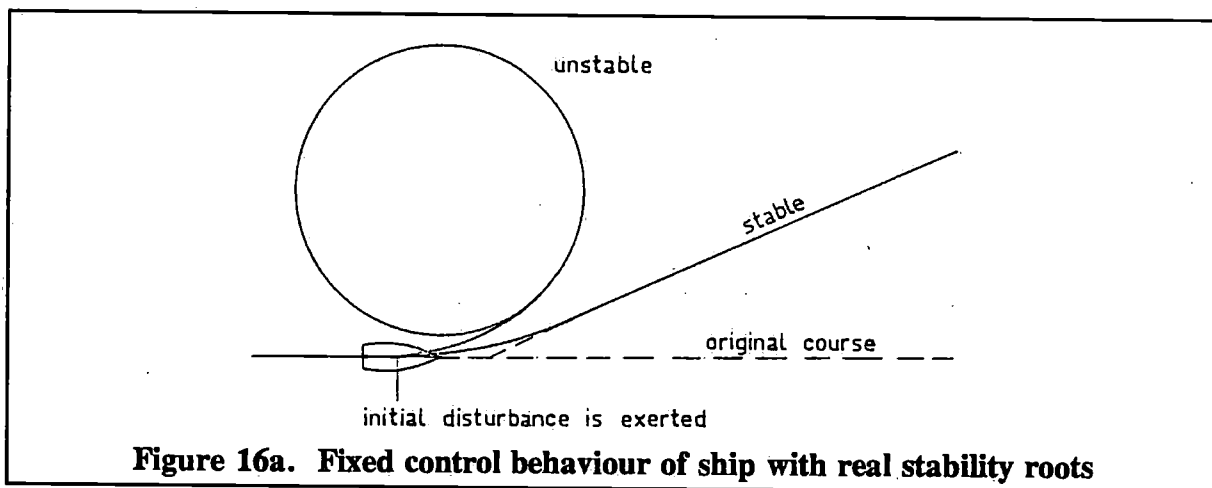
(4.2.1)

$$N_v \cdot v + N_{\dot{v}} \cdot \dot{v} + N_{\dot{\psi}} \cdot \dot{\psi} + (N_{\ddot{\psi}} - I_{zz}) \ddot{\psi} = 0$$

where: v = the sway velocity
 \dot{v} = the sway acceleration
 ψ = the yaw rate
 $\dot{\psi}$ = the yaw angular acceleration
 m = the mass
 Y_v, Y_{vv}, etc = derivatives of the sway force
 N_v, N_{vv}, etc = derivatives of the yaw moment

Table 5. Dimensionless stability roots of the coupled sway-yaw equations of motion

ship	S_1	S_2
model 2811-1 (Spens [2])	- 0.45	- 2.51
model 2811-2 (Spens [2])	- 1.66	$\pm 0.53 i$
model 2988 (Spens [2])	- 1.37	- 2.94
half ton yacht, $F_n = 0.243$ (1)[3]	- 2.60	$\pm 2.87 i$
half ton yacht, $F_n = 0.468$	- 1.37	$\pm 2.82 i$
Stormy with original bulb keel	- 2.32	$\pm 2.95 i$
Stormy with feen keel	- 2.06	$\pm 2.89 i$
Columbia, $F_n = 0.168$	- 1.60	$\pm 0.34 i$
„ , $F_n = 0.251$	- 1.53	$\pm 0.33 i$
„ , $F_n = 0.335$	- 1.47	$\pm 0.44 i$
Valiant , $F_n = 0.163$	- 0.33	- 3.03
„ , $F_n = 0.244$	- 0.25	- 2.91
„ , $F_n = 0.325$	- 0.58	- 3.88



The solution of the two equations gives the stability roots which determine the behaviour of the ship after an initial disturbance from the equilibrium condition, while the rudder (control) is fixed. If all roots are real and negative, the ship will, after an initial disturbance, come to a straight path again, see Figure 16a. It is called: fixed controls stable or it is said to have a positive fixed controls stability. If one of the roots is positive the ship is ultimately going to turn around a circle, still with the rudder fixed in the centre position, and is called to be fixed controls unstable.

If the roots are complex the fixed controls behaviour of the ship is oscillatory, see Figure 16b. The oscillation is damped and the ship is fixed controls stable if the real parts of the complex roots are negative. In the case of positive real parts the oscillation is undamped, which means a fixed controls instability.

In the first reports about manoeuvrability on sailing yachts [2],[3] the conclusions concerning the controllability were based upon the stability roots of the coupled sway-yaw equations (4.2.1.). These roots are mentioned in Table 5.

(1) Froude number is: $F_n = V/\sqrt{gL}$

where: V = ship speed in m/s
 g = acceleration of gravity in m/s²
 L = waterline length in m

The real parts of all roots are negative, which means that all ships have a fixed controls stability if they are considered to perform only swaying and yawing motions. In principle freedom in roll has to be considered too. Owing to the relatively large vertical distance between the lateral centre of keel and rudder and the centre of gravity, a sway or yaw motion introduces a rolling moment, while a roll motion gives sway forces and yaw moments. This hydrodynamic coupling in sway, roll and yaw cannot be neglected and must be expressed in the equations of motion, which are:

$$Y_v \cdot v + (Y_{\dot{v}} - m)\dot{v} + Y_{\phi} \cdot \phi + Y_{\dot{\phi}} \cdot \dot{\phi} + Y_{\ddot{\phi}} \cdot \ddot{\phi} + (Y_{\psi} - m)\dot{\psi} + Y_{\ddot{\psi}} \cdot \ddot{\psi} = 0 \quad (4.2.2)$$

$$K_v \cdot v + K_{\dot{v}} \cdot \dot{v} + K_{\phi} \cdot (\phi + K_{\dot{\phi}} \cdot \dot{\phi} + (K_{\ddot{\phi}} - I_{xx})\ddot{\phi} + K_{\dot{\psi}} \cdot \dot{\psi} + K_{\ddot{\psi}} \cdot \ddot{\psi} = 0$$

$$N_v \cdot v + N_{\dot{v}} \cdot \dot{v} + N_{\phi} \cdot \phi + N_{\dot{\phi}} \cdot \dot{\phi} + N_{\ddot{\phi}} \cdot \ddot{\phi} + N_{\dot{\psi}} \cdot \dot{\psi} + (N_{\ddot{\psi}} - I_{zz})\ddot{\psi} = 0$$

where: (in addition to the list of symbols after (4.2.1))

ϕ = the roll amplitude
 $\dot{\phi}$ = the roll angular velocity
 $\ddot{\phi}$ = the roll angular acceleration
 $K_v, K_{\dot{v}}, etc$ = derivatives of the roll moment

In Delft a technique has been developed to measure the sway force, roll moment and yaw moment when the yacht model performs forced harmonic oscillations in one of these modes of motion.

Compared with the roots of the basic sway-yaw system (Table 5) the calculated stability roots of the coupled sway-roll-yaw system (Table 6) show that the coupling with roll has a destabilizing influence. In some cases the system described in this way is even unstable.

Table 6. Dimensionless stability roots of the coupled sway-roll-yaw equations of motion

ship		S_1	S_2	S_3	S_4
half ton yacht,	$F_n = 0.243$	- 2.54 ±	2.99 i	- 0.53 ±	5.62 i
„ „ „ ,	$F_n = 0.486$	- 1.62 ±	3.14 i	- 0.22 ±	2.52 i
Columbia ,	$F_n = 0.168$	- 1.60 ±	0.34 i	0.11 ±	7.46 i
„ ,	$F_n = 0.251$	- 1.53 ±	0.33 i	0.10 ±	5.08 i
„ ,	$F_n = 0.335$	- 1.49 ±	0.40 i	- 0.20 ±	3.81 i
Valiant ,	$F_n = 0.163$	- 0.32	- 3.04	- 0.39 ±	8.39 i
„ ,	$F_n = 0.244$	- 0.24	- 2.94	- 0.51 ±	5.45 i
„ ,	$F_n = 0.325$	- 0.53	- 3.88	- 0.43 ±	3.97 i

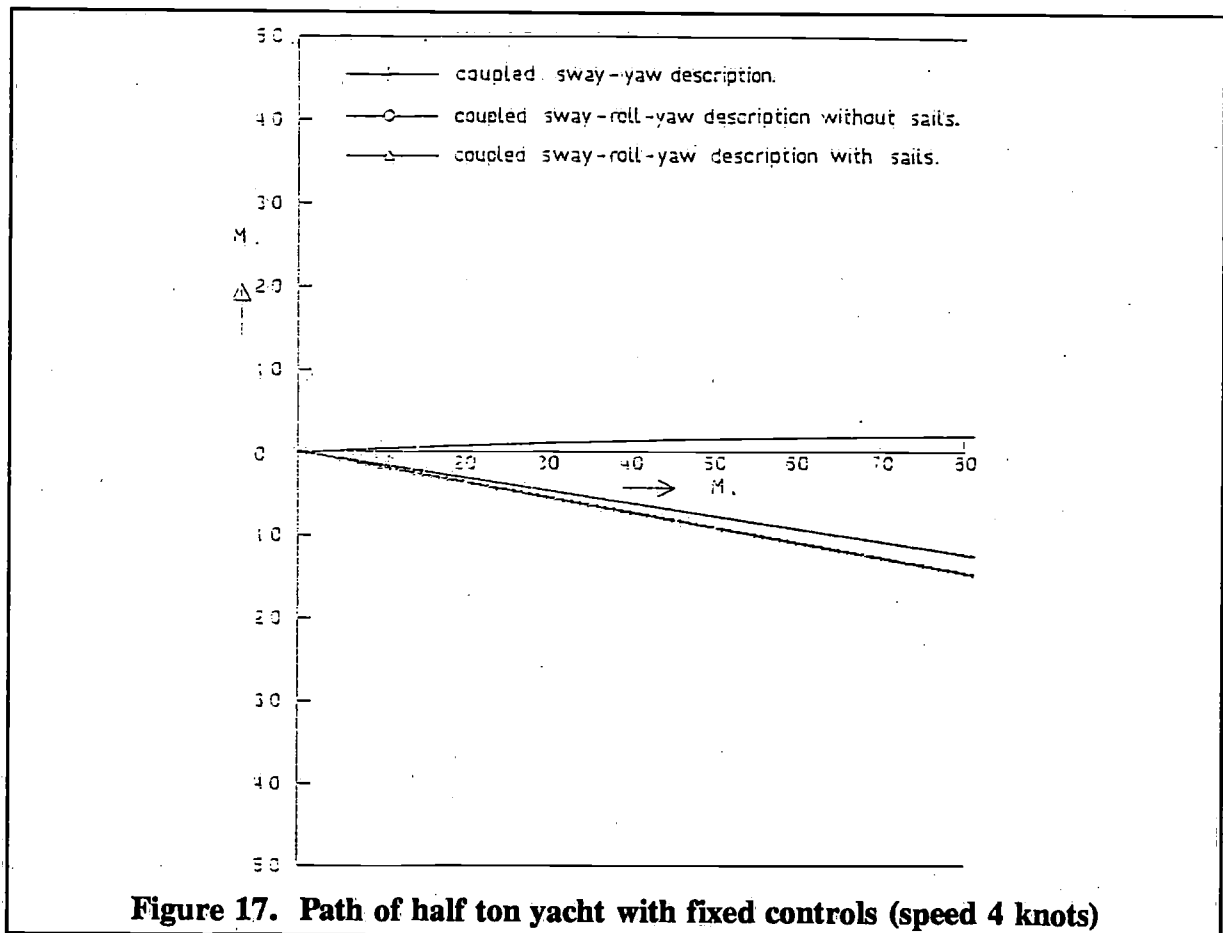


Figure 17. Path of half ton yacht with fixed controls (speed 4 knots)

For sailing yachts it is necessary to make another extension to the equations (4.2.2). Every motion changes magnitude and direction of the apparent wind, which has its influence on the sail force.

By using in the downwind condition the simple concept of a mainsail and spinnaker which blows in the apparent wind direction and gives only forces because of its drag properties, the changes in sail force can be calculated. Because of its mutual independence hydrodynamic and

aerodynamic forces can be added to form a new set of equations of motion. They are similar to the system shown in (4.2.2), except for additional terms dependent upon the course deviation ψ .

These follow from the dependency of the aerodynamic forces on the wind direction and cause the appearance of a fifth stability root (see Table 7).

Table 7. Dimensionless stability roots of the coupled sway-roll-yaw equations of motion including aerodynamic forces

ship		S_1	S_2	S_3	S_4	S_5
half ton yacht,	$F_n = 0.243$	- 2.50 ±	2.98 i	- 1.54 ±	5.51 i	- 0.02
” ” ” ,	$F_n = 0.486$	- 2.27 ±	1.35 i	- 1.72 ±	3.22 i	0.32
Columbia ,	$F_n = 0.168$	- 1.61 ±	0.36 i	- 1.13 ±	7.38 i	-0.02
” ,	$F_n = 0.251$	- 1.56 ±	0.35 i	- 1.19 ±	4.94 i	- 0.01
” ,	$F_n = 0.335$	- 1.60 ±	0.48 i	- 1.61 ±	3.37 i	0.04
Valiant ,	$F_n = 0.163$	- 0.38	- 3.08	- 1.78 ±	8.19 i	0.04
” ,	$F_n = 0.244$	- 0.37	- 3.01	- 1.91 ±	5.08 i	0.09
” ,	$F_n = 0.325$	- 0.74	- 3.97	- 1.76 ±	3.59 i	0.16

It can be seen from the value of this root that the extension of the system with aerodynamic forces has a further destabilizing influence in most of the cases.

The influence of the way in which the moving system is described (coupled sway-yaw, coupled sway-roll-yaw without sails or coupled sway-roll-yaw with sails), on the predicted controls fixed behaviour of the half ton yacht is demonstrated in Figure 17 for a finally stable condition and in Figure 18 for a finally unstable condition.

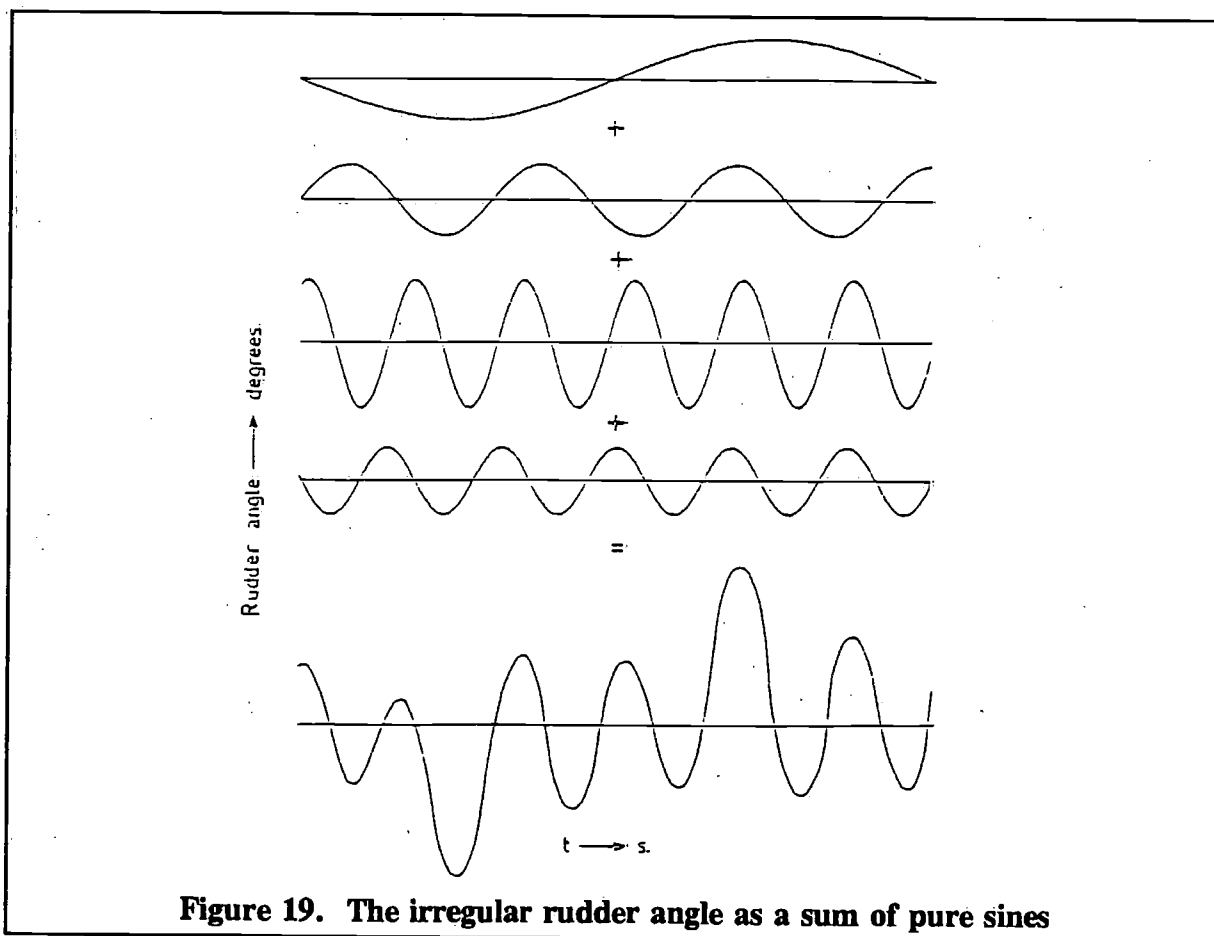
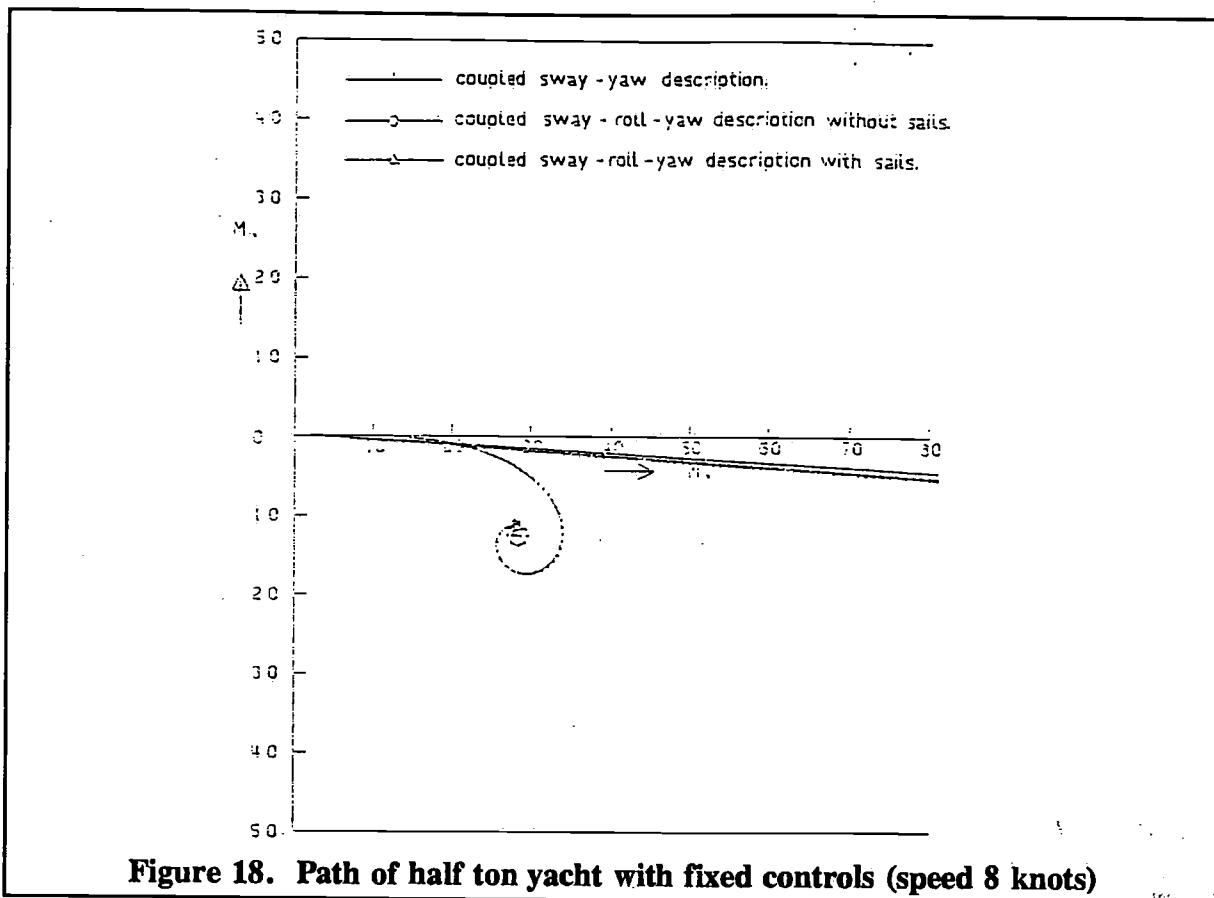
The most realistic description of the motion of a sailing yacht is the coupled sway-roll-yaw equations of motion, including hydrodynamic and aerodynamic forces.

Before continuing this paper attention will be paid to the significance of the stability roots, to realise what the fixed controls behaviour means in the process of steering a sailing yacht. The helmsman of a big merchant ship, like a supertanker, will not continuously react to any course deviation, but only change the rudder angle if the course deviation has surpassed a certain threshold. From then on, the rudder will be kept in the same position until the threshold is reached in the other direction. If the ship, because of its mass, is reacting very slowly, the period between two successive rudder actions will be long. Consequently the path and motions of a large heavy ship will mostly be governed by its controls fixed behaviour (with initial conditions), expressed in the degree of stability.

Small ships like sailing yachts, because of their much smaller mass, react much faster and consequently the time delay between a rudder action and its recognisable effect is very small. The helmsman is forced to perform a nearly continuous rudder action to neutralize the effects of disturbances and his own earlier rudder action.

Thus, the analysis of the steering and manoeuvring abilities should be extended to include the helmsman's performance. It is probable that the kind of steering device, wheel or helm, influences the steering tactics, which should be included in the analysis.

The absolute values of the stability roots determine the time constants of the system. As long as these have the same order of magnitude as the time constants of human beings, which is nearly always true for sailing yachts, the system can be steered, whether it has a positive controls fixed stability or not. It can only be said that a very unstable system will probably be much more difficult to steer than a stable, neutral or only slightly unstable one.



The time constants are very clearly visualised in Bode-diagrams, which will be discussed in the next chapter. Not much is known about the influence of the shape of the Bode-diagram upon the helmsman's performance, that is to say upon the "steering compliance" of the ship and its controls.

At last it must be noted that long keel yachts do not have the better controls fixed stability believed by many sailors.

4.3 The behaviour with a continuous rudder action

If the rudder angle variation is assumed to be continuous it can be considered as the sum of an infinite number of pure sines, all with their own amplitude and frequency, see Figure 19. Because the steered yacht (the open loop system in Figure 11) is assumed to be linear, the total response to the irregular rudder angle is equal to the sum of the responses to each sinusoidal component. This response component is also a pure sine. Let us consider one of the components with a circular frequency ω . The rudder angle component, with amplitude ζ_a , is:

$$\zeta(t) = \zeta_a \sin(\omega t) \quad (4.3.1)$$

After adding the forces and moments due to this rudder angle to the equations of motion, the course deviation ψ can be obtained as:

$$\psi(t) = \psi_a \sin(\omega t + \epsilon_\psi) \quad (4.3.2)$$

where: ψ_a = the course deviation amplitude
 ϵ_ψ = the phase angle between rudder angle and course deviation
 t = a time parameter

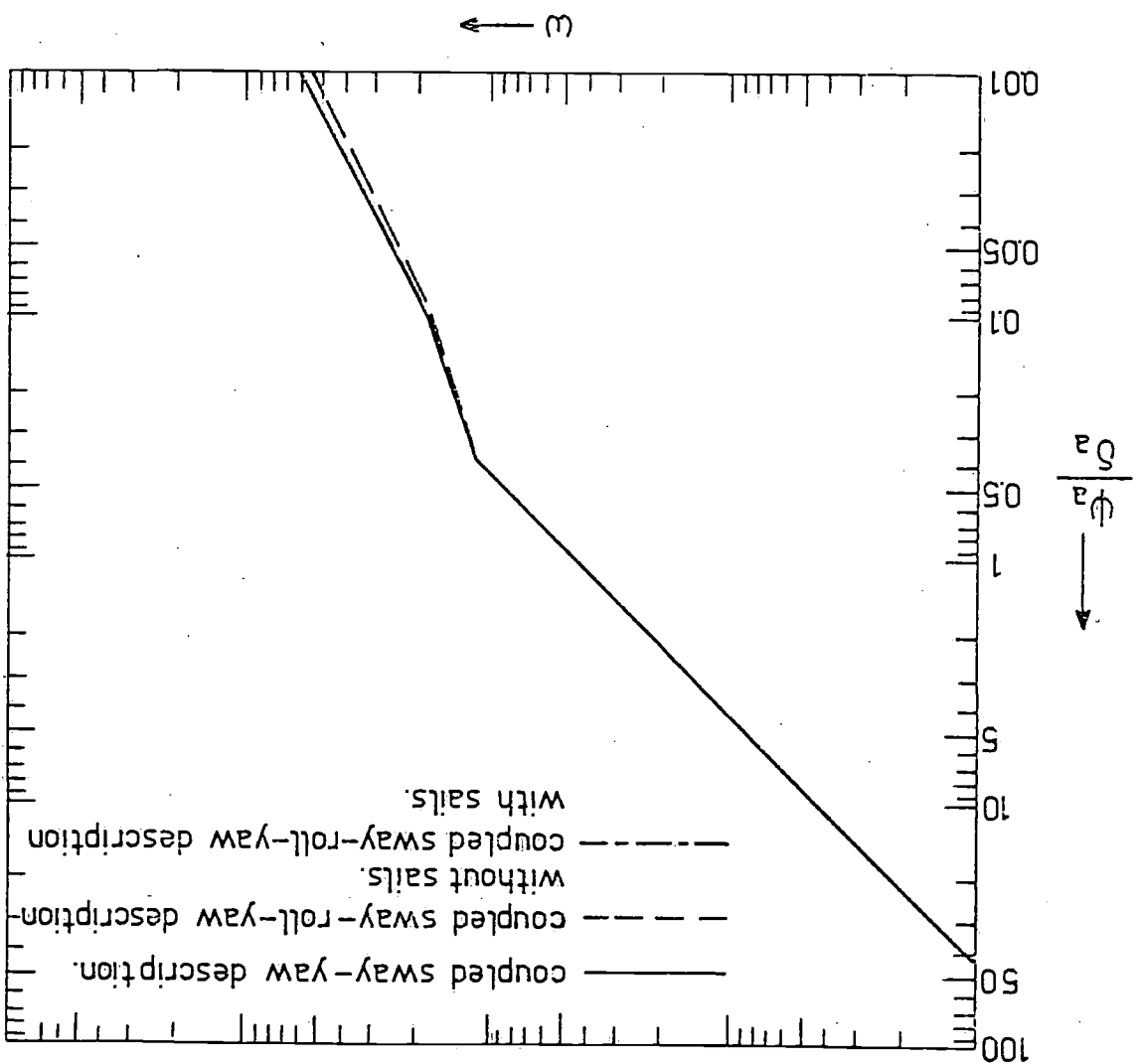
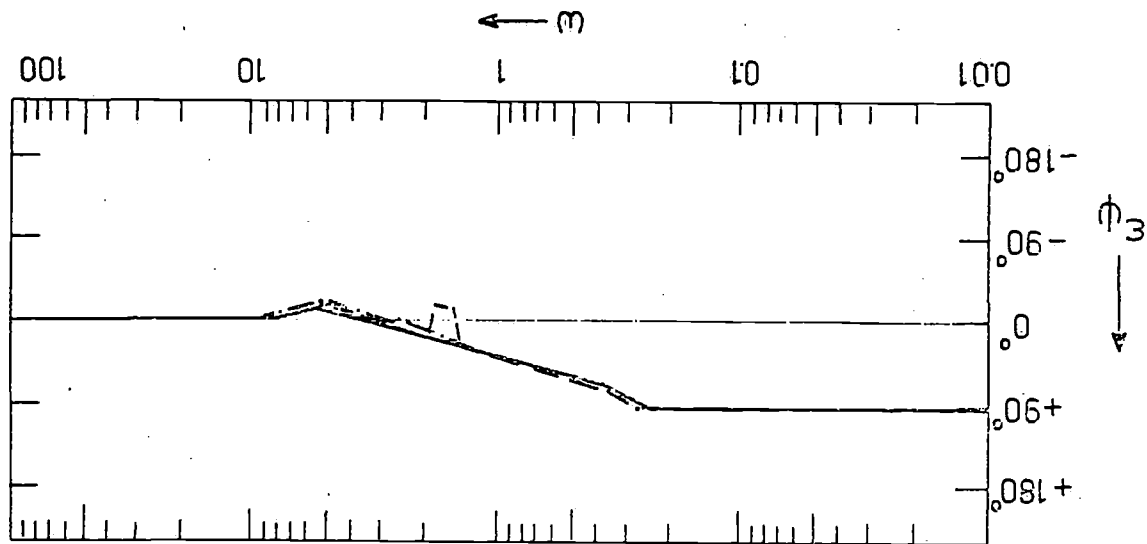
With a given rudder angle amplitude the resulting course deviation amplitudes and phases can be calculated for a range of circular frequencies ω .

In control engineering the plot of the amplification factor or response amplitude operator, defined as ψ_a/δ_a , versus circular frequency ω , is called the Bode-diagram of the system. Following the method of the preceding chapter to construct the equations of motion, the Bode-diagram can be calculated for the yacht considered as a system performing coupled sway-yaw motions (according to (4.2.1) extended with rudder forces), performing coupled sway-roll-yaw motions without sails (according to (4.2.2) extended with rudder forces) or performing coupled sway-roll-yaw motions with sails. This has been done for the half ton yacht at a speed of 4 knots, see Figure 20, and 8 knots, see Figure 21, and for the "Columbia" at a speed of 4 knots, see Figure 22.

The frequency range of interest consists of those frequencies which form a significant contribution in the helmsman's irregular rudder action, say between $\omega = 0.2$ and $\omega = 4$ (periods between 1½ and 30 seconds).

A comparison of the Bode-diagrams in this range shows that there is only a slight difference in the response to a sinusoidal rudder action if only coupled sway and yaw motions are

Figure 20. Bode-diagram of half ton yacht (speed 4 knots)



considered, or if the description of the system is extended with a coupled roll motion and aerodynamic forces.

We arrive at the same conclusion when the general response function is derived from the equations of motion as:

$$\begin{array}{c} \text{sway-yaw} \quad \text{coupling with roll} \\ \text{coupling} \end{array}$$

$$H_{\psi}(s) = \frac{\psi}{\delta} = K_{\psi} \frac{(\tau_d s+1)(\tau_{dd} s^2 + \tau_{ed} s+1)}{(\tau_c s+1)\left(\frac{s^2}{\omega_b^2} + \frac{2\beta_b}{\omega_b} s+1\right)\left(\frac{s^2}{\omega_r^2} + \frac{2\beta_r}{\omega_r} s+1\right)} \quad (4.3.3)$$

$$\begin{array}{c} \text{course de-} \quad \text{sway-yaw} \quad \text{coupling with roll} \\ \text{pendency} \quad \text{coupling} \end{array}$$

The time constants τ , frequencies ω and relative damping factors β can be expressed in the stability derivatives

$$Y_v, K_v, N_v, Y_{\dot{v}}, K_{\dot{v}}, N_{\dot{v}}, Y_{\phi}, \text{ etc.}$$

From an order of magnitude analysis of the derivatives it can be concluded that the terms due to the added coupling with roll nearly cancel each other. Besides, the time constant τ_c , due to the inclusion of the sail forces, is generally so large that $(\tau_c * \delta + 1)$ can be approximated by $\tau_c * \delta$. So, a useful representation of the response function is given by:

$$H_{\psi}(s) = \frac{\tau_d s+1}{\tau_i s\left(\frac{s^2}{\omega_b^2} + \frac{2\beta_b}{\omega_b} s+1\right)} \quad (4.3.4)$$

with: $\tau_i = \tau_c / K_{\psi}$

The response function of the system, regarded as a hull performing only coupled sway and yaw motions has exactly the same form as (4.3.3), while the values of the parameters are nearly equal.

Thus, in considering the response of the sailing yacht to a continuous rudder action by the helmsman, the total system of the swaying, rolling and yawing hull with sails can successfully be simplified to the swaying and yawing hull only.

The parameters in the simplified response function, can be determined with forced oscillation tests, which has been standardized in some towing tanks for manoeuvrability research of merchant ships.

As we have finished the preceding chapter with a judgement of the importance of the controls fixed behaviour, we have to do the same here for the behaviour due to a continuous rudder action.

Every tendency of the yacht to deviate from its course, or even to broach, will be introduced by disturbances due to wind and waves. Because of the fast response of the ship to disturbances, the helmsman nearly immediately recognises this tendency and tries to neutralize it with a rudder action, which in his turn has a quick response. If the steering power of a yacht is translated as the power to neutralize disturbing influences, it is best expressed by the response amplitude operator, or amplification ratio of course deviation and rudder angle. The higher the response amplitude operator, the better the steering power.

This criterion must mainly be applied in the frequency range of the significant disturbances which is, depending upon the ships size, roughly estimated, from $\omega \approx 0.5$ to about $\omega \approx 6$, (periods from 1 to 12 seconds, corresponding with stern waves from 4 to 60 meters length or with wind gusts). Because the value of time constants, deduced from the stability roots, affects also the form of the Bode-diagrams, these relatively simple figures contain all information necessary to judge the steering qualities of a yacht. Unless more research will be done concerning the influence of system characteristics (Bode-diagram) upon the helmsman's behaviour, the interpretation will be difficult from the handling point of view.

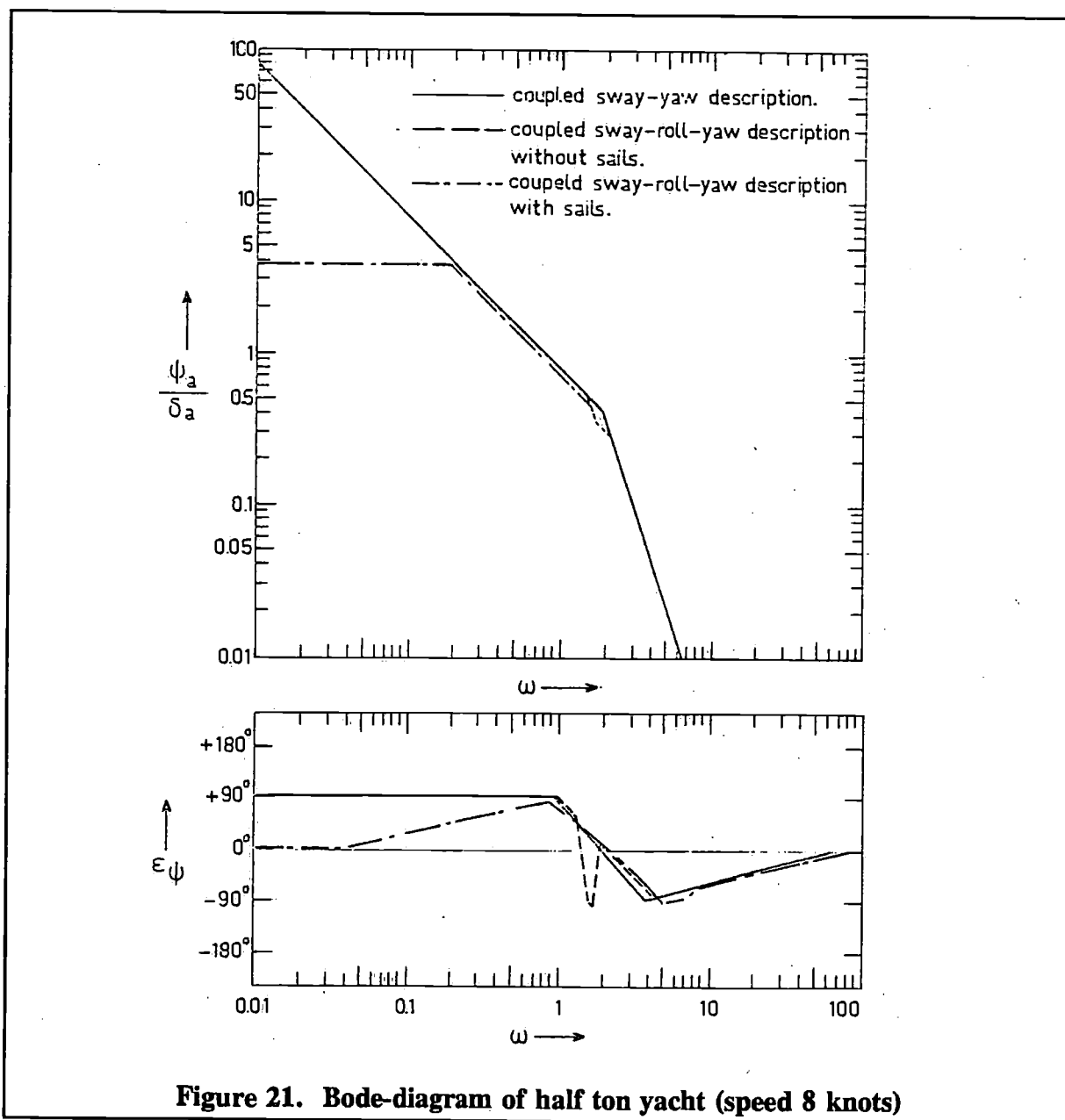


Figure 21. Bode-diagram of half ton yacht (speed 8 knots)

5 Conclusion

5.1 On seakeeping

It may be concluded that a reduction of the longitudinal radius of gyration is favourable for the windward performance of a yacht. If a weight of 1% of a yacht's displacement is shifted from amidships towards one of the ends, a 25% radius of gyration will increase to 25.5%, with a corresponding total resistance increase of about 1%. A more drastic change of the longitudinal weight distribution has of course a larger effect on the yacht's resistance in waves.

When constant draught is considered in a design, large displacement yachts have less efficient fin keels, due to the fact that the deeper hull reduces the span of the fin. Although the large displacement yacht has the lowest resistance per ton displacement in the upright condition and a small advantage with respect to the added resistance in waves percentage wise, the less efficient fin keel seems to be the cause of a less favourable windward performance, when compared with lighter displacement hulls.

Large displacement yacht's have a slightly larger pitching motion in seawaves.

It may also be concluded that model experiments in the still water condition remain a meaningful tool for the designer of sailing yachts.

5.2 On steering

The "steering power" of a yacht can be increased by using a well situated separated fin keel and rudder.

The realistic coupling of roll with sway and yaw; and the inclusion of aerodynamic forces in the equations of motion of a yacht, sailing off the wind, has a destabilizing influence on the controls fixed stability. However, in most cases, the controls fixed behaviour and stability have no direct influence upon the ships course and controllability characteristics.

The fast reaction of a yacht forces the helmsman to a continuous rudder action. The Bode-diagram, from which the response to such an action can be derived directly, contains the necessary information to judge the steering qualities. The assumption of linearity, which must be made for constructing the Bode-diagram, is valid unless uncommon hull or rudder forms or badly located rudders are concerned. In deriving the Bode-diagram the reality of the coupled swaying, rolling and yawing yacht with sails (on a downwind course) can successfully be simplified by considering the coupled swaying and yawing hull only.

Research on the steering behaviour of the helmsman of a sailing yacht is necessary in order to consider all aspects of its controllability.

6 Acknowledgement

The authors are indebted to Sparkman and Stephens who kindly provided detailed information of "Columbia" and "Valiant", to Frans Maas and E.G. van de Stadt who put the designs of respectively the "Systematic Series" and the "Stormy" to their disposal. The motion and added resistance tests of "Columbia" and "Valiant" were carried out by Joost van Santen.

7 References

- [1] K. Davidson,
Experimental studies of the sailing yacht,
The Society of Naval Architects and Marine Engineers, 1937

- [2] P.G. Spens, P. de Saix and P.W. Brown,
Some further experimental studies of the sailing yacht,
The Society of Naval Architects and Marine Engineers, 1967
- [3] J. Gerritsma,
Course keeping qualities and motions in waves of a sailing yacht,
Proceedings of the third AIAA Symposium on the Aero/ hydrodynamics of sailing,
California, 1971
- [4] J. Gerritsma and W. Beukelman,
Analysis of the resistance increase in waves of a fast cargo ship,
International Shipbuilding Progress, 1972
- [5] Yachting World, Annual 1972,
London life books
- [6] P.G. Spens,
Sailboat test technique,
Davidson Laboratory, Stevens Institute of Technology Technical Memorandum no. 124,
1958

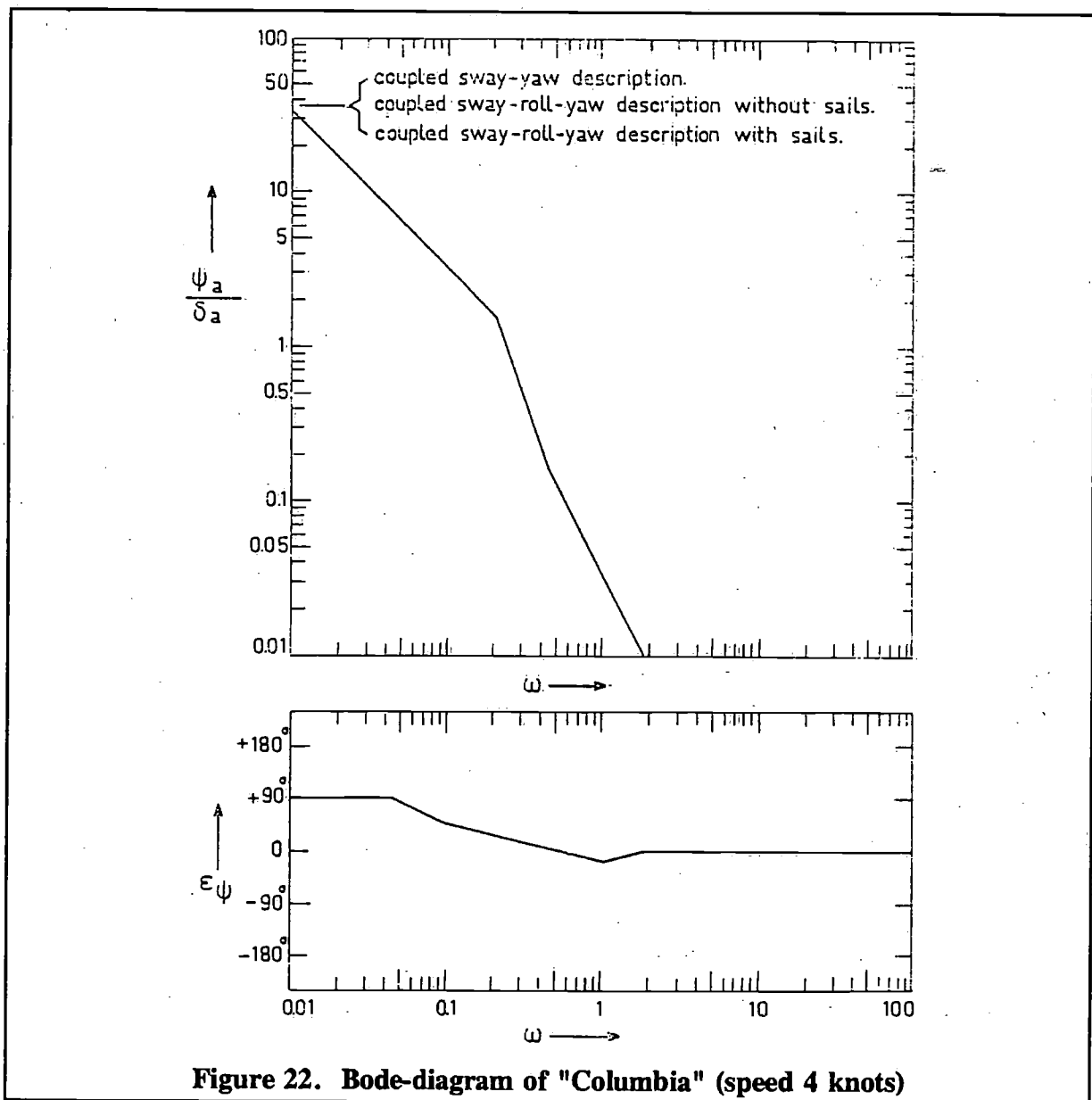


Figure 22. Bode-diagram of "Columbia" (speed 4 knots)

Sailing yacht keels

by Justin E. Kerwin* and Halsey C. Herreshoff**

* Massachusetts Institute of Technology
Cambridge, Massachusetts, USA

** Halsey C. Herreshoff
Boston, Massachusetts, USA

Abstract

Lift and induced drag of a yacht hull is treated by the concept of an "equivalent keel." Lifting surface calculations are used to compare the performance of different keel Planforms. Water tunnel tests show lift and drag comparisons for several configurations of keel tips. Quantitative information on the effects of keel shape variations on lift and drag are provided to assist the designer in the selection of optimum keel proportions.

1 Introduction

One characteristic of current hull design for ocean racing yachts is the appearance of the keel as a distinct appendage. This has been a consequence of several trends:

- a. Hull depths amidships have reduced as a result of decreasing displacement and increasing maximum beam.
- b. Maximum draft has increased as a result of taller rigs and greater stability.
- c. Keel chord lengths have been reduced to minimize wetted surface.

As a result, keels now look like wings or control surfaces, and analytical and experimental techniques for their design should be applicable. Since all keels perform the same function, one might expect that all keels would have similar appearance. This, however, is far from true; some protrude straight down while some are highly swept back; great variations exist in the ratio of tip chord to root chord; some keels have square tips, some have vee shaped tips and some have bulbs.

It would seem instructive, therefore, to examine the influence of such variations on the hydrodynamic characteristics of a keel alone. One should keep in mind, however, that such results must be combined with an evaluation of the keel as a ballast container and as a contributor to the overall wave making resistance. These latter two considerations are not within the scope of this paper.

If the speed/length ratio of the yacht is sufficiently small, wave effects become negligible, and it is proper from a hydrodynamic point of view to consider the flow around the actual keel and its reflection about a rigid plane parallel to the water surface. From the standpoint of keel lift and induced drag this approximation is also reasonably accurate at higher speeds.

It is not correct to consider a keel entirely exclusive of a hull because the existence of the hull above directly contributes lift. Slender body theory [1] provides a means for determining analytically the lift and drag of a yacht-like body with one or more fins. One

consequence of this theory is that for a fixed ratio of body "radius", r_o , to span, b_o , the lift force is given by the expression

$$L = C\rho\pi V^2 b_o^2 \alpha \quad (1)$$

where ρ is the fluid density, V is the speed, α is the angle of attack and C is a coefficient which depends on r_o/b_o . We can interpret r_o as being the depth of the hull and b_o as the draft as shown in Figure 1. For the limiting case when r_o/b_o equals 0, the value of the coefficient C would be unity. This decreases to a value of 0.69 for r_o/b_o equals 0.5.

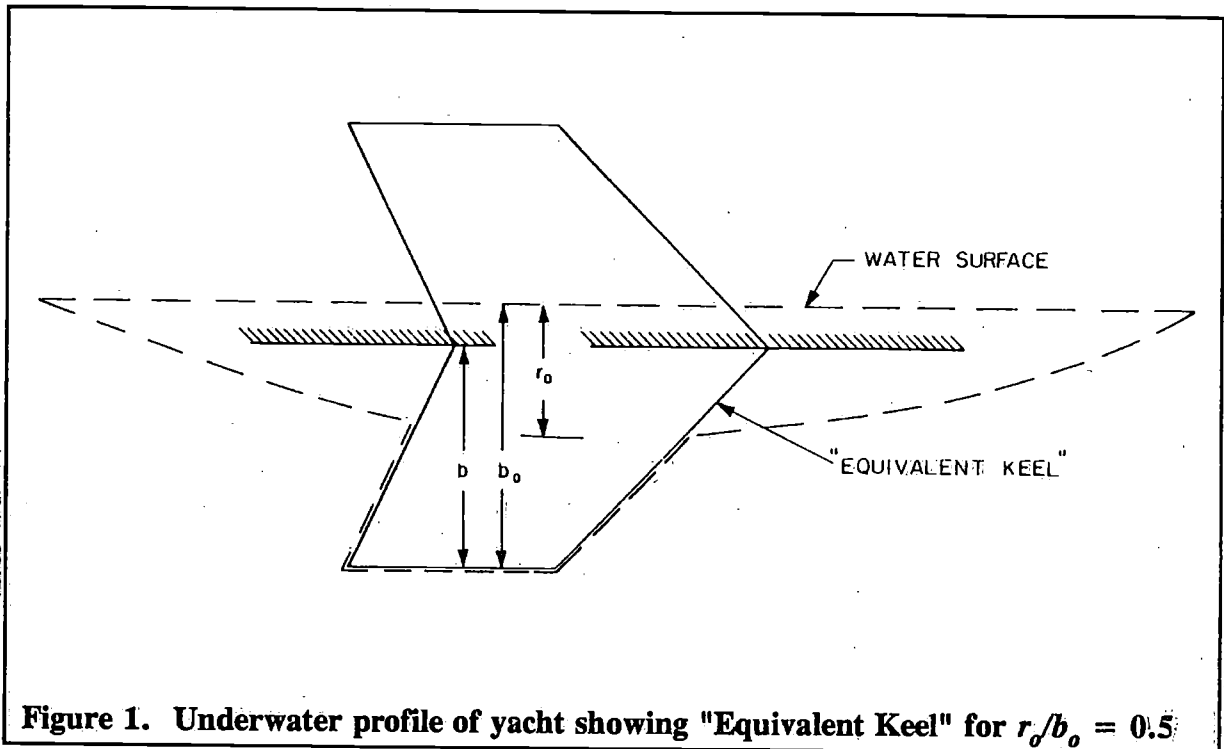


Figure 1. Underwater profile of yacht showing "Equivalent Keel" for $r_o/b_o = 0.5$

For a fixed hull depth and draft, (1) indicates that the lift is independent of the area and particular shape of the keel. If we were to test a hull having a keel with an extremely long chord and gradually shorten the chord, we would find experimentally that the lift would initially be practically unchanged, thus verifying (1). However, as the keel aspect ratio increased sufficiently as a result of shortening the chord, the lift would eventually decrease. This contradiction is due to the fact that the assumptions of the slender body theory are violated if the local aspect ratio of the fin becomes too high. As a result, changes in aspect ratio and shape of a yacht keel, for a fixed draft, do affect performance and cannot be predicted by slender body theory. However, slender body theory still provides the correct conclusion that draft is by far the most important parameter affecting keel performance.

To study a keel alone, both theoretically and experimentally, one possible way of accounting for the hull is as follows. Suppose that we use slender body theory to find the draft, b , of an "equivalent keel" which produces the same lift as the combination of hull and keel for a particular value of r_o/b_o , as shown in Figure 1. For $r_o/b_o = 0.5$, we can see from (1) that

$$b/b_o = \sqrt{.69} = 0.83 \quad (2)$$

Consequently, the equivalent keel protrudes into the hull to a point approximately two thirds of the distance from the hull-keel juncture to the water surface.

The "equivalent keel" concept permits us to make both theoretical and experimental studies of the keel alone. Overall lift and details of flow at the tip should be well portrayed by such a theoretical or experimental model. However, details of the flow in the neighborhood of the hull-keel intersection could not be expected to be reproduced exactly.

2 Lifting-surface theory calculations

The effective aspect ratio of typical modern ocean racing yacht keels is in the range from one to three. This is too high for low aspect ratio theory and too low for high aspect ratio theory to be valid. Consequently, the effect of planform variations on lift and induced drag can only be obtained theoretically by means of numerical computation employing lifting-surface theory.

Until recently, only a limited number of computed results were available in this aspect ratio interval in the literature. Computer programs for this purpose are now much more readily available, so that it is practical to obtain systematic results for planform variations in a range suitable for yacht keels.

A series of calculations is presented in this paper, made with a computer program recently developed at M.I.T. to predict the performance of flapped rudders [2]. This program was written specifically to accept general trapezoidal planform shapes of any aspect ratio, α ; quarter-chord sweep angle, Λ , and taper ratio, λ .

The method of calculation employs a vortex lattice technique consisting of a large number of concentrated vortex lines. One set consists of spanwise elements running along lines of constant percent of chord and a second set running in the streamwise direction. The circulation distribution is assumed to be approximated by a 36 term series consisting of six spanwise and six chordwise modes of unknown amplitude. The velocity is computed at 64 control points distributed over the surface, and the unknown circulation mode amplitudes are obtained by least-squares.

The results of the first series of computations appear in Figure 2. In this case the geometric aspect ratio is held constant at $\alpha = 0.81$, and the effective aspect ratio, obtained by reflecting the planform about the root section is $\alpha = 1.62$. The taper ratio, λ , is 0.66. Four values of quarter-chord sweep angle, Λ , were chosen, ranging from zero to 51 degrees.

The results given are the lift slope, $C_{L\alpha}$, and the efficiency, η . The induced drag coefficient C_{Di} may be obtained from this efficiency as follows:

$$C_{Di} = \frac{C_L^2}{\pi\alpha\eta} \quad (3)$$

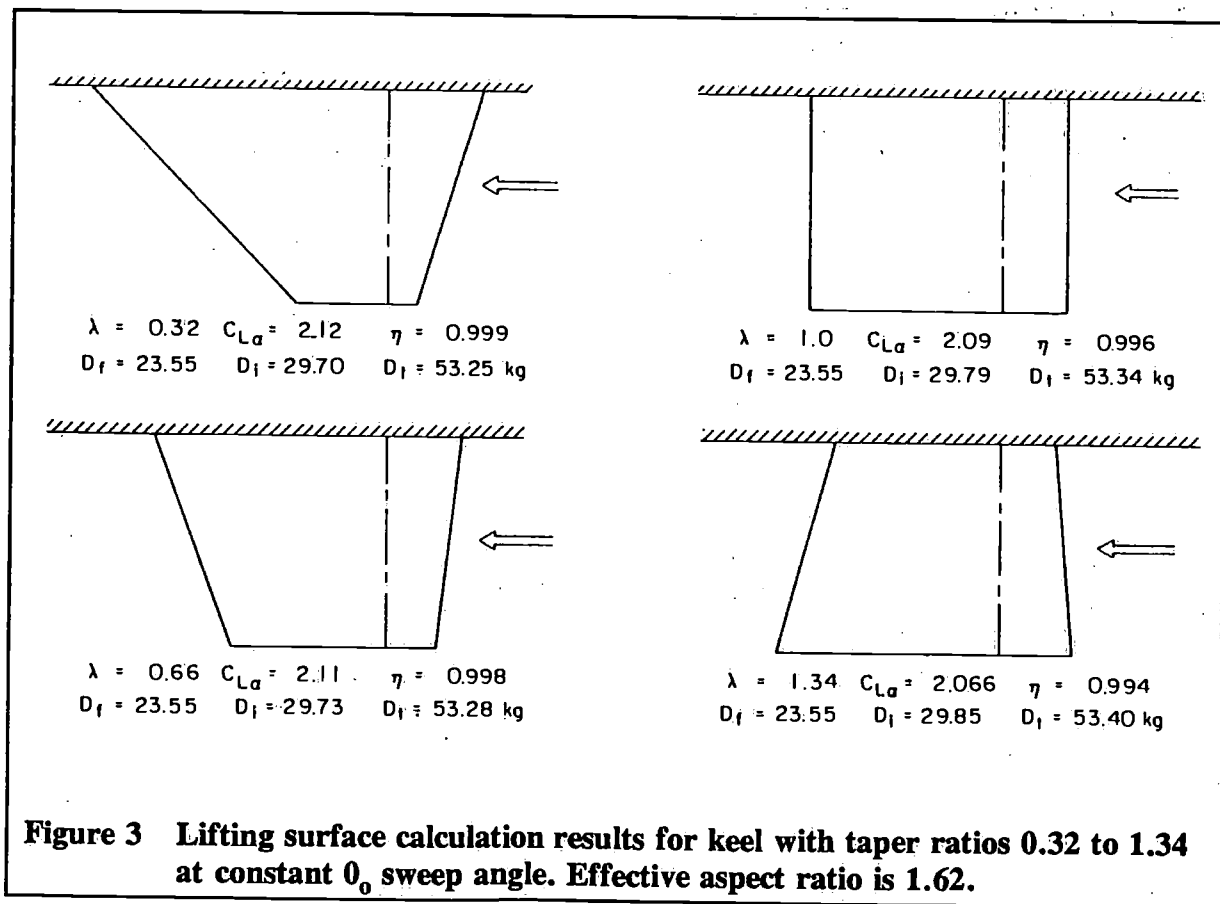
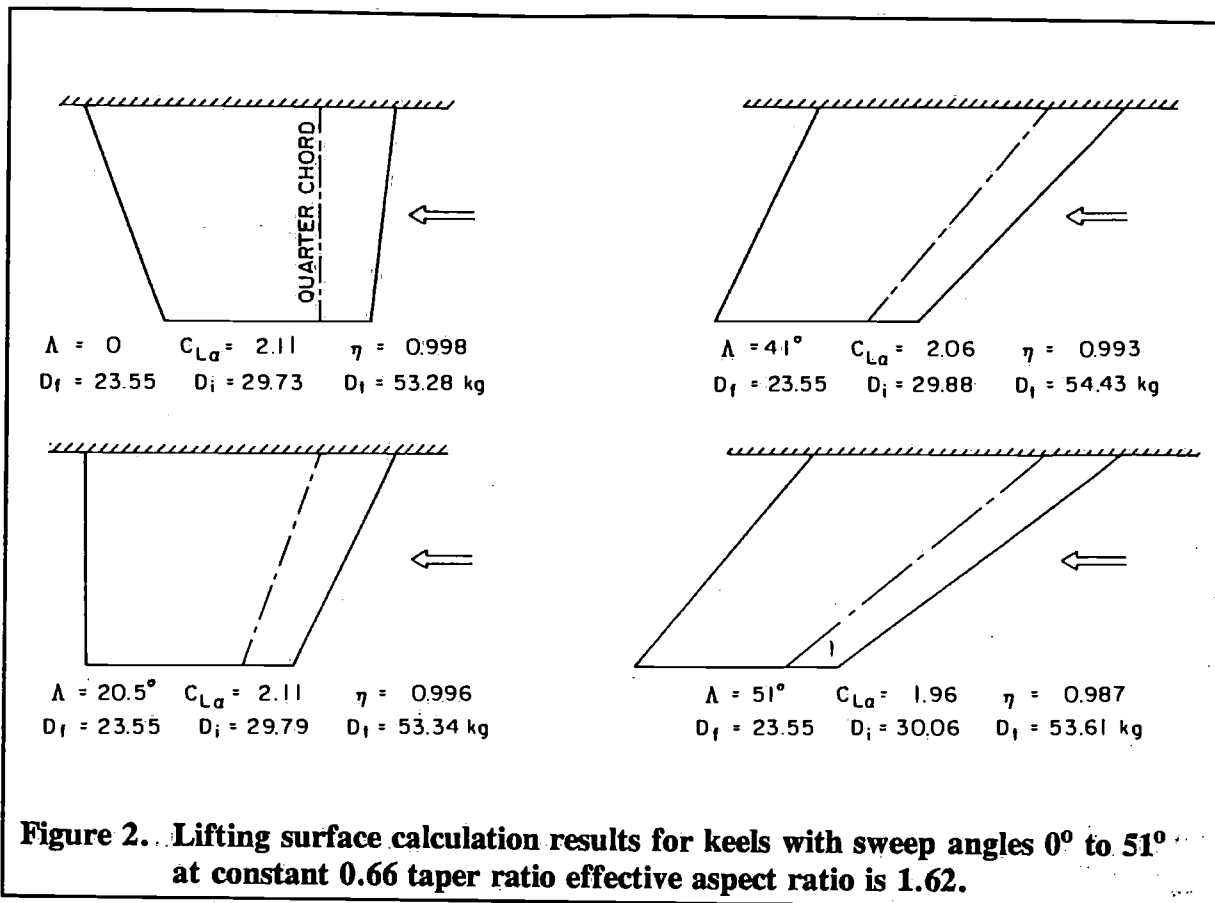
so that an efficiency of 100 percent would indicate a keel with minimum induced drag corresponding to elliptical spanwise loading.

In addition to these non-dimensional results, the frictional, induced and total drag in kilograms is indicated for a specific choice of keel area and lift force corresponding to design II of [3] sailing to windward at a speed of 6.74 knots. The frictional drag, of course, does not come from the theory, but is based on an assumed drag coefficient of

$$C_{Df} = 0.0085 + 0.0166 C_L^2 \quad (4)$$

based on previous test work and NACA two-dimensional data [4].

These calculations indicate that the lift slope is reduced by about 8% and induced drag is increased by about 1% as the sweep angle is increased up to 51°.



A wide tip chord is advantageous from a consideration of ballast, and these calculations would indicate that the latter does not involve a great penalty in hydrodynamic performance.

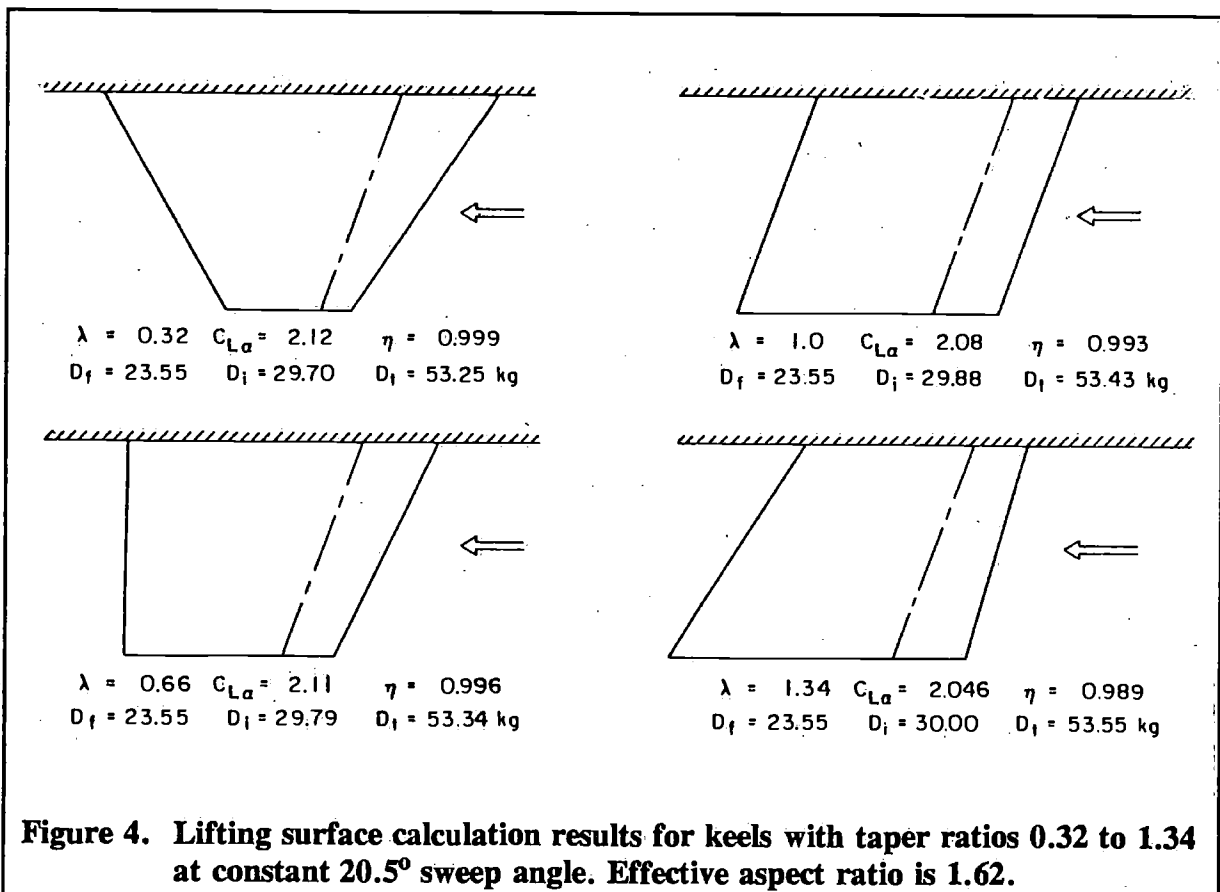
Figures 4 and 5 illustrate the same influence of taper ratio with sweep angles of 20.5° and 41° . The losses of efficiency due to sweep and increasing tip chord are cumulative, so that the combined effect is not necessarily negligible in influencing yacht performance.

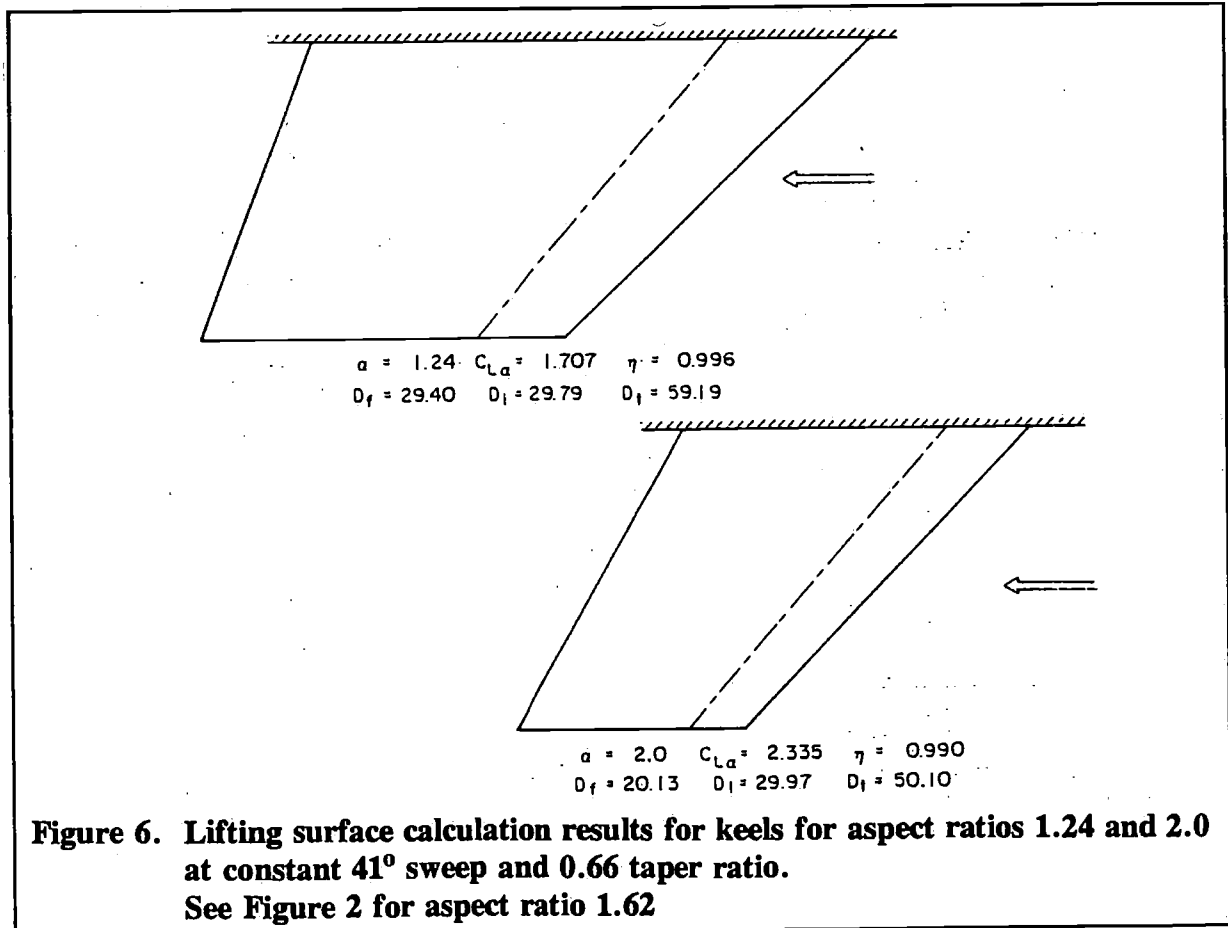
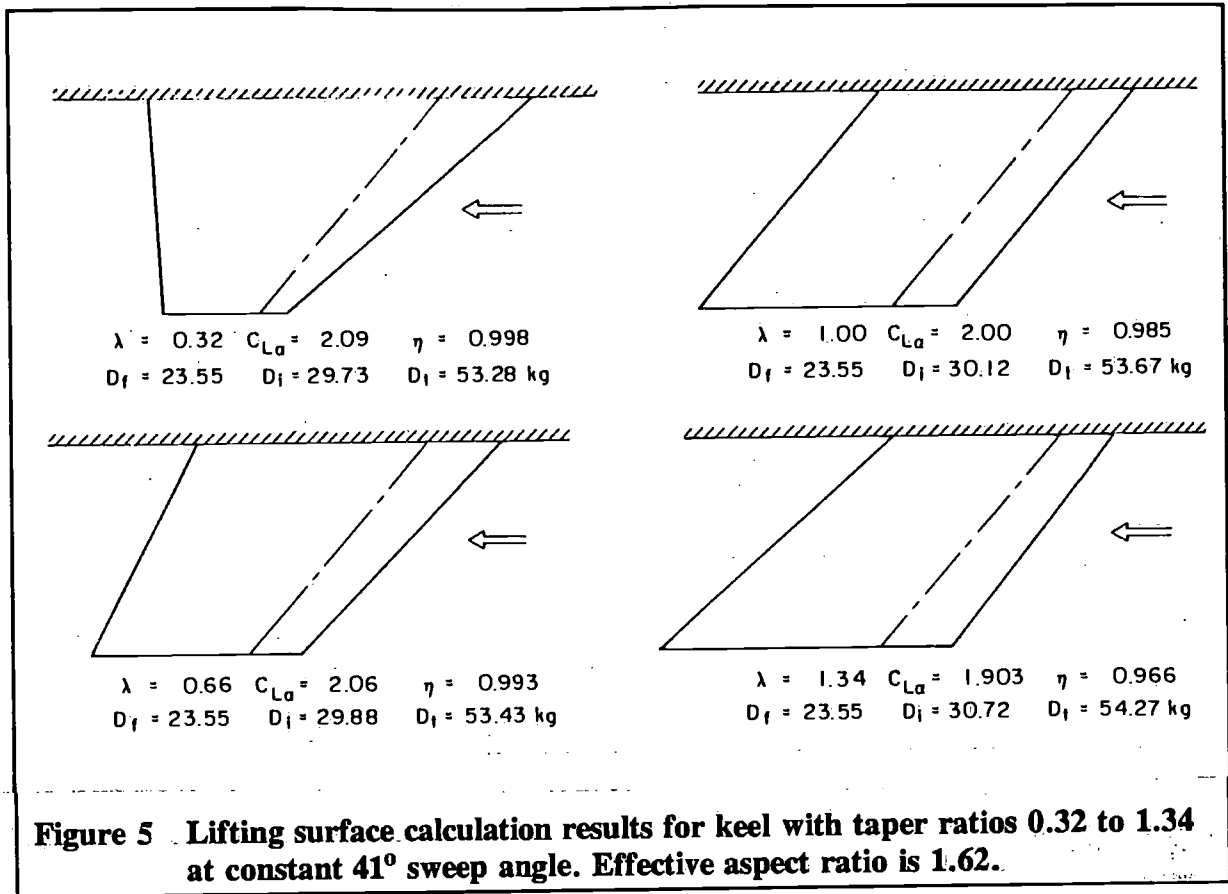
The last sequence of calculations, shown in Figure 6, involves variations in effective aspect ratio from 1.24 to 2.0 for fixed values of $\Lambda = 41.0$ and $\lambda = 0.66$. Here, of course, the lift slope increases noticeably with increasing aspect ratio. The efficiency decreases slightly with aspect ratio in this case, since in effect, it is harder to achieve an elliptical circulation distribution as aspect ratio is increased.

To compare these last results with the preceding calculations one must decide whether aspect ratio is to be increased by increasing the draft or decreasing the chord of the keel. If we chose the latter, so that the yacht rating is unaffected, the induced drag actually increases slightly with aspect ratio, while the frictional drag decreases due to the shorter chord. The numerical values given in Figure 6 indicate a substantial reduction in total drag with increasing aspect ratio. The conclusion depends, of course, upon the particular assumption used for estimating frictional drag. Obviously if the aspect ratio is increased to an extreme stall will occur. In addition, the increased angle of attack will cause greater hull drag.

The high value of efficiency and the insensitivity of induced drag to this extreme planform change is characteristic of relatively low aspect ratio lifting surfaces. The spanwise loading tends to be very nearly elliptical for any shape. It can be concluded, nevertheless, that the swept keel is a less efficient lifting surface, having a lower lift slope and higher induced drag.

The next series of calculations, shown in Figure 3, illustrates the effect of taper ratio at zero sweep angle. These indicate that taper is beneficial both from the point of view of lift slope and induced drag, but that this influence is extremely weak.





3 Model tests

Eight modifications of a keel from the previous series were tested in the M.I.T. Water Tunnel [5].

Tests of a complete yacht model in a towing tank using Froude scaling result in a ratio of model to full scale Reynolds Number equal to the $3/2$ power of the scale ratio. For example, this ratio is 3.7% for a $1/9$ scale ratio which introduces the likelihood of scale effects. Another disadvantage is that the small absolute force differences between respective keels might well be masked by uncontrollable minor variations in the total measurement.

Tests of the keel portion by itself in a high-speed water tunnel with no free surface present advantages and disadvantages. Testing at a speed inversely proportional to size allows exact Reynolds scaling corresponding to any sailing speed. Water velocities of 18 knots were used for the tests described herein. Thus, for a $1/9$ scale keel a test is exactly equivalent to the yacht sailing at two knots, or stated differently, a Reynolds Number 30% of that for the yacht at 6.74 knots. This Reynolds Number is sufficiently high to avoid most scaling problems.

The disadvantage of water tunnel tests is the need to neglect the pressure effects of a hull moving through a free surface and the practical necessity to place a model keel against one of the test section walls. This makes necessary the assumption of the "equivalent keel" already discussed. Also, the test tunnel wall boundary layer is proportionally thicker than that at the hull where a keel is attached. A favorable or unfavorable pressure gradient along the keel to hull joint is not duplicated and this may be an important factor in interference drag.

Not with standing these objections, the water tunnel test is best for detailed study of the keel problem. Reference [5] includes a complete description of the M.I.T. Variable Pressure Water Tunnel. Eight inch span models were placed in the 20" x 20" square test section adjacent to one wall with a gap of 0.032". A six component strain gauge dynamometer measured forces through the range of ± 8 degrees angle of attack. Tunnel wall interference is dealt with in accordance with conventional wind tunnel procedure:

- a. ANGLE OF ATTACK. $\Delta\alpha = 1.55 C_L$ where the coefficient is a function of the keel area and span related to the test section. For the subject test the angle correction was under 0.5° .
- b. DRAG COEFFICIENT. $\Delta C_D = 0.027 C_L^2$. This correction amounted to addition of about 8% drag to the maximum test values.

Figure 7 gives the design properties of the keel models. Tests covered the following modifications to the tip portion.

<u>Model Number</u>	<u>Bottom Planform</u>	<u>Tip Shape</u>	<u>Toe Shape</u>
1.	Flat	Square	Square
2.	Flat	Square	Round
3.	Flat	Round	Round
4.	Flat	Vee	Round
5.	Exponential	Square	Round
6.	Exponential	Round	Round
7.	Exponential	Bulb Protruding Aft	
8.	Exponential	Bulb Protruding Forward	

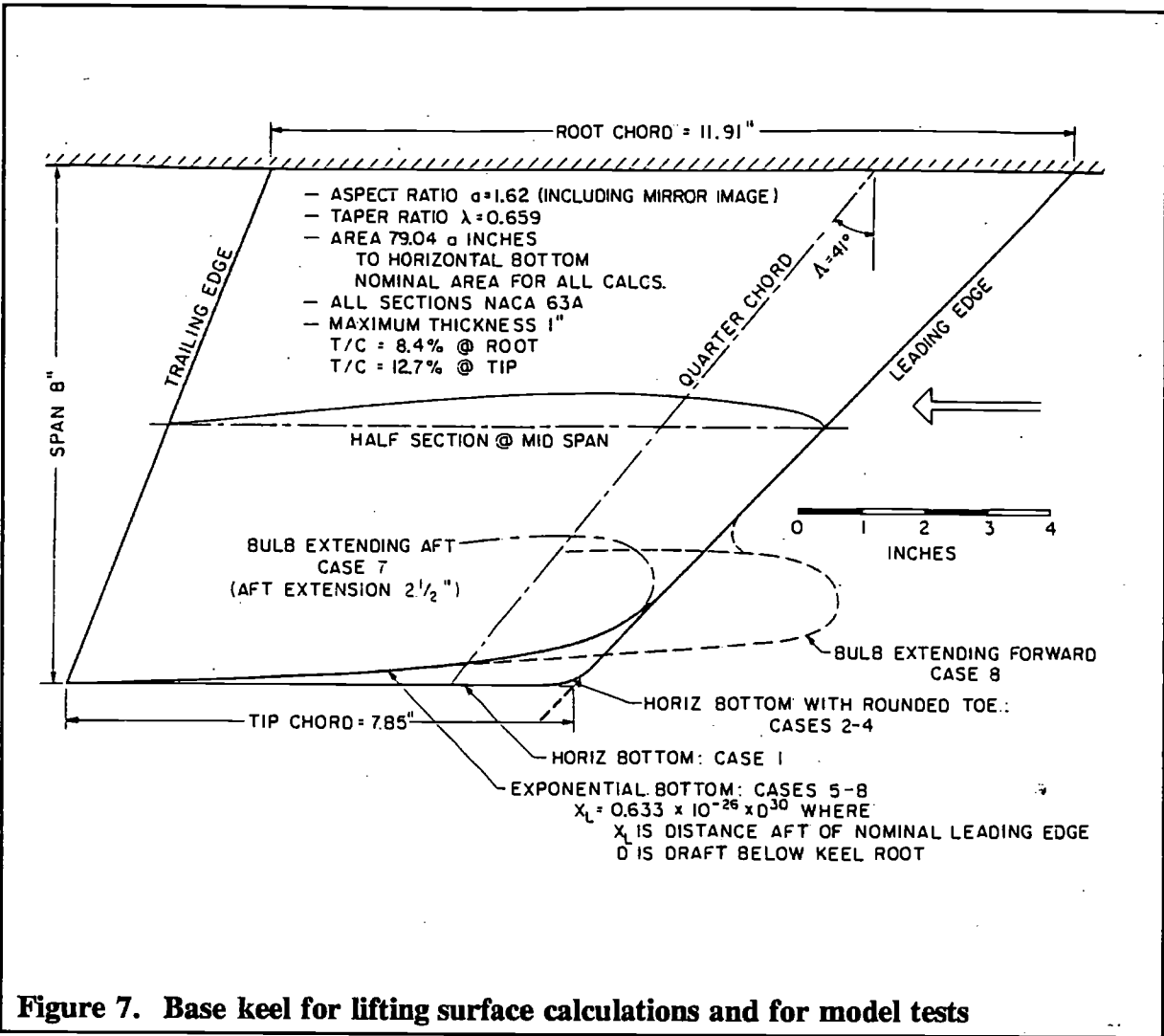


Figure 7. Base keel for lifting surface calculations and for model tests

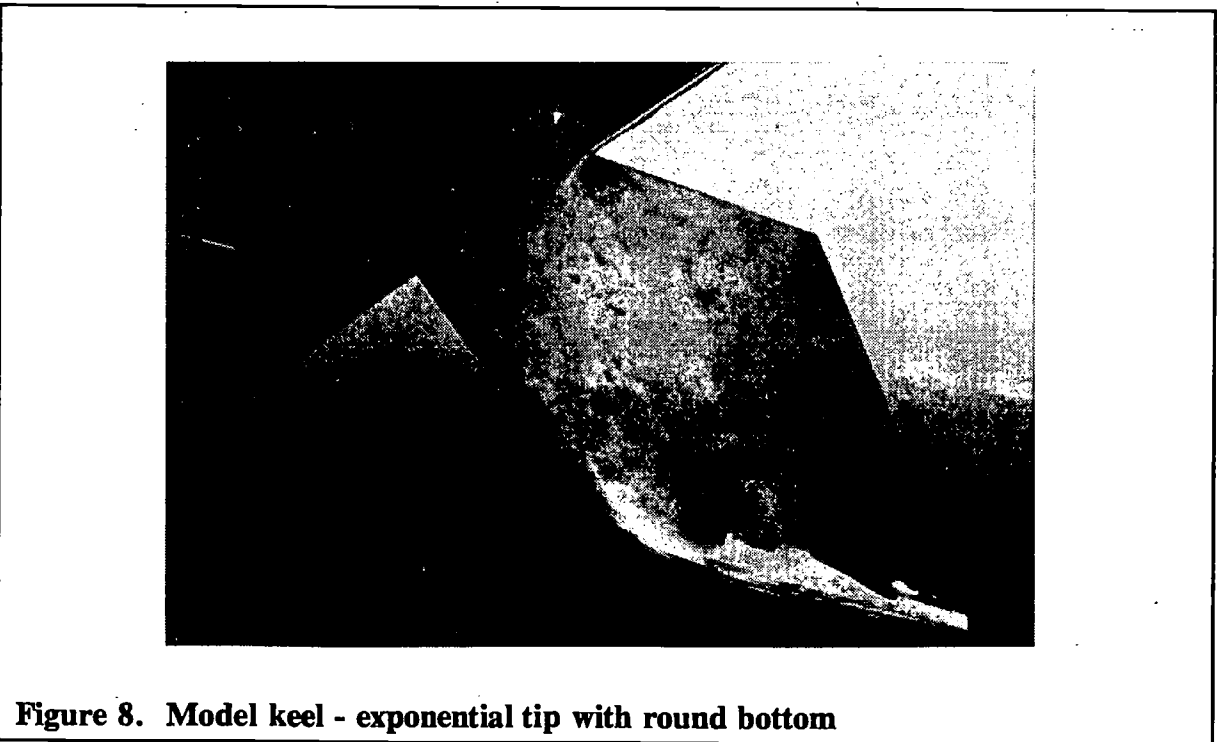


Figure 8. Model keel - exponential tip with round bottom

Figure 9 gives the lift coefficient vs. angle of attack for modifications 1 - 4. Since the range of angles is well below the stall point, lift is nearly linear. The slightly concave upwards nature of the curves is accountable to the crossflow drag contribution to lift from displacement of the tip vortex from the plane of the keel. Figure 11 is a photograph showing the curled path of the vortex.

For tests 1 - 4 the lift differences are attributable solely to tip shape because (except for toe rounding after Test 1 that had negligible effect) all four models have identical profiles. From Figure 9 it is seen that the square tip gives approximately 4% more lift than the round or vee tips.

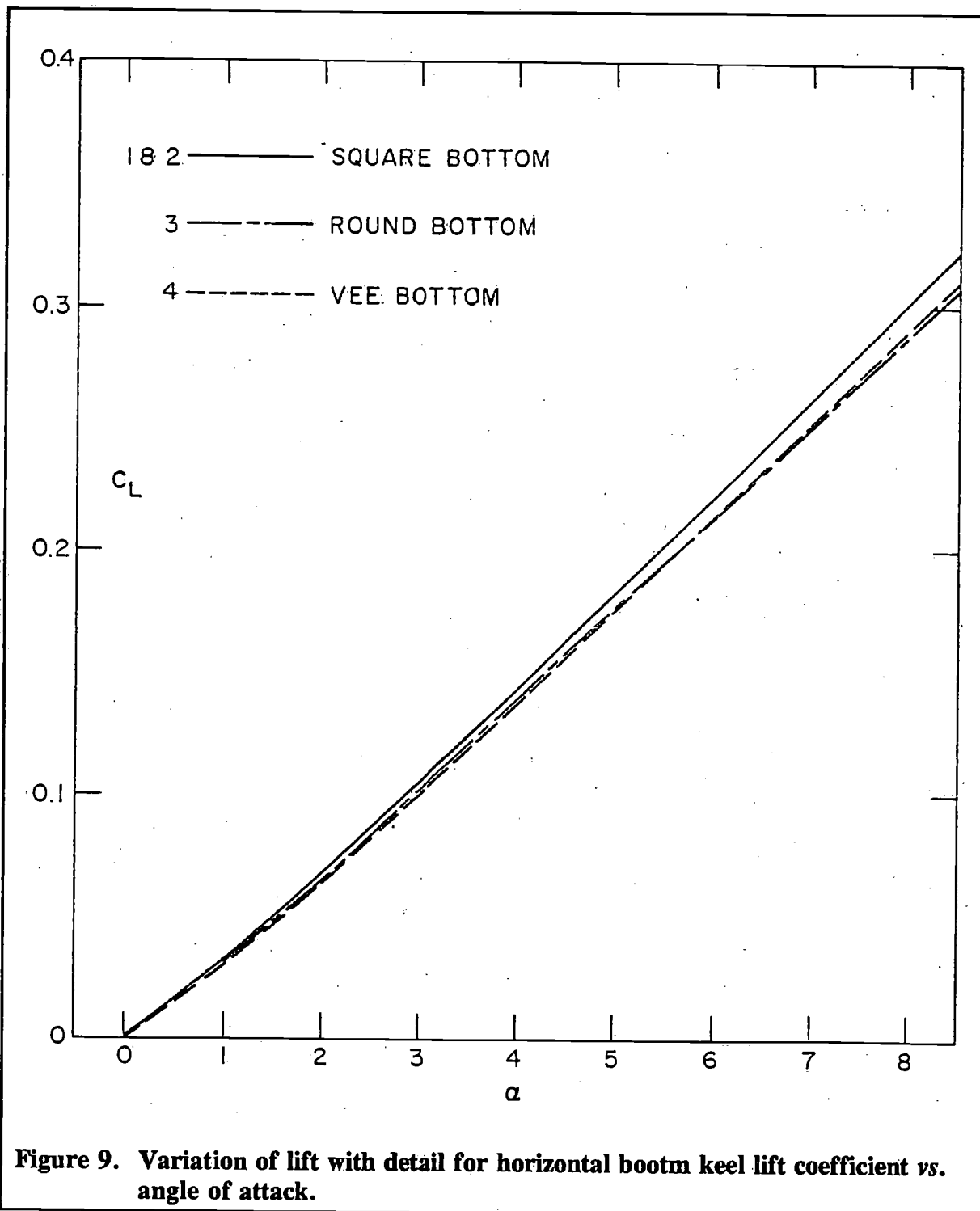
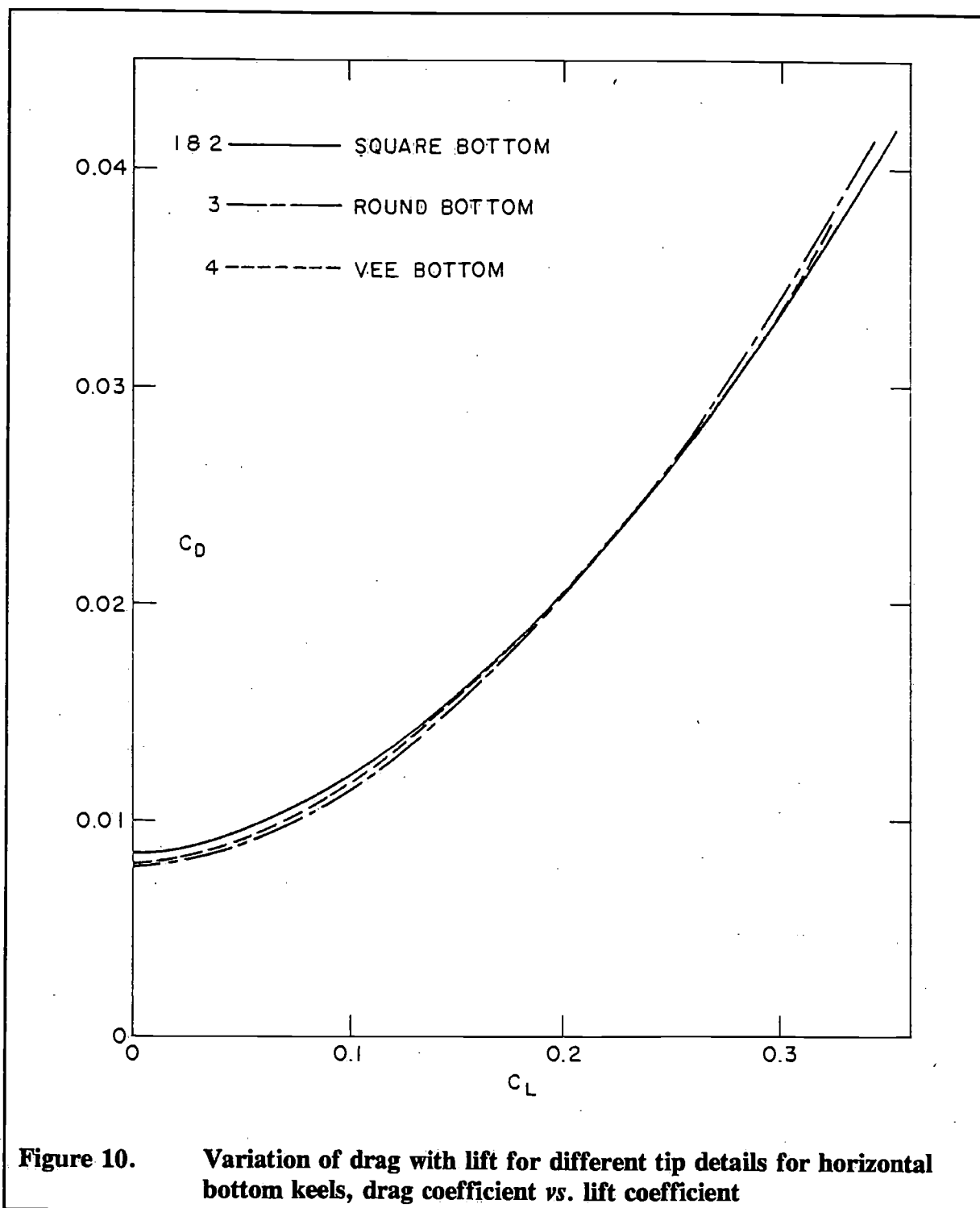


Figure 9. Variation of lift with detail for horizontal bootm keel lift coefficient vs. angle of attack.

Figure 10 is a plot of Drag Coefficient vs. Lift Coefficient for modifications 1 - 4. Since all curves are based on a nominal area these results may be considered an indication of absolute lift and drag for the "equivalent keel" exclusive of a hull. In making overall design selections attention must be given the fact that equivalent lift coefficients for the various keels correspond to different angles of attack.



For straight ahead motion the round bottom has the least drag, vee slightly more and the square bottom the most. For high values of lift, the ranking is reversed. One might easily jump to the conclusion that these differences are of trivial magnitude, but this is not so.

For example, applying the results of Figures 9 and 10 to a 33.6 ft. rating boat, hull II of [3] shows for example that:

- a. **UPRIGHT AT 6.74 KNOTS.** A boat with a square tipped keel would have 1.5 kg. more drag representing 1.2% more total resistance than another boat different only in rounding of the keel tip. The difference represents 0.02 knots loss of speed or 1.5 second/mile increase corresponding to 0.28 ft. rating difference!
- b. **YAWED 5% AT 6.74 KNOTS.** The indicated 0.5 kg. drag disadvantage of a vee tipped keel with respect to one with a round bottom corresponds to a rating disadvantage of 0.1 ft.

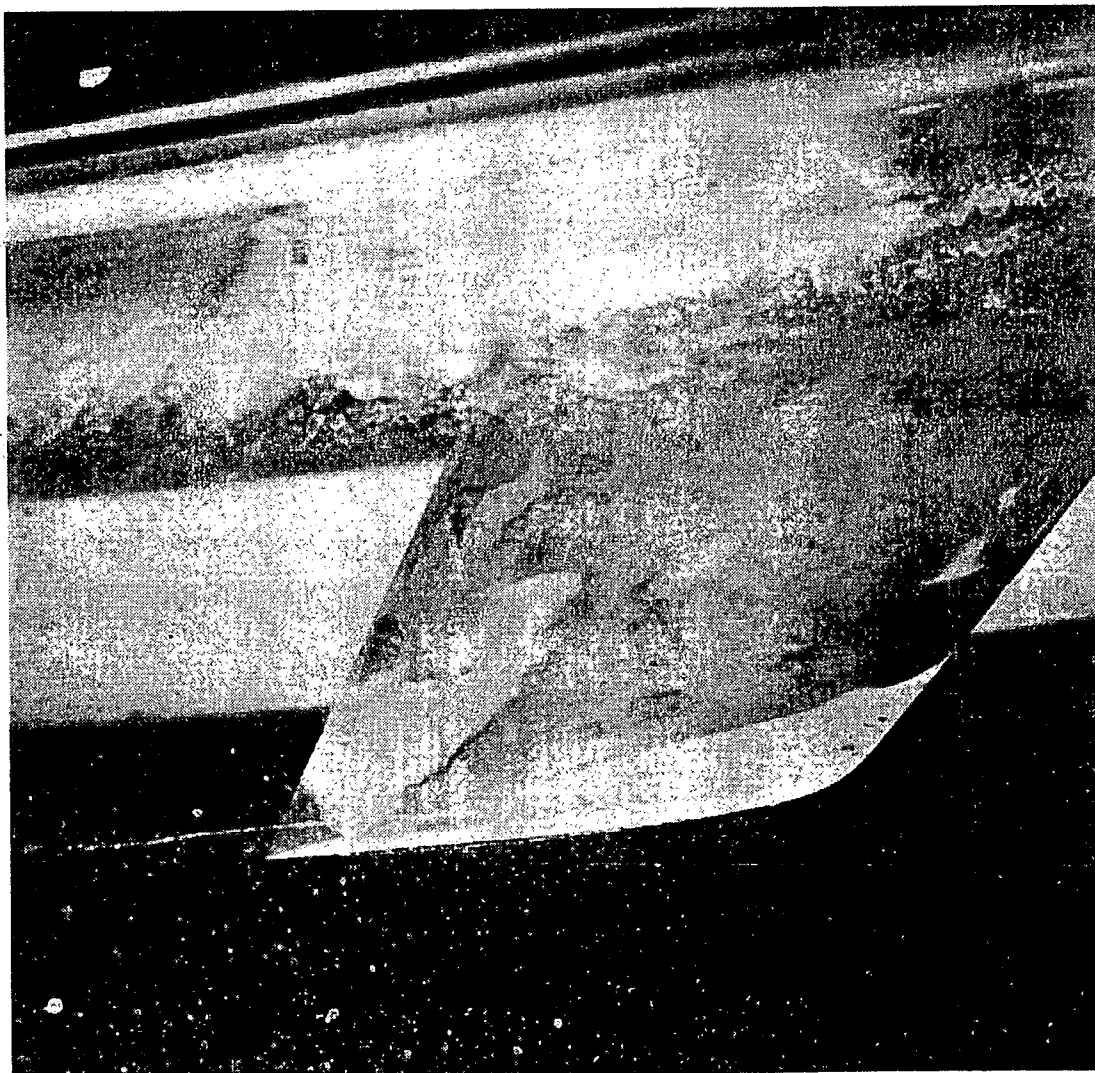


Figure 11. Keel model - flat bottom with rounded toe. Tip vortex made visible by reducing tunnel pressure.

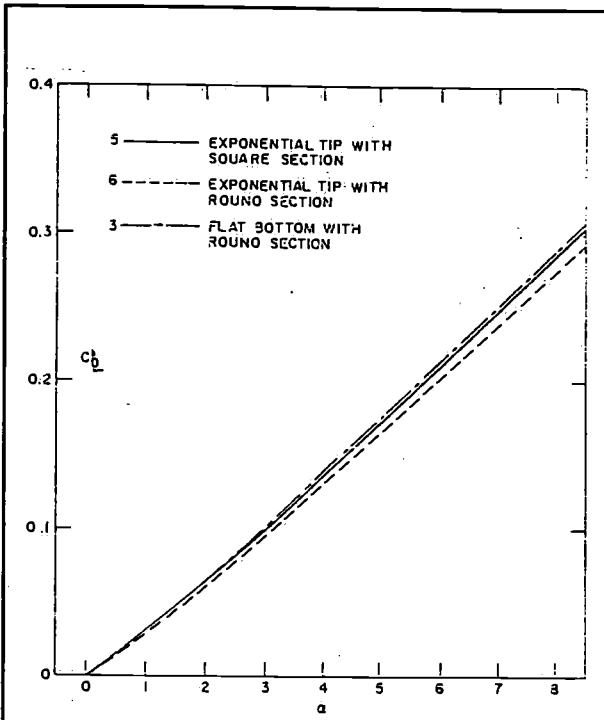


Figure 12. Variation of lift with keel tip planform and shape lift coefficient vs. angle of attack.

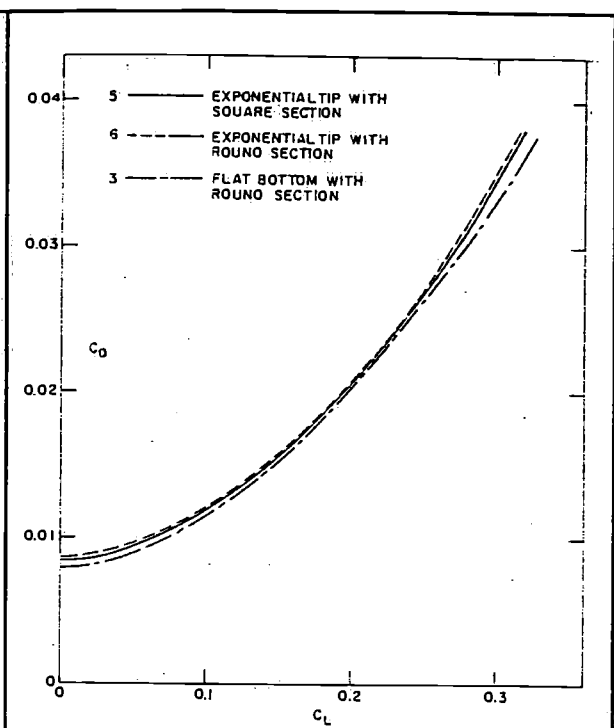


Figure 13. Variation of drag with lift for different tip planforms and shapes. Drag coefficient vs. lift coefficient

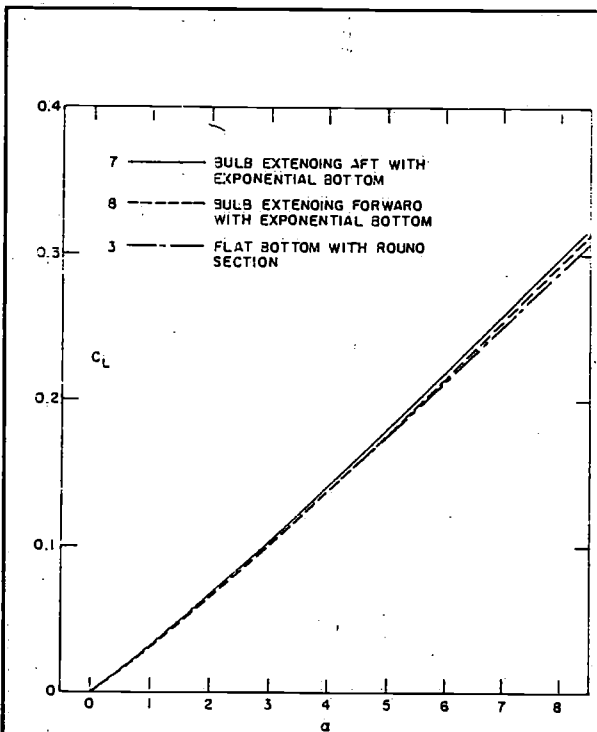


Figure 14. Lift vs. angle of attack for bulb keels.

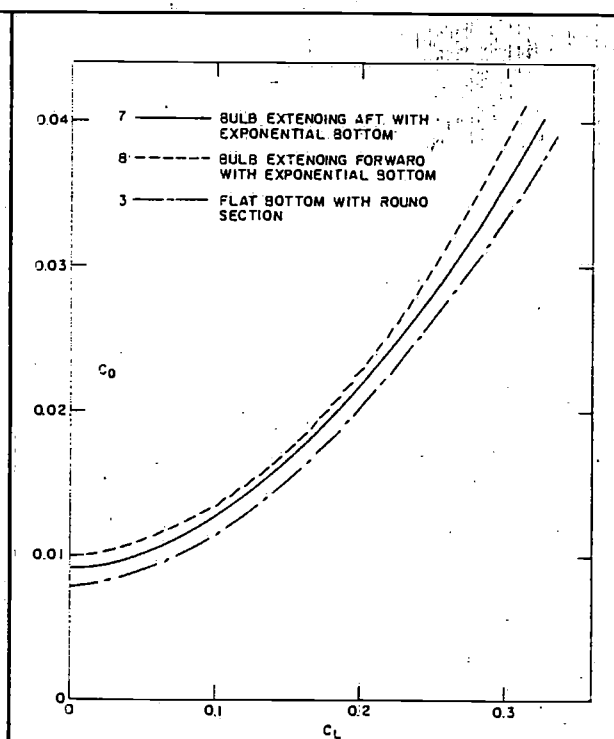


Figure 15. Drag vs. lift for bulb keels.

Figure 12 shows the lift for keels with exponential tips. To provide a basis for comparison the results for modification 3 are repeated. The differences between lifts for the square and round tips are identical to the differences between modifications 2 and 3. Keels with exponential tips give slightly less lift than the respective modifications with horizontal bottoms.

Figure 13 shows the drag vs. lift for these same modifications. The exponential tip keels have higher drag than their counterparts with horizontal bottoms. The exponential bottom thus seems inferior from considerations of both lift and drag. The drag difference between modifications 5 and 6 at high lift are consistent with the differences between modifications 2 and 3; however, the reverse is found at zero lift. This trend appears inconsistent.

The results of the bulb tip modifications are given in Figures 14 and 15. As would be expected, the bulbs produce only slightly more lift and substantially more drag. The advantage of a bulb tip can only be established by considering possible gains due to increased stability.

Further refinements in bulb tip design might be possible through systematic modifications coupled with flow visualization. Figure 16 shows the tip vortex path for modification 7. The flow about modification 8 is shown by yarn tuft photographs in Figure 17 at two angles of attack.

4 Theory and experiment

The lift slope predicted by lifting surface theory for the keels with horizontal bottoms used in the experiments is $C_L = 2.06$, which corresponds to a lift coefficient of $C_L = 0.288$ at an angle of attack of eight degrees. While this agrees almost exactly with the average of the experimental data for the square, round and vee bottom models, this result is actually a fortunate coincidence. It can be seen from Figure 9 that the lift curves are not straight lines, but are slightly concave upwards, which is characteristic of all low aspect ratio experimental results. The linearized lifting surface theory used here provides only the slope of the lift curve at zero angle of attack, which can be seen to be higher than the experimental value. The deviation of the measured lift curve from a straight line is generally accounted for by an empirically determined cross-flow drag factor, C_{DC} , such that

$$C_L(\alpha) = C_{L\alpha} \alpha + C_{DC} \alpha^2 \quad (5)$$

For rectangular wings with round leading edge airfoil sections, Flax and Lawrence [6] suggest values of C_{DC} of 1.0 for round tips and 2.0 for square tips. Whicker and Fehlner [7] indicate that for non-rectangular planforms, the value of C_{DC} should be reduced by an amount very nearly equal to the taper ratio. For the experimental keel with a taper ratio of 0.66, the increment of lift at $\alpha = 8^\circ$ due to cross-flow drag would then be 0.0129 for the round tip and 0.0257 for the square tip. The difference between these two values agrees very closely with the measured difference between square and round tips, so that these choices of C_{DC} seem plausible. By subtracting out the above values of lift due to cross-flow drag, we obtain an experimental value of lift slope of 1.98, which is approximately five percent below the value obtained from lifting surface theory. This discrepancy can certainly be attributed to gap and interference effects at the tunnel wall, as noted in earlier experiments run in the same facility [5].

The experimental values of drag coefficient at zero lift fall in between the smooth and rough two dimensional test results for the NACA 63-A section [4] which seems reasonable. However, the total drag in the region of lift coefficients between 0.2 and 0.3 are about twenty

percent higher than the theoretical values obtained from (3) and (4).

It appears that this discrepancy must be due to interference at the tunnel wall, and indicates that this effect has a greater influence on drag than on lift. While a similar effect must be present at the hull-keel intersection of the actual yacht, one would suspect that its magnitude would be less due to the proportionally thinner boundary layer on the yacht.

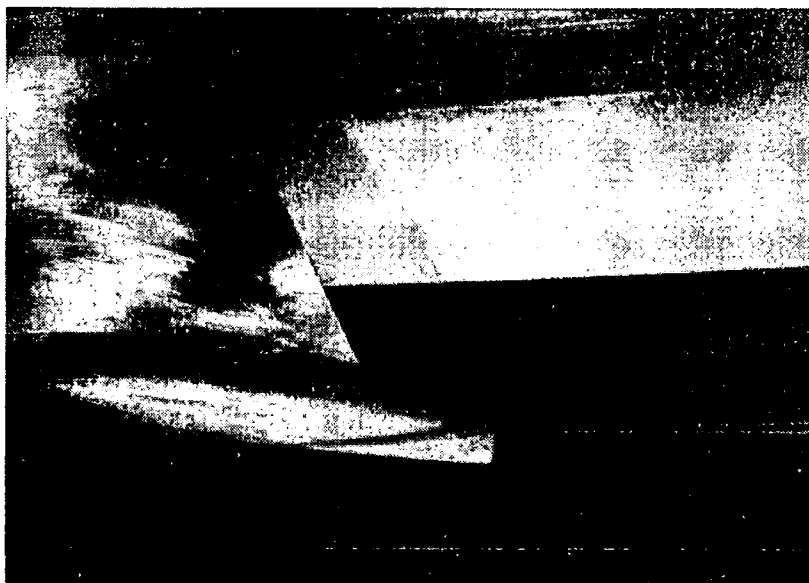
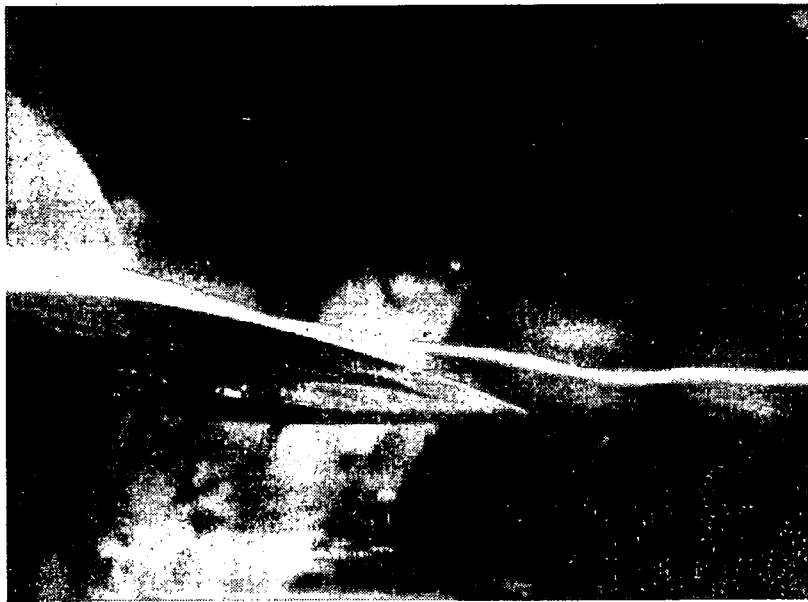


Figure 16. Keel model - bulb extending aft tip vortex made visible by reducing tunnel pressure.

One immediate conclusion is that a more complete understanding of the reason for this discrepancy in measured drag should be gained before continuing a systematic experimental program. The relative differences in performance due to changes in tip shape given in the present work should nevertheless be valid.

It is also interesting to consider the lifting surface results applied to the keel of Model II of [3], which has a sweep of 45° and a semispan (draft) of 1.785 meters assuming $2/3$ of the immersed hull draft is effective as part of the "equivalent keel." On this basis the area is 3.84 sq. meters and $\alpha = 1.66$. Interpolating between results of Figure 2 and Figure 6, assuming 45° sweep is not effectively different from 41° , gives $C_{L\alpha} = 2.07$ and $\eta = 0.988$.

It is stated in [3] that "when sailing to windward with a speed of 6.74 knots, the still water resistance is increased due to drift and heeling angle by approximately 66% for design II." It is assumed that side force is three times drag force and that the hull is heeled 20° so that the body axis side force becomes 652 kg corresponding to a lift coefficient of 0.270. From (3) the induced drag coefficient is calculated to be 0.0141, and from (4) the frictional drag coefficient is 0.0097. Therefore, the total drag coefficient is 0.0238.

These values yield the keel components of drag which comprise portions of the total drag increase of 81 kg between upright and windward conditions reported in [3].

	C_D	Drag-kg.
Frictional Drag at Zero Lift	0.0085	20.6
Frictional Drag due to lift	0.0012	2.9
Induced Drag	0.0141	34.1
Total Keel Drag	0.0238	57.6

It is noted that of the 81 kg less than half of the increase (37 kg) is directly attributable to lift effects on the "equivalent keel." Even adding twenty percent for the possible interference drag increment would account for little of this difference.

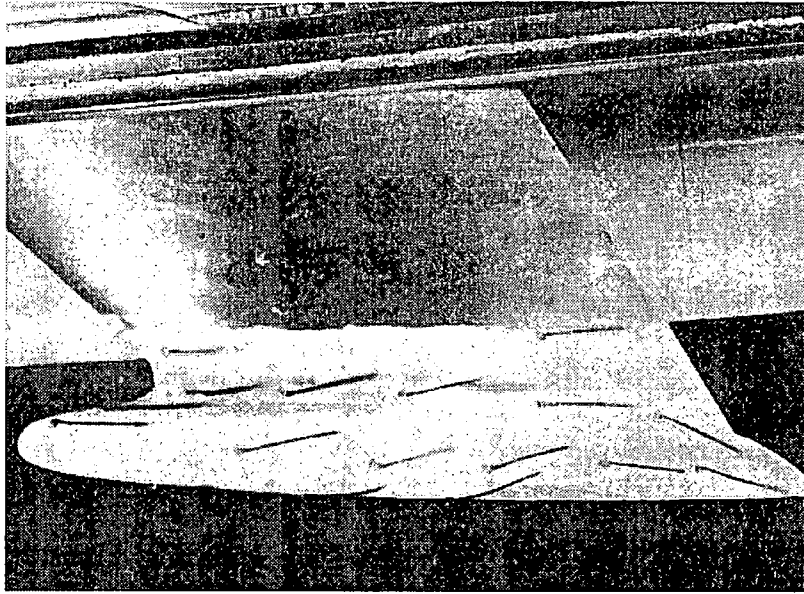
5 Conclusions

It is concluded that the selection of an appropriate keel may sensibly be based in part upon lifting surface theory calculations and model experiments in a water tunnel. The former are suitable for choice of span, aspect ratio and planform. The latter can provide information about details such as tip shape and root filleting.

The demonstrated differences between theory and experiment are attributable to interference effects at the tunnel wall and to cross flow drag at the tip. While the flow phenomenon at the root is understood in principle, further work is needed for quantitative values relating to that problem.

A common pitfall in the designing of yachts is failure to recognize the vital performance influence of certain characteristics where absolute force differences may seem small; the keel design problem is a case in point. Span and aspect ratio are significant to windward performance. Area and detailing of the keel contribute markedly to high or low drag on other points of sailing.

The aspect ratio series of calculations reveal important variations of drag vs. lift. While for these calculations span is considered constant, the designer will generally interpret results in terms of more and less draft as well as more or less area; such an analysis will always show advantage for the deep high aspect ratio keel which may or may not be offset by rating increase with draft or increased drag for the downwind sailing situation. Drag has been shown to increase with sweep angle, but the effect is small for moderate sweep angles.



6° angle of attack

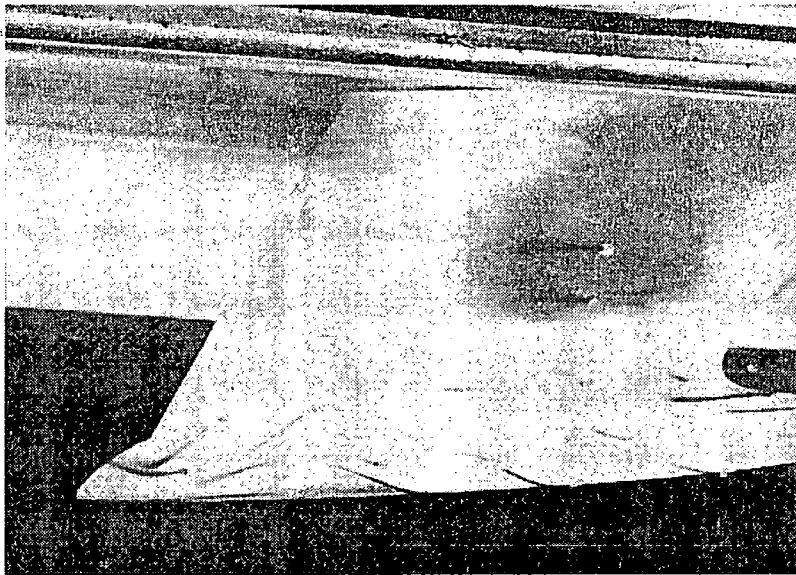


Figure 17. 11° angle of attack - beginning of stall bulb forward keel model.

Optimum taper ratios, from a hydrodynamic point of view, are less than would be desired from considerations of ballast.

The horizontal tip planform is superior to the exponential tip. An interesting conclusion from both test data and flow observation is that the effective span is set more by the leading

edge span than that of the trailing edge.

Vee or round bottom keel tip sections are superior to square bottoms for drag at zero lift. The square bottom produces greater lift slope than the others. Since the drag becomes about equal near C_L of 0.2, it is concluded that the square bottom is increasingly superior above 4° angle of attack.

This has been a study of keels, not a design analysis. Further inputs are required by a designer in the selection of the best keel for a boat: weight and vertical center of gravity of the lead, volume of the keel and its influence on total yacht hull drag, hull drag dependence on drift angle, and the detailing of the keel to hull joint.

This latter is one of several special areas deserving of further research. Also, wider variations of design parameters for keels should be considered by the experimental and theoretical techniques.

6 Acknowledgements

The authors wish to acknowledge the contribution of Dean Lewis, Research Engineer, and Charles Riley and William Connelly, Technicians, at the Marine Hydrodynamics Laboratory. Part of this study was accomplished as a class project by Neptune Rodriguez and Bohdan Oppenheim, graduate students in the Department of Ocean Engineering. Computer and publication costs were supported by contributions to Yacht Research at M.I.T.

7 Nomenclature

A	=	Planform area (span \cdot mean chord)
α	=	Aspect ratio = span/mean chord
b	=	Semi-span of "effective keel"
b_o	=	Semi-span of body with fin from [1]
C	=	Section chord length
C_D	=	Drag coefficient = $D/1/2\rho AV^2$
C_{DC}	=	Cross-flow drag factor
C_{Df}	=	Frictional drag coefficient = $D_f/1/2\rho AV^2$
C_{Di}	=	Induced drag coefficient = $D_i/1/2\rho AV^2$
C_L	=	Lift coefficient = $L/1/2\rho AV^2$
$C_{L\alpha}$	=	Lift slope per radian
D_i	=	Induced drag
D_T	=	Total drag
L	=	Lift
r_o	=	Body radius from [1]
T	=	Maximum section thickness
X_L	=	Distance of leading edge aft of nominal leading edge for exponential bottom keels.
V	=	Flow velocity
α	=	Flow angle of attack
η	=	Efficiency = induced drag / induced drag with elliptical loading
Λ	=	Sweep angle of quarter chord
λ	=	Taper ratio = tip chord / root chord
ρ	=	Mass density of fluid

8 References

- [1] Newman, J.N. and T.Y. Wu, "A Generalized Slender-Body Theory for Fish-Like Forms", *Journal of Fluid Mechanics*.
- [2] Kerwin, J.E. and B. Oppenheim, "A Lifting Surface Computer Program for Trapezoidal Control Surfaces with Flaps", M.I.T. Dept. of Ocean Engineering, Report 73-3.
- [3] Gerritsma, J. and G. Moeyes, "The Seakeeping Performance and Steering Properties of Sailing Yachts", 3rd HISWA Symposium on Yachts, Amsterdam, 21-22 March, 1973
- [4] Abbott, I.H. and A.E. Von Doenhoff, "Theory of Wing Sections", Dover, 1959.
- [5] Kerwin, J.E., P. Mandel and S.D. Lewis, "An Experimental Study of a Series of Flapped Rudders", *Journal of Ship Research*, December 1972.
- [6] Flax, A.H. and H.R. Lawrence, "The Aerodynamics of Low-Aspect-Ratio Wings and Wing-Body Combinations", Third Anglo-American Aeronautical Conference, 1951.
- [7] Whicker, L.F. and L.F. Fehlner, "Free Stream Characteristics of a Family of Low Aspect Ratio Control Surfaces", DTMB Report 933, May 1958.

The influence of fin keel sweep-back on the performance of sailing yachts

by W. Beukelman and J.A. Keuning

Delft University of Technology
Shipbuilding Laboratory

Abstract

On a model of a sailing yacht, fin keels with sweep-back angles of 0, 20, 40 and 60 degrees have been investigated to determine the influence of the mentioned Parameters on the performance. Two aspects ratios have been considered and for each aspect ratio series, the areas of the keels remained constant. The performance has been determined from towing test results using the wellknown Gimcrack-sail force coefficients.

Results of an analysis with respect to lift and induced drag are presented. Side force measurements in upright and heeled conditions have been compared with "equivalent keel" calculations. An empirical method is proposed to determine the position of the centre of effort in the horizontal and vertical direction.

Contents

- 1 Introduction
- 2 Experiment
 - 2.1 Ship-, keel- and sail data
 - 2.2 Upright condition
 - 2.3 Heeling condition
- 3 Performance calculation
- 4 Analysis of experiments
- 5 Calculation of side force
- 6 Discussion
 - 6.1 Induced drag and total resistance for a given lift
 - 6.1.1 Upright condition
 - 6.1.2 Heeling condition
 - 6.2 Induced drag and lift for a given angle of leeway
 - 6.3 Sailing performance
 - 6.4 Calculation of the side force
- 7 Conclusions
- 8 Acknowledgement
- 9 Nomenclature
- 10 References

1 Introduction

Systematic investigations concerning the influence of fin keel sweep-back in connection with sailing performance are scarce. An experimental study was presented by DeSaix [1] for

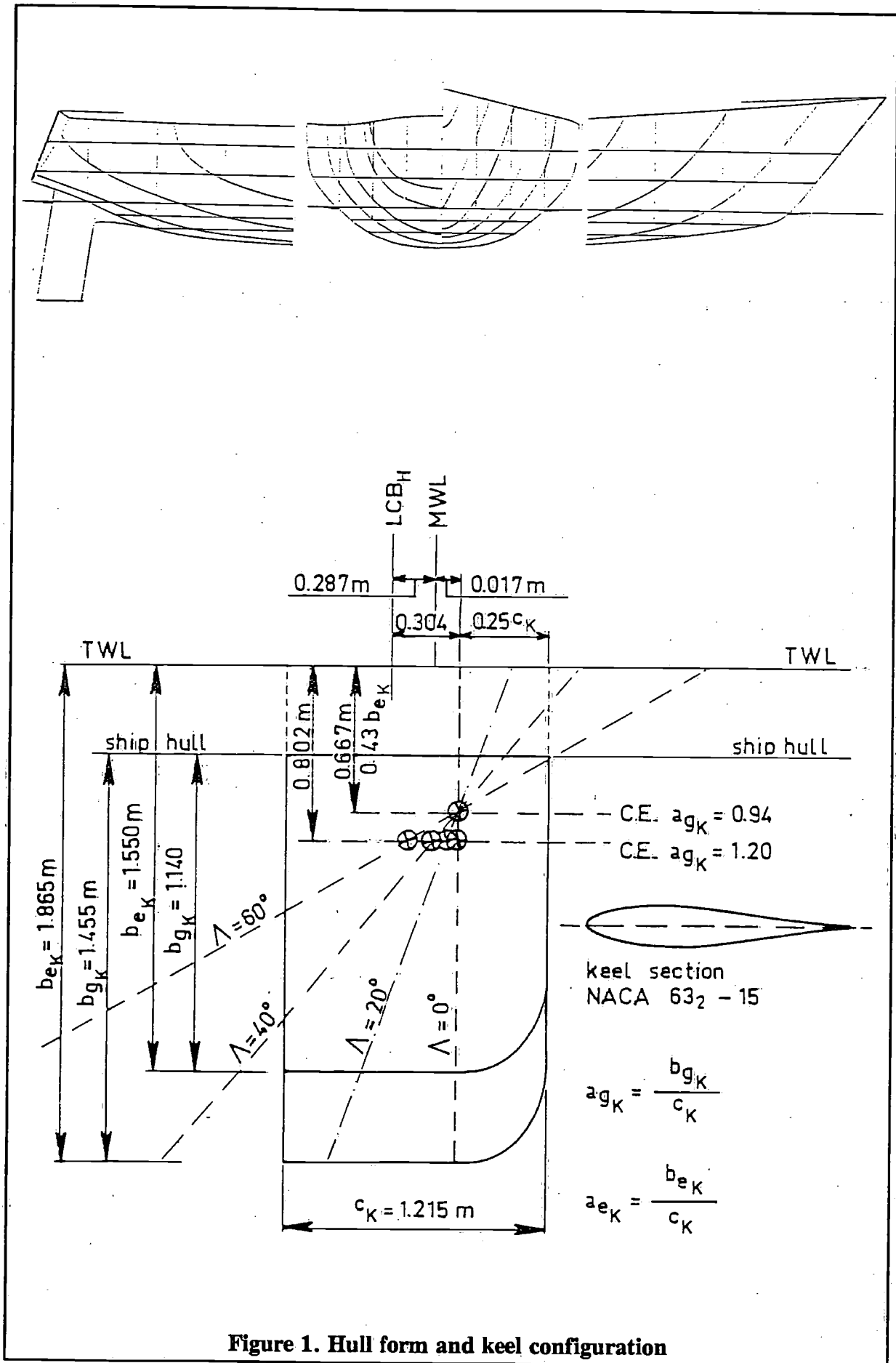


Figure 1. Hull form and keel configuration

sweep-back angles of 0, 25 and 30 degrees and a variation in aspect ratio from 0.5 to 1.52. All keels had the same lateral area and the same taper ratio. Optimum sweep angles, dependent on aspect ratio, had been determined.

Later, routine windward tests had been carried out for these optimum keels from which higher aspect ratio keels appeared to be more favourable.

An experimental and theoretical study on isolated fin keels was carried out by Herreshoff and Kerwin and had been reported in [2]. Lifting surface calculations, according to the concept of an "equivalent keel" had been undertaken to compare the performance of keel plan forms.

Induced drag was shown to increase by about 1% and lift slope was reduced by about 8% as the sweep angle was increased up to 51°. All of these keels had been investigated in the upright position and the keel-hull interaction had not been taken into account.

Wind tunnel tests carried out by Mac Lavery [3] on a double model of a 5.5 m yacht for keels from 30 - 65° sweep-back showed a decrease in drag with increase of sweep-back for a given side force.

Contrary to this result has been the conclusion of the report of the Advisory Committee for Yacht Research of the University of Southampton [4] which stated, that increase of sweep-back causes an increase of induced drag for a given side force.

For the present investigation performance tests were carried out on a model of the sailing yacht "Spirit 28". Keels had been fitted with sweep-back angles of 0, 20, 40 and 60 degrees for two aspect ratios of 0.94 and 1.20 to determine the influence of these Parameters.

In addition the experiments were extended to include tests on the bare model-hull with and without rudder. These results are not included in the present report.

The series of experiments consisted of three parts viz.:

1. tests without heel and leeway to determine the upright resistance and to determine downwind performance.
2. tests in the upright condition with leeway to determine side force production and induced drag.
3. test with 10, 20 and 30 degrees heel with leeway to determine heeled side force production and resistance and to calculate close-hauled performance.

The windward performance has been calculated with the normal Gimcrack sail coefficients. Extended analysis of the experiments has been carried out to find out whether a tendency could be established in the lift and drag induction with respect to sweep-back and aspect ratio. To a certain extent hull influence has always been included in the results.

The measurements of the side force for both the upright and heeled conditions were compared with the results of calculations according to the "equivalent keel" procedure as presented by Gerritsma in [5, 6]. Some corrections derived from the measurements have been proposed for the calculation of the centre of effort of the side force in horizontal and vertical directions both for the upright and heeled conditions.

2 Experiments

2.1 Ship-, keel- and sail data

The main particulars of the sailing yacht, have been presented in Table 1 and the hull-form is shown in Figure 1.

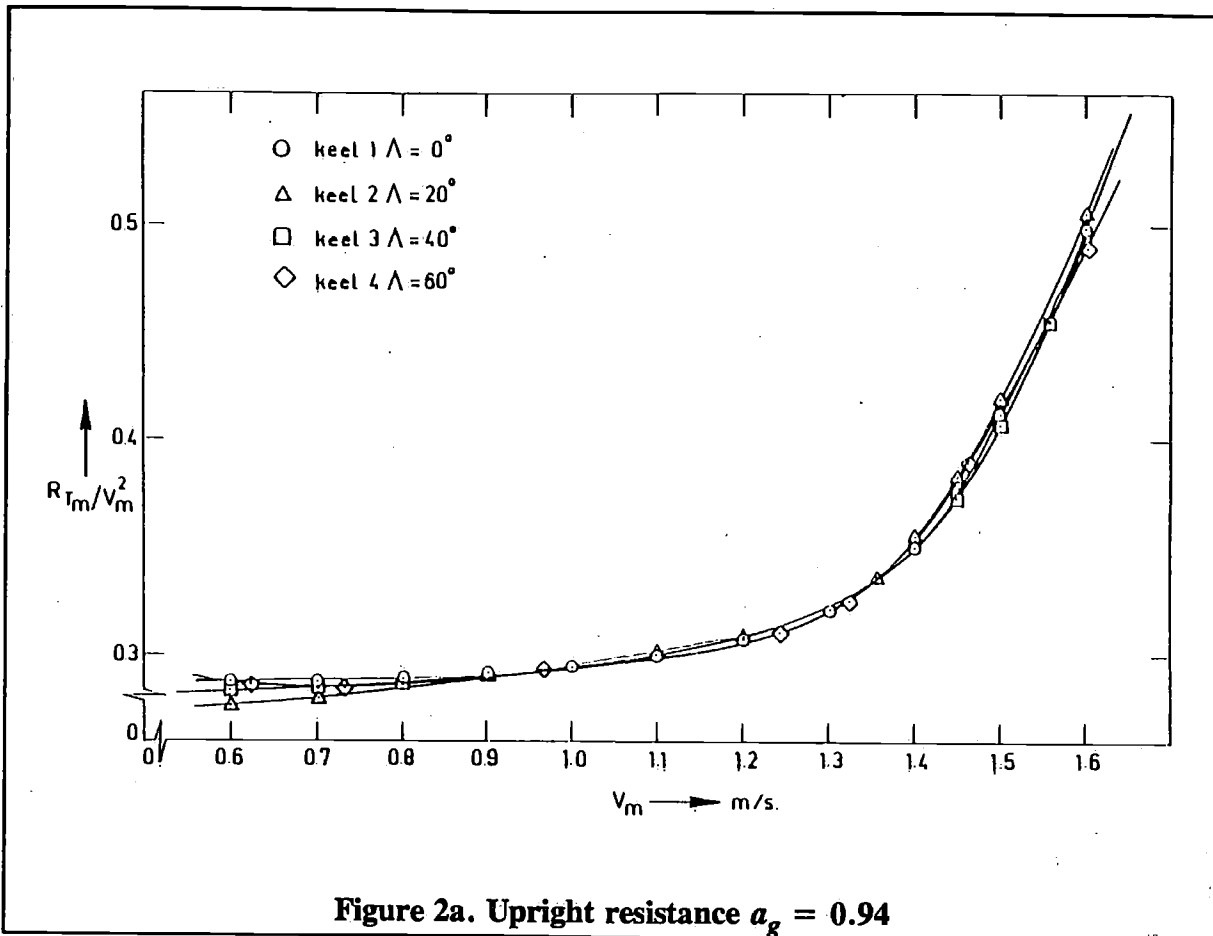


Figure 2a. Upright resistance $a_g = 0.94$

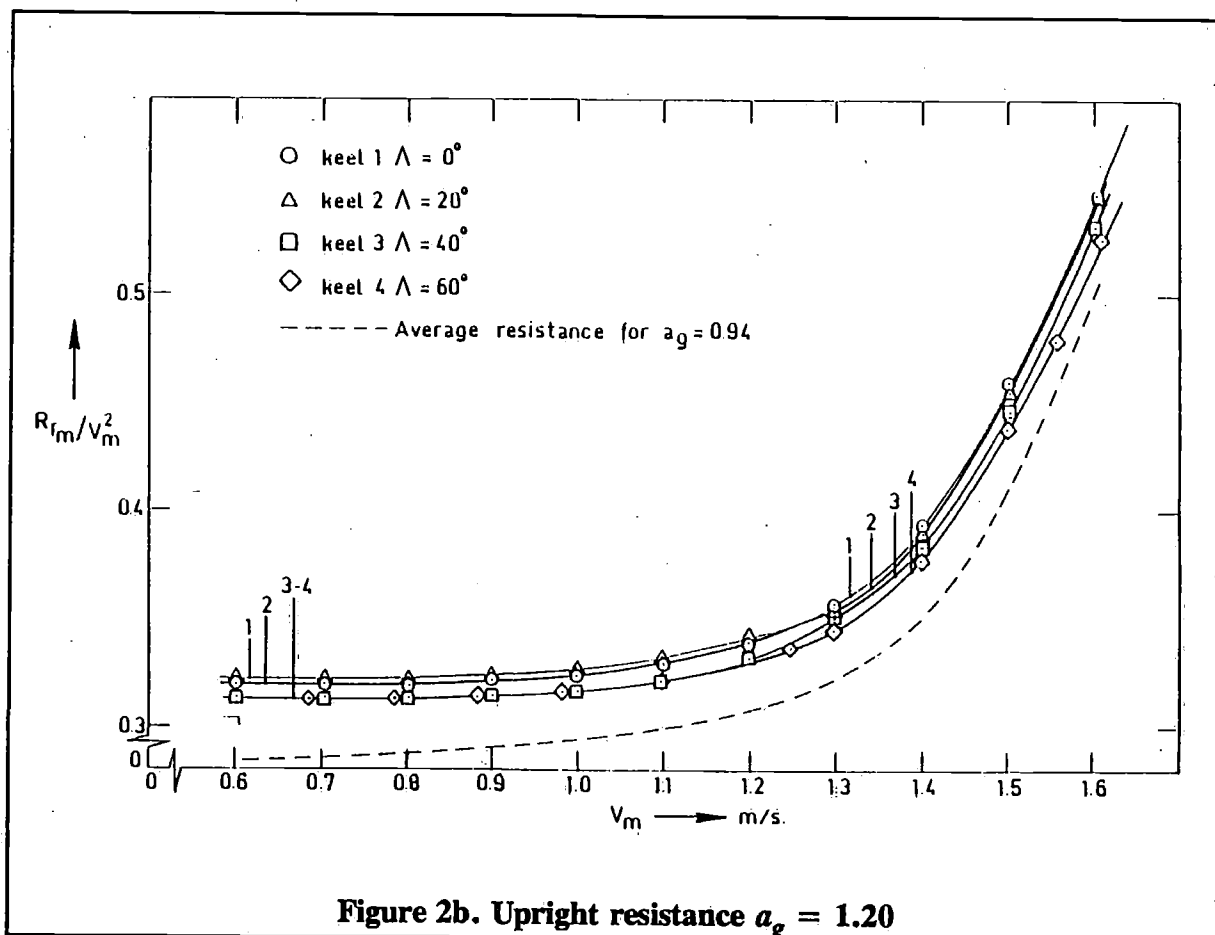


Figure 2b. Upright resistance $a_g = 1.20$

The keels have been investigated for two geometric aspect ratios viz.: $a_g = 0.94$ and $a_g = 1.20$. The definition of geometric and effective aspect ratio as used in this paper is also presented in Figure 1 and in the nomenclature (chapter 9).

For one aspect ratio the keels had the same lateral area, taper ratio ($\lambda = 1$) and section profile NACA 63₂-015 derived from [7].

The keels have been fitted to the hull in such a way that for the aspect ratio $a_g = 0.94$ the theoretical centre of effort of the effective keel (i.e. the keel extended to the waterline), remained at the same point as shown in Figure 1.

With the deeper keels this centre of rotation has been kept at the same position, which means not at the assumed centre of effort for these keels.

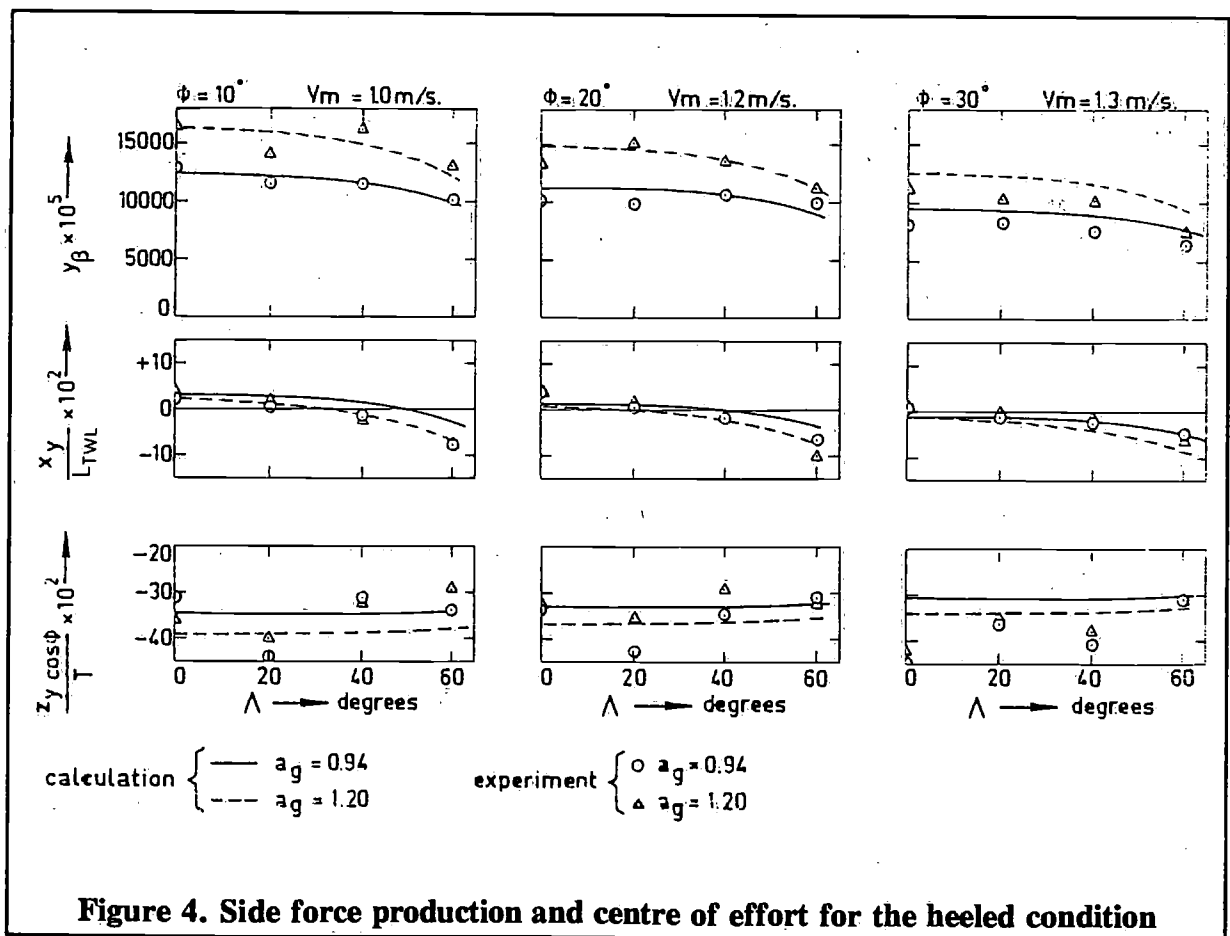
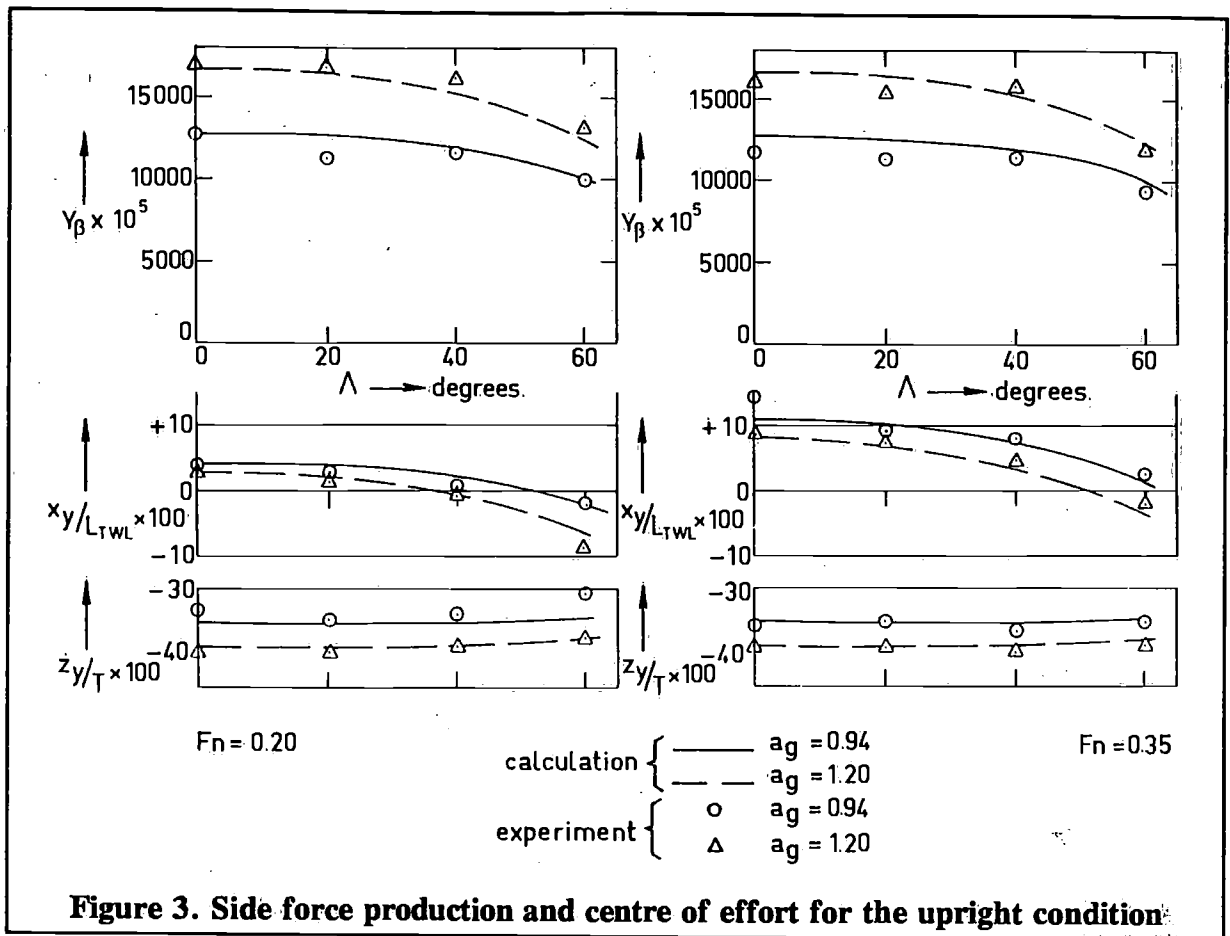
The centre of effort initially approximated to be on the quarter chord at a distance of 43% of the total draught below the waterline. The height of the centre of gravity remained the same for all models. The applied sail data have also been presented in Table 1.

Table 1

Ship Data		name:	Spirit 28
Model scale 1:4.5		designer:	E.G. van der Stadt
Description	Symbol	Unit	Quantity
Length over all	L_{OA}	m	8.40
Length on test waterline	L_{TWL}	m	6.90
Maximum breadth	B_{MAX}	m	2.81
Hull draught	T_H	m	0.41
Total draught (= effective keel span)	T	m	1.55-1.87
Hull displacement		kg	2547
Total displacement		kg	2719-2763
Length centre of buoyancy of hull before MWL	LCB_H	m	-0.29
Hull prismatic coefficient			0.579
Centre of gravity under	L_{TWL}	m	0.010
Effective sail area beating		m ²	27.8
Effective sail area down wind		m ²	71.1
Effective centre of effort beating above	L_{TWL}	m	4.68
Keel span	b_g	m	1.14-1.46
Keel chord	c_K	m	1.22
Geometric aspect ratio of keel	a_{gK}		0.94-1.20
Keel sweep-back angle	Λ_K	degree	0-20-40-60
Rudder span	b_{gR}	m	1.03
Average rudder chord	c_R	m	0.45
Geometric aspect ratio of rudder	a_{gR}		2.29
Rudder sweep-back angle	Λ_R	degree	8

2.2 Upright condition

At first the upright resistance without heel and leeway has been measured for the models with the different keels. For the lower aspect ratio, the differences in this upright resistance appear to be negligible, but for the keels with the higher aspect ratio ($a_g = 1.20$) the resistance has



decreased with the increase of sweep-back angle above $\Lambda_K = 30^\circ$ to $\Lambda_K = 60^\circ$ by about 5%. The resistance curves are shown in Figure 2.

Afterwards the side force and resistance have been determined in the upright position of the model with leeway for two speeds viz.: $F_n = 0.20$ and 0.35 .

The side force is shown in Figure 3 for each aspect ratio in relation to the sweep-back angle Λ . The side force is expressed in non dimensional form:

$$Y_p = \frac{Y}{\frac{1}{2}\rho V^2 L_{TWL}^2 \beta} \quad (1)$$

in which:

- Y = $F_H \cos \phi$ = hydrodynamic side force
- ρ = mass density of water
- V = speed
- L_{TWL} = length on test waterline
- β = angle of leeway in radians

Also in Figure 3, the vertical and horizontal position of the centre of effort of the side force for the different keels is shown as actually measured.

These positions have been presented as a percentage of the waterline length with respect to the middle of the test waterline (*MWL*) (forward is positive) and as a percentage of the maximum draught with respect to the waterline respectively.

For further analysis relative to induced drag and lift see chapter 4.

2.3 Heeling condition

For heeling angles of 10, 20 and 30 degrees a minimum number of three angles of leeway and three speeds have been considered to determine the resistance and side force and, finally, the close hauled performance as described in chapter 3.

The side force and the position of the centre of effort in the heeling condition, derived from the measurements, have been shown in Figure 4 in the same way as described for the upright position in chapter 2.2.

The results are presented for the conditions in Table 2.

Table 2

Heeling angle ϕ	Speed m/sec
10	1.0
20	1.2
30	1.3

The Figures 5 and 6 show the wave pattern of the model with a keel-sweep-back angle of 0 and 60 degrees and for heeling angles of 10, 20 and 30 degrees for the cases of normal leeway and without leeway.

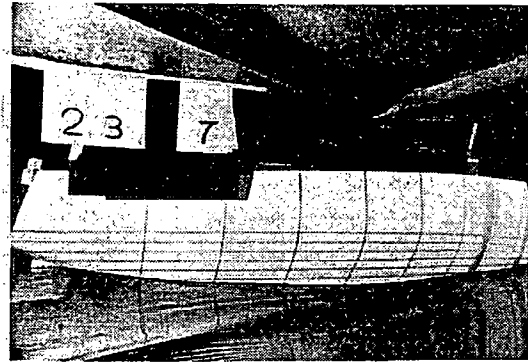
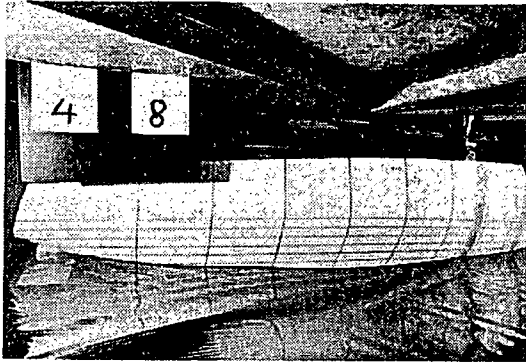
For the last condition the model was artificially heeled at the predetermined angle. The photographs are related to the higher aspect ratio series only.

It is obvious from these pictures that the wave amplitude due to heel is strongly dependent on the keel loading and increases significantly with heel, and decreases with sweep-back.

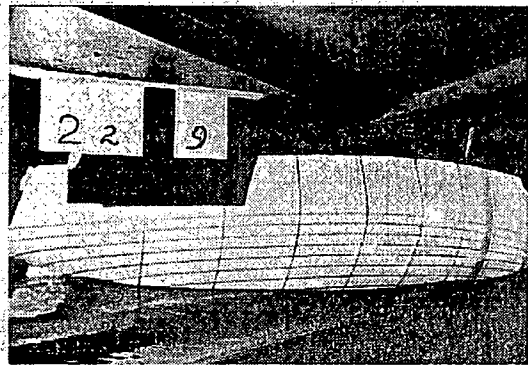
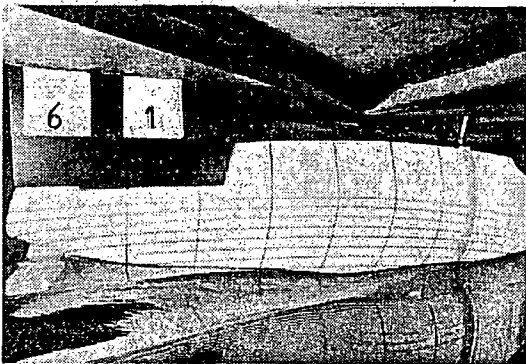
with leeway

$\Lambda = 0^\circ$

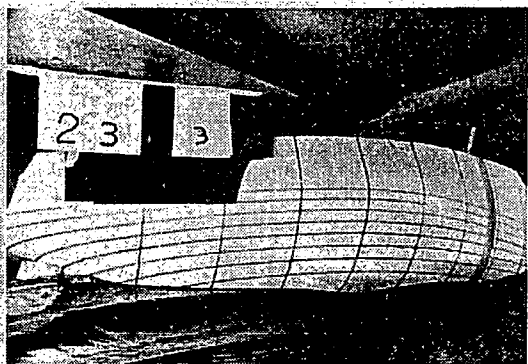
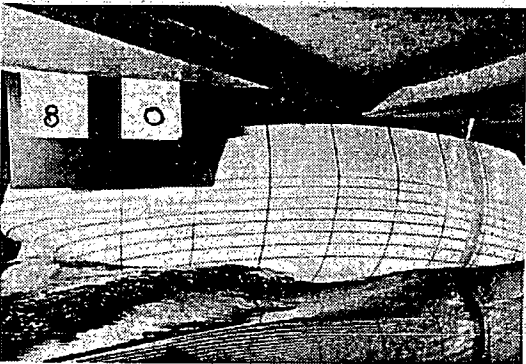
without leeway



$\phi = 10^\circ$



$\phi = 20^\circ$



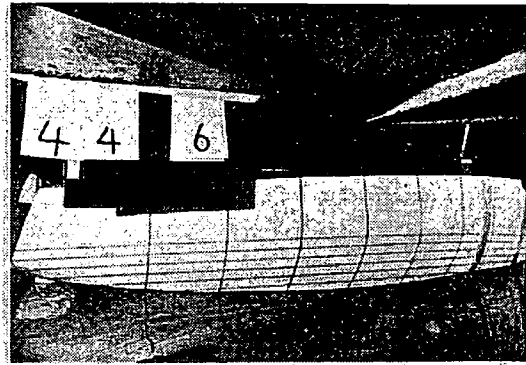
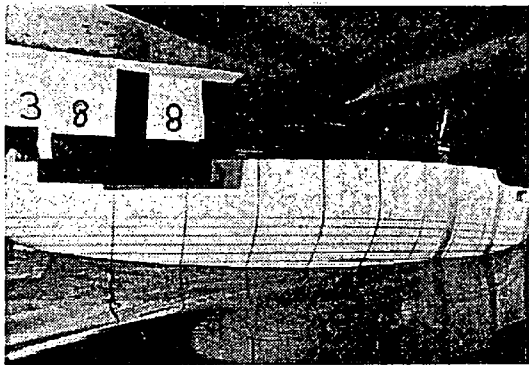
$\phi = 30^\circ$

Figure 5. Photographs of the wave pattern under heel with and without leeway for a sweep-back angle $\Lambda = 0^\circ$

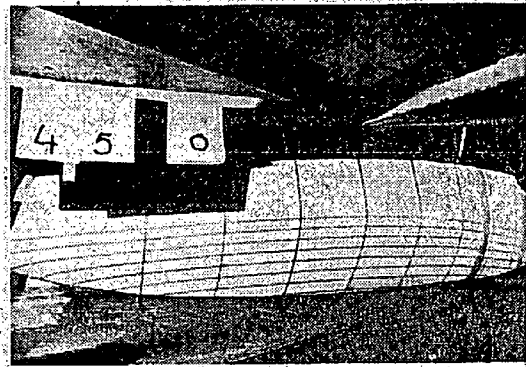
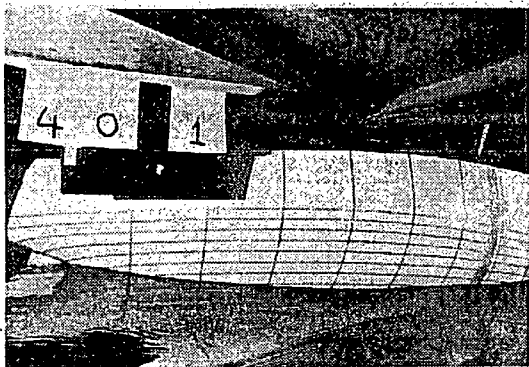
with leeway

$\Lambda = 60^\circ$

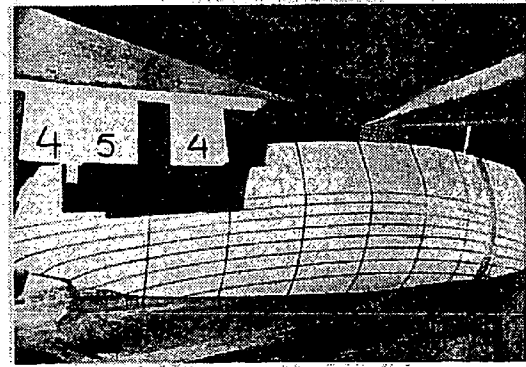
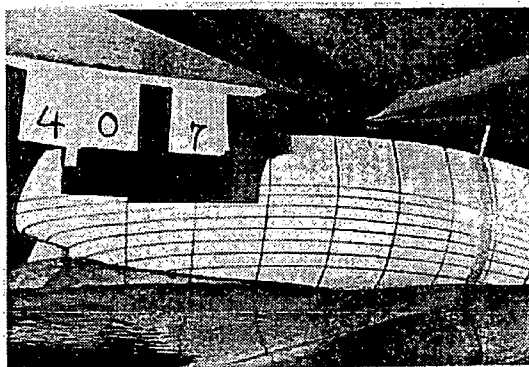
without leeway



$\phi = 10^\circ$



$\phi = 20^\circ$



$\phi = 30^\circ$

Figure 6. Photographs of the wave pattern under heel with and without leeway for a sweep-back angle $\Lambda = 60^\circ$

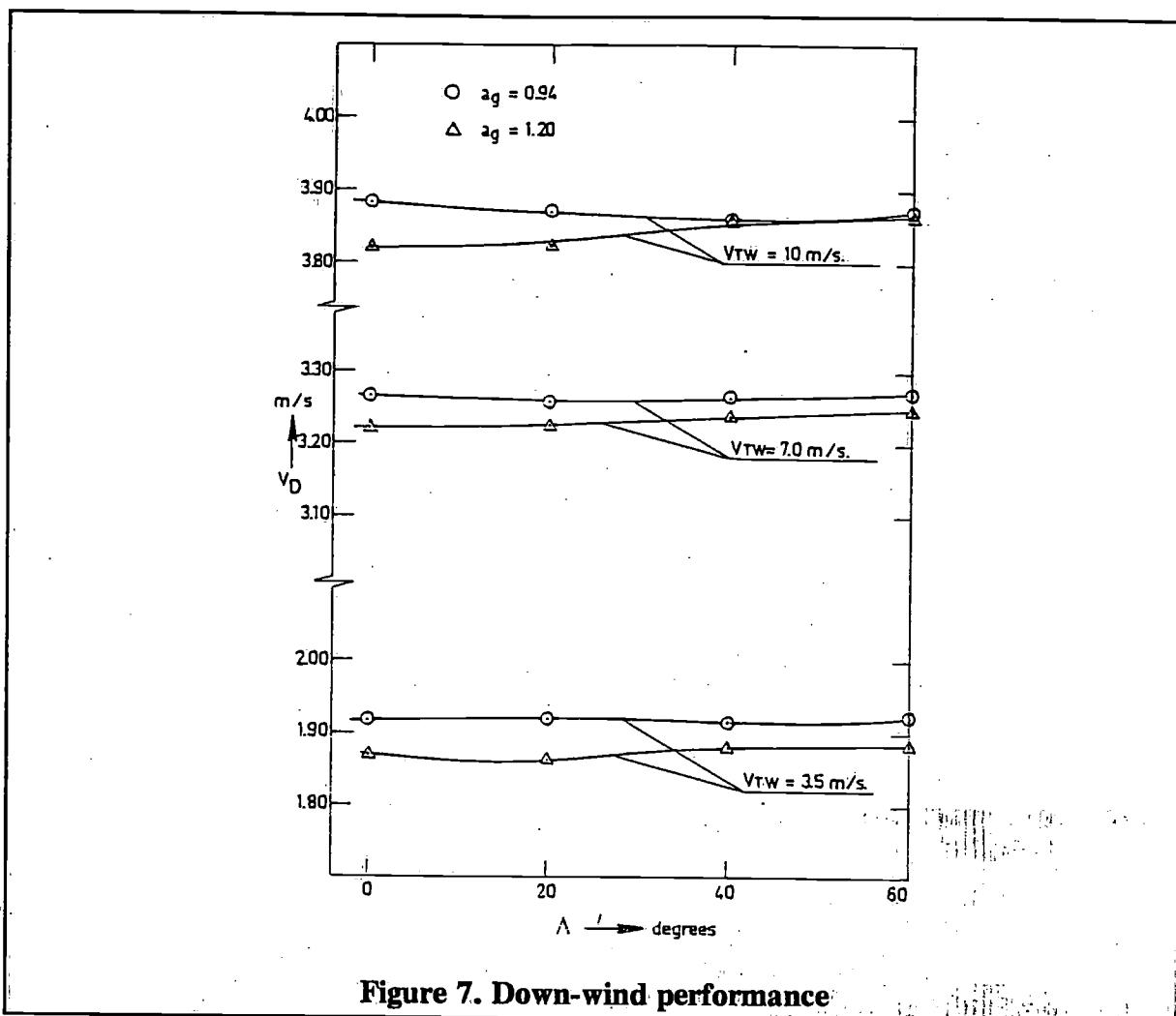


Figure 7. Down-wind performance

3 Performance calculation

The performance in running conditions for the ship with different keels, is shown in Fig. 7. As the sail area remains constant for the two aspect ratios, it can be seen that the ships with the higher aspect ratio have a lower down-wind performance because of the resistance increase due to the larger lateral keel area. This is to be expected. The difference in speed between both aspect ratios appears to be smaller for keels with corresponding high sweep-back, which is due to the lower upright resistance for the keels with higher aspect ratio and high sweep-back.

The optimum windward performance has been determined from the test results in the usual way with the normal Gimcrack sail coefficients.

When considering the aspect ratio as a constant, Figure 8 shows that the speed-made-good is almost the same for all sweep-back angles considered.

There is an exception, however, with strong winds and a high aspect ratio. For this case the keels with high sweep-back angles look attractive.

A disadvantage, however, is the high angle of leeway. The leeway angle appears to increase rather rapidly for the keels with maximum sweep-back angle, as shown in Figure 9 for true winds of 3.5, 7 and 10 m/sec. The speeds-made-good, as a result of the windward performance calculations, are shown in Figure 8b. This was done on the basis of sweep-angle for the true winds previously mentioned.

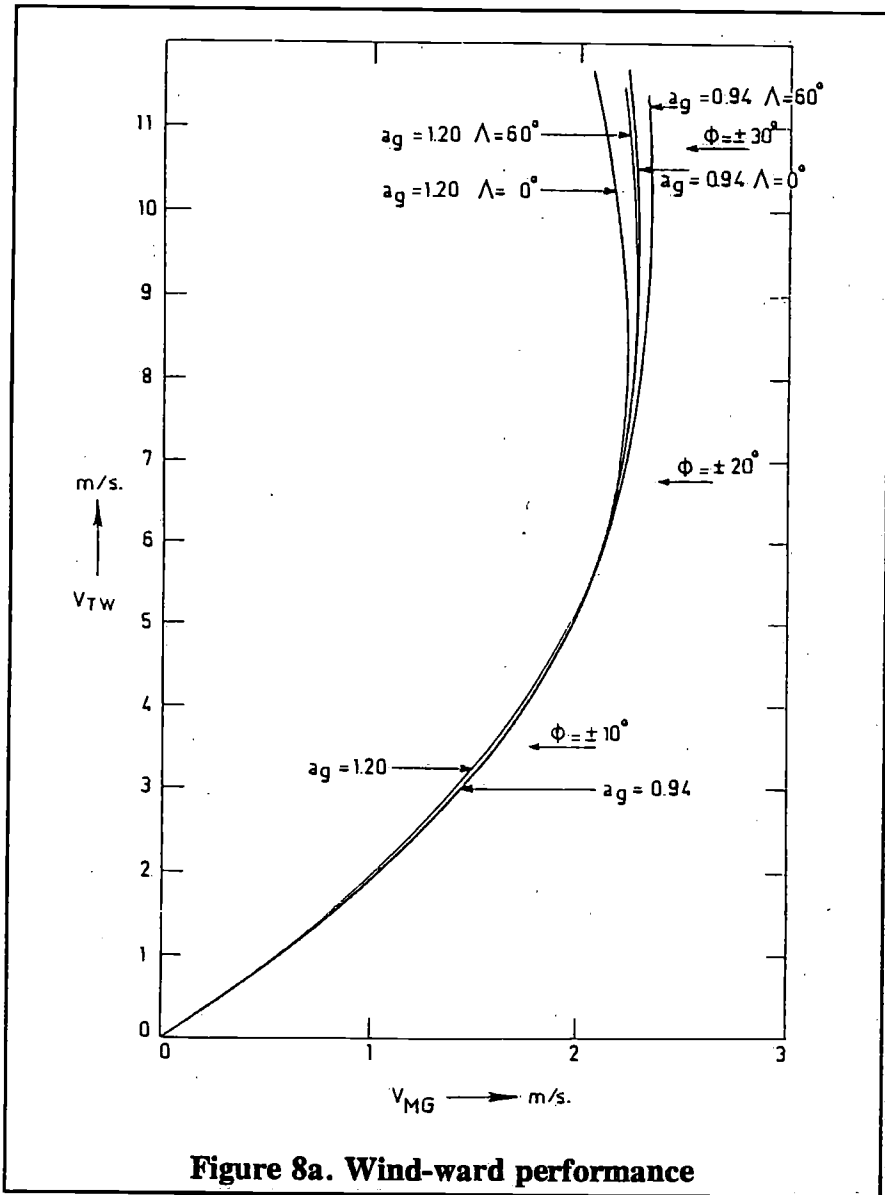


Figure 8a. Wind-ward performance

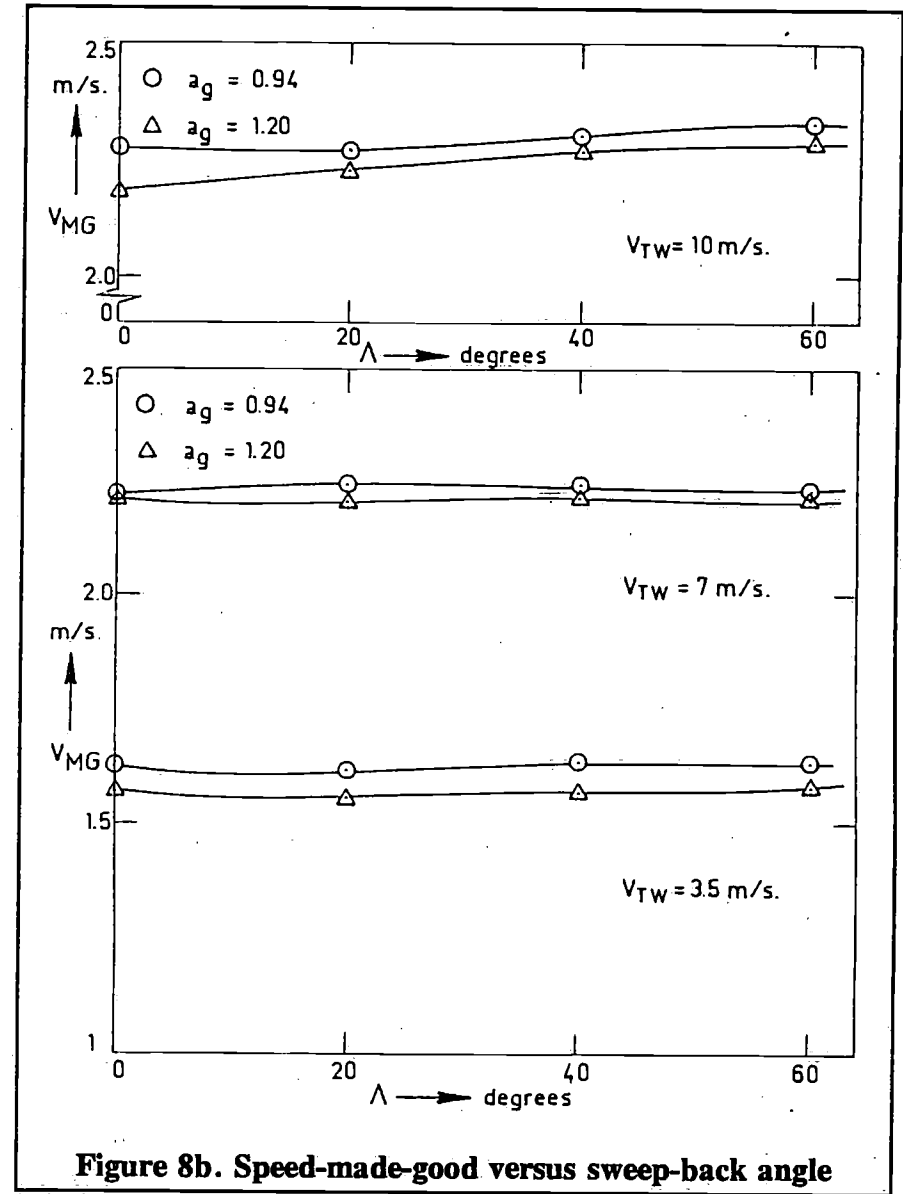
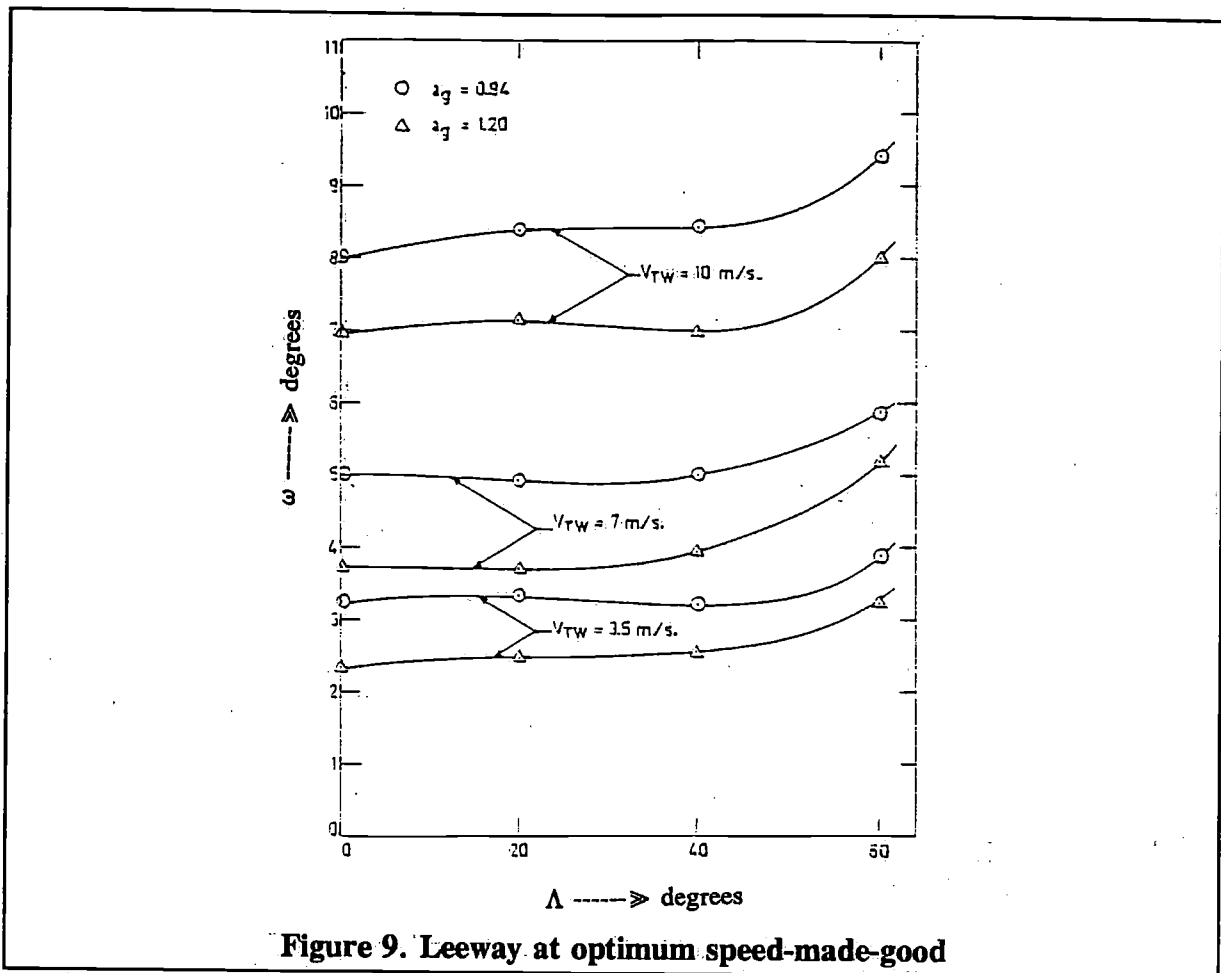


Figure 8b. Speed-made-good versus sweep-back angle



4 Analysis of experiments

For this analysis, induced drag D_i is characterized by the drag increase above the resistance measured in an upright condition without heel and leeway. It should be remembered, that this upright resistance is not the same for all keels, but reduced for keels with the higher aspect ratio and high sweep-back. This influence is not included in the induced drag, while on the other hand the resistance variation with respect to the upright resistance, is included. This arises from alteration in the wave pattern of hull and keel due to leeway and heel.

The lift and induced drag coefficient are defined as follows:

$$C_{D_i} = \frac{D_i}{\frac{1}{2} \rho V^2 A_T}$$

(2)

$$C_L = \frac{L}{\frac{1}{2} \rho V^2 A_T}$$

in which:

$L = Y =$ Hydrodynamic side force

$A_T =$ the lateral area of the equivalent keel and rudder ($= b_{eK} c_K + b_{eR} c_R$), which means the keel and rudder extended to the waterline

For the different keels and each aspect ratio, the induced drag coefficient versus the lift coefficient is presented in Figure 10 for the upright condition.

Figure 11 shows that for the heeling condition and speed as denoted in Table 2 of chapter 2.3. The lift coefficient versus leeway is shown for the some conditions in Figures 12, 13, 14 and 15.

For a given lift coefficient the upright condition and for lift force values in the heeling condition near the optimum speed-made-good, the total resistance and induced drag on the basis of sweep-back angle are shown in Figure 16 respectively. Also combinations of heeling angle and speed as denoted in Table 2 are presented for this case.

5 Calculation of side force

Side force calculations have been carried out by means of the "equivalent keel" procedure as introduced by Gerritsma in [5, 6]. The keel and rudder are considered to be extended to the waterline, while the presence of the hull is assumed to be replaced by the extended part of keel and by the extended part of the rudder, if this does not intersect the water surface already. As a resumé, the procedure, including the proposed corrections, is described briefly here-after. To determine the slope of the lift curve use has been made of the expression according to Whicker and Fehlner in [8]:

$$\frac{\delta C_{L_{K,R}}}{\delta \alpha_{K,R}} = \frac{5.7 a_{e_{K,R}}}{1.8 + \cos \Lambda \frac{\sqrt{a_{e_{K,R}}^2}}{\cos^4 \Lambda_{K,R}}} \quad (3)$$

in which:

- K,R = index for keel or rudder
- $C_{L_{K,R}}$ = lift coefficient
- $\alpha_{K,R}$ = angle of incidence in radiands
- $a_{e_{K,R}}$ = effective aspect ratio
- $\Lambda_{K,R}$ = sweep-back angle of quarter chord line

For keels and for a rudder not intersecting the waterline, the aspect ratio is taken as:

$$a_{e_{K,R}} = \frac{2 b_{e_{K,R}}}{c_{K,R}} \quad (4)$$

with:

- $b_{e_{K,R}}$ = span or draught of effective keel
- $c_{K,R}$ = chord length

If the rudder does intersect the water surface the aspect ratio may be chosen as:

$$a_{e_R} = \frac{1.6 b_{e_R}}{c_R} \quad (5)$$

For small angles of incidence, the side force of a keel or rudder may be estimated from:

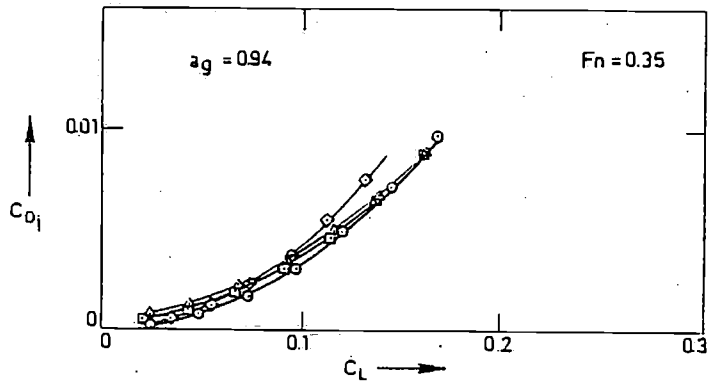
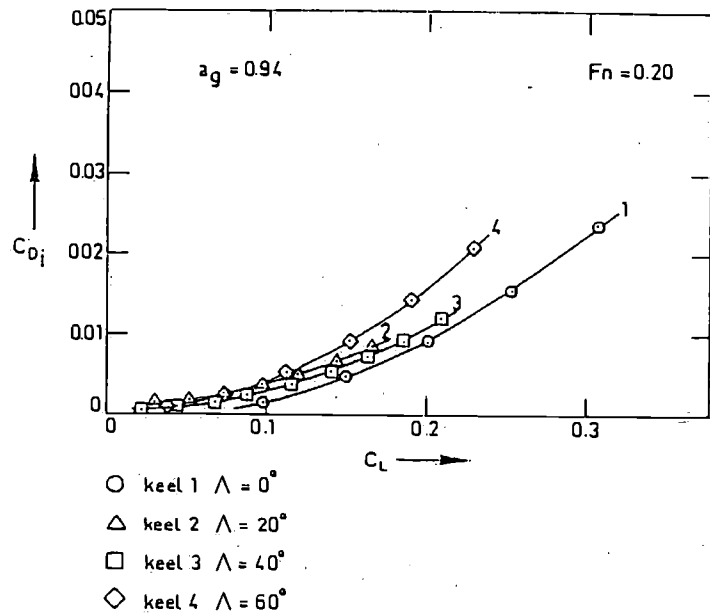


Figure 10a. Induced drag-versus lift coefficient for the upright condition

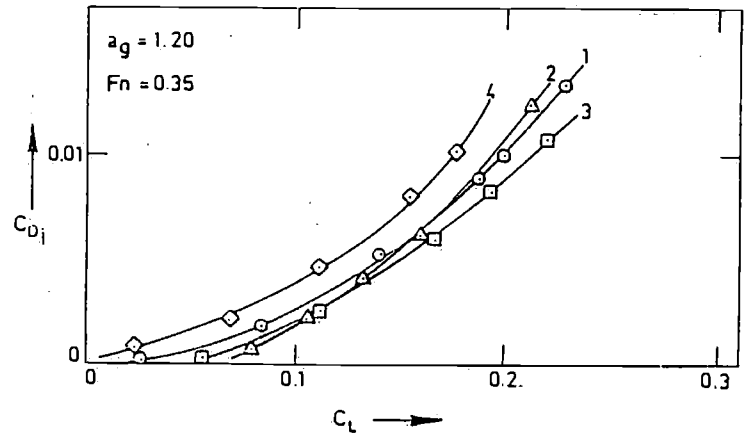
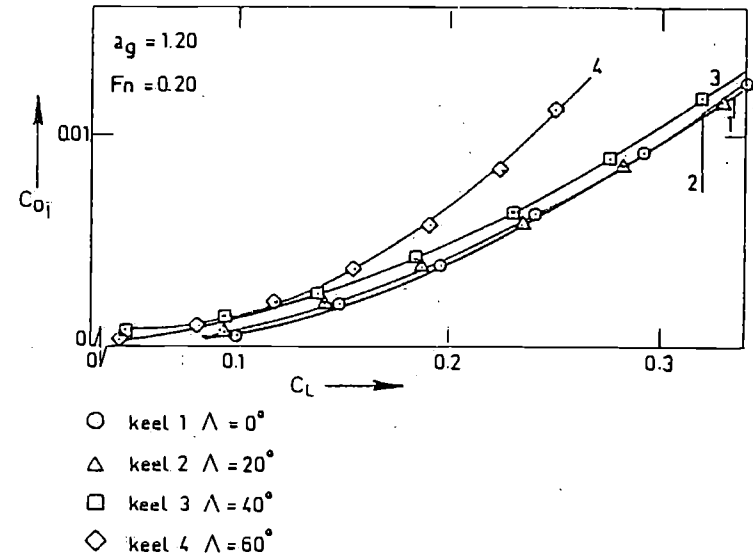


Figure 10b. Induced drag-versus lift coefficient for the upright condition

$$L_{K,R} = \frac{1}{2} \rho V_{K,R}^2 A_{K,R} \left(\frac{\delta C_{L_{K,R}}}{\delta \alpha_{K,R}} \right) \alpha_{K,R} \quad (6)$$

in which:

$$\begin{aligned} V_{K,R} &= \text{water velocity at keel or rudder} \\ A_{K,R} &= \text{lateral area of keel or rudder } (= b_{eK} c_K \text{ resp. } b_{eR} c_R) \end{aligned}$$

The water velocity at the keel may be set equal to the ship speed, and so

$$V_K = V_s \quad (7)$$

while this velocity at the rudder is estimated as :

$$V_R = 0.8 V_s \quad (8)$$

The angle of incidence for the keel may be put equal to the leeway angle, so :

$$\alpha_K = \beta \quad (9)$$

while the angle of incidence for the rudder after correction for "side-wash" of the keel, can be estimated as :

$$\alpha_R = \left\{ 1 - \frac{1.6 (\delta C_{L_K})}{\pi a_{eK}} \right\} \quad (10)$$

If the situation of the centre of effort for keel and rudder is known, it is possible to determine the situation of the centre of effort for the total side force in horizontal and vertical direction respectively from :

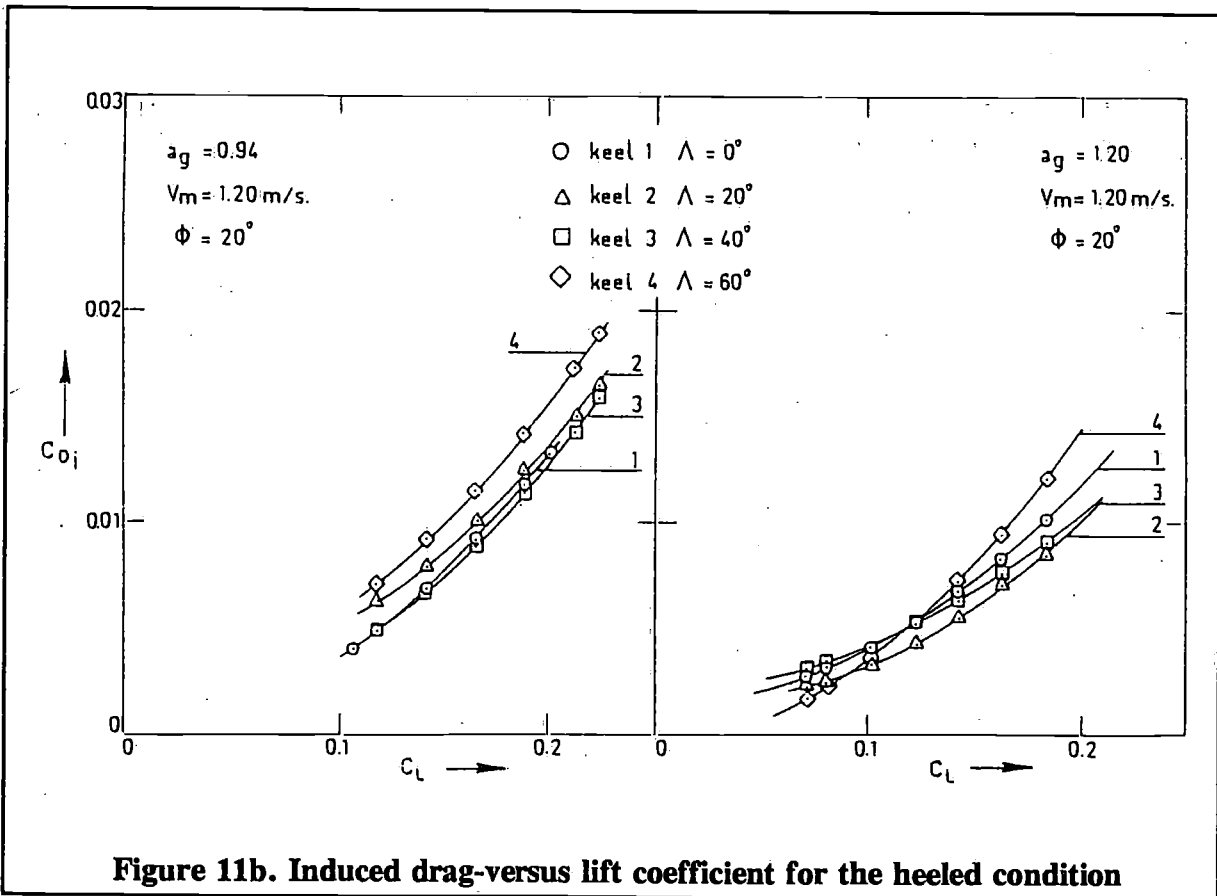
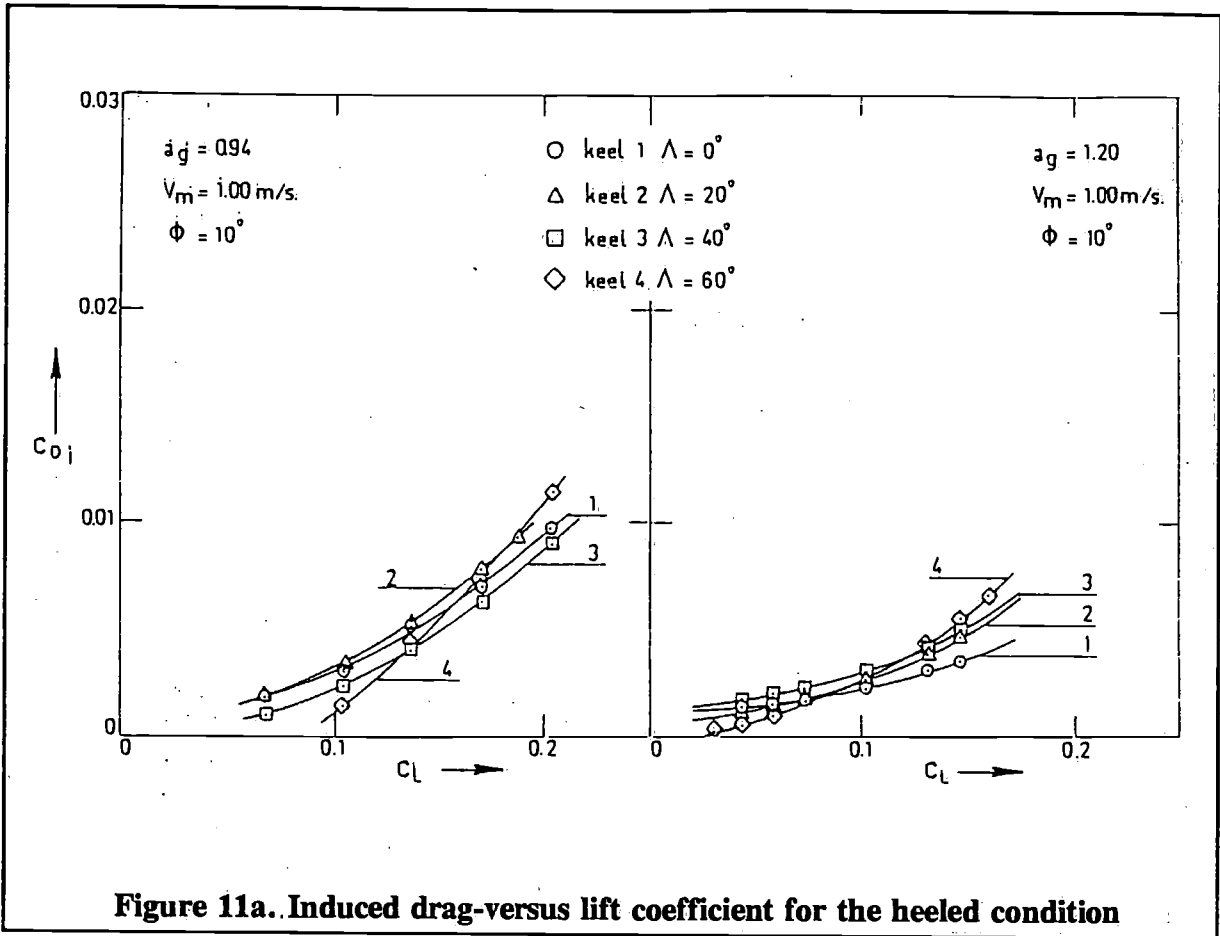
$$x_Y = \frac{L_K x_{Y_K} + L_R x_{Y_R}}{L} \quad (11)$$

$$z_Y = \frac{L_K z_{Y_K} + L_R z_{Y_R}}{L}$$

in which :

$$\begin{aligned} L = L_K + L_R &= \text{the total side force} \\ x_{Y_{K,R}} &= \text{the horizontal distance of the centre of effort of keel or rudder} \\ &\quad \text{from the middle of the test waterline (positive in forward} \\ &\quad \text{direction)} \\ z_{Y_{K,R}} &= \text{the vertical distance of the centre of effort of keel or rudder} \\ &\quad \text{from the test waterline (positive upwards)} \end{aligned}$$

For a spanwise elliptical loading, it is assumed, that the centre of effort is situated on the quarter chord line at 43% of the effective span below the waterline.



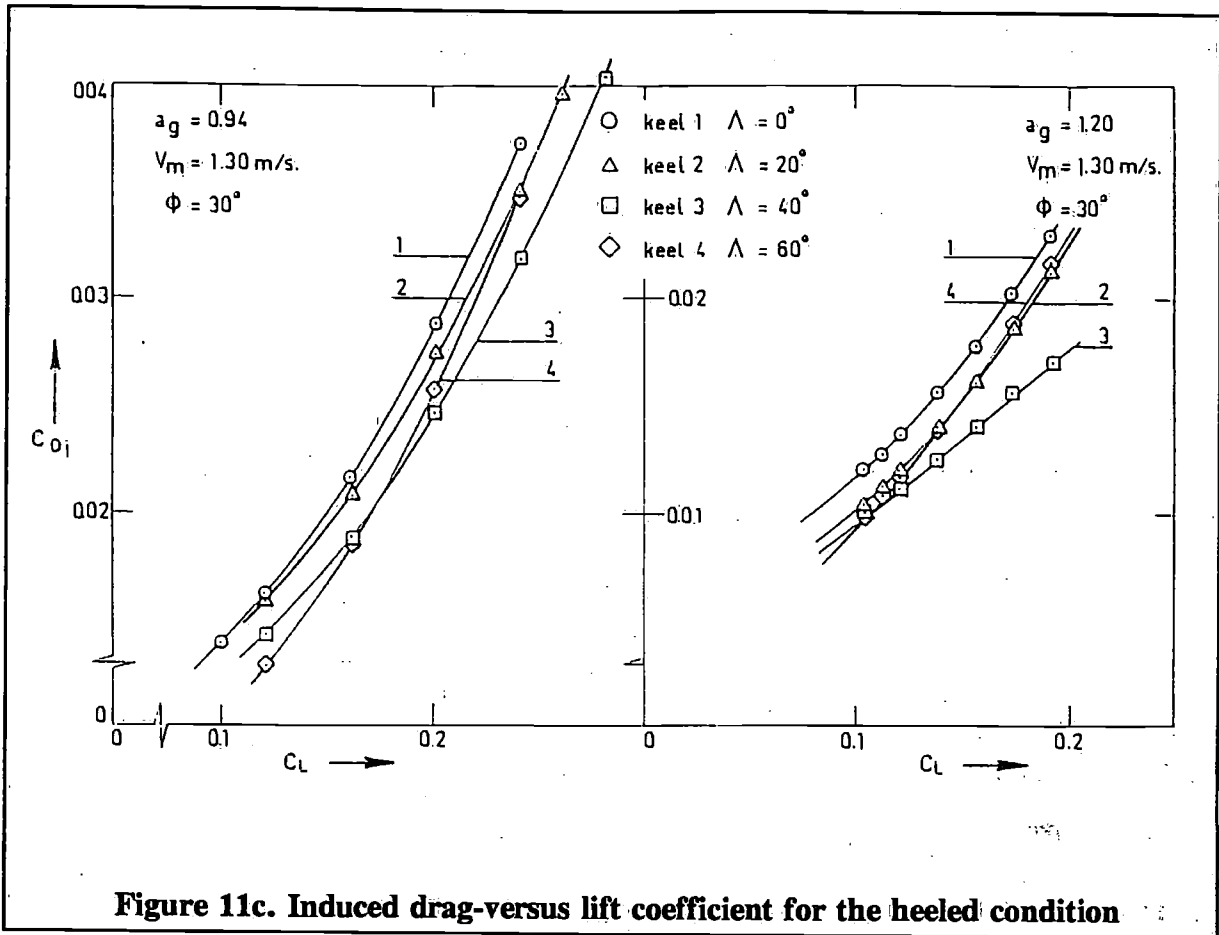


Figure 11c. Induced drag-versus lift coefficient for the heeled condition

It appears, however, that particularly for the horizontal direction, the centre of effort, calculated in this way, shows a rather large deviation from the measurements on the model with keel and rudder. This is a consequence of hull and speed influence. A regression analysis has been made from the experimental results and leads to the following preliminary proposals for the horizontal and vertical situation of the centre of effort.

For the keel the vertical distance of the centre of effort as a ratio to the effective span should be chosen on the quarter chord line as :

$$z_{Y_K}/b_{e_K} = 0.50 - \frac{0.1245}{a_{g_K}^{1.5}} \quad (12)$$

in which: a_{g_K} = the geometric aspect ratio of the keel.

The horizontal distance of the centre of effort, defined off the middle of the test-waterline (MWL) is related to the length of this waterline. Calculated as shown above with x'_Y/L_{TWL} and corrected for speed, hull influence and heeling angle this relative distance may be estimated as:

$$x_Y/L_{TWL} = x'_Y/L_{TWL} + \frac{0.425}{a_{g_K}} Fn \cos \Lambda_K (1 - \sin \phi)^2 \quad (13)$$

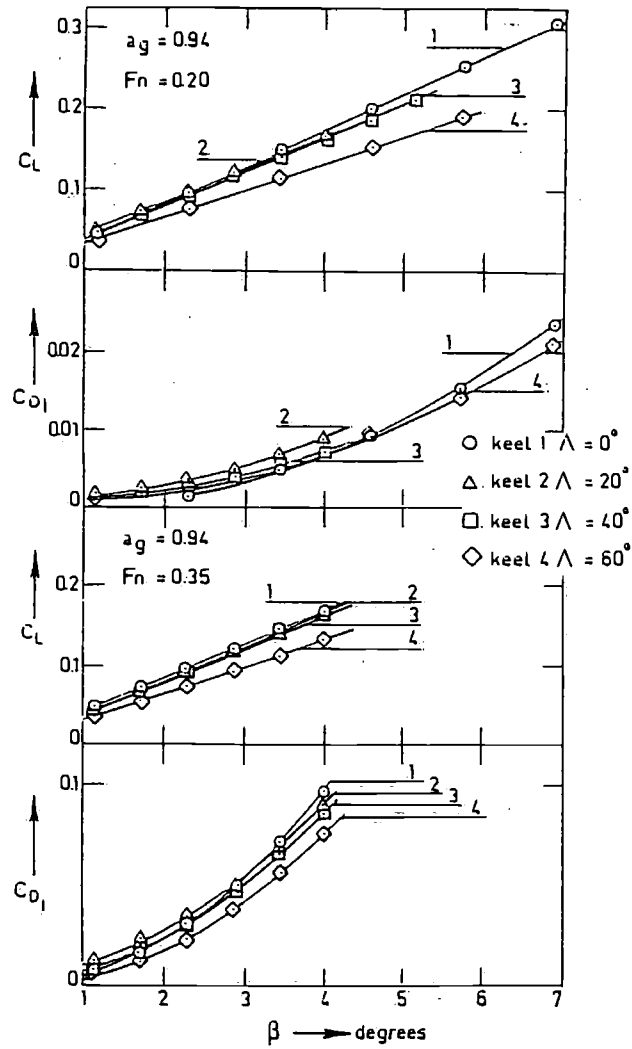


Figure 12a. Induced drag- and lift coefficient versus leeway for the upright condition

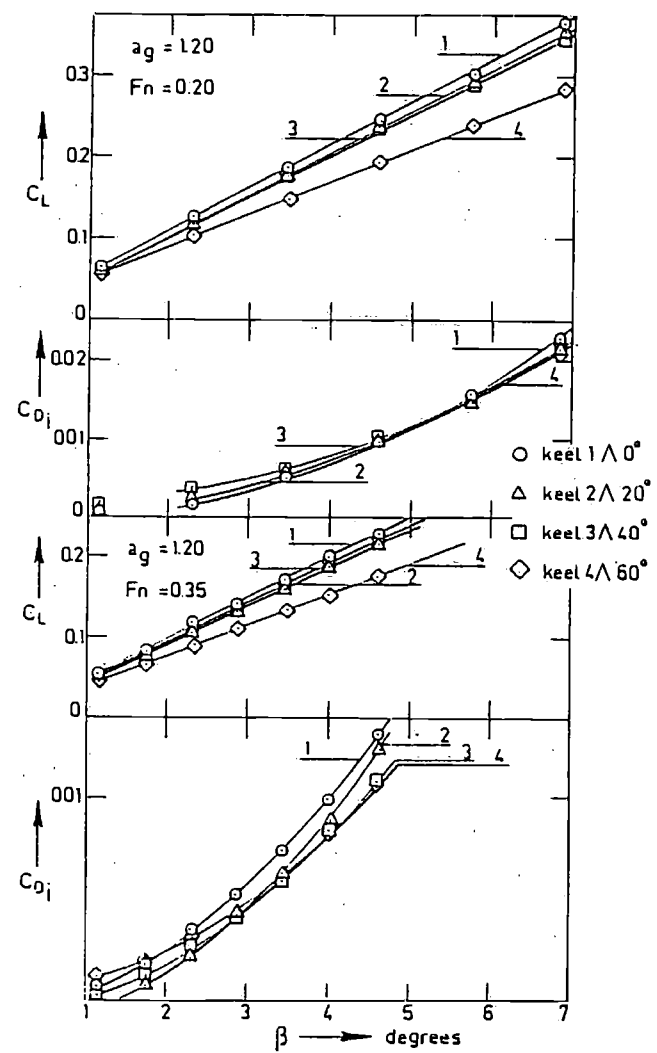


Figure 12b. Induced drag- and lift coefficient versus leeway for the upright condition

in wich:

L_{TWL}	=	length on the test waterline
$Fn = V/\sqrt{gL_{TWL}}$	=	Froude number
Λ_K	=	sweep-back angle of keel
ϕ	=	heeling angle

The calculated results are shown in Figure 3 and 4 both for the upright and heeled condition and are presented in the same way as described in chapter 2.2 for the experimental results on the understanding that :

$$L = Y = F_H \cos \phi \quad (14)$$

The proposed corrections are only a first step because more extended statistical investigations are needed for different hulls and keels to obtain more reliable results.

6 Discussion

To obtain a clear judgement about the test results, the following aspects are taken into consideration:

- 1 induced drag and total resistance for a given lift
- 2 induced drag and lift for a given angle of leeway
- 3 sailing performance
- 4 calculation of the side force.

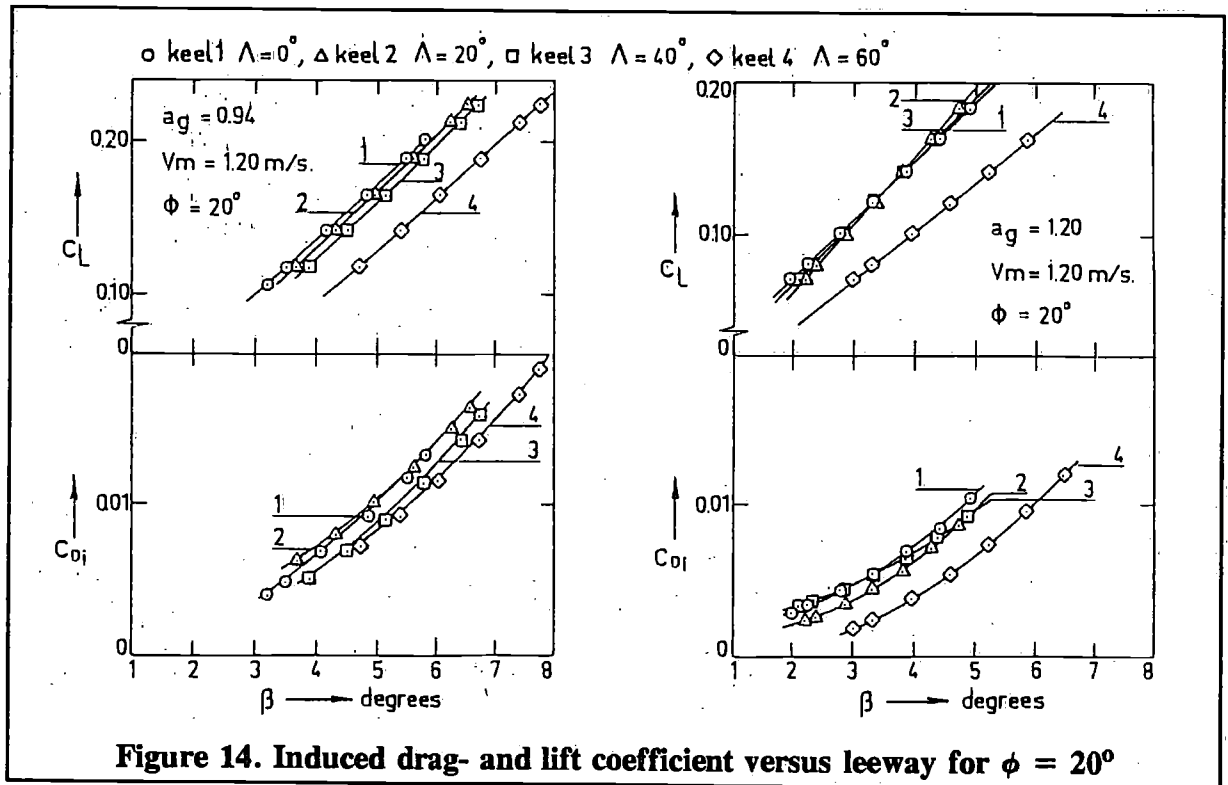
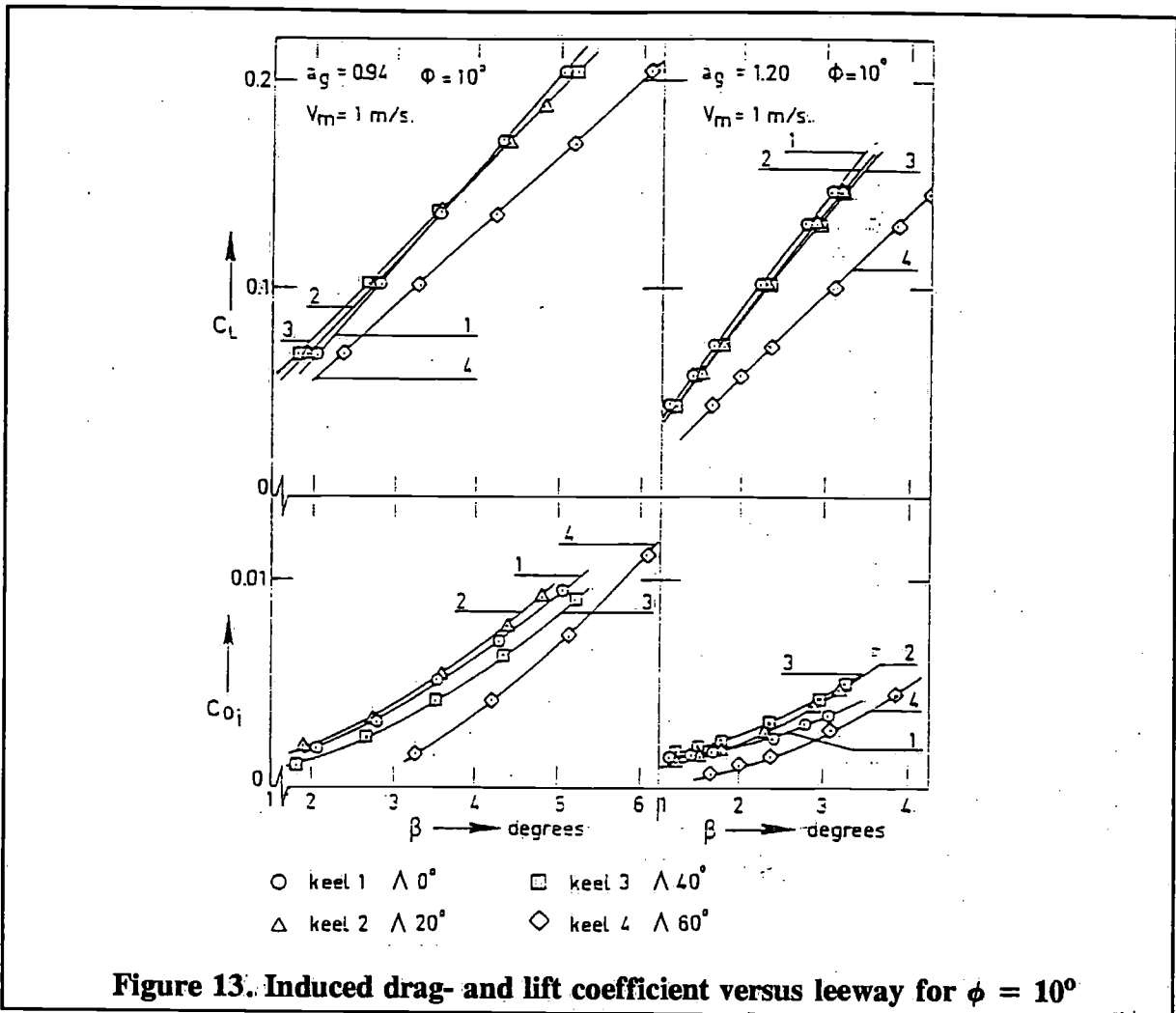
For comparison, the results with respect to the total resistance or induced drag and the resulting speeds of the sailing performance, it should be remembered, that the total resistance or induced drag is more sensitive than the speed.

For the upright condition without heel and leeway, it is clear from Figure 2 that the differences in resistance are small for the lower aspect ratio, while for the higher aspect ratio the resistance is reduced by about 5% for a sweep-back angle of 0 to 60 degrees. This phenomenon has an important influence on the final results, as will be shown later.

6.1 Induced drag and total resistance for a given lift

6.1.1 Upright condition

It is evident from the results shown in Figure 10, that for the upright condition with leeway, the induced drag is increasing with sweep-back angle for a given side force. This tendency is in agreement with [2] and [4]. The percentage of increase is dependent on the value of the lift force, but generally far more than 1% of that calculated by Herreshoff and Kerwin in [2]. For a certain lift coefficient e.g. $C_L = 0.05$ with respect to the higher aspect ratio, the total drag increases with sweep-back angle of 0 up to 60 degrees by about 6%. For this aspect ratio, especially, one should remember that the upright resistance without leeway reduces by about 5% for a sweep-back angle of 0 to 60 degrees. It should be remarked from Figure 10 that increase of induced drag with sweep-back angle is most clearly demonstrated for the higher aspect ratio and the lowest speed in the case of the upright position. Further, the influence of the keel wave may be expected to increase with speed and to decrease with aspect ratio.



6.1.2 Heeling condition

The relation between induced drag and sweep-back angle, as found for the upright position, changes a great deal under heel. This may also be caused by the behaviour of the keel wave: the amplitude of this wave increases with heel and decreases with sweep-back angle as remarked in chapter 2.3. This phenomenon appears to be a dominant factor for the induced drag and consequently, for the total resistance.

For the higher aspect ratio and the smallest heeling angle, the tendency is the same as that for the upright position:

induced drag increases with sweep-back angle for a given side force. It is easily understood that for this case the influence of the keel wave is rather small. For the other heeling angles with higher aspect ratio and for all heeling angles with the lower aspect ratio, it is possible to indicate a minimum value of the induced drag with respect to the sweep-back angle for a given side force as shown in Figure 16. The same procedure can be used to determine the minimum total resistance relative to sweep-back angle. For the considered lift coefficients, where values have been chosen near those of the optimum speeds-made-good, the minimum total resistance is mostly found at sweep-back angles of 40-50 degrees. It should be emphasized that for the determination of the optimum sweep-back angle on a basis of the minimum total resistance, also the leeway angle should be taken into consideration. The performance calculations in chapter 3 and Figure 9 show that the variation in leeway is very small for sweep-back angles of up to 45 degrees which can be regarded favourably.

6.2 Induced drag and lift for a given angle of leeway

Both for the upright and heeled condition, it is clear from the Figures 12-15 that induced drag, as well as side force, is decreasing with sweep-back angle for a given angle of leeway. From this relation, it follows that side force production as well as induced drag may be expected to be maximum for a sweep-back angle of zero degree. The reduction of the side force production for a certain angle of leeway is both for the upright and heeled condition clearly shown in Figure 3 and 4. It is surprising that for a sweep-back angle of 20 degrees a rather strong reduction of the side force production has been observed, which perhaps might be due to an unfavourable interference of the keel and hull wave.

6.3 Sailing performance

With respect to the results of the performance calculations, it can be shown from Figure 7 that the down-wind speed with the lower aspect ratio keel is almost equal for all sweep-back angles, while for the higher aspect ratio keel, the maximum sweep-back angle appears to be the most favourable.

This fact is due to the reduced upright resistance for this case as previously mentioned. The lower speed with the higher aspect ratio in comparison to the lower ratio, is of course caused by the higher frictional resistance due to the larger keel area. The results of the windward performance calculations are shown in Figure 8. It is again clear, that the higher aspect ratio keels deliver lower speeds-made-good than the lower aspect ratio keels because of the higher frictional resistance.

Nevertheless, it is noteworthy that for moderate winds, the differences between the speed-made-good values obtained with both aspect ratios, are almost negligible as shown in Figure 8 and 9.

This fact might denote that an increase of aspect ratio with equal keel area, within certain limits seems favourable for moderate winds (± 7 m/sec).

For strong winds the high sweep-back angle seems to be advantageous, especially, for the higher aspect ratio keel. This gain in speed-made-good is also mainly due to the reduction of

the upright resistance for the high sweep-back angle.

It should, however, be kept in mind that the leeway angle, which appears to increase rather significantly by about one degree for the maximum sweep-back angle (Figure 9), is not accounted for sufficiently in the usual calculation procedure of the speed-made-good. In practice, it generally holds that the smaller leeway the more a vessel can be sailed close to windward.

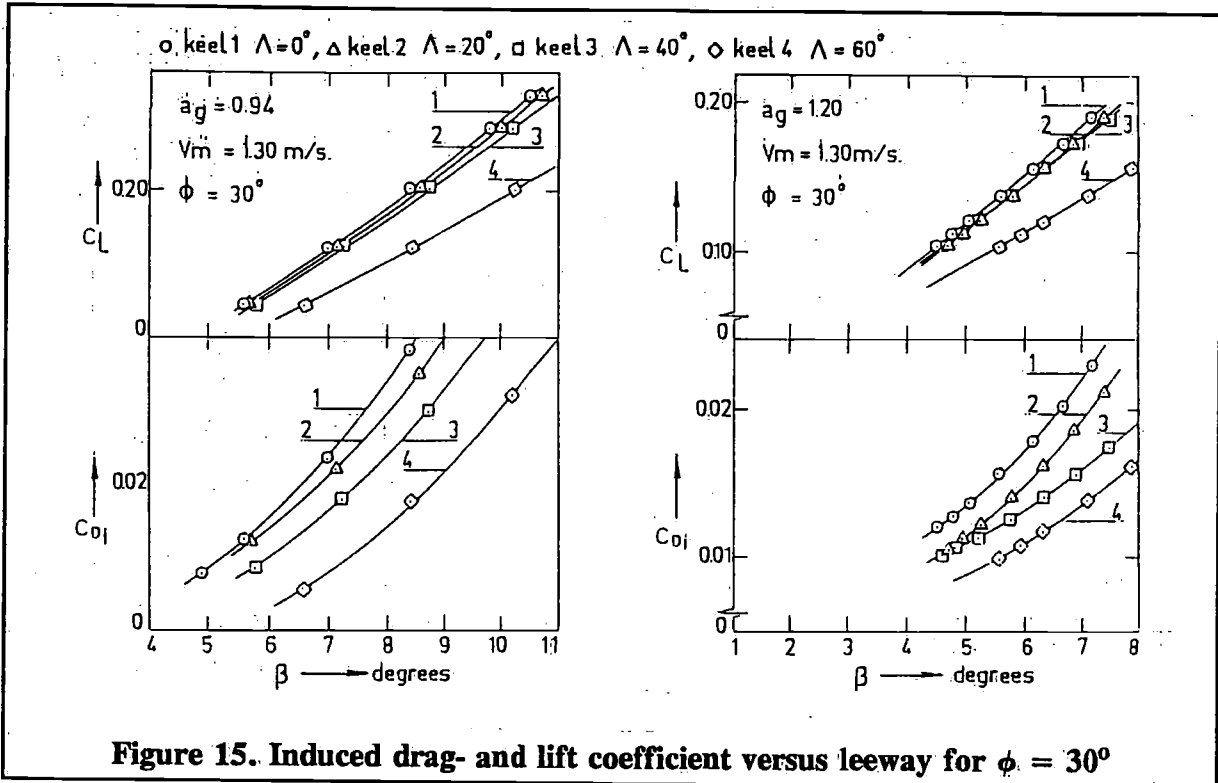


Figure 15. Induced drag- and lift coefficient versus leeway for $\phi = 30^\circ$

6.4 Calculation of the side force

The calculated values of the side force production for each angle of leeway agree very well with the measurements even for the heeling condition as shown in Figure 3 and 4. The centre of effort shifts backwards in horizontal direction with the increase of the sweep-back angle and appears to be affected strongly by speed, heeling angle and aspect ratio. For this reason, these parameters are accounted for in the proposed correction. In the vertical direction, the centre of effort remains almost constant and is mainly dependent on the aspect ratio. The proposed correction for the vertical position of the centre of effort is related especially to the upright condition.

The measurements for the heeling condition show a rather large dispersion with again remarkably exceptional values for sweep-back angles of 20 degrees.

The proposed corrections have a preliminary character because they are, probably, related strongly to the hull form considered.

7 Conclusions

The upright resistance has proved to be almost independent of sweepback angle for an aspect ratio of 0.94, while a reduction of about 5% is found for an aspect ratio of 1.20 at a sweep-back angle of 60 degrees. The tendency that induced drag increases with sweep-back for a given lift in the upright condition, was shown not to be valid under heel. This was caused by the significant influence of the interference of keel and hull wave dependence on sweep-back angle. This important surface influence should not be disregarded for keel design. Under

heel, at optimum sailing conditions, the minimum total resistance has been observed at sweep-back angles of 40-50 degrees. Side force production and induced drag decrease with sweep-back if the same angle of leeway is considered. This holds true for both the upright and heeled condition. For 20 degrees sweep-back angle, a strong reduction in side force has been observed. Performance calculations show that leeway proves to be nearly constant with aspect ratio for all angles of sweep-back. An exceptional increase of about one degree has been found for a sweep-back angle of 60 degrees. The leeway angle should be accounted for more satisfactorily in the wind-ward performance calculation. But neglecting this imperfection, the results of the usual windward performance calculation lead to high aspect ratio keels for moderate winds while highly swept back for strong winds. The centre of effort in a horizontal direction shifts backwards with sweep-back angle and is greatly dependent on speed, heeling angle and aspect ratio. The centre of effort in a vertical direction with aspect ratio is rather constant with the exception of 20 degrees sweep-back angle. In conclusion, calculated values according to the "equivalent keel" procedure appear to be in good agreement with the measurements for the side force, whereas the proposed calculation of the position of the centre of effort needs further investigation.

8 Acknowledgement

The authors wish to acknowledge the contribution of Carl R. Witmer and Joel S. Mac. Minn, students at Webb Institute of Naval Architecture, who carried out the performance tests with the lower aspect ratio keels during their stay at Delft.

They are also indebted to A.J. van Strien and R. Onnink of the Delft Shipbuilding Laboratory for their assistance in the experiments and analysis.

The authors are indebted to E.G. van de Stadt, who put the design of the "Spirit 28" at their disposal.

Furthermore, they are particularly grateful for numerous discussions with Prof.ir. J. Gerritsma and ir. G. Moeyes of the Delft Shipbuilding Laboratory, who stimulated the present project.

Finally special acknowledgements are made to P.W. de Heer for the lay-out and manufacture of the graphs and figures.

9 Nomenclature

Symbol	description	unit
A	= lateral area	m^2
$A_T = b_{eK}c_K + b_{eR}c_R$	= total lateral area of effective keel and rudder	m^2
$a_{eK} = b_{eK}/c_K$	= aspect ratio of effective keel i.e. keel extended to the test waterline	
$a_{eR} = b_{eR}/c_R$	= aspect ratio of effective rudder i.e. rudder extended to the test waterline	
$a_{gK} = b_{gK}/c_K$	= geometric aspect ratio of keel	
$a_{gR} = b_{gR}/c_R$	= geometric aspect ratio of rudder	
B	= beam	
b_{eK}	= span of effective keel i.e. keel extended to the test waterline	m
b_{eR}	= span of effective rudder i.e. rudder extended to the test waterline	m

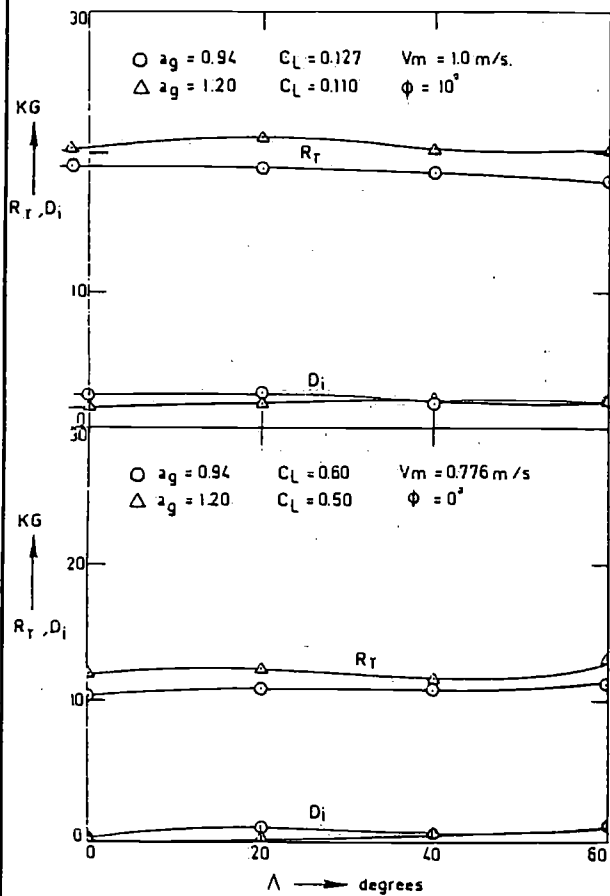


Figure 16a Induced drag and total resistance for a given side-force

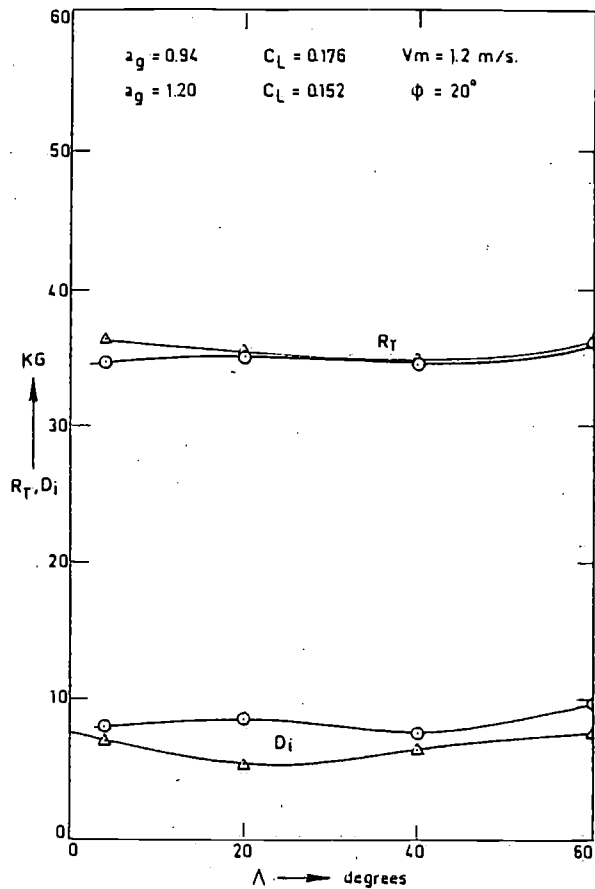


Figure 16b Induced drag and total resistance for a given side-force

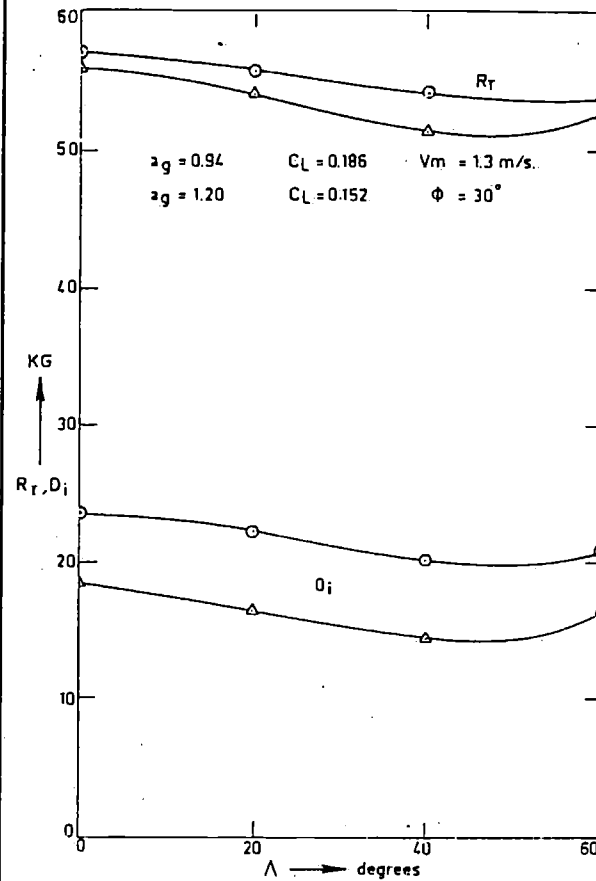


Figure 16c Induced drag and total resistance for a given side-force

Symbol	description	unit
b_{gK}	= span of keel from tip chord to root chord at the hull	m
b_{gR}	= span of rudder until the hull	m
$C_{Di} = D_i / \frac{1}{2} \rho V^2 A_T$	= induced drag coefficient	
<i>C.E.</i>	= centre of effort	
$C_L = L / \frac{1}{2} \rho V^2 A_T$	= lift coefficient	
c_K	= chord of keel	m
c_R	= chord of rudder	m
D_i	= induced drag	m
F_H	= sail force	kg
$Fn = V / \sqrt{gL_{TWL}}$	= Froude number	
g	= acceleration of gravity	m/sec ²
H	= hull as a subscript	
K	= keel as a subscript	
L	= ship length, lift	m, kg
LCB_H	= position of centre of buoyancy of hull in length with respect to <i>MWL</i>	
L_{OA}	= length over all	m
L_{TWL}	= length on test waterline	m
<i>MWL</i>	= middle of test waterline	
R	= resistance; rudder as subscript	kg
R_T	= total resistance for ship	kg
R_{Tm}	= total resistance for model	kg
T	= draught	m
$V = V_s$	= ship speed	m/sec
V_D	= speed down wind or speed in running condition	m/sec
$V_{MG} = V_s \cos(B + B_{TW})$	= speed-made-good to windward	m/sec
V_m	= model speed	m/sec
V_{TW}	= true wind speed	m/sec
x_Y	= horizontal distance of centre of effort from <i>MWL</i> (positive forward)	m
Y	= hydrodynamic side force	kg
$Y_B = Y / \frac{1}{2} \rho V^2 L^2_{TWL} B$	= dimensionless side force per angle of leeway	
z_Y	= vertical distance of centre of effort from the waterline (positive upwards)	m
α	= angle of incidence	degr/rad.
B	= angle of leeway	degr/rad
B_{TW}	= angle between course and true wind	degrees
λ	= taper ratio	

Symbol	description	unit
ϕ	= heeling angle	degrees
ρ	= mass density of fluid	kg s ² /m ⁴
Λ	= sweep-back angle of quarter chord line	degrees

10 References

- [1] DeSaix, P.,
"Yacht keels on experimental study", Journal "Sail", May 1974
- [2] Herreshoff, H.C. and Kerwin, J.E.,
"Sailing yacht keels", 3rd HISWA Symposium on Yachts, Amsterdam, March 1973
- [3] Mac Lavery, K.,
"Tests of a 5.5 meter yacht form with various fin sweep-back angles", University of Southampton, SUYR report 17, 1966
- [4] Annual Report of the Advisory Committee for Yacht Research, University of Southampton, 1967
- [5] Gerritsma, J.,
"Course keeping qualities and motions in waves of a sailing yacht", Proceedings of the third AIAA Symposium on the Aero-hydrodynamics of sailing, California, 1971
- [6] "Symposium onderzoek aan zeiljachten" (in Dutch),
Report no. 350, Shipbuilding Laboratory, University of Technology, Delft
- [7] Abbot, I.H. and Doenhoff von, A.E.,
"Theory of wing sections", Dover Book, 1959
- [8] Whicker, L.F. and Fehlner, L.F.,
"Free stream characteristics of a family of low aspect ratio control surfaces", DTMB Report 933, May 1958

On noise reduction aboard motoryachts

by J. Buiten and M.J.A.M. de Regt

TNO Inst. of Applied Physics, Delft

Summary

A brief introduction to the fundamentals of acoustics and on noise measuring and rating is given and this is used to a better understanding of a table of acceptable noise levels for various compartments of motor yachts taking into account the owners intended use. It is argued that effective shipboard noise insulating measures with respect to the noise generated by the main propulsion system affect so essentially the design as to make the acoustical planning an indispensable part of the early design stage. Toward this aim a calculation method is given for an engineering estimate of the noise levels on board a yacht due to the primary noise sources. The system proposed is applied in detail to two typical yacht designs and good agreement is demonstrated between calculated and measured A-weighted sound levels; in addition several possible improvements in noise levels are indicated.

1 Introduction on noise prevention

Effective noise countermeasures on board ships do affect essentially the design and construction of a ship. In this respect much is known especially from extensive investigations and practical experience on board large sea-going commercial and naval vessels. Little of this experience appears to be applied in motor yachts, however. It is the purpose of this paper to try and summarize the main aspects of acoustical designing in naval architecture as far as it is relevant to motor yacht building.

There is a large selection of materials that may be recommended for noise abatement such as viscoelastic damping layers, porous absorbing materials, rubber or plastic sheets etc. Intuitively they could all be expected to have a marked effect on noise transmission, their effectiveness, however, is often very disappointing. This arises from the very complex nature of the problem and a warning on their use is given. The important point is that these materials can furnish an effective and economical solution when properly applied and again underlines the necessity of acoustical planning at an early stage in the design of a yacht.

Clearly there is a need for a calculating method to estimate probable noise levels based on data available in the first design stage. This may be confined to those noise sources and those hull parts, a modification of which at a later stage would be prohibitive. The primary aspects to be considered are the propulsion engines and reduction gears, the propellers and water on-flow, the airborne and the structure-borne sound transfer and insulation. This does not imply other noise sources are not important, they may even largely spoil the achieved results by the main acoustical measures, but for these sources remedial measures later on are possible without affecting the ship's design. Of course, the noise level estimates must be rated as to their acceptability. The present paper contains therefore a noise rating recommendation for motor yacht designers and owners.

2 Noise, measuring and rating

Sound as heard by the ear is physically an alternating pressure, a "ripple on the static air

pressure", brought about by a vibrating source region and propagated by the air. If the source vibrates in such a manner as to show a sinusoidal displacement as a function of time, then we would hear a pure tone, the number of cycles per second being called the frequency, provided this frequency was within the audiofrequency range: between 16 cycles per second (very low audiofrequencies) and up to 16 000 Hz (hertz) for the very high frequencies.

The sound pressure itself is not normally used to describe the magnitude of sound. A logarithmic scale of a function of the sound pressure gives suitable values for the pressures occurring in practice. Moreover this appears useful in view of the measuring accuracy required and of the fact that man judges loudness in a more or less logarithmic manner. As the reference value for the logarithmic scale a pressure of 2×10^{-5} N/m² (or P_a = pascal) is the international standard. The sound pressure level (L_p) expressed in decibel (dB) is defined by

$$L_p = 10 \log_{10} \frac{P_{eff}^2}{p_0^2} = 20 \log_{10} \frac{P_{eff}}{p_0}$$

in which $p = 2 \times 10^{-5}$ Pa.

Sound can be radiated by vibrating surfaces. The vibrations of these surfaces can be measured with the aid of vibration pick-ups, mostly accelerometers. In accordance with standardization these vibrations may be described in terms of velocity level (in this paper the reference velocity is 5×10^{-8} m/s) or of acceleration level (reference 10^{-6} m/s²).

A sound phenomenon can be described by its frequency and its level. However, usually machines do not generate one single frequency but a great number of pure tones or more or less "white noise" which makes it difficult to describe the frequency content and the strength of the signal as dependent on frequency. To overcome this difficulty the audio-frequency range can be divided into pass-bands with a width of one octave (the upper and the lower limiting frequencies of each band have a ratio of 2:1). These octave-bands are often designated by their standardized centre frequencies 31.5, 63, 125, 250, 500, 1000, 2000, 4000 and 8000 Hz. This rather rough division appears to be fine enough for most noise abatement problems. For the description of noise aboard motor yachts the frequency range may even be limited to 63-2000 Hz. Octave bands levels can be measured easily so the numerical description of noise does not lead to serious problems.

The prediction of the reaction of people to noise is however not that simple. Man judges a low-frequency sound less loud than an equally strong high-frequency. A simple way of taking into account this subjective judgment is to introduce a frequency dependent constant; standardized as the so-called *A*-weighted sound level in dB(*A*) [1, 2]. An *A*-weighted sound level meter is equipped with a filter network that attenuates the low frequency pressures relatively compared to the higher ones; for example pressures at 30 Hz are weighted some 40 dB lower than those at 3000 Hz. Its use for rating motor yacht noises is practical and seems to be justified in general.

This single number measure for a noise is insufficient for planning countermeasures, however. For that purpose one needs insight into the frequency ranges causing the annoyance. In general octave band spectra will give sufficient information. For rating these noise spectra there exist successively numbered Noise Rating (*NR*) curves [1, 3]. The *NR*-curve tangent to the octave band spectrum determines the noise rating number of the corresponding noise. There are at least 5 aspects of noise annoyance on board motor yachts:

1. impairment of hearing (engine room)
2. speech interference (saloon, wheelhouse, open deck)
3. audibility of whistles (poor visibility, at sea, rivers etc.)
4. general comfort (cabins, saloons, open decks)
5. radiated external noise (environment, harbours, banks).

The first three have been investigated extensively and specific recommended noise limits have found wide acceptance, at least as a working proposal for the time being [3 to 9]. The fifth will not be considered in this paper whereas the fourth needs some explanation.

Legislative noise limits for commercial ships might be used as a starting point for motor yachts [5 to 8]. The limits for crew cabins appear to be within the range 45-60 dB(A) where 60 dB(A) is a "just acceptable" level. These limits are intended for the hours of rest for the crew. When the yacht only will be used during day-time hours slightly higher levels will be accepted by the crew, e.g. 65 dB(A).

However it is probable that the owner of a luxury yacht wants to obtain more comfort in his compartments than "just acceptable" and a lower limit than 60 dB(A) has to be recommended in that case, e.g. 50 dB(A).

The owner of a fast sailing motor yacht, who uses the top speed for only a few hours a day will accept much higher levels. The limit will be influenced in that case only by the interference of speech, for which a realistic limit will be 70 dB(A). These and similar considerations lead to

- a. a classification of motor yachts according to their use
- b. a division into comfort classes of the various spaces on board according to the required acoustical comfort.

It is with these aspects in mind that the authors propose the summary of recommended noise limits of Table 1 as a guidance to the designers and the owners of motor yachts.

3 Noise, sources and paths

On board a ship a large part of the noises heard is being radiated by the decks and bulkheads into the air. Nearly always it is possible to discern a source region, various transfer paths and a receiving region.

In general sound sources are distinguished in the way the sound is propagated from the source to its surroundings. So airborne sound sources radiate sound which is propagated by the air (e.g. loudspeaker, exhaust of engine, ventilators). For structureborne sound sources the first part of the transfer path is the ships structure (diesel engines, gearboxes). Propellers initiate waterborne noise where the first part of the sound path is via the water to the ships hull.

In practice a machine will produce airborne as well as structureborne sound and both aspects need to be considered. Figure 1 gives an impression of the various sound paths between a propulsion engine and an accommodation space located just above the engine room. As can be seen in the figure the hull in the engine room and the separating deck are excited by structureborne as well as by airborne sound. The vibrations of these parts of the ship's structure will be propagated to the boundaries of the accommodation which will radiate sound into the accommodation space.

The way in which sound is propagated through solid materials is very complicated.

Table 1 A-weighted noise levels not to be exceeded; see footnotes (1) and (2).

(motor)yachts spaces	sea-going speed ≥ 16 kt	sea-going speed < 16 kt	inland cruiser	fast in- shore powerboat	sailing yacht using auxiliary propulsion engine
owners' accommodation					
1 (1, etc.)	50	50	fore: 60	80	60
2	55	60			
3	60	70			
guests' cabins					
1	55	55	aft: 65		
2	60	65			
3	65	75			
public rooms					
1	55	55			
2	60	65			
3	65	70			
recreation decks					
1	50	50	50		
2	65	65	60		
3	70	80	65		
crew cabins					
1	55	55			
2	60	65			
3	65	75			
crew dayroom					
1	55	55			
2	65	65			
3	70	75			
wheelhouse	65	70	open: 65 closed : 60	90	65
bridgewing	70 dB(A) at 260 Hzt 68 dB at 500 Hzt 63 dB				
engine room occupied	90				
non-occupied	110				
control room	80				
externally radiated at 1 m from ship at 15 m (2)	50	50	50	80	50

Footnotes: (1) The comfort classes are to be understood as follows:

1. really comfortable; not to be exceeded when in harbour
2. reduced but still acceptable comfort
3. limit of acceptability: complaints when exceeded.

(2) According to SAE recommended measurement procedure [10].
Local legislative noise limits have to be observed, however!

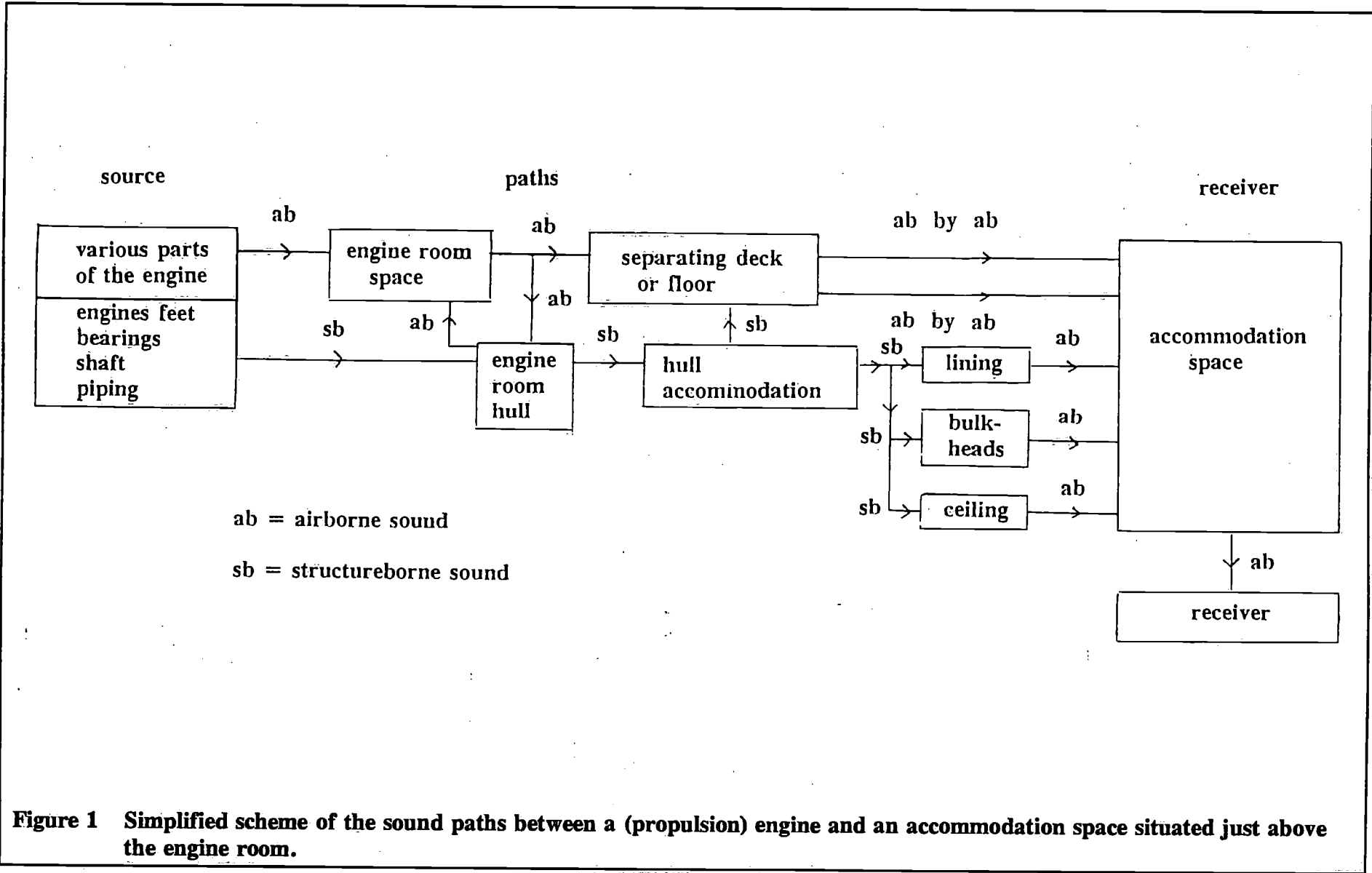


Figure 1 Simplified scheme of the sound paths between a (propulsion) engine and an accommodation space situated just above the engine room.

A mixture of torsion and bending, longitudinal and transverse waves forms the transfer mechanism. Moreover the wave-lengths are not very small compared to the dimensions of the structural parts. All these factors imply that for efficient noise reduction not only the form and the dimensions of the insulating structure itself but also the acoustical properties of the contiguous parts of the sound path are of utmost importance.

So, for example, a heavy and airtight steel bulkhead may be a very good insulating structure between two cabins, it is a very poor insulator of waterborne propeller noise. A layer of air bubbles, on the other hand, close to the plates may isolate very effectively propeller noise from the hull. A resilient mount, although very good in general, may give no improvement when for example it is mounted under an extended engine foot.

A special instance is that of visco-elastic damping layers. These are very successful in several applications but nearly never on board of ships, partly because other elastic-dissipative mechanisms are incorporated naturally in the ship's structure already, partly because these layers cannot be made sufficiently stiff.

In general effective barriers in sound paths are either heavy layers between light and compressible media or compliant layers between heavy and stiff media.

4 Noise reduction design

In principle, the following noise countermeasures are at the naval architect's disposal:

- quiet machinery and propeller
- resilient mountings and acoustical enclosures
- enlarged distances between machinery and accommodation
- special insulation in way of accommodation
- sound absorption in accommodation and/or in machinery spaces

An early decision about most of these is required because they may affect the whole design of a ship quite considerably. After the ship is built nearly all of them can be applied only at very considerable expense and even then the result is sometimes dubious!

From the several acoustical and shipbuilding aspects that should be weighted against the owner's requirements it has to be considered that the data in Table 4. of the calculation scheme (section 5) on shipboard noise sources in general are a fair average of the noise levels occurring in practice. It may be worthwhile to compare different machines under consideration with respect to their actual noise production.

This applies to diesel engines, reduction gears and also more or less to flexible couplings, either between engine and reduction gear or in the propeller shaft. Also the "average" calculation scheme arguments (section 5) deserve careful consideration. For example resilient mountings and acoustic enclosures for engines are more efficient as general noise countermeasures than special insulation in way of the accommodation. Compare in this respect step 2, step 4 and step 6 with step 9 etc.

It seems that applied research in the field of propeller noise could yield most useful results. In conventional propeller design only costs and efficiency are parameters. For a "quiet" propeller an improved design (less cavitation) with greater hull clearance and carefully controlled water onflow in the wake field are essential.

Another possibility to reduce propeller noise is the application of a compliant layer to the waterside of the hull above the propeller.

Such a layer may consist of closed-cells foam rubber covered by a watertight layer of e.g. glassfibre reinforced polyester. The total area treated should be approximately 20 times the

propeller disk area and may bring about a propeller noise reduction of some 8 dB(A).

In an endeavour to avoid complicated measuring procedures and extensive calculations, a simplified calculation scheme was set up to estimate probable values of sound levels-A that could be expected on board a new yacht design. This calculation is based on some fair average values for "source strengths" of various machinery and for "transfer functions" that probably will be typical for constructions used in yachts. At present it can not be much more than a good working hypothesis, based as it is on experience with large sea-going ships of various types and with only a few yacht-like motorboats and yachts, see references [11, 12, 13]. Its character is that of an engineering estimate and it may be considered reliable if the large majority of the measured results from many actual yachts deviate by not more than 5 dB(A) from the levels calculated.

A number of measures and their estimated effects based on the calculation scheme of section 5 have been summarized in Table 2 (remember that this scheme considers only, the primary acoustical designing aspects, and not for example exhaust noise or rattling doors etc.).

The 8 m yacht would present no special technical difficulties except for the cabin aft where the noise is mainly caused by the propeller. The resilient mounting of the diesel engine can be improved by installing a flexible coupling in the propeller shaft. Clearly the airborne path is very important; it can be influenced by means of an engine enclosure. The level in the wheelhouse could be reduced further by installing a better sound insulating floor based on steel plate (see step 9 of the scheme in section 5).

Aboard the 40 m yacht a considerable noise reduction can be brought about by mounting resiliently the two main engines including their reduction gears. In the accommodation all sound radiating surfaces have to be installed resiliently in order to attain sufficiently low noise levels.

As the airborne path from the engines is less important than the structureborne path the influence of an engine enclosure is negligible.

In order to illustrate how the scheme can be handled, in sections 5.1 and 5.2 the sound levels-A have been calculated respectively for the open wheelhouse of the 8 m yacht and for the guests cabin on board the 40 m yacht.

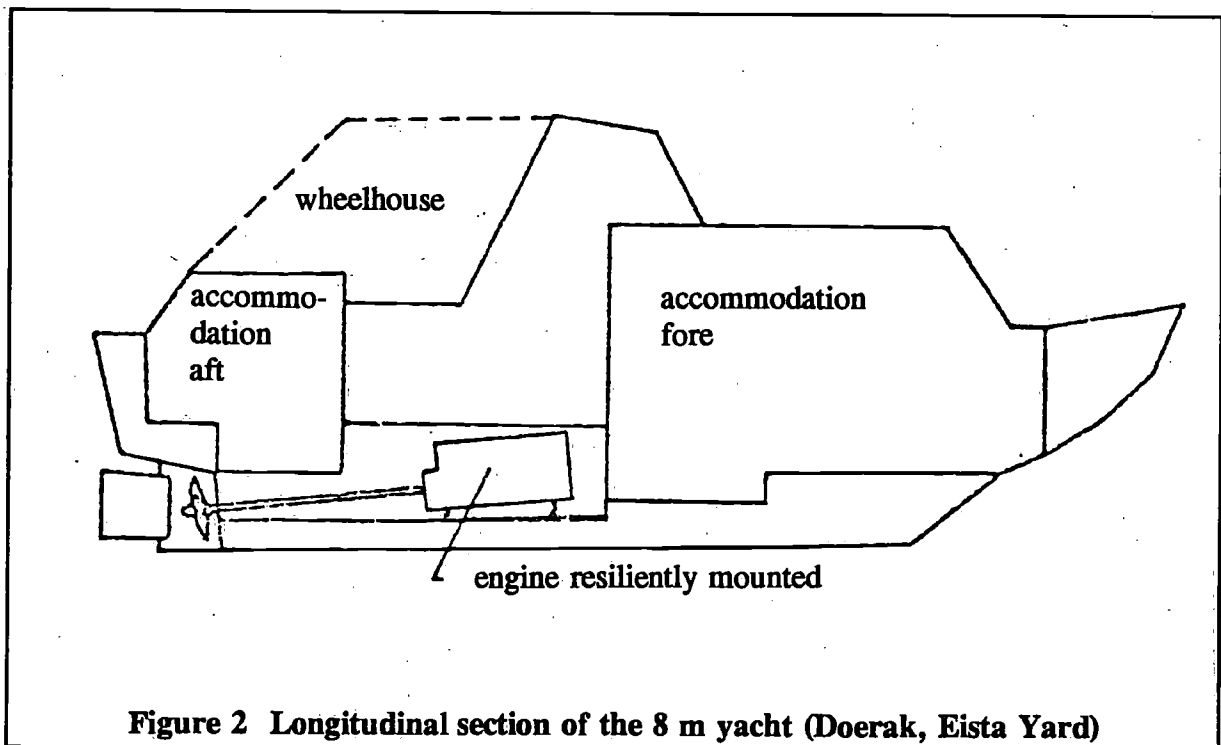


Figure 2 Longitudinal section of the 8 m yacht (Doerak, Eista Yard)

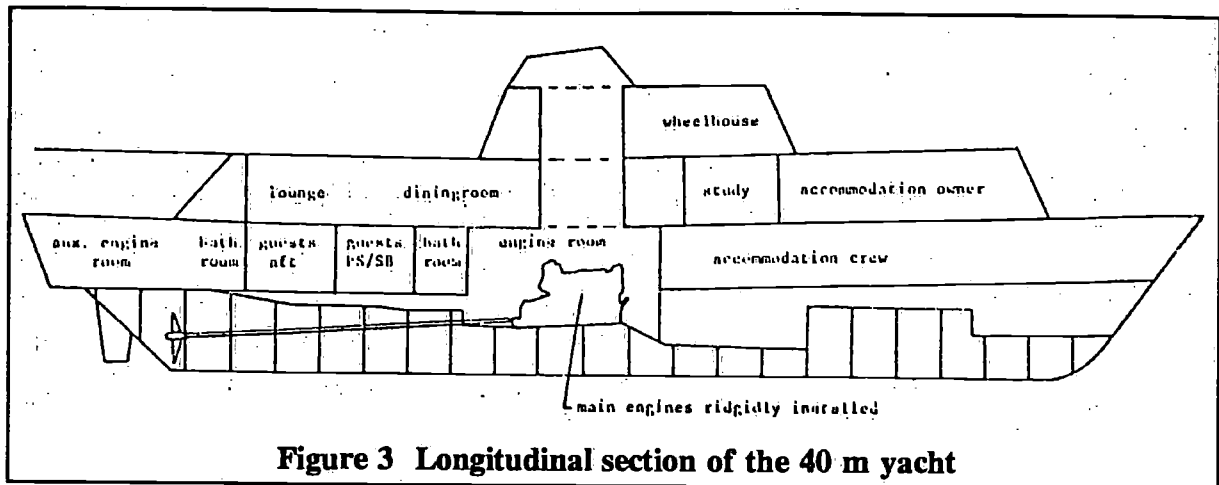


Figure 3 Longitudinal section of the 40 m yacht

Table 2 Comparison of recommended limits, of measured values and of calculated estimates of sound levels-A for various conditions

location	limit	measured	improved resilient mounting for engine (1)	engine in enclosure (2)	measures (1) and (2) combined
8 m yacht					
wheelhouse	65	73	73	64	63
cabin fore	60	68.5	67	64	61
cabin aft with conventional noisy propeller	65	74	72	71	71
cabin aft with special design quiet propeller	65		68	65	62
			main engines with reduction gears mounted resiliently	additionally floor, bulk-heads ceiling mounted resiliently	additionally main engines in enclosures
40 m yacht					
guests PS/SB	60	75	65	60	59
lounge	60	71.5	65	60	59

5 Calculation scheme for estimating primary noise levels

Only three types of noise sources are considered of primary importance:

- Diesel engines
- reduction gears
- propellers.

In the Figures 4 to 8 "flow diagrams" have been given for a calculation scheme including structureborne and airborne sound transmission. The necessary numerical data on the sources and on typical ship hull transfer functions have been given in Table 4 and in the Figures 9 to 11.

Finally the following examples of calculation are given:

1. open wheelhouse of a 8 m yacht
2. cabin on board 40 m yacht.

Extensive noise measurements have been carried out aboard 2 yachts of which all relevant constructional details are known. Profiles are given in Figures 2 and 3. The 8 m yacht is a typical small, Dutch inland motorcruiser, the other a 40 m luxury sea-going yacht for cruises all over the world. For both yachts some sound level estimates have been calculated according to the scheme. The results are compared with the measured values in Table 3.

Table 3 Comparison between measured and calculated sound level-A on board 2 yachts

	measured	calculated
8 m yacht		
wheelhouse	73	74 dB(A) (see also section 5.1)
cabin fore	68.5	70 "
cabin aft	74	72 "
40 m yacht		
guests PS/SB	75	76 dB(A) (see also section 5.2)
guests aft	74.5	74 "
diningroom	75.5	74 "
lounge	71.5	71 "
study	66.5	69 "

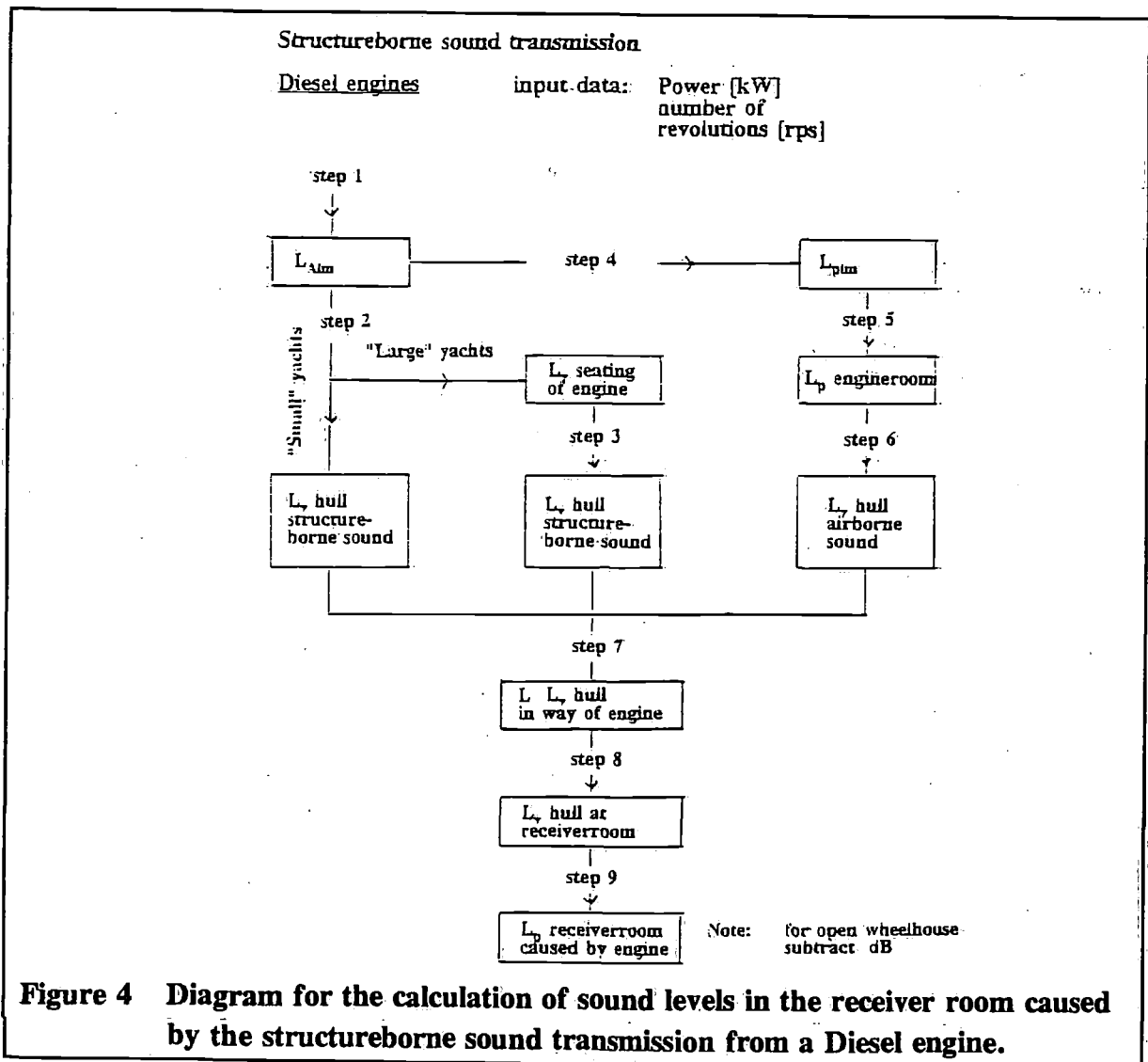


Figure 4 Diagram for the calculation of sound levels in the receiver room caused by the structureborne sound transmission from a Diesel engine.

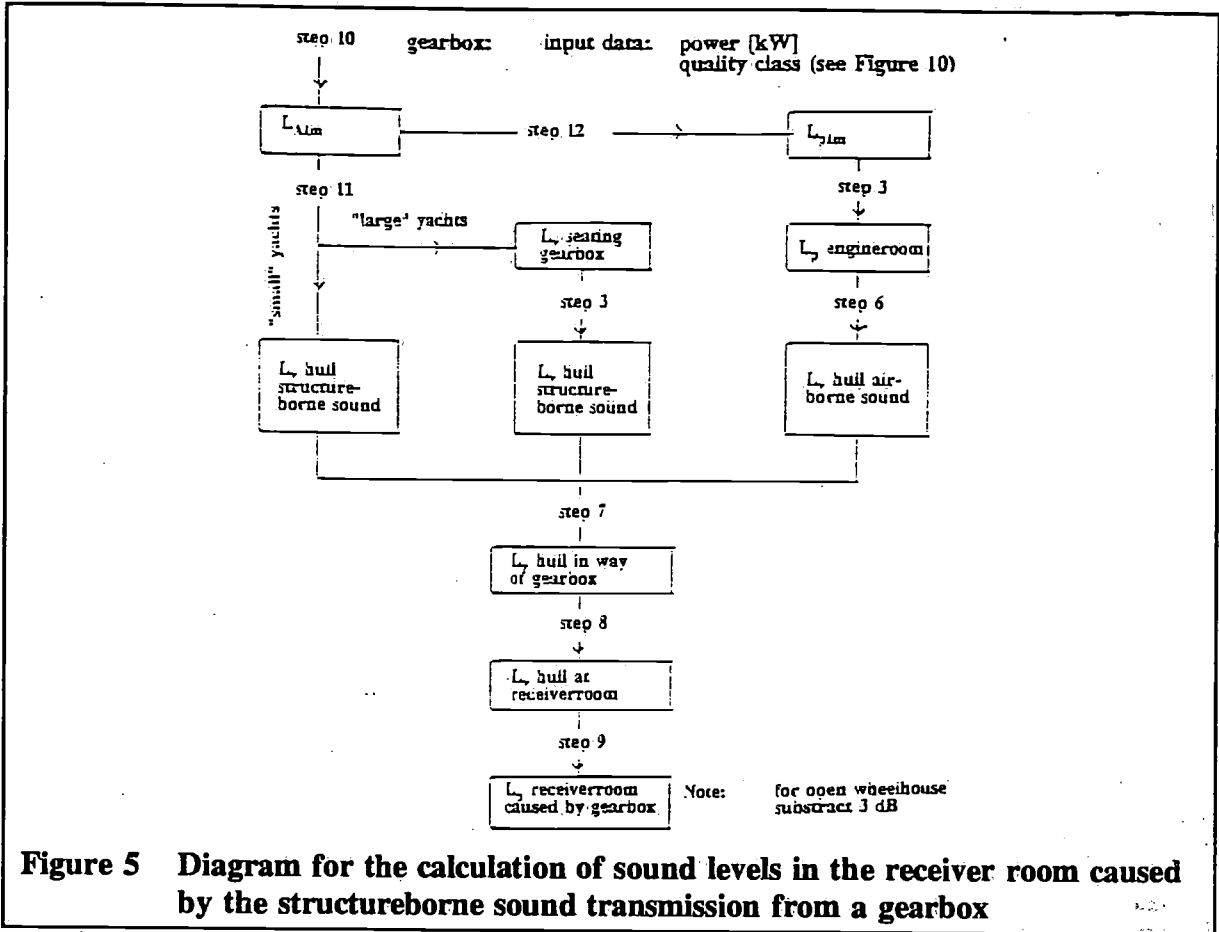


Figure 5 Diagram for the calculation of sound levels in the receiver room caused by the structureborne sound transmission from a gearbox

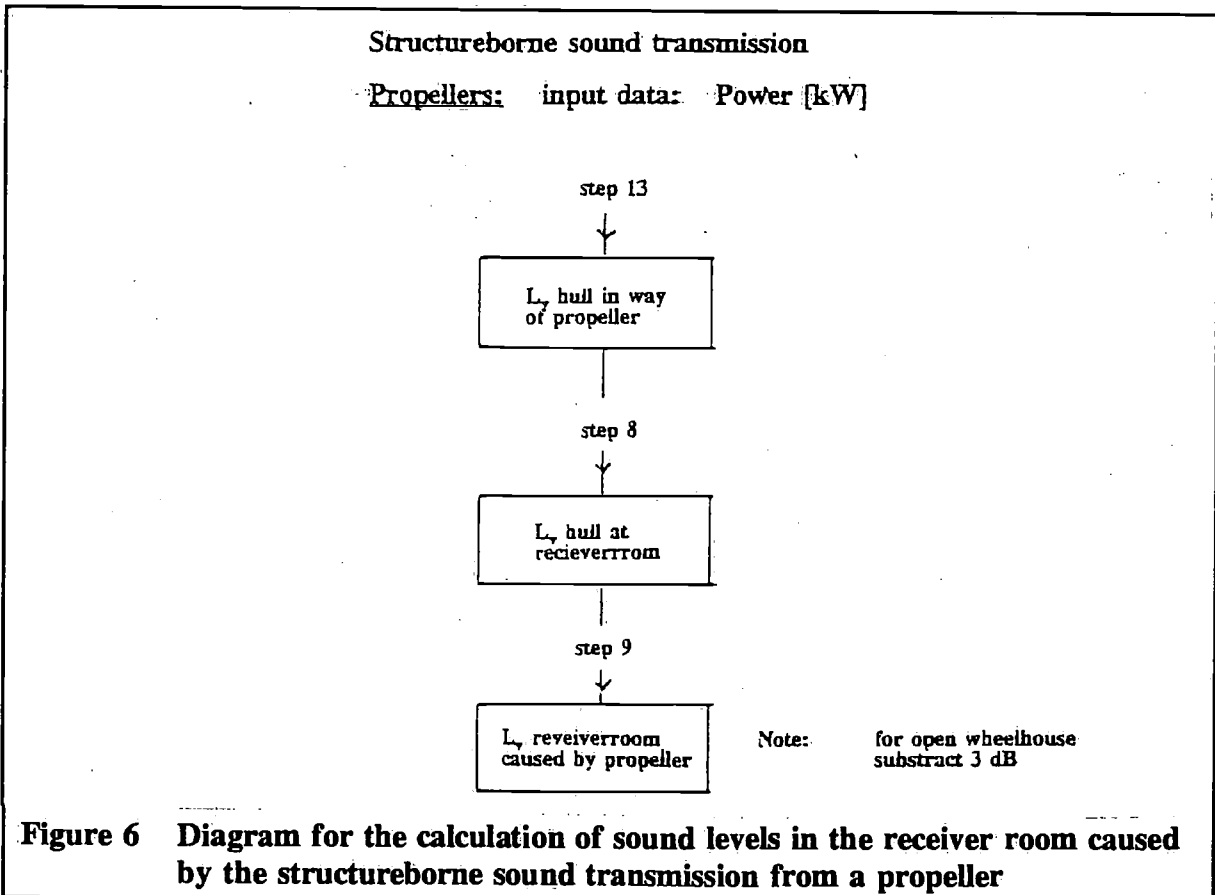
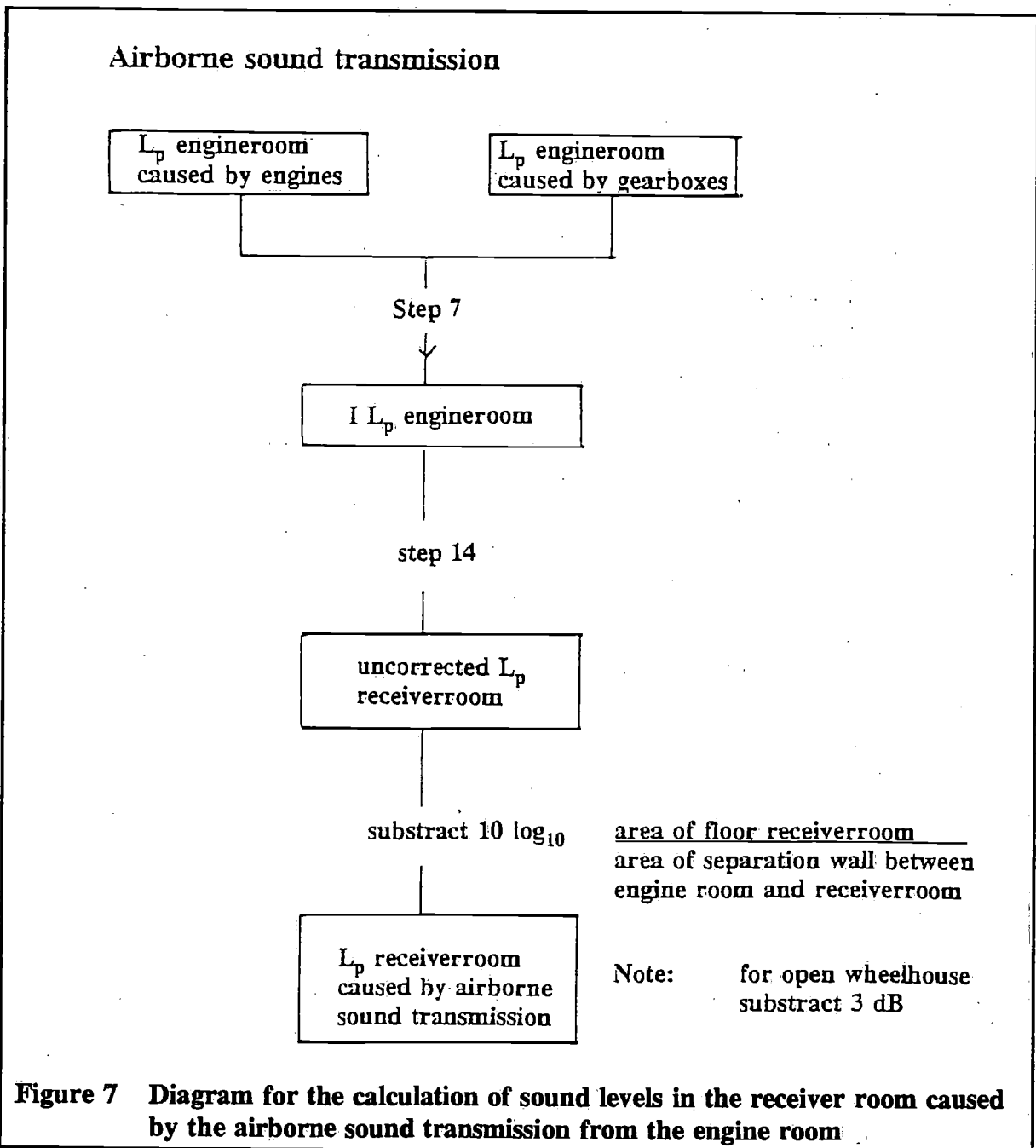


Figure 6 Diagram for the calculation of sound levels in the receiver room caused by the structureborne sound transmission from a propeller

The agreement is very promising indeed, the more so as the calculated octave band levels show a good agreement also with the respective levels measured actually in both yachts (not shown in this paper).

Aboard the 8 m yacht an analysis could be made of the contributions of the air-borne and structureborne sound to the resulting level in the wheelhouse. The contributing levels were 73 and 66 dB(A) respectively. Following the calculation of section 5.1 these levels are 73 and 68 dB(A) respectively. Also the octave band levels of measured and calculated contributions show a satisfying agreement. If the insertion losses of acoustical measures, as being incorporated in the data of Table 4, are reliable for both types of paths a reliable prediction of the resulting sound level due to an acoustical measure may thus be expected.

Of great interest, of course, is the question what acoustical measures should be taken in order to comply with the recommendations of Table 1.



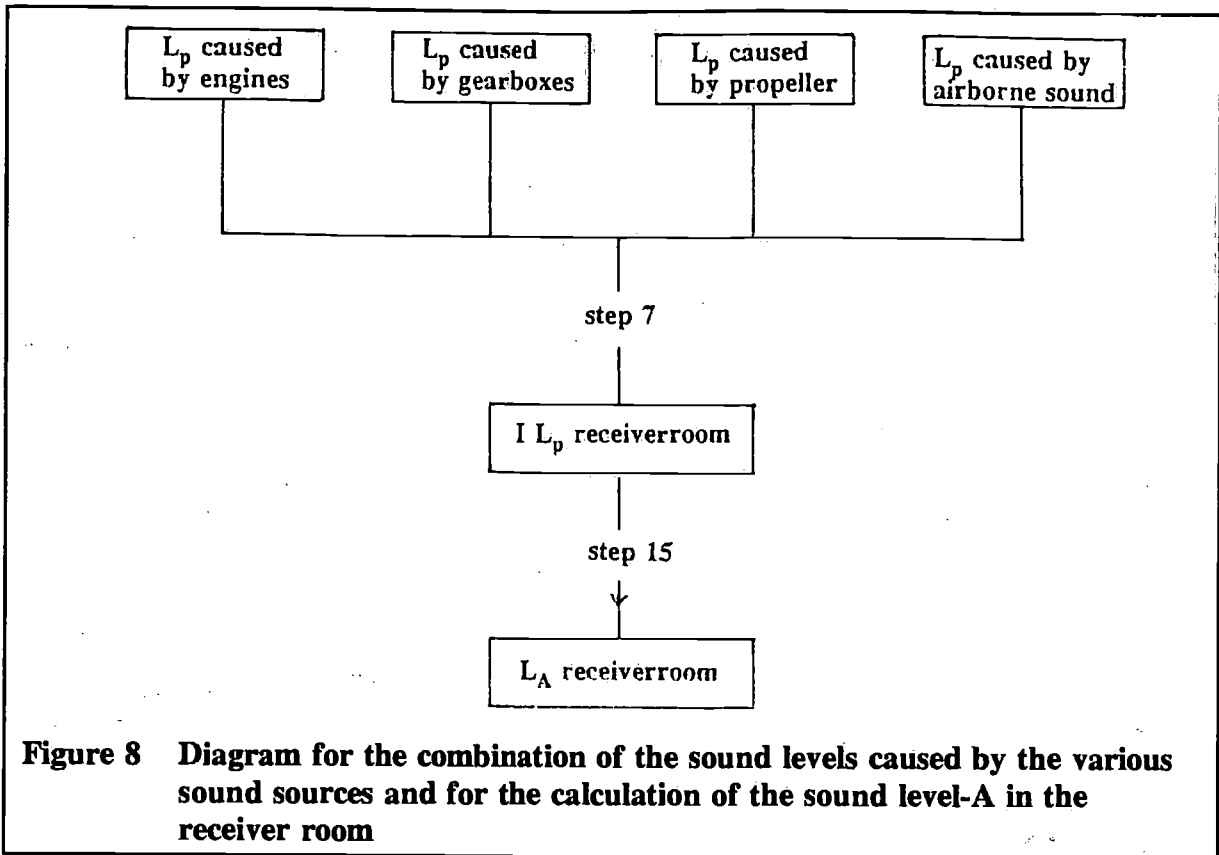


Figure 8 Diagram for the combination of the sound levels caused by the various sound sources and for the calculation of the sound level-A in the receiver room

Table 4 Data for the calculation of sound levels in engine room and accommodation according to the diagrams of the Figures 4 to 8.

Step 1

$$L_{A1m} = 10 \log_{10} \frac{n}{n_o} + 5.5 \log_{10} \frac{N}{N_o} + 56 \text{ db}$$

- L_{A1m} = sound level-A at a distance of 1 m under free field conditions
- n = number of revolutions [rpm]
- n_o = one revolution per minute
- N = radiated power output of engine [kW]
- N_o = one kilowatt

Step 2 L_v hull (or seating) - L_{A1m} caused by structureborne transmission.
 L_v hull = velocity level of hull in dB re 5×10^{-8} m/s.

	centre frequencies in octave bands (Hz)					
	<u>63</u>	<u>125</u>	<u>250</u>	<u>500</u>	<u>1k</u>	<u>2k</u>
engine rigidly mounted:	-13	-11	-13	-15	-17	-24
engine resiliently mounted						
a) normal:	-21	-28	-35	-37	-39	-45
b) rather stiff:	-16	-23	-30	-32	-34	-40
c) very low eigenfrequencies	-26	-33	-40	-42	-44	-50

Step 3 L_v hull - L_v seating of engine
(only for yachts) ΔL_v :

-1	-5	-7	-12	-15	-20
----	----	----	-----	-----	-----

Step 4 $L_{p1m} = L_{A1m}$ for diesel engines
 L_{p1m} = sound pressure level in
dB re 2×10^{-5} N/m² at a distance
of 1 m under free field conditions

engine without enclosure:	-12	-9	-7	-4	-3	-7
engine in enclosure:	-15	-17	-19	-20	-22	-27

Step 5 L_{Pr} engine room = $L_{p1m} + K$ for
the value of K . See Figure 9.

Step 6 L_v hull - L_p engine room (dB)
 L_p engine room = sound
pressure level in
dB re 2×10^{-5} N/m² in engine
room near to hull or deck above

hull: 3 mm steel:	-17	-20	-27	-32	-38	-41
3 mm steel, 100 mm rockwool:	-18	-22	-32	-40	-41	-51
5 mm steel:	-20	-23	-30	-35	-41	-44
5 mm steel, 100 mm rockwool:	-21	-23	-35	-43	-51	-54
4 mm aluminium:	4	-1	-11	-19	-24	-29

Step 7 Combining decibels:
deference in dB between
levels to be combined

0 - 1	3
2 - 4	2
5 - 9	1
> 9	0

add the following number of
dB to the highest level

example: 78 dB + 75 dB = 78 + 2 = 80 dB

Step 8 L_v hull receiver room - L_v hull engine room (dB)
attenuation in fore and aft direction: 1 dB/meter
attenuation in vertical direction: 6 dB/deck

Step 9 L_p reciever room - L_v hull at receiver room (dB)

	center frequencies in octave bands (Hz)					
	<u>63</u>	<u>125</u>	<u>250</u>	<u>500</u>	<u>1k</u>	<u>2k</u>
wooden floor, linings, bulkheads and ceiling fixed:	4	-1	-1	-3	-3	1
wooden floor including linings, bulkheads and ceiling resiliently mounted:	1	-5	-7	-10	-13	-7

steel floor, bulkheads and ceiling fixed:	-4	-4	-2	0	3	8
steel floor (resiliently mounted), wooden bulkheads and ceiling fixed:	1	-4	-4	-6	-6	-2
Step 10 L_{Alm} gearbox: see Figure 10						
Step 11 L_v hull (or seating) - L_{Alm} gearbox (dB)						
gearbox rigidly mounted:	-45	-36	-26	-17	-17	-27
gearbox resiliently mounted on one raft with engine:	-48	-48	-43	-34	-34	-43
Step 12 $L_{plm} - L_{Alm}$ gearbox (dB)						
gearbox without enclosure:	-20	-14	-8	-5	-3	-8
gearbox in enclosure:	-24	-23	-20	-21	-22	-28
Step 13 L_v hull in way of propeller; see Figure 11						
Step 14 Sound level differences between engine room and adjacent rooms L_p receiver room - L_p engine room (dB)						

	center frequencies in octave bands (Hz)					
	<u>63</u>	<u>125</u>	<u>250</u>	<u>500</u>	<u>1k</u>	<u>2k</u>
3 mm steel + stiffeners:	-15	-23	-28	-32	-34	-35
3 mm steel + stiffeners + 16 mm plywood rigidly secured:	-13	-23	-30	-40	-45	-49
5 mm steel + stiffeners:	-17	-30	-34	-35	-39	-36
5 mm steel + stiffeners + 16 mm plywood rigidly secured:	-15	-30	-36	-43	-50	-50
5 mm steel + stiffeners + 16 mm plywood resiliently mounted (sound absorbing material between steel and lining):	-18	-35	-46	-53	-61	-61
25 mm plywood:	-18	-22	-25	-30	-30	-30
4 mm aluminium + stiffeners:	-12	-15	-20	-25	-27	-25

Step 15 Calculation of sound level-A from calculated or measured octave band levels.

Values to be subtracted from octave band levels:	26	16	9	3	0	-1
Combine the for the A-weighting network corrected octave band levels according to step 7 example:						
calculated octave band levels:	100	95	90	85	80	75

A-corrected levels:
 combine the A-corrected
 levels starting with the
 highest ones until the level
 difference between the
 combined level and the
 remainder octave band levels
 is larger than 9 dB.

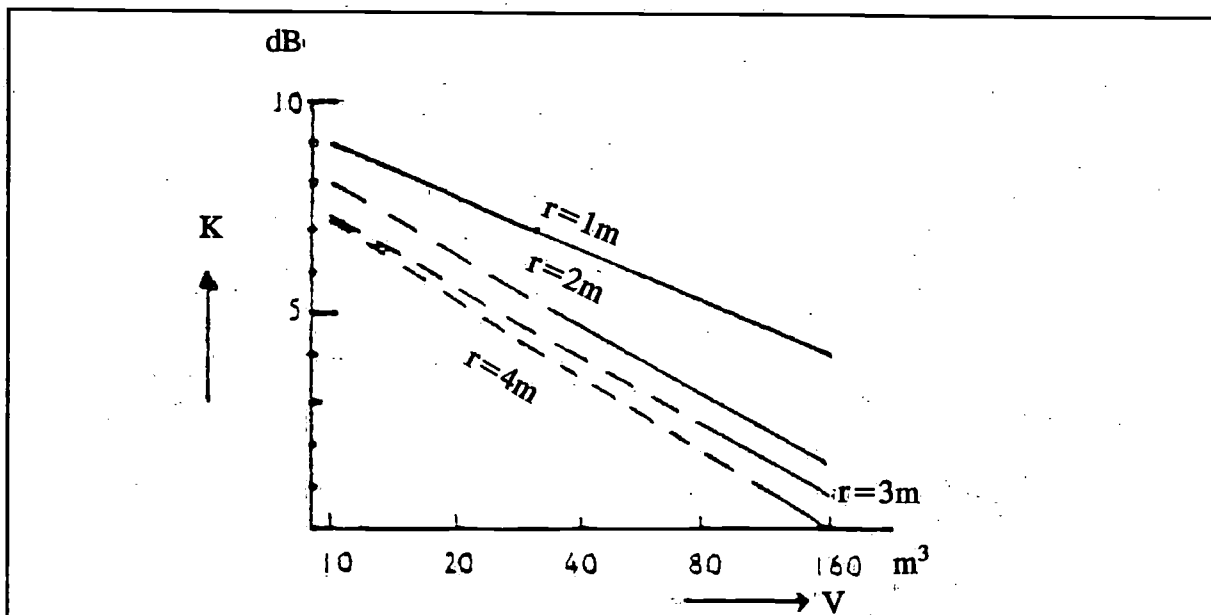
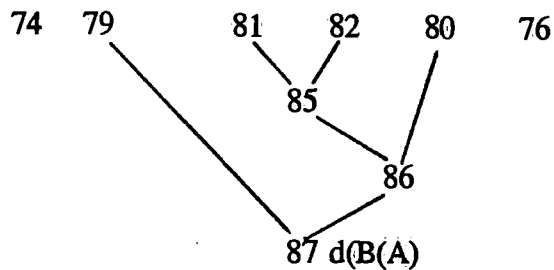


Figure 9 The correction K to be added to the sound pressure level at 1 m under free field conditions (L_{p1m}) to arrive to the sound pressure level at a distance r in an engine room with volume V : $L_{pr \text{ engine room}} = L_{p1m} + K$

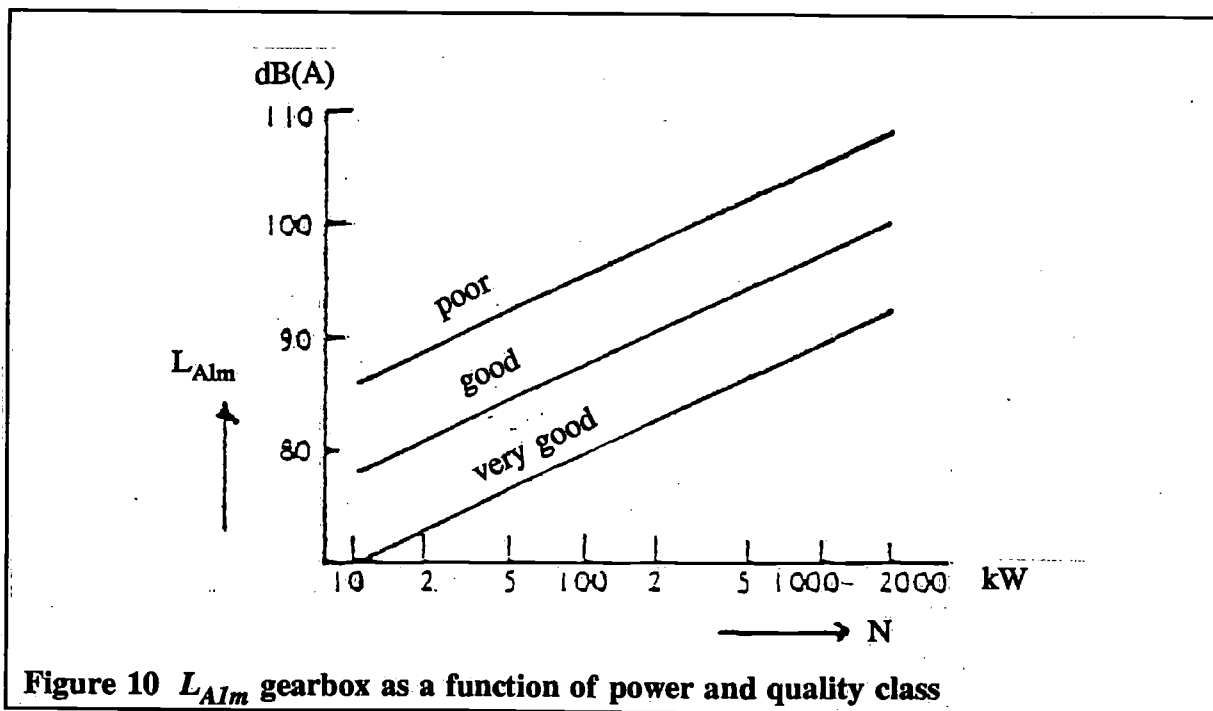


Figure 10 L_{A1m} gearbox as a function of power and quality class

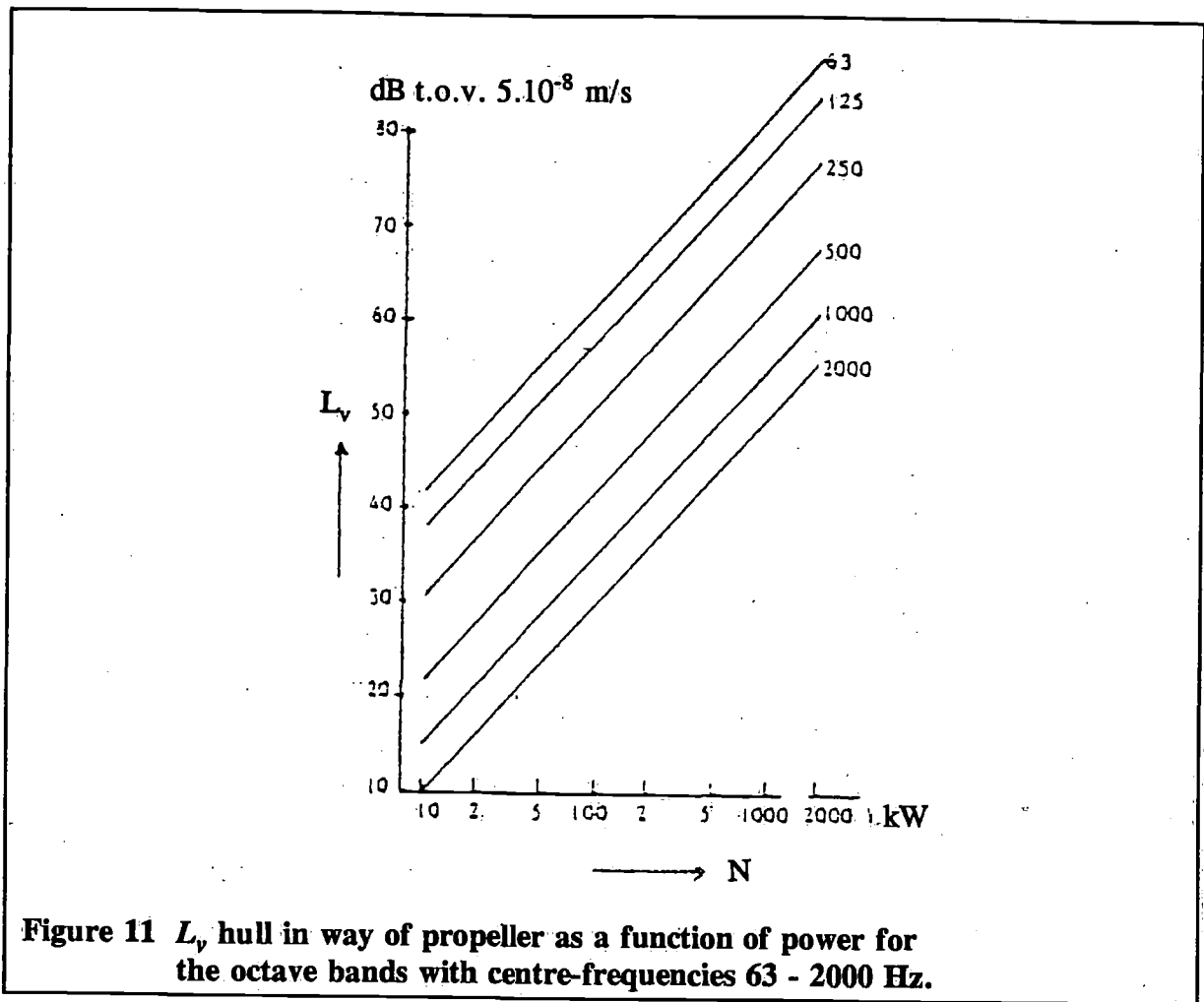


Figure 11 L_v hull in way of propeller as a function of power for the octave bands with centre-frequencies 63 - 2000 Hz.

5.1 Example 1: Calculation of the sound level-A in the open wheelhouse of the 8 m yacht

data: diesel engine 29 kW, 2000 rpm, resilient mounting of main engine rather stiff (see Figure 2)

5.1.1 Contribution of structureborne sound transmission

main engine: input data: 29 kW, 2000 rpm

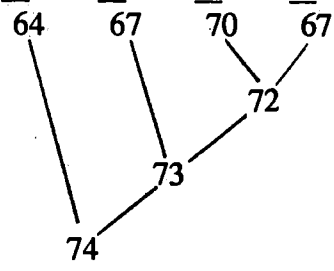
Step 1 $L_{Alm} = 10 \log 2000 + 5.5 \log 29 + 56 = 97 \text{ dB(A)}$

		center frequencies in octave bands (Hz)					
		63	125	250	500	1k	2k
Step 2	L_v hull = 97 +	-16	-23	-30	-32	-34	-40
	L_v hull structureborne sound =	81	74	67	65	63	57
		(a)					
Step 4	engine without enclosure						
	$L_{p1m} = L_{Alm} (=97) +$	-12	-9	-7	-4	-3	-7
	$L_{p1m} =$	85	88	90	93	94	90

Step 5	$V_{\text{engine room}} \approx 16^3$ distance hull to centre engine about 1.5 m Figure 9 gives correction $K =$ L_p engine room =	8	8	8	8	8	8
		93	95	98	101	102	98
Step 6	hull: 3 mm steel L_v hull = L_p engine room + L_v hull airborne sound =	-17	-20	-27	-32	-38	-41
		76	76	71	69	64	57
							(b)
Step 7	EL_v hull (combine a en b) =	82	78	73	71	67	60
Step 8	no attenuation, so L_v hull = L_v hull at receiverroom						
Step 9	Wooden floor, linings and bulk- heads fixed L_p receiver room = L_v receiverroom L_p receiver room = correctyion open wheelhouse = L_p wheelhouse caused by structure- borne sound =	+4	-1	-1	-1	-3	-1
		86	77	72	68	64	61
		-3	-3	-3	-3	-3	-3
		83	74	69	65	61	58
							(c)

5.1.2 Contribution of airborne sound transmission

	center frequencies in octave bands (Hz)					
	<u>63</u>	<u>125</u>	<u>250</u>	<u>500</u>	<u>1k</u>	<u>2k</u>
L_p engine room =	93	96	98	101	102	9
Step 14 floor 25 mm plywood:						
L_p receiver room = L_p engine room +	<u>-18</u>	<u>-22</u>	<u>-23</u>	<u>-30</u>	<u>-30</u>	<u>-30</u>
L_p receiver room =	75	74	73	71	72	69
correction open wheelhouse:	<u>-3</u>	<u>-3</u>	<u>-3</u>	<u>-3</u>	<u>-3</u>	<u>-3</u>
L_p wheelhouse caused by air- borne sound =	72	71	70	68	69	65
						(d)
EL_p wheelhouse (combine c and d):	83	76	73	70	70	66
"A" correction =	<u>-26</u>	<u>-16</u>	<u>-9</u>	<u>-3</u>	<u>0</u>	<u>1</u>
A-corrected levels =	57	60	64	67	70	67



L_A wheelhouse = 74 dB(A)

5.2 Example 2: Calculation of the sound level-A in the cabin guests PS/SB of the 40 m yacht

data: 2 diesel engines 770 kW, 1300 rpm, 2 gearboxes 770 kW, 1300 → 400 rpm diesel engines and gearboxes rigidly mounted (see Figure 3).

5.2.1 Contribution of the structureborne sound transmission main engine:

input data: 770 kW, 1300 rpm

Step 1 $L_{Alm} = 10 \log 1300 + 5.5 \log 770 + 56 = 103 \text{ dB(A)}$

		center frequencies in octave bands (Hz)					
		63	125	250	500	1k	2k
Step 2	("Large" yachts) L_v seating = 103 + L_v seating =	-13 90	-11 92	-13 90	-15 88	-17 86	-24 79
Step 3	L_v hull = L_v seating + L_v hull structureborne sound +	-1 89	-5 87	-7 83	-12 76	-15 71	-20 59
Step 4	engine without enclosure $L_{plm} = L_{Alm} (=103) +$ $L_{plm} =$	-12 91	-9 94	-7 96	-4 99	-3 100	-7 96
Step 5	$V_{\text{engine room}} \sim 100 \text{ m}^3$ L_p engine room = $L_{plm} + K$ Figure 9, $r = 2 \text{ m}$ gives $K =$	+3	+3	+3	+3	+3	+3
Step 6	hull: 5 mm steel + 100 mm rockwool L_v hull = L_p engine room + L_v hull airborne sound =	-21 73	-25 72	-35 64	-43 59	-51 52	-54 45
Step 7	EL_v hull caused by main engine (combine e and f)	89	87	83	76	71	59
Step 8	distance between engine and cabin: 4 m no vertical attenuation: $\Delta L_v =$ L_v hull at cabin =	-4 85	-4 83	-4 79	-4 72	-4 67	-4 55
Step 9	wooden floor, bulkheads and ceiling fixed L_p cabin - L_v hull at cabin + L_p cabin caused by main engine =	4 89	-1 82	-1 78	-3 69	-3 64	1 56

(I)

5.2.2 gearbox:

input data: 770 kW

quality class: poor

Step 10 (see Figure 10) $L_{Aim} = 105$ dB(A)

	center frequencies in octave bands (Hz)					
	<u>63</u>	<u>125</u>	<u>250</u>	<u>500</u>	<u>1k</u>	<u>2k</u>
Step 11 ("Large" yachts)						
L_v seating = L_{Aim} (= 105) +	<u>-45</u>	<u>-36</u>	<u>-26</u>	<u>-17</u>	<u>-17</u>	<u>-27</u>
L_v seating =	60	69	79	88	88	78
Step 3 L_v hull = L_v seating +	<u>-1</u>	<u>-5</u>	<u>-7</u>	<u>-12</u>	<u>-15</u>	<u>-20</u>
L_v hull structureborne sound =	59	64	72	76	73	58
						(g)
Step 12 L_{p1m} = L_{Aim} (= 105) +	<u>-20</u>	<u>-14</u>	<u>-8</u>	<u>-5</u>	<u>-3</u>	<u>-8</u>
L_{p1m} =	85	91	97	100	102	97
Step 5 L_p engine room = L_{p1m} + K ; K =	3	3	3	3	3	3
Step 6 L_v hull = L_p engine room +	<u>-21</u>	<u>-25</u>	<u>-35</u>	<u>-43</u>	<u>-51</u>	<u>-54</u>
L_v hull airborne sound =	67	69	65	60	54	46
						(h)
Step 7 EL_v hull caused by gearbox						
(combine g and h)	68	71	73	76	73	58
Step 8 distance between gearbox						
and cabin: 3 mm;						
no vertical attenuation: ΔL_v =	<u>-3</u>	<u>-3</u>	<u>-3</u>	<u>-3</u>	<u>-3</u>	<u>-3</u>
L_v hull at cabin =	65	68	70	73	70	55
Step 9 L_p cabin = L_v hull +	<u>4</u>	<u>-1</u>	<u>-1</u>	<u>-3</u>	<u>-3</u>	<u>+1</u>
L_p cabin caused by gearbox =	69	67	69	70	67	56
						(II)

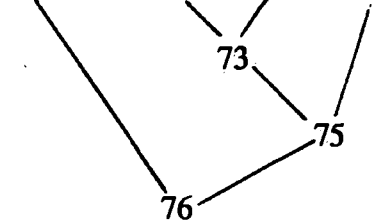
For the total sound pressure level in the cabin, combine (I) and (II);

$EL_p =$

89	82	79	73	69	59
----	----	----	----	----	----

Step 15 "A"-corrected levels:

63	66	70	70	69	60
----	----	----	----	----	----



$L_{A\text{cabin}} = 76$ dB(A)

6 Conclusions

- 1 The acoustical design of a yacht can and must be realized at an early design stage.
- 2 Adequate measures to meet realistic noise specifications are available to the designer.
- 3 The calculation method presented in this paper gives an engineering estimate of the noise likely to obtain in the various compartments.
- 4 When selecting machinery it is advisable to take into account the noise emission of the primary noise sources.

7 Acknowledgements

The authors would like to thank the owners of the yachts described for their permission to use on board measured data. Very helpful information was given by the Eista yard and by mr. Roger.

8 References

- [1] International Organization for Standardization, ISO Recommendation 1996: "Noise assessment with respect to community response".
- [2] International Electrotechnical Commission (I.E.C.); Publication 179: "Precision sound level Meters" (recommendation).
- [3] Buiten, J., "A proposal on noise criteria for sea-going ships", Report nr. 125S of the Netherlands Ship Research Centre TNO, Delft, 1969.
- [4] Int. Organization for Standardization, ISO Recommend. 1999: Assessment of noise-exposure during work for hearing conservation purposes.
- [5] Richtlinien für zulässige Schallpegel auf Seeschiffen; See-berufs-genossenschaft Hamburg, 23 januari 1968.
- [6] Vorläufige Vorschriften für die Lärmbekämpfung auf Schiffen; Deutsche Schiffs-Revision und -Klassifikation, DSRK 6.8, 1964.
- [7] Normen voor toelaatbare geluidniveaus op zeeschepen en voorschriften ter voorkoming van schadelijke invloeden door geluid; USSR 24/IX 1962, no. 416 - 62; vertaling Nederlands Scheepsstudiecentrum TNO
- [8] Sjöfartsverkets bestämmelser och rekommendationer om skydd mot buller på fartyg; Sjöfartsverkets Meddelanden, Stockholm 1972.
- [9] Convention on the International Regulations for Preventing Collisions at Sea, 1972; Annex III: Techn. Details of Sound Signals Appliances; IMCO.
- [10] Exterior sound level measurement procedure for pleasure motorboats SAE J34; Society of Automotive Engineers, New York 1973.
- [11] Buiten, J., ir. J.H. Janssen, H.F. Steenhoek and ir. L.A.S. Hageman: "Prevention of noise and vibration annoyance aboard a sea-going passenger and car-ferry equipped with diesel engines"; Part I: Line of thoughts and predictions. Report nr. 139 S of the Netherlands Ship Research Centre TNO, Delft 1971
- [12] Buiten, J., ir. J.H. Janssen, H.F. Steenhoek, and ir. L.A.S. Hageman: "Prevention of noise and vibration annoyance aboard a sea-going passenger and car-ferry equipped with diesel engines"; Part II: Measures applied and comparison of computed values with measurements. Report nr. 140 S of the Netherlands Ship Research Centre TNO, Delft, 1972.
- [13] Janssen, J.H. and J. Buiten: "On acoustical designing in naval architecture; Proceedings of Inter-Noise '73, page 349-356.

Sail plans and deck layouts for ocean going cruising yachts

by G. Dijkstra jr

Ocean Sailing Development BV
Amsterdam, Netherlands

Summary

Sail plans for yachts, intended to make long distance ocean passages are being considered in a general way. Both the planform - and the division of this planform into seperate sails are discussed. The comparison of the sail plans is based on experience, however in some cases it has been possible to find theoretical backing of this experience in the literature.

In selecting a sail plan for a boat it is important to include the possible deck layout, with regard to the sail handling. Some remarks in this respect are included in the paper.

Most long distance passages are made with a small crew, so the sail plans are being discussed with the singlehanded handling of the boat - and sails taken into account.

On several occasions references are made to the racing yacht. Although this paper deals with the cruising yacht it would be a waste to disregard the experience gained with racing yachts, as some cruising yachtsman are intended to do.

Contents

- 1 Introduction
- 2 The planform
- 3 The division of the sails
- 4 The sails for a solo-racer
- 5 Roller-furling sails
- 6 Several classic - and alternative sail plans
- 7 Definitions of head sails
- 8 Literature

1 Introduction

This paper concerns itself with the sail plans and, to a lesser extend, with the deck layouts of ocean going cruising yachts. I feel the above to be a field that has been rather neglected by the general trend in the modern design of sailing yachts. This is probably due by the fact that there are few boats designed specially as an ocean going cruising yacht, although the advertising in yachting magazines make one believe that nearly all the boats offered are, at least, ocean going. Fortunately there is now a slow beginning with the manufacture of production boats that are real long distance cruisers and not floating caravans or slightly adapted racers. The rationalisation, so clearly demonstrated in the uncompromising design of the modern racing yacht, is slowly finding its way in the design of the cruising yacht. This is a slow process indeed, and more often then not it is the owner who slows down the process.

The yachtsman chooses his boat according to his experience, his readings on the subject and according to the advice he gets from, hopefully, qualified persons. This all in respect to the available budget. For the racing sailor the above scheme is a good one and allows rapid development within the racing rules. During a hard racing season one can gain a lot of experience, there are plenty of experienced people to talk to and there is enough good literature. Furthermore, the designers of the yachts are actively taking part in the races and they can judge the result of changes in design and equipment quickly. Also the turnover of top racing yachts is fast, it isn't uncommon for the owner of such a yacht to have a new build every two years.

For the cruising yachtsman, who likes to make long distance passages, the situation is less ideal. In general he gathers his experience much slower than the racing sailor, most of the books on cruising yachts are technically not very up to date, it is seldom the designer who engages on long distance passages and the cruising sailor tends to keep his yacht longer than the racing sailor. So most of the development regarding equipment etc. is left to the amateur. Though in several cases this has led to remarkable results there are, unfortunately, many armchair sailors under the cruising sailors. A lot of problems they have with their boats and equipment could be solved by plain sailing, and plain experience.

In addition the so called cruiser/racer concept is a problem for the development of the long distance yacht. Though the cruiser/racer is a highly desirable yacht, its existence slows the commercial development of the real cruising yacht. This results in sailors taking this type of yacht, for budget reasons, when they would prefer a real cruiser instead of the mentioned cruiser/racer. It isn't only the trade who is at fault here, but also the sailor who has a tendency to buy a boat with a "racy" background. Even in cases when he really would make much better use of a cruising yacht.

It isn't surprising that it has taken events as the single-handed transatlantic race to push the development of designs and gear for long distance sailing. Naturally some of the designs used for the race aren't everybody's taste of a cruising yacht, but if one defines cruising as "not racing" also the extreme designs used have a purpose. Also, what is cruising for one sailor might be seen by another sailor in an entirely different light. The gear developed in the single-handed race is certainly very worthwhile. I mention in this respect the windvane steering gears, the small auto pilots, battery charging systems, the junk rig, roller furling jibs, of-course alarms, trimtabs, steering with the sails etc.

But also IOR races have provided useful equipment for the short-handed cruising yachtsman. For instance: the self tailing winch, safety equipment, mainsail reefing systems and, apart from equipment, improved hull, keel and rudder design. It is my opinion that the IOR rule promotes sound types of hulls, apart from the always present exceptions, which are perfectly good for cruising purposes. In general it is possible to make those hulls more comfortable at sea, if required, by adding ballast and/or constructing the hull more heavy if the boat isn't a heavy displacement type already. Also a little sheer added to increase the stem height and the comfort on the foredeck would be changes to be considered for a cruising yacht.

As stated in the beginning of this paper there is now a trend showing of sail boats that have taken advantage of developments in the solo - and IOR races. The cruising yacht with a rational approach to the problems of short-handed cruising is no longer a rarity. It is no longer the old timer, heavy, equipped with a long keel and gaff rig, that is considered the only type of real cruising yacht.

The modern cruising yacht is a yacht which performs well under sail, is very sea-worthy, and has a rational approach to the sail handling and the protection of the crew on deck. It are mainly these last two points where a cruising yacht differs from a racing yacht. One should bear in mind that a cruiser like this, even if produced in series, isn't cheap. The number of sails are less then onboard a racer, the winches can be more simple since speed in the sail handling is less important, but in other aspects one is adding to the bill. Roller furling gear, self-steering gear can be expensive, as are gadgets to facilitate single-handed handling of the boat. In this respect it is worthwile to point to the light displacement type of vessel, which can be propelled by a relative small sail plan, with the consequent reduction in costs.

There are many types of ocean going cruising yachts, from motor sailers, conventional sail boats to multi hulls. The type of yacht dealt with here is the long distance passage maker. Performance (speed) under sail is thereby a requirement since, also on a long passage, I prefer to sail and not to merely drift with the current and the wind. Furthermore this speed and, combined with this, the ability to weather a lee shore, are safety factors that shouldn't be taken to light. The sail plans here considered are able to give a hull a speed which is getting close to the speed the boat would have under a racing rig. However; course directional stability, ease of handling, durability (chafe) and comfort have to be taken into account and small losses in speed are accepted to further these ends. It depends on the skipper of the yacht how much speed he is prepared to give away, in order to gain on the cruising requirements of the rig. This trade-of should be done carefully, since it is often seen that, to simplify the sail handling just a little a lot of efficiency of the rig is lost. An example is for instance the stowing of twin poles along the mast [6].

Also light weather cruising rigs are considered. In this respect the cruising yacht can often be better equipped then the racing yacht, since there are no rating rules to be considered. Ofcourse it is possible to start the engine under the conditions when light weather sails are called for. But this takes the fun out of the sailing and it isn't practical to take the amount of fuel onboard that even only a few days-of calm will require during an ocean passage.

This paper is in no way condemming the old timer as a cruising yacht. It merely shows the advantage of modern technology for the cruising sailor, without taking the fun out of the sailing. I can very well see the point of the sailor who feels it is more sporting to challenge the ocean with less perfect aids, as was done by our ancestors. However they didn't have any choice between the use of their equipment or the equipment anno 1975. A storm is a storm, and the modern cruising yacht is superior in sea-worthiness to the old timer.

2 The planform

The performance of a sail boat depends largely on the sails, but in contrast with this it are the hull characteristics that are rather well known at present. This is caused by the difficulties that arise when measuring the forces working on a sail. Although this particular field is gaining interest, very little information is available for the design of rigs for cruising yachts. But even if sail force coefficients are known it is still difficult to compare different sail plans theoretically. It isn't sufficient, unfortunately, to compare the driving - and side force coefficients from the sails. The heeling moment coefficient is at least as important for the performance of the yacht. It is only possible to find the effect on performance of a change in some factor (sheeting angle, sail shape, planform etc.) which will influence the sail coefficients, by considering the balance of hull and sail characteristics combined. For when the yacht is sailing the wind - and water forces are in balance. This procedure will yield good results, but requires testing of both hull and sails combined with lengthy *Vmg* calculations. It is very well

possible for one planform to increase the performance of one type of hull and have the adverse effect on another hull.

For running - and reaching courses the comparison of sail plans is less complicated and it is general possible to judge the effect on performance by comparing the sail coefficients apart from the hull, or calculate in a simple way for instance the V_s/V_t ratio.

In a general way it is possible to judge the windward performance of a sail plan or sail setting in comparison to other sail plans or - settings, when the variation in sail coefficients is known. If the leeway angle λ is increased, the side force and resistance (mainly induced drag) increase rapidly. If the heeling angle θ is increased, the resistance will only increase slowly and the developed side force will remain constant or fall slightly.

Thus if one sail can produce the same forward force coefficient with a smaller side force coefficient then another sail, at the same angle ($\beta-\lambda$) to the apparent wind or less, improvement in performance will result, if also the heeling moment coefficient is the same or lower. Results of wind-tunnel tests on various sail plans are described in [2], [6] and [7].

The above mentioned methods require systematic information on the sail force coefficients, to be of value to the sailor. Very little data is available and, the data that is available, relates mainly to problems of importance for racing yachts. Until more is known the designer has to go on his experience by the design of cruising sail plans. This isn't so bad, since for cruising yachts one is concerned with the general performance and not with increasing the performance with 0.1% or so. One also has to bear in mind that, in general, the cruising sailor will not give the same attention to sail setting as will the racing sailor. Small performance difference between rigs are not important, however some basic research for cruising sail plans seems to be very worthwhile. Gaining experience with full size rigs is a slow process which could be speeded up with model testing. Since there are no rating rules to restrict the development, some interesting rigs could result.

A first evaluation of a ketch cruising rig is given in [2] where the importance of the size of the staysail in the fore triangle is shown. An analysis concerning the use of one - or two sails is given in [3]. The conclusion arrived at favors a two sail rig above one large single sail rig, except when the rig is for a yacht with an extreme good stability, which operates at high speeds and at small angles to the apparent wind. This can be seen in practice as racing multi-hulls and ice-sailing yachts are the only type to operate one-sail rigs successfully. For the cruising yacht the two - or more sail rig has the advantage. This advantage goes for performance as well as for course directional stability and ease of handling (smaller sail areas).

There are many types of sails and sail plans of use to the sailor as can be seen in chapter 6 and 9. However for conventional yachts it is hard to beat the normal sloop rig as used aboard the racing yachts as far as performance for sail area is concerned. Also for cruising purposes this seems to be the best rig. For ease of handling, course directional stability, durability and comfort one can consider the cutter, schooner - or ketch configuration, to improve the cruising characteristics of the rig. However this should only be done if the size of boat does warrant a further division of the number of sails set at one time. In general it can be said that, if more than two sails are set to windward, the windward performance will decrease. This effect is most strongly in moderate winds. In light- and heavy going the pointing angle is usually increased and the windward performance is hardly affected by the use of more than two sails. In very heavy weather the use of a cutter rig to windward might even be of advan-

tage for the bigger boats since the sail shape is better kept under control, then the shape of one larger genoa. On smaller boats the sails of a cutter are getting to close to each other which a poor effect on performance. For extreme light winds one should divide the sail area as little as possible and one big sail would be best. So when drawing the planform the above mentioned points should be kept in mind, since the planform basically dictates the possibility for the subsequent division of the separate sails.

It is difficult to assess the performance of a planform in an exact way. A rough guide, apart from experience, to the overall performance of the planform will be given by the IOR rating of the planform if a conventional set up is used. Also the systematic data given in [1] can be used.

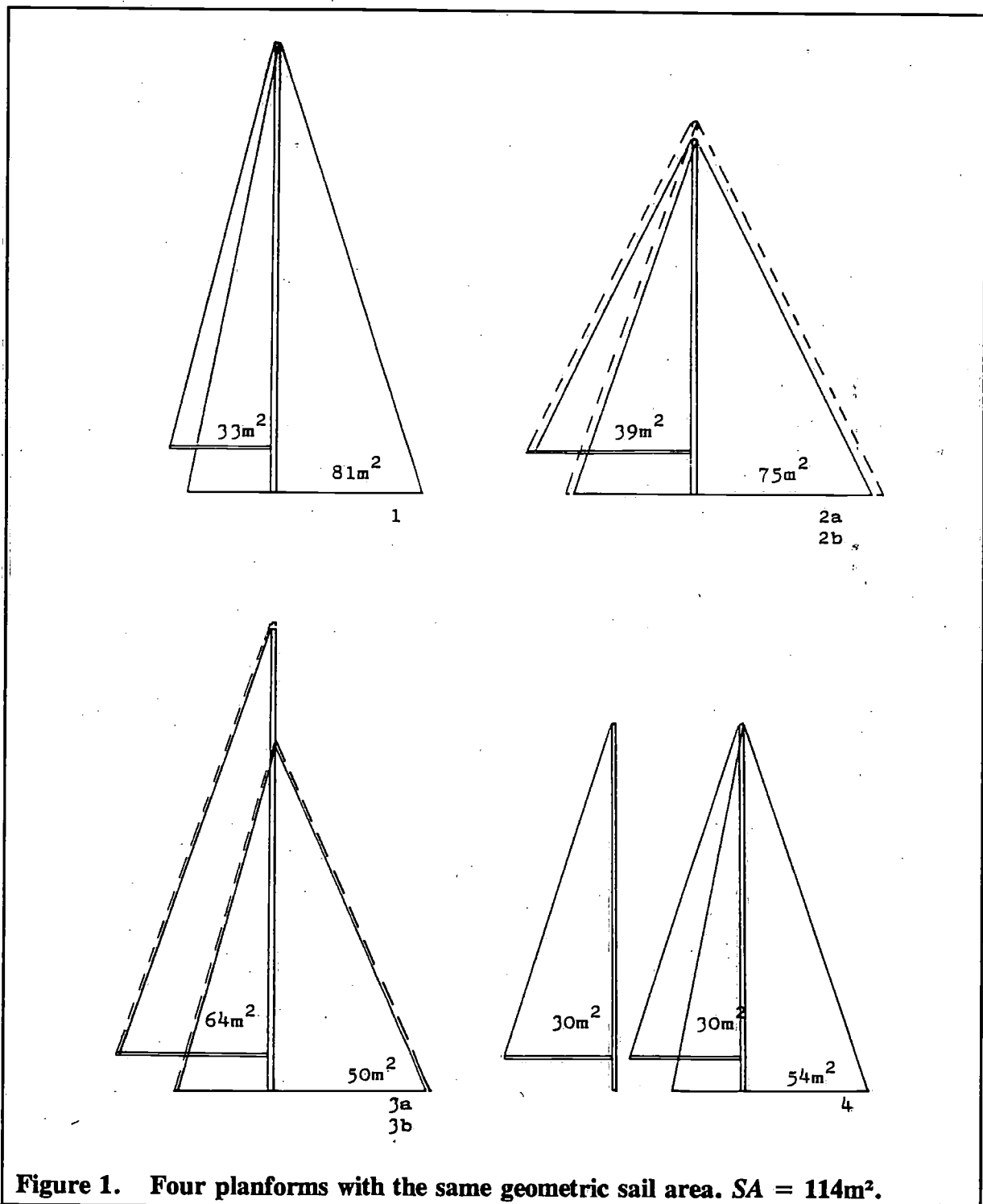
Figure 1 shows four planforms with the same geometric area. 1-1 Shows a modern IOR planform with high aspect ratio sails. 1-2 Is a rather extreme low a.r. planform while 1-3 and 1-4 are representative for the 3/4 rigged sloop and the modern schooner. In regards to allround performance 1 will be superior, this is also expressed by the IOR ratings of the sail plans. With [1] the characteristics of the four planforms was calculated. Unfortunately the tables in [1] only give the sail coefficients for a true wind angle of 45° , so for a modern hull this isn't an angle at which optimum *Vmg* to windward is to be expected. By comparing the planforms for an apparent windspeed of 23 m.p.h. planform 1-4 is slightly better than 1-1. The developed side force and forward force are equal to 1-1 but the angle of heel is nearly one degree less. However for smaller true wind angles 1-1 will definitely give a better *Vmg*. Also running will be better for 1-1 since this rig can more easily carry large running sails. Reaching will be better with 1-4 since it is possible to carry a wide variety of sails in between the two masts. The real advantage of 1-4 for the cruising boat lies in the better course stability and the easier handling of the smaller sails. If the size of boat does warrant it, 1-4 would make the best cruising sail plan, if small losses in efficiency in extreme light winds and small losses in the *Vmg* to windward in moderate conditions are accepted. The *Vmg* to windward in heavy going of 1-4 will be very close again to 1-1, since the fore sail will then be furled and the yacht will be sailing under head sails and schooner sail.

The course keeping ability of the schooner (or ketch) rig is described in [4], in general it can be said that by increasing the number of sails set aft of each other, the better the course keeping characteristics. Taberly has done much to develop the schooner rig for racing (RORC and solo) and gives an account of his experiences in [5]. Although his sail plans do include a large number of sails, they will do excellent for cruising rigs if only the basic sails are used.

The remaining planforms are less efficient, both by IOR standards and according to table [1]. Even if the sail areas are increased (dotted lines) to give the same angle of heel as 1-1, the low a.r. sloop and the 3/4 sloop produced less driving force and more side force. Though 1-3 is again considerably better in this respect than 1-2.

The ketch rig is hardly mentioned since there is little reason to use this type of planform, if a two masted rig is called for. The use of an equal mast-height schooner seems a better choice, if a ketch rig is used it would be best to make the mizzen mast rather tall. The small mizzen does add to the course keeping stability and also permits a yacht to hove to more comfortably. It seems however a waste to carry an extra mast for only these purposes, since the driving force of a small mizzen is hardly worthwhile. Most modern yachts, with a large separate rudder well aft, are sufficient course stable to enable a windvane steering gear or

auto pilot to be used. If one wants to hove to it is possible to use a small "jib" hoisted along the back stay to serve as a device to keep the stem to the seas if required. If the course keeping stability of the yacht is not too good it is possible to use the staysail of a cutter for improvement in this respect. For best results it is then necessary to make the sheeting angle of the staysail adjustable. This can easily be done if a self-tacking staysail is used. Only in very bad cases the use of a mizzen in addition to the staysail is warranted. In a case like this it will be the main and the jib or genoa topsail that will drive the yacht, and the mizzen combined with the staysail will be sheeted in such a way as to keep the yacht on course, with the subsequent loss in performance.



3 The division of the sails

Once the type of planform - and the basic sail area is determined the sails to be used to fill this planform have to be chosen. Though in general the basic planform of a cruising yacht will differ little from the racing yacht, the actual sails used will vary. It is the ease of handling and/or course keeping stability that dictates the difference. The racing yacht will reach his maximum windward performance as soon as possible and once this condition is reached, will want to keep this conditions if the wind increases. She will carry a large number of sails to suit the windconditions. In Figure 4 a graph is shown of the sails that are used in windstrengths from zero till 60 m.p.h., this is the apparent wind speed at mast top level. It is clearly demonstrated that the cruising yacht can do with a smaller number of sails then the racing yacht since the losses in performance resulting from the "steps" in the decrease of the sail area are acceptable for the cruising yacht, since the required sail changes are kept to a minimum.

A graph or sail setting chart does give a good insight in the effect of sail changes and will prevent any inefficient sails (sails of use in a narrow wind range) to be carried onboard.

It takes a long time to compile sail setting charts by actual sailing with a yacht, especially in the higher wind range. One doesn't often meet the heavy sailing conditions, but it is nevertheless important to know exactly the behaviour of the yacht in them. It is a good precaution to take the boat out in a gale for a proper shake down, instead of waiting till one is caught out at sea by a gale in a position which isn't one's own choice. If the sail setting chart includes sheeting positions etc., it will provide an aid for safer navigation, since in a gale one is apt to get influenced by the environment and a loss in the appreciation of the performance of the yacht might prove dangerous.

The graph of Figure 4 shows an example of a yacht that will reach her maximum performance to windward at rather low apparent wind speeds. This yacht has an ample basic sail plan (150% *LP* genoa) which is further increased with the addition of a 180% *LP* genoa. The determination of the size of the basic sail plan is an important part of the design of a cruising yacht. It is the owners option to sail with a "lazy" sail plan, a sail plan which will give good performance only in the higher wind range. However, it is often better to have a fair sized sail plan for a cruising yacht and, if one wants to take it easy, it is very simple to leave the bigger sails in the bag.

But it are naturally design parameters like, wetted area, displacement and righting moment who determine the maximum size of sail area aswell. Also the main cruising grounds where the yacht will be sailed are to be taken into account.

The type of hull has influence in the determination of the number of sails to carry. A relative narrow yacht is less affected in her performance by changes in the angle of heel, then the beamy type. The narrow yacht can carry sails over a wider wind range and thus requires less sail changes. Also in small boats, where crew weight is detrimental to the stability, relative few sail changes are required.

After the basic sail plan is designed and the wind speed is determined, by calculation, experience and/or model testing, at which the yacht will reach her optimum V_{mg} to windward it is usefull to prepare a sail setting chart to further determine the amount - and type of sails in the sail inventory. This can be done based on experience with similar types of yachts, it is however also possible to use the heeling moment developed by the sails as an aid.

The maximum *Vmg* is reached at a certain angle of heel, which in its turn depends on the heeling moment generated by the sails and the righting moment of the hull. The righting moment can be considered linear with the angle of heel, so if the heeling moment is kept constant this is a guide to design the sail setting chart by:

$$Hm = \frac{1}{2}\rho \cdot V^2 \cdot A \cdot Chm$$

<i>A</i>	= sail area m ²
<i>Hm</i>	= heeling moment kgm
$\frac{1}{2}\rho$	= 0,063
<i>Chm</i>	= heeling moment coefficient, which consists of the side force coefficient and the height of the centre of effort of the side force
<i>V</i>	= the apparent windspeed

The relation between these parameters and the apparent wind speed is shown in Figure 4a and 4b. The heeling moment increases with the square of the apparent wind speed, so drastic reduction in sail area is needed to keep the heeling moment constant. Apart from sail area, the heeling moment is also influenced by the sail shape and sheeting angles which is seen in changes in the sail coefficients. These play an important part in the lower wind range where there isn't enough sail area to reach the maximum performance. The 180% *LP* light genoa gives in this respect a fair sized advantage for the cruising yacht. In the 30 knot wind range the sail area curve often shows a slight "lump", this irregularity is caused by the wider sheeting angles and flatter sail shapes that are now used. A similar effect gives the transition of the sloop rig to a two headsail rig. It appears that this type of rig needs more sail area than would be necessary for a single sail.

There are so many parameters in the design of cruising rigs that it is impossible to cover all applications and variations in this paper. The examples, discussed in more detail, are directed towards a cruising yacht with the emphasis on performance or good sailing abilities. However indications are given how handling and course keeping characteristics can be traded for this performance. In chapter 6 several rigs in actual use are described in a general way.

The Figures 1, 2a/g, 5a, 8a/c show examples of planforms and the related division in separate sails for the same basic geometric sail area of 114 square meter. These planforms are all drawn on the same light displacement hull, so in cases where the base of the planform is lengthened this could be done, in all but one case, without the aid of a bowsprit. This latter would present a difficulty if the same comparison of sail plans was done in connection with a heavy displacement hull. In order to carry enough sail area, if none overlap head sails are used, a bowsprit becomes inevitable on the heavy displacement hull. The other solution, a taller mast to increase the sail area with, will only be acceptable if the yacht has ample stability.

The sail plans discussed are nearly all sloops and/or cutters. The reasoning behind the division of the fore triangle can also be used for the fore triangle of the ketch or schooner. In general the latter rigs will have less sails in use in the fore triangle, since part of the decrease in sail area is done by reefing - or furling of the mizzen or fore sail. In general the basic cruising rig is based on the racing rig with 150% *LP* genoa's. On several occasions however the advantage of a basic rig with less overlap or even no overlap is shown.

Figure 2a

A cruising sloop with a minimum number of four head sails, two reefs in the main and a single spreader rig. The last reef in the main is used as a trysail. It would be advisable to have a separate trysail aswell. The rig shown is about the most simple rig possible for an ocean voyage. Only on very small boats a further reduction in the number of headsail could be warranted. Apart from the normal sails also a light feather genoa is drawn in the sail plan. Since the rig is used on a light displacement hull the fore stay is well inboard, a fact which does improve sail handling, also the rather high clews of the sails do improve handling, prevent waves hitting the sails and increase the vissibility for the helmsman. When lowering the main, the boom is allowed to drop on the deck. This prevents the wind getting under the sail and greatly facilates the sail handling.

On moderate - to heavy displacement hulls the fore stay will have to be right at - or near the stem.

Figure 4a shows the sail setting chart for the rig, though the steps are rather large, they are acceptable for cruising purposes. The - - - line shows the steps followed by a racing yacht, of simmilar size.

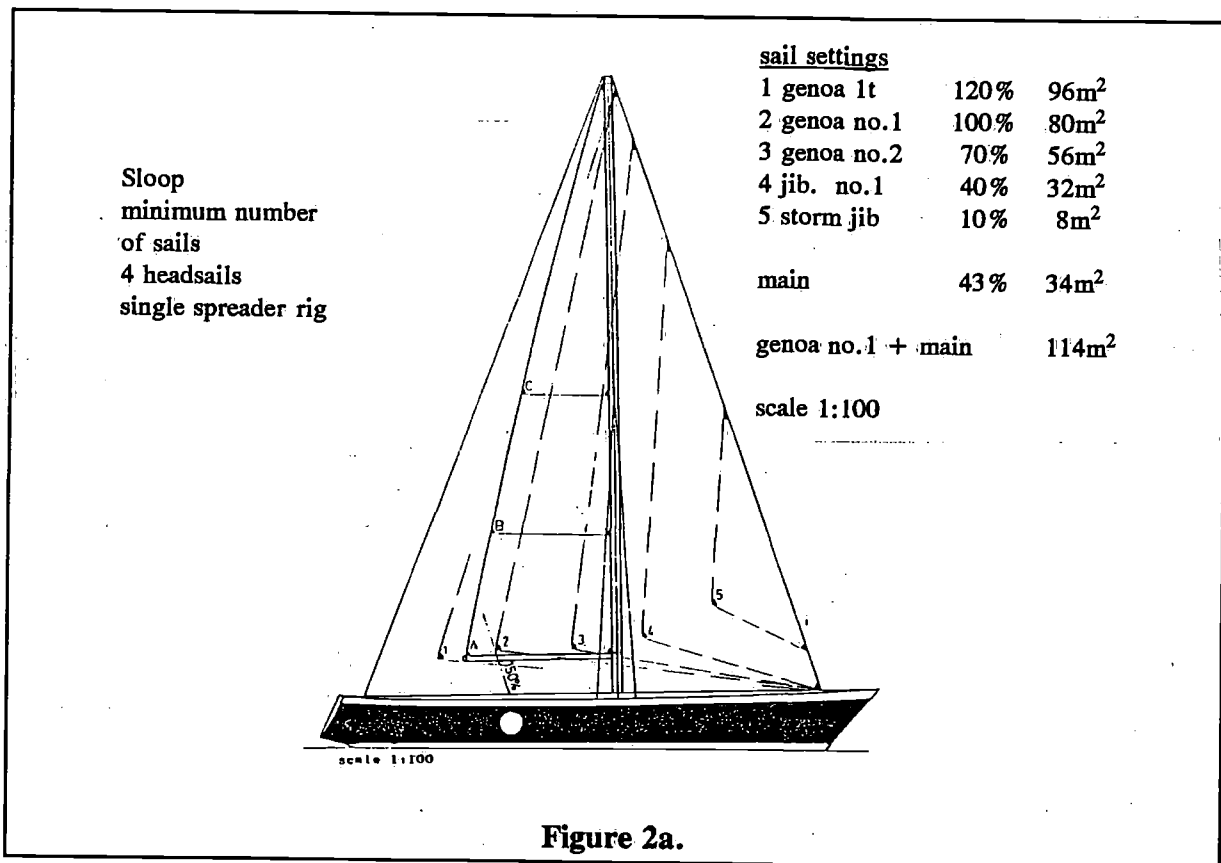


Figure 2a.

Many innovations are possible to make the rig easier to handle, some of them are shown in the chapter concerning the roller furling sails, but all arrangements lead easly to a reduction in performance and in this field the rig shown is hard to beat.

To make the rig easier to handle in strong winds it is possible to design the rig with the forestay more forward, so the clew of sail 3 will be in front of the mast and the sail can be made self tacking. Either with a boom or with the system shown in Figure 3. If a boom is

used the sail could be fitted with a reef, such as is fitted in the main. Sail 3 will then be kept permanently hanked on to the forestay and, if reefed, will act as sail 4. Now only sail 5 and sail 2 will have to be hanked on and - of. The use of a double forestay will further reduce the sail handling, and also sail 2 can be kept permanent hanked on. However a double forestay is a far from ideal solution on long trips due to chafe problems, damage to sail hanks, lack in forestay tension, windage etc. It seems better to do a little more work and bypass these problems.

For a sail area (main + genoa no.1) of 114 square meter the rig is rather large and the individual sails are about the maximum what one man can handle. The rig as drawn here would be more usefull for smaller boats. Many sailors would prefer a cutter or a schooner for this sail area, also with the better course keeping stability of these rigs in mind. Another advantage will be the better position of the storm sails. The storm jib as drawn in Figure 2a is really moving the centre of effort of the sail plan too much forward. Figure 2b shows a better position for the storm jib. The position of the light weather genoa is more or less ideal, for sail efficiency it would be better to move the luff of the sail forward but if this is done the yacht will quickly develop an unacceptable lee helm when sailing to windward. When preparing a sail setting chart, it aren't only the sail area's, but also the position in fore and aft direction of the centre of effort of the rig that have to be kept in mind.

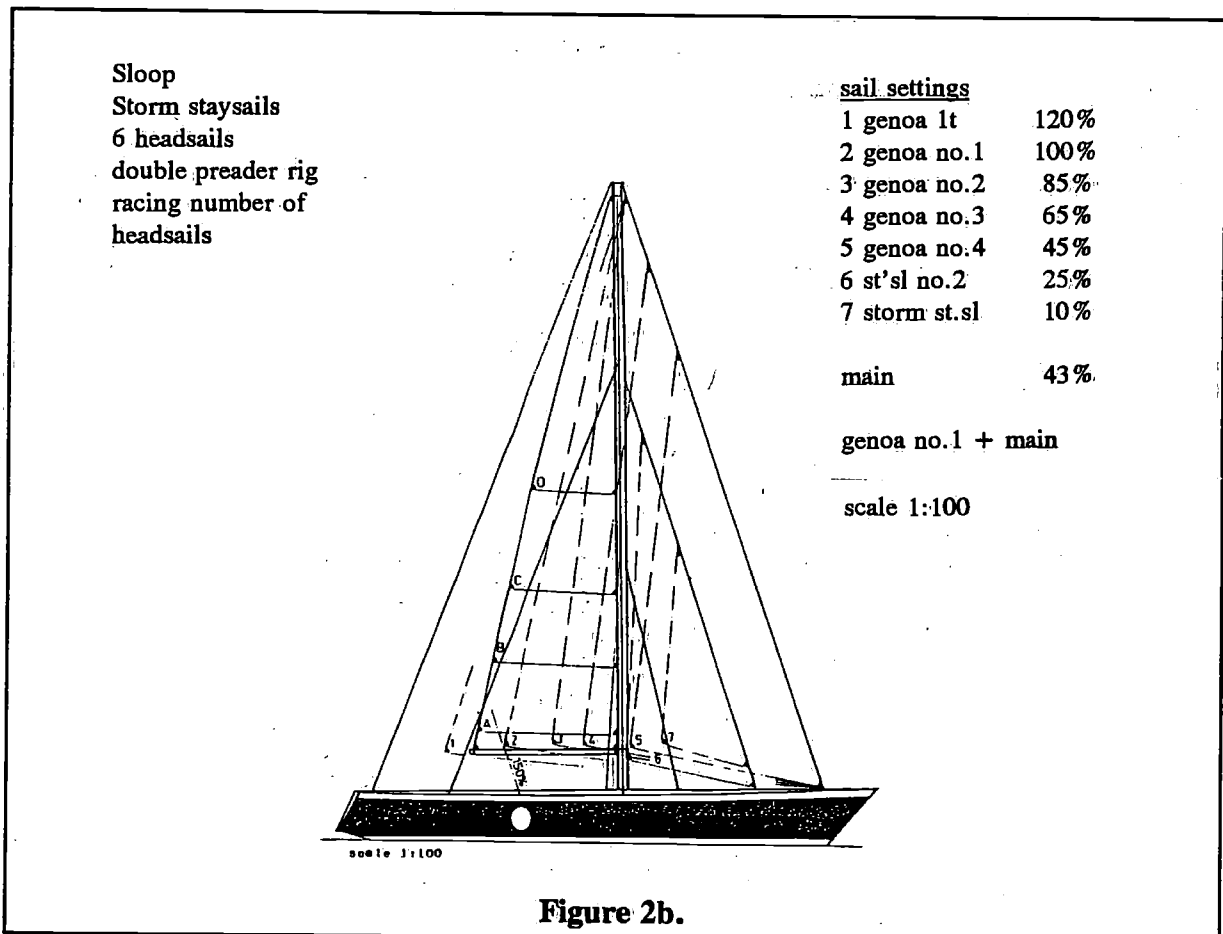


Figure 2b

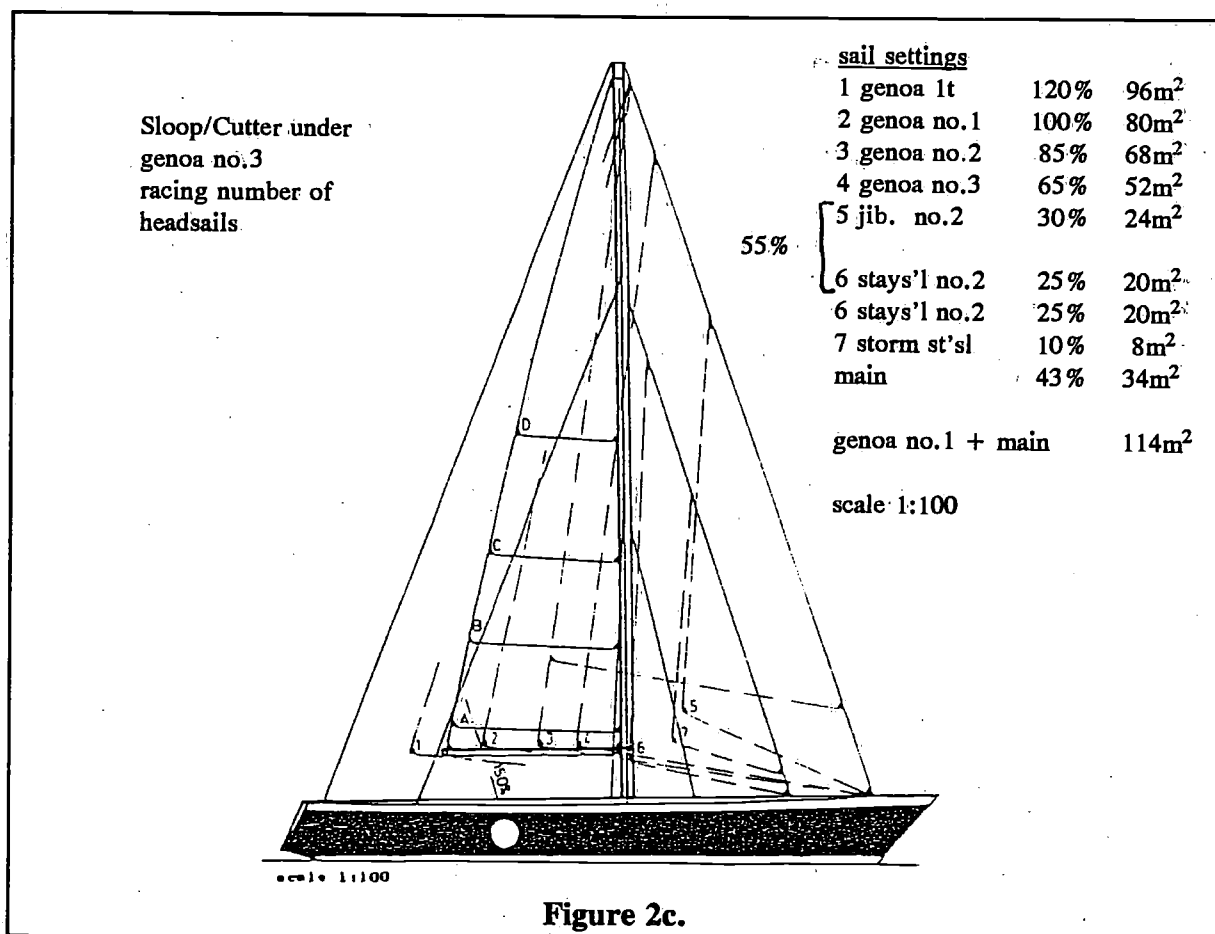
This sloop shows the number of head sails and the number of reefs that are in use aboard racing yachts. The sail plan drawn only differs from the racing sloop in the extra large genoa light, the extra height of the clews of the genoa no's 1, 2 and 3 and reef D in the main.

Normally the racing sloop only carries the flattening reef A and the reefs B and C. Instead of reef D a try sail is used. The racing sloop will carry several genoa's of the same area, they differ in cloth weight - and shape to suite the wind conditions. If the cruising sailor wants to use light weather sails, he might aswell make them as big as possible to take full advantage of the wind.

The sail area curve of this rig is shown in Figure 4a, the sail changes are thus spaced that, combined with the trim of the sails, optimum performance over the whole windrange from 23 knots upward is achieved if the sail inventory starts with the 150% LP genoa. As was said for sloop 2A, it is now also possible to reduce the number of different sail area's used for smaller boats. Five would be a good number for a smaller boat and for a bigger boat sloop 2C will give best results.

Figure 2c

This would be the sail plan for a large racing sloop with a much larger basic sail area then 114 square meter. The genoa no.2 can be reefed down to the genoa no.3. This procedure can only be followed if the required cloth weight for the two sail area's is the same. In general the reefing of head sails is succesfull if used for boomed jibs and although the reefing of regular genoa's is used by racing yachts the idea is probably not too good for a long distance cruiser in view of the durability of the sail.



For the cruising yacht sloop 2C is much better then sloop 2B, which has little to offer in this respect. In addition to the cruising modifications already shown in the drawing and discussed for sloop 2B, sloop 2C could be further modified as follows; Use the main of sloop 2A, com-

bine sail 3 and - 4 to one genoa no.3 of 75% and change to the cutter rig in the "racing" manner after this. The steps will now be, 100%, 75%, 55% (two sails), 25% and the last one will be to the storm jib 10%. A good compromise for a boat with the basic sail area of 114 m². A further ease in sail handling will be reached by changing to a cutter rig right after genoa no.1 as is shown for sloop 5A.

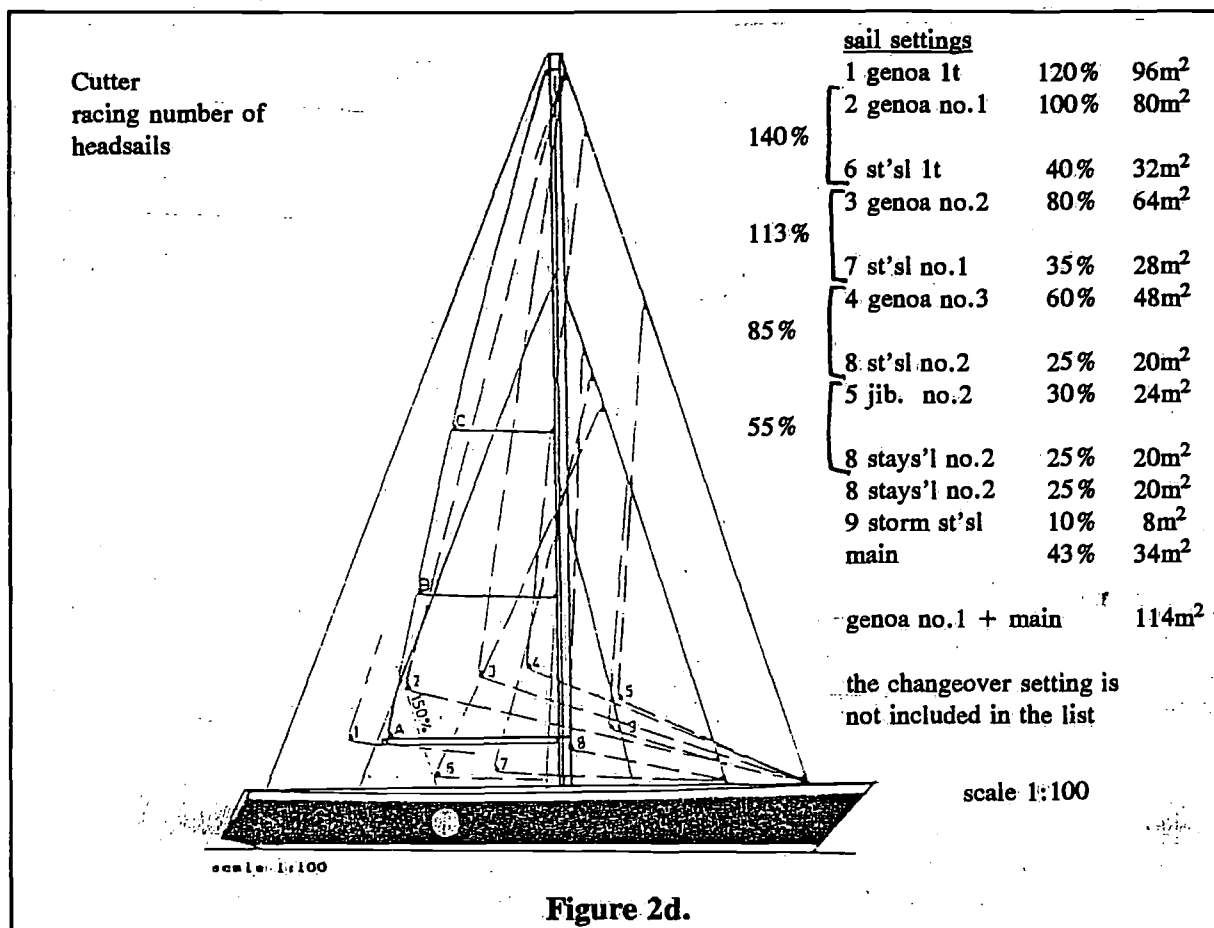


Figure 2d.

Figure 2d

Though a cruising main is drawn, the division of the fore triangle is for a racing cutter. In its true form the racing cutter isn't much used nowadays since one head-sail performs better to windward than two. The only exception are big boats in strong winds. For ocean passages it doesn't make sense to point too high when sailing to windward and under these conditions a cutter could come in its own. Also for reaching in strong winds the cutter is a good configuration. The cutter as shown here, or in a slightly simpler form, makes only sense for boats where the genoa no.1 is too big to be handled. The genoa no.1 would then be replaced by sail 3 and - 7, this means a reduction of 20% in the largest sail. If light weather sails are demanded the genoa light can be replaced by sail 2 and - 6, with again a reduction of 20%. This reduction is less than would be expected since the combined area of the two sails set at one time, is bigger than the area of the single sail they replace. A fact born out in practice, the heading angle of the cutter rig is bigger and a higher speed is needed to be able to maintain the same *V_{mg}* to windward, as the sloop. The cutter rig requires more, but easier sail changes and thus will follow a sail area curve in relative small steps. If the cutter rig is used in combination with a second mast, it becomes possible to sheet the sails farther aft and thus the clews can be designed higher from the deck. The interference between the two headsails will become less and the performance of the rig better. This interference can be very severe

and, with a small boat, careful sail trimming is needed to get good results out of the rig. In general it would be better to consider a schooner or a typical cruiser cutter rig as shown in Figure 2f if the genoa is going to be too much to handle, for cruising purposes.

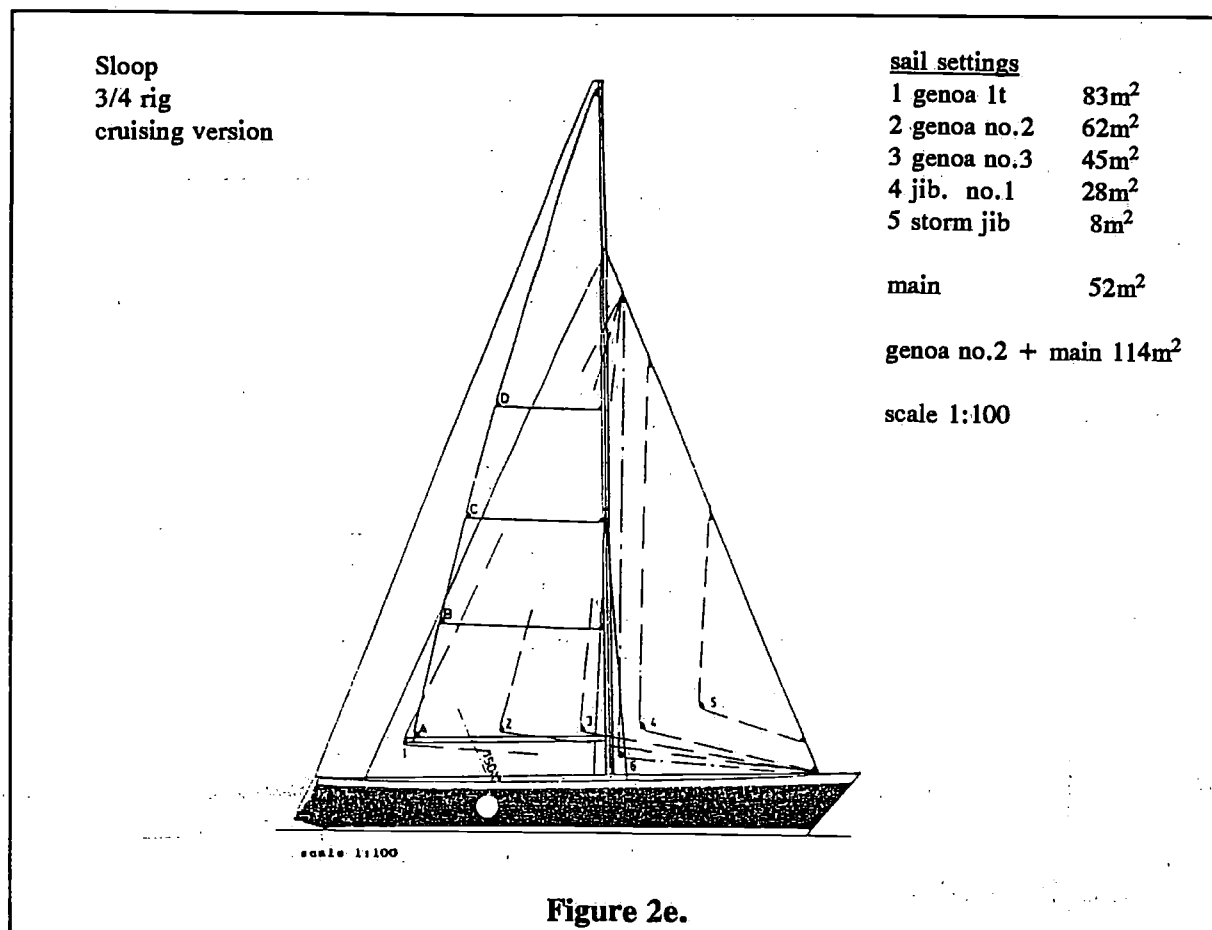


Figure 2e

An interesting alternative for cruising purposes gives the 3/4 rigged sloop. Actually a 4/5 rigged sloop would be still better since it appears that with this type of rig sail 3 and 6 would have been the same, which means that the genoa no.3 will be self-tacking. The number of head sail changes is brought to a minimum and due to their reduced size they are fairly easy to change. The main is rather big, but with the latest reefing systems the handling should be easy. It is less work to reef a main than change a headsail. Performance to windward will be good, but reaching and running will be suspect. The rig requires runners but, in strong winds, when the main is reefed the runners could be set permanent. A serious drawback of the rig for a basic sail area of 114 m² is the course directional stability, or rather the lack of it. A yacht with this much sail requires a staysail to improve course directional stability and reduce steering requirements, if the wind is strong or gusting and the boat isn't hard on the wind. A staysail like sail 5 in Figure 2f would be useful, especially if equipped with a traveller as shown in Figure 3. Also [4] and [9] give information in this respect. Although in a slightly less severe way this lack of course stability is also apparent with sloop 2A and only if the hull, windvane or auto pilot could provide the course stability these rigs can be used for long distance passages.

Figure 2f

The rig shown here is very satisfactory for cruising purposes. The performance will be less

then for instance the performance of the cruising version of sloop 2C or - 5A, but this is partly compensated by a slight increase in the basic sail area. In designing this sail plan the basic concept of the 150% LP genoa is abandoned. After establishing this standard rig for the yacht and after the sail inventory has been decided, these data are used to design the cruising rig, with the emphasis on the desired cruising characteristics. Common sense is used to make sure this trade-of of cruising characteristics against racing performance is not too drastic. Unfortunately very little theoretical work has been done in this field and no systematic data concerning sail coefficients for typical cruising sails is available.

The lack in performance will be evident in the moderate wind speed range. If the genoa light is used the boat will certainly move in the very light conditions and the cutter rig will be efficient enough in heavy going.

The runners are usually in a fixed position just aft of the lower shrouds and assist the jumper stays in taking the load from the cutter stay. In very heavy going the jumper stays should be able to keep the mast straight but it will be better for the performance (straighter cutter stay) and safer to use the runners in the normal way. If the sail is reefed the runners could be set permanent aft.

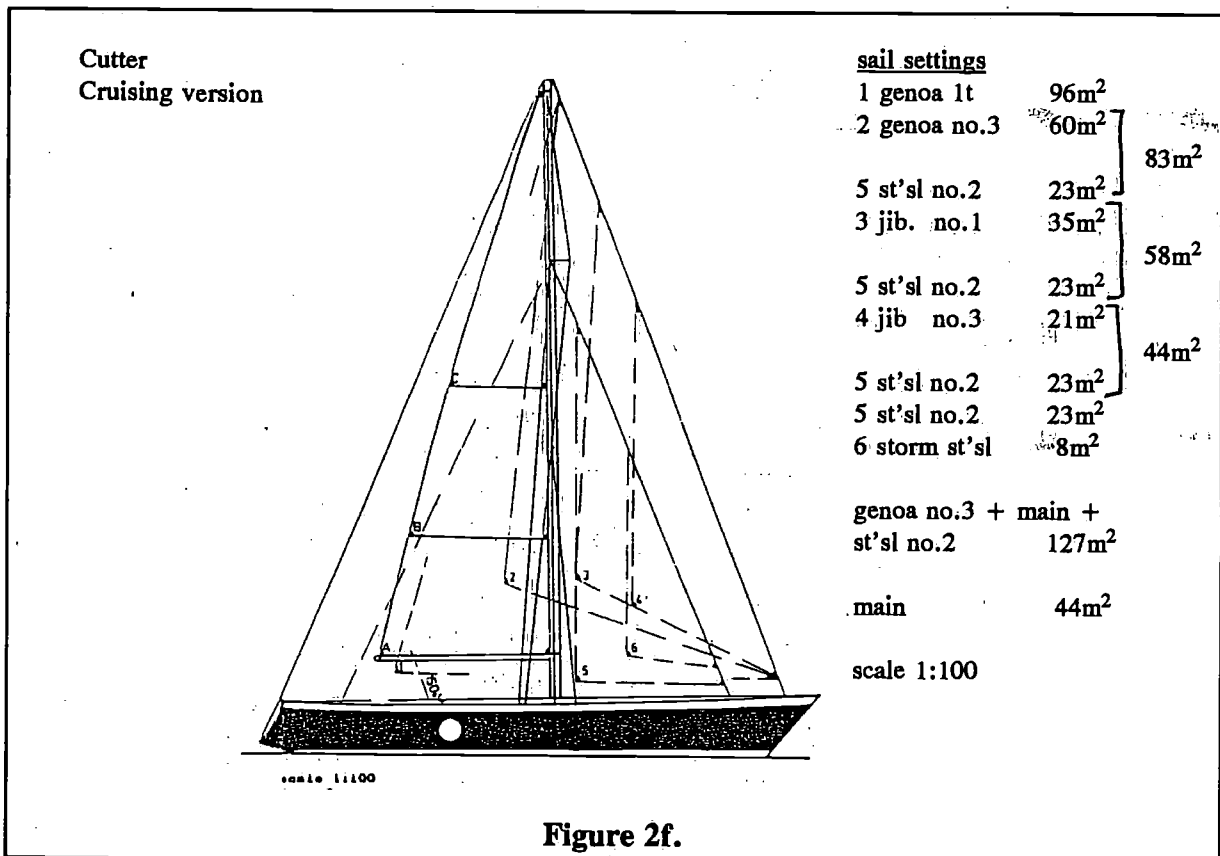


Figure 2f.

The high clews of sails 1, 2 and 3 enable the sheeting positions to be kept on the toe rail. Which means the sheets are outside the life lines at all times and no chafe occurs when the sheets are started on a reach. Also the deck area will be much cleaner without the genoa track. Sail 4 can be sheeted to a pad eye and adjustments to the sheeting angle can be made by moving the sail up - or down along the fore stay. It is necessary to bend the stanchions aft 10° inside to prevent the sheets touching the life lines when hard on the wind. The system works very satisfactory if the transom of the yacht isn't too wide. Care has to be taken how-

ever for flogging sheets, which are now near the sheet handling area.

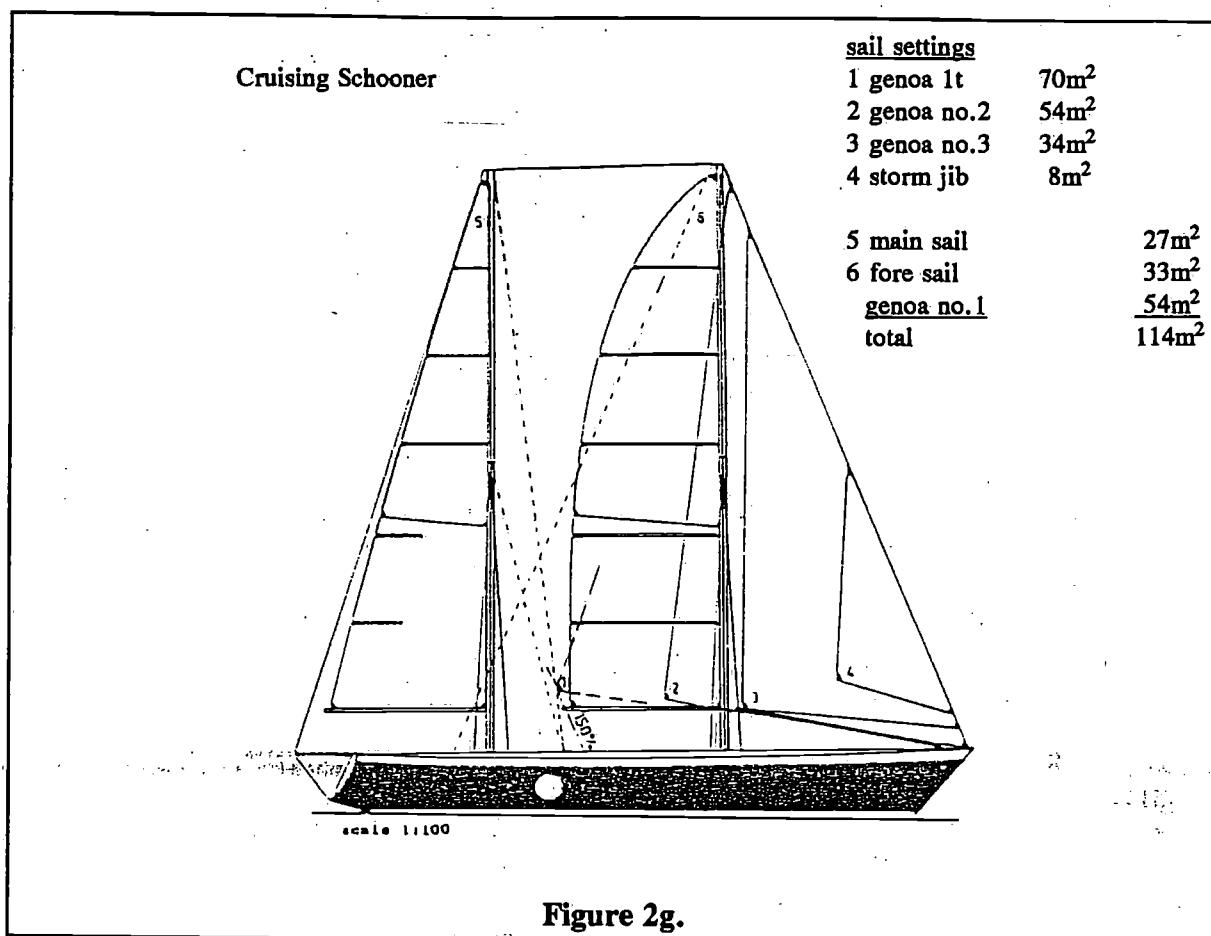


Figure 2g

The schooner, with equal masts, is also a very promising cruising rig, if the size of the sail area does warrant the use. The distance between the masts, or rather the distance between the leech of the fore sail and the luff of the main, is an important parameter. The farther apart this two sails are, the better. Figure 10 shows what can be done in this respect. If there is enough room in front of the main mast a second genoa could be set from this mast and used to windward with advantage in light going.

The sail plan shown has a fairly conservative aspect ratio and a further improvement in performance could be expected from a higher aspect ratio, this will also increase the distance between the main and fore sail. The number of headsail changes is an absolute minimum indeed and the reefing of the main and fore sail should be easy. The rig is self-tacking with sail 3. The rig has many possibilities on a reach as can be seen in Figure 13. *Vmg* to windward in moderate conditions and also in light conditions are suspect, also the running sails are rather small due to the reduced mast height. The ease of handling - and course directional stability are however excellent. The rig really offers advantages for sailing crafts that rely on speed and not on heading angle to obtain a good speed-made-good to windward, an example is given in Figure 11.

The masts rely on each other for staying purposes, which does give a neat looking arrangement. For safety purposes it is probably better to make a separate set up for each mast as is shown by the dotted lines. The shape of the fore sail will have to be adapted.

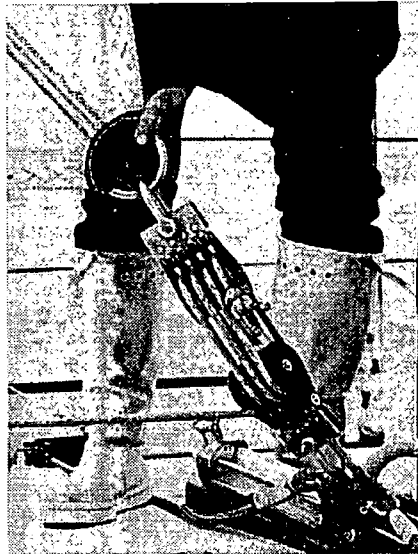
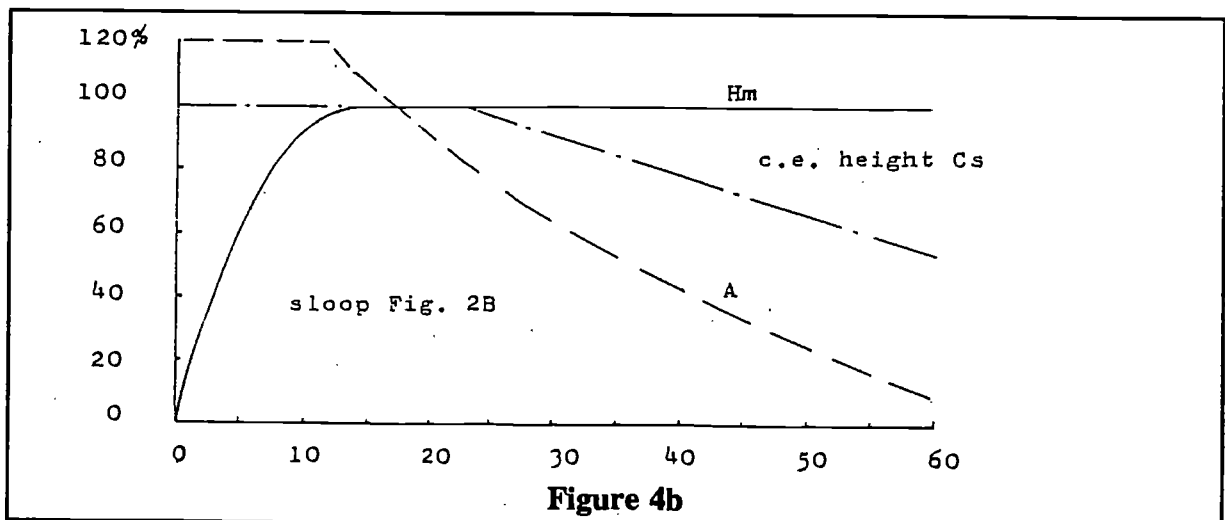
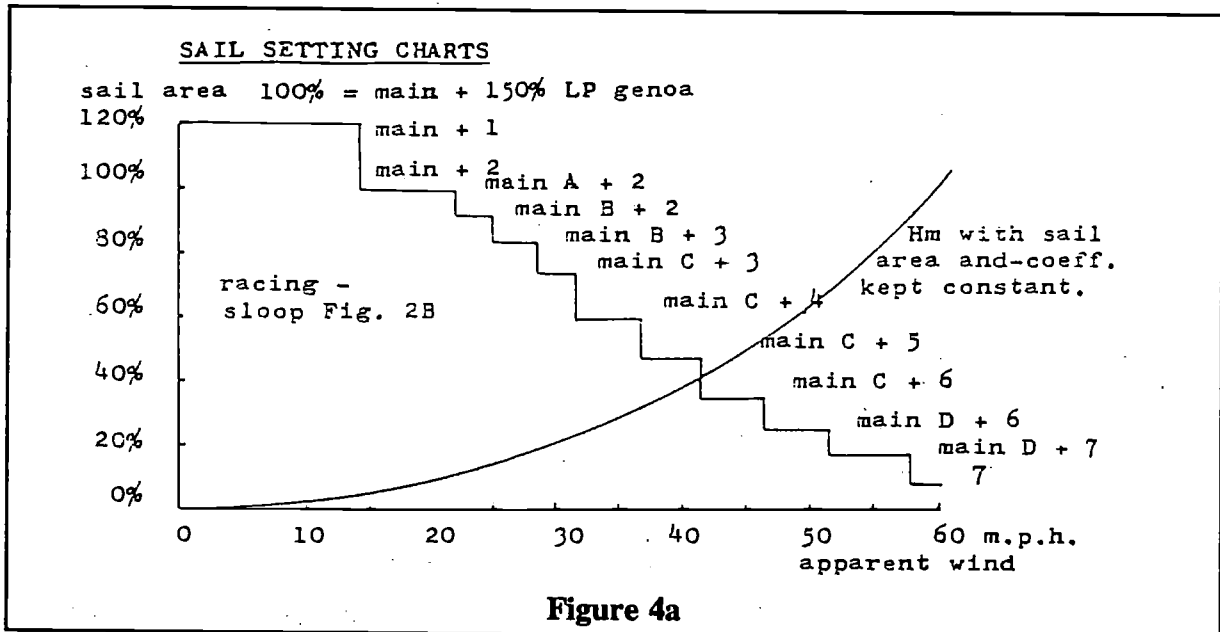
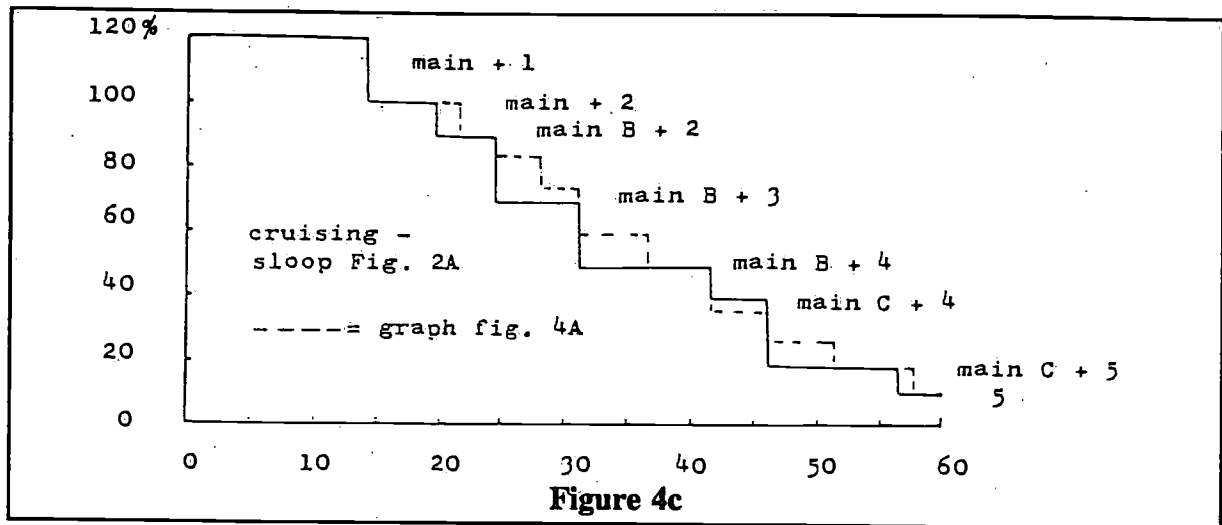


Figure 3. Traveller arrangement for self-tacking staysail





4 The sails for a solo-racer

Figure 5a and b illustrates the windward - and running sails for a single-handed transatlantic racer. The dimensions of the yacht are: *l.o.a.* 16.50 m, *l.w.l.* 14 m, beam 3.30 m, draft 3.30 m, displacement 9 tons and a basic sail area of 114 m². The separate sail settings used are visualized in Figure 6a/g and the corresponding deck layout in Figure 7.

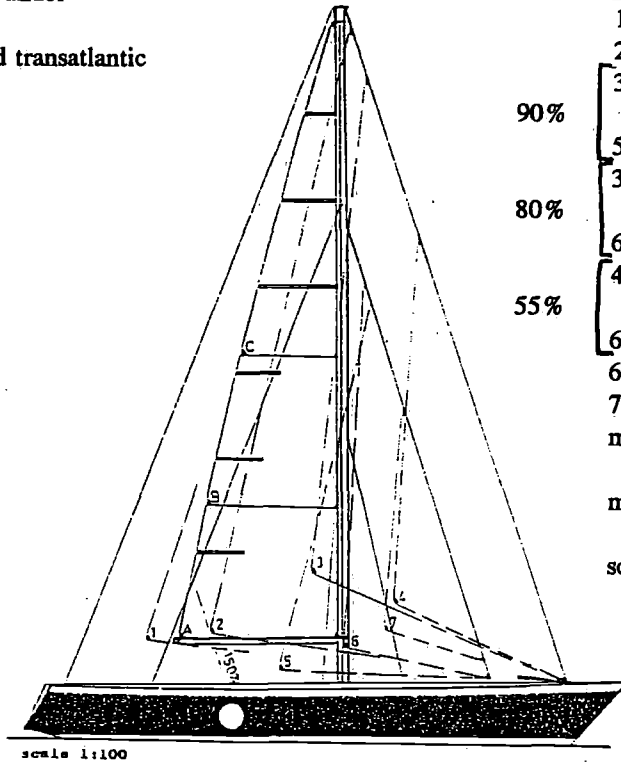
The sail plan is a modification of the IOR racing sloop 2C. The sloop is cutter rigged below genoa no.1 to prevent the handling of a genoa no.2, in a blow, of 68 m². Both, the genoa no.2 and the genoa no.3, are replaced by a double head rig. The consequences for windward performance are rather small since the moderate conditions are being sailed with a genoa no.1 with optimum performance and the double head rig is only starting when it already blows a bit. Since the boat is used for a transatlantic race the reduction in heading angle with the use of the double head rig is acceptable. To get the best out of the double head rig the staysail 6 isn't self-tacking and used more for performance than for course keeping characteristics. The main has only two reefs and the flattening of the main, when still full size, is done by luff - and foot tension without the use of cunningham holes. The latter makes only sense when the rating has to be considered. The sail battens, full length near the top, improve the sail shape in strong winds without the use of heavy - and though to handle sail cloth. Also the shaking (chafe) of the sail in strong winds is less this way.

The light weather performance is increased by the use of a 180% LP genoa light, which can be roller furled or set in the usual way. Sail handling is further facilitated by the possibility to drop the main boom to the deck when furling the main. The genoa no.1 is permanent attached to the fore stay and stows in its own bin under the deck.

The solo-racer is narrow, with good stability, and can operate to windward at fairly high angles of heel. For this type of yacht the moment to change sail is less critical than onboard a yacht with more beam and the genoa no.1 can be carried to windward fairly long in increasing winds. So it should be possible to bypass the change from genoa no.1 to the first double head rig and go directly to the combination of genoa no.3 and staysail no.2. Staysail is added to increase the possible sail settings when sailing with slightly eased sheets or when reaching.

When reaching it is possible to use the spi poles to push the clews of the genoa's to leeward, a technique prohibited in IOR races, which will greatly increase the efficiency of the sails on this course.

Sloop/Cutter under
 genoa no.1
 single-handed transatlantic
 race version

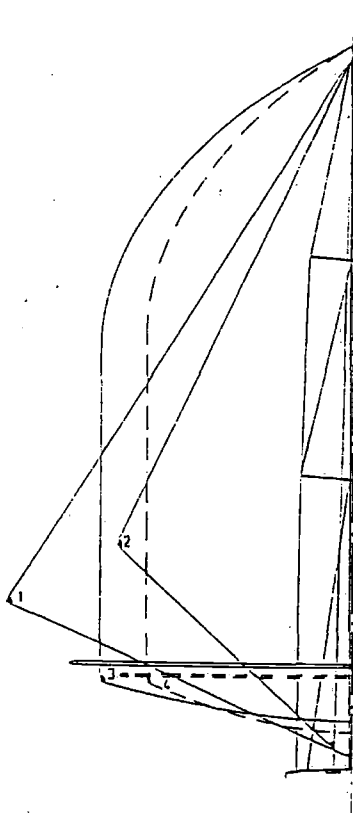


sail settings

	1 genoa 1t	120%	96m ²
	2 genoa no.12	100%	80m ²
	3 genoa no.3	55%	44m ²
90%	5 st'sl no.1	35%	28m ²
	3 genoa no.3	55%	44m ²
80%	6 st'sl no.2	25%	20m ²
	4 jib no.2	30%	24m ²
55%	6 st'sl no.2	25%	20m ²
	6 st'sl no.2	25%	20m ²
	7 storm st'sl	10%	8m ²
	main	43%	34m ²
	main + genoa no.1		114m ²

scale 1:100

Figure 5a



Running sails

Single-handed transatlantic
 race version

sail settingd

- 3 spinnaker for 190% LP
 appr. 220 m²
- 2 heavy weather twin
 2 x genoa no.3 96m²
- 3 middle weather twin
 2 x genoa no.1 160m²
- 4 IOR 150% LP fore triangle
 spinnaker and spi pole
 spi appr. 175m²

scale 1:100

Figure 5b

The rigging is conventional, 1 x 19 stainless wire is used for the standing rigging since this will leave a greater safety margin than would be possible with rod rigging. The lower shrouds are well inboard to facilitate the sheeting of staysail no.1 to windward. In case the main is reefed to trysail size it is possible to set the runners permanent.

There are three sail settings for running. For running in light winds a spinnaker, corresponding with a IOR spinnaker for a 190% *LP* fore triangle, is used. The length of the spinnaker pole for this spinnaker (1.9/1.5 x *J*) coincides with the length of pole needed to make efficient use of the genoa no.1. This gives a pole length/genoa *LP* ratio of 0.85, which is considered a minimum. It is now also possible to use the genoa's as twins with the wind not dead aft. The absence of lower fore shrouds further increases the wind/course angle at which the twins can be used. The genoa no.1, hanked to the fore stay, and the roller furling genoa light are the moderate wind running sails. If the wind isn't dead aft it will be profitable to set the genoa no.1 to windward and the larger genoa light to leeward, however the genoa light will have to be partly furled to suit the length of the pole anyway.

The spinnaker will be equipped with "sally" furling. The sally consists of a number of nylon rings with approximately 30 cm diameter. These rings can be pulled up to release the spinnaker or pulled down over the spinnaker pole for furling before taking the spinnaker down. The rings are kept apart by a distance line or by a spicon made out of cloth.

For running in heavy conditions two genoa's no.3 are set in front of the mast. They will form an inverted "V" to the wind, a very stable rig. The two genoas no.3 are hanked on to removable jack stays to control the sails during setting and furling. For this purpose it is possible to use the genoa halyards as the jack stay and hoist the sail with the spinnaker halyard. After hoisting the genoa halyard should be slackened off to prevent chafe of the halyard in the sheave box.

An interesting method to use one of the heavy weather twins, set to windward, for course directional stability and self steering is given in [9]. If a combination of sails is set, [10] will give an easy procedure to visualise the airflow (two dimensional) around the sail plan and the interaction between the sails can be seen.

5 Roller-furling sails

Roller furling sails can be divided into two types. First there are the sails that can be both roller furled and roller reefed, the other type can only be roller furled. There are many gears for roller furling sails on the market nowadays, a description of them is given in [11].

The possibilities for the roller furling/reefing gear are wide spread and the application of this gear for cruising rigs has only just started. The problem with the roller furling/reefing concept is the sail and not the gear. The partly reefed sails set poorly since the leech and foot of the sails are getting too tight and the centre areas are getting too full. The tension in the wire or rod of the roller furling gear should be the same as the tension used in a normal fore stay. This requirement is often difficult to satisfy, particular in the case where the gear has to be easy removable. Due to these difficulties and due to the price of the more sophisticated gears the roller furling sail is still not very popular, however this might change in the near future. Though the price of the gear is high, it also saves one - or two sails so this will cancel the extra expenditure.

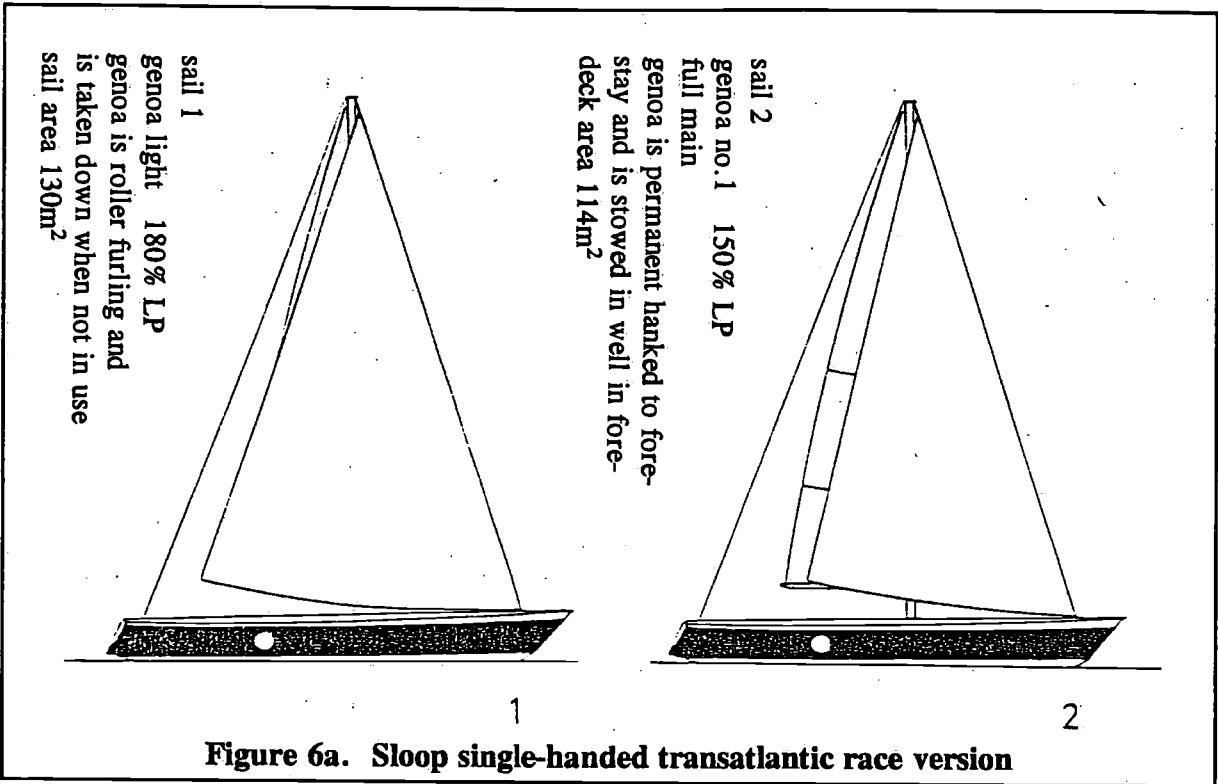


Figure 6a. Sloop single-handed transatlantic race version

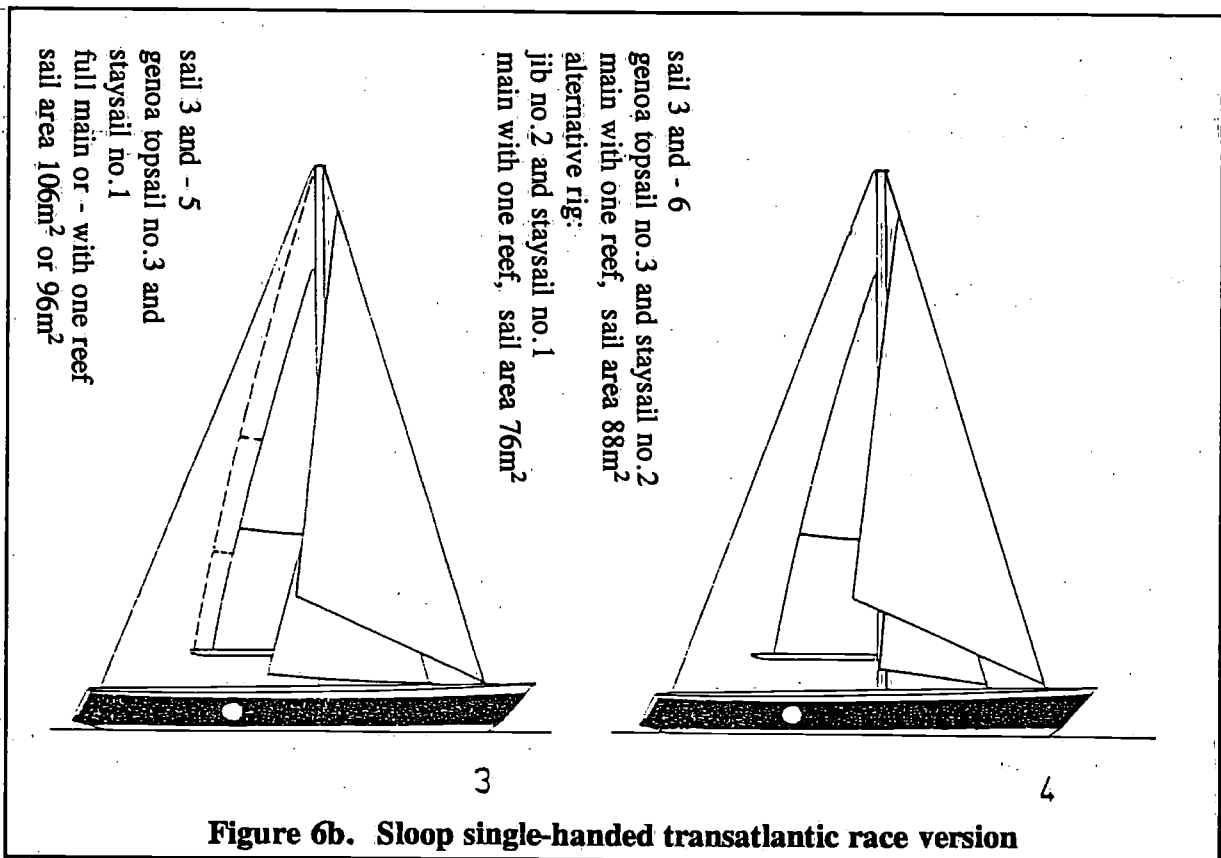


Figure 6b. Sloop single-handed transatlantic race version

Some roller furling/reefing gears are strong enough to take the tension of the fore stay, they can actually replace the fore stay. However, for long passages this is bad practice since the fore stay has to be available to set light weather sails from and/or the storm jib. Also a spare working sail should be kept onboard in case of gear failure.

Figure 8a shows an entirely with roller furling sails equipped sloop. Though the concept looks attractive at first glance the performance of the rig will be rather poor since the sail shapes are hard to control. It is ofcourse impossible to change the cloth weight of the genoa during the reefing process, so the cloth should be strong enough for the heavy conditions. This required weight of cloth will set poorly in light winds and the sail will distort during the reefing and set badly in strong winds. If one wants to enjoy his sailing this rig doesn't look attractive to use. For very small boats, and moter sailors, the rig could be usefull.

The roller twin shown looks more promising and gives a good solution for the problems of the cruising sailor when running before the wind. If the rig has a cutterstay it would be not possible to use the one piece roller twin in front of the mast. Two seperate sails will be required.

An interesting application of the roller twin is the combined use of this sail for running and for sailing to windward. The gear will then run from the stem to the masttop and with the two clews tied together it is used as a two ply genoa. For running one simply unties the clews, set up the poles and pull the sails apart.

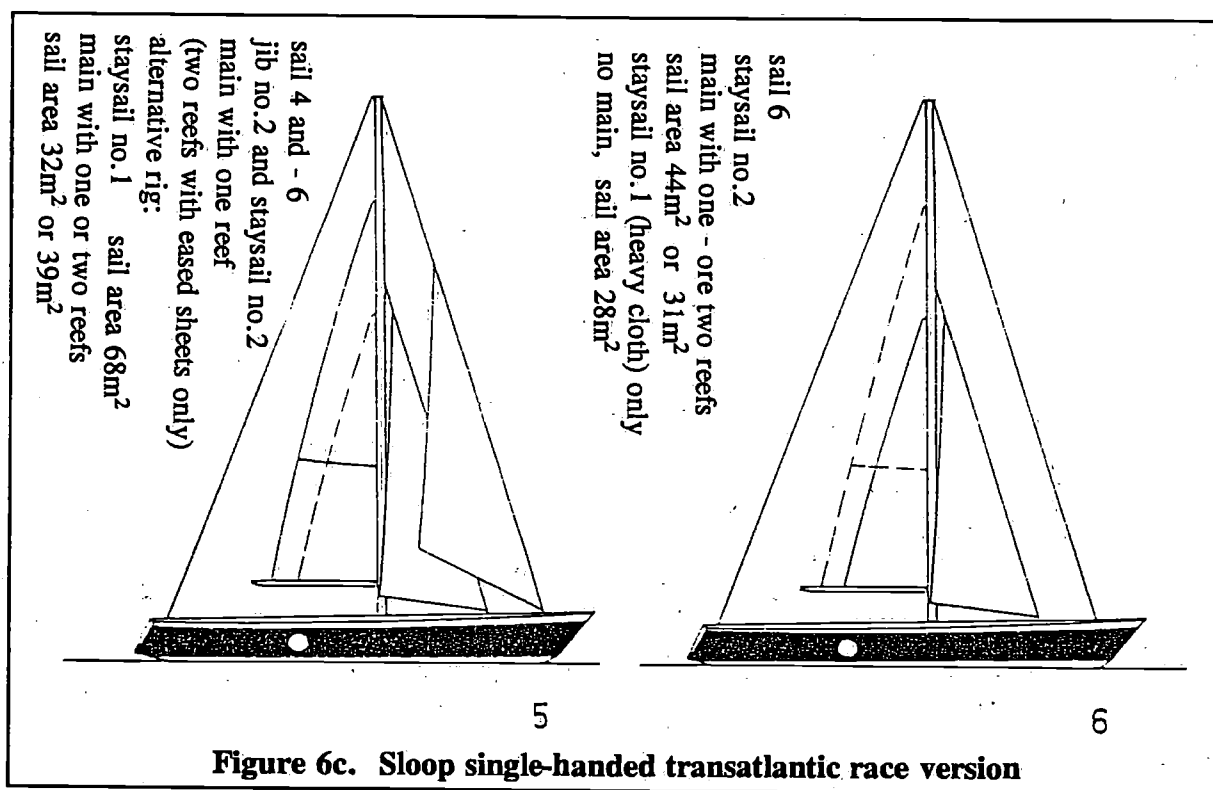
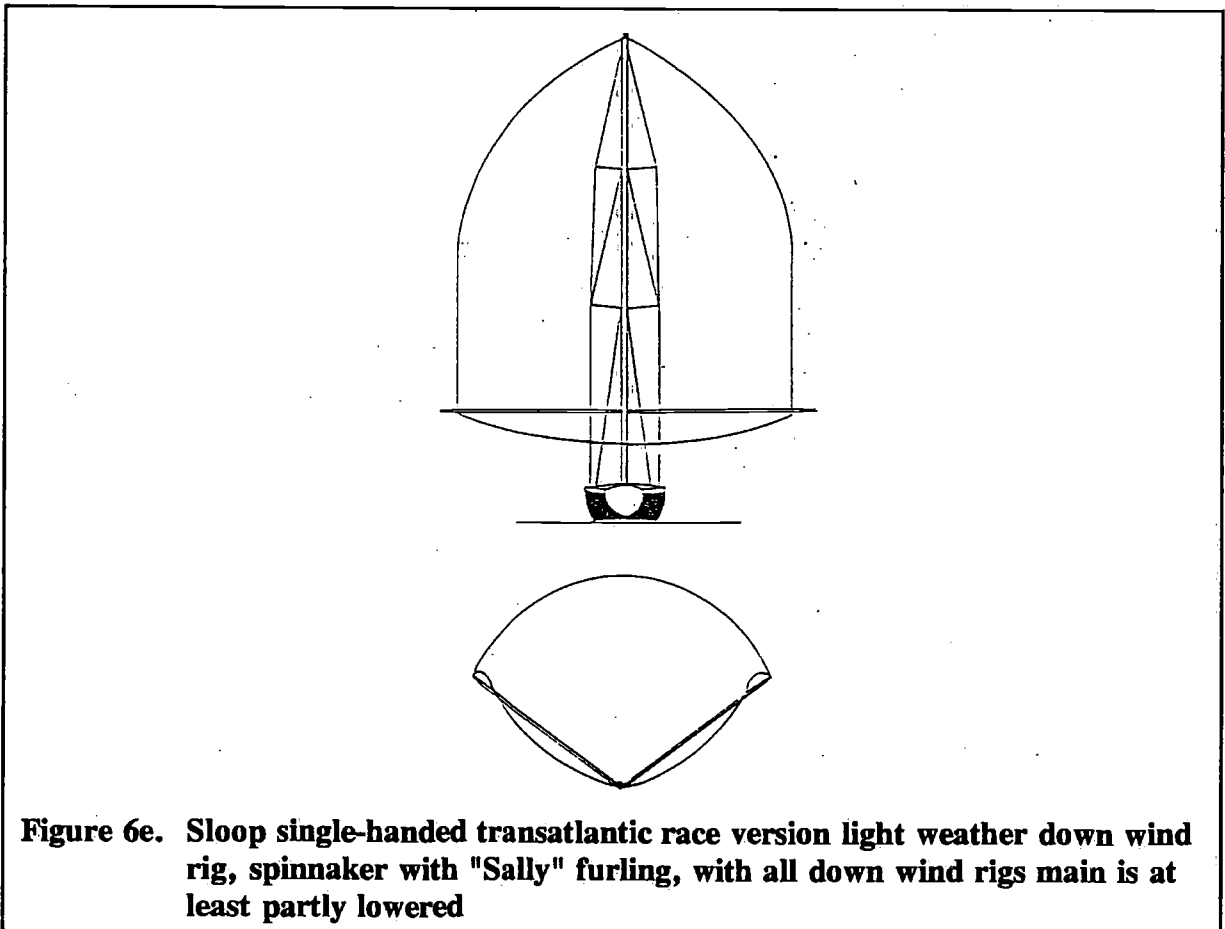
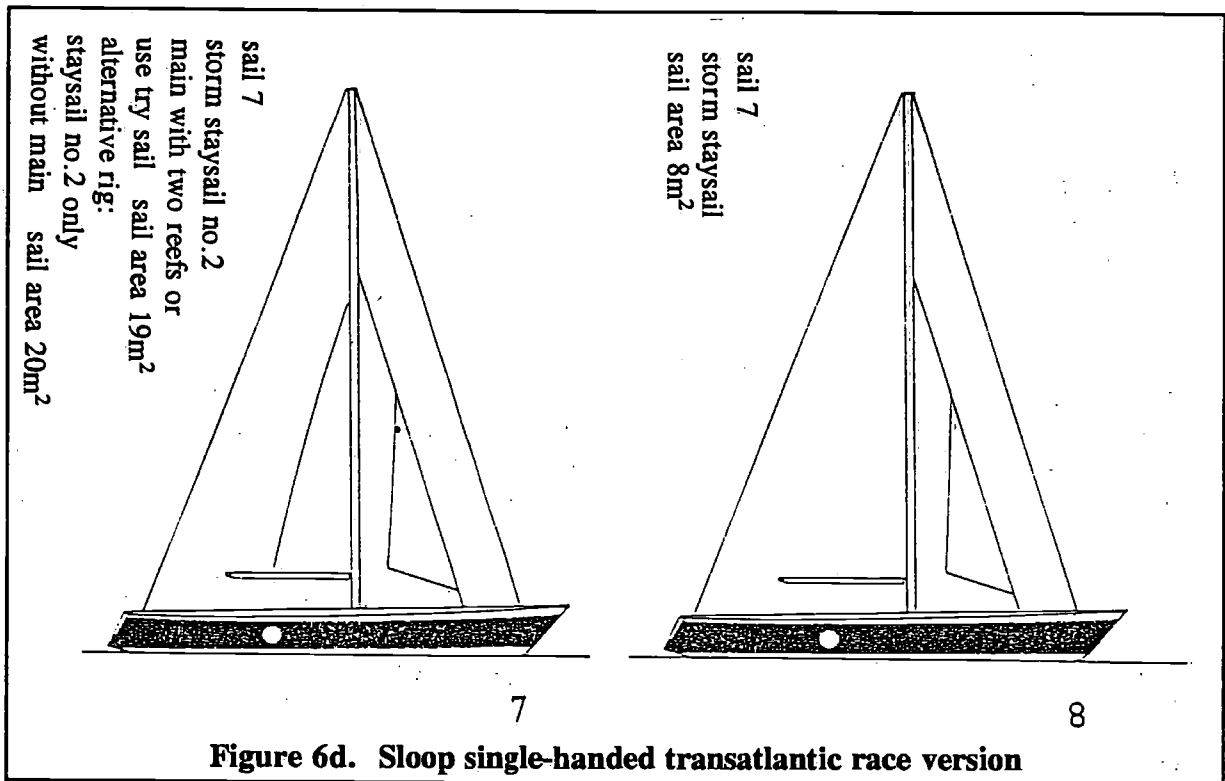


Figure 8b shows a better application of a roller furling/reefing sail. The genoa has been much reduced in size and if the sail is only partly reefed a reasonable performance can be expected. The fore-stay is used for the genoa light and for the storm jib. Another cruising application of the roller furling sails is seen in cutter 8C, which is otherwise identical in planform to cutter 2F. The main is fully battened and, combined with the lazy jacks, handling of the main should be no problem at all.

For running sails and light weather sails the furling/reefing sails are very usefull, in other applications they are also usefull but, unfortunately, give rather poor results sailing wise. However for moter sailors and small cruising yachts this isn't so. Here they can be used in all applications with a fair amount of succes. The furling only sails could be used succesfully

if some means are found to set the sails in an easy way, without jeopardising the required tension along the luff, and still be able to lower the furled sails on a moments notice.



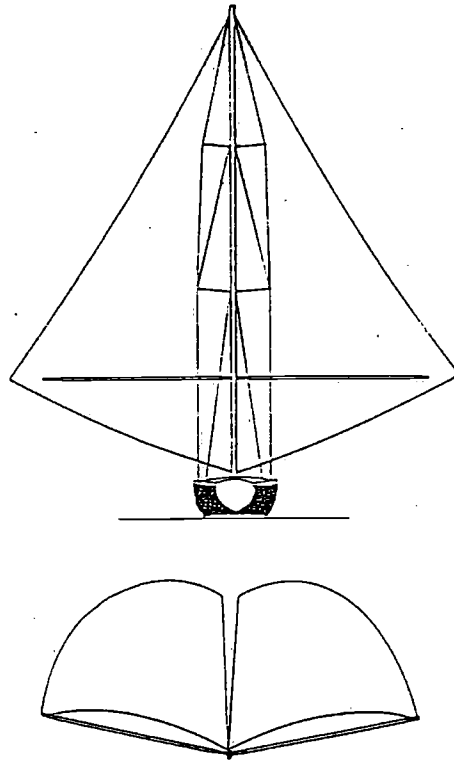


Figure 6f. Sloop single-handed transatlantic race version, middle weather twins, two genua's no.1 or genoa no.1 with partly roller furied genoa light

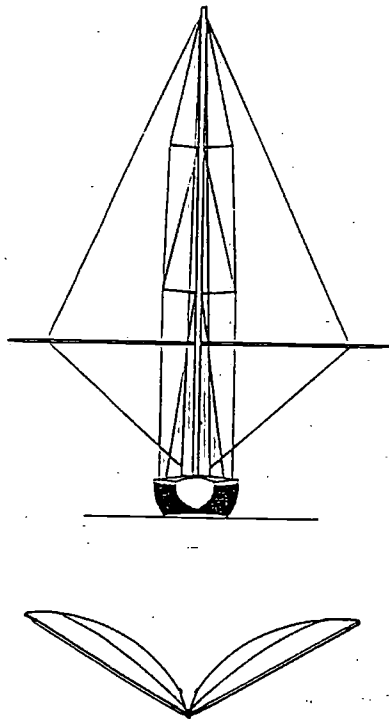


Figure 6g. Sloop single-handed transatlantic race version, heavy weather twins, two genoa topsails no.3 hanked to jack stays or two roller furling sails which are taken down when not in use

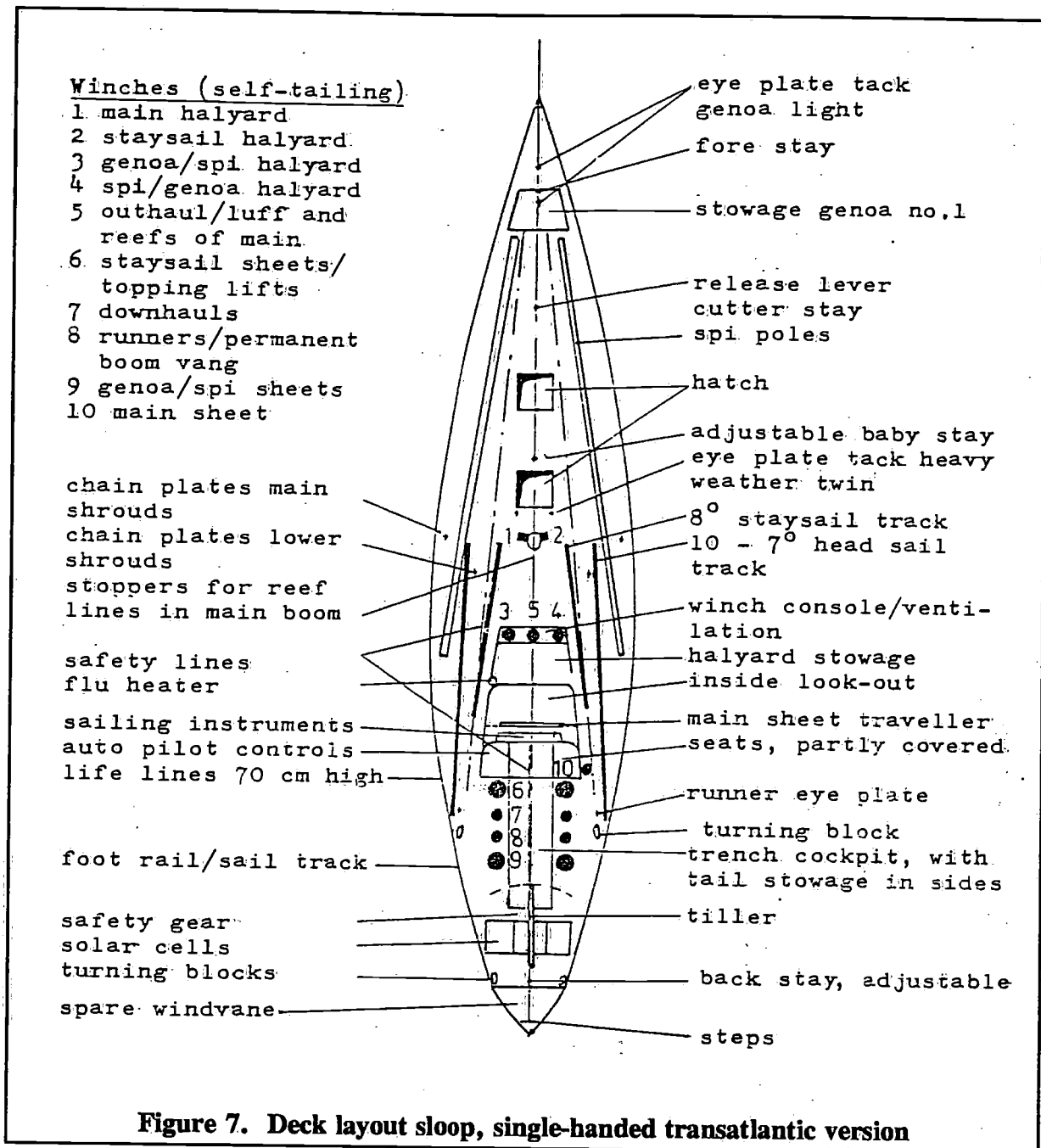
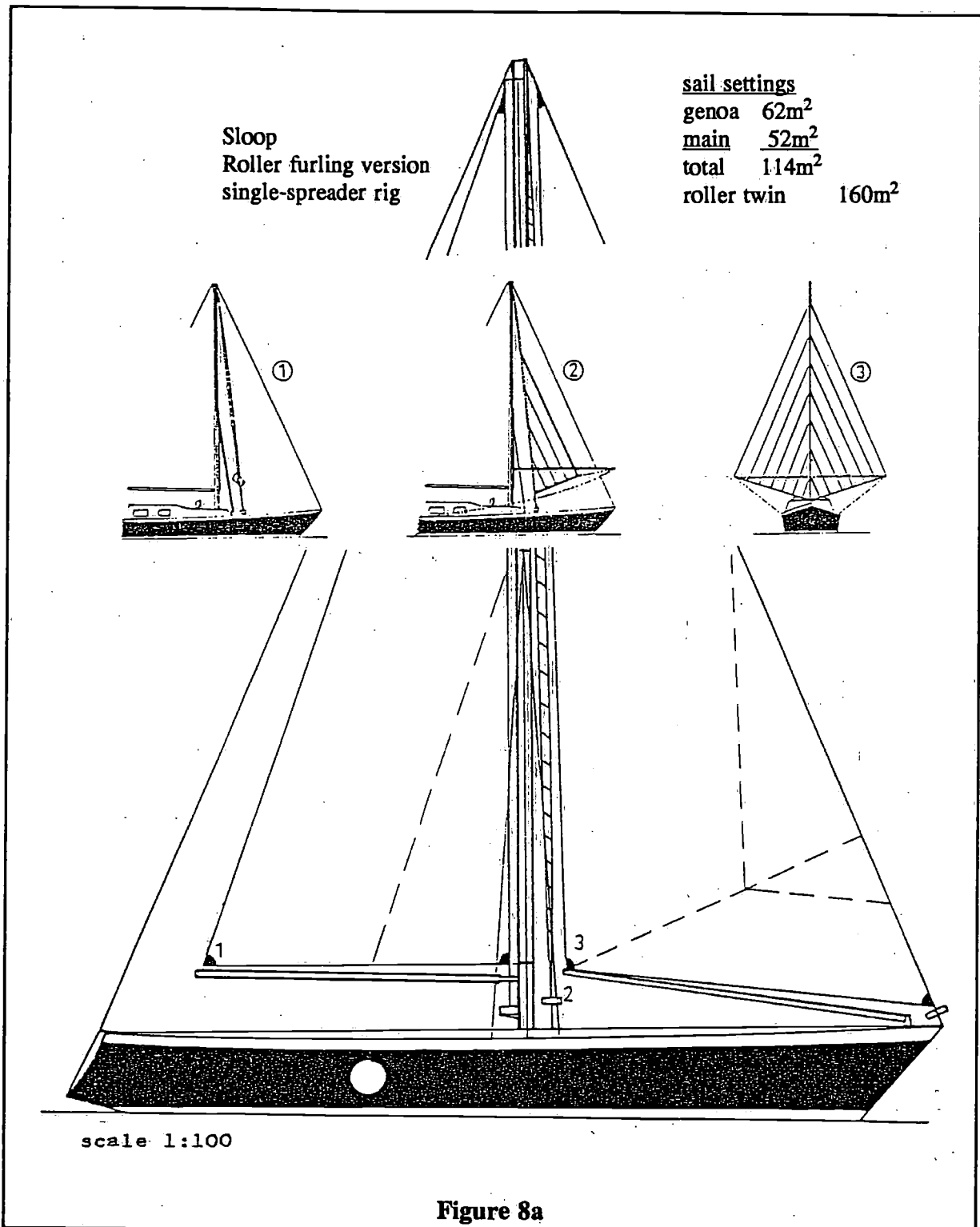


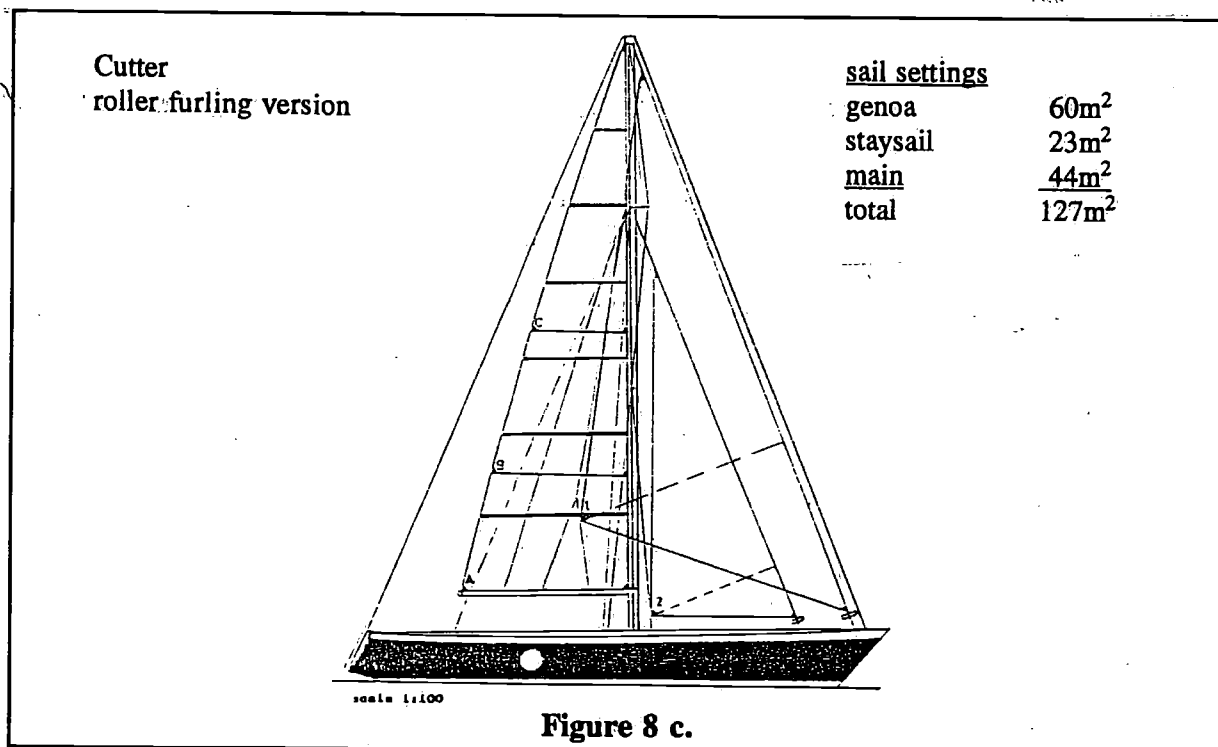
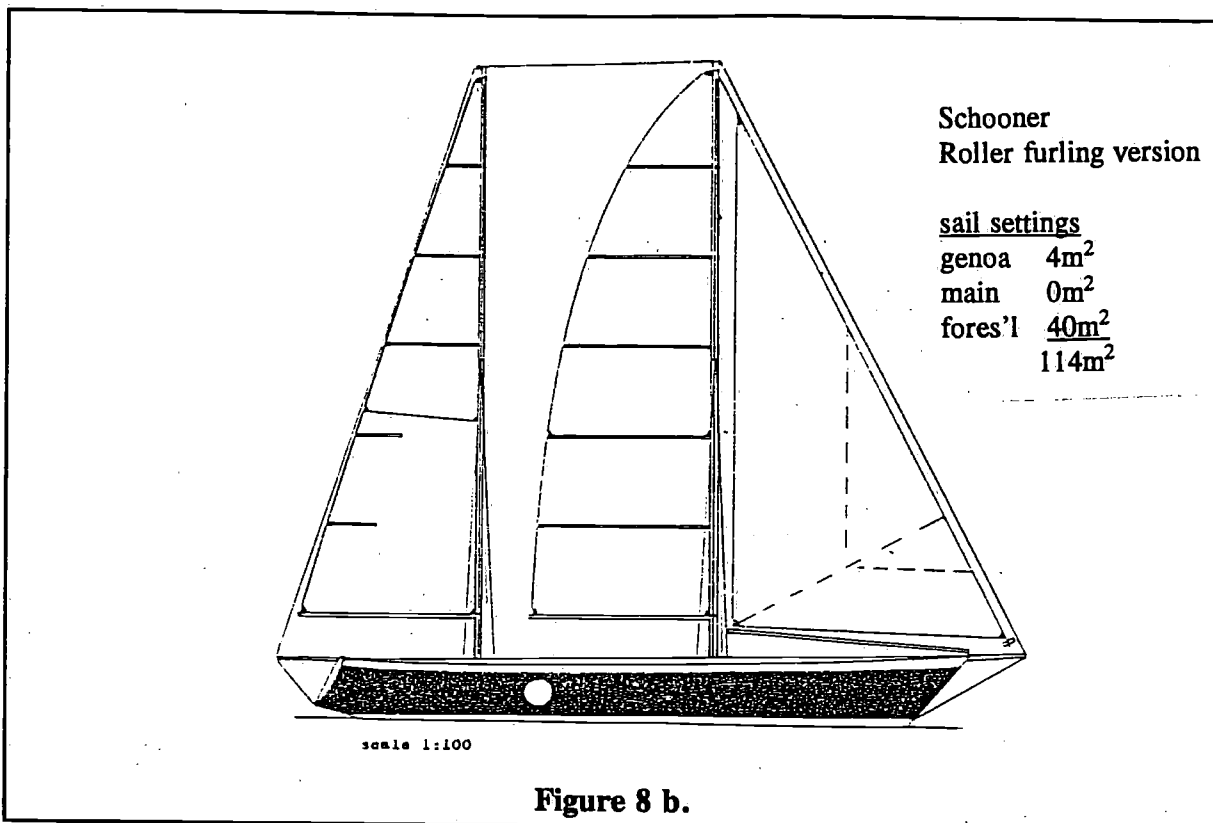
Figure 7. Deck layout sloop, single-handed transatlantic version

6 Several classic - and alternative sail plans

The Figures 9 - 35 are a collection of the various possibilities that are invented to catch the wind in order to propel a yacht through the water. Most of the conventional type of rigs have been discussed in the previous chapters and the illustrations speak for themselves. It would be beyond the scope of this paper to discuss the various alternative rigs in detail. However one exception is made for the junk rig. The possibilities of this rig are shown in Figures 29, 30 and 32, it is a rig which is very easy to handle, has no concentrations of tensions in one point since the sheet isn't a single rope, can be relative cheap and is equal effective on all points of windward work and reaching. The disadvantage is the poor light weather performance, the rigid sails stall very easily unnoticed and it is difficult to put enough area in the sails. Also the unstayed mast, which is necessary to take full advantage of the rig, can be a weak point. Apart from the solid foil rigs, this is the only rig that can be handled entirely from the inside of the yacht.



One sail which isn't illustrated or mentioned before, but could be a sail of interest for the ocean voyager, is the anti-rol sail described in [8]. Though the model tests were carried out for a Finn rig, the sail might well prove useful on cruising yachts. It would greatly increase the comfort on board if the rhythmic rolling, experienced while running for a sea, could be reduced. The sail could be described as a small mainsail (20% of the area) set from the forward side of the mast to weather with the aid of a small boom. The luff of the sail runs in a track along the mast. The angle of the sail to the wind resembles the angle the weather sail of the heavy weather twins is making.



In coming to a conclusion concerning the use of the conventional rigs mentioned it appears that, for a basic sail area of 114 m², sloop 2B will give the best allround performance, cutter 2F and schooner 2G are comfortable cruising rigs with a reasonable performance to windward and good cruising characteristics. For a single-handed transatlantic racer sloop 5A would be best. For smaller basic sail area's the plain sloop importance, while for larger basic sail area's with equal masts will gain in desirability as a cruising rig.

7 Definitions of head sails

In general the genoa no.1 is considered to be 100%, the genoa no.1 usually has a *LP* of 150%. This means that the perpendicular from the clew - to the luff of the sail is 1.5 times *J*, where *J* is the distance from the forward side of the mast to the point where the forestay intersects the deck. Usually a genoa with this area can be carried to windward till an apparent windspeed of 20 m.p.h. on a tender boat and up till 25 m.p.h. on a stiff boat, if the boat is designed with a conventional planform. In this case the main will be between 40 - and 50% of the area of the genoa no.1, if the boat is sloop rigged.

If the clew of the genoa is well above the main boom, and the clew of the jib is high above the deck (more then 1.3 times the height of the main boom from the deck, if a conventional main boom height is used), the suffix "topsail" is added to the sail name.

The sail area's are geometric, the curves of the foot - or leech of the sails is not included.

Usually the weight of the sail cloth will be constant from genoa no.2 upwards, for a given sail plan. This also includes the weight of the staysail no.2 and the storm staysail. The other headsails will vary in weight according to the windstrengths in which they are used. Racing yachts will carry more then one genoa no.1, with different cloth weight but the same area. For cruising yachts it seems practical to increase the area and use lighter cloth for the light weather sails.

The sails are defined in relation to the size of the fore triangle for the sake of simplicity. They could also have been defined in relation to the sail area of the total basic rig or according to the windstrengths in which they will be used.

Drifter	100% or more	Staysail light	50 - 40%
Genoa light	idem	Staysail no.1	30 - 35%
Genoa no.1	idem	Staysail no.2	25 - 15%
Genoa no.2	90 - 80%	Storm Staysail	10%
Genoa no.3	75 - 60%		
Genoa no.4	55 - 45%		
Jib no.1	40%		
Jib no.2	35 - 30%		
Jib no.3	25 - 20%		
Jib no.4	15%		
Storm jib	10%		

8 Literature

- [1] Milgram, J.H.,
'Sail Force Coefficients for Systematic Rig Variations',
T&R Report R-10, SNAME 1971
- [2] Marchaj, C.A.,
'Rig Development Tests of a 1/16.6 Scale Model of an 80 ft Cruising Ketch',
SUYR Report No.36, 1974
- [3] Meijer, M.C.,
"Zeilen en Zeildoek",
TH Delft, Laboratorium voor Scheepsbouwkunde, Rapport No.350, 1972

- [4] Letcher jr., J.S.,
'Self-Steering for Sailing Craft',
International Marine Publishing Co., 1974
- [5] Taberly, E.,
'Pen Duick', Adlard Coles Ltd, 1971
- [6] Marchaj, C.A.,
'Sailing Theory and Practice Dodd',
Mead & Co, 1964
- [7] Marchaj, C.A.,
'Results of Windtunneltests',
Lands' End Yachtman's Equipment Guide, 1975
- [8] Marchaj, C.A.,
'Instability of Sailing Craft-Rolling',
HISWA Symposium Yacht Architecture, 1971
- [9] 'Self Steering',
Amateur Yacht Research Society, 1967
- [10] Gentry, A.E.,
'The Aerodynamics of Sail Interaction',
AIAA Symposium, 1971
- [11] Dijkstra jr., G.,
'Rolzeilen',
Maandblad Watersport No.1 en 2, 1974

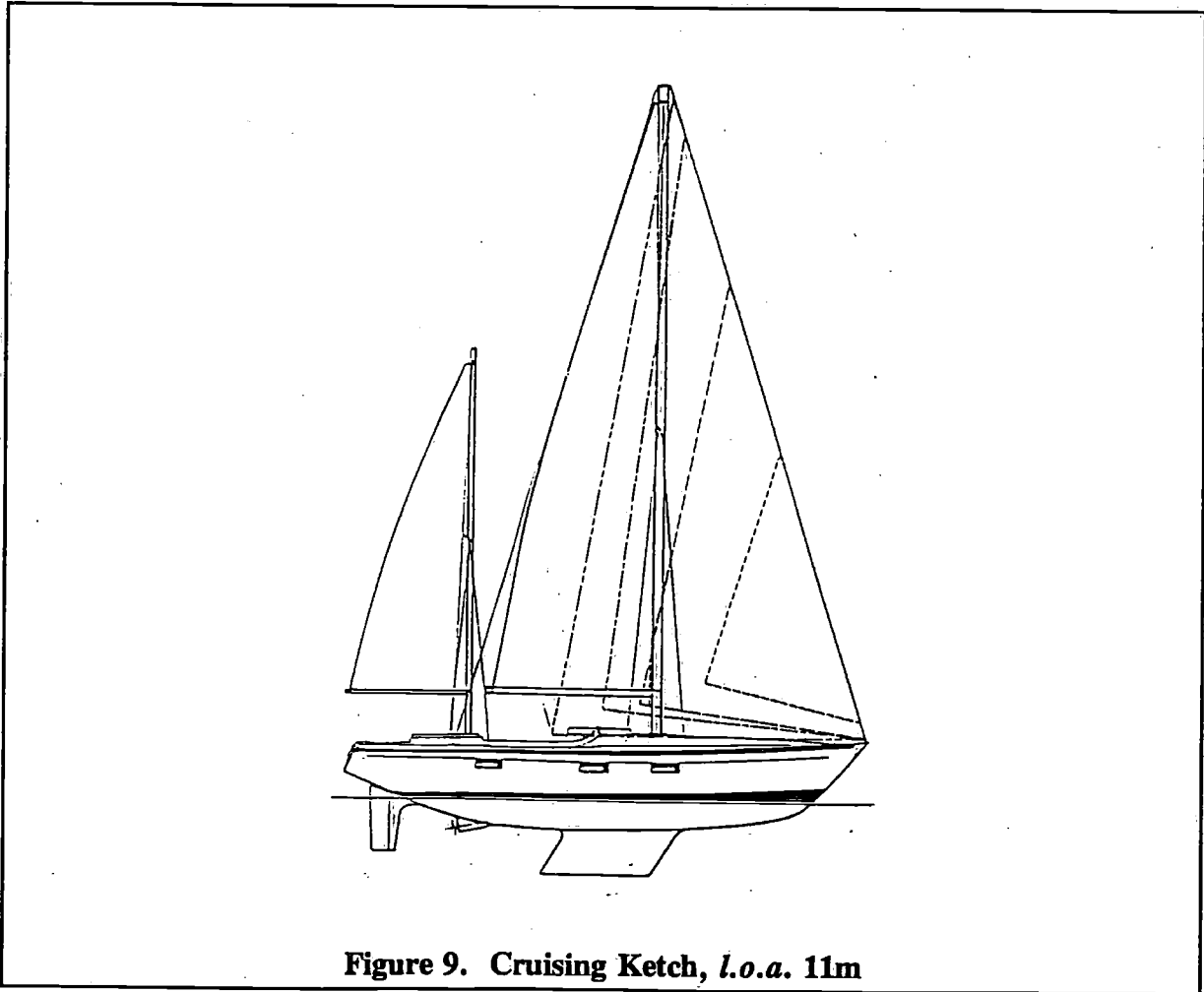
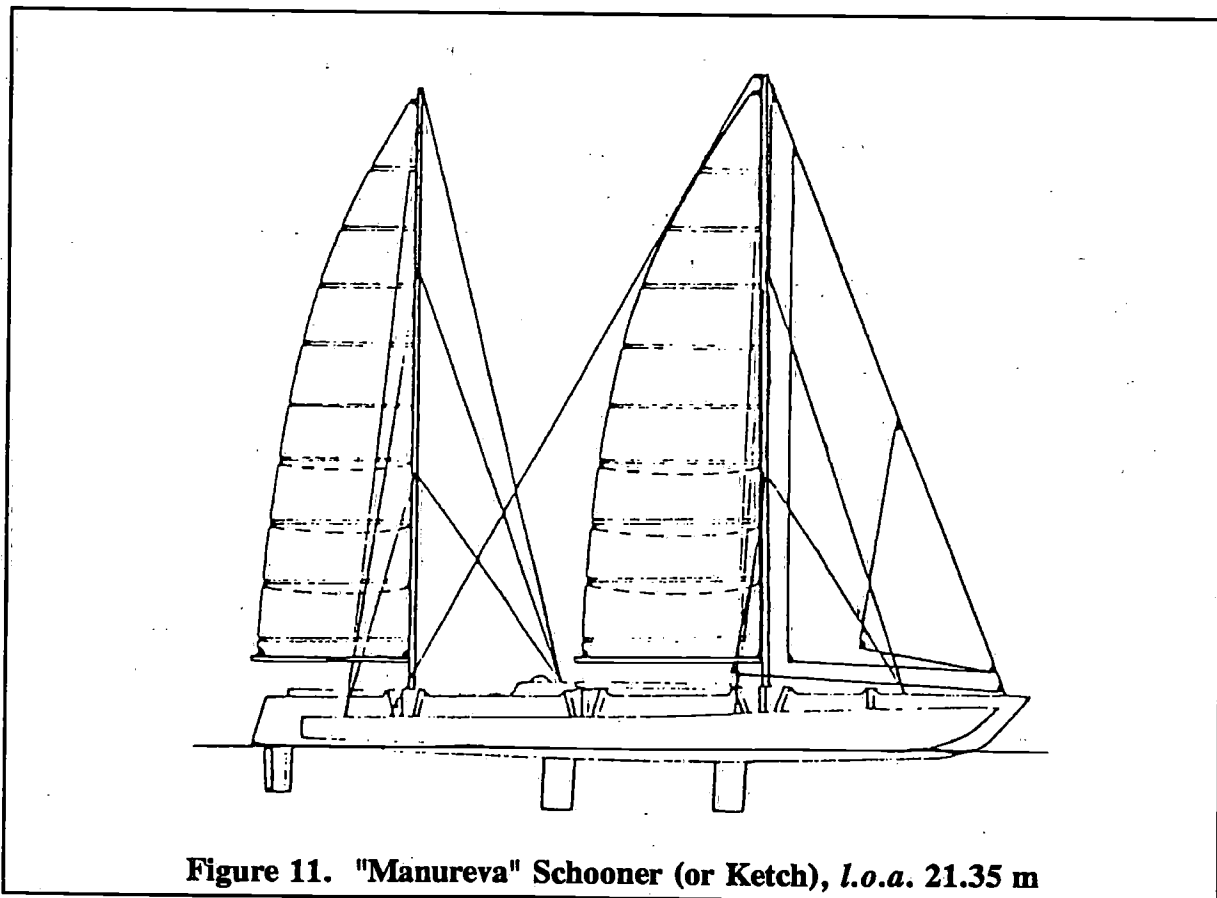
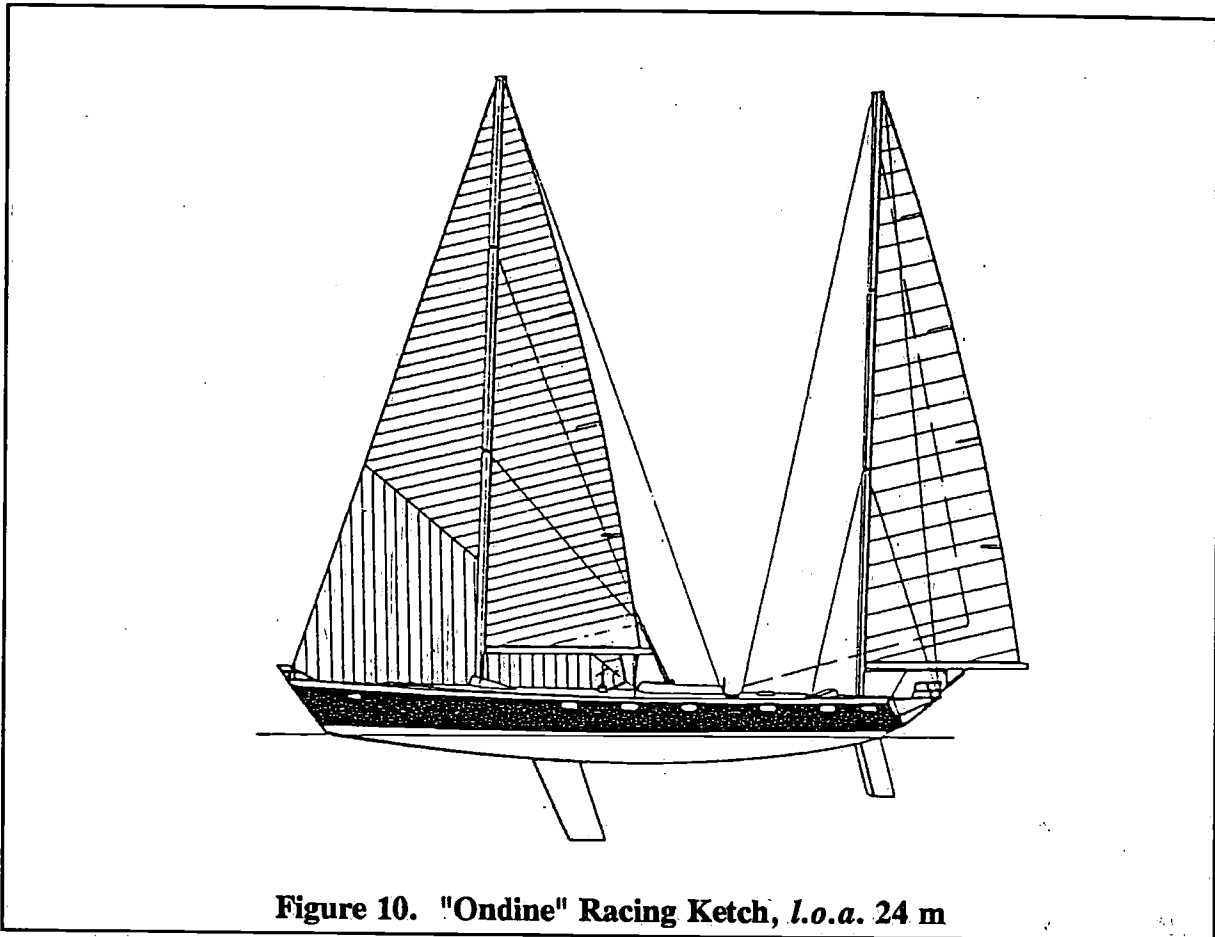


Figure 9. Cruising Ketch, *l.o.a.* 11m



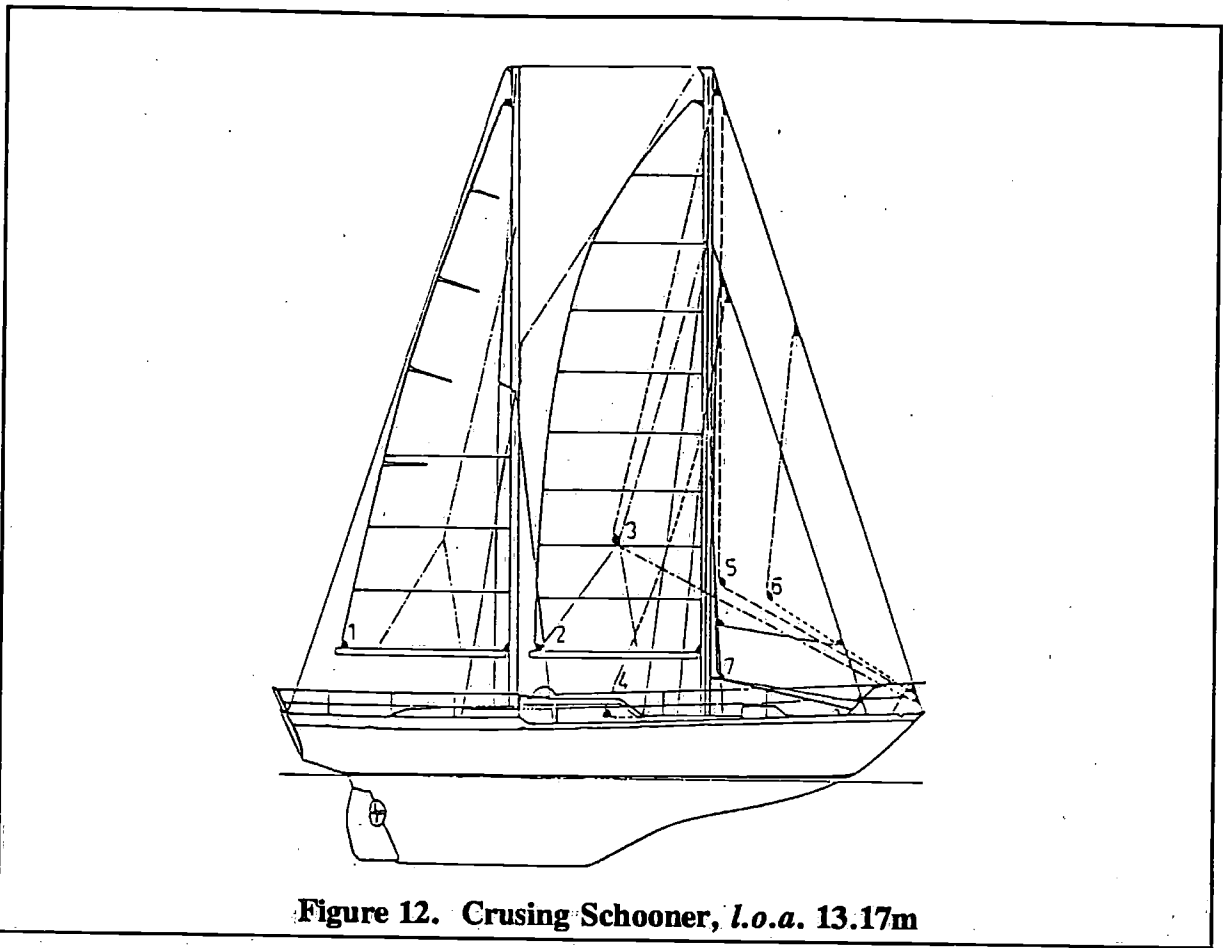


Figure 12. Cruising Schooner, *l.o.a.* 13.17m

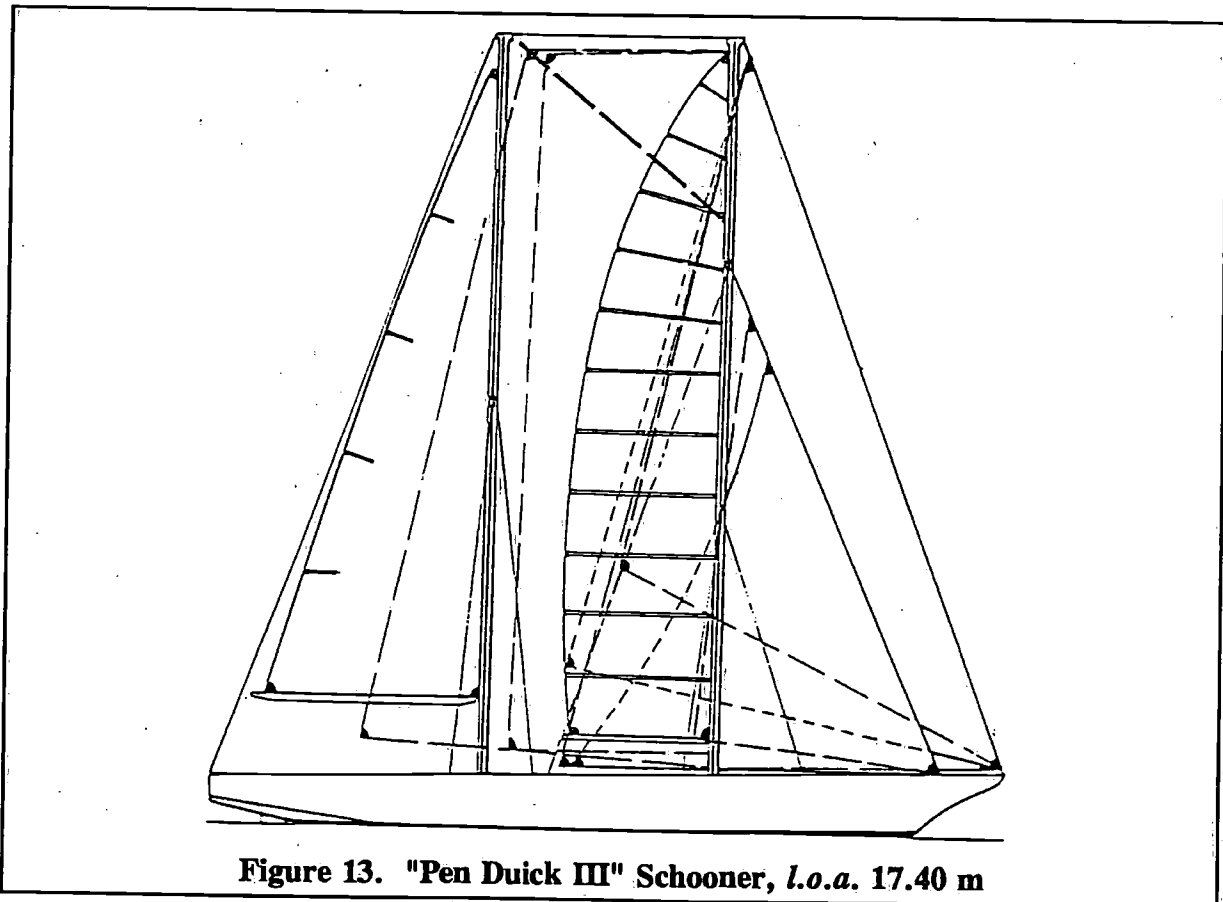


Figure 13. "Pen Duick III" Schooner, *l.o.a.* 17.40 m

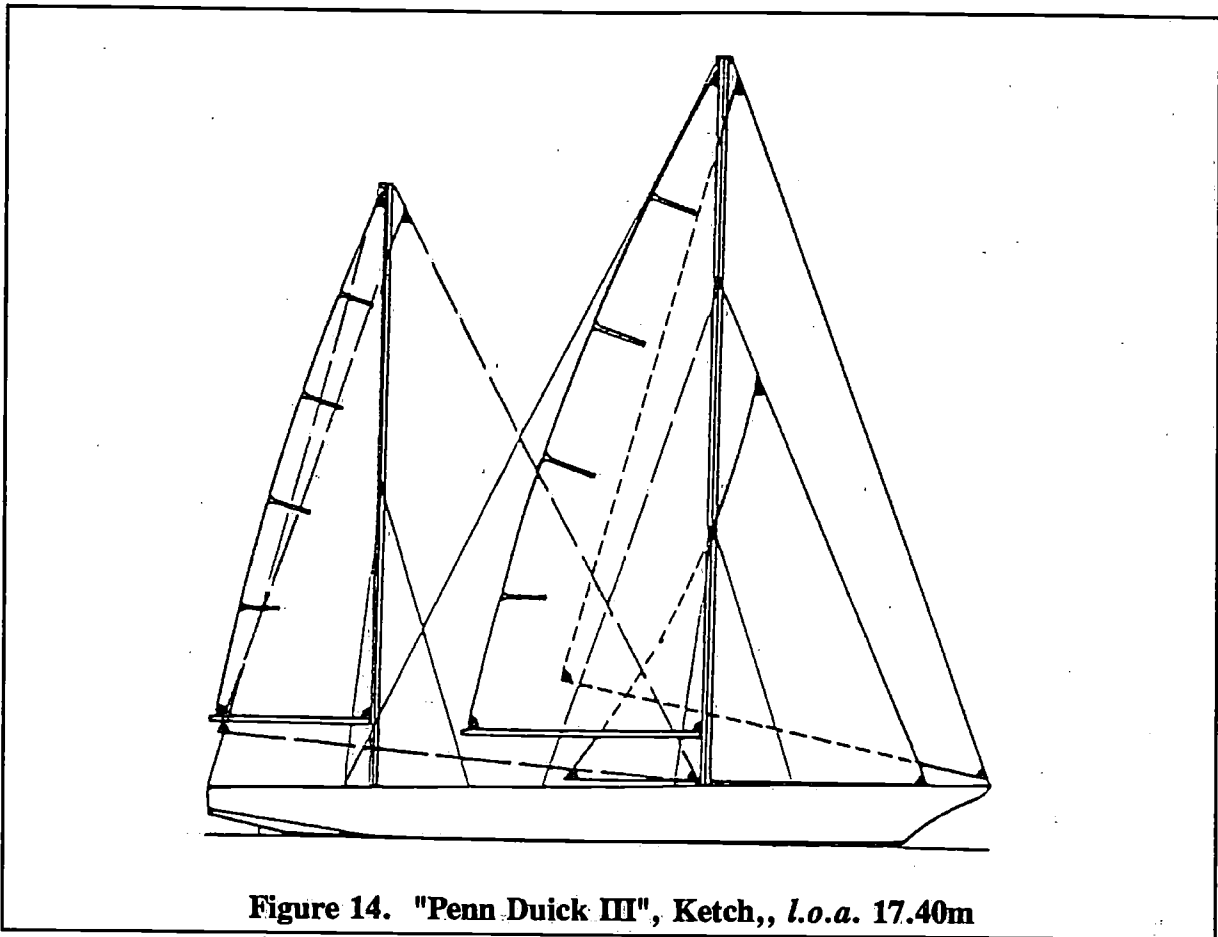


Figure 14. "Penn Duick III", Ketch, *l.o.a.* 17.40m

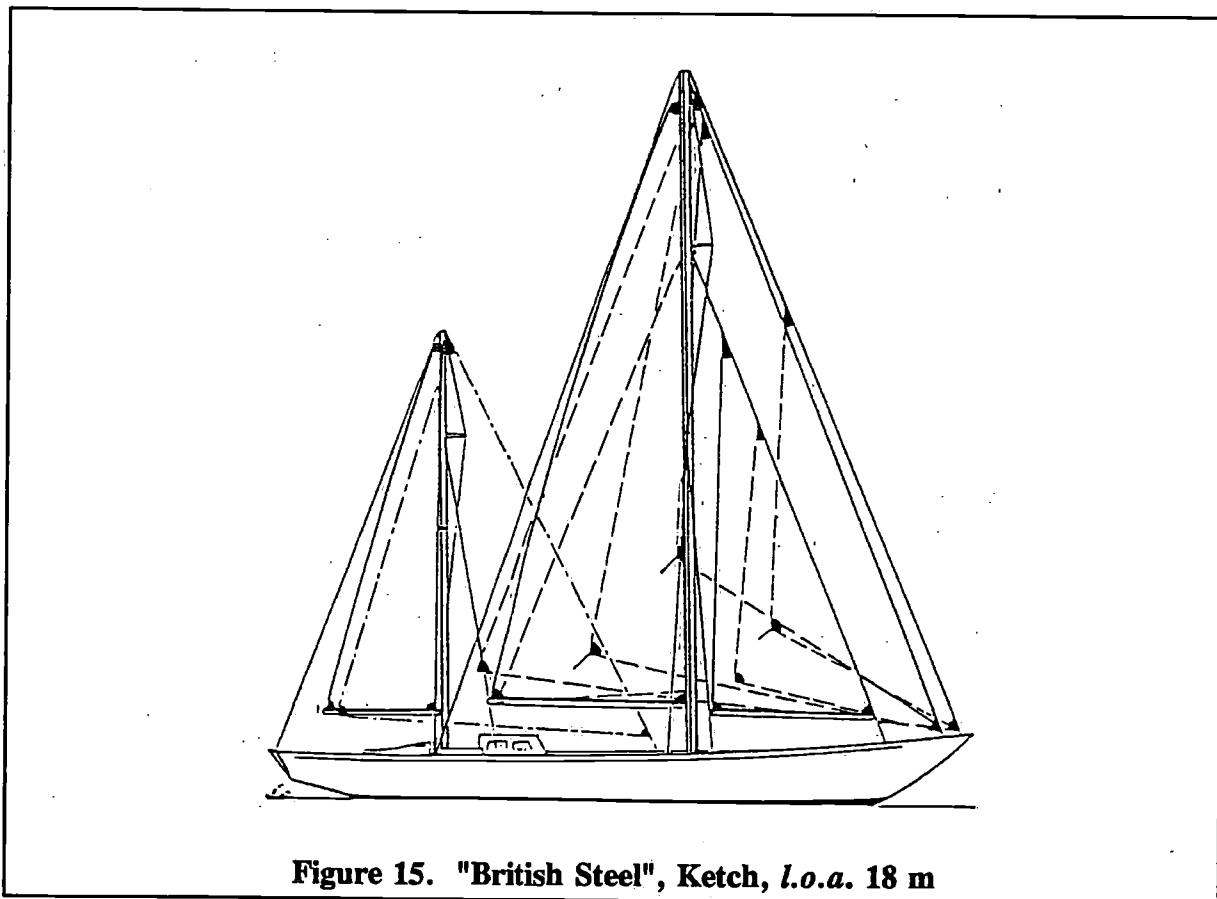


Figure 15. "British Steel", Ketch, *l.o.a.* 18 m

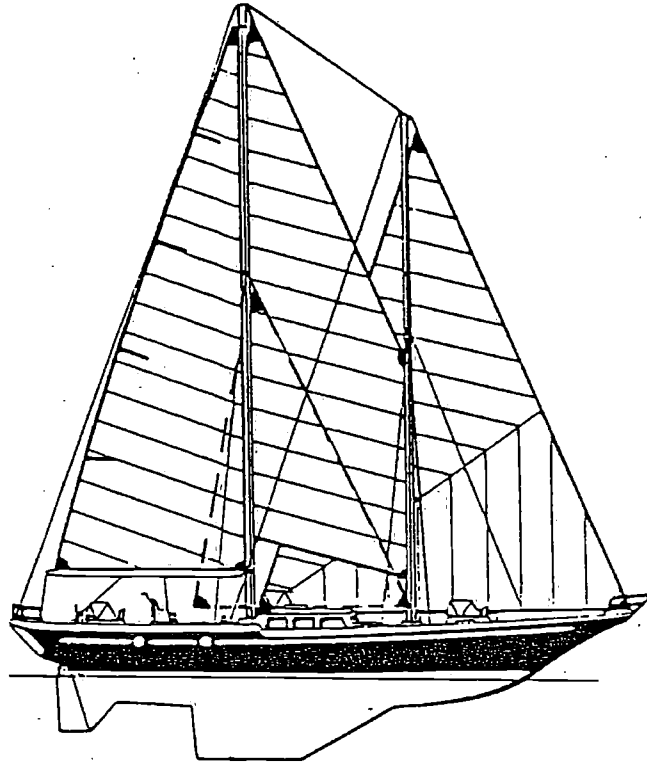


Figure 16. "Grand Louis" Schooner, *l.o.a.* 18.40m

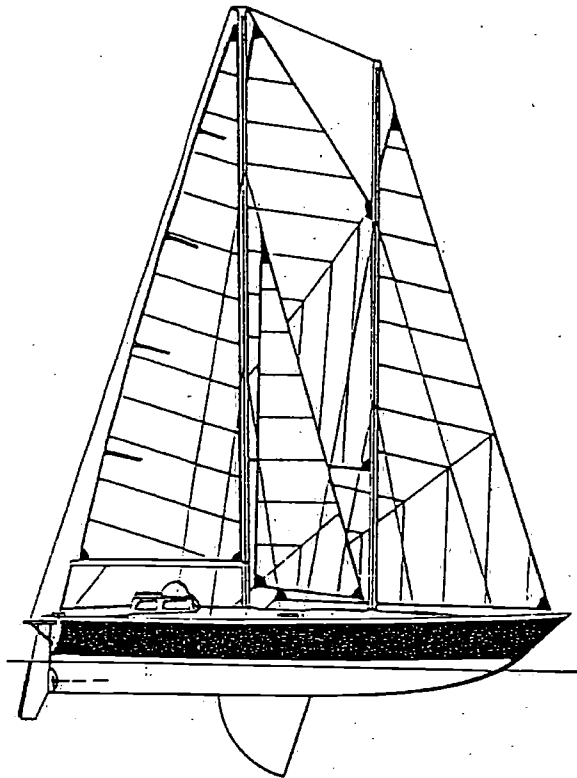


Figure 17. "Damien II", Schooner, *l.o.a.* 14.14m

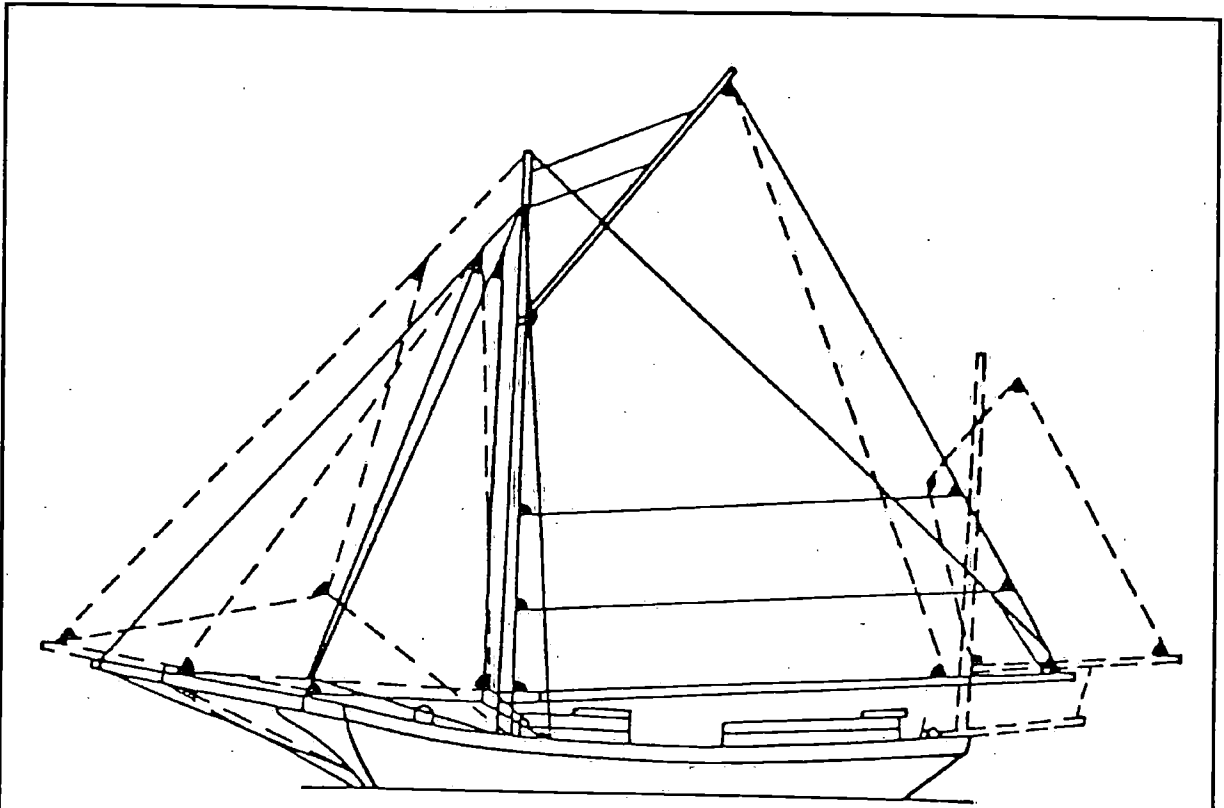


Figure 18. "Spray", Joshua Slocum's famous gaff cutter, later converted to yawl rig, *l.o.a.* 11m

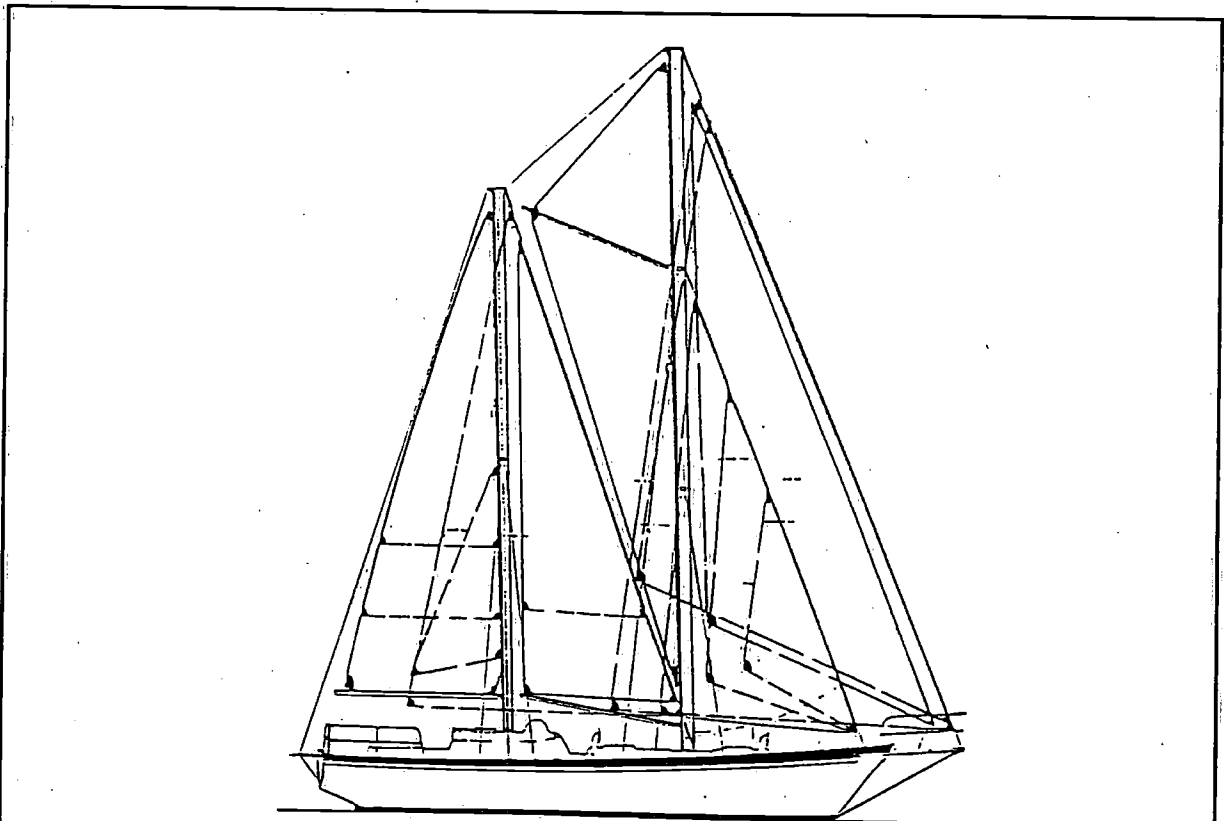


Figure 19. "Bylgia", Wishbone Ketch, *l.o.a.* 12m

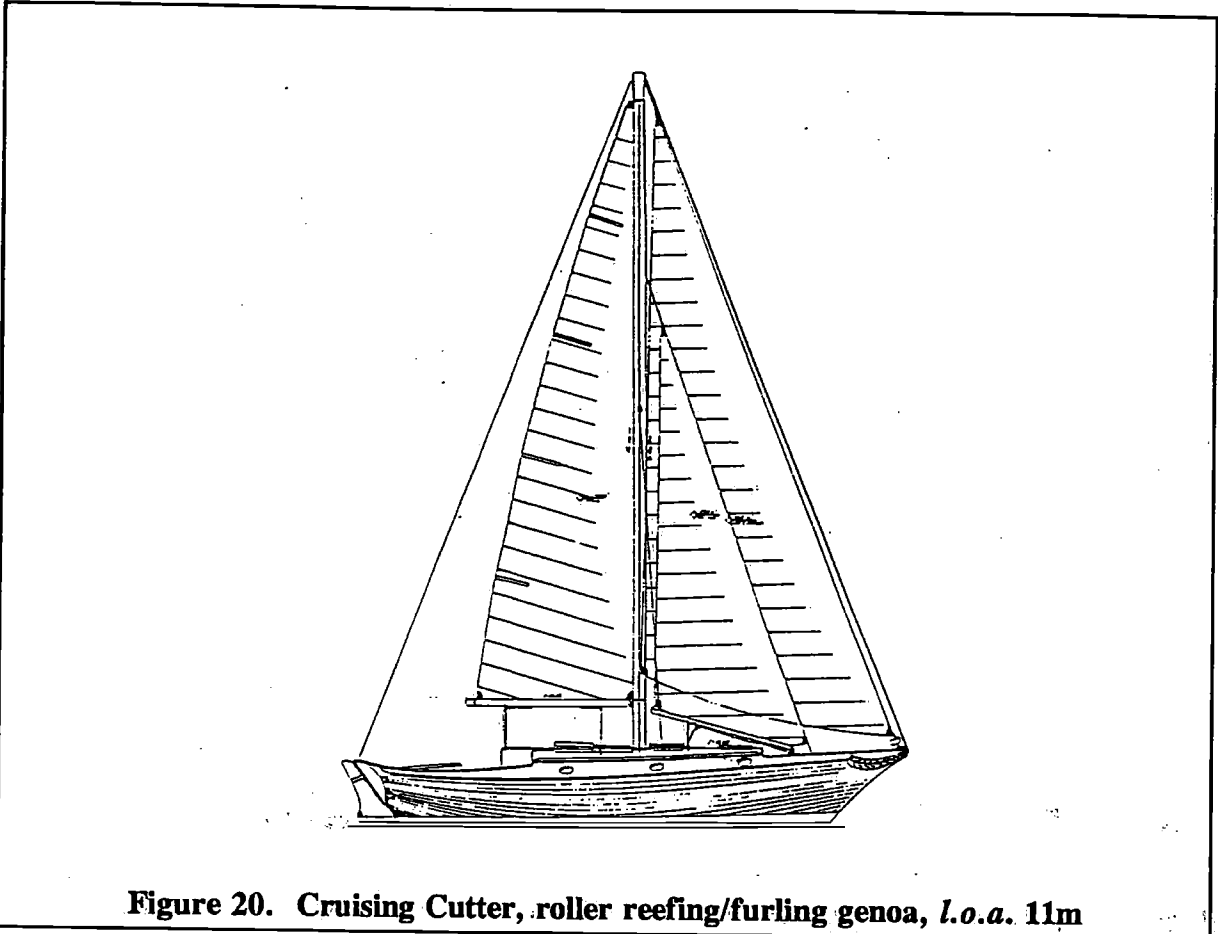


Figure 20. Cruising Cutter, roller reefing/furling genoa, *l.o.a.* 11m

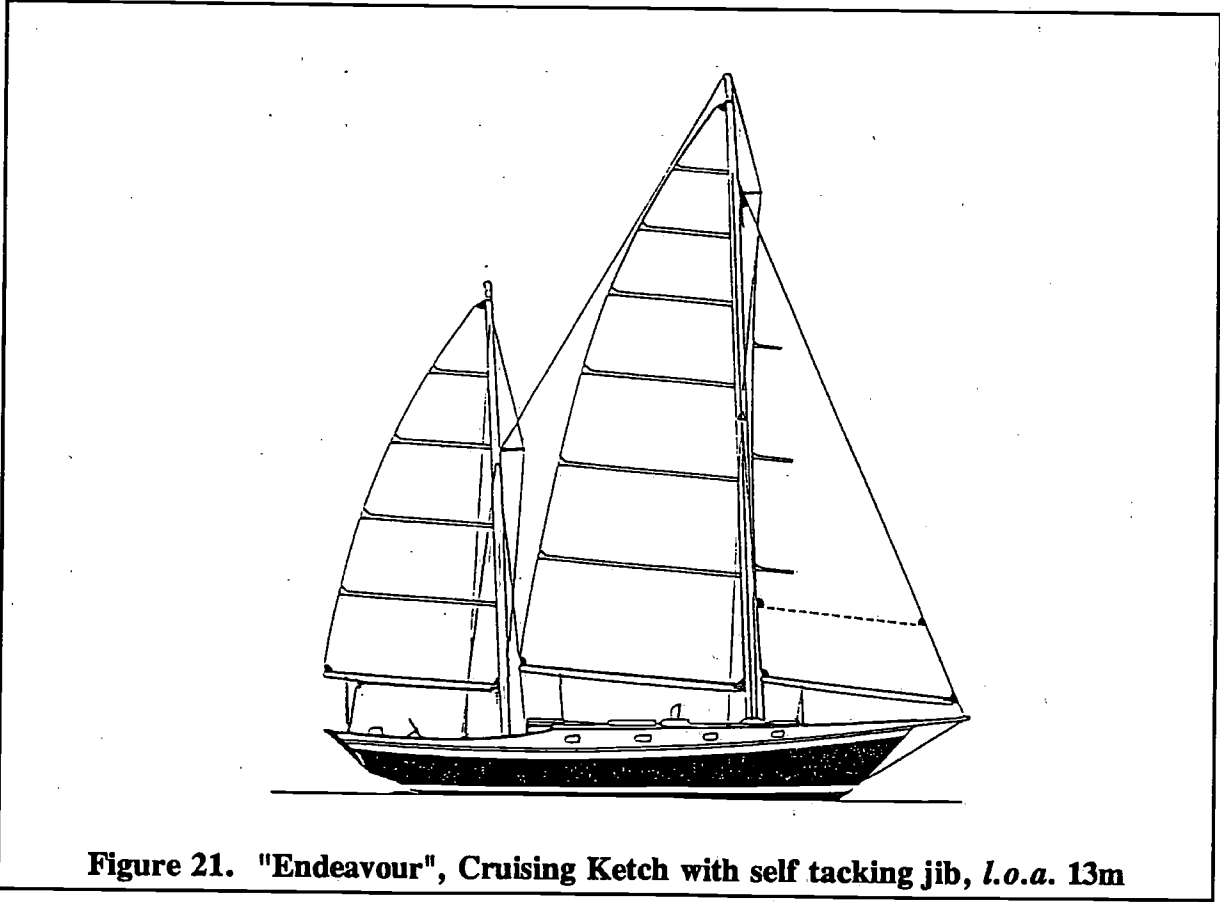


Figure 21. "Endeavour", Cruising Ketch with self tacking jib, *l.o.a.* 13m

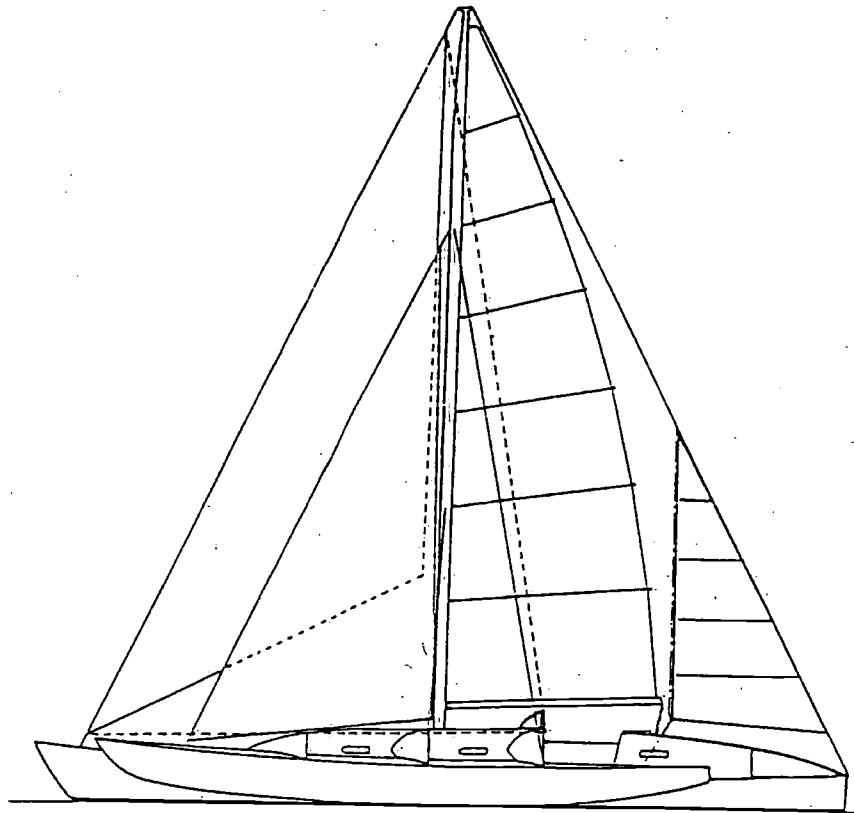


Figure 22. "Gulf Streamer", Cutter, *l.o.a.* 18.30m

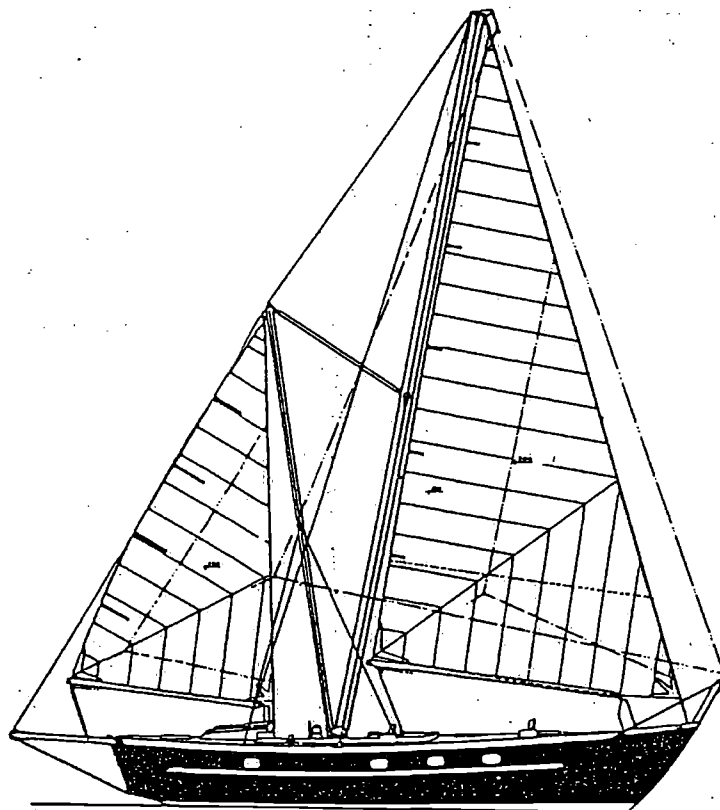


Figure 23. "Diomedea Exulans", self-tacking cruising rig, *l.o.a.* 13.90m

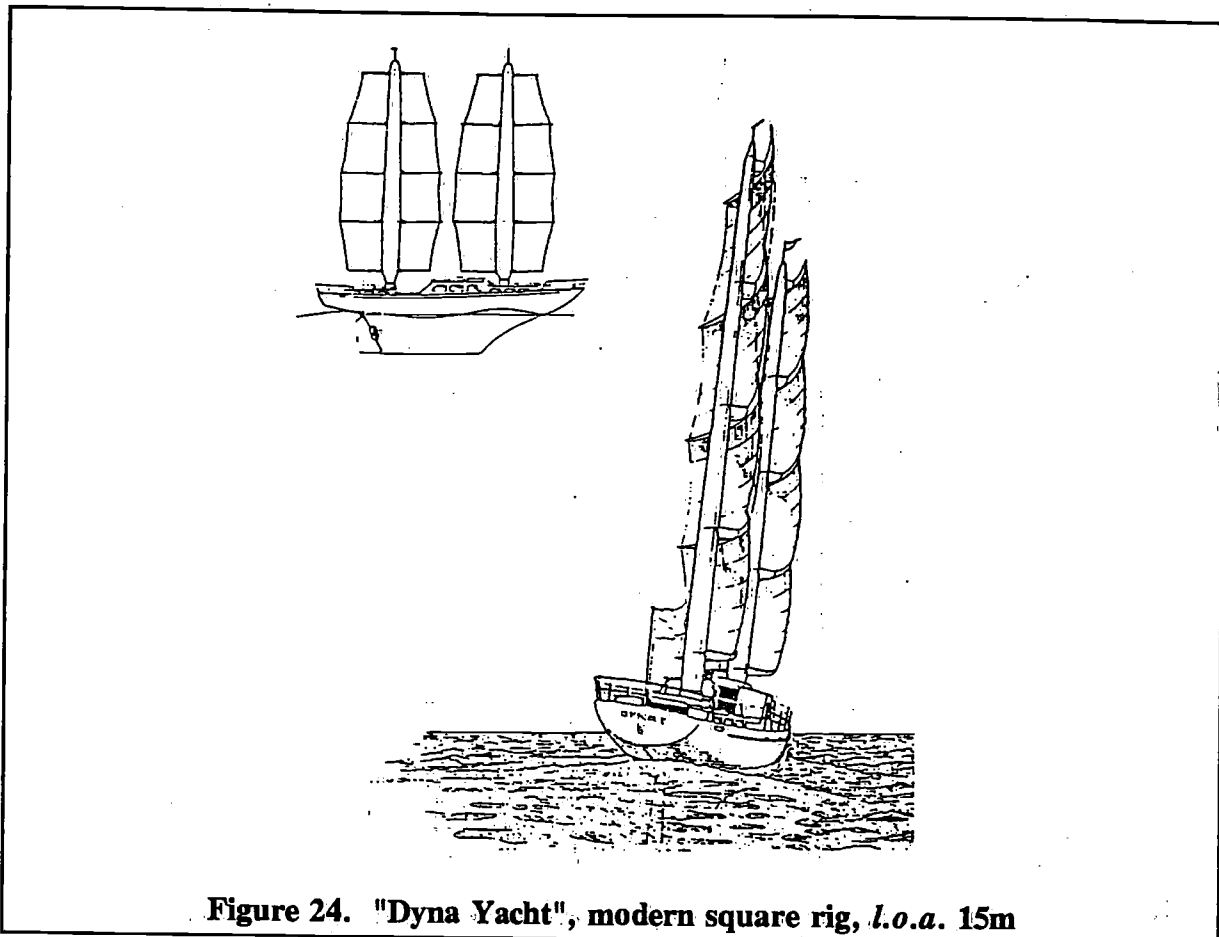


Figure 24. "Dyna Yacht", modern square rig, *l.o.a.* 15m

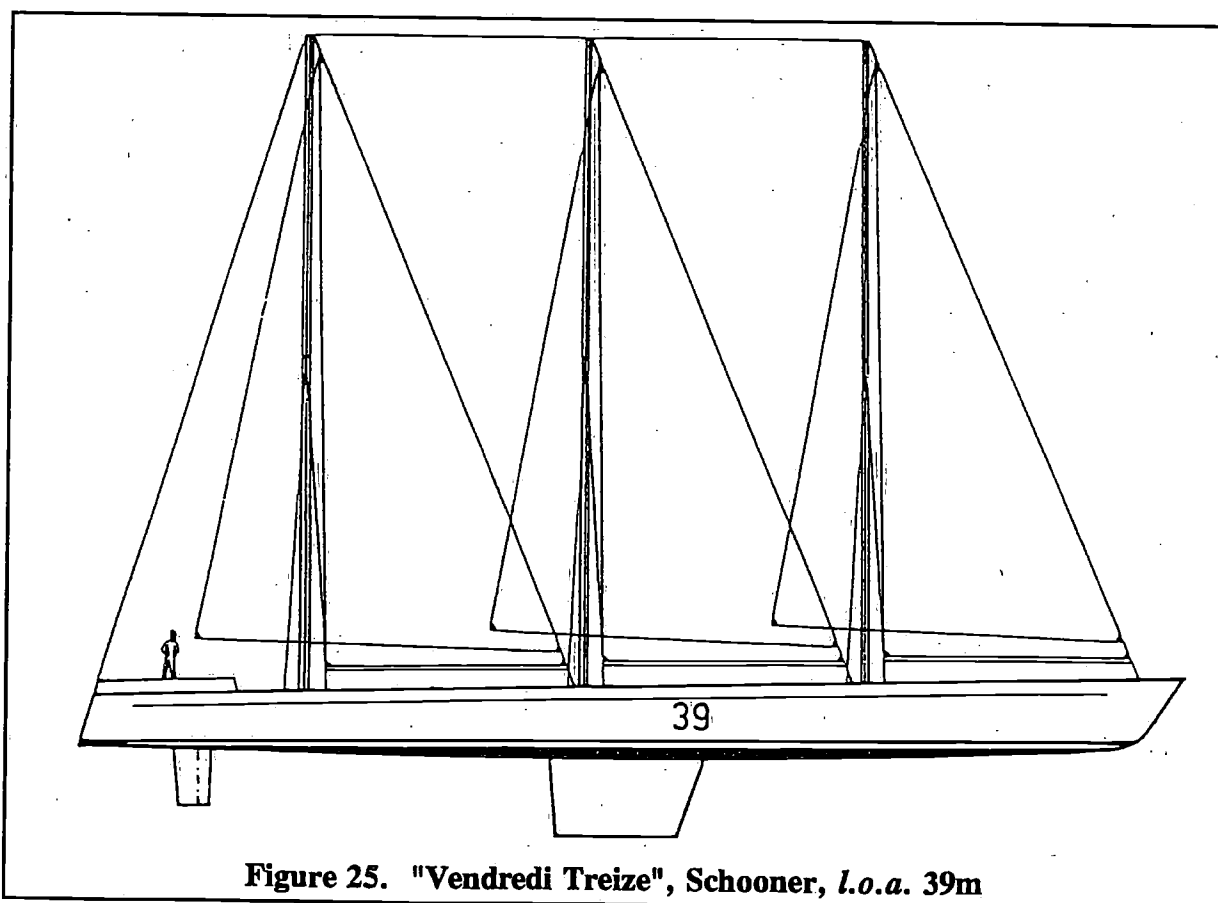


Figure 25. "Vendredi Treize", Schooner, *l.o.a.* 39m

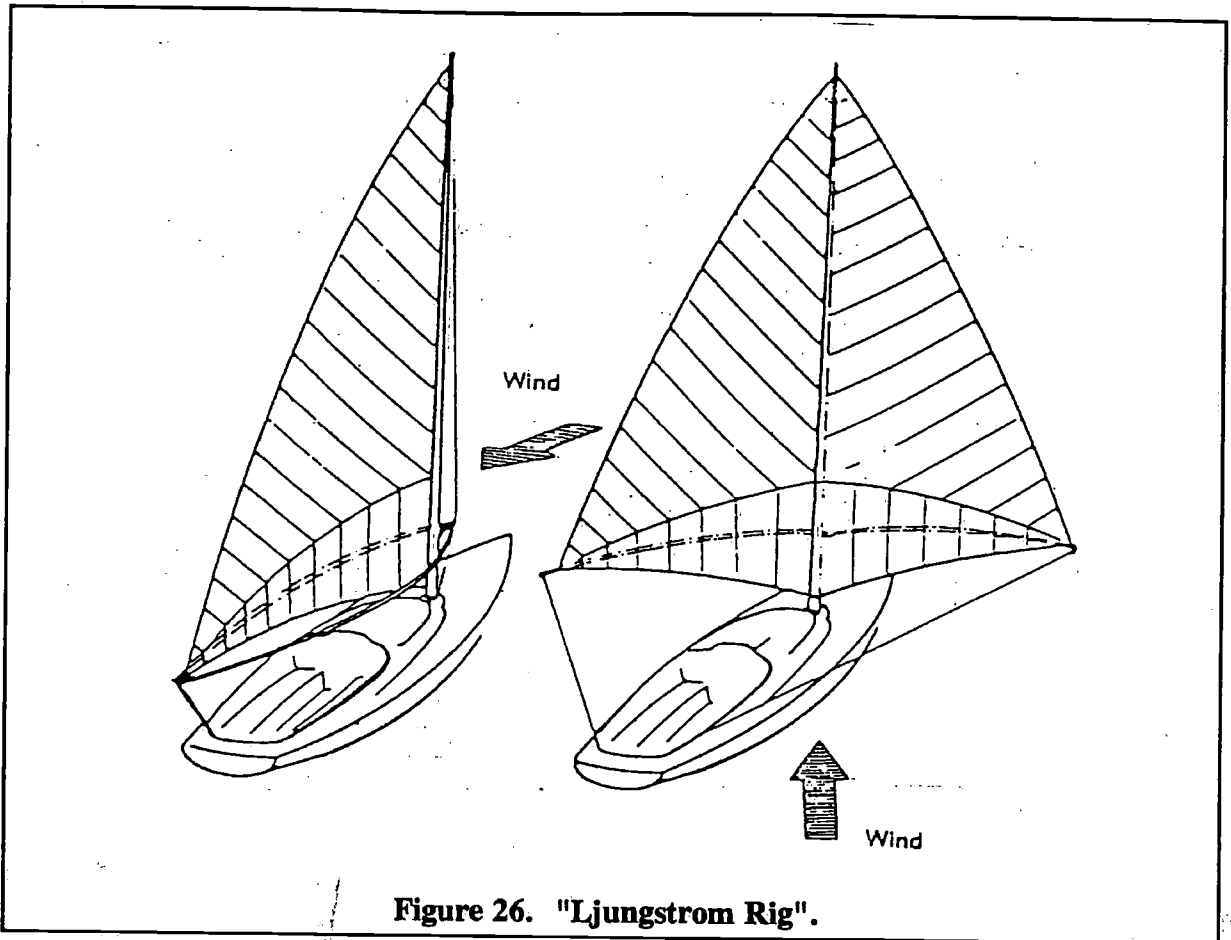


Figure 26. "Ljungstrom Rig".

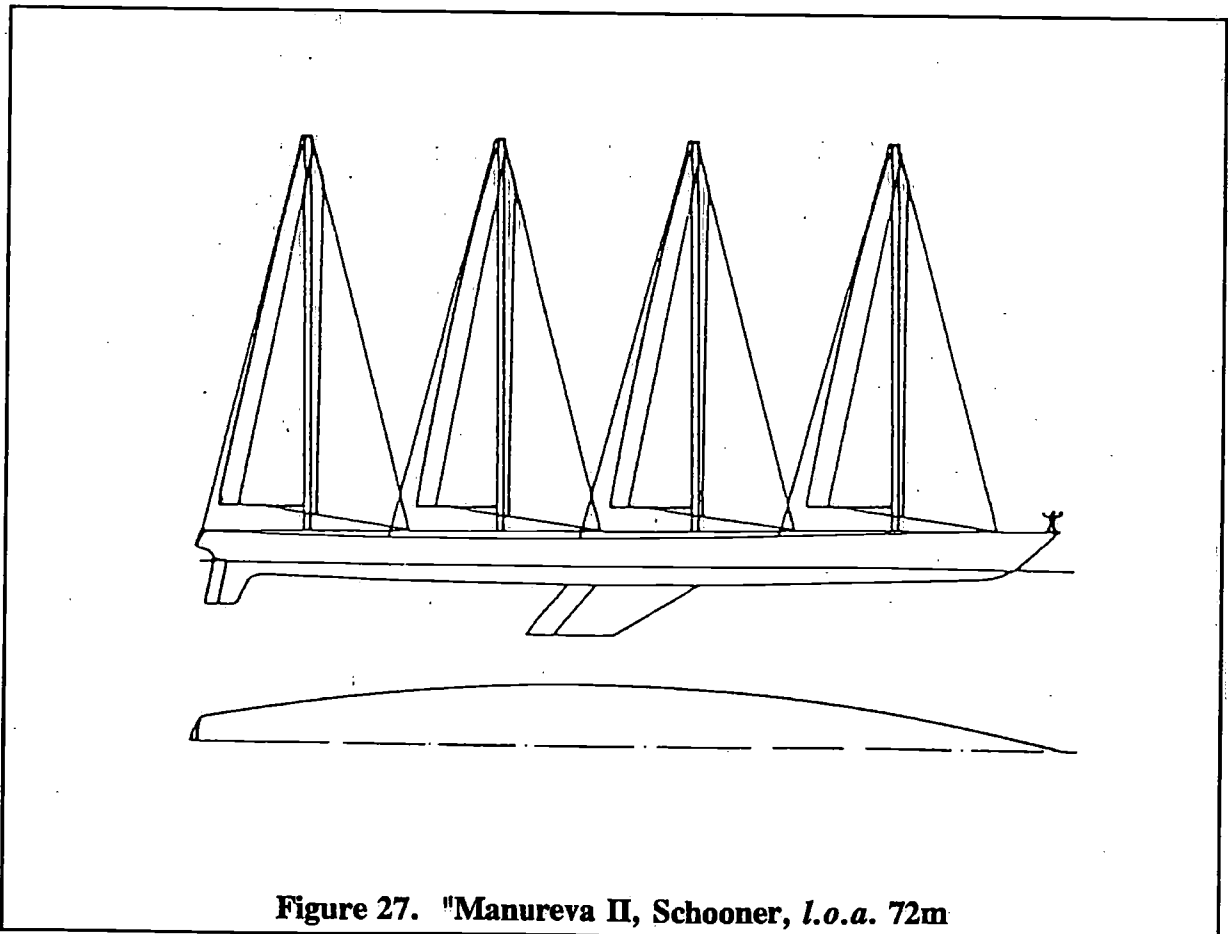
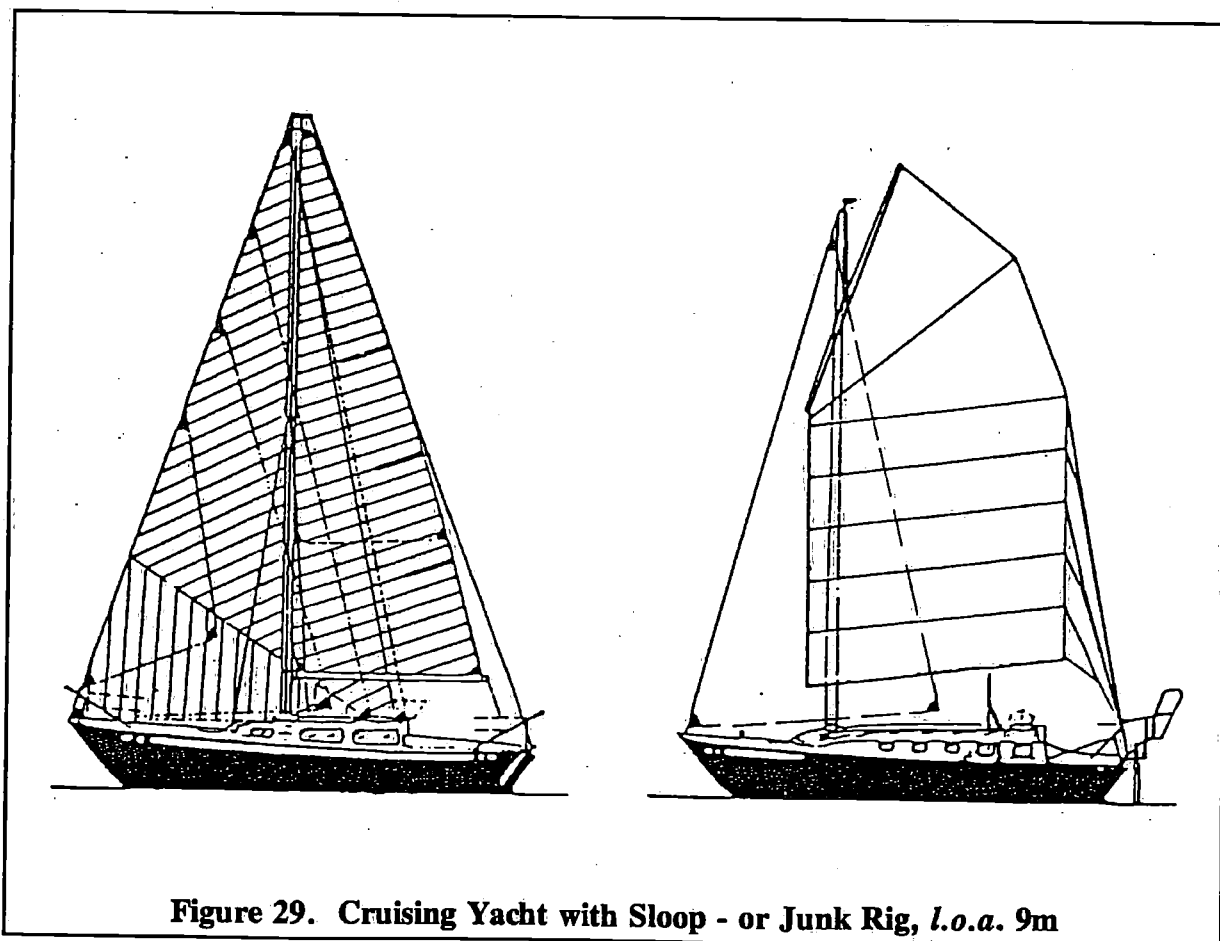
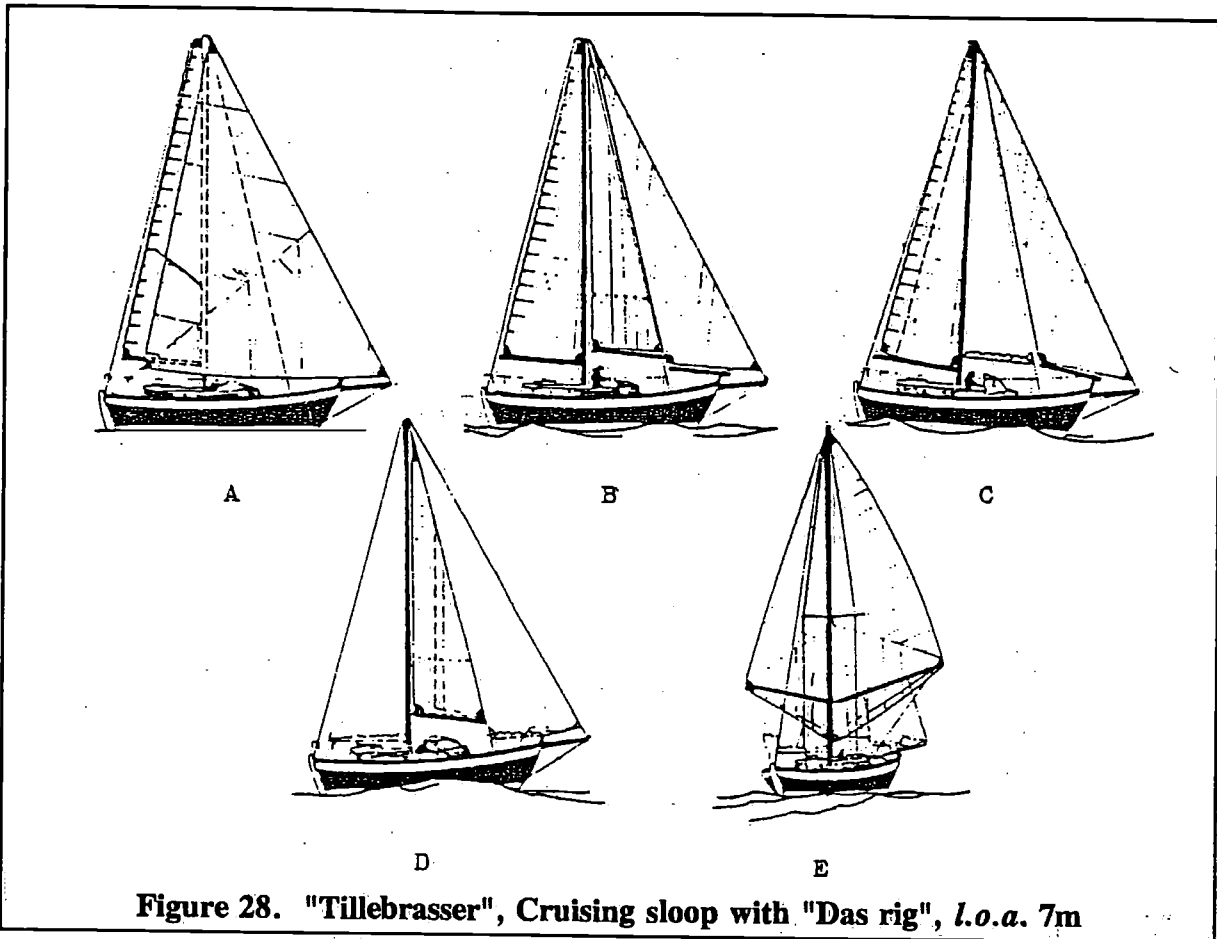


Figure 27. "Manureva II, Schooner, *l.o.a.* 72m



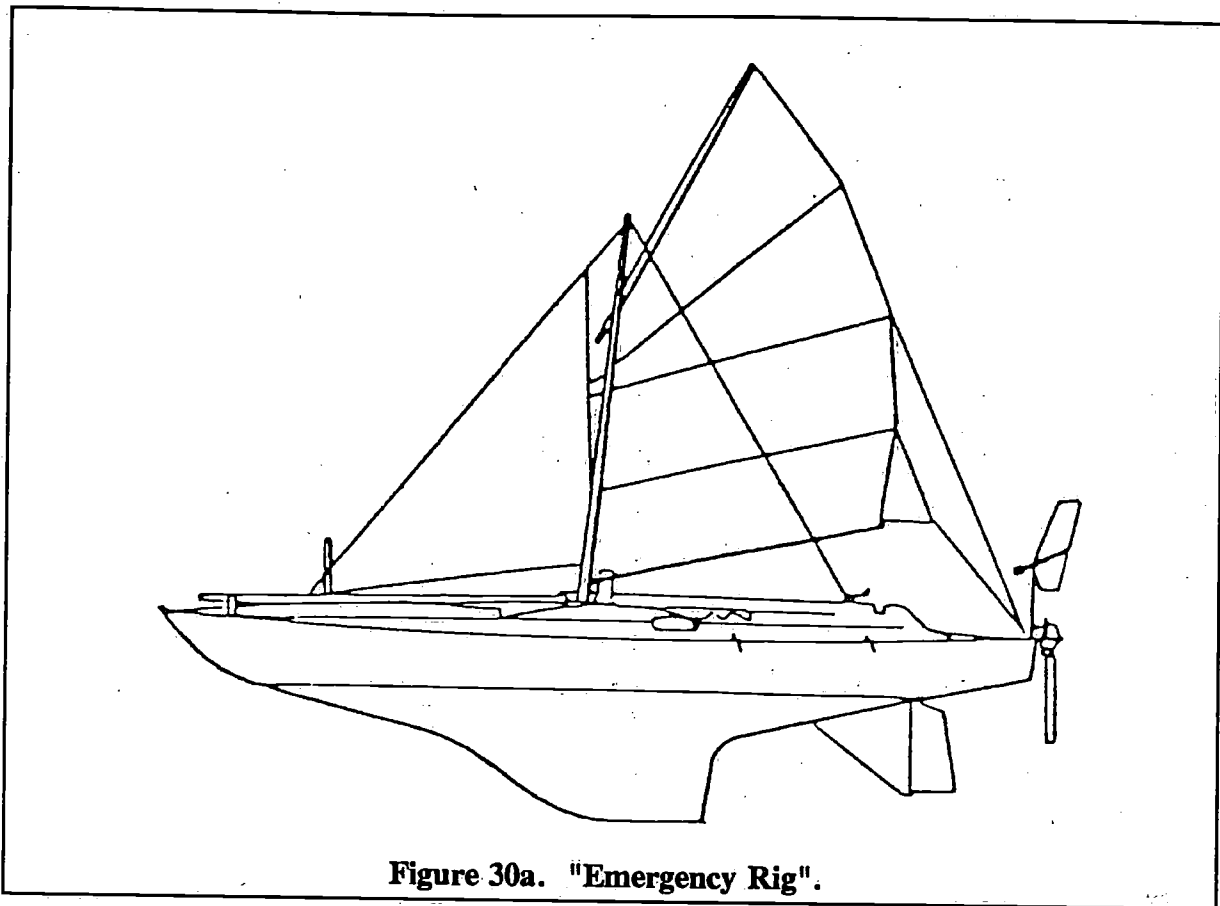


Figure 30a. "Emergency Rig".

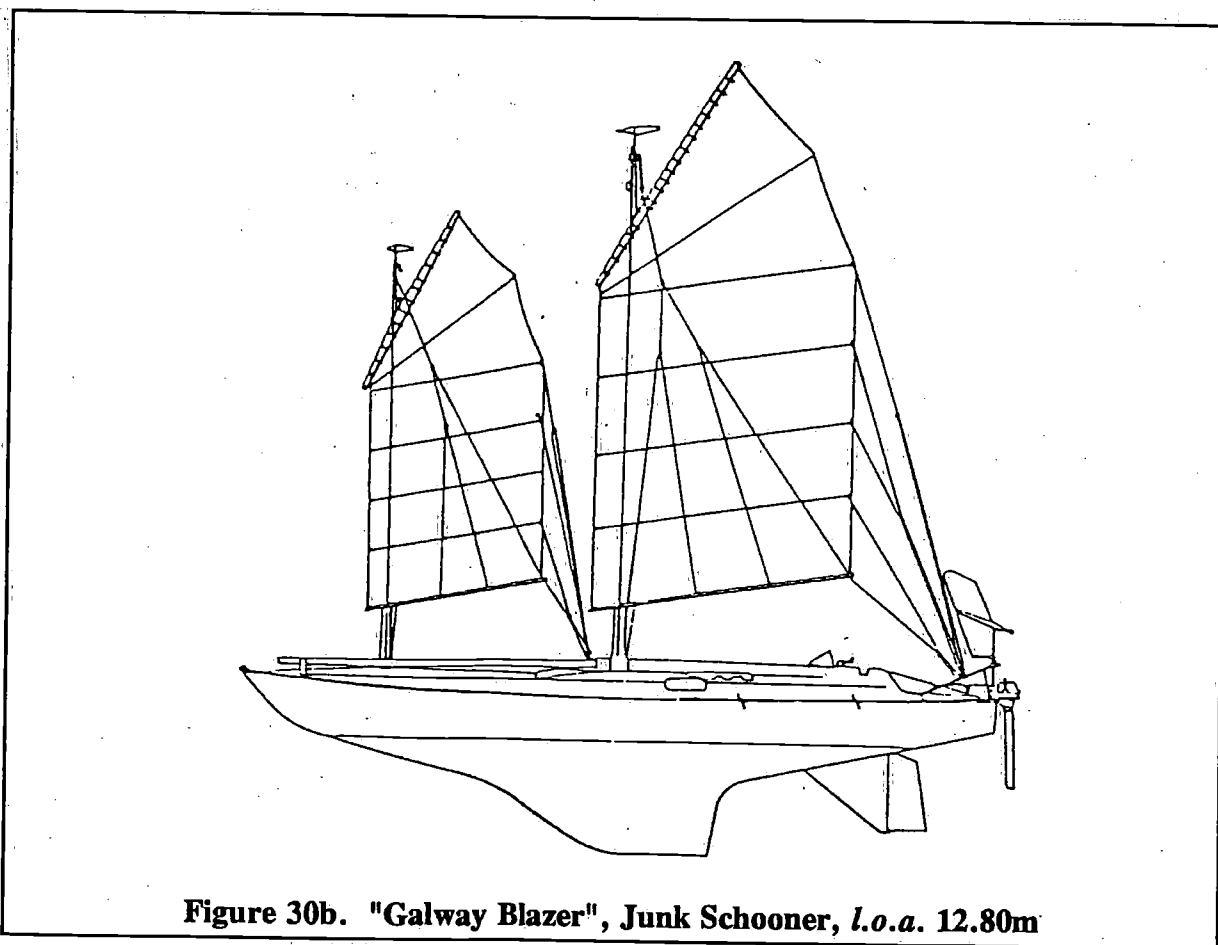
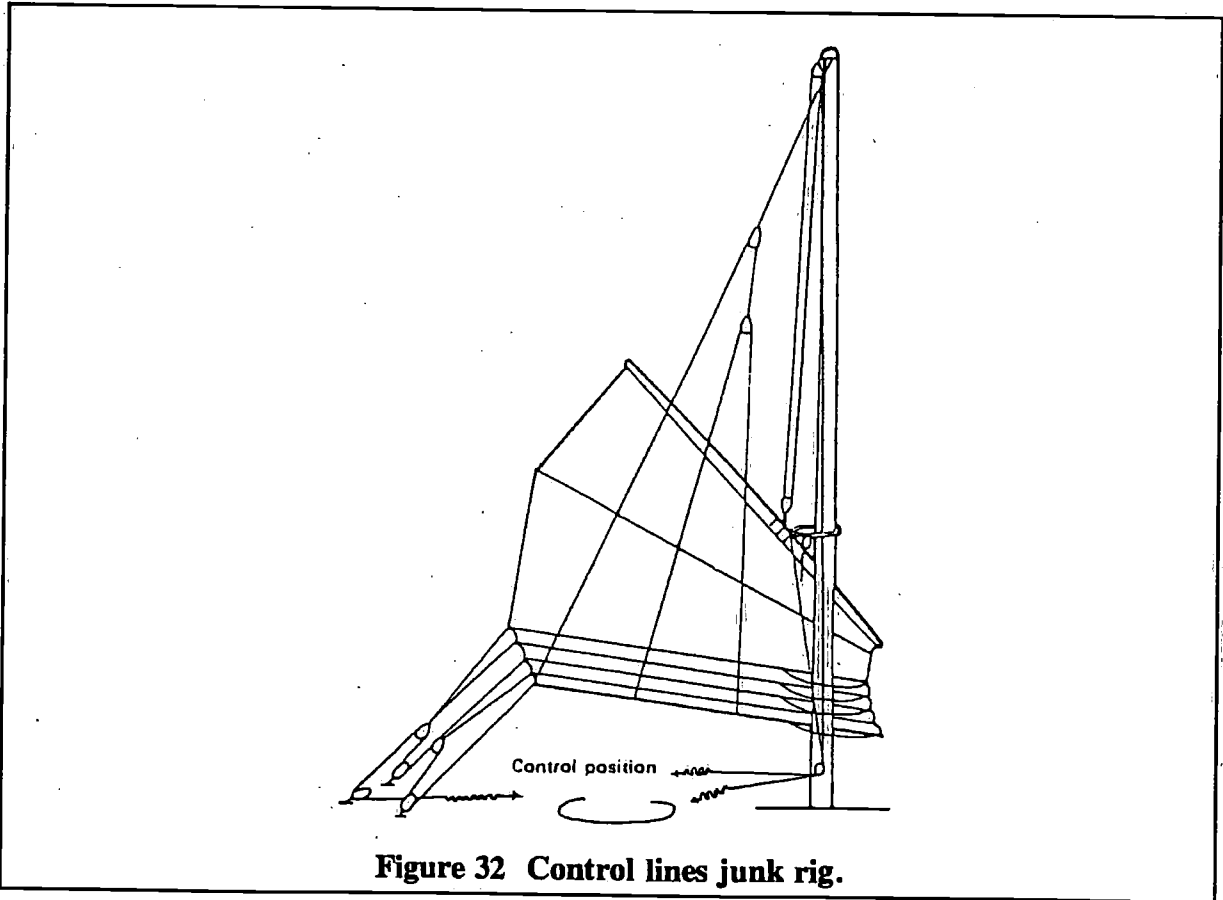
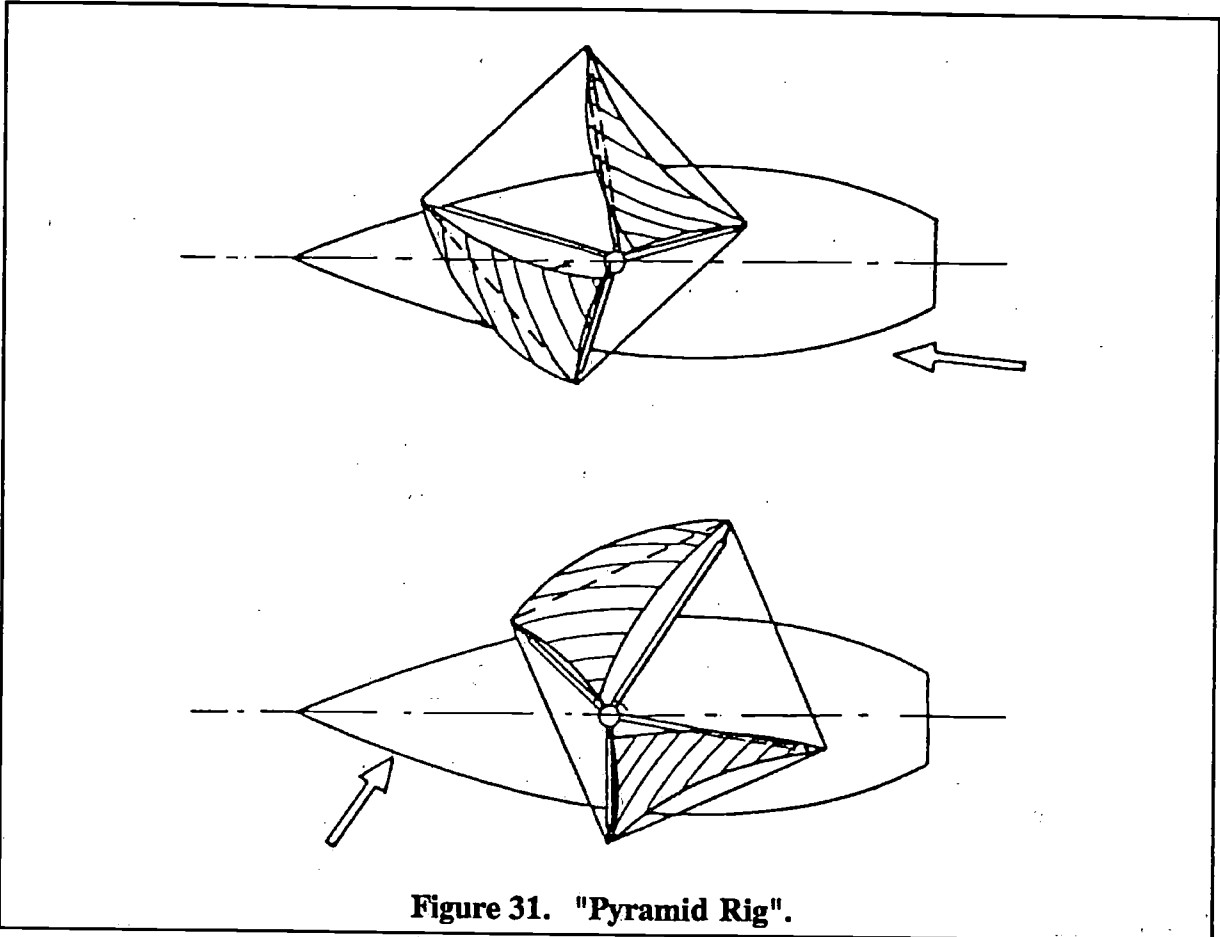
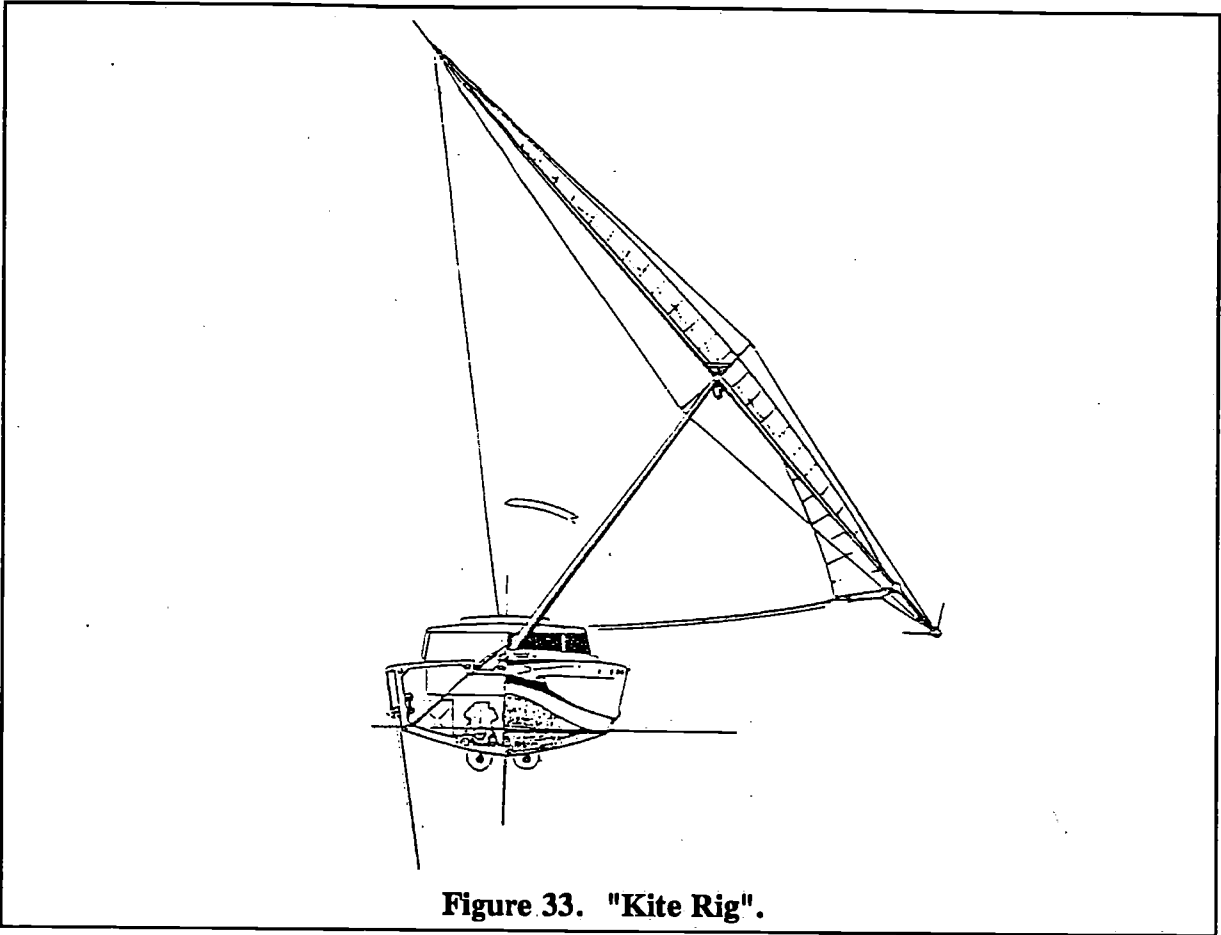


Figure 30b. "Galway Blazer", Junk Schooner, *l.o.a.* 12.80m





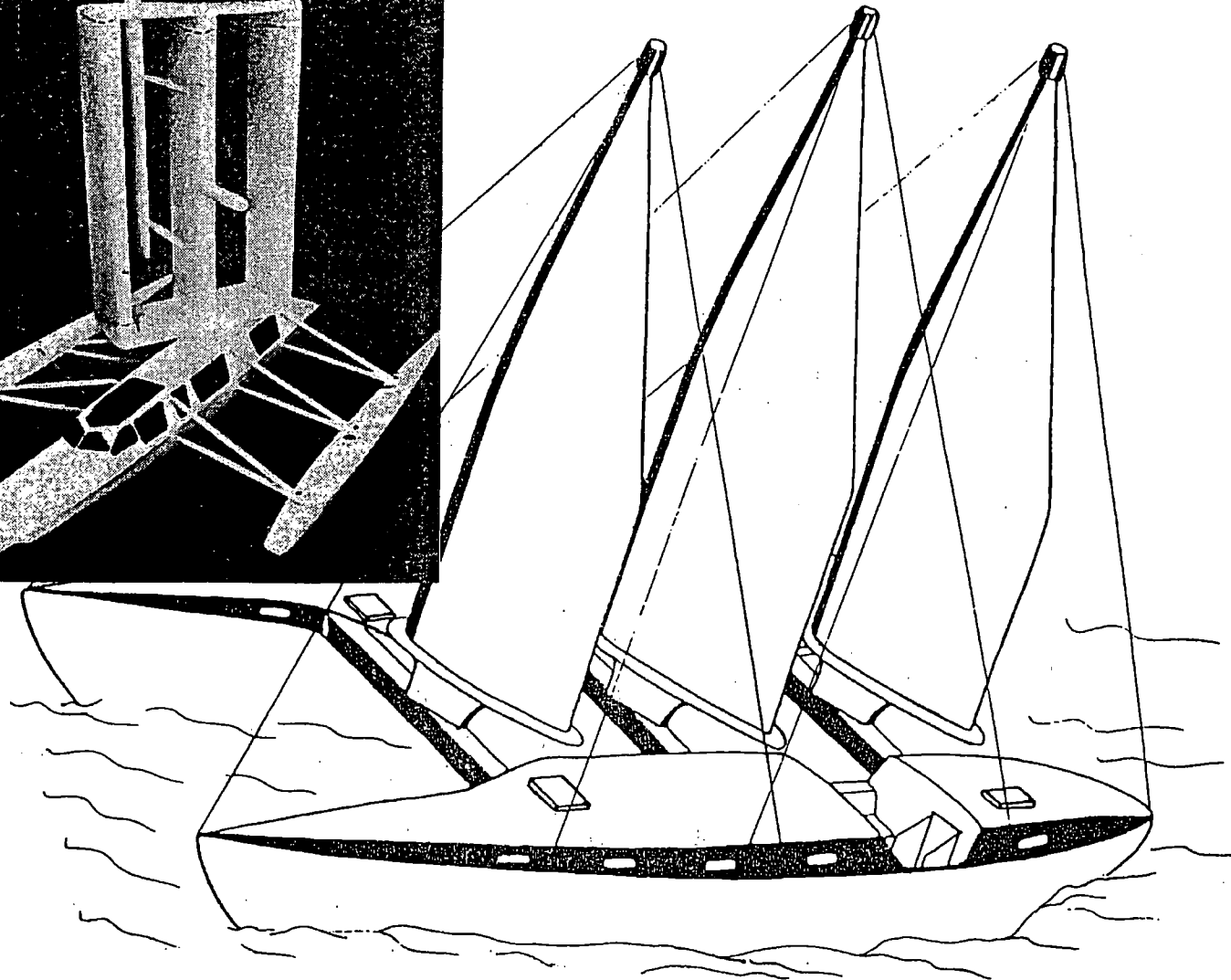
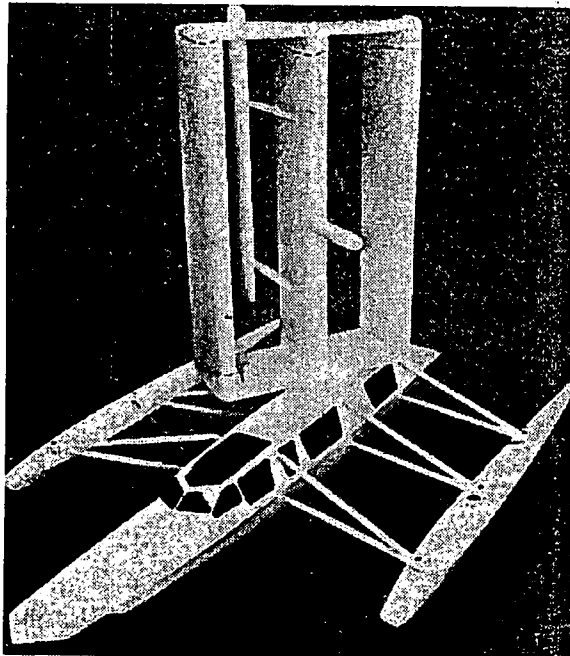


Figure 34 "Planesail", Solid Foil Rig.

Figure 35 "Shadowfax", Solid Foil Rig, *l.o.a.* 15.25m

Noise reduction aboard small yachts

by J. Buiten and H. Hendriks

TNO Institute of Applied Physics,
Delft, The Netherlands

Summary

Measurements aboard two small boats with respect to the existing noise levels are reported. The one, being a 10 m long motor inland cruiser, has carefully been investigated to obtain a firm basis for the assessment of the influence of noise abatement measures.

Aboard the other one, a 8.5 m long polyester sailing cruiser, the influence of a simple acoustical measure installed to reduce the noise caused by the inboard auxiliary propulsion engine has been investigated.

The measurements are discussed and some general conclusions with respect to acoustical measures aboard yachts are given.

Introduction

Within the frame-work of a research sponsored by HISWA an analysis has been made of the noise situation and of the noise path aboard a 10 m long steel-made inland motor cruiser. The yacht chosen for this purpose represents a very popular type of motor yacht in the Netherlands. Some important data of this yacht are:

- Builder : Kempers B.V., Alphen a.d. Rijn, The Netherlands
- type : Kempala
- length : 10 m
- width : 3.1 m
- diesel engine : 4-cil.-Peugeot DTP 50, 37 kW at 2600 rev./min.
- cruise speed : 13 km/h. at 2000 rev./min. of the engine (26 kW)
- propeller : 3 blades

The investigation is a follow-up of the work done in the past in this field by the authors [1]. It was now tried however to obtain detailed information about the acoustical behaviour of the yacht to arrive in the future to a firmly based relationship between the profits and the costs of noise control measures aboard the considered type of yacht.

For that purpose a great amount of measurements were carried out aboard and analysed afterwards in the laboratory.

In the following chapters the results of the measurements will be given and discussed.

The second yacht discussed in this paper is a glassfibre reinforced polyester sailing cruiser, also a typical family-ship. Aboard this ship the owner installed in cooperation with the builder of the yacht sound insulating material in way of the auxiliary propulsion engine. Some data of the yacht are:

- Builder : Zaadnoordijk B.V., Heerenveen, The Netherlands
- type : Compromis 850
- length : 8.5 m
- dieselenigne : 2 cil. - Buck, IS kW at 3000 rev./min.

The authors had the possibility to carry out measurements before and after the acoustical measure was applied.

The principle results are given in this paper.

In a previous paper [1] an introduction to the physicals of noise and the reaction of people on noise were given already; for the definitions of sound pressure level (L_p), velocity level (L_v), frequency (Hz), octave bands, A-weighted sound level (dB(A)) etc. we refer to that paper.

Results of measurements aboard the motoryacht

In Figure 1 the spectra of the sound measured in the three spaces aboard the motoryacht are given. In Table 1 the sound levels A of the spectra are given and compared, with the limits recommended by Buiten and De Regt [1].

Table 1. Measured and recommended sound levels in dB(A)

	recommended	measured
wheelhouse	60	75
cabin fore	60	66
cabin aft	65	72

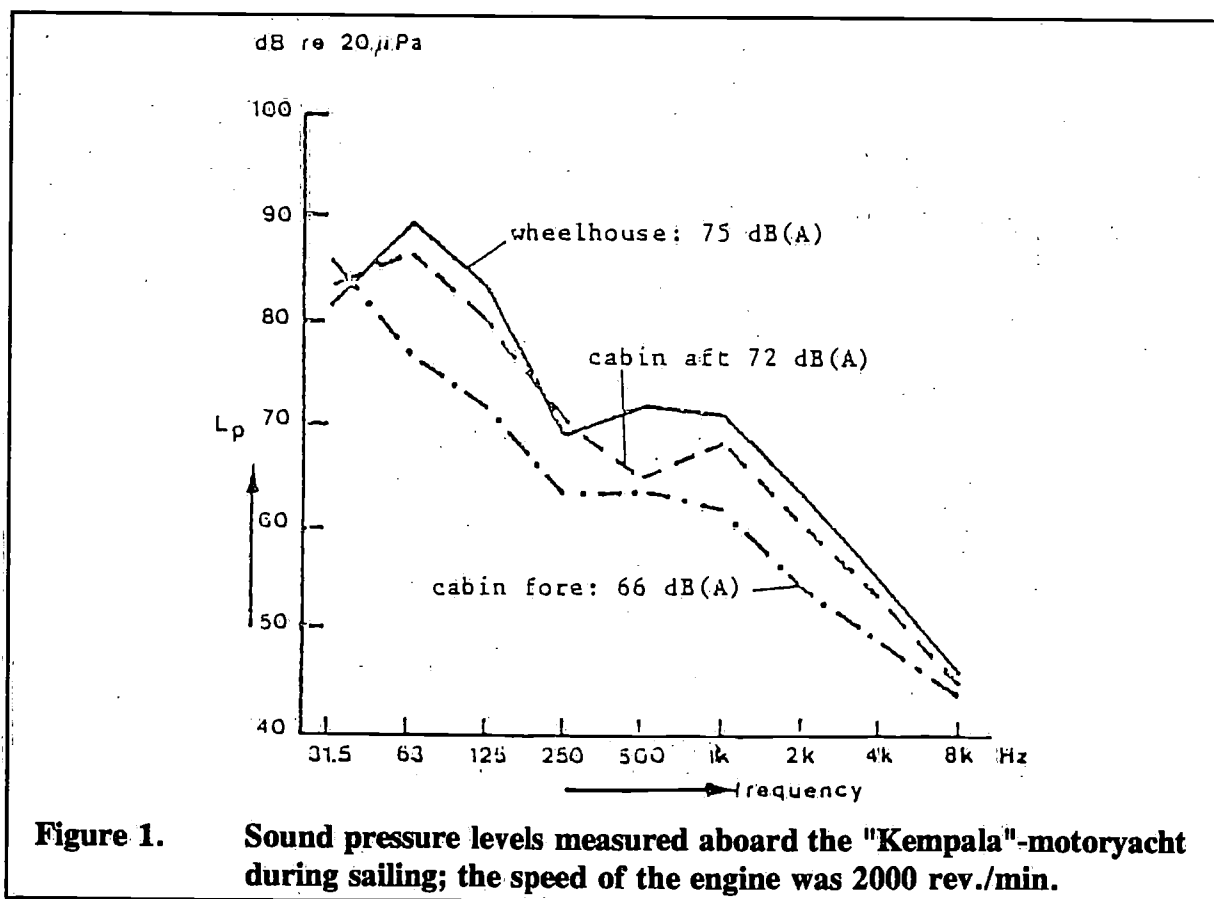


Figure 1. Sound pressure levels measured aboard the "Kempala"-motoryacht during sailing; the speed of the engine was 2000 rev./min.

The measurements were made during normal cruising speed (13 km/h.); the speed of the engine was 2000 rev./min.

The separation between wheelhouse and cabin fore appears to result in a difference of 9 dB(A) between the sound levels in these spaces.

It is clear that though the sound levels are quite usual (8 m yacht in [1]: 73, 68.5 and 74 dB(A) following the order of Table 1) they are 6 - 15 dB too high.

Discussion of the results

The origin of the noise in the wheelhouse is without doubt the diesel engine.

From Figure 2 it appears that the sound pressure levels measured aboard and corrected for a distance of 1 m between microphone and engine and corrected for acoustically "free field" circumstances are certainly not higher than might be expected based on a relation, described by Hempel [2], between sound level A and power and speed of the engine.

The relation between L_A (1 m, free field) and the octave band levels given in [1], which is based on measurements of a great number of engines, is used to obtain the "average" spectrum of the considered engine from the calculated sound level A . Measurements in the laboratory with respect to the same type of engine give a spectrum that is close to the results obtained aboard when it is considered that in the laboratory the engine was not loaded.

The L_p (1 m, free field) were also calculated using the velocity levels (L_v) measured at three positions on the engine and an average radiation efficiency. Especially at the lower frequencies, with exception of the level in the 31.5 Hz-octave band, the agreement between the two methods is not bad. Of great importance is the nice agreement in the 63 Hz-octave band which indicates that in this band, in which the firing frequency is located, the possibility of an important contribution of noise radiated by the airsuction openings can be eliminated.

In the wheelhouse the sound radiated by the floor is dominating as is shown in the Figures 3, 5 and 6. The sound radiated by each surface is calculated from the averaged velocity level of a surface and its radiation efficiency, the latter obtained from Maidenik [3] and Josse and Lamure [4]. In the wheelhouse about ten measuring positions per square meter are used to obtain the desired precision with respect to L_v .

Besides some supplementary experiments were carried out to be sure about some sound path e.g. by using an artificial air-borne sound source.

For the floor hatches situated just above the engine air-borne sound excitation is dominant but the other parts of the floor are mainly excited by structure-borne sound.

This is due to the high velocity levels of the hull and the steelwork attached to it.

It could be calculated that the sound levels radiated by the parts of the floor near the ship's sides are composed by the following contributions:

- via air-borne sound excitation: 64.5 dB(A)
- via structure-borne sound excitation caused by the hull: 70.5 dB(A)
- via structure-borne sound excitation caused by the supporting frame: 66 dB(A)

The agreement between the measured sound levels and the total of the sound levels calculated by using the measured L_v appears to be good (Figure 4).

From the data given and the discussed graphs it is clear that the structure-borne sound path via the hull is a very important one and noise reducing counter measures have to be related to this path in the first place.

Figure 7 shows that the velocity levels of the bottom of the ship underneath the engine can be explained fairly well when it is supposed that air-borne excitation due to the sound radiated by the diesel engine exists.

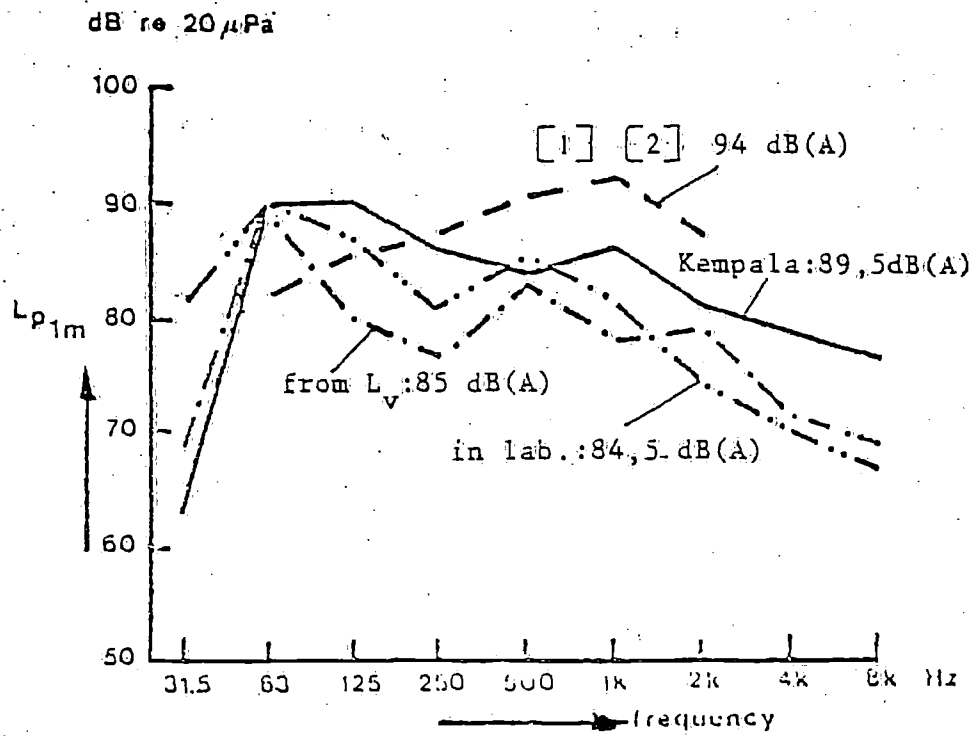


Figure 2. Sound pressure levels at 1 m corrected for acoustical free-field circumstances as being measured aboard and in the Laboratory. Also data obtained using velocity levels (L_v) of the diesel engine aboard are given. Using relations given in [1] and [2] calculated data are added.

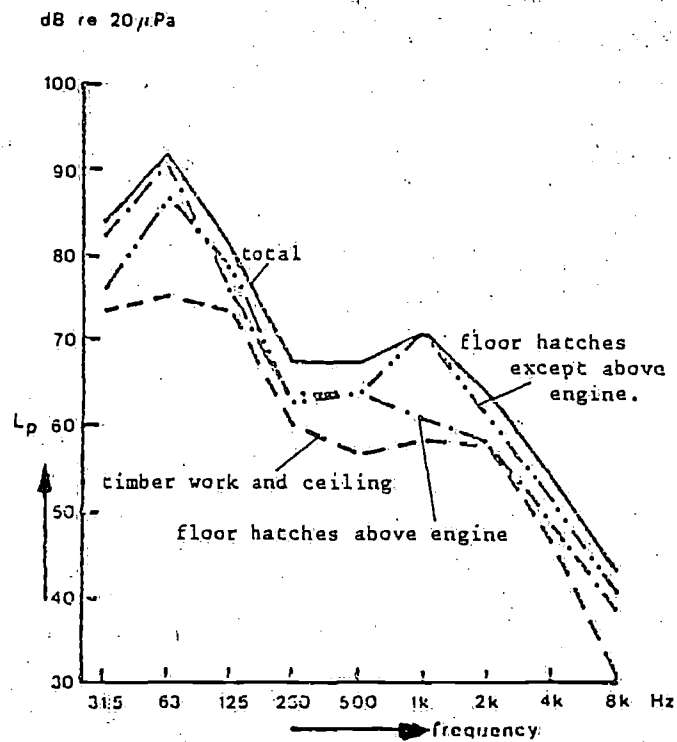


Figure 3. The contributions of the boundaries of the wheelhouse to the sound pressure level in the wheelhouse calculated using the measured velocity levels of the boundaries. Condition: sailing, engine speed: 2000 rev./min.

The foundation vibrates much less and because of the thicknesses of bottom and foundation are nearly equal (4 and 6 mm) it may be concluded that the latter is excited by the bottom instead of the reverse. Even the "whine" produced by the gearbox seems to excite the ship's bottom plating via the air-borne path though this does not appear from Figure 7. But, while there is a large difference between the velocity levels of the fore- and aft feet of the engine (16 dB in the 1000 Hz octave band), underneath the mounts the levels are equal.

Besides it may be expected that the sound level underneath the gearbox is higher in this band than the space-averaged level used in the calculation.

So to avoid structure-borne sound excitation of the hull the production of airborne-sound generated by the diesel engine has to be reduced! Only in the 31.5 Hz octave band the velocity level of the bottom is more than 10 dB higher than the air-borne induced level which indicates that in this band structure-borne sound excitation is dominating. This is in agreement with the fact that the six "eigen" frequencies of the resilient system are in the range of 16 - 34 Hz, the one in the vertical direction being 26 Hz.

However this octave band is of no importance with respect to the reduction of the sound level A in the wheelhouse, as can be learned from Figure 8.

Noise reducing measures

The A -weighted octave band levels given in Figure 8, obtained from Figure 3, show that though the levels in the octave bands with centre frequencies higher than 250 Hz certainly must be reduced, the levels in the 63 and 125 Hz-octave bands caused by the floor must be decreased with at least nine dB to arrive at a level of 60 dB(A). This fact reduces the possible noise reducing measures at a large extent.

The possible counter measures are in principle:

- to use a diesel engine with reduced noise production
- insulation in way of the engine
- insulation in way of the accommodation.

The first would always be the most simple one.

However, the selection of the engines with respect to their noise production is not a simple task because the number of manufacturers who possibly can produce graphs like Figure 2 is very limited.

The insulation in way of the accommodation can be made effective at high frequencies. Certainly aboard the yacht concerned, it is impossible to obtain an insertion loss (IL) of more than a few dB in the 63 Hz-octave band because of the weight of the material to be applied. This is due to the fact that the IL of measures such as "floating" floors or "floating" decks at low frequencies depends among others on the "eigen" frequency of the system [5].

To obtain an "eigen" frequency which is low enough, in the case of the yacht discussed ca. 40 Hz, the mass of the floating floor would be about 80 kg/m².

However, a higher IL can be obtained when the wooden floor would be replaced by a steel one on top of which a floating floor would be applied. In this case a higher "eigen" frequency may be chosen because in the frequency range below the "eigen" frequency the radiation efficiency of the steel is the most important quantity with respect to the sound radiation of the floor.

With respect to the uncovered wooden floor an IL of ca. 6 dB in the 63 Hz-octave band is then attainable. In the 1 kHz band the IL of the described measure can exceed 20 dB so L_A radiated by the floor could be reduced to about 60 dB(A).

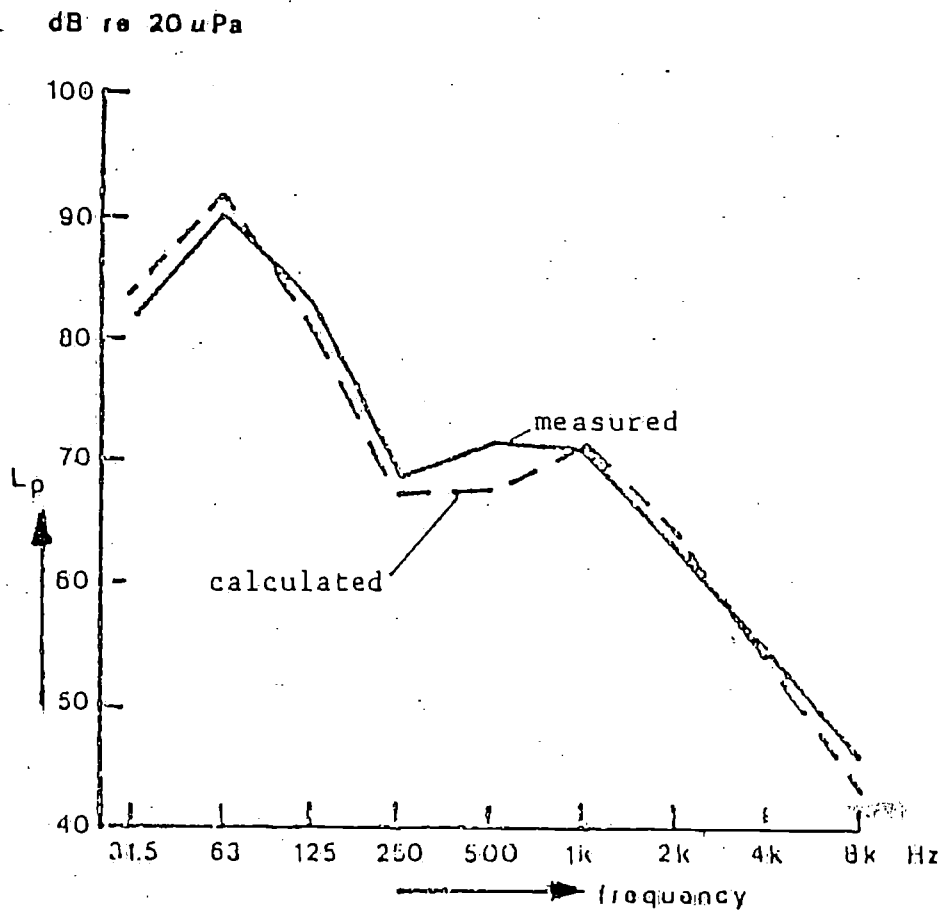


Figure 4. The measured and the calculated sound pressure levels in the wheelhouse, the latter obtained from Figure 3.
Condition: sailing, engine speed 2000 rev./min.

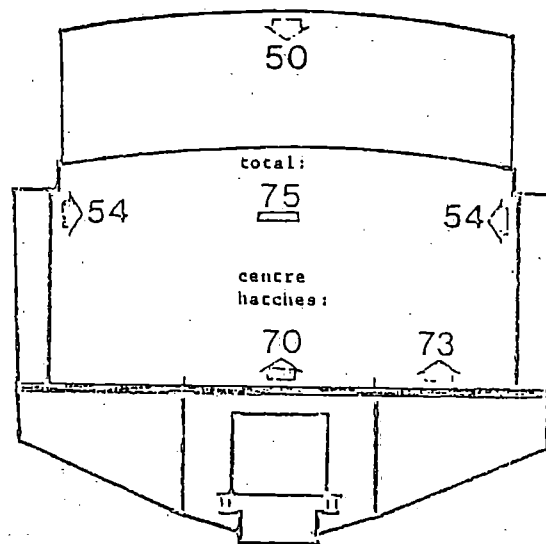


Figure 5. The contribution of the different sound radiating boundaries of the wheelhouse in dB(A) to the total sound level.
Condition: sailing, engine speed: 2000 rev./min.

The contribution of the sound radiated by the walls has to be reduced to about 50 dB(A). This implies an *IL* of about 8 dB at high frequencies which is attainable by decoupling the timber work from the steelwork by using small rubber mounts.

So when the practical problems which undoubtedly are connected to the measures described are solved, the measures in way of the wheelhouse can reduce the sound levels from 75 to 60 dB(A). For the cabin aft similar measures would have to be carried out as described for the wheelhouse to arrive to 65 dB(A). In the cabin fore, the floor and the bulkhead aft should be decoupled from the steelwork, which should be effective in the 500 and 1000 Hz octave band. When 2 mm thick, small rubber pieces are inserted between steel and furnishing the wanted effect would be attained.

The insulation in way of the engine is the most logical counter measure, because the measure is concentrated at one place. Of course only the noise produced by the engine is decreased and e.g. the propeller induced noise is left unchanged. Aboard the yacht concerned this seems not to be a problem however.

As stated before the excitation of the hull can be reduced by decreasing the air-borne sound levels in the vicinity of the engine. This can be achieved by installing an enclosure made of steel sheet around the engine.

The enclosure has to be air-tight and has to be provided with cooling air suction- and discharge-silencers. Also the not to be avoided openings (propeller shaft, exhaust pipe) have to be designed as close fitting ducts (length: 2 x diameter) provided with a layer of mineral wool or a similar material at the inner side (thickness: ¼ diameter).

The enclosure must be installed resiliently using soft rubber mounts. At the innerside the enclosure has to be provided with a layer of mineral wool (or similar material) with a thickness of 50 mm.

For some constructional details of enclosures we refer to [6] and [7].

The effect of enclosures is wellknown and described by several authors. Some results are given in Figure 9. From an investigation carried out in the laboratory it appears that up to 18 dB lower, *IL*'s in the 125 and 250 Hz octave bands were measured when an engine was installed in the enclosure, than when an artificial air-borne sound source was used.

At the harmonics of the firing frequency an increase of sound pressure levels in the enclosure with respect to the free-field conditions cause the reduction of *IL* in the 125 Hz octave band. This can be avoided by applying a sufficient amount of sound absorbing material in the enclosure.

Figure 9 shows that it is likely that the *IL* of an enclosure made from 2 mm thick steel sheet is in about the middle of the range given in [6].

These values, being 3, 8, 12, 16, 19, 20 dB for the octave bands 63 up to 4000 Hz respectively are given in [1] and are used for the yacht discussed here.

In Figure 10 the resulting sound levels are given. The total sound pressure level is 64 dB(A) which is caused by the floor still. So some additional measures e.g. the insertion of small pieces of rubber sheet between floor hatches and steelwork are still necessary.

The sound levels in both of the cabins are decreased by the same amount as is the case for the wheelhouse: 11 dB(A).

If the enclosure is only a kind of hood i.e. the enclosure is not closed at the bottom side, the bottom will still be excited by the air-borne sound radiated by the diesel engine. So the structure-borne path via the hull still exists and the decrease of the sound level in the wheelhouse will only be 3 dB(A). The conclusion thus be that insulating the engine as well as insulation

measures in way of the accommodation are possible; it will depend on the practicability of the measures described and the costs which one is preferable for a yacht.

Noise reduction aboard a polyester yacht

Aboard the fibre glass reinforced polyester yacht the space in which the engine is installed was provided with an airborne sound insulating covering. The covering was composed by a layer of foam plastic (thick 40 mm) on top of which a lead-vinyl-sheet was 2 glued (thick 3 mm, density: 18 kg/m²). Much attention was paid to avoid acoustical leakage to the cabins. For practical reasons the bottom was not covered at all. In the Figures 11 - 13 the results of the measure are given.

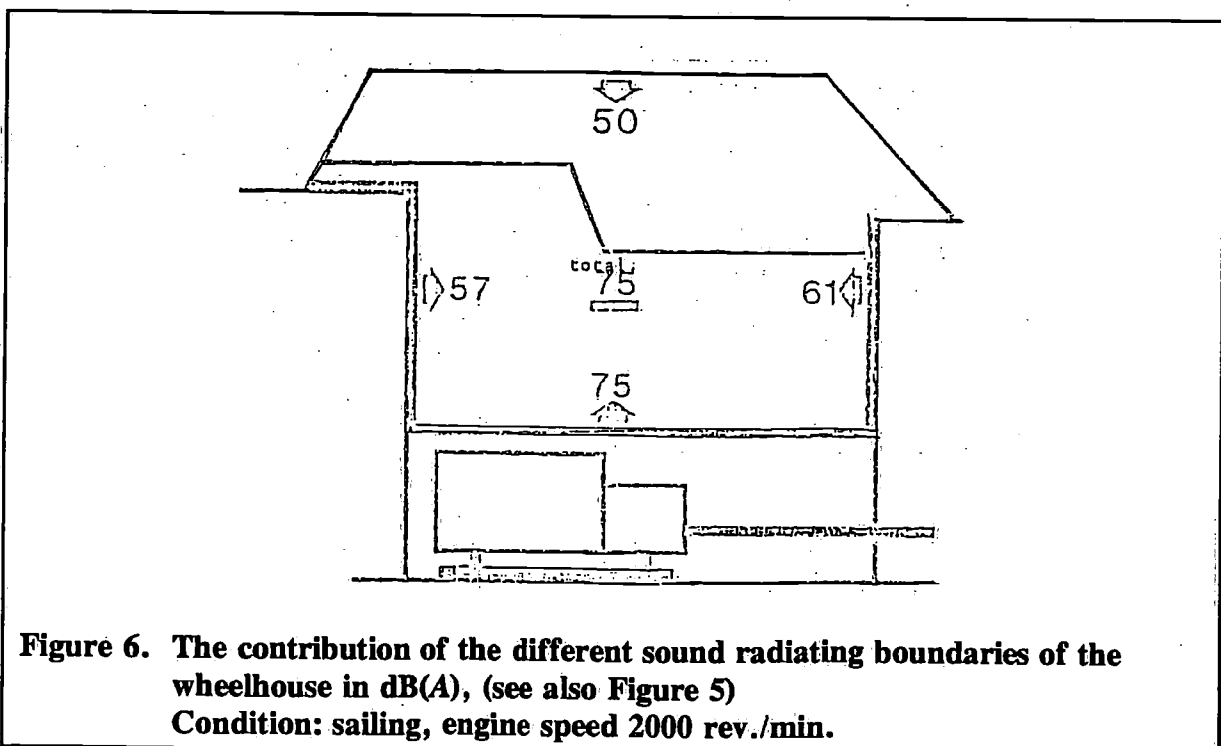
The reduction of the levels is in the cabins larger than in the cockpit 7 - 8 dB(A) against 4 dB(A) respectively. These values are too low when the proposed limits given in [1] have to be reached (cockpit 65 dB, force: 60, aft 65 dB(A)).

One reason of the low reduction is the existence of the uncovered bottom underneath the engine. Figure 11 shows that the noise in the cockpit is caused by all boundaries with exception of the floor, which is in top of the engine! So similar reasons for the low values of the *L* as described for the motoryacht are present: the path is via the hull due to structure-borne sound which is excited by the air-borne sound radiated to the bottom.

A second reason is that the insulation of the material chosen is low at low frequencies. Both causes mentioned can be avoided to some extent whereby practical problem's ask for inventive solutions.

Acknowledgements

The authors thank the HISWA for their financial support in the research to silent yachts and the director mr. Van Vollenhoven for the fruitful cooperation. Also the owners and builders of the yachts investigated are owed thanks for their fine cooperation and great patience during the measurements.



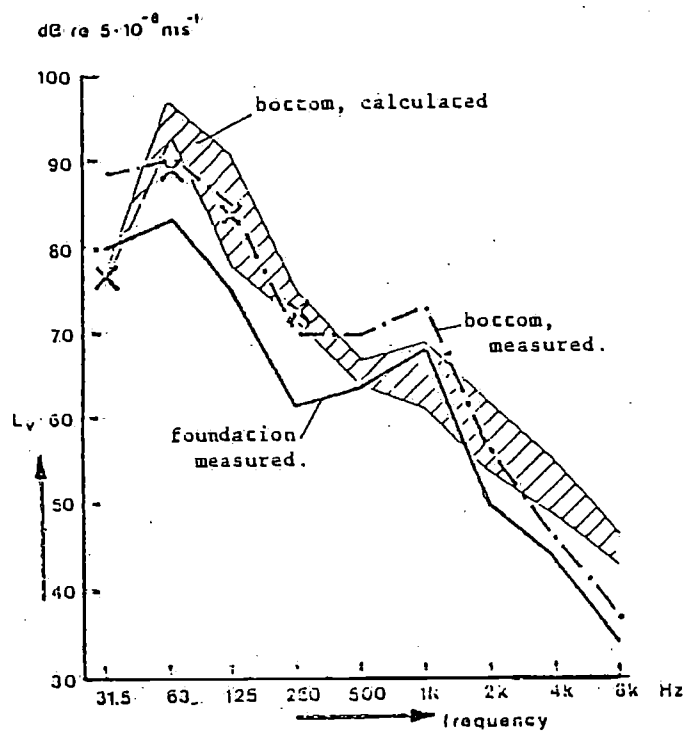


Figure 7. Measured and calculated velocity levels of the bottom of the yacht underneath the diesel engine. The calculated data are derived from measured L_p 's with floor hatches closed resp. opened (given by X). The velocity levels were measured when the hatches were opened.

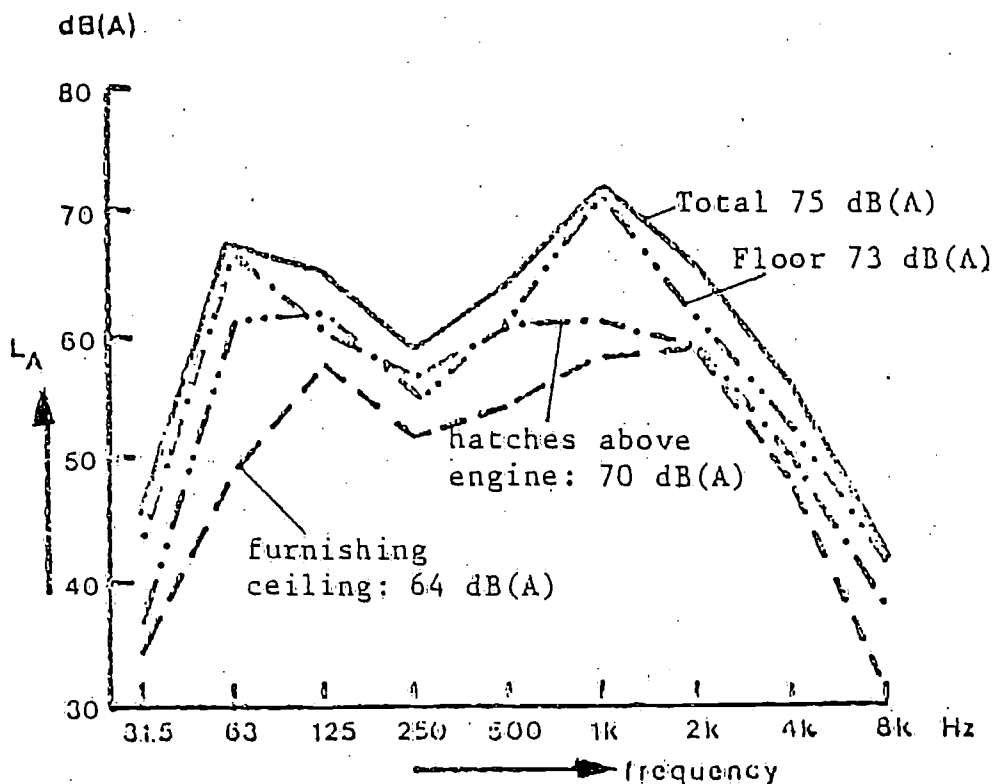


Figure 8. The contributions of the sound radiated by the boundaries of the wheelhouse to the total level given by the A-weighted levels of Figure 3.

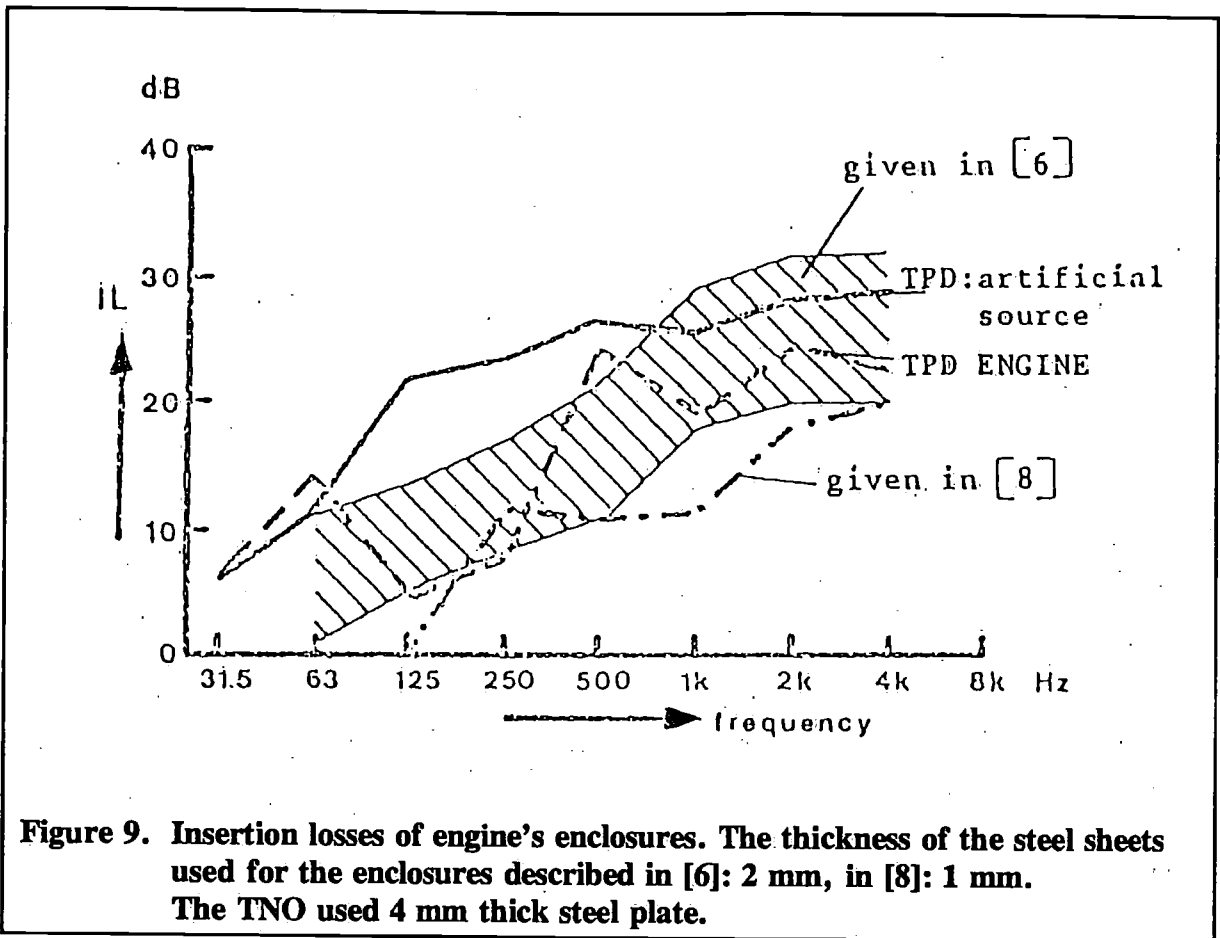


Figure 9. Insertion losses of engine's enclosures. The thickness of the steel sheets used for the enclosures described in [6]: 2 mm, in [8]: 1 mm. The TNO used 4 mm thick steel plate.

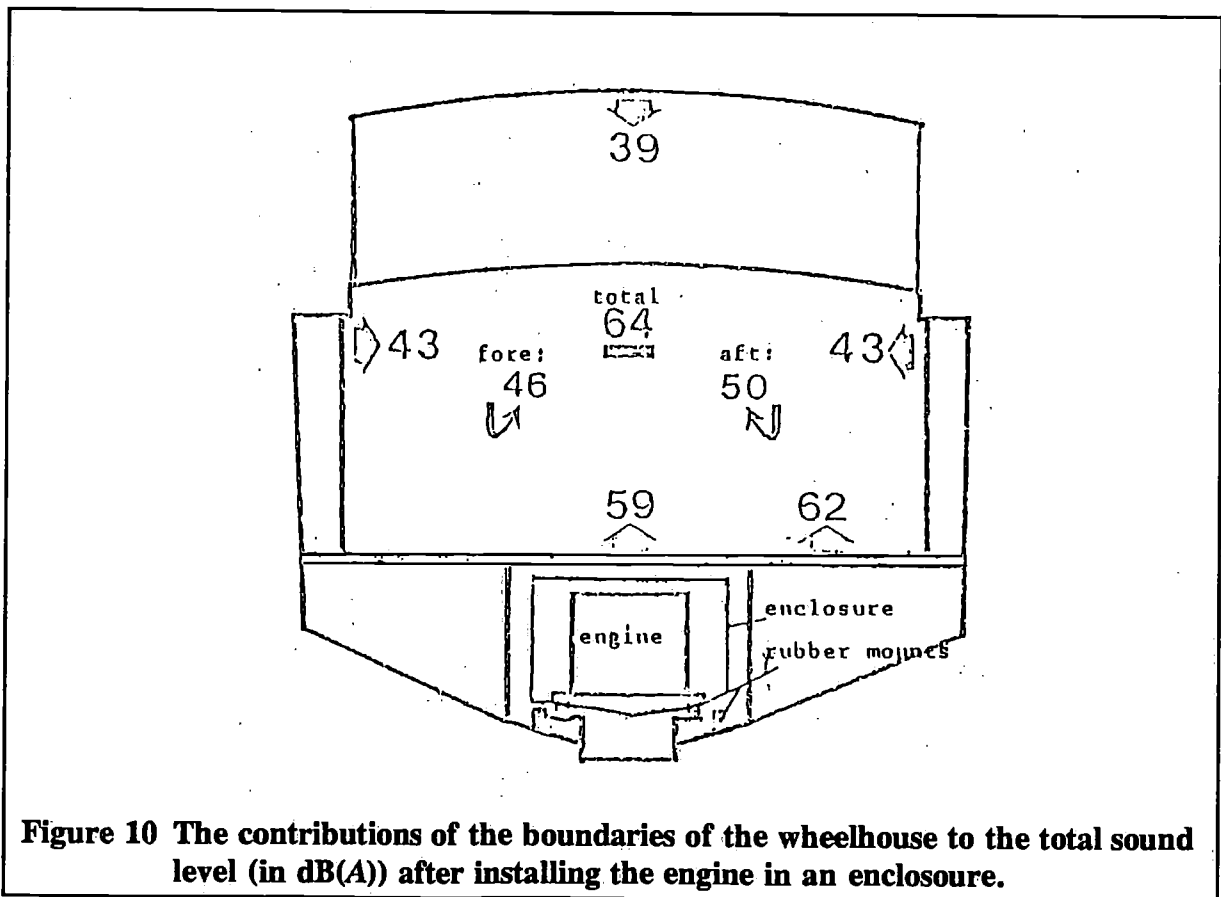


Figure 10 The contributions of the boundaries of the wheelhouse to the total sound level (in dB(A)) after installing the engine in an enclosure.

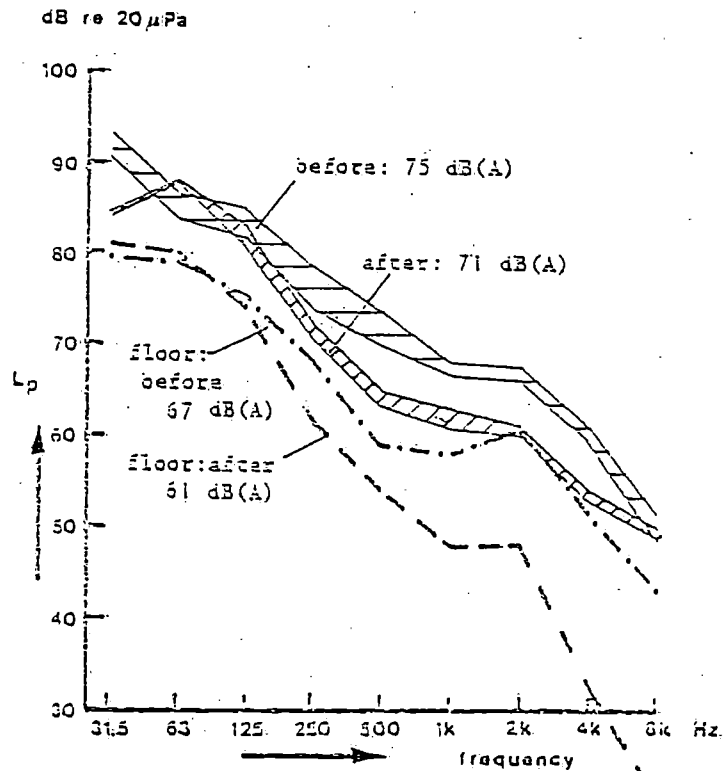


Figure 11 The sound pressure levels in the cockpit measured at ear-height near the helm aboard the compromis before and after the sound insulating measure was installed. Besides the contributions of the floor are given.

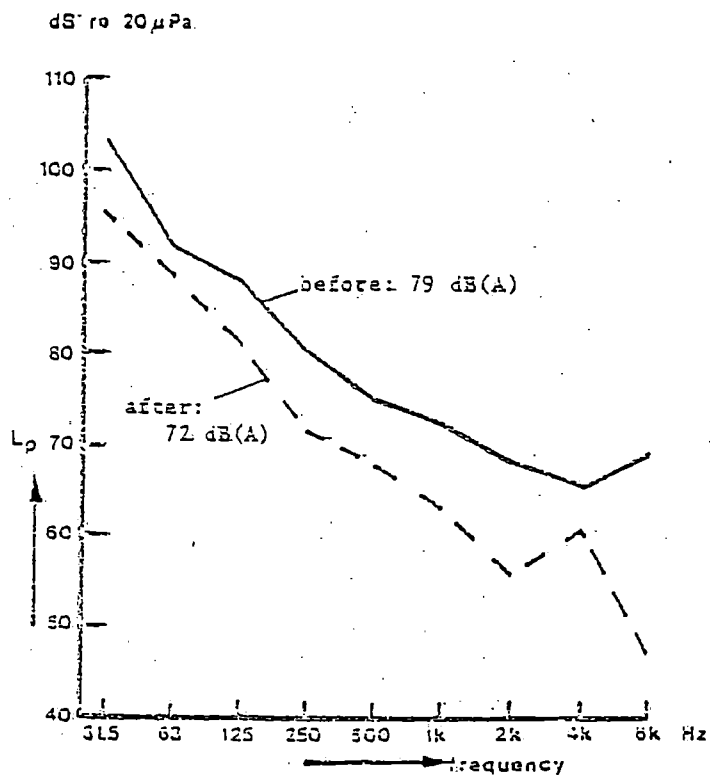


Figure 12 The sound pressure levels in the cabin fore aboard the compromis before and after the sound insulation was installed.

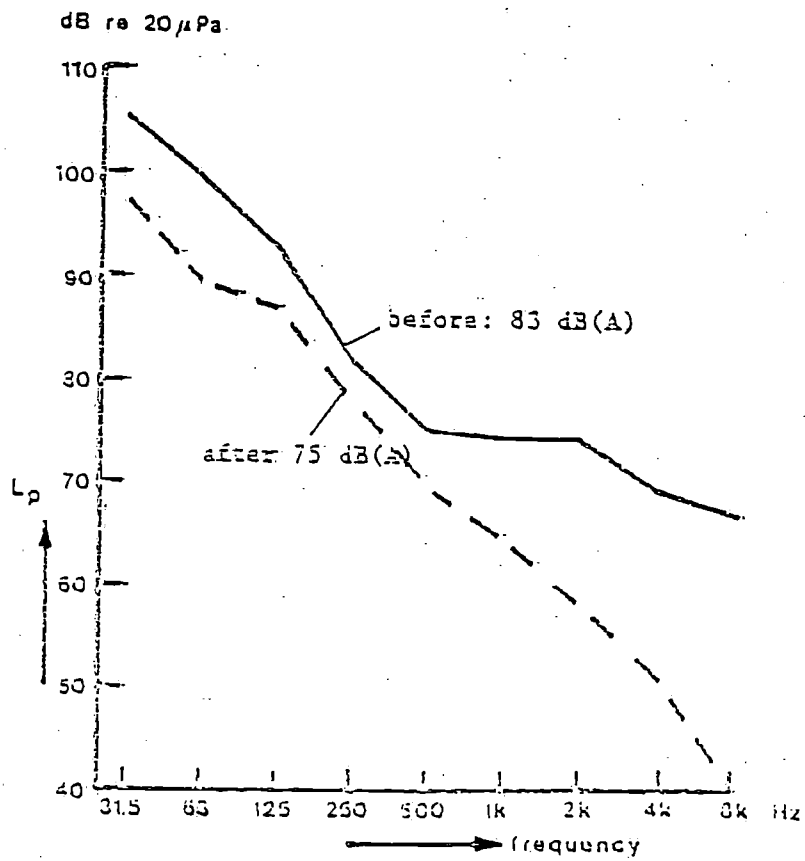


Figure 13 The sound pressure levels in the cabin aft aboard the Compromis before and after the sound insulation was installed.

Test results of a systematic yacht hull series

by J. Gerritsma, G. Moeyes and R. Onnink

Delft University of Technology
Ship Hydromechanics Laboratory

Contents

- 1 Introduction
- 2 Geometric description of the systematic series
- 3 Experimental set-up and discussion of test results
 - 3.1 Experimental set-up
 - 3.2 Upright resistance
 - 3.3 Side force and leeway
 - 3.4 Heeled and induced resistance
- 4 Sailing performance
 - 4.1 Determination of sailplan and stability
 - 4.2 Downwind speed
 - 4.3 Speed-made-good to windward
 - 4.4 Performance with respect to rating
- 5 Acknowledgement
- 6 References

List of symbols

A_w	: waterplane area
A_x	: maximum sectional area
AR_E	: effective aspect ratio
B	: centre of buoyancy
B_{MAX}	: maximum breadth
B_{WL}	: waterline breadth
BAD	: height of boom above deck
BM	: metacentric radius
C	: average chord
C_{Di}	: induced drag coefficient
C_F	: frictional resistance coefficient
C_H	: weight coefficient of hull
C_L	: lift coefficient
C_P	: prismatic coefficient

D	: depth
E	: length of mainsail foot
F	: freeboard
F_n	: Froude number
F_H	: heeling component of sail force
G	: centre of gravity
g	: gravity acceleration
GM	: metacentric height
$GM \sin \phi$: arm of static stability
h	: height of centre of effort of sails above waterline
HB	: breadth of mainsail headboard
I	: foretriangle height
I_L	: longitudinal moment of inertia of waterplane
I_T	: transverse moment of inertia of waterplane
J	: length of foretriangle base
K	: keel point
$k(\phi)$: dimensionless residuary stability
KB	: height of centre of buoyancy above base line
KM	: height of metacentre above base line
L	: length
L_{OA}	: length over all
L_{WL}	: waterline length
LCB	: longitudinal position centre of buoyancy
LCF	: longitudinal position centre of flotation
M	: metacentre
$MN \sin \phi$: arm of residuary stability
MR	: measured rating
P	: length of mainsail luff
R	: rating
R_F	: frictional resistance
R_H	: heeled resistance at zero sideforce
R_i	: induced resistance due to leeway
R_n	: Reynolds number
R_R	: residuary resistance
R_T	: total resistance in upright position
R_ϕ	: total resistance with heel and leeway
RM	: righting moment
S	: wetted area
SA	: sail area
SA_{eb}	: effective sail area to windward

SA_{ed}	: effective sail area downwind
SR	: stability ratio
T	: draught
TMF	: time multiplication factor
V	: speed
V_d	: downwind speed
V_{mg}	: speed-made-good to windward
V_{tw}	: true wind speed
W_H	: hull weight
Y_B'	: sideforce curve slope, made dimensionless by $\frac{1}{2}\rho V^2 L_{WL}^2$
Z_{CE}	: height of effective centre of effort of sail force above waterline
α	: linear scale ratio
β	: leeway angle
Δ	: weight of displacement
∇	: volume of displacement
ϕ	: heeling angle
γ	: kinematic viscosity
ρ	: specific density

Subscripts

b	: refers to base boat
c	: refers to canoe body
k	: refers to keel
r	: refers to rudder

1 Introduction

Systematic research on the hydrodynamic characteristics of yacht hull forms has only been carried out on a rather limited scale.

Already during the discussion of Davidson's classical paper on experimental studies of the sailing yacht, in 1936 [1], two of the discussers focussed the attention to the necessity of a systematic investigation of yacht hull forms, to give a more rational base for design methods and performance analysis. In this respect a parallel was drawn with the well-known Taylor Series, the results of which are still in use with naval architects to determine the resistance of merchant- and naval ships in the design stage [2].

This discussion took place some forty years ago, but already at that time those concerned with yacht research and yacht design were well aware of the fact that systematic design for sailing yachts could be extremely useful to analyse the influence of hull form and sailplan variations. The possibility to determine the performance of a yacht by varying the sail geometry and the stability of a given design, based on the results of one particular model test had been available for some time, and it was also possible to include in the analysis a variation of the yacht's size, keeping the same geometrical form.

An additional possibility, to include form variations could be considered as a useful and even necessary extension of the existing methods.

In this respect the rating of racing yachts is a special area of interest. The determination of

a yacht's rating as a function of hull geometry, sail dimensions and stability is important because designers of racing yachts try to optimize hull and sails to produce an optimum combination of rating and speed potential. Rule makers aim at equal performance at equal rated length for fair competition.

There is no doubt that designers of cruising and racing yachts would benefit from the results of systematic model tests, although the problems are of such a complexity, that the full scale experiment, a "one off" will continue to play an important role in development of yacht designs.

Systematic model tests have been carried out for 12-meter yachts, because in this case the research costs for one individual design is not a very restrictive factor. Unfortunately most of the results of such tests are confidential and concern a rather extreme class of yachts.

An interesting systematic model series of yacht hulls has been presented by DeSaix on the 2nd HISWA Symposium in 1971 [3]. He varied the lines of the parent model, Olin Stephens "NY 32", to study the effect of the beam-draft ratio (5 models) and the prismatic coefficient (3 models).

DeSaix remarks in his paper:

"It is hoped the work will encourage others in the same position as the author to contribute systematic data for the use of the individual yacht designer."

Gerritsma and Moeyes published the results of a small systematic series consisting of three models with equal waterline length, breadth and rating, but with a considerable variation in the length-displacement ratio [4].

With regard to fin keels and rudders, isolated or in connection with the hull, a reasonable amount of systematic work has been carried out by DeSaix [5], Millward [6], Herreshoff and Kerwin [7], Beukelman and Keuning [8], and others.

This summary is not considered as complete, but it may serve to give an impression of the hydrodynamic research on sailing yachts, other than model testing of individual designs.

The entire problem of yacht performance is very complex and includes also the sail forces. The combined knowledge of hull forces and sail forces can be used to simulate sailing conditions, for instance to determine the speed-made-good and the heel angle under given wind conditions.

Computer techniques allow the analysis of a large amount of data and consequently many combinations of hull forms and sailplans can be considered when the basic hydrodynamic and aerodynamic data are available.

To this end sail forces have to be known as a function of wind speed and apparent wind angle for the considered sail configuration. For the close-hauled condition the well known Gimcrack coefficients are commonly used. Some forty years ago these coefficients have been derived by Davidson from full scale tests with the yacht "Gimcrack" and corresponding yacht model tests [1]. The assumption being made was that in the equilibrium condition, defined by forward speed, heel angle and leeway angle, the driving sailforce is equal in magnitude but opposite in sign with the longitudinal water resistance force. The same holds for the heeling sailforce and the sideforce, acting on the under water part of the yacht. The hydrodynamic forces can be determined from experiments with a model running in the same conditions (speed, heel angle, leeway angle) as during full scale tests and consequently the sailforces follow from the above mentioned equalization of sail- and hull forces. It is assumed that the sail force coefficients, derived in this way are independent of the planform of the sails.

Although the Gimcrack coefficients are restricted to the close-hauled condition, the method can be extended to other points of sailing.

A theoretical calculation of sail forces with sufficient accuracy is not yet available, although attempts have been made by Milgram [15] to investigate the influence of planform on sailforces with vortex sheet calculations. In some special cases wind-tunnel measurements with model sails have been carried out [9],[10]. Systematic model experiments with a sail configuration of a cruising sloop, for all points of sailing have been carried out by Wagner and Boese [11].

These wind tunnel tests included the main sail, the working jib, genoa and spinnaker, in combination with the part of the hull above the waterline, as well as the aerodynamic forces on the hull only.

The various sail combinations were also tested without the hull.

In view of the age of the Gimcrack measurements two new determinations of sailforce coefficients have been carried out in 1974, using Davidson's method to combine model tests and full scale data. They concern the American yacht "Bay Bea" [12] and the Dutch yacht "Standfast" [13]. In the latter case the extensive model test program included the applied rudder angle, which could therefore be added to define the sailing condition to match the model and full scale results. The new data cover all points of sailing. The sailforce coefficients derived with these experiments are larger than the "Gimcrack" values, which may be due to the more efficient sailplans and the modern materials, used for sail cloth.

The experience of testing a fair number of individual yacht designs in the Delft Ship Hydromechanics Laboratory led to the conclusion that, within the time available for yacht research, much more knowledge could be obtained by testing a systematic series of yacht hulls, with variations in hull form. This series was planned to contain primarily variations of length displacement ratio, prismatic coefficient and longitudinal position of the centre of buoyancy, and should consist of approximately 27 models to cover most types of yachts. In an early stage of planning a cooperation of Delft with the Department of Ocean Engineering of the Massachusetts Institute of Technology, Boston has been established in view of their H. Irving Pratt Ocean Race Handicapping Project. This cooperation comprises generating the lines and manufacturing polyester hulls and keels of the first 9 models by MIT; towing tank testing has been carried out by the Delft Ship Hydromechanics Laboratory. Unfortunately the funds of the Pratt-project do not permit MIT to cooperate in the testing of further models. The test results will be used by MIT to look for fair handicap systems, while after terminating the whole series the analysis of Delft intends to provide above all the designer with basic hydrodynamic design knowledge and performance estimation methods.

In this paper the results of the first nine models are discussed. A standard performance calculation has been carried out for each of the nine models, assuming a waterline length of 10 meters, a realistic sailplan and a stability conforming the present design practice for I.O.R. designs. This exercise enables the comparison of the performance of the nine models with the rating according to the I.O.R.

2 Geometric description of the systematic series

The main form parameters of the first nine models are given in Table I, in which model 1 represents the parent form. All models have approximately the same longitudinal location of the centre of buoyancy. The prismatic coefficient has a nearly equal value for models 1 - 7, whereas model 8 has a high and model 9 a low prismatic coefficient. The relations between the various main parameters are presented in Figure 1 for models 1 - 9 (black spots) as well as for thirteen models to be investigated in the near future (open circles). The lines of the nine models are shown in Figure 2.

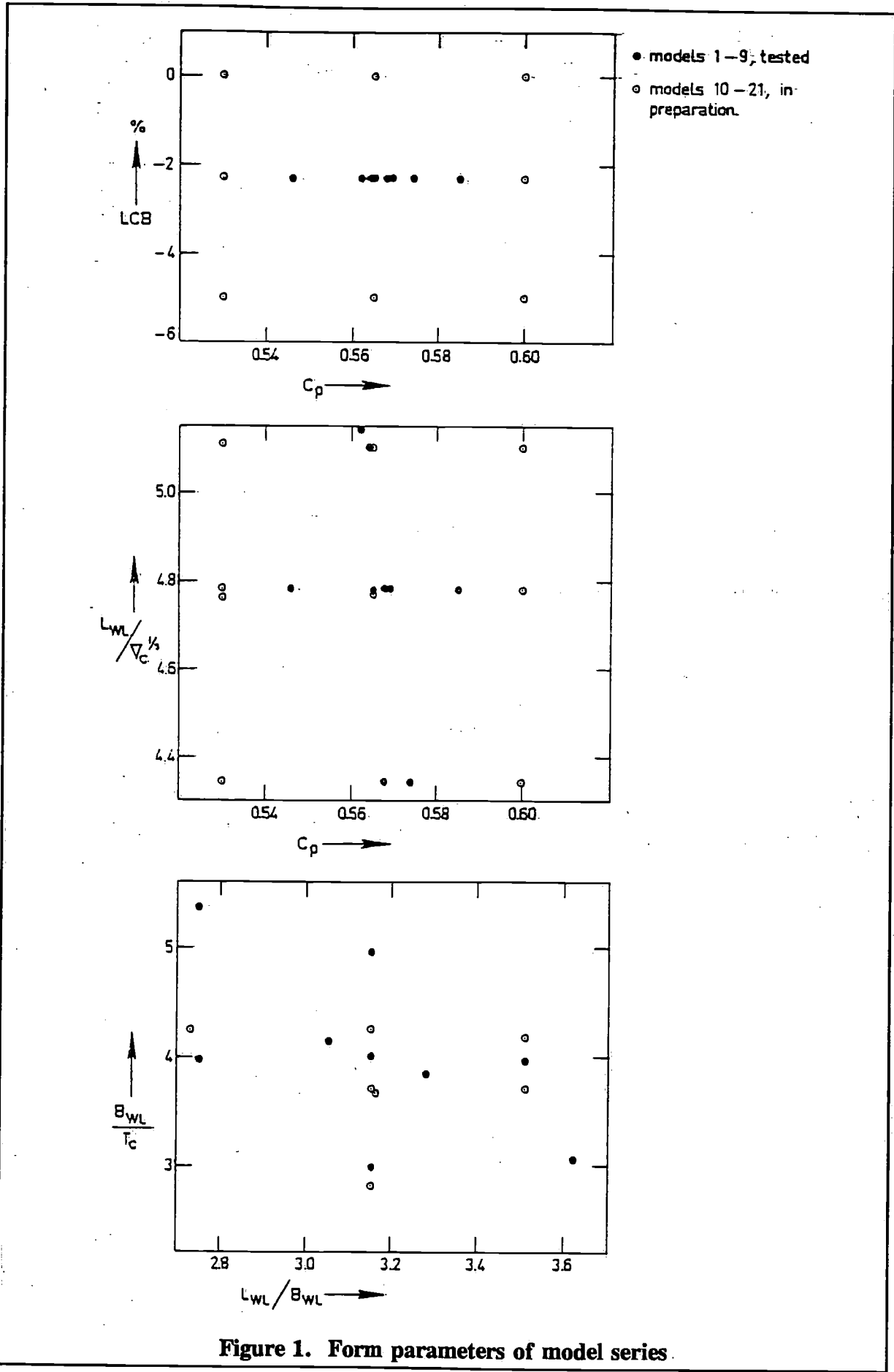


Figure 1. Form parameters of model series.

Table I. Main form parameters

Model nr.	L_{WL}/B_{WL}	B_{WL}/T_c	C_p	$L_{WL}/\nabla_c^{1/3}$	LCB_c %
1	3.17	3.99	0.568	4.78	-2.29
2	3.64	3.04	0.569	4.78	-2.29
3	2.76	5.35	0.565	4.78	-2.31
4	3.53	3.95	0.564	5.10	-2.32
5	2.76	3.96	0.574	4.36	-2.44
6	3.15	2.98	0.568	4.34	-2.38
7	3.17	4.95	0.562	5.14	-2.31
8	3.32	3.84	0.585	4.78	-2.37
9	3.07	4.13	0.546	4.78	-2.19

Wider, narrower, deeper and shallower models have been derived from the parent model by multiplication of coordinates with a factor which is constant for the underwater part and gradually going to 1 for the above water part of the hull. The resulting cross-sections, waterlines and buttocks were faired by computer graphics with spline cubic equations, while slight corrections of the profile ends fore and aft were introduced, when necessary, to obtain more regular and realistic forms.

These corrections cause the minor differences in LCB and prismatic as shown in Table I. Variation of the prismatic coefficient was accomplished by shifting cross sections to obtain the desired curve of cross sectional areas belonging to the prescribed C_p and LCB .

The parent model, which resembles closely the successful "Standfast 43" designed in 1970 by Frans Maas of Breskens, has a moderate form with regard to ratio's of main dimensions. It has clean lines, without bustles or other extreme variations in the curvature of the hull surface.

With regard to the parent model, model 2 is narrow and deep, whereas model 3 is wide and shallow, where draught is referred to the canoe body. They have the same displacement as the parent. Models 4 and 5 have a constant beamdraught ratio, but nr. 4 is lighter and nr. 5 is heavier than the parent hull. Models 6 and 7 are variations in displacement at constant length-beam ratio, thus having variations in the beam-draft ratio. Model 6 is heavier and deeper, whereas model 7 is lighter and shallower. Model 8, with the high prismatic has fuller ends and Model 9 with the low prismatic coefficient has fine end sections.

Because hull form variations were the main object of the series, all models have been tested with the same fin keel and rudder. Consequently deep- and shallow hull forms have an equal keel span, although this is not common design practice.

A NACA 63₂ - 015 airfoil section has been used for the fin keel and a NACA 0012 section for the rudder. The arrangement of keel and rudder is shown in Figure 3.

The waterline length of the corresponding full scale "Standfast 43" is 10 meters, so for a first analysis of the experiments the scale factor of all models has been set to $\alpha = 6.25$ and test results have been extrapolated to 10 m waterline yachts. The main dimensions of these nine yachts and some other hull data are summarized in Tables IIA and IIB. Some of the derived quantities, such as wetted surface, metacentric radius etc. are given for the canoe body as well as for the combination canoe body plus keel plus rudder. The series of nine models is too small to derive empirical relations between the main dimensions and for instance the metacentric radius BM or the height of the centre of buoyancy above the keel KB . It has to be noted that the keelpoint K is assumed to lie on the base line, which is the horizontal tangent to the canoe body.

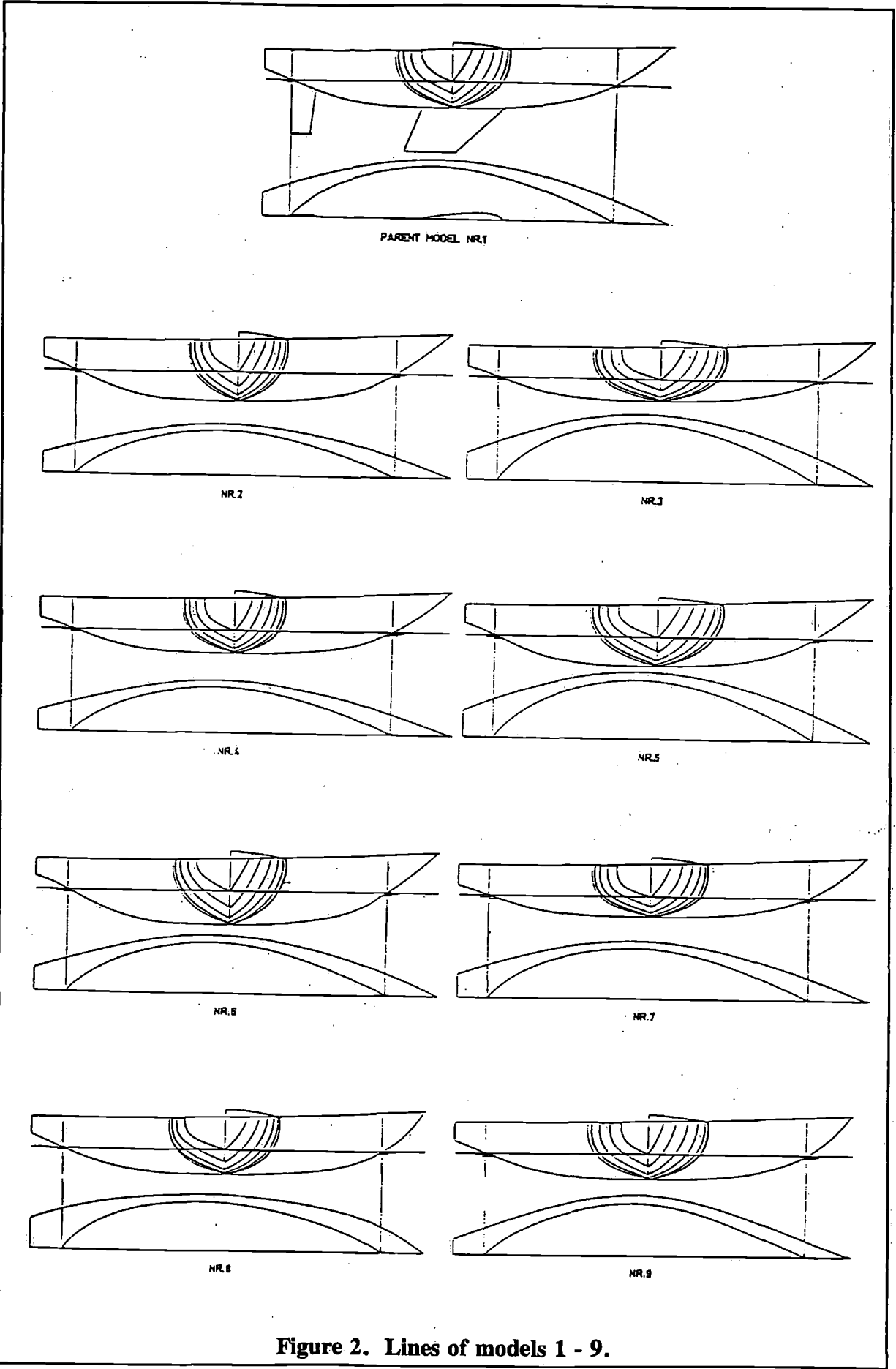


Figure 2. Lines of models 1 - 9.

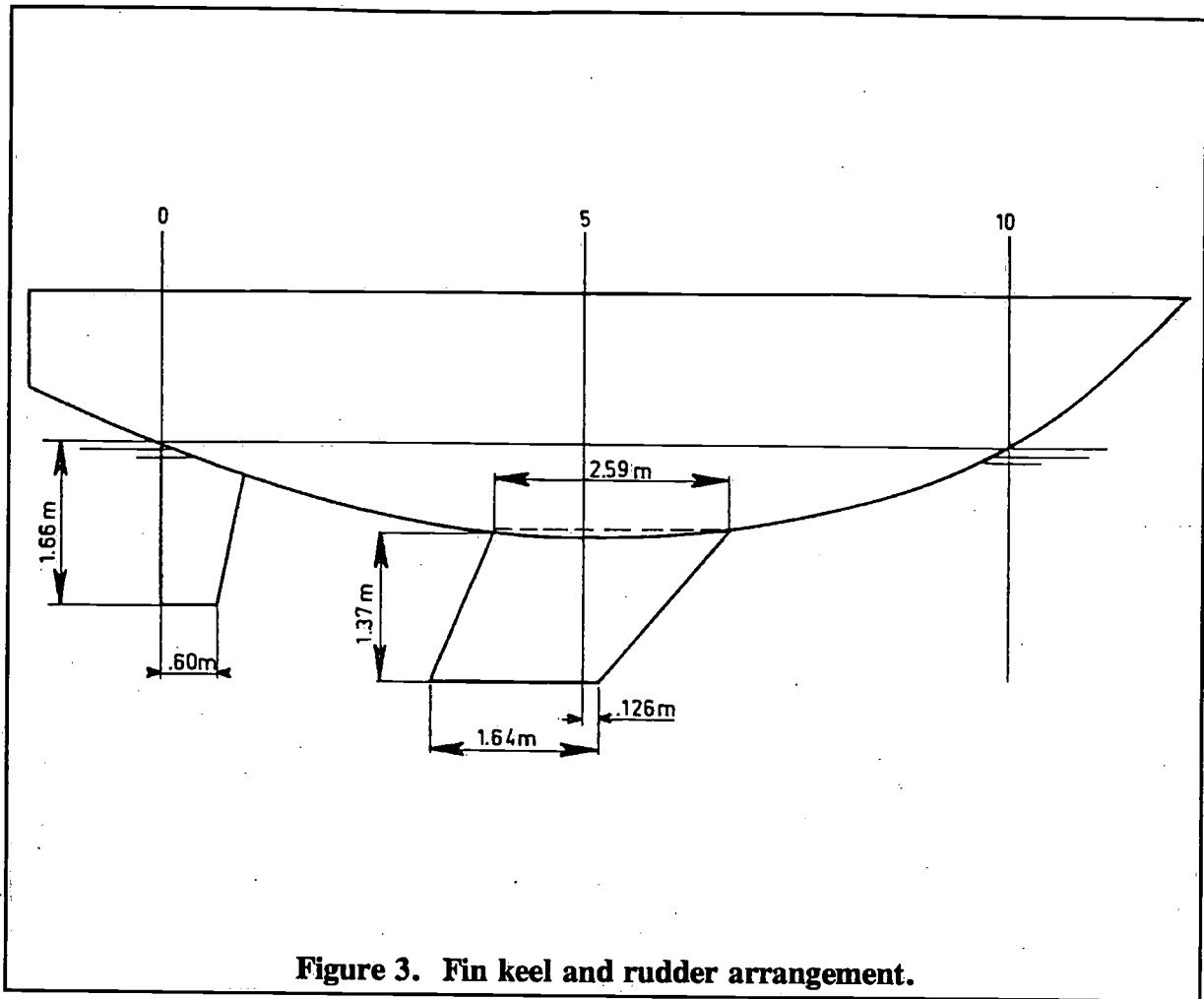


Figure 3. Fin keel and rudder arrangement.

Table IIa. Main dimensions and derived quantities

Nr.	L_{OA} m	L_{WL} m	B_{MAX} m	B_{WL} m	T_c m	D m	F m	∇_c m ³	S_c m ²	A_x m ²	A_w m ²
1	12.65	10.04	3.67	3.17	0.79	1.94	1.15	9.18	25.4	1.62	21.8
2	12.65	10.04	3.21	2.76	0.91	2.06	1.15	9.18	23.9	1.62	19.1
3	12.65	10.06	4.25	3.64	0.68	1.83	1.15	9.16	27.6	1.63	25.2
4	12.65	10.06	3.32	2.85	0.72	1.87	1.15	7.55	23.0	1.34	19.8
5	12.65	10.05	4.24	3.64	0.92	2.07	1.15	12.10	29.1	2.15	25.3
6	12.65	10.00	3.66	3.17	1.06	2.21	1.15	12.24	27.5	2.16	21.9
7	12.65	10.06	3.68	3.17	0.64	1.79	1.15	7.35	24.1	1.31	21.8
8	12.65	10.15	3.54	3.05	0.79	1.94	1.15	9.18	25.4	1.57	22.1
9	12.65	10.07	3.81	3.28	0.79	1.94	1.15	9.18	25.0	1.68	21.5

	Volume m ³	Wetted area m ²
keel	0.639	6.01
rudder	0.055	2.15
total	0.694	8.16

Tabel IIb. Main dimensions and derived quantities

Nr	I_T m ⁴	I_L m ⁴	LCF %	LCB %	KB^* m	BM^* m	KM^* m	KB^{**} m	BM^{**} m	KM^{**} m
1	12.89	113.2	-3.32	-2.29	0.53	1.40	1.93	0.45	1.30	1.75
2	8.64	99.2	-3.31	-2.29	0.60	0.94	1.54	0.56	0.87	1.43
3	19.88	131.1	-3.30	-2.31	0.45	2.17	2.62	0.38	2.02	2.40
4	9.60	102.8	-3.30	-2.32	0.48	1.27	1.75	0.39	1.16	1.55
5	19.99	131.2	-3.32	-2.44	0.61	1.60	2.21	0.55	1.51	2.06
6	12.85	113.2	-3.34	-2.38	0.71	1.05	1.76	0.64	0.99	1.63
7	12.85	109.8	-3.29	-2.31	0.43	1.75	2.18	0.34	1.60	1.94
8	12.66	120.6	-3.43	-2.37	0.53	1.38	1.91	0.45	1.28	1.73
9	13.21	105.3	-3.07	-2.19	0.52	1.43	1.95	0.45	1.33	1.78

* canoe body

** canoe body + keel + rudder

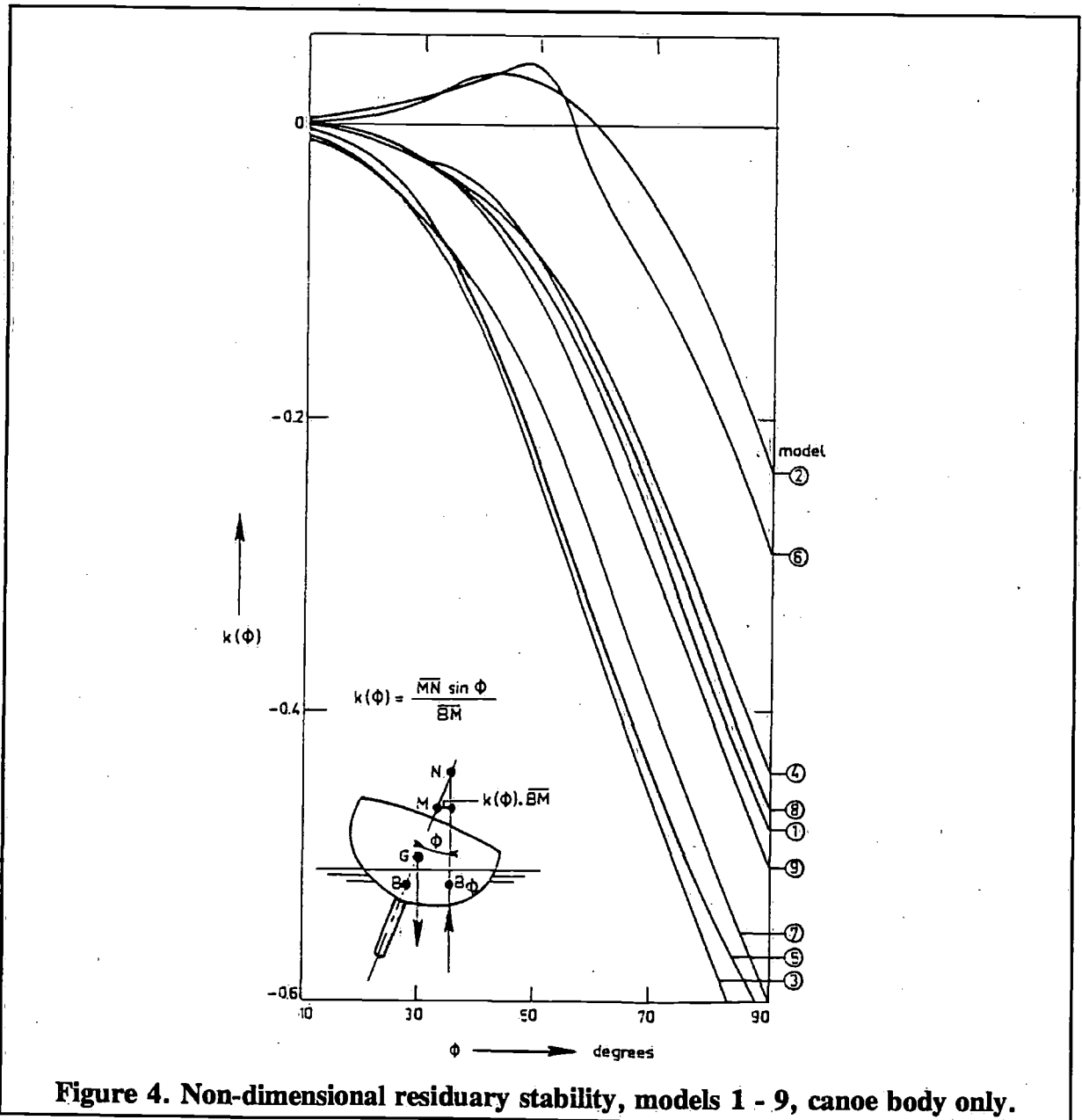


Figure 4. Non-dimensional residuary stability, models 1 - 9, canoe body only.

From Table IIB it may be concluded that the influence of the keel and rudder volume on the vertical position of the metacenter M is quite large. This influence should not be neglected in a calculation of the initial stability of a yacht.

The computed static stability for heel angles up to 90 degrees is given in dimensionless form in Figure 4, where the residuary stability $k(\phi)$ is plotted on a base of heel angle ϕ for each of the nine models.

The definition of the dimensionless residuary stability is given by:

$$k(\phi) = \frac{MN \sin \phi}{BM} \quad (1)$$

and the meaning of MN in this expression is clarified in Figure 4.

For geometric similar hull forms, which could have different dimensions, the arm of the static stability moment at a heel angle ϕ follows from:

$$GN \sin \phi = GM \sin \phi + k(\phi) BM \quad (2)$$

where GN and BM correspond to the considered dimensions of the yacht. The relative importance of the residuary stability $MN \sin \phi$ is shown in Figure 5a and 5b, where the stability curves of models 2 and 3 (narrow and wide) are compared, assuming realistic values for the height of the centre of gravity G . For model 2 the influence of the residuary resistance is not important, whereas for model 3 $MN \sin \phi$ is relatively large.

It is concluded that for detailed studies of a yacht's stability the determination of the initial stability ($GM \sin \phi$) is not sufficient. In particular for wide beam hulls the residuary stability is rather important. The effect of the yacht's own wave system is not considered in this static stability calculation.

3 Experimental set-up and test results

3.1 Experimental set-up

All models were constructed of GRP, corresponding to a linear scale ratio 6.25 and a waterline length of 1.6 m. This size, which implies an overall length of about 7 feet, fits the usual measuring apparatus of the Delft Ship Hydromechanics Laboratory and gives in combination with the applied turbulence stimulator an adequate guarantee for consistent test results. This turbulence stimulator consists of carborundum strips on hull, keel and rudder, which arrangement is shown in Figure 6. The carborundum has a grainsize 20 and is applied on the models with a density of approximately 10 grains/cm².

Upright resistance tests for model speeds of 0.5 m/s - 1.8 m/s (Fn 0.13 - 0.46) are carried out twice, with a "single" and a "double" sand strip to enable the extrapolation of the measured resistance values to zero sand strip width. It is then assumed that the extra resistance due to the sand strips varies with the speed squared and the strip width. Mean values of the resistance coefficients of the strips were determined in the middle of the tested speed range ($V = 1.0 - 1.6$ m/s) to avoid influence of special flow phenomena (laminar flow or wave-making).

All tests have been carried out in tank nr. 2 of the Delft Ship Hydromechanics Laboratory, which has a wetted cross section of 1.22 x 2.75 m.

In view of tank blockage effects the models 1, 6 and 7 have also been tested in tank nr. 1 (wetted cross section 2.55 x 4.22 m).

All resistance values, as measured in the small tank were corrected for blockage using the method given in [14] after checking the corrections with the tank nr. 1 results.

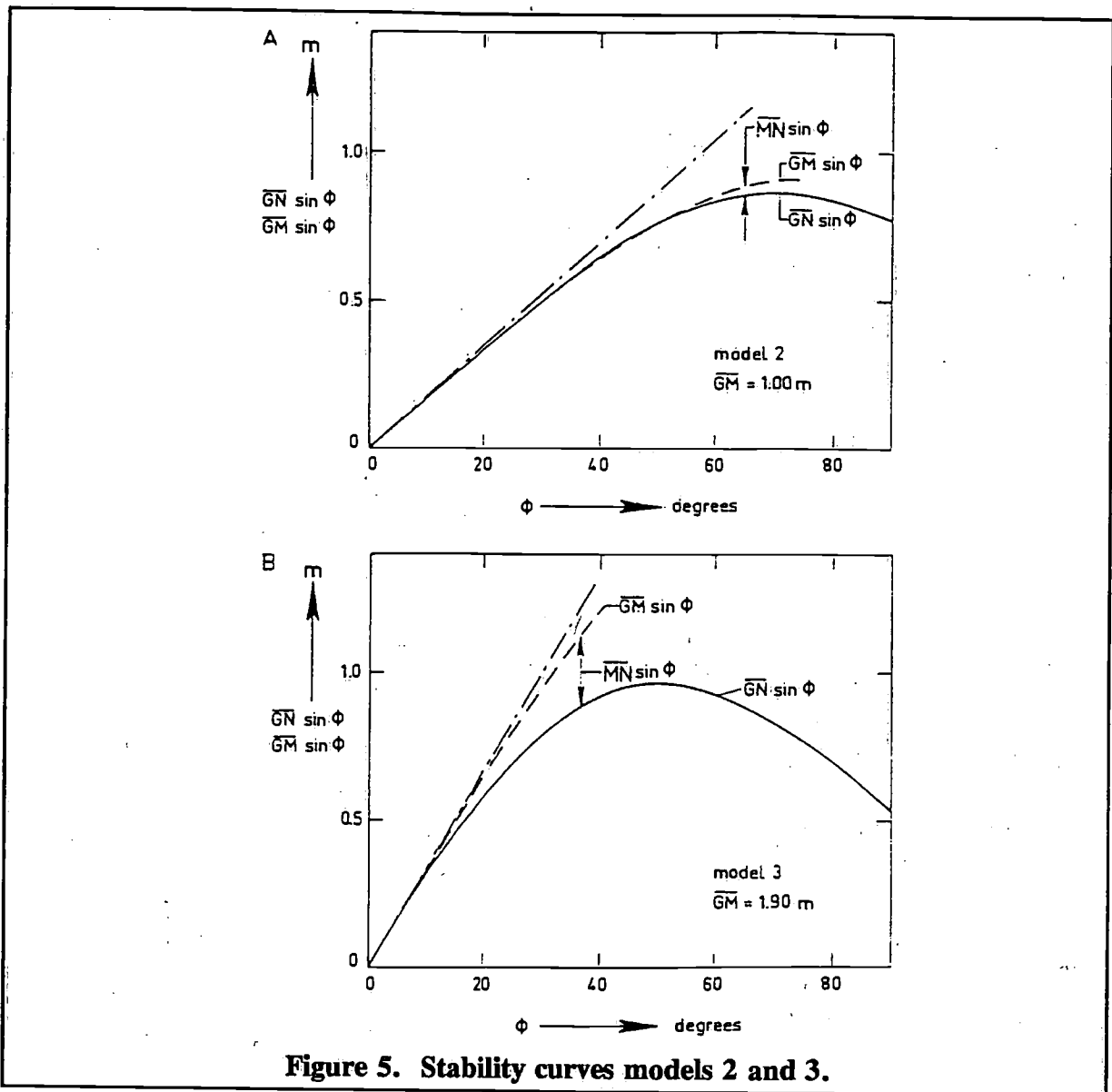


Figure 5. Stability curves models 2 and 3.

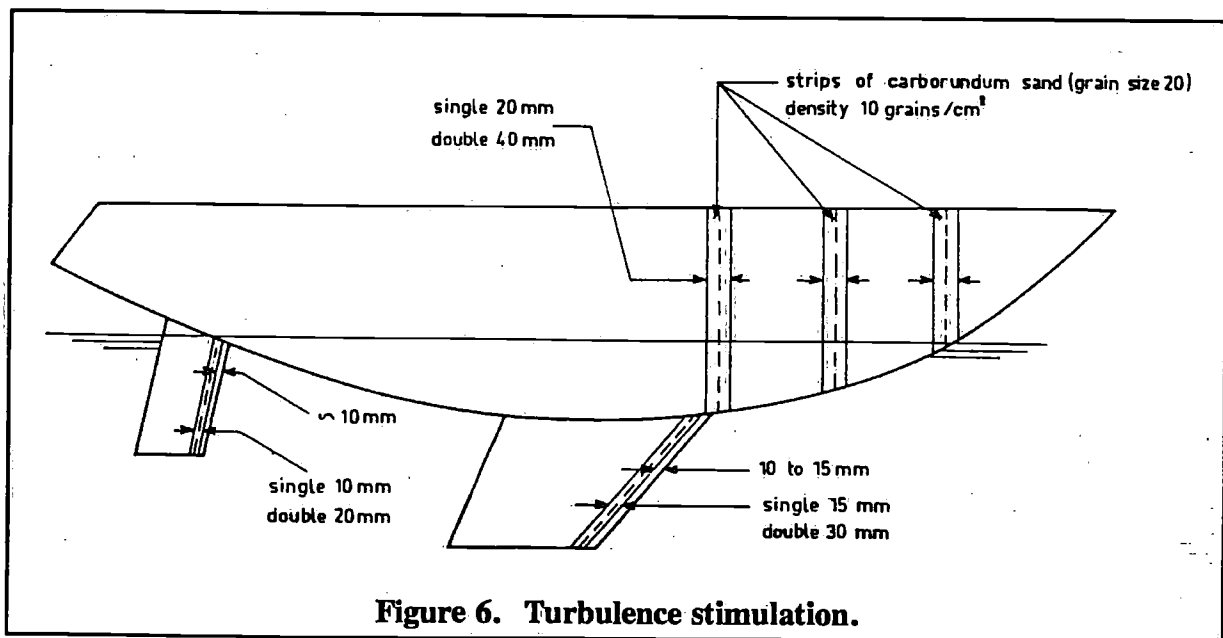


Figure 6. Turbulence stimulation.

In addition to the upright resistance tests, for each of the nine models heeled and leeway tests are carried out. Heel angles of 10, 20 and 30 degrees and leeway angles up to 10 degrees have been considered. Model speeds are chosen as 1.0, 1.2 and 1.4 m/s at 10 degrees, 1.2, 1.4 and 1.6 m/s at 20 and 30 degrees heel. With these combinations of variables all practical sailing conditions may be covered.

During the tests heel angles are the result of the side force due to leeway and forward speed and to a moment produced by a weight p to be shifted transversely over a distance t . This additional heeling moment is necessary first of all because the model is fixed sideways to measure the sideforce, and the locations where the reaction forces are measured do not correspond with the centre of effort of sailforces.

Secondly the model centre of gravity is not scaled down exactly from full scale size, which necessitates a correction for stability.

The additionally applied moment is varied in magnitude to allow for an analysis with various positions of the centre of sailforces (sail plan) and centre of gravity (stability).

3.2 Upright resistance

For each of the nine models the residuary resistance per ton displacement of the canoe body R_R/Δ_c is given in Table III as a function of Froude number $F_n = V/\sqrt{gL_{WL}}$. For this comparison only displacement of the canoe body is considered because the influence of keel and rudder on residuary (mainly wave-making) resistance is considered to be of minor importance. For geometric similar hull forms the residuary resistance is found from:

$$R_R = \frac{R_R}{\Delta_c} \cdot \Delta_c \quad (\text{kgf.}) \quad (3)$$

where: Δ_c = the displacement of the canoe body.

The corresponding speed is:

$$V = F_n \cdot \sqrt{gL_{WL}} \quad (4)$$

where: g = 9.81 m/s.

L_{WL} = nominal length of waterline in m.

To find the total resistance R_T the frictional resistance R_F is added,

$$R_T = R_R + R_F \quad (5)$$

For yachts with separated fin keel and rudder the frictional resistance is found as the summed contributions of canoe body, keel and rudder:

$$R_F = \frac{1}{2} \rho V^2 (S_c C_{F_c} + S_k C_{F_k} + S_r C_{F_r}) \quad (6)$$

where: S_c , S_k and S_r are wetted area of canoe body, keel and rudder respectively C_{F_c} , C_{F_k} and C_{F_r} is frictional resistance coefficient for respective parts.

ρ = density of water at 15° C
 = 101.87 kgm⁻¹s² for fresh water
 = 104.61 kgm⁻¹s² for salt water

The frictional resistance coefficient is calculated according to the definition by the International Towing Tank Conference 1957.

$$C_F = \frac{0.75}{(\log R_n - 2)^2} \quad (7)$$

where the Reynolds number is calculated for canoe body, keel and rudder as respectively:

$$R_{n_c} = \frac{V \cdot 0.7 L_{WL}}{\nu}$$

$$R_{n_k} = \frac{V \cdot \bar{C}_k}{\nu} \quad (8)$$

$$R_{n_r} = \frac{V \cdot \bar{C}_r}{\nu}$$

with: $\nu = 1.1413 \times 10^6$ for fresh water of 15° C

$\nu = 1.1907 \times 10^6$ for salt water of 15° C

\bar{C}_k and \bar{C}_r are the average chord length of keel respectively rudder in m.

The factor 0.7 in the definition of the Reynolds number for the canoe body allows for the particular profile and waterline shape of a yacht and gives a kind of average wetted length. The data in Table III is obtained from measurements being corrected for the effects of sand strips and tank blockage.

Table III. Residuary resistance per ton hull displacement

F_n nr	R_R / Δ_o kg / ton								
	1	2	3	4	5	6	7	8	9
0.127	0.12	0.05	0.10	0.20	0.17	0.14	0.29	0.21	0.16
0.153	0.29	0.19	0.32	0.37	0.24	0.28	0.47	0.41	0.34
0.178	0.50	0.40	0.59	0.69	0.37	0.46	0.74	0.68	0.58
0.203	0.82	0.70	0.92	0.97	0.58	0.76	1.12	1.01	0.90
0.229	1.26	1.13	1.40	1.43	0.93	1.19	1.66	1.44	1.31
0.254	1.94	1.69	2.12	2.09	1.43	1.83	2.36	2.11	1.86
0.267	2.36	2.05	2.57	2.50	1.84	2.18	2.84	2.57	2.24
0.280	2.79	2.52	3.19	2.98	2.30	2.72	3.25	3.16	2.66
0.292	3.38	2.97	3.85	3.56	2.84	3.20	3.73	3.88	3.12
0.305	3.99	3.50	4.47	4.20	3.37	3.72	4.35	4.64	3.67
0.318	4.61	4.16	5.10	4.75	4.16	4.35	5.23	5.33	4.35
0.330	5.30	4.99	6.01	5.56	4.92	5.07	6.27	6.16	5.23
0.343	6.38	6.24	7.30	6.92	6.07	6.27	7.53	7.31	6.45
0.356	7.99	7.99	9.20	8.81	7.91	8.02	9.05	8.78	8.33
0.369	10.51	10.45	11.70	11.19	10.26	10.57	11.35	10.85	11.04
0.381	13.55	13.79	14.96	14.55	13.83	14.21	14.43	13.62	14.71
0.394	17.89	18.52	19.15	18.76	17.95	18.85	18.32	17.25	19.51
0.407	23.04	24.46	24.26	24.07	23.70	25.07	23.21	21.75	25.25
0.419	29.31	31.39	30.48	30.38	30.40	32.66	29.23	27.21	32.09
0.432	37.05	39.42	37.86	37.79	38.89	41.27	36.15	33.67	40.01
0.445	45.88	48.31	46.43	46.21	48.10	51.58	44.03	41.24	49.18
0.458	55.45	57.33	55.89	55.51	59.21	62.55	52.74	49.60	59.73

As an example the total and residuary resistance of model 4 are given in dimensionless form in Figure 7 to show the relative importance of the resistance components. At a Froude number $F_n = 0.35$, which is approximately the maximum speed in the close-hauled condition the frictional and residuary resistance are about equal in magnitude.

To compare the upright resistance of the hull form variations Figures 8a, b, c and d give the total resistance in upright condition for a waterline length $L_{WL} = 10$ m.

Four groups are considered:

Figure 8a compares the parent model with models 2 and 3 (equal displacement, narrow and deep versus wide and shallow).

Figure 8b compares models 1, 4 and 5 (equal B_{WL}/T_c , medium, light and heavy displacement)

Figure 8c compares models 1, 6 and 7 (equal L_{WL}/B_{WL} , medium, heavy and light displacement)

Figure 8d compares models 1, 8 and 9 (medium, high and low prismatic).

The Figures show the primary importance of the length-displacement ratio with regard to resistance (models 4, 5, 6 and 7), the relatively small influence of the beam-draught ratio and the beneficial effect of a high prismatic coefficient at speeds above $6\frac{3}{4}$ knots for the considered length of waterline.

Table III and equations 3 - 8 enable the determination of the upright resistance of geometric similar yacht forms of given dimensions.

Within the range of variation the data can be used for systematic studies of yacht hull resistance.

3.3 Sideforce and leeway

In any asymmetrical position the hull, keel and rudder develop a sideforce due to hydrodynamic action.

The dominant parameter in this respect is the leeway angle β , but also the heel angle ϕ and the rudder angle are causing sideforces, of which the horizontal component is denoted by $F_H \cos \phi$, (see Figure 9).

Although the rudder angle is important in this respect [13] this parameter is not considered here, because the object of the systematic series is to study the influence of hull form variations only.

In Figure 10a plot has been made of model sideforce versus leeway angle for heel angles 10, 20 and 30 degrees and model speeds respectively 1.2 m/s, 1.4 m/s and 1.6 m/s (corresponding to Froude numbers: 0.30, 0.35 and 0.40). These speeds are somewhat higher than optimal sailing speeds in the close-hauled condition, but the figures may serve to illustrate some general conclusions regarding the ability to generate sideforces for each of the nine models. However it should be remembered that all models had the same fin keel and rudder.

Figure 10c shows that model 6 (heavy displacement, deep hull) needs approximately half the leeway angle at equal sideforce as compared with model 3 and 7. Both nr. 3 and 7 have a large beam-draught ratio. A good deal of the difference is due to the zero sideforce leeway angle, which is large for the hulls with a large beam-draught ratio. Apparently the large B_{WL}/T_c hull has a larger asymmetry when heeling. The corresponding sideforce due to the hull is directed to the leeside of the yacht in all of the considered cases.

Figure 10 shows that the slope of the lines $d(F_H \cos \phi)/d\beta$ increases with increasing draught of the canoe body.

The data indicate that in the considered range of leeway angles a linear relation between

sideforce and leeway angle exists at constant forward speed and heel angle. Within practical limits, the sideforce varies as V^2 at constant leeway and heel angle, as suggested by Kerwin [13].

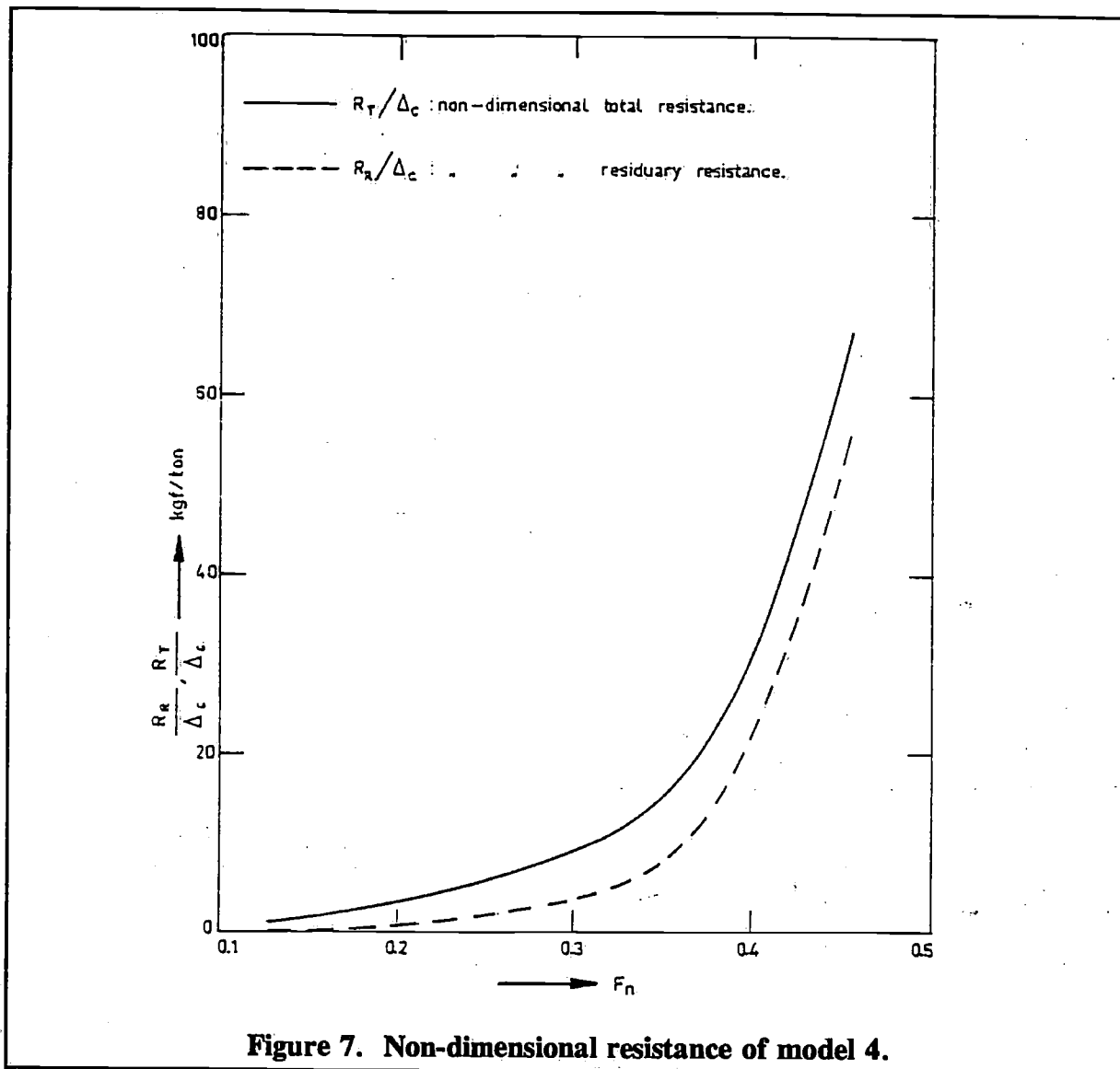


Figure 7. Non-dimensional resistance of model 4.

Measurements of sideforce and resistance at various leeway angles but zero heel are carried out for all nine models at speeds corresponding to Froude numbers of 0.20 and 0.35.

Although in the ocean sailing practice side-force is commonly associated with both leeway and heel, these tests may provide useful basic information on sideforce production.

A plot of measured sideforce versus leeway angle represents the lift curve of the complete underwaterbody. Its slope in the origin, which indicates the effectiveness of sideforce production, is given for all nine models in Table IV. The values are made non-dimensional by dividing by $\frac{1}{2}\rho V^2 L_{WL}^2$.

In confirmation of the statements above the most effective sideforce production, e.g. the steepest sideforce curve, may be expected with the deepest draughts. The slight speed dependency is caused by the corresponding generated wave systems.

In Table IV the experimental values are compared with calculations according to a method introduced by Gerritsma [16]. This method is valid for fin keel and rudder yachts and is based on a virtual extension of keel and rudder to the waterline as shown in Figure 11, after

which aerodynamic theories may be applied on both fins. The extensions are assumed to represent the contribution of the hull. A graphical comparison of experimental and calculated values in Figure 11 shows that the method gives useful predictions. The root mean square relative error of the prediction is 4.4 % and 4.5 % for Froude number .20 and .35 respectively.

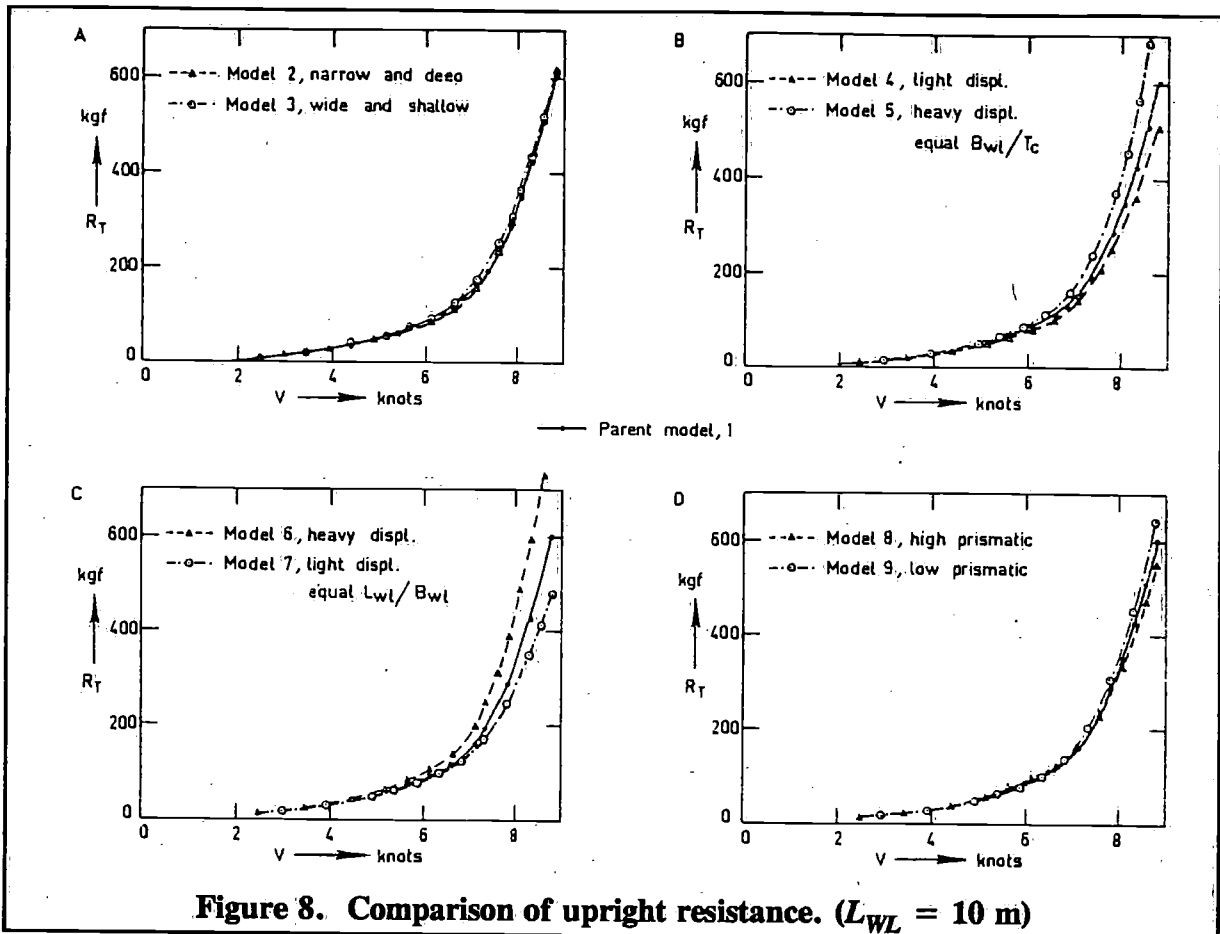


Table IV. Calculated and measured side force curve slopes

Nr.	T (m)	$Y'_B \cdot 10^5$		
		measured		calculated
		$F_n = .20$	$F_n = .35$	
1	2.16	12400	12400	12630
2	2.28	12700	12800	13654
3	2.05	11800	12300	11618
4	2.09	11400	11600	11962
5	2.28	13000	13600	13688
6	2.43	14500	15500	15118
7	2.01	10800	11200	11260
8	2.16	12800	13600	12630
9	2.16	12450	13150	12630

$$Y'_\beta = \frac{dF_H}{d\beta} / \frac{1}{2} V^2 L_{WL}^2$$

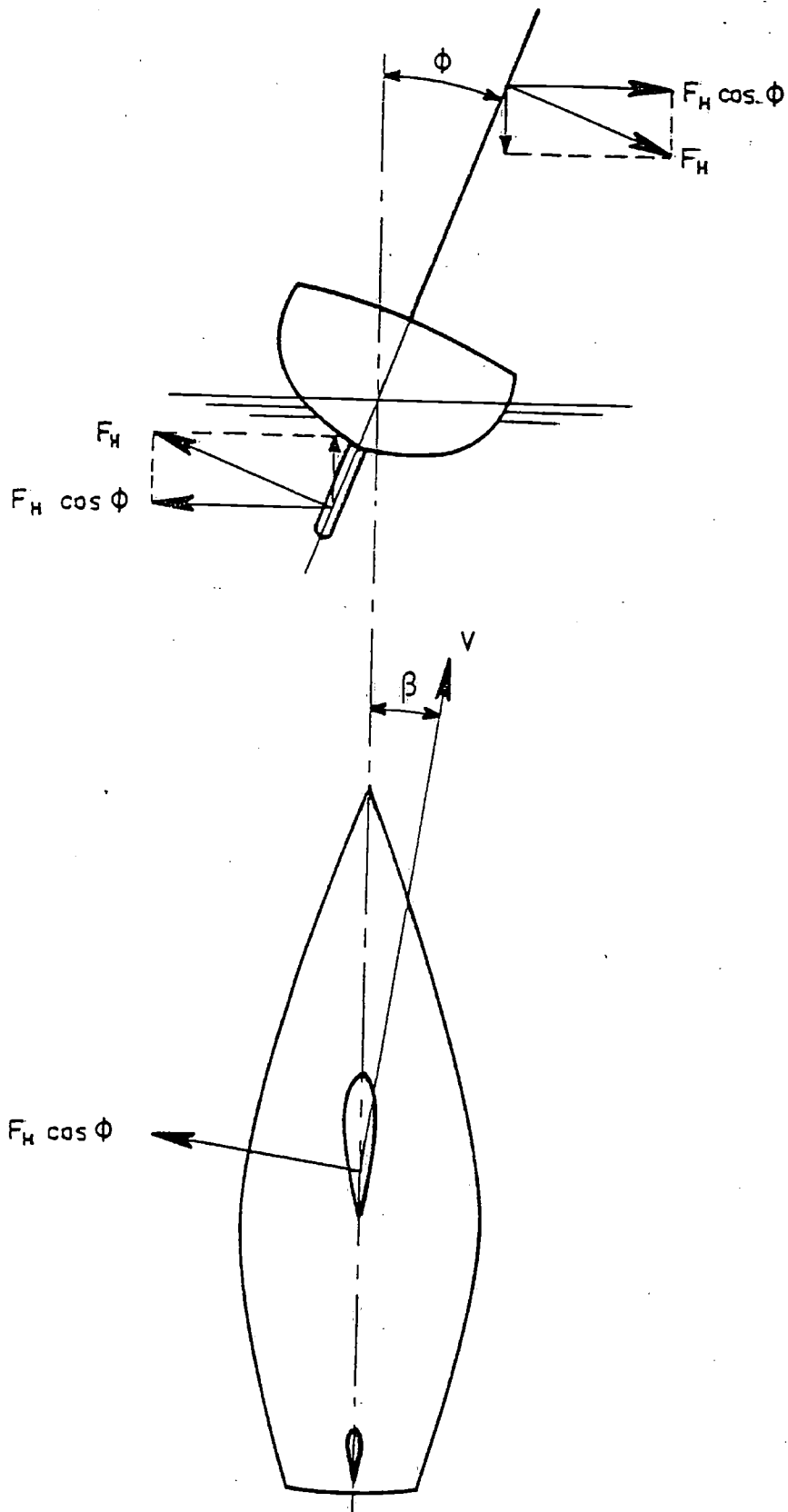


Figure 9. Sideforce and sailforce

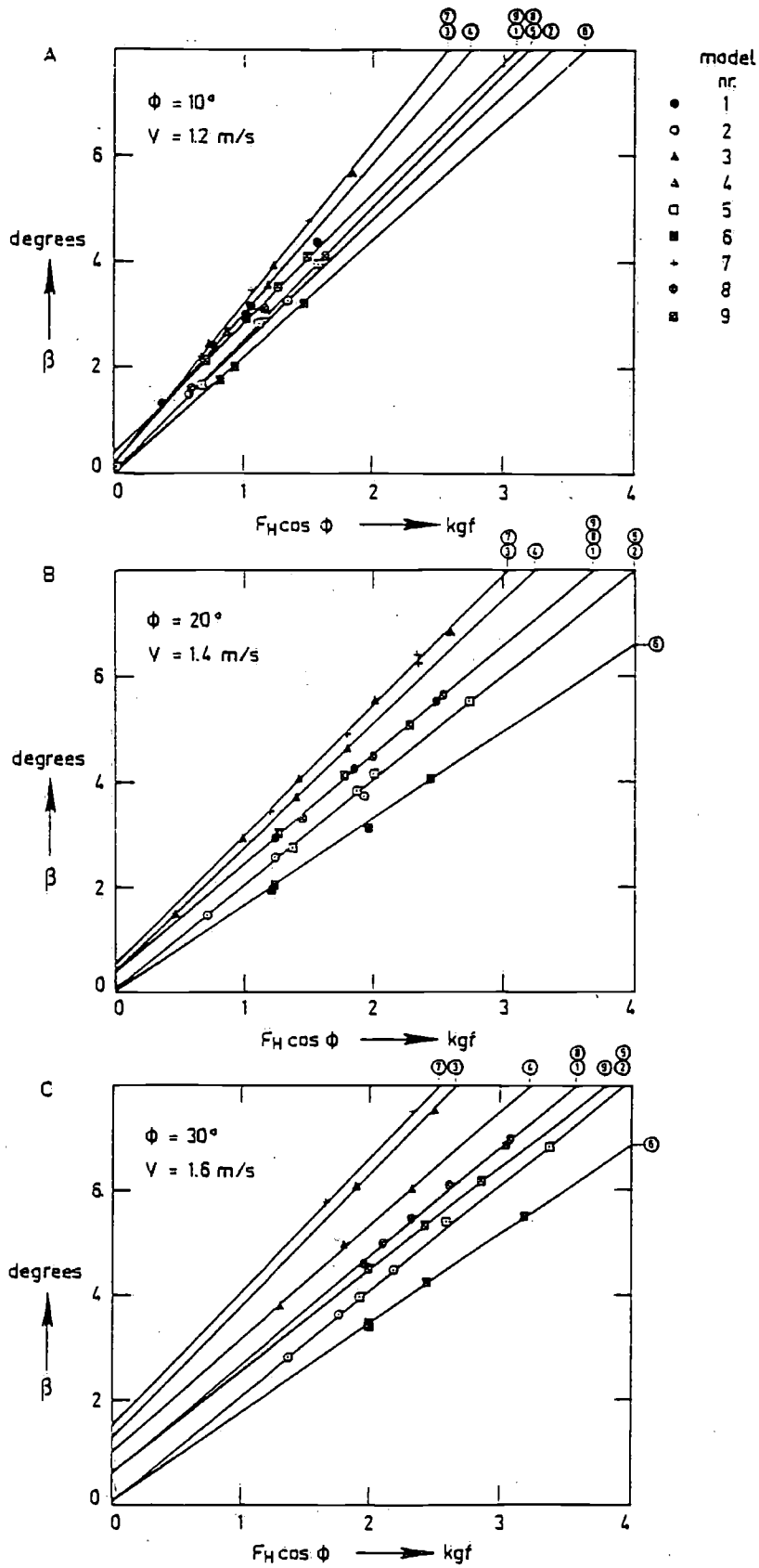


Figure 10. Sideforce versus leaway (model values).

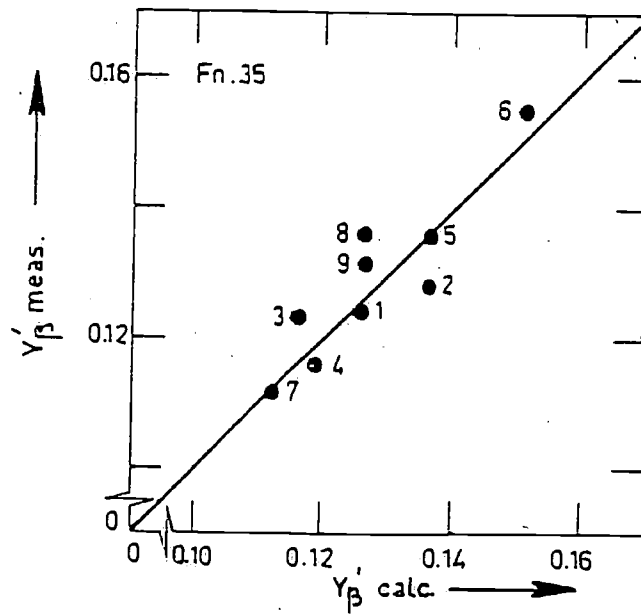
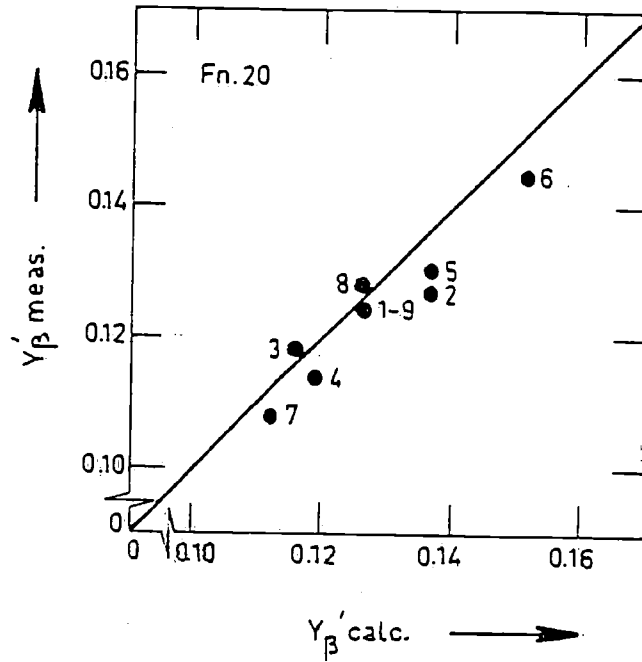
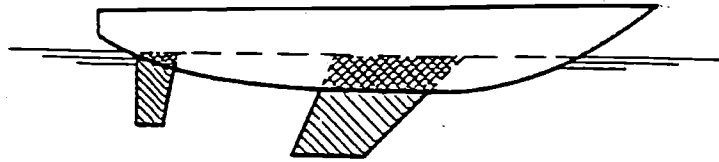


Figure 11. Calculated and measured sideforce curve slopes.

3.4 Heeled and induced resistance

In addition to the upright condition, a sailing yacht experiences an extra resistance force due to heel and sideforce. This resistance component is important as shown by the analysis of model test data. For instance at the maximum attainable close-hauled yachtspeed (approximately: $F_n = 0.35$) the frictional-, residuary- and heeled + induced resistance are roughly equal in magnitude. On other courses and forward speeds the relative importance of the various resistance components is different.

The heeled resistance can be defined as the extra resistance at zero sideforce, although as shown in Figure 10, this condition requires a leeway angle to counteract the sideforce produced by the asymmetrical immersed part of the hull. Following this definition the heeled resistance and the resistance induced by the sideforce can be distinguished in Figure 12 for the case of a thirty degrees heel angle with:

$$R_\phi - R_T = R_H + R_i \quad (9)$$

where: R_ϕ = total resistance with heel and leeway angle
 R_T = total resistance in upright position
 R_H = heeled resistance at zero sideforce
 R_i = induced resistance due to leeway

The highest values for the heeled and induced resistance are found for models 3 and 7 (both shallow hull forms) and the lowest values correspond with the largest draught (model 6). The differences between the highest and the lowest values are significant in the considered case ($\phi = 30^\circ$, $V = 1.6$ m/s, model value). Apparently this is due to the differences in the effective aspect ratio of the combination of keel + rudder + underwater part of the hull, which varies from model to model due to variations in hull form. From airfoil theory the following relation between the induced resistance and the lift is known:

$$C_{D_i} = \frac{C_L^2}{\pi AR_E} \quad (10)$$

where: AR_E - the effective aspect ratio of the wing. For the present purpose this can be written as:

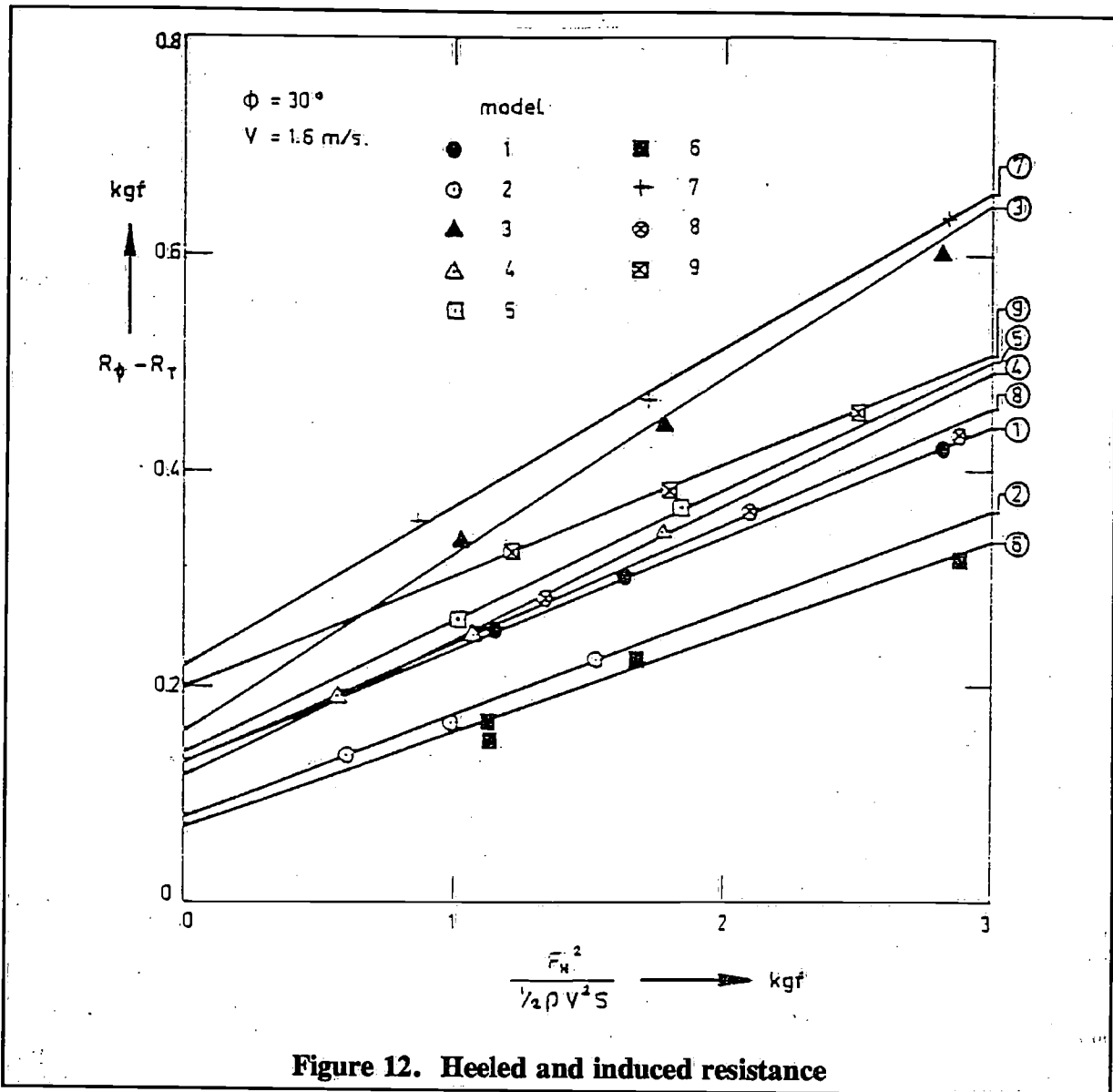
$$R_i = \frac{F_H^2}{\frac{1}{2}\rho V^2 S \cdot C} \cdot f(\phi) \quad (11)$$

where: S - the total wetted surface or a representative area of hull, keel and rudder combination.

In [13] Kerwin suggested for $f(\phi)$:

$$f(\phi) = C_1 + C_2\phi^2 \quad (12)$$

where C_1 and C_2 are constants to be determined from the experiments. To show the relation between the heeled and induced resistance versus sideforce as indicated by equations (9) and (11), the extra resistance $R_\phi - R_T$ is plotted on a base of $F_H^2 / \frac{1}{2}\rho V^2 S$ in Figure 12.



4. Sailing performance

4.1 Determination of sailplan and stability

To predict sailing performance stability and sailplan must be determined for each model in a systematic way and matched consistently to the given hull dimensions.

The following method has been chosen:

a) Hull weights, including crew and equipment, are calculated with

$$W_H = C_H \cdot L \cdot B_{MAX} \cdot D$$

where:

- C_H is a constant, for which a value of 65 represents current construction methods, materials and crew size
- L is length in m, taken as the average of overall length and waterline length (resp. 12.65 m and 10.00 m for all models).
- B_{MAX} is maximum breadth
- D_H is depth of the hull, which equals the constant freeboard (1.15 m) plus the draught of the canoe body.

The centre of gravity of hull weight (including crew) is assumed to be at 80% of the depth above the base line and in the centre plane of the ship. So in the stability calculations no allowance is made for asymmetric crew positions.

- b) The available weight for ballast is obtained by subtracting the estimated hull weight from the given weight of displacement. It is cast as lead into the keel, assuming a specific weight of 11000 kg/m³. Thus it fills up to a certain height and gives the position of the centre of gravity of ballast.
- c) The position of the total centre of gravity is obtained by adding hull and ballast parts. Stability moments are calculated.
- d) Basic proportions of the sail plan as indicated in Figure 13 are assumed. Though these assumptions are in fact arbitrary they reflect the actual design practice on a base of IOR regulations and may thus represent common yachts.
- e) Maintaining the proportions mentioned under "d" the mast height is varied in such a way that the ratio of heeling moment to stability moment at 30° heel is equal for all ships. This ratio is represented by:

$$SR = \frac{SA \cdot h}{(RM)_{\phi} = 30^{\circ}} \quad (13)$$

with: $SA = \frac{1}{2} \cdot I \cdot J + \frac{1}{2} \cdot P \cdot E$
 $h = Z_{CE} + 0.4 \cdot T_T$

where: SA = represents sail area to windward
 h = represents the arm of heeling moment
 I, J, P, E are sail dimensions according to Figure 13
 Z_{CE} = height centre of effort of sail area SA above the waterline
 T_T = total draught

For the present analysis the value of SR has been chosen as 10.

The heel angle of 30° has been selected because this value is often encountered in conditions where stability becomes an important factor to performance.

Results of the above calculations are shown in Table V for weight and stability and in table VI for sail dimensions and derived parameters. The resulting ballast ratios (Table V) have normal values. The position of the centre of gravity is in some cases probably a bit low compared to normal practice. This may be caused by the wide variations in total draught, due to the use of a standard keel under different hull shapes. This is contrary to the standard total draught stimulated by the IOR.

The obtained sail plans have normal dimensions. It must be noted that the effective sail areas downwind and to windward, as given in Table VI, are calculated different from the area SA used above, though they are linearly related to SA .

The downwind area SA_{ed} consists of mainsail and spinnaker and is estimated as:

$$SA_{ed} = 1.4 \cdot I \cdot J + \frac{1}{2} \cdot P \cdot (E + HB) \quad (14)$$

where: HB = standard breadth of mainsail headboard.

The sail area to windward consists of mainsail area, neglecting roach, plus the area of a standard IOR 150% genoa.

Table V. Weight and stability data

Nr.	BR %	Z_G m	GM m	RM at $\phi = 1^\circ$ kgm	RM at $\phi = 30^\circ$ kgm
1	47	-0.34	1.30	224	6095
2	51	-0.48	1.00	173	4915
3	42	-0.19	1.90	327	7873
4	44	-0.29	1.12	161	4376
5	49	-0.40	1.54	343	9492
6	54	-0.56	1.14	256	7026
7	40	-0.15	1.45	204	4682
8	49	-0.38	1.32	227	6223
9	45	-0.30	1.29	222	5966

BR = Ballast Ratio

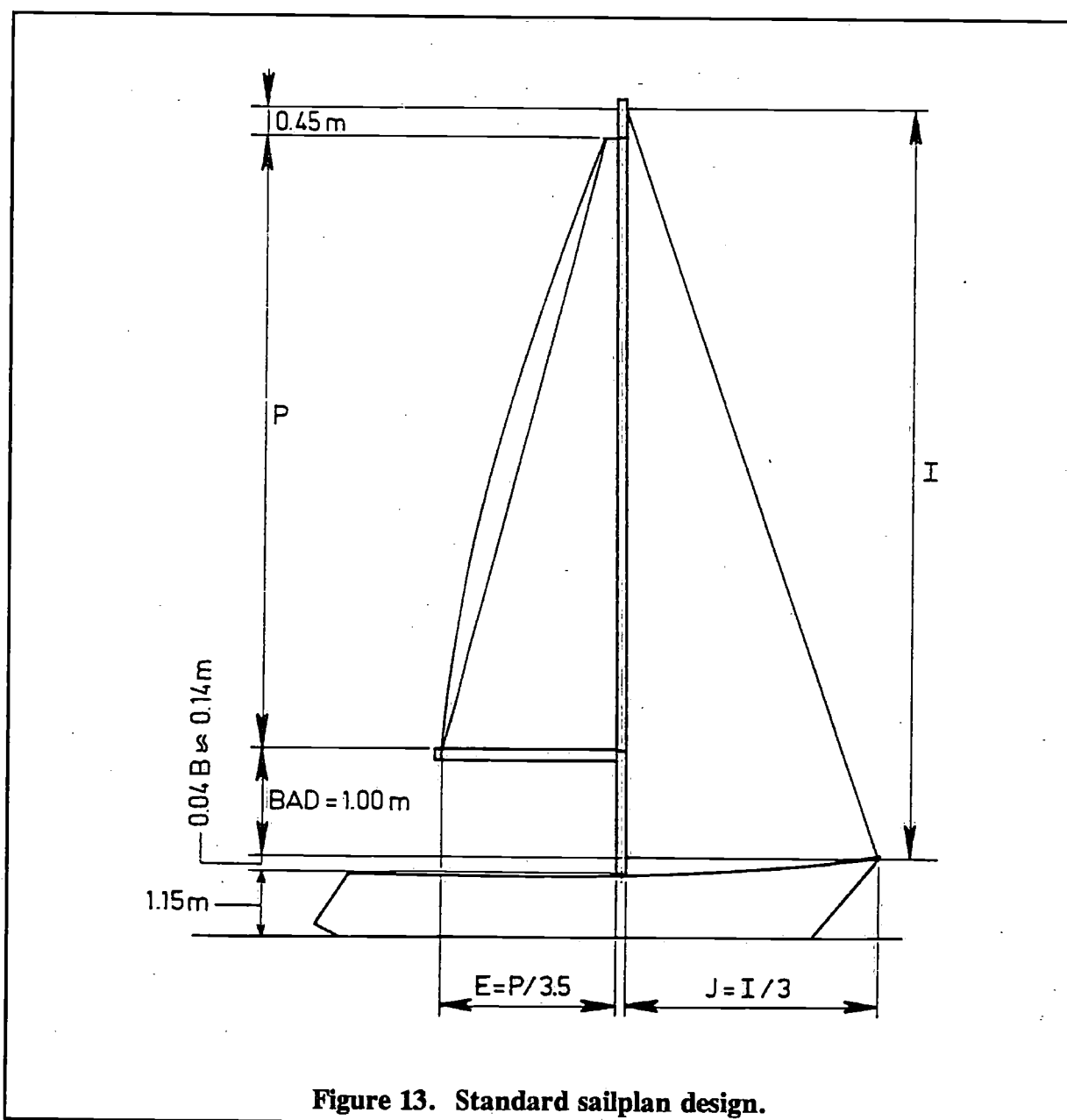


Figure 13. Standard sailplan design.

Although height and area of the rigs are selected in a fixed relation to stability moment, the sail area to wetted area and sail area to displacement ratios still vary considerably. The light models 4 and 7, with low ballast ratios and according low positions of the centre of gravity, have a small sail area compared to wetted area.

A low stability moment due to a small breadth, like with model 2, results also in a relatively under canvassed boat.

Contrary, a wide hull, when combined with a normal or heavy displacement, like model 3 and 5 results in relatively large rigs.

Finally the rating of the resulting designs has been calculated, assuming an equal engine weight and position and equal propeller dimensions and immersion. From Table VII it appears that the rating of this series covers a margin of abt 4 feet, which is appreciable for ships with equal length.

Table VI. Sail dimensions

Nr.	<i>I</i> m	<i>J</i> m	<i>P</i> m	<i>E</i> m	SA_{ed} m ²	SA_{eb} m ²	Z_{CB} m	$(SA_{ed} / S)^{1/2} \cdot$	$(SA_{ed} / \Delta^{1/3})^{1/2} \cdot$
1	16.47	5.49	15.02	4.29	159.8	104.7	6.99	2.18	5.89
2	15.23	5.08	13.78	3.94	136.3	89.1	6.56	2.06	5.44
3	18.07	6.02	16.62	4.75	192.9	126.7	7.55	2.32	6.48
4	14.64	4.88	13.19	3.77	125.6	82.1	6.36	2.01	5.55
5	19.24	6.41	17.79	5.08	219.2	144.0	7.95	2.43	6.33
6	17.27	5.76	15.82	4.52	176.1	115.5	7.26	2.22	5.65
7	15.02	5.01	13.57	3.88	132.5	86.6	6.50	2.03	5.74
8	16.61	5.54	15.16	4.33	162.6	106.6	7.04	2.20	5.94
9	16.34	5.45	14.89	4.25	157.3	103.0	6.95	2.18	5.84

*) The ratios of windward sail area to wetted area and displacement are proportional to the downwind sail area ratios

Table VII. Rating parameters

Nr.	<i>MR</i> m	<i>R</i> ft	<i>TMF</i>
1	10.62	34.2	1.0646
2	10.05	33.2	1.0528
3	11.40	36.7	1.0930
4	10.09	32.5	1.0443
5	11.17	36.3	1.0886
6	10.48	34.9	1.0727
7	10.30	32.9	1.0492
8	10.73	35.6	1.0807
9	10.33	33.1	1.0516

4.2 Downwind speed

The downwind speed is calculated from the upright resistance tests, assuming a drag coefficient for the sails of 1.2. Furthermore it is assumed that sailing downwind does not give heel and does not necessitate a rudder angle.

The results are given in Figure 14. To show the additional influence of sail area above the resistance as shown in Figure 8, the different models are grouped in the same way.

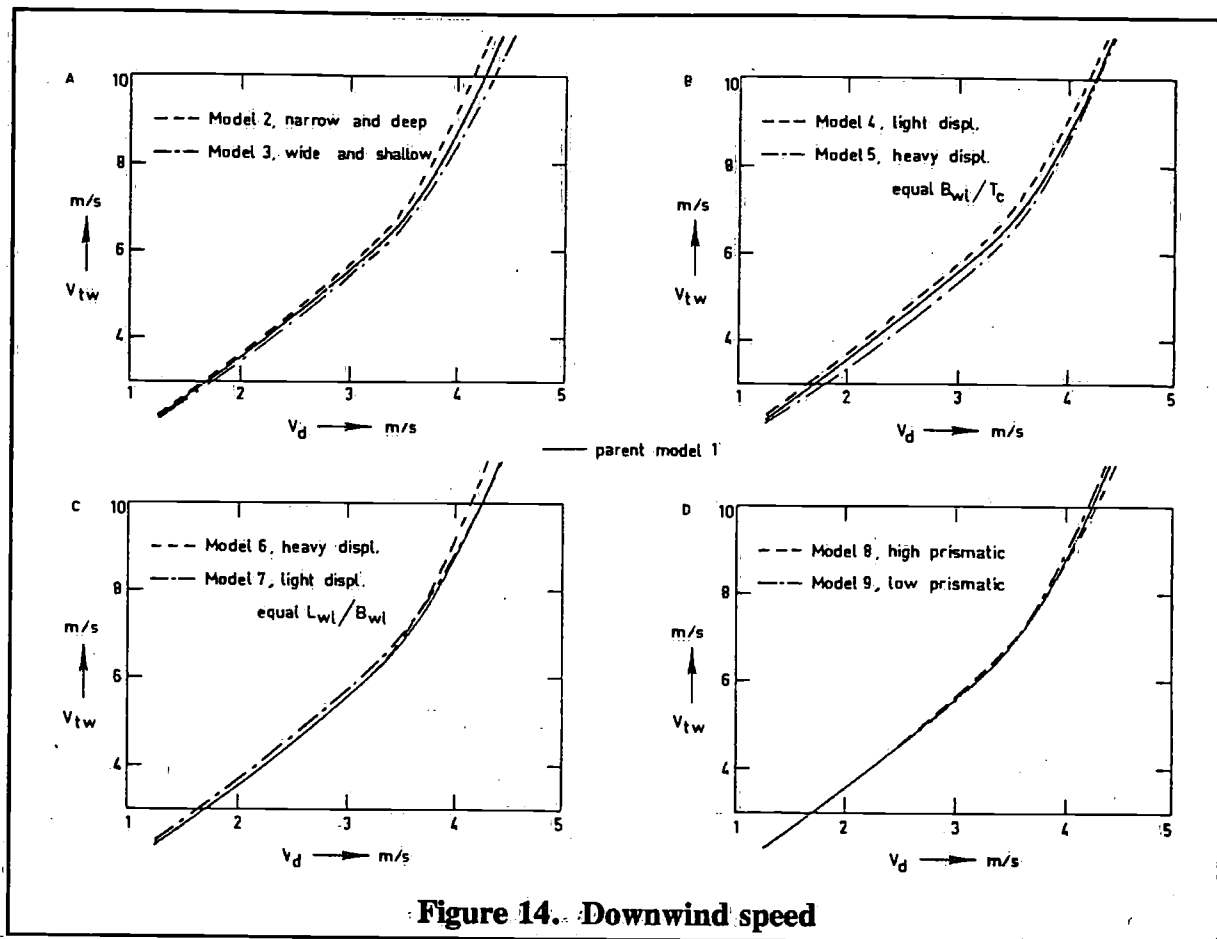


Figure 14. Downwind speed

While the resistance of models 1, 2 and 3 (Figure 8a) is nearly equal, the downwind speed differs greatly due to the difference in sail area. As said before model 2 has less sail area because its narrow beam and according low initial stability does not permit to carry more sail to windward.

The beamy model 3 is just the opposite.

A comparison of models 1, 4 and 5 shows again the important effect of sail area. Though the light displacement model 4 has less resistance than 1 and 5, its downwind speed is still lower than the others because its more strongly reduced sail area.

According to Figure 14c the difference in resistance between models 1, 6 and 7, as observed in Figure 8c is apparently better compensated by sail area than the foregoing combinations. The improving performance of the light displacement yacht with increasing wind speed, and the reversed characteristics of the heavy boat may be noted.

As shown in Figures 8d and 14d the influence of prismatic coefficient is of second order, at least if otherwise hull dimensions and displacement are comparable.

However, the slightly favourable effect of a high prismatic at higher boat speed and wind velocity is noticeable from both Figures.

If downwind speed as related to resistance is compared with the sail area-wetted area and sail area-displacement ratios from Table VI, it may be concluded that high ratio values favour the downwind performance. As may be obvious the sail area - wetted area ratio greatly governs the lower wind speed range, while the sail area-displacement ratio may indicate the downwind speed at higher wind speeds.

4.3 Speed-made-good to windward

The speed-made-good to windward of all 9 models is calculated according to Davidson's method [1], using the Gimcrack sail coefficients.

However, as a result of recent investigations [13] the Gimcrack coefficients are applied to the geometric area of mainsail and genoa, including overlap, instead of the reduced effective area proposed by Davidson. This modification takes into account the improvements in sail cloth and rig design during the last decades and gives a better prediction of heeling angle without affecting the qualities of Davidson's method.

The results of the calculations are shown in Figure 15, arranged conform Figures 8 and 14. The influence of sail area and stability on windward performance above that of hydrodynamic resistance and sideforce properties may be indicated by comparing these figures.

Figure 15a presents the characteristic differences between speed-made-good curves of a narrow and deep respectively wide and shallow hull.

At lower wind speeds, if only a moderate sideforce production is required, resistance and driving force characteristics are dominant. So in this case the beamy model 3 with its large sail area attains the highest speeds, both to windward and downwind. The narrow model 2 may still be considered as under-canvassed in these conditions.

When wind speed increases the balance between stability and heeling moment and the efficiency of sideforce production becomes more important. As discussed in paragraphs 3.3 and 3.4 the deep draught model 2 requires smaller leeway angles to generate a prescribed sideforce (Figure 10c) than the shallow model 3, and does this with much less resistance increase (Figure 11). From these hydrodynamic characteristics it may be expected that at high wind speeds model 2 is better than model 3 as shown in Figure 15a. In the case of extreme wide and shallow hulls large drops in windward performance may occur with increasing wind speed and heel angle.

With respect to models 2 and 3 it must be remarked that in practical designs model 2 should be equipped with a somewhat smaller keel, to reduce wetted area and model 3 with a more extended keel, to improve sideforce production.

Figure 15b demonstrates that the differences which models 4 and 5 show in downwind conditions are likely retained when sailing to windward. This must be largely due to maintaining a constant breadth-draught ratio when varying displacement. This results in a comparatively low stability for the light model 4, combined with a relatively low sail area as a consequence of the design rules given in paragraph 4.1. The heavy model 5 has just opposite characteristics. Besides, the shallow draught of the light model 4 results in relatively poor sideforce and induced resistance properties (see paragraphs 3.3 and 3.4) and will therefore adversely affect the speed-made-good curve at high wind velocities. In practical designs the light displacement of model 4 might have been obtained with a somewhat wider hull and combined with a deeper keel and slightly larger sail plan.

An analysis of the differences between models 1, 6 and 7 is probably more speculative. Though the beam of model 6 should expect a sufficiently large sail area, this is apparently not enough if related to wetted area, to obtain a light weather performance which is equivalent to models 1 and 7. The relatively worsening qualities of model 6 and the improving qualities of model 7 at true wind speeds near 9 m/s might be attributed to the shallow respectively deep draught and consequently worse and better efficiency of sideforce production. As can be seen from Figures 10c and 12 the light, shallow draught model 7 operates at very high leeway angles and gives an appreciable resistance increase due to heel and leeway, whereas the deep model 6 demonstrates good properties within this respect.

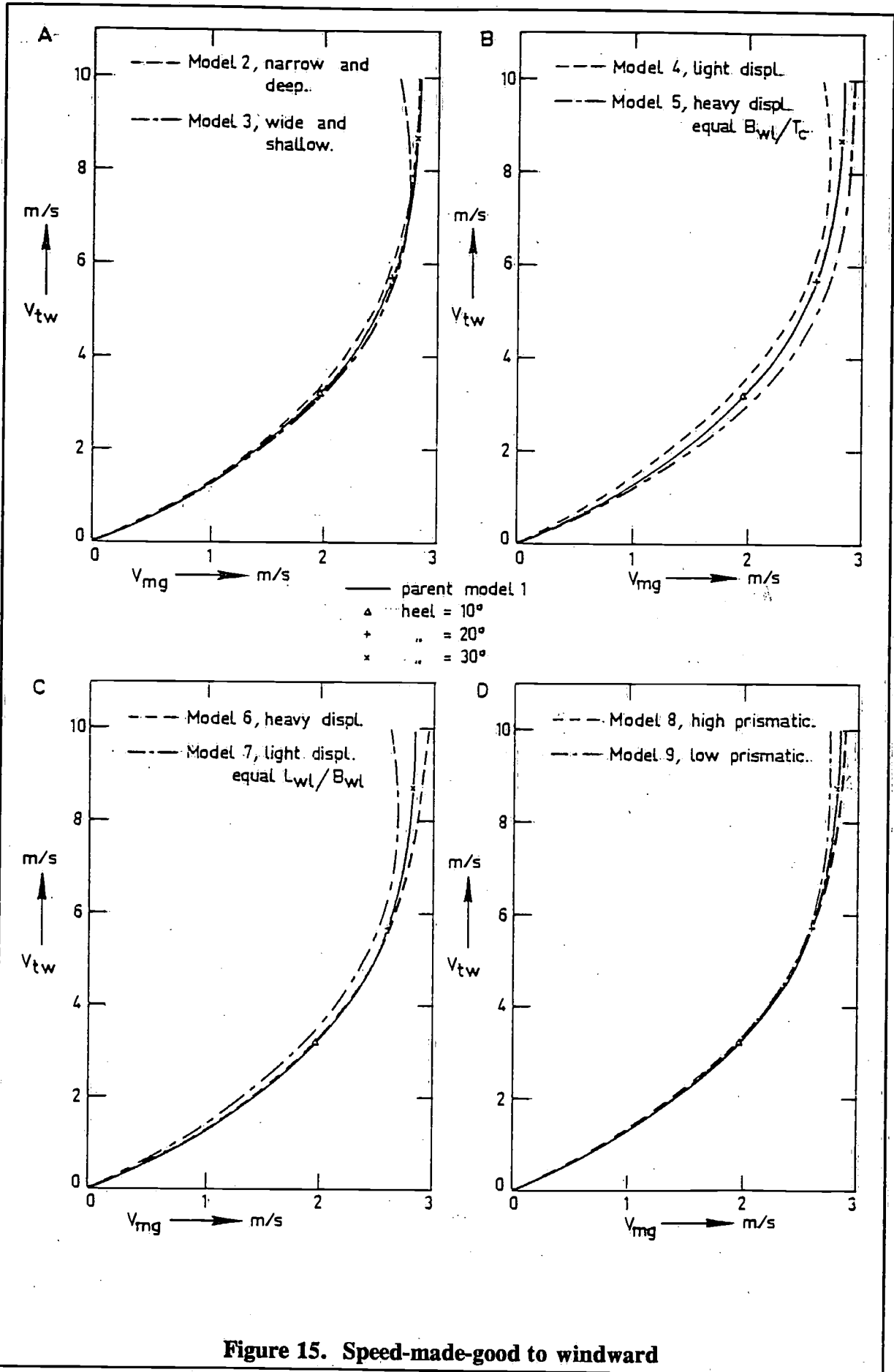


Figure 15. Speed-made-good to windward

The influence of prismatic coefficient, with otherwise comparable hull dimensions and sail plan is also demonstrated in the windward performance of models 8 and 9. In the high wind speed and consequently high boat speed range, the high prismatic model 8 shows advantages above the low prismatic model 9. This phenomenon does completely agree with the resistance curves (Figures 8d) and downwind speed (Figure 14d).

As a general conclusion it may be stated that a high sail area-wetted area ratio works advantageous in light weather, whereas at higher wind speeds a deep keel and right balance between stability moment and sail area might improve the performance to windward.

4.4 Performance with respect to rating

For racing yachts the attainable speeds have to be related to a predetermined handicap. In most European ocean races during the 1976 and 1977 seasons the handicap consisted of multiplying the elapsed time with a *TMF* (Time Multiplication Factor), which was based as follows on the IOR-rating [17].

$$TMF = \frac{A\sqrt{B}}{1 + B\sqrt{R}}$$

where: R = rating in feet
 A = 0.2424] for yachts with rating
 B = 0.0567] above 23 feet (class I - IV)

or: A = 0.4039] for yachts with rating
 B = 0.2337] under 23 feet (class V - VIII)

Rating R and TMF are calculated for all 9 models and given in Table VII.

The rating formula intends to give an estimate of the yacht's speed potential, whereas the handicap system is constructed in such a way that the derived TMF ought to be directly proportional to speed.

Figure 16 shows the speed at standard true wind speeds of 3.5, 7.0 and 10.0 m/s versus TMF , where model 1 has been used as base boat, with suffix b . Speed is distinguished in downwind speed, speed-made-good to windward and the average speed on a standard track parallel to the wind direction, which has to be sailed to windward and downwind.

Based on the assumption that speed and TMF should be proportional to each other, lines have been drawn through the points with the aid of the least squares fit. The root mean square of the deviation of all points with respect to this line is also shown in Figure 16 with rms. Secondly the correlation coefficient of all speed- TMF combinations is determined, based on an assumed linear relationship. The results are for all sailing conditions given in Figure 16 under r . If it is realised that the standard way in which hull forms, keel-rudder arrangements, stability and sail plans of this series are determined might give deviations from optimal designs, and if it is furthermore realised that it is impossible to set one single handicap being equally fair in all sailing conditions, the IOR-rating system seems to be a surprisingly good speed estimator. A root mean square error of the speed prediction which is less than 2% in most conditions may be considered very satisfactory from an engineering point of view.

Yet, racing sailors will require even less "probability" in their competition results.

From Figure 16 it appears that the IOR is especially aimed at average wind conditions, represented by the 7 m/s wind velocity. Downwind speed seems to be better predicted than speed-made-good to windward. This indicates that the IOR rates fairly well the upright hull with

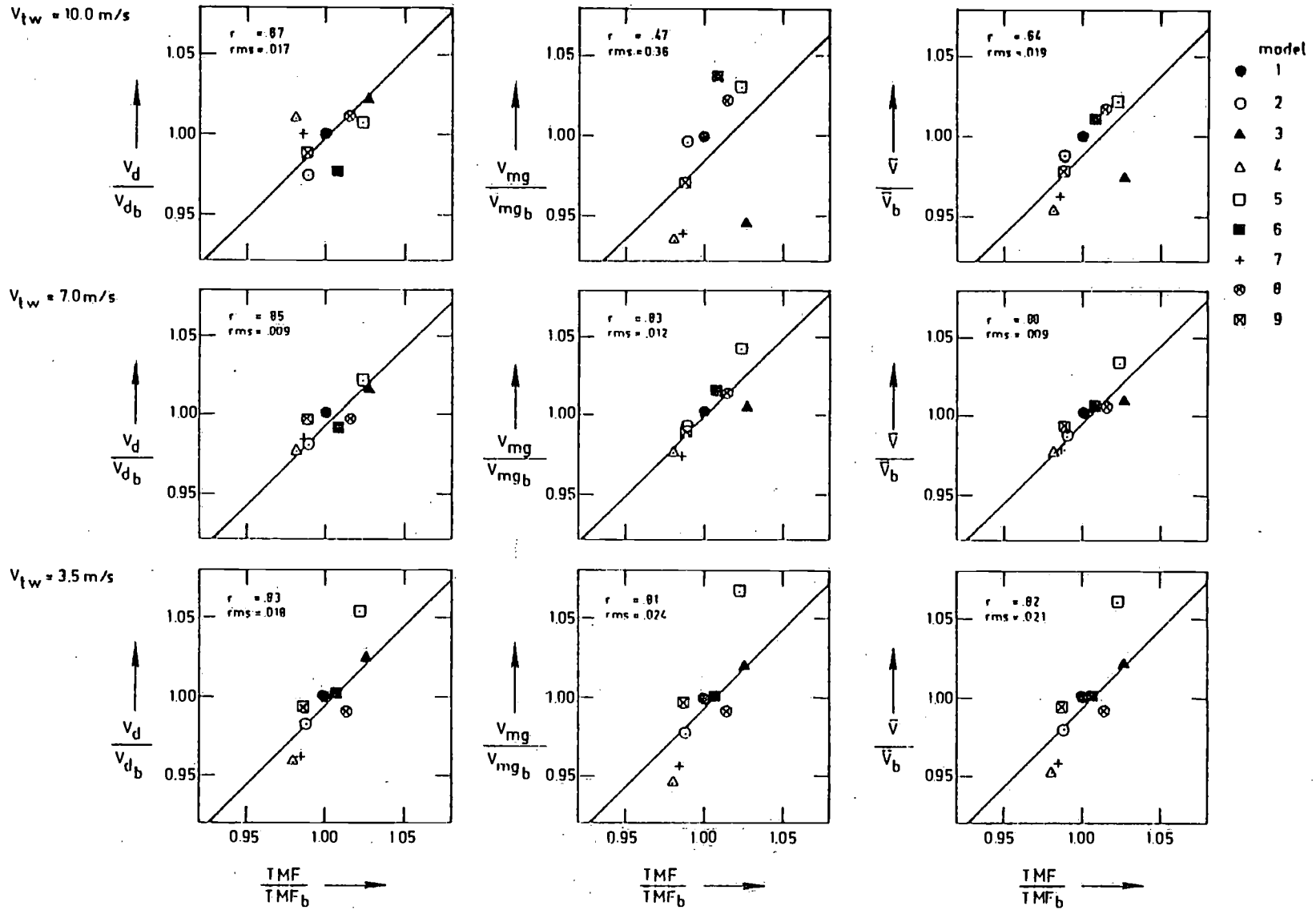


Figure 16. Downwind, made-good and average speed related to rating ($L_{WL} = 10$ m)

according resistance and the downwind sail area, but has problems in discovering all significant effects of stability and the keel-rudder configuration, when going to windward. It will indeed be difficult to imply these effects in one single formula. All statements and conclusions above are based on calculations with yachts of equal hull length, but further strongly varying parameters. Further calculations with length as additional variable may necessitate a revision of the *TMF*-formula with respect to its proportionality to speed for a wider length range, but will otherwise probably confirm the conclusions above.

5 Acknowledgement

The authors want to mention the good and fruitful cooperation with Professor J.E. Kerwin, Professor J.N. Newman and O.H. Oakley, with the Massachusetts Institute of Technology at Boston, who contributed to a great deal to the success of the reported series. Further, they are indebted to Frans Maas, Breskens, for permission to use his design as parent model, and E.G. van de Stadt & Partners for their practical advices in consistently determining stability and sail plan.

Finally, thanks go to Mrs. J. de Jager and P.W. de Heer for carefully typing this manuscript and drawing the figures.

References

- [1] Davidson, K.S.M.,
'Some experimental Studies of the Sailing Yacht',
Society of Naval Architects and Marine Engineers 1936, N.Y.
- [2] Taylor, D.W.,
'The Speed and Power of Ships', Washington 1933.
- [3] DeSaix, P.,
'Systematic Model Series in the Design of the Sailing Yacht Hull',
2nd HISWA Symposium 1971, Amsterdam.
- [4] Gerritsma, J. and G. Moeyes,
'The Seakeeping Performance and Steering Properties of Sailing Yachts',
3rd HISWA Symposium 1973, Amsterdam.
- [5] DeSaix, P.,
'Fin Hull Interaction of a Sailing Yacht Model',
SIT, DL, Technical Memorandum 129, 1962.
- [6] Millward, A.,
'The Design of Spade Rudders for Yachts',
University of Southampton, Report 28. 1969.
- [7] Herreshoff, H.C. and J.E. Kerwin,
'Sailing Yacht Keels',
3rd HISWA Symposium 1973, Amsterdam.
- [8] Beukelman, W. and J.A. Keuning,
'The Influence of Fin Keel Sweep Back on the Performance of Sailing Yachts', 3rd
HISWA Symposium 1973, Amsterdam.
- [9] Marchaj, C.,
'Wind Tunnel Tests of a 41 scale Dragon Rig',
University of Southampton, Dept. of Aeronautics, SUYR Paper, no. 14, 1964.
- [10] Herreshoff, H.C.,
'Hydrodynamics and Aerodynamics of the Sailing Yacht',
Society of Naval Architects and Marine Engineers 1964.

- [11] Wagner, B. and P. Boese,
'Windkanal Untersuchungen einer Segelyacht',
Schiff und Hafen 1968.
- [12] Kerwin, J.E., B.W. Oppenheim and J.H. Mays,
'A Procedure for Sailing Performance Analysis based on Full Scale Log Entries and
Towing Tank Data', M.I.T. Report no. 74-17, 1974.
- [13] Gerritsma, J., G. Moeyes and J.E. Kerwin,
'Determination of Sail Forces based on Full Scale Measurements and Model Tests',
4th HISWA Symposium 1975, Amsterdam.
- [14] Principles of Naval Architecture
Editor J.P. Comstock 1967 N.Y.
- [15] Milgram, J.H.,
'Sail Force Coefficients for Systematic Rig Variations',
SNAME Technical & Research Report R-10, 1971.
- [16] Gerritsma, J.,
'Course keeping Qualities and Motions in Waves of a Sailing Yacht',
3rd AIAA Symposium on the Aero/hydrodynamics of sailing, California, 1971 also:
Delft Ship Hydromechanics Laboratory, report 200, 1968.
- [17] International Offshore Rule IOR Mark,
III Offshore Rating Council, IYRU.

Sail plans, spars, rigging and sails.

by Roderick Stephens Jr.

Index

Introduction.

1.00 Sail Plans

- 1.01 The Sloop Rig
- 1.02 The Yawl Rig
- 1.03 Ketch Rig
- 1.04 The Schooner Rig
- 1.05 Fore Triangle
- 1.06 Size of Headsails
- 1.07 Effect of Measurement Rules
- 1.08 Discourage Rig Extremes

2.00 Spars

- 2.01 Spruce to Aluminum
- 2.02 Tangs
- 2.03 Mast and Boom Tracks
- 2.04 Selection of the Right Section
- 2.05 The Spar Design
- 2.06 Masts Stepped Through Deck
- 2.07 Spinnaker Poles
- 2.08 Jockey Poles
- 2.09 Mast Jacket for Cold Weather

3.00 Standing Rigging

- 3.01 Wire vs. Rods
- 3.02 1 x 19 Wire
- 3.03 Swaged Terminals
- 3.04 Norseman Terminals
- 3.05 Turnbuckles
- 3.06 Avoid Closed Barrels
- 3.07 Avoid Blind Terminals
- 3.08 Rods Strongly Secured
- 3.09 Rods Threading
- 3.10 Lenticular Rods, "Singing"
- 3.11 Swaged Rods
- 3.12 Toggles
- 3.13 Cotter Pins
- 3.14 Rod vs. Wire Headstays
- 3.15 Special Attachment of Headsails to Headstay
- 3.16 Hydraulic Tensioning
- 3.17 Avoid Combined Hydraulics
- 3.18 Removable Forestays

- 3.19 Lubrication
- 3.20 Adequacy of Standing Rigging
- 4.00 Running Rigging
 - 4.01 Natural Fibers to Synthetics
 - 4.02 Calvanized to Stainless
 - 4.03 Wire Sheave Diameters
 - 4.04 Reduced Stretch Rope for Halyards
 - 4.05 Reduced Stretch Rope for Sheets and Guys
 - 4.06 Avoid Reel Winches
 - 4.07 Swing from Roller to "Jiffy" Reefing
 - 4.08 Suggestions for "Jiffy" Reefing
 - 4.09 More About Reefing
 - 4.10 Internal Halyards
 - 4.11 Halyard Replacement
 - 4.12 Replacement of Lines Inside Rooms
 - 4.13 Extra Halyards
 - 4.14 Vangs
 - 4.15 Boom Support
 - 4.16 Topping Lifts
 - 4.17 Topping Lifts for Roller Reefing
 - 4.18 Winches
 - 4.19 Lock-Offs
 - 4.20 Lock-Offs Doubtful Against a Rotating Surface
 - 4.21 Lock-Offs on Spinnaker Halyards
 - 4.22 Chain and Cable Steering
 - 4.23 Centerboard Pennants
- 5.00 Sails
 - 5.01 Synthetic Sails
 - 5.02 Sail Covers
 - 5.03 Sails Primarily for Cruising
 - 5.04 The Double Head Rig
 - 5.05 Mizzen Staysails
 - 5.06 Plastic Compounds to Protect Stitching
 - 5.07 Roller Furling Headsails
 - 5.08 Roller Furling Mainsails
 - 5.09 Need for Effective Sail Limitation
 - 5.10 Oversized Spinnakers
 - 5.11 Storm Sails
 - 5.12 Stretchy Headsails
 - 5.13 Foot Grommets and Head Pennants
 - 5.14 Sail Stowage
 - 5.15 Headsails for Groove Stay Systems
 - 5.16 Sail Stopping
 - 5.17 Halyard Marking
 - 5.18 Mainsail Luff Gauge
 - 5.19 Battens
 - 5.20 Change Down Early When Cruising
 - 5.21 Reefing Headsails
 - 5.22 Low Booms
 - 5.23 To Raise Boom End When Running

Introduction

The aim of this paper is to review in sequence current practices concerning sail plans, spars, standing rigging, running rigging, and sails, as currently utilized on fast auxiliaries designed with emphasis on capability for fast offshore passages, be this racing or cruising.

Emphasis is placed on practical accomplishment of arrangements that are rugged, and avoid compromises in security too often encountered when perhaps too much emphasis is directed toward maximum efficiency.

It is hoped that the information discussed is of sufficient practical value to compensate for a lack of theoretical information which normally would be expected by those attending this Symposium.

The following delineates desirable characteristics relating to Sail Plans 1.00, Spars 2.00, Standing Rigging 3.00, Running Rigging 4.00 and Sails 5.00.

1.00 Sail Plans

1.01 The sloop rig

The sloop rig is the logical starting point, and most suitable up to the range of 30 to 45 foot waterlines, the yawl rig being the next step.

1.02 The yawl rig

The yawl rig offers more flexibility for sail reduction, plus the possibility of carrying some sail aft if required for balance in extreme conditions. A tremendous advantage, considerably obscured by present day reliance in auxiliary power, is steering control in tight places, when the mizzen can be used as an adjunct to steering when loss of way makes normal steering ineffective.

1.03 Ketch Rig

Finally in the range above 45' waterline there is the logical selection of ketch rig, for racing or cruising to minimize the size of the individual sails required.

1.04 The Schooner Rig

The schooner rig in the past enjoyed wide use for large commercial vessels and for many of the earlier cruising and cruising-racing yachts. In the range currently under consideration there seems nothing strong to recommend its use.

1.05 Fore Triangle

Whether a sloop, yawl, or ketch, optimum use of the fore-triangle is the most important consideration. This is best achieved by going to the masthead, which provides maximum horsepower for competitive sailing and maximum simplicity by utilizing a permanent backstay. If over 30' to 35' waterline, the masthead fore-triangle should be sub-divided for added mast support in competitive sailing, and for effective use of divided headsails for cruising purposes, and for either cruising or racing in heavy weather.

1.06 Size of Headsails

The ocean racer will have numerous large headsails, supplemented by double-head rig occasionally for light air, and again when conditions are rough. The cruiser should minimize the large headsails preferably having one combination drifter, reacher, light genoa and then

go to a fore staysail used with one or more jib topsails. This is advantageous for minimizing sail stowage problems and keeps the crew work lighter by using individually smaller sails.

1.07 Effect of Measurement Rules

Measurement rules have a profound effect on rigs, and this has produced an all but standard rig with minimum mainsail and large foretriangle. This has been countered with increased charges for headsail area and reduction for unit charge for mainsail area which has started a trend already noticeable in the smaller classes for smaller 7/8-ths or 3/4-ths foretriangle with larger mainsails, and there have been some competitive boats with a cat rig or a cat ketch rig utilizing the more favorable charge for mainsail area. Any relative increase in size of mainsail, and reduction of foretriangle, minimizes sail stowage problems and as long as a reasonable fore-triangle remains, it could be considered a desirable tendency. This tendency would also reduce the problem of wild broaching which is a by-product of large spinnakers matching the maximized foretriangle dimensions.

1.08 Discourage Rig Extremes

Accepting the profound effect of measurement rules on rig development, a better combination of racing and cruising could be achieved, if rig extremes could be discouraged. To attain a balance, a sliding scale would seem clearly needed, so that when one segment - as for example the foretriangle - is out of proportion, the pro rata charge would increase. On the other extreme a large mainsail with little or no area in the foretriangle, would be limited by the rapidly increasing charge for mainsail area as its relative size increases.

2.00 Spars

2.01 Spruce to Aluminum

Here we have seen a swing from hollow spruce spars, accepted standard to the period just before WW II, to virtually complete acceptance of aluminum alloy spars. This material has been satisfactory, being reasonably corrosion resistant but longevity is assisted by correct anodizing or by maintenance of effective paint protection.

2.02 Tangs

The mast attachment of standing rigging now utilizes tang fittings, normally outside, but under competitive pressure, frequently inside the shell, to reduce windage. Normally stainless straps are utilized with bolt and tap screw attachment. Tang alignment must be exact and thickness sufficient to eliminate flexing which would lead to fatigue.

2.03 Mast and Boom Tracks

Mast and boom tracks or grooves may be attached or may be part of the extrusion.

2.04 Selection of the Right Section

Selection of the right section is of extreme importance and there is constant pressure from the competitive side to cut down excessively which of course is most undesirable for obvious reasons. Basically the mast design should tie right in to the basic stability, utilizing chainplate width and foretriangle height, as the important factors for the required section. There are bound to be some spars undersized so that if some penalty could be devised that would not exclude any particular boats but would certainly discourage undesirable practice, this would be a helpful addition to measurement rule.

2.05 The Spar Design

The spar design, primarily for masts, must be based on the estimated loads which are in turn

generated by stability of the boat primarily, but secondarily by additional loads generated by tensioning of the fore and aft rigging principally to improve windward performance and minimize tendency of headsails to become more drafty as the breeze increases. By making reasonable assumptions for appropriate factors of safety, it's possible to generate dimensions for masts as well as booms giving moments of inertia both longitudinal and transverse after which review of available sections leads to selection of what is most appropriate to use.

2.06 Masts Stepped Through Deck

It seems important to stress desirability of stepping masts through the deck and on the keel as this arrangement combined with the proper securing where the mast passes through the deck at the partners can contribute tremendously to the stability of the mast tending to reduce fore and aft pumping and, for a given spar dimension and weight, provides a more secure rig, minimizing the necessity of additional fore and aft support. There should be a transverse bolt to prevent mast heel coming out of step in case of accident.

2.07 Spinnaker Poles

Spinnaker poles have changed from considerably tapered hollow spruce spars to parallel alloy tubing which is lighter for requisite strength and can better carry the bending loads resulting from the present ability to use spinnakers relatively close reaching, rather than simply for running.

2.08 "Jockey Poles"

"Jockey Poles", also tubular aluminum alloy, are widely used to better the angle of spinnaker guy, when spinnaker reaching, reducing both compressive loading, chafing and damage to life rail.

2.09 Mast Jacket for Cold Weather

A simple but effective accessory, applicable to alloy spars is a quilted jacket on that part of the spar below deck, for use in cold areas where the lower part of the spar will always follow the air temperature, and if not jacketed, will waste much heat.

3.00 Standing Rigging

3.01 Wire vs. Rods

Today the basic choice is between 1 x 19 stainless wire or rods, and the rods may be round in section or may be lenticular, which latter provides some reduction in drag when sailing close hauled. Where emphasis is on cruising it would seem a very simple and single obvious selection that would be the 1 x 19 wire. The first place where one could consider utilizing rods is in the masthead shrouds, where rods become advantageous if the spreaders are shortened for competitive purposes, which in turn increases loading and in this case, the lesser stretch of the rod permits the mast to stand straight with less initial tension than required for wire. Such rod upper shrouds are particularly beneficial, when competitive sailing emphasizes heavy loads at the masthead, as when carrying a heavy genoa in the fresh breeze. Lenticular rods should be used only where there's the maximum emphasis on performance in long-shore racing; never for long distance sailing.

3.02 1 x 19 Wire

The 1 x 19 construction minimizes stretch for wire while at the same time providing just a little desirable elasticity to take the shock out of peak loading. This wire is available in two types- 302/304 alloy generally used in the U.S. and 316 generally used in Scandinavia and in U.K. and perhaps other parts of Europe. The 316 is more resistant to corrosion, but the

standard used in U.K. averages about 13% under the maximum breaking strengths available elsewhere.

3.03 Swaged Terminals

The best wire terminals are the swaged fittings commonly known as "Tru-Lock". A word of caution in regard to these swaged fittings - the barrels should be periodically inspected and any sign of a longitudinal crack should dictate replacement. Any swaged terminal that is not absolutely straight should be rejected. The life of swaged fittings may be extended by spraying with sealant to exclude water.

3.04 Norseman Terminals

An alternative where swaging is not available, and particularly suited for on board repairs, is the Norseman mechanical fitting. It is somewhat more bulky than the True-Loc type and below in maximum strength but appears to have a longer life as the pressure of swaging the True-Loc type sooner or later leads to longitudinal cracks in the barrel which in turn leads to the necessity of replacement. Also the Norseman type can be inspected and it's perhaps more easy to ascertain that a correct installation has been made. In either type it is of vital importance that the fittings match exactly the wire on which they are applied and there is room for problems between metric and inch measurements. Further in the case of the swaged type it is important that enough pressure be applied - not excessive pressure - and the swaging be not done too rapidly, to avoid lamination. Swaging equipment should never be used for diameters greater than the maximum for which the tooling has been designed. Occasional proof testing of sample assemblies of each size is a vital safeguard. For long trips, spare wire with a terminal at one end and of sufficient length to replace any particular piece and appropriate sized Norseman type of fittings makes it quite easy to produce an on-board replacement, where some deterioration is encountered. Also a shroud or stay can be shortened on board, if this should become necessary.

3.05 Turnbuckles

With the 1 x 19 wire, normal turnbuckles should be employed, although in areas where the at rest tension is minimal it is feasible to use a half turnbuckle which minimizes the chance of anything coming undone because of failure of cotter pins or whatever locking device is used. Filister head machine screws are good in place of cotter pins on large turnbuckles. Any locking device should be sealed and padded with silicone sealer and then taped.

3.06 Avoid Closed Barrels

With further regard to turnbuckles, the open center type, as furnished for years by Merriman, makes it easy to see that sufficient thread is buried as compared to the tubular or closed barrel types where there is no way to see how much thread is buried. This makes the latter type most inappropriate and it is strongly advised that they never be used.

3.07 Avoid Blind Terminals

The same problems occur with rod rigging, the rod frequently threaded on each end, so that with its terminals it becomes in effect a very long turnbuckle. End terminals must be slotted to show amount of thread and permit use of cotter pins.

3.08 Rods Strongly Secured

In connection with rod rigging, there is a particular danger because the lee rigging inevitably bows out to leeward with the slack which occurs, and when the boat pitches into sea, this produces a very strong rotating moment not present with wire, for which reason locking

cotter pins should be of generous diameter and stainless steel which can do a real job. Alternately, an undersized brass cotter pin can be sheered off, or the bar can be turned by merely bending the pin down pretty flat against the threaded portion, after which it can unscrew itself while sailing.

3.09 Rods Threading

A most important safeguard for threaded rods is to have right hand threads on both ends except for the final lowest member which would have right and left hand threads to enable the final tensioning to be accomplished but this makes it literally impossible for the upper rigging to become disconnected even if there has been some shortcoming in the locking, and with deference to the fact that it's harder to check on things aloft as compared to the lowest vertical which can be clearly watched on deck. The round ball headed Navtec rods avoid this danger, as they can rotate without changing adjustment. And in connection with bar rigging, when it is being assembled there must be most meticulous cleanliness as any grit which causes undesired friction in the threads can lead to galling - after which it is generally impossible to either adjust or even disassemble the piece in question, calling for its replacement.

3.10 Lenticular Rods "Singing"

Another danger is the tendency for certain combinations of tension and length to create a high-frequency vibration which comes through with a very audible humming or singing. This leads to rigging failure and should be eliminated by adjustment for example by reducing tension if the singing occurs at anchor. If the singing occurs only under sail, it's necessary to add a small but sufficient weight perhaps in the center of the span, as for example a number of wraps of rigging tape to affect the frequency and stop the singing. With lenticular rod is the need for keeping it precisely aligned which in turn leads to the use of compression lock nuts which are not satisfactory as they loosen under load, and furthermore there is no visual inspection that will determine whether they are right. Thus the terminals of the lenticular rigging should be slotted and the rigging should be locked with stainless steel cotter pins.

3.11 Swaged Rods

Round section rods available with the swaged end fittings and also with up-set ends seated in an appropriate end terminal as made by Navtec, have the advantage of eliminating any torque as the slack bar can turn at liberty without changing adjustment and of course eliminates undesirable loading on the cotter pin used to secure the adjustment which involves either a turnbuckle or a half turnbuckle.

3.12 Toggles

Regardless of what type of standing rigging, wire or bars, it's absolutely essential that all lower ends are fitted with toggles to provide for angular freedom thereby preventing fatigue on terminals. Toggles are required aloft only on headstay and forestay to take care of the misalignment occurring as a result of the diagonal loading put on the stays by the headsail that's being carried. Toggles should be kept as short as possible to minimize eccentric loading and they are not a substitute for the proper alignment of chainplates and all lower and/or upper end fittings for standing rigging.

If toggles don't correctly fit the chainplate or possibly a masthead web, shims or washers should be used to center them carefully for optimum load distribution. It's important to avoid the use of cast toggles which have proved unreliable. They should be forged, machined or welded but never cast.

3.13 Cotter Pins

While consistently abused and hence disliked, are the best all around method of securing all parts of the standing rigging. The correct length should be $1\frac{1}{2}$ times the diameter of the piece that they are used to secure, and use of unreasonably small cotter pins should be avoided. The hole that they go through is normally at the extreme end of the pin to be secured so there's no harm in making this hole large enough. A $\frac{1}{4}$ " bar or threaded section should have a $\frac{3}{32}$ " cotter pin and the hole should be just larger than the cotter pin and slightly counter sunk on each end to facilitate entry of the cotter pin. $\frac{3}{8}$ " diameter requires $\frac{1}{8}$ " cotter pin; $\frac{1}{2}$ " diameter, $\frac{5}{32}$ " cotter pin; $\frac{3}{4}$ " diameter, $\frac{3}{16}$ " cotter pin; and 1" diameter, $\frac{7}{32}$ " cotter pin.

When the cotter pin has been cut to length, all sharp edges at the end must be carefully rounded and when it has been installed, the cotter pin should be spread not more than 20° included angle (10° each side) and the cotter pin should be turned so that when it is doing it's blocking job, each of the spread ends, will block at the same time, which means the spread should normally be vertical in standing rigging. Silicone sealer should be used to hold the cotter pins in the right position and to pad them prior to application of good heavy rigging tape. All terminals or turnbuckles should have dacron or similar boots after thoroughly lubricating them. See 3.19 below.

3.14 Rod vs. Wire Headstays

Prior to late 1960s it was not unusual for competitive boats to use a rod headstay, sometimes mated with rod backstay. It was easier to secure maximum desired tension due to less elastic stretch to be taken in. With rods normal hanks were used to secure headsails to headstays. It's most important to realize that for performance it is desirable to minimize sagging of the headstay. The inevitable tendency of the stay to sag is a function of the tension so that presuming the reasonable maximum load is applied the stay will be exactly the same whether it's wire or rod, or expressed in another way, it's much better to have the reliability of wire as the use of rods is not a magic way to reduce undesirable sag. Also the very slight ability of the wire to give in the face of excessive peak loading, clearly adds to the overall safety and security of the rig.

3.15 Special Attachment of Headsails to Headstay

There were a few tries at tracks secured to wire (1933 VAMARIE) and tracks on spruce spars serving as compression members, but no real acceptance until the Sea Stay (Hood) in 1969. This was a stainless member formed to a "C" which accommodated the luff rope, utilizing an ingenious feeder. This has been followed by various systems retaining one, and later two luff ropes (some can accommodate 3 but there's little benefit from this) which greatly expedite headsail changes. These schemes are of interest to competitive sailors but are not recommended for cruising, primarily because a sail that is lowered is immediately disconnected and needs more beef to keep it under control. Therefore, stay with hanks on all headsails, and slides on luff and foot of mains and mizzens.

3.16 Hydraulic Tensioning

With almost universal swing to masthead foretriangle, hydraulic cylinders have been accepted for tensioning various fore and aft stays, with the most productive applications on the permanent backstay. These units facilitate adjustment of pressure for variations in wind strengths and different points of sailing primarily of interest for racing and basically an unnecessary complication for cruising. The great danger is the temptation of overtensioning for up-wind speed. Never exceed $\frac{1}{3}$ of rigging strength, and ease off when rough.

3.17 Avoid Combined Hydraulics

One important recommendation on hydraulics is not to combine - keep systems independent so one failure will not effect several functions, and to minimize confusion in operating controls. The safest arrangement is to simply use hydraulic on the backstay and the best unit to use is the Hydra Tensioner made by Krueger, which is a very well designed and constructed complete unit, combining storage, pump and pressure gauge, and this is fitted with the turnbuckle and it is desirable that lengths be worked out so that if there was hydraulic failure, the turnbuckle could provide reasonable tension.

3.18 Removable Forestays

For removable forestays many systems have been used starting with a turnbuckle fitted with captive handles and fast pin, to lever, to hydraulics (too slow) to rein-forced roller slides on suitable track or suitable blocks and tackle, which latter systems permit very quick release in the middle of a rough water tack and facilitates operation without exposure on foredeck.

3.19 Lubrication

An oft neglected detail applicable to all parts of the standing rigging is the proper lubrication. The most obvious place is the turnbuckles where corrosion can build up on the threads and often make the necessary adjustments difficult to accomplish and occasionally leads even to over-stressing turnbuckle with torque, so it is very important that the correct lubrication be employed. It also applies to pins which hold the upper terminals to the mast tangs and the lower terminals to the turnbuckle. This is a place where there's lots of motion on the lee side and without lubrication it can lead to quite rapid wear which again leads to a future weakness. Finally, in the same area, toggles which are used to minimize eccentric loading can tend to freeze and then fatigue is created in the wire or the terminal, or maybe the tang fitting. Also as a safety matter if the cotter pins were properly lubricated, they can be extracted quickly if the need for adjustment or, more important, to disconnect in the event dismasting, can be of great importance. The most desirable material from my own personal experience, is anhydrous lanolin which is a greaselike product available from drug stores. Alternately, Forbes Morse has recommended Exxon P290, a development for World War II aircraft which is resistant to oxidation and water and changes very little with temperature.

3.20 Adequacy of Standing Rigging

A simple rule for judging adequacy of standing rigging, related to inclining moment, is attached. (see Appendix A).

4.00 Running Rigging

4.01 Natural Fibers to Synthetics

In the post-war period there has been a complete transition from natural fibers-hemp, linen or even cotton to dacron with some nylon and other fibers.

4.02 Galvanized to Stainless

In the same period, for wire rope there has been a transition from hot-dipped galvanized to stainless steel and this change has been expedited by the fact that currently the only galvanized wire available is electro-plated which appears to be porous and provides very little protection. It's unfortunate because a good, hot-dipped galvanized plow steel was more fatigue resistant than the average stainless steel, though this latter varies considerably depending on the amount and rapidity with which it has been drawn. The more drawing, the more rapid drawing builds up tensile strength, which is not primarily a problem, and increases hardness, which hastens fatigue as a result of cold working where passing over a

sheave, particularly critical in the case of headsail halyards. Suggested halyard diameters keyed to headstay are found in Appendix B.

4.03 Wire Sheave Diameters

For any wire halyard, sheave diameter as well as the sheave score, is very critical. A diameter at sheave center of less than 16 times the wire diameter should never be used. The score which contacts to the wire should be a good fit. Sheaves can be made of bronze with appropriate bushings, also appropriate aluminium alloy - again with more emphasis on the bushings and also some grades of plastic as for example Delrin or Celcon, but not softer plastics like Nylon or Teflon, which cold flow under heavy load.

Tuffnol, made of what would appear to be impregnated cloth under high pressure, is quite unsatisfactory for wire as it will delaminate under heavy load and particularly after abrasion.

4.04 Reduced Stretch Rope for Halyards

An interesting and relatively new development is special rope with lower stretch - the most common of which comes from Germany - the firm Gleistein, marketing it as "Cup" rope. The elasticity of this material is somewhere midway between a good grade of dacron and normal 7 x 19 wire, making it entirely suitable for halyards for any type of cruising and some racing, getting away from the difficulty of rope and wire splices and presumably more resistant to fatigue than any type of wire. "Cup" rope, combined with a suitable 2-speed winch provides the safest, quickest and easiest way to handle main, mizzen and headsail halyards. Normal Dacron provides just the right elasticity to be best for spinnaker halyards.

4.05 Reduced Stretch Rope for Sheets and Guys

For normal sheets various types of Dacron rope are excellent, though again for spinnaker guys, the Gleistein "Cup" rope can be a substitute for wire without complicating the problem of winch drums which must be bronze or preferably stainless steel or Titanium, if wire is used, but can be aluminium alloy, saving in weight and expense, if rope, only, will be used. A compromise is possible where wire can be laid up inside of rope but it is more expensive and less handy than the stretch resistant rope.

4.06 Avoid Reel Winches

Another important consideration in running rigging, particularly the main halyard, is the danger of reel winches. These offered a short cut, freeing the crew of the need of coiling down a halyard, either after hoisting, or more important, before lowering. It added a considerable price of injury to crew members, because of the basic fact that with the reel winch the drum must turn for lowering and most people erroneously try to utilize the crank to get a more careful control over lowering. Under unexpected loads or lurches, the crank can spin around with extremely serious results.

4.07 Swing from Roller to "Jiffy" Reefing

Roller reefing provided a quick and easy method of sail reduction as long as mainsails were quite flat and clews were high enough to provide an angle comfortably under 90° at the clew. The advent of more drafty synthetic sails with low clews and short booms has brought about an almost complete switch to what is now called "jiffy" or "Slab" reefing.

4.08 Suggestions for "Jiffy" Reefing

Several details have expedited and simplified the reefing operation. Primarily the shorter booms and the use of very stable and strong synthetic cloth so that full pressure can be placed on the sail as soon as the luff and the leech reef cringles have been brought to the correct

point without having to wait to tie up individual reef points which were necessary on cotton sails, and time consuming when coupled with a long boom. Hooks are generally used at the gooseneck, one each side for the luff reef cringles, and the hooks can be made smaller and lighter if D-rings are fastened to the sail in place of the otherwise sometime bulky circular grommets. The leech reefing pennant is now frequently led inside the tubular aluminium alloy booms, coming out at the gooseneck and a very effective lock-off device as normally included but the pennant also leads over a deck block into a powerful conveniently located deck winch which greatly expedites the application of the necessary tension to bring the leech cringle home. It is perhaps not amiss to mention the importance of lashing the leech cringle to the boom before the few reef points are tied otherwise if the pennant is inadvertently slackened without lashing on the leech cringle and with the reef points tied, the sail will be seriously damaged.

4.09 More about Reefing

The normal arrangement for the conventional scheme going historically back, includes two cheek blocks, one each side of the boom at each reef, but there are limitations here. First of all, as the pennant is being hove in, it's possible to damage the sail by pulling it partially into the block; secondly, if you are lucky enough to have more than one mainsail, you get a whole lot of different points as generally two mainsails don't have exactly the same depth of reef and if the depth of reef is the same it may not be the same distance due to variations in draft. All this can be overcome by using an asymmetric scheme where the pennant comes from a cheek block or sheave right at the extreme boom end going through the leech cringle and dead-ending on the boom at a point dictated by the particular sail, ideally by having a grommet in the foot of the sail at the appropriate point a couple of inches outside of the final position. With this scheme there is no way that the sail can be pulled into the sheave and it is feasible to reef any sail on any boom.

4.10 Internal Halyards

Another development under running rigging is the general acceptance of internal halyards which had started simply with the afternoon racing boats, particularly 6, 8, 10 and 12 meters, and only just shortly before the war began to be requested by ocean racers. The initial reaction was that it was quite inappropriate for offshore but as a result of persons who insisted, schemes have been worked out which provide reliable installation and generally ready replacement, preferably something that can be put outside in case weather conditions are unfavorable but where proper replacement inside is made as simple as possible.

4.11 Halyard Replacement

The internal halyard replacement has been further facilitated by use of simplified exits generally eliminating the two sheaves set in a box with number of fastenings usually very difficult to remove. Instead, a simple oval slot with appropriate replaceable chafing strips for wire halyards makes it easy to fish out a halyard that has been dropped down from the masthead, only requiring a metal coat hanger formed into a properly shaped hook. The recommended halyard exit is shown in Appendix C. Finally, the internal halyards minimize the problem of the hauling end getting around the spreaders and minimize the problem of quieting halyards when tied up under windy conditions. All in all, they can be considered acceptable for cruising as well as competitive purposes. For the main halyard it is frequently feasible to have a messenger permitting pulling in a spare halyard from the deck without having to be a hero by going aloft.

A back-up capability of rigging external halyards is most desirable.

4.12 Replacement of Lines Inside Booms

In practice may include two or more reef pennants inside the boom and possibly a clew outhaul tackle and possibly a topping lift. If carefully laid out so the lines are all clear this is a good way to clean up the rig but it should only be employed when a simple method for replacement of any of these lines is clearly available. Most important are ample openings on each end of the boom to see what is going on and to facilitate reefing lines clear. Along with this is the need to have a snake - this can be plastic tubing or 1 x 19 wire or something similar, it must have a good eye to carry a lanyard which in turn can secure it to the flemish eye in the end of any piece of line that is placed inside the boom. With these provisions the need for replacement will almost automatically be reduced but if it's needed it should go quickly and easily.

4.13 Extra Halyards

Along with the acceptance of internal halyards has been the desirable arrangement to include extra halyards - generally two genoa halyards initially to provide a spare but today to provide for sail changing where various luff systems allow for two sails at once. Spinnaker halyards - initially a spare - but today with the numerous spinnakers of different shapes, the double halyards permit quick spinnaker changes, virtually eliminating any lost speed in the course of the change.

4.14 Vangs

There is nothing at all new to hold the boom forward and from a competitive standpoint to hold it down, but recently the bigger boats have picked up something originating with very small ones, where there is a center or permanent vang to hold the boom down without need to adjust it as the main sheet is either trimmed or slack-ened. This vang can be a powerful tackle and more recently has been mechanical, frequently double acting so that it can also support the boom. Hydraulics has gotten in and provides a very easy way to get power, the disadvantage being it may be too easy to pull too hard. Whatever the system - hydraulic or mechanical - it is desirable to have some shock absorber to minimize peak loads occurring when gybing in a heavy breeze just at the moment the leech flicks across. If there is no give in the vang something has to go - perhaps the boom or gooseneck or vang or its attachment to the boom or the mast, or the main headboard. Hence a strong but always available "give" under peak tension load is desirable. Further, with the central vangs, a very important advantage is that if the boat rolls the boom heavily in the water, the boom is always free to come inboard, which is not the case if the tackle has been set up to the lee deck, a little bit forward of the position of the boom to hold it both down and forward. With the center vang it's still desirable to use the preventer but this should be reasonably light and in heavy weather it should be led to the boom end, so that if the boom dips heavily it has to come back with the rush of the water, the boom itself will not be damaged. Long light nylon provides desirable give and remember all vangs and guys should be secured amidships to facilitate release in case of knockdown.

4.15 Boom Support

Presuming the vang is double acting, also supporting the boom, there must be something to take compressive shocks occurring either when there is a failure in the headboard or the main halyard, or when the sheet is being trimmed vigorously without appropriate adjustment to the vang. The very best stiff vangs have had long ranging compression springs so even if the boom had been held up, and the mainsheet was being trimmed quickly the tendency to bend either boom or vang was eliminated by the vang peacefully accepting the added compression and later being appropriately adjusted. A strong fixed gooseneck is best with a permanent

vang.

4.16 Topping Lifts

Except for cases where there is a totally reliable double acting vang, the main boom lift is a most important piece of running rigging and except for boats small enough to accept the boom's dropping down on your head without more than momentary inconvenience, the topping lift should always be used. The most common fault with a topping lift is the tendency to use the spare main halyard sheave aloft or else possibly hang a block at the masthead. In either case there is inevitable chafe plus the normal tendency of a wire to fatigue as there's a lot of motion in the topping lift which is slack as the boat is sailing along. For this reason the only seamanlike arrangement is a standing end aloft, most certainly with a toggle or shackle so it's completely free and any adjustments required accomplished at the lower end preferably with a nylon tackle so that assuming halyards inadvertently released or the headboards pulls out of the sail, etc. as the boom drops the nylon will provide a cushion and shock absorber for the topping lift pennant.

4.17 Topping Lifts for Roller Reefing

With the roller reefing there should be a small multi-part pennant right at the boom end to keep the boom clean for the rolling but with conventional reefing the hauling part can come along the side of the boom or even can be led into the boom. An important point, just as mentioned for the mast, is the arrangement that facilitates replacement of any lines that are led inside the boom whether it be reefing line's or topping lift or outhaul tackle, just so long as there is a line there, there is a possibility of its being inadvertently pulled out or possibly just breaking from old age, or overloading.

4.18 Winches

Winches have been accepted more and more and gotten bigger and bigger - not to mention more and more expensive, but they do a good job and virtually all halyards and sheets are organized with a view to leading to a winch. A relatively new development is very effective self-tailing capability which is helpful to the cruiser as well as the competitive sailor as once the line comes under tension by taking just half a turn around the self-tailing head of the winch it is possible to devote all energy to cranking the winch, and nobody is needlessly taking in the slack.

4.19 Lock-Offs

Finally, there has been continued development of "lock-off" devices which essentially permit one winch to do two jobs or possibly more. Perhaps the most appropriate place for these devices is in connection with leech reef pennants. In the past these might be led to a small winch on the boom but this tends to slow down the reefing process as a good deal of power is needed to get the leech reef cringle home, particularly in competitive sailing where you want to keep the boat speed up during the process, but this also applies to offshore cruising where it is desirable to minimize the flogging of the mainsail. To get the necessary power on the leech reef pennant, it is more appropriately led to the gooseneck down to the deck and to a good sized winch, most appropriately the spinnaker halyard winch, as with the current relative sizes of mainsail and foretriangle, there is no excuse for setting a spinnaker with anything but the full mainsail. In any case, assuming the leech pennant is led to a powerful deckmounted winch, it's desirable to free up the winch and also so the lead will be clear of a center permanent boom vang, etc., so the lock-off in or near the gooseneck is most appropriate.

4.20 Lock-Offs Doubtful Against a Rotating Surface

Lock-offs have also been furnished on the foot block commonly used to turn the genoa sheet through 180 degrees prior to leading to a winch perhaps located more amidships, but any lock against a rotating sheave requires the load be taken on one side of the rope and in fact, it just doesn't work under high load. For a lock to be really effective it must work against a fixed surface, shaped to generate friction without damaging the rope, plus an adjustable cam surface which shares the holding job and has proven quite effective.

4.21 Lock-Offs on Spinnaker Halyards

The spinnaker halyard is a very logical though seldom used line on which a lock-off could be very helpful. Either at the mast exit, or if it's an external halyard perhaps affixed to the mast about 7' above the deck, there can be a lock-off device which can be deactivated. Its function is to prevent the spinnaker halyard getting away when the sail is being set. This can be helpful any time a spinnaker is being used though obviously of greatest help in the competitive area. Once the sail is fully hoisted and secure, the lock-off would be deactivated so there would be no interference when it comes time to take the spinnaker in.

4.22 Chain and Cable Steering

While it's not literally running rigging, the chain and cable in the normal steering gear should be treated in the same general way in that the sheave should be oversized as much as mechanically feasible with a score that fits the wire and with precise alignment also closely fitted with quards preventing a slack cable from dropping off the sheave which would immediately inactivate the gear. It's most important to have a complete spare chain and cable assembly with the center of the chain marked to match the kingspoke and most important to be certain that there's sufficient access and clearance and necessary tools to permit quick installation of this spare assembly. In order to install the replacement cables, it's frequently necessary to have the end of the wire free with no pre-applied terminals. The normal wire clamps are only effective if the cable is carefully taped and then tightly serve and if this is omitted much of the holding power is lost. Appendix D shows a desirable clamp for the steering cable, which also furnishes the equivalent of a thimble to minimize chafing and fatigue and maximum hold is developed without special serving - only an end serving to keep the wire from undesirably becoming unlayed.

4.23 Centerboard Pennants

The use of nylon line is recommended to eliminate electrolytic problems, thus minimizing possible failure. Arrangements should be such that it's feasible on board, and simply by swimming, to replace the centerboard pennant. It is also desirable that the centerboard pennant can easily be inspected throughout its entire length, without need for any shipyard or shoreside help. A recommended scheme is basically a two part pennant, with a standing end reasonably above the deepest waterline, and covered with a waterproof cap and gasket. The pennant passes over a single sheave in the centerboard, the hauling end comes out on deck, where the Luke type (formerly Merriman) davit winch is utilized, to spool on the nylon line. The pennant should be clearly marked, and long enough to have two turns on the drum, when the board is fully lowered. With the board fully down and against a stop, the pennant can be further slackened and disengaged from the drum. It should have a flemish eye on which a messenger can be attached, and then from the standing end, the entire pennant can be pulled out. This permits a complete inspection, after which the pennant can be immediately pulled back, secured to the winch drum; and the whole unit is back in operation. Obviously, a replacement pennant can be put on with no loss of time, should it be desirable. A sketch indicating this arrangement is in Appendix E.

5.00 Sails

5.01 Synthetic Sails

The use of synthetic sails (also hulls) is undoubtedly harmful from a long-range ecological standpoint, but in other respects it is a help to the sailor - be he racing or cruising oriented. The necessity for long slow periods for proper sail break-in are eliminated, and more important, there is little worry of harm from sails being stowed when wet.

5.02 Sail Covers

A common mistake is neglect of sail covers, which should be religiously used, not to keep the sail clean but to keep off the by-products of sunlight, which shortens the sail life. Don't forget that the neatest and easiest and lightest covers don't go around the mast - just over the headboard, lashed below gooseneck and at boom end and rubber with hooks below boom allowing adjustment to the excellence (or not) of the furl.

5.03 Sails Primarily for Cruising

In a given sail plan, the cruiser will have fewer sails and in smaller and lighter packages, to facilitate stowage and handling. Mainsails will be lighter to furl more easily and be lighter to hoist. Sails should secure to spars with reinforced nylon slides on alloy tracks and to stays with conventional hanks.

5.04 The Double Head Rig

A large light, and small heavy jib topsail plus forestaysail and storm staysail will cover a good range. A large light reacher - drifter with raised clew would be next, and spinnaker only on smaller vessels with ample crew power. There is a desirable refinement that patches be sewn over the normal hanks on the luff of the forestaysail, the patch being sewn across the top and the bottom and along the luff but opened aft and pulling tight when the sail is fully hoisted. These patches tend to minimize chance of cutting or chafing the jib topsail which must run over the forestay and the hanks, and minimize the chance of the jib topsail sheets either unhooking or in any way damaging the forestaysail hanks. It is a simple refinement but most appropriate with the regular staysail when any jib topsail may be set ahead of it.

5.05 Mizzen Staysails

Yawl or ketch will have a large light triangular mizzen staysail and a schooner probably large and small topmast staysails.

5.06 Plastic Compounds to Protect Stitching

With cotton, all good offshore sails were hand sewn to pull the stitching into the cloth, protecting it from chafe. This has gone with synthetics, where quite durable machine sewing is accepted. Applications are becoming available to physically shield the stitching. But never let a slack lee backstay runner rub the sail; take it forward.

5.07 Roller Furling Headsails

Roller furling headsails are facilitated by the several devices which hold the luff to the stay; unacceptable sag and unreasonable halyard loads are eliminated. They do not provide the variation of weight, nor do they set well partially rolled, so their use compromises efficiency. Generally roller sails are most suitable for fair weather and for motor sailers, where a compromise in efficiency is of lesser importance. They are not suitable for hard offshore sailing where both the weight and shape of the sail should be optimum for conditions being encountered.

5.08 Roller Furling Mainsails

In addition to the obvious difficulty of maintaining optimum shape when partially rolled (the same problem as comes up with roller headsails), the fundamental rolling mainsail as set on a wire which added additional compression to the mainmast without furnishing the steadying influence that a normal mainsail has as it is secured all along its luff. Recently Ted Hood has been promoting a variation in which the mainsail is rolled up in a cavity in a separate after compartment in the mast so that when pressure comes on the sail it is supported by contact with the cavity exit, thereby minimizing additional compressive load, and having some steadying influence on the mast.

5.09 Need for Effective Sail Limitation

There's been an unfortunate omission which tended to drive apart the all out competitive sailer and the fast cruiser who is interested in some racing. Happily, recent action by the Offshore Racing Council is encouraging, as numerical limits have been applied which will be helpful. Appendix F gives the details for the numbers of headsails and spinnakers which key to the I.O.R. rating. It would seem desirable if this could lead to further limitation hopefully reducing the rather exorbitant number of spinnakers and more important requiring that certain of the headsails not exceed certain percentages of the overall maximum size to avoid the situation where the light weather optimist tries every conceivable useful light sail and is, because of this judgment, in a rather serious situation if heavy weather is encountered. It would seem desirable if the rule would permit three additional sails, one not over 47; the second not over 68; and the third not over 85 per cent of the largest headsail in area, and decrease by these three sails the total number of sails allowed which would work for everything except the mini-class where the total number of headsails is only three plus the storm jib, so they should have something perhaps like 47 and 80 per cent of the maximum, plus one maximum sail. It would still seem desirable not to permit a headsail being set outside of the spinnaker sheet, even though the blooper has many supporters in the racing fleet. It still complicates sail reduction as in rapidly deteriorating conditions, and really slows down the possibility of returning to a man overboard or getting out of unexpected shallow water, etc. I.O.R. Sail Limits for I April 1977 - Appendix F.

5.10 Oversized Spinnakers

There is another area where sails are excessive, and that is the modern spinnaker whose effective area has grown to compound the problem of increased foretriangle dimensions. Downwind spinnaker sailing is accelerating - literally and figuratively, up to a point. Then one encounters problems that are not easy to control. The foot width should not be larger than maximum headsail L.P., and width aloft should be limited. Poles should not exceed foretriangle base.

5.11 Storm Sails

Most certainly storm sails should be clearly required, with their size limited. Of course they are seldom needed but they are the best possible ultimate insurance and their absence or neglect has played a prominent part in real storm difficulties. Not only should they be required (on board) but all hands should become acquainted with them to facilitate their use, however rarely required. The storm jib should most certainly be fitted with hooks and set on a stay. Thus, a boat that had some device on the headstay that would not accept hooks, would need a separate forestay, which presumably would be desired anyway for mast support, but the important thing is that the storm headsail should go on hooks, which latter dictates a wire so the sail could be used even if there had been some damage to some one of the more sophisticated luff groove systems. On a large boat where the stacked mainsail piles quite high it's desirable

to have a separate track for the storm trysail which track should come down very nearly to the deck so that the storm trysail can be put on in advance, to make ready for poor weather, and can be furled close to the deck if its use is temporarily not required, but continued heavy weather may be expected. The separate track seems preferable to the little feeder track coming into the main track with some kind of a switch. These switches have seldom operated smoothly and they frequently interfere with the normal mainsail hoisting and lowering, and more important, can delay the setting of the storm trysail at a time when it's required quickly.

5.12 Stretchy Headsails

In the racing scene the "stretchy" headsail first publicized in 1962 America's Cup competition is now generally accepted and permits ready adjustment of draft, increasing range of maximum efficiency of a particular sail. A fringe benefit for the cruiser is less halyard problems previously encountered with an overloaded wire - luffed sails. The lighter rope luff also facilitates sail stowage.

5.13 Foot Grommets and Head Pennants

All low clewed overlapping headsails should have a strongly reinforced grommet near the midpoint of the headsail foot to permit use of what we call a tacking line, which leads from this grommet through a snatch block near the headstay and back to a convenient point on the deck helping the sail to be pulled forward hence facilitating tacking. The same grommet or a similar one located perhaps just $\frac{1}{3}$ of the way back from the tack, can help to lift the foot of the sail to keep it out of the bow wave, when the sheet has been eased for reaching, and it is important that any headsail that is not full length on the luff be fitted with a head pennant. The head pennant should be short enough so the sail can be pulled up on a tack pennant at least 4 or 5 per cent of the foretriangle height to minimize conflict with the bow wave when the sheet has been eased.

5.14 Sail Stowage

Generally synthetic sails do not react well to being stuffed into a bag - rather they should be folded and rolled and tied securely before dumping into the bag, which will then pass through a much smaller opening, with less profanity. Fundamentally, the most important arrangement is to have a workable sail stowage plan so that it's possible for the crew to live below with all the sails and it's necessary to get away from what is too often seen where sails are put on deck when the crew must go below and the boat is in port, while all hands must pitch in to getting the sails back down below as the crew comes on deck to go sailing or racing. It's not an easy problem but nothing is insoluble, and with really effective sail limitation and proper planning it not only can, but most certainly should be accomplished.

5.15 Headsails for Groove Stay Systems

Headsails for groove stay systems have their own sausage shaped covers, which pass through smaller openings and may be laid ready on fore deck for a quick racing change.

5.16 Sail Stopping

Sail stopping is used only on the larger end of competitive sailing, and stops are generally rubber bands instead of cotton twine. Spinnaker fills quickly (sometimes much too quickly) when set without stops, just hoisted from a deck located "Turtle" into which they have been carefully packed.

5.17 Halyard Marking

The combined use of stretchy sail and masthead foretriangles places emphasis on precise,

indestructible halyard reference marks to warn when maximum hoist has been reached. A mark incorrectly located, or one which can slide, is much worse than no mark. Copper bell wire tucked through alternate strands of the wire is a very effective marking, with reference numbers on mast or deck to dictate optimum settings for specific sails under specific conditions.

5.18 Mainsail Luff Gauge

There is one device that's better than even the best halyard marking, that is that each normal mainsail or mizzen should be fitted with what could be called a luff gauge wire - a light stainless wire secured to the forward corner of the headboard coming down through the seam at the luff of the headsail coming out perhaps 2' above the tack, and of a length that when the sail is fully hoisted to the upper band about 1 foot of this wire is exposed but is pulled lightly down toward the tack by a short piece of shock cord. Then a reference mark is placed on the after quarter of the mast in line with the bottom of this exposed wire eye when the sail is at the band and it will show you immediately if you have come below the band due to increased tension and stretch on the halyard (particularly important with rope halyard) or whether on the other side you may be actually above the band due to lightening wind slacking the mainsheet, slacking the main cunningham, etc. It's a relatively simple detail but is of great importance to competitive sailor and useful for cruising sailor to avoid damage aloft from overhoisting.

5.19 Battens

Properly tapered and more or less indestructible fiberglass battens are most useful. Always maximum rule length for the racer, but for cruising, the inner ends of top battens should be outside the span of main shrouds to permit pulling sails down when off the wind.

5.20 Change Down Early When Cruising

In the shorthanded cruiser, sails should be changed down early - and it is then feasible to run off, reducing apparent wind and water on deck. Not feasible, however, if you have already carried on too long. The racer will change, when feasible, while maintaining maximum speed on optimum course.

5.21 Reefing Headsails

For heavy weather reaching a heavy No.2 or No.3 genoa can use a diagonal reef, with cringle about seven feet above deck, and a few points to tie up the lower corner and keep that part out of water. The genoa Cunningham (used as on main, to flatten a genoa already at maximum hoist) can be used to allow sail to be somewhat raised after attaching the reaching sheet. The present tendency for crosscutting genoas makes reefing seem more feasible but it is still doubtful that a reefed headsail is really shipshape when windward sailing, which must involve tacking.

5.22 Low Booms

Low booms, particularly with a low clew, are very dangerous and should be avoided.

5.23 To Raise Boom End When Running

Applicable to racer and cruiser alike. With slab reefing, the boom end can be raised, without undesirably slacking the leech (when running in rough weather) by heaving the leech reef pennant, if you have had the foresight to prepare this in advance. For roller reefing there should be a sliding gooseneck permitting the boom to be raised parallel by rolling, without slacking the halyard.

Appendix A - Paragraph 3.20

A simple guide to diameter of standing rigging related to righting moment

- 1 Righting Moment for 1 degree - This is available on Certificate.**
- 2 Maximum expected Righting Moment - Multiply the moment for 1 degree by 45.**
- 3 Maximum expected total load on shrouds, divide the maximum expected Righting Moment by the distance from the centerline to the main shroud chainplate. This assumes that the chainplates are more or less evenly spaced from the centerline - where there is a difference of note this can be averaged.**
- 4 Individual Maximum Shroud Loads determined as follows:**
 - a Top shroud single spreader 45% of Three above.**
 - b Top shroud double spreader 30% of Three above.**
 - c Intermediate shroud double spreader 30% of Three above.**
 - d Single-lower-single-spreader shroud on the centerline, 55%.**
 - e Single-lower-single-spreader, but when the lower shroud is set aft, 60%.**
 - f Double lowers, total should equal 65%.**
 - g Single lowers with double spreader rig, 40%.**
 - h Single lowers, double spreader when the lower shroud is set aft of the centerline, 45%.**
 - i Double-lower shrouds, double spreader rig, total 50%.**
- 5 The amount by which various rods, wires and turnbuckles exceed the calculated maximum loads would be the expected factor of safety, and the Figure of about 2.25 is a reasonable minimum to be considered acceptable.**
- 6 A very simple rule of thumb, and quite accurate up to a half-inch diameter, is to take the diameter, express it in 16ths, square it, and divide by two, and this will give you the number of thousand pounds that is reasonable to expect from one by 19 wire. Some bars are offered at the higher strengths; but I do not feel there is enough background on this to make it really acceptable for Offshore sailing, so the same rule of thumb is reasonable when applied to bar shroud into the wire part of the halyard, with a normal rope and wire halyard.**

The other alternative being all wire with a reel winch which is not recommended due to the inherent danger created by the handle, when a reel winch spins back.

Appendix B - Paragraph 4.02

Headstay 1x19 stainless		Jib Halyard					Main Halyard				
		7x19 stainless		Gleistein Cup Rope			7x19 stainless		Gleistein Cup Rope		
Diam. (in.)	Break Load (lbs)	Diam. (in.)	Break Load (lbs)	Rope Tail Diam. (in.)	Diam. (in.)	Break Load (lbs)	Diam. (in.)	Break Load (lbs)	Rope Tail Diam. (in.)	Diam. (in.)	Break Load (lbs)
3/4	59.700	7/16	16.300	3/4	—	—	3/8	12.000	5/8	3/4	16.000
5/8	46.800	3/8	12.000	5/8	3/4	16.000	5/16	9.000	9/16	5/8	12.900
9/16	39.000	5/16	9.000	9/16	5/8	12.900	9/32	7.800	9/169/1	5/8	12.900
1/2	29.700	5/16	9.000	9/16	5/8	12.900	9/32	7.800	6	5/8	12.900
7/16	23.400	9/32	7.800	9/16	5/8	12.900	1/4	6.400	1/2	9/16	9.000
3/8	17.500	1/6	6.400	1/2	9/16	9.000	7/32	5.000	7/16	9/16	9.000
5/16	12.500	7/32	5.000	7/16	9/16	9.000	3/16	3.700	3/8	7/16	6.400
9/32	10.300	3/16	3.700	3/8	7/16	6.400	5/32	2.400	3/8	3/8	4.600
1/4	8.200	5/32	2.400	3/8	3/8	4.600	1/8	1.760	5/16	5/16	2.500
7/32	6.300	5/32	2.400	3/8	3/8	4.600	1/8	1.760	5/16	5/16	2.500
3/16	4.700	1/8	1.760	5/16	5/16	2.500	3/32	.920	5/16	1/4	1.500
5/32	3.300	1/8	1.760	5/16	5/16	2.500	3/32	.920	5/16	1/4	1.500
1/8	2.100	3/32	.920	5/16	1/4	1.500	3/32	.920	5/16	1/4	1.500

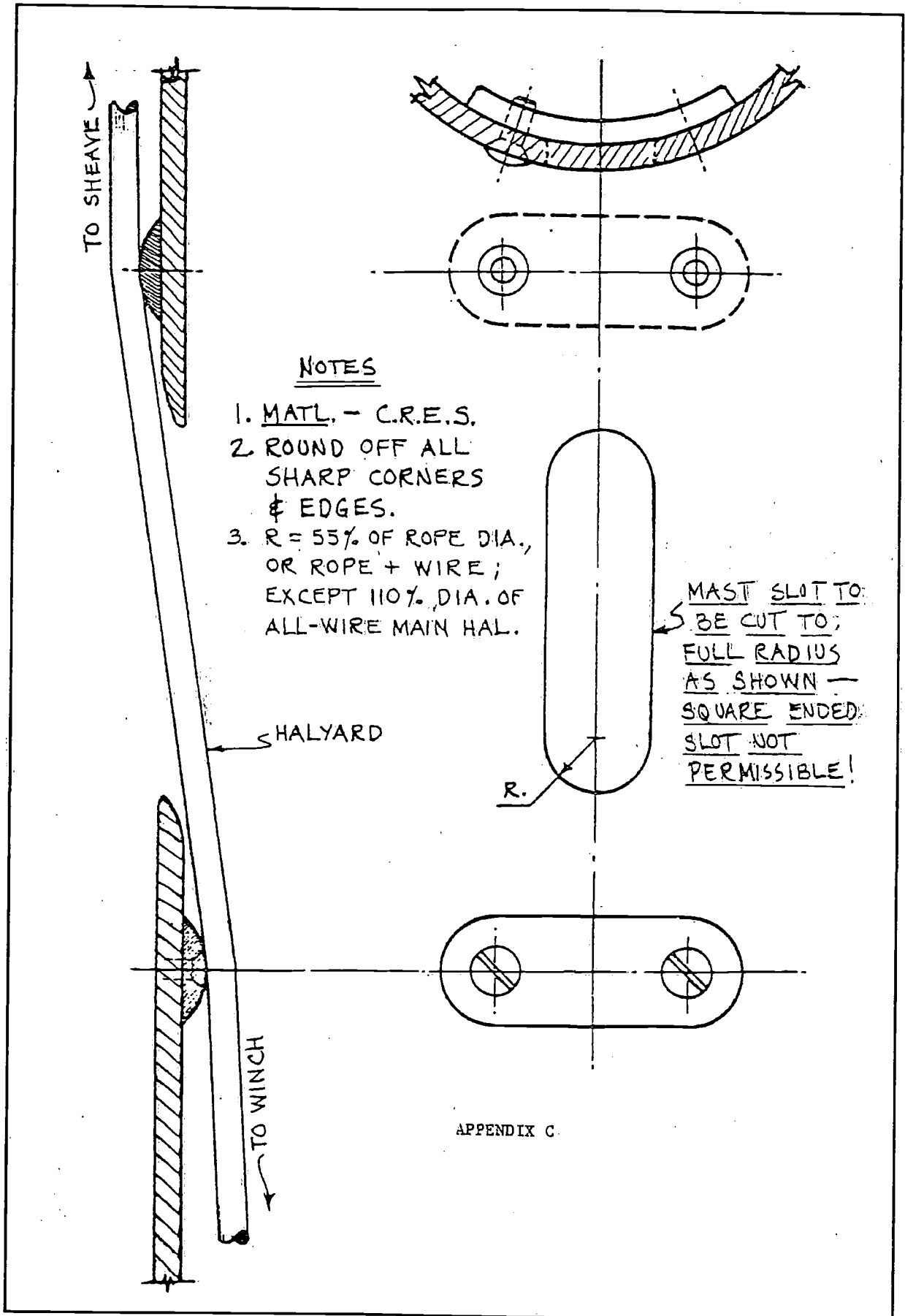
Normal practice is to utilize a rope and wire jib halyard having enough wire to provide four turns on the halyard winch plus allowance of about 3% of the fore triangle height for the fact that headsails don't always go all the way and to permit advantage to be taken of the stretchy luff characteristics. This presupposes that smaller or shorter headsails will have appropriate head pennants to extend them so the wire will properly reach the halyard winch.

The development of reefing headsails complicates this and poses the problem of either sailing on the tail, including the splice, or having excess wire which at best is unpleasant and hard for any one but the most expert to cope with.

There is an alternative and that is to eliminate the wire and utilize rope construction that minimizes stretch which first has the advantage of simplicity by eliminating the need for rope and wire splice and further eliminates the possibility of the very unpleasant situation when some strands in the wire break and stick out. The rope completely eliminates the problem when the headsail is reefed. The type rope presently most suitable and in use for several years is called Gleistein "Cup" rope, and it can be purchased from Nicro Corp., 2065 West 140th Avenue, San Leandro, California 94577.

Same choice prevails for the main halyard but here reefing is a completely accepted fact which complicates it by virtually necessitating excess length of wire. This again puts emphasis on desirability of a no-stretch all rope halyard, which latter also makes it much quicker and easier to hoist the mainsail hand-over-hand eliminating the delay particularly created when you run.

Appendix C



NOTES

1. MATL. - C.R.E.S.
2. ROUND OFF ALL SHARP CORNERS & EDGES.
3. $R = 55\%$ OF ROPE DIA., OR ROPE + WIRE; EXCEPT 110% DIA. OF ALL-WIRE MAIN HAL.

MAST SLOT TO BE CUT TO; FULL RADIUS AS SHOWN - SQUARE ENDED; SLOT NOT PERMISSIBLE!

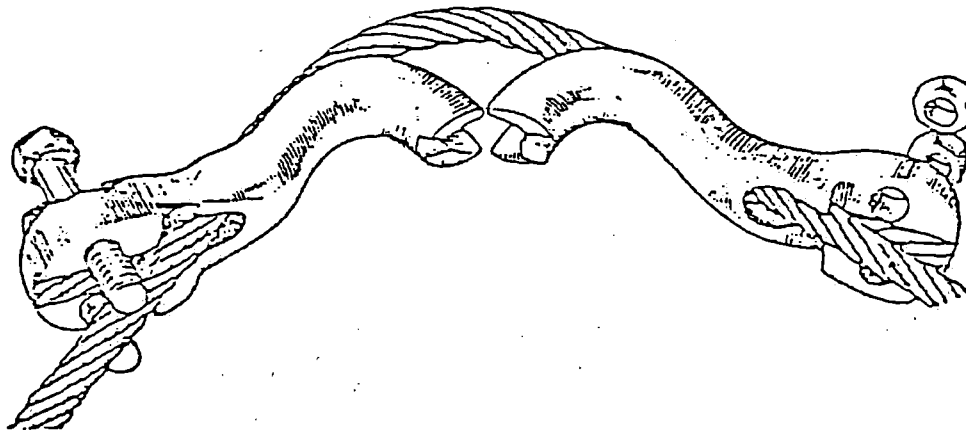
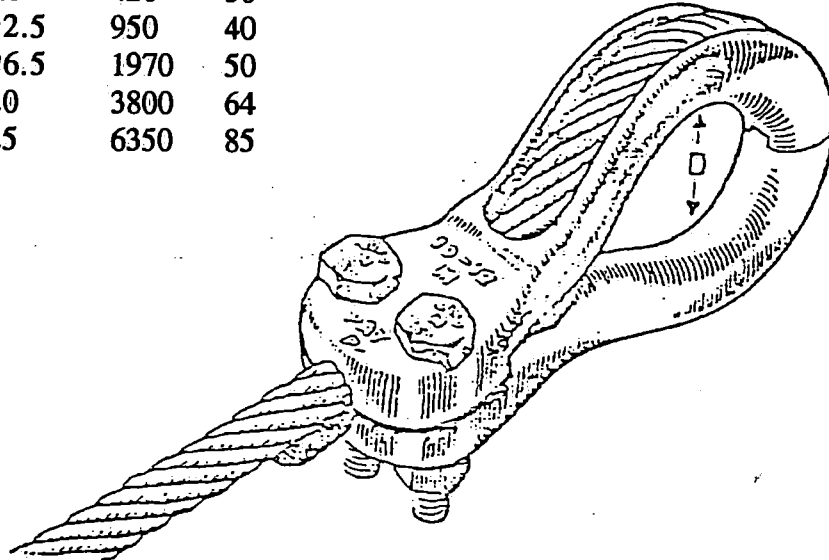
APPENDIX C.

Appendix D

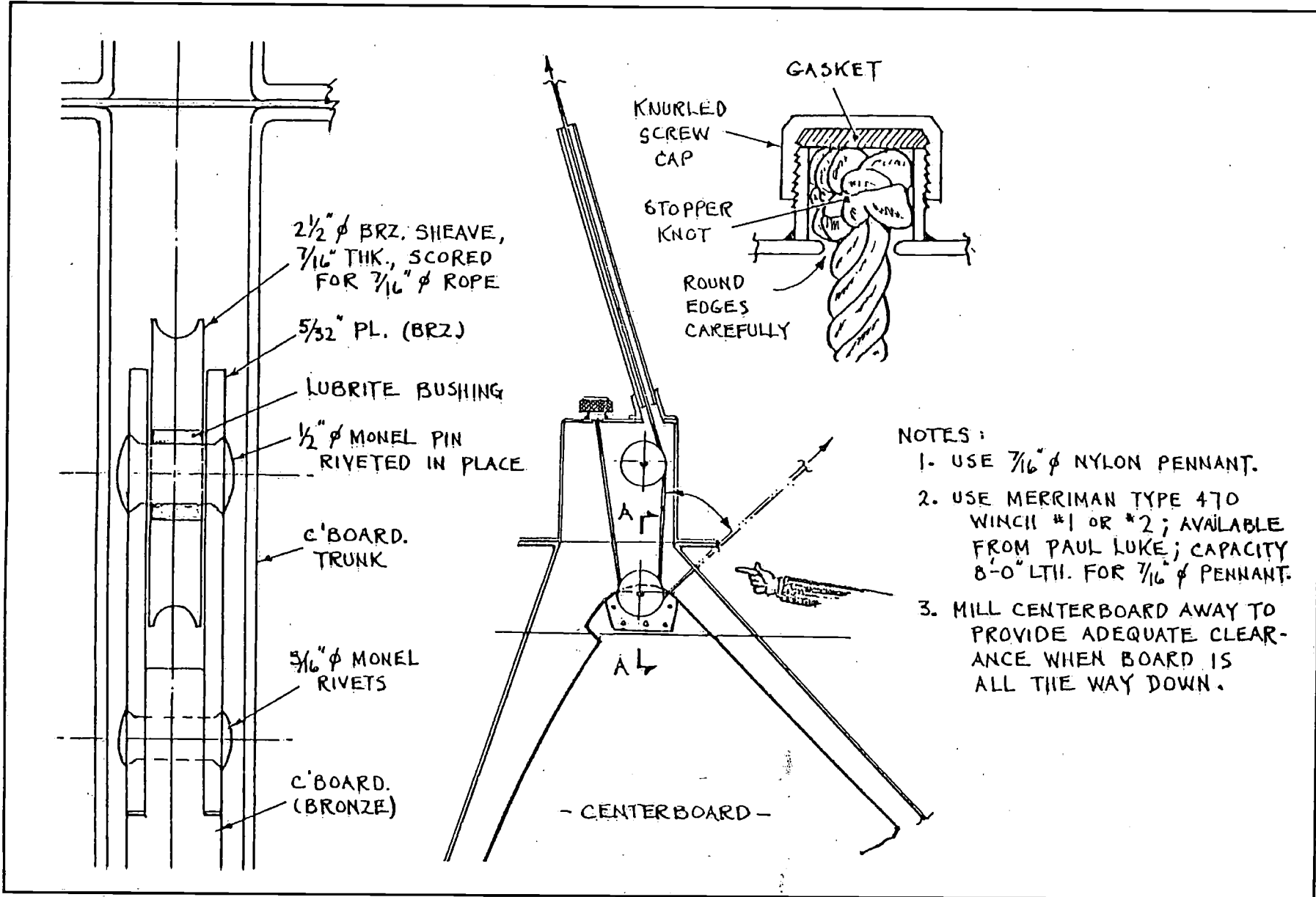
KLAMMERKAUSSER

Kombination av linlås och fast kaus. Konstruktionen är godkänd av Kungl. Arbetarskyddsstyrelsen för användning även på hisslinor.

Typ	Lindiameter mm	Vikt gr.	D mm
KK-M5	5 - 6	150	22
KK-M6	7 - 8	250	19
KK-M9	7 - 9.5	420	30
KK-M12	10 - 12.5	950	40
KK-M16	13 - 16.5	1970	50
KK-M20	17 - 20	3800	64
KK-M25	21 - 25	6350	85



Klammerkausen är delbar och försedd med BUFO bult och mutter av seghärdad stål.



Appendix F - Paragraph 5.09

Sail number limitation (Effective 1st April 1977)

892. Sails on board a yacht in a race shall be limited to not more than:

1 One mainsail.

One spare mainsail complying with 851.2.

One storm trysail complying with 851.3.

One storm jib (of an area (MSA) not exceeding 0.0512 and with a luff not exceeding 0.651).

2 In addition to the above yachts may have headsails, according to their rating, not exceeding the numbers in the table below.

Mark III Rating	Jibs shall not number more than	Spinnakers shall not number more than
16.0 ft	3	1
16.1 to 19.4 ft.	5	3
19.5 to 22.9 ft.	6	3
23.0 to 28.9 ft.	6	4
29.0 to 36.0 ft.	7	5
36.1 to 43.0 ft.	8	5
43.1 to 51.9 ft.	9	6
52.0 to 62.0 ft.	10	6
62.1 and above	11	6

3 Two masted yachts may have in addition to the above:

A Yawls and ketches rated for RSAY:

One mizzen and three mizzen staysails.

Schooners rated for RSAB:

One foresail and three other sails to be set between the masts.

Yachts rating 52.0 ft. and above may carry one mizzen staysail or between mast sail in addition to the above.

B Schooners rated for RSAG:

One foresail.

4 For the purpose of this rule, a gaff headed sail plus topsail shall count as one sail.

Suggestions relate to 892.2 - Headsails

16.0 Rating - 3 jibs allowed, of which one may not be more than 60% area of maximum headsail, and a second not more than 85% of maximum headsail, with weights consistent for their intended purpose, windward sailing in fresh breezes.

For all ratings above 16.0, one of the jibs allowed must be not more than 50% area of maximum headsail, a second not more than 70%, and a third not more than 85%, with weights consistent for their intended purpose, windward sailing in fresh breezes.

The use of a wood-resin composite for marine construction

by Meade A. Gougeon

President - Gougeon Brothers, Inc.

Abstract

Wood is an excellent engineering material with unique physical properties that ideally suit it for use in constructing lightweight marine craft.

Being a hygroscopic material, wood is plagued by a number of serious problems that are moisture related. Because of these problems and the introduction of more modern materials, the use of wood has declined greatly.

With the help of modern technology, most of the problems with wood can be solved by incorporating wood into a composite with a proper resin material.

Three different construction methods are presently being used to construct hulls with the wood-resin composite.

The use of a wood-resin composite for marine construction

Before we can present a meaningful discussion of the wood-resin composite, the main ingredient, wood, must be fully understood from the engineer's viewpoint. Unfortunately, the physical properties of wood are not widely known or understood in the marine field. This is not too surprising when one considers that even the best naval architecture schools give wood only token mention concentrating their efforts on the metals and fiber reinforced composite. Wood is an immensely complex subject, and we can only cover those pertinent points in this paper that are necessary to develop a clear understanding of the wood-resin composite.

Wood as an Engineering Material

In considering wood as an engineering material, it is pertinent to note that "wood" is not a single material with one fixed set of mechanical properties, but rather includes many species which possess a wide range of properties, which depend upon both the species and the density selected. The range of properties is considerably wider than what is generally available with most other types of materials, where some variation of properties can be attained by means such as alloying or tempering, but where little variation of material density is possible. Wood, on the other hand, can be selected over somewhat more than a full order of magnitude in density, from 6 lbs/cuft or even less for selected grades of balsa, to over 60 lbs/cuft for certain species of hardwood. The flexibility this can provide the wood structure designer is obvious; since low-density species can be selected for efficient use as core materials, or for panels or beams where stiffness or buckling resistance is of primary importance. High-density species can be selected where there is a need for high strength and modulus per unit volume, such as in panel skins or in structural members which must occupy constrained geometric volumes. The full range of intermediate densities provide a match for requirements anywhere

between these extremes. In this regard, it is worth noting that the physical properties of wood are roughly proportional to its density, regardless of species, since the basic organic material is the same in all species. Thus, changing density is rather like compressing or expanding the net strength and elastic stiffness into different cross-sectional areas with little net variation to total properties per unit mass.

Given that the strength and modulus of wood vary approximately in proportion to its density, it is easily shown that the length of a solid wooden panel which is stable against buckling will vary inversely with its density, while the length of a solid wooden column stable against buckling will vary inversely with the square root of its density. Therefore, approximately a factor of ten in unsupported panel length, or a factor of three in unsupported column length, is readily available to the designer of wooden structures. Designers of structures using other materials can perhaps best appreciate what this means by imagining that a factor of ten of density variation were somehow readily available for the steel, or aluminum, or composite, with which they regularly work.

Granted that the density variation of wood can be of advantage to the wooden structure designer, one must also inquire how good are its net properties per unit mass relative to other structural materials. There are, after all, other light variable density materials available, such as the expanded foams. For modern structures where weight is an important issue, the strength-to-density ratio (specific strength) and modulus-to-density ratio (specific modulus) are two very important numbers to consider, since they determine how much strength and stiffness you can get for a given mass of material.

A typical grade of Douglas fir, a moderate density species, will possess approximately the following properties:

Fir

Density	: .52 (32.5 lbs/cuft)
Compressive Strength	: 7500 psi
Tensile Strength	: 15,000 psi
Modulus	: 2×10^6 psi

To easily compare this to other materials, the table below indicates the strength and modulus required of the other materials to achieve exactly the same strength-to-weight, and modulus-to-weight, possessed by Douglas fir:

Equivalents of Fir

	Steel	Aluminum	Fiberglass Composite
Density	7.8(487 lbs/cuft)	2.7(169 lbs/cuft)	1.9 (119 lbs/cuft)
Compressive	112,500 psi	38,942 psi	27,403 psi
Tensile	225,000 psi	77,885 psi	54,807 psi
Modulus	30×10^6 psi	10.38×10^6 Psi	7.3×10^6 psi

Those familiar with the typical properties of steel, aluminum, or fiberglass composite, will recognize that these numbers indicate Douglas fir to be a competitive structural material on a per unit weight basis. It might also be noted that the number cited for the fir do not represent unusually good samples or unusually dry samples. Typical shop laminates we have produced, in fact, exceed the strength and modulus numbers cited.

It should be pointed out at this time that the preceding considered the properties of wood along its grain direction. The same piece of fir which displays 15,000 psi tensile strength along its grain direction will have something like 300 psi tensile strength across its grain. That is a 50 to 1 variation in tensile strength depending on the load direction. The other physical properties of wood are also distinctly anisotropic, although not to as great a degree. What this means is that the wooden structure designer may have to take explicit measures to deal with crossgrain or shearing forces within the wooden structure which could safely be regarded as negligible by the designer who uses a conventional material with isotropic properties, such as steel or aluminum. It also means that in cases where large loads flow in more than one direction, that wood fiber will have to be arranged to align with all of these loads. For cases where the large loads are confined to a single plane, a structure such as laminated veneer or plywood can meet the requirements. Where loads in all three axis exist, the designer must use more sophisticated approaches tailored to the loads and geometry. One of the key elements in our success with lightweight wood composite boat structures has been an ability to identify directional loads so that we could align our wood fiber accordingly.

Wood has an exceptionally high work of fracture (around 10^4 j/M^2) with an almost total resistance to crack propagation that is so familiar with metals. By its very nature as a fibrous material, wood has excellent resistance to repetitive fatigue loading. When one considers that nature has spent millions of years in the serious business of competitive survival to develop strong trees which must stand repeated and highly variable loads from wind for long periods of time (some redwoods are several thousand years old), it is not surprising to find that wood is an efficient structural material with very respectable fatigue properties. Unfortunately, the fatigue testing done with wood has been minimal in comparison to other materials; but results to date indicate that infinite fatigue life occurs somewhere between 30% to 40% of ultimate. When building high performance racing craft where safety margins are not particularly important, we often use as high as 100% of ultimate with surprisingly good long term performance. This is probably due to the unusual failure mechanism of wood.

In boats, wood is usually used in bending so that tension and compression forces occur in the same part. Failure will always be in compression which is the weakest part of wood. As compression loads are applied to the individual wood cells, they can deform considerably before initial failure begins to occur. This deformation allows the wood cell to share some of the burden with those cells closer to the natural axis which, in effect, transfers some of the load to the tension side. In this way, the actual load on a wooden beam before total collapse occurs may be up to twice the theoretical compressive stress. No doubt this ingenious mechanism was designed by nature to allow trees to withstand occasional violent gusts of wind. For boats, this failure mechanism together with good fatigue life and resistance to stress concentrations make wood a potentially very safe material; and to quote Mr. J. E. Cordon, "a material with which one can vary nearly get away with murder".

It appears that nature happened on a very good thing when it invented a cellular structural material in which a significant portion of its volume is composed of air. Man has tried to duplicate this phenomena with the development of expanded foams, but even the best of man-made foams is a poor match for wood on a weight-to-strength or stiffness basis. Efforts to develop superior materials have generally centered around the exotic high-modulus fiber composites such as boron or carbon. While these materials exhibit an extremely high Young's modulus per unit weight, they do not have the desirable low-density resistance to buckling of wood. Rather than continue his pursuit of high-modulus fibers, man might better spend his time developing a material with holes in it. The efficiency of low-density materials is clearly

illustrated in Table 1 where wood (spruce) is compared with a number of materials in various roles.

Table 1. The efficiency of various materials in different roles

Young's modules, specific gravity					
Material	EMN/m^2	p grams/c.c.	E/p	$\sqrt{E/p}$	$\sqrt[3]{E/p}$
Steel	210.000	7.8	25.000	190	7.5
Titanium	120.000	4.5	25.000	240	11.0
Aluminium	73.000	2.8	25.000	310	15.0
Magnesium	42.000	1.7	24.000	380	20.5
Glass	73.000	2.4	25.000	360	17.5
Brick	21.000	3.0	7.000	150	9.0
Concrete	15.000	2.5	6.000	160	10.0
Carbon-fiber composite	200.000	2.0	100.000	700	29.0
Wood (pruce)	14.000	0.5	25.000	750	48.0

Where :

E/p is specific Young's modulus

$\sqrt{E/p}$ is weight-cost of carrying a compression load in column

$\sqrt[3]{E/p}$ is weight-cost of a panel in buckling

Taken from the book "Structures" by J.E. Gordon.

While the Young's modulus of wood is low in comparison to other materials, its efficiency as a panel is superior to even that of a carbon fiber composite. Panel stiffness is the single most important physical property of a material for boats. A boat hull and deck has significant amounts of surface area that must all be adequately supported against high-point loading at the least cost in weight.

Lightweight panels can be built with higher-density materials by bonding two separate skins on either side of a lightweight core of foam or end grain balsa. Unfortunately, this procedure is quite expensive both in cost of materials and labor to produce, but even then will probably not provide a panel that is as efficient as wood. Certainly the complexity and difficulties of engineering structures with cored laminates are well known.

Conclusion

Wood is an engineering material that possesses some unique potential for boat construction that is unavailable with any other material. Specifically, wood has high-weight-to-strength values, is almost immune to crack propagation, is resistant to stress concentration, and has excellent resistance to fatigue loads. The density range of wood seems to be ideally suited for boats to provide the highest stiffness at the least cost in weight. These are all the advantages; but like all engineering materials, wood has its share of problems which we shall discuss in detail.

Historical Problems with Wood and a Modern Solution

With the development of modern engineering materials, such as steel, aluminum and fiber reinforced plastic composites, the use of wood as a serious engineering material for sophisticated structures has greatly diminished. The reasons for this are generally well known, wood

can deteriorate from rot, and be dimensionally unstable. The fact that the consistency of wood can vary within a single tree together with fluctuation in physical properties because of moisture level change can cause difficult quality control problems.

We feel that the demise of wood as a serious engineering material is both unfortunate and premature. With the help of modern technology, most of the problems with wood can be solved in a practical manner. For the past ten years, we have used wood in composite with plastic resins to build high-performance sailing craft; specifically, iceboats and multihull craft that must be built at high strength and stiffness-to-weight ratios in order to be successful. In part, our success has been due to the fact that wood itself is an excellent engineering material; but our ability to solve the moisture problem with wood, however, has been the key to the development of wood as a practical engineering material especially for use in a hostile marine environment.

To better understand what we have done to achieve our solution, a discussion of the inter-relationships between moisture and wood is needed.

Moisture is a major ingredient of all wood in the living tree. Even wood that is properly dried or cured will have a significant percentage of its content by weight being moisture. This will typically range from 8% to 15% of the oven dry weight of the wood, depending upon the atmospheric conditions in which the wood exists. Figure 1 shows the ultimate moisture content of wood when subjected to various relative humidities at a temperature of 70°F. Unfortunately, the subject is a little more complicated than the chart portrays because 50% relative humidity is much different at 40°F. than at 70°F. (warm air holds more moisture than cold air); but every area will have an average year around moisture and temperature level that will determine the average wood moisture content level. In our Great Lakes area, wood seems to equalize at about a 10% to 12% moisture content when dried in a sheltered but unheated area. The real problem with wood is that its moisture level is rather quickly influenced by short term changes in atmospheric conditions. In the Great Lakes area, we continually have extremes of dry and humid climate conditions that are compounded by temperature extremes of 100° F. between winter and summer.

Wood cells are quite resistant to the invasion of moisture in a liquid form, but moisture vapor as a gas has a sudden and dramatic effect on wood by being able to easily and quickly pass through the cell wall structure. Responding to the changes in atmospheric conditions is thought to be the leading cause of wood to age prematurely¹. Conversely, wood in its natural state as a living organism will remain at a relatively constant moisture level during its entire lifetime until it is harvested.

This sponge-like capacity to take on and give off moisture at the whim of the surrounding environment in which it exists, is the root cause of all of the problems with wood. Specifically, varying moisture levels in wood are responsible for:

- 1 dimensional instability,
- 2 internal stressing that can lead to checking and cracking of the wood,
- 3 potential loss of strength and stiffness of the wood,
- 4 wood decay due to dry rot activity.

1 *Wood has been taken out of the tombs of Egypt that has been over 3,000 years old. Because of the constant temperature and humidity in which it was stored, the wood has lost none of its original physical properties there, in fact, must be rather exact conditions in order for dry rot spore activity to occur.*

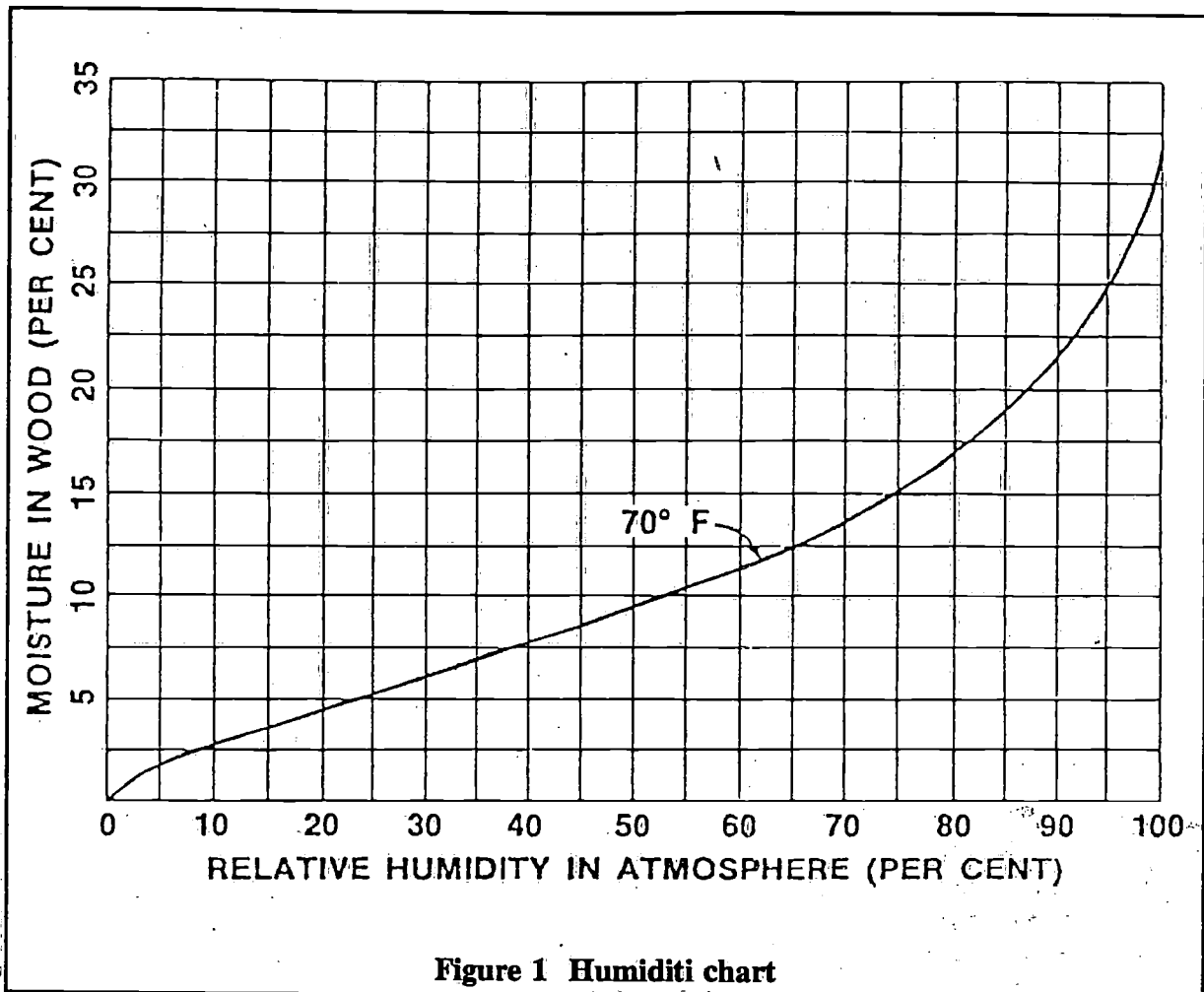


Figure 1 Humidity chart

Dimensional instability has always been a limiting factor for the use of wood in many engineering applications where reasonable tolerances must be maintained. To complicate matters, the dimensional instability of wood has never been constant and varies widely between species of wood, with radial grain wood (cut perpendicular to grain) in most species being more stable than is tangential wood (cut parallel to grain). The dimensional change of wood due to moisture change always occurs first on the outer surface causing differing moisture levels to occur within the same piece of wood. This can lead to internal stressing that often is the cause of check-ing and cracking on the wood surface.

Moisture has a significant effect on the strength of wood. Dry wood is much stronger and stiffer than is wet wood. The reason for this is the actual strengthening and stiffening of the wood cell walls as they dry out. If wood is taken at its fiber saturation point of 20% and allowed to dry to 5% moisture, its end crushing strength and bending strength may easily be doubled and in some woods tripled. The result is that wood has the potential to be an excellent engineering material when dry but only a mediocre material when wet. This causes a vexing problem for the engineer who may not be able to determine the level of moisture content that can be maintained in the structure he is designing and must assume a worst case situation.

Of all of the problems with wood, dry rot decay is the most known and feared. Dry rot is a misleading term since dry wood does not rot; there, in fact must be rather exact conditions in order for dry rot spore activity to occur.

- 1 The moisture content of wood must be at or near the fiber saturation point of 25% (rot is unknown in wood with a moisture content less than 20%).
- 2 There must be an adequate supply of oxygen available to the rot spore fungi, i.e. the wood must not get too wet.
- 3 The temperature must be warm, 76° to 86° F. is ideal although fungi have been known to be active at temperatures as low as 50° F.
- 4 There must be the proper kind of food. Some woods such as western red cedar are resistant to rot because of the tannic acid in their cellular makeup.

Although there are many types of rot fungi that can destroy wood, in North America there are two species of the brown rot family that predominate. They are very hardy creatures that seem to survive large temperature extremes in a dormant state waiting only for the right conditions to occur to become active. Efforts to control the brown rot family have had only limited success and generally center around poisoning the food supply with various commercial wood preservatives. Our approach to solve this problem is quite different as will be explained.

Wood's benefit of being a low-density material becomes a disadvantage when it must be joined. The use of fasteners as a joining medium is a limiting factor on the load transfer capacity between wood parts. Only a properly designed adhesive bonded joint can utilize the full potential of wood. Historically, this has created a problem because wood bonding has only been totally successful when performed under ideal conditions. Complicated structures such as boats present difficult bonding conditions with potential for failure; thus, most designers or builders have been reluctant to use this joining method and revert to the less efficient but more predictable fastener concept of joining wood parts.

The Wood-Resin Composite

As we have discussed, most of the problems that we have with wood are moisture related. Therefore, a primary goal of incorporating wood into a composite with a resin is to provide maximum protection against moisture to the wood fiber. Our basic approach is to seal all wood surfaces with our proprietary resin system¹.

This same resin system is used as the bonding adhesive to make all joints and laminates with the goal that they too will be secured from moisture. The lamination itself can usually be counted upon to offer secondary moisture protection. To build our structures, we usually laminate thin veneers together and count on the glue line between each veneer to serve as a secondary moisture barrier. For instance, when using 1/8 inch thick veneers in a 1 inch thick laminate, we would provide 7 glue lines that must each be penetrated to increase or decrease the moisture content of the entire laminate.

The success of the wood-resin composite-method depends on the ability of the resin employed to resist moisture passage. Our resin system is the most effective moisture barrier that we know of and has proven itself through actual usage over many years in marine construction. We can not claim that this resin system forms a perfect moisture barrier, but it does slow the passage of moisture into the wood to such a great extent that any moisture change within the wood itself is minimal.

¹ *We began the development of our resin system in 1969 specifically to solve the problems that we had with wood. The makeup of our resins are trade secrets of our company. For the past eight years we have marketed these resins and associated products under the WEST System trademark.*

If dry wood encapsulated in our resin were put in a steam bath and left there for several months, the moisture in the wood would eventually rise. However, the rate of moisture change in a wood-resin composite is so slow under normal changing atmospheric conditions that the wood inside remains at a virtually constant moisture level that is in exact equilibrium with the average annual humidity and is able to easily resist violent seasonal moisture fluctuations. With the moisture content of the wood stabilized at constant levels, we are able to maintain a set standard of physical properties together with excellent dimensional stability. Dry rot is eliminated as a problem by keeping the moisture content below that required for dry rot activity and also by completely sealing the wood from an oxygen source that is a necessary ingredient for the rot spores to survive. Our testing has shown that even if wood should reach a moisture level high enough to support rot spore activity, the rot spores still can not exist without adequate oxygen.

We, of course, did not invent the principle of laminating wood; this process had been commonly used for a number of years. There are, however, some significant differences with our method. First, a wood-resin composite laminate as we construct it is composed of a very high resin content by weight, considerably higher than what is considered normal. This high percentage of resin-to-wood ratio is desirable for several reasons. Enough high-density plastic is available in the composite to provide sufficient moisture protection to all of the wood fiber. Secondly, our resin has excellent physical properties with the potential to improve the composite structurally. Wood is considerably stronger in tension than it is in compression. The resin that we have developed is just the opposite, being much stronger in compression than it is in tension. By properly mating the two materials, one compliments the weakness of the other with the potential for more strength than either would be capable of on its own. How much extra strength that is developed is dependent on several variables which include wood density, wood resin ratios, and geometric configuration of the laminate.

Most wood laminating adhesives require high pressures (up to 75 psi) and heat to assure effective bonds. Achieving high laminating pressure can be very expensive with a high capital expense for tooling. High pressures also severely limit the size of a laminated part that can be made. With our adhesive system, we are able to make perfect bonds¹ at very low laminating pressures. In many cases, only contact pressure is needed between wood pieces because our adhesive has sufficient physical properties to easily span small gaps. Low laminating pressures have the positive effect of lowering the cost of wood bonding and also makes bonding practical in situations that once would have been considered too risky. In our custom boat construction, we rely primarily on staples that are supplied by air powered staple guns for laminating pressure together with various simple mechanical clamping mechanisms. When warranted, we use vacuum bag pressure against a mold that can provide up to 13 psi laminating pressure at nominal costs for equipment and tooling. Vacuum bag pressure techniques are especially effective with low volume production which is so typical of the marine industry.

Economics and Manufacturing Methods

Labor continues to be the largest single cost element in boat construction no matter what material is used. Wood has always been a labor intensive material, and our efforts to reduce labor hours with our wood-resin composite approach have only met with limited success. We

1 *The term "perfect bond" indicates that a bonded joint tested to destruction will have a failure mode within the wood fiber itself rather than the resin bond, i.e. the bond is stronger than the grain strength of the wood.*

are presently cost competitive with any other construction material in the custom or semi-custom range; and in some sizes and types of boats, we seem to have a definite cost advantage. In production quantities, *C.R.P.* construction with its use of a female mold has an obvious advantage over any competitive method that we can presently offer. With small boats, however, this advantage is mainly in reduced finishing time (a molded gel coat finish in comparison to a hand applied finish). We and others have laid up small boat hulls (up to 20 feet in length) using male molds with vacuum bag pressure in labor hours that approach being competitive with a *G.R.P.* layup of the same size. We are presently experimenting with female molds in a program to develop large wood-composite windmill blades with the goal of developing a molded gel coat type finish. If this program proves successful, we may be able to use the same technique with wood-composite boat hulls to lower expensive finishing costs.

Methods of Hull Lamination

In our own boatbuilding practice, we have used three basic methods of laminating hulls with the goal of providing the best product at the least amount of cost to the customer. We have titled these three methods the "mold method," the "strip plank method," and the "stringer frame method." Each method can be varied to provide a great deal of flexibility. Each of the methods also has advantages and disadvantages for a given boatbuilding situation which we will discuss briefly.

A male mold or a plug is a form over which wood veneer can be laminated into the shape of the hull desired. The mold merely serves as a base upon which pressure can be exerted to facilitate a bond between wood laminates until the adhesive element cures. Usually, either staples or a vacuum bag is used to apply this pressure. When staples are used for pressure, a very simple riband-type mold can be used where perhaps only 50% of the mold surface is solid. With the vacuum bag process, the mold must be both solid and air tight to create a vacuum; and, of course, this more thorough type of mold is more expensive to produce.

The biggest advantage of the mold method is reproducibility; you can make any number of identical hulls from a single mold. An adequate mold can be built with minimal cost in man hours and materials allowing economical low unit cost for tooling. Even a sophisticated mold for a vacuum bag pressure system would only cost at most a quarter of that tooling needed for similar size *G.R.P.* hull production.

The disadvantage of the mold method is that even a simple mold presents an expense that may be difficult to justify if only one hull is to be built. The larger the boat, the bigger this problem becomes. Thus, the strip plank method of construction was a natural evolution of the mold method where the mold, in effect, becomes a permanent part of the hull. Most molds are stripped planked anyway; and with a little alteration, we found that it was easy to allow the strip planking to become a permanent part of the structure rather than remain on the mold frames. Besides the obvious efficiency in savings of labor and materials, a further benefit is derived with this method with the capability to install all bulkheads, frames, and other interior items directly in the setup stage rather than having to laboriously install these items later into an already completed hull which is necessary with the mold method. We also found that this method is structurally efficient with the strip planking providing the longitudinal fiber in a hull scantling system. Subsequent layers of veneer are then bonded on the exterior strip plank surface to provide both diagonal and athwartship strength and stiffness. Well placed bulkheads and interior appointments are used to further strengthen and stiffen the hull laminate. Thus, we are able to efficiently produce an exceptionally rigid and strong monocoque hull structure

and, at the same time, produce a smooth interior that is almost devoid of the normal interior framework associated with wooden boats.

Table 2. Approximate energies required to produce various materials

Material	$n =$ energy to manufacture Joules $\times 10^9$ per ton	Oil equivalent tons
Steel (mild)	60	1.5
Titanium	800	20
Aluminium	250	6
Glass	24	0.6
Brick	6	0.15
Concrete	4.0	0.1
Carbon-fibre composite	4.000	100
Wood (spruce)	1.0	0.025
Polyethylene	45	1.1

Note: All these values are very rough and no doubt controversial; but I think that they are in the right region. The value given for carbon-fibre composites is admittedly a guess; but it is a guess founded upon many years of experience in developing similar fibres.

Taken from the book "Structures" by J. E. Gordon.

Table 3. The structural efficiency of various materials in terms of the energy needed to make them

Material	Energy needed to endure a given stiffness in the structure as a whole	Energy needed to produce a panel of given compressive strength
Steel	1	1
titanium	13	9
Aluminium	4	2
Brick	0.4	0.1
Concrete	0.3	0.05
Wood	0.02	0.002
Carbon-fibre composite	17	17

(These tables are based on mild steel as unity. They are only very approximate.)

Taken from the book "Structures" by J. E. Gordon.

We usually choose low-density wood for our strip planking so that we can achieve the thickest hull skins at the least amount of weight to provide the maximum panel stiffness to further reduce the need for any supporting framework on the interior. A side benefit of the extra-ordinarily thick hull skins has been the very good insulating and sound deadening qualities which are desirable for boats cruising in northern climates. Unfortunately, there is a minimum hull skin thickness of around $\frac{7}{8}$ of an inch in which a hull can practically be built with this method. This is due to the fact that it is impractical to strip plank material less than $\frac{1}{2}$ inch thick. In addition, to eliminate the normal interior frame structure, we feel that a minimum of three laminations of $\frac{1}{8}$ inch veneer are needed over the exterior surface of the strip planking. This results in the minimum $\frac{7}{8}$ inch thick hull skin panel which will weigh approximately 2 pounds per square foot. This panel weight limits the practicality of the strip plank method to boats of 30 foot and up although there have been some heavier displacement cruising boats in the mid-20 foot range built with this method.

Some of the more successful boats with this method are the Ron Holland designed *Golden Dazy*, a Canada's cup winner, and the Britain Chance designed centerboarder *Bay Bea*, a U.S. Admiral's cup contender.

The stringer frame method of laminating is probably the most widely used method of building a custom one-off laminated hull. The basic procedure is to erect frames at a given interval (some may be only temporary) which are then covered with longitudinal stringers in sufficient numbers to serve as a beginning molding surface. Like the strip plank method, the stringer frame method eliminates the need for a mold. It also has the advantage that you can install interior members such as bulk-heads and permanent frames during the setup. The biggest advantage of the stringer frame method is that you can use it successfully with just about any size and type of boat. The stringer frame method has become very popular because it has the advantage of requiring the least amount of hours to produce a hull for a custom one-off boat. This method also has the potential to produce the best strength and stiffness-to-weight ratio hulls, particularly in situations where there is little compound curvature such as exists in catamaran or trimaran type hulls.

The stringer frame method also has its share of disadvantages. The main problem is that the builder must begin laminating the hull skins over what in reality is an inadequate mold. A good deal of skill on the part of the builder is necessary to overcome this initial obstacle when applying the first two laminations of veneer. With the longitudinal stringers set at 5 to 8 inch intervals, the first laminations must be installed with great care to insure a fair molded surface. It is only after the first two laminations are bonded in place that a good solid mold surface exists over which normal molding can take place. A further disadvantage of the stringer frame method is that it results in a cluttered interior. Unlike the mold or strip plank methods which result in smooth interior walls, the stringers and frames inherent with this method not only take valuable interior room but are also more difficult to keep clean.

The concept of the load-bearing skin, well supported by a stringer frame system, was first developed by the aircraft industry. By substituting load-bearing skin panels in place of fabric, aircraft designers found that they could build substantially better strength-to-weight structures which became a significant factor in the development of modern aircraft. With the development of plywood, the marine industry borrowed the load-bearing skin concept and, with a few modifications, were able to construct light-weight hull and deck structures. Because boats use water as their medium rather than air and because hulls sink when punctured, thicker skins are usually necessary as a practical measure in relationship to the supporting framework that

Table 4. Mechanical properties¹ of selected woods²

Species	Specific gravity	Static bending			compression parallel to grain-maximum crushing strength	Compression perpendicular to grain fiber stress at proportional limit	shear parallel to grain-maximum shearing strength	tension perpendicular to grain maximum tensile strength	Side hardness load perpendicular to grain	Impact bending height of drop causing complete failure
		Modulus of rupture Psi	Modulus of elasticity ³ Million Psi	Work to maximum load pounds per cubic inch	Psi	Psi	Psi	Psi	Pounds	Inches
Ash, white	.55	9,600	1.44	16.6	3,990	0.670	1,380	0.590	0.960	38
Balsa, medium	.60	15,400	1.74	17.6	7,410	1.160	1,950	0.940	1.320	43
Birch, yellow	.17	2,900	0.58	—	1,805	0.100	0.300	0.118	0.100	—
Cedar, Alaskan	.55	8,300	1.50	16.1	3,380	0.430	1,110	0.430	0.780	48
Cedar, Northern white	.62	16,600	2.01	20.8	8,170	0.970	1,880	0.920	1.260	55
Cedar, Port Orford	.42	6,400	1.14	9.2	3,050	0.350	0.840	0.330	0.440	27
Cedar, Western Red	.44	11,100	1.42	10.4	6,310	0.620	1,130	0.360	0.580	29
Douglas fir, coast	.29	4,200	0.64	5.7	1,990	0.230	0.620	0.240	0.230	15
Hickory	.31	6,500	0.80	4.8	3,960	0.310	0.850	0.240	0.320	12
Lauan, light red	.39	6,600	1.30	7.4	3,140	0.300	0.840	0.180	0.380	21
Mahogany, Honduran	.43	12,700	1.70	9.1	6,250	0.720	1,370	0.400	0.630	28
Mexican, dark red	.31	5,200	0.94	5.0	2,770	0.240	0.770	0.230	0.260	17
Meranti, dark red	.32	7,500	1.11	5.8	4,560	0.460	0.990	0.220	0.350	17
Okoume/Gaboon	.45	7,700	1.56	7.6	3,780	0.380	0.900	0.300	0.500	26
Pine, loblolly	.48	12,400	1.95	9.9	7,240	0.800	1,130	0.340	0.710	31
Pine, longleaf	.64	11,100	1.57	23.7	4,580	0.840	1,520	NA	NA	74
Pine, white	.72	20,000	2.16	25.8	9,210	1.760	2,430	NA	NA	67
Ramin	.41	7,500	1.44	NA	3,750	NA	0.840	NA	0.500	NA
Spruce, black	.44	11,300	1.67	NA	5,750	NA	1,090	NA	0.590	NA
Teak	.45	9,300	1.28	9.6	4,510	NA	1,310	NA	0.700	NA
Walnut, black	NA	11,600	1.51	7.9	6,630	NA	1,290	NA	0.810	NA
Yew	.43	8,600	1.50	8.8	4,450	NA	NA	NA	0.560	NA
—	—	12,100	1.63	11.7	6,970	NA	NA	NA	0.630	NA
—	.37	7,300	1.14	—	3,900	NA	NA	NA	0.380	NA
—	.47	7,300	1.40	8.2	3,510	0.390	0.860	0.260	0.450	30
—	.51	12,800	1.79	10.4	7,130	0.790	1,390	0.470	0.690	30
—	.54	8,500	1.59	8.9	4,320	0.480	1,040	0.330	0.590	35
—	.59	14,500	1.98	11.8	8,470	0.960	1,510	0.470	0.870	34
—	.34	4,900	0.99	5.2	2,440	0.220	0.680	0.250	0.290	17
—	.35	8,600	1.24	6.8	4,800	0.440	0.900	0.310	0.380	18
—	.59	9,800	1.57	9.0	5,395	NA	0.994	—	0.640	NA
—	NA	18,400	2.17	17.0	10,080	—	1,514	—	1,300	NA
—	.38	5,400	1.06	7.4	2,570	0.140	0.660	0.100	0.370	24
—	.40	10,300	1.53	10.5	5,320	0.530	1,030	—	0.520	23
—	.37	5,700	1.23	6.3	2,670	0.280	0.760	0.250	0.350	24
—	.40	10,200	1.57	9.4	5,610	0.580	1,150	0.370	0.510	25
—	.57	11,000	1.51	10.8	5,470	—	1,290	—	1,070	—
—	.63	12,800	1.59	10.1	7,110	—	1,480	—	1,030	—

¹ Results of tests on small, clear straight grained specimens. (Values in the first line for each species are from tests of green material, those in the second line are adjusted to 12% moisture content) Specific gravity is based on weight when oven dry and volume when green, or at 12% moisture content.

² We and others use these species with WEST System products.

³ Modulus of elasticity measured from a simply supported, center loaded beam, on a span depth ratio of 14 to 1. The modulus can be corrected for the effect of shear deflection by increasing it 10%.

are common in normal aircraft construction scantling systems. Even so, skin thicknesses on boats built with the stringer frame system are usually much less when compared to the skin thicknesses necessary with either the mold or the strip plank method. The basic concept behind both the mold and strip plank method is to produce a total monocoque self-supporting load-bearing skin; the stringer frame supported skin, however, is only a partial monocoque in that it can only be load bearing when properly supported by framework.

With hulls that have significant amounts of compound curvature, we usually prefer a thick skinned total monocoque-type hull; but with hulls that have significant amounts of flat or straight runs, the framework supported partial monocoque is preferred. Our decision between the two, other than for purely technical reasons, is usually influenced by economics and the personal taste of the client.

Our basic laminating material has been $\frac{1}{8}$ inch thick sliced veneers. We have also used thinner plywood from $\frac{1}{8}$ to $\frac{1}{4}$ inch thick; but structurally, plywood is not as efficient as veneer on a weight-to-strength or stiffness basis. (Because of several extra glue lines within a plywood laminate, it is usually considerably more dense than veneer.) Plywood also costs at least twice as much as does veneer on a per square basis. Sliced veneer should not be confused with the more normal rotary cut veneer that is used in most plywood panels. Rotary cut veneer is made by rotating a log in a lathe with a sharp knife, then peeling off a thin layer of veneer from the rotating log. Sliced veneers are made by first cutting the log into quarters, then slicing off a given thickness of veneer by moving the quartered piece down upon a fixed blade, slicing off a veneer that usually measures from 8 to 15 inches in width and anywhere up to 17 feet in length. The slicing process provides edge grain orientation within the veneer providing a very stable and flat material which makes the laminating process much easier, i.e. less pressure is needed to secure the veneer laminate in proper position. One-eighth inch thickness is about the maximum that can be sliced without damaging the wood fiber during the slicing process.

Fortunately, the $\frac{1}{8}$ inch thickness seems to be an ideal choice for most laminating situations. Larger hulls can be laminated with thicker stock, but the cost of sawing and the associated waste and material is usually not worth any benefit that can be gained (there is no waste in the slicing process).

Material Cost for the Wood-Resin Composite

Contrary to popular belief, the cost of high-quality wood is quite low especially when compared to other efficient competitors in the marine field such as aluminum or a cored *G.R.P* laminate. The cost of wood, of course, varies by species, quality and dimensional size. One of the more common species that we use is Douglas fir which can be purchased in sawn dimensional stock at approximately 40c per pound or slightly less than one dollar per board foot. Sliced and trimmed $\frac{1}{8}$ inch Douglas fir veneers ready to use would cost approximately 80c per pound or 30c per square foot. The price of our resin is at present \$1.80 per pound; and assuming that it is used in a ratio of 20% resin to 80% wood fiber to form a composite, the resultant per pound cost of one dollar is lower than the cost of aluminum or a foam cored GRP laminate on a weight basis. To be added to this is always the possibility that on a per pound basis wood may be the more efficient material for a given application, saving some weight and cost of material in the process.

The most interesting aspect of wood is its future cost potential. Over the past five year period, the price increases on top quality (clear) Douglas fir have been considerably less than the inflationary rate. This in part is due to the fact that very low levels of energy are needed

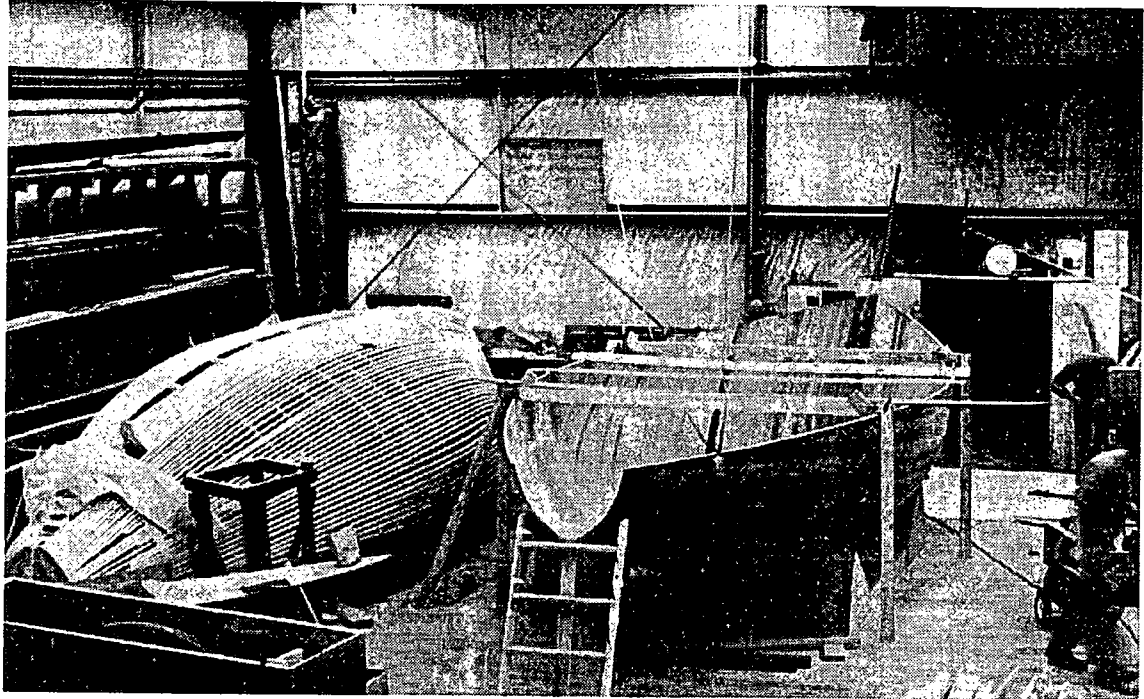


Figure 2. A simple riband mold is used to produce a 30 foot hull laminate which consists of 6 layers of $\frac{1}{8}$ inch thick veneer



Figure 3. The $\frac{1}{8}$ inch thick veneers were held in place with staples until a resin cure could take place. After the first two layers were bounded, the alloy staples were left in place on subsequent layers to save time.

to turn a tree into usable stock (veneer or dimensional boards). In comparison, many materials such as aluminum require high levels of energy to produce and have increased in price at a much higher rate. Figure 1 shows the relative amounts of energies required to produce all of the common materials while Table 3 shows the structural efficiency of various materials in terms of the energy needed to manufacture them. In both cases, wood is by far the most efficient material per unit of energy required to produce. We feel that as energy costs continue to escalate in proportion to other costs, the price of wood will decrease in relationship to the other materials because of its minimal dependence on energy. Rising energy costs should further favor the use of wood by putting a premium on lightweight construction.

It is difficult to predict the future of the wood-resin composite. We feel that its use in custom and semicustom boat construction will continue its present rapid increase in popularity, but its future as a production material is less clear. As we have discussed, the rising cost of energy will have a positive effect but will probably never be enough to overcome present high labor costs. An improvement in present technology will be needed to make the wood-resin composite an economically competitive material in volume production. Over the past 30 years, GRP technology has developed to its present fine art. In comparison, wood-resin composite manufacturing technology is quite new; and there is a great deal yet to be learned. The next five to ten year period will see a period of intense activity by ourselves and others to develop better manufacturing techniques to solve this last major problem with wood. For sure, we can safely predict that we will all see a steady increase in the use of wood in the marine field in the years to come.

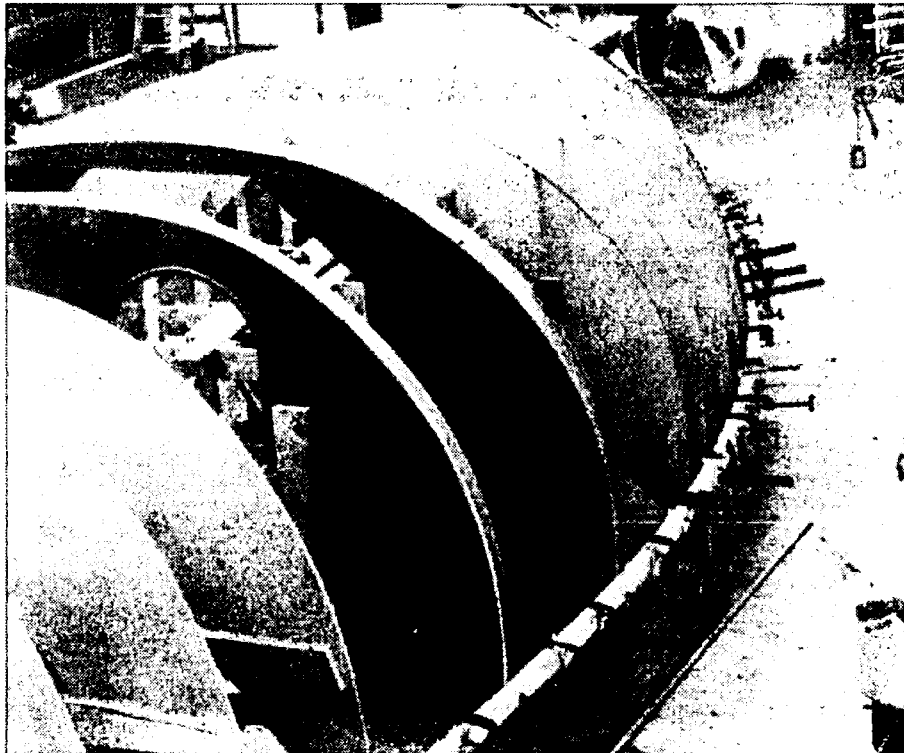


Figure 4. A set-up for the strip plank method incorporates temporary frames that are later removed, but permanent bulkheads and frames can be installed in the setup stage to save time.



Figure 5. Strip planking that is neither tapered nor beveled (to save time) is temporarily fastened to the mold frames until the bonding adhesive between the plank edges reaches a cure. The planks are also bonded to any permanent members in the set-up.

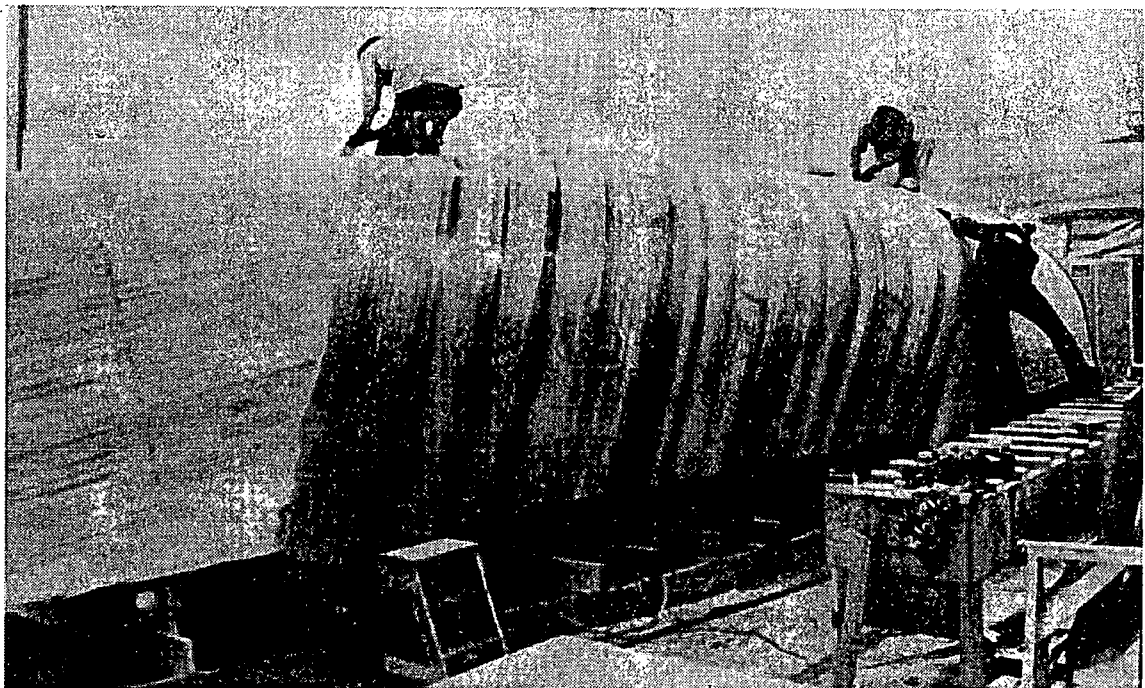


Figure 6. The first layer of $\frac{1}{8}$ inch thick veneer is applied at a diagonal angle over the strip planking.

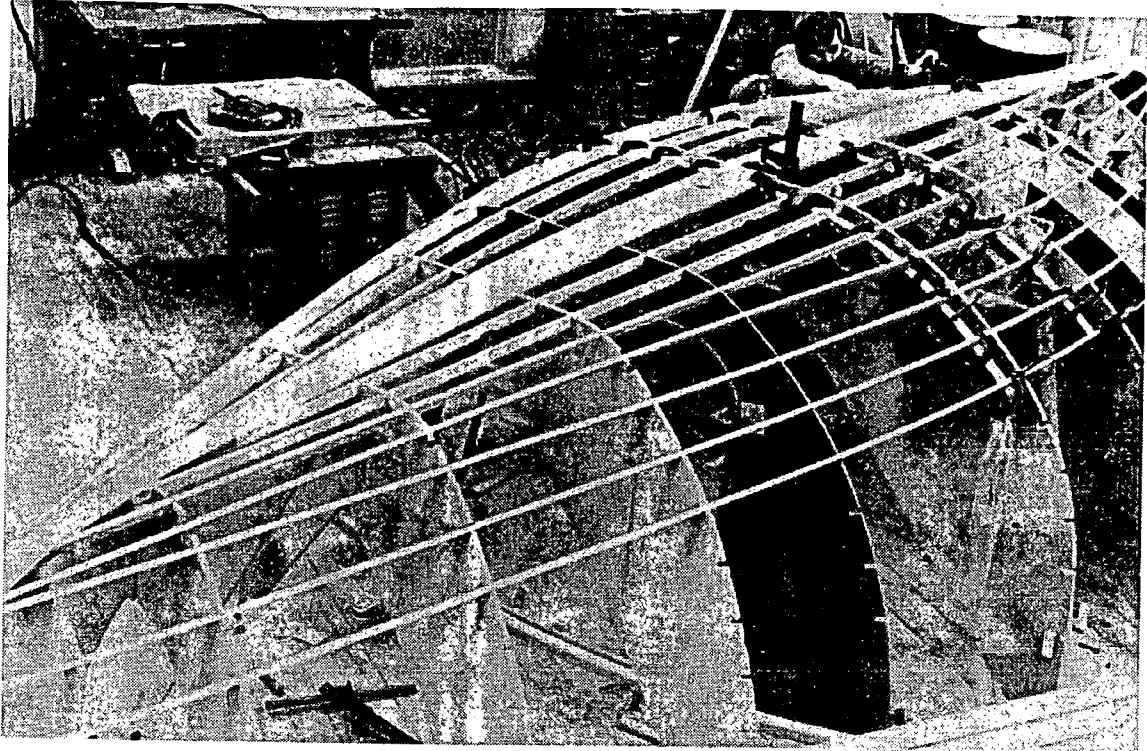


Figure 7. The setup for the stringer frame method also uses temporary mold frames, but bulkheads, frames and other interior items can be efficiently installed at this point.

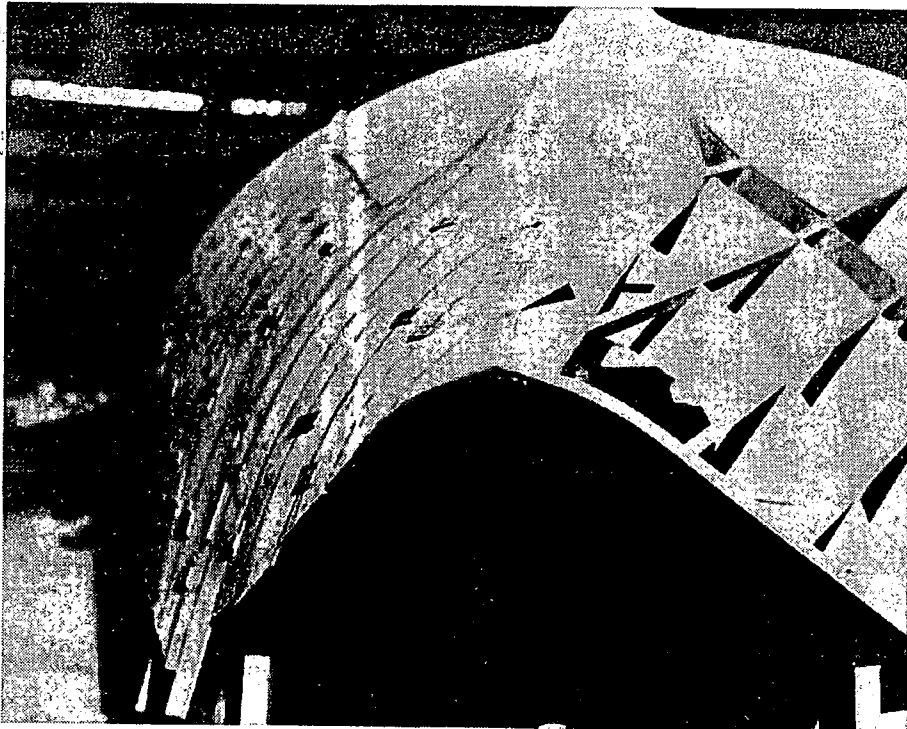


Figure 8. The first layer of veneer is very carefully installed over the stringers. The pads serve to help line up the veneer edges between stringers where they are not supported.

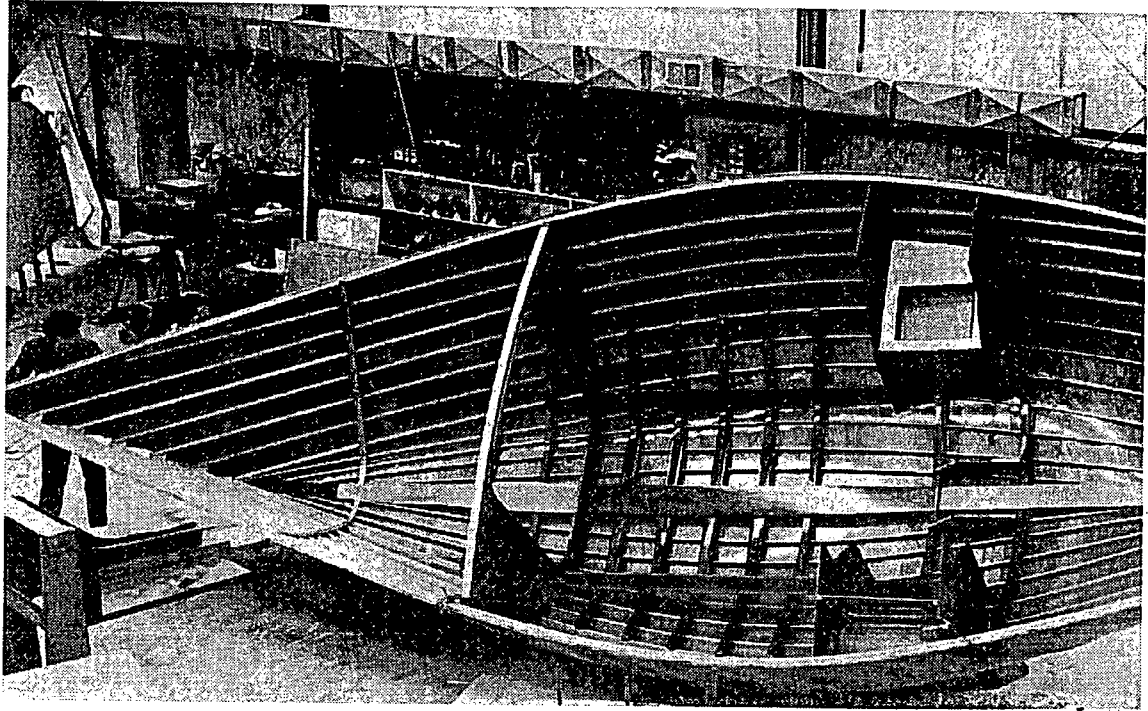


Figure 9. The completed hull is being rolled over. Note the heavy resin coating of all the interior parts.

Considerations relative to a trimaran design for myself

by Richard C. Newick

Summary

Half of the author's 40 years of boating experience has been in multihulls. This paper explores the thinking that went into the design of a boat for him and his wife to live aboard for at least six months of each year.

Requirements

1. good performance
2. reasonable safety
3. convenient operation with a small crew
4. modest comfort for two with two occasion guests
5. moderate building and operating budget
6. efficient use of materials

General discussion

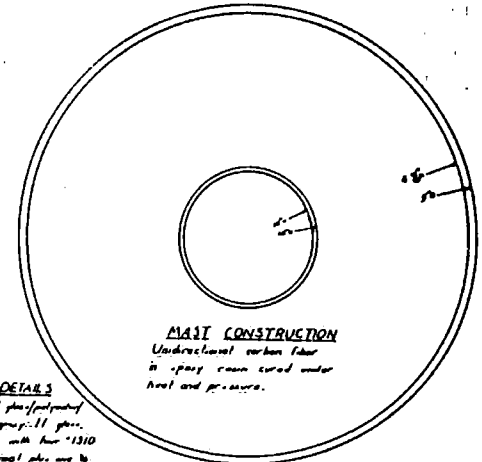
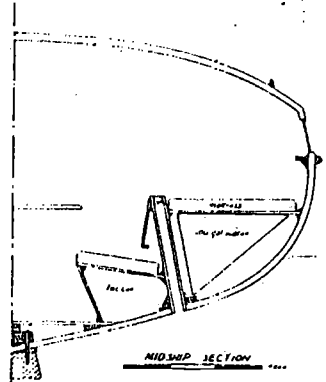
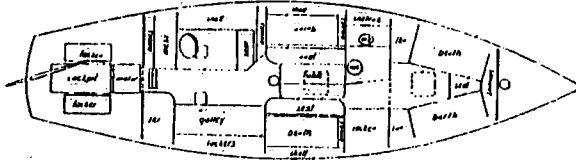
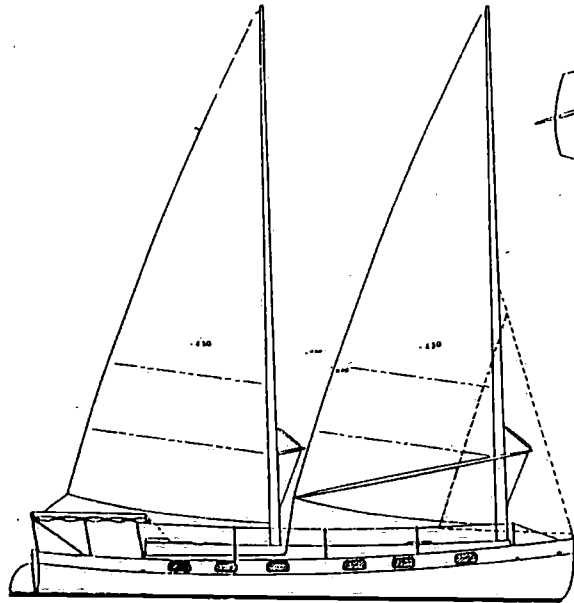
Polynesian terminology:

ama - outerhull

aka - connecting structure between the hulls

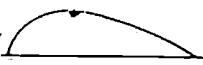
To establish an open minded approach, the author first designed a "monomaran" (Figure 1) considering the above requirements for an intended cruising area of the U.S. east coasts, hence the unusually shallow draft. This design uses a feature now common in the author's multihulls; every station in the hull is made from the same pattern. The sheer and keel are lofted conventionally in plan and elevation views. The stations of sheer and keel are then transferred to the body plan and each station's points are joined by laying a "master pattern" on them, keeping a reference point on the pattern on a reference line drawn on the body plan. After some experience choosing a master pattern and appropriate reference lines, this method can give a quickly generated set of fair multihull lines with little or no compromise in desired qualities.

The monomaran was vetoed for our use because she lacked one essential quality; the sparkling performance that multihull sailors learn to love. Figures 2 and 3 show a 50 foot trimaran, the author's design #50, which is the subject of this paper. She is expected to fulfill the above requirements. Figures 4, 5 and 6 show SIB (a name inspired by the title of E.P. Schumacher's book 'Small is Beautiful'). She is a 31' trimaran and might be considered a prototype for design #50. SIB was launched in 1978, conceived by Phil Weld, Jim Brown and the author was a simple sailing workboat, but she has so far generated more interest among yachtsmen than among commercial seamen.

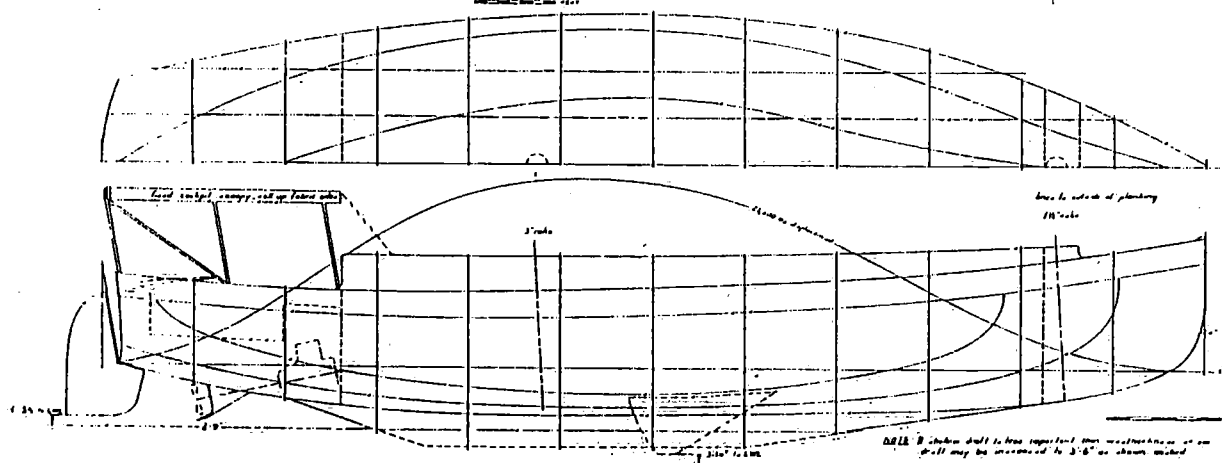


CONSTRUCTION DETAILS
 May be built either of glass/polyester
 from sandwich or unidirectional 11 ply.
 use 3/4" PVC foam core with four 1310
 Unidirectional tubular ply use 1/2"
 as mast outside three 1310 inside Wood
 construction shown here: planking and decking
 double diagonal 3/4" wood of beam 20 to 36 lbs/ft. H.
 weight over laminated with frame 2 1/2" - 2 1/2" spaced
 10". keel and stem laminated of 3/4" ply.
 shear clamp with. All drilled with three ply
 of 4 oz. polypropylene use WEST epoxy resin
 throughout.

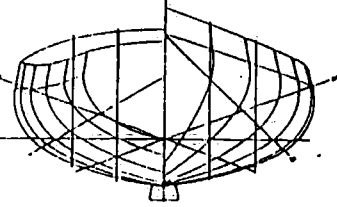
MAST CONSTRUCTION
 Unidirectional carbon fiber
 in epoxy resin cured under
 heat and pressure.



MAST STEP ASSEMBLY
 use wood for this part



LOA	48'-0"
LWL	45'-7"
BOA	13'-3"
BWL	11'-8"
Draft	2' -9"
Sail	860-970 sq.H.
Disp.	27.200 lbs
Ballast	9.000 lbs



NOTE B shows draft to true top surface then weatherline as on
 shell may be increased to 3'-6" as shown marked

Figure 1 Lines Plan Model A

Rig

SIB's unstayed schooner rig with a Ljungstrom style foresail has served well. Unstayed masts are both ancient and modern. Today's Windsurfers, Lasers, and Finns make the most of their flexible rigs. Dr. Ljungstrom's designs and, more recently, the Freedom 40, have pioneered in larger sizes, disposing with weight, windage and expense of standing rigging. Aircraft, benefiting from larger research and development budgets, eliminated exposed wires in the early 1930's. Modern materials make further development of this theme possible. Carbon Fiber, "S" glass and wood are all feasible materials, using epoxy as the bonding agent. Production economies are making high modules and high strength carbon fibers cost effective where light-weight strength is vital. Aluminium's advantages for stayed masts is lessened in unstayed larger spars where fatigue resistance is an important factor.

A trimaran's wide sheeting base can be used to especially good advantage with the Ljungstrom rig, securing optimum sheeting angles with barber haulers led to the amas. Quick reefing and furling by simple amst rotation gives clear decks both in harbor and under sail. The sails open up, doubling their area off the wind, which may not be as efficient as spinakers, drifters and mizzen staysails, but it is cheaper and simpler. Chafe of the doubled sail on itself is not a serious problem if the seams are staggered. Halyards will seldom be used so long as it is acceptable to furl the sails around the mast.

Given the trimaran's great initial stability there is some concern about mast whip in a seaway. Consequently, ama sections on this design are unusually sharp and overall beam is moderate to give an easy motion. In addition, the slightly flexible akas are stayed with 6" wide nylon webbing with a tensile strength of over four times the vessel's displacement. Tension on these aka stays will be varied with lanyards at their outboard ends until they provide the desired amount of support and freedom to flex.

Design

Panels for each side of all three hulls of the 31' prototype SIB were built on the same inexpensive mold (Figure 4 and 6) using Jim Brown's Constant Camber (patent pending) concept with both the athwartships and longitudinal radii constant to make sections of a torroid which, when joined together in a spherical triangle of proper skin thickness, gives a light-weight, strong hull structure requiring no framing. This same mold can be used for a wide variety of hulls by varying the panel outlines, which are then joined at keel and sheer. Tooling cost for low volume or one-off production is modest, but the tripbe diagonally planked panel construction is rather labor intensive if mechanical fasteners such as staples or nails are used for gluing pressure. Vacuum bagging the glued veneers is now being developed.

Larger molds with different constant camber (patent pending,) radii are used in the subject design. They are part of a series of molds developed by SIB Associates. (Jim Brown, Chris White, John Marples, and the author) for various sizes and types of craft. Twist of the panels can give finer bows or fuller midsections as required. It is essential to accurately reproduce the boundary shape of each hull side to assure a straight centerline and smooth sheerlines in the assembled hull; keels are joined with epoxy/glass tapes, sheers have laminated sheer clamps glued in place to accept deck fastenings. Bulkheads and interior furniture are glass/epoxy taped in place before the hull is decked. The frameless interior can be finished bright for an easily maintained, attractive finish.

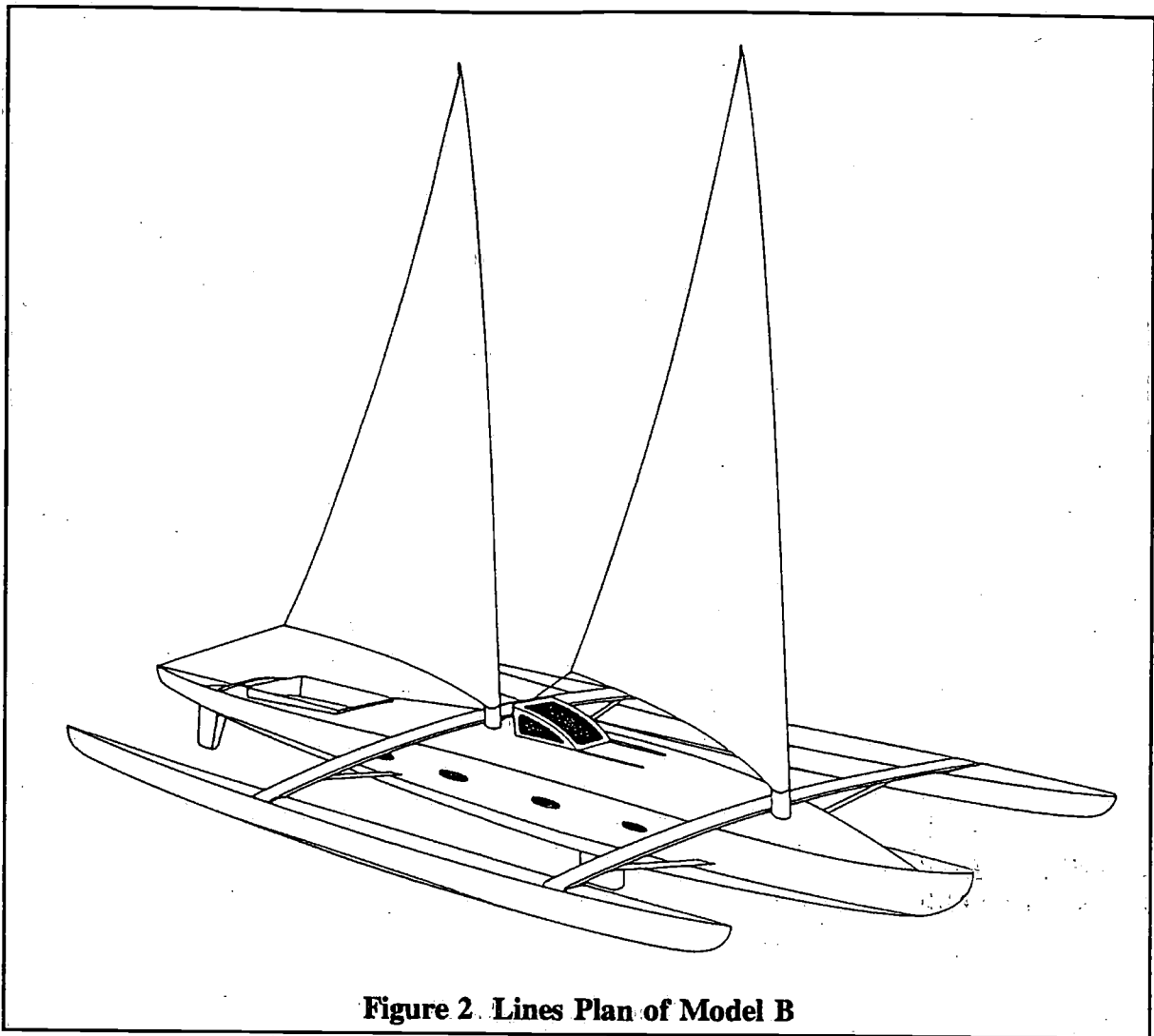


Figure 2. Lines Plan of Model B

Assembly/disassembly of the hulls and akas is facilitated by use of stainless steel straps and bolts, which makes building in shops with average sized doors remote from the launch site practical.

Material

Principal material is wood, 3 Plies of $\frac{1}{4}$ " (0.6 cm.) white cedar (juniper) in the hulls and decks. Wood is a renewable resource that is pleasant to work with. It is fastened and sheathed with epoxy and the exterior is further protected by a layer of Polypropylene cloth, tougher and lighter than fiberglass. Epoxy can be made from coal tar derivatives, decreasing demand for scarce petroleum. Polypropylene hull sheathing along with Dacron sails and running rigging are petroleum derived. These we consider a good use for our share of this much desired commodity and will consequently reduce our use of heating and propulsion fuels.

Spars will use carbon fiber/epoxy if tests are favorable. The per pound expense may be justified by the fewer pounds required as well as by savings from the elimination of standing rigging. "S" glass and wood alternate spar choices. (SIB's masts, 6", (0.15 m.) square at the deck are 30' (9.2 m.) long and weigh about 90 lbs. (41 kilo's) each). They have come through severe tests with no problems, as have her 3 ply hulls of $\frac{1}{8}$ " (3 cm) vertical grain douglas fir veneers. New linear polyurethane paint that can be brush or roller applied eases the maintenance of large areas of hull surface.

All materials are chosen with the realization that we have an obligation to use scarce resources wisely. This vessel will provide shelter and transportation for two people for at least half of each year and will require a minimum of outside services to maintain.

Equipment

The Tillermaster autopilot has helped to win several transocean races, drawing an average of 1/3 amp at 12 volts, with a battery fed by solar generated electricity (which gives two amps at 12 volt in sunlight). This Solar Power Co. charger takes up about as much deck space as a hatch. The clean, quiet efficiency of this combination is impressive. An extra long shaft 15 H.P. outboard motor will cruise this craft at six knots in a calm and will seldom be used otherwise. Mounted on a pivoting arm near the cockpit it is handy for those rare times it is needed, it gives no drag when not working and can be easily serviced ashore if necessary. The deck hardware list of standard items is short. Bearings for the rotating masts are still being researched.

Accommodation

Cabin space is small indeed for a 50 footer (15.2 m). The useable cabin length of 38' (11.3 m), waterline beam of 4 1/2' (1.3 m) and overall hull beam of just under 8' (2.4 m) limit us to double berths at each end with head, galley and dining area amidships. We cheerfully accept these modest comforts - and their moderate price - in order to enjoy sparkling performance, one of our major reasons for having a yacht. The cockpit has a shallow "W" cross-section which nicely fits the seated figure and has worked well on the author's first trimaran which has sailed for 19 years in the Caribbean day charter business. Deck area is supplemented by nets stretched between akas and hulls which afford easily accessible storage for two kayaks.

Aesthetics

In this part of the world we often hear that multihulls "do not look like a boat" and, indeed, many of them would not be considered pretty or graceful in any part of the world. The designer still finds this particular main hull less pleasing than he would wish. Perhaps if there is an opportunity to visit remote Pacific islands some old folks' eyes will sparkle as they exclaim, "Now that's what a boat should look like!"

Cost

This vessel is a bargain for her length, costly for her accommodation and downright cheap for her average speed under sail. Since boatyards and marinas will be avoided, most charges based on length are not a concern.

Multihull proponents of twenty years ago were often over-enthusiastic about low cost. We have found that a good multihull cannot be much cheaper than a good ballasted craft - insofar as they can be compared. The only great cost advantage realized by multihulls is on a per knot basis.

Safety

The safety of any vehicle is largely dependent on its operator. A vessel that might capsize is less tolerant of mistakes than a vessel that might right herself if rolled over by a big wave, which in seagoing multihulls is the biggest risk. Since no small craft can be guaranteed uncapsizable we are concentrating on limiting the likelihood of this happening and, if it does, of assuring the crew's survival and, if possible, their ability to right the vessel and sail on.

<i>L_{OA}</i>	50'	15.24 m
<i>L_{WL}</i>	44'	13.41 m
<i>B_{OA}</i>	27'	8.23 m
<i>B_{WL}</i>	4.6'	1.37
Draft	2.3'-7'	0.68-2.13 m
SA	700	65.1 m ²
Disp.	8500	3859 K
B	1.3	

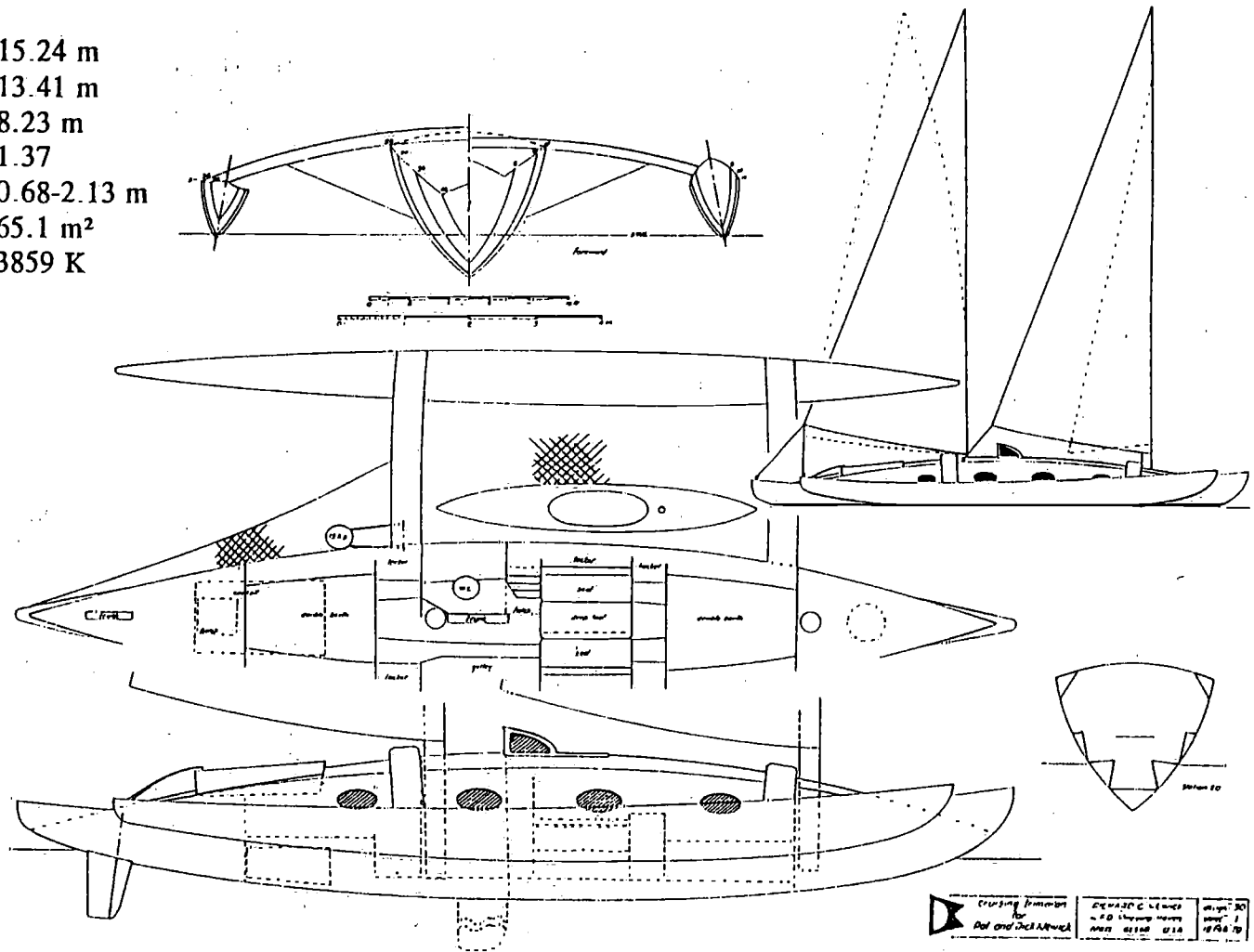


Figure 3 Lines Plan of Model C

This design does not lend itself to self-righting methods as first proposed by Carlos Ruiz of San Salvador, Central America at the Multihull Symposium in Toronto, Canada in 1976. He demonstrated with models the feasibility of flooding forward (or aft) compartments of a capsized multihull and using either buoyancy winched down to the masthead or boomed out water ballast, to induce bow (or stern) down righting. At present, the largest craft to have proven this method at sea is the 23' (7 m) Tremolino. Most of the author's stock designs now incorporate these features. Since the necessary compartmentation would have been unduly restrictive in this particular design, we have given special consideration to preventing capsize and are starting to experiment at sea with simple weighted drogues streamed from the amasterns in extremely bad weather to slow the quick reaction of a light vessel to a breaking sea from abeam. These drogues must be "tuned" to each particular vessel's characteristics in order to prevent her from being swept by a breaking sea while at the same time preventing a hull from being thrown into the air, the first phase of a capsize. We who prefer multihulls realize that capsize is our biggest problem. It is getting much serious attention.

It should be unnecessary to point out that any vehicle that offers a performance advantage will have speed exploited by those who wish to set records. Such attempts stress ultimate speed above other considerations. Failures should be judged in this context instead of sensationalized, as they often are, by semi-informed journalists who are just as ready to exploit a spectacular failure as they are to publicize a great new record.

Conclusion

These non-technical remarks may indicate today's rather primitive state of the multihull art. Important advances have been made with the help of basic engineering common sense but we are now at the stage where further progress will benefit from the attention of more technical talent.



Figure 4 "SIB" - 31' - Trimaran

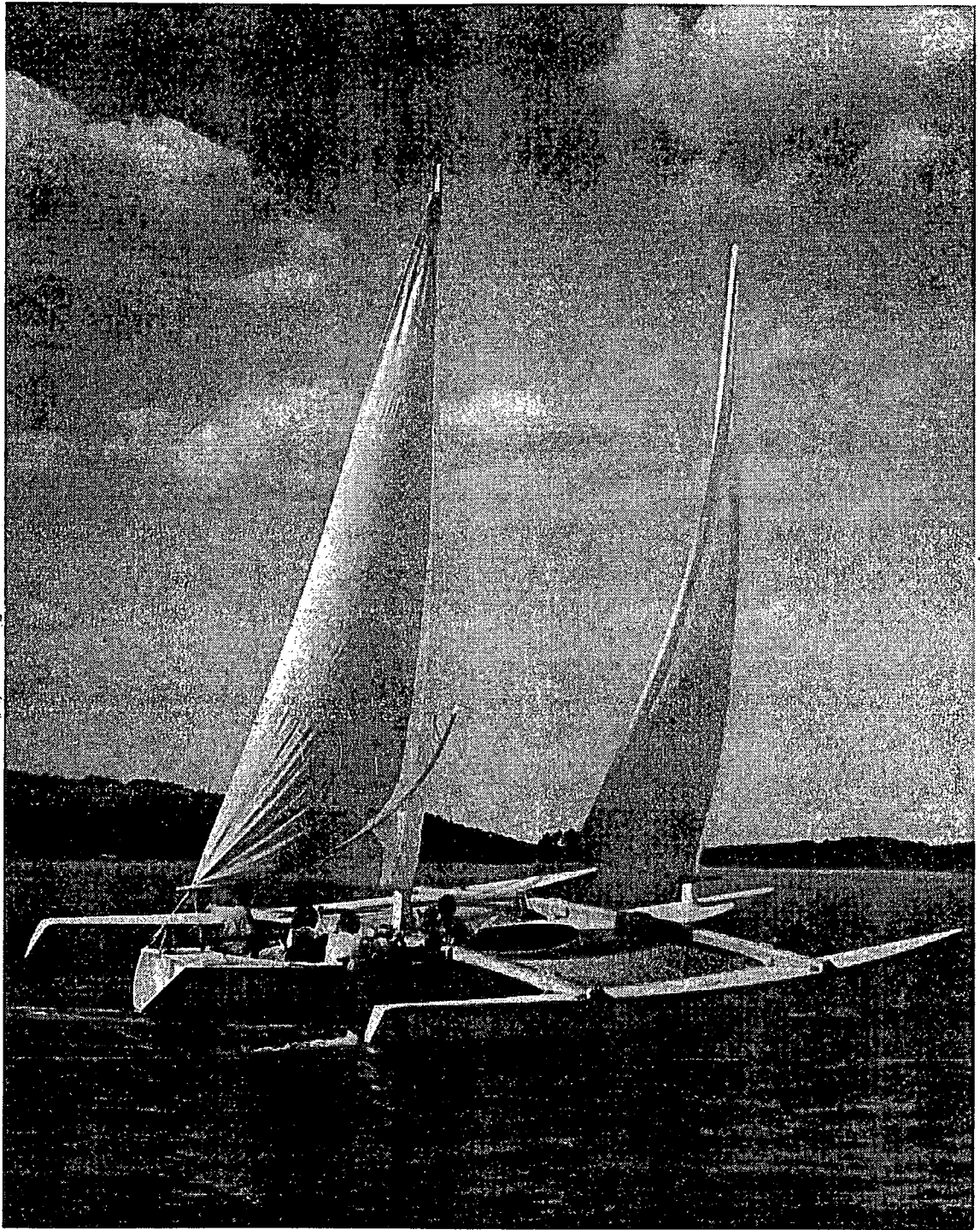


Figure 5 "SIB" - 31' - Trimaran

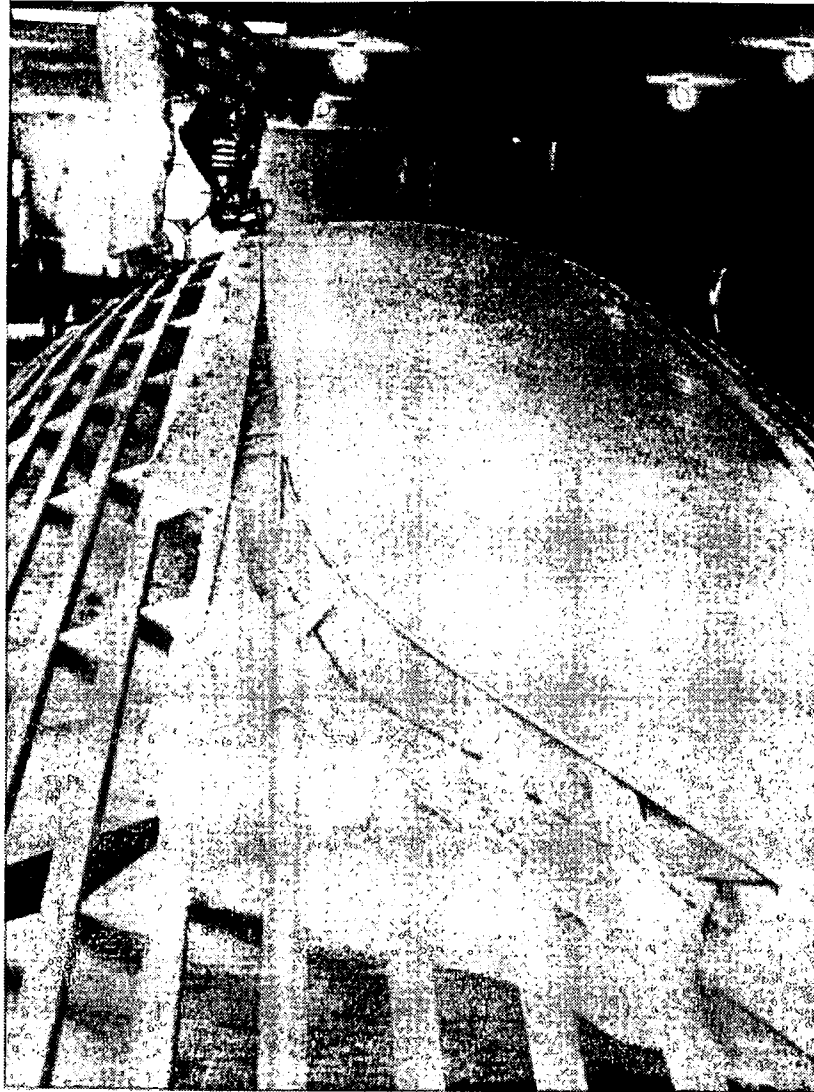


Figure 6 "SIB" - 31' - Trimaran

Appendix

To compare multihull designs the author relies on two different ratios, the Bruce number ($B\#$) and Stability number ($S\#$).

$$B\# = \frac{\sqrt{\text{sail area in square feet}}}{\sqrt{\text{displacement in pounds}}}$$

For the subject design $B\# = \sqrt{700} / \sqrt{8500} = 1.3$

$$S^* = \frac{\frac{\text{displacement in lbs.}}{2} \times \text{distance in feet between vessel } C_L \text{ and ama } C_L}{\text{sail area in square feet} \times 3 \times \text{distance in feet between center of sail area and center of lateral area}}$$

(* 3 pounds per square foot wind pressure at 28 knots)

For the subject design:

$$S^* = \frac{\frac{8500}{2} \cdot 14.2}{700 \cdot 3 \cdot 23} = 1.09$$

Comparison of S^* and B^* - author's designs:

Name	L_{OA}	B^*	S^*	Remarks
CHEERIO	32' (9.8 m)	1.57	.67	mini 1980 OSTAR (proa)
VAL	31' (9.5 m)	1.46	.69	2nd 1976 OSTAR
TRICIA	36' (11 m)	1.47	.69	fast cruiser for two
THREE CHEERS II	46' (14 m)	1.50	.79	racer/cruiser for four
ROGUE WAVE	60' (18.3 m)	1.57	.87	racer/cruiser for five
(unnamed)	56' (17 m)	1.70	.67	maxi 1980 OSTAR racer
DESIGN #50	50. (15.2 m)	1.30	1.09	simple cruiser

Comparison of the above boats which are primarily racers indicates that Design #50 will be reasonably fast and able to carry full sail longer than any of them.

Special considerations in trimaran design concern relative placement of the ama's centers of displacement and centers of lateral effort about 10% forward of these centers of the vessel at rest. This assures an easy helm when heeled.

Bibliography

Canoes of Oceann	Haddon & Hornell, Bishop Museum Press, Honolulu, Hawaii, U.S.A.
Multihull Seamanship	McMullen, Donald Mckay Co., New York, U.S.A.
The Case for the Cruising Multihull	Jim Brown, Nautical Publishing-Go., Camden, Maine 04843
Amateur Yacht Research Society	(various publications) The Hermitage, Newbury, Berkshire, U.K.
Multihull International	(periodical) 2 South St., Totnes, Devon, U.K.
Multihulls	(periodical and special publicantions such as The Symposium Book and The Capsize Bugaboo Book) 421 Hancock St., North Quincy, Mass. 02171
SIB Associates	(Constant Camber information Box 14, North, Va. 23128

Balance of helm of sailing yachts

- Shiphydrodynamics Approach on the Problem -

by K. Nomoto and H. Tatano

Motoyama-Minami
Kobe, 658 Japan

Abstract

Tank tests of three typical sailing hulls are carried out. Colin Archer redningskoite, a medium displacement cruising cutter and an IOR Q-tonner are taken. An emphasis is laid upon lateral resistance and its centre of action, namely *C.L.R.*

The experimental results are compared with existing methods of estimating lateral resistance and/or *C.L.R.*, including the popular method of geometric *C.L.R.*, slender body lift theory and the method of Gerritsma.

Then we propose a new method; a combination of Gerritsma method and slender body theory. This proved effective for most yacht hull types of the present day.

Finally we deal with a performance prediction based upon the tank test. Sail force data is taken from another experimental source. Balance of helm and its physical mechanism are discussed.

Preface

Balance of helm of sailing vessels has long been a popular topic. Sailors have a keen interest in "weather-helm" and "lee-helm" of their ships; naval architects often refer to "Centre of Effort (*C.E.*)" and "Centre of Lateral Resistance (*C.L.R.*)" and "Lead". Yet this problem has been dealt with largely on the empirical basis; rather few scientific approach on it [1]. Here we will introduce some experimental and analytical studies on the problem. These studies were performed at the Ship Experiment Tank of Osaka University as a part of a research project on shiphydrodynamics of sailing vessels.

1 Tank tests of three typical yacht hulls

1.1 Mode Types

We take three typical hull forms: the Colin Arche's "redningskoite" at one end, a light IOR Q-tonner at the other and a medium displacement cruising cutter in between. The lines are shown in Figures 1, 2 and 3 and their principal particulars in Table 1.

Models A and B are fabricated of polyuretane foam plastics with thin outer coat of polyester resin and inboard lining of GRP. Model C is of GRP sandwich construction with PVC-foam core. Our practice for turbulence stimulation to establish a turbulent boundary layer is two rows of square-section studs put on the hull surface. Arrangement is shown in the lines plans (Figures 1, 2 and 3). We have a good ship correlation with this technique [2].

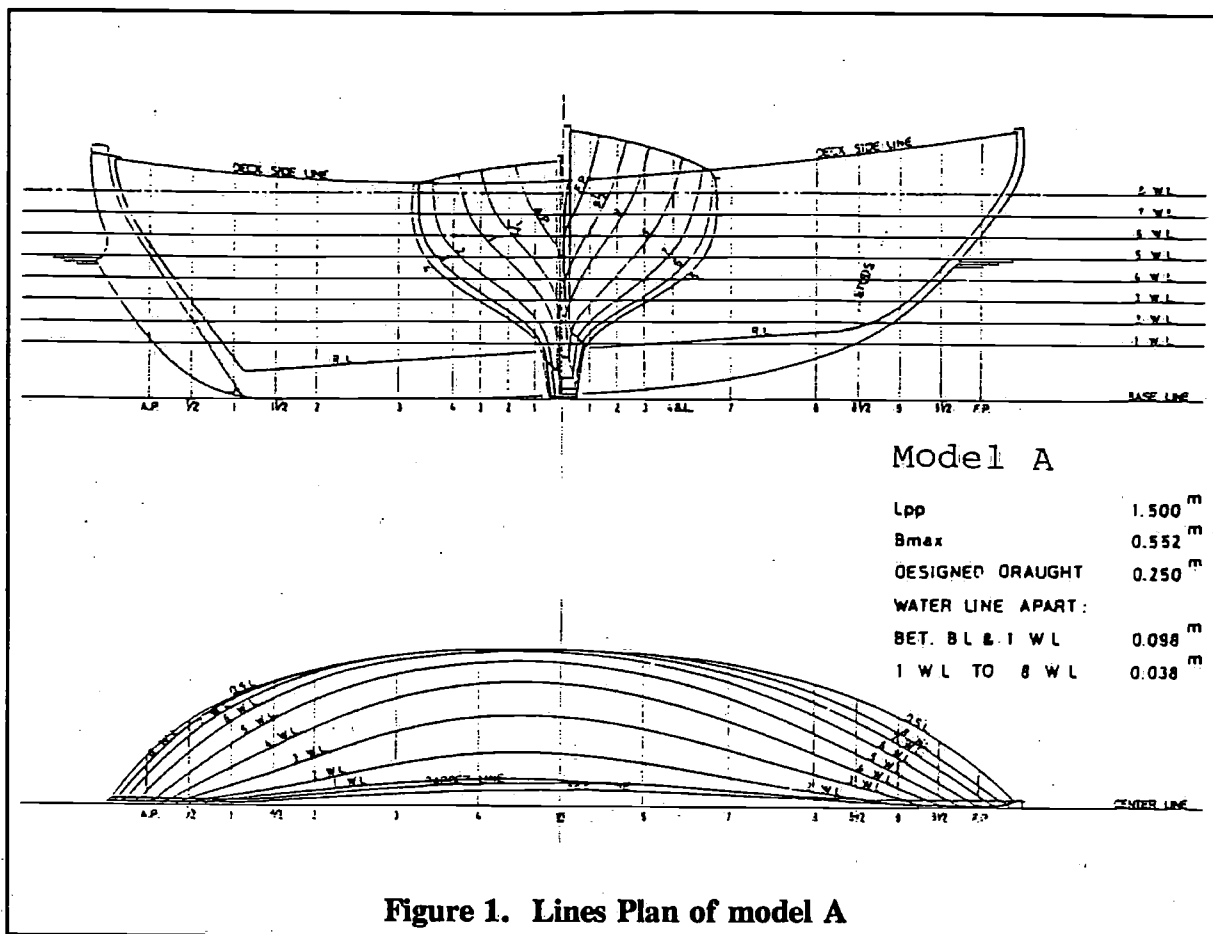


Figure 1. Lines Plan of model A

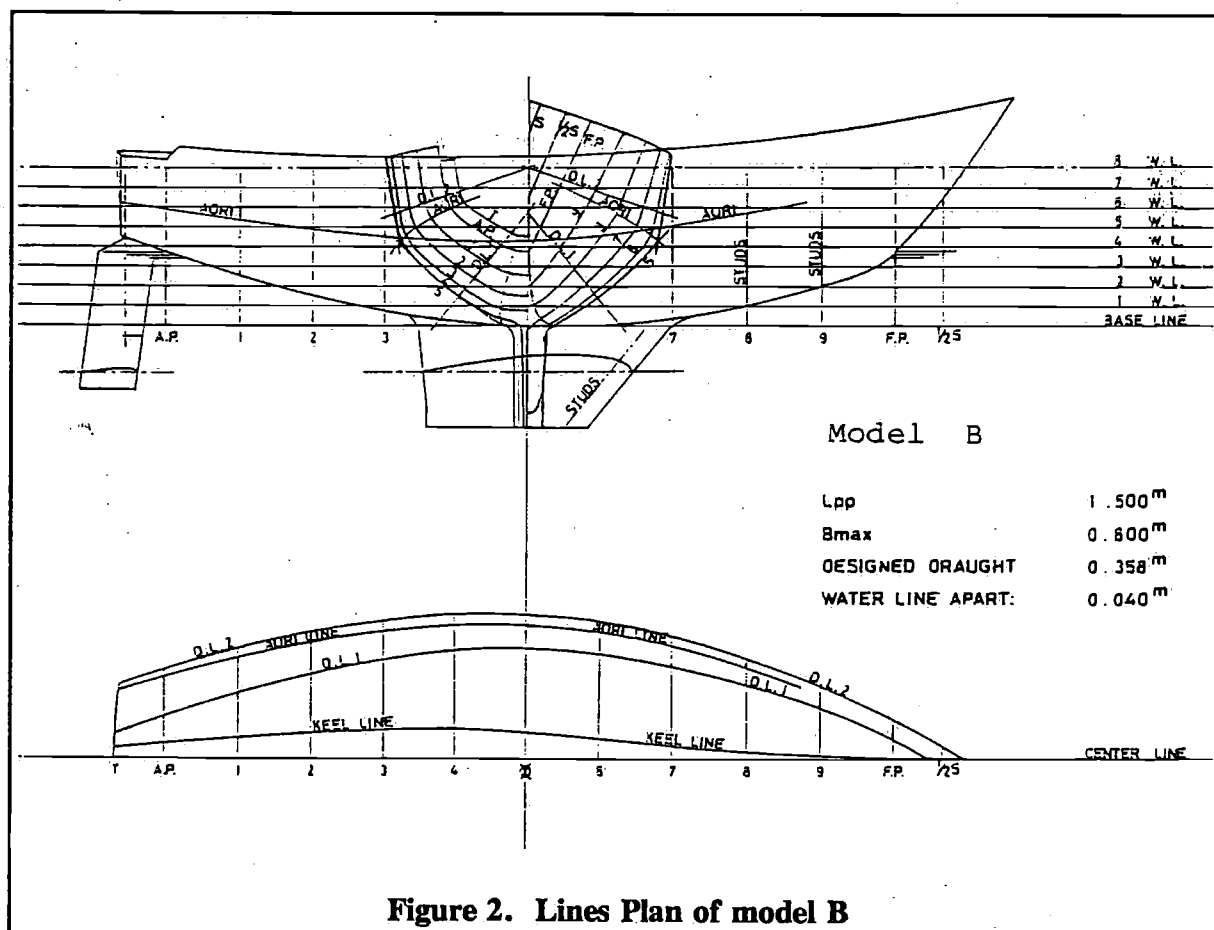


Figure 2. Lines Plan of model B

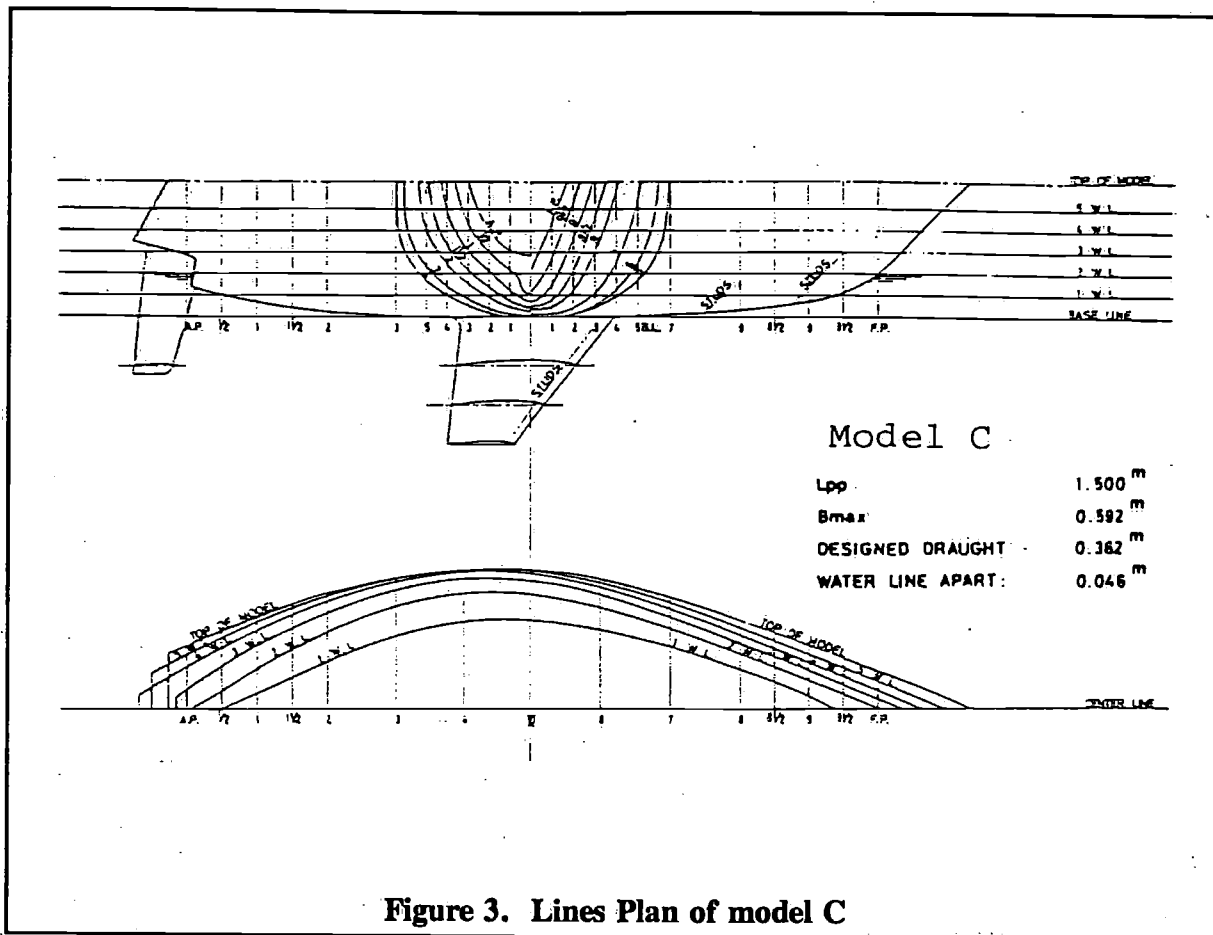


Figure 3. Lines Plan of model C

Table 1. Principal Particulars of Models

		Redningskoite Model A	Cruising Cutter Model B	Q-Tonner Model C
L_{pp}	(m)	1.500	1.500	1.500
L_{oa}	(m)	1.648	1.846	1.848
L_{wl}	(m)	1.545	1.686	1.594
B_{max}	(m)	0.552	0.600	0.592
B_{wl}	(m)	0.504	0.504	0.489
d_{max}	(m)	0.250	0.358	0.362
d_h (hull)	(m)	0.143	0.150	0.0925
∇ (total)	(m ³)	0.04414	0.04344	0.02847
∇_h (hull)	(m ³)		0.03898	0.02740
A_h	(m ²)	0.2927	0.1554	0.1133
A_k	(m ²)		0.0905	0.0644
A_R	(m ²)	0.0222	0.0318	0.0213
$A = A_h + A_k + A_R$		0.3149	0.2777	0.1990
$\Delta/(L'/100)^3$		347 *	263 *	204 *
d_h/L_{wl}		0.162 #	0.089	0.058

A_h : main hull lateral area,
 A_R : rudder area (including skag, if any)
 * : indicates values on sea water

A_k : fin keel lateral area
 L' : L_{wl} in feet
 # : d_{max}/L_{wl}

1.2 Experimental Scheme and Set-up

The tank test was carried out at the Ship Experiment Tank of Osaka University, 100 m long, 7.8 m wide and 4.6 m deep. We measured the resistance, lateral resistance and the centre of lateral resistance at a number of combinations of leeway angle, rudder angle, heel angle and speed.

The set-up is shown in Figure 4. We hold a model hull with a 4-component dynamometer at fixed angles of leeway and heel. Trim and sinkage of the hull are free. The dynamometer is one of the ready-made types supplied by Nisho Electric Instruments Co. Ltd. and it is essentially a multicolumn force sensor with bond wire strain-gauge pick-ups.

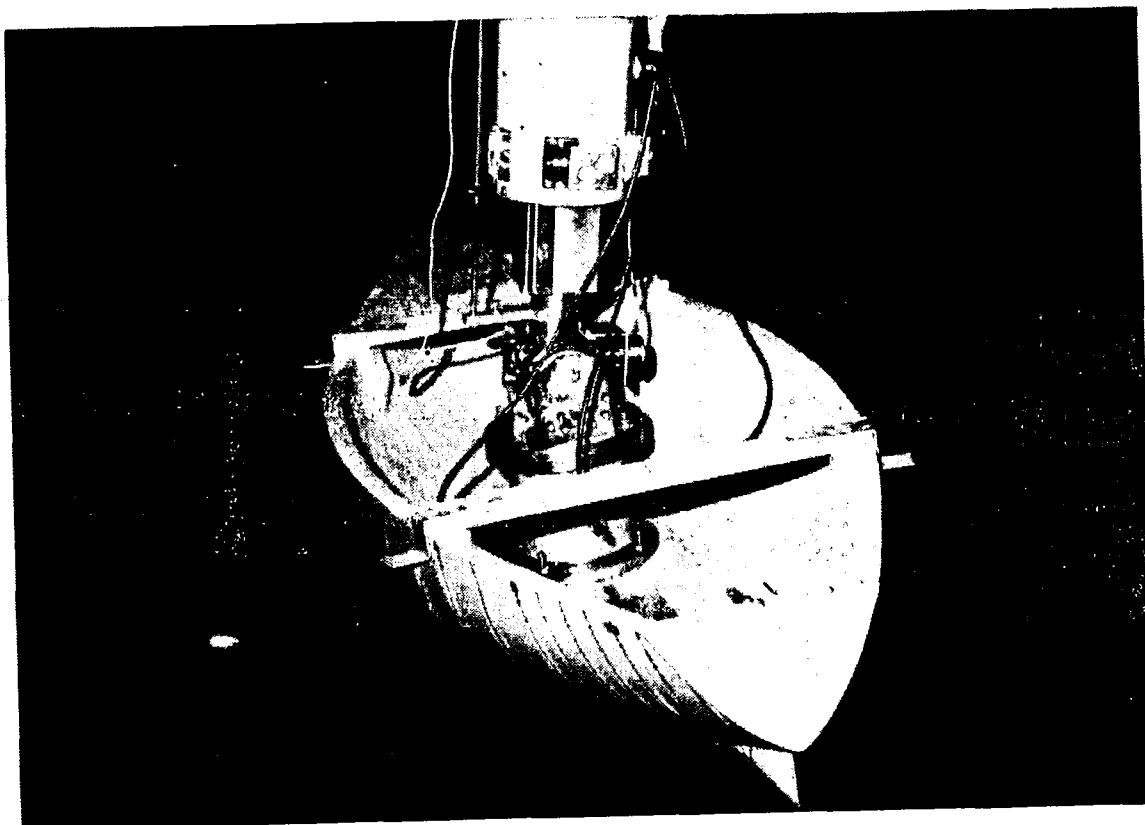


Figure 4. Experimental Set-up

1.3 Experimental Results

Figures 5, 6 and 7 shows the resistance test results without leeway and heel. The total resistance coefficients of different models should not be compared directly however, since the appendage configurations (ballast keel and skeg and rudder) differ immensely among three types. This is interesting but another subject and we will leave it to another occasion.

Figures 9 through 20 illustrate how the lateral resistance and its centre show themselves with different angles of heel and leeway. The effect of rudder deflection to correct a helm balance is also indicated. The figures also show the heeling moment of the lateral resistance.

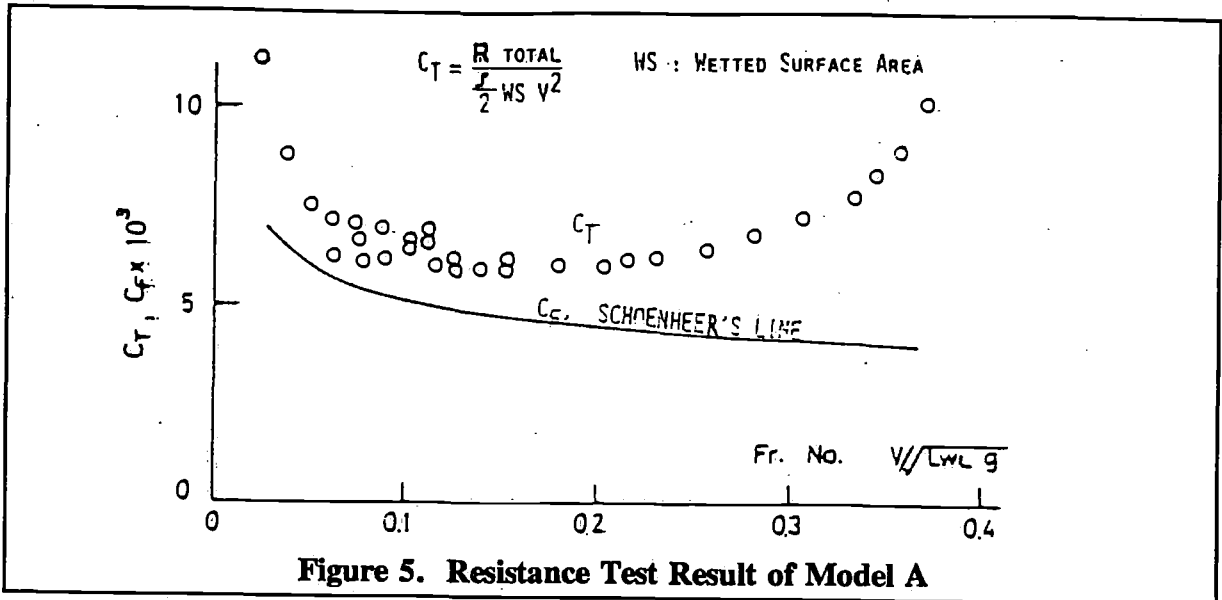


Figure 5. Resistance Test Result of Model A

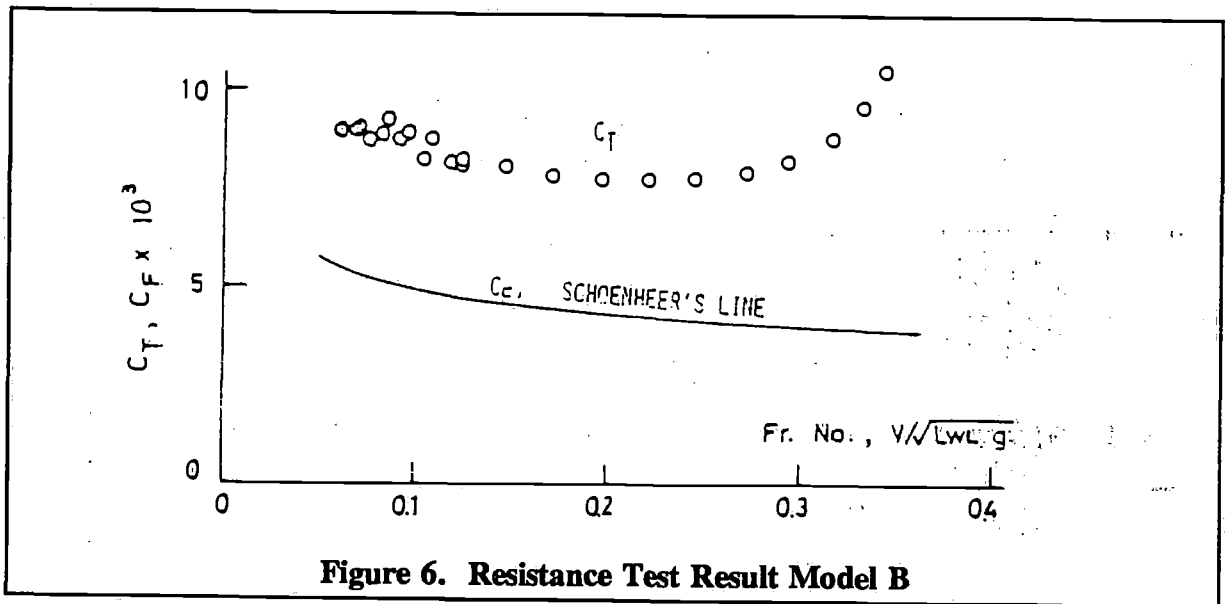


Figure 6. Resistance Test Result Model B

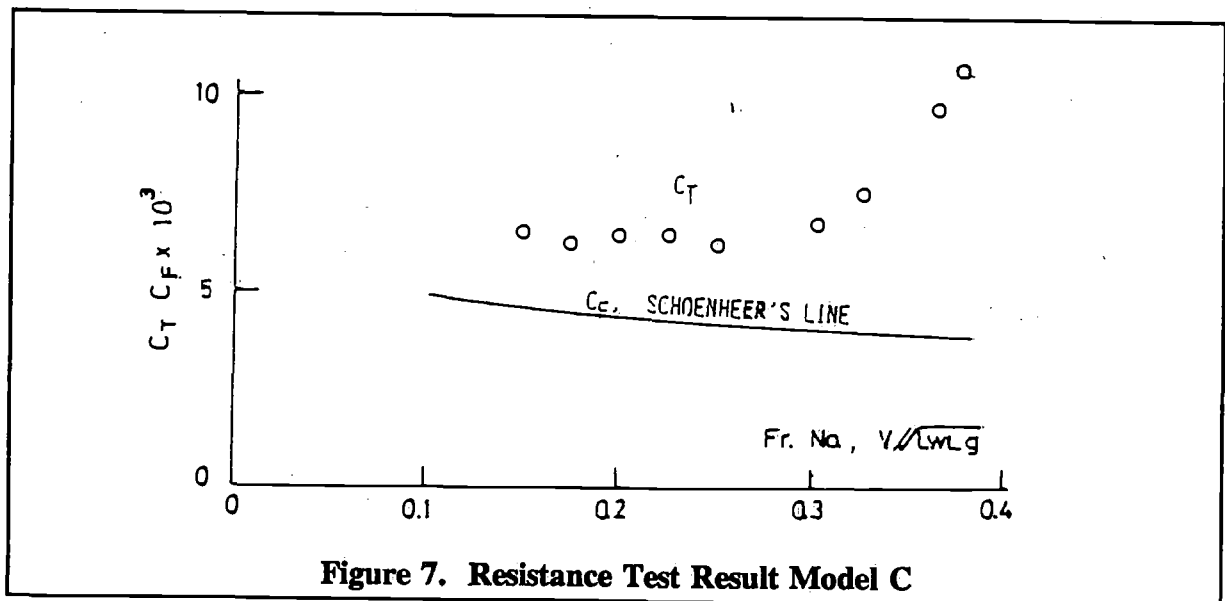


Figure 7. Resistance Test Result Model C

The notations employed are (cf. Figure 8):

β : angle of leeway, positive to port

ϕ : angle of heel, positive to port

δ : rudder angle, positive to starboard rudder

v : ship speed in m/sec.

ρ : water density in $\text{kg m}^{-4}\text{sec}^2$

A : lateral projected area of underbody including keel, skeg and rudder

$X' = X / \frac{1}{2}\rho AV^2$, X : Longitudinal resistance, negative sign corresponds to aftward force

$Y' = Y / \frac{1}{2}\rho AV^2$, Y : Lateral resistance

$N' = N / \frac{1}{2}\rho AL_{wl}V^2$ N : hydrodynamic yaw moment about the midship

$CLR' = N' / Y'$: distance of centre of lateral resistance from the midship in fraction of L_{wl}

$L' = L / \frac{1}{2}\rho AdV^2$, L : heeling moment of lateral resistance about the point "O", that is the middle point of water line on the midship section at upright condition (cf. Figure 8)

d : maximum draught (bottom of keel)

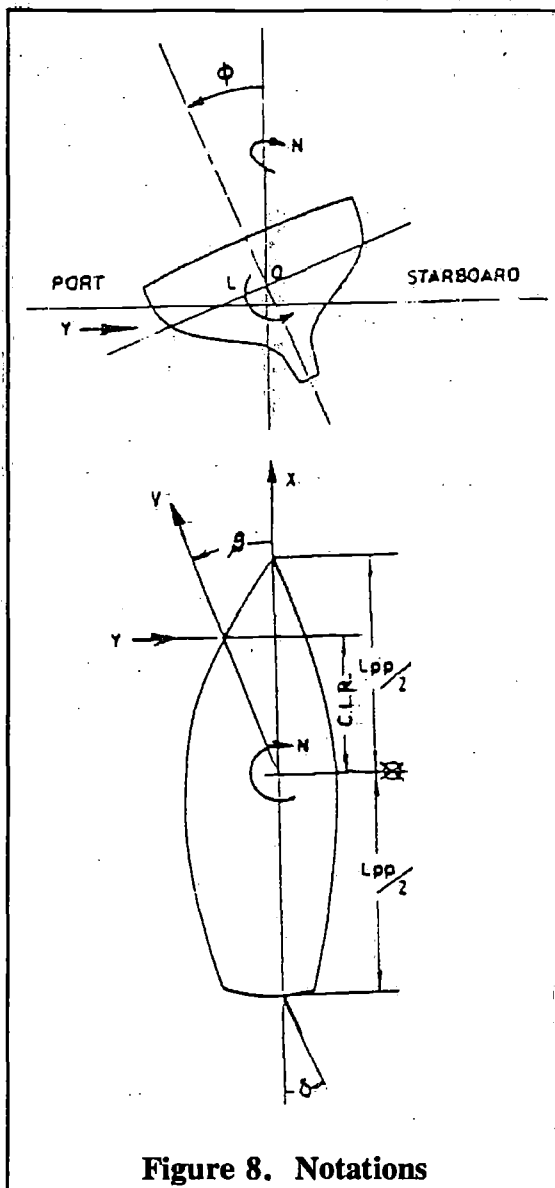


Figure 8. Notations

The lateral force Y is normal to the fore-and-aft axis of the yacht, and the resistance X parallel to the axis. The lift and drag of the hull, referring to the wing theory, are then

$$\text{Lift} = Y \cos \beta - X \sin \beta \quad (1)$$

$$\text{Drag} = Y \cos \beta + X \sin \beta$$

As a remark in interpreting the result, Y is nearly equal to the lift but the drag and X are quite different from each other.

Findings from the tank tests are:

1. The lateral resistance of the long-keel model A is considerably smaller than that of the separate rudder models B and C (Figures 9, 13 and 17). The lift-drag ratio of the hull is accordingly relatively small for A. Windward ability of long-keel boats will not be as good as separate rudder and fin-keel designs.
2. The centre of lateral resistance of Model A, with the helm amid-ship, is at 15-20% of L_{wl} forward of midship. For Model B, 5-10% L_{wl} forward, and for Model C it is nearly at the midship. (Figures 9, 13 and 17)

3. The effect of rudder deflection to correct the helm balance is impressive. Only 3° of rudder deflection will move the centre of lateral resistance as much as 10 % of L_{wl} for all three models. (Figures 11, 12, 15, 16, 19 and 20).
4. The effect of heel on the centre of lateral resistance is rather small. For example, 10° heel shifts the *C.L.R.* by 6% L_{wl} forward for Model A and 2 - 3 % L_{wl} forward for Models B and C. It can be cancelled by a very slight rudder deflection. (Figures 11, 12, 15, 16, 19 and 20). This suggests that the common trend of weatherhelm in heeled condition can hardly be explained from the hydrodynamic force acting on a heeled hull. We will discuss this point later.
5. The lateral resistance produces a heeling moment L . We can define the vertical position of the centre of lateral resistance by L/Y . The vertical *C.L.R.* thus defined is nearly at the bottom of the main hull (canoe body) for all three models. (Figures 9, 13 and 17). This can be used in calculating the heeling moment under sail.

2 Theoretical estimation of lateral resistance and *C.L.R.* Comparison with tank test results

We have a number of theories on the lateral force acting upon an obliquely sailing hull. They range from a simple approximation to highly sophisticated computation, but none of them is, in author's view, established one. What we have done here is first to apply a few typical theories to the present three hull forms, Models A, B and C, comparing the results with the tank test data. Next we introduce a new method of estimating the lateral force and moment, based upon a general review on the problem from the hydrodynamics point of view. This is in a sense an improvement of the method of Gerritsma [3] by applying the slender body lift theory to the hull moment. Its result is also compared with the tank test data.

2.1 Geometric Theory ----- *CLR*, *CE* and Lead

This should perhaps be called a design practice rather than a theory, but it is the most popular procedure of getting a good balance of helm in design stage. *C.L.R.* is defined as the centre of projected lateral area of the underwater part, hull, keel, skeg and rudder all included. In Figure 21 we indicate the "geometric *C.L.R.*" thus defined, compared with the "hydrodynamic *C.L.R.*" obtained by tank test.

At a glance we find the real centre of lateral resistance (hydrodynamic *C.L.R.*) is considerably forward of the geometric *C.L.R.* The lead of hydrodynamic *C.L.R.* over geometric *C.L.R.* is 24% of L_{wl} for Model A, 14% for B and 9% for C.

Naval architects use *C.E.* and Lead together with the (geometric) *C.L.R.* *C.E.*, Centre of Effort of Sails are defined as the centre of area of sails, all sheeted in amidship. Lead is the distance between *C.E.* and *C.L.R.*, normally in percentage of L_{wl} . Most naval architects would choose the lead of about 20% for single-masted rig.

At any rate, the real centre of effort of sails is more or less apart from the geometric *C.E.*; the aerodynamic centre is not the geometric centre; easing a sheet in a reach run brings the real *C.E.* aftward. The geometric *C.L.R.* is not the real *C.L.R.* either. An empirical factor, "lead" is then called upon to compensate both errors. It should be noted, however, that the fore-and-aft balance of sails and underwater body does not only relate to helm balance under steady sailing. It does also have an essential effect on manoeuvring under sail, i.e., luffing, tacking, paying-off and heaving-to. Being an empirical factor, the lead reflects consideration of these performances, not only of the balance of helm under steady sailing.

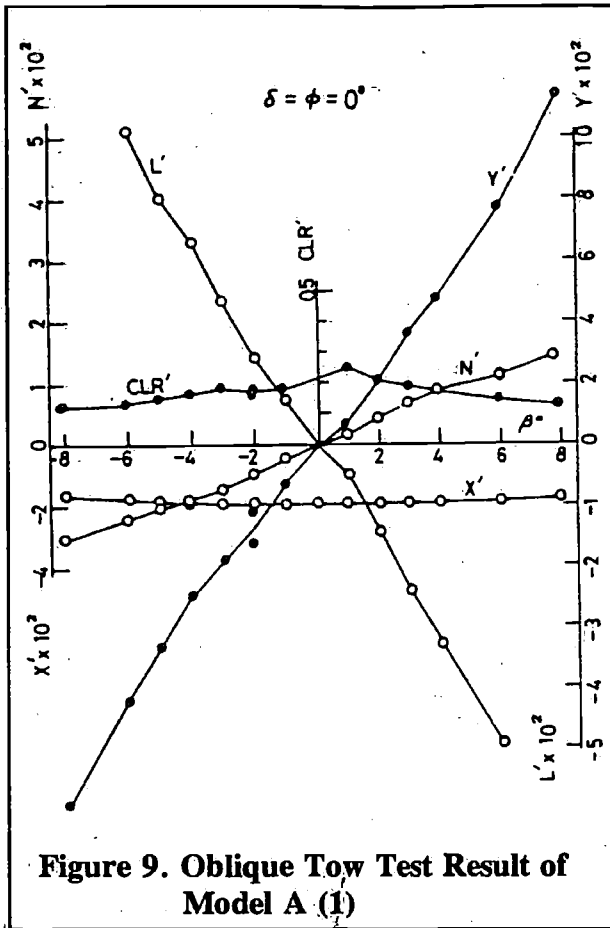


Figure 9. Oblique Tow Test Result of Model A (1)

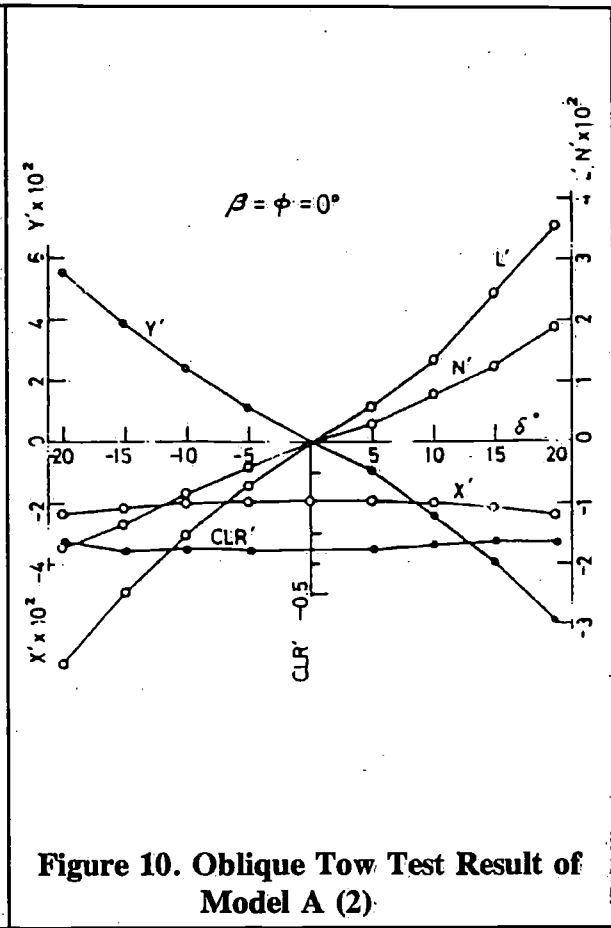


Figure 10. Oblique Tow Test Result of Model A (2)

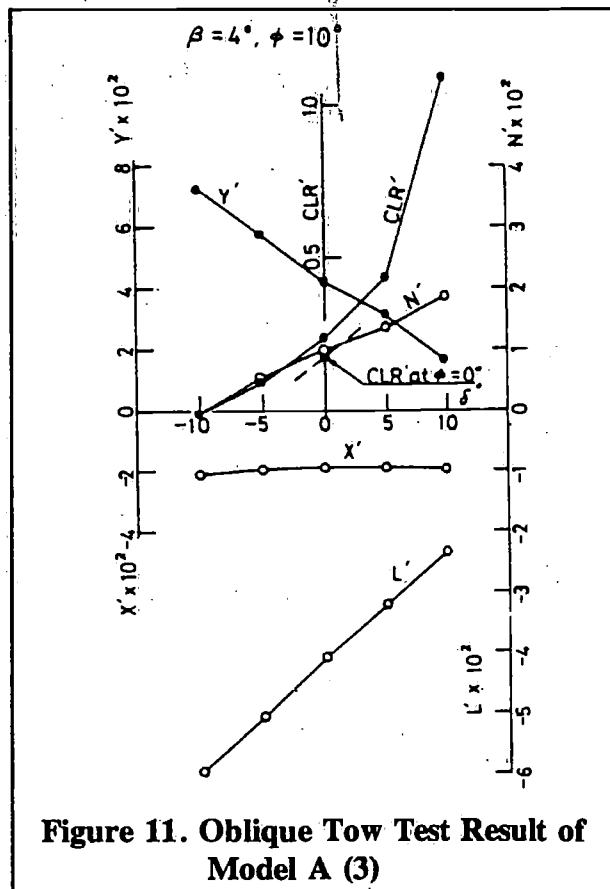


Figure 11. Oblique Tow Test Result of Model A (3)

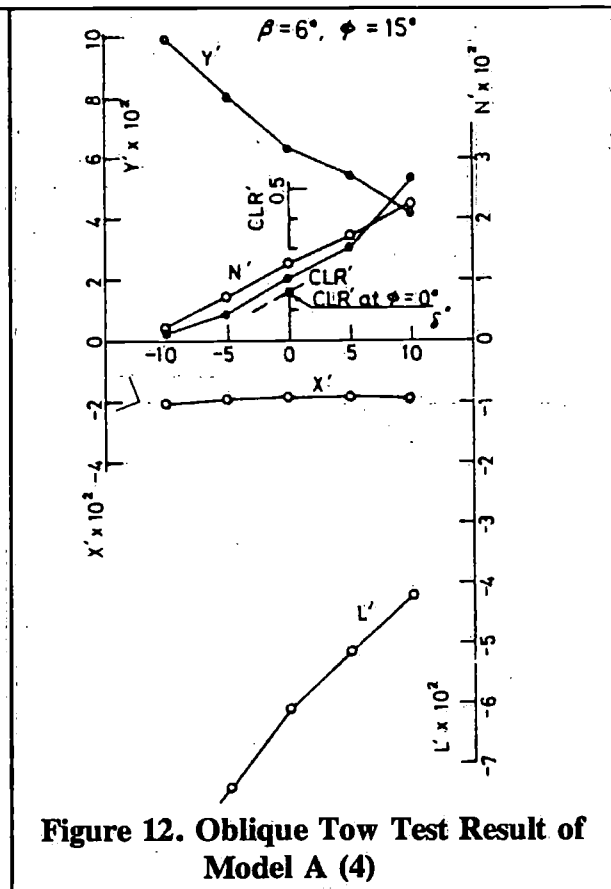


Figure 12. Oblique Tow Test Result of Model A (4)

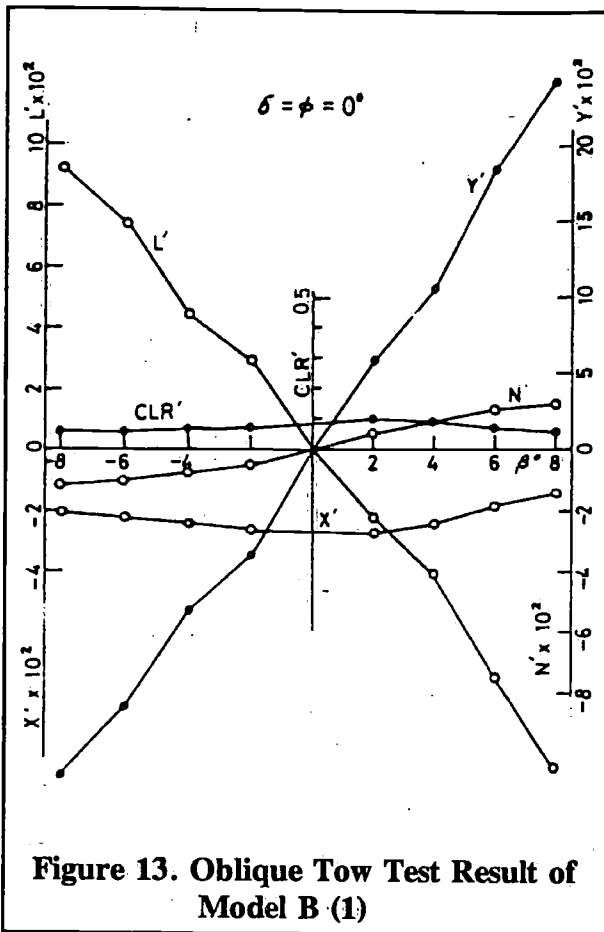


Figure 13. Oblique Tow Test Result of Model B (1)

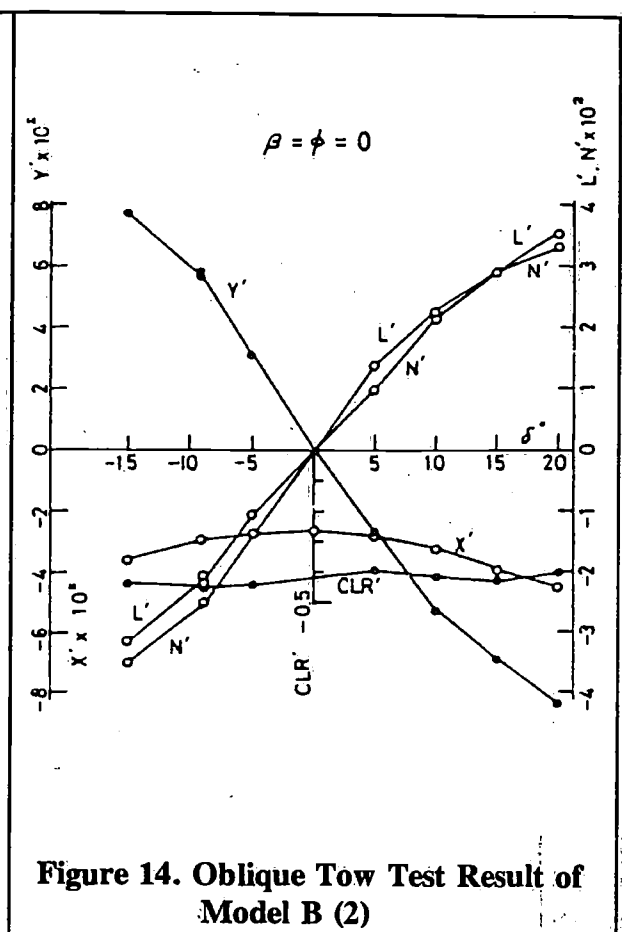


Figure 14. Oblique Tow Test Result of Model B (2)

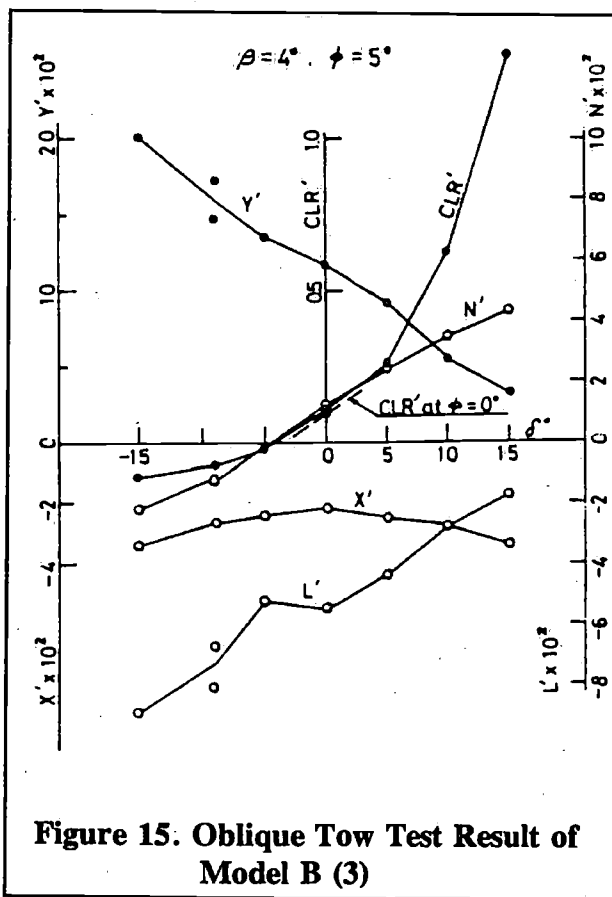


Figure 15. Oblique Tow Test Result of Model B (3)

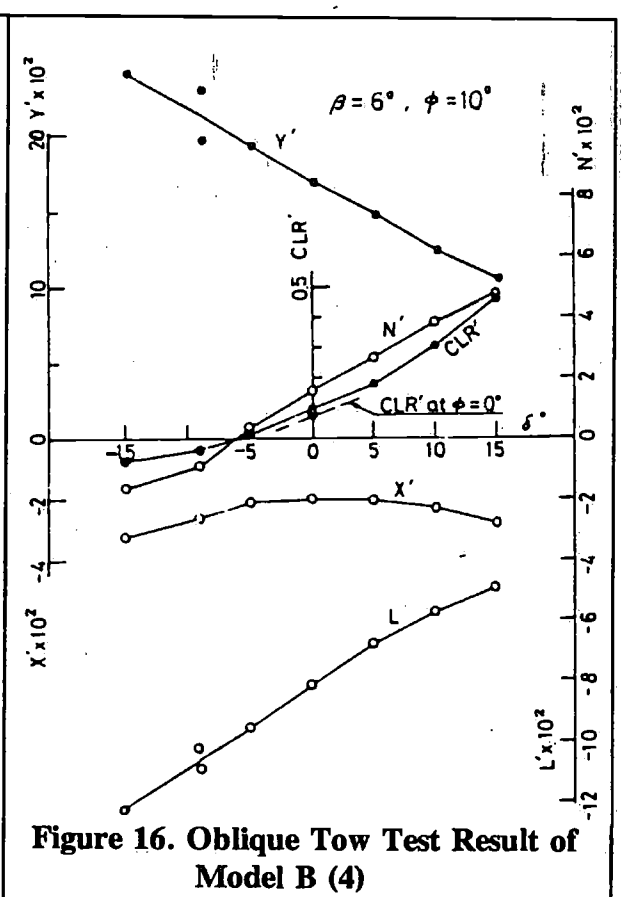
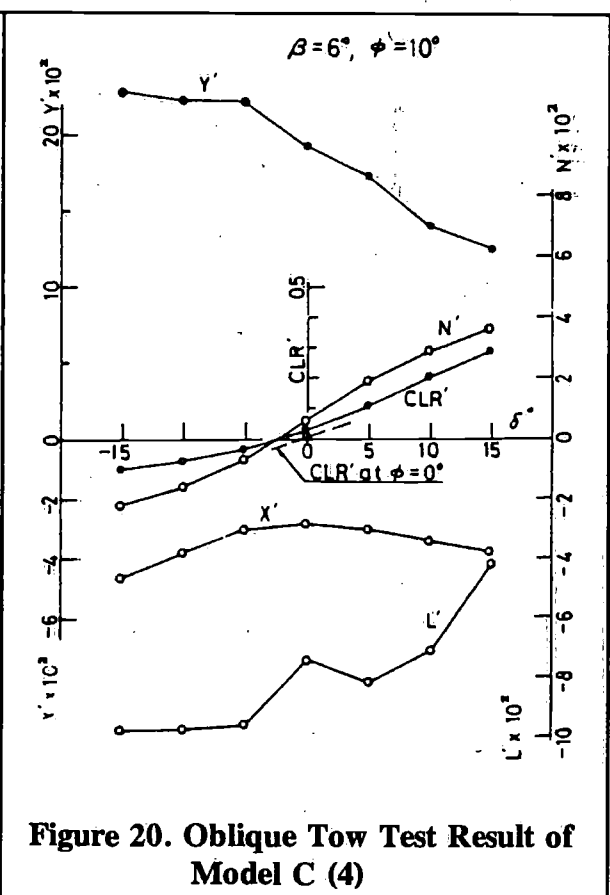
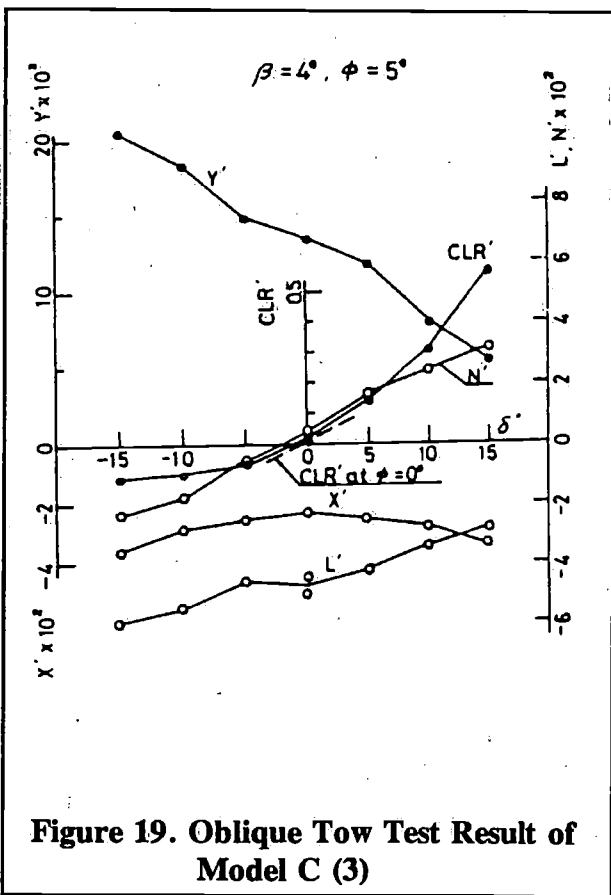
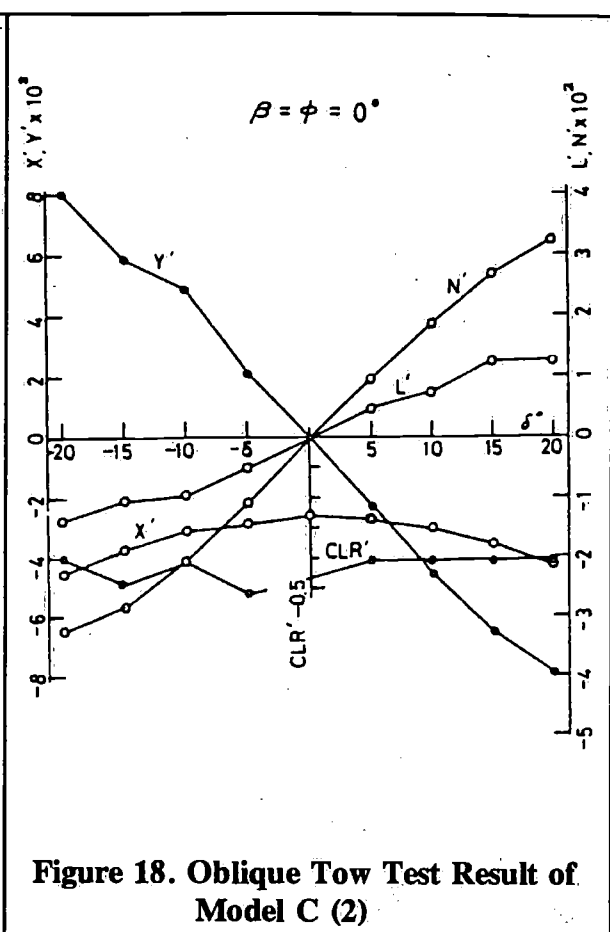
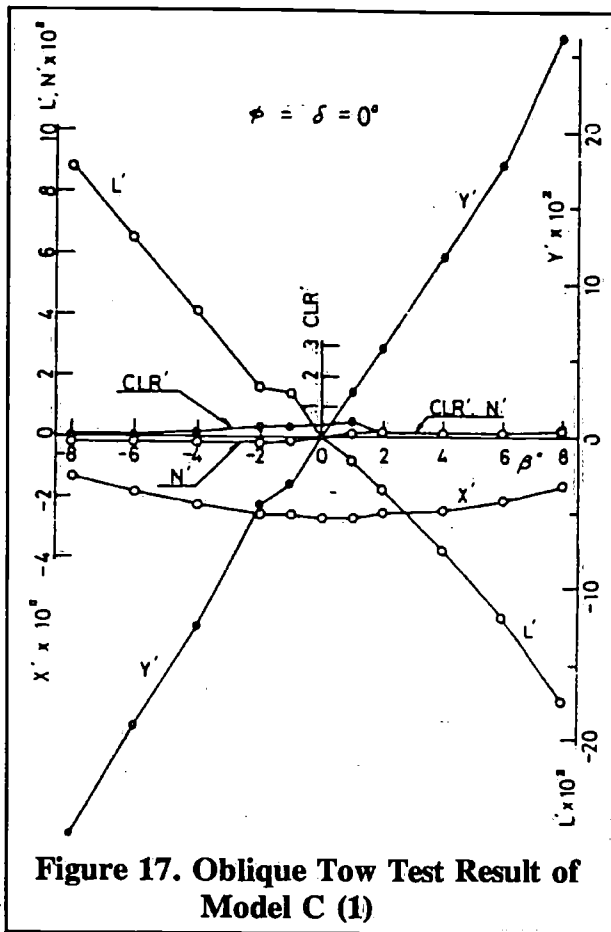


Figure 16. Oblique Tow Test Result of Model B (4)



2.2 Slender Body Theory

The basic idea of this theory is "dynamic displacement effect" of a body moving through a liquid. Static displacement produces buoyancy. Dynamic displacement induces momentum change in the surrounding liquid, which generates a force acting upon the body.

A slender body means a body whose breadth and depth are much smaller than its length. We can compose the flow field around such a body by "laminating" two-dimensional lateral flow at each cross section plane. This is a great benefit for the analysis.

Now taking a slender body moving through a liquid obliquely with a leeway angle, the hydrodynamics tells us that:

Lateral momentum of the liquid in a plane perpendicular to the body's axis is $vA(x)$, where v is flow velocity normal to the body's axis and $A(x)$ is additional mass of the cross section of the body on the plane, x being measured along the axis. (cf. Figure 21).

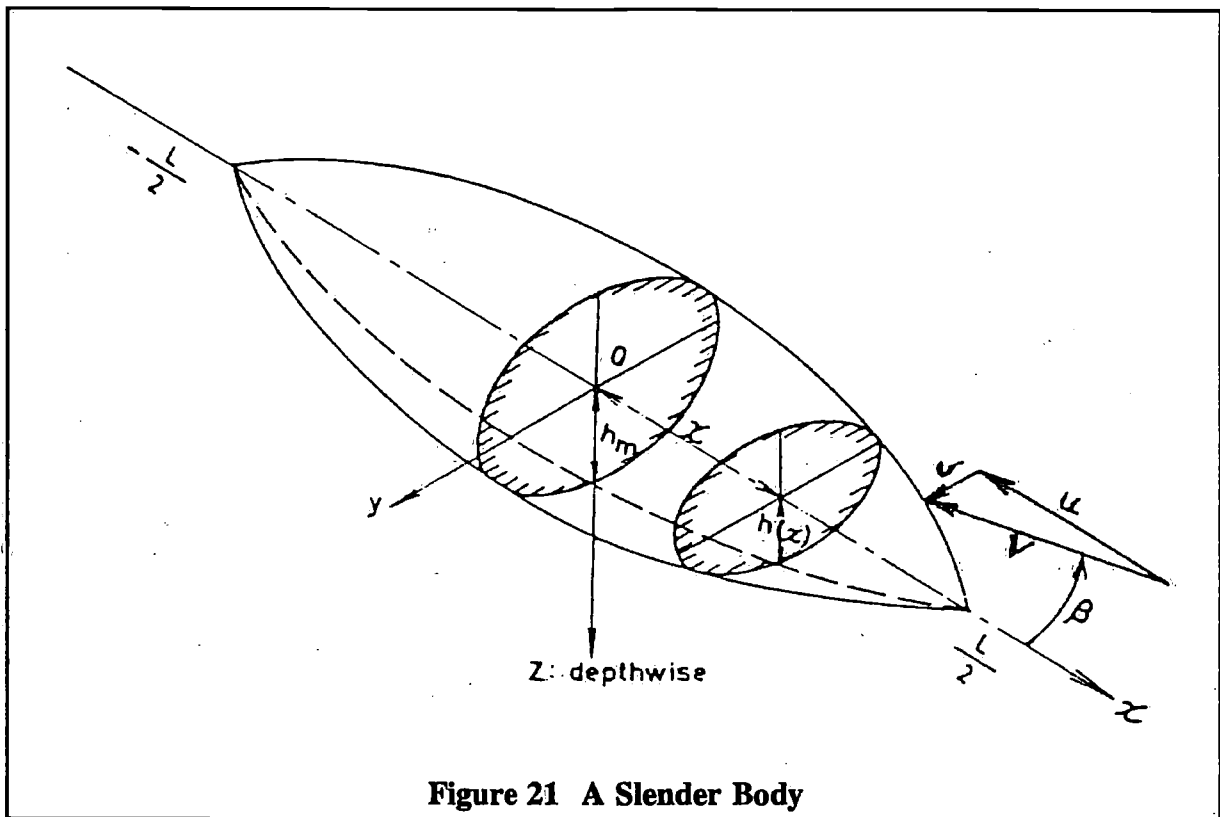


Figure 21 A Slender Body

Rate of change of lateral momentum in the plane is then:

$$u v \frac{d}{dx} A(x) \quad (2)$$

where u is flow velocity along the body's axis.

The additional mass A is approximately:

$$A(x) = \pi \rho h^2(x)$$

where $h(x)$ is half the local depth of the body as is shown in Figure 21.

The rate of change of momentum equals to local force acting on the of the cross section of the body.

The resultant lateral force and its moment are:

$$Y = \pi \rho u \int_{\frac{-L}{2}}^{\frac{L}{2}} v \frac{d}{dx} h^2(x) dx \quad (3)$$

$$N = \pi \rho u \int_{\frac{-L}{2}}^{\frac{L}{2}} v x \frac{d}{dx} h^2(x) dx \quad (4)$$

This simply becomes:

$$Y = \pi \rho u^2 \beta \int_{\frac{-L}{2}}^{\frac{L}{2}} dh^2 = \pi \rho u^2 \beta \left[h^2(x) \right]_{\frac{-L}{2}}^{\frac{L}{2}} = 0 \quad (5)$$

$$N = \pi \rho u^2 \beta \left(\left[x \cdot h^2(x) \right]_{\frac{-L}{2}}^{\frac{L}{2}} - \int_{\frac{-L}{2}}^{\frac{L}{2}} h^2(x) dx \right)$$

$$= - \pi \rho u^2 \beta \int_{\frac{-L}{2}}^{\frac{L}{2}} h^2(x) dx \quad (6)$$

We get no lateral force (d'Alembert's paradox) but do get a moment even in an ideal fluid. This moment is often called Munk moment.

In the real fluid with viscosity, however, cross flow rounding the bottom of the body generates vortices trailing out from there. These vortices induce "wash down" flow which reduces the inflow angle to the afterbody. Accordingly on the afterbody, the lateral velocity v of Eqs. (3) and (4) becomes much smaller than leeway velocity $u\beta$. As the result the integral of Eq. (3) does not vanish, unlike Eq. (5), and we get some amount of lateral force. At the same time the moment N become smaller than of Eq. (6), Munk moment.

A popular assumption to deal with this effect is simply to cut off the integrations over the afterbody, [4] that is, to stop the integrations where $h(x)$ is maximum. This results in

$$Y = \pi \rho u^2 \beta h_m^2 \quad (7)$$

$$N = -\pi \rho u^2 \beta \left(x_m h_m^2 + \int_{x_m}^{\frac{L}{2}} h^2(x) dx \right) \quad (8)$$

where h_m : maximum half-depth of the body,
 x_m : x where $h(x) = h_m$

In applying this to sailing yachts we should halve the Y and N according to the principle of image on the waterplane. The lateral resistance is simply

$$Y = \frac{\rho}{2} \pi V^2 \beta d_m^2 \quad (9)$$

where $V \cong u$ = ship speed in m/s.
 d_m = the maximum draught,
 β = angle of leeway in radian
 ρ = 104 kg. m⁻³ sec⁻² for sea water.

The centre of lateral resistance is then

$$CLR = \frac{N}{Y} = x_m + \frac{1}{d_m^2} \int_{x_m}^{\frac{L}{2}} h^2(x) dx \quad (10)$$

where x_m = horizontal distance between the midship and the station where the draught is maximum ($h = d_m$), positive to forward of the midship.
 $h(x)$ = local draught, i.e., depth of the yacht below water line at station x .

The integration of Eq.(10) is performed by Simpson rule.

We applied this procedure to the Models A, B and C, Table 2 and Figures 22 and 23 indicates the results. We have a fair result for the long-keel model A but at a small angle of leeway, say $\beta < 2^\circ$ (cf. Figure 23). It is not surprising for the slender body lift theory is valid by its nature at an infinitesimal angle of attack. In larger leeway angle the covering effect of trailing vortices on the afterbody becomes less prominent. Consequently the rudder and stern deadwood produce an appreciable amount of lateral resistance: lateral resistance gradient Y'/β increases and *C.L.R* moves aftward. This is a remarkable feature of the long-keel model A, unlike the fin-keel Models B and C. The lifting surface theory of low aspect ratio is useful to take account of this effect. We will discuss it in Section 2.4. The lifting surface approach requires a fair amount of computation, however. So Eqs.(9) and (10) can perhaps be a practical procedure of evaluating the lateral resistance and *C.L.R* of long-keel boats with deep fore-foot (typical in Model A).

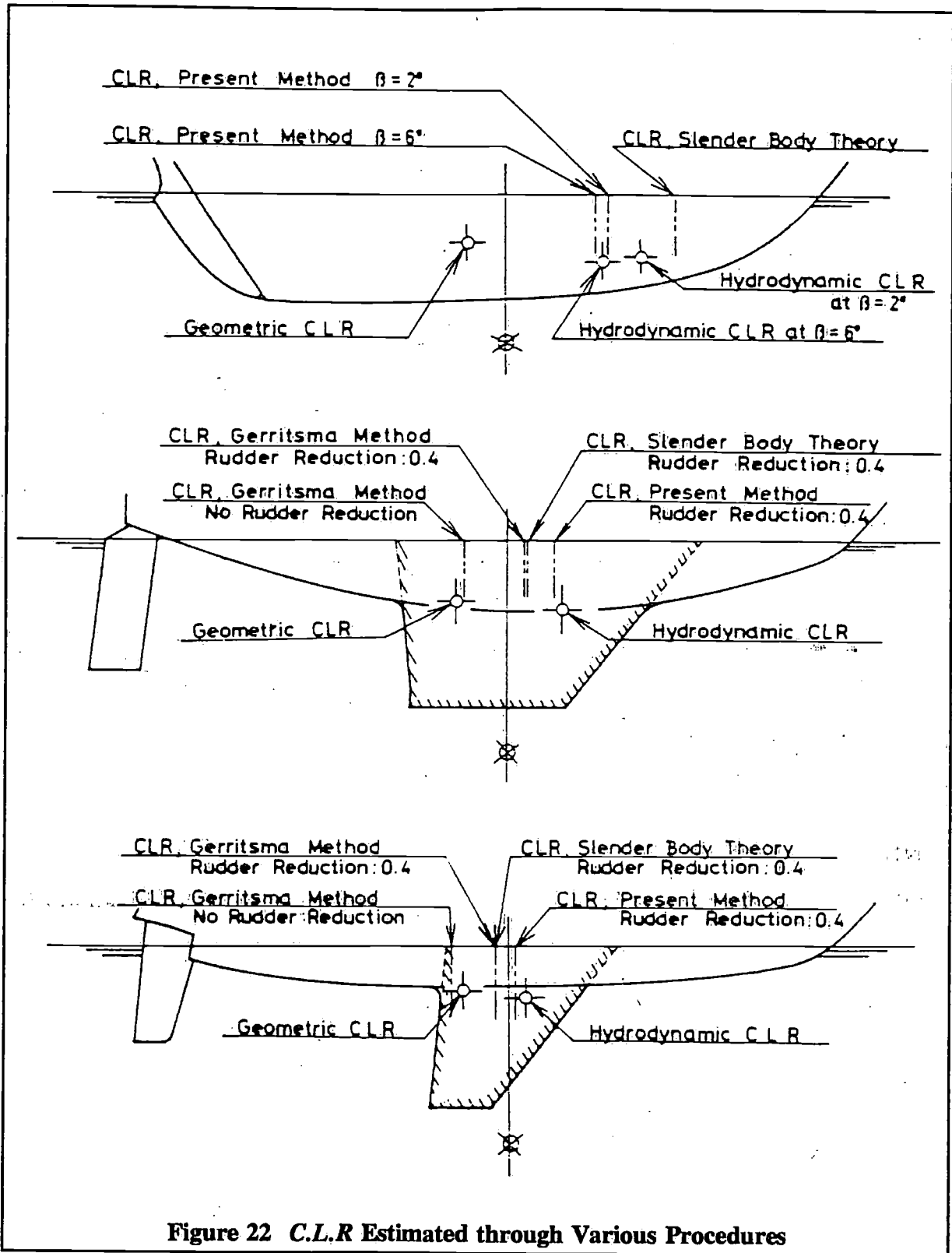


Figure 22 C.L.R Estimated through Various Procedures

We should remember in that case, however, that the lateral resistance gradient increases and C.L.R moves aftward both appreciably at larger leeway angle.

The whole underwater bodies of Models B and C including the fin-keel and rudder are not really slender; maximum draught is some 20% of L_{wl} . Nevertheless Table 2 show that this theory is not too bad to apply to these types of hulls.

Table 2 Lateral Resistance and C.L.R Estimated through Various Procedures

Procedures	Model A		Model B		Model C	
	Y'/β	$C.L.R'$	Y'/β	$C.L.R'$	Y'/β	$C.L.R'$
Tank Test	0.55, $\beta=2^\circ$ 0.77, $\beta=6^\circ$	0.200, $\beta=2^\circ$ 0.146, $\beta=6^\circ$	1.62	0.073	1.74	0.024
Geometric C.L.R		-0.078		-0.068		-0.067
Slender Body No Rudder Force	0.62	0.257	1.45	0.15	2.07	0.047
Slender Body, Rudder Reduction: 0.4			1.80	0.026	2.36	-0.018
Gerritsma, No Rudder Reduction			1.70	-0.058	1.77	-0.082
Gerritsma, Rudder Reduction: 0.4			1.43	0.024	1.52	-0.018
Present Method No Rudder Reduction for Model A	0.527, $\beta=2^\circ$ 0.761, $\beta=6^\circ$	0.155, $\beta=2^\circ$ 0.135, $\beta=6^\circ$				
Rudder Reduction: 0.4 for Models A and C			1.69	0.064	1.67	0.010

Y'/β and $C.L.R'$ indicate average values over $\beta=2^\circ$, 4° , 6° and 8° unless otherwise remarked

Errors in evaluating the lateral resistance are some 15%, and $C.L.R$ error ranges 3 - 6% of L_{wl} , if we cut off the afterbody, including the rudder, at the maximum draught station. To cut off entirely the contribution of the rudder to lateral resistance is perhaps an oversimplification. A correction for this is to apply the same approach independently to the rudder to have rudder lateral force and then modify it by rudder force reduction factor. This reduction is assumed to come from the trailing vortices outflowing from the fin-keel. Table 2 and Figure 22 involves the results of such calculation with rudder force reduction factor of 0.4.

2.3 Method of Gerritsma

This plain theory is recognized to give a good evaluation of the lateral resistance. To extend the fin-keel and rudder to the water surface and to take the image on the surface is a reasonable assumption from the hydrodynamics point of view. The bound vortex generated on the keel can not vanish at the bottom of the hull by the nature of vortex. Instead it induces a circulating flow around the hull about the vertical axis, and this effect is well represented by extending the bound vortex up to the surface.

The same reasoning can be applied to the rudder, though the trailing vortices coming out from the fin-keel reduces the inflow angle to the rudder considerably [5]. Table 2 and Figure 22 contain the lateral force and $C.L.R$ calculated for Models B and C, following to this method. The reduction factor of 0.4 for the inflow angle to the rudder is based upon an analysis on the induced velocity (wash down) of the trailing vortices coming out from the keel.

This procedure without rudder force reduction gives a nice result in estimating the lateral resistance but the predicted $C.L.R$ is rather too aft. The rudder force reduction improves the $C.L.R$ prediction but the lateral resistance estimated is rather too small then.

2.4 A Combined Method of Vortex Wing and Slender Body Theory

The method of Gerritsma, based on the vortex wing theory, evaluates well the lateral resistance of the fin-keel and separate rudder. That is certainly the essential part of lateral resistance of modern yacht hulls. What is lacking is, however, the contribution of the hull forebody, in the authors' view. Its share in lateral resistance may not be large, but it may have a considerable effect on yaw moment, and then on *C.L.R.*

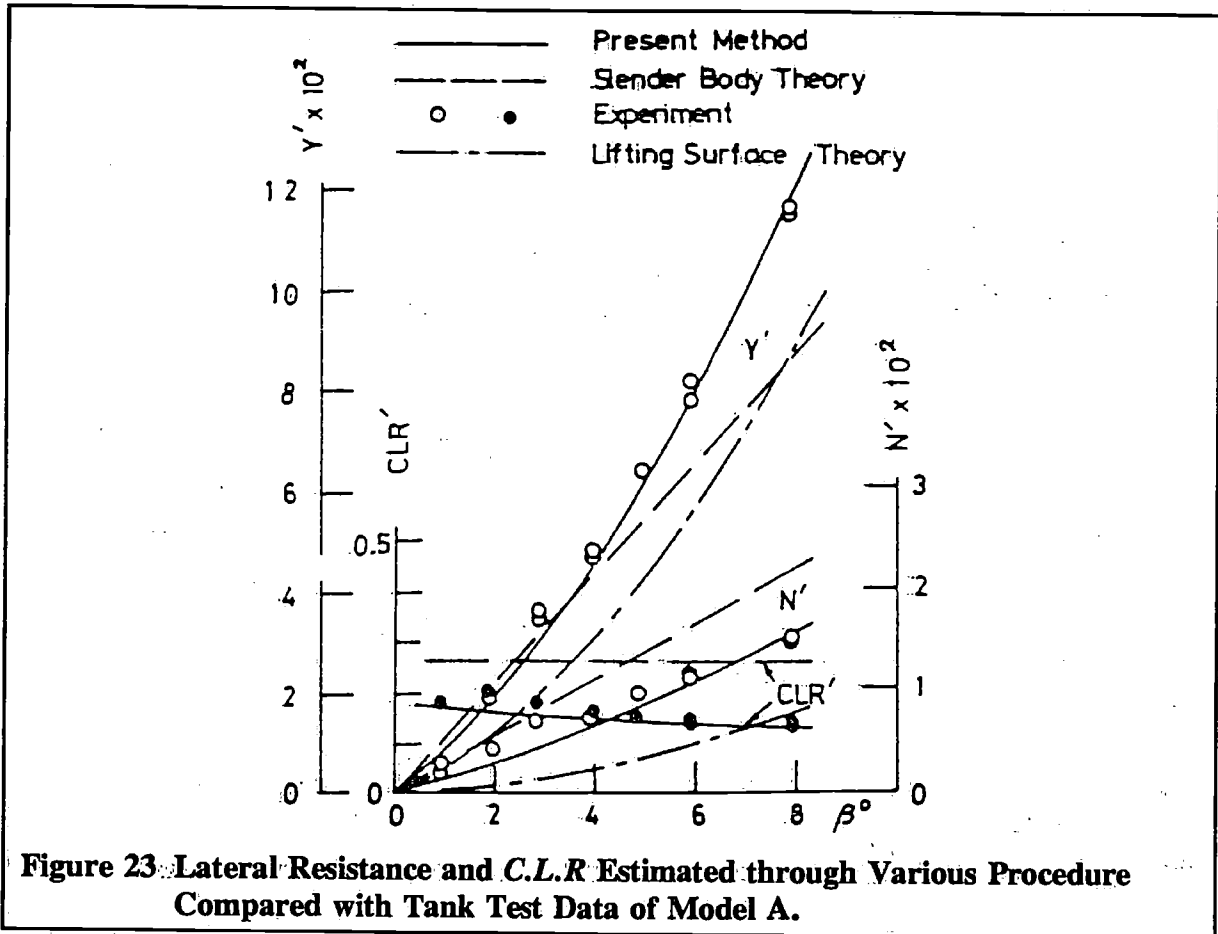


Figure 23. Lateral Resistance and *C.L.R.* Estimated through Various Procedure Compared with Tank Test Data of Model A.

This idea leads us to a combined method: to apply the vortex wing theory on the fin-keel and rudder (Gerritsma method) and the slender body lift theory on the forebody. The afterbody is exposed to the wash-down flow induced by the trailing vortices flowing out from the forebody and fin-keel. This eliminates the contribution of the afterbody to lateral resistance. (Jones assumption, cf. Section 2.2, ref. 4). Strong wash down produced by the fin-keel will well justify this assumption.

The procedure is:

- 1 to get the lateral resistance of the fin-keel and its moment about the midship, following to Gerritsma method, the lift gradient

$$p = \frac{\partial C_L}{\partial \alpha} = \frac{5.7 a_e}{1.8 + \cos \Lambda \sqrt{\frac{a_e^2}{\cos^4 \Lambda} + 4}} \quad (11)$$

is used;

- 2 to get the lateral resistance of the rudder and its moment similarly but with the rudder force reduction factor of 0.4;
- 3 to use Eqs.(9) and (10) to obtain the lateral resistance of the fore-body and its moment about the midship, the draught $h(x)$ in this case being that of the main hull (canoe-body);
- 4 to sum up the above three to get the lateral resistance and *C.L.R* of the yacht.

The rudder reduction factor will vary configuration to configuration. 0.4 is perhaps a good average according to a hydrodynamic analysis on wash down flow behind a fin-keel.

Table 2 and Figure 23 tell us that this procedure works well for fin-keel models B and C. It will hopefully work also for a deep keel yacht with a shallow fore-foot and the rudder attached to the aft edge of the keel. In this case the rudder and deep keel should be regarded together as a single wing (like a fin-keel).

The long-keel, deep fore-foot Model A raises a problem: we can hardly define the keel to apply the vortex wing theory; the aspect-ratio of the equivalent wing must be very small any way, so that the lift gradient formula (11) may not be proper and the centre of pressure uncertain.

We tried a lifting surface approach instead of lifting line wing theory normally used in Gerritsma Method. The very low aspect-ratio of the long-keel Model A led us to the idea. The basic scheme is:

- 1 to take a thin wing whose plan form is identical with the profile of the whole underwater body of Model A but including its image on the waterline;
- 2 to distribute bound vortices continuously over the thin wing;
- 3 to assume spanwise (depthwise) distribution of circulation uniform by the nature of very low aspect-ratio wing and consequently the same strength of free vortex trails out from the bottom of the keel;
- 4 chordwise (lengthwise) distribution of circulation is assumed to be

$$\gamma(x) \sqrt{\frac{1 + 2x/L}{1 - 2x/L}}$$

where $\gamma(x)$ is an unknown function of x , x being positive to forward;

- 5 to get wash down velocity on the centre-line of the wing (i.e. waterline of the yacht) induced by all the bound and trailing vortices;
- 6 to equate the wash down velocity with leeway lateral velocity $v\beta$ to have an integral equation to define $\gamma(x)$;
- 7 to approximate $\gamma(x)$ by a trigonometric series with a number of unknown constants and put it into the integral equation to deliver a set of simultaneous equations to define the unknown constants;
- 8 to get the resultant lateral force and its moment by summing up all the bound vortex circulations thus defined.

The lateral force and its moment obtained in this manner for Model A is indicated by chain lines in Figure 23. The upward curvature of lateral force curve is clearly seen.

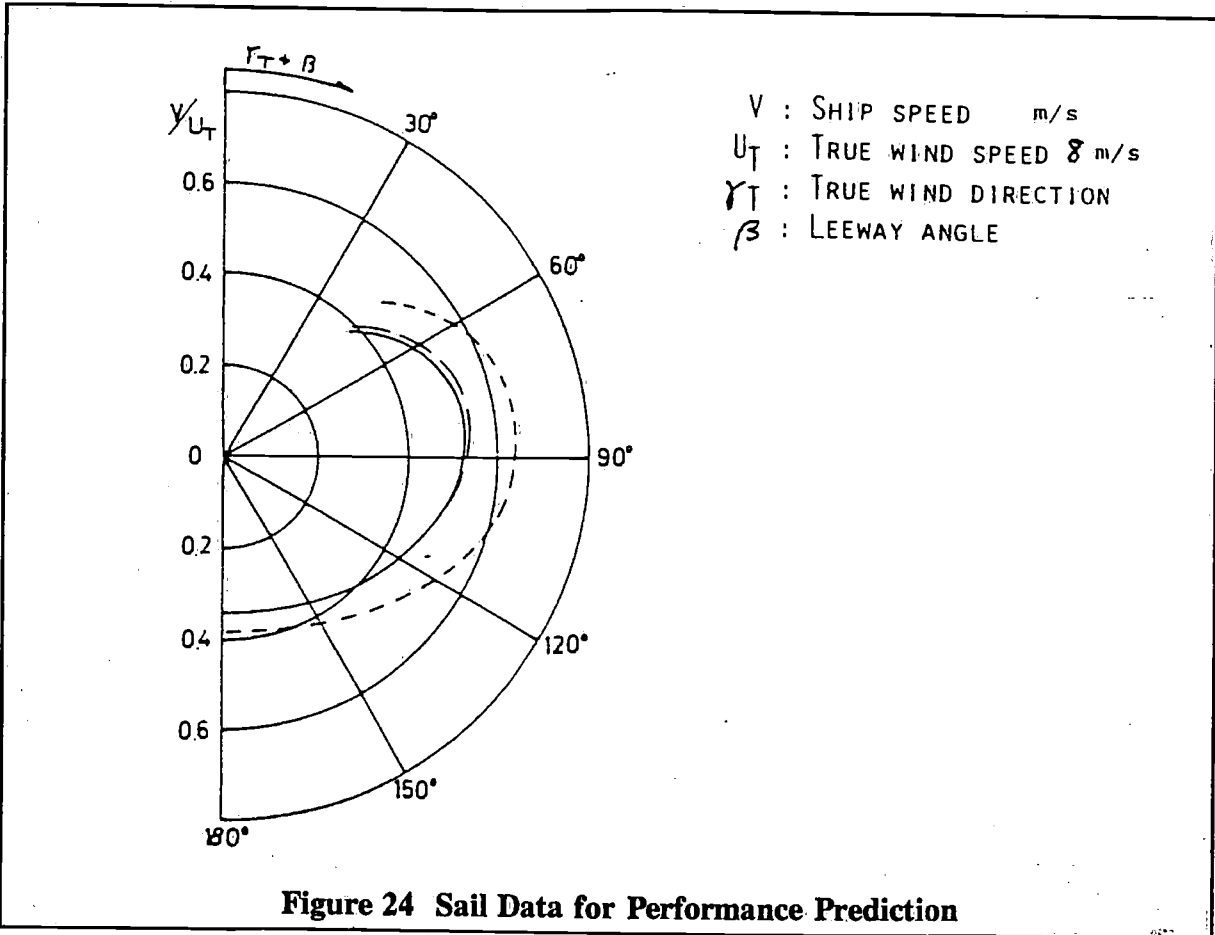


Figure 24 Sail Data for Performance Prediction

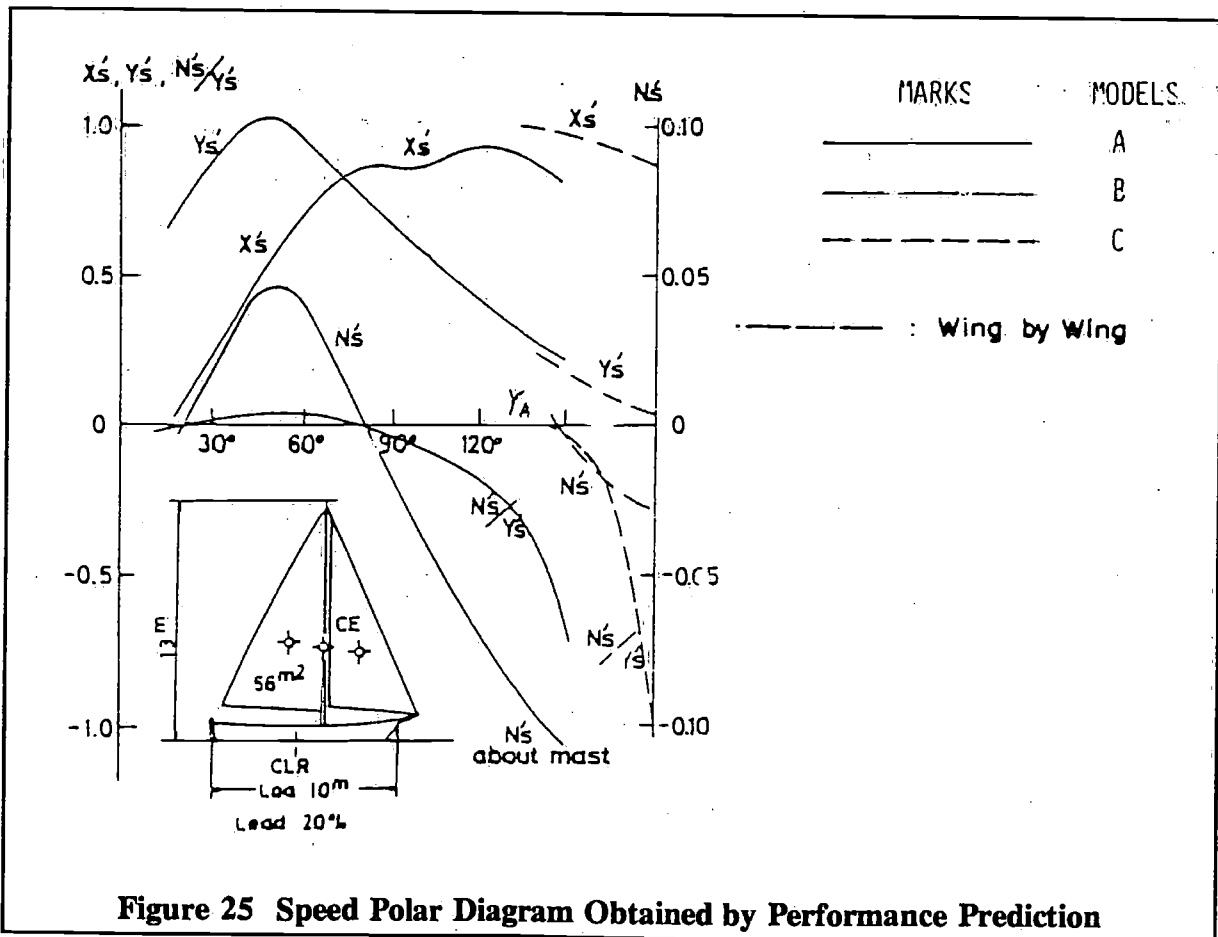


Figure 25 Speed Polar Diagram Obtained by Performance Prediction

To add the lateral force and moment of the canoe-body upon the ones obtained through this lifting surface approach can be controversial. We tried this, however, and the result looks good indeed at least in this case. A possible interpretation is that the lifting surface approach evaluates the lift of the skelton thin wing and the slender body theory the dynamic displacement lift of the main hull (canoe body). The lateral force and moment of the canoe-body is given by Eqs.(9) and (10) also in this case.

3 Performance prediction and elements of balance of helm

3.1 Performance Prediction

Let us assume a jib-headed sloop rig for all the three Models A, B and C. The length over all of actual vessels is assumed to be 10 metres.

Sail area is 56m² and the mast height above the surface 13 metres (cf. Figure 24). The aerodynamic data of this rig is provided by model sail test [2] as is illustrated in Figure 24 in a non-dimensional form. The notations employed are:

$$X'_s = \frac{X_s}{\frac{1}{2} \rho_a S U^2}$$

X_s = longitudinal (thrust) component of sail force

$$Y'_s = \frac{Y_s}{\frac{1}{2} \rho_a S U^2}$$

Y_s = lateral component of sail force

$$N'_s = \frac{N_s}{\frac{1}{2} \rho_a S^{3/2} U^2}$$

N_s = yaw moment of sail force about the mast

ρ_a = density of air in kg.m⁻⁴sec²

S = sail area in m²

U = apparent wind speed in m/sec.

Now we can make a sailing performance prediction of the yachts A,B and C by incorporating the sail data with the tank test data of section 1.

The fundamental equations are :

$$X' (V, \beta, \delta, \phi) \frac{\rho A}{\rho_a S} \left(\frac{V}{U} \right)^2 = X'_s (\gamma_A, \phi) \quad (12)$$

$$Y' (\beta, \delta, \phi) \frac{\rho A}{\rho_a S} \left(\frac{V}{U} \right)^2 = Y'_s (\gamma, \phi) \quad (13)$$

- δ_1 : due to unbalance of *C.E.* and *C.L.R.*
- δ_2 : due to shift of *C.L.R.* induced by heel
- δ_3 : due to leeward shift of drive force of sails induced by heel

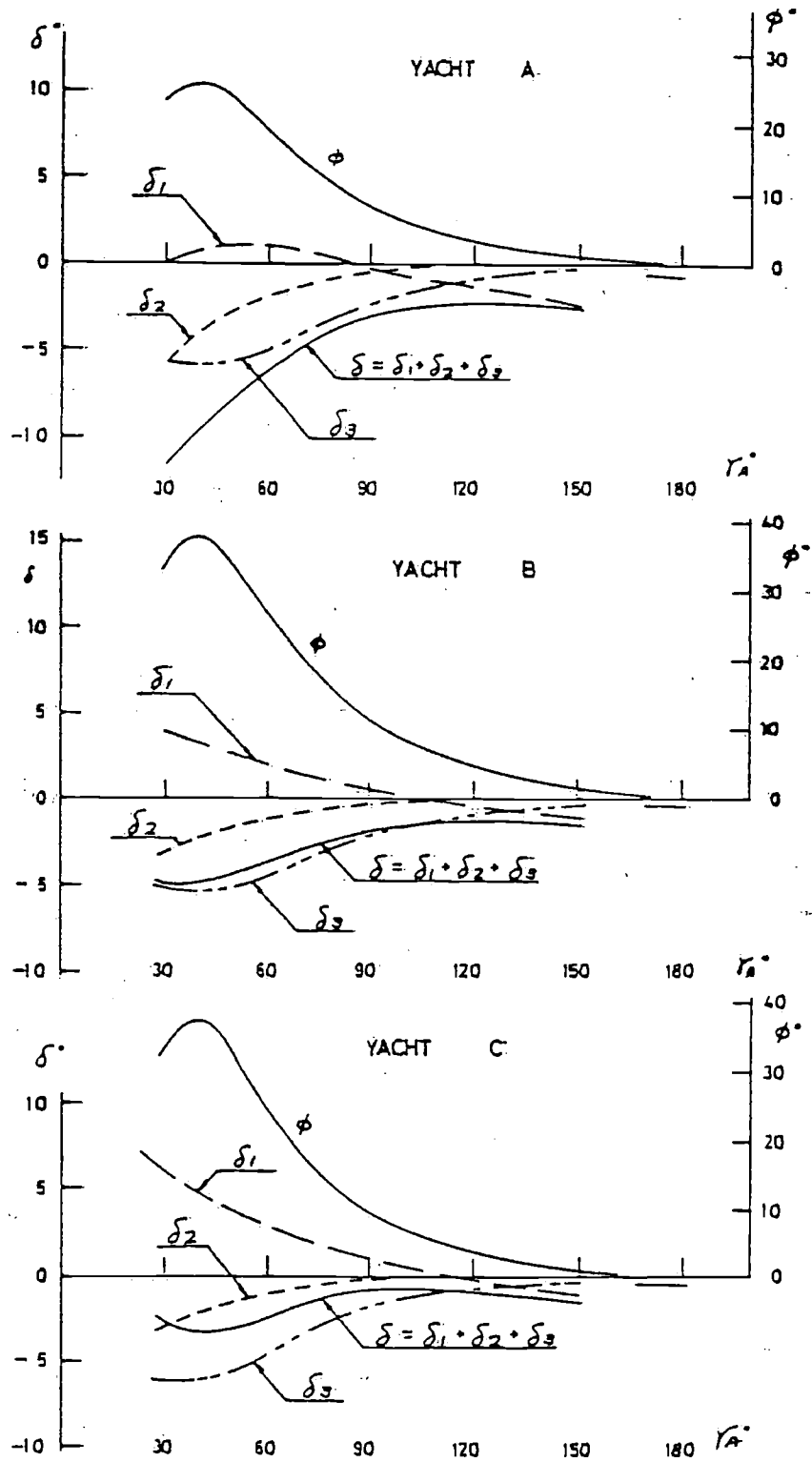


Figure 26 Rudder Angle Needed for Helm Balance at Steady Sailing and Its Components

$$N'(\beta, \delta, \phi) \frac{\rho ALwl}{\rho_a S^{3/2}} \left(\frac{V}{U}\right)^2 = N'_{so}(\gamma_A, \phi) \quad (14)$$

$$W GZ(\phi) = \frac{\rho_a}{2} S^{3/2} U^2 L'_s(\gamma_A, \phi) \quad (15)$$

where

γ_A = apparent wind direction.

N'_{so} = yaw moment of sail force so about the midship (converted from N_s)

The sail trim is adjusted so as to produce the maximum thrust (X force) for a given γ_A .

Given apparent wind condition i.e., U and γ_A , we obtain heel ϕ , leeway β , speed V and rudder angle δ from the four equations, (12), (13), (14) and (15). Then we get the true wind speed U_T and its direction γ_T by vector calculation. By interpolation finally we get V , β , δ and ϕ for a given U_T and γ_T .

Figures 25 and 26 illustrate the result. The true wind speed is 8 m/s. Superior speed of the light displacement IOR racer is impressive. At the same time the 19th century redningskoite competes well with the medium displacement cruiser of the present day, though her windward ability is the worst among the three.

3.2 Elements of Balance of Helm

Figure 26 illustrates the rudder angle versus apparent wind direction, as obtained by the performance prediction. These rudder angles are called upon to balance the helm at different point of steady sailing. Sorting out the calculation of the performance prediction stage by stage tells us that the rudder angle at steady sailing are composed of three components:

- 1 the first is a rudder angle required to counteract a couple generated by sail and hull lateral forces; i.e. δ due to unbalance of aerodynamic $C.E$ and hydrodynamic $C.L.R$;
- 2 the second is to counteract a yaw moment acting on a heeled hull, i.e. δ_2 due to shift of hydrodynamic $C.L.R$ induced by heel;
- 3 the last is to counteract a yaw moment generated by leeward shift of sail driving force accompanied with heel, δ_3 .

The last yaw moment is evaluated approximately by:

$$X_s \frac{h}{2} \sin \phi = X \frac{h}{2} \sin \phi$$

where X_s and X are sail thrust and hull resistance respectively, and h is the mast height above the surface; $h/2$ is then approximately the $C.E$ height above the water.

As is seen in Figure 26 the last element of rudder angle is the largest in most cases. In other words the common trend of weather-helm accompanied with steep heel is primarily due to the leeward shift of driving force of sails. The forward shift of centre of lateral resistance induced by heel certainly has some effect but it is rather small, perhaps somewhat contrary to the common belief among sailors.

References

- [1] Letcher Jr., J.S., 'Balance of Helm and Static Directional Stability of Yachts Sailing Close-Hauld', Journal of the Royal Aeronautical Society, Vol. 69, April 1965.
- [2] Nomoto, K., H. Tatano and T. Kaneda, 'Hydrodynamic Analysis on Sailing', (1st Report), Journal of the Kansai Society of Naval Architects, Japan, No. i70, September 1978.
- [3] Gerritsma, J., 'Course keeping qualities and motions in waves of a sailing yacht', Proceedings of the third AIAA Symposium on Aero-hydrodynamics of Sailing, California, 1971.
- [4] Jones, R.T., 'Properties of Low Aspect Ratio Pointed Wings at Speeds above and below the Speed of Sound', NACA Tech. Report/ 835, 1961.
- [5] Beukelman, W. and J.A. Keuning, 'The Influence of Fin Keel Sweep-Back on the Performance of Sailing Yachts', 4th HISWA Symposium on Yacht-Architecture, 1975.

A philosophy of yacht design

by Olin J. Stephens II

My philosophy, if it deserves that name, is a practical one, so my discussion will be pragmatic and descriptive. I hope that I have learned something over the years, although I am not sure that the designs of the seventies are any better than those of the thirties. However, I shall try to suggest some of the changes in method and philosophy that I have seen since I began to work professionally in 1928.

In retrospect, a pragmatic approach has been applied according to certain principles, which have also developed and changed as time has passed. As well as I can recall, such principles were applied quite unconsciously, i.e., the early days while the desire to improve one's work demanded analysis later on. In youth, confidence came easily. Recognition of a search for the best way followed later.

In the discussion that follows, I shall compare methods where I can, so as to review the results of changing patterns of work as time has passed. The focus has been a gradually increasing emphasis on analysis as it has replaced intuition as a design tool. To the writer, this direction has seemed correct and inevitable in the light of increasing theoretical knowledge and computing power, but it must be granted that in a competitive field, and one that is even highly technical, analysis has often yielded to intuition as the way to success.

The methods of procedure and examples discussed here are primarily directed toward evaluation of and improvement in sailing yacht performance in which sense they apply most directly to racing yachts in which speed is the primary design objective. Yet, some understanding of design factors as they may influence speed is useful in any design if only in providing benchmarks for the evaluation of needed compromises such as relatively greater than normal displacement or less than normal draft, often needed in a cruising yacht. Therefore, while emphasis is on performance, the well behaved cruising yacht must be seen as just as important as the winning racer.

Experience on the water from my youngest days led me to yacht design and I never considered any other vocation. When I was very small, my family had motor boats on Lake George, in New York State, but after the first World War, we spent our summers on salt water and we all became sailors. My brother, Rod, and I, each, in his way, became addicted to sailing and to such technical facets of the sport as we could understand.

We have worked together since that time although Rod did not join our firm until 1934, and we have been fortunate in having generally complimentary talents so that where my tendency to generalize might have missed details, he has applied his interest and talent in a way that was absolutely necessary, and which I never could have done. With a mind and an eye for detail, he has specialized in hull and rig construction and shipyard inspection while I have looked after general design and administration with a special interest in hull lines. We have, I think, tacitly held a common philosophy stemming from our early sailing together. We have enjoyed fast, lively and responsive boats which, however, must have been strong and safe. We have respected the force of wind and water and we have recognized the limitations existing in the strength of boat building materials.

Not without difficulty and error, we have tried to combine strength, reliability and performance. We have also considered a sailing yacht a self-sufficient entity to the greatest extent possible, to which, end, complexity should be avoided. To achieve suitable results, we have tried to avail ourselves of the best materials and workmanship. These have been targets not always hit.

Our sailing began in small day boats and went on to a cruising phase. A bulky cruising ketch may have conditioned our desire for speed, and we started racing, first in a small, light one design schooner, then in an older six metre from which we went on to offshore racing, first with various owners and then in our own DORADE. Her success in winning the Trans-Atlantic and Fastnet Races in 1931 brought us other commissions even during a period of financial depression.

Rod and I both studied navigation and racing tactics, while I was happiest steering and Rod took charge of the foredeck and crew. This again made a good combination enabling us to get the most out of our own designs, sometimes after others had failed.

The first boats of Sparkman & Stephens design came out in 1929. From that year through 1935, our Six Metres and offshore boats were highly successful and in 1936, our office was asked to collaborate with Starling Burgess on a new J Class design for Harold S. Vanderbilt which became RANGER. We both worked on the plans and sailed in the afterguard.

Gilbert Wyland joined our firm after serving as Chief Draftsman on the RANGER project. Again we were fortunate not only in his sound technical ability as a graduate of the Webb Institute of Naval Architecture, but also in his practical philosophy which made his aims the same as Rod's and my own. Before joining Sparkman & Stephens, Gil had worked in the field of power yachts as well as with the Electric Boat Co., a contractor to the Navy, and his abilities in that area led directly into small vessel work for the Navy Department as the war approached.

It is only as this is written that I realize how long we worked for the government. The period lasted almost twenty years, beginning in 1939 and ending in terms of an enlarged office in 1958. During that time, our office staff numbered eighty to one hundred technical people, while the normal yacht work has been handled by a much smaller group of from eight to twelve people.

My partner, Drake Sparkman, was an important part of the firm's background, which I have reviewed here. Although he was little involved with our designs, technically his position was important both practically and philosophically. A good salesman, who invariably served the best interest of his clients, he had confidence in our designs and as Chief Executive of our firm, his judgment was conservative and sound.

Drake and I became partners in 1928 and incorporated Sparkman & Stephens the following year. My technical training was almost nil as I had spent less than a year at M.I.T. after graduating from high school. I had studied and pretty well absorbed some of the standard books on the subject of naval architecture, such as Atwood, and White, as well as Skene on Yacht Design. I was an avid reader of the yachting magazines as well as books on both racing and cruising and the English writer and sailor, Claud Worth, was an authority I almost wholly accepted. It is hard to evaluate his influence today as our views on technical matters are now far apart although I think we would still share the basic philosophy that the best solution is the only solution. Thus, he helped to direct me in the right way.

In the content of my early reading, I cannot help noting that the English yachting press was then and I think still is, oriented in a more technical direction than that of the U.S.A. through most of this period, although no longer. American design, construction and equipment, and even handling in many cases, has been at a high technical level. This seems a strange paradox.

Philosophically, in the early thirties, I had technical grasp of the statics of yacht design, but

I was totally intuitive with respect to dynamics, more advanced than the work of William Froude and the calculation of upright resistance from models, or Taylor's standard series. I did not particularly like drawing except the drawings of lines which I had done since my early teens with a good deal of care as to balance between the ends as well as fairness and appearance. In my mind, then and now, a quality of sweetness seemed to mean a great deal.

I use the phrase "seemed to" because looking back at those of the old designs which were built to a rule such as that of the Six Metre Class, I can see that I did then, as I should do now, look hard at the measurements taken according to the rule so as to take advantage of its provisions.

As a statement of belief, or philosophy, I have held that a good design came from a good combination of features, rather than any single minded approach. According to the consistency of the combination, one characteristic may dominate one boat and another show up in a competitor and yet the competition between very different racing yachts may be very close. I have tried always to respect the fundamentals of performance in the most basic sense by looking at the balance between a yacht's drag and the power or driving force. Whatever could decrease the one or increase the other should be a part of the design. This attention to basics helps not only in the search for improvement, it also demands the balanced characteristics that are such an important part of a good design.

This early philosophy was sound but simplistic. Good principles were observed. These called for sweet and well balanced lines, a fair compromise between sail carrying power and the best practical relationship of sail area to wetted area. I believed in the importance of the prismatic coefficient not so much as an absolute value but as a basis of comparison. If too low, high speed performance was limited and a cresting wave came up on the weather quarter. Too high a value seemed to increase resistance at the normal windward sailing speeds. Rigs were intended to be clean and strong and full advantage was taken of winches which were just coming into general use on smaller boats. I had a strong sense of what a yacht should be. The design was intended to embody a preexisting form. In this sense, the work was intuitive.

A major step toward analysis which I took in the early days was model testing. I was acquainted with Dr. Kenneth Davidson during the early stages of his work which became the main support for my design development through forty years. Also, the work with Ken Davidson was a great help personally as a substitute for a serious lack of formal education. Recent years have brought new views of the place of models in yacht design which I shall touch on below.

During the most recent decade, the computer has played an increasingly important role. I have accepted its promise gratefully. A philosophy of yacht design must recognize the computer as a primary tool. The power it provides must be used thoughtfully.

By its nature, intuition is harder to define or explain than analysis, so it may be worth adding that the use of intuition is not necessarily unscientific, and it is certainly not anti-scientific. Surely the intuitive designer uses all the technical "know how" he can, but his comparisons are qualitative rather than quantitative. A new design will be placed over an older one to see whether the lines are longer or shorter, or that displacement or wetted area is more or less. If wetted area is less, is lateral plane too small? Such and such a boat had an equally small keel and sailed well to windward so the small keel should be o.k. Or may be wetted area is less and displacement more. Judgment had to decide whether this was for better or for worse. Today, we have numbers to support the judgment, but accepting competition as close, can we rely on the numbers? Today, I would do so but I could well be wrong.

Although, through impatience, I passed up a good opportunity for schooling, I have always tried to be well informed. My meeting with Dr. Kenneth Davidson just as he was starting the work which made him a pioneer in analytical yacht design was most fortunate for me.

His project then was the testing of small models which he had started in the college swimming pool in which he towed a model yacht, measuring the upright drag. The methods that he developed have been fully treated in the literature, especially Ref. [1]. Through the availability of models, designs and actual full scale yachts (primarily GIMRACK), it was possible to help with this project and a rather close association developed which taught me all I could absorb personally and put our office in a strong position with respect to design development through model testing.

Philosophically, Davidson's work marked a long step in the direction of analysis but I am afraid that my bias toward intuition and comparison postponed the acceptance of present methods which are more fully analytical. Also, I was earning my bread and butter as a yacht designer, working for individual clients, who wanted specific yachts, in each case for some particular class or purpose. This is why nothing corresponding to a standard series was done until the recent joint work of Professors Newman, Kerwin and Gerritsma (Ref. [2]).

Controversy existed in the thirties as it has done in the seventies regarding the value of small model testing. In my opinion, Davidson introduced, in a practical and useful way, two major steps. First, the small economical models provided useful information and second, a reliable method based on model results was developed to calculate windward performance at sailing speeds. As it occurred, downwind performance was overlooked, partly through personal bias although the relatively heavy International Rule boats, Sixes and Twelves, sailed almost side by side downwind and the even heavier offshore racers had similar characteristics. So the emphasis was on windward work and the tank provided answers that stood the comparison between calculation and competition. I think it is fair to say that all of the present methods of performance predication stem from Ken Davidson's work. The plot of sail coefficients now has been completed to apparent wind angles up to 180 degrees and the computer has automated the plotting. These steps have made it possible to predict performance under all conditions of wind strength and sailing angle.

I believe that this predictive ability has added a dimension to yacht design methods without changing the fundamental approach. So far, the designer's work has not been simplified. Conversely, new possibilities have been demonstrated and now any new design should be checked for performance. The by products of this procedure are probably more important than the speed calculation itself. That is, the structuring of a performance program necessarily causes the designer to review and evaluate all the speed related factors. This brings us back to the fundamentals. Understanding is increased even if the final prediction is wrong.

I should like with all my heart to put a few words into this paper that would justify the time spent in listening or reading, and which would repay the compliment that the organizers have done me by their invitation to take part in this meeting. My experience has shown me no simple rules, and most surely no secrets. I have often tried to diagram a design path, but never been satisfied with the results, it is too much of a chicken and egg affair. The logic seems always to become circular and the assumptions that must be made by experienced comparison or intuition are controlling. After making some pretty important assumptions, logic can take over if desired in the form of a computer, and a consistent set of dimensions will result. One possible sequence follows:

1. Length - assumed
2. Displacement/Length ratio - assumed
 - 2.1 Displacement
3. Beam - assumed as an appropriate B/L
4. Draft
5. Approximate hull weight demanded by 1, 2 and 3

6. Approximate wetted area consistent with 1, 2, 3 and 4
7. Approximate sail area consistent with 2, 4 and 6
 - 7.1 Rig Height
8. Approximate rig weight consistent with 7
9. Approximate ballast consistent with 2, 5 and 8
10. *BM* consistent with 1, 2.1, 3 and 4
11. Location of *B* from 2.1 and 4
12. Location of *G* consistent with 4, 5 and 9
13. *GM* consistent with 10, 11 and 12
14. Stability from 7 and 13
15. Depending on results, modify parameters and loop.

Note that the subjective element has not been eliminated and note also other assumptions could be taken as beginnings and many other paths could be taken to the end.

An active, practicing organization or individual will normally make better use of comparison with existing known designs and will use steps such as those described primarily to list consistency rather than as a working design tool.

Here a distinction should be made between working practice and design study or philosophy. As a study tool, a predictive algorithm leads to sensitivity analysis which can offer the means of answering the many obvious questions about the optimization of proportions and characteristics. The interesting questions are of course those to which the answers are uncertain and to the best of my knowledge, we do not fully understand such fundamental relationships as those between beam and resistance, heel angle and even wetted area. This is to say that valuable as speed predictions may be, their use is again circular just as is a design program. There are very few fixed points in the procedure.

Just as design parameters must be balanced, so must be the designer's attack on his problem. He must use all he believes as hypotheses to establish a design and proceed confidently, while yet remaining alert to the fact that in a new context, the most firmly held beliefs may be upset.

An important element of the writer's design philosophy has been an interest in rating rules. A natural curiosity about the relationship between shape, size and performance has led to a lifetime of rule activity. While one hopes that the sport has been helped to some degree, all that can be said with certainty is that rule work has provided a very valuable learning experience. In a technical sense, one is forced to reach decisions on all the important speed relationships and then see the decisions tested. My principal complaint is that most critics fail to appreciate the limited and often contradictory evidence on which many decisions have to be based. Bad results come mainly from lack of knowledge rather than intention. Rule committee work makes one think. As with design decisions, one must have confidence without stubbornness. It seems worth noting here that the predictive method seems ideally suited to the purpose of rating. The fact that speed is predicted under varying conditions in place of a single number called a rating should make adjustments easier to apply and control and the correspondence between design and speed should be more easily recognized.

A fundamentally important point about rating rules which should be mentioned here is the dual nature of any possible rule. First, the measurements must be defined and taken. The method is likely to have an important influence on the boat's shape. Then the measurements are combined by formula, a step which broadly influences proportions. Measurements have become many and complicated in an effort to avoid putting great pressure on particular points and to the writer, it appears that the vertical taking off of the lines will come as the next logical step in rule development. When the lines become available to the computer, a speed

predicting formula can be applied, possibly in the form of an algorithm as in the American MHS, but I think preferably in a formula, possibly a Taylor series which might be made to essentially reproduce the results of the predictive algorithm and yet be more readily transparent in its application.

Although some of my colleagues in rule studies find appeal in a rule which is hard for the designer to penetrate, I prefer a rule which is as easy as possible to understand and apply so as to open the field of design as wide as possible and thus encourage development as well as wide participation.

To repeat, I wish I could write a more useful paper. Although the generalities are relatively easy to discuss, the most successful designs seem to come from a fortunate combination of proportions and details. Such a combination surely can be closely approximated through analysis but only fully achieved through the right feeling. The right feeling must be fed by an accurate knowledge of hydrodynamics, structures and all that goes into a yacht. I think a good practical knowledge of sailing is also essential.

Yacht design and yacht designers have been very good to me. I have particularly appreciated the generosity of the professional societies and the academic society which I slighted as a younger man. I am fully aware of the gaps in my knowledge and technical equipment. Today I recommend all the schooling one can get. But more is necessary than even technical and practical knowledge, which I say knowing that I could have done better with the greater application of determination and energy. It is easier to visualize the work that should be done than to do it. Understanding is cumulative and the study that can be made now provides a step toward the future. Understanding must be applied with confidence and drive, and variations on the best current work must be studied and applied. Mathematical modeling whether in simple or complex terms can be revealing. The total of a large number of small figures has always surprised me. The combination of a number of small improvements in a design has a similar, large effect. Enthusiasm and the steady effort to put together small gains can lead to the break through. That method may not be easy but it works.

References

- [1] 'Experimental Studies of the Sailing Yacht', SNAME Transaction Vol. 44, 1936.
- [2] 'Test Results of a Systematic Yacht Hull Series',
J. Gerritsma , G. Moeyes and R. Onnink,
Symposium Yacht Architecture, 1977.

Some applications of aeronautical engineering in the construction of yachts

by F.A. Jacobs

National Aerospace Laboratory,
The Netherlands

Summary

Some recent developments of the masts and standing rigging of racing-yachts and, on the other hand, the failures of a number of masts and rudderstocks led to the application of aeronautical engineering. Load spectra of the standing rigging of a 10.00 m racing yacht are given and the application of them in a lug. Some information is given on stress-raisers and on materials. Finally some test-applications are mentioned.

Contents

- 1 Introduction
 - 2 Assessment of loads
 - 3 Stresses and stress raisers
 - 4 Materials and heat-treatments
 - 5 Miscellaneous
- References

Motto, by William Thompson and Lord Kelvin:

"When you can measure what you are talking about, and express it in numbers, you know something about it".

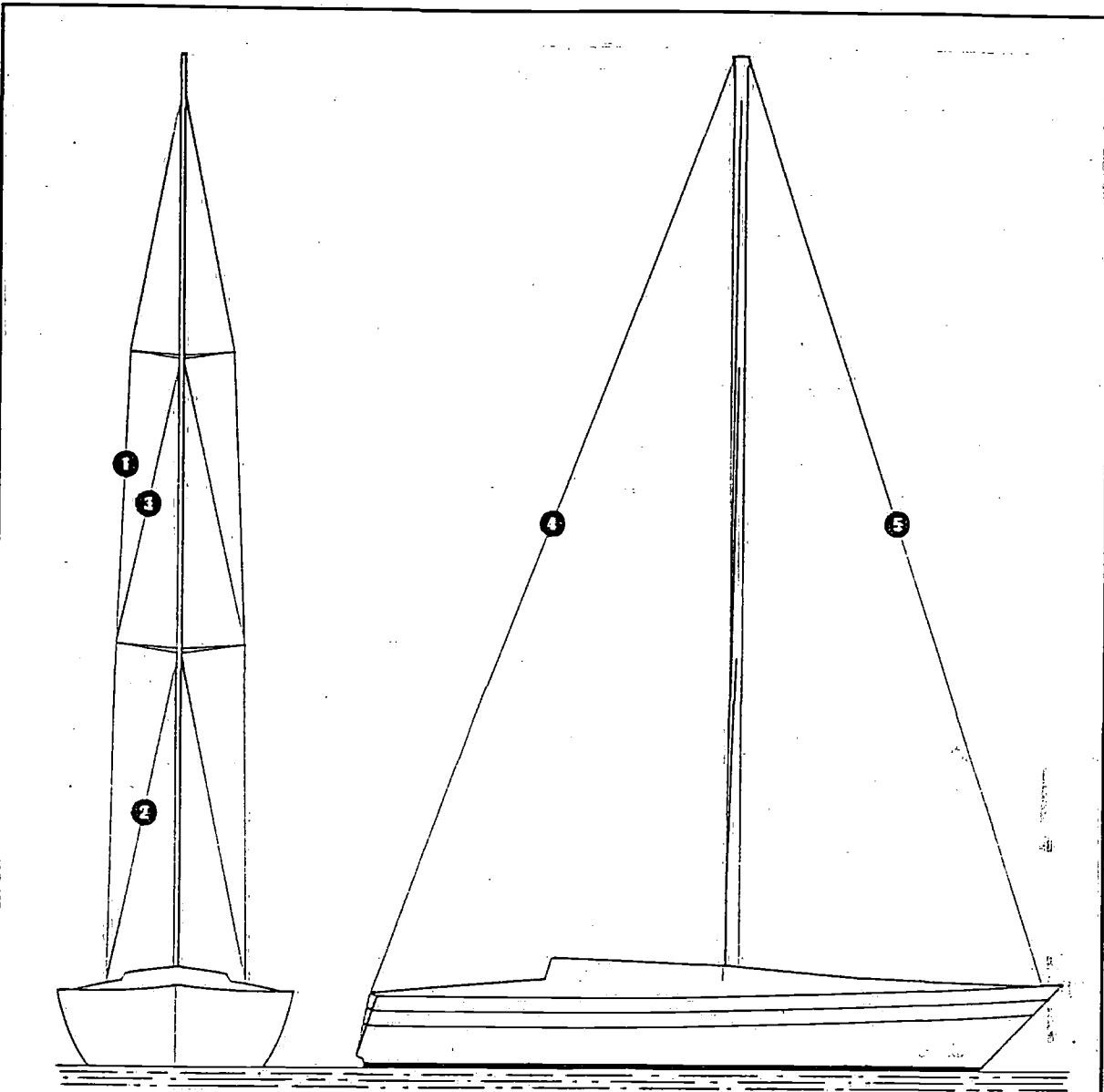
1 Introduction

One of the important goals of aeronautical engineering is to achieve strong and reliable constructions with a low weight. Since the latter requirement is imperative, the strength-weight ratio of airborne constructions is very high as compared with other vehicles (cars, trains) or with other products of mechanical engineering. This certainly is necessary to keep air transportation economically feasible, which means that there is a non-lessening pressure to save weight where- and whenever possible.

For example: saving 1 kg construction weight in a Boeing 747 (take-off weight ~ 350.000 kg) or in a DC-10 (take-off weight ~ 250.000 kg) results in saving \$ 100 nett per year. So, in general it appears to be worthwhile to save weight by all reasonable means.

Weight reduction can be achieved by detailed stress research, by the application of advanced materials and by extensive testing. The latter varies from small parts or specimens to full-scale environmental testing (like the Concorde).

A considerable part of the knowledge gathered in aeronautical engineering is available for the application in other engineering branches with a demand for constructions with a high strength-weight ratio, for instance sailing yachts! This will be especially usefull if the concept



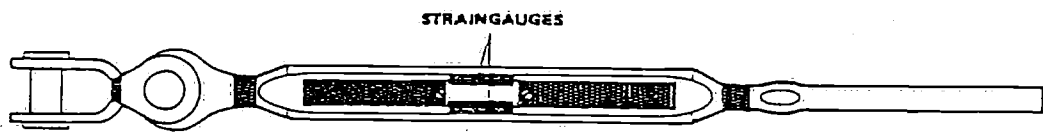
0 0.4 0.8 1.2 1.6 2.0 m

KALIK 33, DESIGN J.H. DE RIDDER

LOA : 10.00 m
 BEAM : 3.35 m
 DISPLACEMENT : 4.800 kg
 I : 13.15 m
 J : 4.20 m
 P : 11.11 m
 E : 3.45 m

LOAD TRANSDUCERS BUILT IN.

CHANNEL 1 : UPPER SHROUD
 CHANNEL 2 : LOWER SHROUD
 CHANNEL 3 : INTERMEDIATE SHROUD
 CHANNEL 4 : BACK STAY
 CHANNEL 5 : FORE STAY
 CHANNEL 6 : MAST
 CHANNEL 7 : VOICE.



RIGGING SCREW PROVIDED WITH TWO ACTIVE STRAINGAUGES

Figure 1 The object of the load measurements

of such a yacht resembles an airplane: built from aluminium alloys. But also in yachts made of other materials, there are many parts which can be treated in a aeronautical way, as for instance the standing rigging and spars or the rudder shaft.

Paying attention to realistic loads, stress raisers and new materials, weight can be saved on one hand while on the other hand unexpected failures, like the many mast and ruddershaft failures of today's (big) racing yachts, can be prevented.

2 Assessment of loads

The loads acting on airplane flying in still air at 1 g can be calculated rather easily. But then immediately the question rises how these loads are influenced by gusts and/or manoeuvres. To answer this question numerous recordings from counting accelerometers and from strain gauges, bonded in critical areas had to be analysed to arrive at load spectra, mostly for the wing, and always related to a specific type of airplane. Based on these data, reasonable overload factors have been established to make possible realistic stress calculations. The testing of parts and finally a static and dynamic full scale test has to prove the integrity of the construction.

A similar development to assess the dynamic loads in the rigging and other critical areas of racing yachts has, to my best knowledge, never taken place. Contrary: to calculate the dimensions of the parts of the standing rigging the approach is fully static: i.e. the yacht is assumed to be heeled by aerodynamic forces until the maximum righting moment is reached. These forces are spread in a rather peculiar way over the mastlength, inducing the loads in the rigging wires (Ref. [1]).

In the applied, more or less empirical formulae, overload- and/or safety factors are included, probably comprising dynamic load effects as well. As Gary Mull in his 1981 HISWA lecture mentioned (Ref. [2]) there has been and still goes on a trial and error type of approach, which, if the causes of the errors are not investigated and understood, will never end. Therefore, to obtain weight reduction without the penalty of failures, the true loads and the number of occurrences in the critical areas of the yachts have to be assessed.

As a first step to obtain some insight in this matter, in the Spring of 1982 measurements have been carried out on a 30 ft racing yacht, the data of which are given in Figure 1. These activities have been executed in close cooperation between the Ship Hydromechanics Laboratory of the Technological University Delft, one of its scientists who made available the racing yacht, INTECHMY which made available an instrumentation recorder and the Structures and Materials Division of the NLR.

Since in this case the standing rigging was of primary interest, straingauges were applied on the rigging screws of the port shrouds and of fore- and backstay. In the barrel of the rigging screw two active straingauges were glued, wired and sealed. Then, with a calibration in a tensile testing machine, the load factor, i.e. the tensile load versus the electrical output, had been assessed (Table 1). The rigging screws were mounted and the wires for the supply and output connected to the instruments according to the block-scheme given in Figure 2. The 7 track (one track being a voice channel) SE 3500 recorder made possible the simultaneous recording of 6 transducers. The pen recorder provided a quick look (Figure 3) and a back-up for malfunctioning of the SE 3500. After preloading the rigging screws according to common practice, the test set-up was ready.

As is shown in the Tables 2 and 3, various conditions were encountered during the 11 runs made, each run lasting for about 20 minutes. Unfortunately only runs 8, 9, 11 and 12 appeared to have usefull results for all channels. Since run 8 and 9 were comparable: same weather- and sea-condition but going windward (run 8) and reaching with spinnaker (run 9), it was decided to process the data of these runs. The analogue (frequency modulated) output of the SE 3500 was recorded on a strip chart recorder (Figures 4 - 9). Via an analogue/digital

Table 1: Data of load transducers and pre-loads

Channel No.	Location of load transducers	Load Factor kN/V	Pre-Loading of Transducers kN	
			before	after
			Pressurizing the back stay actuator	
1	Upper Shroud	14.95	4.20	4.20
2	Lower Shroud	13.89	3.56	3.16
3	Intermediate	10.69	1.64	1.64
4	Back Stay	18.92	3.24	6.90
5	Fore Stay	14.15	2.89	3.70

Table 2: Conditions during the measurement runs

	Run									
	1	2	3	3'	4	8	9	10	11	12
Date (1982)	23/4	23/4	24/4	24/4	25/4	27/4	27/4	27/4	30/4	30/4
Course	windw	windw	windw	reach	windw	windw	reach	*	windw	windw
Wind (8 Bf)	4-5	5	6-7	6-7	4	5	5		4	5-6
Sails	M+G4	M+G4	M2r	G4	M+G2	M+G4	M+8		M+G2	M+G4
Waves (m)	0.5-1	0.7-1	+		0.5	1.0	1.0		1.0	1.0
Speed (kts)	5.5-6	5.5-6		5.5-6	5	6	6.5		5-6	5
Heel Angle (°)	30	30-35	5.5-6 >30		30	30	15		30	30

*: Zero-check of all channels in Harbour

M = Main, G4 = Genoa #4, M2r = Main with two reefs

S = Spinnaker

General remarks: - During Runs 1, 2, Probably 3, 4, 8 and 9 the Lee-shrouds Showed Slack
 - Wind, Waves and Heel Angle Estimated

Table 3: Survey of useful tape recordings (indicated with x)

Recorder Channel	Location	Run												
		1	2	3	3'	4	5	6	7	8	9	10	11	12
1	Upper shroud	-	-	*	*	-	-	-	-	x	x	x	x	x
2	Lower shroud	x	x			x	-	-	-	x	x	x	x	x
3	Intermediate	x	x			x	-	-	-	x	x	x	x	x
4	Back Stay	x	x			x	-	-	-	x	x	x	x	x
6	Fore Stay	x	x			x	-	-	-	x	x	x	x	x
7	Mast	-	-			-	-	-	-	-	-	-	-	-

* Recorder damaged by saltwater.
 Pen recordings available.

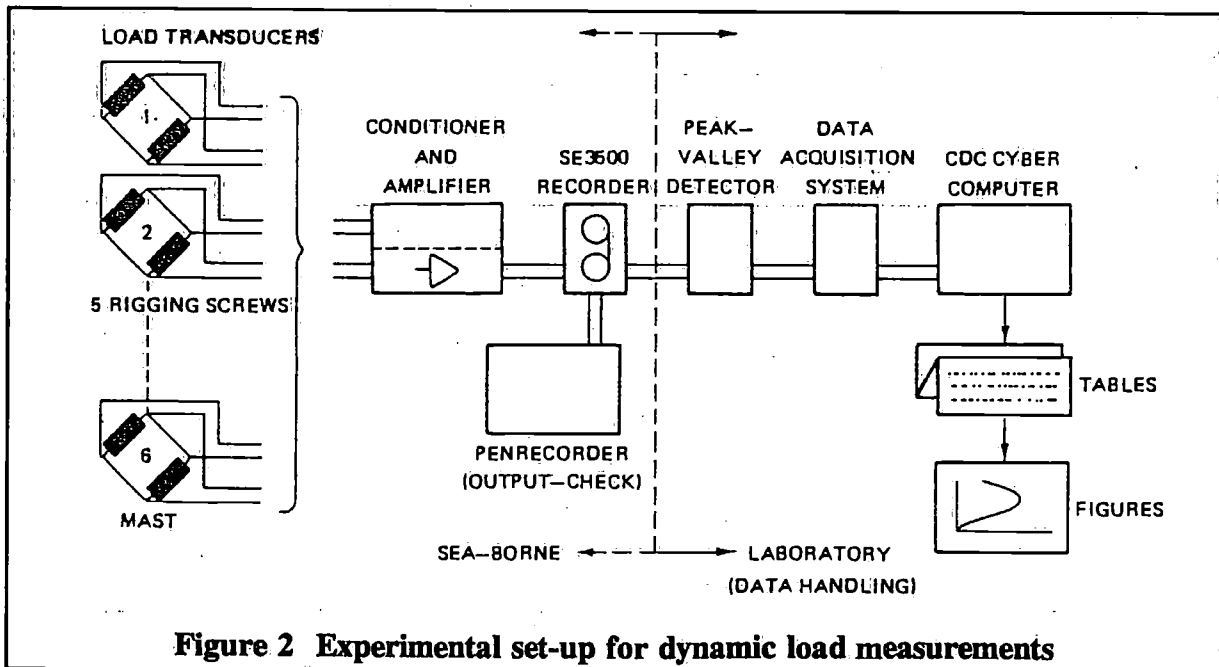
converter the same signal was passed to a peak-valley detector presenting its digitized results as a sequence of numbers representing the milli-voltage of the peaks, respectively valleys. Load direction changes smaller than 40 mV (representing ~ 60 kgf as an average for all channels) were omitted. This sequence of numbers was compared with the strip-chart recording to check for EMI - and switching errors. The now corrected sequence was then handled by computer to produce Tables 4 and 5 and Figures 10 - 13 representing level crossings and range countings (NLR range-pairrange or rainflow counting; Ref.[3] and [4]). A review of the important data are represented in Table 6. All designers are invited to apply their favourite formulae on the sailplan of Figure 1 to check whether or not the results of these do agree with the measured loads.

From the figures with level crossings and range countings a danger looms up: the apparent dynamic character of the loads in shrouds and stays implies metal fatigue. With this aspect a completely new approach in construction is necessary if an optimal construction is pursued. An example may illustrate that this is not unreasonable. If it is assumed that:

- The yachtlife is 16 years.
- In 25 weekends per year the yacht is sailing for 10 hours.
- 50% of that sailing time is according to conditions of run 8.
- The elapsed time of run 8 was 20 min.

Then the accumulated load history is:

$16 \times 25 \times 10 \times 0,5 \times 60 = 6000$ times the content of run 8. For the lower shroud the number of loads in class 13, which is ~ 50% of the highest measured load, is ~ 130. So during its life the yacht will be exposed to $130 \times 6000 = 780.000$ loadcycles of that magnitude. The number of loads in class 19 (75% of highest measured load is 10, which means that the yacht will experience in its lifetime 60.000 of these loadcycles.



Probably a number of mast failures in the past can be explained by this enemy in (especially aeronautical) constructions. It is even more probable that, although some parts of the rigging have been constructed too light others were too heavy, by simply applying a safety factor of 4 or 4.5 (Ref. [1]).

The same reasoning with respect to the loads in the rigging applies to other critical parts; rudder stock (Figure 14), lugs, steering cables and last but not least the mast section itself.

Table 4: Range countings according to range-pair-range method (rainflow-method)

Run		8				9			
Channel		1	2	3	4	1	2	3	4
Range	1	1209	143	1501	1169	1099	1581	1281	1021
	2	1121	1339	1235	1155	969	1279	898	979
	3	897	1087	991	983	572	673	490	617
	4	681	947	813	785	330	355	293	349
	5	499	807	627	600	203	207	163	223
	6	336	701	502	428	130	129	106	134
	7	191	584	374	308	78	86	66	86
	8	112	481	240	182	54	64	49	63
	9	46	395	157	138	31	47	32	59
	10	22	307	99	77	23	31	20	49
	11	8	226	62	43	21	25	17	39
	12	6	169	36	25	16	18	10	29
	13	0	129	20	19	13	10	6	19
	14	0	71	10	18	6	10	5	11
	15	0	53	6	16	4	4	3	7
	16	0	32	3	8	4	4	1	5
	17	0	26	1	6	2	1	0	3
	18	0	14	0	6	0	0	0	3
	19	0	10	0	6	0	0	0	2
	20	0	5	0	4	0	0	0	2
	21	0	3	0	3	0	0	0	2
	22	0	2	0	2	0	0	0	2
	23	0	1	0	1	0	0	0	2
	24	0	0	0	1	0	0	0	2
	25	0	0	0	0	0	0	0	2
	26	0	0	0	0	0	0	0	2
	27	0	0	0	0	0	0	0	1
	28	0	0	0	0	0	0	0	1
	29	0	0	0	0	0	0	0	0
	30	0	0	0	0	0	0	0	0
	31	0	0	0	0	0	0	0	0
	32	0	0	0	0	0	0	0	0

Thus an extensive field has presented itself to be explored. It seems worthwhile to start its exploration. Some final remarks on the discussed strip chart recordings and range countings may be useful:

- The similarity of upper, lower and intermediate shroud is apparent. Although different in magnitude, the peaks and valleys follow the same pattern.
- A marked difference between run 8 and run 9 is shown in Figure 10. While in run 8 the lower shroud is subjected to loads which dominate in number and magnitude, the loads on the back stay are contrary to this. In run 9, however, the effect of the empty spinnaker which suddenly fills, resulting in a shockload, can be seen clearly.
- In run 9 the differences between the loads in shrouds and back stay are relatively small as compared with run 8. The affect of the spinnaker-top load can be recognized.

3 Stresses and stress-raisers

It is supposed that the dimensioning of important structural parts is not based on rules of thumb but on stress calculations. It means that, after having assessed the loads, these have to be translated to stresses in the material of the parts involved.

It may be that the construction has to be resistant to plastic deformation. Then the maximum local stress shall not pass the yield limit of the material. If plastic deformation is accepted, the ultimate stress can be applied. Nevertheless, to cope for deficiencies in the stress calculation and/or in the materials applied, a safety factor has to be introduced. It is plausible that this factor which covers uncertainties, can be smaller when reliable data are available with respect to loads, stresses and materials.

Based on a good understanding of loads and stresses and on tight material requirements, in aeronautics a safety factor of only 1.5 is an accepted standard. Compare this with the factor 4 which is often used in yachtbuilding.

As long as a stress can be calculated, for instance in tension, as: load divided by cross sectional area, uncertainties are small. Unfortunately this is seldom the case. Stress raisers tend to be everywhere, even when not expected: for instance the damage induced by fretting corrosion. An example of this danger can be the light alloy lug of Figure 15 (Ref. [4]). It is made of the Al-Cu-Mg-alloy 2024-T3 with its typical mechanical properties: ultimate tensile stress $S_u = 49.5 \text{ kg/mm}^2$ and yield limit $s_{0.2} = 35.2 \text{ kg/mm}^2$. With a safety factor of 1.5 a nett stress level of 33.0 kg/mm^2 seems to be applicable. The fatigue life however of this lug for a stress varying between zero and 33.0 kg/mm^2 is only ~ 2000 load cycles.

This is far less than the expected 6000 max-load cycles for a 16-year life time, based on the range counting discussed earlier. The reason for this unexpected low fatigue life is twofold: a stress concentration factor (defined by local peak stress/ nominal stress) of 3.5 raises the local stress in the wall material next to the hole, to the same extend and, on top of this, fretting corrosion is introduced by the motion of pin and wall material during the load cycle (Figure 16).

Should a safety factor of 4 have been applied on S_u , which yields a maximum nett stress of 12 kgf/mm^2 , then the fatigue life should be about 100.000 loadcycles.

Based on the data given in Figure 10 this is comparable with the number of load cycles at level 18 (lower shroud). 18 times the earlier mentioned factor 6000. Since level 18 is 67% of the maximum load this is discouraging because the luglife is consumed completely by this load level. Fortunately the actual load history has the stochastic character as shown before: few high loads mixed with many low loads. It seems nevertheless worthwhile to eliminate doubts by executing simulation - or at least programme tests (a simpler fatigue test with few load levels and the loadcycles grouped) on lugs.

Because the dimension of lugs in various applications will differ strongly, Figure 17 is given, from which the stress-concentration factor for other lugs can be deduced. It is evident that the stresses next to the hole can reach unexpected high levels.

Another interesting approach of the dimensioning of lugs is in reference [5].

Unfortunately, unexpected stress raisers can be found in many constructions.

Therefore a number of them with the relevant stress concentration factors are given in the Figures 18a, b and c taken from reference [6]. This handbook contains an extensive databank of stress concentration cases, presented in graphical form as shown in the Figures 18a, 18b and 18c. Similar data are given for plates with a variety of holes, shapes and patterns for shafts with and without holes or steps, etcetera.

Apart from the problem to assess the concentration of stresses is how to cope with these crack starters, It will be clear that the prevention of grooves and working scratches perpendicular to the load direction, of inclusions and indentations will save already much trouble.

Table 5: Level crossings

Run		8			
Channel		1	2	3	4
Level	1	0	0	0	0
	2	0	0	0	0
	3	0	0	0	0
	4	0	0	0	0
	5	0	0	0	1
	6	0	0	0	1
	7	0	0	0	3
	8	0	0	0	5
	9	0	1	4	6
	10	0	5	12	8
	11	0	17	39	10
	12	7	41	89	13
	13	84	91	194	31
	14	283	177	329	87
	15	453	266	430	213
	16	901	349	516	344
	17	462	428	501	463
	18	355	499	444	513
	19	226	526	340	473
	20	125	490	219	363
	21	48	434	128	236
	22	18	351	61	123
	23	4	277	27	58
	24	0	203	8	29
	25	0	128	1	6
	26	0	75	0	3
	27	0	31	0	2
	28	0	18	0	1
	29	0	6	0	0
	30	0	1	0	0
	31	0	1	0	0
	32	0	0	0	0

9			
1	2	3	4
0	0	0	1
0	0	0	1
0	0	0	1
0	4	1	1
0	13	4	1
0	49	18	1
0	111	78	2
0	205	155	5
0	322	230	9
1	418	296	15
8	416	298	17
48	320	266	24
134	191	183	41
254	102	99	75
328	47	51	101
332	32	25	108
273	16	11	150
167	10	6	203
100	6	1	238
55	1	0	236
34	0	0	239
19	0	0	174
11	0	0	116
8	0	0	63
4	0	0	27
3	0	0	7
0	0	0	2
0	0	0	1
0	0	0	0
0	0	0	0
0	0	0	0
0	0	0	0

Table 6: Important results from the runs 8 and 9

Channel	Run 8			
	1	2	3	4
Elapsed time of run (min/sec)	20'7"	20'2"	19'47"	20'6"
Number of load cycles (C)	605	718	743	585
Average freq. (Hz)	0.50	0.60	0.63	0.49
Max. Load (kgf)	1102	1450	1169	1292
Min. load (kgf)	531	402	395	206
Load range (max-min) (kgf)	571	1048	774	1086

Run 9			
1	2	3	4
18'1"	18'42"	19'3"	18'26"
550	791	643	511
0.51	0.70	0.56	0.46
1243	960	910	1292
468	181	197	61
775	779	713	1231

Also, the building-in of internal stresses is worthwhile in many cases. This is possible by shotpeening or other forms of cold deformation including the expansion of holes in lug-pin combinations. A good example of the effect of hole expansion is given in Figure 19 (Ref. [7]) while the effect of shotpeening is shown in Figure 20 (ref. [8]).

The mentioned methods have been applied for many years in aeronautics. Why should yacht designers and - yards neglect them while they are generally available?

4 Materials and heat treatments

A rule of thumb for metal alloys which a designer often has to cope with is what can be considered as the retaining total of the properties of an alloy. The meaning of this rule is: If boosting one property of an alloy, whether it be a steel or an aluminium alloy, this nearly always results in one or other property getting worse. Now the properties of interest for the yacht designer are: ultimate tensile strength (S_u), yield strength ($S_{0.2}$), elongation (δ), corrosion resistance, weldability, susceptibility for fatigue and for stress-corrosion cracking. For example: boosting S_u and, consequently $S_{0.2}$, by cold working, this will reduce δ . The penalty for the latter very often will be an increased sensitivity for fatigue and/or for stress corrosion cracking. Therefore a part subjected to a fatigue load has to be made from a material with an elongation of at least 12%, if possible 15%. On the other hand, in the area of a construction, not threatened by fatigue, an alloy can be applied with a temper, which shows a much higher S_u and $S_{0.2}$.

An example is the stainless steel swaged terminal for $i \times 19$ rigging wire. The material applied has to be strong enough to prevent failure at the lug or at the end of the bore in the shaft. Commonly AISI 316 material, $\frac{1}{4}$ or $\frac{1}{2}$ hard is used. By the swaging process (cold deformation) the elongation δ is reduced again and therefore the susceptibility for stress-corrosion cracking is increased. Placed in a saline (= corrosive) environment, as strong as for instance in the Gulf of Mexico, then, cracks will start in the shaft, induced by the residual tangential stresses after the swaging process.

For aluminium alloys the retaining total of properties (a gain at one property means a loss at another) is shown in Figure 21 which was derived from reference [9].

The effect of cold working on S_u , $S_{0.2}$ and δ is evident. Based on the above mentioned minimum elongation level of 12% it is advisable to apply the tempers -H12 of -H32 (i.e. $\frac{1}{4}$ hard). Should fatigue loads be absent, then the tempers -H14 and -H34 may be acceptable.

Figure 22 (Ref. [10]) shows the relationship of the mentioned properties for the existing series of aluminium alloys. It appears that for sheet and plate the Al-Mg (5000) series offers an attractive compromise, especially the alloy AA 5083 in the temper -H321 and also AA 5086 in the temper -H116. Resistance to corrosion and stress corrosion cracking is very good. Weldability is good. Strength is moderate to good. Fatigue strength is moderate. Elongation is sufficient, even if some cold deformation is necessary.

It seems attractive to apply alloys from the 2000 or 7000 series, developed for the aerospace industrie, because of their favourable tensile strength (Figure 23). Other important properties, however, a low resistance to corrosion and stress corrosion cracking and bad weldability-, prevent a simple application unless special manufacturing methods (for instance bonding and preservation by coating) can be used.

Special attention is necessary for heat-treatable aluminium alloys like the Al-Mg-Si (6000) series. An AA 6061 mast section in the -T6 temper (artificially aged) will lose locally its -T6 properties after having been welded. The material has arrived then in the -O (annealed) or, after a short-time, in the -T1 temper which show substantially lower strength levels. To arrive at an optimum strength level, after the extrusion the material has to be treated into the

-T4 or -T5 temper. Then the welding can be executed followed by full artificial ageing to the -T6 temper of the completed mast. It is a rather expensive way to prevent local weakness by a low $S_{0,2}$ in the mast section by the welding (which unfortunately often is combined with a stress concentration). However, if this is a method to prevent local buckling and consequently mast failure, it seems to be worthwhile.

With respect to steels: a heat treatable steel like the ARMCO 17-4 precipitation hardening steel apparently is a perfect replacement for AISI 316 where high strength is required. Since the strength of it can be varied between 80 and 150 Kgf/mm² by varying the ageing temperature it is possible to obtain exactly the combination of properties as required.

Otherwise it should be noted that the notch-sensitivity of steels is slightly worse than of aluminium alloys, especially in the case of small radii.

Finally, a titanium alloy should be mentioned (Ti6Al4V) as a material for special purposes, like rudder stocks. Being light (specific gravity of 4.43) and strong ($s_u = \sim 112$ kg/mm²) but very expensive (Dfl. 80,-/kg) it can solve a constructional problem when no other material is able to do this. Although a number of Ti alloys is available, only the above mentioned alloy is applicable for its good corrosion resistant capability.

5 Miscellaneous

There is no doubt that the aerospace institutes can assist yacht designers in many more cases than in the above mentioned: Loads - Stresses - Materials. Some examples may be given:

- For the evaluation of kevlar rope for sheets, bending fatigue tests with pulleys according to sheaves in practice can be executed (Figure 24). It has been done with interesting results.
- For the assessment of the construction weight of a yacht, an aircraft weighing kit can be applied. This weight assessment can be carried out with and without keel (ballast) and/or without gear inventory. A better understanding of the composition of the total displacement is possible then.
- The tensile testing of welds, either for the evaluation of new welding techniques or to check the quality of welding equipment and/or the welder. MIG and TIG welding systems are routinely used for welding aluminium alloys and regular check-up is very useful.
- The tensile testing of newly developed connections of standing rigging wires to the mast section.
- Bonding techniques for secondary loaded connections in parts like booms.

It has not been the goal of this paper to describe in detail the results of the above mentioned tests. These have been executed for a well known yacht yard in Holland and can be repeated for anybody interested in facts and figures. Finally, it is interesting to quote, a postulation of the famous scientist who's expression was lent as a motto on the first page of this paper, namely:

"Flying machines are impossible; they always will appear to be too heavy".

By measuring, calculating and testing, history has denied this. Yacht designers can make use of it, to complete future missions that may now be considered impossible.

6 References

- [1] Kinney, F.S., 'Skene's elements of yacht design', A. and C. Black, London (edition 1973)
- [2] Mull, G.W., 'A rational approach to the structural design of sailing yachts', HISWA Symposium 1981; Supplement.
- [3] Jonge, J.B. de, 'The analysis of load time histories by means of counting methods', NLR MP 83039 U (1982).
- [4] Schijve, J. and F.A. Jacobs, 'The fatigue strength of aluminium alloy lugs', NLR-TN M.2024 (1957).
- [5] Hobbit, F.M., 'Analysis of lugs and shear-pins', Aluminium and steel alloys, Lockheed Aircraft Corporation report LAC-R-8025 (1952).
- [6] Peterson, R.E., 'Stress Concentration Factors', John Wiley and Sons, New York (1973).
- [7] Schijve, J., D. Broek and F.A. Jacobs, 'Fatigue tests on aluminium alloy lugs with special reference to fretting', NLR report M 2103 (1962).
- [8] Graaf, E.A.B. de, F.A. Jacobs and J.H. Nasette, 'Influence of residual compressive stresses upon the fatigue strength of notched and unnotched 7079 specimens. NLR TR 71105 (1971).
- [9] Anonymous: 'Aluminium standards and Data', The Aluminium Association Inc., Washington (1978).
- [10] Wanhill, R.J.H., 'Fatigue and fracture- toughness in Aluminium', NLR MP 82058 (1982). (In Dutch).

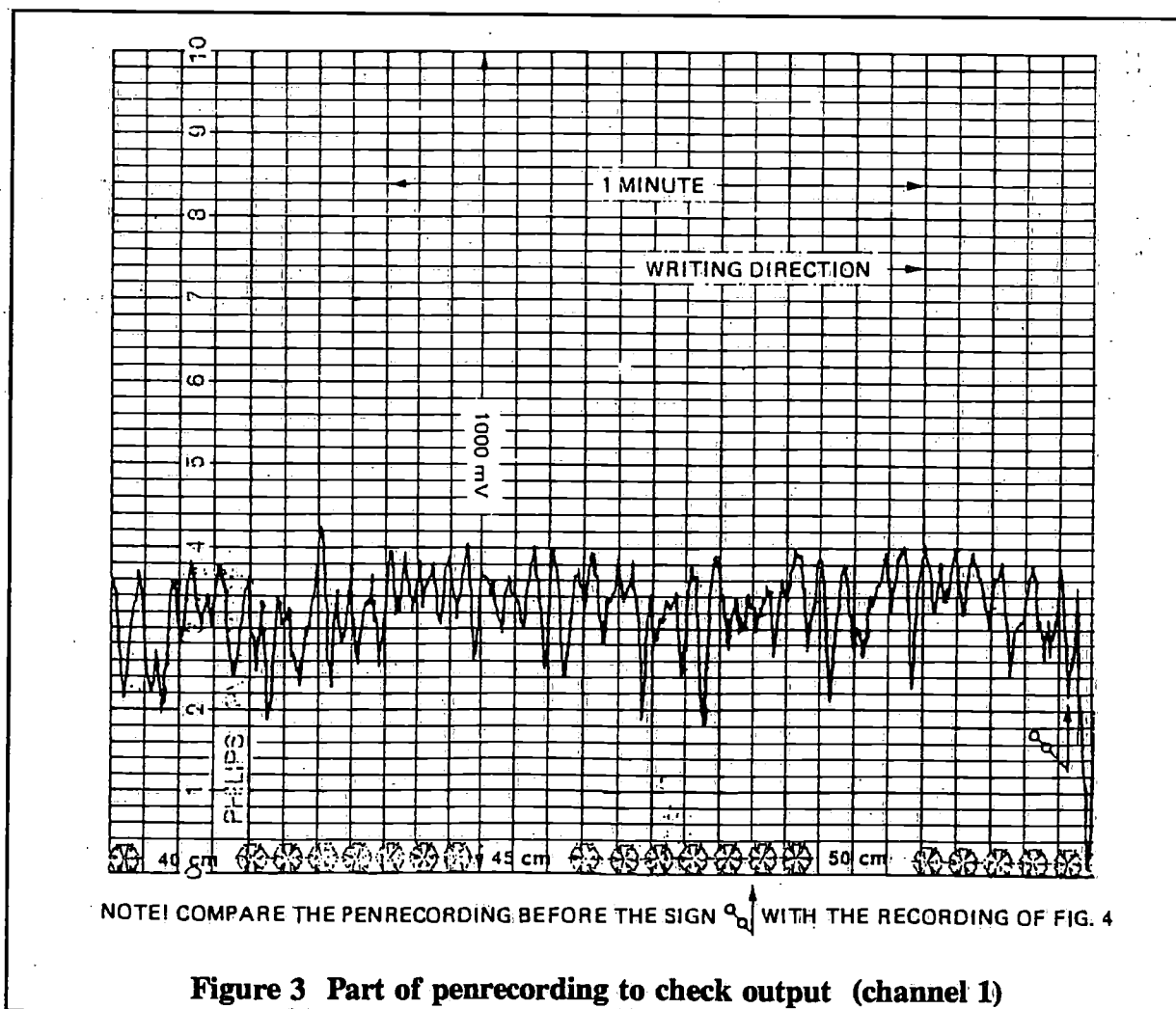


Figure 3 Part of penrecording to check output (channel 1)

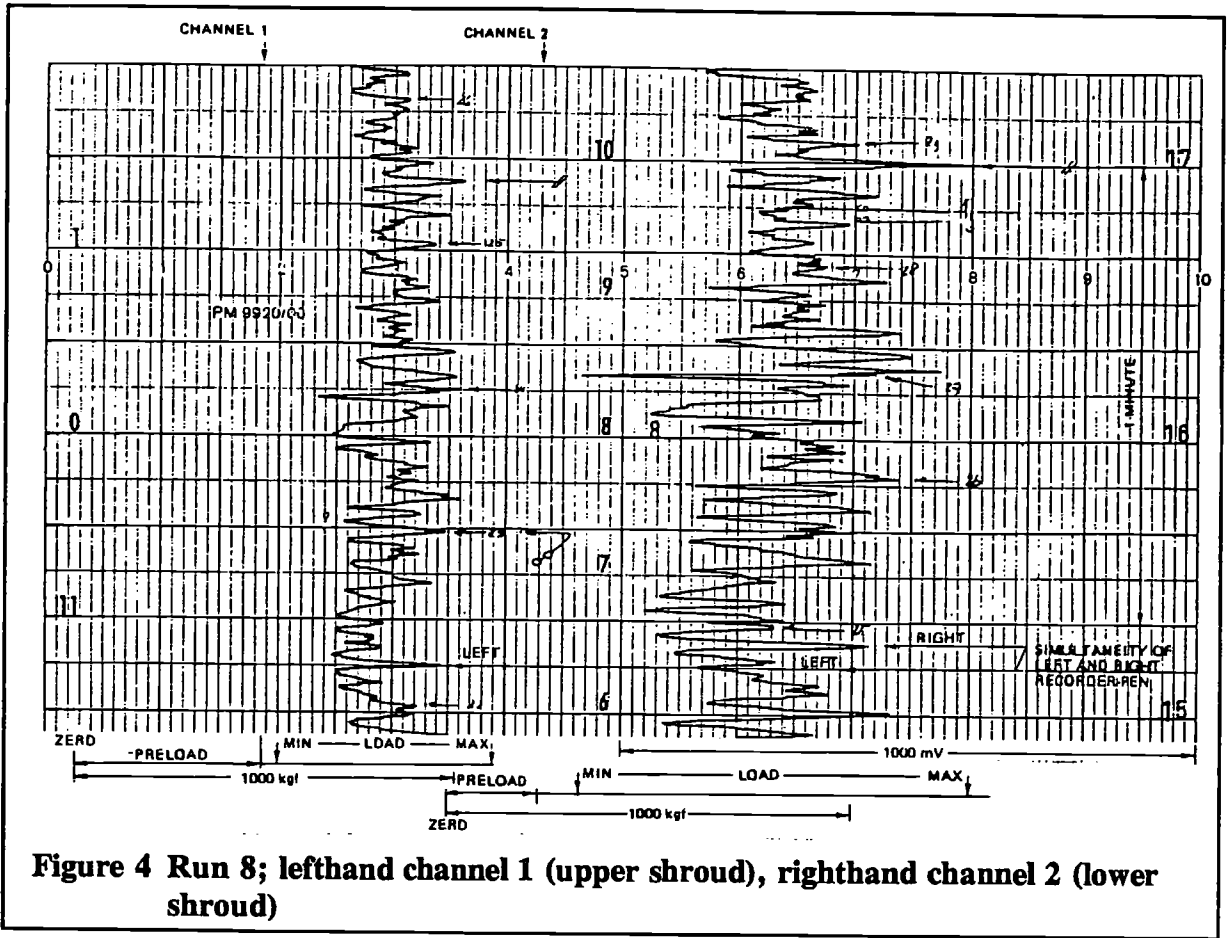


Figure 4 Run 8; lefthand channel 1 (upper shroud), righthand channel 2 (lower shroud)

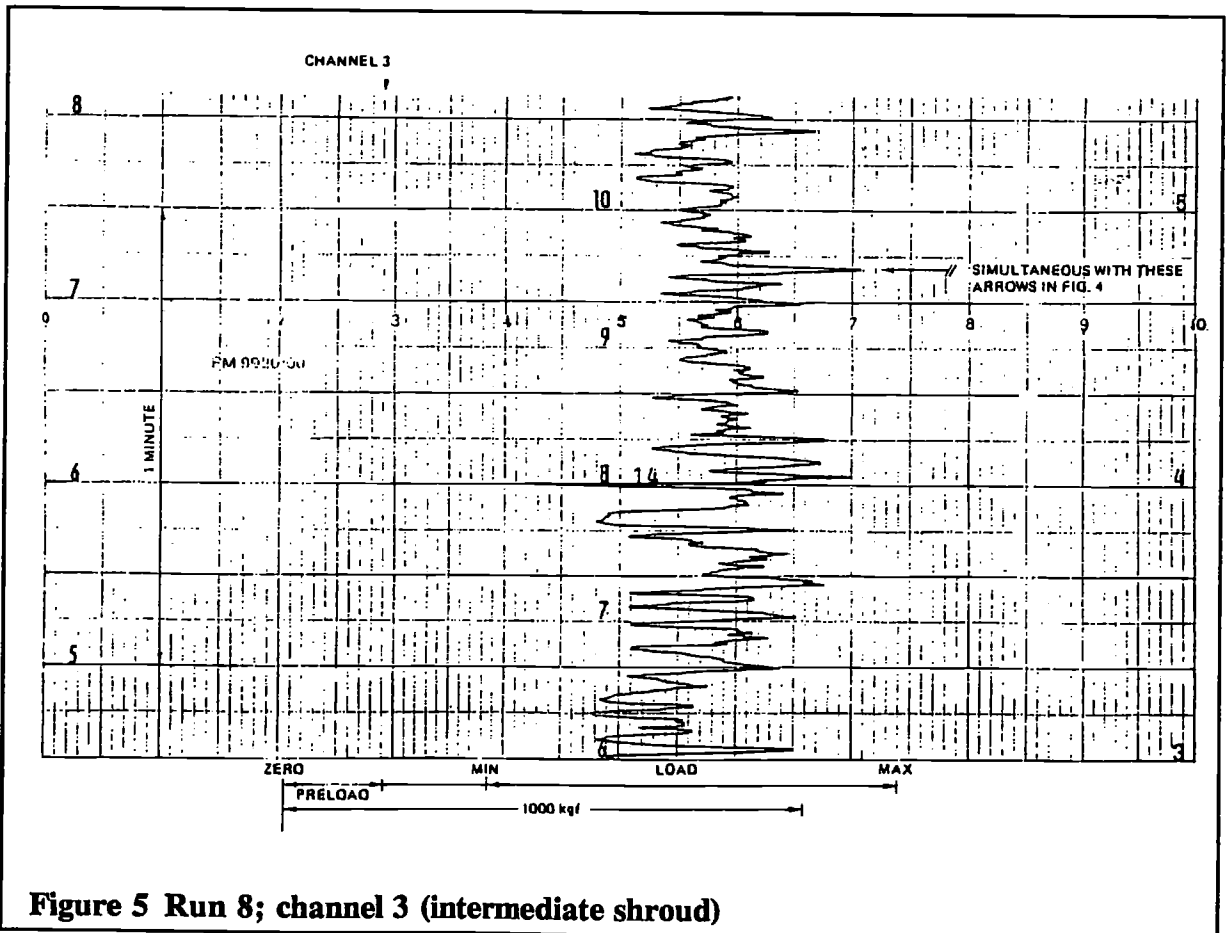
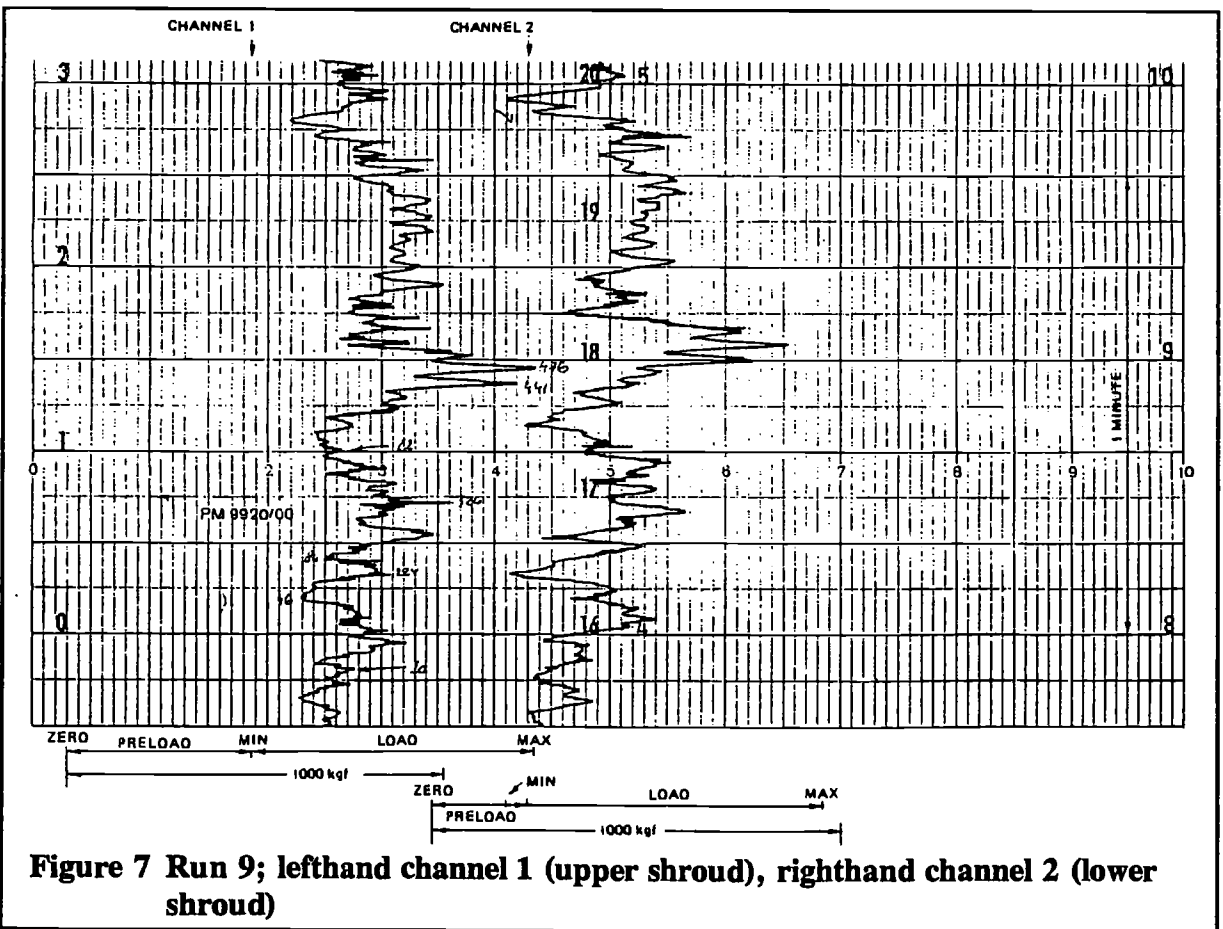
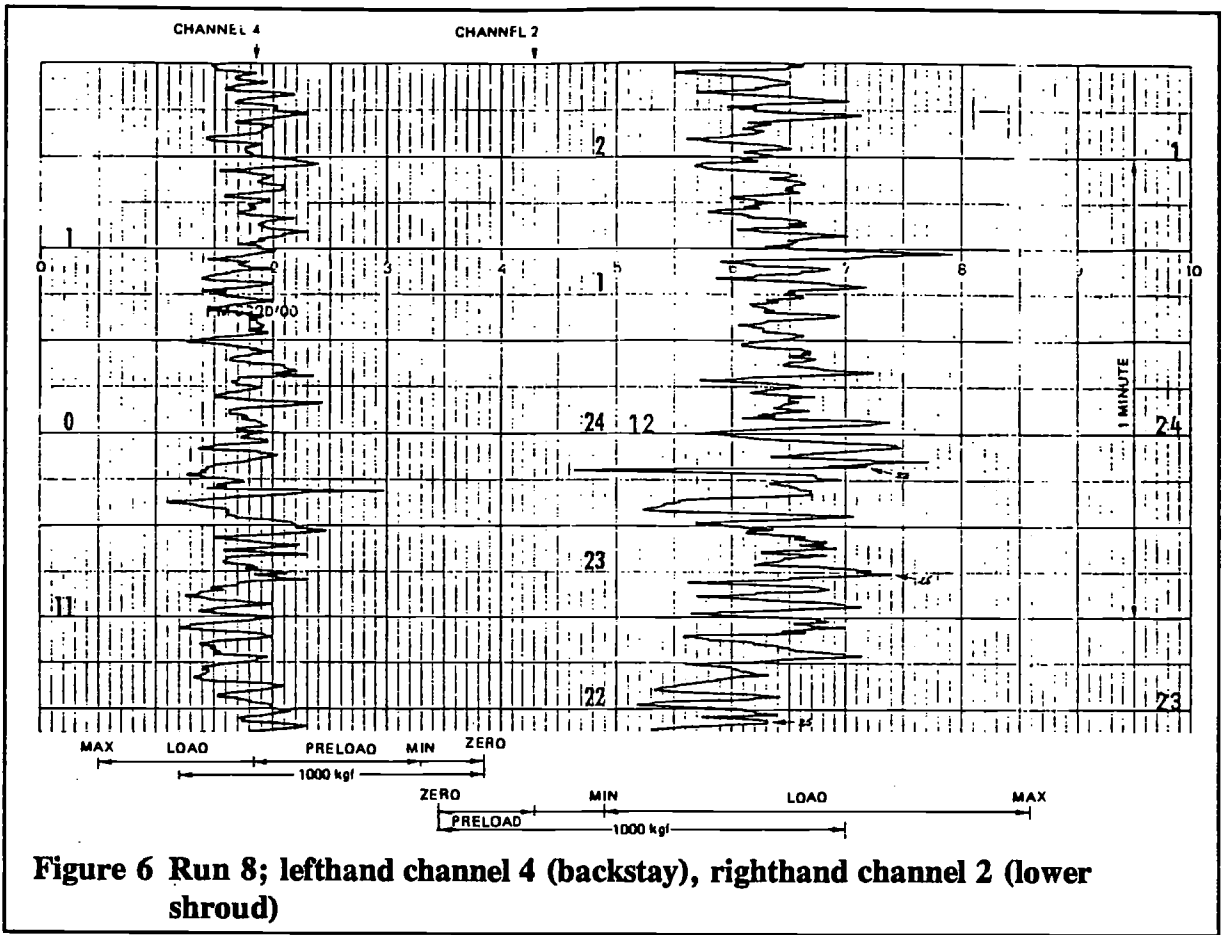


Figure 5 Run 8; channel 3 (intermediate shroud)



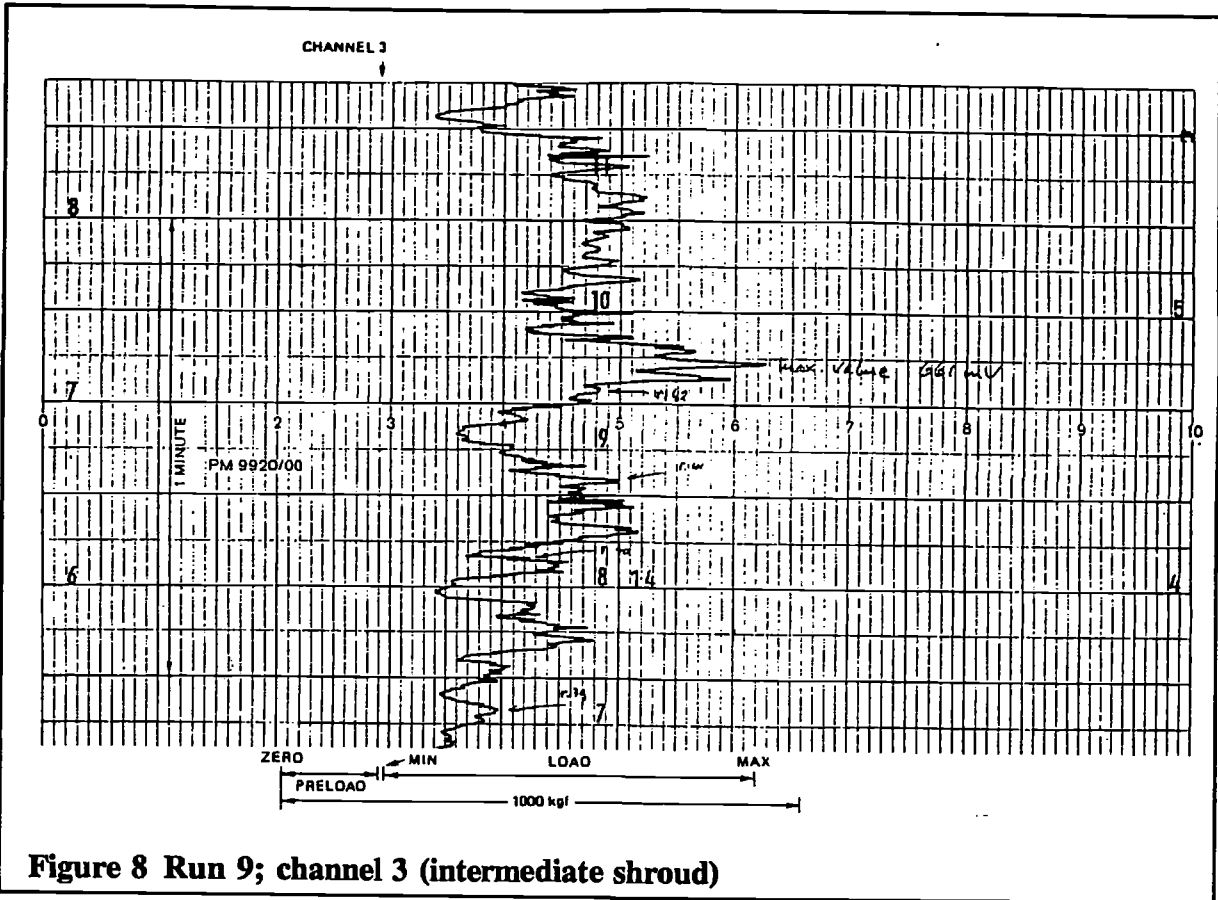


Figure 8 Run 9; channel 3 (intermediate shroud)

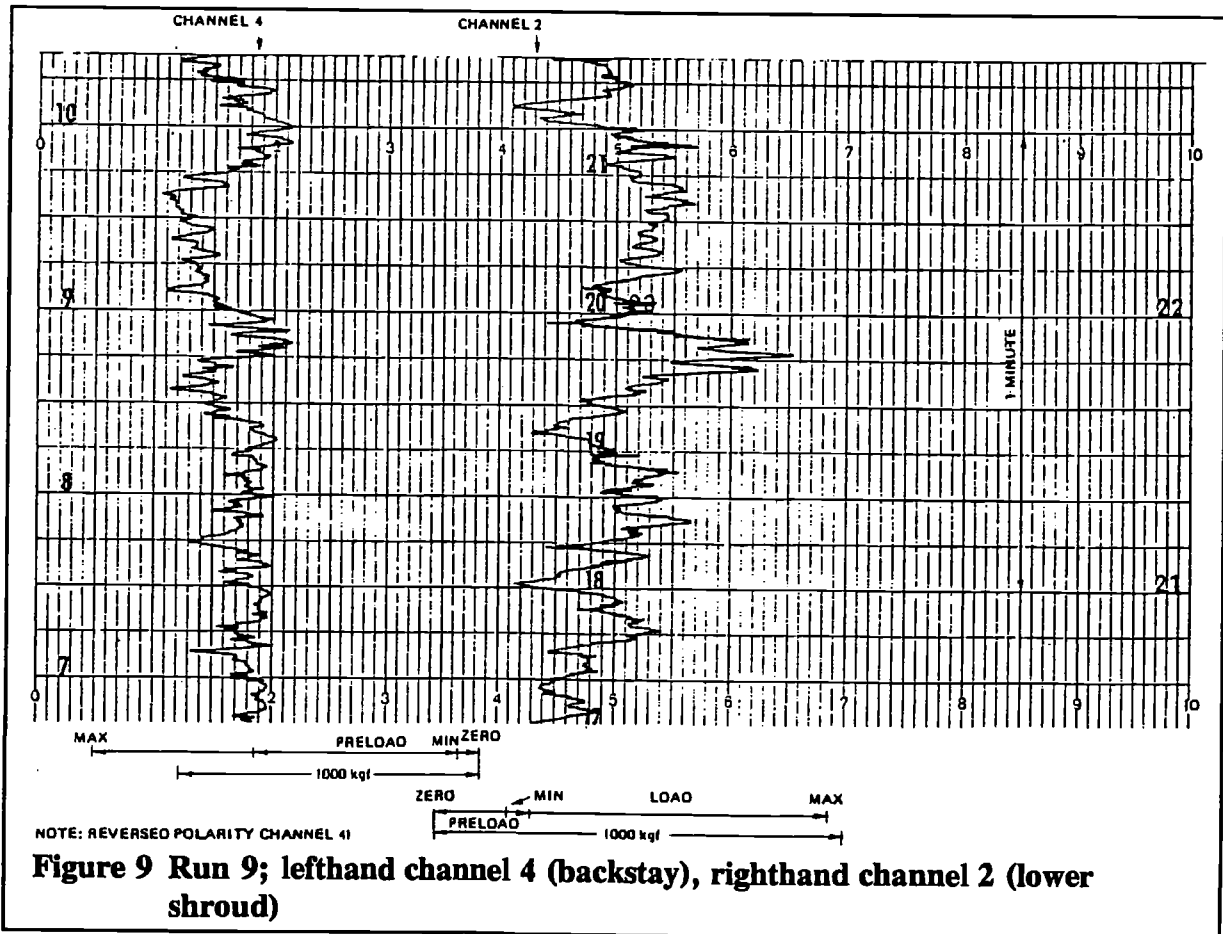
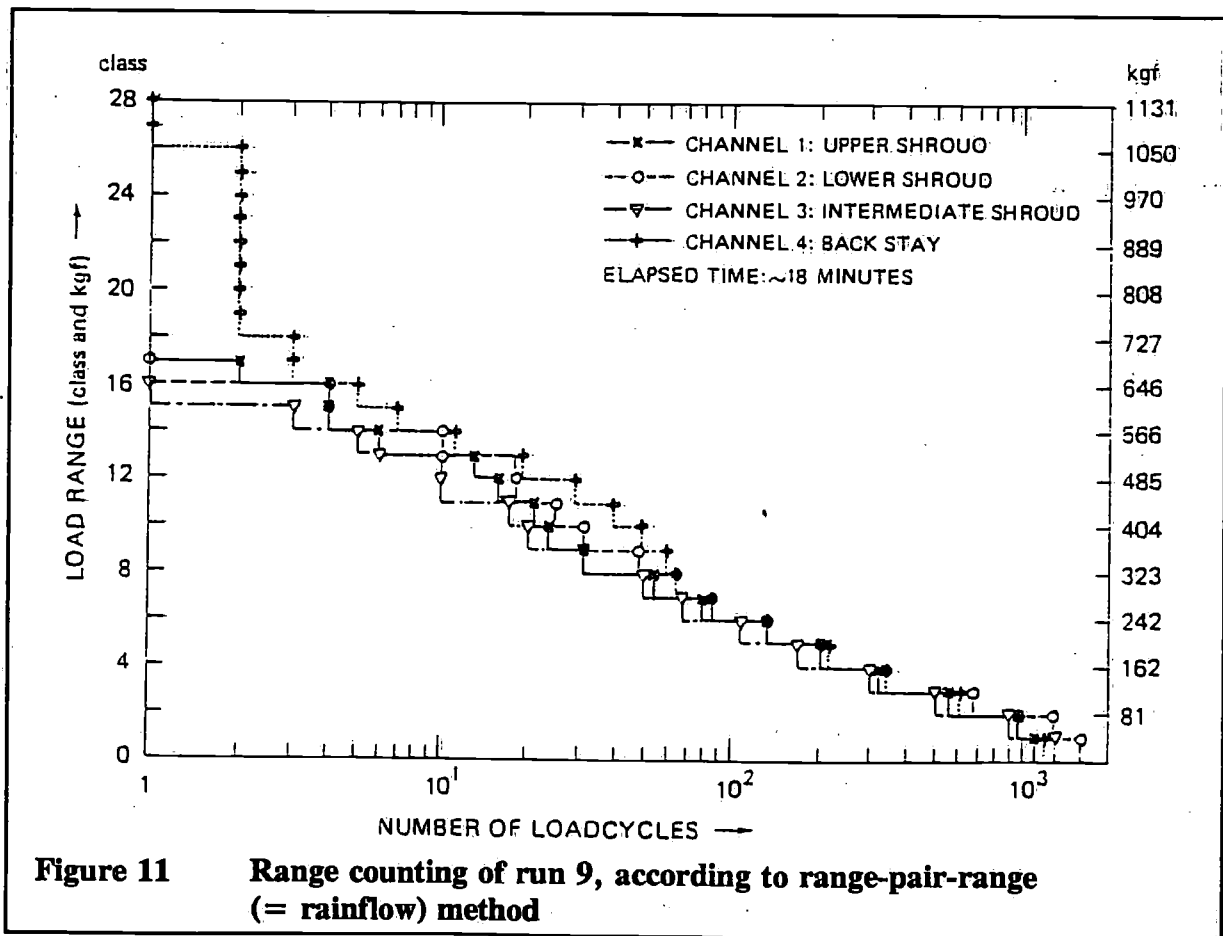
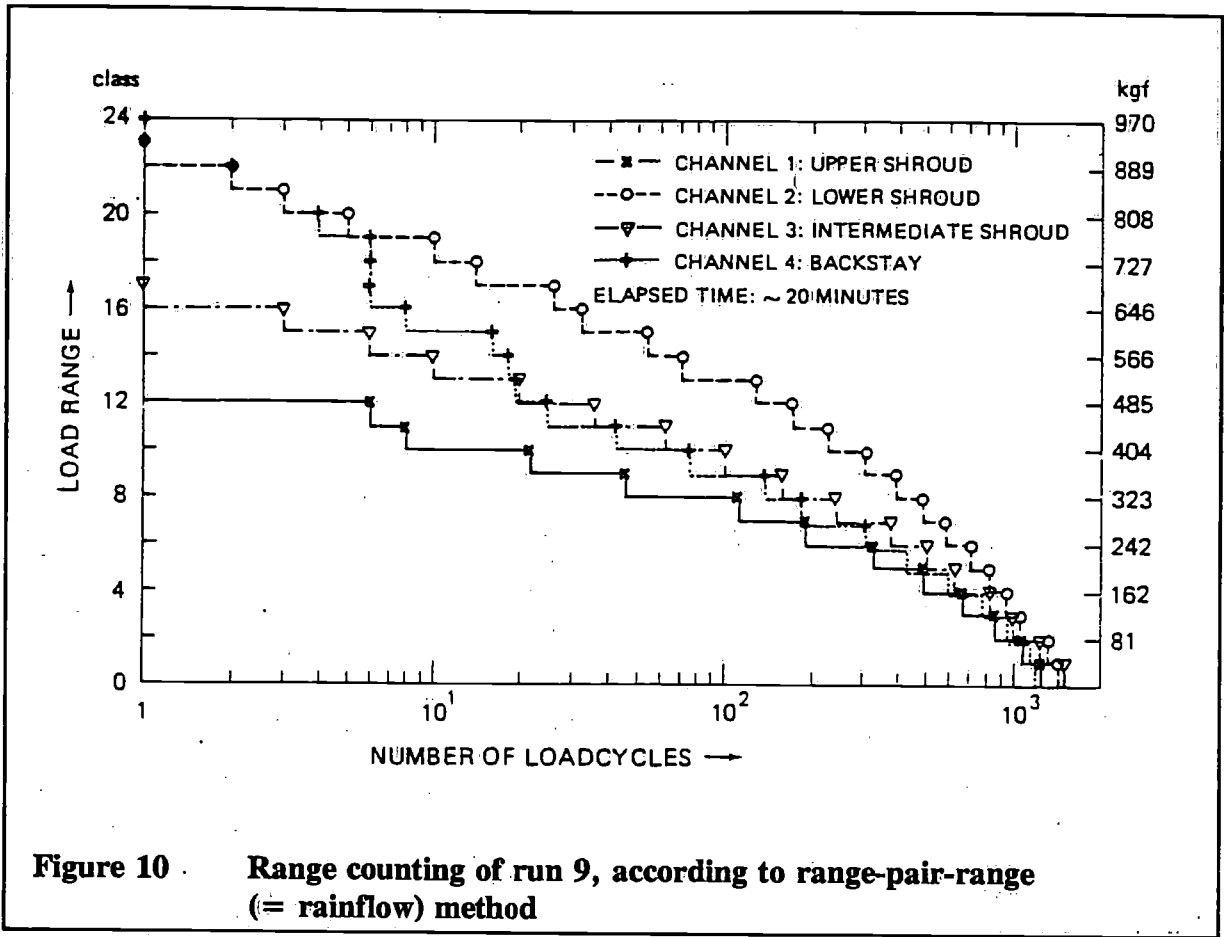
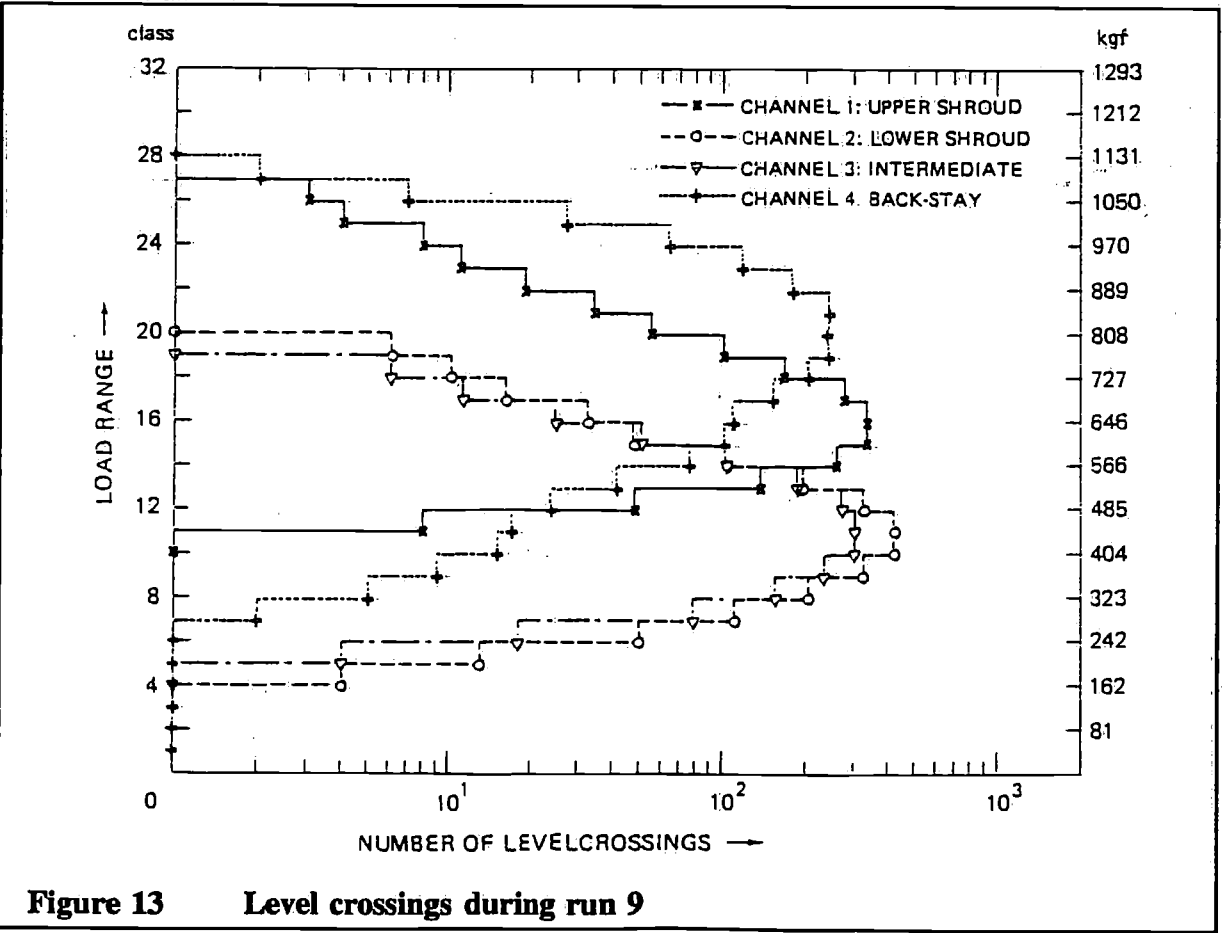
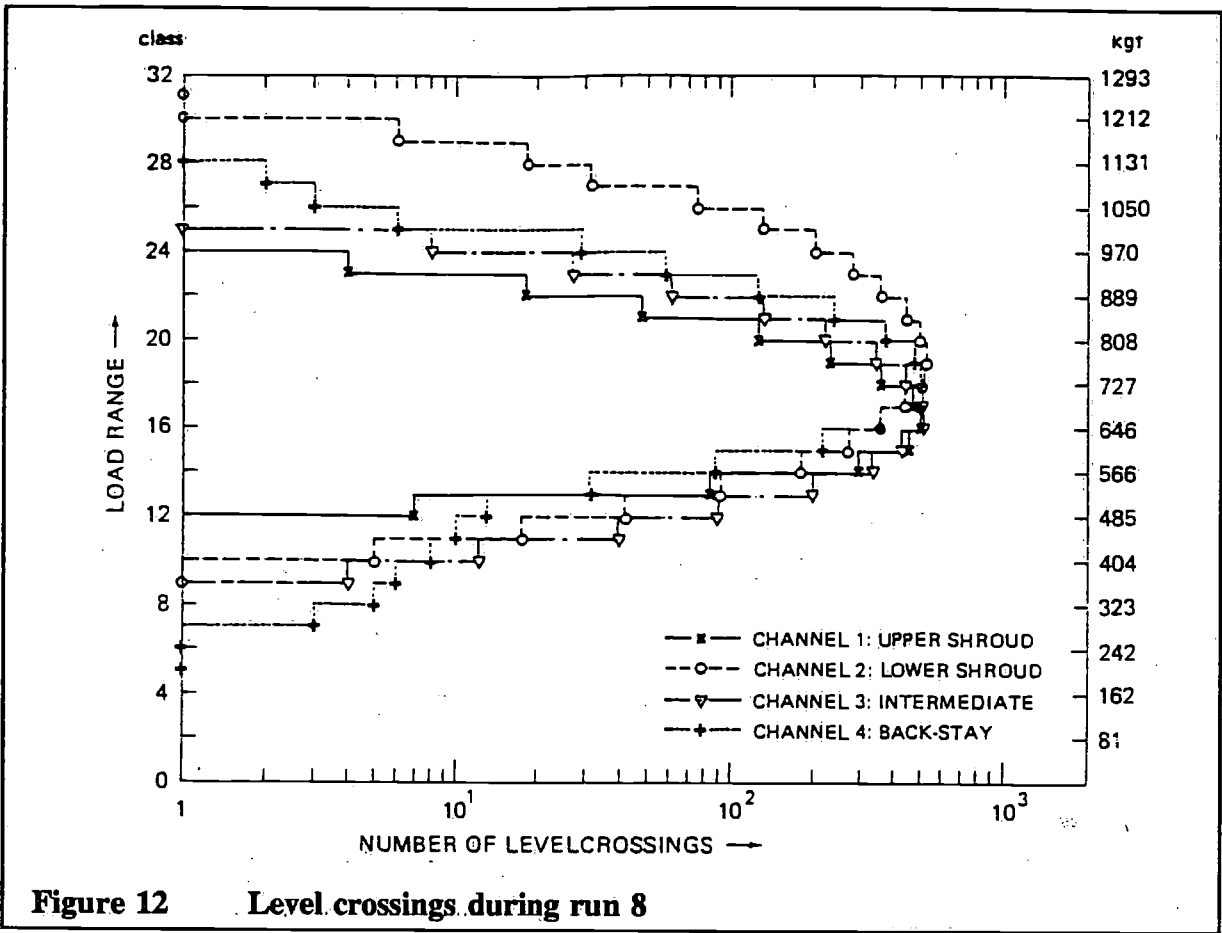


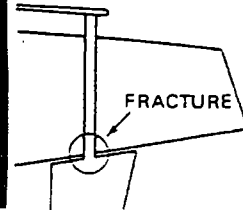
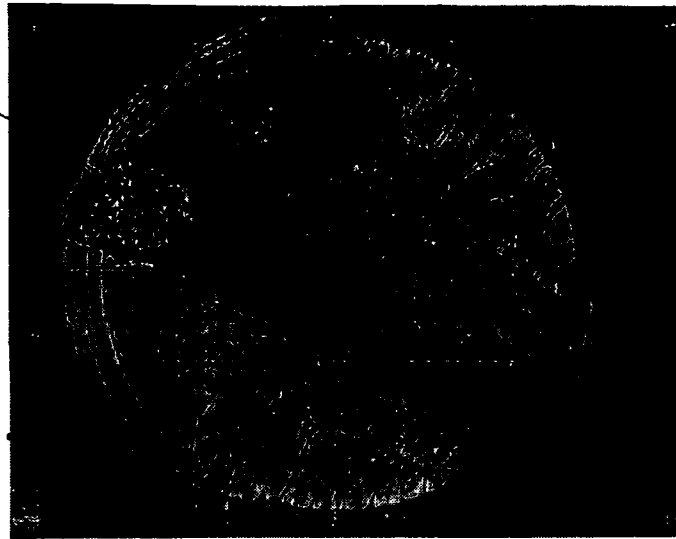
Figure 9 Run 9; lefthand channel 4 (backstay), righthand channel 2 (lower shroud)





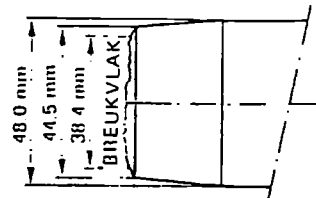
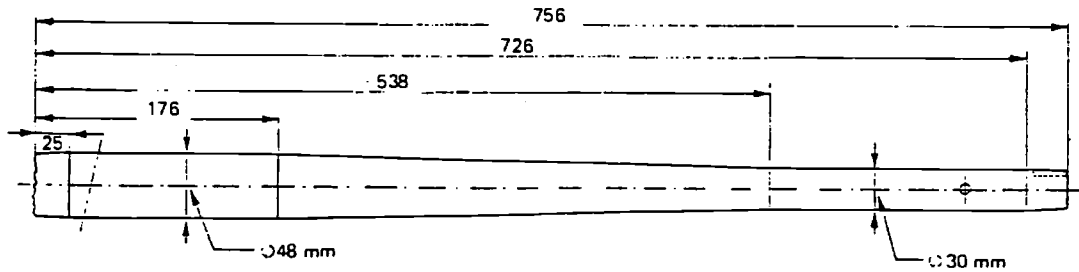
LATERAL PLANE
OF RUDDER STOCK

RESIDUAL
FRACTURE
SURFACE



OBSERVATIONS OF FRACTURE SURFACE OF FIGURE 14

- MANY RADIAL STEPS INDICATE NUMEROUS CRACK ORIGINS PROVOKED BY SHARP TURNING GROOVES IN RUDDERSTOCK. ($K_t \approx 2.6$ AT LEAST)
- BENDING FORCES ARE MAINLY RESPONSABLE FOR THE START AND THE PROPAGATION OF THE FRACTURE. TORSION SEEMS TO BE LESS IMPORTANT.
- THE RESIDUAL FRACTURE SURFACE IS EXTREMELY SMALL AS COMPARED WITH TOTAL SURFACE AREA.
- FROM THE NUMBER OF STRIATIONS IT IS NEARLY POSSIBLE TO ESTABLISH WHEN THE CRACKS STARTED. A CONSERVATIVE COUNT SEEMS TO BE AT LEAST 20 TRIPS.
- REMEDY: PREVENT SHARP NOTCHES BY THE APPLICATION OF A RADIUS > 5 mm. PREVENT TURNING GROOVES DENTS AND SCRATCHES. POLISH CRITICAL AREA AND, EVENTUAL, APPLY SHOT PEENING TO INTRODUCE INTERNAL COMPRESSIVE STRESSES.



PART OF BROKEN RUDDERSTOCK
WITH FRACTURE

Figure 14 Fatigue fracture of (spade) rudder-stock $\phi 45$ mm

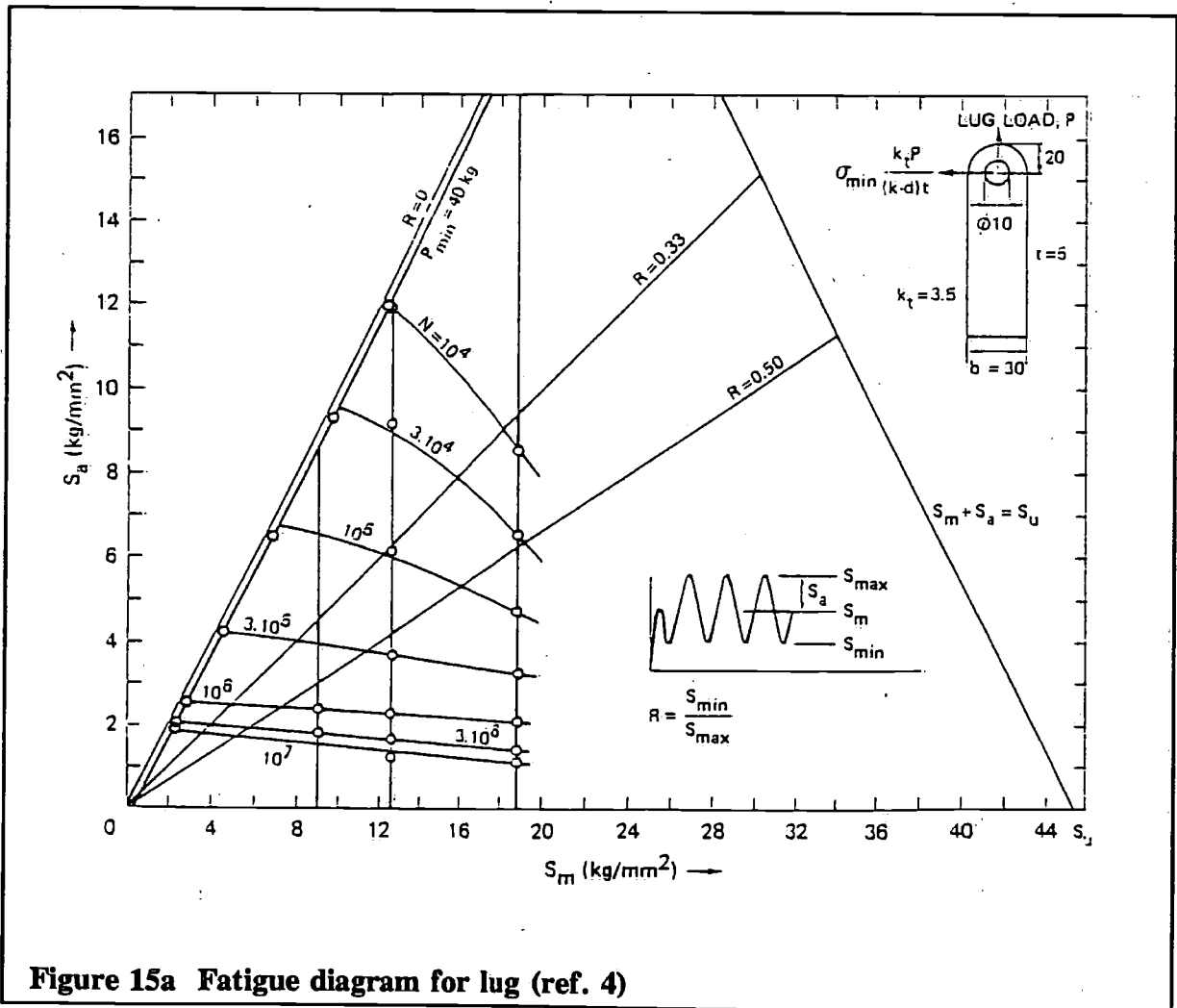
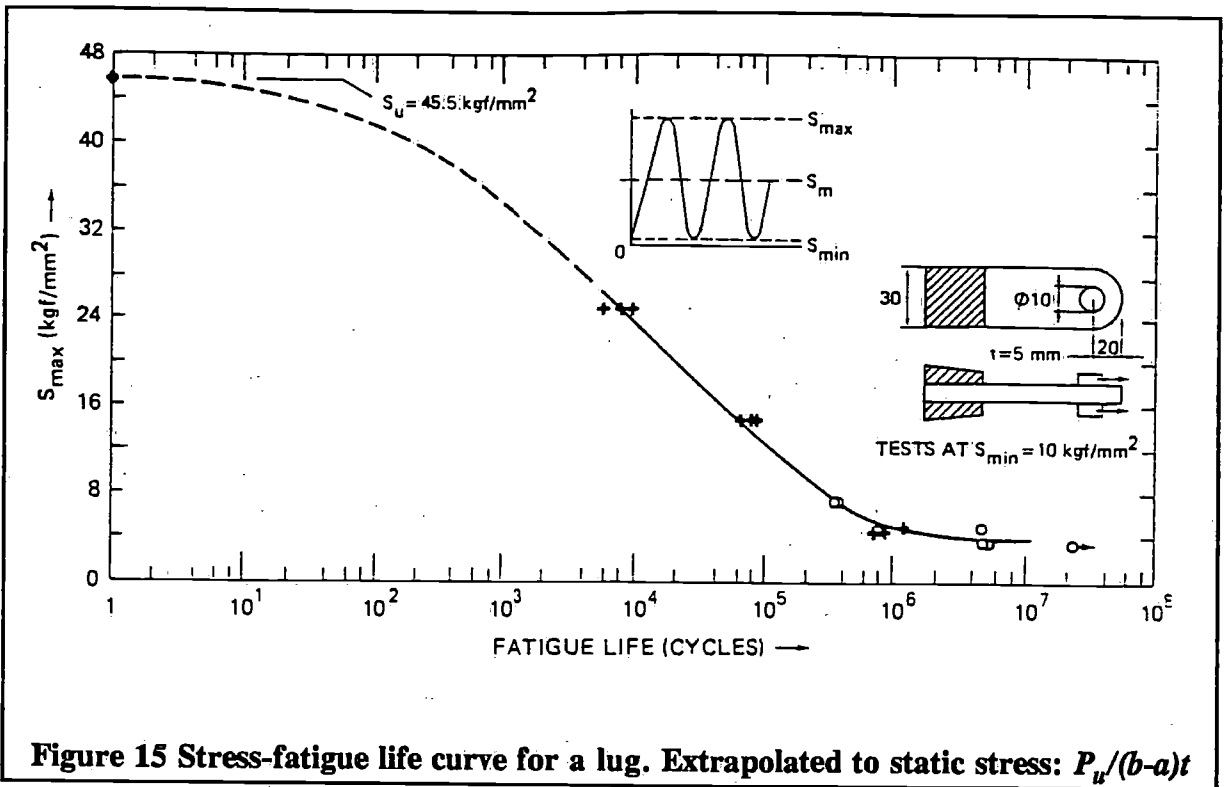




Figure 16 Severe fretting damage in a lug with an expanded hole loaded for 66 million cycles at $S_a = 8 \text{ kg/mm}^2$

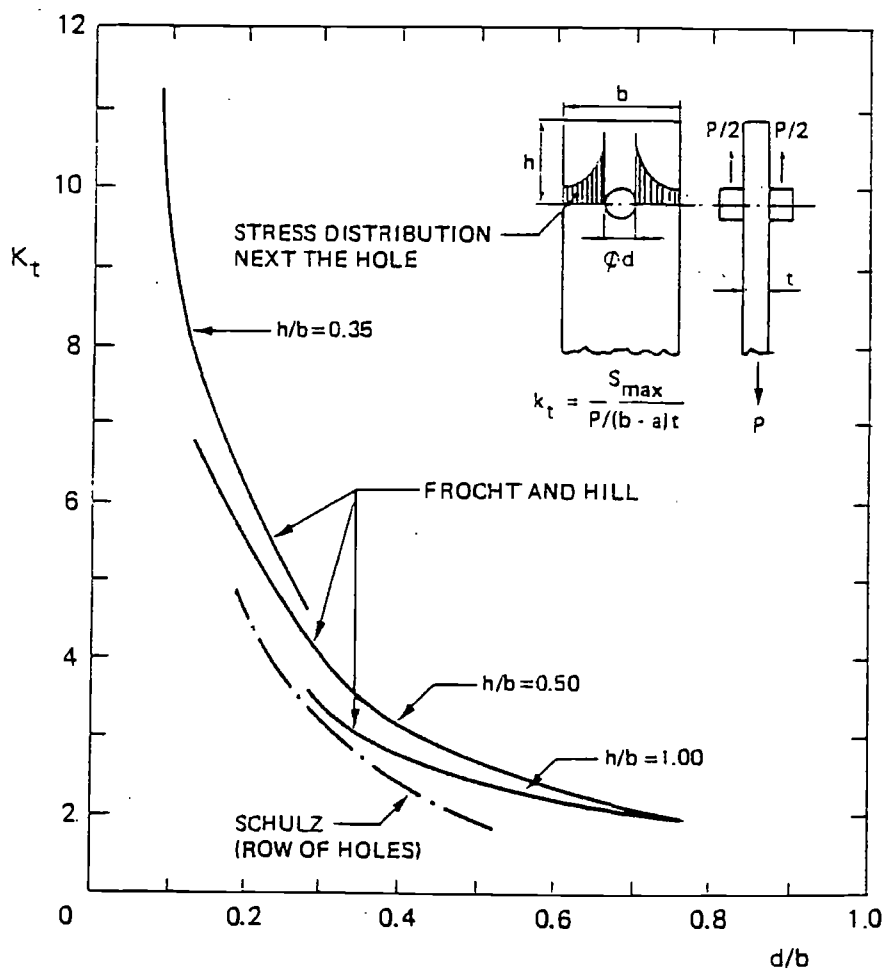


Figure 17 Theoretical stress concentration factor for lugs with a square head according to measurements of Frocht and Hill

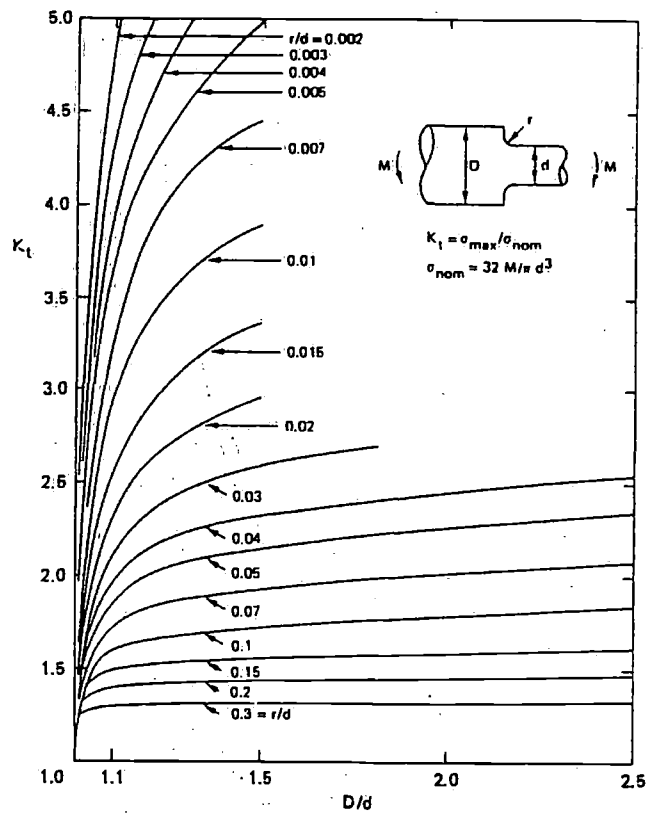


Figure 18a Stepped round bar with shoulder fillet in bending (see Figure 14 for example)

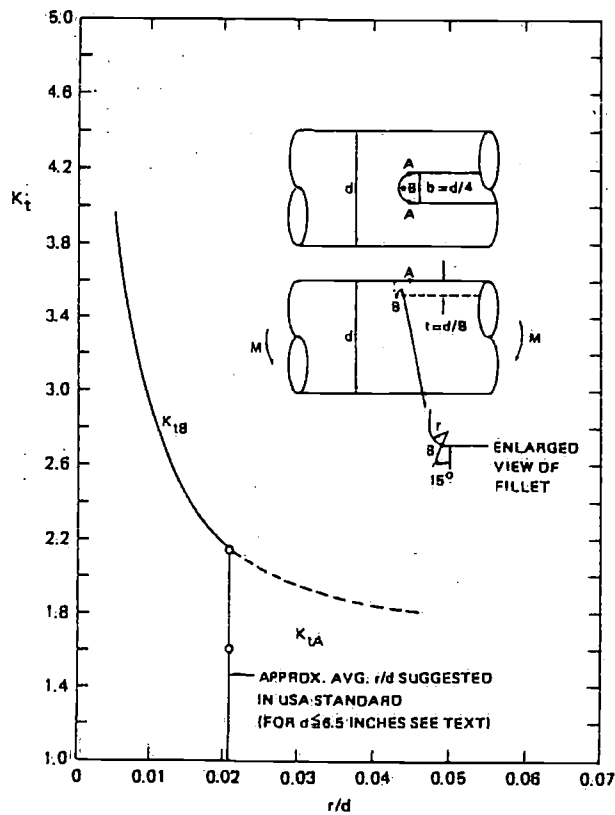
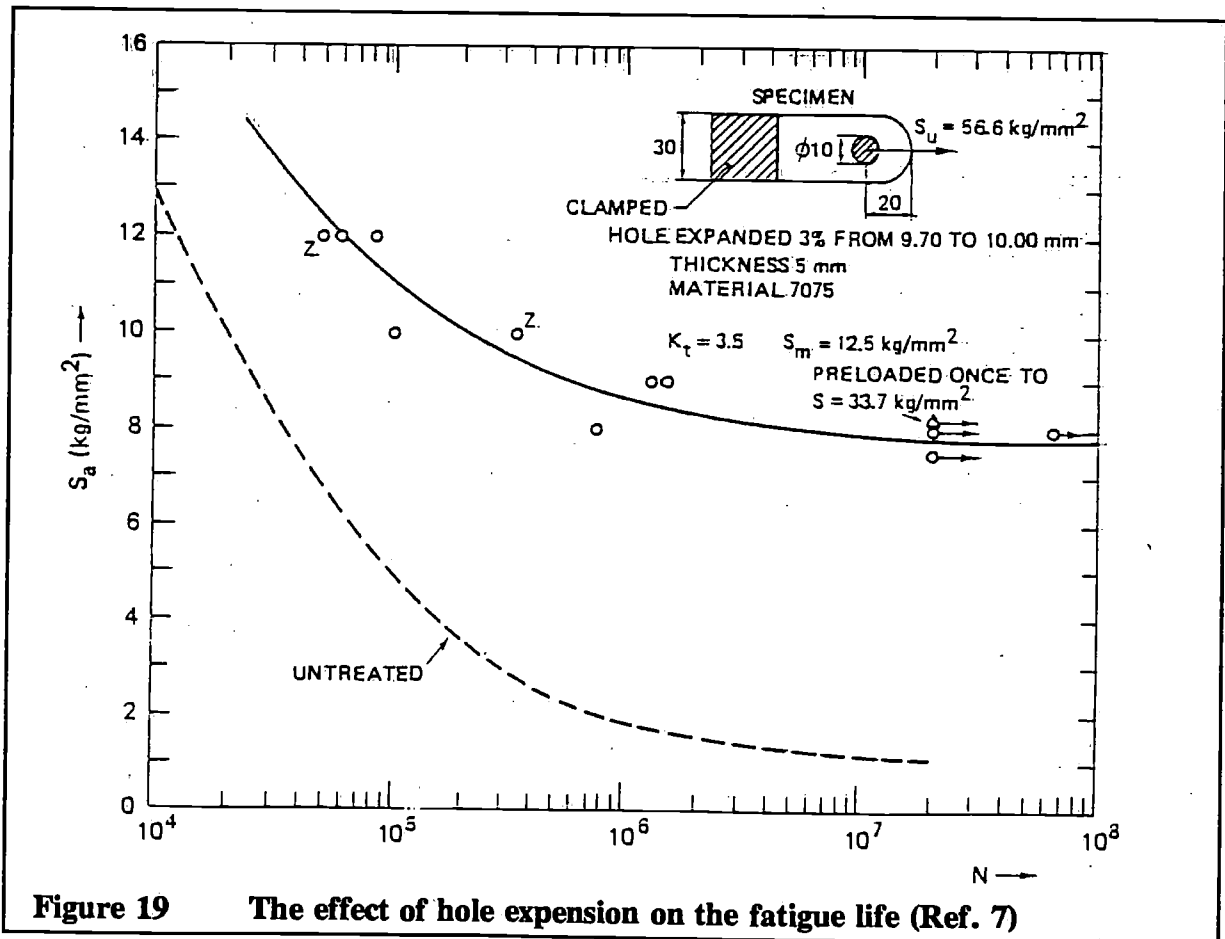
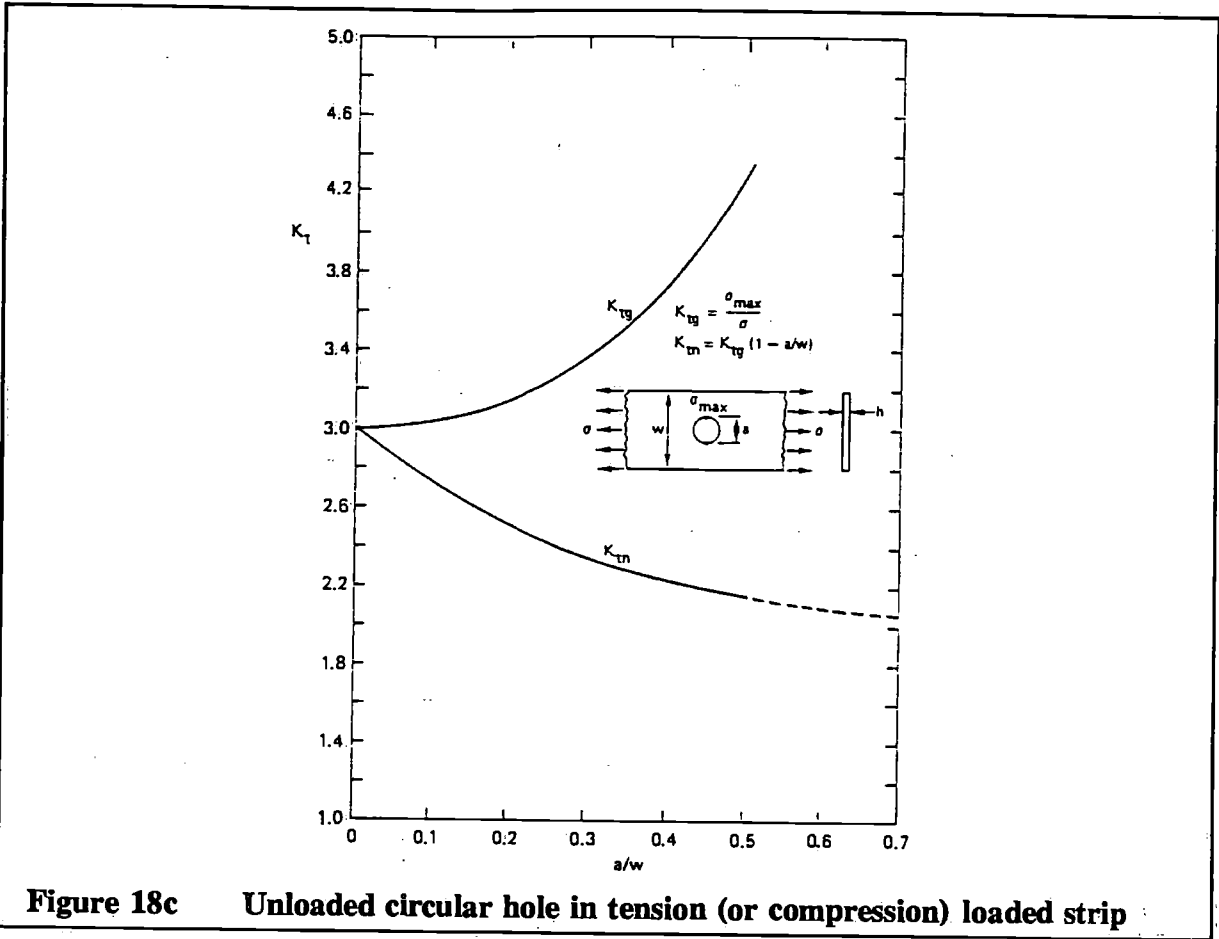


Figure 18b Shaft with semi-circular keyseat in bending



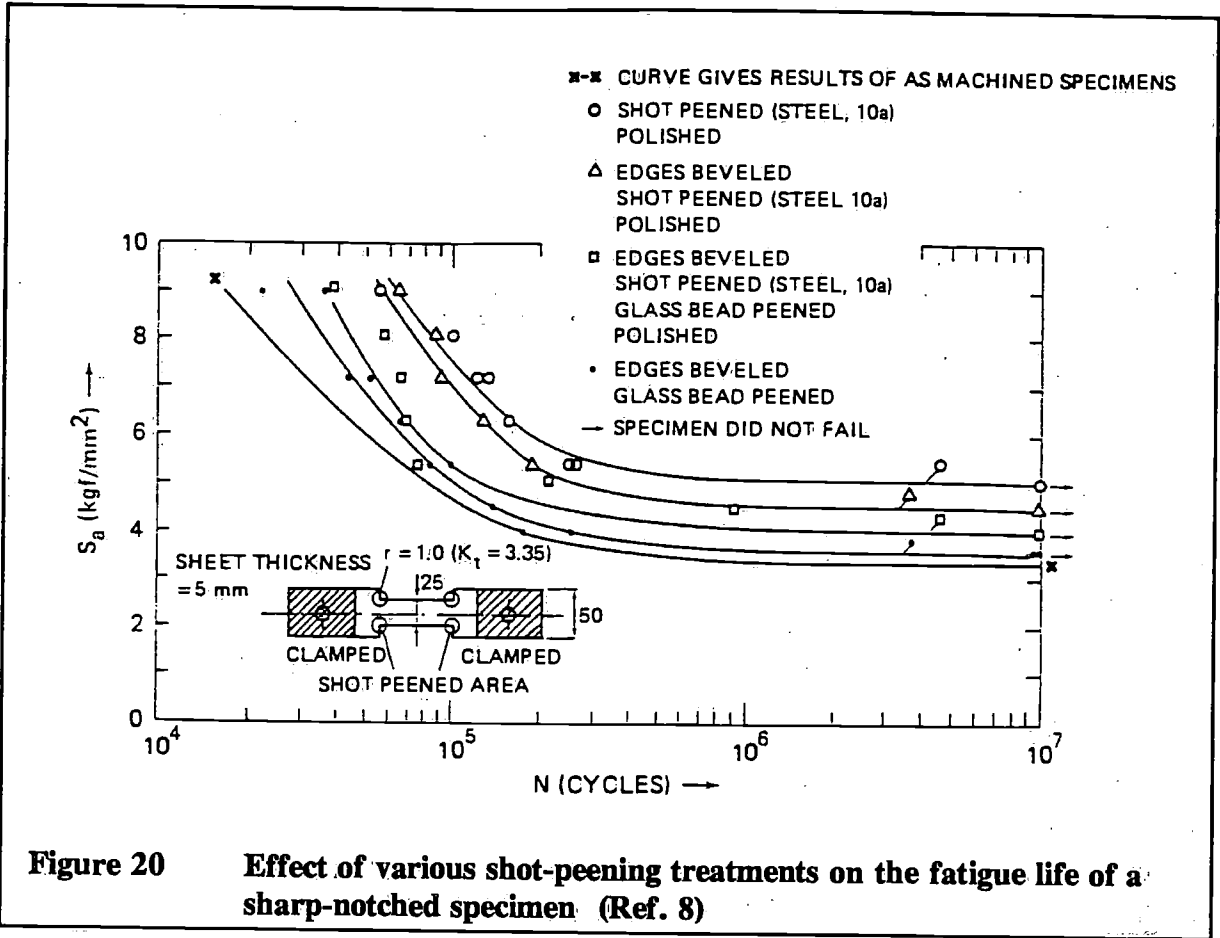


Figure 20 Effect of various shot-peening treatments on the fatigue life of a sharp-notched specimen (Ref. 8)

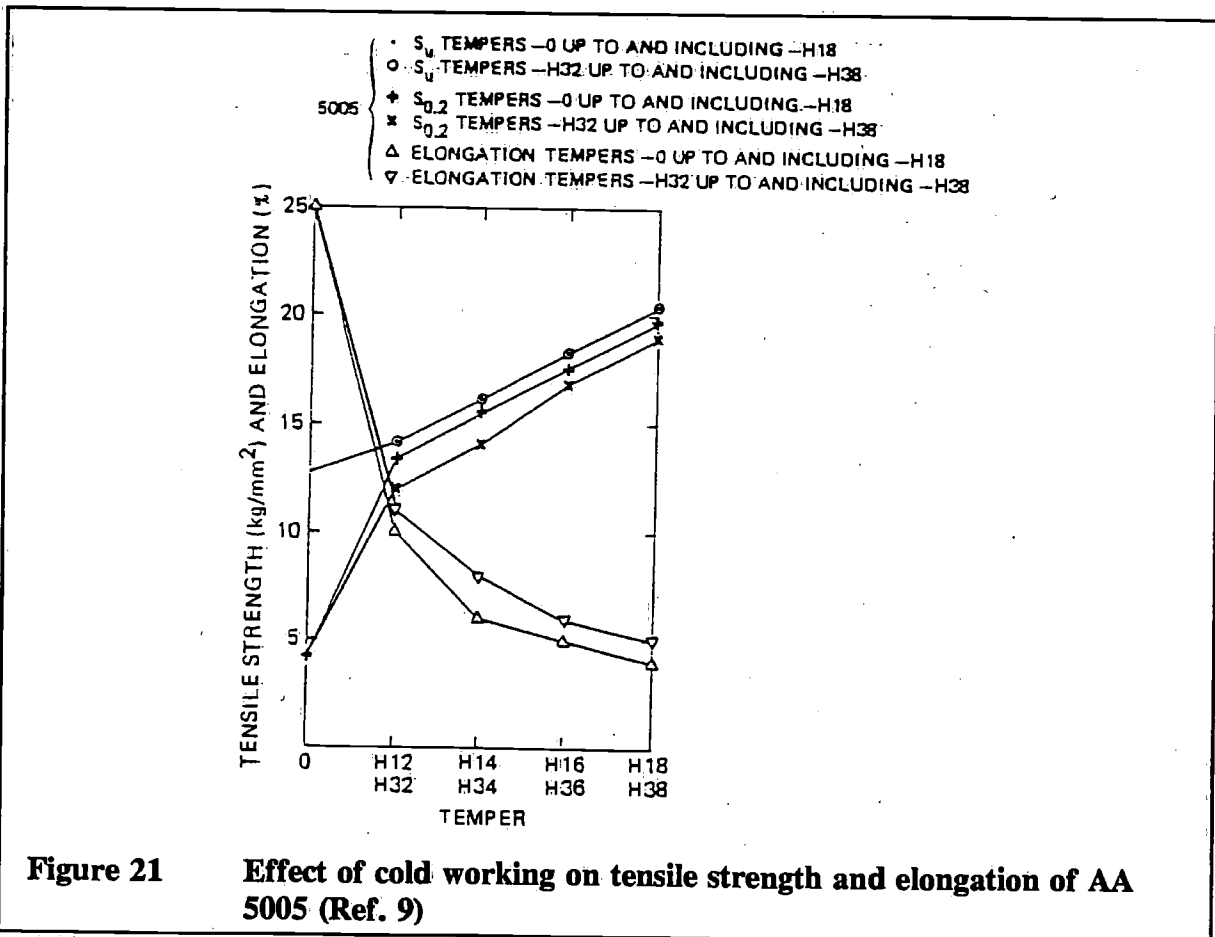


Figure 21 Effect of cold working on tensile strength and elongation of AA 5005 (Ref. 9)

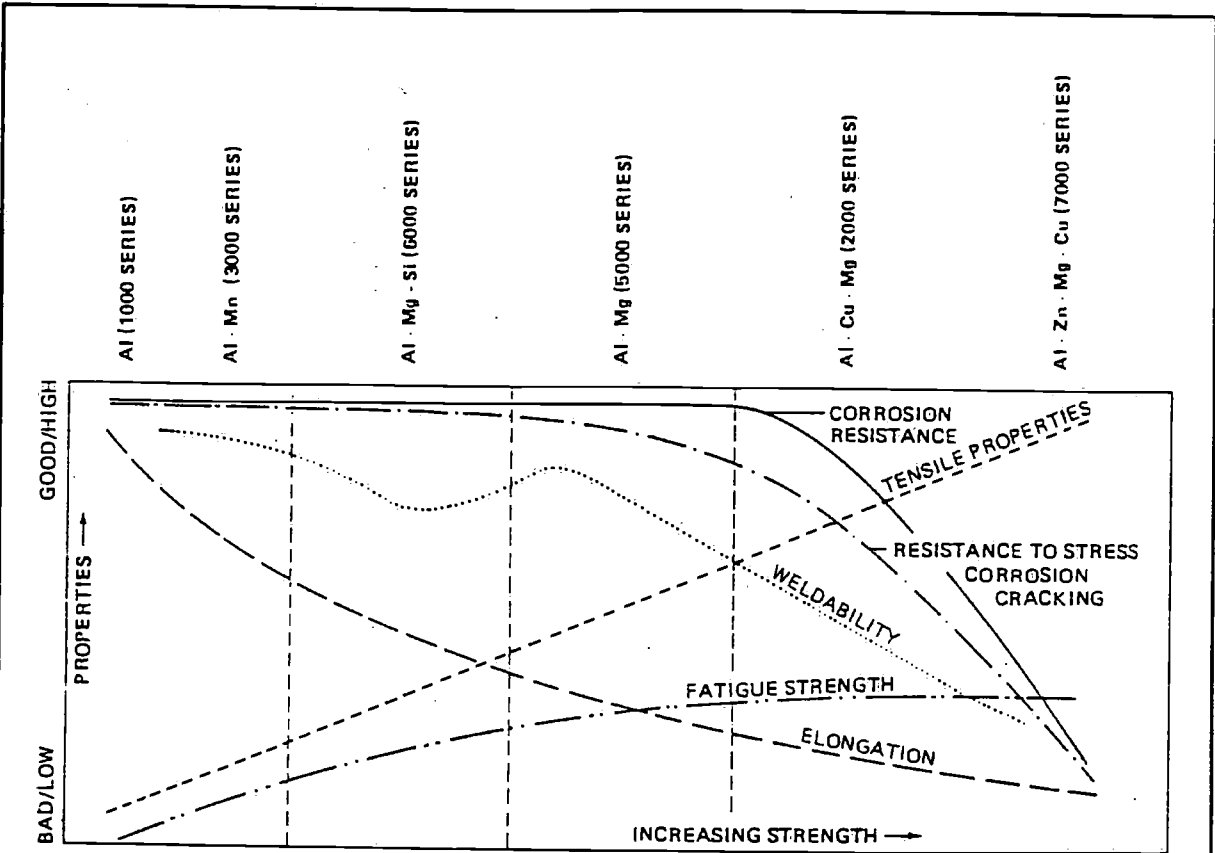


Figure 22 Review of wrought aluminium alloys and their properties (Ref. 10)

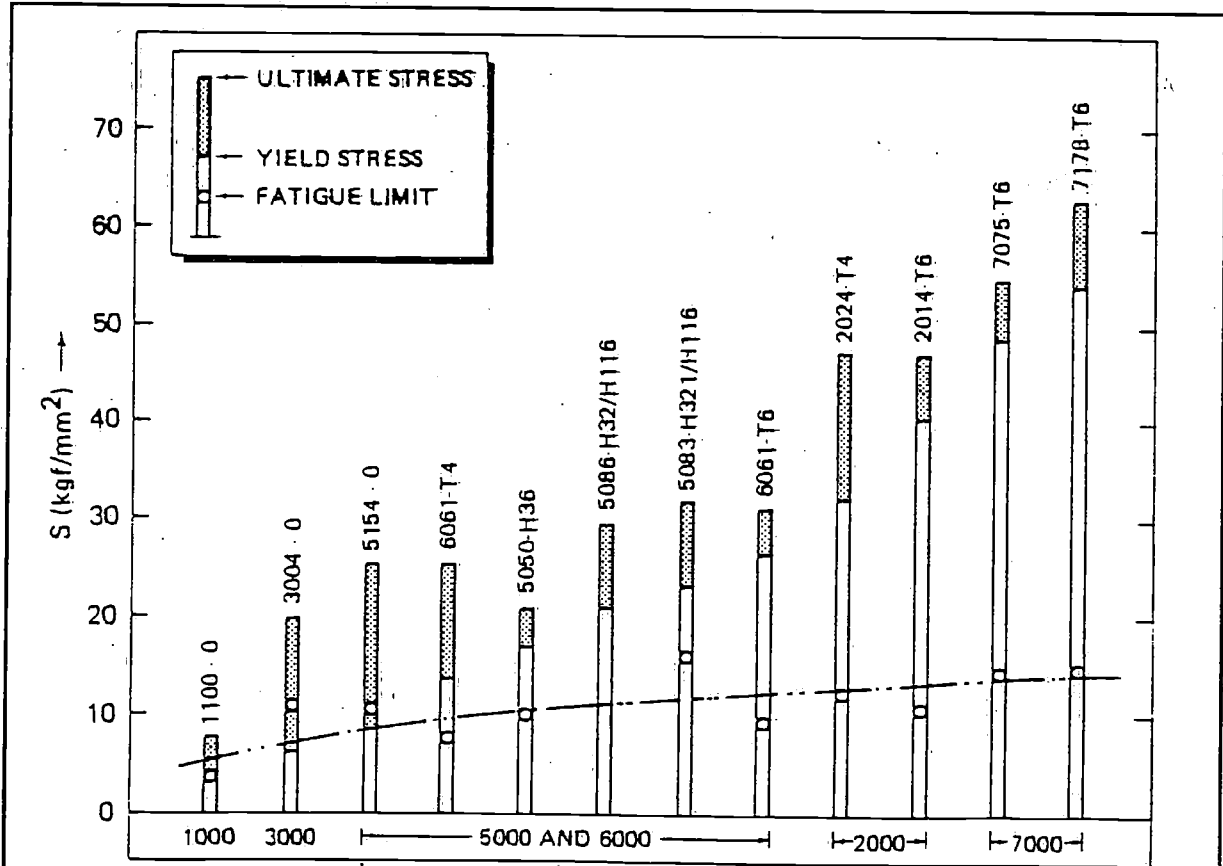
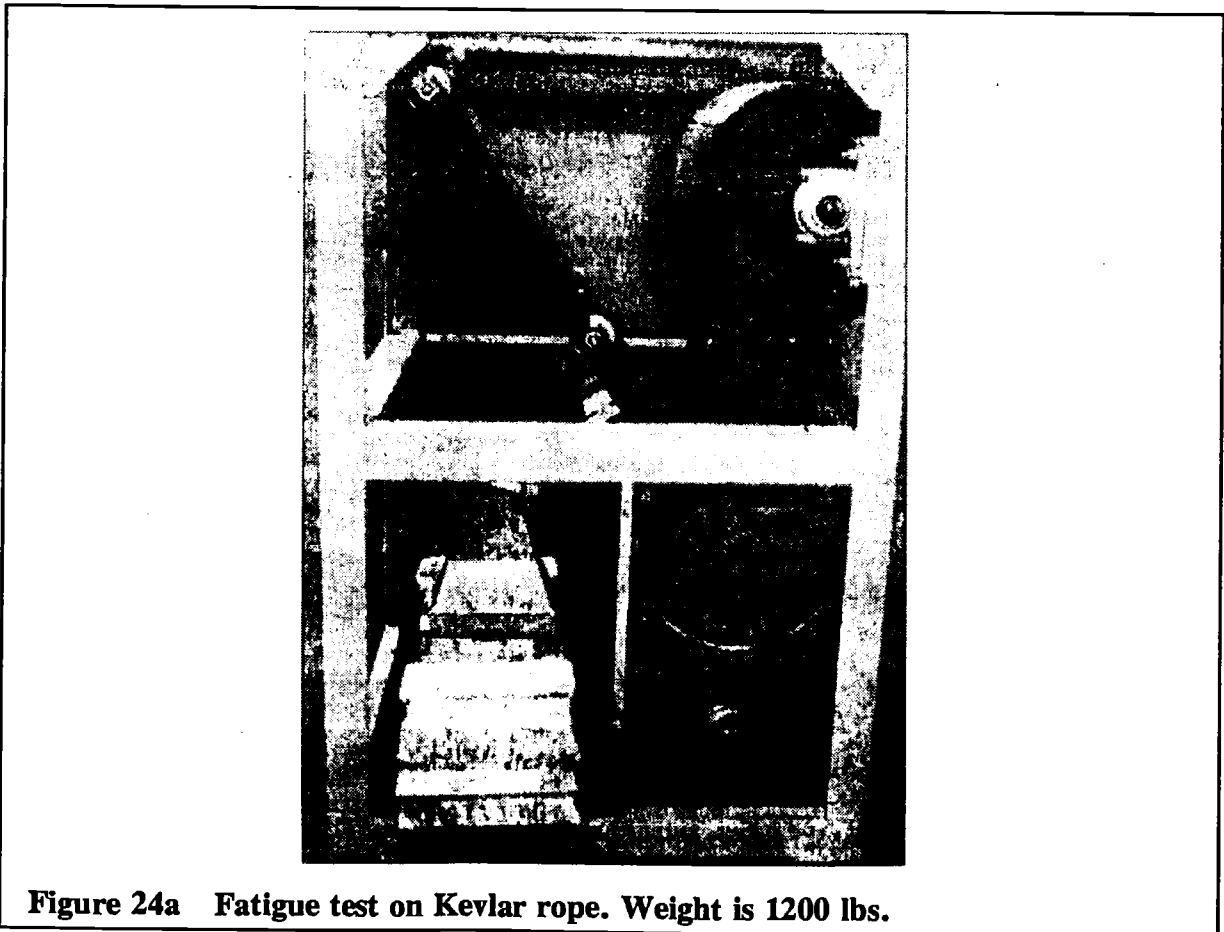
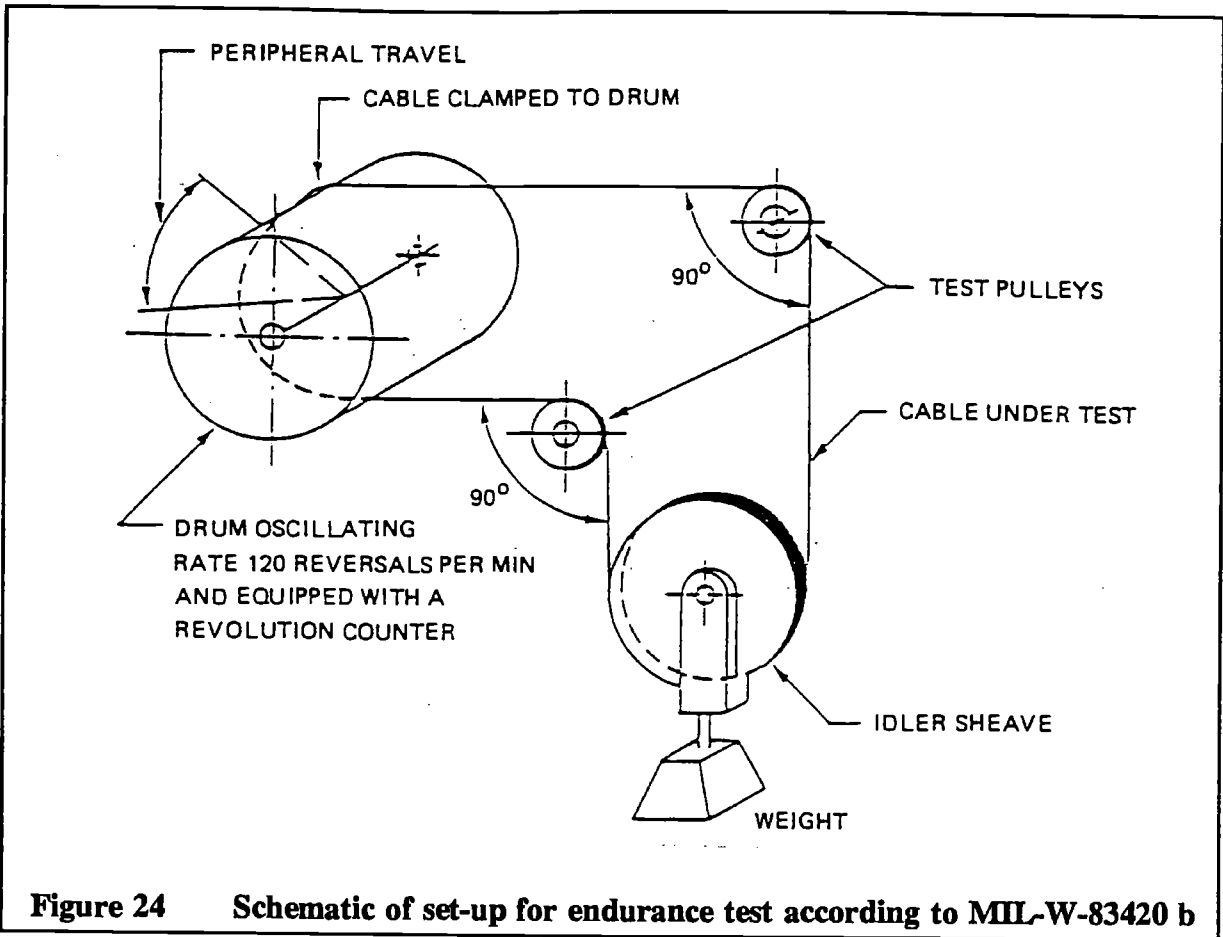


Figure 23 Tensile data of some wrought aluminium alloys (Ref. 10)



The design of offshore cruising yachts

by **D. Koopmans**

Naval Architect

More and more people are dreaming of sailing away or around. Because it is often difficult to find the right yacht in the standard types some of them decide to let the boat be designed and built to their personal specifications and ideas.

This lecture is an attempt to show the possibilities and the restrictions which the designer is confronted with when designing a specific cruiser.

Features like how to inform the client with the right arguments, the relations between design-factors, the use of data from tank tests, the influence of windage of hull and rig in the higher windspeeds and the stability in extreme circumstances are discussed.

- 1 Introduction
- 2 General:
 - Philosophy of yacht design
 - The appearance of the yacht
 - The influence of the current rating rules\
 - A cruiser has to be all-round
- 3 The hull
- 4 Balance
- 5 The rig
- 6 The influence of wind forces on rig and hull
- 7 Stability in extreme circumstances

1 Introduction

The author is an independent naval architect since 1963. He made the choice of this profession because he had an obsession for everything about boating and the sea. As a yachtsman he progressed from sailing on the inland lakes to racing on the IJsselmeer and later the international races in Europe. Some years ago he stopped racing because he felt it impossible to combine racing any longer with the intensive cruising with his family. In his career as a yacht designer he has followed more or less the same line without specialising too much at any time.

In the discussion I shall restrict myself as much as possible to the design of specials, that is to say, especially designed one off cruising yachts. Nevertheless an important part of my thoughts upon the subject are related to those put into practise when designing yachts for serie-production, mostly so called "cruiser-racers", nearly always built in fibre-glass.

Whilst I am sure that the use of multihulls, particularly in the case of the bigger sizes can be of interest in this theme, I am not going to discuss multihulls simply because I don't have enough personal experience on that particular subject.

2 General

More and more people are looking for a sailing yacht for extended cruising. The means they have to live on board for long periods of time in reasonable comfort.

Often they cannot find just the right boat within the market of existing standard boats because those boats do not entirely satisfy the needs of the blue water sailor in general concept and construction.

So people come to the decision to let that very personal "dreamboat" be designed and built as a "one-off". This means that they mostly start with a visit to a professional yacht designer. In general the commissioner will select a designer who attracts him because of his style, his personal approach and his experience. These points have a very important bearing, firstly because of the pré-selection which takes place, and secondly because of the need of a good relationship during the designing and eventually building stage and thereafter.

The first conversation between designer and commissioner is very important. On the one hand there is a man or a couple with a fairly good outlined idea of the new boat and on the other hand the designer who often has to start by bringing the ideas down to realistic levels. Next the designer makes a pré-design and this serves as a starting point for further stages.

In most cases the pré-design also serves to get an indication about the building price.

Philosophy of yacht design

For most people the starting point for their new boat is based on the experiences with the previous one. Shortcomings of the old boat often become the guide to the new one.

It is up to the designer to make clear that the new boat has to suit the requirements and that the requirements have to be formulated with the eye to the expected use and sailing area.

I once read the report of a man who designed for himself a little steel yacht. His design philosophy was that a seagoing boat cannot be strong enough. The result was not only an immensely strong but also an extremely heavy boat!

When the owner recounted the first sailing experiences he remarked: "Fortunately the boat was so strongly constructed, the sea washed right over the cabin top without causing any damage!"

Time after time the designer has to explain that designing a boat is, just like a car or a plane, always a compromise between strength and, in our case, sailing qualities.

Sailing people are often deeply interested in their sport.

They read books about sailing and designing and they talk a lot about theories.

Unfortunately those books were written some time ago referring to experiences with still older yachts. Opinions about seaworthiness and seakindness are often based on the restricted constructive possibilities. The beautiful and often admired curve between hull and long keel was not chosen for better behaviour in a seaway, on the contrary, it was at one time the only way to reach a low centre of gravity without losing too much strength and stiffness.

Nowadays, if someone chooses to have that shape, it has to be based on other, more rational considerations.

The idea "rational" is, when considering yachts, not so easy to describe. When a very functional designed yacht disfigures some beautiful bay where she is anchored it could be questioned whether the owner is happy with his boat. For a yacht, meant for pleasure, the joy of the owner when looking at his boat is one of her functions.

There are always a number of unknown factors in a design of a sailing yacht. The relation between the factors concerning the behaviour in a seaway is so complex that it cannot entirely be understood or calculated. Experience and feeling are essential for the yacht designer to prevent failures.

Most relations and shapes are, when an experienced designer is drawing a current yacht, more or less automatically good. Slenderness, longitudinal center of buoyancy, place of keel and mast can be fixed by most designers by eye.

Here we see a marked difference between the attitude of designers. One starts drawing and calculates to control and correct what he did, the other, who I fear will win the game in the long run, calculates first before drawing a single line, or even restricts himself to looking at line drawings being produced by the computer.

The appearance of the yacht

I already mentioned the importance of the appearance of a yacht. At this point, apart from the personal style of the designer, the fashion of the moment plays an important role.

It is an art to find the right combination between the intended use and the shape of the boat. For a cruising yacht, which can still be considered as a long lasting product, it is important to strive for a more or less timeless look.

From the overall impression of the yacht it has to be clear what the character of the yacht is. A slow cruiser with a streamlined appearance soon looks like a highly unsuccessful racer! Personally I like to see something of the atmosphere of the great sailing clippers in a modern cruiser.

A cruising yacht must have the appearance of a little ship more than of a big boat.

The influence of current rating rules

In yacht design, as in most other techniques and sports, there is a tendency to look for the ultimate properties.

In our case mostly speed. It is quite understandable for racers and it is advocated by the present rating rule, the I.O.R.

In fact this rule is not only important for actual features of boat and rig, but probably of even more influence for what is not measured by the rule. Very important resistance making features like wetted area and moment of inertia are not in the rule.

It is a pity, in comparison with all the trouble, costs and especially the risks for the crew, that improvement in speed is only marginal, and by no means useful. Absolute speed is useless in races where only speed differences count.

Racing in displacement boats is as ridiculous as races between snails seen from the point of absolute speed!

Nevertheless the pressure on the designers of racing yachts leads to too low safety factors, especially because the potential winners tend to overdo things in this respect and set the standards.

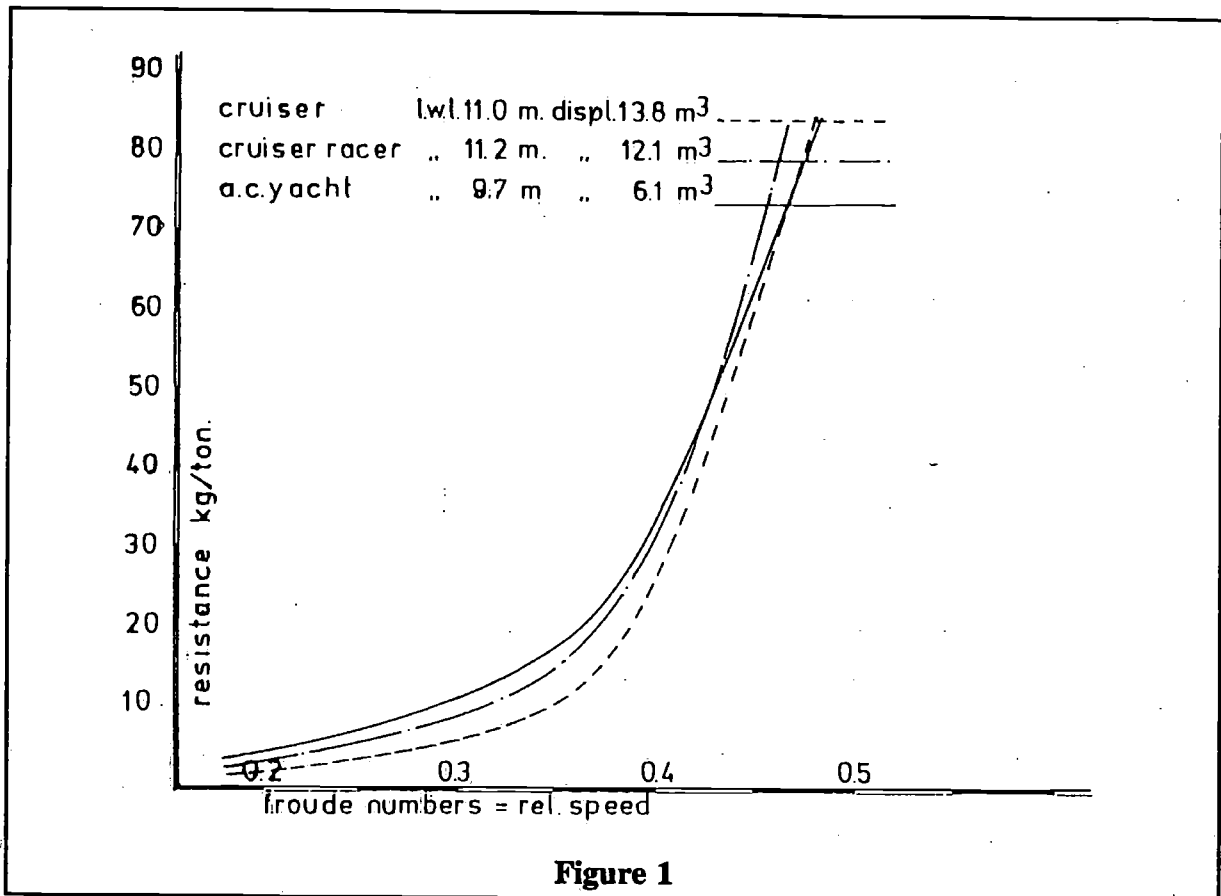
In these developments the rating rules however are not always responsible for the negative effects. Often other factors govern a certain movement. An interesting example is the development of bigger and bigger one tonners, the so called "Jumbo's" until the little Ganbare demonstrated that the I.O.R. rule is not kind to "Jumbo's" at all.

For real cruisers the mentioned considerations might not be of interest, on the other hand we see a strong influence of the racers in the shape and construction of cruisers as well as a change of mind when thinking of acceptable safety margins.

It is a misunderstanding that cruisers are of a less design quality than racers. A cruiser sails under the same law of nature. It is up to the yacht designer to make the best of it.

Cruisers are in practice mostly slower than racers because of factors such as heavier constructed hull and rig, little draught, more devided sail area, fixed propeller and so on.

From tanktests we can see that the quality of hull forms, between cruising and racing hulls, does not differ (Figures 1 and 2)



A cruiser has to be all-round

A good cruising yacht must have a reasonable "range" of properties. By this I do not only mean the properties under sail and power, but also the ease of upkeep, the construction and lay-out etc. The designer has to be aware of the fact that the boat can be used in other ways and circumstances than those which he intended. This means for example that the shell must be strong enough to support the boat when she is dried-out or to withstand the treatment she will get in some busy commercial harbours.

A winch, carefully placed and attached to serve a certain sheet, can be used for other purposes in another direction and so on.

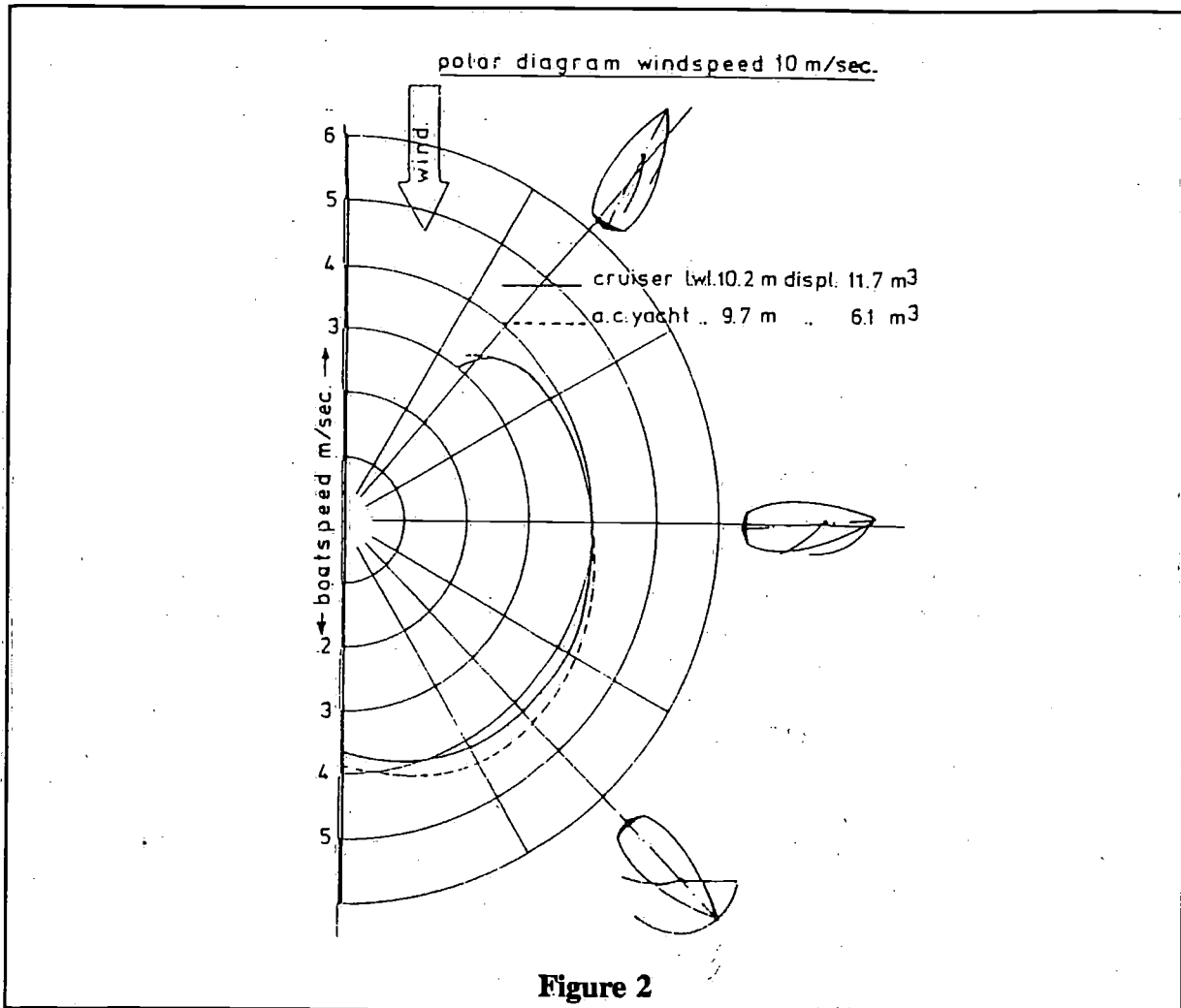
One of the complications for the designer of cruising yachts is lack of controllable feed-back. The designer of a flat out racer is as good as her pricelist, for the cruiser the judgement is more complicated.

Most owners love their own boats, a fact which can be very profitable for the designer from the commercial point of view, but he seldom hears about the faults of the boat before she is sold!

In my own boat I have got an anchorwinch and chain for the first time in my life. I soon discovered that the chain did not fill the chain locker in the way I assumed. Clients who I asked how they solved the problem told me that they had to rear-range the chain twice to get it in the locker which they considered quite normal even where there was enough place for a better arrangement.

It will be clear that I consider the personal sailing experience of a yacht designer as essential, nevertheless there are disadvantages as well. The designer who normally sails with his own boat or own design will tend to find his own solutions the best, simply because he is accustomed to them.

Another difficulty is when the designer has got much more sailing experience than his client. For example: It takes a lot of time to design a good looking galley, especially in the bigger boats, that can be used in reasonable safety and comfort in a seaway. Such a galley is also good for harbour use though not optimal. Lots of people however are unknown to cooking in a heavy sea and want a "Harbour galley" which is much easier to design but more or less useless as well as dangerous in a seaway.



In the last few years a lot of research work has been carried out especially in Holland. Most of the research was done on yachts of the cruiser-racer type, nevertheless some typical cruisers were also towed and analysed.

I do not think that scientific research leads to super yachts, better than best is difficult. However, the research has led to a marked improvement in the general design quality. The risk of bad designs is considerably reduced by a better understanding of the theory and the availability of better statistic material concerning factors like: resistance, steering, behaviour in a seaway, shape of keel and rudder and so on.

For a long distance cruiser a high topspeed is useless because normally the sails are reefed or changed long before.

It is possible now to chose for optimum hull factors for a lower speed (Figure 1 and 2). Speed to windward is important for a cruiser, but normally cruising people plan their routes carefully to prevent windward courses as much as possible, and when they are on the wind they often sail under reefed canvas for comfort.

Nevertheless I consider good windward capacities as essential also from the point of safety unless one would depend on the auxiliary.

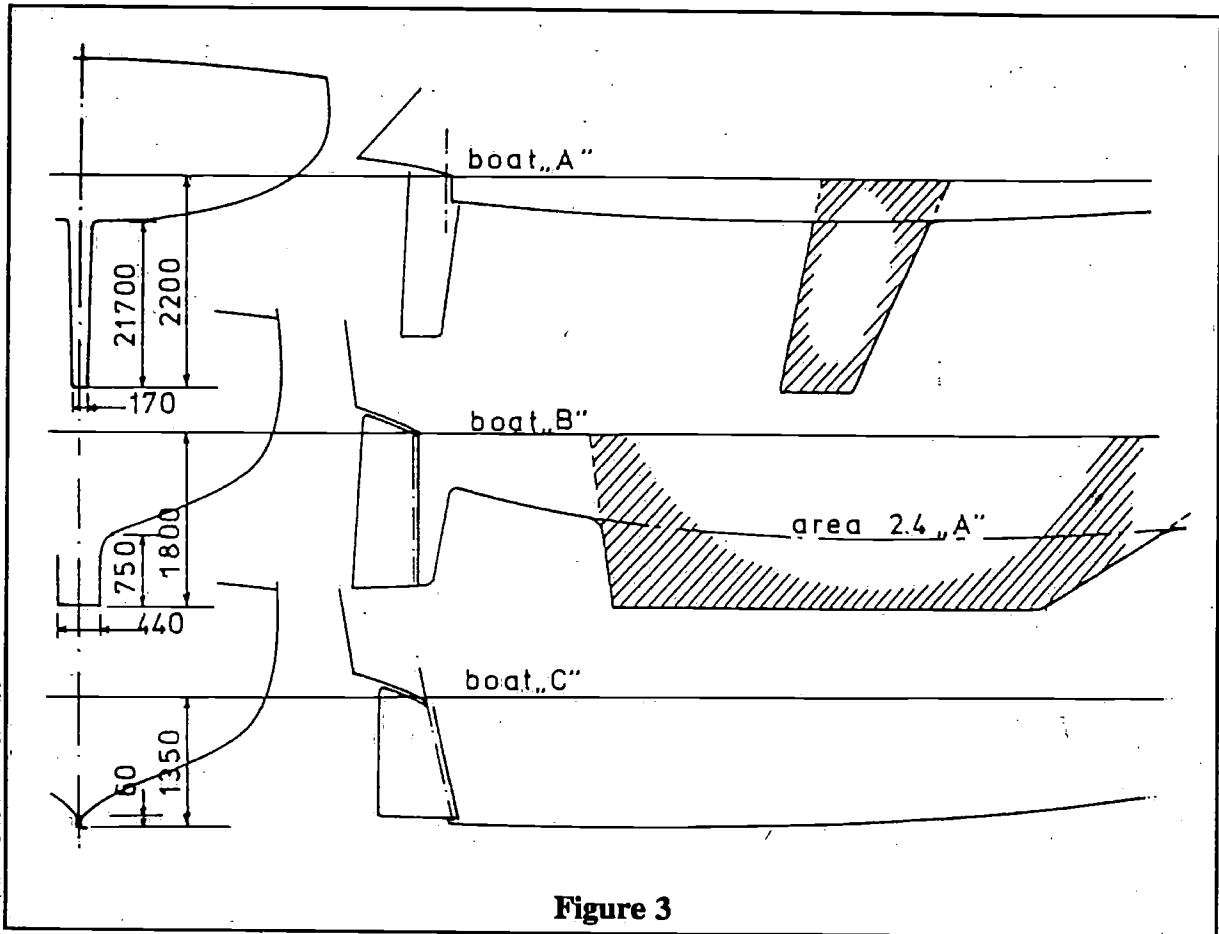


Figure 3

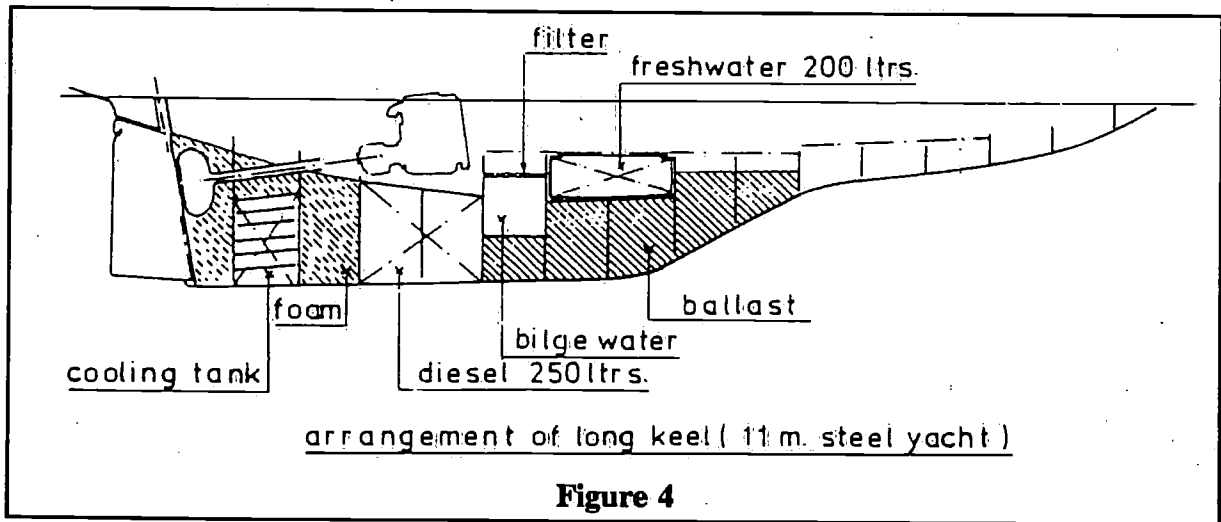


Figure 4

3 The hull

The discussions about advantages and disadvantages of the long keel with attached rudder are over now.

It is clear to most sailors that the concept of the short deep keel with separated rudder is superior in terms of speed and control. It took a long time for the design-ers to adjust the hull lines to the new concept before the advantages became clear.

By way of exception this better system is cheaper to produce as well, especially in series-production.

Nevertheless for the cruising man who wants to explore different areas there are still good arguments to consider the long keel. The long keel offers a lot of store for ballast, fresh water, diesel and bilgewater (Figure 3). The boat can dry-out easily and propeller and rudder are well protected.

If the owner wants to restrict the draft considerably the choice becomes almost apparent. In figure 4 are given the underwater parts of:

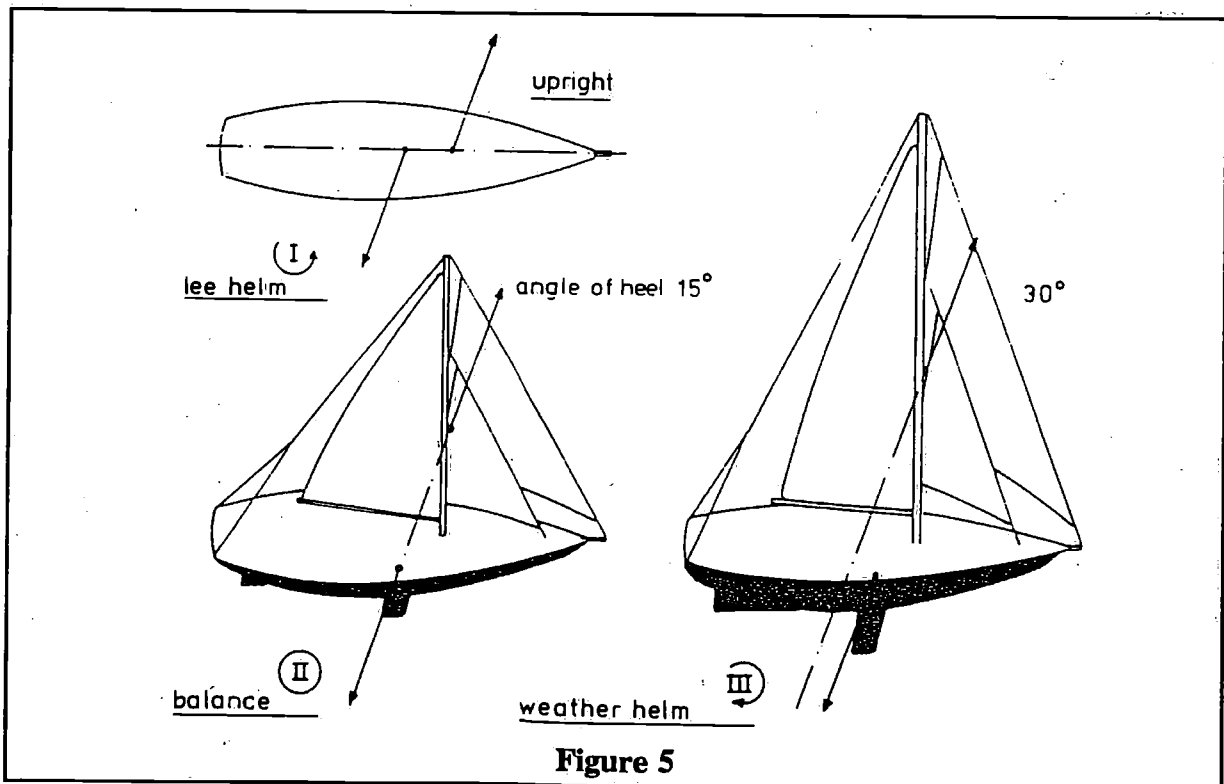
- (A) a light racer with maximum draft
- (B) a heavy cruiser with moderate draft and
- (C) a heavy cruiser with shallow draft.

It can be seen that the real keel-height of the cruiser (B) is much less than could be expected from the difference in draft due to the difference in hull draft (Here is in my opinion one of the advantages of the very light boats under the I.O.R. rule where the maximum draft is a function of L).

Using the calculating model of T.H.Delft (report 260, in Dutch) the hatched area of (B) is 2.4 times (A) for the same leeway angle I feel that in practice this model is too optimistic for keels like the example (B), probably the relation thickness/height also plays a role.

When the space between the back of the keel and the front of skeg or rudder is too small the rudder is working in the downwash of the keel. In that case it is better to choose the old concept of the attached rudder of Figure 3. Here the rudder works together with the keel because the pressure also works on the aft part of the keel, reason to keep the propeller aperture as small as possible.

Lateral forces can also be generated by other means as is demonstrated by Figure 4 type (C). In spite of the absence of a real keel this boat sails reasonably well to windward and, in spite of her heavy displacement, she is fast on all other courses.



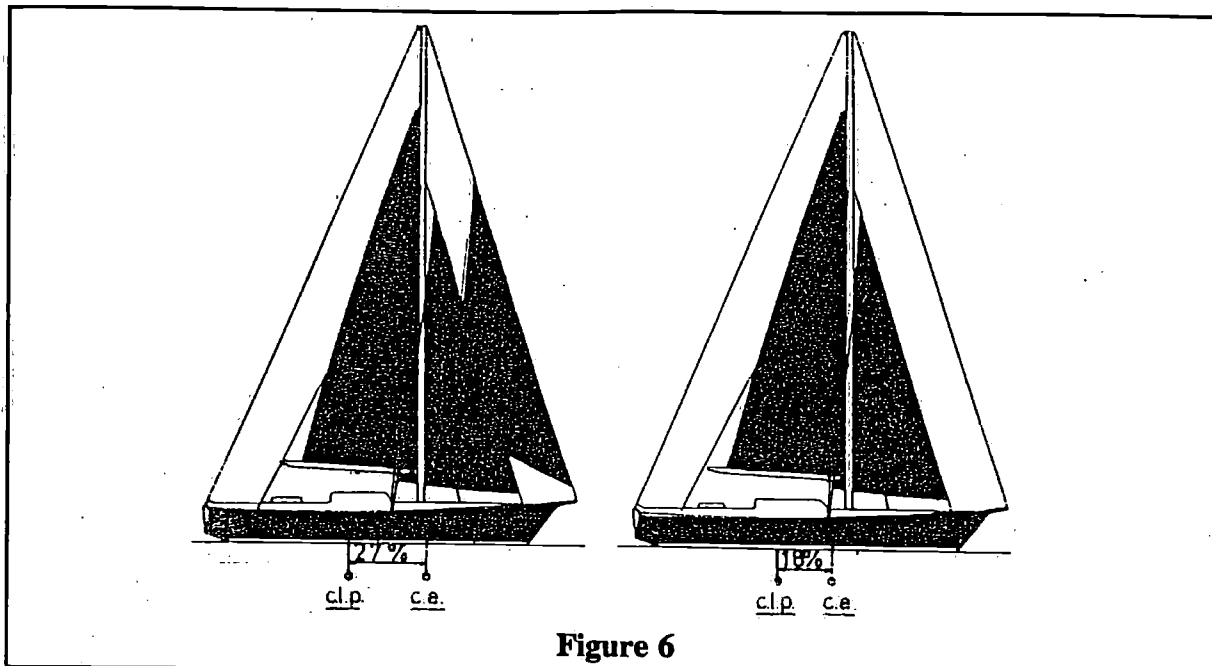


Figure 6

4 Balance

The modern yachts are characterised by big beam and narrow entry-angle of the waterlines. The result is a strongly curved midship part. This shape has proved to be attractive from the point of view of accomodation, sailing comfort and speed to windward. It is however not the best way to attain a good balance. Heeling such a hull has nearly always a luffing moment as a result.

For a cruiser a good balance is extremely important especially when the rudder, due to the moderate draft, is less efficient which in turn means bigger rudder forces and/or rudder angles.

Under water the centre of attack of lateral forces is moving along a horizontal axes dependant of speed and leewayangle.

The longer the keel the more it moves.

This holds true for the sails, the more the sail area is underdivided the less the centre of attack of the windforce moves.

The angle of heel of the yacht, and thereby the stability, plays an important role. A hull normally generates her own luffing moment due to heeling. An extra luffing moment can be seen because the centre of attack of the sailforces moves to leeward (Figure 5).

In practice the methode to start the game with a certain lead between centre of lateral plane and the centre of efford of the sails (Figure 5 and 6) is widely used.

It will be clear that this distance, expressed as a percentage of LWL is a pretty rough guide. Figure 6 shows my boat in two situations. Sit. 1 the lead is 27%. If the wind increases too much for the stability I simply lower the yankee reducing the lead to 18% to find the boat perfectly balanced again (Figure 6, sit. 2).

Whereas it is nearly always possible to balance a sailing boat when on the wind this does not hold so for courses from the wind. Now the balance of the hull itself and the efficiency of the rudder are important. Unfortunately balanced hulls as well as narrow hulls have a tendency to roll, which can be the cause of bad steering...! as can be understood from Figure 5. It will be clear that it is impossible to calculate more or less accurate the right balance. Till now it is mainly a question of feeling and experience.

The preference of so much cruising people for a long keel from the point of balance has more to do with the slow rate at which divergences occur as with the real offcourse angles.

5 The rig

The question "what is the right rig for a typical cruiser"? is often the subject for a hot discussion.

Sometimes people seem to forget that sails are not hoisted for aesthetic reasons or to be easily hoisted but to drive the boat. For the cruiser there are some important facts: The individual sails must be easy enough to be handled by the normal watch on deck. All systems must be such that mistakes are prevented and that, if they come to pass, no major damage can occur. The prevention of wear and chafe and fatigue stresses is also high on the list.

With modern developments like roller reefing of foresails and mainsails watches can handle bigger and bigger sails. People must realise however that they make themselves more and more dependent upon expensive and complex gear for the price of which they could have sailed for a long period using just that small amount of bodily effort to keep themselves in good condition!

6 The influence of windforces on rigging and hull

Tank testing of sailing boats in general stops when the maximum real speed is reached.

For sailing to windward this point is reached at a windspeed of about 10 m/s (6 Bf.)

The point when a sailing yacht stops making progress to windward is reached sooner than most people think.

When the autumn gales blow over the yachtharbour you see that most yachts heel considerably when the wind is abeam, in fact most yachts already consume an important part of their stability without any sail set.

Most cruising yachts are heavily rigged. The seaworthiness and the durability can be improved just like that, but the price which has to be paid is windward ability, another form of seaworthiness.

To show the influence of the windforces on rig and hull I made some calculations based on the full scale measurements of "Standfast" (HISWA Symposium 1975) and used the results for my own boat, "Jantine IV", a typical cruiser.

From the Standfast results with sails no. 1 and 6 (Figure 8a) I took the total wind-forces and detracted the calculated windforces of rigging, hull and the part of the mast above and under the mainsail. I allowed for windgradient and other factors given in Figure 7.

The so derived real sailforces were applied to the situations given in Figure 9 with the addition of the matching rig and hull forces. From the known righting moment at 30° angle of heel it was possible to calculate the adequate windforces. The results are given in Figure 10. A comparison between the racing rig (from HISWA 1975) and the heavier cruising rig for the same hull is given in Figure 8b.

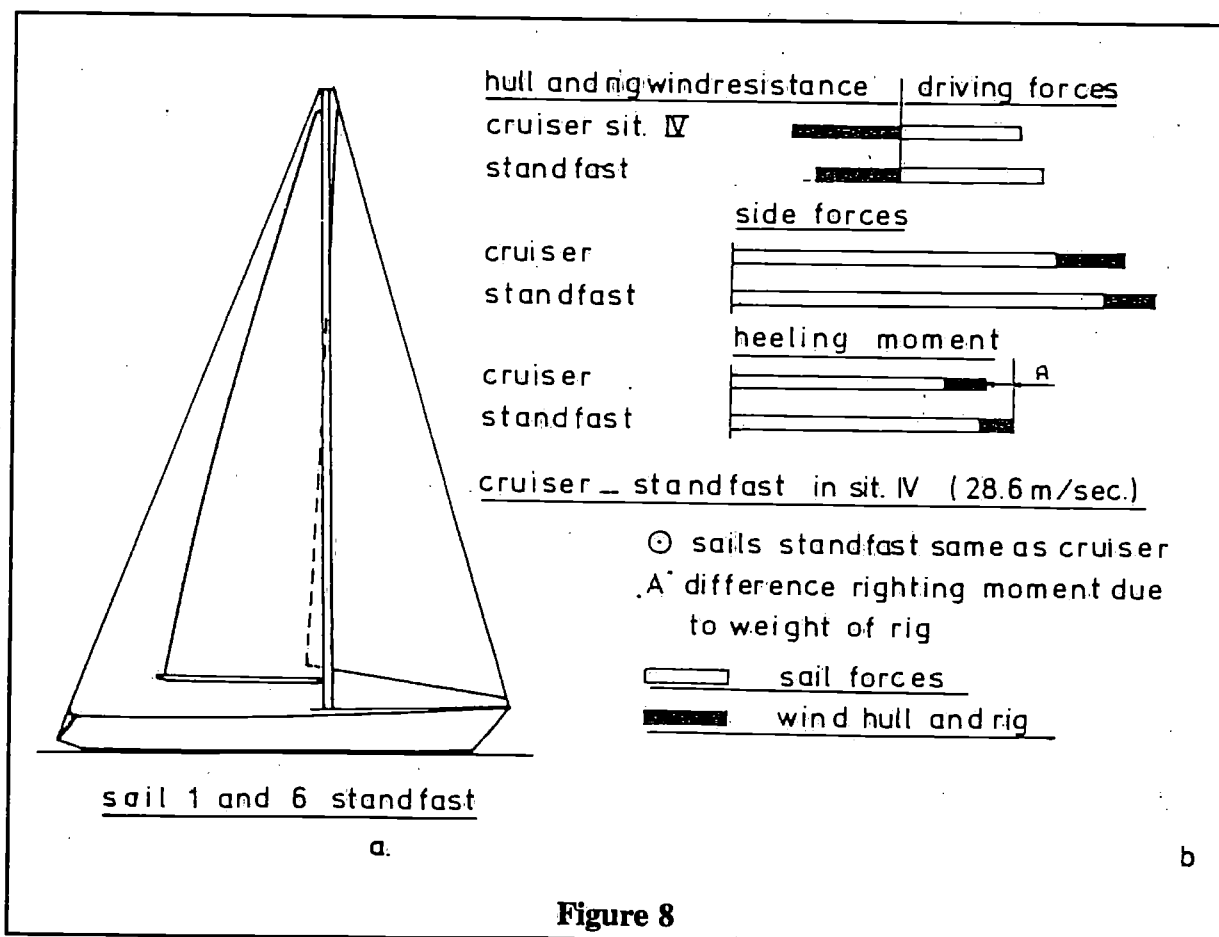
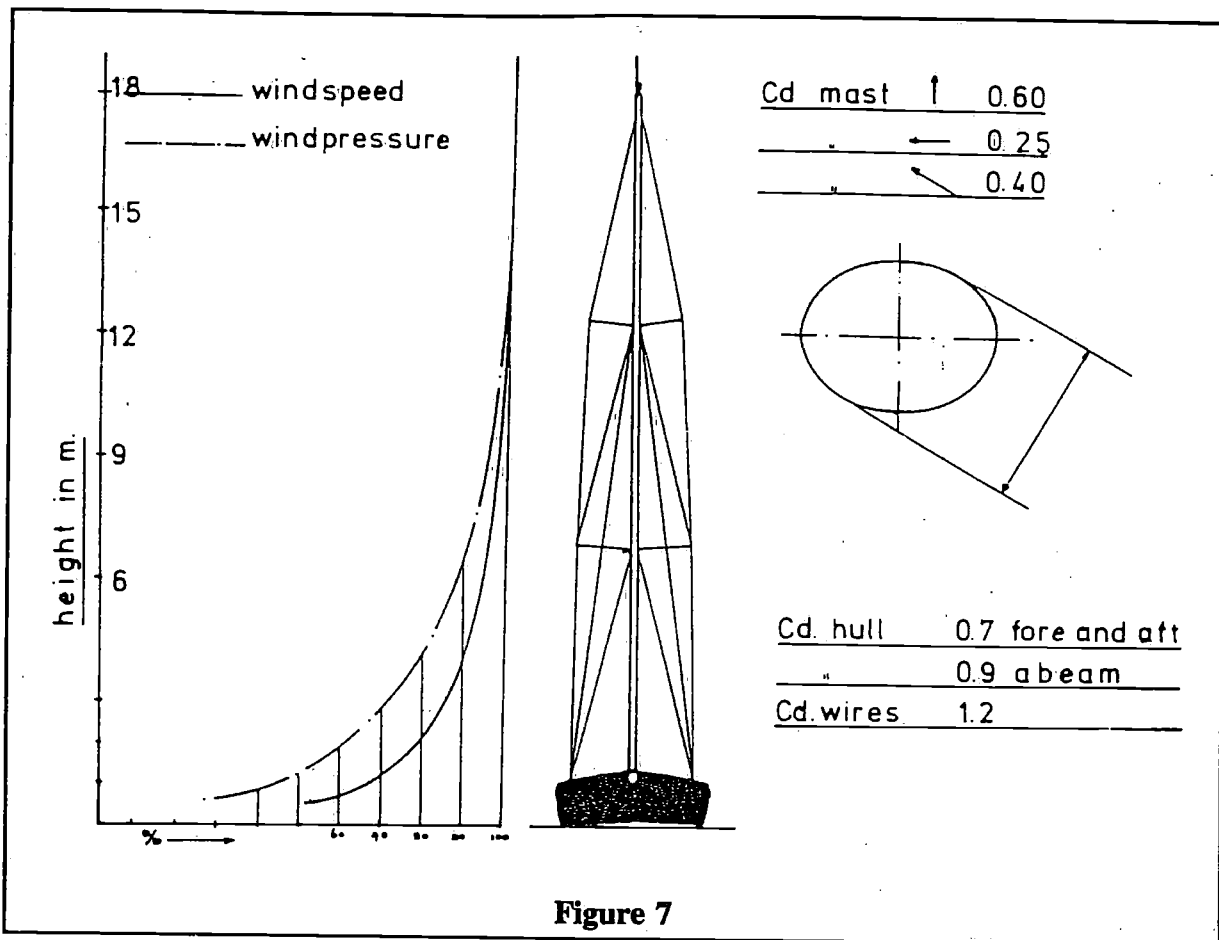
Thereafter I calculated the angle of heel without any sail set and the speed when running under bare poles. These results seem to conform with reality.

Angle of heel lying ahull:

5° ----	15.9 m/s ----	7 Bf.
10° ----	23.7 m/s ----	9 Bf.
15° ----	30.0 m/s ----	11 Bf.

Running

4.21 ----	14.0 m/s ----	7 Bf.
5.91 ----	19.3 m/s ----	8 Bf.
6.71 ----	23.5 m/s ----	9 Bf.
7.41 ----	26.7 m/s ----	10 Bf.



7 Stability in extreme circumstances

A cruiser intended to cross oceans will meet winds of gale force from time to time. Normally a well designed and built yacht will cope with those conditions without problems, provided the crew reacts in the right way. The chosen heavy weather technique will be more dependant upon the circumstances than the safety of the yacht.

It is of utmost importance that the chosen technique is carried, out perfectly.

The possibility of meeting real extreme circumstances is nevertheless always there. Now the chosen technique will be dictated by the state of the sea. It is in those conditions that even big yachts can be completely rolled over.

If the mast under those circumstances will stay in position, which is probably not in all cases desirable with the eye on turning back, the whole rig must not only be very strongly constructed but also it must be such that no bending moments is the mast can be generated.

From the literature and reports, from people who I know well enough to believe, we see that a yacht can capsize in different ways.

Nevertheless it is difficult to realise what really happens and the reconstructions after the event are not accurate because of the accelerations.

It is an experience which makes a very deep impression and few people have gathered enough experience to be able to give a cool report. Nevertheless some conclusions can be drawn:

The risk of capsizing in longitudinal direction is less than abeam, the known cases are always a combination.

Boats being helmed actively seem to be safer than boats which are left to themselves, particularly the light racing boats can probably adopt the fast motorboat techniques.

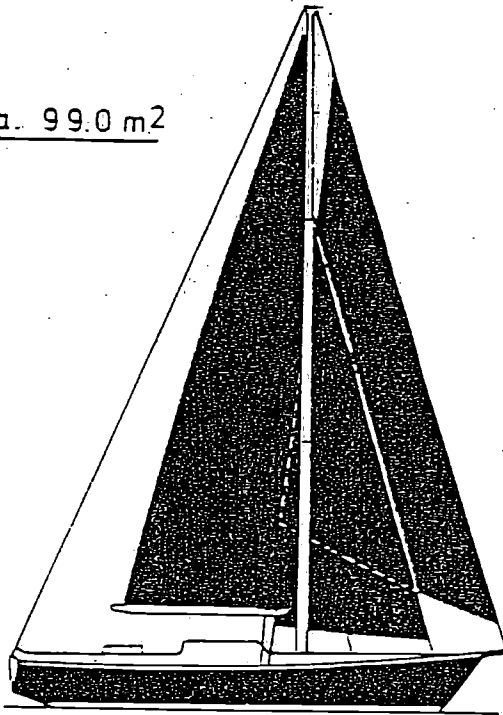
The bigger the yacht the more energy is necessary to capsize, nevertheless a number of really big yachts are actually capsized.

I feel that one of the reasons of capsizing is that the yacht is being thrown away by an unusual steep wave. In a series of pictures I tried to illustrate how the phenomen occurs. The camera moves with the wave speed. Two yachts of the same size are struck by a dangerous steep wave. The first yacht is an I.O.R. type and the other a typical cruiser (see Figure.11)

	displacement	rig	beam	freeboard	draft	vert. centre of gravity
I.O.R.	light	v. light	big	moderate	deep	c.w.l.
Cruiser	heavy	heavy	moderate	moderate	moderate	c.w.l.

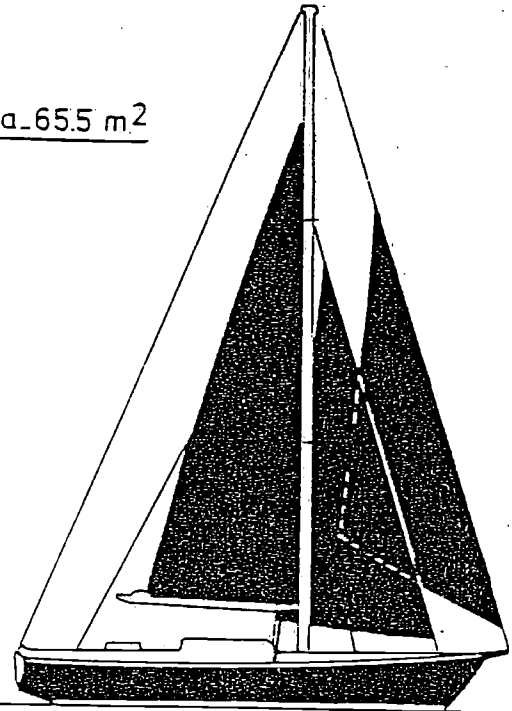
- Sit. 1 Both yachts are more or less stationnary in transverse direction. Both yachts "feel" the nearing wave and start to heel.
- Sit. 2 Both yachts are being hit by the steepest part of the wave. The I.O.R. yacht reacts quicker because of her relatively small mass in relation to the projected area. The deep keel resists the movement thereby adding to the heeling forces.
The cruiser cannot react as quick, her keel, being shallower generates less heeling moment and her heavy rigging has a considerable steadying moment. Of course she takes more water on deck.
- Sit. 3 The I.O.R. yacht is moving with nearly the wave speed.
When the deck takes the water an extra heeling moment is generated and the boat flips over. The angle of heel of the cruiser is still increasing.

s.a. 99.0 m²



sit. I

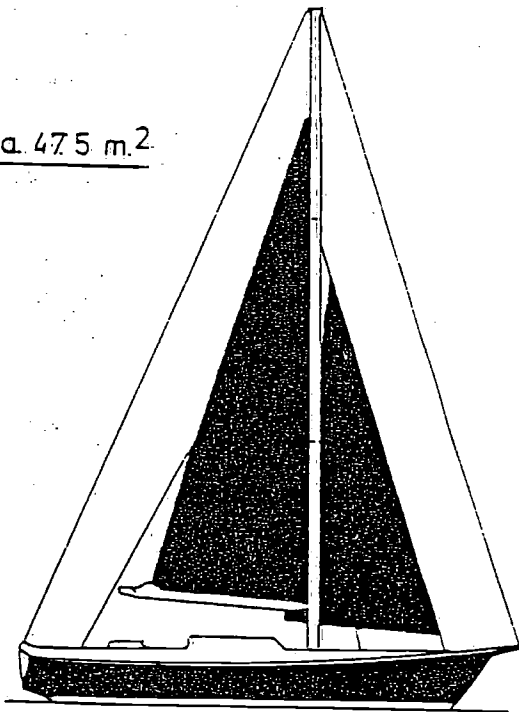
s.a. 65.5 m²



sit. II

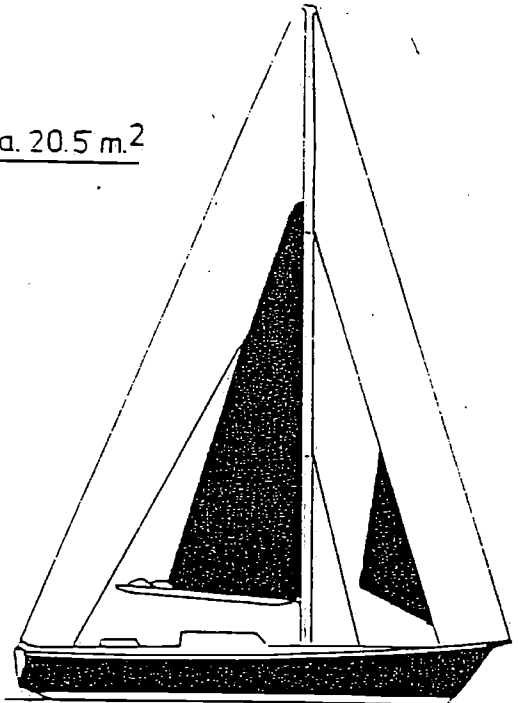
JANTINE IV

s.a. 47.5 m²



sit. III

s.a. 20.5 m²



sit. IV

Figure 9

- Sit. 4 The I.O.R. yacht is actually capsized and whether she rolls 360° or rolls back does not make any difference.
The cruiser, being behind the wave top is slowing down now.
Because of the big mass in relation to her stability she will roll to an alarming angle of heel, a so called knock-down, but she is on the safe side of the wave and will recover.

I feel that the distribution of weight in height is playing an important role. It is striking in this connection to note that yachts having lost their mast seem to capsize more easily. Heavy cruisers with very heavy rigs and high centre of gravity (Joshua, Bylgia, Sentijn, Zeeuwse stromen) have all experienced several knock downs in the Southern oceans but none of them rolled through.

I see capsizing in extreme circumstances as a dynamic happening which is beyond the normal stability calculations of naval architecture. As a matter of fact the normal stability calculations are important, propulsion to windward is based on the righting moment, also important are the calculations of righting arms at angles of heel of more than 90°, be it only to look at which angle the boat comes back to her upright position. It must be born in mind that incoming water has a beneficial influence here!

Summing up:

Positive factors concerning capsizing are:

- size - distribution of weight in height - displacement - low centre of gravity - high freeboard
- shallow draft - little lateral area and indirectly:
- well balanced hull - buoyancy in stem - low gunwale - optimum prismatic coefficient and
- longitudinal center of buoyancy

Negative factors concerning capsizing are:

- small size - relatively light displacement - concentration of weight in height - big beam
- on deck deep draft - low freeboard - big lateral area and indirectly: bad balance - deep
- forefoot - big transom

Factors which are beneficial for speed are:

Length - relatively light displacement - low centre of gravity - concentration of weights - deep draft - little lateral area - ability to plane low freeboard and a lot of beam on deckheight.

References

1. First Symposium Yacht Architecture 1975,
"Determination of sailforces based on full scale measurements and modeltests" by J. Gerritsma, G. Moeyes, J. Kerwin
2. Second Symposium Yacht Architecture 1977,
"Developments in the design of sailing yachts" by C.W. van Tongeren and H.R.F. Körner
3. Laboratorium voor Scheepsbouwkunde, T.H. Delft, Rapport No's. 260, 474, and 518.
4. 1979 Fastnet Race inquiry Report (R.O.R.C.)
5. "Small boats and breaking waves" by Donald J. Jordan, "Sail", Dec. 1982

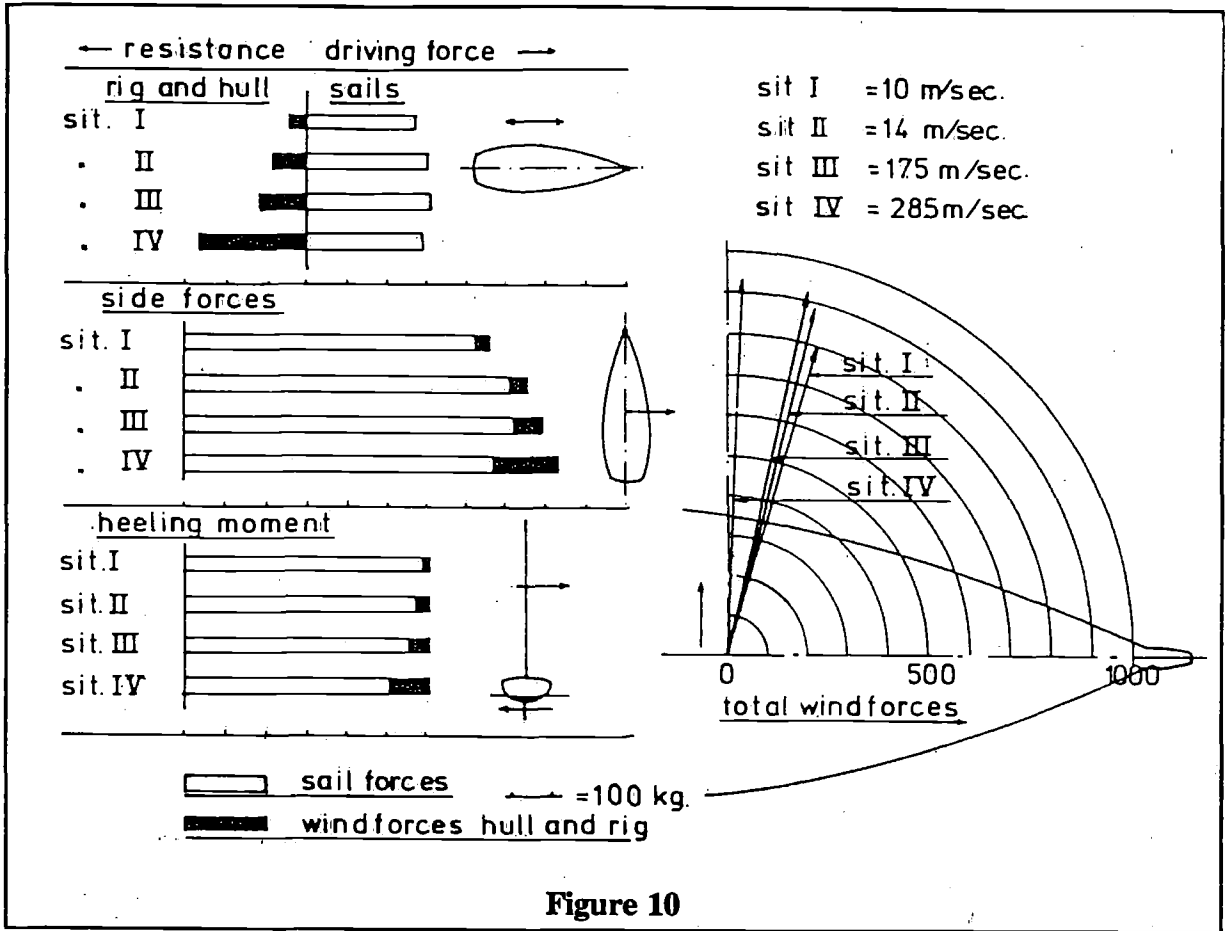


Figure 10

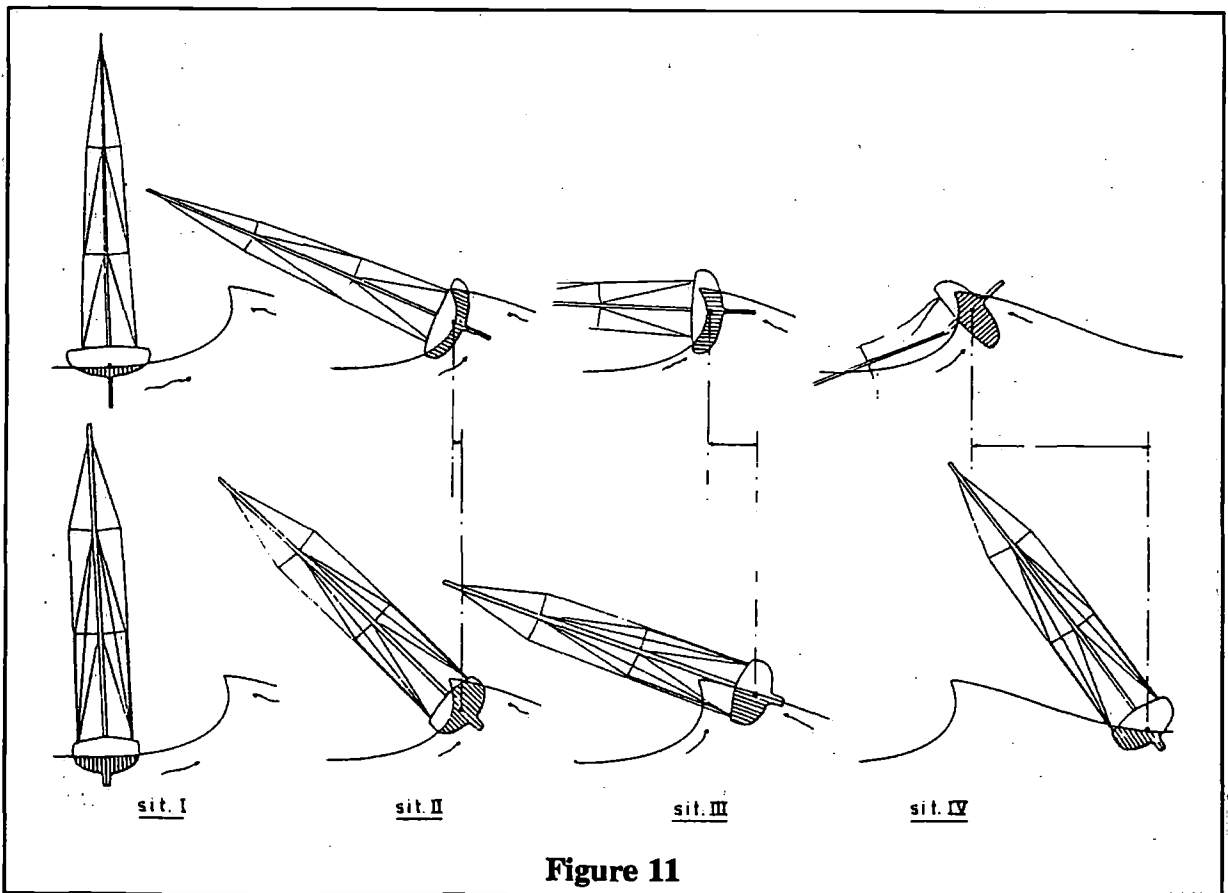


Figure 11

Planing Craft Design and Performance

by Renato Levi

Powerboat designer

The influence of offshore racing upon the design of highspeed planing craft with the introduction of full length V- hulls.

The writer deals with the theory of planing, expressing at the same time his own preference for certain basic shapes. These are based on thirty years practical experience as a designer of many hundreds of different planing craft.

The conclusion suggests a multihull geometry for the future.

In the 60's the design of planing craft changed more than at any other time in its history. During that decade a remarkable transformation took place as designers and builders, slowly at first, started producing what was popularly and rather loosely referred to as deep V- hulls. Offshore powerboat racing was largely responsible for this phenomenon. These open water races clearly demonstrated the superiority of these hulls and underlined in particular their rough water capabilities. The word soon spread as well about their soft riding qualities and within ten years there was almost a complete conversion.

There remained a core of opinion, mainly from those connected with the larger planing boats of over 60 feet, where there was a resistance to change. Their main objection to the deep V- hull was its poor smooth water top speed potential even though the results of fair weather races at that time were disproving this theory. Tank tests carried out before the war on models of flying boat hulls were sometimes quoted as evidence. These results, showed amongst other things, that resistance increased with deadrise and therefore the traditional warped plane with flat or very shallow deadrise aft was still the best.

Perhaps the greatest justification for resisting change in design of the bigger boats was due to the disappointing performance of some 70 and 80 foot cruisers that were built at that time. Most of these craft resembled scaled up versions of their smaller offshore counterparts. They were unsuitable since they neglected to observe any of the fundamental principals involving scale. Elementary reasoning was abandoned in favour of adopting the fashionable high deadrise design trend on boats which had not the speed potential to warrant or indeed benefit by this extreme hull geometry.

The fact is that those early racing designs were around 30 feet and did between 40 and 50 knots. The aft deadrise being adopted varied from 20° to 30° as we felt our way towards the best compromise. It was abundantly clear from the start that the intensity of the slamming depended to a great extent on the amount of deadrise in the impact area and the speed at which this contact was made. The running trim and weight distribution were other contributing factors.

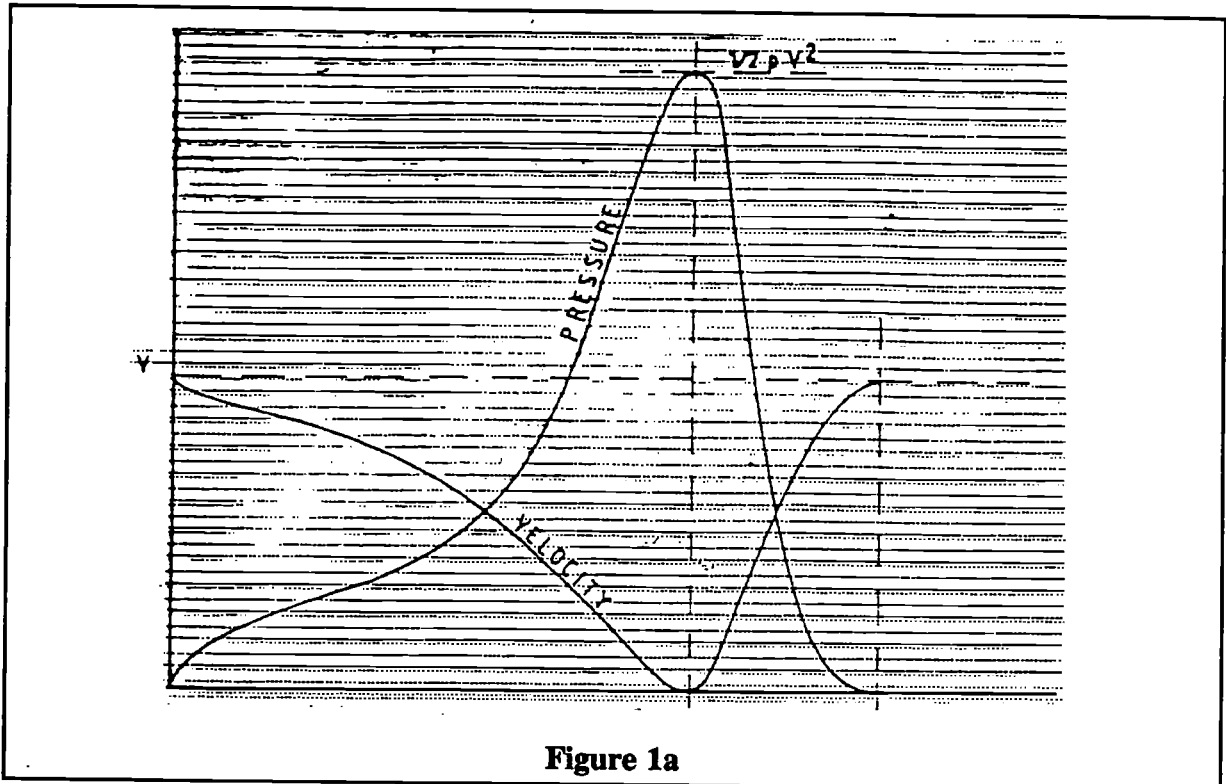


Figure 1a

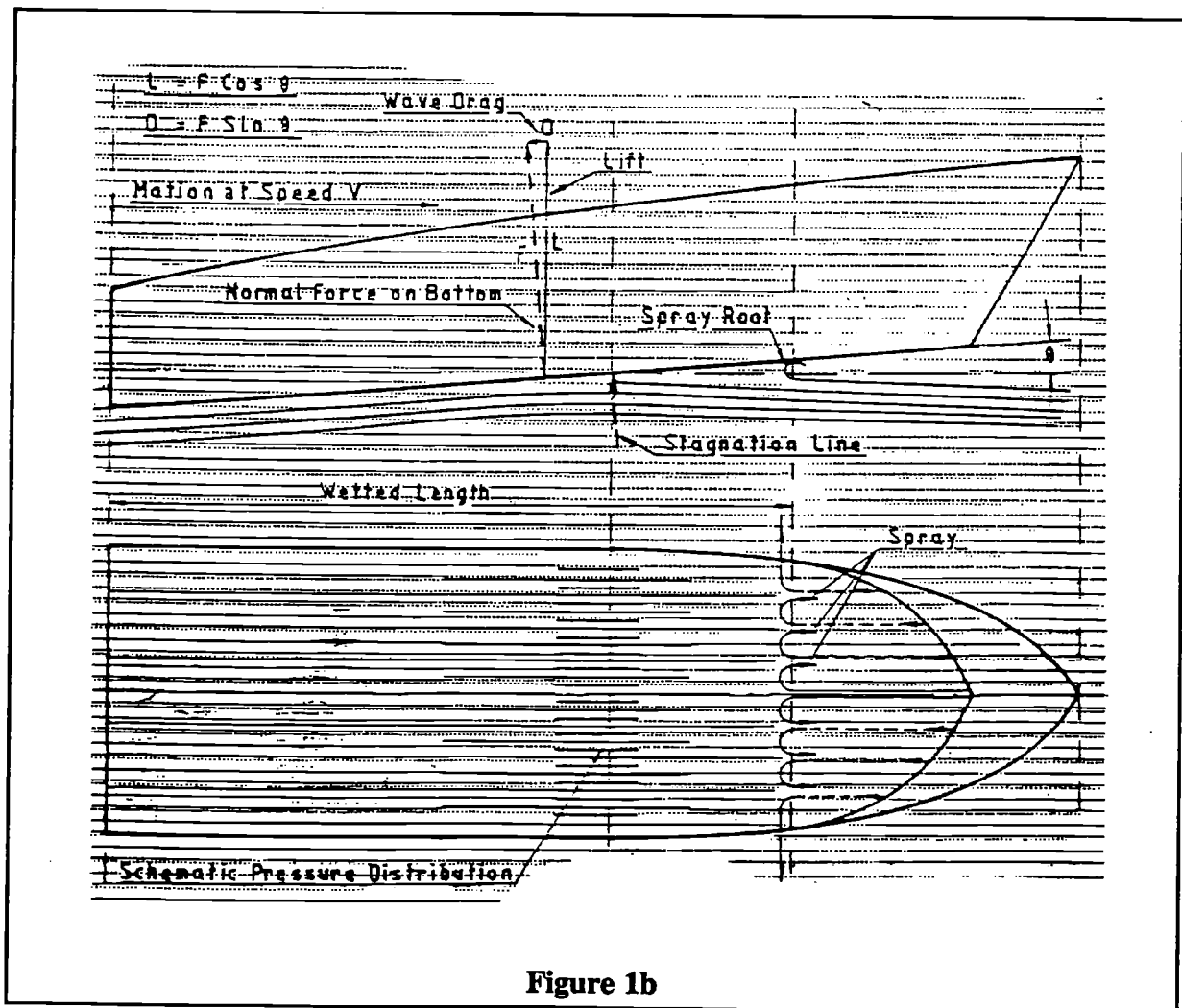


Figure 1b

This was quite well known in the flying boat era of the thirties. Extensive design experimentation and tank testing, already referred to, had produced a lot of interesting information. This included such useful data as the best trim to obtain the optimum Lift/Drag for various angles of deadrise. Fast powerboats however differed in many ways from these flying boats and consequently there were quite a few problems to which answers had to be found.

Since performance is related to size, for the purpose of this text I will employ the most commonly used speed coefficient V/\sqrt{L} . Occasionally arguments are put forward that truer metres of comparison can be made using other dimensions such as waterline beam. The argument being that waterline length varies with speed. The fact is that with Veeed planing hulls all dimensions change with variation in velocity.

The principals underlying planing and the laws governing fluid dynamics are well known. Numerous eminent researchers have studied various aspects of the subject in depth and there is much documentation on these theories and suggested ways of quantifying values under hulls of different geometric forms. A brief look at this by going over familiar ground will highlight the problem and underline the fundamental difficulty encountered in a theoretical prediction of planing performance on a new design.

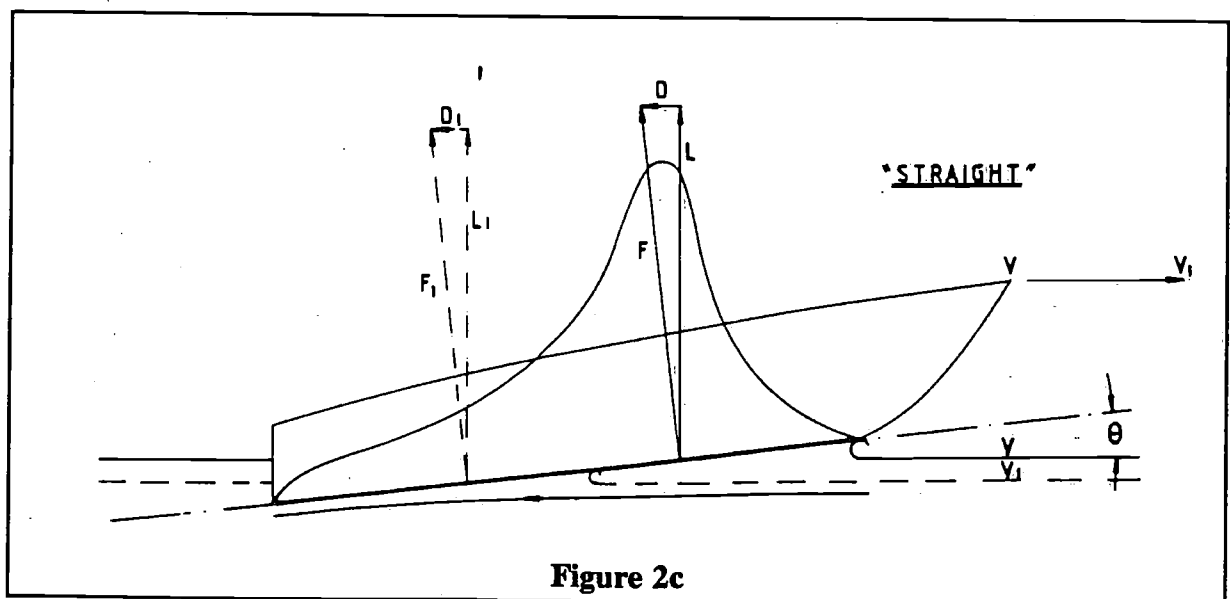
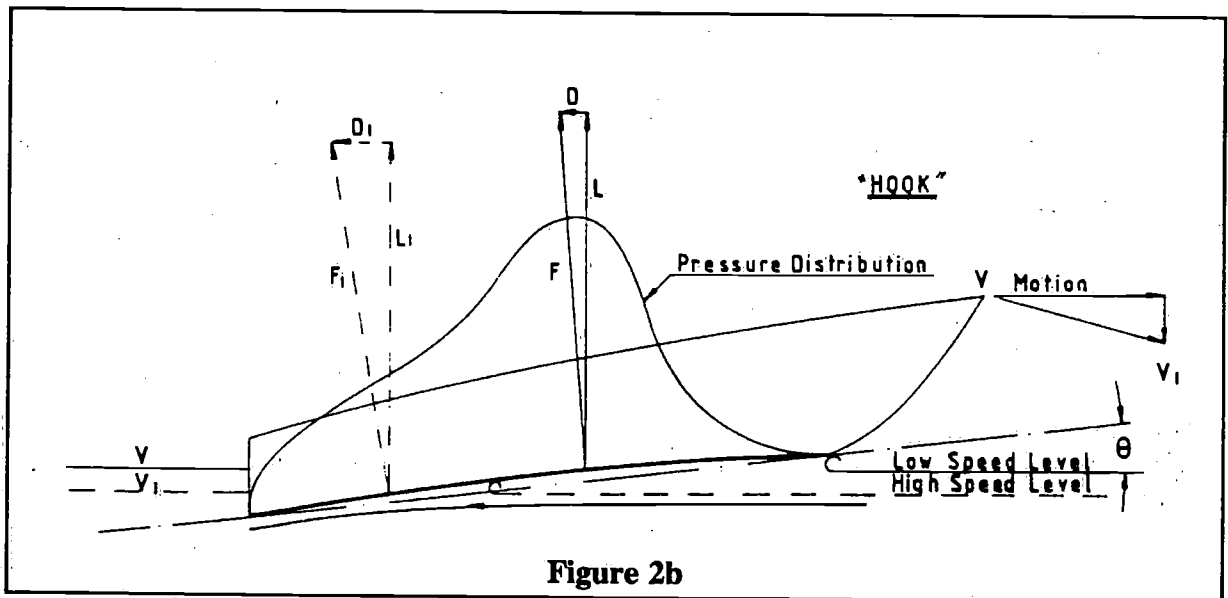
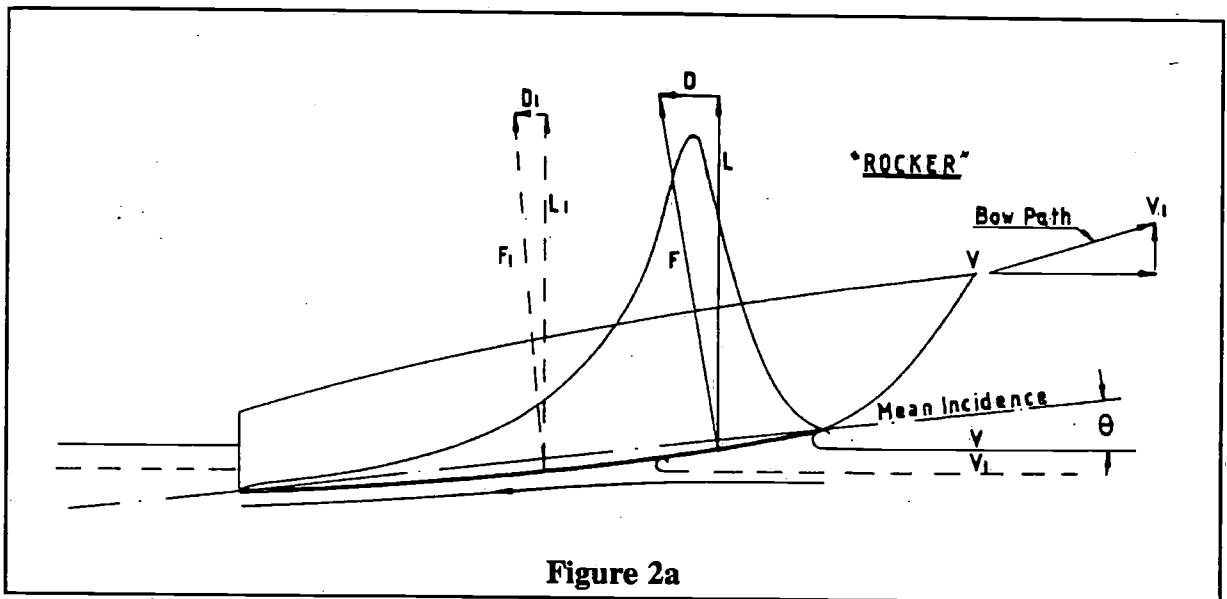
Viewed in a figurative manner, planing occurs when a craft is moving sufficiently fast that it climbs over its bow wave and runs on an inclined pressure plateau. It is held in this vertically elevated attitude by dynamic lift produced by the relatively high forward motion. This dynamic lift is the result of a force acting normal to the bottom and generated by a change of momentum of the deflected stream. The magnitude of this force, due to the high pressure under the hull, will vary with the speed of the craft, its incidence and effective area. The actual distribution of this pressure is related to the relative velocity at any point in the stream. Figure 1a shows the relationship of pressure to velocity which would occur throughout the length of a planing surface. In this case the pressure distribution is suggested for a flat bottomed hull. At the stagnation point where the velocity of the fluid is 0, maximum pressure occurs which is $\frac{1}{2}\rho V^2$. As the velocity of the fluid increases, so the pressure drops until it is restored to atmospheric pressure at the transom where the relative speed is the forward speed of the boat. This is consistent with Bernoullis' Law.

The net effect of this pressure distribution is to produce a force F which will be inclined to the normal as shown in Figure 1b. This reaction may be resolved into a vertical component L which tends to support the craft and a horizontal drag component D which resists its motion:

$$\therefore L = F \cos \Theta \quad \text{and} \quad D = F \sin \Theta$$

It can be appreciated that determining the location and magnitude of the pressure wave force F is fundamental to a theoretical approach to performance prediction of a new design. If we examine the effect deflecting the stream with rocker (convex) Figure 2a or hook (concave) Figure 2b and then with a straight buttock Figure 2c, then Veeing the stagnation line with various deadrise angles, we can see that the variations are endless with considerable shifts of the centre of pressure.

Figure 2a shows that for a given mean plane inclination, rocker produces a high effective incidence which results in a sharply peaked pressure distribution (forward centre of pressure) with a high drag component. If the water surface is made to intersect the plate lower down, such as would occur if the velocity were increased, we see a progressive reduction in



incidence with a corresponding loss of lift. So in order to generate the same lift as before, the incidence must be increased with the accompanying bow up pitching moment and a rapid shortening of the wetted length, *1, which if carried to extremes results in longitudinal instability (porpoising).

Conversely hook, Figure 2b, produces the opposite effect. Note the well rounded pressure distribution curve (aft centre of pressure) *2. At higher speeds the bow down pitching moment results in rapid increase in wetted length, high skin friction drag, accompanied eventually with lateral instability (leaning) and possible loss of directional control.

The straight planing surface shown in Figure 2c is the one which permits the same relationship between lift and drag to be maintained for changes of water surface at a given incidence. It follows that provided equilibrium can be kept through the various surface levels at the best lift over drag ratio, which for a flat surface is around $4\frac{1}{2}^\circ$, then the ideal situation is achieved. Such perfection is unlikely to be realized, but the absence of the bow up or down pitching moment offers the best possibility of approaching the optimum condition throughout the speed range.

In order to avoid peaks of pressure such as would be the case in Figure 1b, Veed sections are adopted in practice as shown in Figure 3a. It can be seen that the stagnation stripe is V-shaped with a much fuller integrated pressure distribution curve and the flow lines under the hull are now diagonal. This in effect means that the deflection of the stream is less than the incidence of the hull. Looking at the pressure under the section and the force acting normal to the bottom, the lift is force $\text{Cos } \beta$.

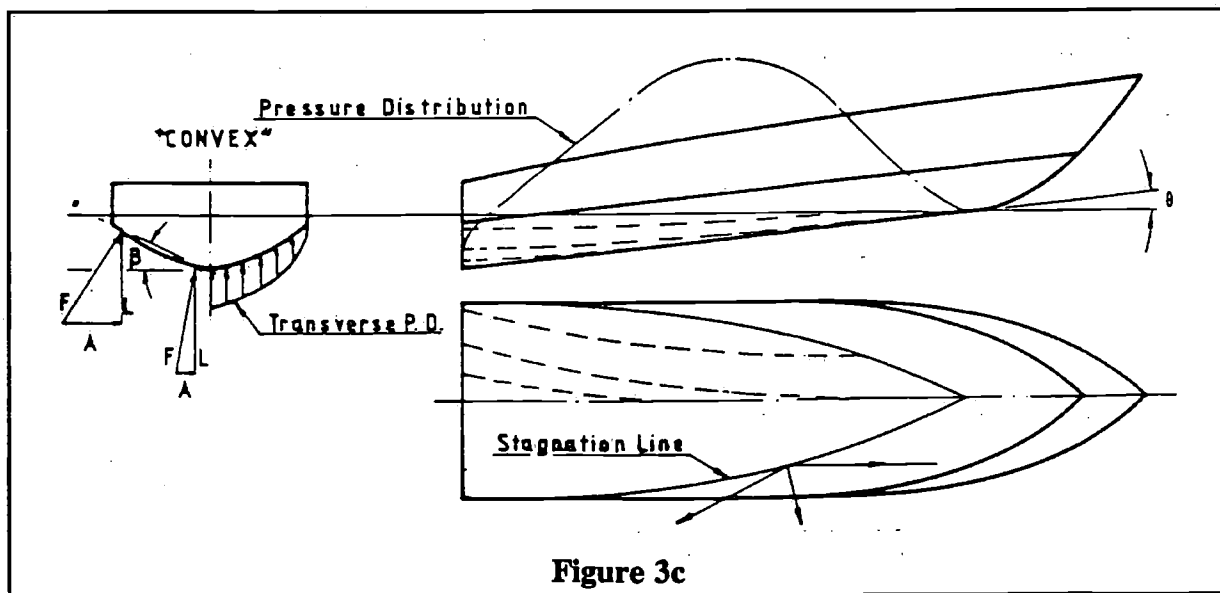
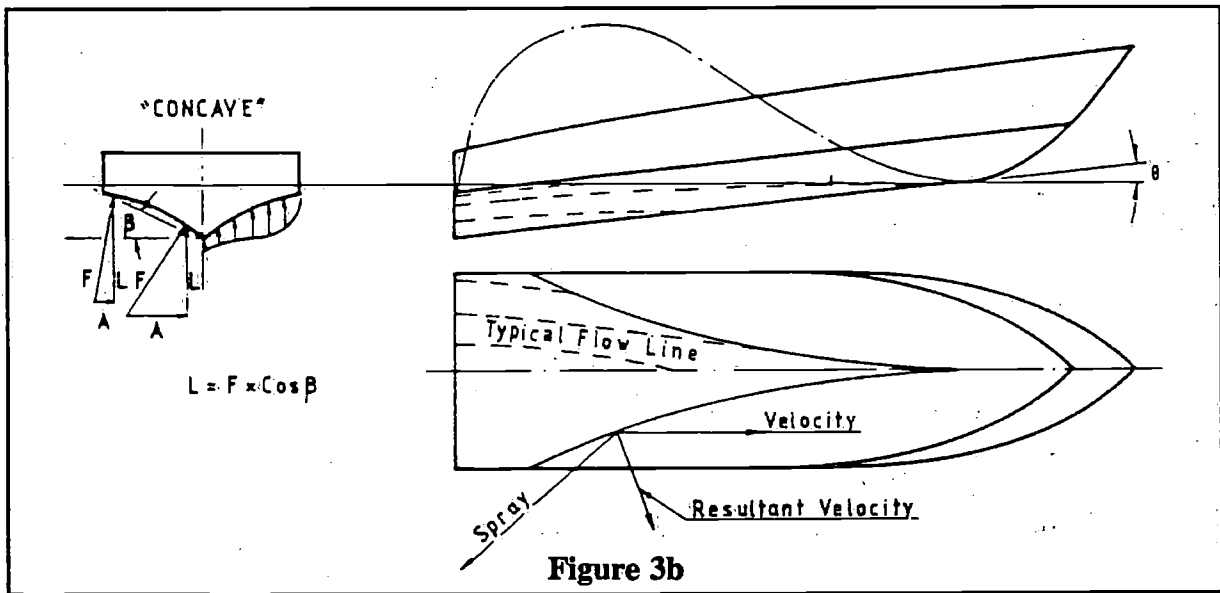
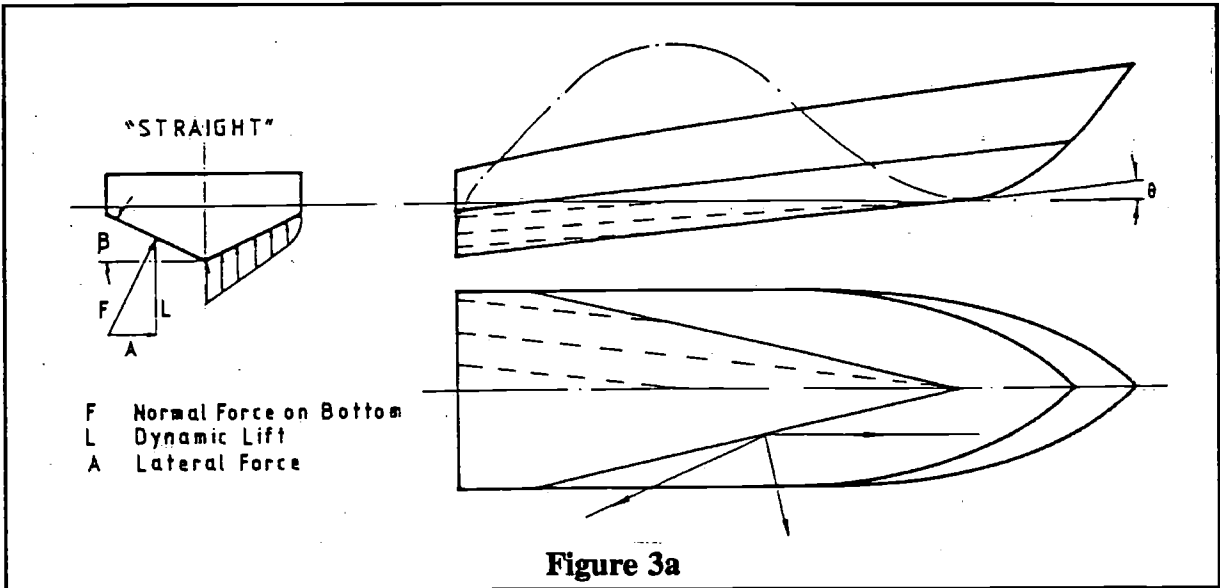
Figures 3b and 3c are variations on Figure 3a and show the effects concave and convex sections have on the flow line and pressure distribution. Briefly the main difference between 3b and 3c can be seen by the pressure pattern under the sections. As the section in 3b gets flatter outboard, it produces progressively more lift, and the reverse is true of 3c. This shows that when the hull rises with the increase in speed, 3b results in a rapid loss of relatively high lifting surface in the initial stages.

Ultimately this leaves an inefficient concave wedged figure of low lift potential, high wetted area and a narrow plane width. It must also be noted that the shallow deadrise portion of the hull occurs at the chine, an area which is prone to pounding. 3c on the otherhand does not have these disadvantages, in fact quite the opposite occurs here, even at very high speed this section shows a significant reduction of wetted area with good lift and a large planing width. In addition, from a structural point of view, a convex section has excellent rigidity of form which can permit lighter scantlings.

Spray rails or lift strakes are now accepted appendages on the bottom of V- hulls. Their purpose is to increase the lift and reduce the wetted area. Since the flow under the V- bottom is diagonal as we have seen in all the examples in Figure 3, these spray rails act as controllers, straightening and deflecting the stream downward to some extent.

*1 Such a condition can be beneficial on very high speed craft if a balancing force such as thrust can create a state of equilibrium.

*2 An aft centre of pressure will be beneficial at low planing speed since there will be high lift for low drag.



The inboard line acts as the high pressure leading edge, whereas the outboard trailing edge where ventilation is adequate (forward), will permit a reduction in hull wetted area, Figure 4. It is possible that further aft, where air starvation could occur, there may be a build up of low pressure along the vertical edge. In this event it is likely that the stream would be further straightened along the hull incrementing the lift.

Spray rails also add to dynamic stability in both yaw and roll. The former causes a build-up of pressure along the vertical faces of the offending side. The latter does so because of an increase in incidence on the bottom faces of the depressed side.

There is a misconception that spray rails are only beneficial in the forebody and are drag inducing in the aft planing area. This is not the case. This assumption has probably been based on hulls that ran too flat with full length rails. In these cases the removal of the rails aft reduced the lift which increased the performance. A greater improvement might have been achieved by altering the *C.G.* and maintaining the lift.

A successful design for an open water craft is one which can run efficiently throughout the required range of speeds. It should be capable of maintaining high speed in broken water with the maximum amount of comfort. For a given size of boat the degree of comfort depends upon the speed, the higher this is, the more uncomfortable is the motion. Increasing the deadrise in the pounding region improves this situation with a penalty on drag at the lower speeds. The locus of the high impact area will shift progressively aft as speed increases till at very high speed $V/\sqrt{L} \geq 8$ it will be well astern. This indicates therefore that deadrise in a design should be varied to best suit the speed. A broad generalization which I have found to be acceptable as a compromise between speed and comfort is the following:

$V/\sqrt{L} =$	Deadrise
3	16°
3.5	18°
4	20°
4.5	21°
5	22°
6	23°
7	24°
≥ 8	25° - 30°

There would be exceptions to these values where for instance the deadrise may be reduced on a fast runabout in the interest of lateral stiffness. Conversely a cruiser or patrol boat which has to ply regularly in choppy waters may benefit with greater *V* as would an offshore rescue craft.

For a given plane deadrise there is an optimum angle of incidence, see Figure 5, and the aim is to approach and maintain this throughout the useful speed range of the craft. In practice this angle is often exceeded at low speed whilst at the higher speeds the incidence is too low. In the first case the excessively high angle of attack generates high pressure wave resistance and in the second case the excessively flat trim causes high wetted area drag. The high angle of incidence at low speed is the result of insufficient area to support the weight (high plane loading) or *C.G.* location too far aft or a combination of the two. Figure 6a illustrates this condition and Figure 6b indicates the ideal attitude to aim for at the low end of the cruising speed range.

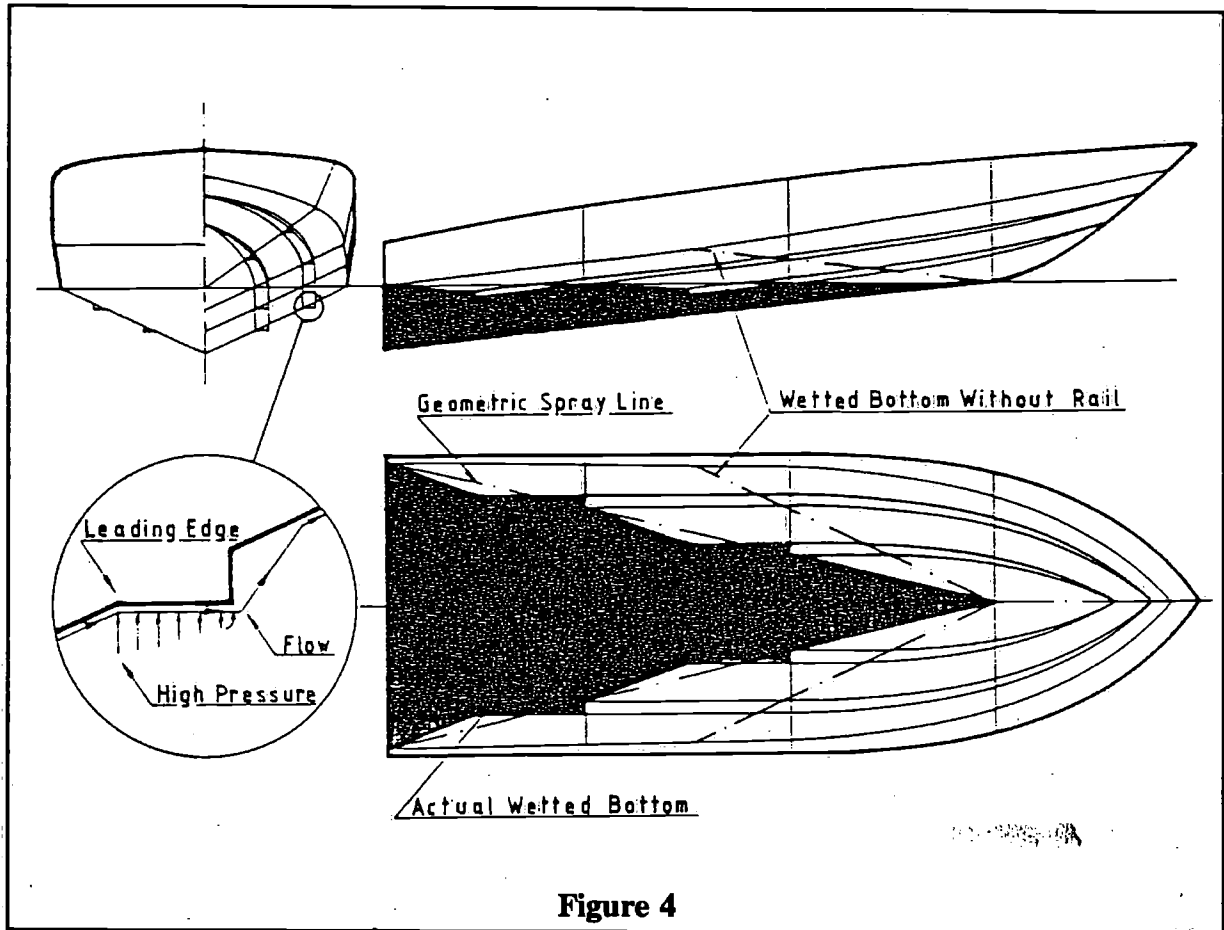


Figure 4

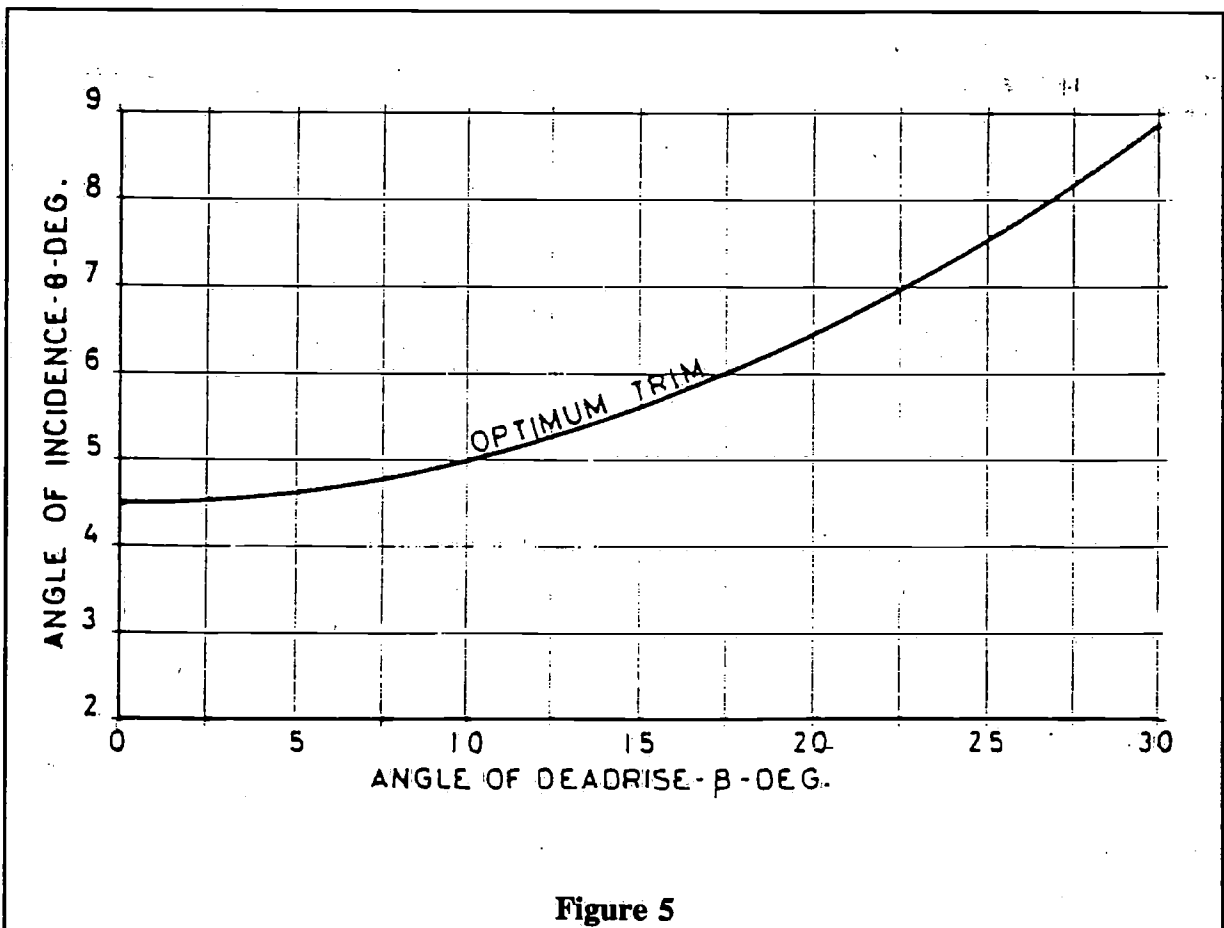


Figure 5

There is also a component of hydrostatic lift which can be quite high at these speeds and could be considered as a balancing force. The analogy which comes to mind in this respect is that of an air-craft during its take off run. At low speed a large proportion of the weight is supported by the undercarriage, the aerodynamic lift being relatively small. With the build up of speed the dynamic lift increases, reducing the weight the wheels have to support. At very high speed, around $V/\sqrt{L} = 8$ the hydrostatic lift is negligible. Photo 1.

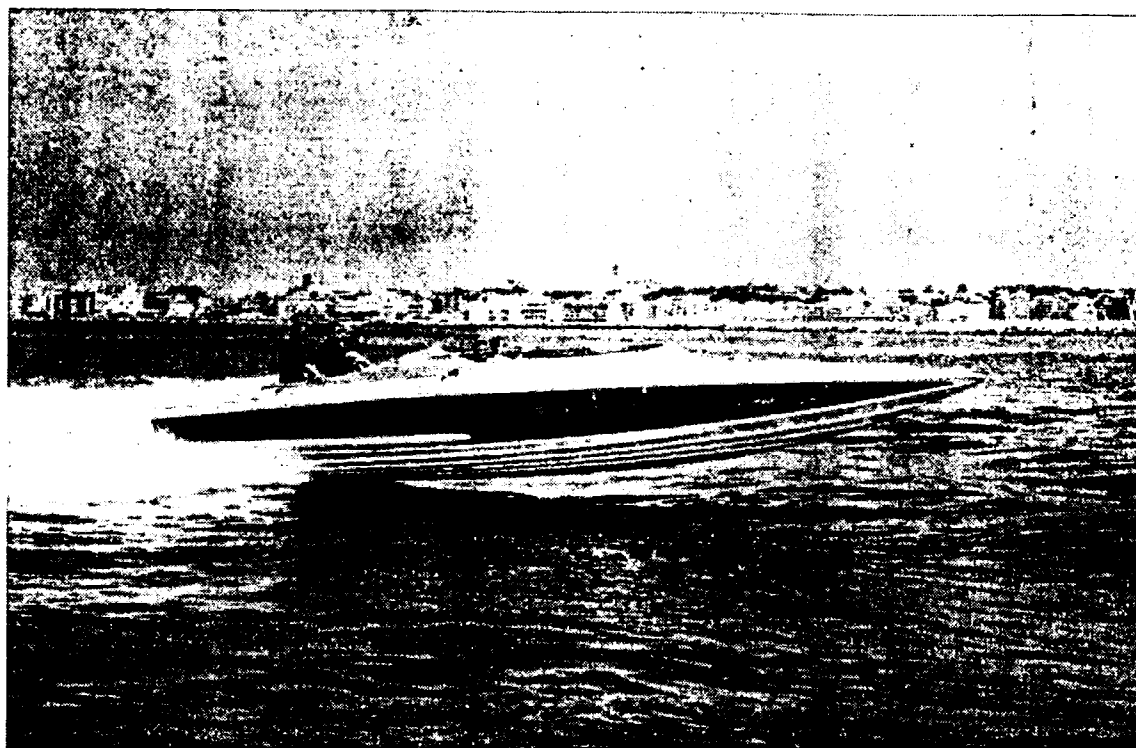


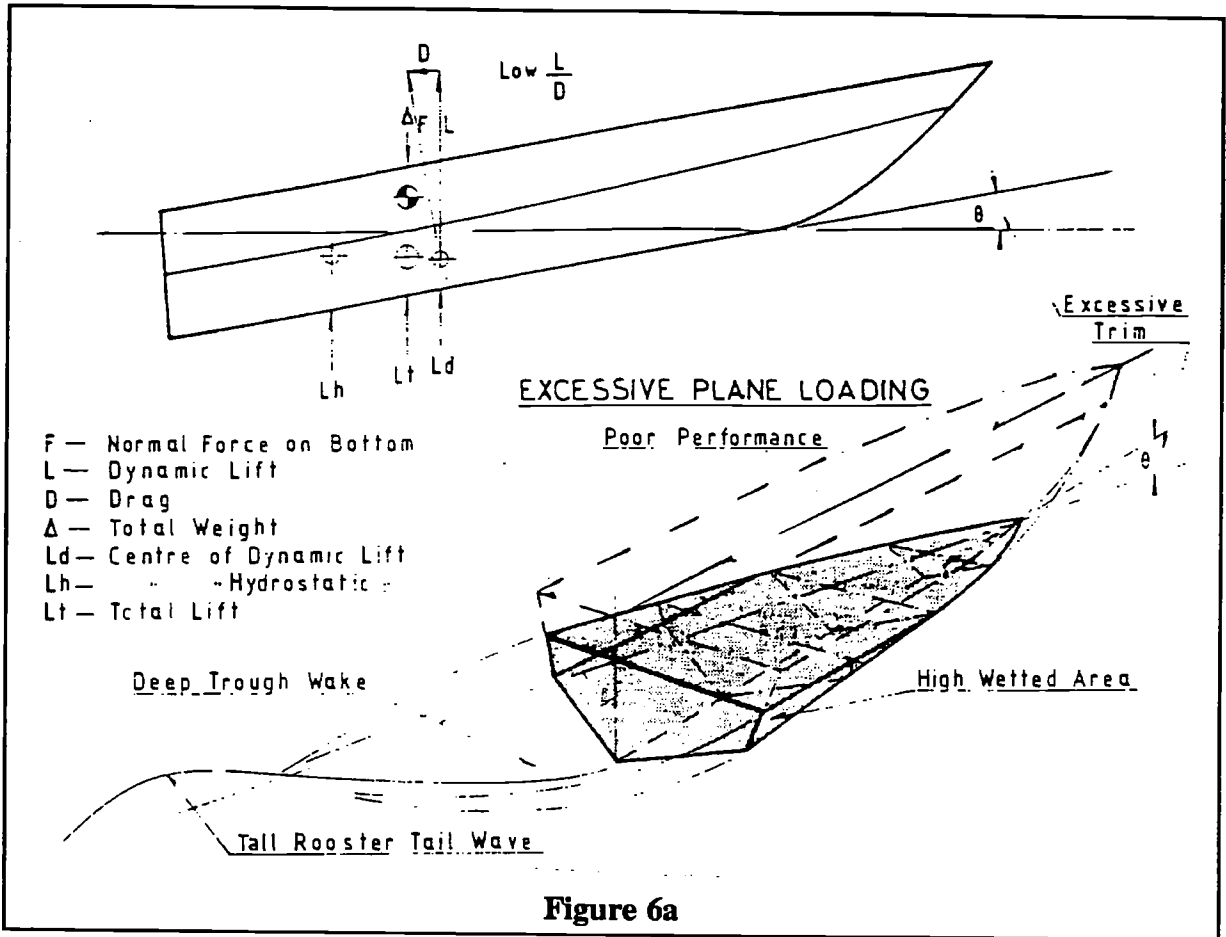
Photo 1 38' Fast Commuter. Waterline is 32'. The craft is travelling at about 50 knots. ($V/\sqrt{L} = 8.8$).

Note: The planing length is short and hydrostatic lift is negligible.

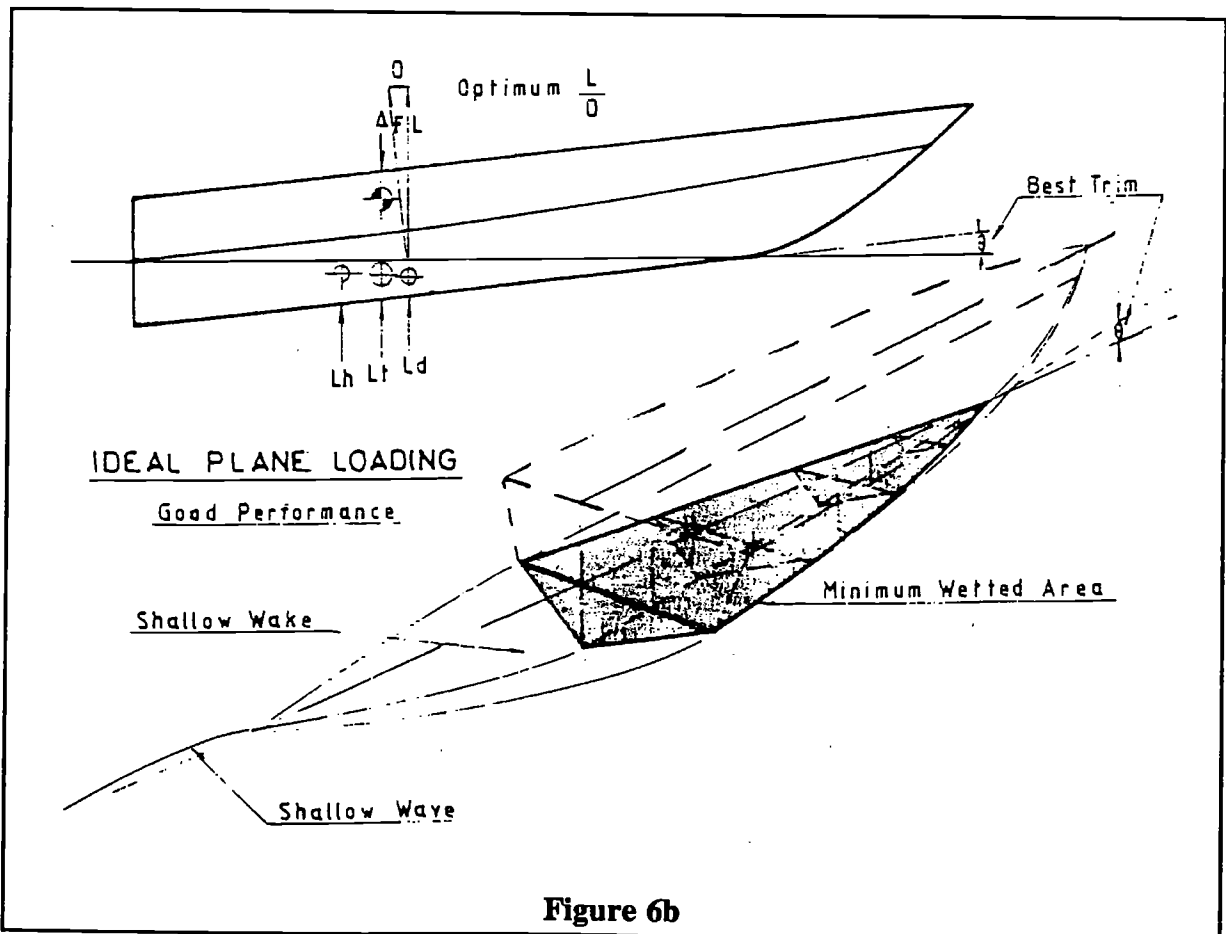
The tendency for the trim to flatten as speed increases is due to the necessity for the water plane to lengthen so as to achieve a state of equilibrium ($C.G$ over $C.P$). Locating the Centre of Gravity further aft would mitigate this condition.

A larger planing area will improve the slow speed performance in a high plane loading situation. This area can either be increased by lengthening or widening the hull. Lengthening the hull will result in the pressure centre being located further aft which would reintroduce the drawback already referred to. So widening is the more favourable choice and fortunately on a Vee hull this additional area need not be drag inducing at high speed.

The most desirable pattern of wetted area reduction due to lift is where optimum incidence is maintained throughout the useful speed range of the craft. It follows that to obtain the best of both worlds, i.e. at high and low speeds, the $C.G$ must be as far aft as required for the top speed consideration and that there is adequate area aft at low speed to avoid squatting. These requirements point to a geometry similar to that in Figure 7 where little or no incidence change is necessary to maintain equilibrium.



- F — Normal Force on Bottom
- L — Dynamic Lift
- D — Drag
- Δ — Total Weight
- Ld — Centre of Dynamic Lift
- Lh — " — Hydrostatic
- Lt — Total Lift



Predicting the performance on a new design, provided it falls within the more common range of speeds, can be done with a high degree of accuracy by means of towed or self propelled models. It must be said that the reliability of such forecasts is largely dependent on the experience of those connected with such work. However, in the case of very high speed craft where for instance, propulsion and the appendage effect plays such a big part, the sea model's results are of doubtful value. On the otherhand some indication of general behaviour will be available, which could prove useful. It can be understood that a purely theoretical approach to the problem, which will necessitate making a number of assumptions, is unlikely to provide trustworthy results.

My own thoughts on design have evolved largely from the experience gained in my earlier work, although I have on numerous occasions relied on models. In spite of developing new designs utilizing earlier familiar hull Forms, a method which would appear infallible, there were surprises. These inconsistencies occurred mainly when systems of propulsion were changed. With hindsight some of the unexpected results were easy to explain whilst others were not so obvious. Certainly the type of propulsion adopted plays a big part in planing boat performance, quite aside from the actual propulsive efficiency. This is not only due to the variation of the actual appendage resistance but also to the effect this has on trim, which can be considerable at the higher speeds. Differing thrust angles are another factor.

The graph in Figure 8 shows the expected performance of hulls from 20 to 60 feet with various power loadings. Horse power per ton of displacement is plotted against corresponding values of the speed coefficient. V/\sqrt{L} together with the recommended aspect ratios. Also indicated for each of the waterline lengths is an average plane loading. These curves are based on data for conventional twin screw propulsion from a wide selection of my own designs and are related to the type of hull form shown in Figure 9.

This represents a set of lines I have come to favour and which when suitably adapted in its main proportions for the performance required, will give reliable results. Briefly, as can be seen, the keel in side elevation is parallel to the static waterline with a well rounded forefoot fairing into a raked stem. The chine is on the waterline aft for about 20% of the waterline length from the transom. This provides the hull with a constant section planing area for this portion of its length. The chine is then raised in a gentle curve till it meets the stem near the sheer. In plan view the chine is widest aft at the transom. This maximum width, obtained from the appropriate aspect ratio, is maintained for 50% of the waterline length and then gradually brought into the centre line with a full curve. Since the sections are of constant curvature, the chine is shaped so as to give a deadrise of around 40° at the forefoot which is about 10% of the waterline length.

The total 0° deadrise area of the spray rails, which would also include the chine flats, will amount to between 20 and 25% of the waterline beam aft. This area is usually split up into 2 or 3 rails plus a flat per side, though sometimes up to 4 rails have been applied. They have been positioned in a variety of ways from following the contours of the waterlines to those of the buttocks. Locating them in either of these extreme ways can cause undesirable effects.

The former will tend to cause tripping (yawing) with poor lift qualities and the latter can induce wetness since there is little spray suppressing effect. Running the rails parallel to the chine seems on the whole to give the best results. Whilst these strakes are indispensable to improving the allround characteristics of a V-hull, they do make the boat hard riding and so should not be overdone. A further important point is that some deadrise should be worked

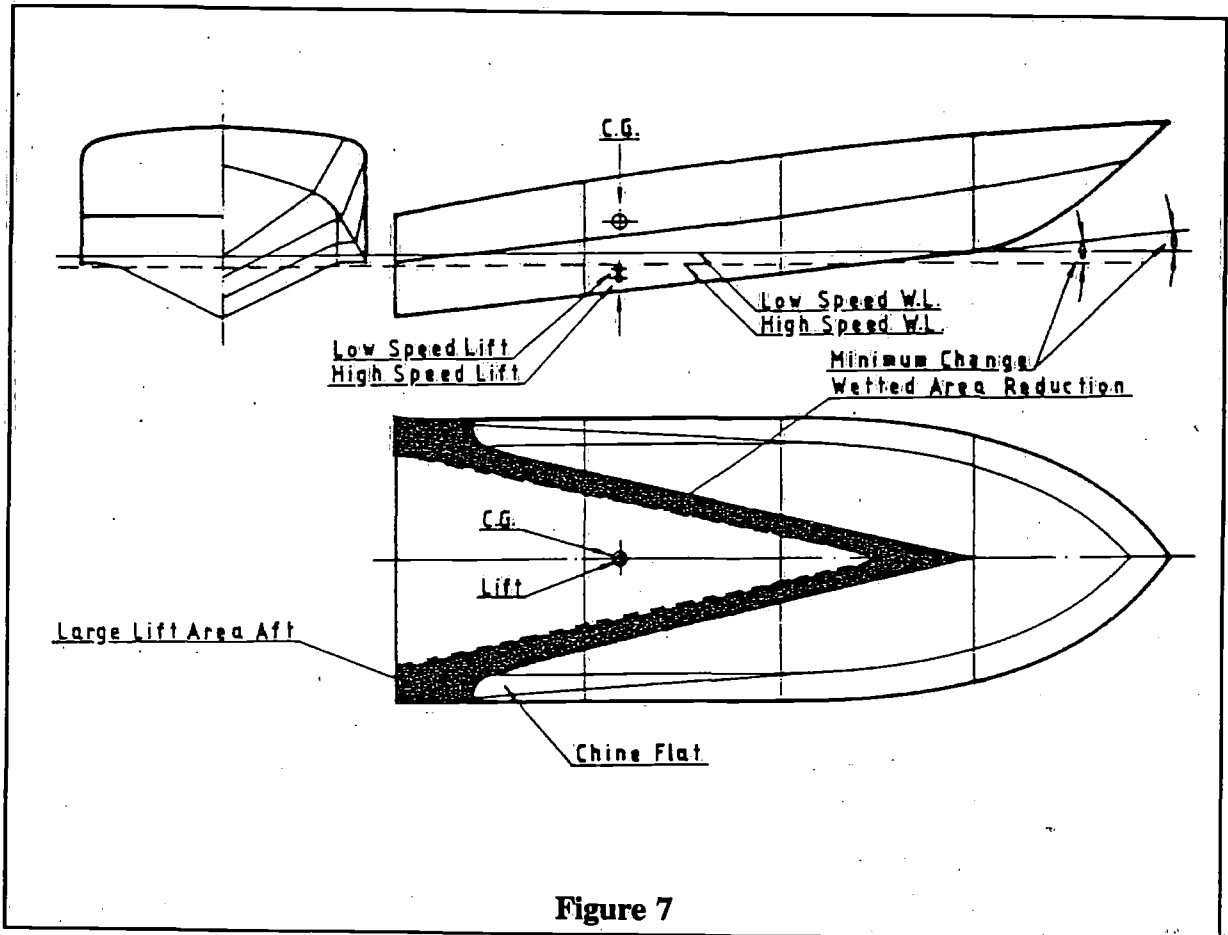


Figure 7

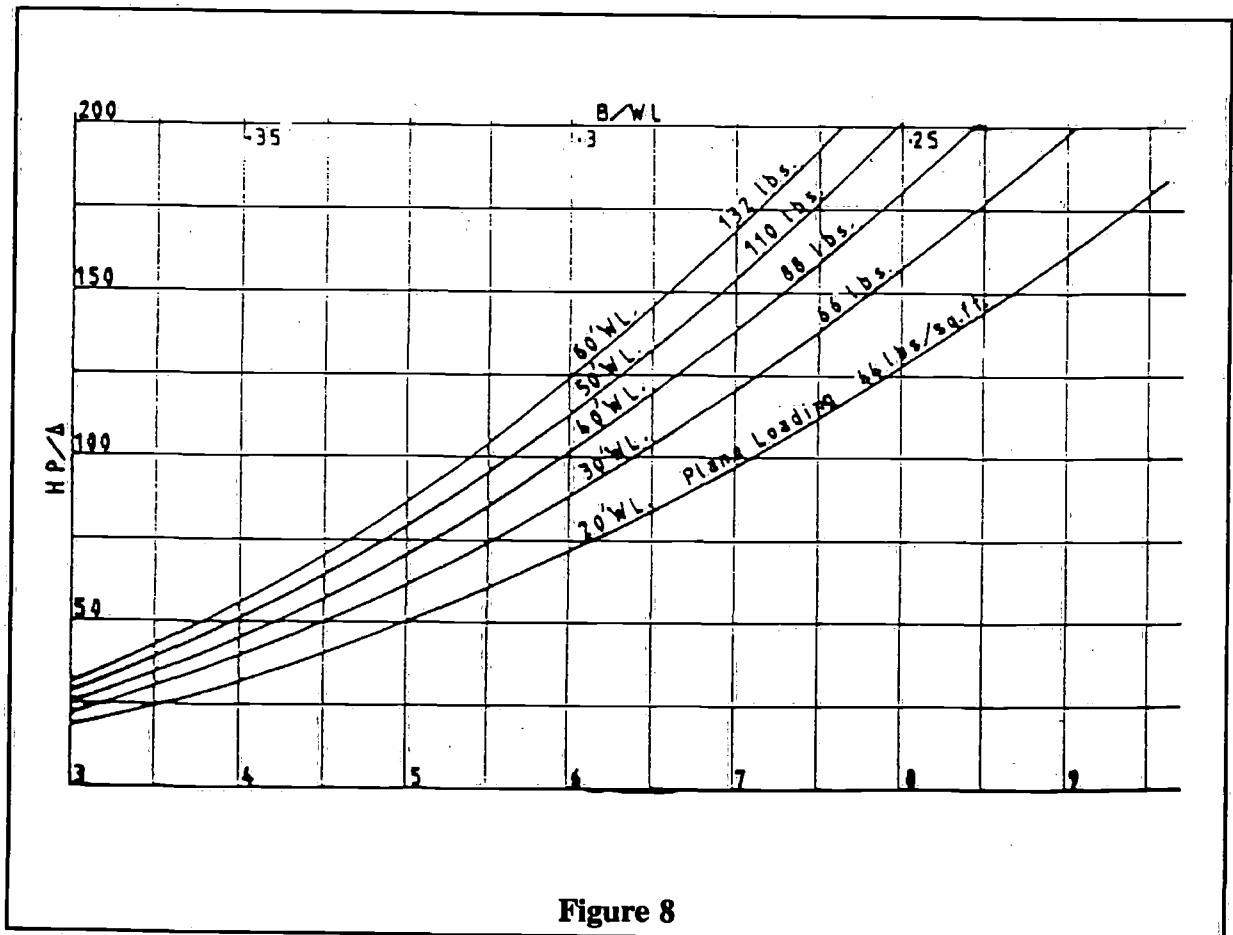
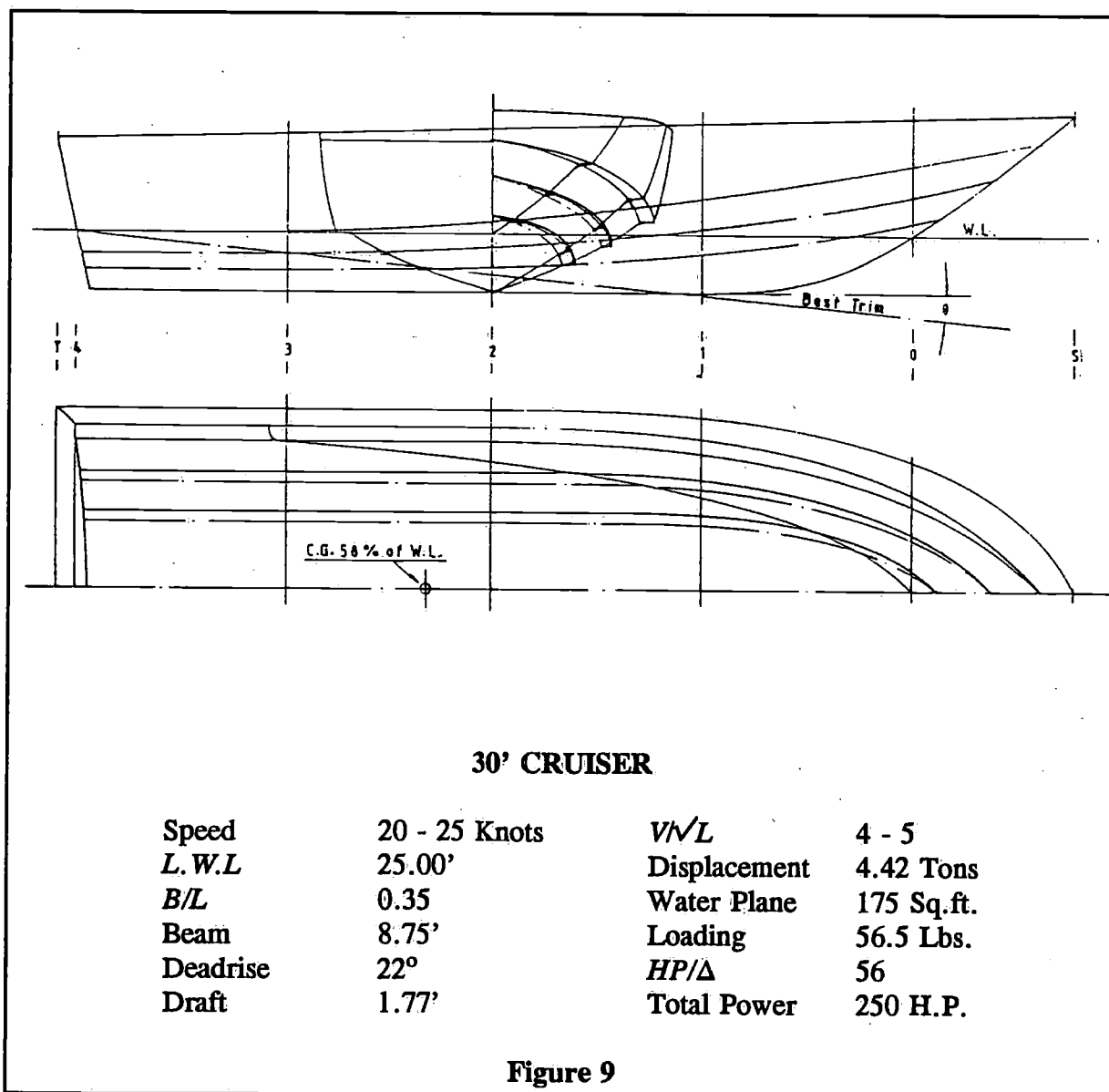


Figure 8

into the rails in the forebody. This will deflect the spray aft, reduce the hardness and avoid the possibility of tripping at high speed.

The water plane and prismatic coefficients will work out at about 0.8 and the longitudinal centre of buoyancy will be located near 60% of the waterline aft of the bows. Trimming such a hull corrects is essential. Broadly, at the low V/\sqrt{L} say to 4, the longitudinal Centre of Gravity should be around 55% of the waterline. At a V/\sqrt{L} of 5 and 6 this should be brought aft to 60% and as far as 70 - 75% for $V/\sqrt{L} > 10$ or more. Power trim (thrust variation possibilities) will be necessary to achieve equilibrium so as to maintain control with *L.C.G.*'s aft of the 75% location. It must be pointed out that whilst these aft *C.G.* positions will give optimum speed, they will make the boat difficult to handle or even dangerous in broken water. For this reason transom mounted flaps are essential, for these have a dynamic correcting effect by shifting the pressure centre further aft and thus holding the bows down. Power trim can also assist in providing this attitude change.

To forecast the performance of a boat similar to the one described above, the following formula will give results which should be accurate to within 2 or 3%:



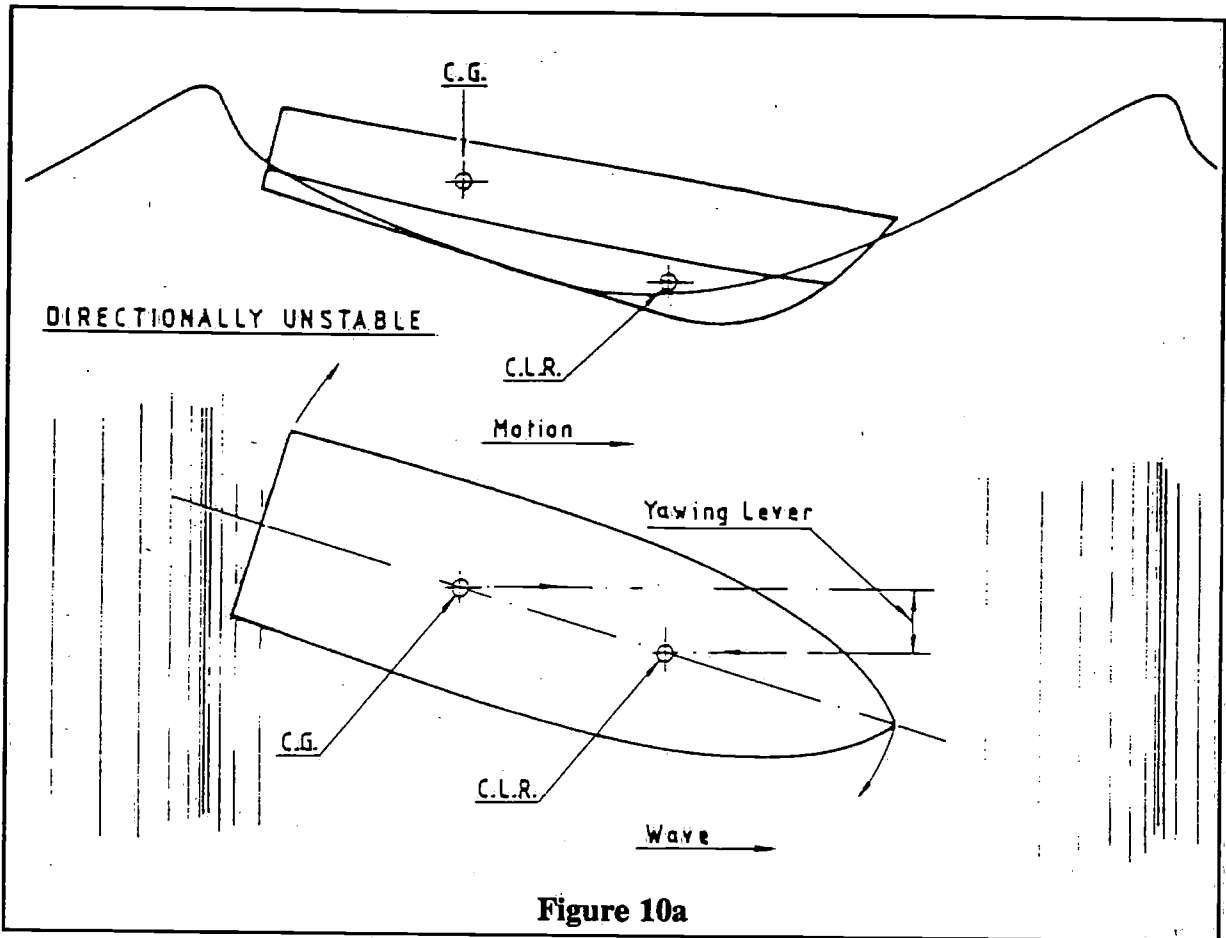


Figure 10a

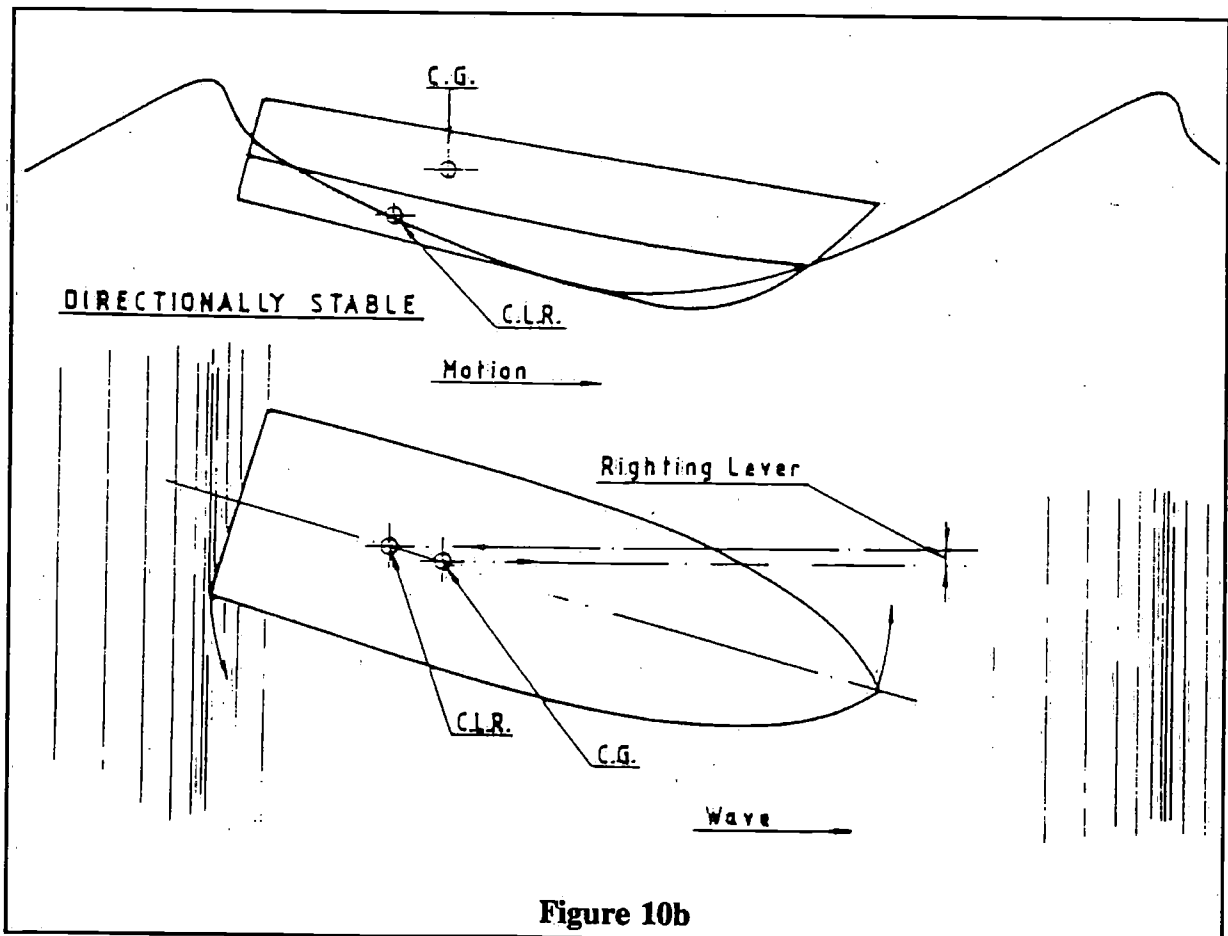


Figure 10b

$$V = L^{.25} K \sqrt{\frac{SHP}{\Delta}}$$

Where: V is expressed in knots, L is the waterline length in feet and Δ is displacement in tons.

K is a propulsion constant which can vary from 1.4 to 1.8.

Here are some examples of K values:

$K =$ Four conventional submerged shafts	= 1.4
Twin conventional submerged shafts	= 1.5
Twin outboards and stern drives	= 1.5 to 1.6
Twin racing stern drives	= 1.8
Twin surface propellers	= 1.8

In the early days of offshore powerboat racing before powertrim was available, front line boats were often designed with rocker in the aft 95% of the running lines, with *C.G.* positions well aft. This was done in an attempt to create equilibrium with high trim angles which gave the least wetted area. To cope with rough water conditions such boats were equipped with water ballast tanks in the extreme bows. Later transom flaps were also adopted to mitigate the behaviour in such circumstances.

Although these early powerboats with conventional submerged shafts had relatively poor top speed potential, they were good in rough conditions. It is perhaps interesting to note that since those days, some twenty years ago, top speeds have doubled, but little impression has been made on improving rough water performance. Certainly no breakthrough has taken place since then in this respect.

The conditions which limit high speed in adverse sea conditions depend largely on two main factors, both of which to some extent are interrelated. The first is the acute slamming which can occur when navigating against oncoming waves. The second is the loss of directional stability which may happen when running with the wave pattern. In either case the intensity of these occurrences will depend upon the speed of the craft, the state of the sea compared to the size of the vessel and the direction in which it is travelling relative to the wave.

The worst conditions occur when proceeding at high speed head on into steep seas and flying off the crest of one wave in to the trough of the next. Such manoeuvres produce very high vertical acceleration which can lead eventually to structural damage or even physical injury. To avoid these dangers one should bear away so as to take a course diagonal to the wave and alter speed as necessary. A bow down trim such as would be possible with the application of flaps, coupled with generous deadrise in the pounding area, will do much to alleviate the otherwise intense discomfort. On the otherhand the V in the forebody should not be too accentuated such as to produce fore and aft imbalance. This will result in the loss of directional stability when running down the steep leeward side of a wave. Speed builds up as the craft slides down the slope, in the trough a rapid slowing down takes place as the bows bury into the next oncoming wave. The fine forefoot produces little hydrostatic or dynamic lift but offers a large lateral area increase which causes a forward shift in the centre of lateral resistance. (See Figure 10a and b). This coupled with the *C.G.* position aft produces a yawing

moment which overcomes the rudder correcting force. The boat veers to port or starboard and in extreme conditions the broach can be violent producing dangerous effects, including the possibility of a capsize. The "spinout" phenomena which front line racing boats are sometimes associated with can also be explained in this way.

The recent past has shown steady progress in planing craft performance. Better design practice has been a contributing factor, though more efficient machinery coupled with improved propulsion systems and availability of new materials have played a big part.

The introduction of new turbo diesels with power to weight ratios approaching petrol engines has made it possible to maintain high speeds and at the same time to reduce running costs considerably. A side from the obvious fuel price advantage, the economy in consumption of the diesel, about one third less than petrol, offers a further bonus in reducing the weight of fuel carried. This is of great benefit when long range is considered.

Innovations in propulsion systems are also contributing to improving performance. In the stern drive category more attention is being paid to fairing the underwater units so as to reduce appendage drag and increase propeller efficiency. More outdrives are available today with "power tilt", this variable thrust facility has done a great deal in permitting boats to be trimmed out to their best advantage. Recent trials carried out on a standard series craft fitted with a new counter rotating stern drive showed something approaching a 10% increase in speed over the conventional mode.

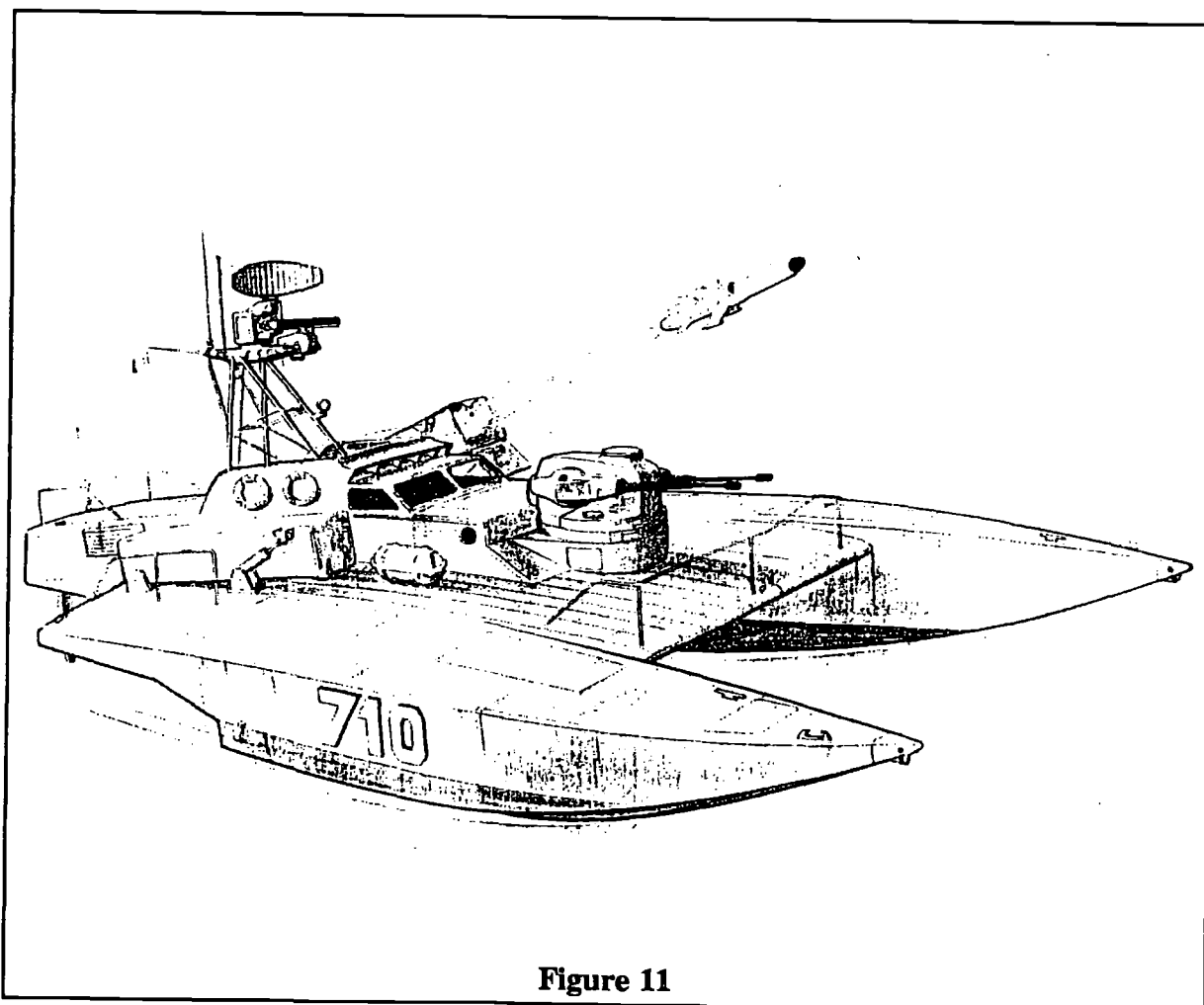


Figure 11

Although surface propulsion first appeared on a production boat over 12 years ago, it is only in the last few years that it has been gaining popularity. The enormous reduction or almost eliminatic of appendage drag that this method offers is the obvious system of transmission for high speed. To quote an example, a 31 foot waterline fast commuter, powered with a total of 750 HP and fitted with twin submerged propellers, did a maximum speed of 41.5 knots on trials. A similar vessel of the same weight with identical engines and surface propellers did close to 50 knots.

This represents a 20% increase in speed due almost entirely to the appendage resistance. Or looked at another way, a further 350 HP or 47% of the original power would have been required to achieve 50 knots with the conventional drives. It is easy to understand that at higher speeds the appendage drag will amount to over half the total resistance. It is also revealing that each shaft line in this case accounts for 175 HP!

Structures are another area where interesting advances can be made to obtain the best strength to weight ratio. Arguably the most suitable structures for these craft could seem to point to monocoque or semi-monocoque types. The reason for this is that extremely high local pressures occur under the bottom of these boats. Resistance to deformation with panel loading is one of the main considerations. For such applications thick light weight panels are best indicated. Laminated timber construction with low density cores have been hard to beat in providing a rigid light weight shell. Even sophisticated metal structures have tended to suffer from deformation which produces the egg-box effect. Various types of glass reinforced plastic hulls have been successful, although their weights were comparable with laminated timber. Today with carbon fibres and Kevlars, well-engineered around foam sandwiches of varying thicknesses, structures can be produced with up to a 30% saving in weight.

On the future of Veed monohull designs, as far as pure speed is concerned it would seem that the limit is in sight. The very narrow planing width on which these boats are now travelling makes lateral stability precarious. Another factor, which is perhaps more inhibiting, is that of maintaining longitudinal equilibrium at the best trim angle on such a short waterline with the thrust as a balancing Force. A stepped nonohull would overcome this but very likely increase the wetted area. In any event this would not eliminate the lateral tenderness.

Recent offshore powerboat race results, when the weather has permitted, have shown the net superiority of catamarans, or tunnel hulls as they are sometimes known, which rely on a good measure of aerodynamic lift for their success. In rough water fast craft spend a good deal of time totally airborne and catamarans are no exception. Upon reentry the forces that build up even under a well Veed mono-hull can be extremely high. In the catamaran there are large flat or near flat surfaces between the hulls which are exposed to the oncoming waves with relatively low clearance. It is not surprising in these circumstances that these areas aft under the tunnel are subjected to intense pounding which eventually leads to structural failure. It must also be said that the twin hull geometry is not the easiest of structures to engineer so that it holds together in the high stress portion of the stern. Because of such shortcomings this type of hull in its present form has given disappointing results in rough weather.

About ten years ago I designed a class II offshore racing powerboat which made use of aerodynamic lift but at the same time tried to overcome the rough water drawbacks of the conventional multihulls. An inverted tricycle configuration was adopted. This consisted of a rectangular aerofoil platform with twin hulls forward and a central hull aft which housed the two crew and single 550 HP engine. The reasoning behind this strange layout was simple; the air-lift would be provided by the Y tunnel and the high pounding area would be eliminated by

the central hull. The craft was driven by a single surface propeller and steered with a deep blade rudder of wedge section. Photo 2.

Technically the design was most successful proving superior to monohulls of similar power, both in calm and rough conditions. It was slower than the catamarans in the smooth water, which was expected since the aerodynamic lift was inferior due to the obstructed tunnel. This boat gained a world speed record of 125 km/hr for its class. Unfortunately mechanical failure plagued the craft throughout its racing career, though it won the only race it completed.

Looking to the immediate future, it seems to me that a vessel embodying the principals I have just described would offer many noteworthy advantages over existing craft for high speed offshore. The artistic impression of an 80 foot military version, Figure 11, illustrates the type of vessel I have in mind.



Photo 2 35' Class II Offshore Racer. Inverted tricycle geometry with aerodynamic lift properties. Top speed is 67.5 knots.
Note: Surface propeller and deep blade rudder for control.

Advanced materials for yacht construction

by A. Cocquyt

AMTEC N.V.

Summary

The lecture deals with different available composite materials and how they are used in yacht construction. Properties and advantages as well as disadvantages of these materials are discussed and confronted with those of other commonly used yacht materials.

Different structure techniques, namely sandwich and single-skin technique, are also discussed and compared.

Finally a short discussion on structural research, illustrated by some examples, is given.

Contents

- 1 Introduction.
- 2 Growing use of F.R.P.- materials in yacht construction.
- 3 Used materials and their properties.
- 4 Single-skin versus sandwich.
- 5 Structural research: necessary?
- 6 Final remarks.

1 Introduction

There's no field into which advanced composite materials have been more rapidly and readily expanded or accepted than the field of high-performance yacht-building.

This consequently has had an enormous impact on the yards using this materials. In the early stage the only problem was to use G.R.P. or steel. Nowadays however F.R.P. itself has diversified so greatly that a one-line approach would make a yard run aground immediately.

To construct reliable high-performance yachts material properties have to be known quite exactly. It must be noted that figures, provided for by industry, must be handled with caution and that, in certain circumstances, it can be usefull to run a series of material tests.

In view of the still developing materials, construction techniques have to be updated continuously. This makes it almost necessary for a yard to run an intensive research program if it wants to remain state of the art.

2 Growing use of F.R.P.- materials in yacht construction

When we look at the many excellent characteristics that F.R.P.- materials have to offer it's only normal that their use as a construction material is still increasing. High strength to weight ratio, ease of maintenance and repair, durability and resistance to the marine

environment, toughness, non-magnetic and dielectric properties and low thermal conductivity are some of the many advantages of the use of F.R.P.- materials. The most important reason however for their growing application is that they are far more flexible both to design and to process than conventional metals. As for design the orientation of fiber reinforcement can be chosen so to suit specific structural requirements, making the structure lighter and more efficient. As for the production process on the other hand, many costly secondary assembly processes are eliminated. (e.g. welding or riveting).

In the early stage however, i.e. after W.W. II the use of F.R.P. was very limited. Their advantages were poorly distinguished, mainly for the following reasons:

- technical knowledge of the material was very limited F.R.P.- builders still didn't think in terms of composites. They only applied rules of steel construction to F.R.P.- construction. No need to say that this led to erroneous structural concepts.
- poor quality products, as made by many low skilled manufacturers made vanish the already low confidence regarding these new materials.
- last but not least the conservative thinking of many steel builders obstructed greatly the growth of the F.R.P.- shipbuilding industry.

As for this latest argument however, opposite reasoning can also be considered. By rejecting the use of F.R.P.- materials, although several reports (see for example [1]) clearly pointed out the advantages of their application even for superstructures in large ships, steel builders promoted the separation of a new totally independent F.R.P.- shipbuilding industry. This industry started building yachts that were completely made out of G.R.P.

Indeed, in the early stage, some disastrous decisions were taken but, as a matter of fact, this separation led to the high-tech composite building yards as we know them today.

To understand more the astonishing aspect of this development a comparison with aviation industry is uttermost revealing. Manufacturers in this area approached the F.R.P.- business in a totally different way. They started using this new materials in very small quantities, thus giving F.R.P. a chance to develop inside the big aviation industry.

Today also approach of aviation industry to the F.R.P.- business is still different from that of yacht industry. There's no discussion that today, anyone who should want to build a Boeing 747 completely out of F.R.P.- materials would be advised to go to a psychiatrist as soon as possible.

3 Used materials and their properties

Before going into detail on the properties of the different types of resins and fiber reinforcements used in yacht construction, a comparison between F.R.P. and other commonly used yacht materials is interesting to be made.

The decision on which material to use for a yacht seldom involves an objective analysis. No "straight-line" reasoning can be expected if one knows that both customer and designer are prejudiced and prefer certain materials or production systems; that each manufacturer proves his material to be the best one by overwhelming the decision makers with non realistic figures and that last but not least most yards are capable to work with only one type of material.

In the following however we will try to make an objective comparison between different

construction materials. Figures that are mentioned in the different tables should only be considered relative to each other unless dimensions are mentioned as well. Data are taken from references [2] and [3].

Table 1 lists the acquisition cost comparison for the different materials. Exact calculation of this quantity can be found in [3].

As for the ownership cost statistical data on F.R.P. - craft are very scarce. However, several yachts in fiberglass have proven to have a durability that is higher than the average value for other materials. With regard to maintenance requirements and ease of repair F.R.P. offer fundamental advantages. Except for a periodic inspection no maintenance is required and repair can be done by low skilled or even unskilled workers using ordinary hand tools.

Tables 2 and 3 are a summary of the engineering properties of the most common boatbuilding materials. Table 4 is in a way deduced from Tables 2 and 3 (see [3]) and gives a structure comparison.

In this Table, for F.R.P., the properties of fiberglass are taken and applied to a single-skin structure. A complete discussion of this figures is beyond the scope of this lecture but following things can be marked. On the basis of strength and stiffness alone, F.R.P.- materials do not have a clear advantage particularly when it is noted that their elongation to fracture is much lower than metals with comparable strength. The advantages of composite materials appear when their high modulus and high strength per unit weight are considered, thus meaning considerable weight saving is possible for structural components.

This high strength to weight ratio, combined with a high stability in the marine environment and high durability under service conditions makes F.R.P. an excellent tool for boat construction. However, one has to remain realistic. Figure 1 for example [1] gives the construction cost for a large GRP cargo vessel compared with that for a steel one. Although the same reference mentions possible cost and weight savings when G.R.P. is applied to certain superstructures of large ships, it is clear that a much more promising area is the area of small ships and certainly the area of the high performance yachts. Several disadvantages as there are high material cost, low resistance to major impact, lower Young-modulus exist but probably the most dangerous point is that F.R.P.- materials have to be fabricated on the yard. If this process is not optimised, many, if not all, advantages will vanish.

We will now have a closer look at the properties of the different F.R.P.- materials used for yacht construction. Data are from ref. [2] and [4].

Resin-systems

Unsaturated alkylstyrene type polyesters have found wide use in marine applications. Since a few years however more and more vinyl ester resins and epoxy resins are used, especially when it comes to high-performance applications. Table 5 lists typical properties of the three systems used.

Polyester resins offer a greater flexibility with regard to handling and curing characteristics and are less costly than the other resin types. Variation of resin/hardener ratio and of the curing cycle from optimum values however will influence final mechanical properties of the cured resin.

The curing cycle for polyester as well as vinyl ester resins is started by adding a catalyst/accelerator. In marine applications these types of resin are only used for hand lay-up

Table 1. Boatbuilding materials cost comparison

	5086 Aluminium	Ferro- cement	Mat/W.R. Composite Glass + Polyester	All woven Roving Glass + Polyester	Steel	Solid- mahogany
Material cost index	100	20	64	72	26	33
Structural weight index*	49	104	55	52	100	105
Structural cost index	100	42	72	76	53	71

* Based on weight for "equally sound" structure (see Table 4)

Table 2. Engineering properties of boatbuilding materials (continued in Table 3)

	Density <i>Mg m⁻³</i>	Young's modulus <i>GN m⁻²</i>	Tensile strength <i>MN m⁻²</i>	Elongation to fracture %
High strength Al-Zn-MG alloy	2.00	72	503	11
Steel	7.85	207	2050 - 600	12 - 28
Solid Mahogany	0.54	10	88	-
Ferrocement	2.40	10	25	-
Glass fiber polyester-U.D., $V_f=0.5^*$	1.93	38	750	1.8
Carbon fiber epoxy-U.D., $V_f=0.6^*$	1.62	220	1400	0.8

* Properties in the direction parallel to the fibers

Table 3. Engineering properties of boatbuilding materials

	Specific Youngs modulus <i>GN m⁻²</i>	Specific tensile strength <i>MN m⁻²</i>
High strength Al-Zn-MG alloy	25.7	180.
Steel	26.4	261 - 76
Solid Mahogany	18.5	163
Ferrocement	4.2	10.4
Glass fiber polyester-U.D., $V_f=0.5^*$	19.7	390
Carbon fiber epoxy-U.D., $V_f=0.6^*$	135	865

* Properties in the direction parallel to the fibers

Table 4. Comparison of small craft structures

	5086 Aluminium	Ferro- cement	Mat/W.R. Composite G.R.P	All woven roving G.R.P	Steel	Solid Mahogany
Thickness for equal def.	1.43	2.84	2.85	2.47	1.0	2.84
Thickness VS safe bending stress	1.04	4.38	1.04	0.98	1.0	1.84
Weight for "equally sound" structure	49	100	55	52	100	75
Relative minor damage resistance	362	200		3800	100	570

processes. First the resin is catalysed and then applied with layers of (mostly) fiberglass cloth to a mold using a roller. When needed, thixotropic agents may be added to minimize resin run-off.

Epoxy resins on the other hand are required when superior mechanical or physical properties are needed. Whereas polyester resins can be cured at room temperature with no significant loss of mechanical properties, for epoxy resins however, it is highly advised to apply the recommended heat cycle as close as possible. This curing cycle is started by adding what is called a curing agent.

As for epoxy as a matrix material the most common processing method used for yacht construction is hand lay-up. Some yards however are starting to use the more advanced prepreg-technique. Prepreg stands for preimpregnated fibers, indicating that fabrication occurs in two distinct stages. The first stage is the production of a sheet or tape of fibers impregnated with resin that is partially cured to produce a flexible aggregate with excellent alignment of the fibers in unidirectional layers and an exactly known and controllable fiber-resin ratio. The second stage is to stack up different layers of prepreg on a mould, consolidate it by pressure or vacuum and heat it up to achieve the final cure.

A comparison between the three resin systems leads to the following conclusions. Epoxy resins offer excellent adhesion qualities. Those of vinyl ester resins are much worse and those of polyester are rather poor. When it comes to weight saving there is no way but to go for epoxy resins. Epoxy resins also offer the best mechanical properties i.e. higher tensile strength and higher tensile modulus. Also concerning elongation to break, shrinkage on curing, fatigue, durability in a marine environment, epoxy resins offer outstanding properties in comparison with the other resin systems. When it comes to cost however epoxy resins are almost twice as expensive as polyester or vinyl ester systems. When the total price of the resin is of second importance in comparison with the other costs, as is the case for a high-performance yacht, epoxy certainly is the best choice.

Fiber-reinforcements and composites

Dealing quite exclusively with performance oriented yachts, only fiber-epoxy composites will be considered when laminate properties are mentioned. Those properties will only be looked at in a very general way. Reason for this is that there's a mass of different materials and data available so that by only presenting a few of them one can grossly misrepresent the case.

At the present time borosilicate type "E" glass fibers are used for most yachts. In the area of high-performance yachts however there is high interest in higher modulus fibers, such as graphite, boron or aramid (Kevlar). Those fibers offer superior mechanical properties combined with even less weight (Table 6). Boron is almost solely applied in aerospace structures and will therefore not be considered further.

Two types of fiberglass are used as reinforcement materials, namely E-glass and R-glass. Typical properties of both are shown in Table 8. The R-type obviously has better mechanical characteristics than the E-type. The cost however is five times as high which is the reason that in 90% of the cases, E-glass is used.

Two types of aramid fibers were developed by Dupont de Nemours of which almost only the Kevlar 49 type is being used in marine applications. Kevlar 49 offers a higher tensile strength and impact strength than other fibers. It can be used in structures that have to be light, strong and stiff as well as in highly stressed structures.

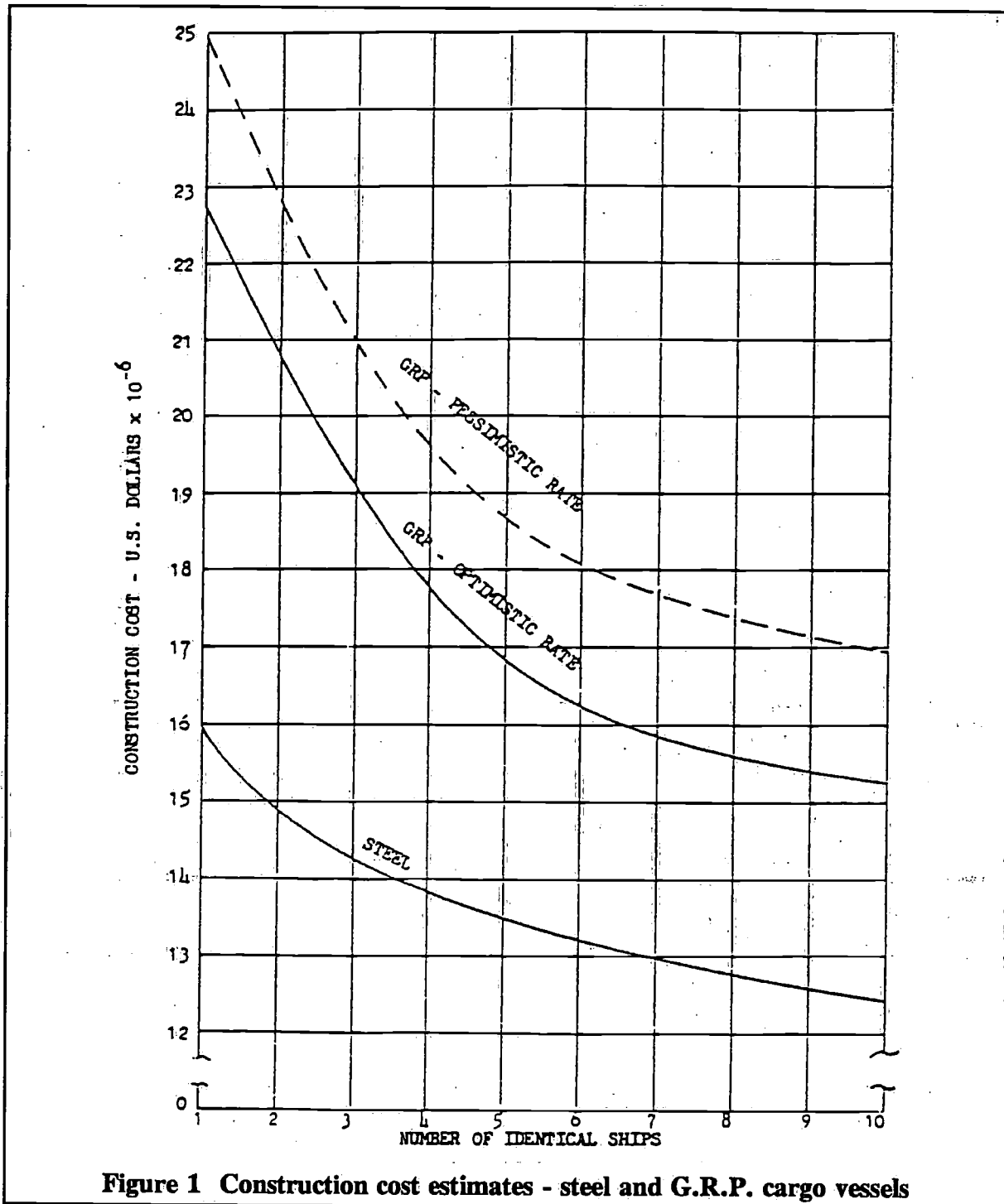


Figure 1 Construction cost estimates - steel and G.R.P. cargo vessels

Table 5. Typical properties of polyester, vinyl ester and epoxy resins

		Polyester	Vinyl ester	Epoxy
Density	$Mg\ m^{-3}$	1.2 - 1.5	1.1 - 1.3	1.1 - 1.4
Young's modulus	$GN\ m^{-2}$	2.0 - 4.5	3.0 - 3.3	3 - 6
Poisson's ratio		0.37- 0.39	0.4	0.38- 0.4
Tensile strength	$MN\ m^{-2}$	40 - 90	80	35 - 100
Compressive strength	$MN\ m^{-2}$	90 - 250	100 - 200	100 - 200
Elongation to break	%	2	4.4 - 5.5	1 - 6
Shrinkage on curing	%	4.0 - 8.0	4 - 8	1 - 2

Carbon fibers were originally developed for application in aerospace structures. Since a few years however their use in highperformance yachts is firmly growing. Reason for this is their extremely high modulus and strength per unit weight, combined with excellent fatigue and vibration characteristics. Carbon fibers therefore are mostly used as stiffeners in hulls or masts. Only when extreme priority is given to high performance and low weight, carbon fiber composites are used as a hull material.

Tables 7 and 9 list several physical and mechanical properties of the different fiberepoxy composites used in yacht construction. It can be noted that E-glass must not be used where high tension is expected. A more critical aspect for yachts however is the hull stiffness. It is here that carbon fiber composites come in as stiffeners in bulkheads, framing and hull. When it comes to compression it can be seen that kevlar has rather poor properties and therefore must not be used in places where large compression values are expected! As already mentioned kevlar possesses excellent impact characteristics. Carbon on the other hand has rather poor impact resistance and should therefore not be used without kevlar reinforcement in places near the bow where high slamming pressures may occur.

Fiber-fabrics are available in several varieties as there are chopped strand mats (only for glass fibers), ravings, woven rovings and UD's (unidirectional fibers). More information on weaving techniques can be found in specialized literature. It be noted that there are a variety of weave patterns each to meet specific design or construction needs. For high-performance yachts only woven ravings and UD's are used.

Special woven forms are the so-called hybrid fabrics. They are a combination of different types of fibers, thus at the same time lowering cost and improving properties. For example a carbon-kevlar hybrid, to get the high carbon-stiffness and at the same time the excellent kevlar-resistance to impact. Some properties of a typical hybrid composite are shown in Table 11.

Finally, a relative cost comparison is shown in Figure 2. A standard fabric of 200 g/m² is considered. The indicated values are selfexplaining

Table 6. Typical properties of high-modulus fibers

Fiber Material	Variety of fibers available	Range of properties			
		Tensile strength ksi (MPa)	Young's modulus msi (GPa)	Density lb/in. (g/cc)	Costs* \$/lb (\$/kg)
Glass	4	500 - 600 (3400 - 4100)	10 - 12 (69 - 83)	0.092 (2.549)	0.7 - 6 (1.54 - 13.2)
Boron	2	400 - 500 (2700 - 3400)	55 (379)	0.092 - 0.098 (2.549 - 2.715)	180 - 225 (396 - 495)
PRD 49-III	3	400 - 430 (2700 - 2900)	12 - 19 (83 - 130)	0.05 (1.385)	20 (45)
Graphite	26	200 - 470 (1400 - 3200)	20 - 75 (138 - 517)	0.054 - 0.071 (1.496 - 1.967)	20 - 200 (45 - 450)

* For 100 lb (45.36 kg) quantities in 1981.

Table 7. Physical properties of typical marine laminates

Physical property	Chopped strand mat laminate, low glass content	Composite laminate, medium glass content	Woven roving laminate high glass content
Percent glass by weight	25 - 30	30 - 40	40 - 55
Specific gravity	1.40 - 1.50	1.40 - 1.50	1.65 - 1.80
Flexural strength psi x 10 ³ (MPa)	18 - 25 (124-172)	25 - 30 (172-207)	30 - 35 (207-241)
Flexural modulus psi x 10 ⁴ (GPa)	0.8 - 1.2 (5.5-8.3)	1.1 - 1.5 (7.6-10.3)	1.5 - 2.2 (10.3-15.2)
Tensile strength psi x 10 ³ (MPa)	11 - 15 (76-103)	18 - 25 (124-172)	28 - 32 (193-221)
Tensile modulus psi x 10 ⁴ (GPa)	0.9 - 1.2 (6.2-8.3)	1.0 - 1.4 (6.9-9.7)	1.5 - 2.0 (10.3-13.8)
Compressive strength psi x 10 ³ (MPa)	17 - 21 (117-145)	17 - 21 (117-145)	17 - 22 (117-152)
Compressive modulus psi x 10 ⁴ (GPa)	0.9 - 1.3 (6.2-9.0)	1.0 - 1.6 (6.9-11.0)	1.7 - 2.4 (11.7-16.5)
Shear strength perpendicular psi x 10 ³ (MPa)	10 - 13 (69-90)	11 - 14 (76-79)	13 - 15 (90-103)
Shear strength parallel psi x 10 ³ (GPa)	10 - 12 (69-83)	9 - 12 (62-83)	8 - 11 (55-75)
Shear modulus parallel psi x 10 ⁴ (GPa)	0.4 (2.8)	0.45 (3.1)	0.5 (3.4)

Table 8. Typical properties of E- and R-glass fiber grades

		E-grade	R-grade
Density	MG m ⁻³	2.54	2.48
Tensile strength	MN m ⁻²	3500	4600
Young's modulus	GN m ⁻²	72.4	85.5
Elongation to break	%	4.80	5.70

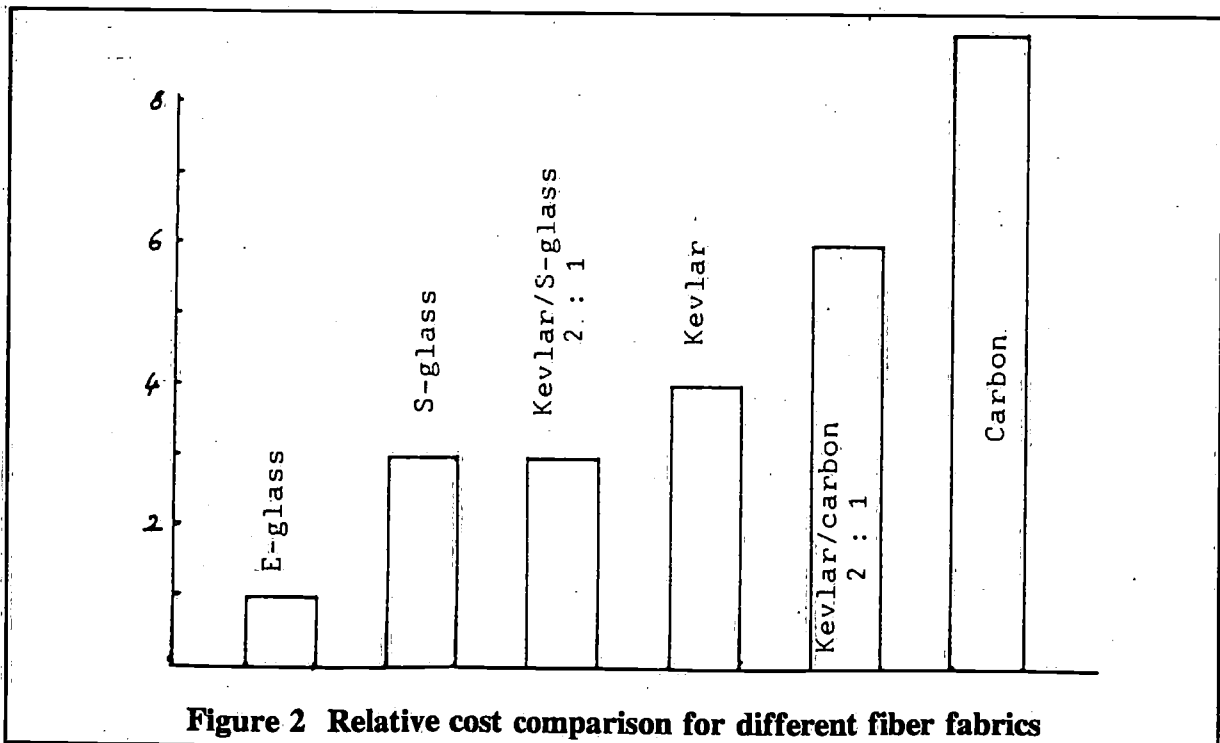


Figure 2 Relative cost comparison for different fiber fabrics

Table 9, Mechanical properties of some structural materials

Material	Young's modulus E, psi x 10 ⁶ (GPa)	Ultimate tensile strength σ , psi x 10 ³ (MPa)	Density ρ , lb/in. ³ (kg x 10 ³ /m ³)	Specific modulus E/ ρ , in. x 10 ⁸ (m x 10 ⁷)	Specific strength σ/ρ , in. x 10 ⁶ (m x 10 ⁶)
E-glass fiber*	10.5 (72.3)	460 (3170)	0.092 (2.55)	1.1 (2.8)	5.00 (1.24)
S-glass fiber*	12.0 (82.7)	600 (4130)	0.090 (2.50)	1.3 (3.3)	6.66 (1.65)
E-glass in epoxy	7.5 (51.7)	200 (1380)	0.070 (1.94)	1.1 (2.8)	2.86 (0.71)
S-glass in epoxy	7.5 (51.7)	300 (2070)	0.070 (1.94)	1.1 (2.8)	4.29 (1.07)
Aramid fiber*	20.0 (137.8)	500 (3445)	0.060 (1.69)	3.3 (8.1)	8.33 (2.04)
Aramid in epoxy	12.0 (82.7)	280 (1930)	0.055 (1.40)	5.9 (3.6)	5.09 (1.38)
HM graphite fiber*	55 (379)	300 (2070)	0.069 (1.90)	7.8 (19.8)	4.3 (1.09)
HT graphite fiber*	35 (241)	350 (2410)	0.064 (1.77)	5.6 (14.2)	5.5 (1.36)
AS or T-300 fiber*	30 (207)	400 (2760)	0.067 (1.85)	6.0 (11.2)	6.0 (1.49)
HM graphite in epoxy	30 (207)	135 (930)	0.058 (1.61)	5.2 (13.2)	2.3 (0.58)
HT graphite in epoxy	22 (152)	205 (1410)	0.054 (1.50)	4.1 (10.4)	3.8 (0.94)
AS or T-300 in epoxy	17 (117)	230 (1580)	0.056 (1.55)	4.1 (10.4)	4.1 (1.01)
Boron filaments*	60 (413)	400 (2760)	0.095 (2.63)	6.3 (16.0)	4.2 (1.05)
Boron in epoxy	31 (193)	220 (1520)	0.075 (2.08)	4.1 (10.4)	2.9 (0.73)
Maraging steel	28 (193)	300 (2070)	0.289 (8.00)	0.97 (2.5)	1.0 (0.26)
Aluminium 7075	10 (68.9)	82 (656)	0.100 (2.77)	1.00 (2.5)	0.8 (0.20)
Titanium 6Al-4V	15 (103)	155 (91070)	0.155 (4.29)	0.97 (2.5)	1.0 (0.25)
Beryllium	35 (241)	90 (620)	0.066 (1.83)	5.3 (13.5)	1.4 (0.34)

* Fibers only: does not include resin.

Note: Fibers and composites are unidirectional. Metals are isotropic

Table 10. Typical mechanical properties of foam and honeycomb core materials

	Density kg/m ³	Compressive strength MPa	Shear strength MPa
Polyurethane foam	21 - 400	0.1 - 13.8	0.14 - 3.1
PVC - foam	48 - 96	0.65 - 1.38	0.45 - 0.83
Al - Honeycomb	16 - 192	0.13 - 14.6	0.22 - 6.55
Nomex - Aramid - paper honeycomb	24 - 144	0.31 - 12.2	0.31 - 6.92

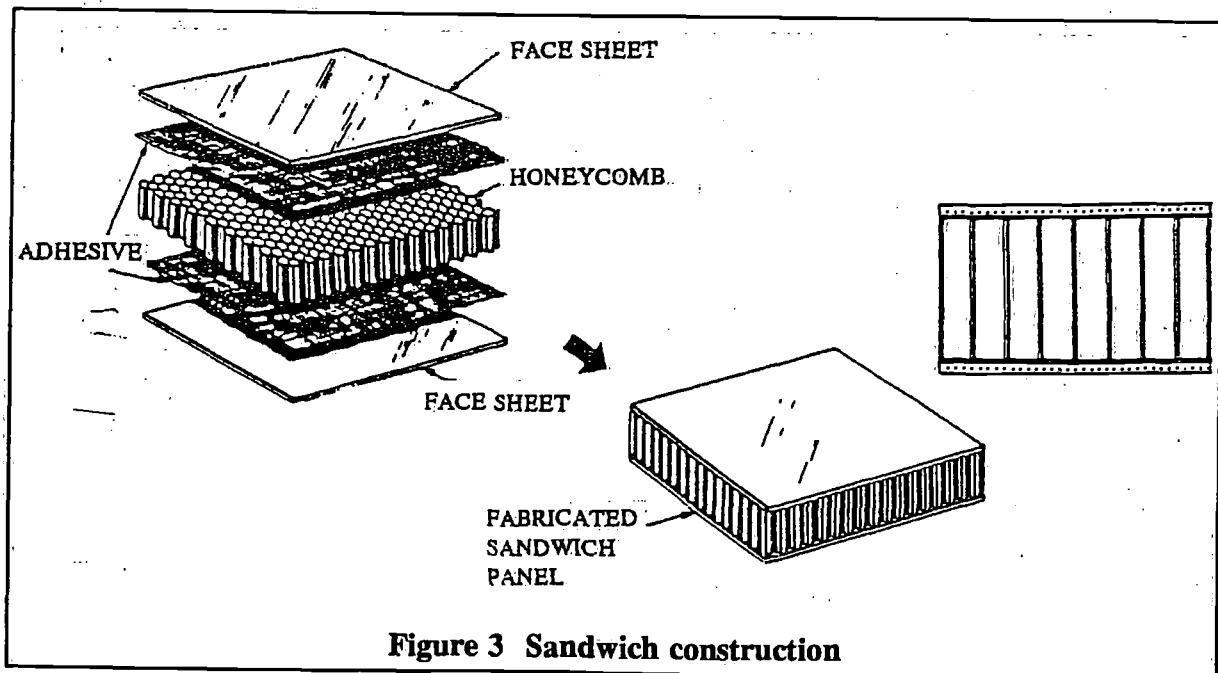


Figure 3 Sandwich construction

**Table 11. Properties of Thornel 300-Kevlar 49/Epoxy Hybrid Balanced Fabric Composites (Nominal 60 Volume % Fiber Content);
Balanced Fabric Contains Equal Number of fiber in the (0-deg) and Fill (90-deg) Directions**

Ratio of Thornel 300 to Kevlar 49 Fibers, %	Resin	Specific Gravity	Modulus		Tensile strength		Compression				Short beam shear strength	
			GPa	(Msi)	MPa	(ksi)	Stress at 0.02% offset		Ultimate stress		MPa	(ksi)
							MPa	(ksi)	MPa	(ksi)		
0/100	Fiberite 934	1.40	35.9	(5.2)	545	(79)	76	(11)	152	(22)	26	(3.8)
50/50	Fiberite 934	1.49	48.3	(7.0)	400	(58)	159	(23)	228	(33)	29	(4.2)
75/25	Fiberite 934	1.47	57.2	(8.3)	434	(63)	221	(32)	317	(46)	32	(4.7)
100/0	Fiberite 934	1.60	60.0	(8.7)	434	(63)	324	(47)	558	(81)	40	(5.8)
50/50	American Cyanamid BP-907	1.44	46.0	(6.7)	434	(60)	165	(24)	290	(42)	48	(7.0)

Table 12. Mechanical properties of Balsa wood when used as a sandwich core

Density			6 lb/ft ³ (96 kg/m ³)		11 lb/ft ³ 176 kg/m ³)		15.5 lb/ft ³ (248 kg/m ³)	
			psi	MPa	psi	MPa	psi	MPa
Shear values	End grain strength	Typically high	500	3.45	1.450	10.0	2.310	15.9
	End grain strength	Typically low	750	5.17	1.910	13.2	2.950	20.3
Tensile values	End grain modulus	Typical	333.000	2275	768.000	5295	1.169.000	8025
	End grain strength	Typically high	84	0.58	144	0.993	198	1.36
Compressive values	End grain strength	Typically low	50	0.34	100	0.689	145	1.0
	Flat grain modulus	Typically high	16.000	110	37.000	255	55.000	379
Tensile values	End grain strength	Typically low	5.100	35.1	13.000	89.6	19.900	137
	End grain strength	Typically high	1.375	9.48	3.050	21.0	4.525	31.2
Compressive values	End grain strength	Typically high	112	0.77	170	1.17	223	1.54
	End grain strength	Typically high	72	0.49	118	0.814	156	1.07
Compressive values	Flat grain strength	Typically low	180	1.24	360	2.48	522	3.59
	Strength	Typically high	158	1.09	298	2.03	425	2.93
Compressive values	Strength	Typically low	16.000	110	37.000	255	55.000	379
	Modulus	Typical						

4 Single-skin versus Sandwich

First the sandwich-technique will be described briefly, followed by a comparison with the single-skin method on processing and building techniques.

To make things clear however a few notes on single skin have to be made. Single-skin construction is quite similar to conventional wood or metal construction. A single thickness of F.R.P. laminate is used which is supported by frames to reduce panel sizes and to provide overall rigidity to the hull. This type of construction is considered the most simple to fabricate.

The purpose of a sandwich construction is to increase the rigidity of a panel by increasing its thickness with relatively little increase in weight. The principle of this is clearly shown in Figures 3 and 4. Two skins are used, separated by a thick, lightweight core that is bonded to the facings by an adhesive. When loaded, one skin will act in compression, the other one in tension. The core resists the compression and transverse shear loads while the adhesive must be capable of transmitting high axial and shear loadings from the facings to the core.

As for the facing materials, there's no substantial difference with the materials already described in the foregoing section so that they will not be discussed here.

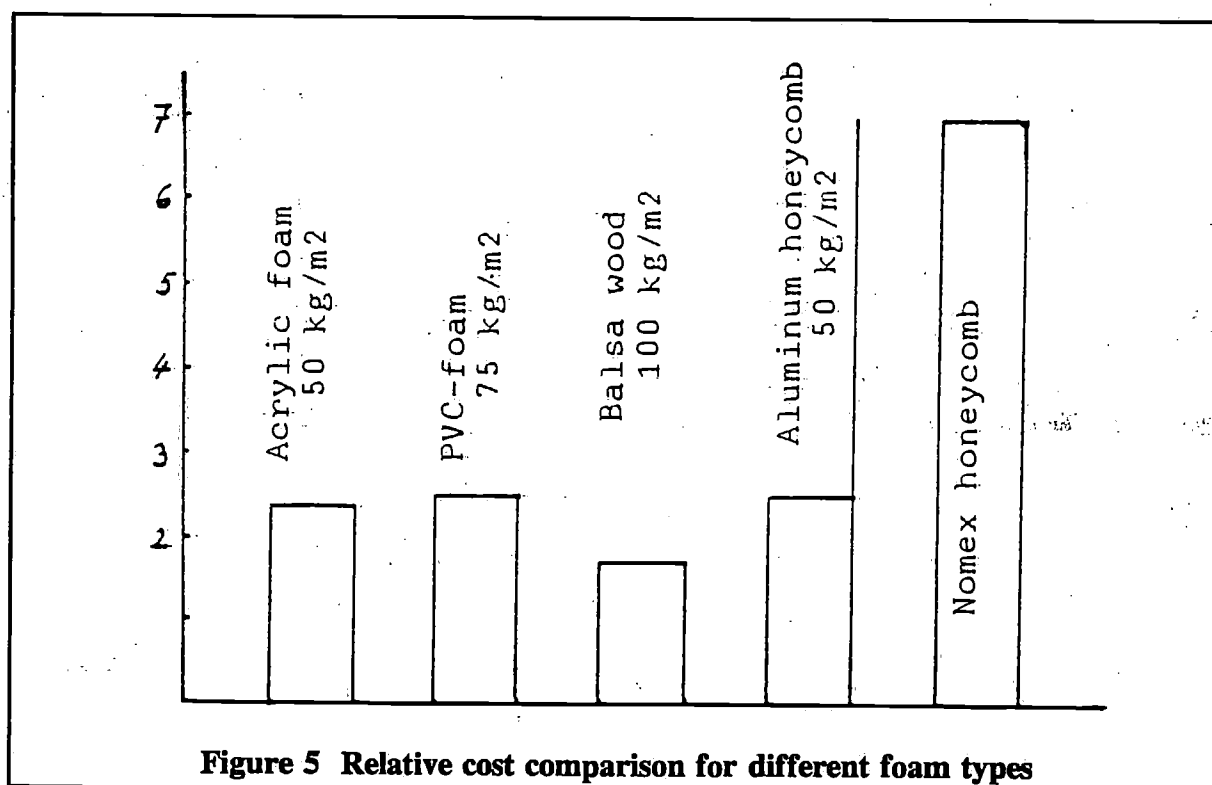
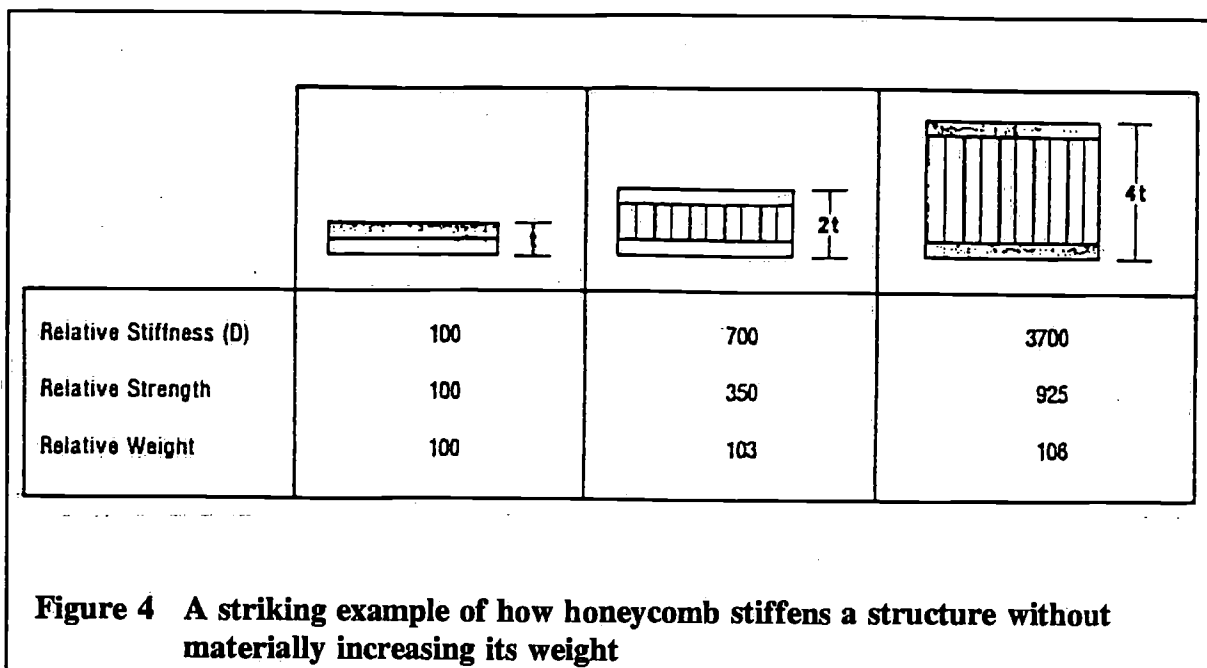
There are mainly three types of core materials used for yacht sandwich construction, namely wood, foam and honey-comb. Representative mechanical properties are listed in Tables 12 and 10. Relative cost is shown in Figure 5.

For wooden cores mostly endgrain balsa is used. It has very good mechanical properties but also a rather high density which obviously is a disadvantage. Also the high resin absorption during curing process is a problem that has to be looked at. Even so, the ease of use and excellent durability of the end product, combined with high compressive strength and modulus has led to sharply increased usage, especially for large hulls when high strength is needed. Since cost of balsa is increasing sharply too, this may become a problem for future applications.

Foam is being widely used as a structural core. Several types of foam exist as there are polystyrene, polyvinyl chloride (PVC), polyurethane and acrylic foams. For each type a broad range of densities is available. The very low cost polystyrene foams nowadays are being used almost only for surfboards. They have a low density, are very easy to shape but their mechanical properties are rather low. As a matter of fact they are not applied for high-performance structures. The same conclusion holds for the polyurethane foams. In spite of their good mechanical properties, problems with existing urethane structures concerning resin-foam bond have resulted in a firmly decreasing use of the polyurethane foams.

The acrylic foams have a high strength and stiffness to weight ratio and, to a certain extent, they are even temperature resistant. They are rather hard to use when it comes to curved surfaces. This is probably the reason why the PVC foams are used more. They combine good mechanical characteristics with good processing characteristics. New developments have led to high-temperature PVC foams that, as a result, can be used with prepreg facings.

For high tech applications, foam and wood have been largely replaced by the more efficient high density (aramid) honeycombs. This is a logical evolution if one looks at the specific needs for a core material and compares them with the excellent properties that honeycombs



have to offer. They have a very high compression strength, a very high transverse shear strength and, above all, they are very light. The two most known types of honeycomb are the aluminium honeycomb and the aramid paper honeycomb. Almost only the aramid one is being used for yacht construction, the aluminium one being much too sensitive to the marine environment. The most important disadvantage of the aramid "Nomex" honeycomb core is its price, being as three times as expensive as the other core materials. On the other hand it is extremely tough and damage resistant; it possesses a unique ability to survive overloads in local areas without permanent damage.

It is obvious that the best characteristics are offered by the honeycomb cores, resulting in an increasing use for high performance yachts. Balsa and foam cores however possess also very good mechanical properties at a considerably lower price!

A discussion of the different adhesive materials is far beyond the scope of this lecture. It be noted though that, when using honeycomb cores, only adhesives with excellent mechanical properties may be taken into account, core-skin contact area being very small.

To end this section, an elementary comparison between single skin and sandwich technique on processing and building methods may be made. As for processing methods there's no substantial difference between the two techniques except for, in the case of sandwich technique, temperature and pressure are required to get a perfect skin to core bond. Different ways of providing this pressure are possible, for example vacuum bagging or autoclave molding.

Hand lay-up techniques are still widely used as a processing method for yacht construction (see Figure 6). For advanced applications however it is highly advised to employ bag molding methods as there are vacuum bag, pressure bag and autoclave molding (see Figure 7). These techniques offer better consolidations and densifications of the lay-ups, resulting in practice in increased inter-laminar bonds, diminutions of voids and removal of excess resin.

Bag molding methods are combined with "wet" lay-up techniques as well as with prepreg techniques, the latter ones undoubtedly leading to superior results, (see Figure 8). As already mentioned the use of prepregs results in an excellent alignment of the fibers in unidirectional layers and in an exactly known and controllable fiber-resin ratio.

As for building methods on the other hand there are several differences between the single-skin and the sandwich technique. Single-skin hulls are generally laid up in a female mold. Since the outer surface takes on the quality of the mold surface, further finishing is unnecessary. In a secondary bonding operation, frames, foundations and decking are installed.

Sandwich skin hulls on the contrary are often laid up over a male plug. Two different procedures exist. In the so-called nomold process first the core material is tacked to a lattice construction; then the outer skin is laid up and cured; hull and lattice construction are separated and the hull is turned over, and finally the inner skin is laid up and cured. In the second procedure, first the inner skin is laid up over the mold and cured; the core is adhered to the inner skin and finally the outer skin is laid up on the core material. Both procedures require considerable work to achieve a smooth outer surface.

Much has been said on whether sandwich or single-skin technique gives best results. Single skin is generally cheaper and all the laminate is in the outside skin of the hull, where it can resist the local impact abuse encountered in service. It probably is the most simple type of construction to fabricate, certainly in the case of sailyachts when relatively little framing is needed. Construction of sandwich panels is generally more difficult because of the steps necessary to ensure a good bond between the skins and core. But, for equal stiffness, a sandwich panel will be both lighter and less space-consuming because no framing is needed.

One can continue reasoning. It is my opinion however that none of both techniques is the best one. They both have their own advantages and disadvantages and it is therefore dangerous to maintain a one-sided reasoning on this point, as almost all yards do. For each case again one has to consider whether sandwich or single-skin technique should be used!

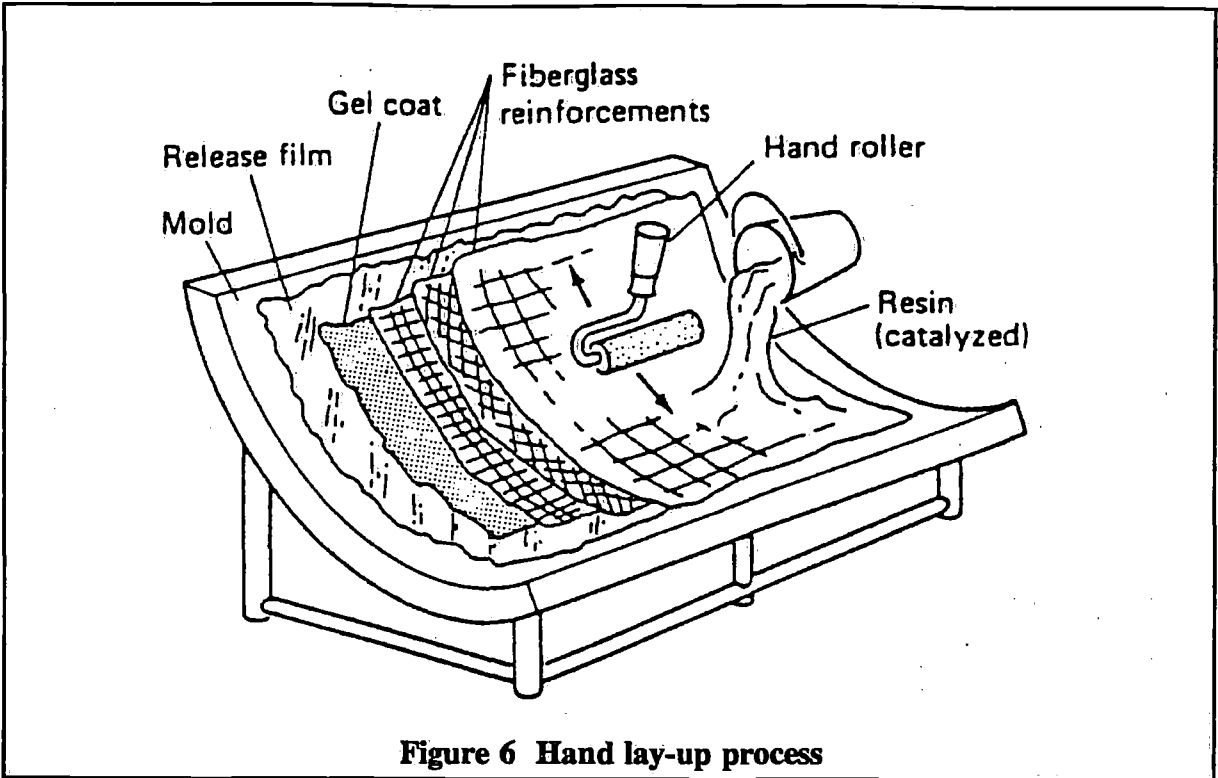


Figure 6 Hand lay-up process

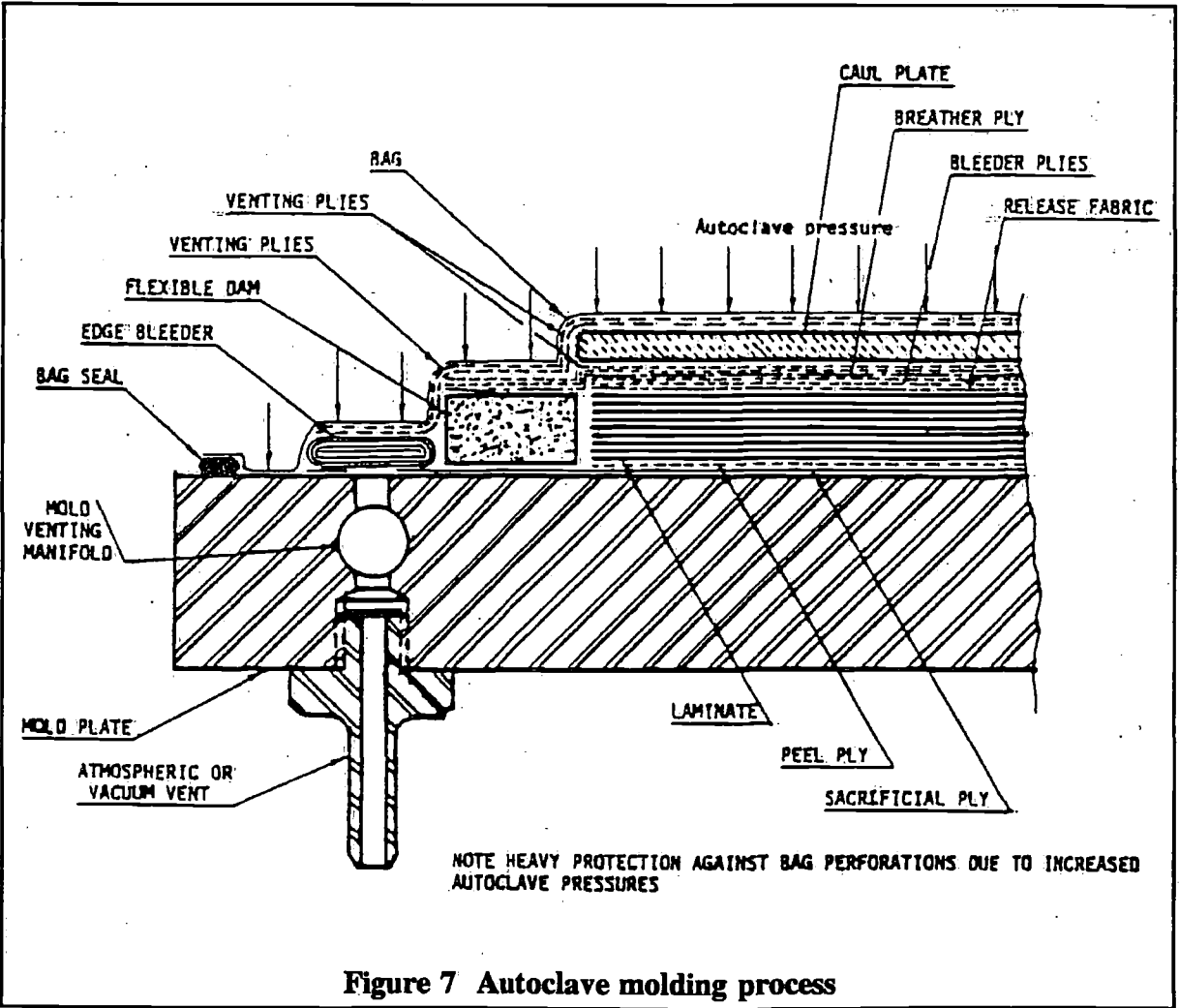


Figure 7 Autoclave molding process

5 Structural research: necessary?

This question should not be answered but positive. The only reason to pose this question is that many manufacturers have answered this question negative in the past and they still do in the present!

It has to be stressed though that many aspects of composite materials are insufficiently known or investigated. When we look at it from the point of view of a ship-design, things are becoming even more complicated.

When designing a ship, three basic things have to be considered or computed:

- design loadings
- selection of construction material
- structural analysis

As for the design loadings, until now very conservative rules have been applied. Only recently some research projects on this topic have been launched.

The selection of a construction material is another very difficult point. Exact data on material properties are nonexistent and it is highly advised to run several series of material tests if one wants to know the characteristics of the material that's used.

For a long period, structural analysis in ship-building was identical to application of rules for steel construction. This of course resulted in structural misconceptions. Since a few years however, calculations are done with finite element methods resulting in much more accurate structures. Only as an example, Figures 9, 10 and 11 show some finite element results on sandwich structures, done by Amtec engineering on NISA.

Conclusion can be short but clear: structural research definitely is necessary. It has only just begun!

6 Final remarks

The foregoing sections have clearly pointed out the many advantages that are inherent to advanced composite materials. If one is able to work with F.R.P. -materials in a proper way, one is also able to realize structures with unequalled characteristics.

When this is combined with a certain amount of, let's say "realistic", common sense and if several yards want to keep up extremely intensive research programs, in the near future "think composites" will certainly become a reality for yacht construction industry.

References

- [1] Report SSC-224,
"Feasibility study of glass reinforced plastic cargo ship".
- [2] Lubin. George, "Handbook of composites",
Van Nostrand Reinhold Company.
- [3] University of Michigan, "Small craft engineering structures"
College of Engineering, Report 121,
- [4] Hull. Drek, "An introduction to composite materials",
Cambridge press.
- [5] Hexcel Report TSB 124, "The basics on bonded sandwich construction",
1981 Revision

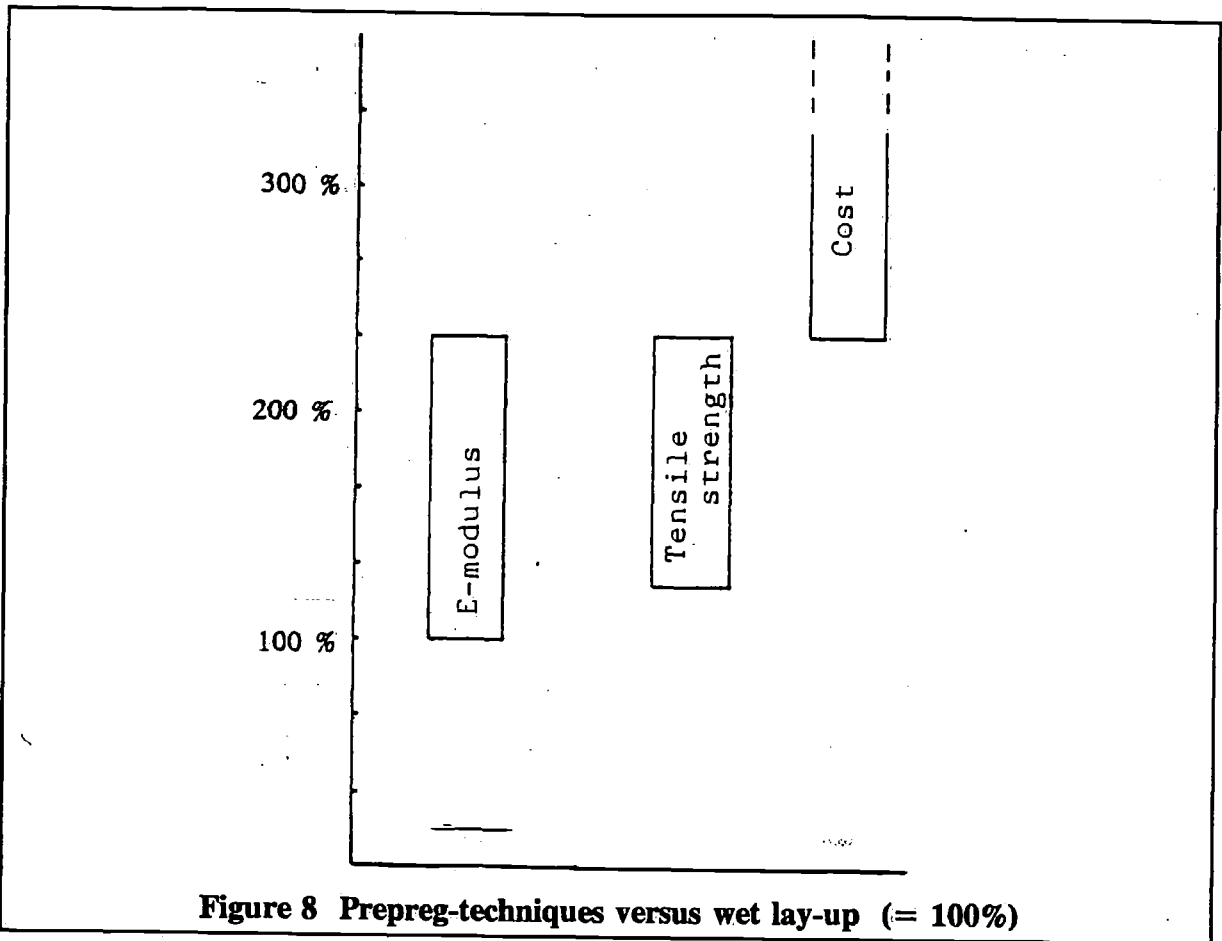
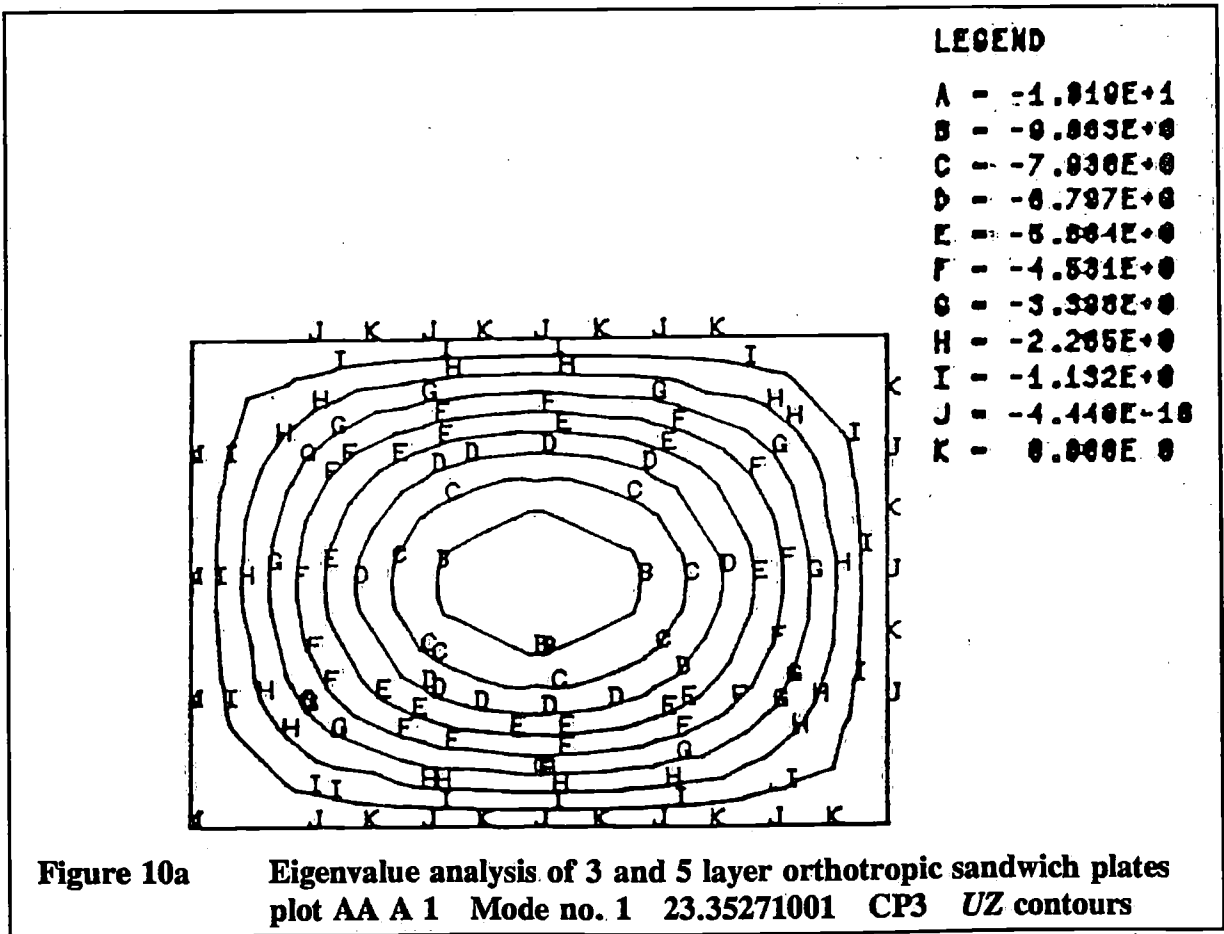
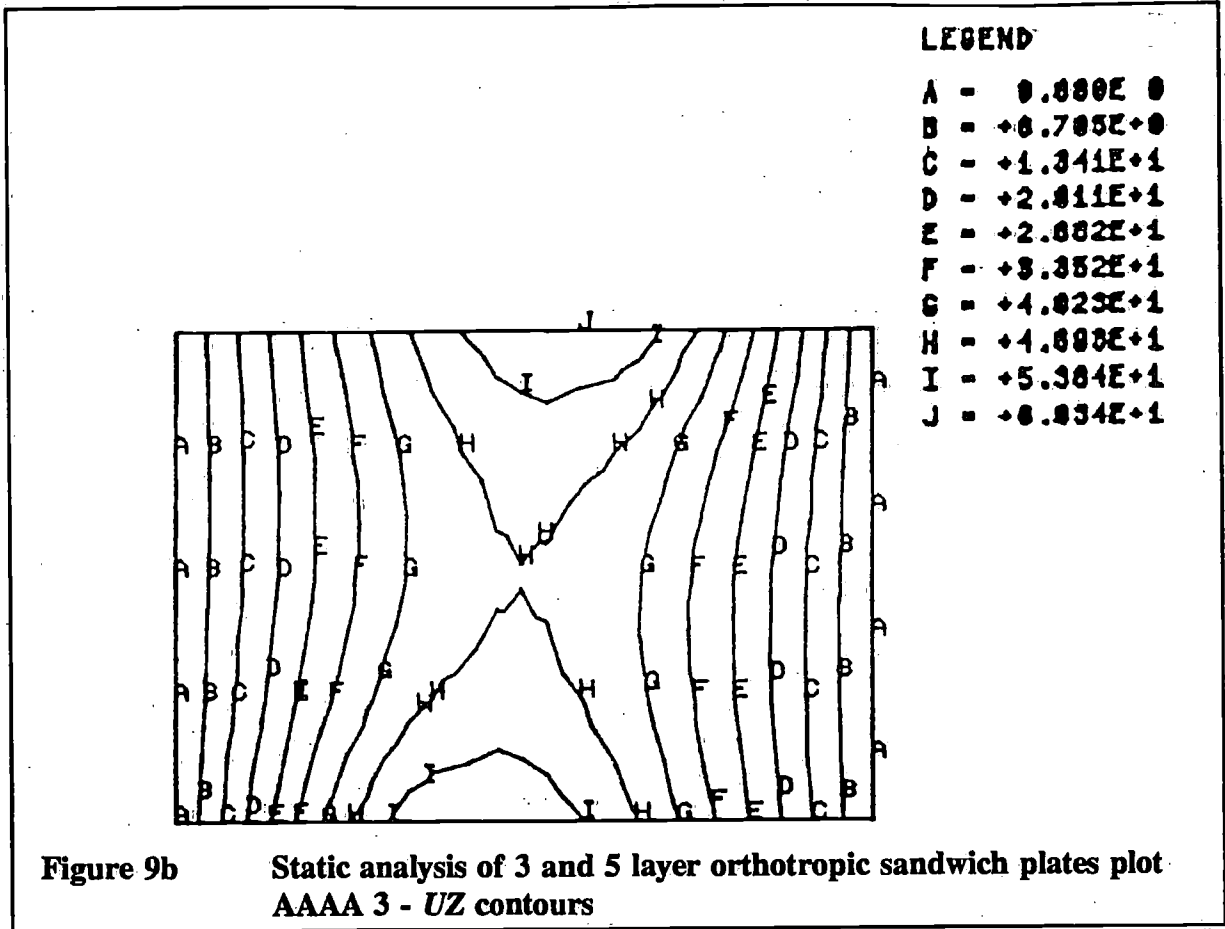
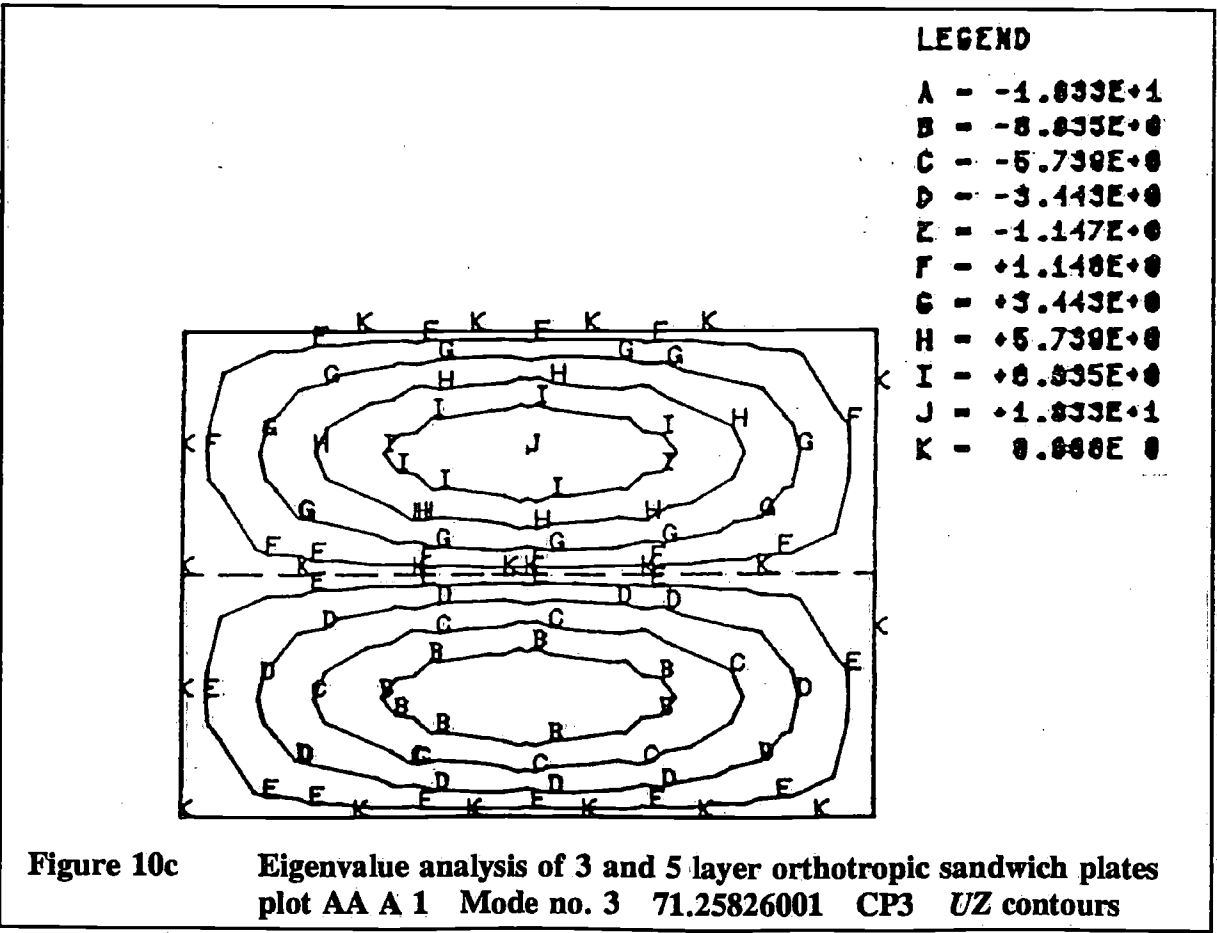
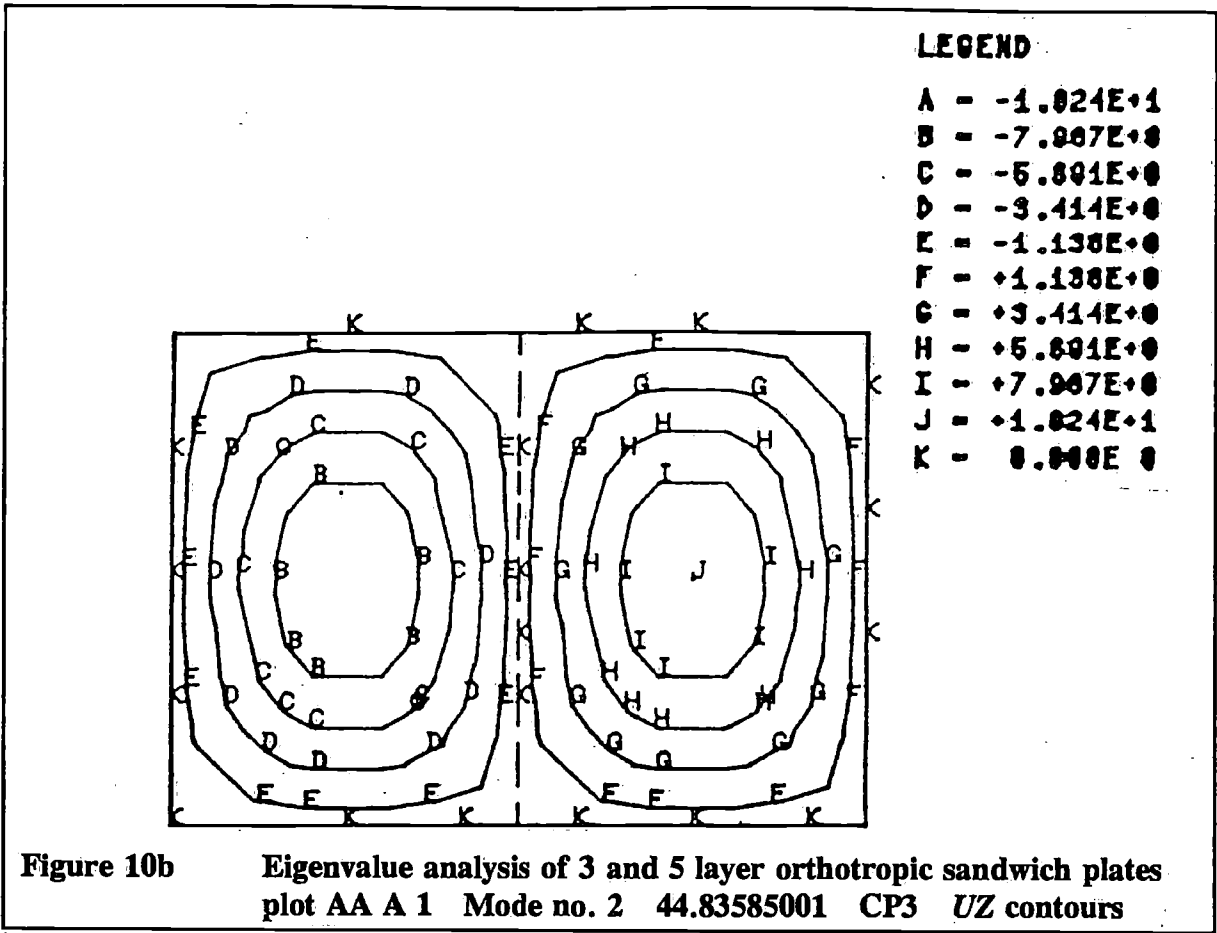


Figure 8 Prepreg-techniques versus wet lay-up (= 100%)

19	20	21	22	23	24
13	14	15	16	17	18
7	8	9	10	11	12
 1	2	3	4	5	6

Figure 9a





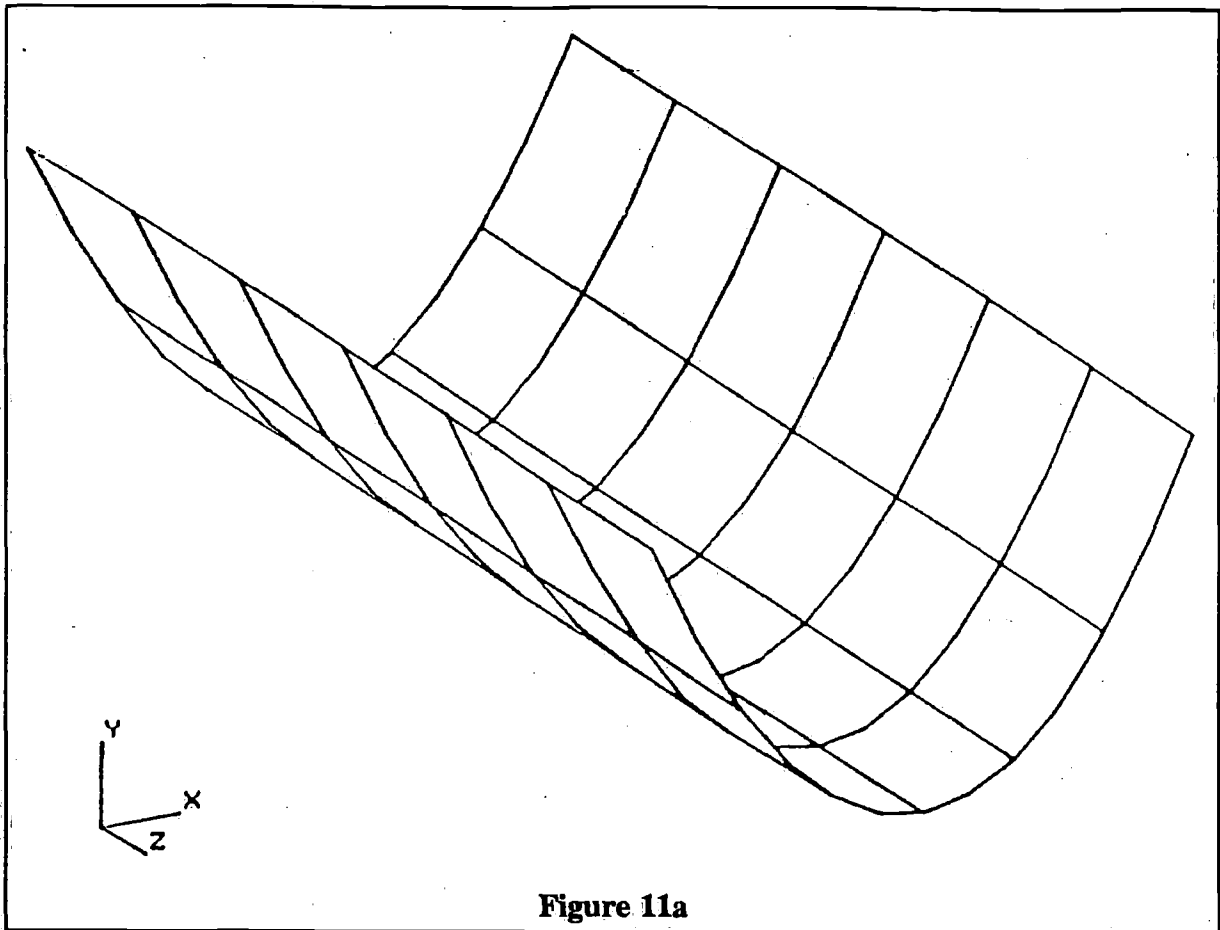


Figure 11a

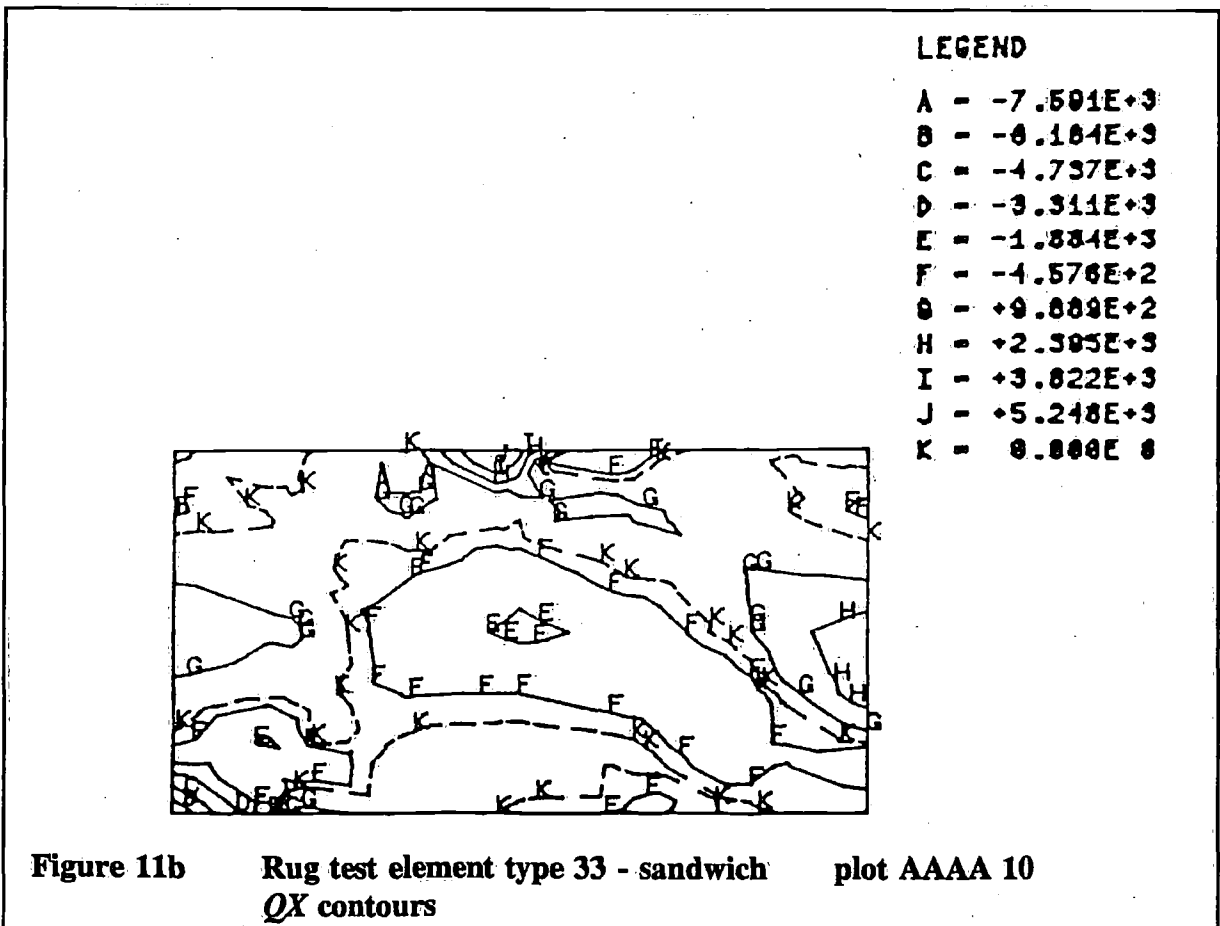


Figure 11b Rug test element type 33 - sandwich plot AAAA 10
QX contours

LEGEND

- A - $-1.348E+4$
- B - $-9.751E+3$
- C - $-5.079E+3$
- D - $-2.228E+3$
- E - $+1.525E+3$
- F - $+5.278E+3$
- G - $+8.838E+3$
- H - $+1.278E+4$
- I - $+1.853E+4$
- J - $+2.828E+4$
- K - $0.000E+0$

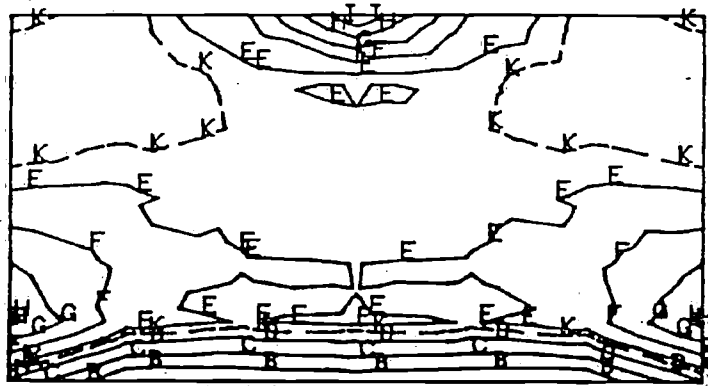


Figure 11c Rug test element type 33 - sandwich plot AAAA 7
3XY layer No. 2

Sail design and panel calculation

by Ir. J.A. Keuning and A. Versluis

Delft University of Technology
Ship Hydromechanics Laboratory

Contents

Abstract

- 1 Introduction
- 2 The Design process
- 3 Panel definition
- 4 Panel calculation
- 5 Examples
- 6 Future Development
- 7 Acknowledgement

References

Abstract

Sail design and panel calculation

In this paper a method, developed at the Delft University of Technology, is described to calculate the panels of a sail of a given geometry and shape.

First the contours of the sail are determined and presented as three dimensional curves, the leech, the luff and the foot of the sail. Subsequently a number of crosssection shapes at different heights along the sail with prescribed camber and distribution of camber along the cord-line are selected.

With these data the computerprogram calculates a complete three dimensional polynomial representation of the sail and visualises the sail from different angles of view for the designer on a plot or visual display unit. In this way the designer may evaluate the sailform and change it if necessary.

If the designed sail is considered to be in accordance with the shape wanted, the designer places the panels over the sail in the way he feels most adequate for handling stresses and distortion of the sail in use, simply by specifying the ends of the seams of each panel. The computerprogram now calculates the shape of each seam in the sail as a three dimensional curve and calculates the offsets of the panels with the aid of a method used to calculate the shape of developable surfaces.

The output of the program is presented in such a way that the panels either can be plotted by hand or, if possibly, with the aid of a numerically controled cutting machine.

In the paper various results of the program are presented as well as some of the experience gained over the years by using this method both on the design-proces as on the construction of the sails. Advantages and short-commings are outlined.

Finally some thoughts about future development are presented.

1 Introduction

In this paper a method is described to design a sail and to calculate the shape of the panels. The initial work on this project started as early as 1976 with a design and calculation procedure for genoas, using traditional panel layout. Much of this work has been kept restricted for use by the participants in the project only, i.e. the Delft University of Technology and Gaastra Sails. Later on this project has evolved to an all-round and versatile design and production method for all kinds of sails, the final version of which is now reported in this paper. Until a decade or so the art of sailmaking was largely based on experience and intuition. This experience was gained using a trial and error technique: by cutting the sails, examining the actual product afloat and correcting it when and where necessary.

The experience thus gained made it possible to construct sails without major faults but predicting the actual shape was hard to be done and progress was slow.

In the last decade a tremendous change in the sailmaking art has occurred due to the availability of new materials and the pressure from the users to find new and even faster shapes in sails with less overall weight.

Detailed theoretical calculations of the optimal shapes for sails will not be available for many years to come, so these will have to be found in practice. A valuable tool for optimising the shape of sails is a possibility to cut the sails in such a way that the shape designed on the drawing board is actually there in the sail. Sails will no longer be defined by the amount of broadseaming on different locations in the sail, thus leaving the actual shape unknown, but by specifying the amount and position of camber and twist all over the span of the sail and leaving it to the computer to calculate the shape of the panels to generate that specifically defined sail.

By knowing that a given shape is in the actually build sail it is possible to compare the merits of each shape and by doing so to find the optimum sail.

Also difficulties encountered by traditional sailmaking in specifying the shape of the panels when completely new panel layouts must be used, as is nowadays common practice by the advent of hightech materials and the search for lighter and stronger sails, may easily be overcome by using this new technique. Any sailshape can be made by proper shaping of the individual panels it is made of. One of the restrictions of the method is that the shape of the panels of the sails are being calculated as if they were developable surfaces. A developable surface is one which may be unrolled into a plane without distortion. In practical terms this means that only the four sides of each panel may be any kind of curved line but no cross-seams perpendicular to the side of the panel may be used. Cones and cylinders are known examples of developable surfaces.

Traditionally these kind of panels are used when making a sail, except perhaps in the foot of mainsails, so this restriction poses no real problems. When planning the panel layout careful consideration must be given to this limitation so that no "unbuildable" sails are designed.

A second limitation of the present procedure is that no account has been taken of distortion of the sail due to the loading on the sail in actual use. Some of the distortion may be accounted for in the design procedure, by making for instance a less full sail with little or no twist, and the camber positioned a little more forward, but furthermore this assumption must be justified by using strong and stretch resistant new materials. However a large number of test sails have been made using regular Dacron and this yielded very good results. Deformation of the sail under load was dealt with in practice using sheet and halyard tension just as usual, but much less of all this was necessary to keep the optimum shape. Since the shape of the panels is completely defined it is no longer necessary to layout the sail as a whole in the loft for specifying the luff, leech and foot of the sail. Even all positions of battens, reinforcements patches and reefs can be drawn upon the individual panels before sewing the sail together, which means a considerable saving of time and space in the saillofts.

The output of the computerprogram is a digital format: at regular intervals the coördinates of the points forming the sides of each panel are presented. Plotting these points by hand is a labourous affair, which has been done many times in the beginning stages of the project and yielded very good results.

But the output is much more suited for numerically controlled cutting of the panels by machines such as known for instance in the shipbuilding- and clothing industry.

By coupling the computer, which calculates the panels, direct to a numerically controlled cutting machine, using a hot-knife or a laser beam, the panels can be cut instantaneously.

2 The Design process

First step in making a sail by using the method described in this paper is defining the shape of the sail in three dimensions and to check whether the designed sail is feasible as a membrane under tension, i.e. that no hollows anywhere in the sail do occur. This is one of the major problems in the new method since sailmakers were not used to specify the section shape, amount of camber, position of maximum camber and twist over the height of the sail. So no experience did exist, from which these data could be collected.

One way to obtain this information is by using the method as first described by Haarstick in Ref. [1]. He sets-up a kind of linesplan of the combined sails in three dimensions of the yacht under consideration using all the information available of the yachts rig and deck layout. In the set-up of the linesplan he tries to take account of the mutual interaction between the mainsail and the genoa. An example of such a drawing is presented in Figure 1.

By using expertise, experience and intuition, as well as information known from aerodynamics, the distribution of the amount of camber and the position of maximum camber as well as twist, mast bend and forestay sag are put in the design at different heights in the sail. Starting with the mainsail, specified for different conditions, the genoa is so designed as to match the main given the circumstances. This can be done for all different sail combinations. Although this method appears to be attractive much of the information needed to set-up the design is unknown and much experience, which is only to be gained by using this method, is necessary to exploit all benefits of this design procedure.

During the development of the project another method was commonly used. In this method it was determined by experience how much forestay sag, mast bend, twist and camber distribution over the height of the sail should be used for defining a good sail, while considering the sail just as an isolated foil.

Further on it is assumed that one way or the other the wanted geometry of the sail is roughly known.

When using the method to design sails, as is described in this paper, the designer is asked to specify in three dimensions the boundaries of the sail under consideration, i.e. the luff, the leech and the foot of the sail. He must specify the coordinates of the corner points of the sail, the amount of forestay sag (or mast bend) in three dimensions both longitudinal and athwartships, the shape of the leech of the sail, in three dimensions, i.e. the amount of curvature and twist, and the shape of the foot of the sail. Then at arbitrary heights along the span of the sail a number of horizontal cross-sections of the sail have to be specified. First of all a choice has to be made between a number of nondimensional cross-section shapes which may be used in the computerprogram, i.e. a hyperbolic function, a parabolic function, the segment of an arc or any arbitrarily chosen cross-section the designer wants to use and which, in that case, has to be specified by him. The choice of cross-section shape depends on the type of sail and the circumstances under which it will be used and is therefore best left to the designer.

For each of the selected horizontal cross-sections of the sail the maximum camber and the position of maximum camber must be specified.

The cross-section in the program are defined as nondimensional offsets. This means that the

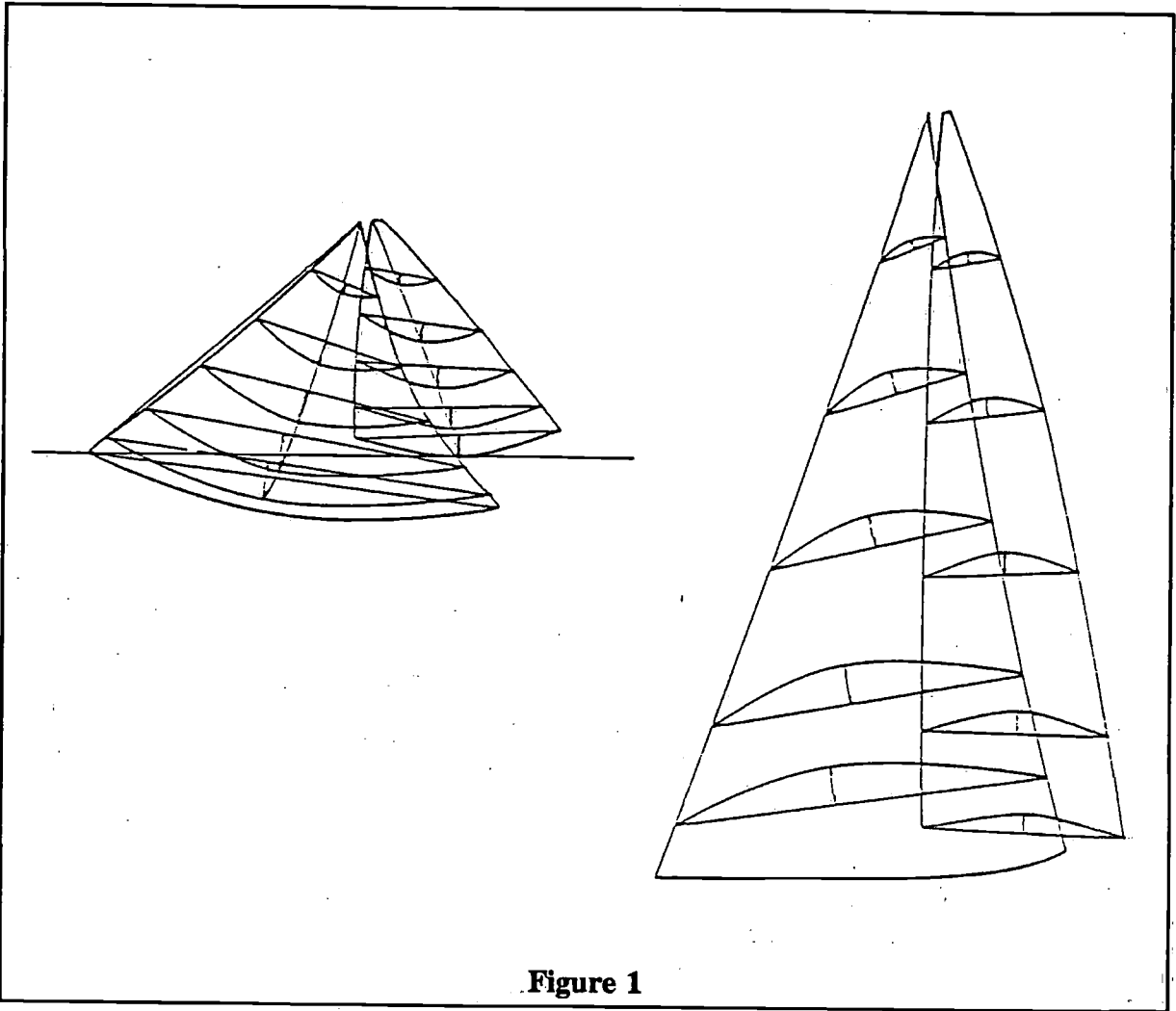


Figure 1

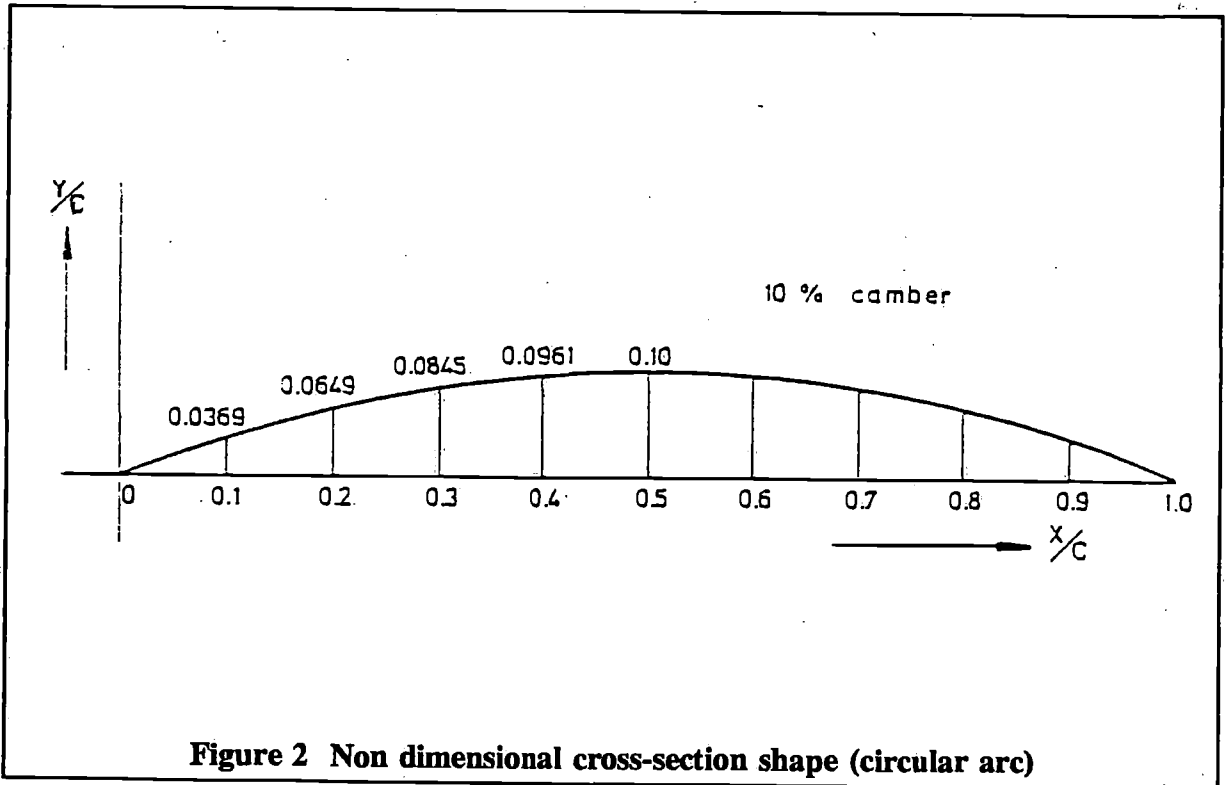


Figure 2 Non dimensional cross-section shape (circular arc)

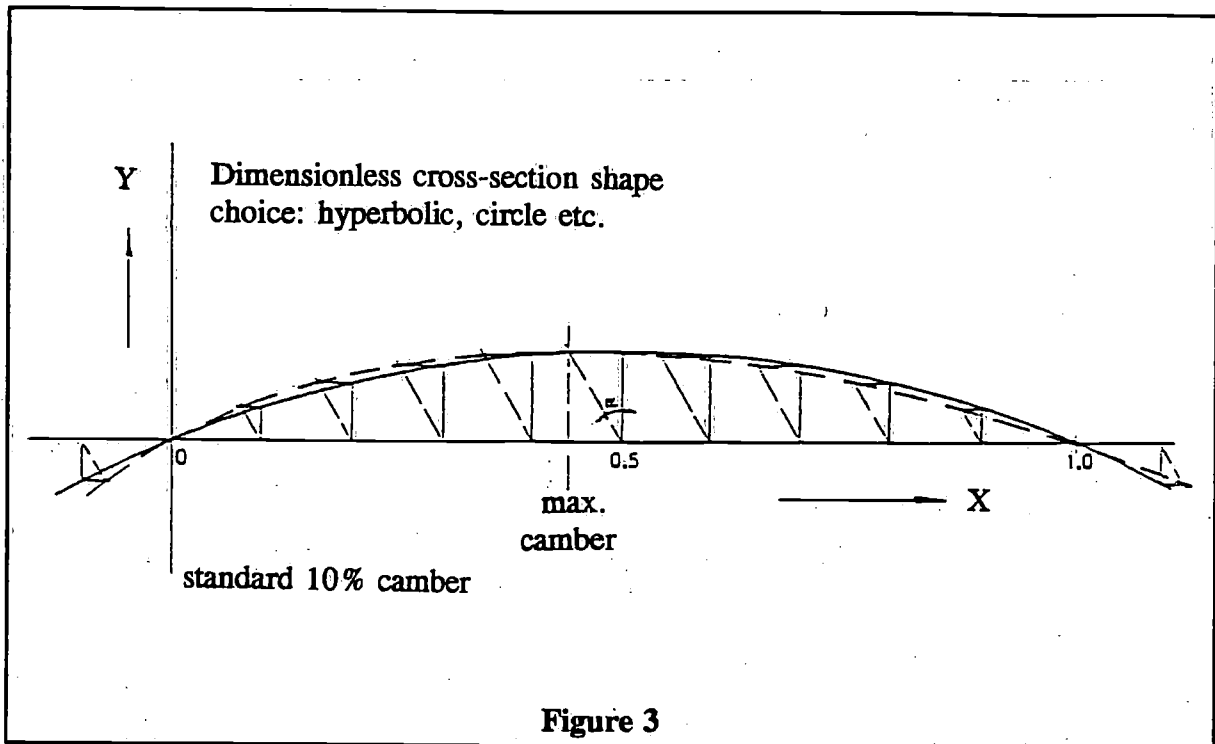


Figure 3

length of the cord is equal to unity and the depth offsets are related to this length of the cord and represent the cross-section of a foil with a maximum camber of 10% positioned at half the length along the cord. As an example the nondimensional circular arc is presented in Figure 2.

For different percentages of camber and position of camber at a given cross-section in the sail as may be specified by the designer, this standard shape is transformed by multiplying all offsets with a constant factor calculated from the difference in camber, i.e. 1.5 for 15% camber instead of 10%, and by shifting all offsets over a constant angle α as defined by the shift in position of maximum camber along the cord. This procedure is visualised in Figure 3.

Finally by multiplying all values with the actual cord length of the cross-section under consideration the actual cross-section shape is obtained. The number of cross-sections thus defined may be limited to 5 or 6.

All these data are used to calculate a three dimensional presentation of the sail. An example is presented in Figure 4. The first drawing in this figure shows the input as given by the designer, the other drawings are generated by the computer herefrom. Emerging from the top of the sail twenty five radial cross-sections will be calculated using constant cordlines over the imputed horizontal cross-section. By means of a spline interpolation polynomial expressions of the third order for each point of these radial cross-sections the depth can be determined. Using these vertical cross-sections a large number of equidistant horizontal cross-sections is being calculated and plotted.

By means of the limited number of horizontal cross-sectional shapes as defined by the designer the depth of any point in the sail can be calculated by finding the cord fraction of the section for the point in which the depth must be calculated. The depth is calculated by constructing a constant cord cross-section emerging from the top over the horizontal input sections using that particular cord fraction. By means of the Theilheimer spline interpolation polynomial the depth at the specific point is found.

Using this technique only a limited number of coefficients in the polynomial expression has to be calculated, which decreases the time necessary for the calculations. See Figure 5.

Now the depth of the sail is known at any point a limited number of radial cross-sections

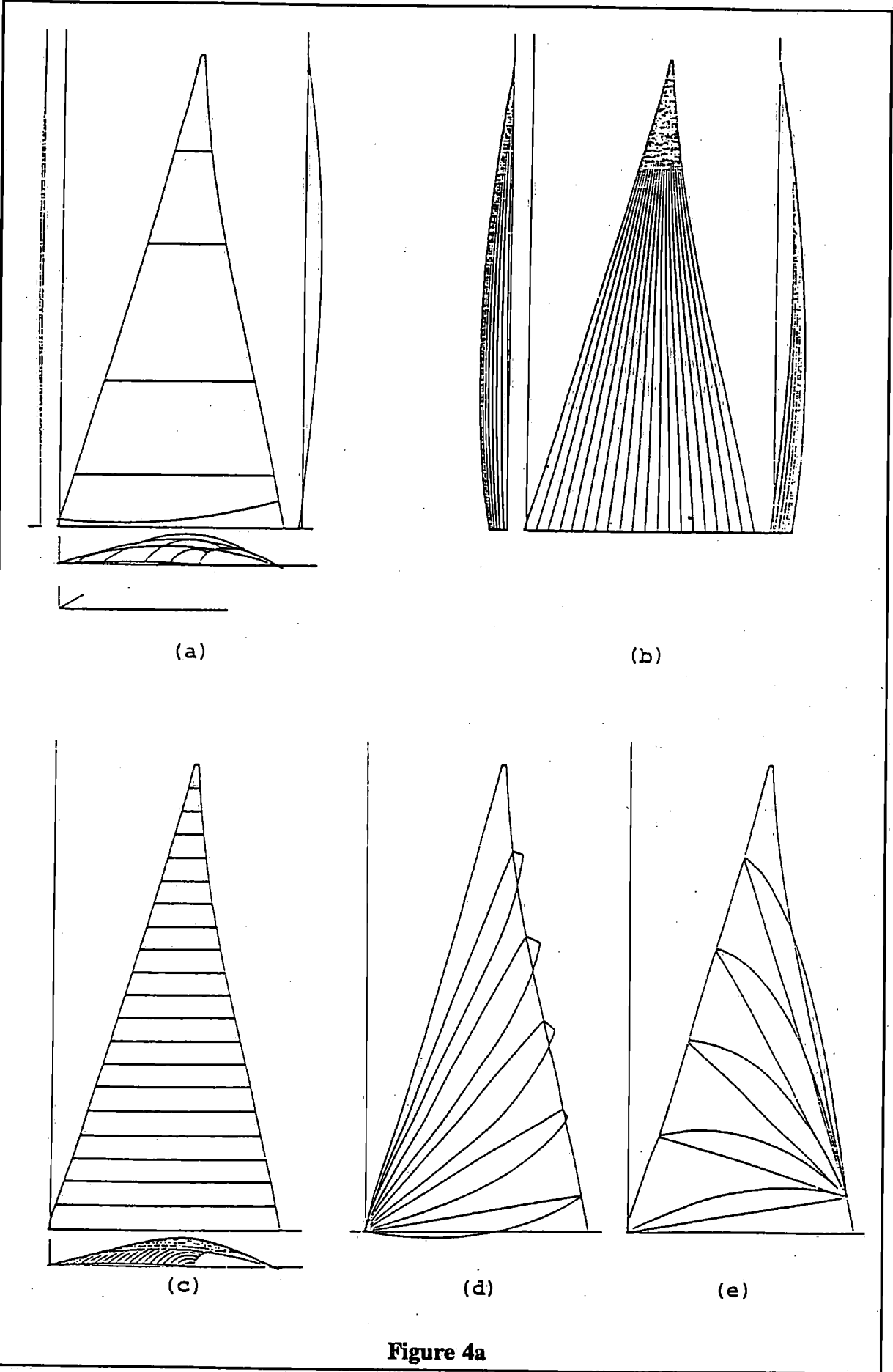


Figure 4a

emerging from the clew and the tack will also be calculated. Figure 4d and 4e. All these cross-sections are used to check the designed sail on its designed shape and on the possible occurrence of hollow regions both visually by means of the plots or by calculating the second order derivative of each cross-sectional shape.

If these regions are found the shape of the sail must be changed. The perspective views are added to give the designer an impression of the shape of the sail he designed when looked upon from different standpoints Figure 4f and 4g. If the shape of the designed sail is in correspondence with the shape wanted.

The designer passes on to the panel calculation procedure.

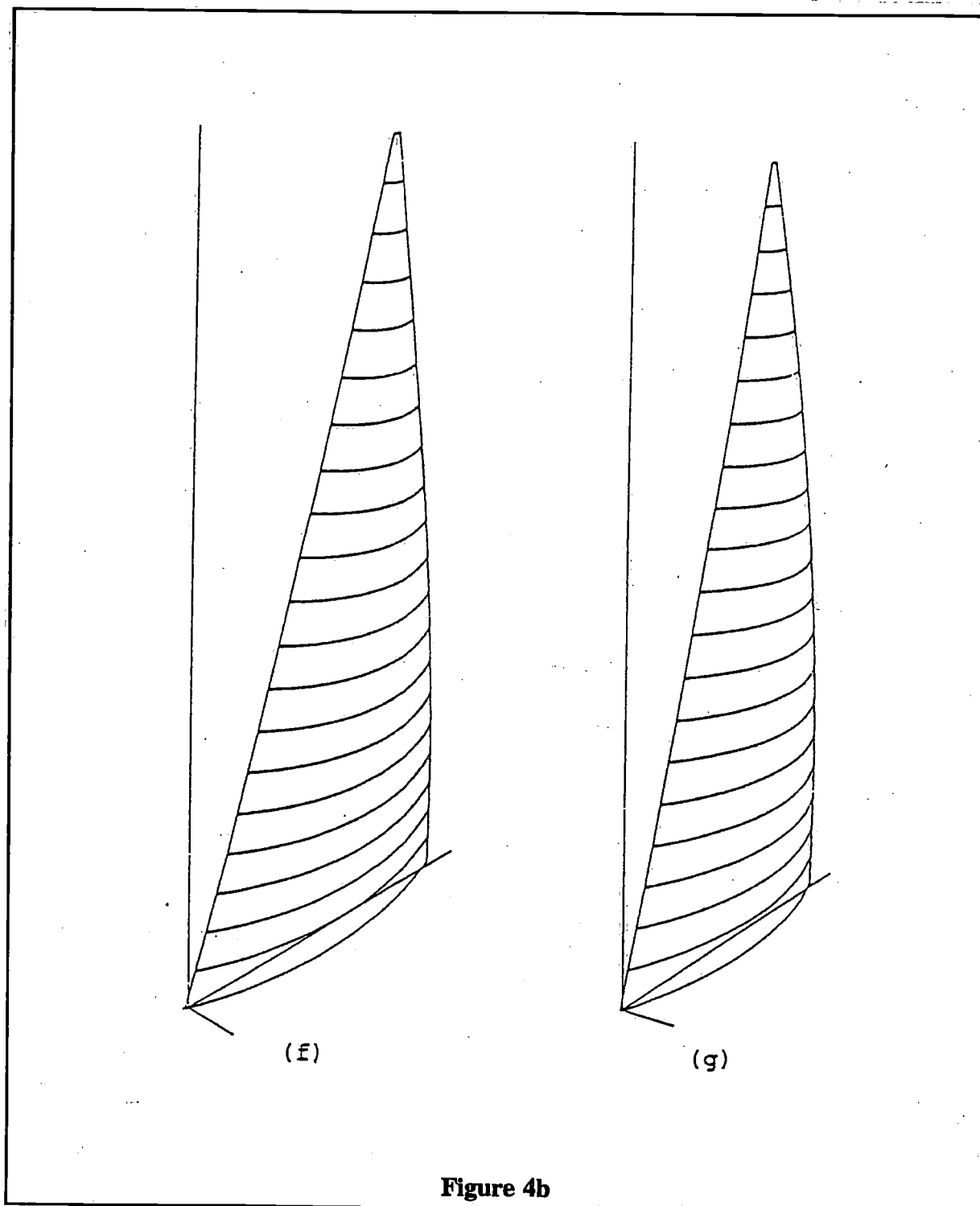
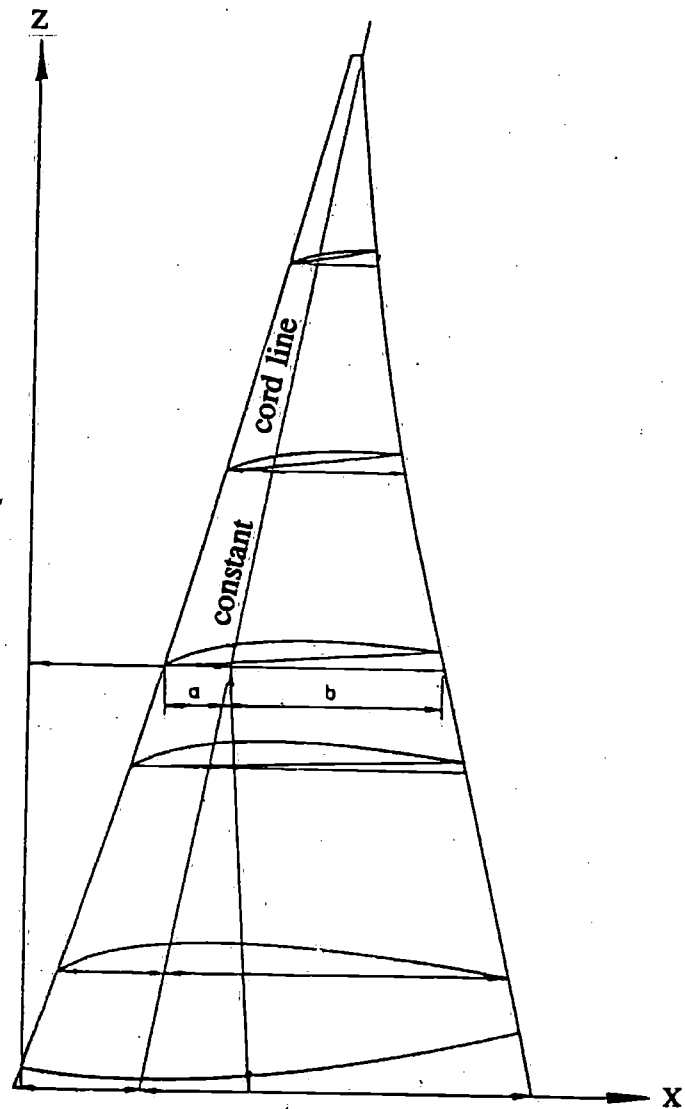


Figure 4b

cord fraction of point p in which depth is to be known $a:b$



Theilheimer:

$$f(x) = C_1 + C_2x + C_3x^2 + C_4x^3 + C_5(x - x_3)_+^3 + \dots - C_{N-1}(x - x_{N-3})_+^3 + C_N(x - x_{N-2})_+^3$$

where

$$(x - x_i)_+^3 = (x - x_i)^3 \text{ if } x > x_i$$

$$= 0 \quad \text{if } x \leq x_i$$

Constant cordline used to calculate depth at any point in the sail using Theilheimer polynomial expression over the horizontal crosssections.

Figure 5 Procedure to find depth in any point of the sail

3 Panel definition

This routine in the computerprogram calculates the outline of the panels of which the sail is to be constructed. A large variety of panel orientations can be used, i.e. horizontal, vertical, radial from all corners and combinations of all these.

The only limitation imposed on the designer when planning the panel layout is that the sail must be "buildable". This means that panels which are no developable surfaces by their nature may not be used, i.e. building half a sphere from one panel is not possible but approximating this half sphere to a very large extend by using a number of radial panels emerging from the center is quite well feasible. In the procedure, which will be described in more detail in paragraph 4, the computer calculates the shape of each panel which is uniquely defined by the shape in three dimensions of its four (or three) sides, i.e. the seams.

The designer now specifies from where to where each seam of the panel extends into the sail designed. In the vertical projection of the sail in the ($x - z$ plane) the seams of each panel must be defined. This is done by entering in successive order the points where the seams determinate and specifying at the same time by means of a code whether it is positioned on the leech (2), the luff (1), the foot (3) or somewhere in the middle of the sail (4). Also the character of the seams spanning these points must be specified by a digital code dependent on whether they are part of the leech (2), the luff (1), the foot(3), the sail surface (4) or part of a radial patern of panels emerging from a corner (5).

Seams of type 1, 2 and 3 are completely defined in three dimensions already by the fact that they are part of the given edges of the sail. The shape of seams of type number 4 and 5 must be calculated by adding to their straight (4) or curved (5) projection in the $x - z$ plane the depth of the sail at a large number of points along the line of the seam using the method earlier described. Finally the direction in which the panel can best be developed is added to these data.

In Figure 6 the different types of terminating points of the seams are visualised and in Figure 7 the different types of seams are presented.

The panel is now completely defined by the shape of its boundaries in three dimensions. By considering it to by a developable surface the shape of the panel can now be calculated.

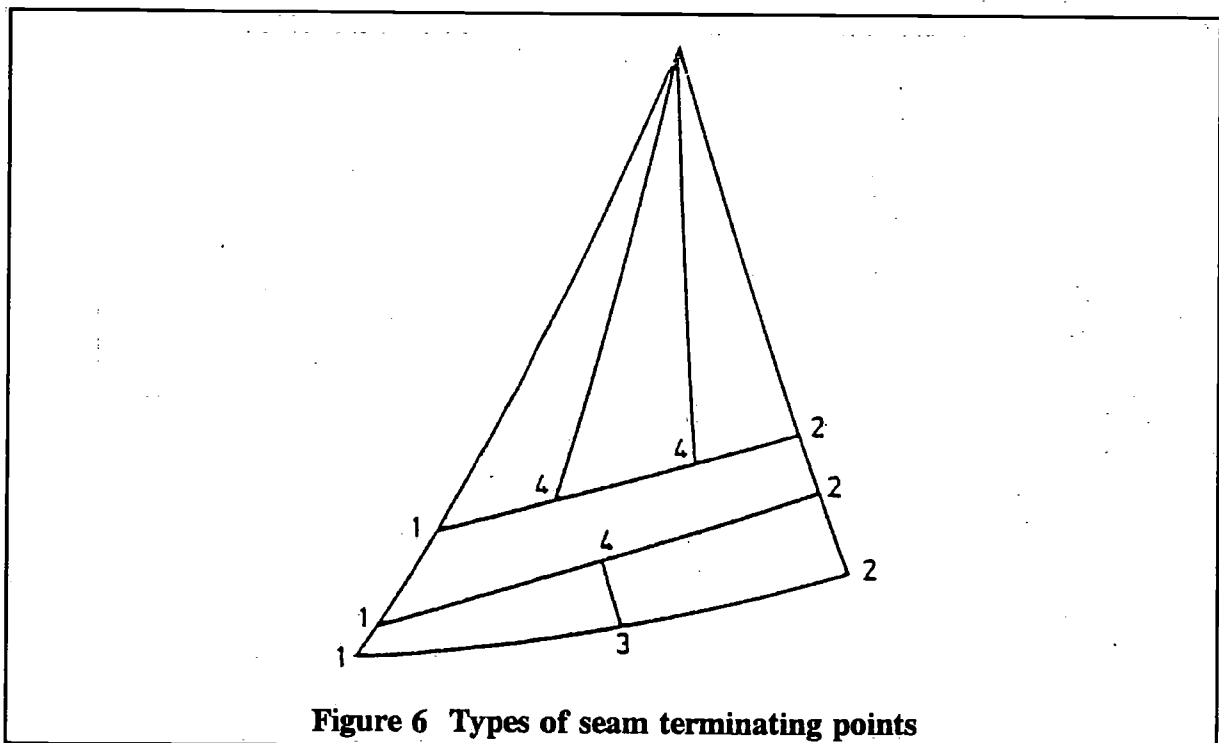


Figure 6 Types of seam terminating points

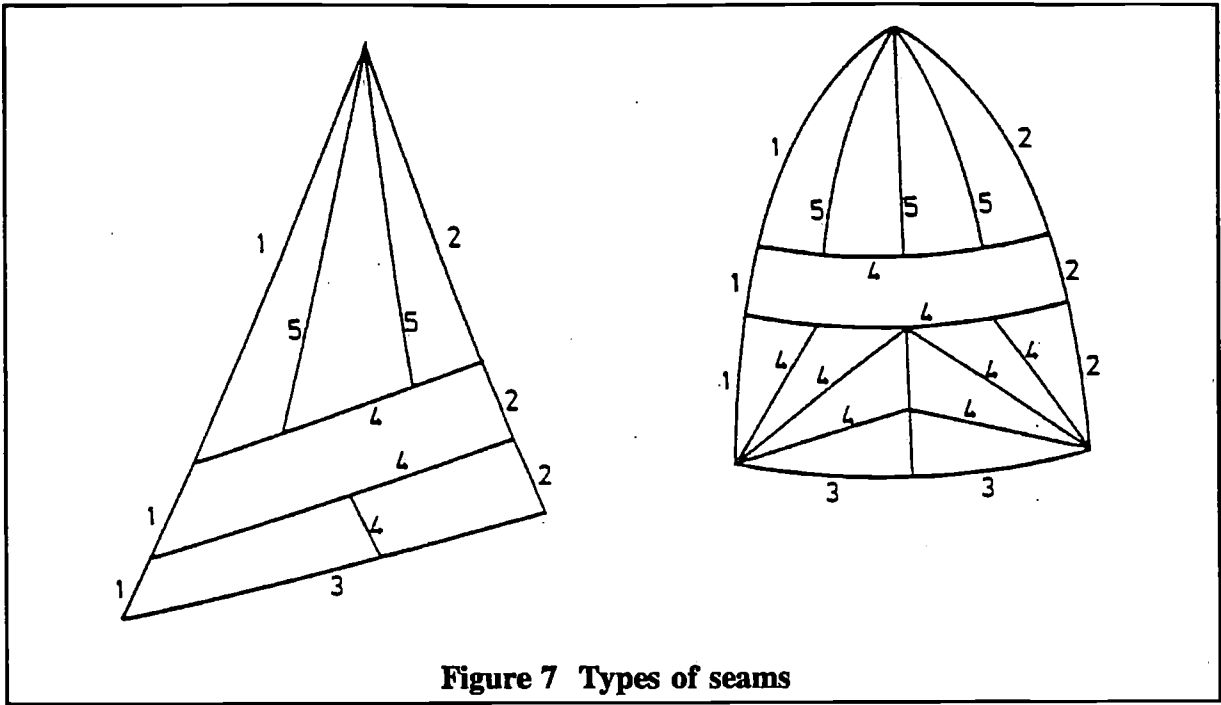


Figure 7 Types of seams

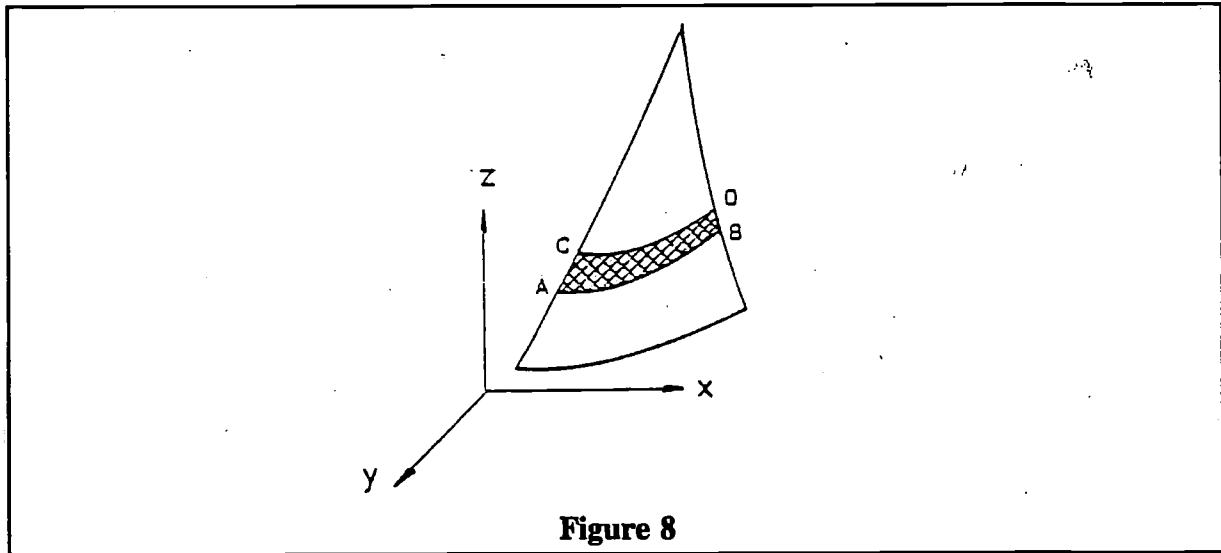


Figure 8

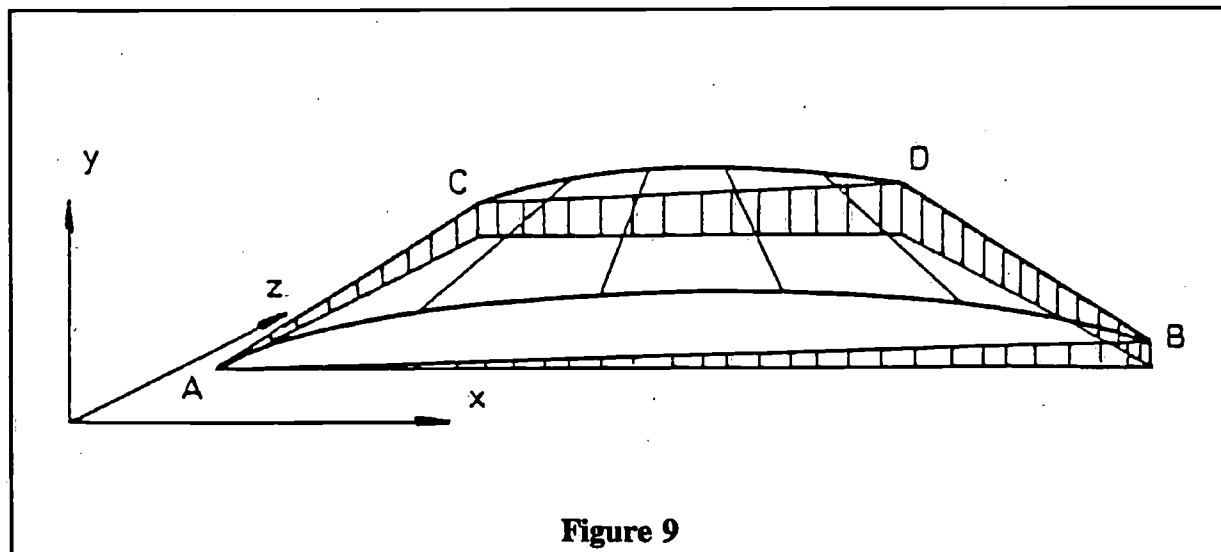


Figure 9

4 Panel calculation

The method used in our program to develop the panels of the sail originates from the ship-building industry. A large variety of methods to develop the rather complex three dimensional shape of a ship into a plate are available. The method used in our program is the so called "cross-mould-method" and is used here because it lends itself quite well for numerical computations.

Only a short outline of the procedure will be given in this paper. For more detailed information reference is made to the literature [2].

The method is based on covering the surface of the panel by a large number of adjacent triangles and developing the lengths of the sides of all these triangles using an approximation for the length of a curved line through three well defined points in space. The geometry of the triangles is completely defined by the length of their respective sides. By using a large number of overlapping triangles and coupling all these together over the length of the panel, starting from a well defined straight line, the shape of the panel may be laid off.

In our situation the surface to be developed is a part of the sail, for instance such as shown in Figure 8. This is just one of the many situations that might occur, but in principle these are all similar.

The panel is defined in space by the curvature along the four sides AB , BD , CD , AC and the geometry of the surface in between these boundaries. This part may be isolated as shown in Figure 9.

Both sections AB and CD are now discretized in a total of 25 points along the cords at regular intervals and the corresponding points of both cords connected by straight lines. Half way in between both sections a new auxiliary section is defined to increase the accuracy. This is shown in Figure 10.

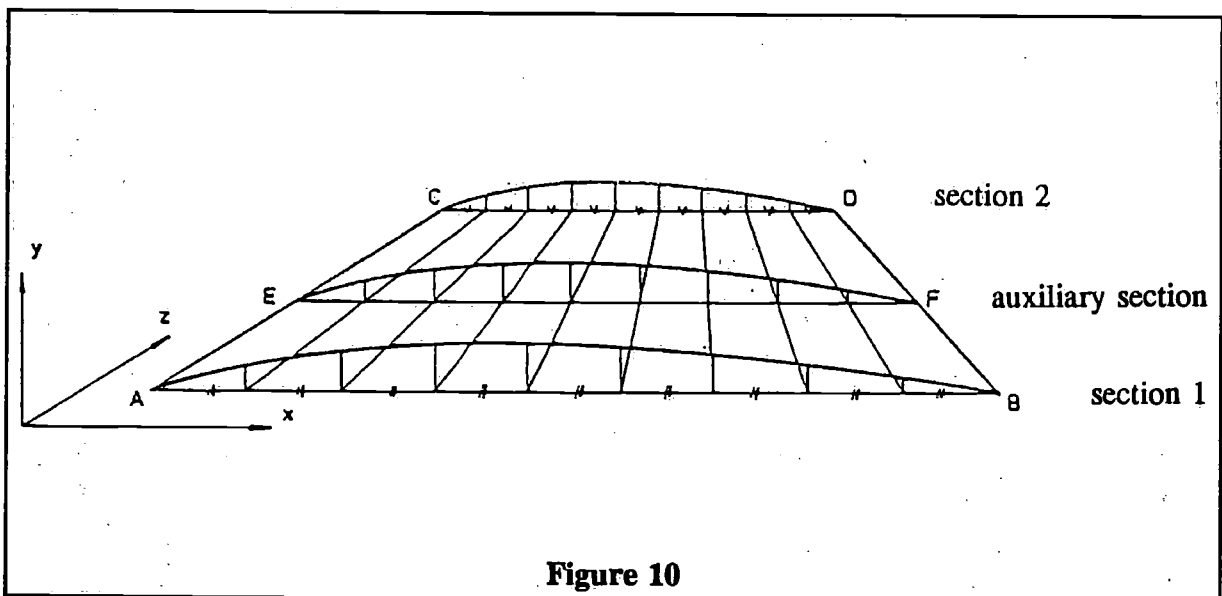


Figure 10

The depth (y) of the profile at each point of the section is calculated using the routine mentioned earlier and by doing so all the points are explicitly defined by their x , y and z -coordinates respectively. Note that only the depth at the specific points needs to be known. Curved lines are drawn which do interconnect these points as shown in Figure 11 (for a small part of the panel only).

The developed length of all the line segments between the points A , E etc, is calculated. To do this use is made of the developed length of the curve of a parabolic function spanned by three points in space.

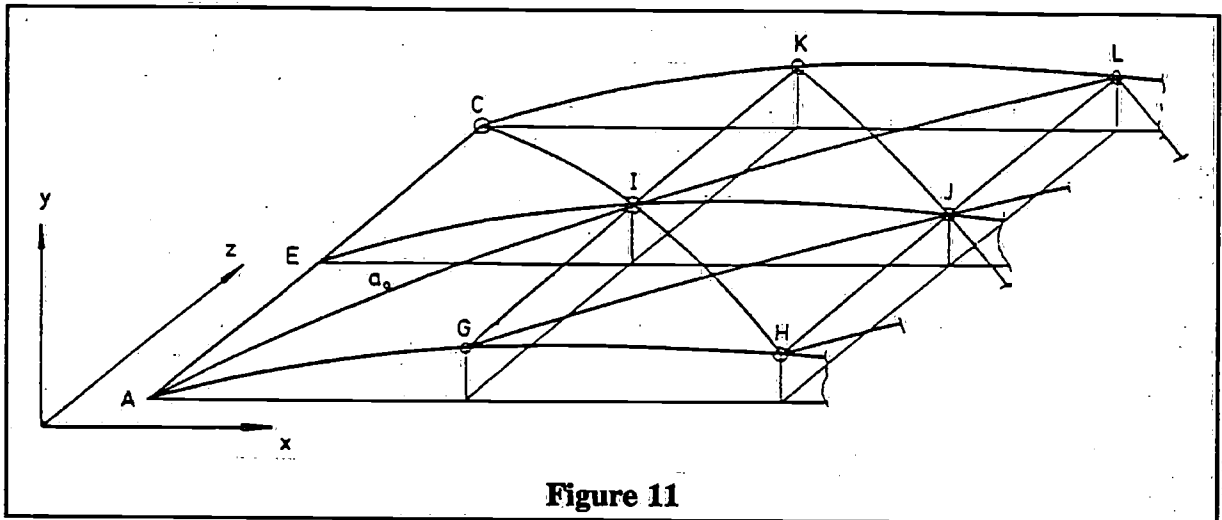


Figure 11

For instance for length of the segment AI the points A , I and L are used, to define the parabolic function, for segment EI the points E , I and J and so on. The developed length is calculated using the known formula for the length of a parabolic curve between three points, i.e.:

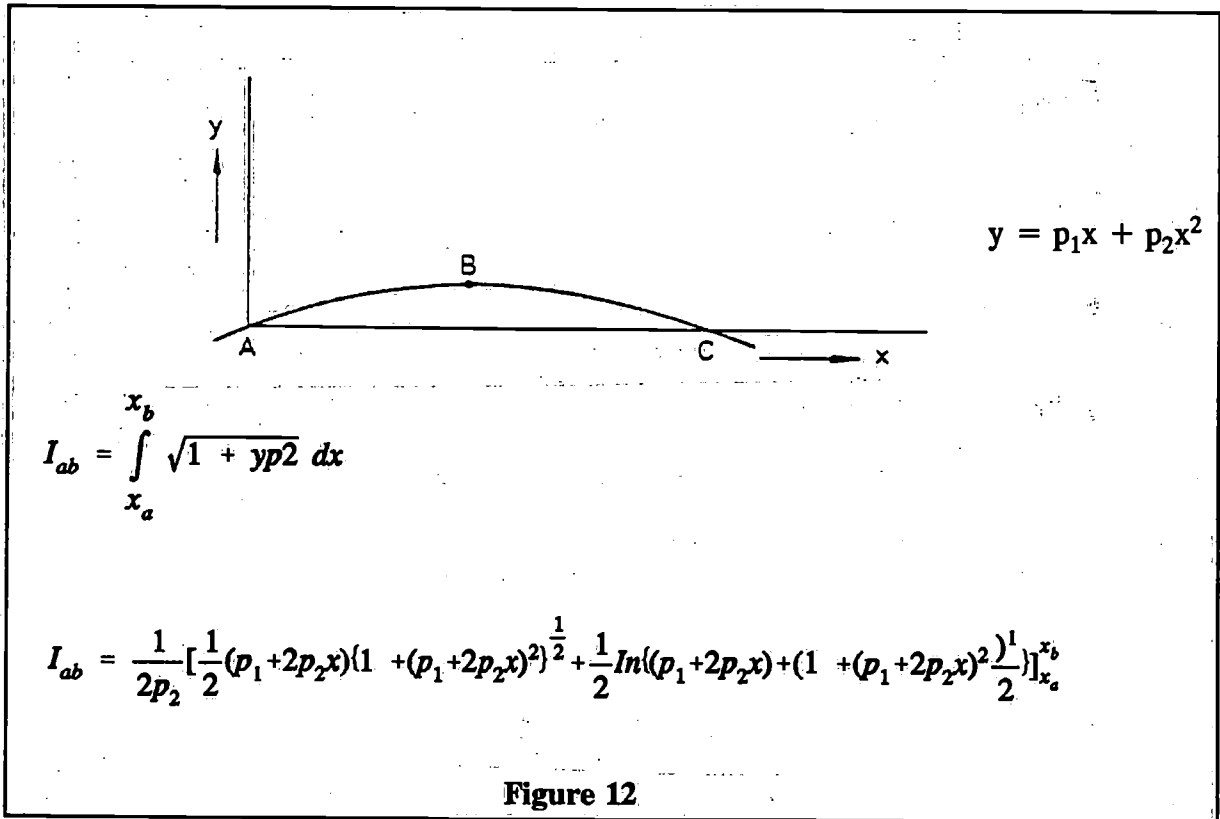


Figure 12

The discrepancies between the length of the actual curve through the three points and that of the parabolic function are neglectable in all practical cases if the points are not too far separated along the cords.

Using this formula all the lengths of the generated triangles are calculated respectively. The layout of the panel is now constructed by adding all these triangles together. Beginning with a straight line AC the developed lengths of the sides of the first triangle ACI are set-out as straight lines to yield point I . See Figure 12.

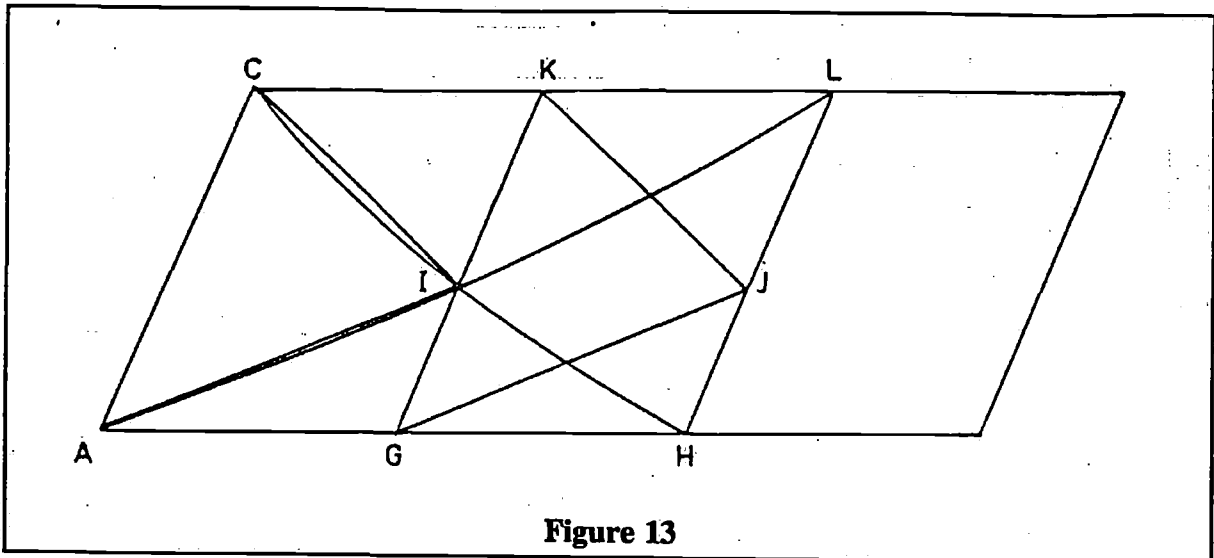


Figure 13

The other triangles CKI and AGI are added yielding KG . Starting from here KGJ , KLJ and GHJ are laid off. Consequently the shape of the part of the panel $ACLH$ arises.

However a correction has to be made because the developed length of AI has been set-out as a straight line, but since point A , I and L are not on a straight line the actual distance between A , C and I must be corrected for this discrepancy. This is done using the same parabolic function as described before.

The correction is applied to the lines AI and CI and by doing so the position of point I is corrected to yield a new triangle with the exact developed lengths between points A , C and I , measured along the actual surface, now corresponding to the lengths along the curved lines connecting these points.

This yields a new line KIG which on its turn now is the starting line for the next triangulation.

This procedure is repeated for all triangles.

The final result is the shape of the developed panel.

The output of the procedure is the shapes of the panel in a large number of offsets representing the boundaries of the panel. These may either be plotted by hand or directly linked to an automatic numerically controlled cutting machine.

5 Examples

From experience gained during full scale experiments with a number of different sails with various dimensions, it appeared that the results of the panel calculation method are very accurate. The panels of the sail fit together without any problem. Adjacent sides of two panels, forming one seam together, are exactly of the same length. The layout of the sail is in correspondence with the design and so are the overall dimensions. Finally the shape designed into the sail corresponds with the shape of the actual product. This may be seen when comparing the shape in photographs with the plots of the designed sail. See Figures 14a and b. This is the mainsail of a fractional rigged three quarter tonner.

The other sail in Figures 15a and b, is the design of a surfsail.

From all the tests with the testsails it appeared that the actual shape of the sails corresponds very much to the designed shape although some corrections in the design are necessary to compensate for distortion of the sail under load. Further distortion of the sail under actual sailing conditions can be corrected in the same way as with usual sails, i.e. halyard tension, sheet tension, lead position etc., the same "instruments" that may be used to change the shape of the sail if felt necessary.

The construction of the sails tended to take less time since laying out the complete sail on the floor for cutting the leeches etc. was no longer necessary. On the other hand it took a little more time to sew the sometimes rather curved seams together.

As an advantage of using a computer in the design process of a sail it should be mentioned that it is very easy to reproduce sails if wanted, because all the data may be stored either on permanent memory of the computer or on paper as plots and tables and remains available at any time without much difficulty. If comments concerning the actual product afloat are added to this data a valuable databank arises within a short time from which much knowledge may be gained for the proper design of new sails.

6 Future Developments

Because of the fact that a method to design sails and to calculate the shape of the panels is now available a number of other possibilities arise.

First of all, it has been mentioned before, a numerically controlled automatic cutting machine for the panels is feasible. This is not new, such machines do exist already, but in most cases they use moulds as an input. In combination with the panel calculation method however it is possible to cut any panel of any sail direct from the drawing board on which the design originates. Such a cutting machine equipped with a laser beam cutting device is now under construction at Gaastra Sails BV at Sneek.

As has been outlined before the fact, that any shape designed can now be reproduced in the sails, makes it possible to experiment with different sail shapes and combinations while knowing exactly what shape is "on". By doing full scale experiments with different sails or combinations of sails a much more reliable and accurate search for the optimum - shapes can be performed than in the case with the traditional sailmaking.

In the search for stronger and lighter sails it is a great benefit to be able to change the panel layout and orientation while knowing that the shape of the sail remains unchanged. This too enables a quicker and more reliable search for the optimum.

When a large amount of experience has been gained in the design and the construction of the sails it may become feasible to nondimensionalize a proven design of an explicit type of sail, for instance a genoa light, a genoa heavy, a mast top main etc.

The sail must be nondimensionalised using a number of main - dimensions of the sail.

When such a nondimensional sail is stored in the computer memory, a new sail with different dimensions may easily be generated using the proper dimensions of the sail wanted. The design process may be shortened considerably using this technique. The new sail will fulfill all the requirements of the sail wanted since it is proven by previous experience.

7 Acknowledgement

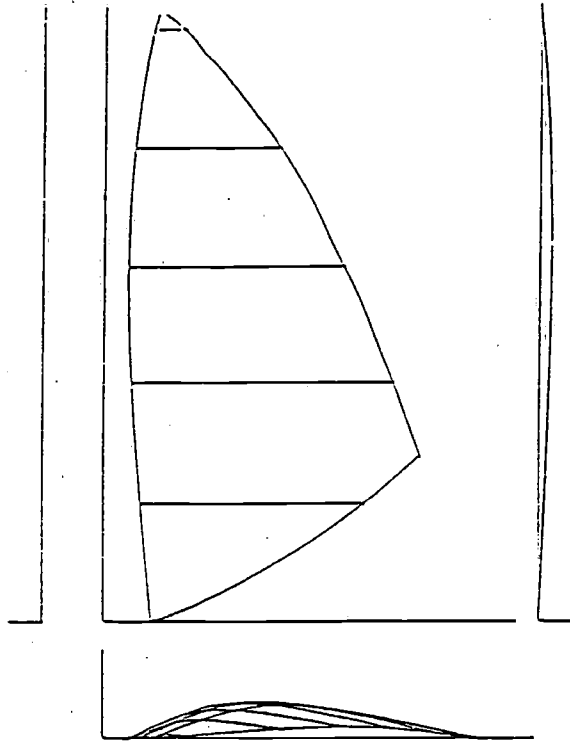
The contributions and guidance of Prof.ir. J. Gerritsma is gratefully acknowledged.

The cooperation with Gaastra Sails in this project was highly appreciated by the authors.

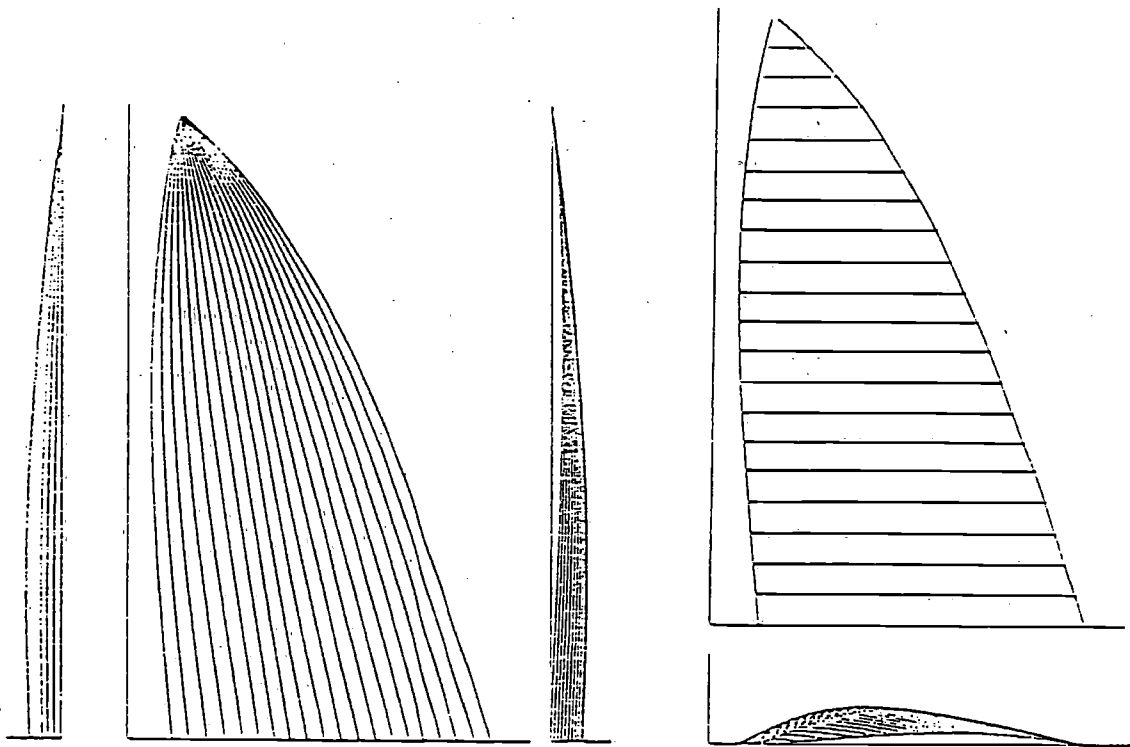
References

- [1] Haarstick, Stephen,
'Principles of Sail Design',
Chesapeake Sailing Yacht Symposium, SNAME, January 1977
- [2] Versluis, A.,
'Beschrijving computerprogramma voor het berekenen van de baanuitslagen van zeilen',
Rapport No. 505-M, juli 1980,
Laboratorium Scheepshydronechanica, TH-Delft (in Dutch).

Surf sail

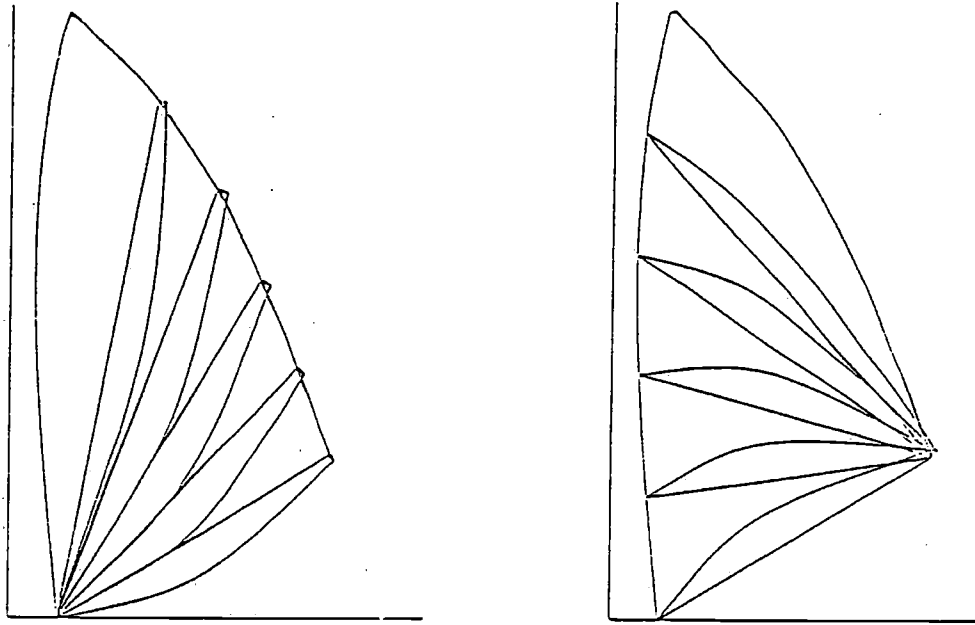


Input data

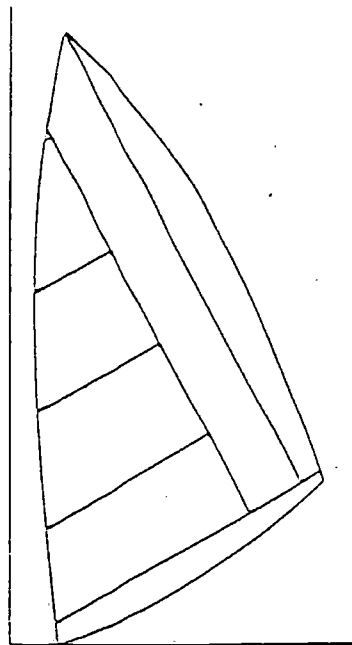


Vertical and horizontal cross sections

Figure 14a

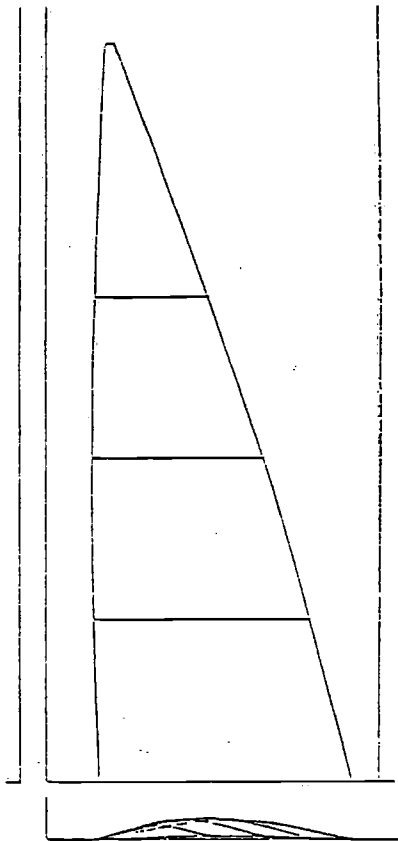


The shape of the radial cross sections

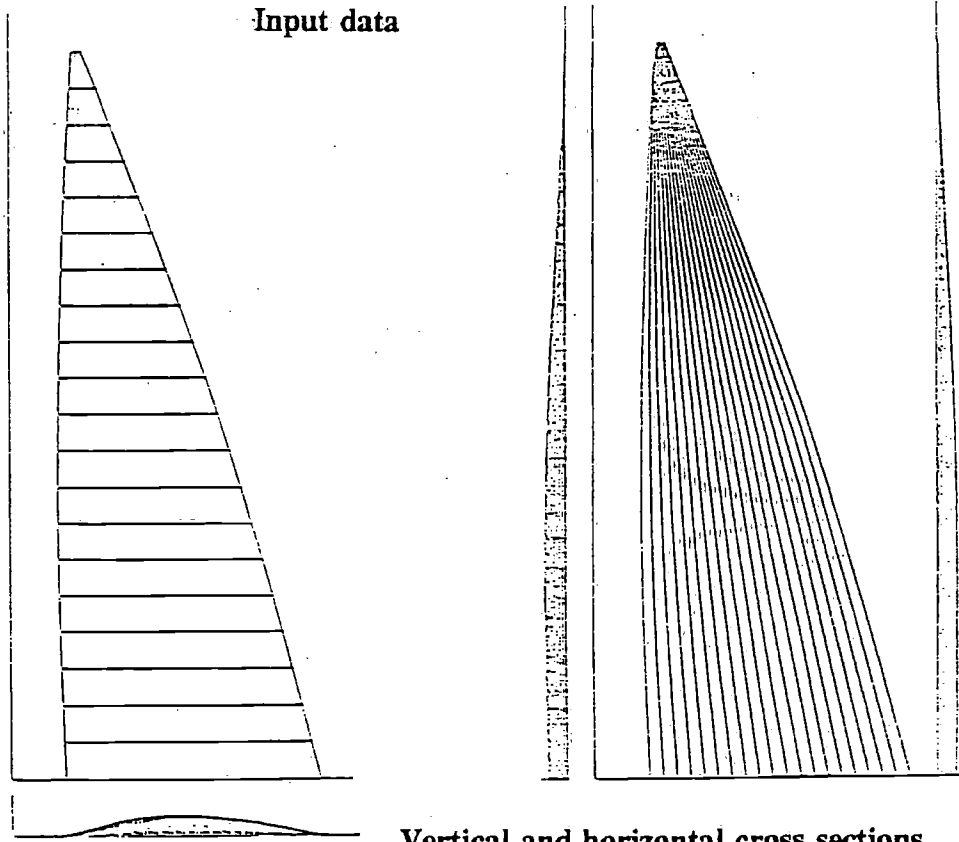


Panel definition

Figure 14b

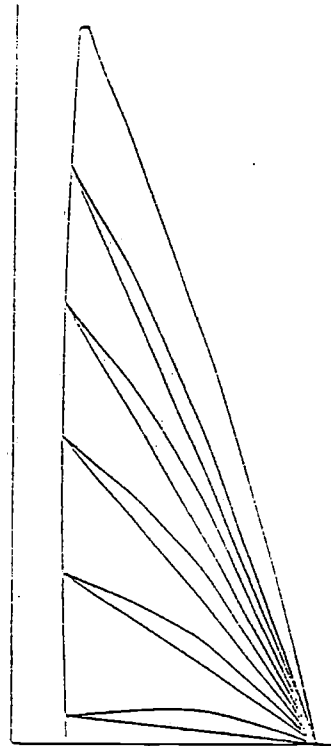
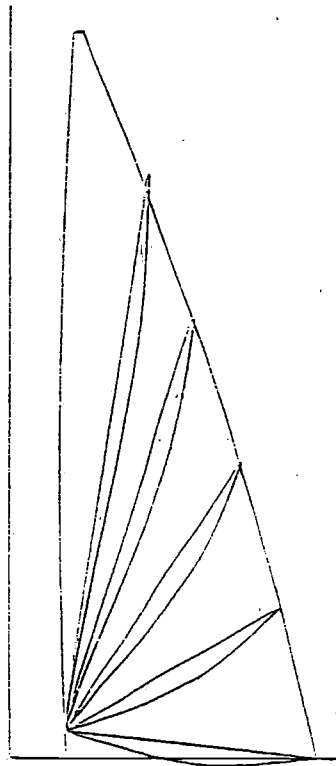


Input data

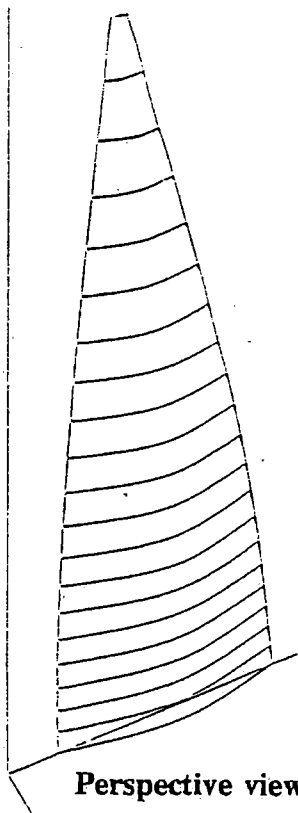


Vertical and horizontal cross sections

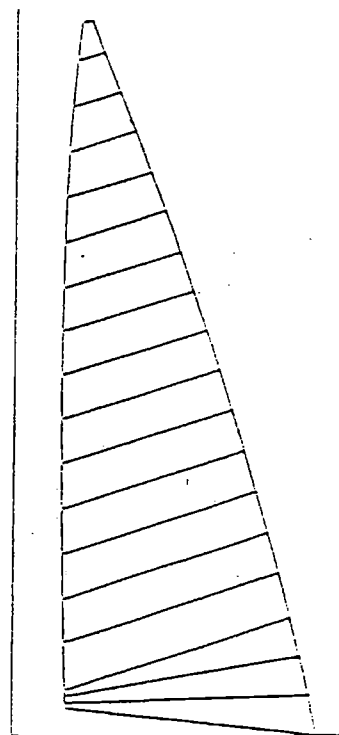
Figure 15a



The s. The shape of the radial cross sections



Perspective view



Panel definition

Figure 15b

Strength and Stiffness of Rigs

by T.F.van der Werff and P.J.Keuning

- 1 Introduction
 - 2 The external loading on the rig
 - 3 Finite element modelling
 - 4 Criteria
 - 5 Computational results
 - 6 Conclusions
- Nomenclature
Appendix I
Appendix II
Appendix III
Appendix IV

1 Introduction

General

The rig as a combination of mast, spreaders and stays is a statically undetermined system. In the past it was very cumbersome to determine the resulting loading on such a system with only analytical tools available. The commonly used calculation method for rig dimensioning is based on the procedure as given by Skene. Ref. [1].

It determines the loading in the stays and the axial compression forces in the mast for an ultimate loading condition.

In this procedure a force in transverse direction in the top of the mast is assumed, which equals the maximum righting moment of the yacht. Because of this load condition the results are representing the loading caused by a genua or spinnaker. No data is gathered about the bending of the mast.

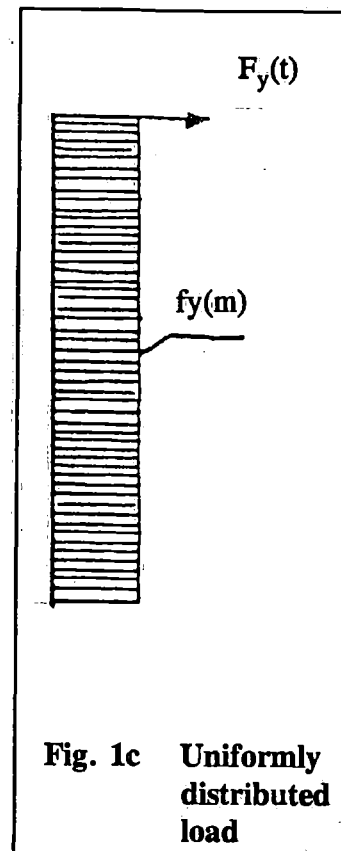
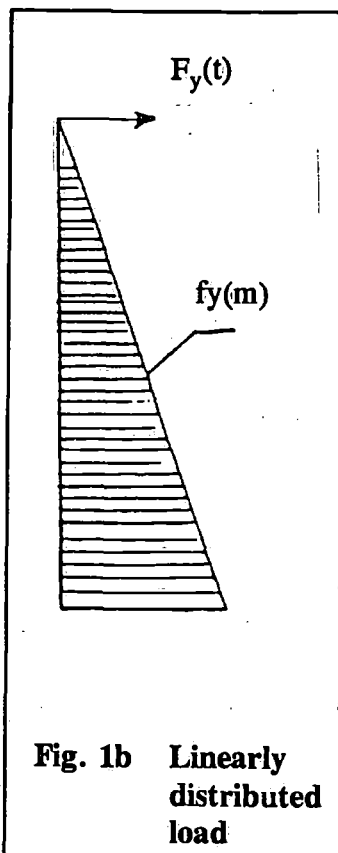
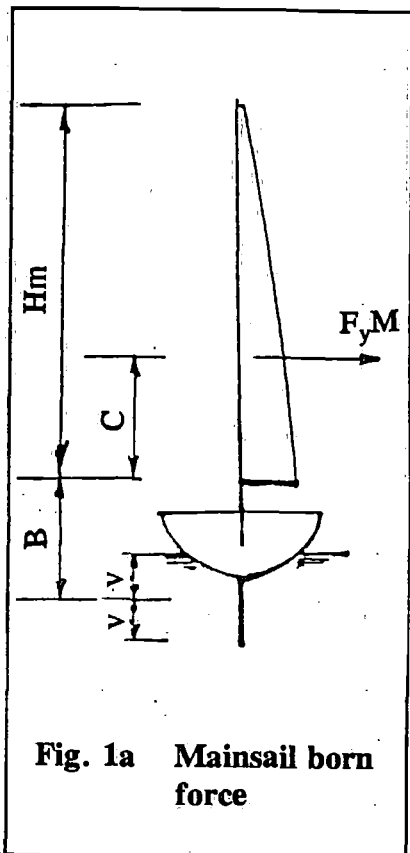
For a better understanding of the actual rig loading a more complex evaluation needed.

Nowadays with the widely available personal computers the computation of the resulting forces in the rig under complex loading conditions is possible using Finite Element Modelling (FEM) techniques. However, the general application of the FEM codes is still limited because a thorough knowledge of the limitations of these FEM codes is necessary to ascertain reliable results.

The main problems to be solved using FEM techniques for rigs are:

- Determination on the external loads on the rig
- Generating the correct FEM model for the specific loading
- The non linear behaviour of the rig
- Determination of the buckling load of the mast.

The loads imposed on the rig are very difficult to assess exactly, and can differ very much



depending on the sails carried by the yacht. An engineering approach is used to determine the most relevant loadcases for rig analysis.

The modelling required for rigs is discussed, in which special attention is given to the influence of pretensioning of the rig to the model. The required criteria for rig design are discussed, with special emphasis on the buckling load determination.

Computational results are presented for different loadcases on two rig geometrics.

A systematic approach to the different types of loading is used here. This systematic approach is chosen in order to get a better insight in which conditions are of relevance for the rig design. It also enables the establishment of the sensitiveness of the results to the assumptions made.

It also demonstrate the possibilities of simple FEM calculations for mast design.

2 The external loading on the rig

General

The rig of a sailing yacht is subjected to forces of different origins. The most obvious ones are the aerodynamic forces on the sails, which introduce loads on the mast, boom and stays. Apart from these other forces act upon the rig as well.

For instance, pretension on the backstay introduces compressive loads in the mast. The same holds for the pretension in the transverse stays. An other kind of loading originates from the mass of the rig. In static conditions this is expressed in its own weight. However in a seaway or due to a windgust the mass of the rig and ship is subjected to accelerations. These can sometimes be sufficiently high to exert heavy loads on the rig.

It must be kept in mind that an exact determination of these often very complex loads is not always possible.

So in the following an engineering approach is assessed regarding nature and order of magnitude of external forces, which are considered relevant in rig design.

2.1 Forces originating from the mainsail

The mainsail born loads are schematized as discussed in appendix I. The following consumptions are made:

- The mainsail forces are transferred by the leech and mast. The latter taking 75 %, the former 25 % of the total sailforce-component, perpendicular to the plane through the mast and the boom
- The vertical distribution of the load is difficult to determine.

In literature several assumptions can be found. Here two alternatives are considered:

- linear distribution, zero at the top, having a maximum at the foot of the sail. This is further referred to as loadcase 2.
- uniformly distributed load, further called loadcase I.

See Figures 1a, 1b and 1c.

The last one is considered to be the most closely related to the actual one for sailing to windward; the other for reaching and reefed condition.

First only the athwartship will be looked at.

Assuming that the heeling moment of the ship is caused by the mainsail only, it is found that the loads vary between the following limits:

- The total of the distributed load along the mast:
$$1.0 \text{ to } 1.4 \cdot M(\phi)/H_m \quad (1)$$
- the pointloads at the mast-top and boom-end, due to the leech:
$$0.16 \text{ to } 0.18 \cdot M(\phi)/H_m$$

The lowest value for the mast-top belongs to the highest value at the boom-end.

The most important components of the forces by the mainsail in its plane with respect to their impact upon rig behaviour, are the transverse forces at the mast-top, $F_y M(t)$, and the end of the boom, $F_y M(c)$. These can only exist due to the sagging of the leech (Figure 2a). In fact the transverse forces are the athwartship component of the tensile force in the leech of the mainsail, F_l .

The following simplification is made:

$$F_l \cdot \theta_1 = F_y M(t) \text{ and } F_l \cdot \theta_2 = F_y M(c) \quad (2)$$

Mainsail born loads are restricted to the loadset shown in Figure 2b. The tension in the leech F_l gives also rise to a force in longitudinal direction at the top of the sail. This is especially relevant for fractional rigs and masthead rigs with a reefed mainsail. The magnitude of this force is approximately the component of F_l along that axis. In the boom of the mainsail also compressive forces are generated. For wind-ward sailing conditions the leech tension is assumed to be directly transferred to the mainsail sheet in most conditions. So no high forces at the goose-neck result.

For off wind conditions the leech tension is applied by means of the boom vang. This generates high forces both in the goose-neck and the boom-vang attachment points. The magnitude of these forces can be derived from equilibrium equations for the boom, once a F_l value is assumed.

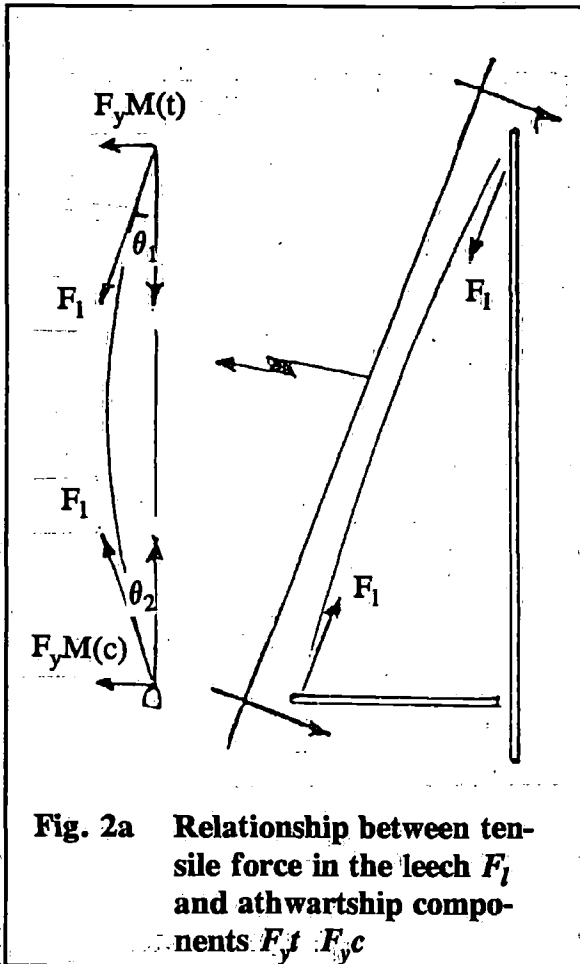


Fig. 2a Relationship between tensile force in the leech F_l and athwartship components F_y , $F_{yM(t)}$, $F_{yM(c)}$

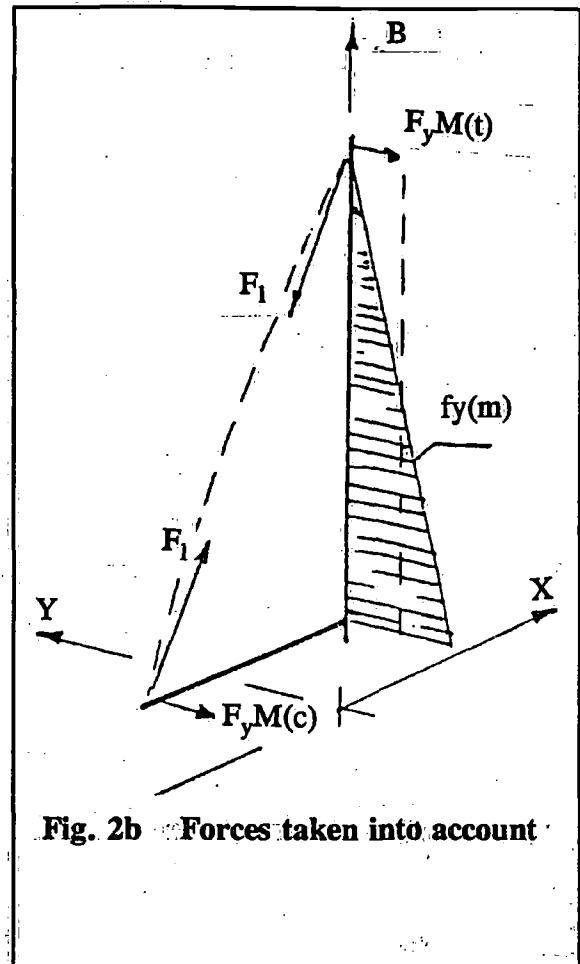


Fig. 2b Forces taken into account

2.2 Forces originating from the headsail

In appendix II and assesment of the athwartships forces initiated by the headsail is given. The following assumptions are made:

- The load distribution over the height of the sail is varied in the same way as for the mainsail
- The total force is transferred to the ship by the tack and clew of the sail at decklevel and by the top of the sail at the mast-top.

Assuming that the heeling moment of the ship is caused by the headsail only the mast-top component of the sailforce varies between:

$$0.75 \text{ to } 0.85 \cdot M(\phi)/H_g \quad (3)$$

The derivation of this expression is given in appendix II.

Spinnaker loading are treated the same way as headsail loadings, resulting in approximately the same values at the mast top.

A quasi static amplification factor may be considered on these force, to accomodate the dynamic influences of broaching. This is however not further elaborated in this paper.

In the following attention is paid to mechanisms leading to realistic headstay forces. For the headstay the same holds as earlier mentioned for the mainsail leech. The transverse component can only be generated by the sag of the stay to leeward. This sag however will occur in both transverse and alongship direction. For the relationship between the tension in the headstay, its athwartship component, the fore-triangle geometry and the total sag of the headstay

the following expressions can be derived:

$$F_h / F_y H(t) = \sqrt{(\text{tg}^2 (\tau - \beta) + \text{tg}^2 \alpha + 1) / \text{tg} \alpha} \quad (4)$$

See appendix III.

Here additional assumptions are made with respect to the headstay behaviour:

- the tangents to the luff of the sail are in one plane. The angle between this plane and the plane of symmetry of the yacht is γ
- The sag of the headstay is in this plane only. The result is γ_0 is γ , projected on a horizontal plane, a 'spatial sagging angle' between the loaded headstay and its position at rest.

It is evident that the force in the headstay can only reach realistic values if sag occurs in the stay. A totally straight stay pushes the required force in the stay to infinity.

On the other hand, sag is a result of the elongation of the headstay under the load F_h , together with the deformation of the structure of the yacht and the mast as a result of the force F_h . The apparent wind angle has a certain relation with the angle γ_0 which is somewhat larger than this apparent wind angle.

For a given angle different curves can be drawn, representing the ratio F_h/F_y as a function of the heeling angle of the yacht ϕ . See Figure 3a. In Figure 3b, a three-dimensional surface is given for F_h , ϕ and δ for a specific geometry and value of Cross-sections through this surface for a constant value of ϕ provide graphs as given in Figure 3c. The same is presented in Figure 3d, on basis of a double logarithmic scale.

This may be regarded as the 'exciting force' side in the equilibrium between the external loading imposed by the headsail on the rig and the response of that rig.

It 'asks' for a particular tension in the headstay in combination with a sagging angle.

The 'response' is a headstay with sag, for which a deformation shape has to be assumed along its length. In appendix IV an engineering approach for this complex problem is suggested, which is assumed to be of sufficient accuracy for the problem under consideration. Lets first assume the structure of the yacht and the rig, except the headstay, are infinitely rigid.

The load F_h causes an elongation in the headstay, which results in a sagged wire in the deformation shape assumed.

Or putting it the other way around, the forces causing the headstay sag (the headsail hanging on its luff) ask for a certain headstay tension going with that sag. The total headstay tension F_h consists of a pretension F_o and a induced load F_i .

$$F_h = F_o + F_i$$

This is graphically presented in Figure 3e on the same double logarithmic scale as used in figure 3d.

All the curves for the pretension F_o go asymptotically to the particular pretension value when the sagging angle goes to zero.

For large sag angles the pretension curves merge with the non-pretension curve.

The combination of the Figures 3d and 3e leads to the graph as shown in Figure 3f.

For illustration this final diagram is presented for one of the yachts used in the computations, the KALIK 33, in Figure 4.

The following information can be drawn from the diagram:

A yacht sailing with a heeling angle ϕ and a headstay pretension such that the sag angle is δ_a . When an increase in windspeed is faced, the transverse forces cause the ship to heel further to y_2 . If the sail-rig geometry e.g. headstay sag would stay unaltered, the tension in the stay would increase to the value F_{h1} .

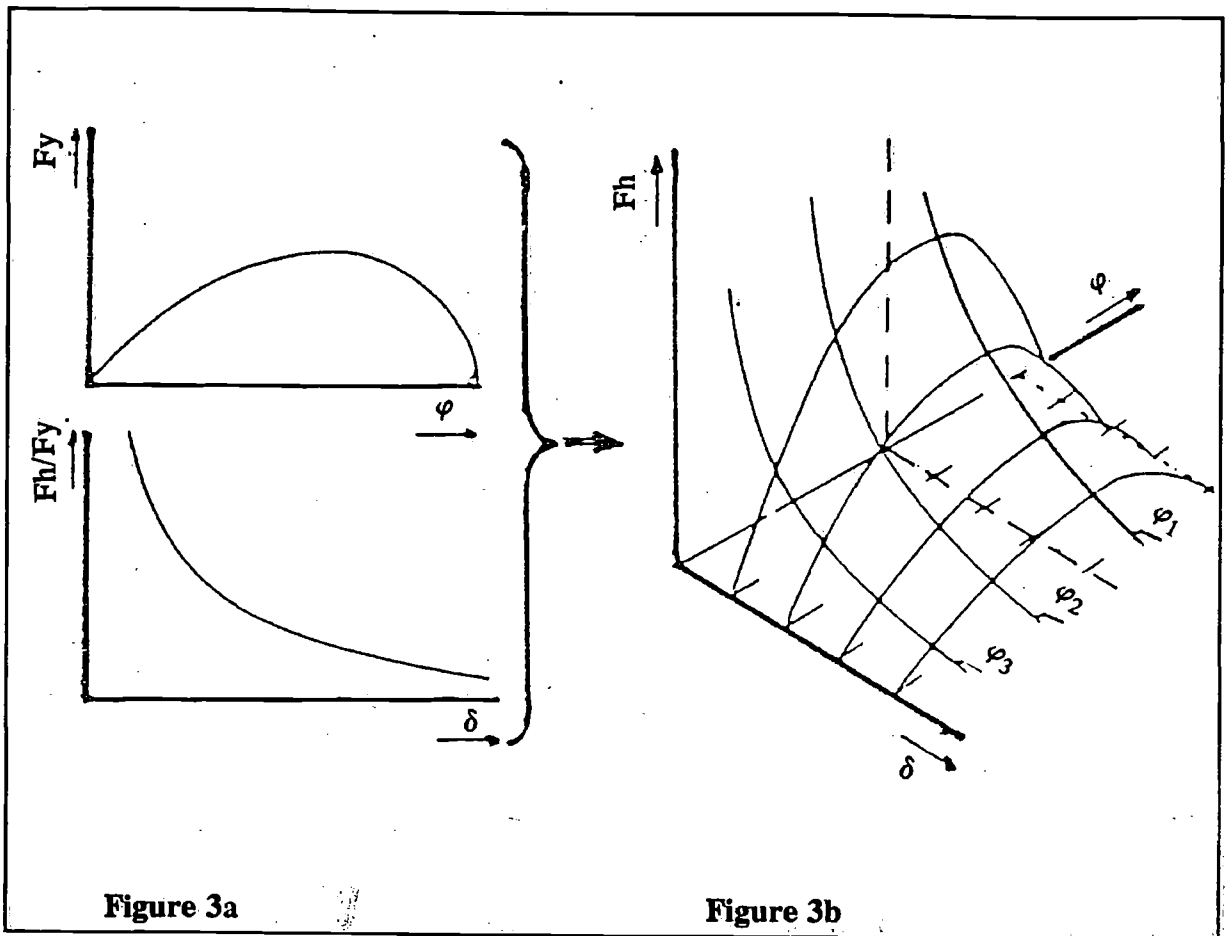


Figure 3a

Figure 3b

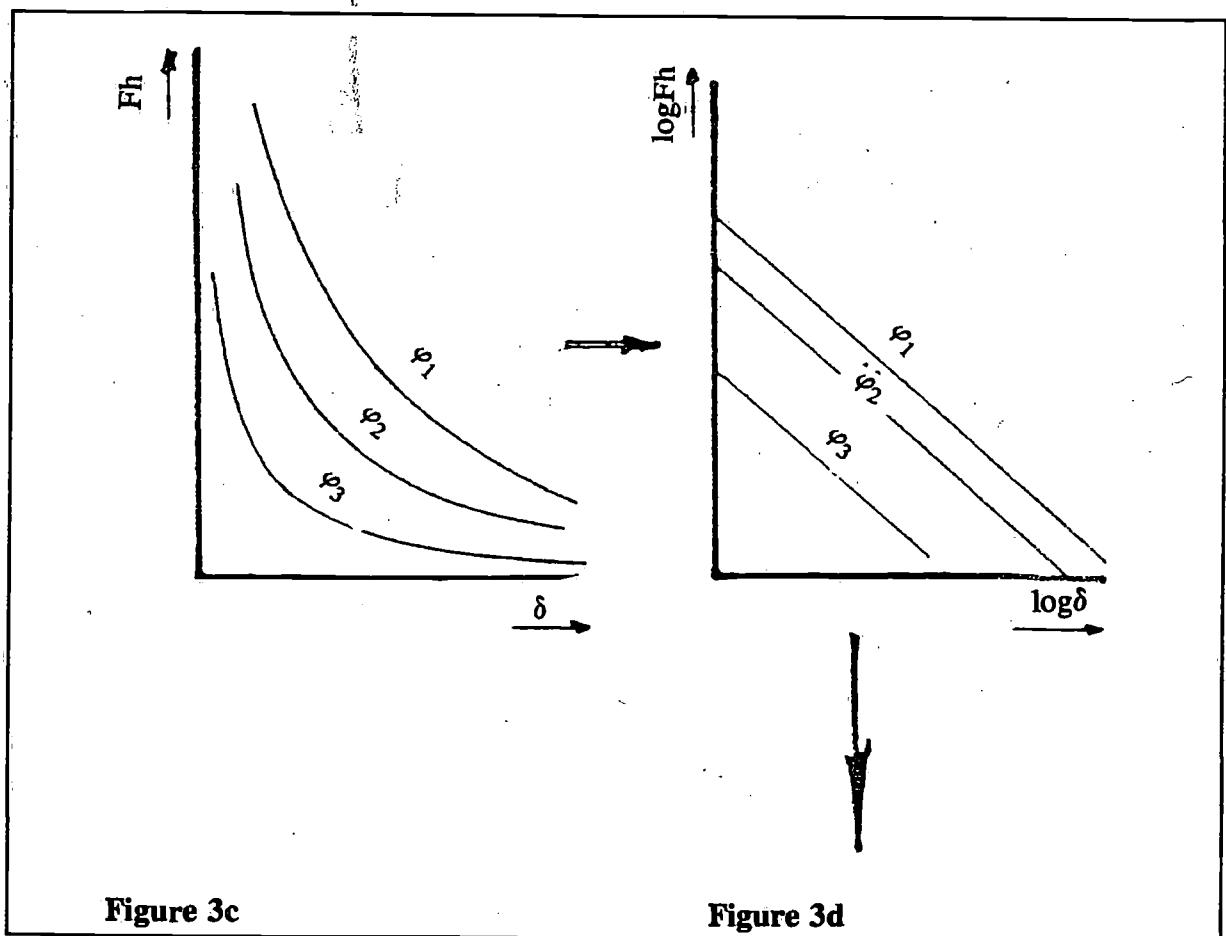
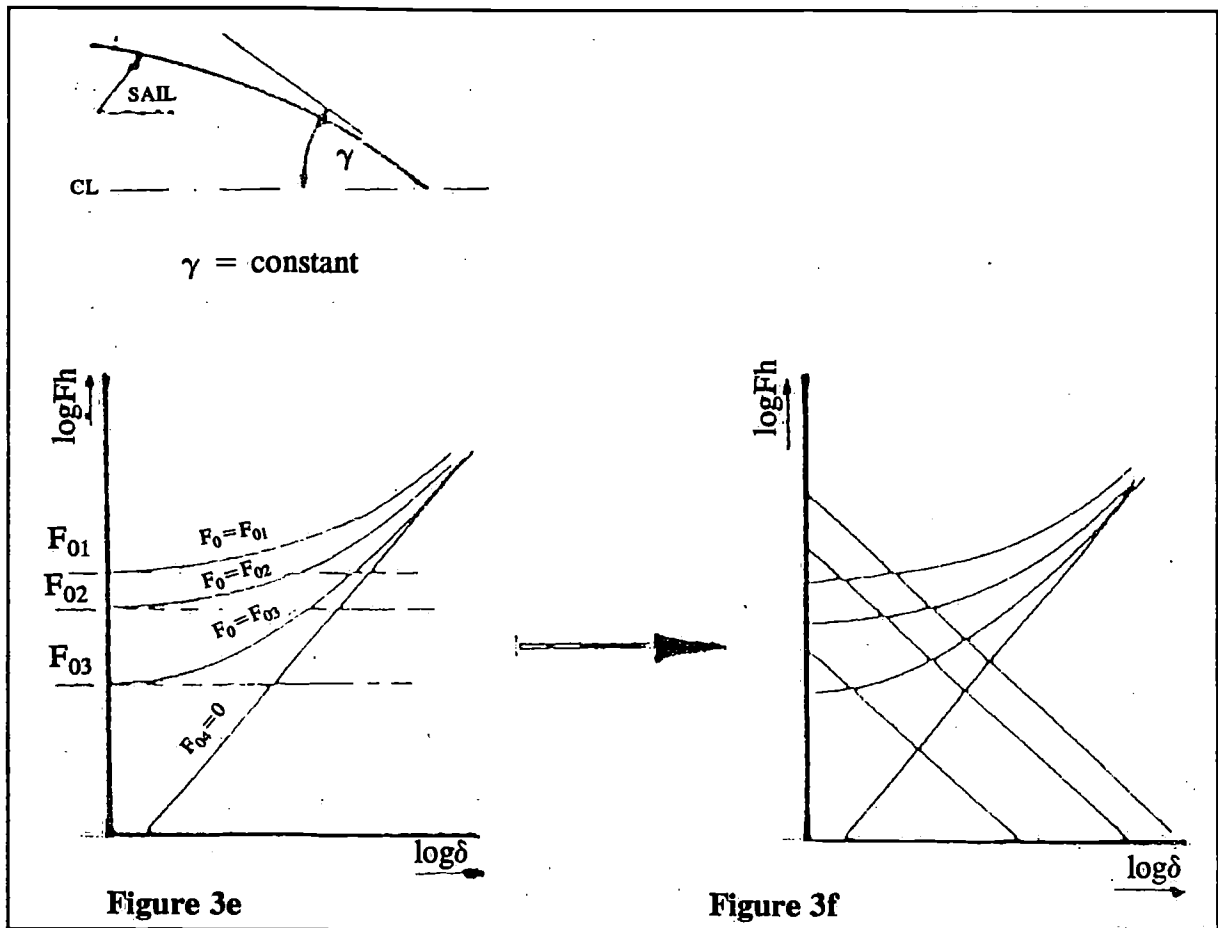


Figure 3c

Figure 3d



When the heeling angle of the yacht increases from 5 to 30 degrees, this could mean a 6 - 10 times increase in tension for windward conditions. This obviously does not happen, the elongation of the headstay reduces the increase in tension in that stay; F_{ho} increases to F_{h2} because the sag angle increase from δ_a to δ_b .

So in this particular case headstay forces are reduced by 60% due to the flexibility of the headstay alone.

Now the consequences of the flexibility of the structure are taken into consideration, especially focussed on the behaviour of the headstay. This non-rigid behaviour results in the following deflections (Figure 5).

- elongation of the back stay
- shortening of the mast due to compression
- deflection of the cross section of the yacht in way of the mast, between the foot of the mast and the chainplates.
- sagging of the entire hull

Two phenomena can be distinguished: a loss of pretension and a stiffness reduction.

In Figure 7 the pretension loss is shown schematically. At a heeling angle of approx. 20 degrees, the leeward shroud is assumed to become slack.

Until that point, marked by (I) in the figure, the deflections are only governed by the pretension, denoted by the starting position marked (O). Neglecting all other influences like keel-forces etc., deflections do not alter until point (I) is reached. The force F_s causes a heeling moment, resulting in a rigid body motion only (ϕ_s).

A further increase of the heeling moment is ofcourse associated with a increase of the

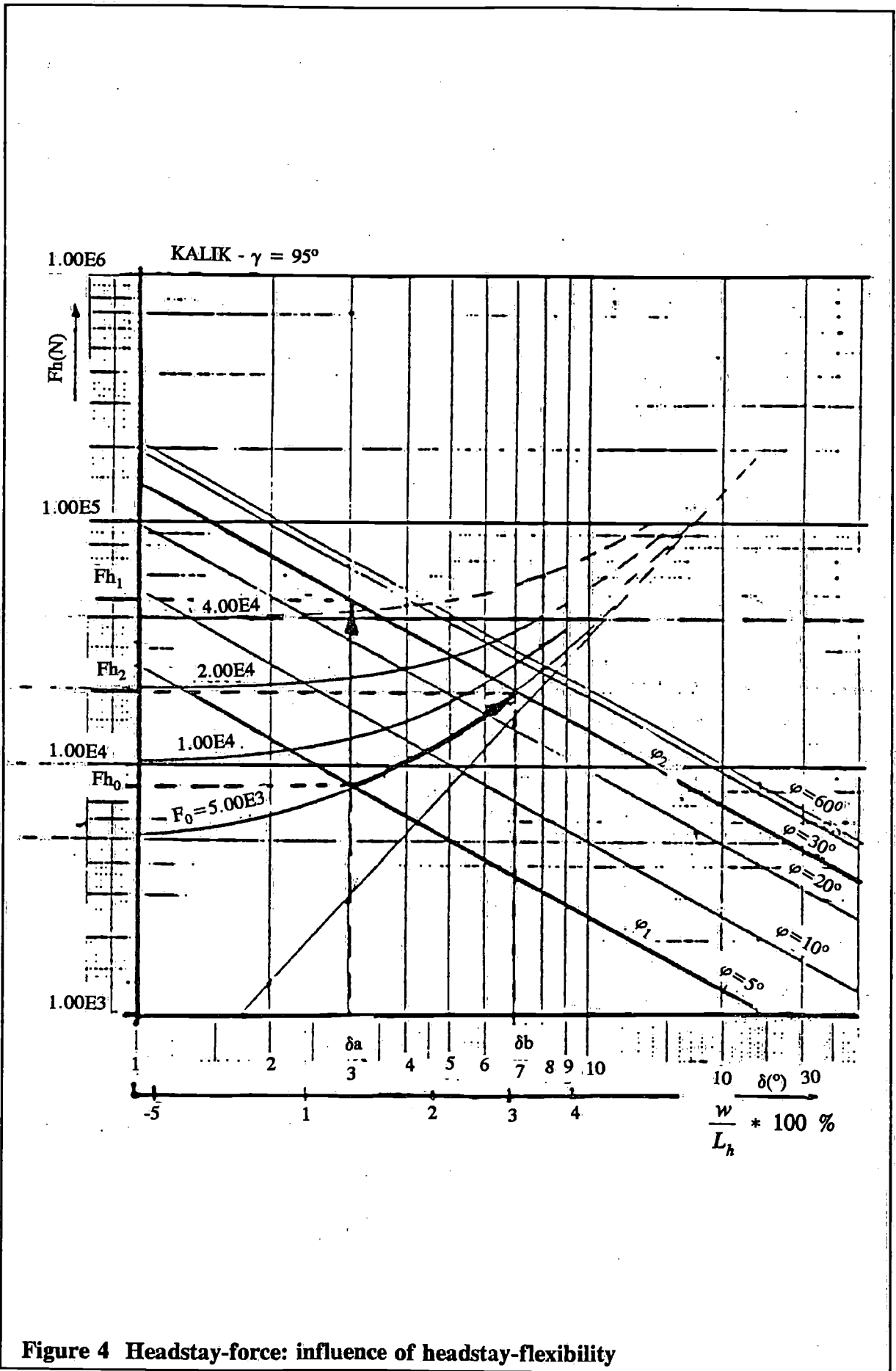


Figure 4 Headstay-force: influence of headstay-flexibility

heeling angle (ϕ_s). In the figure this is marked by the contribution (III). Now the deflections in the cross-section increase as well, due to the contribution marked with II in the figure. In short, this last contribution (II) causes a decrease in the distance between the masttop and deck if heeling angles are 20 degrees and more. To illustrate the order of magnitude of this pretension loss, results for an assumed G.R.P. hull construction are used in conjunction with the earlier presented results for the KALIK 33 in Figure 4.

The combination of the resulting hull deformation and this rig geometry is given in Fig. 6. The pretension in the backstay is set on 7500 N.; the resulting headstay tension becomes then approx. 8500 N. This pretension is, for heeling angles beyond the 20 degrees, gradually lost. This is given by the curve marked (1) in the figure.

Curve (2) represents the headstay force as it would develop for a totally rigid ship structure. Due to the deformation of the hull, the force develops however as given by the curve (3).

It is also worth noticing that for this particular case a further increase of the stiffness of the headstay has little effect on the overall performance, due to the relatively large flexibility of this assumed hull structure. Increasing the stiffness to twice the original value, reduces the sagging in the stay only from 5% to 4.5% of the headstay length.

Finally for spinnaker conditions also spi-pole forces on the mast have to be taken into account. These can be derived from equilibrium equations between the force in the clew and the spi-pole compression force and the force in the sheet and pole-lift. The magnitude of these forces is in the same way as for the boom-vang forces on the mainsail.

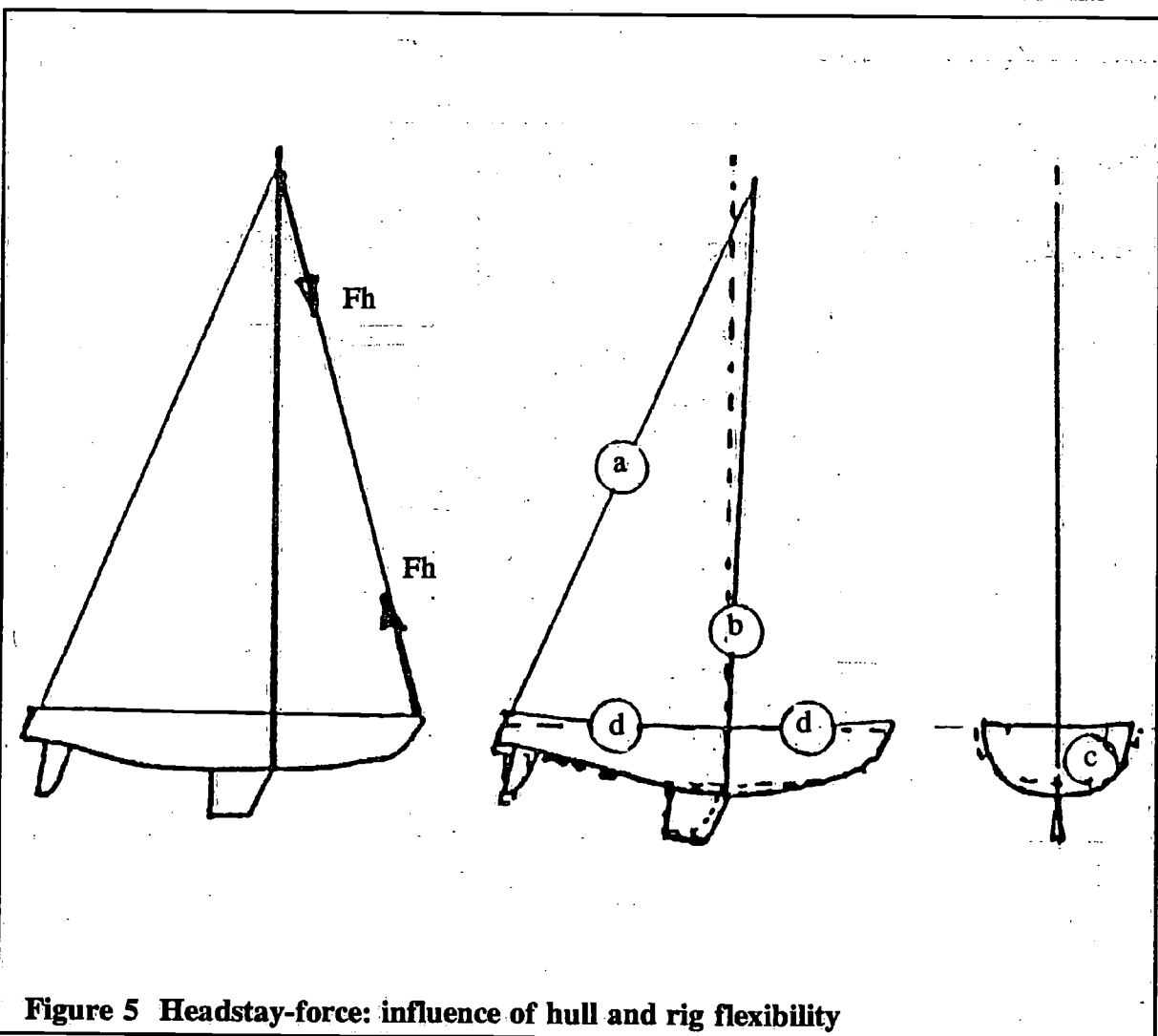


Figure 5 Headstay-force: influence of hull and rig flexibility

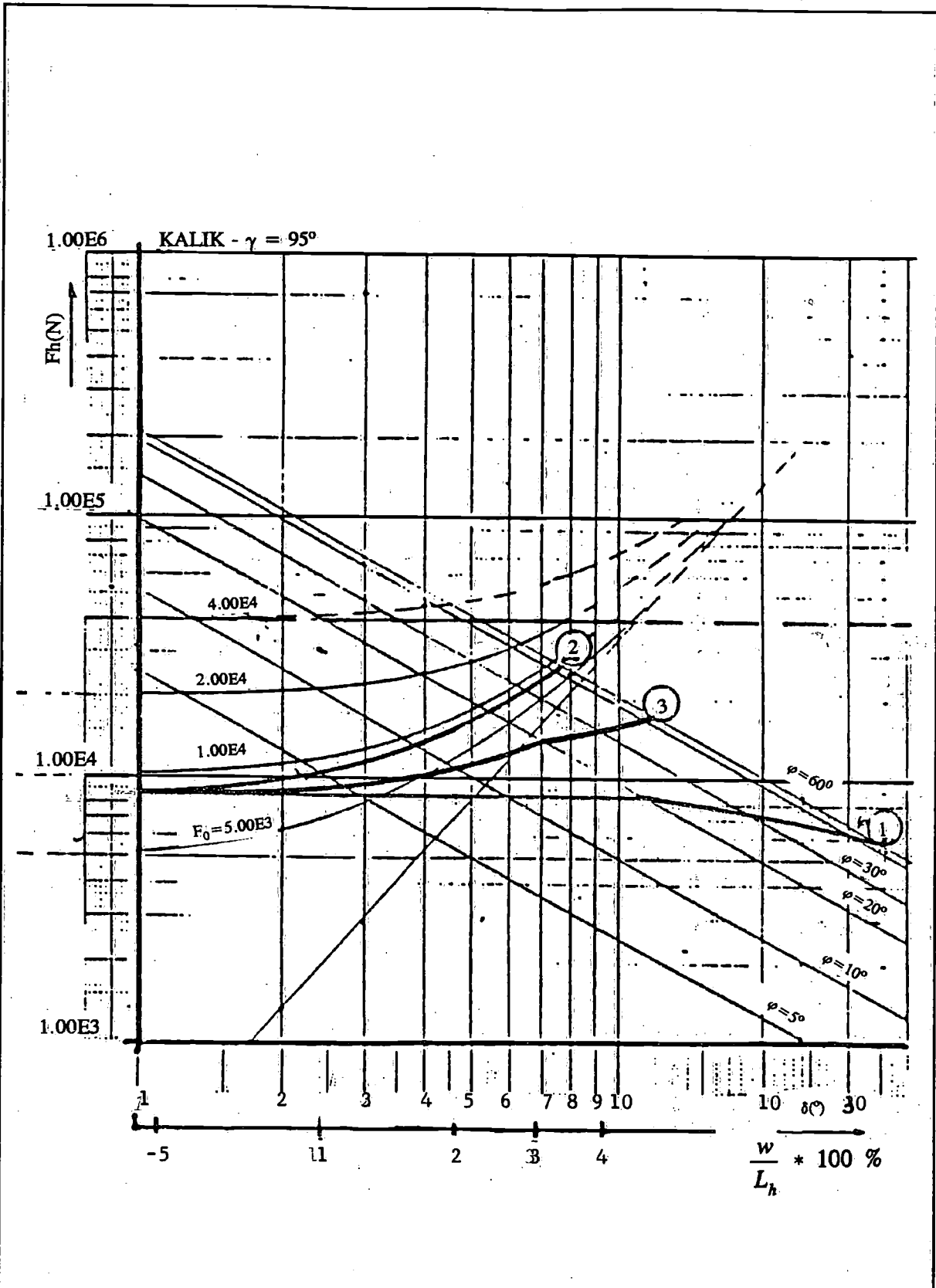


Figure 6 Headstay-force: influence of both hull and rig flexibility
1: pretension
2: headstay-force i.c.o. an infinitely stiff structure
3: realistic force-sagging diagram

3 Finite element modelling for rigs

If the rig system would have been a latticed beam structure, FEM modelling would have been straightforward.

The application of wires in the system is however a complication. The simulation of wires, with no capability to carry compressive loads is not directly possible with simple FEM codes. For a better understanding of the required technique, first a general discussion on the effect of pretensioning on the rig performance will be given.

Pretension Influence

For the sake of simplicity we restrict ourselves in the example to transverse loading of the rig (y -direction) by a force in the top of the mast.

We assume a rig with a certain level of pretension. Of the shroud forces the transverse components, $F_y(1)$ and $F_y(2)$ are considered. Both *SB* and *PS* shrouds exert a force in y -direction on the top of the mast, without any external force on the mast, the mast is at rest, so:

$$|F_y(1)| = |F_y(2)| = F_{y\text{pret}} \quad (5)$$

The stiffness of the wires in y -direction is given by:

$$C_y(1) = C_y(2) = (E \cdot A/l) \cdot (\sin^2\eta) \quad (6)$$

In which η is the angle between mast and wire.

If a small external force $F_y(\text{ext})$ is exerted on the masttop in negative direction the mast will displace in that direction over a distance W . $F_y(1)$ will increase and $F_y(2)$ will decrease to establish a new equilibrium, so:

$$F_y(1) + F_y(2) + F_y(\text{ext}) = 0$$

The change in shroud forces being:

$$C_y(1) \cdot W = -C_y(2) \cdot W = F_y(\text{ext})/2$$

So the leeshroud (2) contributes to the equilibrium, and the total stiffness of the system is given by the summation of the stiffness of the two shrouds. This is the case until the leeshroud becomes slack, which neglecting all other influences happens when:

$$C_y(2) \cdot W = F_y(\text{pret})$$

From there on only the windward contributes, so equilibrium is given by:

$$F_y(1) = F_y(\text{ext})$$

The change in shroud force being:

$$C_y(1) \cdot W = F_y(\text{ext})$$

The total stiffness of the rig now being only the stiffness of shroud 1. The displacement W versus the external force is graphically presented in Figure 8a, which also gives the curve for the case without any pretension. The forces in stays and mast as a function on the $F_y(\text{ext})$ is given in Figure 8b. The axial compressive force in the mast is constant until the moment that the lee-ward shroud becomes slack. Because the load imposed is pure bending and the mast is on the neutral axis of the beam, consisting of mast and both stays.

The displacements of the mast as a function on the external force is less in case of pretension relative to the case without pretension, so pretension stiffens the rig, the total displacement being smaller also when the leeshroud is slack. The forces in the system however are the same for the ultimate loading condition when the leeshroud is slack.

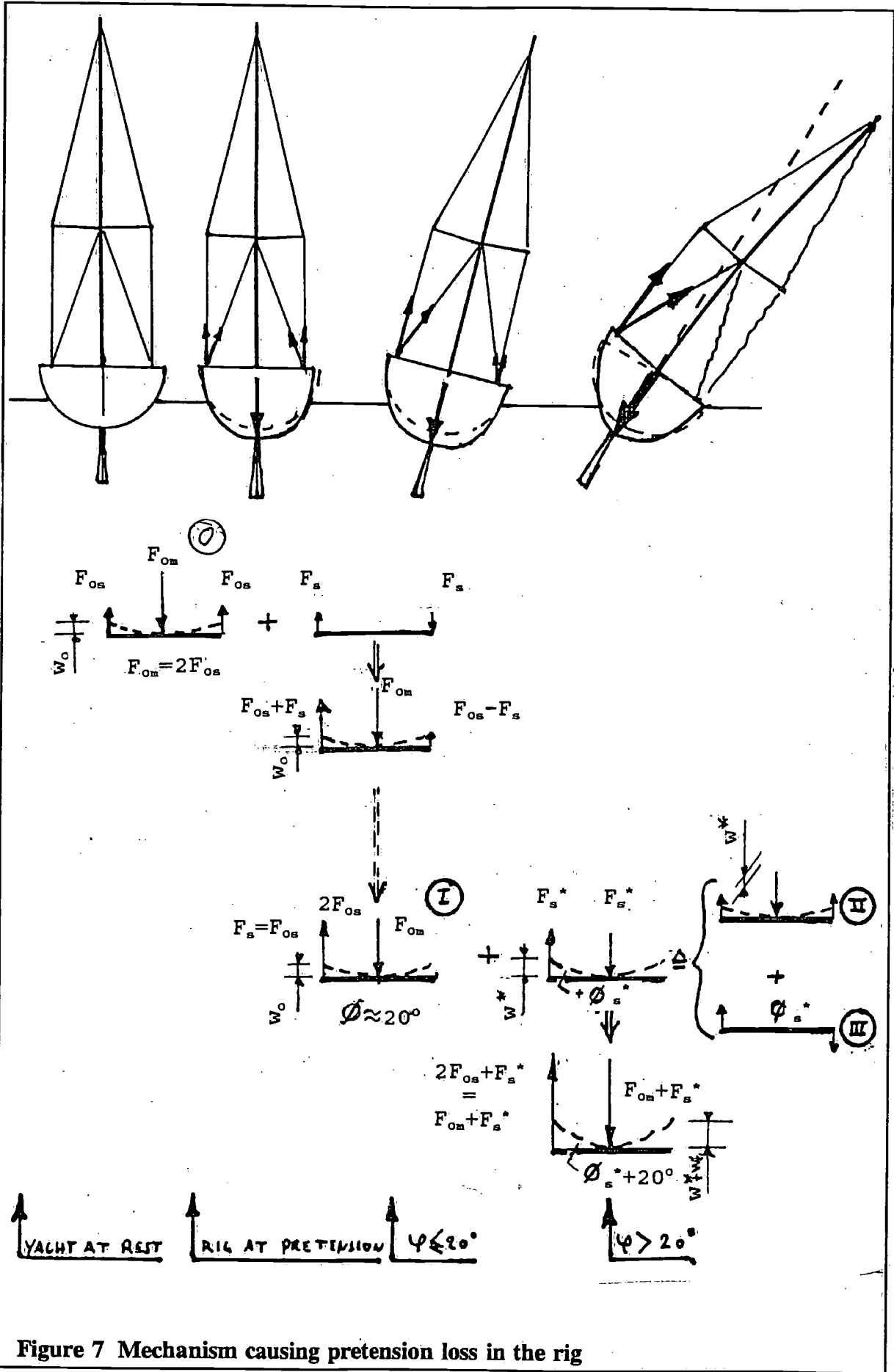


Figure 7 Mechanism causing pretension loss in the rig

So pretensioning does not enlarge the maximum forces in the system. In case of pretension the bending of the mast is reduced, resulting in lower bending stresses, also when leeshrouds become slack.

Modelling

Direct modelling of these phenomena ask for a non linear model in the FEM code. This is however out of the scope of the mast designer using PC facilities. So schematizations are necessary using linear calculation only.

The combination of beams (mast) and wires (shroud) demands a special modelling in case a certain amount of pretensioning of the shrouds is used, which is always the case, the amount of pretensioning however can differ considerably.

In order to incorporate the behaviour in the FEM calculation the pretension of the wires has to be brought in the model and all the shrouds have to be modelled.

When the loading is applied to the mast a check run has to be made to evaluate the shroud forces. If no compressive forces are found in the wires, the calculated results are directly applicable. If however wire-forces become negative, that specific shroud has to be removed from the model and the calculation repeated. The total stiffness then applied in the FEM model, is of course only valid for the high load part of the deflection curve.

This would result in too large deflections of the mast. However, this is not the case because the additional stiffness due to the pretension is simulated in the model through the pretension in the windward shrouds. This causes the mast to bend in the opposite direction, when no external force would be present.

This is graphically represented in the Figure 8a by the line under the axis. It results in both the correct forces and bending moments in the mast.

The calculation procedure given above can be simplified, assuming an 'optimum' pretension; meaning the pretension distribution in the shrouds equals the actual forces on them by the external force. In that case the calculation for conditions in which the leeshrouds are not slack, can be performed with a model without pretension and the leeshroud taking compressive loads; the shroud forces are found by summation of the calculated forces and the pretension. For the ultimate loading condition, assuming slack leeshrouds, the axial compression force in the mast and shroud forces are the same as for the case without pretension. The bending moments in the mast are however smaller.

For ultimate load conditions with slack leeshrouds the model consists only of the windward shrouds. The influence of the pretension on the bending moments is taken into account by subtracting the force necessary for slacking the leeshrouds from the external force, when determining the bending moments for this case.

However for different loading conditions this gives different 'optimum' pretension forces, which will differ from the actual pretensions used. So a schematization is made using this procedure, which may result in an underestimation of the bending forces in the mast.

4 Criteria

For the evaluation of a specific rig design, the computational results have to be compared with several criteria.

These criteria depend upon material properties, rig geometry and operational use.

The main criteria for evaluation are considered to be allowable stresses and buckling safety.

These will be discussed in the following.

Stress criteria

Two different stress criteria are relevant. These are related to two load conditions, which have to be considered in the design.

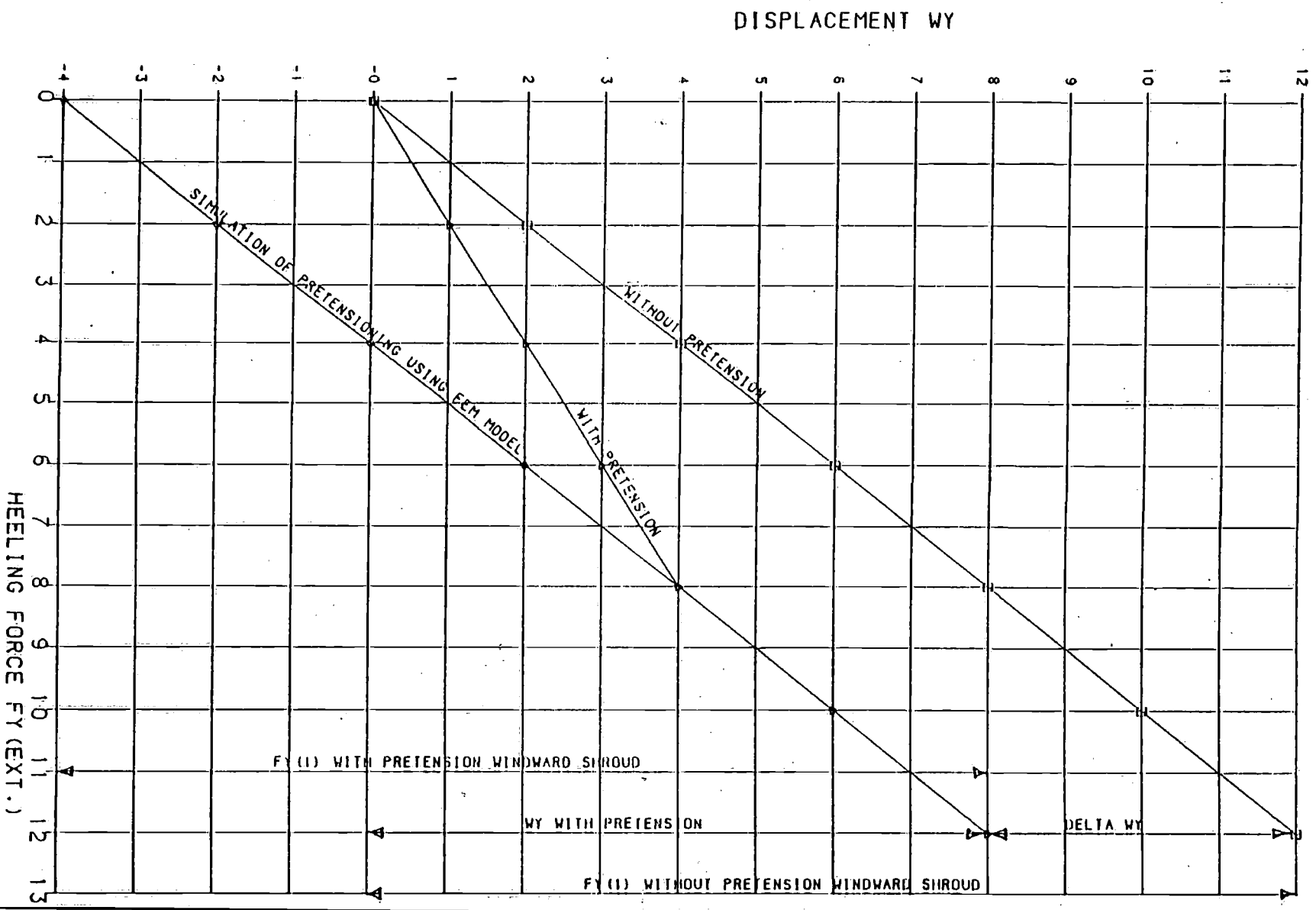


Figure 8a Influence of pretension of the shrouds on rig performance

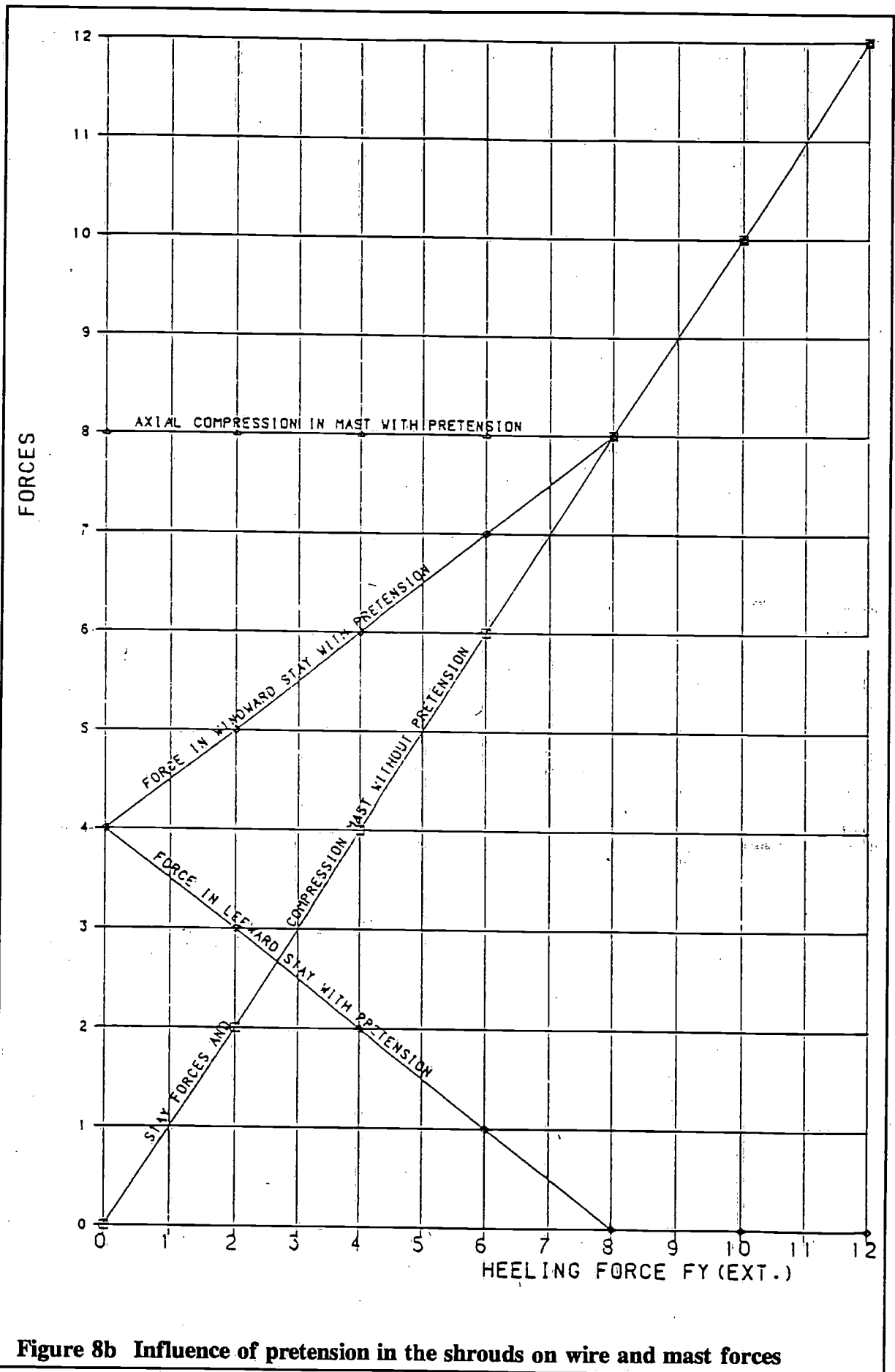


Figure 8b Influence of pretension in the shrouds on wire and mast forces

- ultimate loading condition. This is related to what is considered to be the 'few in a lifetime' survival condition.
Stresses up to ($\sigma_{0.2}$) can be allowable here. (7)
- normal operational conditions. The allowable stresses under these conditions are lower. A typical value being $0.75 \cdot \sigma_{0.2}$. (8)
For the latter conditions the emphasis is also on fatigue life, related to an assumed operational profile of the yacht.

For standard production yachts both the loading conditions to be considered and the operational profile will differ from both the racing yacht on the one side and the ocean passage yacht on the other side. The former one will tolerate lower safety factors. The latter one will probably have higher ultimate loading conditions as well as a reduction in allowable stresses for fatigue.

Classical rig design methods result in a safety factor of approx. 2.5 for the wires in the specified ultimate loading condition.

Dimensions of mast sections are usually only evaluated for buckling. However fatigue should be considered especially with regard to local high stresses due to stress concentrations.

The actual values used for allowable fatigue stress are very dependent on the material used. Special attention should be paid to the fatigue strength of the material affected by welding, because high strength aluminium is prone to considerable degradation due to welding.

Buckling

For the evaluation of the buckling safety two types of buckling have to be considered:

Global buckling

Two modes can be distinguished:

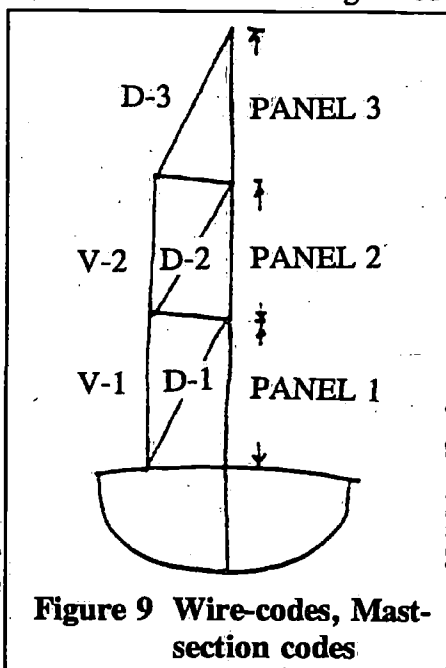


Figure 9 Wire-codes, Mast-section codes

- overall buckling. This refers to the total system of mast and stays. The mast being the element collapsing in its fundamental mode. This is only of relevance for the longitudinal direction, when no innerheadstays or running backstays are used.
- column collapse between the supports. In this case the mast is supposed to be a beam supported at the shroud attachment points. Because of the longitudinal moment of inertia of the mast section being larger than the transverse one, the athwartship mast geometry is determinative.

In the following the different parts of the mast which be referred to as panels. For definition see Figure 9.

These are the collapse modes which are normally considered in the usual design procedures. Critical buckling loads are determined using the classical Eulerian formulation. High safety factors are applied.

However this seemingly high safety factor decreases quite rapidly when additional factors, influencing the critical load, are also considered.

These additional factors are:

- Additional compressive forces in the panels due to the forces of the head- and back-stays, halyards tensions, goose-neck forces etc.
- Additional stresses in the mast due to the bending moments. In determining the critical collapse load, these have to be taken into account. As will be shown later, their contribution to the critical stress in the mast section can easily surpass the compressive forces.
Methods for incorporation of these bending stresses in the critical buckling collapse load calculation can be derived from rules, used in regulations for industrial structures.
- Reduction of the cross section area of the mast due to for instance halyard outlets etc. This results in higher stresses naturally.
- Boundary conditions. The classical Eulerian formulations used are valid for beams with infinitely stiff supports at the ends. For masts however, the supports are the shrouds and ship structure. The inherent flexibility of this support can result in a reduction of the critical collapse load. It is a function of the quotient between the stiffness of the mast and the stiffness of the support. In most cases this influence will be small, however for specific cases reduction to 25% are found.

For buckling evaluation of the rig design these additional factors have to be taken.

Local plate buckling

Usually mast dimensions are not evaluated for this buckling phenomena. The critical buckling load is a function of plate curvature and plate thickness. Rules and criteria are also available in the earlier mentioned regulations.

For masts with relatively large outer dimensions, plate thicknesses will be relatively small for weight considerations. It is found that for these type of masts, this buckling mode is probably determinative for the design and not the global buckling behaviour. Modern type racing yacht masts with small outer dimensions relative to their moments of inertia, have quite thick plating. These are not so sensitive to this buckling mode.

In this case also stresses due to axial compression and bending have to be taken into account. Local reduction of mast cross section deserve special attention.

The following can be noticed from the table with regard to:

a The different loading conditions:

The highest forces in the shrouds occurs for the genua or spi condition. Spinnaker loadings are higher, because the external loading is somewhat higher in the computations.

The only exception being the *D-1* wire.

The distribution of the forces over the wires differs considerably between the loadcase main- or headsail, especially for the masthead rig. The relative differences between mainsail and genua loading for the fractional rig are smaller, because the centre of effort of the mainsail is much closer to the shroud attachment point than for a masthead rig.

b Influence of the different load distribution assumption in height:

The different load distributions for the head sail gives only a 10% difference in the force at the top of the mast, and a equivalent difference in wire forces. These are not further presented here. The two assumed distributions for the mainsail result in 10-30% difference in wire forces.

c The comparison between masthead and fractional rig:

Wire forces are higher for the fractional rig.

This is caused by a combination of several reasons, e.g. a higher stability of the yacht, a smaller base of the rig geometry and, for the mainsail conditions, a much higher centre of effort of the total force relative to the stay attachment points.

The relative differences between mainsail and genua loading for the fractional rig are smaller for that same reason.

For the fractional rig the contribution of the mainsail to the overall loading is larger than for the masthead rig, due to its configuration. So using only the force at the headstay attachment, as design load in the rig dimensioning, as is the case in the before mentioned analytical calculation method, may lead to unreliable results.

5 Computational results

General

For two yachts calculations are performed. Both yachts are of 3/4 ton size, a KALIK 33 (Jac. de Ridder) and a Dehler DB 2 (v.d. Stadt & Partners). One is a fractional rig the other a maststop rig.

The main characteristics are given below:

		KALIK 33	DB 2
L.o.a.		9.98 m	10.30 m
Displacement		4.80 m ³	3.30 m ³
M(ϕ) 60 degrees		3.3 E+6 Ncm	3.6 E+6 Ncm
rig-type		masttop two spreaders keel-stepped	fractional two spreaders keelstepped
mast section	1xx	590 cm ⁴	298 cm ⁴
	1yy	260 cm ⁴	133 cm ⁴

For the calculations a FEM programme for PC was used.

Different loading conditions were calculated in order to evaluate the influence.

The relative behaviour of these load-conditions determine which ones should be considered for the design.

Also investigated is the influence of the different assumptions on load distribution as discussed earlier.

The use of both fractional and mast-top rig enables a comparison between both type of rigs for design purposes.

The calculated loading conditions for both ships are:

- Mainsail with 2 different load distributions, transverse loading only
- Headsail transverse loading only
- Spinnaker alone
- Spinnaker and main.

For this paper the choice was made to calculate the response of the system to the different loading conditions separately.

This enables a better insight in their contribution to the loads in the system, which is valuable or the design of the rig. In this paper the results will be discussed briefly, the main purpose being to demonstrate the possibilities of these techniques and to establish that FEM techniques can be a valuable tool for rig design.

The calculations for the mast-top rig can be compared with experimental results of experiments carried out with that particular ship in 1983, which were reported on a earlier HISWA symposium.

However because the aim of the experiments was not to compare them with theoretical results, they are only partially applicable.

Shroud forces

In Table I the determined wire forces are given for the different loading conditions. The wire codes used are given in Figure 9.

All calculations were performed for the ultimate loading condition, with leeshrouds slack and maximum heeling angle.

Table I Forces in Newton

	V-1	D-1	V-2	D-2	D-3
KALIK, genua	18550	4800	11550	6900	10950
main 1	13200	9900	5200	7800	5100
main 2	9300	10700	3300	5850	3200
spi	21330	5525	13175	7925	12875

DB2, genua	19200	8650	12175	7100	12175
main 1	19300	12100	12900	6450	12900
main 2	14350	14900	7700	6700	7700
spi	21800	9675	13750	8125	13775

Comparison with experimental results

Comparison is possible with the reported results of measurements at sea with the same KALIK. (See Table II)

The comparison is made for the runs 8 and 9 as reported. Run 8 is a windward condition; run 9 a downwind condition with spinnaker.

The difficulty with the comparison is that very rough sea conditions were used during the measurements. The main aim of the experiments was to get insight in the dynamic loading on the wires. For comparison sake this is however not optimal.

Very large force fluctuations were measured.

No averaged values over the whole measurement period were presented. So mean values were considered to be presented by the summation of the minimum value and half the experienced maximum load range.

Table II Presents percentages of wire forces relative to the V-1 wire

	V-1	D-1	V-2	D-2	D-3
KALIK, run 8	100 %	57 %	51 %	49 %	51 %
calc.	100 %	56 %	52 %	47 %	51 %
run 9	100 %	40 %	60 %	40 %	60 %
calc.	100 %	42 %	57 %	42 %	60 %

Comparison is first made on basis of the relative force distribution over the wires.

For run 9 it is assumed that 70% of the loading is contributed by the spinnaker. For run 8

the genua contribution is put on 50%. The relative distributions as given correspond well between measurements and calculations. This implies that the assumed load distribution functions are sufficiently close to the actual ones. Scaling the computational results with the heeling angle, it is found that the measured absolute forces are higher than predicted. This is caused by the very high dynamic fluctuations in the wire forces. The average heeling angle for these runs were resp. 20 and 30 degrees. However there were estimated values, because the heeling angle was not measured. This makes them unreliable for the present use.

These very dynamic loadings on the wires reach the design loads as calculated for the wires, using both analytical of FEM methods. The frequency of the fluctuations coincides with the wave encounter frequency of the yacht. Which suggests that the motions of the yacht cause, directly or indirectly, these high fluctuations.

Some probative calculations were performed for the KALIK mast in order to determine the force fluctuations in the wires. The accelerations in the rig, due to the ship motions, were used as input. The force fluctuation found did not explained the very high values measured. Not more than 20% dynamic fluctuations could be attributed to the oscillatory motions of the yacht in a seaway.

Further work is envisaged to investigate the nature and origin of these dynamic loadings.

It is however quite evident that with the load conditions widely used for rig design, a substantial load amplification factor should be used for dimensioning the wires, to allow for these dynamic fluctuations.

Non linear influence due to large deflections

If the displacements of the rig become large, relative to its overall geometry, linear force displacement relations are not valid any more. It is suggested in literature that non linear behaviour is indeed the case.

Complex non linear calculations are not possible with the FEM code on PC's. Besides they are considered to be out of the scope for the rig designer.

An approximative method is used here, performing iterative calculations. The displacements of the rig are calculated and the deformed geometry is taken as a new starting point. The differences between both results is superimposed on the original values. This process is repeated until the differences become negligible.

Such a calculation was performed for the KALIK geometry. Only transverse loading was considered. The influence for this calculation appeared to be below 5% on the shroud forces. The calculations were performed for the condition without pretension. For a rig with pretension, deformations, and hence these non linear influences, are smaller.

However, it is emphasized here that other types of non linearities can be important. Especially in the longitudinal direction the deflections of the mast reduced by the horizontal reaction forces at the spreaders due to their misalignment caused by the bending of the mast. So for rigs with great flexibility iterative calculations will be a necessary tool for the correct determination of these deformations and the associated spreader loading.

This avoids complex non linear calculations.

For the design of normal rigs, without very great flexibility it is probably not necessary to perform these kind of calculations.

In general the following conclusions can be drawn

The exact loading condition is hard to determine.

The two assumed load distributions were assumed to represent the windward and downwind (or reefed) condition schematically.

Comparison with experimental results showed that these rather coarse assumptions correlated rather well with the actual ones.

The engineering approach used in this paper seems to be justified from a design point of view for the wire loadings.

The genua (or spi) loading is determinative for the design of most of the wires. This also holds if a summation on contributions for a genua and mainsail are taken, especially for the mast-head rig in which the headsail contributes the most to the loading.

However using genua results only, will lead to an under-estimation of the loads on the D-1 wire, for which the mainsail condition is determinative. It is difficult to assess the correct loading distribution over the sails. Carefully executed full scale experiments can be a helpful tool to gather more insight in this load distribution along the mast. As is apparent from the presented wire forces, the relative distribution of the wires can reveal, to a certain extent, this load distribution. However from a design point of view it is important to notice that even for the rather coarse assumption made here for the load distribution, the difference in wire forces are approx. 10-30%, and this mainly for the D-1 wire.

5.1 Loading on the mast

Contrary to the analytical methods FEM calculations give reliable information about the deformations in the rig and the resulting stresses in the mast. For optimal section design a very valuable tool.

Computations were performed for ultimate loading conditions for rigs with little or no pretension, for simplicity reasons.

Axial compression force in the mast

The axial compression forces in the different mast panels is given in Table III.

The forces are due to transverse shroud loading only (Forces in Newton). Difference in axial compression at deck level are directly related to the difference in bending moments in the mast at that place. For the lowest panel the differences are not very significant. For the two upper panels this is however different.

Genua loading leads to higher compression forces in the upper panels. Because of the combination of high bending moments and high compression, the genua load case could certainly be important for buckling for the masthead rig.

The different loading conditions give somewhat smaller differences for the fractional rig for the lowest panel.

Compared with the masthead rig, the two upper panels for the fractional rig are heavily loaded. This is in accordance with the results for the wire forces, which are of course closely related.

Table III

Loading condition	Panel 1	Panel 2	Panel 3
KALIK main 1. case 1	23190	13200	5330
	19830	9110	3230
	23300	18390	11500
DB 2 main 1. case 1	32025	20050	13675
	30225	15525	8900
	28280	23400	14830

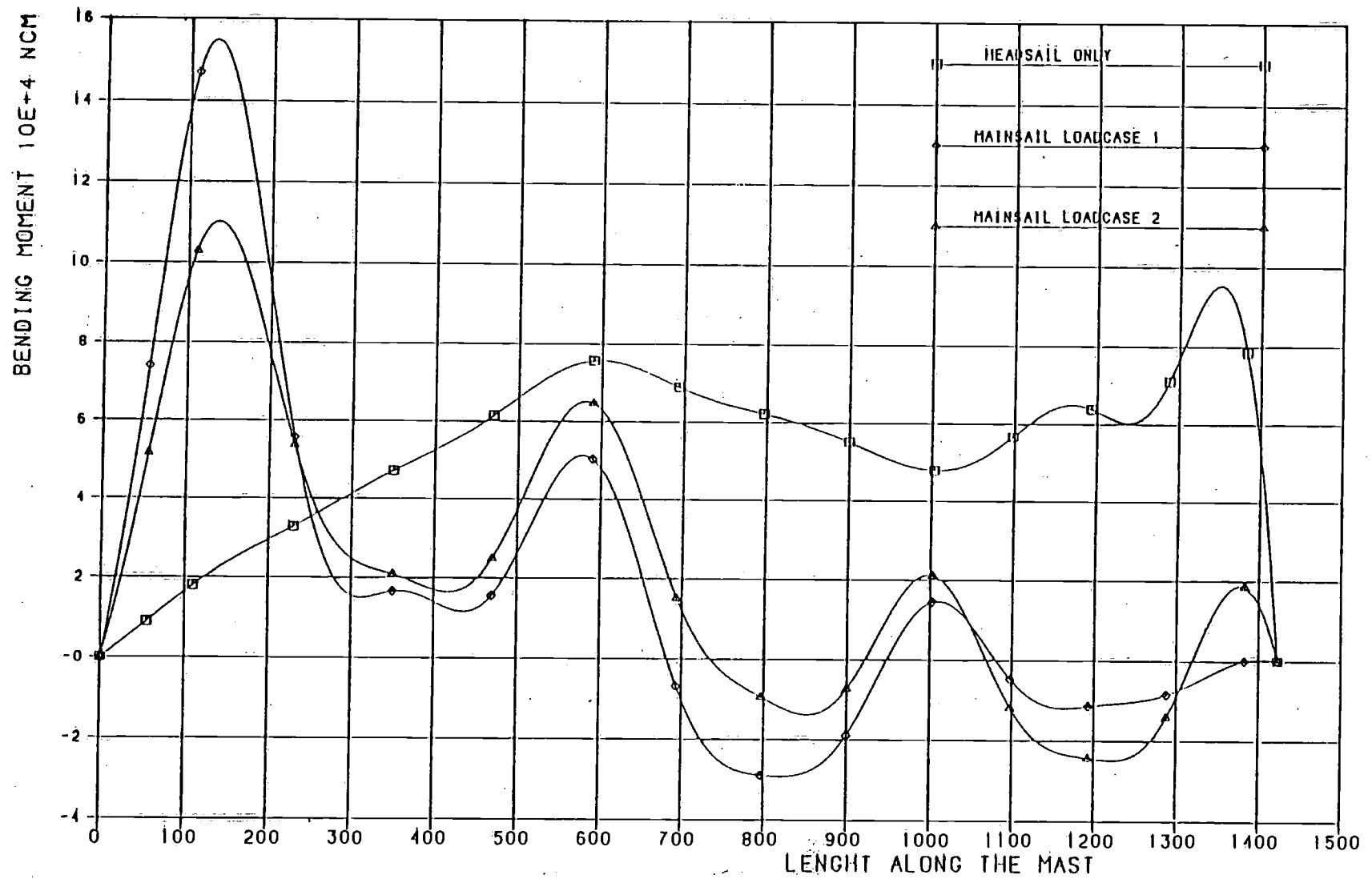


Figure 10a Transverse bending moment masthead rif different loads

5.2 Bending moments

The transverse bending moments for the different load cases for both yachts are given in Figures 10a and 10c.

Also the longitudinal bending moments are given for the load condition of spinnaker in Figures 10b and 10d.

For the fractional rig also the longitudinal bending moment is given for the mainsail load condition. Contrary to the masthead rig the tensile stress in the leech give considerable bending of the mast in that direction. The amount of which is very much determined by the trim considerations of the crew.

The following observations can be made with regard to the bending moment as presented in the figures.

5.3 Influence of loading conditions

Bending moments for the KALIK are relatively small for mainsail loads, for headsail loads they increase in the upper panels. For the fractional rig highest bending moments under headsail occur at the upper spreader. For the masthead rig they are highest at the lower spreader under the same conditions.

For the mainsail load conditional the moment distribution differs of course substantially between the fractional and mast head rig. Highest values are reached at the stay attachment point. This holds for both the transverse as longitudinal bending moment. This is of course due to the unsupported upper end of the mast. The computed values may somewhat exaggerated due to a quite high leech tension assumed. As stated earlier, the actual loading is strongly influenced by trim considerations of the crew. For both the masthead rig and fractional rig, the highest bending moments occur in the lowest panel, for the 'spinnaker plus main' condition. This is caused by the spi-pole and boom-vang forces. This is in line with experience.

For the fractional rig the mainsail conditions is determinative for the middle and upper panel. For the masthead rig the genua loading seems to be the most unfavourable. So genua loading is determinative for these panels.

5.4 Influence of load distribution assumption

For the different load distribution assumption for the mainsail results for the masthead rig in approx. 40% higher bending moments on deck level.

For the fractional rig the differences are much more prominent. The largest differences are for the upper panel of the mast, approx. 70% because of the higher loading on the unsupported upper end of the mast.

At deck level the difference are also approx. 40%.

The bending moments in the mast of the fractional rig are sensitive for the chosen assumption on the vertical load distribution of the mainsail along the mast.

Because they are also much higher than the loads imposed by the headsail they are determinative for the mast design. So as long as there are no data available about this distribution great care must be taken in the choice of this distribution.

5.5 Influence of mast stiffness

As pointed out before, the forces in the different stays can be estimated from simple equilibrium considerations for the system. The main difference with the exact solution being the bending moment in the mast.

So the shroud forces, axial compression in the mast and the bending moment mutually influence each other.

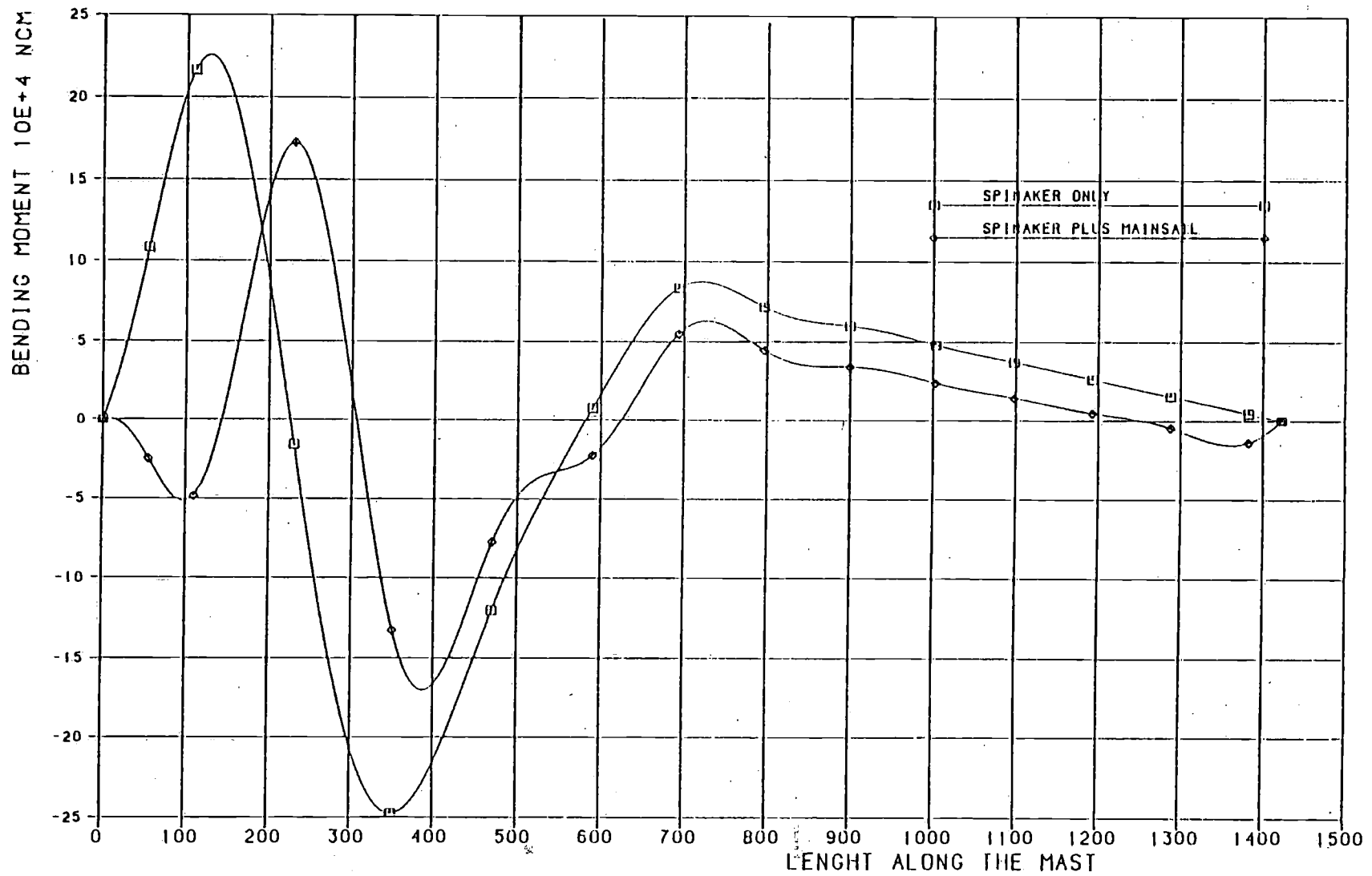


Figure 10b Longitudinal bending moment masthead rig different loads

The stiffness of the mast, especially for keel stepped masts, has an influence on the loading in the systems.

A stiffer mast gives rise to higher bending moments in the mast. This is illustrated by repeating the calculation for the KALIK under genua loading using twice the original moments of inertia of the mast section.

The resulting transverse bending moment is compared with the original one in Figure 10e. Both the absolute value as the longitudinal distribution has changed.

Not given here are the values for the axial compression and wire forces.

These also changed; the compression reduced as well as the wire forces. These changes are however much smaller. The rise in bending moment doesn't have to lead to higher stresses, because in most cases the moduli of the section will increase with the increase of the moments of inertia.

The stiffness of the hull will also have its influence. When this is relatively small, deformation of the mast and the associated bending moments will increase. Especially when the mast has a relatively large section, this may cause a considerable increase in bending stresses. So a very stiff, keelstepped, mast on a very flexible hull, could lead to a critical situation.

For a correct determination of the bending moments in the mast, the used engineering approach for the vertical distribution of the load is satisfactory for the masthead rig, because mainsail loads are not determinative for the designload.

For the fractional rig bending moments in the upper parts due to the mainsail are determinative. The windward condition results in a higher loading than the reaching condition. Based on the rather well correlation with experimental results, it is expected that the differences in bending moment for the actual loading and the one found for the uniform distribution are from a design point of view within acceptable limits.

More sophisticated elliptical load distribution etc, as suggested by others could be avoided then.

6 Conclusions

With the availability of FEM programs on Personal Computers; application of these FEM techniques is now within the possibility of the rig designer.

The use of FEM techniques enables a more thorough evaluation of the rig system, than in the past using analytical procedures. One has to remind however when using these techniques, that the accuracy of the computed results depends on the accuracy of the input. (loadings).

The exact loading conditions are hard to determine. Especially for the dimensioning of the D-1 wire, the mainsail condition has to be taken into account.

Differences between the various load assumptions are within acceptable margins.

The loading on the rig can lead to considerable different results for reefed- and/or stormsail conditions. These should also be considered in mast design.

Dynamic Loading on the rig can lead to a much higher loading for both mast and wires than determined, using maximum stability as the ultimate load condition. Further work is necessary to investigate these dynamic loadings. For a correct determination of the bending moments in the mast, the used engineering approach for the vertical distribution of the load is satisfactory for the masthead rig. For the fractional rig the bending moments in the upper parts due to the mainsail are determinative.

The spinnaker plus mainsail condition is very important for mast design. Especially for the lower part of the mast.

This condition should be incorporated in design evaluation. Reducing the deflections in the mast by means of pretension can not normally be anticipated in the design.

It is suggested therefore to perform the design calculations for a production yacht for the no-pretension condition.

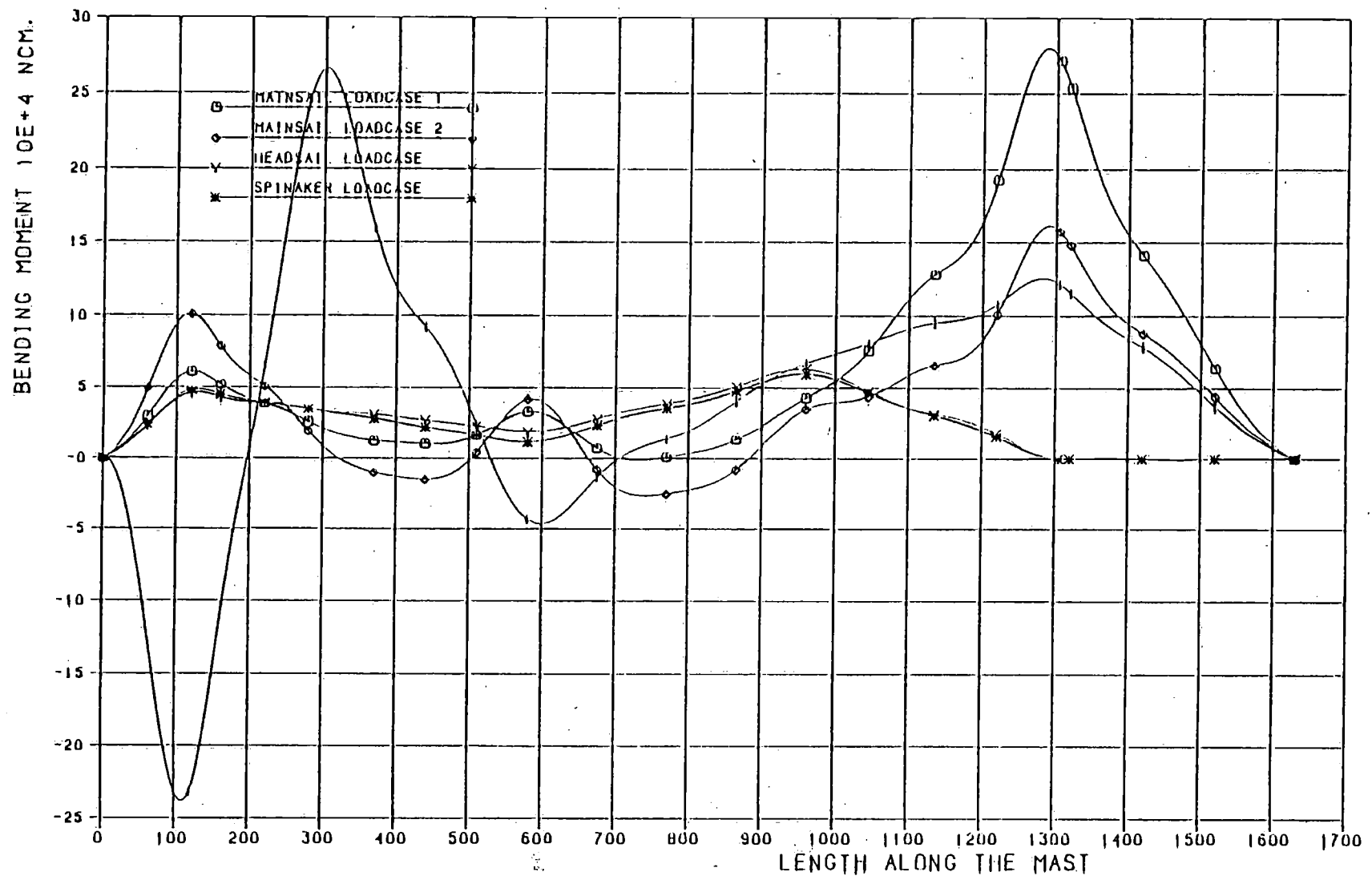


Figure 10c Transverse bending moments fractional rig different loads

Mast section evaluation should be performed for both global and local buckling. Local plate buckling is especially important for mast sections with small wall thickness. The contribution of additional bending moments and compressive forces, as well as cross section reductions must be taken into account, when determining the critical collapse load.

Stress analysis should be performed for both ultimate load as operational conditions. For the latter special emphasis has to be put on fatigue evaluation.

Nomenclature

A	: - cross-sectional area of wires/stays - vertical distance between lateral centre of effort of the yacht's underwaterbody and the decklevel
B	: vertical distance between lateral centre of effort of the yacht's underwaterbody and the mainsail-boom
C_y	: wire stiffness athwartships components
E	: modules of elasticity
F_o	: pretension of the headstay
F_{om}	: compressive force of the mast due to pretension of the shrouds
F_{so}	: pretension of the shroud
F_h	: force in the headstay
F_i	: induced load on the headstay, caused by the headsail
F_l	: force in the leech of the mainsail
F_s	: shroud force
F_s''	: shroud force, in excess of the pretension
$F_y H(t)$: athwartships component of F_h at the top of the headsail
$F_y M(t)$: athwartships component of F_l at the top of the mainsail
$F_y M(c)$: athwartships component of F_l at the clew of the mainsail
$F_y(m)$: mainsail-borne distributed athwartships load on the mast
H_h	: height of the top of the headsail above the deck
H_m	: lufflength of mainsail
L, l	: length of the stay
$M(\phi)$: heeling moment
w_o	: deformation ("sagging" of the yacht's cross-section, due to the shroud's pretension
w_s^*	: deformation in excess of w_o
α	: sagging angle component in yacht's athwartships vertical plane
β	: sagging angle component in yacht's vertical plane of symmetry
δ	: spatial sagging angle between loaded headstay and the line between the top and the tack of the headsail
ϕ	: heeling angle
ϕ_s^*	: heeling angle, in excess of the heeling angle above which pretension is lost
γ	: angle between yacht's plane symmetry and a plane tangent to the luff of the headsail
η	: angle between shroud and mast
Θ_1	: top-angle between F_l and the line through top and clew of mainsail
Θ_2	: clew-angle between F_l and the line through top and clew of mainsail
σ	: stress
$\sigma_{0.2}$: yield stress
τ	: angle between mast and headstay

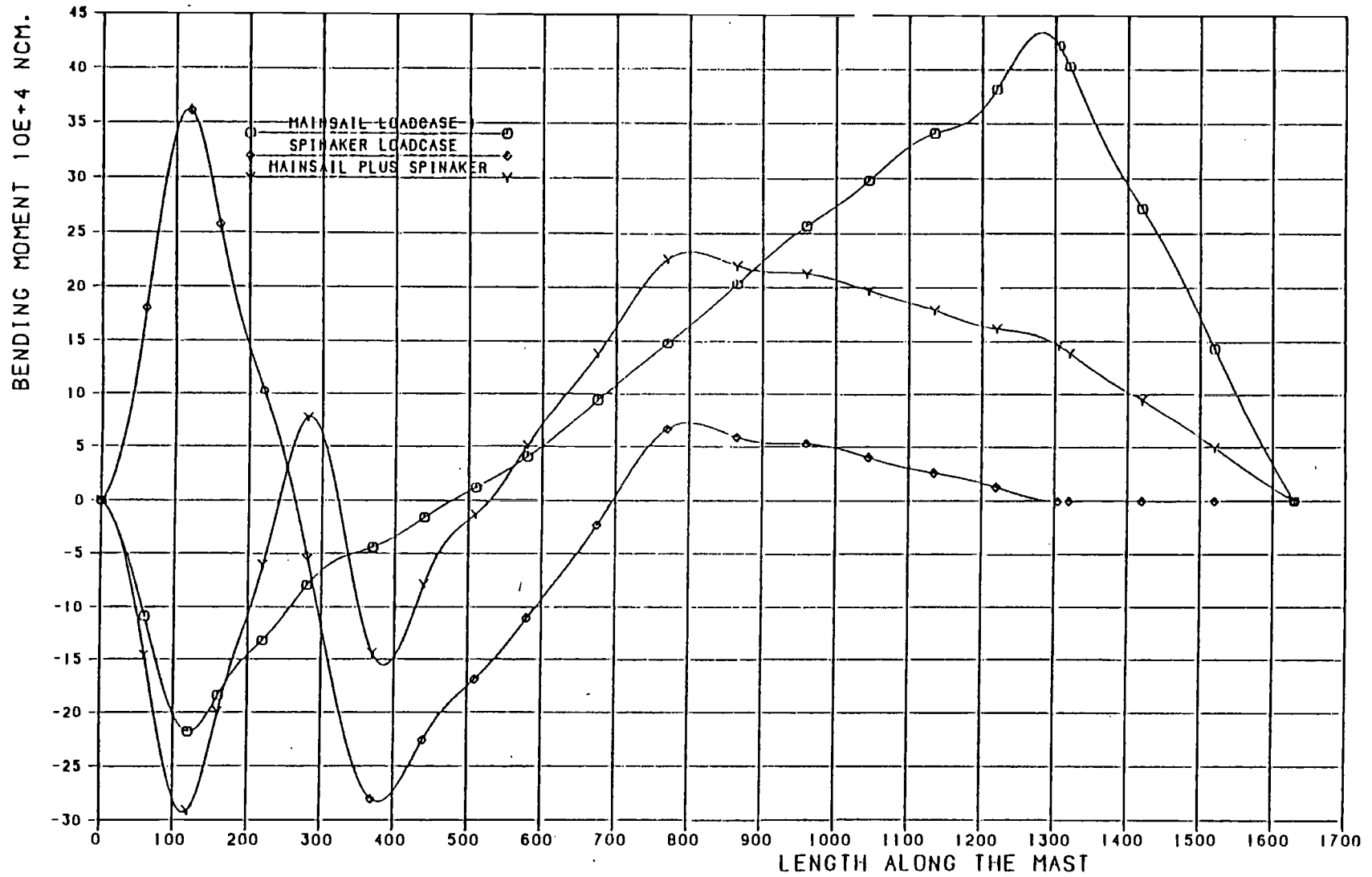


Figure 10d Longitudinal bending moments fractional rig different loadings

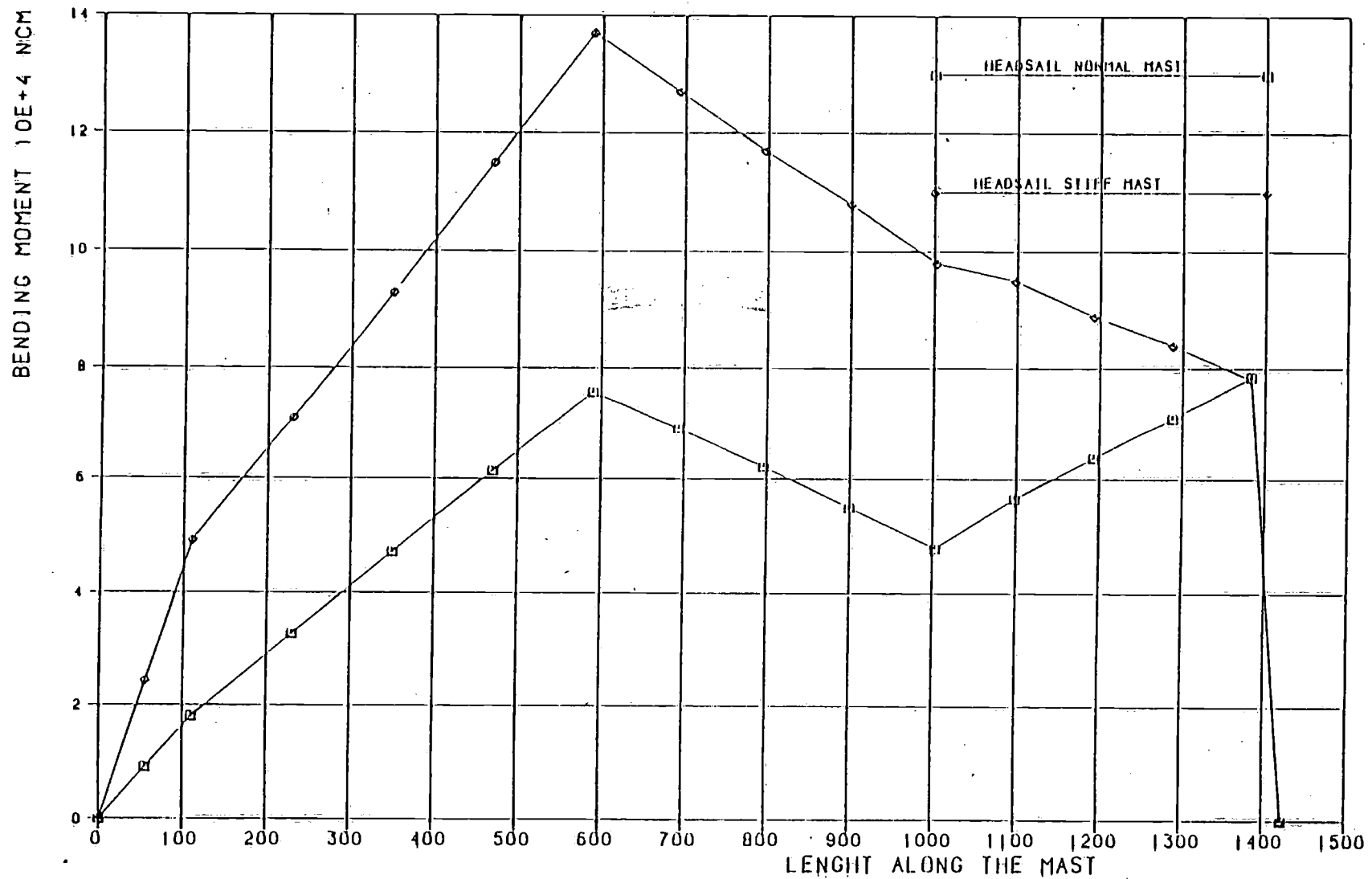


Figure 10e Transverse bending moment headsail only different mast stiffness

Appendix I

Mainsail born forces. (Figure 1)

Transverse loads.

Assumptions made:

- The mainsail force is transferred by the leech and mast.
The mast is taking 75 % of the transverse load, the leech 25%.
- The heeling moment of the ship is caused by the mainsail only.

Two load distribution in height are assumed:

1. Linear distribution:

Zero at the top, maximum at the boom.

$$F_y M = (3 \cdot M(\phi)) / (H_m + 3 \cdot B) \quad (9)$$

Distributed load along the mast:

- at the top : 0
- at the boom :

$$F_y(m) = 9 \cdot M(\phi) / (2 \cdot H_m(H_m + 3 \cdot B)) \quad (10)$$

Concentrated load at the top due to the leech:

$$F_y M(t) = M(\phi) / (4 \cdot H_m + 3 \cdot B) \quad (11)$$

2. Uniform distribution over the height of the mast :

$$F_y M = 2 \cdot M(\phi) / (H_m + 2 \cdot B) \quad (12)$$

Distributed load along the mast:

$$F_y(m) = 3 \cdot M(\phi) / (2 \cdot H_m (H_m + 2 \cdot B)) \quad (13)$$

Concentrated load at the top due to the leech:

$$F_y M(t) = M(\phi) / (4 \cdot H_m + 2 \cdot B) \quad (14)$$

Appendix II

Headsail borne loads (Figure II.1, II.2 and II.3)

Transverse loads only

Assumptions made:

- The transverse load is transferred to the ship at the top and at the deck
- The heeling moment of the ship is caused by the headsail only

Two load distribution over the height of the sail are assumed:

1. Linear distribution Zero at the top, maximum at the deck level.

Total transverse load:

$$F_y H = 3 \cdot M(\phi) / (H_g + 3 \cdot A) \quad (15)$$

Concentrated load at the top:

$$F_y H(t) = M(\phi) / (H_g + 3 \cdot A) \quad (16)$$

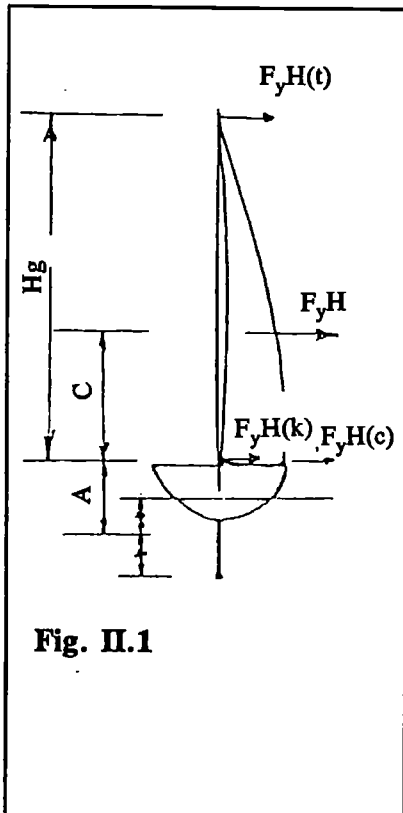


Fig. II.1

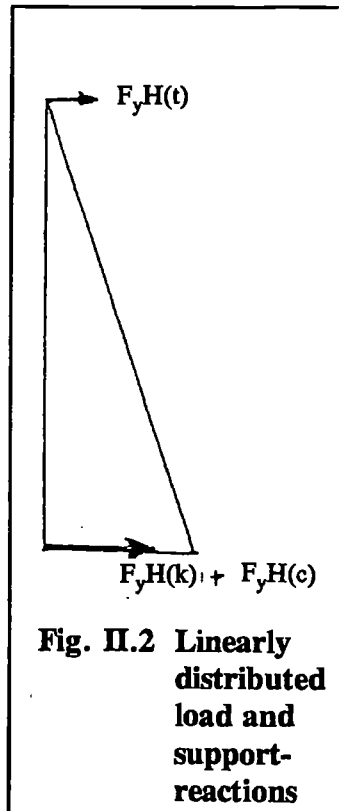


Fig. II.2 Linearly distributed load and support-reactions

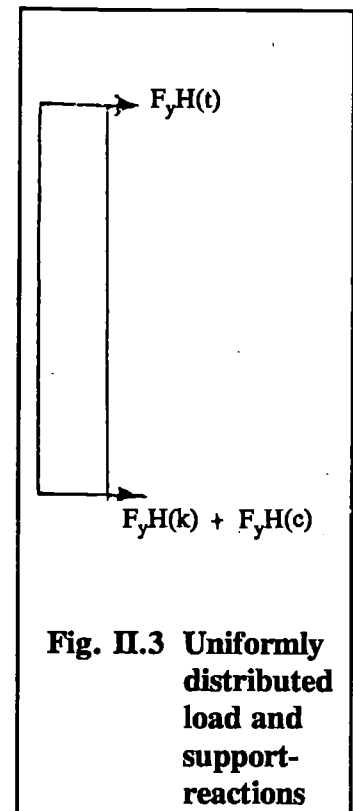


Fig. II.3 Uniformly distributed load and support-reactions

Concentrated force at deck level:

$$F_y H(c) + F_y H(k) = 2 \cdot M(\varphi) / (H_g + 3 \cdot A) \quad (17)$$

2. Uniform distribution.

Total transverse force:

$$F_y H = 2 \cdot M(\varphi) / (H_g + 2 \cdot A) \quad (18)$$

Concentrated force at the top:

$$F_y H(t) = M(\varphi) / (H_g + 2 \cdot A) \quad (19)$$

Concentrated force at deck level:

$$F_y H(c) + F_y H(k) = M(\varphi) / (H_g + 2 \cdot A) \quad (20)$$

The relation between heeling moment of the ship and the total force is given by:

$$M(\varphi) = F_y H(t) \cdot H_g + (F_y H(t) + F_y H(c) + F_y H(k)) \cdot A \quad (21)$$

Appendix III

Headstay force in relation to the required transverse force.

In Figure 8 the relation between the 'spatial' sag-angle δ and its component δ in the athwartships-plane α and in the vertical plane of symmetry given (β)

This is on the basis of the parameters τ (angle between headstay and mast) and γ (angle in the horizontal plane between the vertical plane and the plane of the tangent to the headsail luff).

The following relations hold:

$$\alpha \approx \delta \frac{\cos \gamma_o}{\cos \tau} \quad (22)$$

$$\beta \approx \delta \frac{\sin \gamma_o}{\cos \tau} \quad (23)$$

With the assumption that the parameter τ does not exceed 20 degrees. From Figure 9, the relations between the different force components can be derived:

$$F_x H(t) = F_y H(t) \cdot \operatorname{tg}(\tau - \beta) / \alpha \quad (24)$$

$$F_z H(t) = \frac{F_y H(t)}{\alpha} \quad (25)$$

This results in a force in the headstay as given below:

$$F_h = \frac{F_y H(t)}{\operatorname{tg} \alpha} \cdot \sqrt{\operatorname{tg}^2(\tau - \beta) + \operatorname{tg}^2 \alpha + 1} \quad (26)$$

Appendix IV

Head stay sagging pattern.

The exact sagging pattern of the headstay is difficult to assess.

It depends, among other things, on the actual shape of the headsail.

For simplicity sake the deformed shape of the stay is assumed to be a circle segment.

See Figure 11.

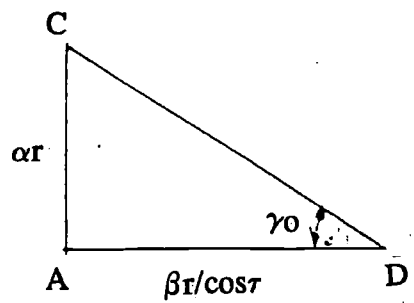
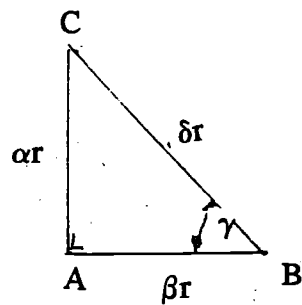
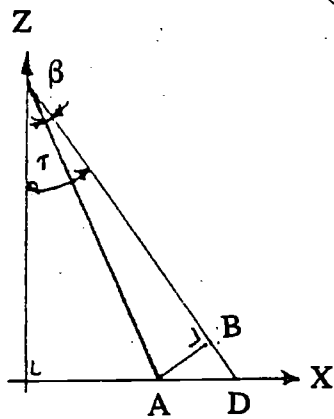
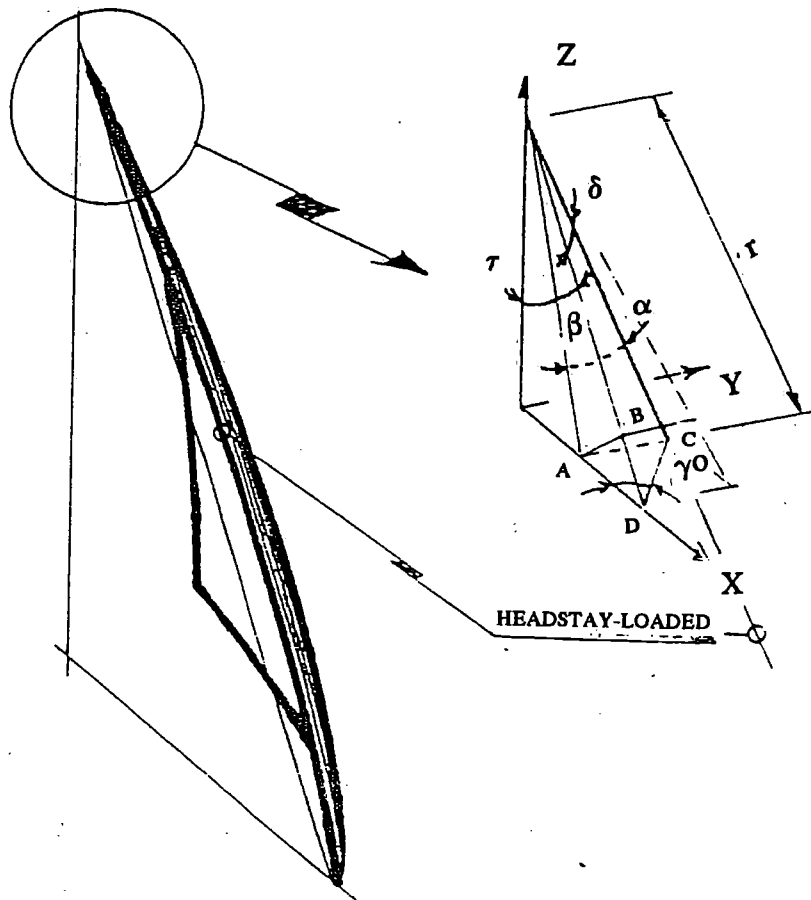
In this case the following relation can be derived for the length of the deformed headstay:

$$\left. \begin{aligned} l &= 2 \cdot \delta \cdot r \\ L &= 2 \cdot r \cdot \sin \delta \end{aligned} \right\} \frac{l}{L} = \frac{\delta}{\sin \delta} \quad (27)$$

Which results in an expression for the force in the stay:

$$F_h = E \cdot A_h \cdot \left(\frac{\delta}{\sin \delta - 1} \right) \quad (28)$$

In which F_h is the rise in tension in the stay relative to its rest position.



$$\alpha = \delta \cdot \sin \delta$$

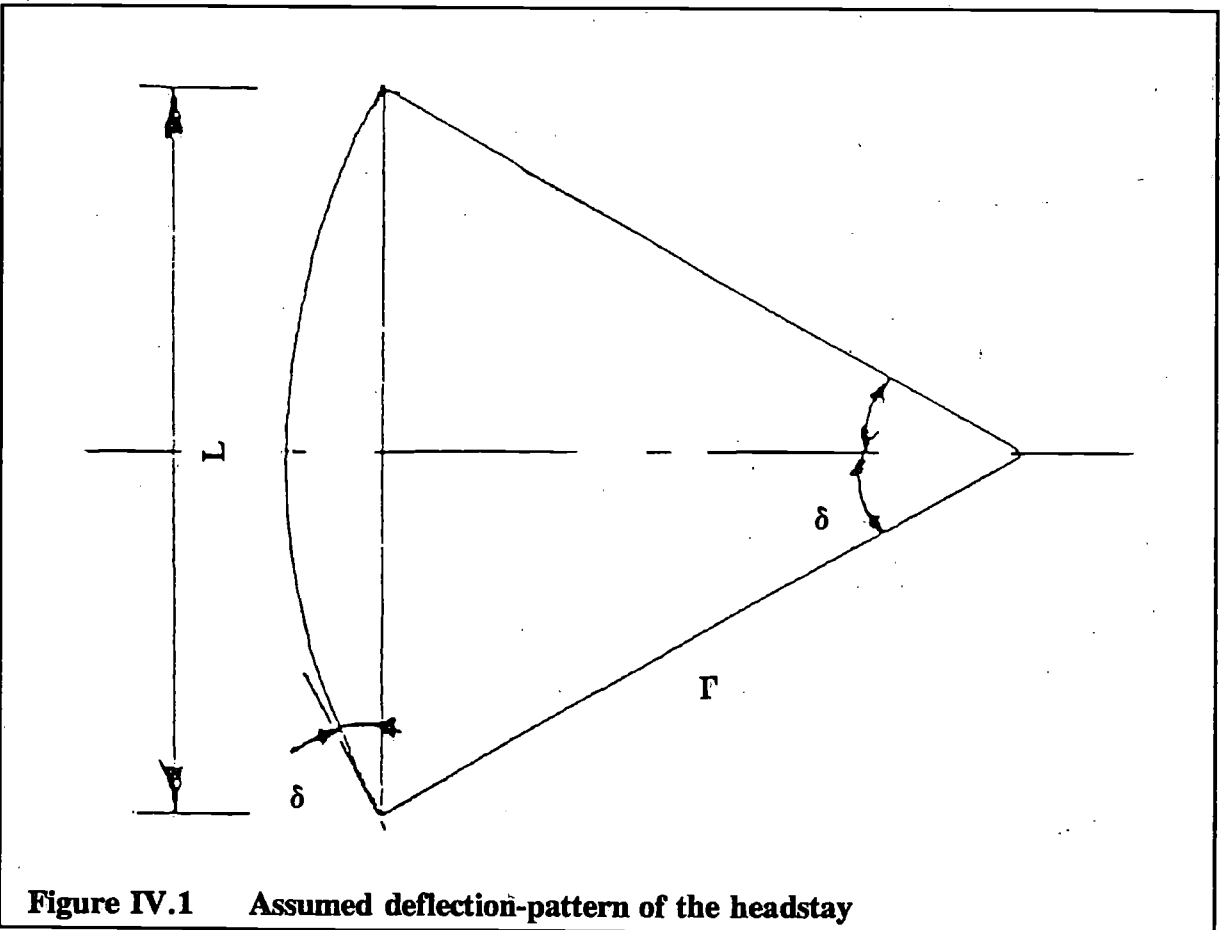
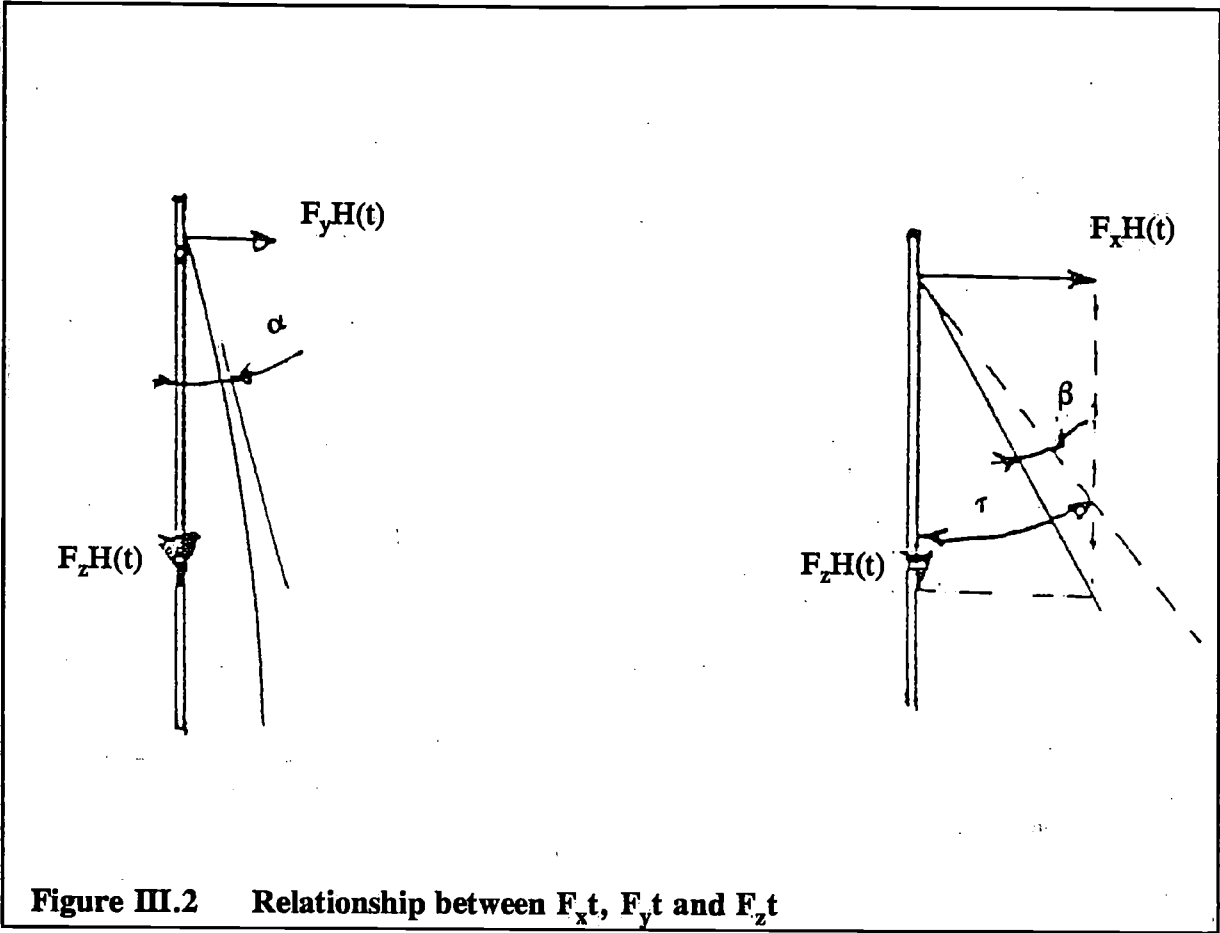
$$B = \delta \cdot \cos \delta$$

$$\gamma = \arctg(\tg \gamma_0 / \cos \tau)$$

$$\alpha = \delta \cdot \sin(\arctg(\tg \gamma_0 / \cos \tau)) \approx \delta \cdot \sin \gamma_0 / \cos \tau$$

$$B = \delta \cdot \cos(\arctg(\tg \gamma_0 / \cos \tau)) \approx \delta \cdot \cos \gamma_0 / \cos \tau$$

Figure III.1 Headstay sag-angle δ in relation to fore-triangle geometry and the angle γ_0



Multi-stage waterjets for over 40 knot craft

by G.H. Davison

C.W.F. Hamilton & Co Ltd
20 Lunns Road, Christchurch
New Zealand

Introduction

In recent years there has been a strong trend for ferries, workboats and patrol boats to travel at ever higher speeds. To accommodate these higher speeds in safety and comfort, hull forms have had to change and to maintain efficiency propulsion units also have had to be reviewed.

Parallel in some respects to the rise in popularity of the pure jet aircraft in the 1960's, jet propulsion in fast marine craft can provide this higher performance and can take seagoing speeds into the 40-60 knot region or higher. At the same time good fuel efficiency, smooth operation and high passenger acceptance accompany this. We will explore the place of the multi-stage waterjet in this advance and some compelling reasons for its utilisation.

Propulsion options

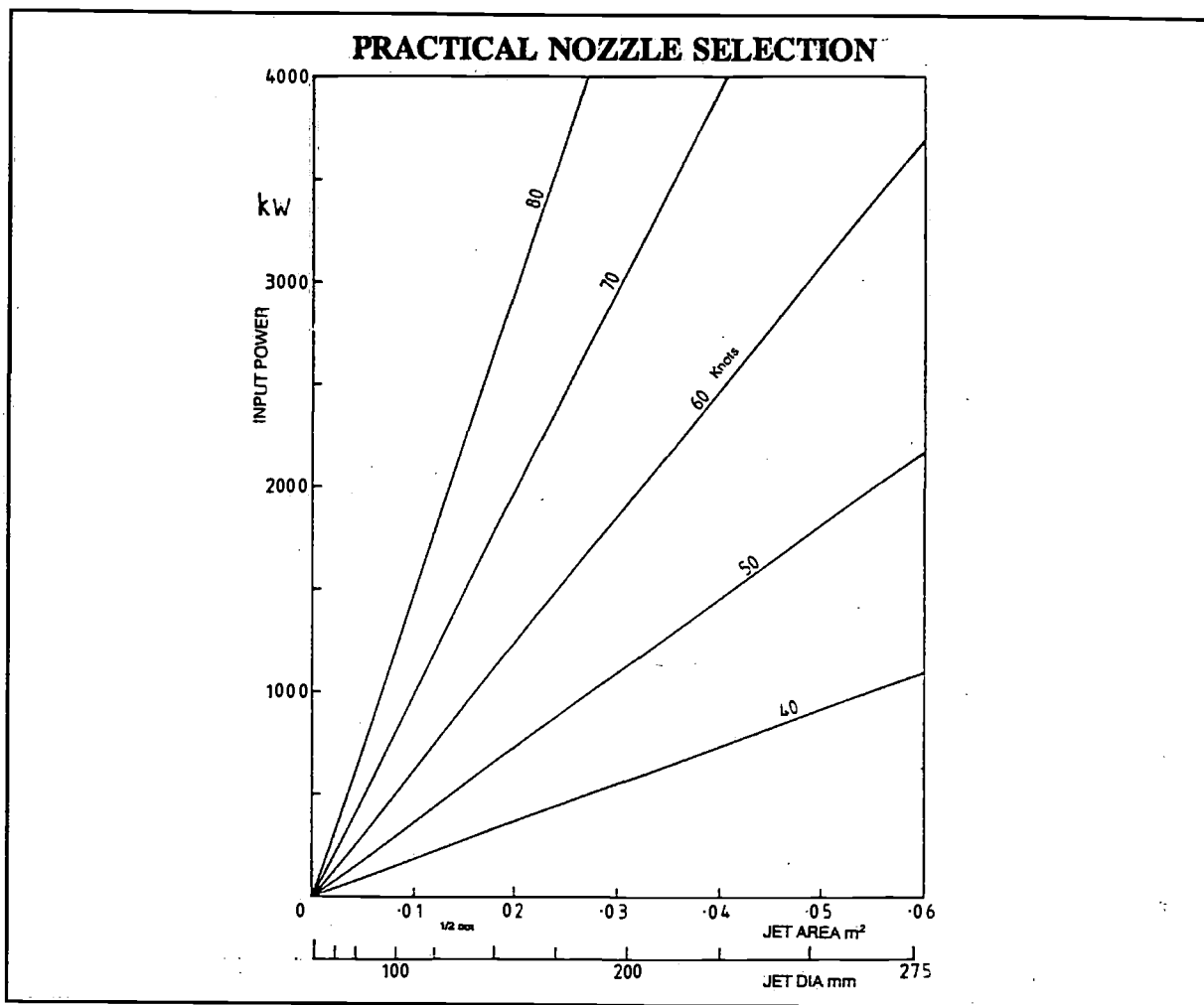
Conventional angled propeller drive and rudders may be approaching their practical speed limits with current craft, due to appendage drag, vibration and cavitation problems. Geared horizontal propellers, especially the forward-facing "tractor" types may become popular with some owners and should perform well although some may be shy of their complexity and vulnerability. Controllable pitch propellers, also complex, will alleviate the loading problems on engines, and surface piercing propellers may certainly have a place on high speeds.

However, it must be apparent that large waterjets are currently almost an Industry standard for fast catamaran ferries and very common on luxury motor yachts. The reasons probably include the quietness and smoothness of the propulsion gear providing the best passenger comfort and the good control in harbours and at terminals.

In addition, there are the attractions of long engine life due to known and constant engine loading conditions at all boat speeds and displacements, minimal downtime for repairs and maintenance, simplicity of driveline and shallow draught.

Freedom from cavitation and demonstrated high propulsive efficiency comparable with the best propeller drives has been the reason for the rise in waterjet popularity worldwide. Hamilton is strong in the ready-to-fit packaged units up to about 1200 kw and Kamewa and Riva Calzoni are active in the larger sizes.

As speeds rise further, waterjets will become increasingly attractive, for reasons we shall describe.



Waterjet design

Jet-drive is not unlike propellers in that the faster the boat speed, the smaller the diameter propeller and the higher the revolutions. The ideal waterjet for slower 20 knot craft is so large and bulky that it is impracticable and is not often attempted. The large slow-revving propeller generally does a better job.

However, as design boat speeds increase beyond 30 knots the waterjet becomes small enough to be acceptable in weight, bulk and cost and overtakes the conventional propeller in overall propulsive efficiency. This is partly due to the elimination of appendage drag which is a significant penalty. This is made up of exposed propellers, shaft, brackets and rudders.

The correct selection criteria for waterjets is by nozzle size. This measurement can be considered equivalent to selection of propeller diameter. The higher the boat speed, the smaller the nozzle size for best efficiency and vice-versa. On most current boats the recommended jet/s are down-sized somewhat from the optimum for reasons of weight and cost, and the small drop in propulsive efficiency is generally acceptable.

But as boat speeds enter the 40+ knot region the ideal waterjet can be employed with the nozzle size closer to the optimum resulting in the best possible propulsive efficiency.

The propulsion machinery becomes compact and light - therefore reasonable cost. This is the area where waterjets come into their own.

A basic nozzle selection chart is attached to this paper, a good initial guide for designers.

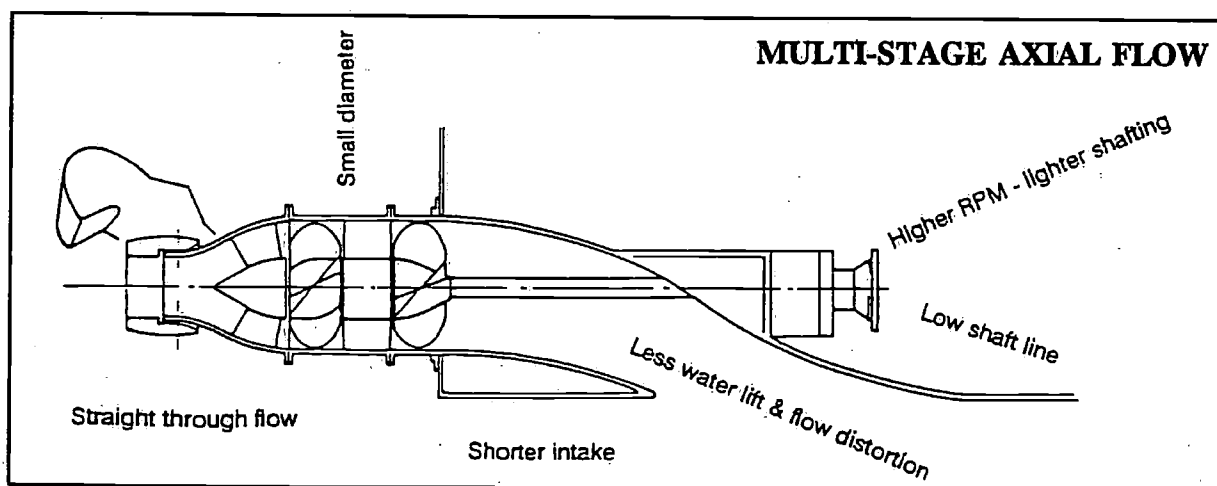
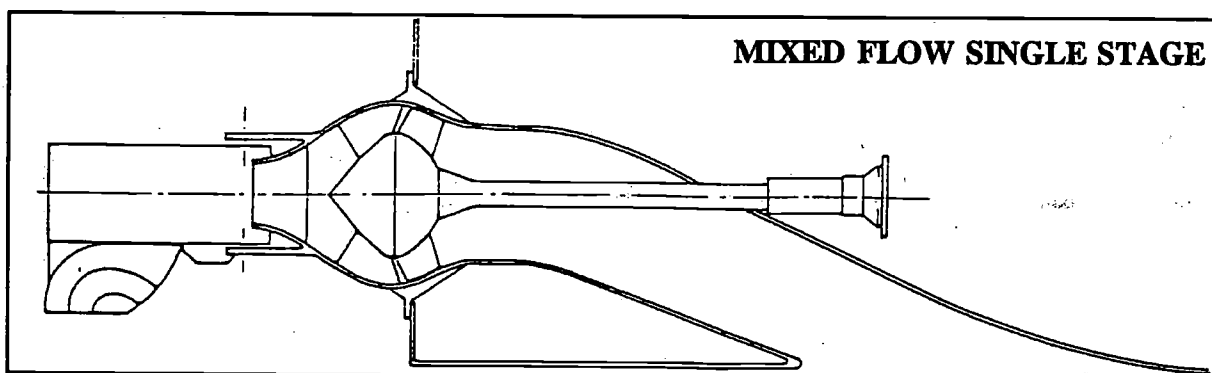
Hull trends for high speed craft

In the field of commercial small craft the fast ferry designers are leading the way. While the conventional vee-bottom monohull continues to be the mainstay for patrol boats and private motor yachts, the demand for improved ride at speed and a large area passenger platform has seen the strong emergence of the fast catamaran design.

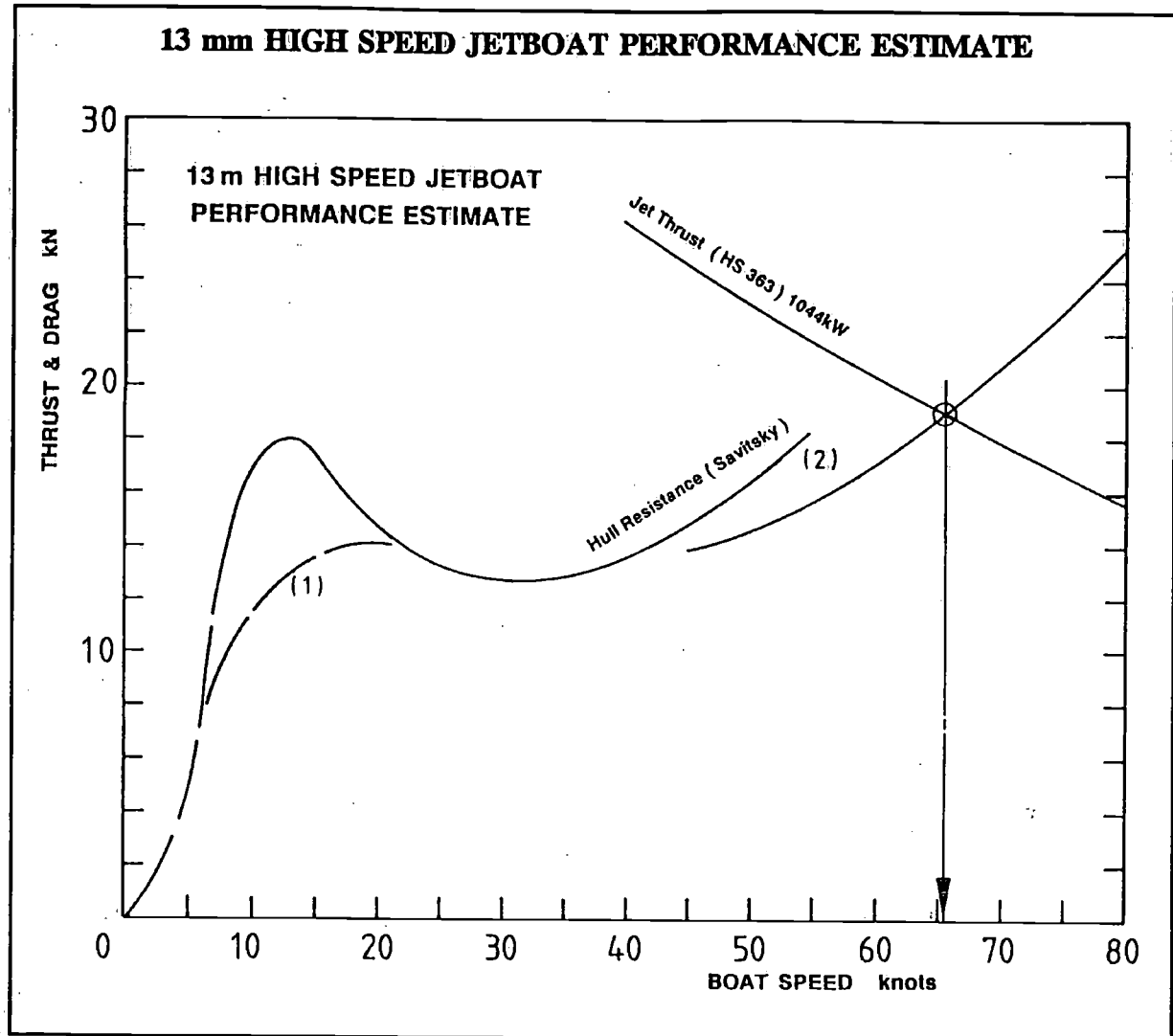
The conventional shape is a pair of long slim displacement hulls with little dynamic lift that can be propelled satisfactorily up to around 30 knots with conventional propellers. The Phil Hercus-designed Incat Wavepiercer and the FBM fast displacement catamaran reduce the water-plane area for improved ride, but generally operate in similar speed regions. Larger designs and the use of waterjet propulsion have extended speeds of this design to near 40 knots. To extend the speed potential further, air-supported side-wall Hovercraft or S.E.S.'s are now more common, and recently the emerging foil-cat design, where part of the hull weight becomes supported on foils to reduce the immersion and therefore the high speed resistance.

These craft are proving successful on relatively sheltered waters where there are moderate wave heights experienced. However, it is clear that these low resistance designs have extended the cruising speeds over the 40 knot mark with acceptable power application and efficiency.

Perhaps naval patrol craft and motor yachts will eventually follow these trends, particularly as modern fast catamarans can also be good-looking and thus appeal to the private owner. The next step is a generation of fast boats capable of over 50 knots employing these low drag hull designs with reasonable installed power, but requiring high efficiency propulsion machinery.



13 mm HIGH SPEED JETBOAT PERFORMANCE ESTIMATE



Waterjet pump design

The prime criteria for correctly selecting a waterjet is the nozzle size. This is the first essential step, which is usually done by the manufacturer.

The pump design ahead of the nozzle is a secondary consideration and various different approaches will be used by different designers. Simple high specific speed-axial flow pump designs or near to it are perfectly adequate for normal boat speeds in the 25-45 knot region.

In a higher speed range the correct nozzle is relatively small and the necessary input power increased, necessitating a higher pressure pump to "drive" the chosen nozzle. Two ways of achieving this are: a mixed flow pump, or a multi-stage axial flow design.

Most of the European waterjets are mixed flow design, and current Hamilton designs have a degree of radial flow due to larger diameter hubs. These are all suitable for current boat speeds, however multi-stage axial flow designs have inherent advantages particularly when applied to modern day high speed hulls.

This design philosophy provides some fundamental technical advantages as follows:

- 1 Multi-stage axial design can run at higher R.P.M. without cavitation, so direct drive can be employed further up the power range. The necessity for a reduction gearbox can be put off for longer and because of the lower torque, lighter shafting can be used.

- 2 The first impeller can be designed as an "inducer" with a lower pressure rise further distancing the onset of low boat speed cavitation.
- 3 The second impeller, receiving already pressurised water can be made to work very hard without risk of cavitation providing the best possible power density.
- 4 The low diameter and profile reduce flow distortions (less "S" bend) in the intake duct improving ram recovery and high speed thrust generation.

In addition, they also have significant physical attractions:

- 1 Slim small diameter housings: This is of particular advantage when mounting waterjets low down in the usually very narrow SES hulls.
- 2 Low Profile (due to small diameter): This provides low water lift, shorter and more efficient intake duct with minimal flow distortion, and low thrust line on hull to maintain best trim at speed. This also keeps entrained water weight to a minimum.
- 3 Common Parts: In many cases, individual parts are simpler and can be repeated in the other stages of the unit reducing manufacturing complexity and component cost.
- 4 Smaller Impeller Hubs: In multi-stage designs the reduced hub diameters keep weight and bulk down and further reduces flow distortions through the pump.
- 5 High Powers: The power density into this design is high providing the maximum thrust from the smallest envelope.

The multi-staging approach has much in common with the aircraft jet engine field, where the multi-stage compressor has completely superseded early centrifugal designs. Many of the same principles apply.

Field experience with multi-stage waterjets

At C.W.F. Hamilton & Co Ltd in New Zealand we have had over 30 years experience with multi-stage axial flow waterjets since the first two-stage units were put into use in 1956. These were in small fast river craft, a sport that continues to this day and demonstrates some interesting points.

Most of the many thousands of units in use have 190mm impeller diameter and are fitted to small vee-bottomed boats around 4-5m in length. High power densities, with 400-900 hp engines being acceleration common, provide outstanding cavitation-free acceleration together with optimum jet velocity for top speeds up to 90 knots or so.

Implications for larger fast craft

These small river craft are, in effect, about 1/5 scale models of full-sized seagoing patrol boats and fast ferries. The most notable lesson to be learned from them is the very high powers than can be applied successfully at low boat speeds for acceleration, and their excellent tolerance to aerated water when compared with single stage pumps. The latter will be important with the new generation of air-cushion and foil-supported catamarans where the waterjet intakes are likely to operate close to an aerated water surface at high speeds.

Some examples of such craft are illustrated along with the water conditions they are required to operate in.

High performance example

In 1987 the Swedish "Smuggler 384" with Scania DSI14 engine and Hamilton 361 waterjet was successfully trialed at 36 knots. The hull was an advanced lightweight composite construction and its deep-vee design capable of higher speeds with suitable machinery.

If this boat was fitted with a multi-stage version of the 361 jet and, say, a Detroit 16V-92TA diesel engine, it is interesting to study the result. Although the more powerful engine adds about 1.8 tonnes to the boat weight, the waterjet would fit on almost the same bottom space and only add about 240 kg to the weight of the propulsion gear.

With properly arranged longitudinal strakes in the bottom, the high speed wetted beam should reduce, perhaps 30% increasing the hull efficiency significantly. See break (2) on graph.

The attached graph indicates a top speed of 65 knots and good propulsive efficiency for this proposal.

Details used for the calculation are:

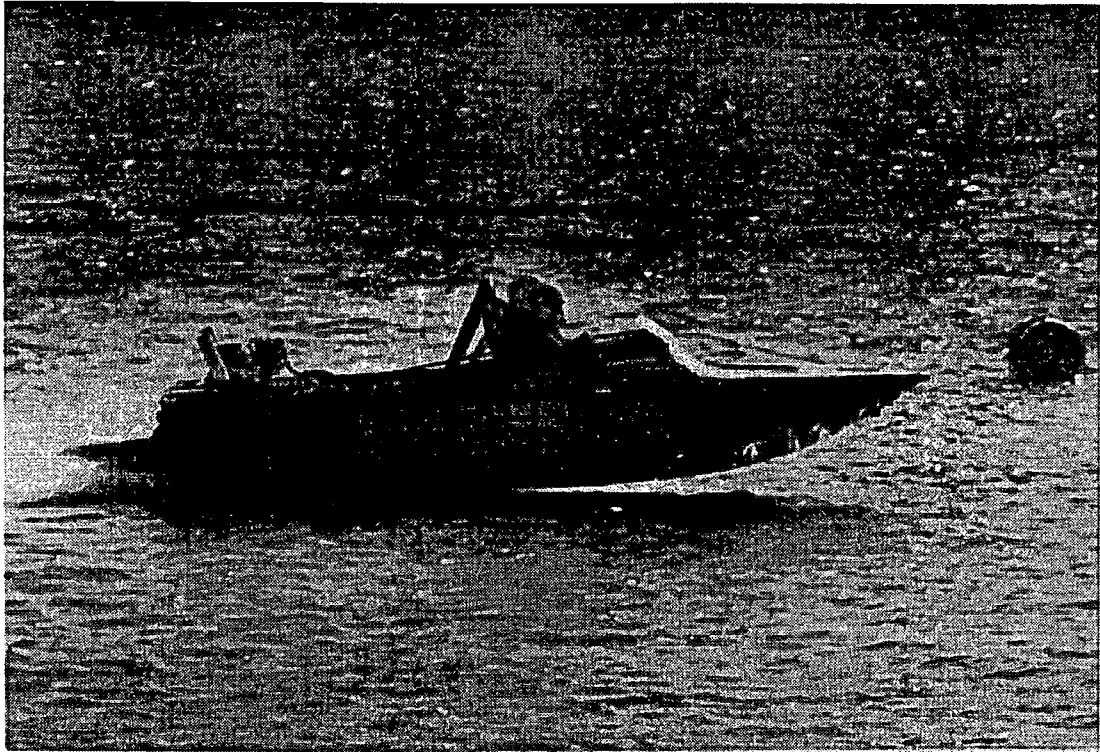
<i>LOA</i>	: 13 m
Displacement	: 7.5 tonnes
<i>L.C.G.</i>	: 2.74 m
Waterline Beam	: 3 m, reducing to 2.1 m at high speeds
Deadrise	: 25°
Frontal Area	: 9.3 m ² , $C_d = 0.5$ assumed
Friction Factor	: 0.0004
Water Conditions	: Calm

Transom flaps would be required in the 10-15 knot region to reduce the excessive trim angles and hump resistance brought about by the aft *L.C.G.* suitable for the upper speed range. See (1) on graph.

This is an example of how to transform an already good performing boat into a very high performance 60+ knot craft. While it is clearly necessary to install the appropriate engine power for the desired speed the fitting of a multi-stage waterjet of the same diameter but little more bulk is a relatively simple and cost-effective operation.

To Summarise:

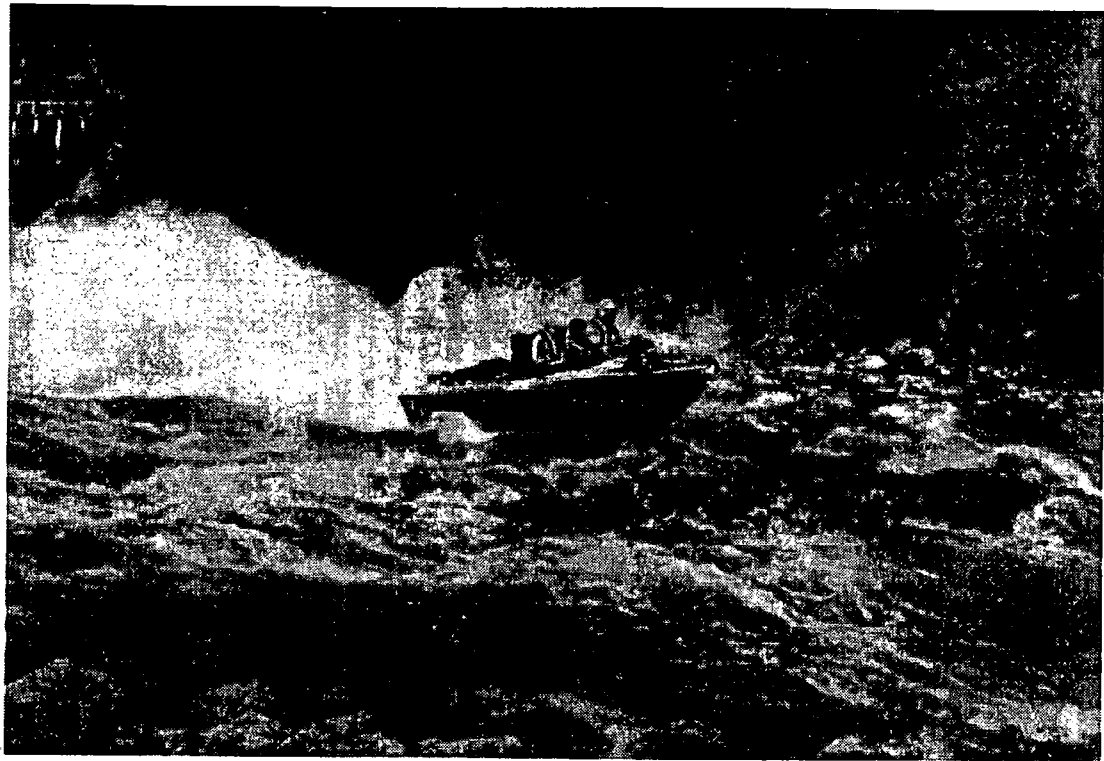
It is our belief that the next few years will certainly see increasing speeds in commercial craft up to about 100 metres in length. The already strong establishment of waterjet propulsion will be extended to these new speeds with the aid of multi-stage pump designs, which have already proved themselves, in smaller sizes, of ably operating in very rough and aerated water conditions. This success will be paralleled in the next generation of larger seagoing craft which will also have to travel fast in the open sea.



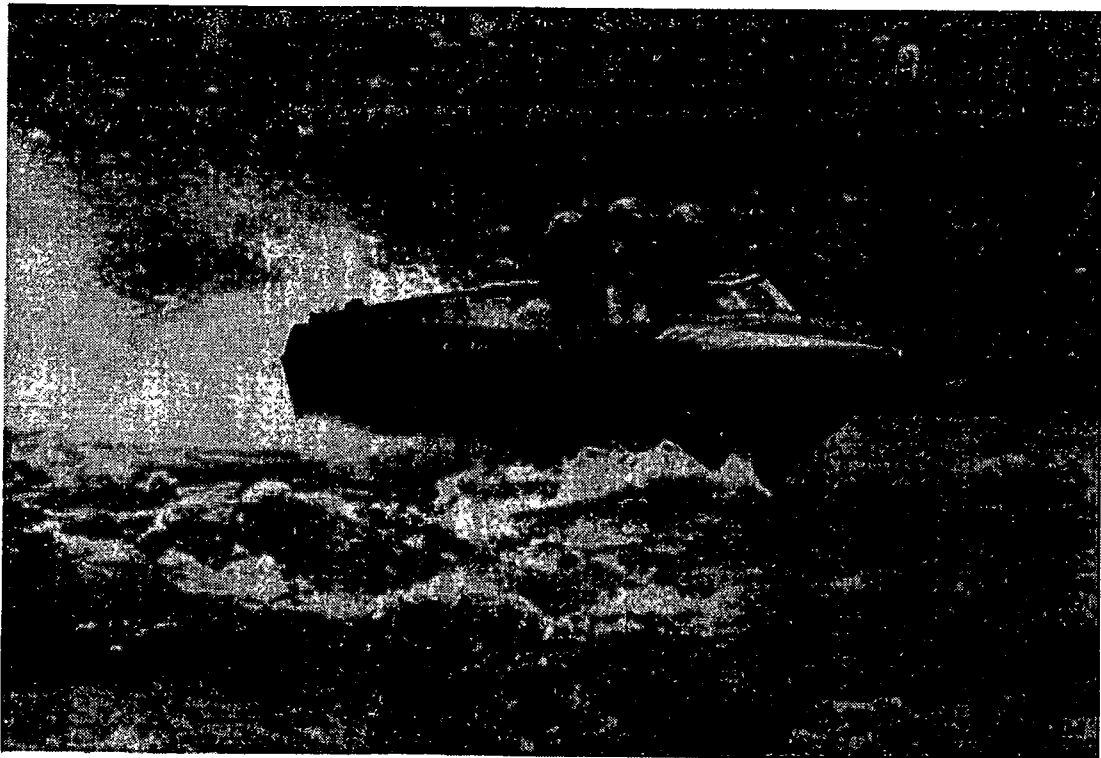
Multi-stage racing craft at 90 knots

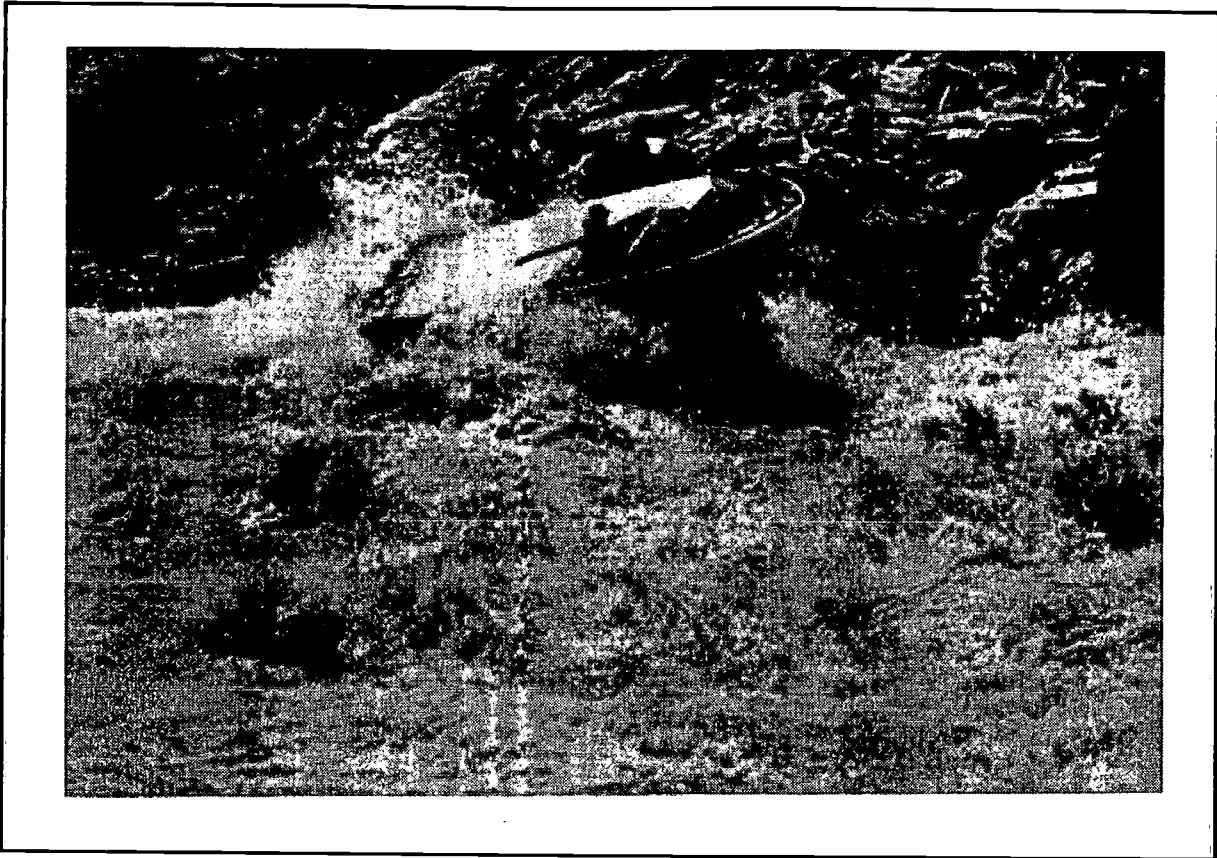


13 m Smuggler 384 jet boat

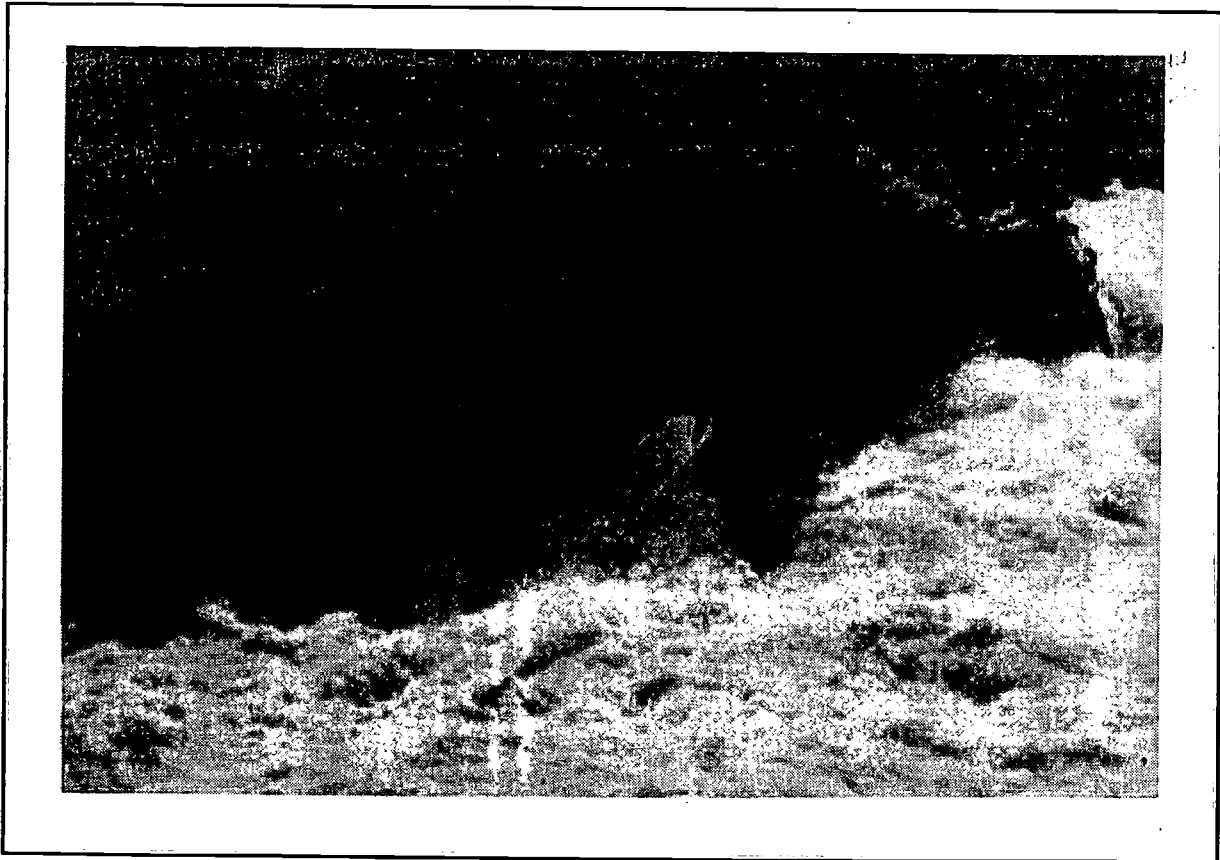


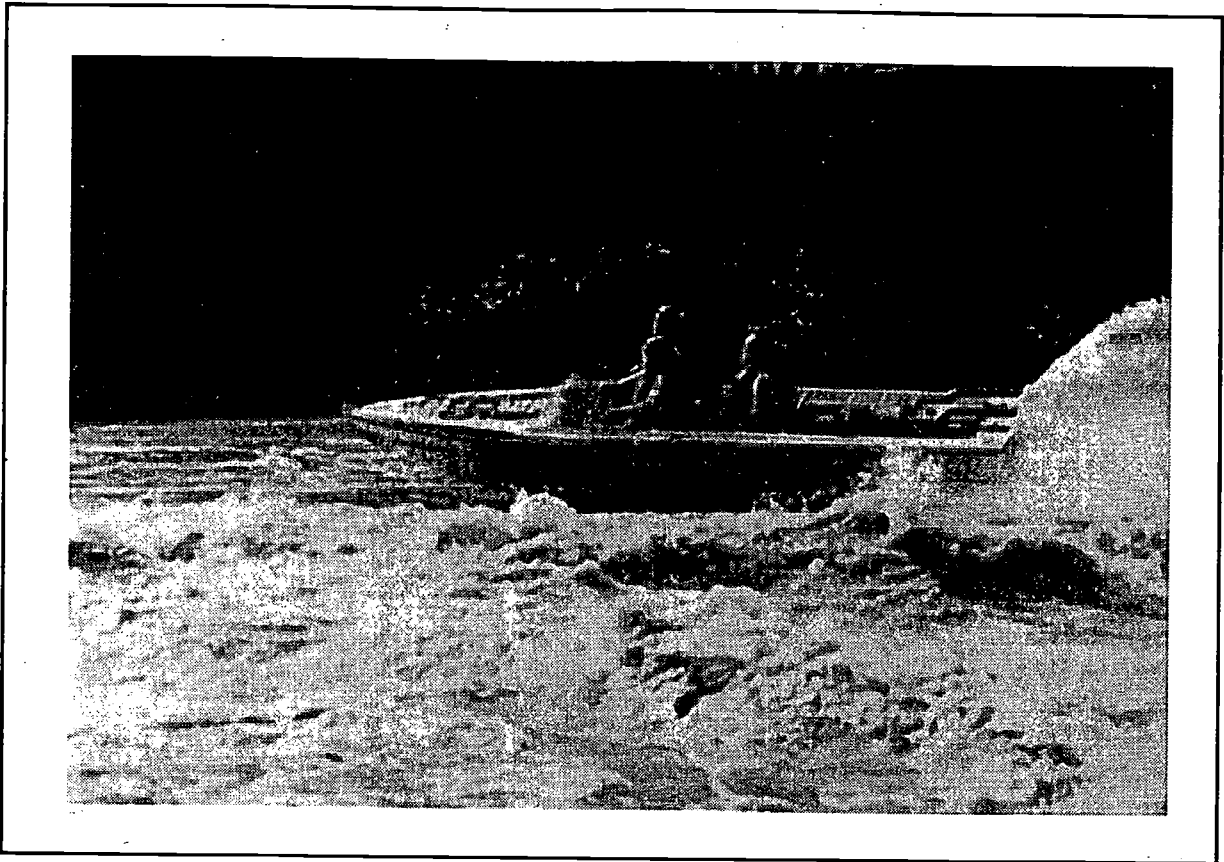
**Examples of High Speed Small Craft operating successfully in rough and aerated water.
All have multi-stage waterjets**



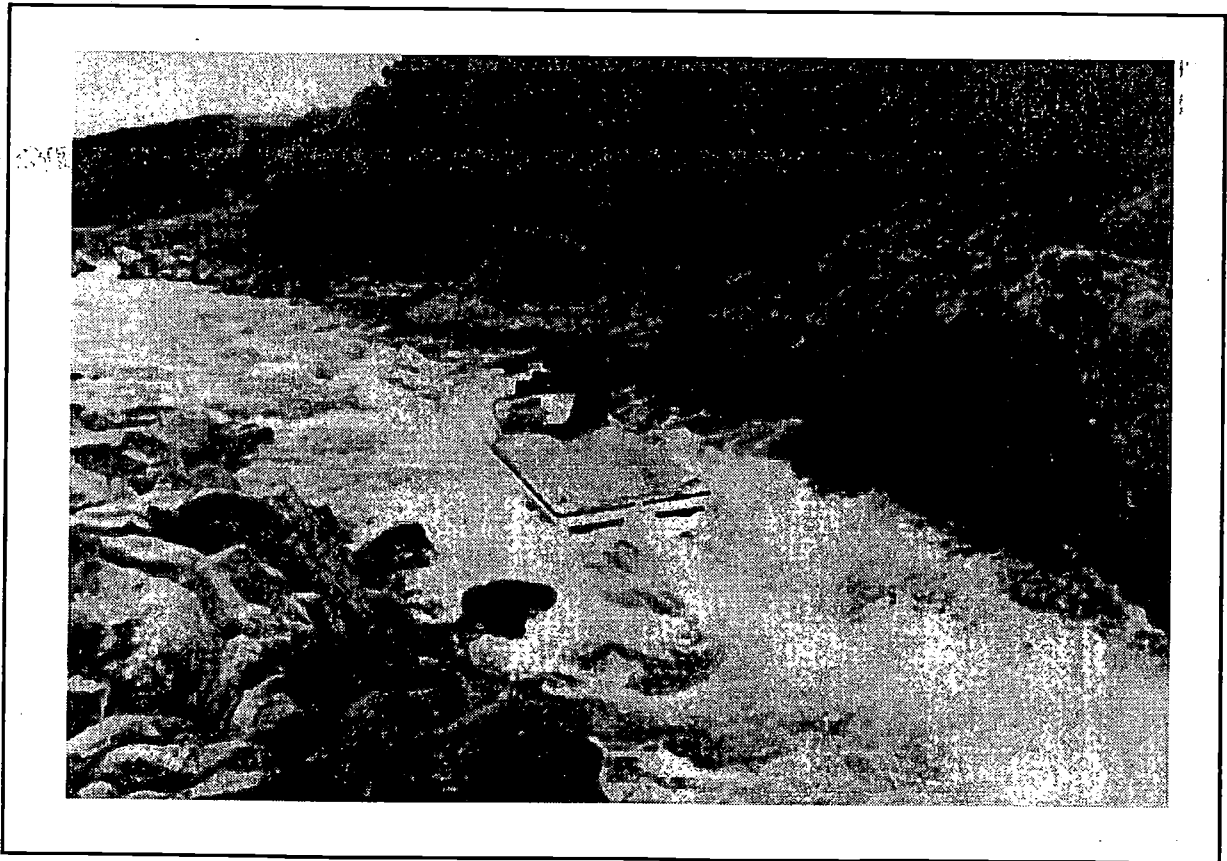


Examples of High Speed Small Craft operating successfully in rough and aerated water. All have multi-stage waterjets





Examples of High Speed Small Craft operating successfully in rough and aerated water. All have multi-stage waterjets



The V.O.C. ship 'AMSTERDAM'

A velocity prediction

by Ir. A. H. Hubregtse

Delft University of Technology
Ship Hydromechanics Laboratory
Delft, The Netherlands

Abstract

A velocity calculation has been made to predict the sailing performance of the V.O.C. ship 'Amsterdam'. The calculations are based upon model experiments in which the upright resistance, the side force production and the induced resistance were measured. A computer model was developed to calculate the sailforces.

Based on this model a velocity prediction program was developed to calculate the equilibrium between the aerodynamic and hydrodynamic forces. The velocity, the heeling angle and leeway angle are calculated for a given true wind speed and angle.

1 Introduction

At the moment two V.O.C ships are being rebuild in the Netherlands. About the sailing performances of these ship very less is known. To get a better insight in the sailing performances of the V.O.C. ships a computer program was developed, based on model experiments, to predict the performance of such a ship. The program is based on the 'Amsterdam', the V.O.C. ship being rebuild in Amsterdam at this moment. In the program no attention is payed to the strength of the rigging or to the sailhandling in the 17th century. Very less was known about these factors so it was better to exclude them.

A lines plan and a sail plan of the 'Amsterdam' were available. Only a few hull parameters had to be estimated.

The calculation of the sailing performance can be split in two parts. First the determination of the hydrodynamic forces by model experiments and the modelling of the results in usable formulas for a computerprogram. And second the development of a model to calculate the aerodynamic forces. This program includes the calculation of special sail coefficients for square rigged sails, the interaction of the sails and the windresistance of hull and rigging.

The equilibrium between the above mentioned forces is calculated in a computerprogram. This program calculates the velocity, heeling angle and leeway angle for a given true wind speed and wind angle.

Also the influence of added resistance due to waves on the performance of the V.O.C. ship can be calculated in the program.

2 The V.O.C. ship 'Amsterdam'

2.1 The ship

The 'Amsterdam' was one of the largest armed merchant ships, build by the V.O.C. in 1748. Unfortunately the ship stranded on her maiden voyage in the English Channel near Hastings. In the museum in Amsterdam a sailplan was kept and also a good model of the hull was available. With three dimensional photography the lines plan of the hull was determined from this model. The main dimensions of the 'Amsterdam' are given in Table 1.1.

The displacement and the height of the centre of gravity of the ship were unknown. Therefore a comparison was made with other ships in Middendorf, 1903 [4], Rees, 1819 [5] and Chapman [1]. In these comparison it appeared that the centre of gravity for ships of the type of the 'Amsterdam' lies near the waterline.

With the linesplan it appeared that the displacement of the hull should lie between the 800 and 1300 tons. With stability calculations for the different displacements and a maximum heeling angle of 20 degrees for shipping green water, see Harland, 1984 [2], the displacement was estimated at 1200 tons. In Figure 1 the stability curves for the different displacements are given. The displacement of 1200 tons leads to a draught of 4.45 metres and a metacentric height of 1.44 metres.

Table 1.1 Main dimensions 'Amsterdam'

L_{pp}	=	42.45 m
Boa	=	11.60 m
D	=	4.45 m
Depl	=	1200 ton
KG	=	4.45 m
Cb	=	0.583
lcb	=	+2.13 m

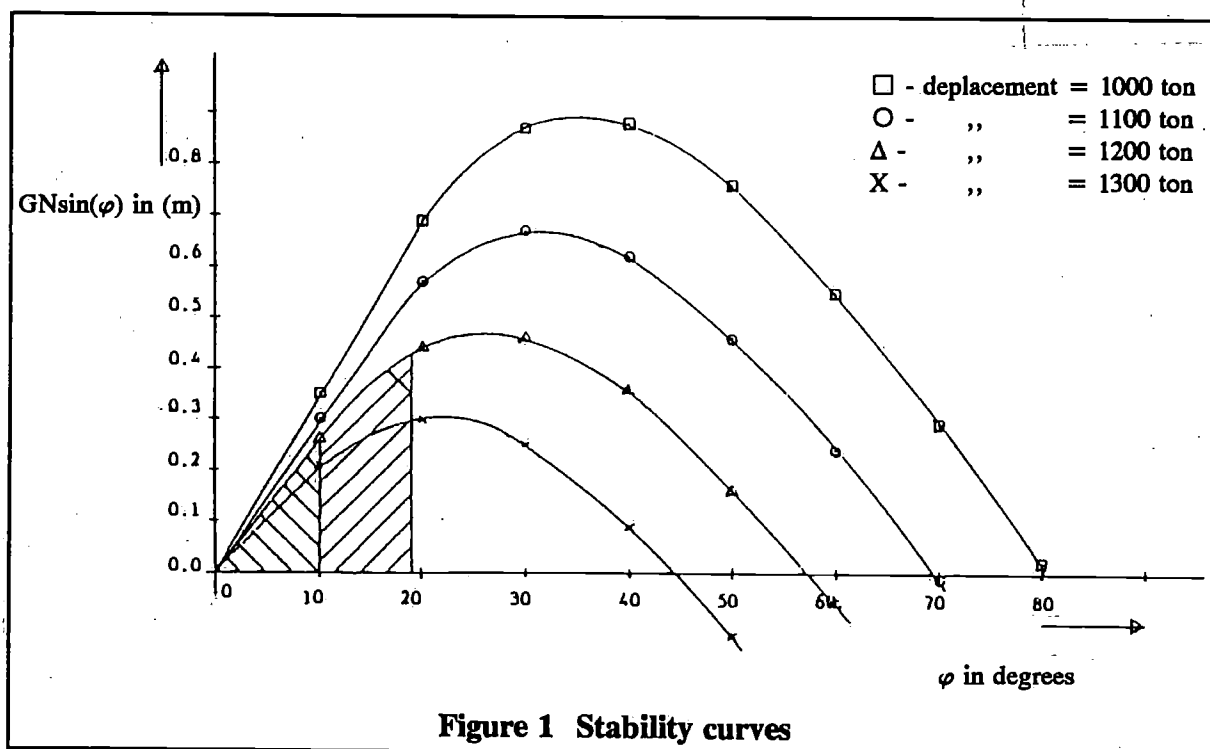


Figure 1 Stability curves

With these parameters and the lines plan of the ship the hydrostatics are calculated for use in the prediction program. These calculations were made on even keel.

The 'Amsterdam' was mainly square rigged. Next to the 9 square sails the ship carries 9 staysails, a mizzen and 2 leesails. This brings the total number of sails to 21 and gives a maximum sail area of 2151 m². A copy of the original sailplan is given in Figure 2.

Due to the minimum sheet angle of 30 degrees, the square rigged sails could only be sailed in apparent wind angles exceeding 60 degrees.

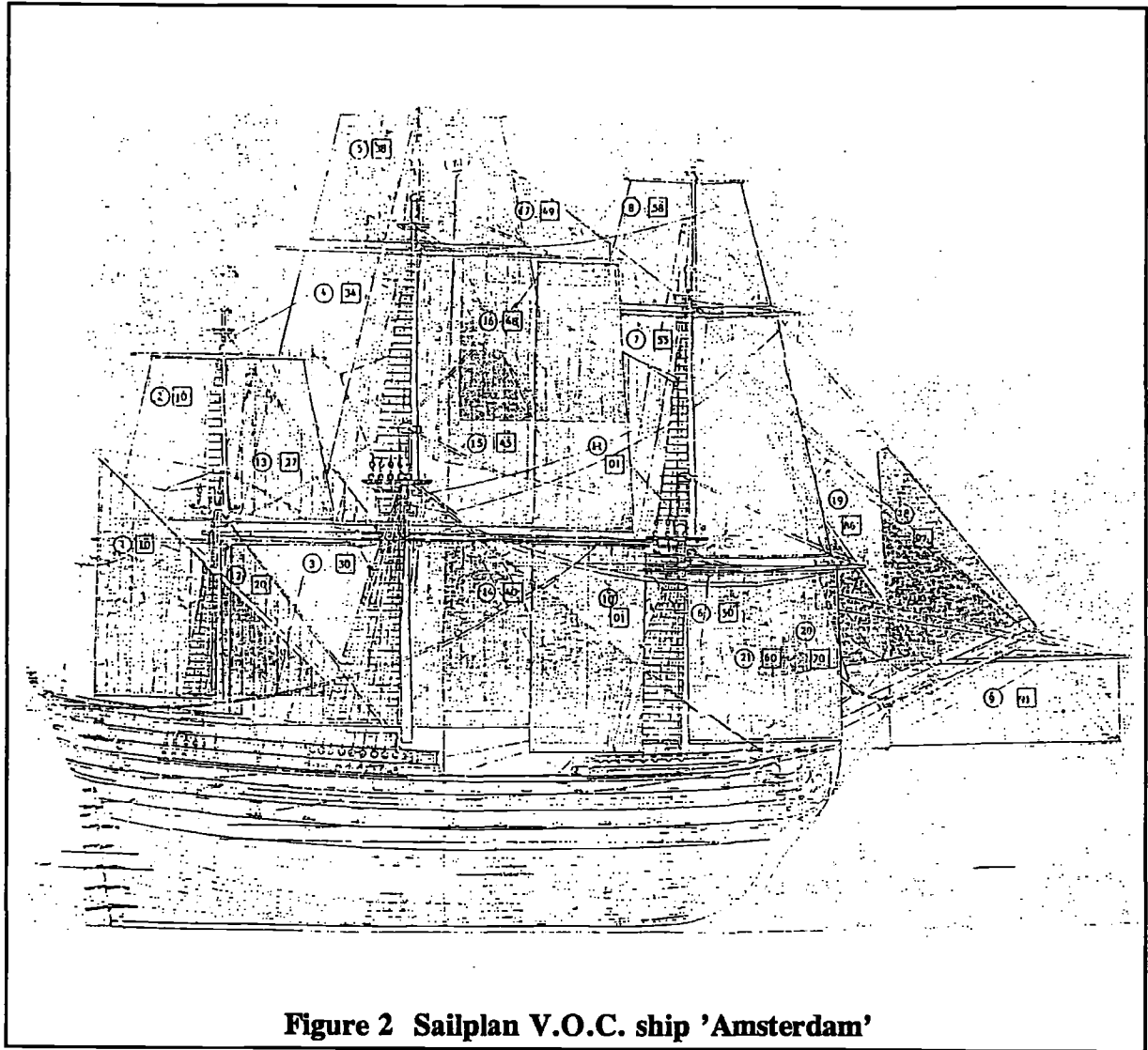


Figure 2 Sailplan V.O.C. ship 'Amsterdam'

3 The wind forces

In this paragraph the methods and conditions for the aerodynamic force calculations are given.

3.1 Sail forces

The sail forces are calculated with the following formulas for the driving- and side sail force:

$$Fr = \frac{1}{2} \cdot p_a \cdot V_{aw}^2 \cdot S_{Ai} \cdot Cr \quad (3.1)$$

$$Fh' = \frac{1}{2} \cdot p_a \cdot V_{aw}^2 \cdot S_{Ai} \cdot Ch \quad (3.2)$$

In which:

Fh'	= Sail force in transverse direction, perpendicular to the sail	(N)
Fr	= Sail force in longitudinal direction	(N)
P_a	= Density of air	(kg/m ³)
S_{Ai}	= Sail area sail i	(m ²)
V_{aw}	= Velocity apparent wind	(m/s)
Ch	= Transverse sail coefficient	(-)
Cr	= Longitudinal sail coefficient	(-)

3.2 Sail coefficients

For these square rigs, with low aspect ratio's, the common sail coefficients can not be used. Special coefficients for this sail forms are given by Wagner, 1966 [6] and Marchaj, 1964 [3]. The value of the sail coefficients depends on the sheetangle of the sails. For the square rigged sails this angle is given by:

$$\alpha = \beta_{aw}/2 \quad (3.3)$$

In which:

α	= Sheetangle, angle between sail and keel
β_{aw}	= Apparent wind angle given of bow

As sail coefficients the Marchaj coefficients are used. These coefficients give better results for the small apparent wind angles. The values of the Wagner coefficients overestimate the force in this area, because these coefficients are based on stiff plate model experiments. In Table 3.1 the Marchaj coefficients are given as a function of the apparent wind angle:

Table 3.1 Marchaj sail coefficients

β_{aw}	α	C_l	C_d	Cr	Ch	C_t
68	34	1.03	0.68	0.70	1.02	1.23
74	37	1.08	0.77	0.83	1.04	1.33
80	40	1.15	0.97	0.96	1.15	1.50
90	45	1.17	1.16	1.17	1.16	1.65
100	50	1.03	1.21	1.22	1.01	1.59
110	55	0.77	1.10	1.10	0.77	1.34
120	60	0.63	1.09	1.09	0.63	1.26
130	65	0.53	1.13	1.13	0.52	1.25
140	70	0.42	1.13	1.14	0.40	1.21
150	75	0.31	1.14	1.14	0.30	1.18
160	80	0.21	1.14	1.14	0.19	1.16
170	85	0.11	1.15	1.15	0.09	1.16
180	90	0.00	1.15	1.15	0.00	1.15

3.3 Interaction of the sails

Interaction of the sails is not included in the sail-coefficients, as in a.o. the Standfast coefficients. Therefore the interaction must be calculated separately. Due to the form of the sail there will be no other interaction than the covering by other sails, depending on the apparent wind angle. This influence will be calculated using the uncovered geometric sail area as sail area.

3.4 Windforce on hull and rigging

Due to the high freeboard and the amount of masts, yards and rigging the wind resistance will have a great influence on the performance of the V.O.C. ship. With the common used formulas for the windresistance for ships and masts, the total force due to wind resistance in the apparent wind direction is given by:

$$F_{aa} = 0.5 \cdot P_a \cdot (V_{aw} \cdot \cos(\phi))^2 \cdot (246.04 + 273.1 \cdot \sin(\beta_{aw}) + Co \cdot \cos(\beta_{aw})) \quad (\text{N}) \quad (3.4)$$

In which:

$$Co = 67.8 \text{ for } \beta_{aw} \geq 90^\circ.$$

$$Co = -72.8 \text{ for } \beta_{aw} < 90^\circ.$$

3.5 Resulting aerodynamic forces and moments

With the above mentioned formulas the following forces and moments are calculated:

- F_x = Aerodynamic thrust force, in forward direction
- F_y = Transverse aerodynamic force
- F_z = Downward aerodynamic force
- M_l = Yaw moment in horizontal plane, calculated to the midship
- M_f = Trim moment, around y-axis, calculated to the application point of the resistance force
- M_h = Heeling moment calculated to the application point of the hydrodynamic side force

3.6 Conditions

Maximum heel angle:

To avoid green water on deck, the maximum heeling angle is limited to 10 degrees. If the heeling angle exceeds the 10 degrees sail area must be reduced.

Maximum yaw moment:

In comparison to the ship dimensions the 'Amsterdam' has a relative small rudder. Therefore the ship must be steered by the sails. The rudder can only be used for small corrections. The maximum rudder moment is determined 70.6 kNm (Calculated to midship). If the yaw moment exceeds this value, the sailplan must be adapted.

4 Experimental results

Model experiments were done to determine the hydrodynamic forces. The tests were done with a 1:20 model of the V.O.C. ship 'Amsterdam'. These tests were carried out in the large as well as in the small towing tank of the Ship Hydromechanics Laboratory of the Faculty of

Mechanical Eng. and Maritime Technology of the Delft University of Technology. During the experiments the resistance, the side force fore and the side force aft were measured for different speeds, heel angles and leeway angles. The tests were carried out to measure the upright resistance, the sideforce and the induced resistance as a function of speed, heel and leeway.

4.1 Upright resistance

The upright resistance was measured in the large as well as in the small towing tank. In this way a correction for the blokkage of the model could be calculated and used for the measurements in the small towing tank. The measured upright model resistance and the calculated ship resistance are given in Table 4.1.

Table 4.1 Upright resistance table

<i>V_m</i> m/s	<i>R_{tm}</i> N	<i>R_{fm}</i> N	<i>R_{rm}</i> N	<i>R_{fs}</i> N	<i>R_{rs}</i> N	<i>V_s</i> m/s	<i>R_s</i> N
.2	.207	.194	.000	652.6	.0	0.9	652.6
.3	.451	.394	.000	1376.4	.0	1.3	1376.4
.4	.823	.655	.053	2339.9	421.1	1.8	2761.0
.5	1.329	.972	.173	3533.9	1384.3	2.2	4918.1
.6	1.918	1.343	.309	4961.5	2474.9	2.7	7426.4
.7	2.629	1.767	.499	6587.3	3993.4	3.1	10580.8
.8	3.405	2.241	.692	8437.0	5533.4	3.6	13970.4
.9	4.413	2.766	1.041	10497.0	8329.5	4.0	18826.4
1.0	5.744	3.339	1.632	12764.0	13057.5	4.5	25821.4
1.1	7.696	3.960	2.739	15235.2	21910.7	4.9	37145.9
1.2	10.809	4.629	4.857	17908.3	38856.8	5.4	56765.2
1.3	15.282	5.343	8.170	20781.0	65361.4	5.8	86142.5
1.4	22.096	6.104	13.578	23851.4	108626.1	6.3	132477.5
1.5	29.567	6.909	19.538	27117.5	156301.7	6.7	183419.2
1.6	37.501	7.760	25.871	30577.8	206969.1	7.2	237546.9

The frictional resistance of ship and model were calculated with the ITTC formulas. No correction was made for the roughness of the hull. The resistance was corrected for the blokkage of the model and the extra resistance due to the sand strips. The last two columns of the table are used in the Velocity Prediction Program (VPP). For intermediate velocities the resistance is determined with second order interpolation in this table.

4.2 Measurements with leeway and heel

For four model speeds, 0.4, 0.7, 1.0 and 1.3 m/s, corresponding with the ship speeds of 3.5, 7.0, 10.5 and 14.0 knots, the side force and the resistance were measured for heel angles of 5, 10 and 15 degrees and for a number of leeway angles. These experiments were carried out in the small towing tank.

Very remarkable was the fact that the measured parameters, sideforce, induced resistance etc., were independent of the heeling angle. With the measured results the following regression equations were derived:

Side force:

$$Fh'' = 8 \cdot (cf1 \cdot \beta + cf2 \cdot \beta^2) \quad (\text{kN}) \quad (4.1)$$

In which:

- Fh'' = Side force
 β = Leeway angle in radians
 $cf1, cf2$ = Velocity dependent regression coefficients given in Table 4.2

Table 4.2 Side force coefficients

V_m	$cf1$	$cf2$
0.4	14.004	46.740
0.7	45.095	118.591
1.0	78.280	273.169
1.3	174.172	175.710

The factor 8 is used to scale the model force (N) to real ship dimensions (kN)

Induced resistance:

The induced resistance was determined by subtracting the upright resistance of the measured resistance with heel and leeway.

$$Rm\beta\phi = R_{tmi} - R_m$$

In which:

- R_{tmi} = Measured resistance with heel and leeway
 R_m = Measured upright resistance
 $Rm\beta\phi$ = Induced resistance

With regression analysis the $Rm\beta\phi$ is now determined as a function of the total side force:

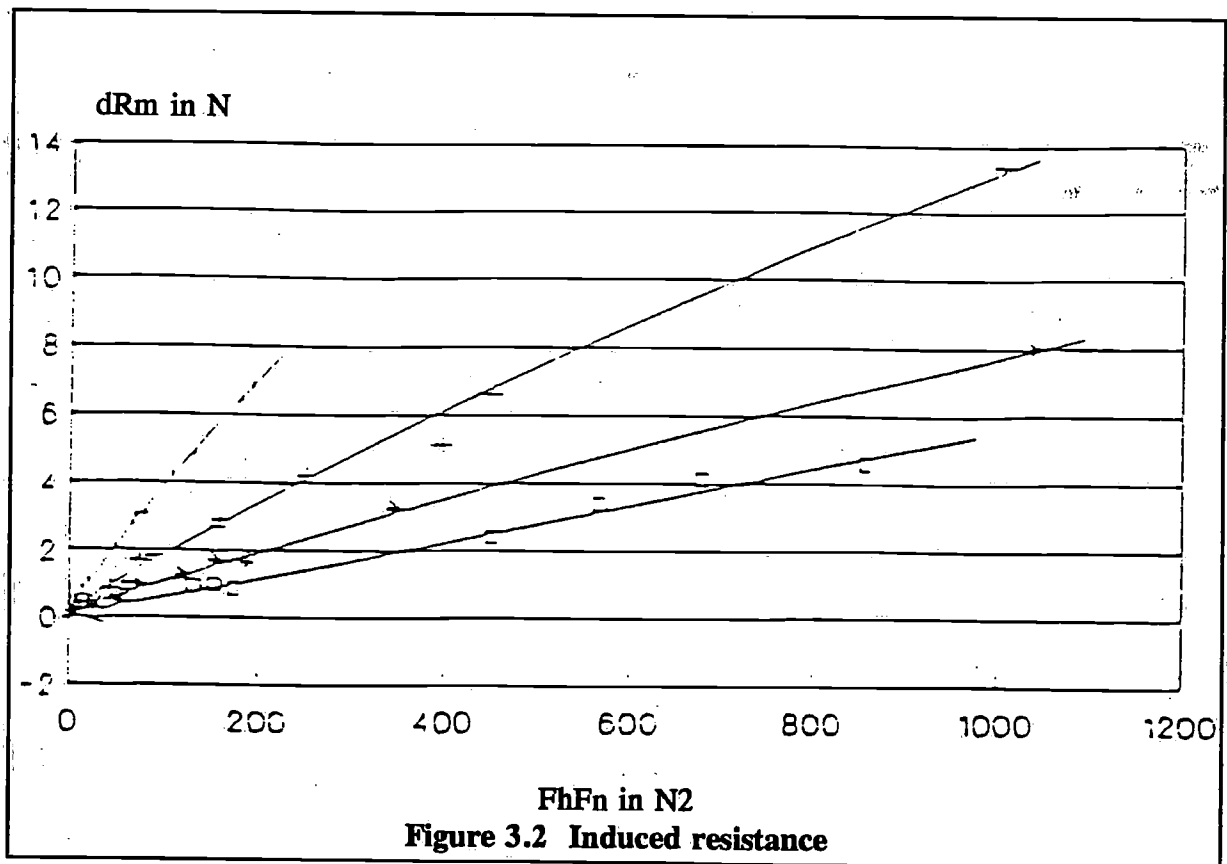
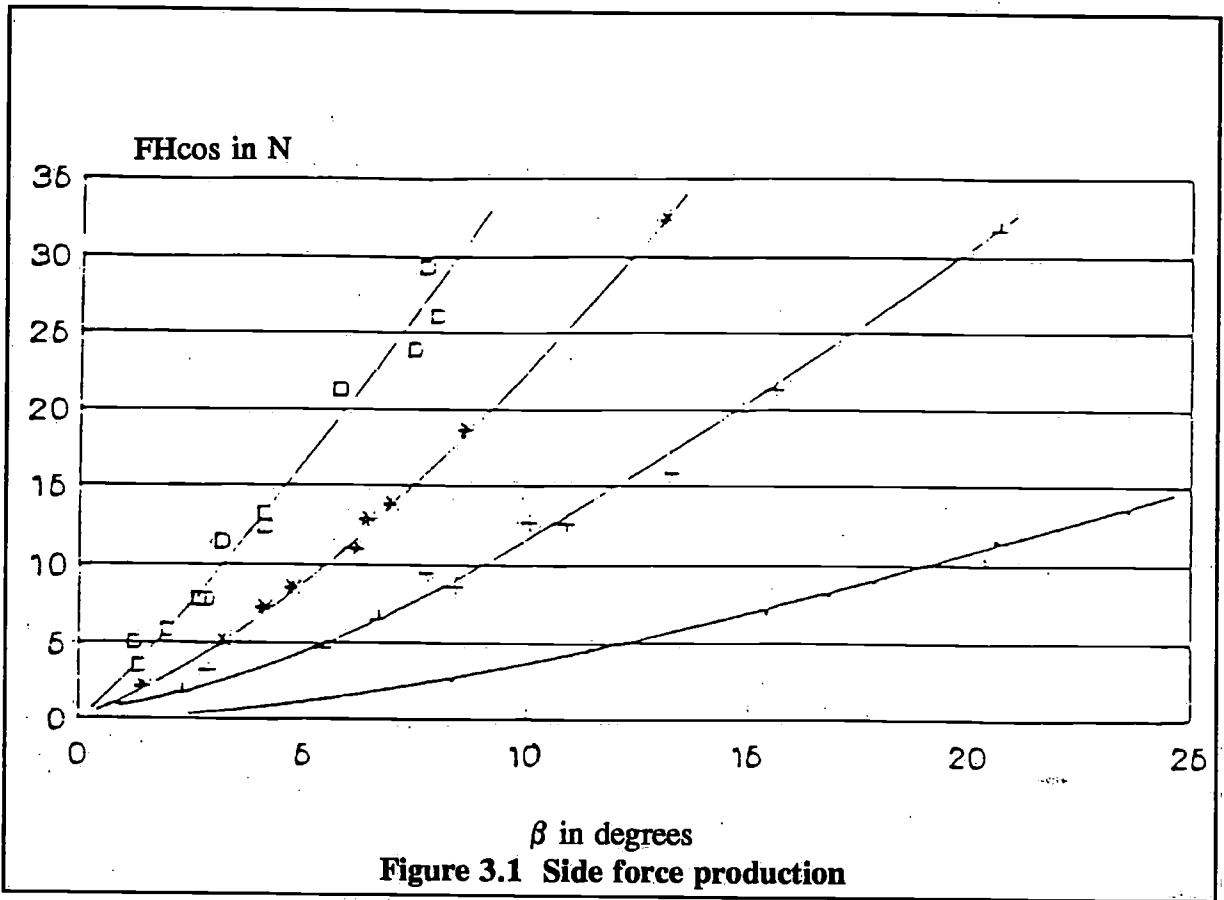
$$Rm\beta\phi = 8 \cdot (cr0 + cr1 \cdot (Fh''/8)^2 + cr2 \cdot ((Fh''/8)^2)^2) \quad (\text{kN}) \quad (4.2)$$

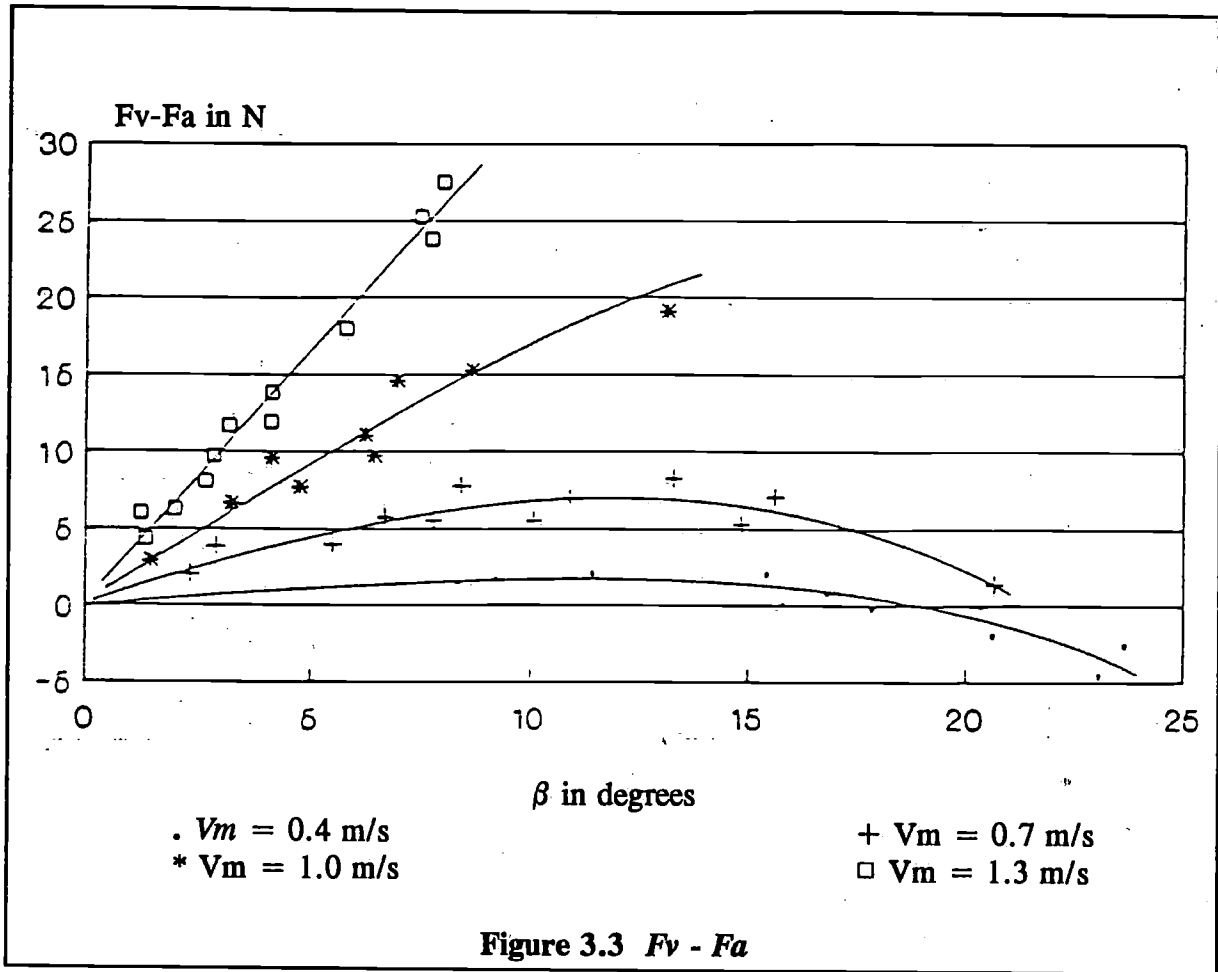
In which:

- $Rm\beta\phi$ = Induced resistance
 Fh'' = Side force in kN
 $cr0, cr1, cr2$ = Regression coefficients

Table 4.3 Induced resistance coefficients

V_m	$cr0$	$cr1 \cdot 10^2$	$cr2 \cdot 10^6$
0.3	0.276	3.894	- 26.930
0.7	0.269	1.470	- 1.691
1.0	0.115	0.9534	- 1.921
1.3	0.132	0.5726	- 0.4127





Yaw moment:

The yaw moment is calculated with the following formula:

$$M_{ls} = \{ [(F_v - F_a)/16 \cdot \cos(\beta) + F_h' \cdot 0.0833 \cdot \sin(\phi)\cos(\beta)] \cdot 160 + R_{ts} \cdot (\frac{1}{2} \sin(\beta) - 0.333 \cdot \sin(\phi)\cos(\beta)) \} \cdot 0.02 \quad (\text{kNm}) \quad (4.3)$$

In which:

- $(F_v - F_a)$ = Difference side force fore - aft
- ϕ = Heel angle
- β = Leeway angle
- R_{ts} = Upright resistance ship

The difference in side force fore - aft is measured and the following regression equation is derived of the measurements:

$$(F_v - F_a) = c_{g1} \cdot \beta + c_{g2} \cdot \beta^2 + c_{g3} \cdot \beta^3 \quad (\text{N}) \quad (4.4)$$

in which:

- $F_v - F_a$ = Difference side force fore-aft
- β = Leeway angle in radians
- c_{g1}, c_{g2}, c_{g3} = Regression coefficients

The measured data and the calculated polynomials are plotted in Figure 3. The last tables are used in the VPP. For a given speed and leeway angle the regression coefficients are interpolated in the tables, and the forces and moments can be calculated.

Application point of the side force:

The last series of experiments were carried out with a leeway angle but with no heel. This was done to determinate the height of the application point of the side force was determinate at 3.24 m above the base line.

Table 4.4 Yaw coefficients

<i>Vm</i>	<i>cg1</i>	<i>cg2</i>	<i>cg3</i>
0.3	16.159	- 15.691	- 112.757
0.7	58.624	- 70.005	- 225.107
1.0	105.523	128.277	- 972.289
1.3	244.666	- 1397.464	7311.794

Table 5.1 Results added resistance calculation

Noordzee, $H_{\frac{1}{8}} = 2.78$ m, $T_1 = 5.5$ s								
β_{tw}	180	160	140	120	100	80	60	40
<i>Vs</i>								
6.0	10.7	9.3	4.7	0.0	0.7	1.9	8.1	21.2
9.0	16.1	14.7	9.2	0.9	0.8	2.3	9.2	25.2
12.0	19.4	19.0	14.4	2.6	0.8	2.7	9.2	26.6
Atlantische Ocean, $H_{\frac{1}{8}} = 3.11$ m, $T_1 = 7.1$ s								
β_{tw}	180	160	140	120	100	80	60	40
<i>Vs</i>								
6.0	8.3	7.2	3.6	0.0	0.6	1.5	6.4	16.3
9.0	12.5	11.4	7.1	0.7	0.6	1.9	7.2	19.1
12.0	15.2	14.8	11.1	1.9	0.7	2.3	7.3	20.1

5 Added resistance in waves

Because of the special hull form it was a point to calculate the influence of the added resistance performance of the V.O.C. ship.

Therefore the added resistance due to waves was calculated for a number of headings and for two wave spectra, a JONSWAP spectrum for the North Sea and a Pierson-Moskowitz spectrum for the Atlantic Ocean.

For both the spectra the added resistance was calculated for three different boatspeeds, 6, 9 and 12 knots. The added resistance was calculated with the method of BOESE, after the motions had been calculated with the ordinary strip theory. The results of these calculations are given in Table 5.1.

This table gives the mean added resistance for the calculated speed range and apparent wind angles. For intermediate velocities and/or wind directions the added resistance is calculated by interpolation in this table.

6 Mathematical model velocity prediction program

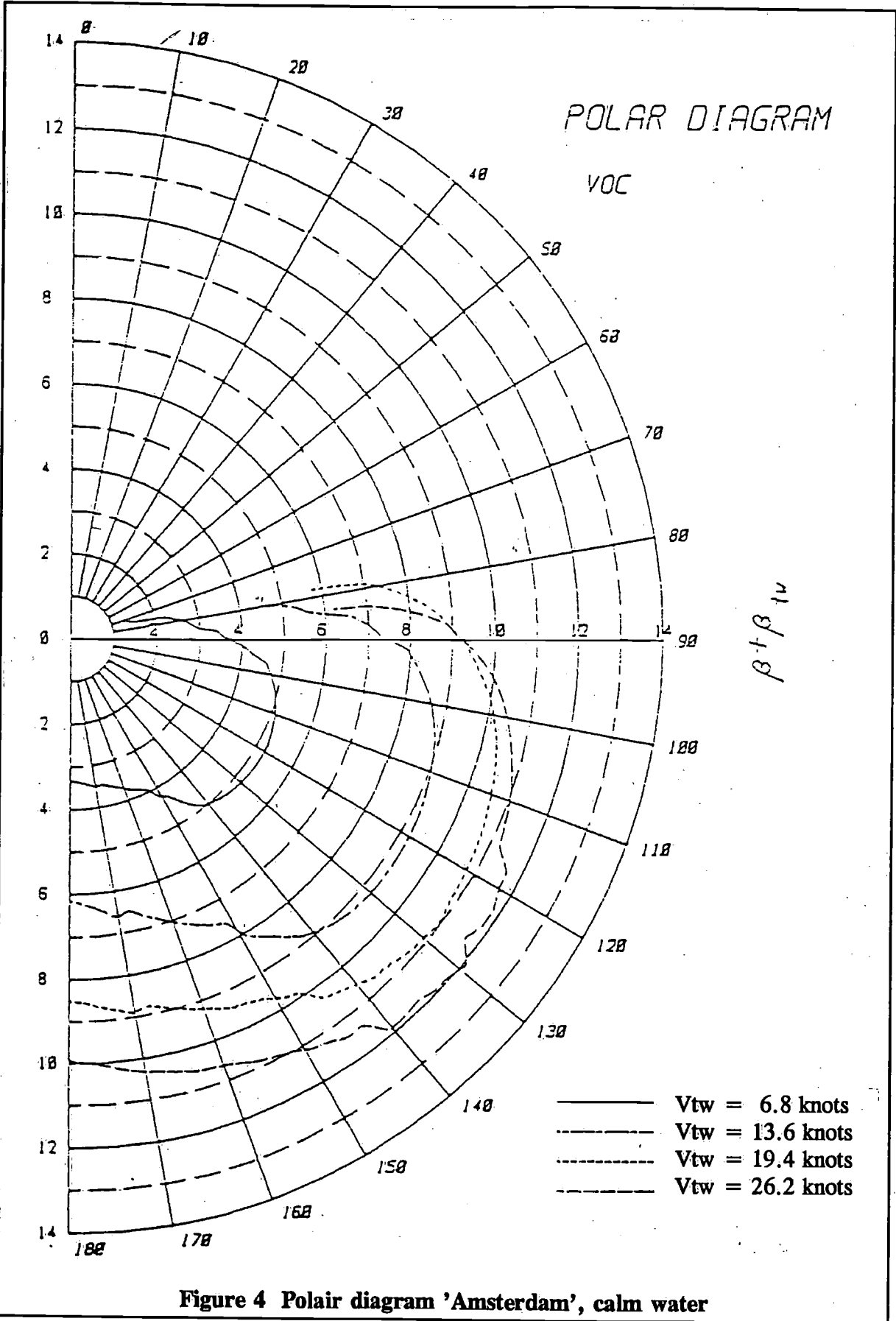
To calculate the balance between the previous mentioned aero and hydrodynamic forces, a computer program is developed. In this program the equilibrium between the forces and moments is calculated for a given true wind speed and wind angle. This results in a prediction of the velocity, the heel angle and the leeway angle.

The maximum possible loads on masts and rigging are unknown. Therefore no sail area is reduced for reasons of possible breaking of any part of the rigging. For the higher windspeeds it is therefore possible that too much sail area is carried and the sailors in the 17th century would have reduced sail earlier for strength reasons. But when they would reduce sail is unknown, and therefore this is not included in the program. If the heeling angle or the longitudinal moment exceeds the maximum values the sail with the highest Ml/Fx or Mh/Fx ratio is removed.

Mathematical model of the VPP:

- 1 Given true wind speed and true wind angle
- 2 Predict velocity, heel angle and leeway angle
- 3 Calculate apparent wind angle and wind speed
- 4 Calculate aerodynamic forces and moments
 - Determine sail coefficients
 - Calculate wind resistance
 - Calculate sail forces for each sail
 - Add the sail forces
- 5 Calculation of heel angle ϕ .
 $Mh = GN\sin(\phi) \cdot g \cdot \text{depl}$
If the heel angle exceeds the 10 degrees the sailplan is adapted.
- 6 Calculation of the leeway angle in (4.1)
- 7 Calculation of δRt

$$\delta Rt = Fx - Rm\beta\phi - Rts - Raw$$



In which:

F_x	= Propulsing sail force
$R_{m\beta\phi}$	= Induced resistance
R_{ts}	= Upright resistance, interpolated in resistance table
R_{aw}	= Added resistance in waves
δR_t	= Difference resistance - propulsion force

The δR_t leads to a new estimation of the speed. With this speed the calculation is redone until δR_t is smaller then 1 % of F_x .

8 Calculation yaw moment.

The yaw moment is calculated with (4.3) and added to the longitudinal moment of the sails. If the total moment exceeds the maximum value, the sailplan is adapted and the calculation is redone.

7 Results velocity prediction

7.1 Prediction in calm water

With the velocity prediction program calculations have been done for four different wind-speeds; 3.5, 7, 10 and 13.5 m/s. For each of this speeds a number of true wind angles were calculated so a polair diagram of the performance of the V.O.C. ship could be made. The polair diagram is given in Figure 4.

Upwind performance:

The upwind performance is very bad. The maximum *VMG* is 1.4 knots. Due to the high wind resistance, the low *Cl/Cd* ratio's of the sails and the absence of a side force producer under water, the velocity is low and the highest course over the ground is 71 degrees. With higher windspeeds this angle increases because the maximum heel angle is exceeded and sail must be reduced.

Running performance:

Running the the V.O.C. ship reaches it's highest speeds. The maximum speed is reached when the sails do not cover each other and the sails area can be used optimal. The knuckles in the lines are results of the removal or adding of sails due to the limits on heel angle and yaw moment.

Downwind performance:

Downwind the speed decreases because the sails cover each other. The wind resistance of the hull has a positive influence on the speed. This force equals about one-third of the total propulsing force.

In Figure 5 the resistance components are given. It can be seen that the induced resistance is very high in the upwind area. This is due to the large leeway angles, necessary to compensate the side force. Compared to the other wind angles, the total propulsing force downwind is very small. The wind resistance of the hull in the upwind conditions is one third of the total resistance.

If the hull of the V.O.C. would be replaced by a keel, as placed on a sailing vessel yacht of the same dimensions, the effective draught would be 2.78 m.

7.2 Performance in waves

The previous calculations were also done in waves. The previous mentioned North Sea and Atlantic Ocean spectra were used. The polar diagrams are given in Figure 6. From this diagrams it can be seen that the influence of the added resistance due to waves is neglectible for upwind and running conditions. Only the downwind speeds decreases due to the added resistance. The resistance components are given in Figure 7. The magnitude of this added resistance is small, only one-third of the added resistance in head waves. But also the propulsing force is very small. Therefore the influence on the velocity is very large.

8 Conclusions

During the model experiments it appeared that the induced resistance and the produced side force were independent of the heeling angle.

The upwind performance of the V.O.C. ship is very bad. This is due to the high wind resistance, the low Cl/Cd ratio of the square sails, and the absence of side force producer under water.

Above a true windangle of 85 degrees the speed increases rapidly until the sails begin to cover each other. The maximum calculated speed is 12 knots. In the calculation no attention is payed to the strength of the rigging. Therefore the predicted speeds could be to high, especially on the running courses. Downwind the speed increases, due to the covering of the sails. The wind resistance has a positive effect in this conditions

The influence of added resistance due to waves can be neglected in the upwind and in running conditions. Only downwind the speed decreases due to the added resistance.

References

- [1] Chapman, Af.,
"Architectura Navalis Mercatoria", Rostock.
- [2] Harland, J.,
"Seamanship in the age of sail", London, 1984.
- [3] Marchaj, C.A.,
"Sailing theory and practice", New York, 1964.
- [4] Middendorf, F.L.,
"Bemastung und Takelung der Schiffe, Berlijn, 1903.
- [5] Rees,
"Naval Architecture", Rees's Aries, 1819-1820.
- [6] Wagner, B.,
"Windkanalversuche mit dem takelage Model einer Viermastbark",
IFS-bericht 172, october 1966. Schiff und Hafen, Heft 1/1967, blz 13.

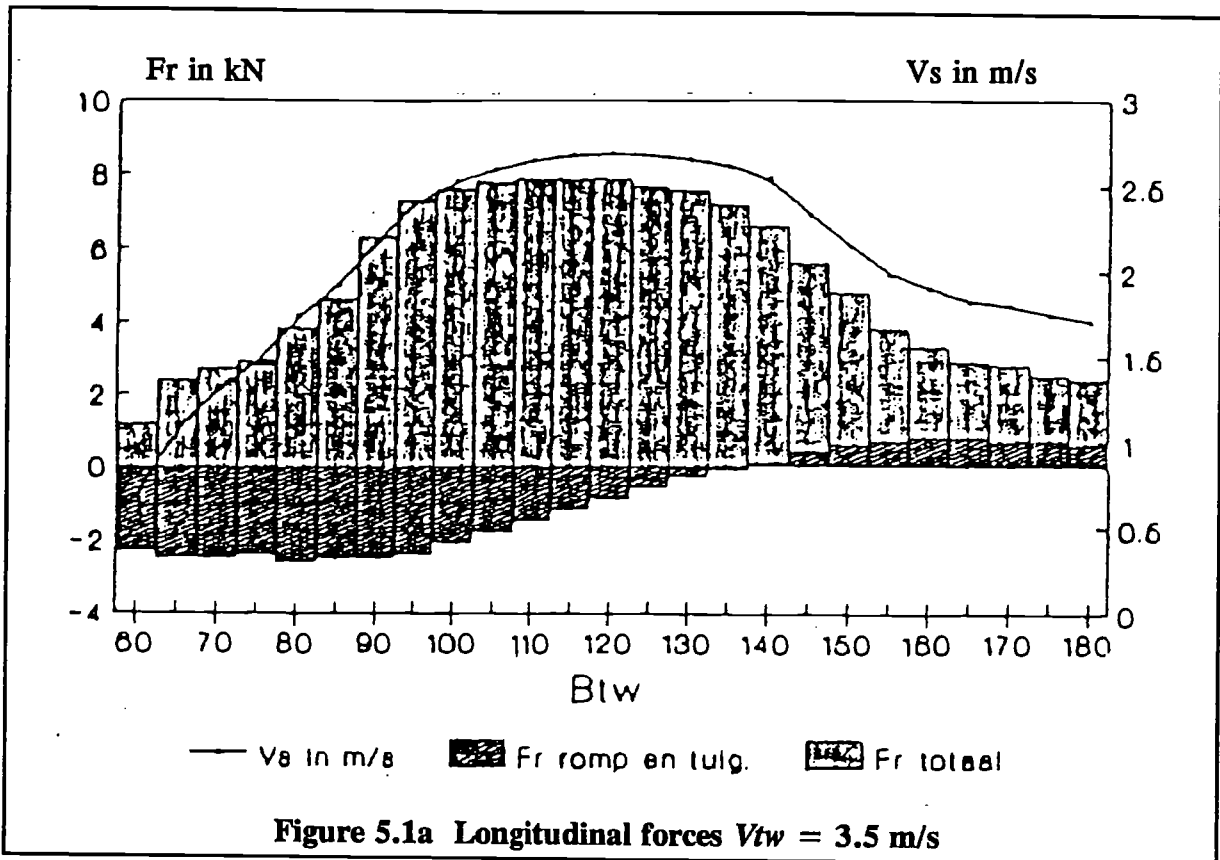


Figure 5.1a Longitudinal forces $V_{tw} = 3.5$ m/s

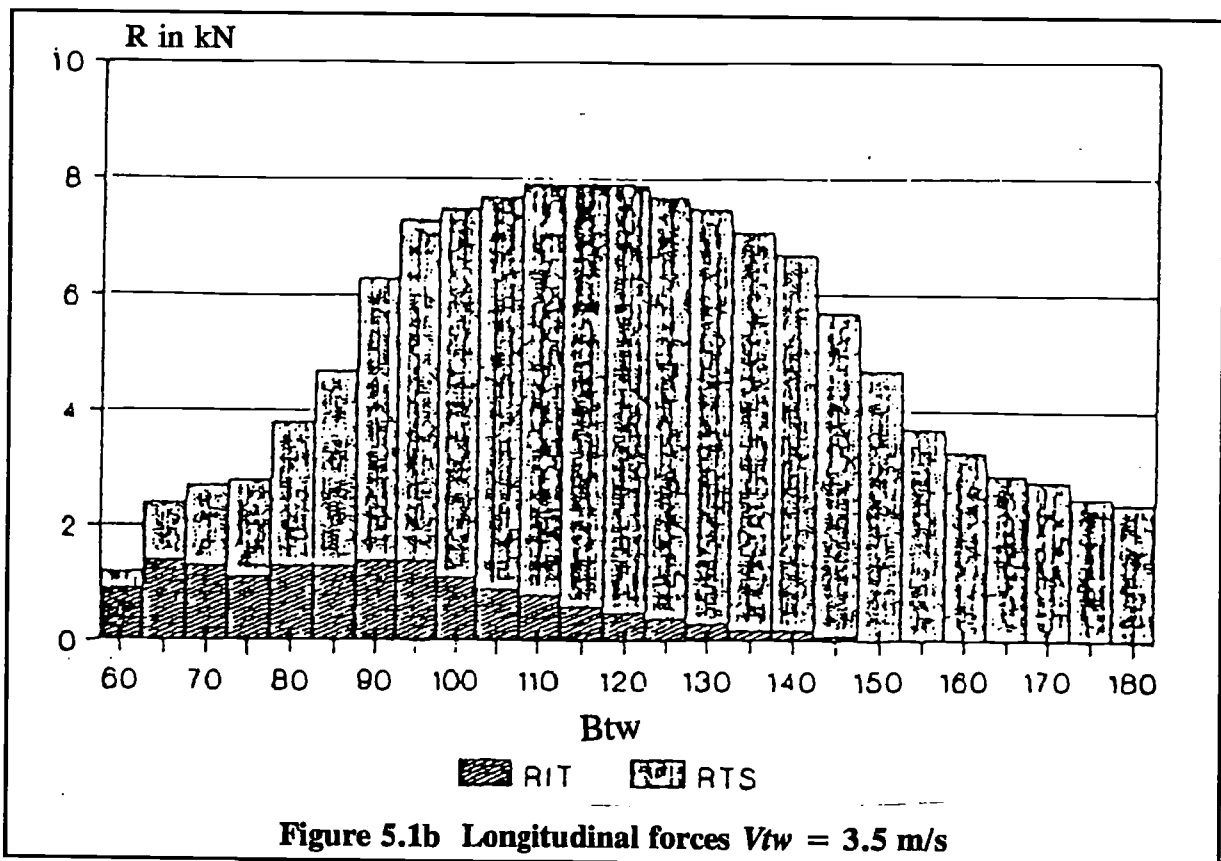


Figure 5.1b Longitudinal forces $V_{tw} = 3.5$ m/s

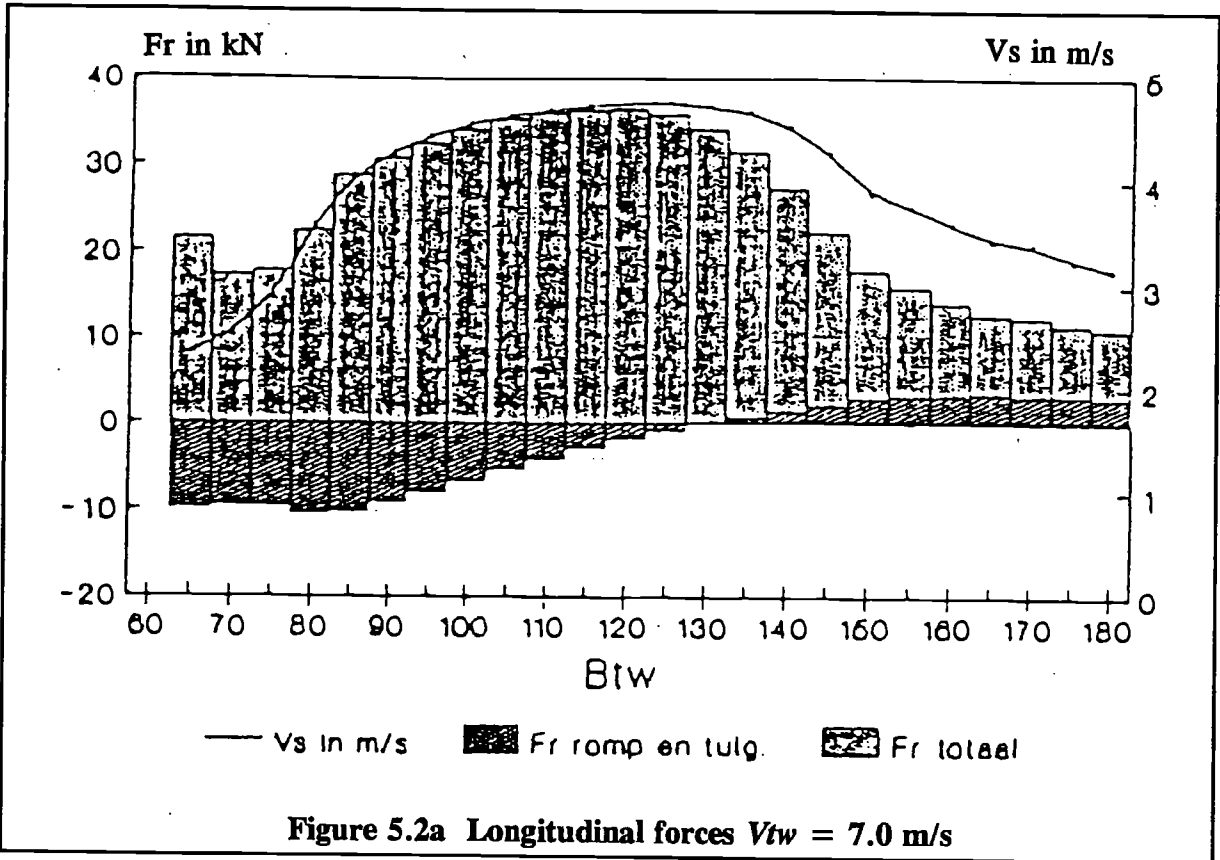


Figure 5.2a Longitudinal forces $V_{tw} = 7.0$ m/s

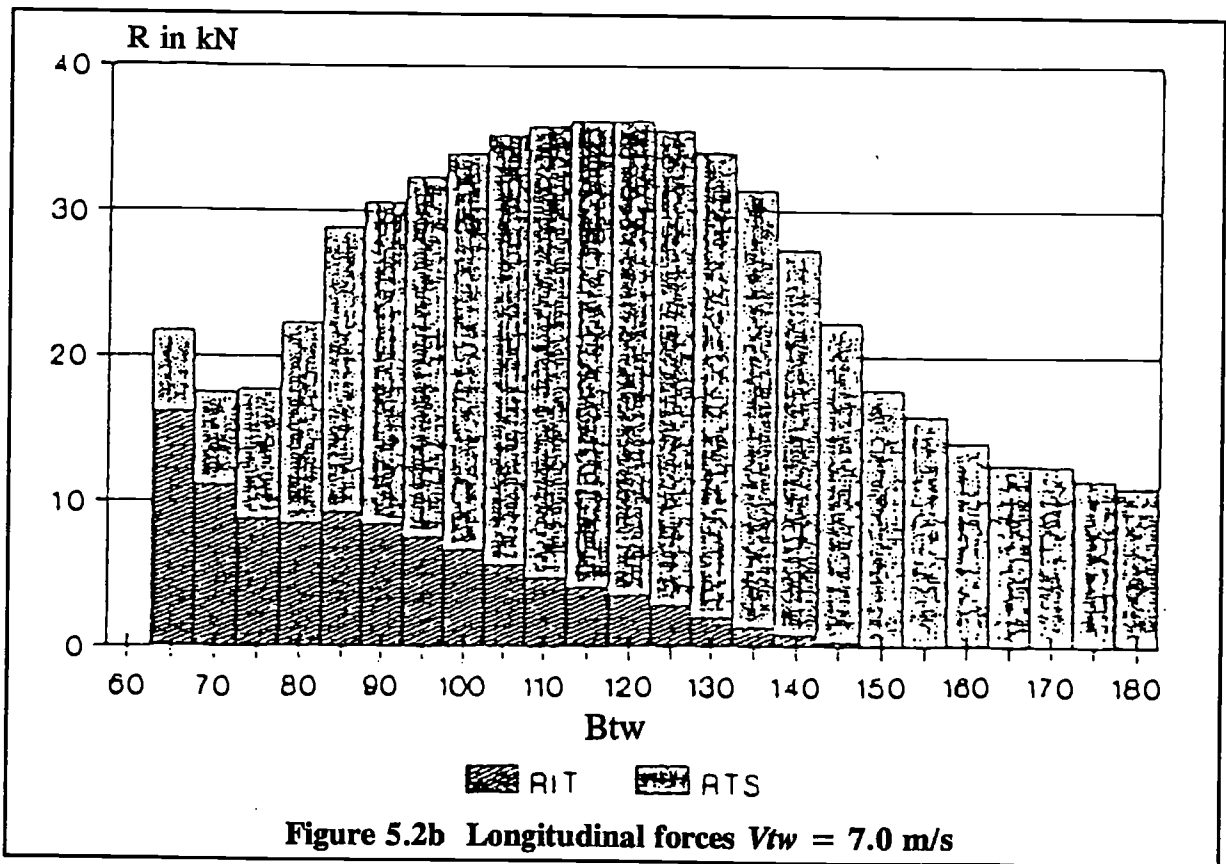
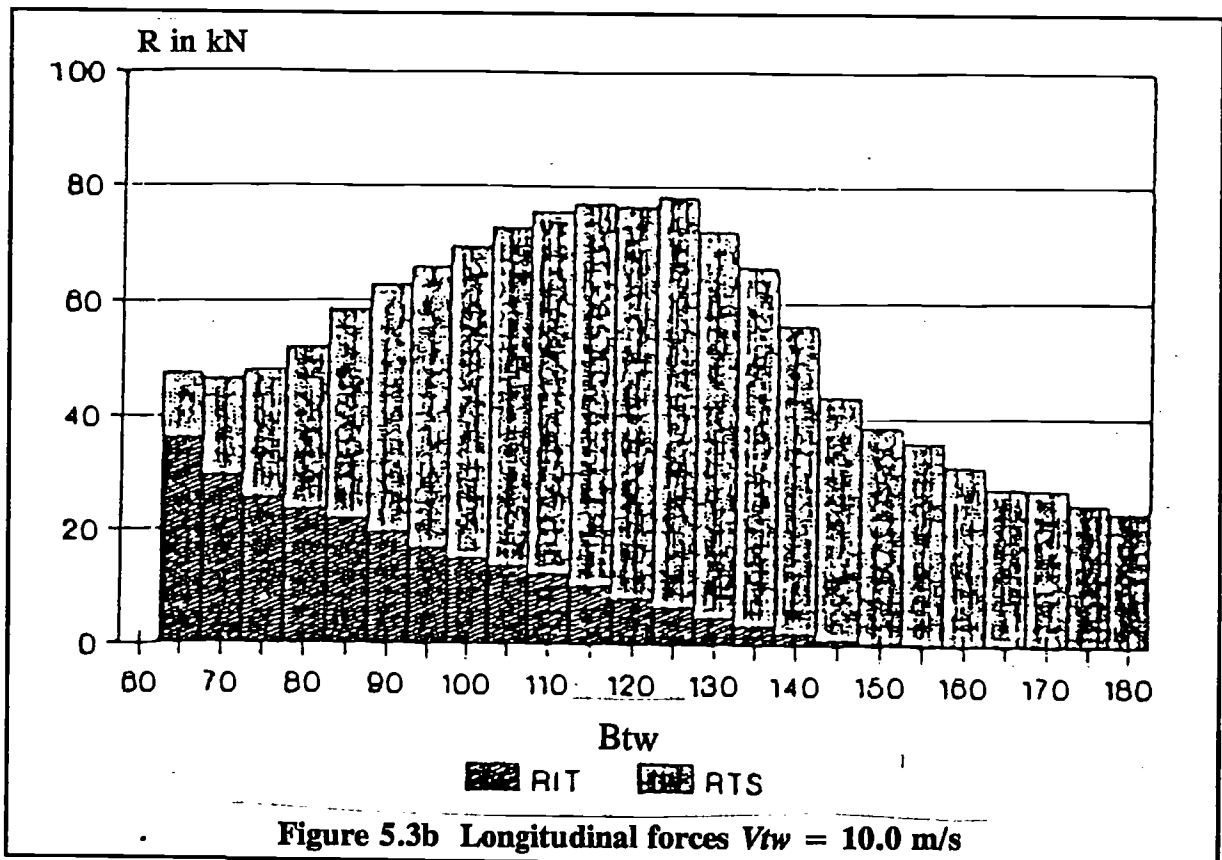
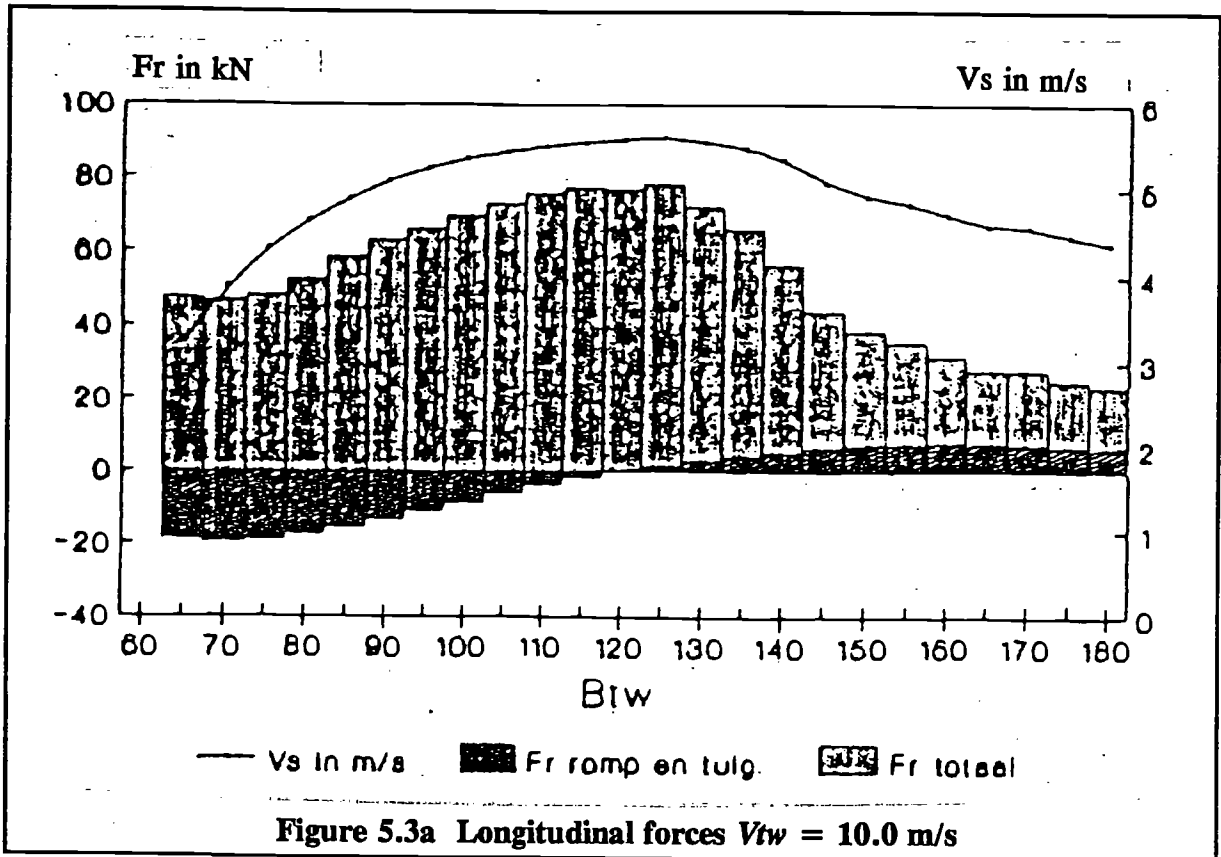


Figure 5.2b Longitudinal forces $V_{tw} = 7.0$ m/s



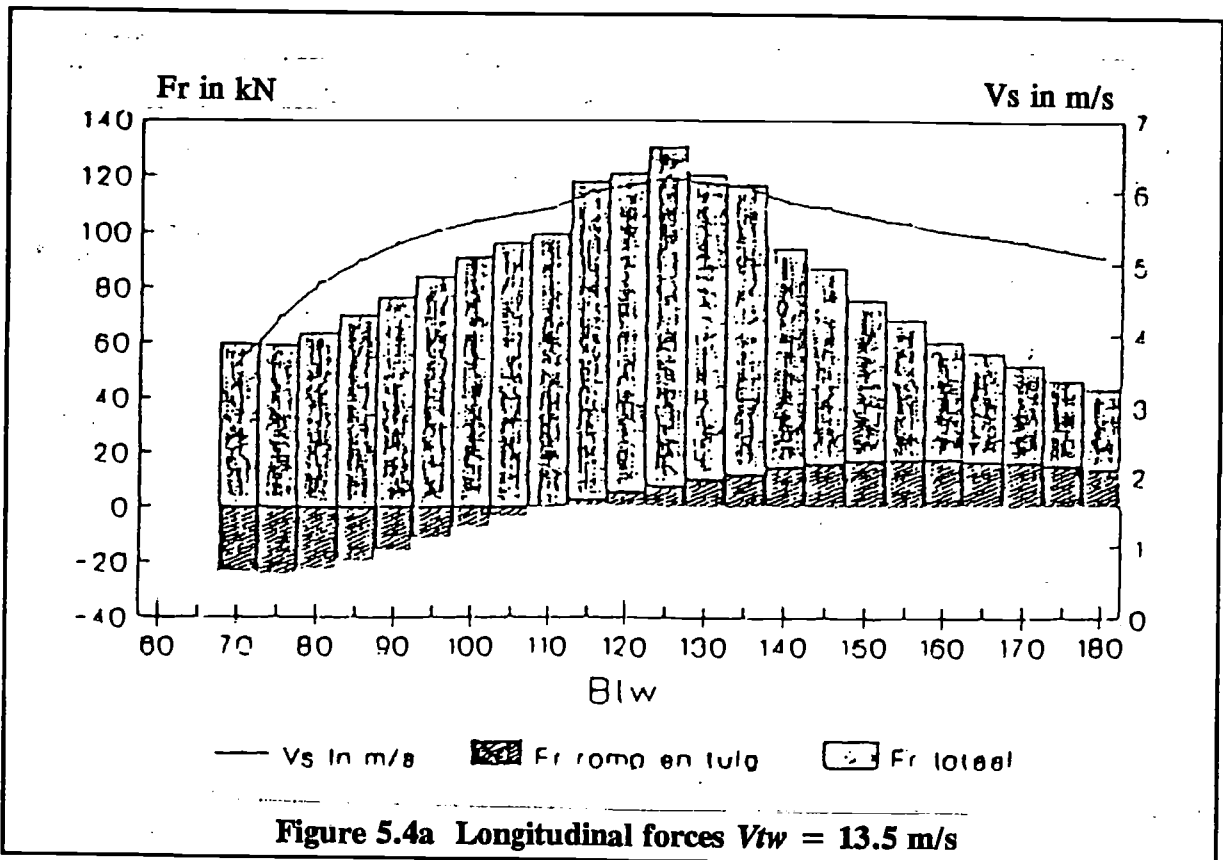


Figure 5.4a Longitudinal forces $V_{tw} = 13.5$ m/s

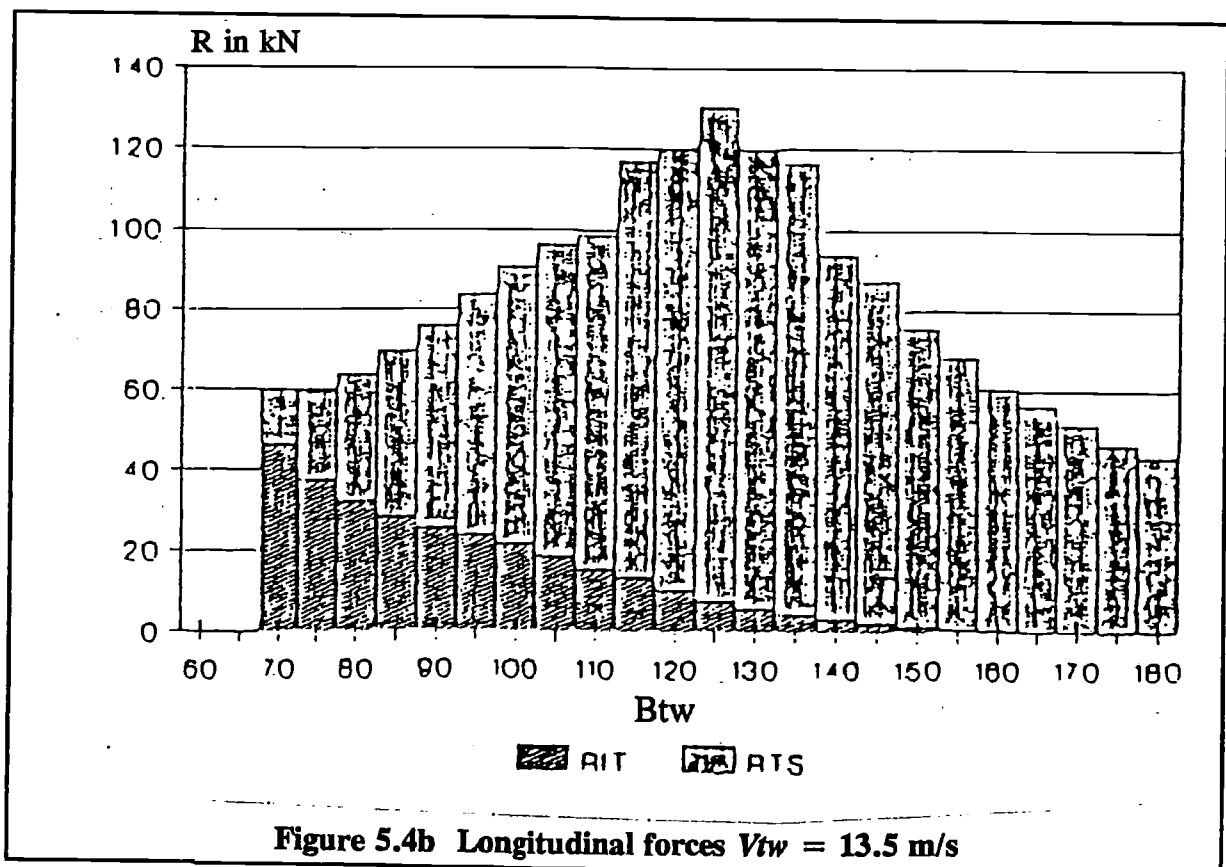
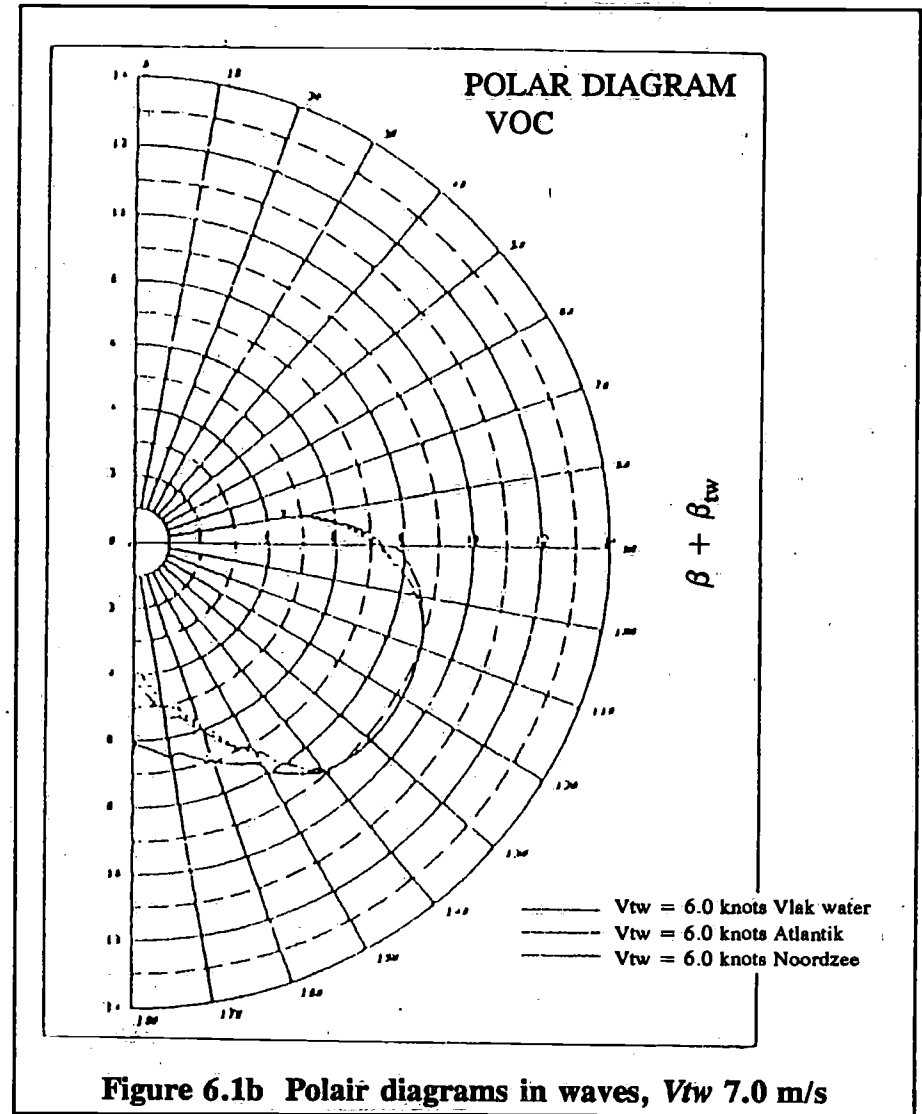
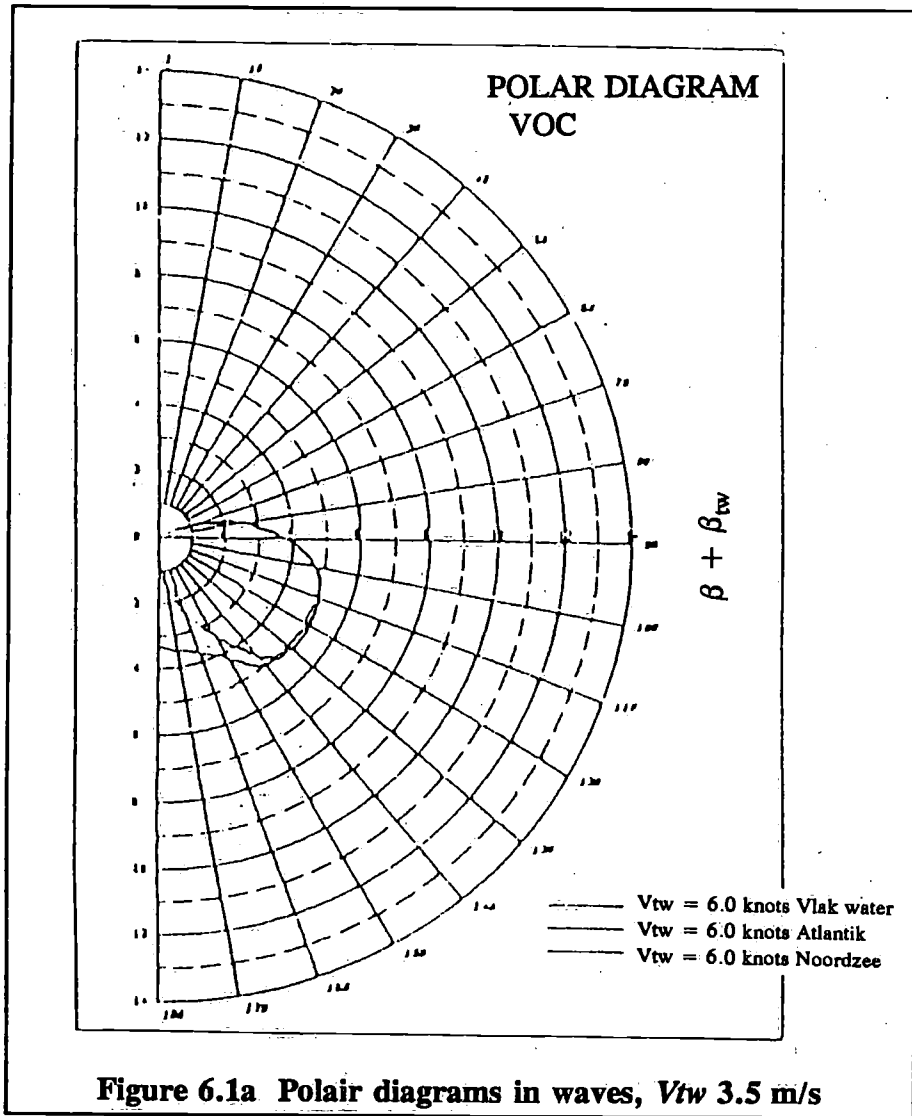
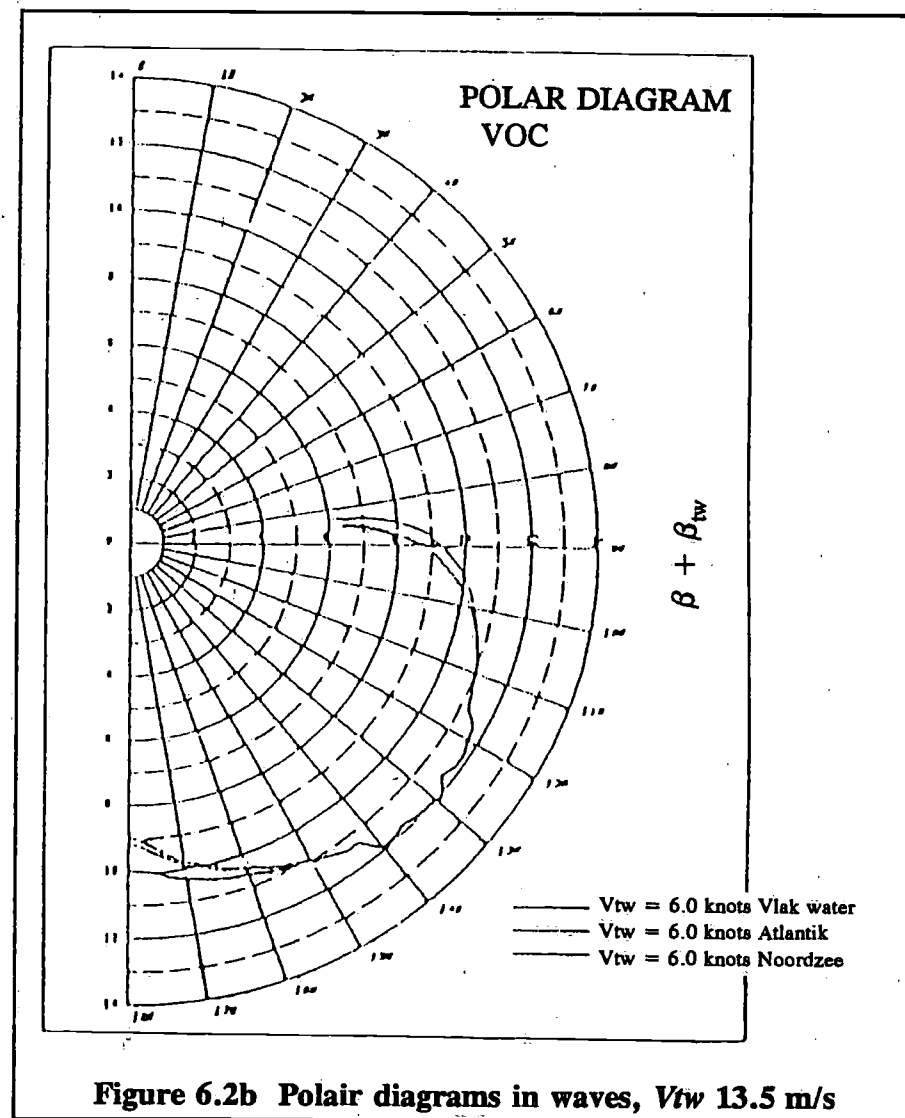
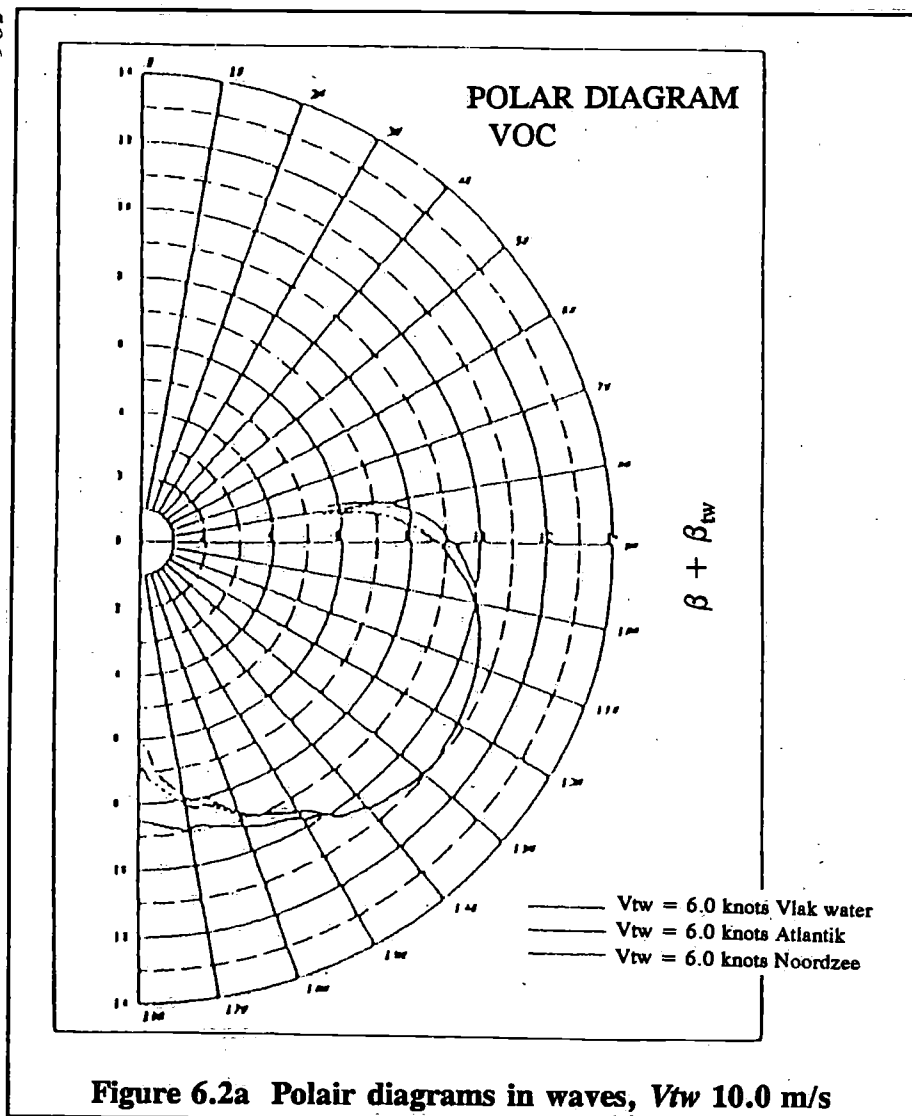


Figure 5.4b Longitudinal forces $V_{tw} = 13.5$ m/s





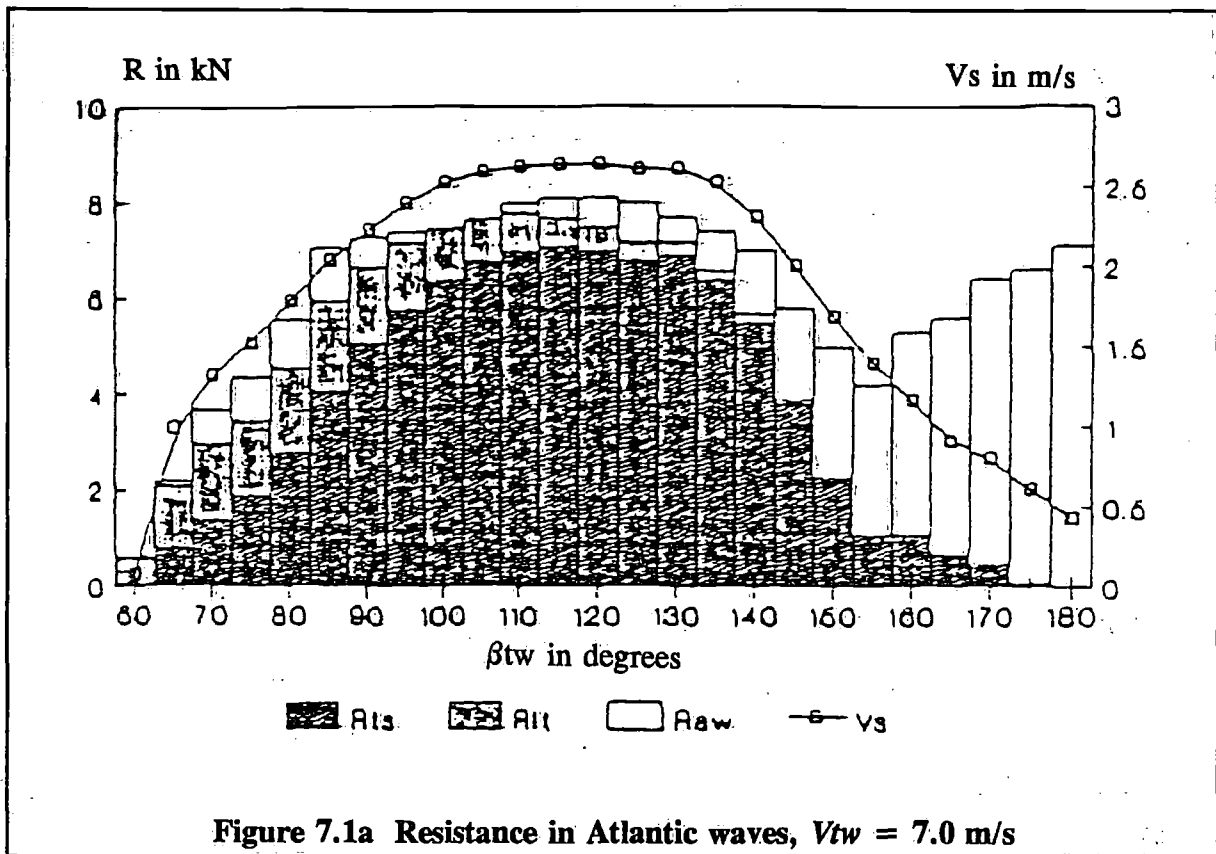


Figure 7.1a Resistance in Atlantic waves, $V_{tw} = 7.0$ m/s

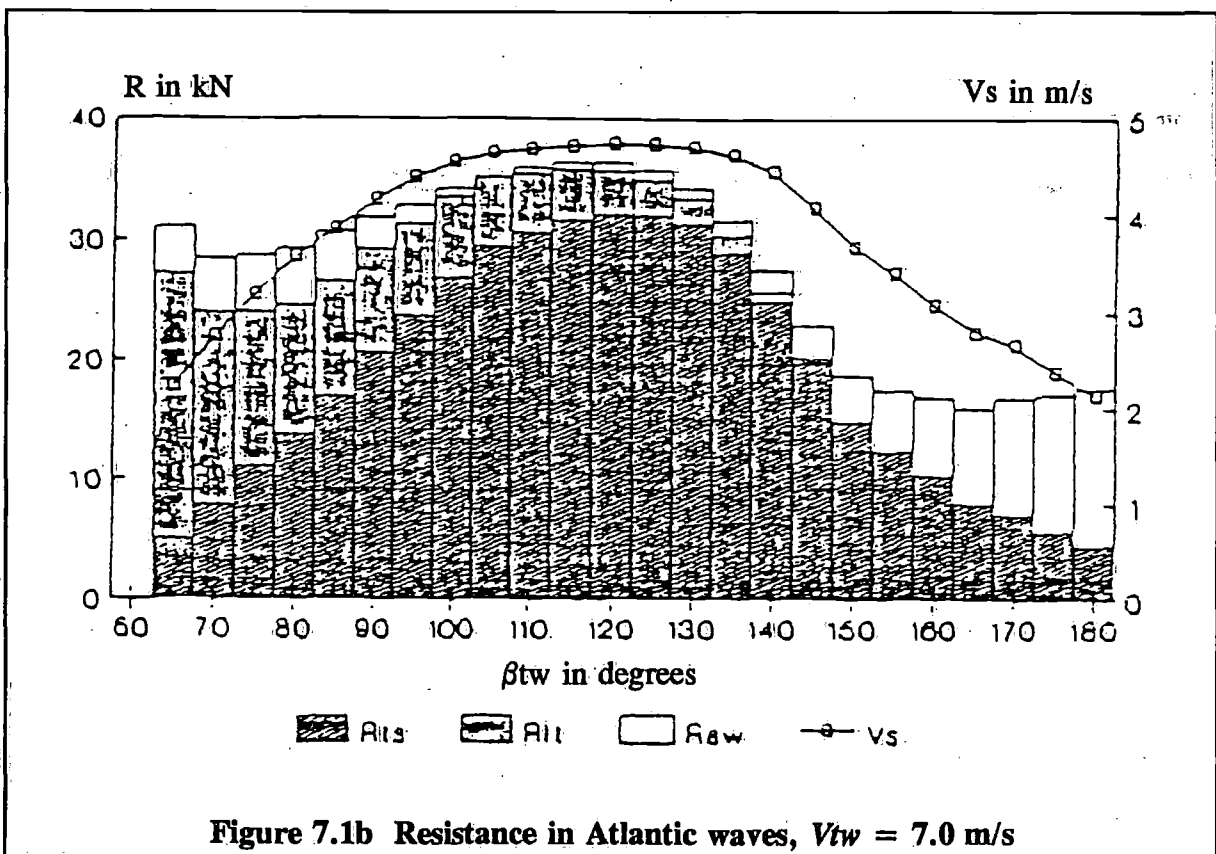


Figure 7.1b Resistance in Atlantic waves, $V_{tw} = 7.0$ m/s

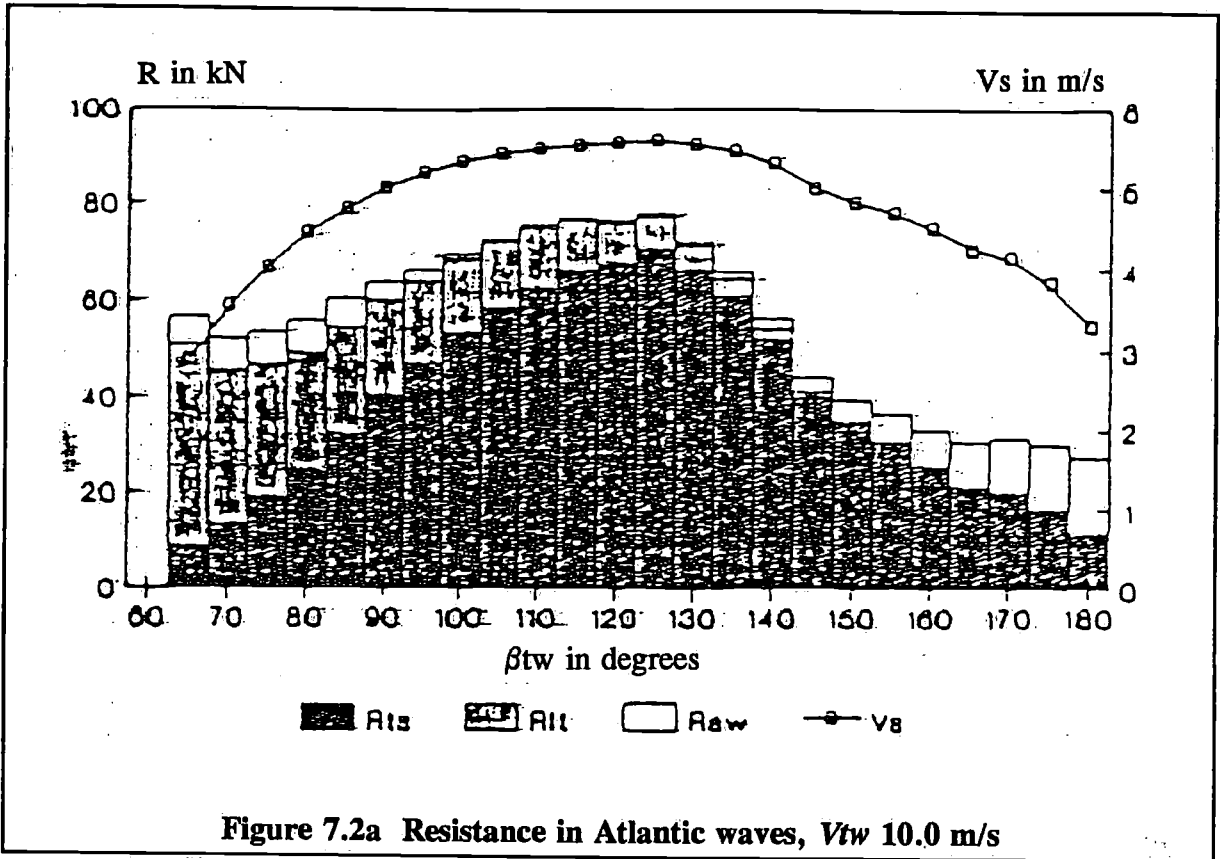


Figure 7.2a Resistance in Atlantic waves, V_{tw} 10.0 m/s

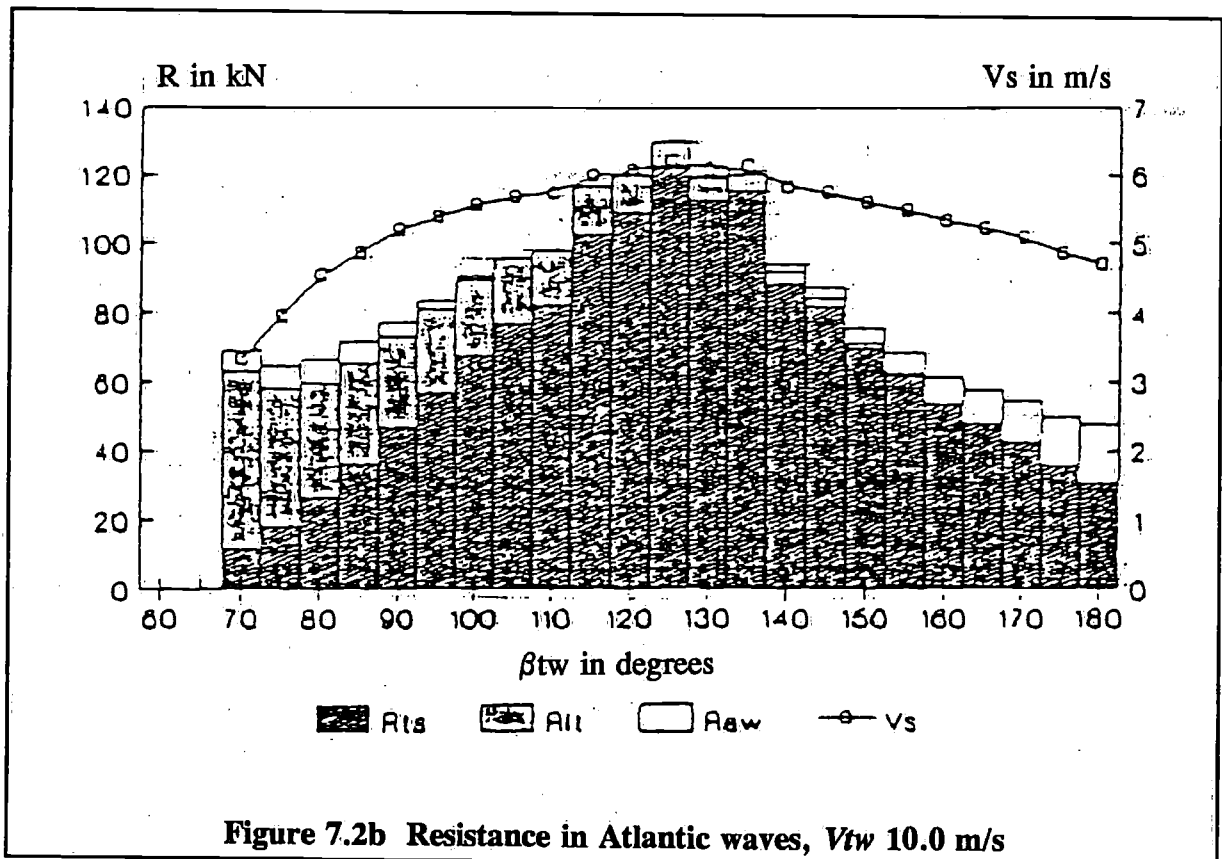


Figure 7.2b Resistance in Atlantic waves, V_{tw} 10.0 m/s

Rig load measurements and comparison with calculations

by P.J.Keuning and T.F.van der Werff

1 Introduction

On the HISWA symposium of 1988, a design methodology was outlined using Finite Element techniques (FE) as a tool for the rig designer [1]. The FE technique enables a simple static analysis of the rig response to the external loads.

This is of special interest for the required cross sectional properties of the mast, because the bending moments induced by the rig loads have to be taken into account for the determination of the collapse load of the mast.

It was pointed out in [1] that bending moments, and shroud forces, differ considerably for the different sailing conditions. So, instead of just one, several load conditions should be considered.

The distribution of the loads, imposed by the sails on the rig, were derived using as a benchmark the measurements as reported by Jacobs in the HISWA symposium of 1986 on a 10 m yacht [2].

It was felt that there was a definite need for more prototype measurement results. These are however difficult to perform.

The Hydronautical Department of the Delft University of Technology (DUT) has been able to perform two measurement campaigns, sponsored by Royal Huisman Shipyard at Vollenhoven and Ocean Sailing Development at Amsterdam. These have provided valuable data, which were made available to the authors for further analysis. The results from these measurements are presented in this paper and used to examine the rigloading.

For the yachts involved also calculations have been performed. Comparison will be made between the measurements and the performed calculations for these rigs.

2 The measurements

During the summer of 1989 two measurement campaigns were performed by the Hydronautical Department of the Delft University of Technology.

The first was on the sloop "YONDER", built by Royal Huisman Shipyard at Vollenhoven. The main objective of these measurements was to determine the loading on the rig in a wide variety of sailing conditions.

For this measurements the yacht was made available by the owner for a considerable time. As much signals were monitored as feasible.

The main particulars of "Yonder" are given below.

Length	: 19.0 m
Beam	: 5.2 m
Displacement	: 2.6E+05 kg
Righting moment	: 237600 Nm Maximum
Mast	: height : 24200 mm
	type : masthead rig
	spreaders : 2

Forces were measured by instrumenting the rigging screws with strain gauges. Because the yacht had discontinuous rods only the force in the D-2 wire could be measured this way. The value for V-2 was afterwards derived assuming force-equilibrium between the wires at the spreadertip. The mast itself was not instrumented with strain gauges, so no information on the bending stresses could be obtained. Of all force transducers and other signals time registrations were made. From these, statistical values were derived.

For two runs the compressive force in the mastfoot could be measured. All force-transducers were calibrated beforehand in the laboratory. After the measurement trials the transducers were again calibrated and checked for zero-drift. This was found to be minimal.

The second yacht instrumented was the well known J-class sloop "ENDEAVOUR". Measurements were performed during the acceptance trials after her restoration on the Royal Huisman Shipyard at Vollenhoven. For this reason the yacht was only available for a limited time, so a more comprehensive measurement campaign was performed.

The main particulars of the J-class yacht "ENDEAVOUR" are given below:

Length	: 140 feet
Beam	: 22 feet
Displacement	: 170.000 kg
Righting moment	: 1989000 Nm Maximum
Mast	: height : 48600 mm
	type : 7/8 rig
	spreaders : 3 plus diamond

Forces were measured in the same way as with "YONDER". Because the yacht also had discontinuous rods, again only the force in the D-2 wire could be measured. The value for V-2 was afterwards derived.

For all runs the compressive force in the mastfoot could be measured. The mast was not instrumented with strain gauges, so no information on the bending stresses could be obtained. All force-transducers were calibrated in the same way as described earlier.

3 "YONDER" results

3.1 Measurement results

The measurements took place spring 1989 on the North Sea from Scheveningen harbour. The wind conditions, ship-speed, apparent wind angle, sails set etc. for the different runs are given in Table 1. As can be seen a wide variety of conditions was investigated. During the weeks that the ship was available, light wind conditions prevailed.

The measurement results for the different runs are given in Table 2. Also given in Table 1 are the additionally measured ship roll and pitch motions.

Values given in the table are the statistical mean and the root mean square (RMS) deviation for the measurement period.

3.2 Determination of $P-t$

From these results the total force in the shrouds at deck-level, ($P-t$) was determined. Multiplied with the distance between the mast and the shroudplates it gives the moment in athwarths ship direction imposed on the rig. In order to determine $P-t$, the influence of the pretensioning of the wires has to be considered.

In calculating $P-t$ from the measured shroud forces distinction has to be made between the lee-ward shrouds slack or tight. If they are tight they contribute, due to their original pretension, to the forces counteracting the sailing loads, and thus in $P-t$. For this reason the determination of $P-t$ from of the measured shroud forces, has to be performed in two ways:

1 Slack lee shrouds.

The value $P-t$ is the summation of the forces in the windward shrouds only.

2 Tight lee shrouds.

The value $P-t$ is the difference between the original pretension in the shrouds and the measured force. The leeward shrouds also contribute.

3.3 Influence of pretension on the measured values

At first glance, the measured values for the wire forces seem to be quite erratic. Closer examination revealed that this was inherent to the measurement procedure used by the DUT. Total force values were presented including the pretension.

This pretension in the $D-1$, $V-1$ and $D-2$ wires was established before leaving harbour. Without the (possible) applied additional pretension on the longitudinal wires. Consequently, for the runs in which the tension in the backstay cylinder was increased, the measured total forces in the shrouds are lower than for the runs in which no additional pretension was applied.

The reason for this is that due to the additional pretension (and halliard tension) the compressive forces in the mast are considerable increased, relative to the condition as measured in the harbour. Due to this, axial deformation of the mast occurs, and a decrease of the pretension in the shrouds results. The absolute values for the wire forces have to be corrected for this effect.

Consequently, the $P-t$ values were determined dividing the runs in different groups as a function of the additional pretension applied and taking into account the influence of pretension in the shrouds as earlier mentioned.

This was found to be as accurate as performing the correction by subtracting the decrease in shroud tension by determining the compressive deformation of the mast due to this additional pretensioning. In this way the deformation of the yacht would be neglected.

The $P-t$ values determined in this way are presented in Figure 1. It appears that, post-processing the measured values in the above mentioned way, the results become quite consistent. The different conditions show the same relation between $P-t$ and the heel angle (ϕ). The transition zone between tight and slack lee-shrouds was found to be between 15-20 degrees heel. This corresponds well with the value derived from direct comparison of the pretension applied and the stability of the yacht. Using the results of Figure 1, the maximum $P-t$ value for the design condition is derived, and compared with the calculated values. The calculated values were found to be approx. 10-15 percent higher than the measured values. The cause for this difference could be that the stability of the yacht is less than the design target used in the calculations. Although a stability mismatch of this value seems quite high.

Table 1 "YONDER", measurement conditions

Run	AWA degrees	Vs knots	ϕ° degrees	$\theta_{..}$ degrees	Main	Jib	Remark
1	77	4.6	- 8.9/2.0	2.8	Yes	Yes	
2	60	5.8	11.2/2.5	1.5	Yes	No	
3	40	8	24.1/6.0	1.2	Yes	Yes	
4	40	8	24.2/5.1	1.5	Yes	Yes	
5	52	7.5	20.8/3.7	1.6	yes	No	
6	40	8.7	24.8/5.6	1.3	No	Yes	
8	20	6.3	0 /3.0	2.5	No	No	on motor
9	47	5.9	11.6/1.6	1.0	Yes	Yes	mastfoot: 260 kN
10	40	4.3	7.7/0.9	1.0	Yes	Yes	
11	-	3.9	5.7/0.9	1.0	Yes	Yes	mastfoot: 300 kN
13	30	4.6	6.9/0.9	0.9	Yes	Yes	
14	30	4.6	2.1/1.1	0.6	Yes	Yes	
15	90	3.3	- 5.9/1.5	0.7	Yes	No	spinnaker
16	33	5.2	13.9/1.0	1.0	Yes	Yes	
17	31	5.4	12.3/0.9	1.1	Yes	Yes	
18	31	5.2	-10 /0.9	0.5	Yes	Yes	
19	34	5.9	-16.1/2.5	2.7	No	Yes	
20	30	6.4	22.2/3.4	2.1	No	Yes	
21	25	5.8	21.3/3.3	2.0	Yes	Yes	
22	60	4.5	12.9/1.7	1.8	Yes	No	

* First value : mean heeling angle

Second value: root mean square deviation

** Root mean square deviation

Remark: negative heel angle means force transducers on leeward shrouds

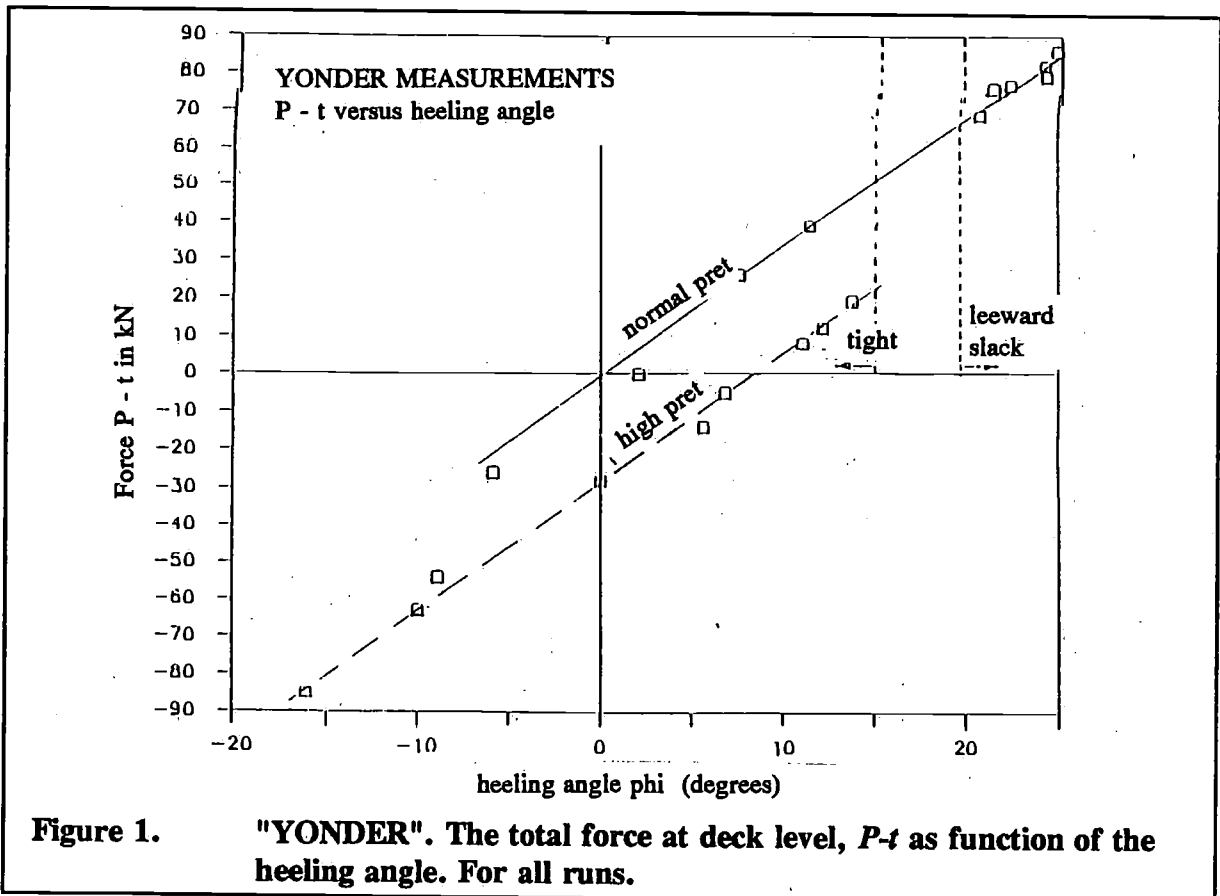
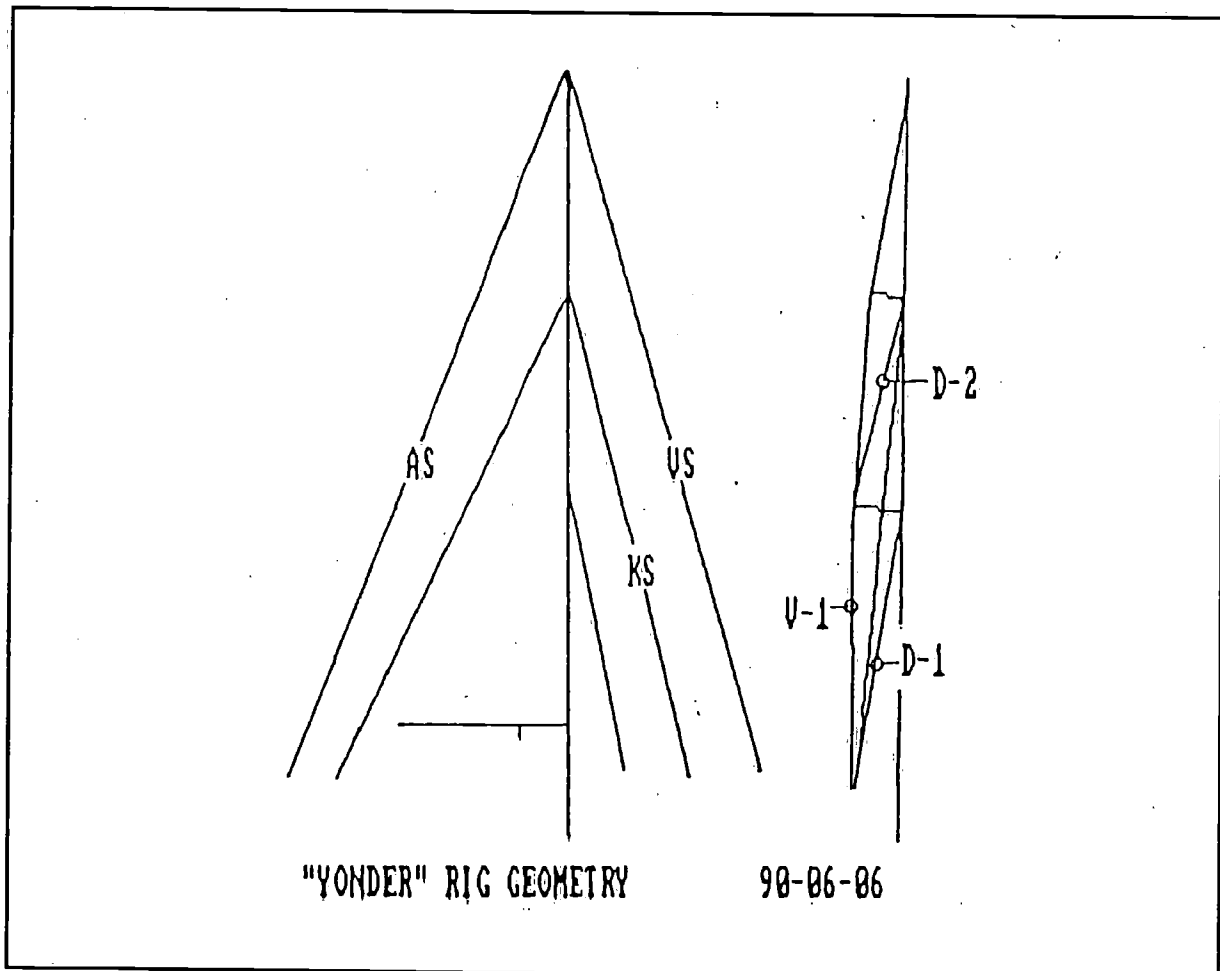


Table 2 "YONDER", measurement results

Run	V-1	D-1	D-2	VS	KS	AS
1	11.3/1.4	10.1/2.3	8.0/1.0	-	9.1	47.4
2	22.9/1.4	28.6/2.2	15.9/1.0	-	9.8	46.6
3	42.5/9.0	39.4/6.1	23.7/3.8	-	9.8	52.1
4	39.1/6.2	40.5/5.1	23.8/2.9	-	7.3	-
5	31.4/2.4	36.9/4.5	19.5/1.6	-	7.2	-
6	47.6/8.7	37.6/5.2	20.9/3.0	-	9.5	-
8	16.4/2.4	18.0/2.8	11.1/1.5	-	10.7	-
9	33.5/1.0	41.8/1.8	30.6/1.4	37.1	18.0	33.5
10	38.1/1.0	27.7/0.8	13.5/0.4	37.0	16.5	23.8
11	26.9/0.8	19.4/0.6	7.1/-	72.0	21.0	60.2
13	31.2/1.8	23.7/2.2	10.2/1.8	71.7	13.5	58.2
14	30.8/1.2	22.2/1.1	10.2/0.6	34.7	11.4	29.5
15	21.9/1.6	18.4/1.2	8.7/0.8	33.8	9.8	31.0
16	35.8/1.3	26.9/0.8	11.0/0.3	69.2	21.2	55.8
17	33.0/2.7	25.8/2.2	10.4/1.0	75.8	20.6	57.5
18	35.5/1.2	5.7/1.0	3.3/0.6	-	25.1	72.5
19	27.5/2.2	3.4/2.5	1.9/1.1	-	-	41.4
20	42.5/3.8	34.2/3.9	18.3/2.4	-	-	44.2
21	41.3/3.7	34.6/4.1	17.8/2.5	-	-	40.6
22	33.9/2.1	28.6/2.4	13.7/1.1	-	-	41.1

First value : mean value forces in kN
 Second value: root mean square deviation



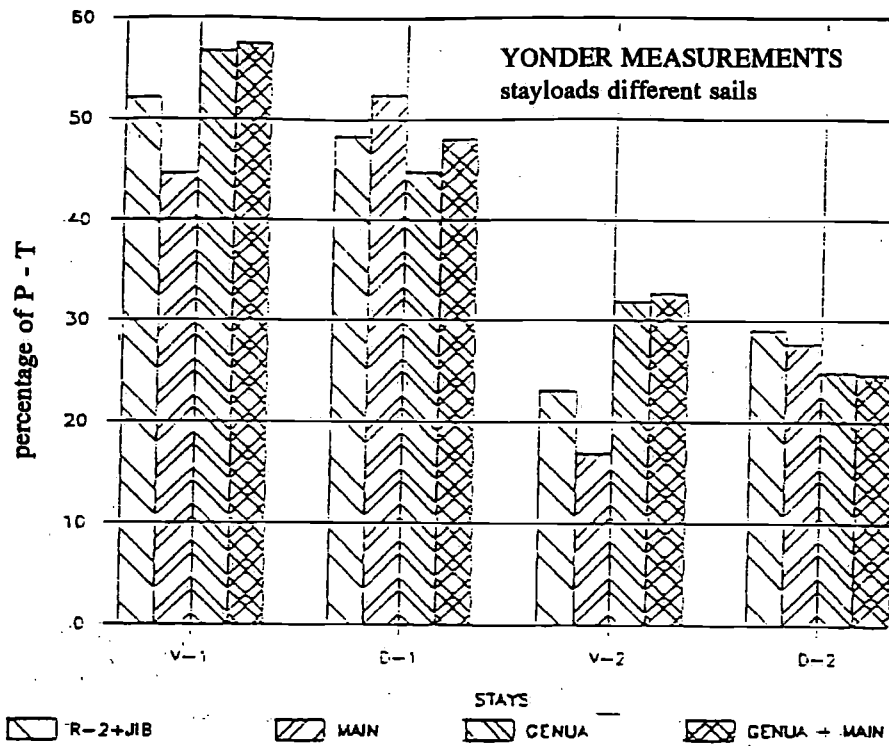


Figure 2. Distribution of the shroud forces for different sailing conditions. As function of *P-t*.

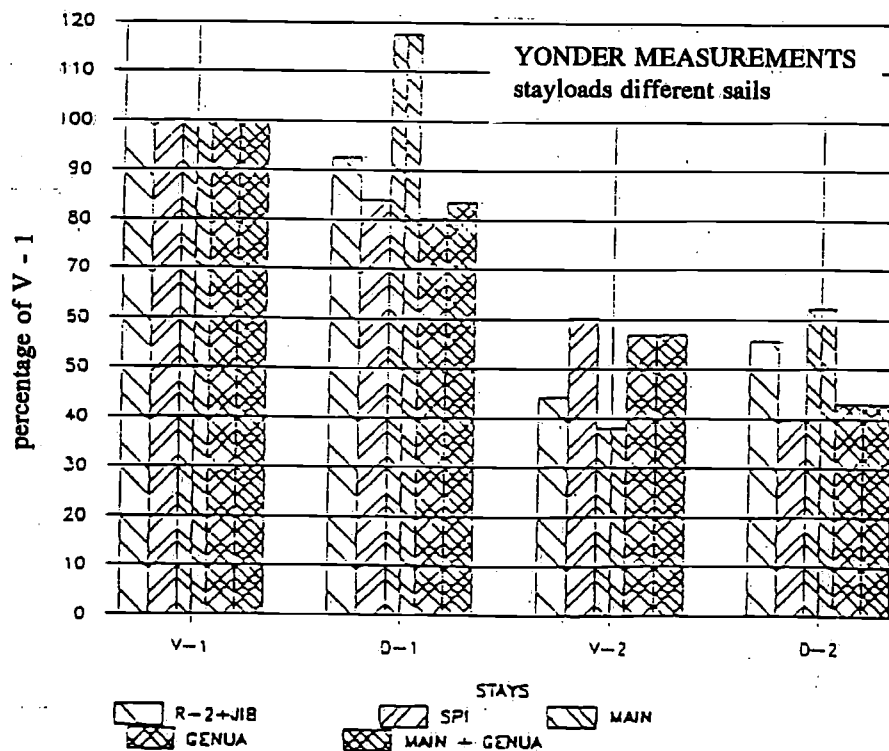


Figure 3. Distribution of the shroud forces for different sailing conditions. As function of *V-I*.

3.4 Distribution of forces in the wires

Influence sailing condition on rig loads. Several sail configurations were used during the trials. This enables the comparison of the loading imposed on the rig between the different configurations and sailing conditions. For the extrapolation of the wire loading for the ultimate load conditions, use has to be made from the runs with slack lee-shrouds (runs 3, 4, 5, 6, 20 and 21). All these runs were for upwind conditions. In Figures 2 and 3 the distribution over the shrouds is given relative to $P-t$ or the force in $V-1$.

As could be expected the "main only" condition gives the highest forces in the D -wires. Noteworthy is that only for this condition the highest force is not in the $V-1$ but in $D-1$ wire. With the "genua only" on the other hand the highest forces are found in the V -wires. This is logical because the loads of the sail are transferred to the rig only at the masttop. Surprisingly the "genua plus main" condition is very similar to the "genua only" condition. A possible explanation could be that the forces exerted by the main are primarily at the top of the sail and the distributed force along the length of the mast is very small for "YONDER" in this condition. Another explanation could be that the mainsail primarily enlarges the thrust of the genua. For the "reefed" condition the distribution reveals higher D -wire forces, caused by the mainsail load applied lower at the mast. The "spi" condition is very similar to the genua condition. With regard to establishing the design load for the different wires it is relevant to note that the variance in loads for the different measurement conditions can be as high as 30 percent of $P-t$. Consequently, calculating the loads for the full sail condition only will lead to an underestimation of forces especially in the D -wires. This is in close agreement with the findings in [1].

The distribution of the loads in $V-1$, $V-2$, $D-1$ and $D-2$ wire for the genua alone (run 20) and main alone (run 5) are compared with calculated results, using the sailload distribution as described in [1]. The results are given below:

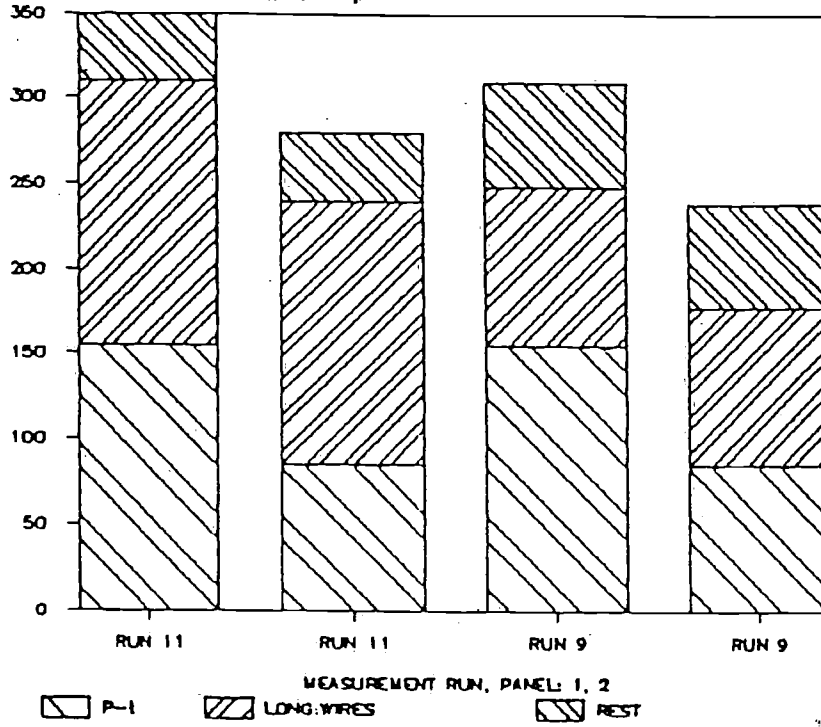
Forces as percentage of $P-t$			
		calculated %	measured %
Run 5	$V-1$	49	46
	$D-1$	51	54
	$V-2$	20	17
	$D-2$	29	29
Run 20	$V-1$	57	55
	$D-1$	31	32
	$V-2$	43	45
	$D-2$	27	24

The measured values correlate rather well with the calculation results.

With respect to the discussion in section 4.3, it is noted here that "YONDER" has a masthead rig and the mast has little prebend. At the "ENDEAVOUR" measurements a totally different mechanism was found. See section 4.3.

The load distribution, suggested in [1], for the combination of main and genua will not correlate with "YONDER" results. The contribution of the distributed load of the main along the length of the mast appears to be much smaller.

YONDER MEASUREMENTS
axial compression mast



ENDEAVOUR MEASUREMENTS
axial compression mast

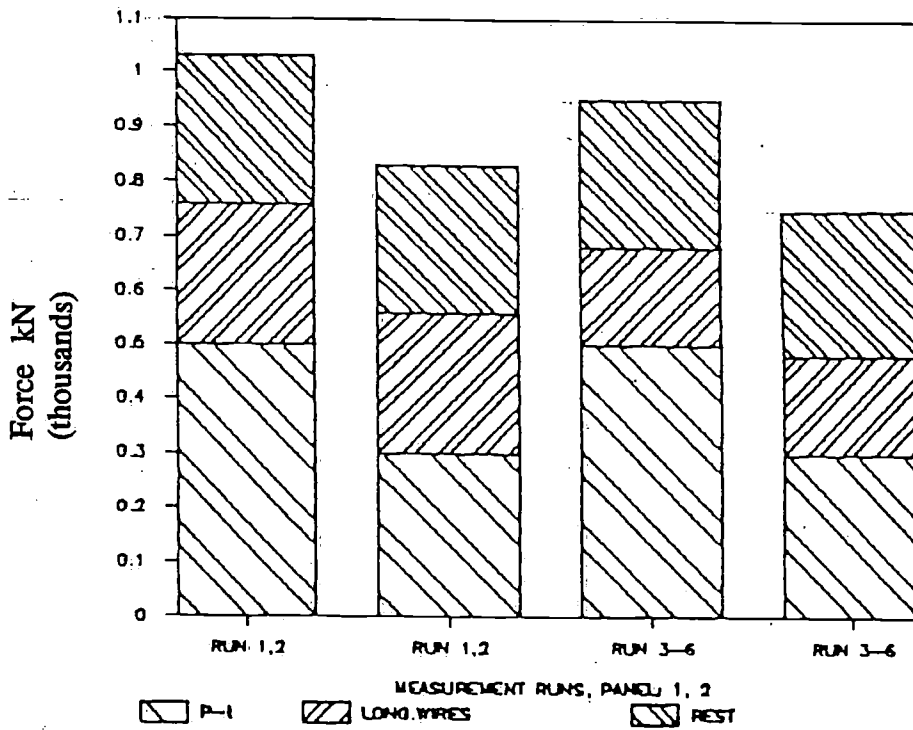


Figure 4. "YONDER" and "ENDEAVOUR". Axial compression at mastfoot for the different runs. For the 1- and 2-panel. Extrapolated to design condition.

The relative distribution of the *V-1* force between *V-2* and *D-2* is of particular importance for yachts with discontinuous rods at the spreader tip. The arrangement of the seatings for the rods in the spreadertip is such that minimal bending moments are introduced in the spreader. For this a load distribution between the wires has to be assumed. The measurements indicate however that this relative distribution can vary quite considerably. Based on this, even more extreme conditions can be formulated, for example:

- 1 Heavy reefed mainsail alone (or trysail).
For this condition the *V-2* wire will be lightly loaded.
- 2 Spinnaker broach.
For this condition the *V-2* wire will be much higher loaded than *D-2*.

Due to the unavoidable mismatch at the spreadertip, bending moments in the spreader will be introduced. The moments of inertia of the cross section of the spreader has to be designed to meet these bending moments in combination with buckling.

3.5 Compressive force in mast

Generally speaking, the total compressive force has three main contributions:

- a The force due to the loading caused by the heeling of the yacht, mainly associated with the load on the sails. So related to *P-t*.
- b The additional force:
 - b-1*: due to the pretension in the longitudinal shrouds.
 - b-2*: due to halliard tension, sheets etc.

Only for runs 11 and 9, data is available on the total compressive force in the mast at the mastfoot. The difference between both runs is the amount of backstay tension applied.

Using the values of run 11 (high pretension of the backstay), the contribution of part *a* and *b-1* can be determined directly. The remainder is considered to be part *b-2*.

Using the measured values for *D-1*, the subdivision in the axial compression can also be derived for the second panel of the mast. The relative contribution of parts *a* and *b* to the total axial compression in the mast is given in Figure 4 for the maximum heel condition.

As can be concluded from these measurements the contributions of parts *b* to the total compressive force are of the same order as the force introduced by the sail loads. For optimal rig design it is therefore important to quantify these additional forces with the same level of accuracy as the sail-induced forces.

A commonly accepted procedure is to use as the design condition the values for 30 degrees heel, multiplied by a certain safety factor, considered to be an allowance for dynamic effects in the loads. Allowance for the additional compressive forces is made by multiplying this value by approx. 2. This introduces however an additional (hidden) safety factor, caused by also enlarging the elements *b* of the compressive force, who have no relation to the loads imposed by the sails.

3.6 Dynamic loads

The dynamic loads in the shrouds for the different runs can be appreciated using the RMS deviation values for the forces, as given in Table 2. The 1 percent exceedance probability value for the force amplitude is approximately 3.3 times this value.

The dynamic loads are mainly associated with two effects:

- 1 The long term variation of the heeling angle due to wind velocity changes.
- 2 The motions of the ship with periods in the order of several seconds.

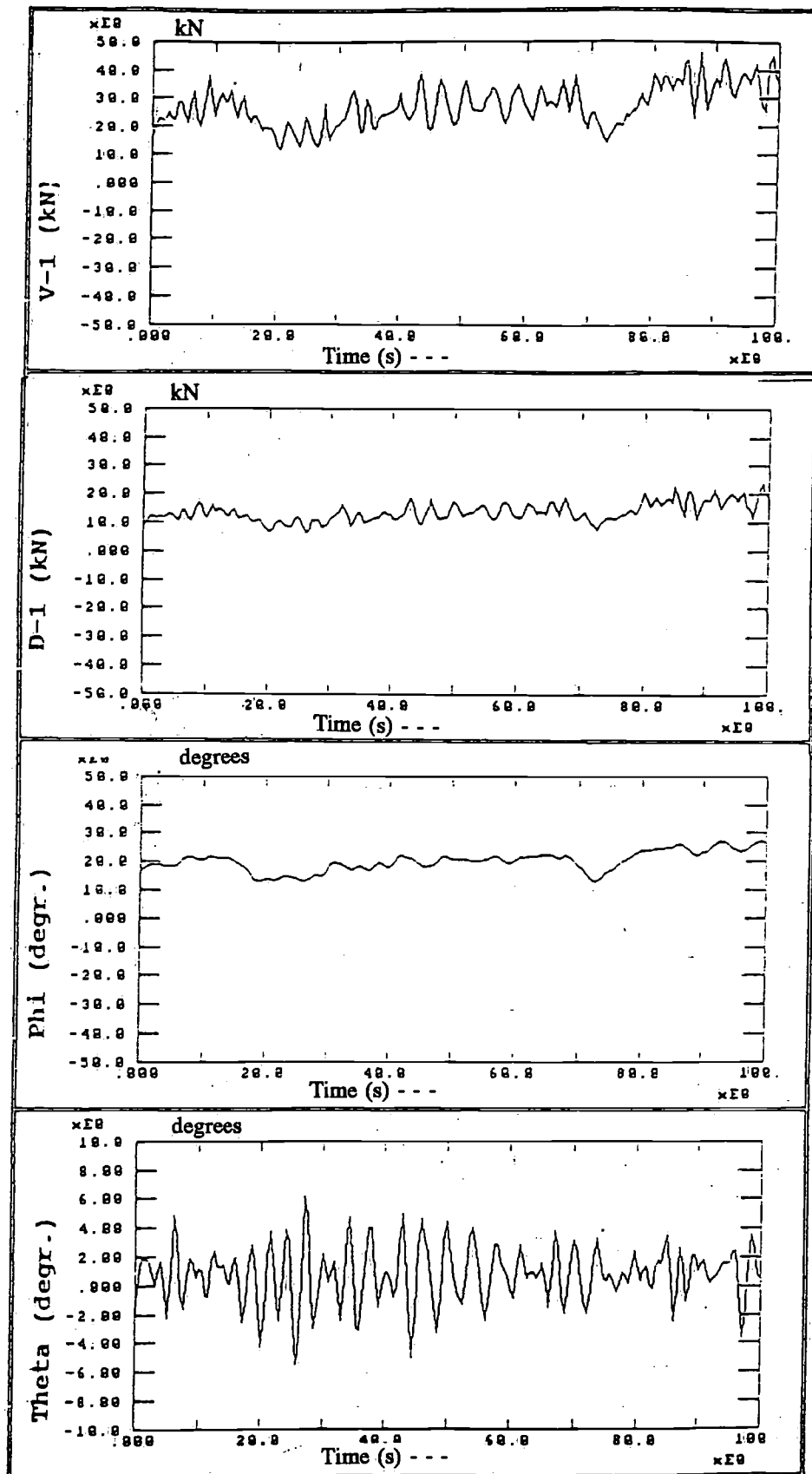


Figure 5. "YONDER". Run 20. Time signals for the shroud forces *D-I* and *V-I*, and the ship motions phi and theta.

The time signals for runs 3 and 20 of some of the force signals *V-1* and *D-1* are given in Figure 5 and 6, together with the simultaneous measured roll- and pitch-angles. Indeed, both types of variation can be observed in the time signals. The "low frequency" variation which corresponds closely with the same variation in the heeling angle caused by windstrength variation. The "high frequency" variation with a period in order of the motions of the ship is superimposed on the long term variation. Also the forces seem to correspond more with the roll motion and not so much with pitch.

Only the runs 1-8 and 19-22 were performed in a relevant amount of seaway, eg. significant waveheight of 1-2 metres. So these are used for establishing the dynamic loads. Assuming the time signals with both contributions still being a Gaussian process, the 1-percent exceedance force increase above the mean level is found to be:

- approx. 50 percent of the mean force in the wires for the upwind runs in sign. waveheight of 1.5 meter, reducing to approx. 35 percent for a waveheight of 1.0 m.
- for beam wave conditions this values are resp. 30 and 23 percent.

It is found that the dynamic loads for the runs without seaway are smaller but still of the same order of magnitude as for the runs in seaway.

Considering the dynamic loading primarily as a high cycle fatigue problem, these force fluctuations as occurring in the normal sailing conditions are of interest.

Considering the selected runs as normal sailing conditions, and taking the top-trough value of the force variations as the measure for the high-cycle fatigue loading, the fatigue loadings for "YONDER" during these runs are typical in the order of:

- approx. 30-40 kN for *V-1*.
- approx. 15-20 kN for *D-1*.
- approx. 10-15 kN for *D-2*.

Table 3 "ENDEAVOUR", measurement condition

Run	1	2	3	4	5	6
AWA	35	30	35	35	25	30
VAW(kn)	25	30	15	20	18	18
Vs (kn)	10.4	10.1	4.4	9.8*	9.6	10.0*
Main	No	No	Yes	Yes	Yes	Yes
Genua	No	No	No	No	No	No
Jib	Yes	Yes	No	No	Yes	Yes
Staysail	Yes	Yes	No	No	Yes	No
ϕ^{**}		10.7/12.6	7.7/1.3	14.0/1.3	18.7/1.6	
θ^{***}	13.8/2.1	0.15	1.6	1.5	1.3	17.0/2.2
	2.1					1.3

* with motor** first figure mean value*** root mean square deviation
second figure: root mean square deviation

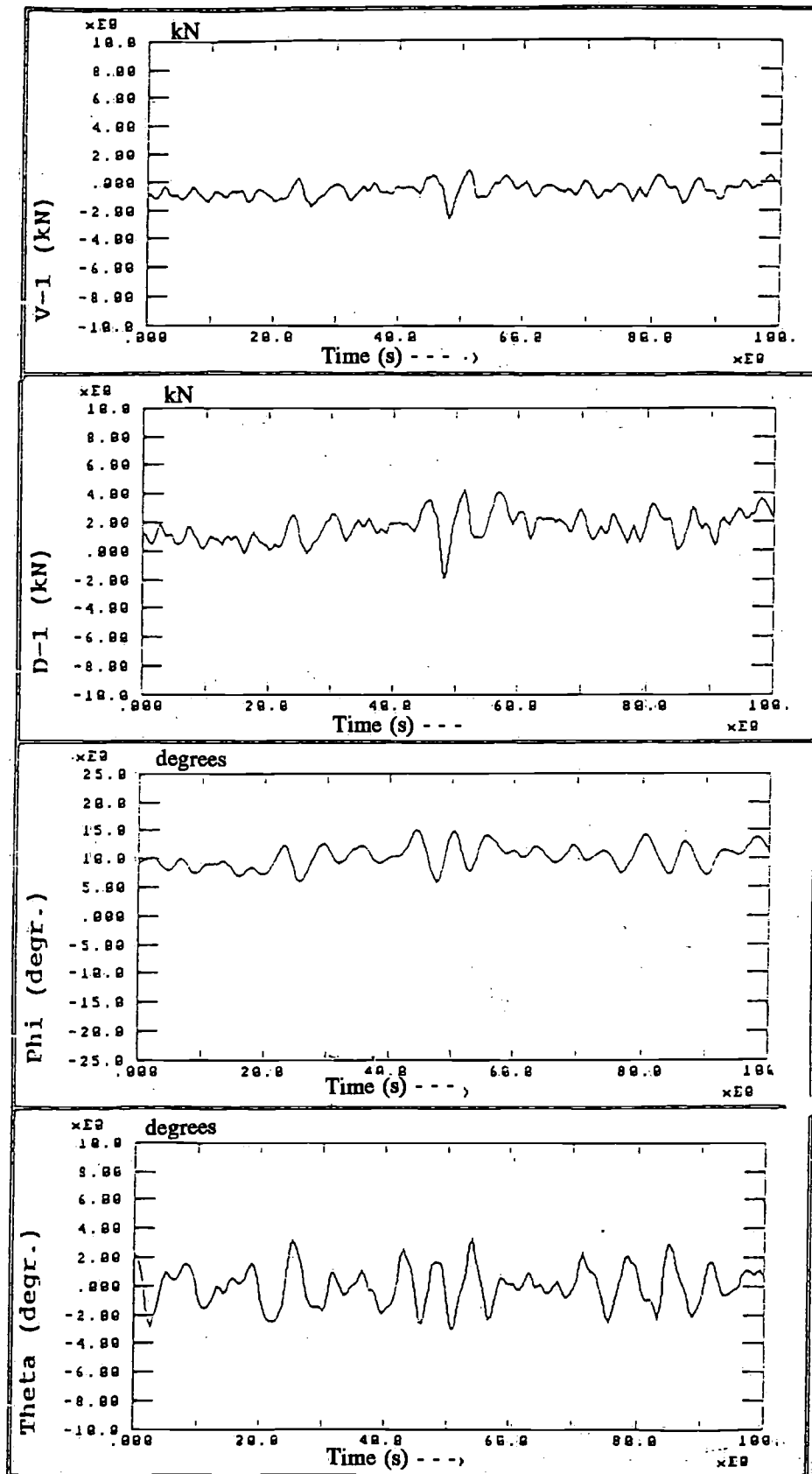


Figure 6. "YONDER". Run 3. Time signals for the shroud forces *D-I* and *V-I*, and the ship motions *Phi* and *Theta*.

4 "ENDEAVOUR" results

4.1 Measurement results

The measurements were performed during the acceptance trials in spring 1989 at the North Sea from Den Helder harbour. On two days measurements could be performed, in total 6 runs.

The wind conditions, ship-speed, apparent wind angle, sails set etc. for the different runs are given in Table 3. The measurement results for the different runs are given in Table 4. Also given in the table are the ship motions, additionally measured. Values given in the tables are the statistical mean and the root mean square deviation.

4.2 $P-t$ determination

From the measured shroud forces, the total vertical force at deck level, $P-t$, is calculated. The result is plotted against the heeling angle in Figure 7. A linear relation is found.

Using $P-t$ value, also the moment $M(\text{meas})$ as produced by the forces in the shrouds is known: $M(\text{meas}) = (P-t) \cdot (2920 \text{ mm})$.

The forces as measured in the shrouds are the combination of the counteracting of the external stability moment and the internal moment due to the weight of the rig. The latter is for this yacht estimated to be in the order of magnitude of 20 percent of the stability moment. The external moment is not only taken by the shrouds. Considering the moment equilibrium for the system at decklevel, the external moment is counteracted by the shroud forces, the horizontal reaction at the mastfoot and the bending moment in the mast at decklevel. For "ENDEAVOUR" the percentage of the moment taken by the shrouds was determined from the calculations and found to be approx. 90 percent.

The stability curve of the yacht, as used in the calculations is the maximum stability ($2.0\text{E}+06 \text{ Nm}$), which is reached at heeling angle $\phi = 57 \text{ degr}$. This is defined as $M(\text{stab})$. The stability curve of the yacht is linear up to 20 degrees. For ease of comparison between the measured and calculated results the heel angle (ϕ) at which this maximum stability value of $2.0\text{E}+06 \text{ Nm}$ is reached, extrapolating this linear relation (beyond this 20 degrees), was derived from the stability curve. This was found to be 35 degrees.

The moment $M(\text{meas})$ for all runs, corrected for the weight influence is determined, and extrapolated to the maximum stability. The ratio between this $M(\text{meas})$ and maximum stability of the yacht $M(\text{stab})$, as used in the rig design is determined:

$$C = M(\text{meas}) / M(\text{stab})$$

This results in the following C -values:

Run 1	: $C = 0.83$	
Run 2	: $C = 0.87$	
Run 4	: $C = 0.87$	Mean value 0.85
Run 5	: $C = 0.80$	
Run 6	: $C = 0.86$	

The values for the separate runs spread 7 percent.

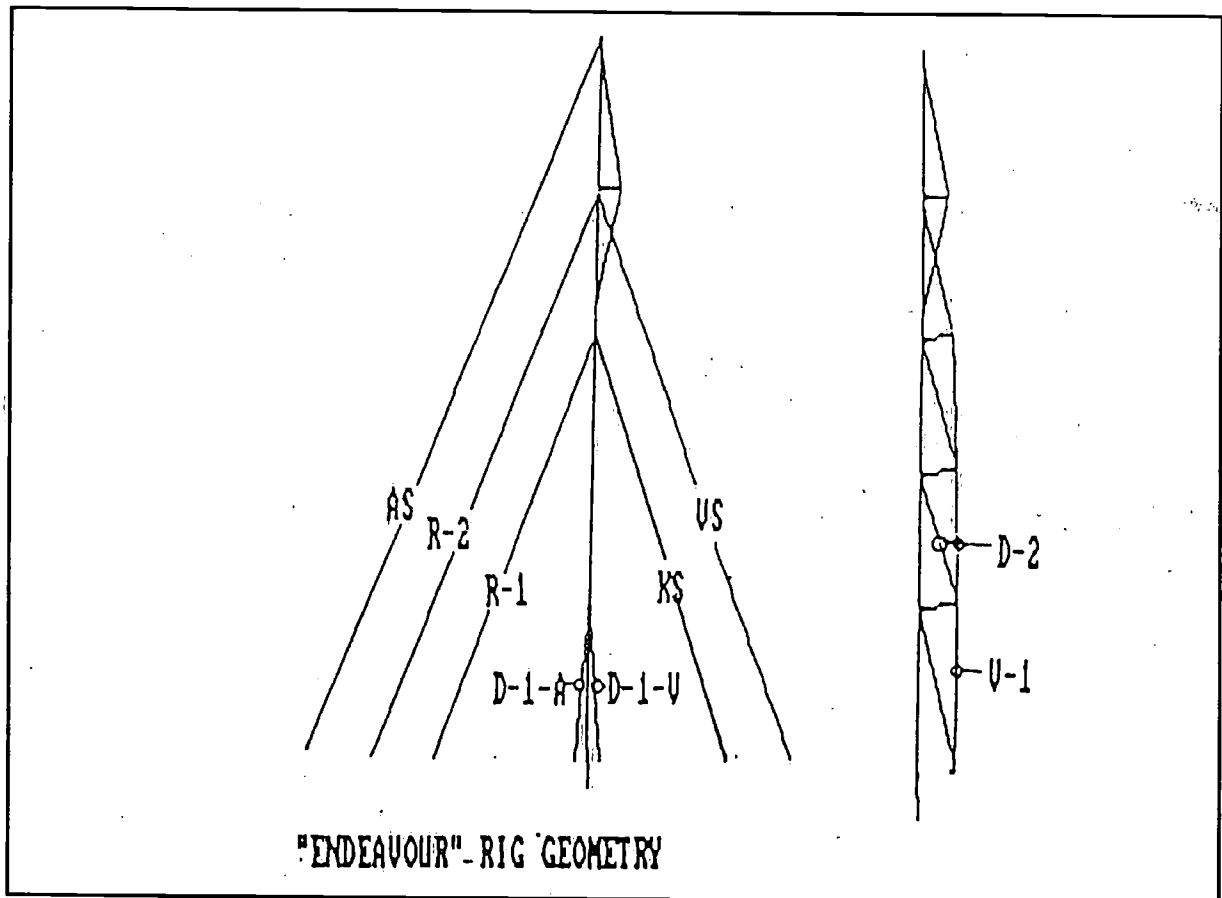
The mean C -value for the measurements is not 0.90 but 0.85. It must be concluded that the forces taken by the shrouds are lower than calculated.

An explanation could be a smaller stability of the yacht as build relative to the value used in the calculation. For the yacht as build no stability data were available.

Table 4 "ENDEAVOUR", measurement results

	Run					
	1	2	3	4	5	6
VS	98 / -	61 / -	70-90/ -	80-90/ -	90 / -	100 / -
KS	53 / -	65 / -	25 / -	27 / -	40 / -	20 / -
AS	13.9/ 1.4	12.5/ 1.6	10.3/ 1.6	9.3/ 1.4	9.8 / 1.5	10.4/ 1.6
V-1	186 /19	156 /22	119 /13	171 /16	220 /20	211 / 25
D-1-V	21.2/ 5.6	12.0/ 5.9	31.5/ 8.6	66.4/ 9.2	60.3/ 9.4	64.8/12
D-1-A	58.4/ 9.7	48.5/11	20.6/ 8.4	44.8/ 9.3	71.1/11	58.5/13
D-2	108 /19	85.3/22	54.4/22	106 /17	147 /20	128 /25
R-1	79.6/ 4.8	75.0/5.6	42.8/ 2.6	40.2/ 3.2	55.8/ 4.6	43.2/ 3.2
R-2	48.2/ 5.2	42.4/ 6.0	19.0/ 2.0	17.8/ 2.0	25 / 3.2	22 / 2.8

* first figure : mean value (kN)
 ** second figure : root mean square deviation (kN)



4.3 Distribution of the forces over the shrouds

The runs were performed with different sail geometries set. See Table 3.

This enables the comparison of the contribution of the forces over the different wires. Also the assumed load distribution as used in the calculations can be compared with the measured results. The comparison is made with the closest comparable calculation condition, e.g.: Full main, headsail #1 and headsail #2. (jib and staysail). The measurement runs closest to this are runs 5 and 6.

The results are given in Figure 8. From this figure it can be concluded that the calculated values for *V-1*, *D-1-A* and *D-1-V* correspond reasonably well with the measured values for runs 5 and 6. The results for *D-2* and *V-2* however differ considerably. The load transferred to the top via the *V-2* wire is apparently less than found in the calculations. The *D-2* wire appears to be more heavily loaded than the *V-2* wire, which is opposite to the calculation results. Several effects are causing this discrepancy:

- a The prebend of the mast. The calculations were performed for a straight mast. However, during the trials the mast had a considerable prebend, of approx 0.60-0.70 m. This has a great influence on the behaviour of the rig, as will be discussed in the following section.
- b In the calculations, a load distribution as suggested in [1] was used. For the mainsail this consists partly of a uniform load, which is supposed to have a linear distribution along the length of the mast. For the relevant runs this may be incorrect. The twist for this extremely large mainsail is more than the much smaller mainsail for which this linear distribution was derived from earlier measurements as best fit. Also the runs were performed with the assistance of the motor, enlarging the twist effect. A load distribution with more emphasis on the lower part of the main would result, which would lead to higher loads in the *D*-wires.

4.4 Influence of prebend

The mast of "ENDEAVOUR" had a substantial prebend during the trials. The influence of this on the behaviour of the rig is quite pronounced. The prebend in the mast is applied in combination with an adjustment of the spreader alignment. The shrouds are kept in line, in order to prevent the introduction of additional bending moments (and torsion) in the mast via the spreaders. This results in the creation of additional stiffness of the rig in longitudinal direction. At the same time also the load distribution over the shrouds changes.

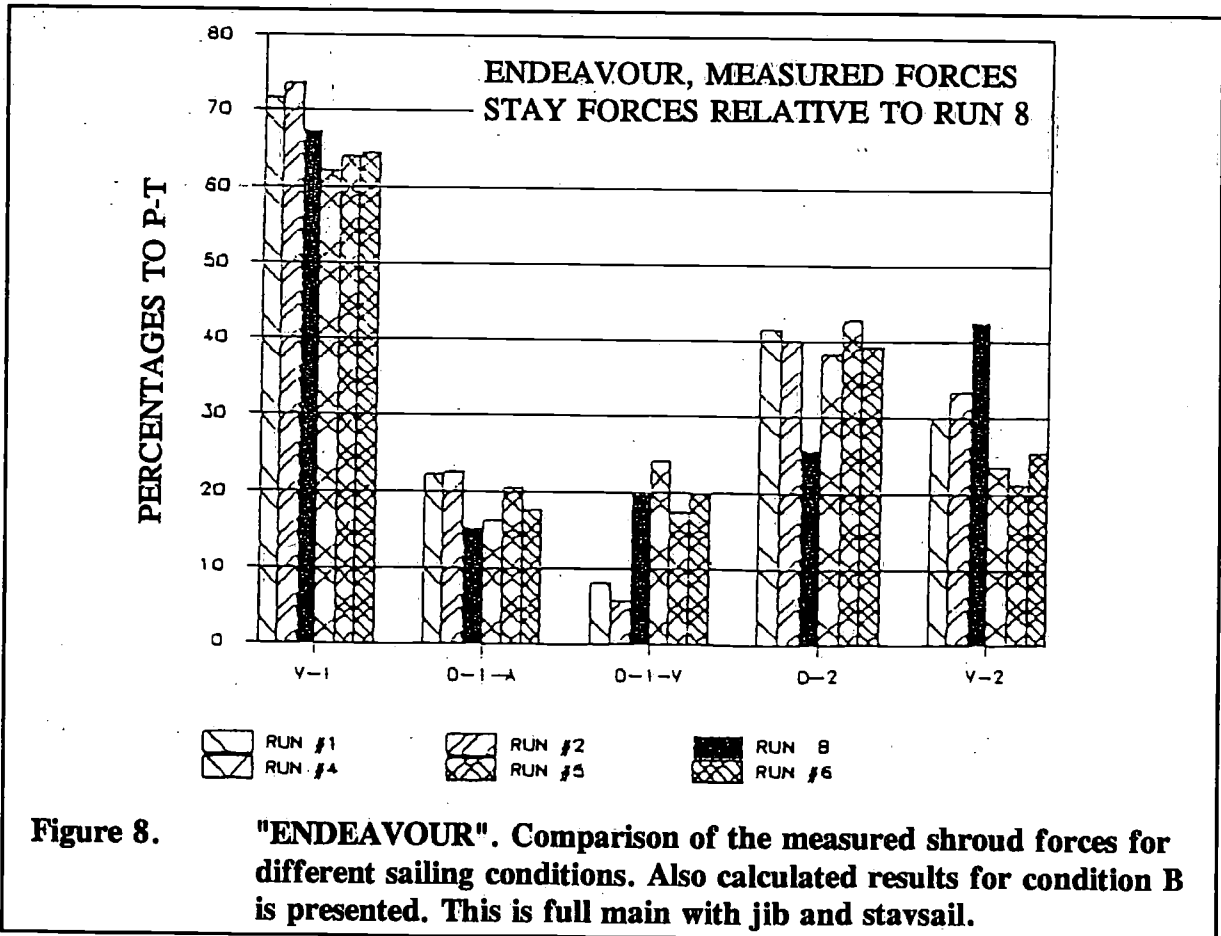
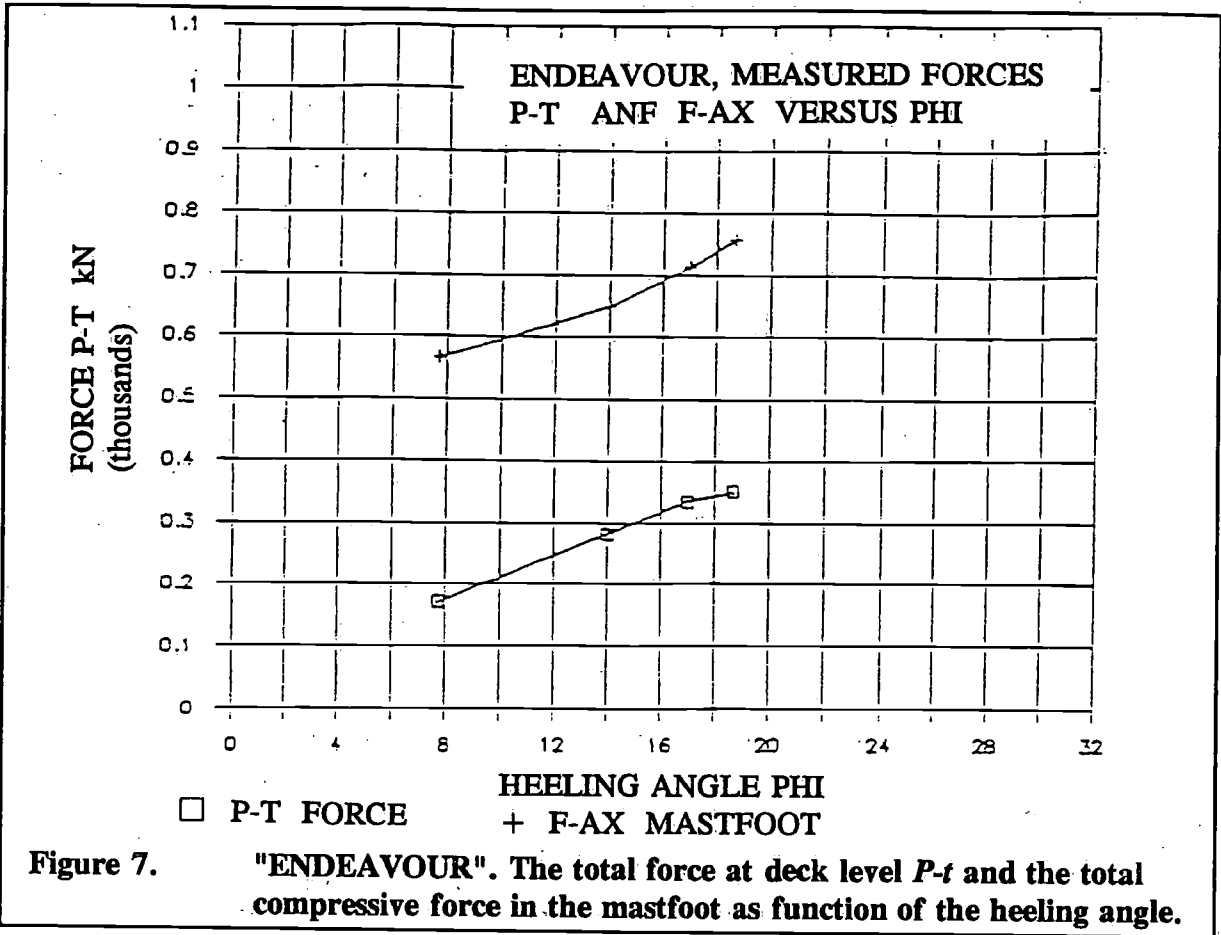
If a sail-load is applied in the masttop in athwartship direction, a compressive force in the mast is introduced. Due to the prebend the mast deforms in longitudinal direction under this compressive load. This longitudinal deformation is counteracted by the additional stiffness in the system introduced by this prebend. This enlarges the forces in the *D*-wires.

Giving a mast prebend produces a more stable system resulting in a higher collapse load in longitudinal direction. The bending of the prebended mast is increased due to compressive force, originating from:

- sailforce F_y
- additional compressive force due to:
pretension in longitudinal wires, halliards etc.

This principle was in an earlier stage already investigated on a simple single spreader rig geometry. The change in loading over the *D-1* and *V-1* wire, as function of the prebend, due to the sailing load in the masttop is given in Figure 9. The *D*-wires become heavier loaded, the *V*-wires less. The runs with "ENDEAVOUR" with genua only, clearly demonstrate this effect, especially for the *D-1* wires. The *D-1-V* shroud has very little load to carry.

For "ENDEAVOUR" being a $\frac{7}{8}$ -type rig, longitudinal deformation (bending) is also introduced by mainsail loads at the top of the mast. For $\frac{7}{8}$ rigs mainsail sheet tension tends to increase the bending of the mast. This also increases the loading in the *D*-wires additionally. This influence of prebend was also investigated for the "ENDEAVOUR" rig. It was found that all shrouds, and especially the *D-1* wires were influenced by the compressive force.



The mainsail effect is more pronounced in the *D-2* wires and higher. In Figure 9a some changes in load distribution over the shrouds are given as calculated. The tendency is confirmed by the calculations, the amount not. For the amount of prebend and mainsheet tension however estimated values were used.

4.5 Axial compression in the mast

The axial compressive force at the mastfoot is given in Figure 10. The measured values are divided in two groups. This subdivision is necessary because on the two days a different amount of pretension in the longitudinal wires was applied. The results of runs 3, 4, 5 and 6 are best applicable. From this figure it can be observed that:

- a The relation with the heeling angle is linear.
This indicates that the pretension in the shrouds was small indeed.
- b By extrapolation, the compression at zero heeling angle is 450 kN. This is however only valid if no pretension is assumed.
- c By extrapolation, the compression at max. stability, 2.0E+09 Nmm is 950 kN.

The 450 kN at zero heeling angle correspond to part b as formulated in paragraph 3.5.

So, the increase in axial compression due to the sailing loads is approx. 500 kN. The calculated value was 480 kN, which is in reasonable agreement.

The higher pretension in runs 1 and 2 result in a maximum compressive force of 1100 kN. The contribution of the different elements in the compressive force, as earlier described in chapter 3.5 are also given for the two lower panels of "ENDEAVOUR" in Figure 4. The same conclusions as given for "YONDER" also apply for "ENDEAVOUR". The additional elements contributing to the total compressive force have to be determined with the same accuracy as the loads due to the sails. In dimensioning the mast, a total compressive force of 1100 kN was used, consisting of 500 kN due to sailloads and 600 kN due to the additional forces (part b) pretensioning, halliard tension, weight of the mast etc.

The contribution due to pretension of the longitudinal wires is approx. 20 kN for runs 3-6 and 30 kN for runs 1-2. Relating this to Figure 4, the contribution of part b 2 is quite substantial for this yacht.

4.6 Dynamic loading on the rig

The root mean square deviation of the forces is given in Figure 11. They vary between 10 and 20 percent of the mean value. The 1 percent exceedance probability value for the force amplitude is approximately 3.3 times this value.

Results are omitted if they were considered unreliable. This holds for run 3, *D-1-A* and *D-2* and run 2, *D-1-V*.

As earlier mentioned the variation in the forces has two distinct contributions, one associated with fluctuation in windstrength and one associated with the yachts motion, mainly roll.

Any relation with regard to the yachts motion in seaway is small, which is not surprising, considering the seastates during the trials and the size of the yacht. So the measurements give no relevant information about the dynamic loading to be encountered by the yacht. The *D*-wires seem to be higher loaded than the *V*-wires. This indicates dynamic loading to be associated with the mass of the rig.

4.7 Buckling of Endeavour mast

Because the usage of the yacht differs from her original one, now being cruising orientated, the original mast cross sectional properties could not be used.

The design of the new rig for "ENDEAVOUR" after her restoration is by Ocean Sailing

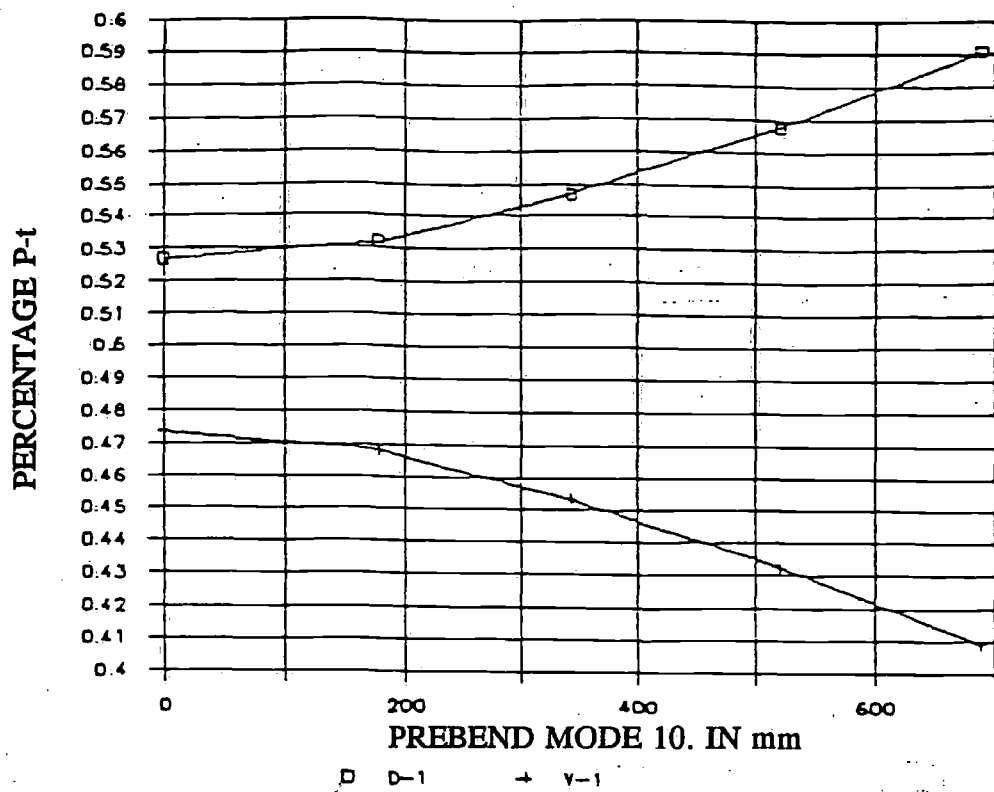


Figure 9. Influence prebend on distribution of forces in D-1 and V-1 shroudes. Shroud forces as percentage of P-t.

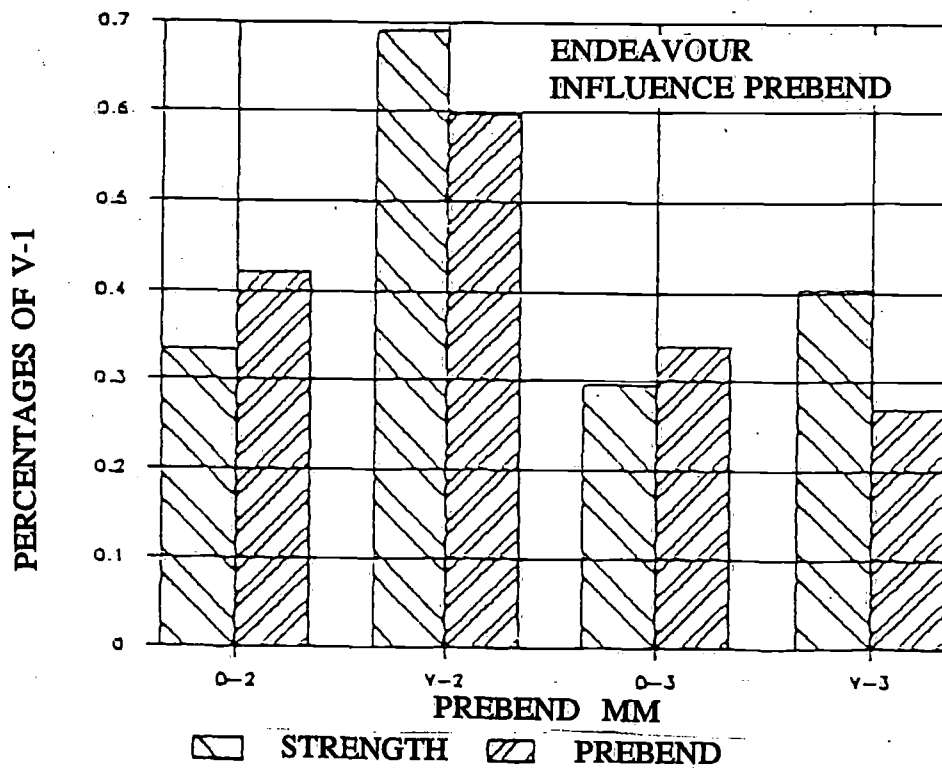


Figure 9a. "ENDEAVOUR". influence of prebend on the distribution of the forces over the D- and V-shrouds.

Development, Holland. In establishing the new cross sectional properties, special attention was paid to the buckling stability in longitudinal direction.

The calculations showed that the lowest buckling mode is in longitudinal direction in the lowest panel (section between deck and inner fore-stay). In this panel also high bending moments are introduced due to the forces exerted by the spi-pole and mainsail boom.

So in order to optimize the mast section modulus the (beneficial) influence of the double *D-1* shrouds on the longitudinal buckling mode was investigated. Beneficial because the angle between the shrouds and the mast introduces an additional stiffness in longitudinal direction. This was investigated by performing a *FE* linear buckling analysis for the whole system.

For the angle of 5 degrees the buckling mode is shown in Figure 12. It can be observed that the additional stiffness changes the buckling mode. The increase of the buckling load as function of this angle is given in Figure 13. For the "ENDEAVOUR" geometry (5 degrees) the increase is approx. 25 percent.

Using this as input, the collapse load of the mast can be determined using the well known formula: $(N / N_{cr}) + (M / M_{cr}) \cdot (1 / (1 - (N / N_{cr}))) < (1 / S.F.)$

In which *N* and *M* are the axial compression and bending moment for each cross section. The *N_{cr}* and *M_{cr}* are the critical buckling load and bending moment respectively. *S.F* is the safety factor. For the compressive force in the mast, the values as extrapolated from the measurements were used. Bending moments were not measured, so calculated values had to be used. As explained earlier in [1], the amount of pretension in the shrouds is of importance when determining these bending stresses in the mast. It is assumed here that the pretension in the shrouds was small. The bending moments introduced by the prebend was taken into account. Using these data, the safety factor for collapse in longitudinal direction was found to have a minimum value of 1.6, all conditions considered.

The buckling mode in athwartship direction is also shown in Figure 13. In athwartship direction the safety factor for collapse is determined in the same way. This was found to have a minimum value of 2.0, for the lowest panel. This is higher than in longitudinal direction. The panels 2 and 3 showed higher safety factors. The cause for this is explained below.

For panel 1, between deck and first spreader, the cross sectional values are increased relative to the other panels, in allowance for the high loads due to spi-pole and mainsail boom.

At first, in normal panel design, the critical buckling loads of the panels were determined for the panels separately. No interaction with the adjacent panels has been considered. This interaction is small indeed if all panels are designed for the same buckling load. If however one of the panels differs considerably from this, the assumed boundary condition for the separate beams being simply supported is no longer valid. A rotational stiffness is introduced. This increases the critical buckling load. This effect can only be quantified if a buckling analysis for the whole system is performed. This calculation confirmed the increased buckling loads for the other panels. So the increased cross section for panel 1 results to an increase in buckling load for the panels 2, 3 and 4. An increase of the *S.F.* for these panels results.

5 Conclusions

Full scale measurements on rig loading on sailing yachts are difficult to organize. Measuring shroud forces by instrumenting the standard turning screws with strain gauges gives the least interference and proved to give reliable results. However instrumenting the mast itself with strain gauges is very difficult to arrange. So prototype information on bending moments will remain scarce. This hampers the verification of the calculated collapse loads of masts.

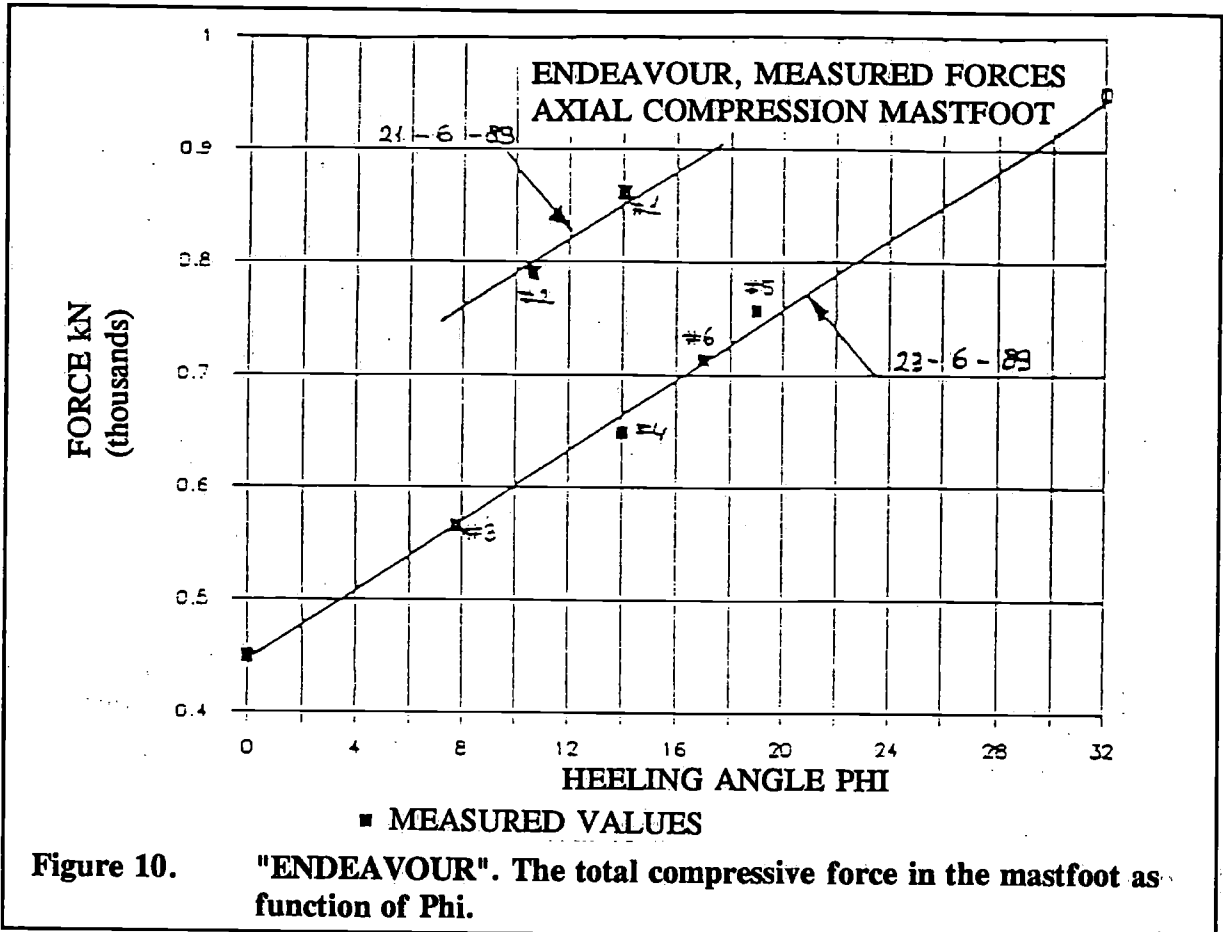


Figure 10. "ENDEAVOUR". The total compressive force in the mastfoot as a function of Phi.

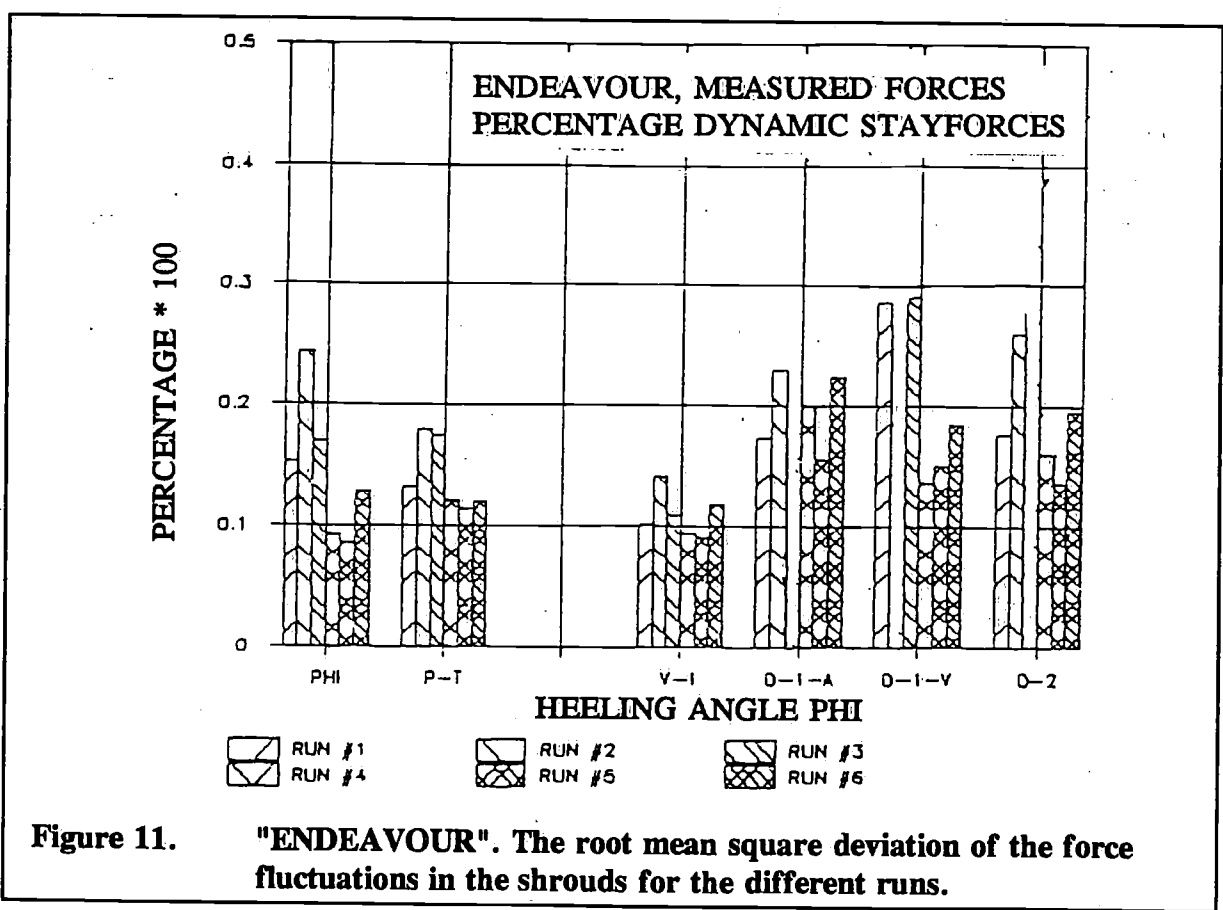


Figure 11. "ENDEAVOUR". The root mean square deviation of the force fluctuations in the shrouds for the different runs.

For both yachts the $P-t$ value as function of the heeling angle, as calculated using target stability values, was higher than derived from the measurements. However, the actual stability properties of the yachts was not established during the measurement campaigns.

The distribution of the shroud forces varies considerably between the different sailing condition and sail configuration. The load distribution on the rig by the separate sails, as proposed in [1], proved to be satisfactory for the masthead rig. The "main plus genua" sail configuration measurement results proved to be different than proposed.

For "ENDEAVOUR" the load distribution differed considerably with the calculations, especially for the $D-2$ and $V-2$ wires. It was found that the prebend of the mast, which was not in the original calculation model, had a considerable influence. The incorporation of all its, non linear, effects is however complicated.

The compression of the mast correlated with the values used in the calculations. It is important to estimate the additional compressive force due to pretension, halliards etc. with the same accuracy as the contribution due to the load imposed by the sails.

Dynamic forces for "ENDEAVOUR" appear to be not relevant, due to the light wave conditions during the measurements. The load increase due to dynamic effects, as measured for "YONDER" are smaller than the results from earlier measurements on a 10 m yacht.

It proved for "ENDEAVOUR" that a buckling analysis for the whole rig system is necessary for accurate rig design. If the geometry of the rig is complicated these kind of calculations have to be considered.

List of Symbols

AWA	aparent wind angle (degrees)
VAW	aparent wind speed (knots)
V_s	ship speed (knots)
ϕ	heeling angle (degrees)
θ	pitch angle (degrees)
$P-t$	total vertical force in shrouds at decklevel (kN)
$F-ax$	axial compressive force in mast (kN)
$V-1$	main shroud (kN)
$V-2$	intermediate shroud (kN)
$D-1$	lower diagonal shroud (kN)
$D-2$	intermediate diagonal shroud (kN)
$RMS(dev.)$	root mean square deviation
VS	headstay (kN)
AS	backstay (kN)
$R-1$	upper runner (kN)
$R-2$	lower runner (kN)
KS	cutterstay (kN)
N	compression force (kN)
M	bending moment (kNm)

List of References

- [1] Werff, T.F.van der and P.J.Keuning, "Strength and stiffness of rigs", 10-th International symposium Yacht Architecture, March 1988, Amsterdam.
- [2] Jacobs, F.A., "Some applications of aeronautical engineering in the construction of yachts", 8-th International HISWA symposium, November 1983, Amsterdam.

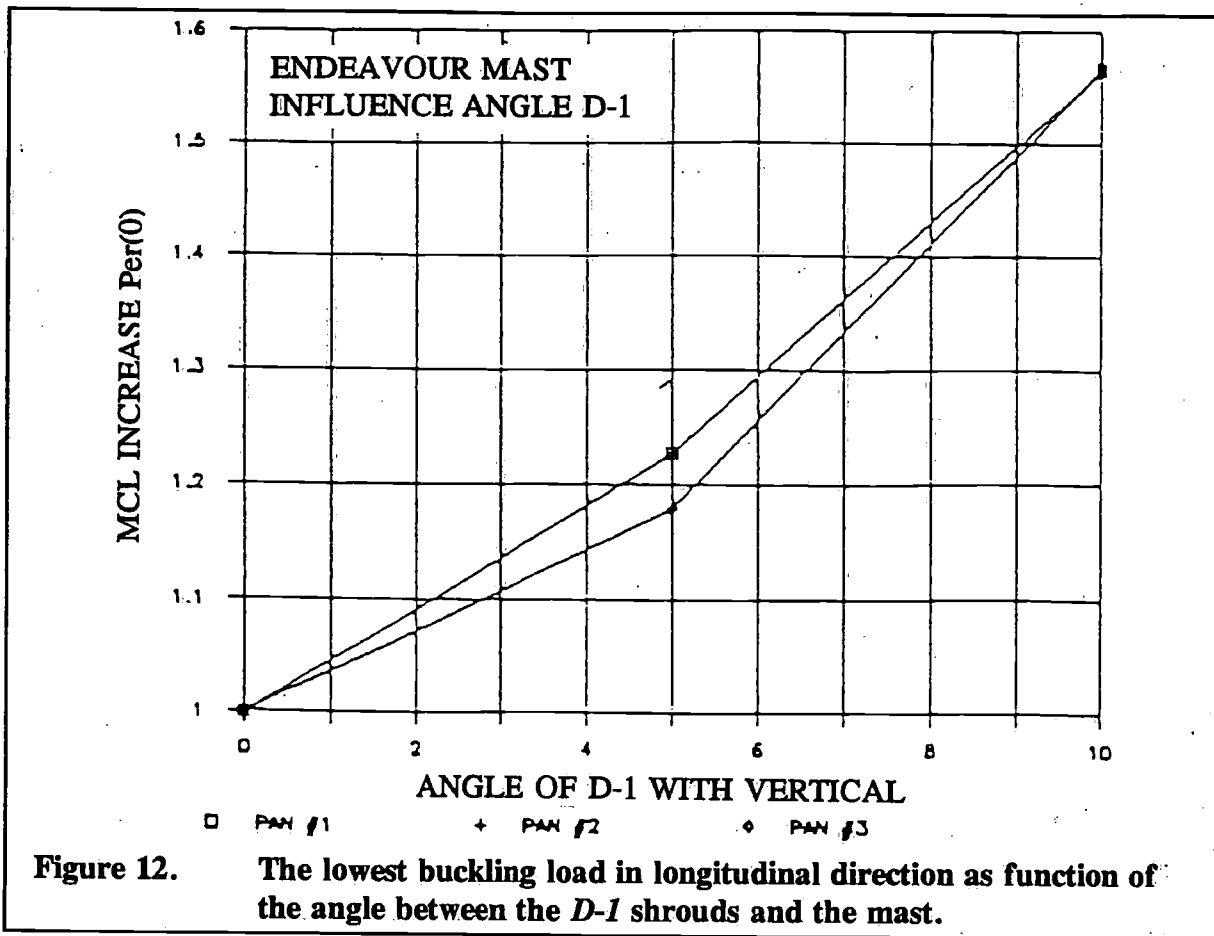


Figure 12. The lowest buckling load in longitudinal direction as function of the angle between the *D-1* shrouds and the mast.

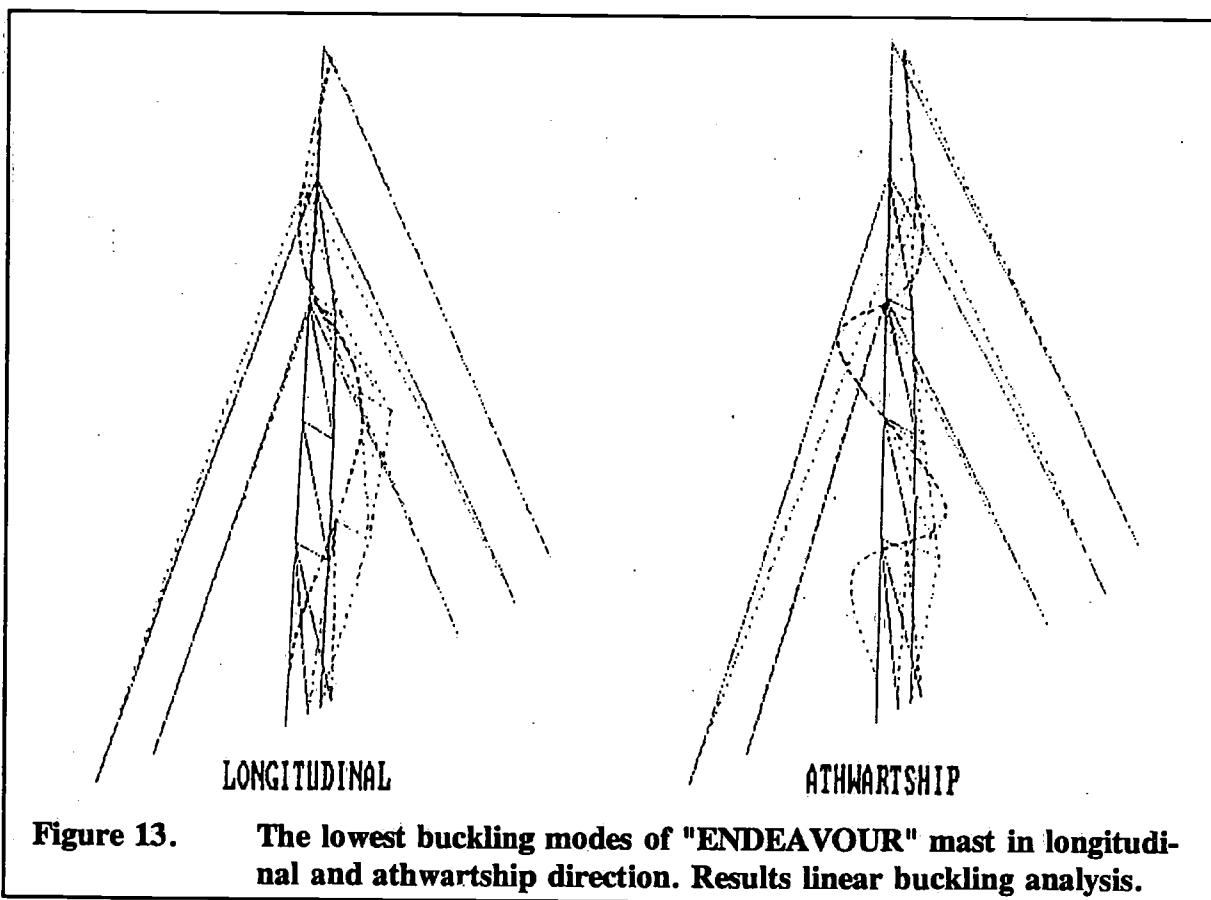


Figure 13. The lowest buckling modes of "ENDEAVOUR" mast in longitudinal and athwartship direction. Results linear buckling analysis.

Amsterdam is building a Dutch-East Indiaman

by Ir.H.J.Wimmers

"Stichting Amsterdan bouwt
Oostindievaarder"

During the last decades in The Netherlands the interest in old ships has been remarkably increased.

Many ships of old age have been kept out of the hands of shipbreakers and are brought again into their original state.

A fleet of ancient sailingvessels, big and small, is sailing on the Dutch waters and abroad. Steamships have been rehabilitated and at special events it is a measure to see them passing by, puffing and whistling.

From several ship-types, which exist no longer, replicas have been built, not only replicas of small vessels but of those of bigger ships as well.

Some years ago the ship-yard "Amels" in Makkum in The Netherlands has built a replica of the 180' Dutch-East-Indiaman "Prins Willem" for Japanese account.

At this moment the replicas of two other Dutch-East-Indiaships are under construction in The Netherlands.

One of them, the "Batavia" is being built in Lelystad while the other one, which has been named "Amsterdam", is under construction in Amsterdam.

This article will describe the building of the latter.

A Volunteer Project

The plan to build a replica of a ship of the "Verenigde Oostindische Compagnie" (V.O.C.) arised in 1980.

For that purpose was chosen the V.O.C.-ship "Amsterdam" which was built in 1748.

It has been decided that the building had to be carried out by volunteers, mostly unemployed woodworkers and young people who are learning the shipwright trade.

In that way, when the ship will be ready, the City of Amsterdam will possess an impressive monument in memory of the V.O.C., which company has played such a prominent part in the development of this city.

At she same time this project has the objective to broaden the historic-maritime interest of the nation.

To realize this plan a foundation has been created named "Amsterdam bouwt Oost-indievaarder".

A part of the necessary funds have been provided by the municipality of the City of Amsterdam, the Ministry of Economical Affairs and the Ministry of Social Affairs whilst many sponsors have been interested in this plan together with an emission of shares on the Exchange.

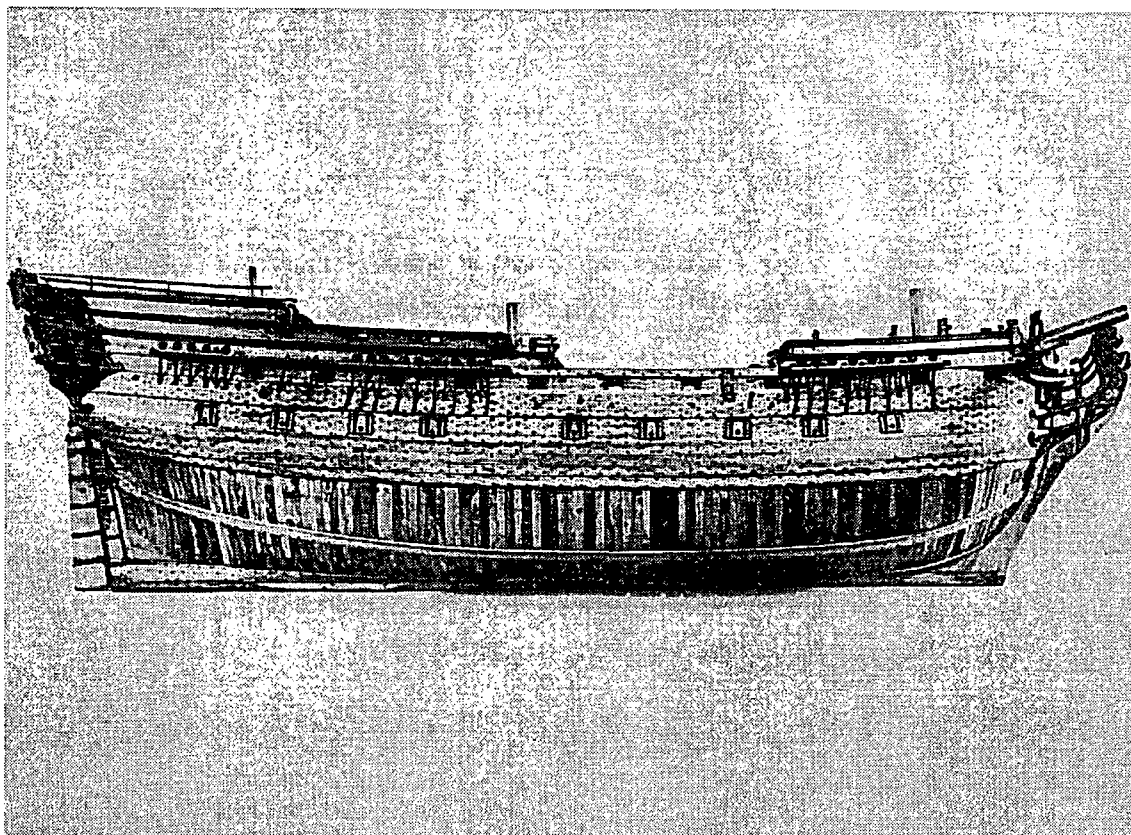


Photo 1 The model of the "Amsterdam", Rijksmuseum in Amsterdam

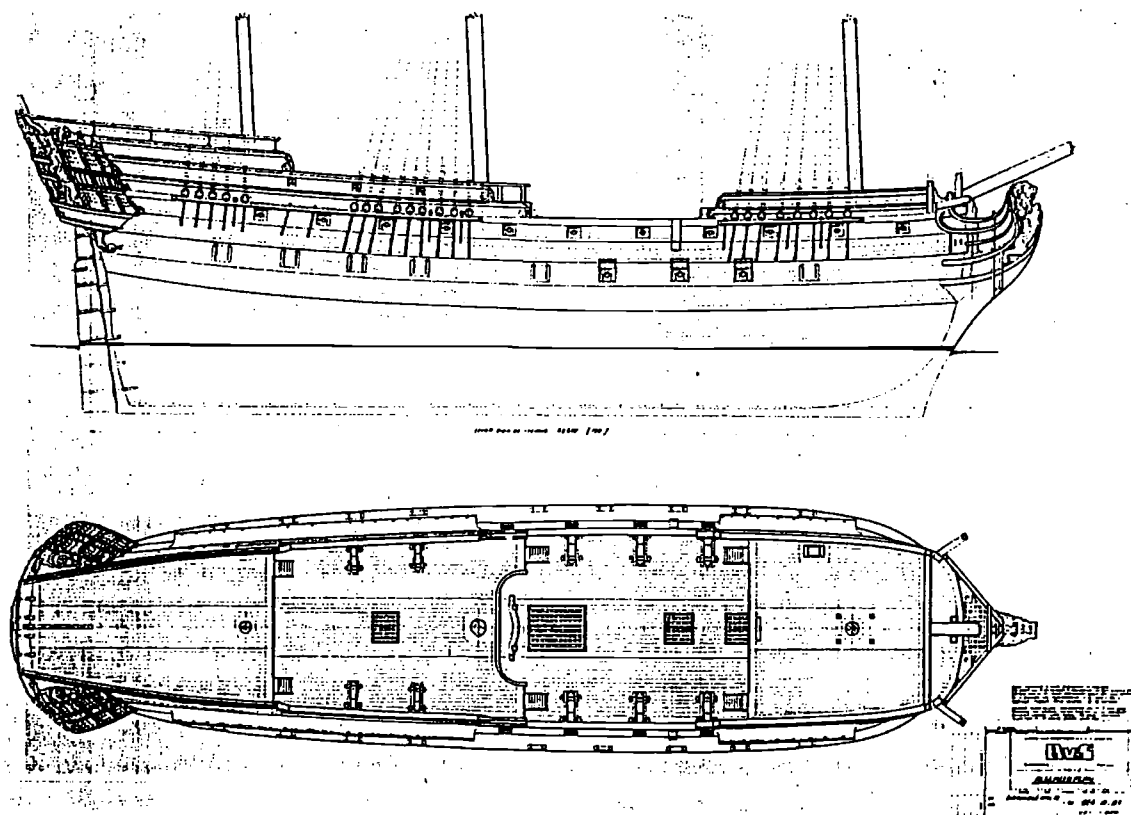


Photo 2 General arrangement replica of the "Amsterdam".

The V.O.C.-ship "Amsterdam"

The original "Amsterdam" has been built on the shipyard of the V.O.C. in Amsterdam in 1748 and was wrecked on her maiden voyage to the Dutch-East-Indies in 1749.

After a short dramatic voyage she stranded during a hurricane on the English coast near Hastings and sank away in shifting sand shortly after.

The length between the stem and the stern was 150 Amsterdam feet (one Amsterdam foot is 0,283 m and is divided into eleven inches). The replica has the same dimensions as the original ship and has a length between stem and stern of 42.45 m, the length overall of the hull is about 48 m while the width on the outside of the frames is 11.65 m.

The distance between the underside of the keel to the top of the transom is 13m. The displacement of the original ship in fully loaded condition was about 1300 tons.

The replica

The specifications and the basic drawings for the replica have been made by "Bureau voor Scheepsbouw" in Bloemendaal in The Netherlands, which design and construction bureau made those for the V.O.C.-ship "Prins Willem" as well.

It was an important advantage that the Rijksmuseum in Amsterdam possesses a reliable scale-model 1:30 of the hull of the "Amsterdam".

This model is very well detailed and contains all parts of the hull-construction.

The directorate of the Rijksmuseum gave fully assistance in using the model for making drawings.

The lines of the ship have not been determined by measurement but have been achieved by the terristic fotogrammetric method.

In following this method the form and the dimensions of an object are recorded by means of stereoscopic photos; which are transformed into accurate drawings by special apparatus.

This method is frequently used in restorations of buildings ect.

Observing the form of the hull it will be noted that this ship had a round stern while the proceeding ships of the V.O.C. used to have flat transoms.

Some years before the "Amsterdam" was built the dockyard of the admiralty of Amsterdam had started in building ships with a round stern instead of a flat transom.

Obviously there existed a contact between the admiralty-dockyard and the V.O.C.-shipyard and the latter has followed this alteration.

The shipyard

To realize the construction of the replica a small park was offered to the foundation at the waterside near the center of the city.

It was one of the conditions that people could observe the construction of the ship from the public road.

The park had to be made ready for the use of a shipyard, the ground had to be hardened, the necessary buildings, workshops with machines, moldloft-floor, slip-way, crane ect.ect, had to be installed. In fact it is strange that this shipyard has been founded for the building of only one ship; when the ship will be ready the place will be a park again.

The Hull

The ship has two decks from fore to aft, the upperdeck and the lowerdeck.

Below the lowerdeck is an orlopdeck, moreover there is a forecastledeck, a poop-deck and an upperpoopdeck.

On the lowerdeck 18 guns of 12 pounds could be placed, on the upperdeck 22 guns of 8 pounds and on the poopdeck 8 guns of 4 pounds.

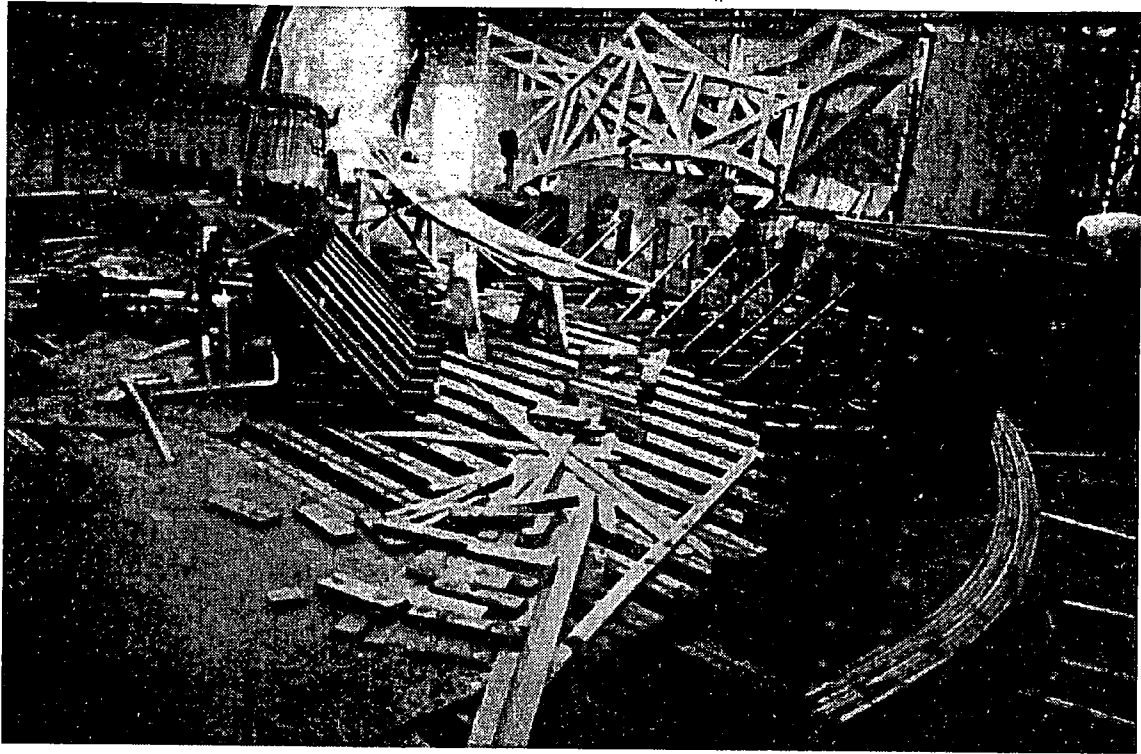


Photo 3 Gluing of a frame

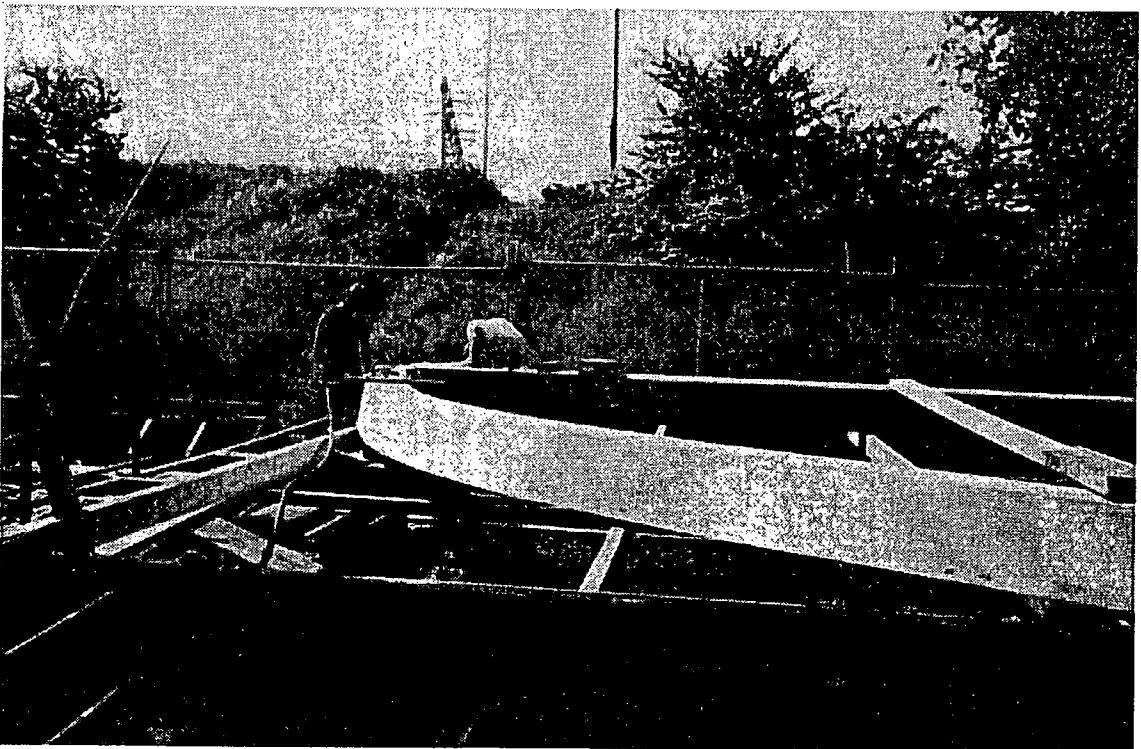


Photo 4 A laminated frame with the right level

The scantlings of the constructionparts have been determined by studying old specifications and with the help of old books in which the hullconstruction has been described in details. To mention some of these books:

"Scheepsbouw en Bestier" written by Nicolaes Witsen (1690)

"De Nederlandsche Scheepsbouw Konst Opengesteld" by Cornelis van IJk (1697)

"Seeman" by W.A. Winschoten (1681).

The keel has a length of about 38.5 m, is 0.60 m high and 0.45 m wide.

The keelson is 0.20 m high and 0.40 m wide, the bilgestringers are 0.30 x 0.15 m.

The frames are bolted between the keel and the keelson.

There are 27 ringframes with deckbeams and knees which contribute importantly to the transversal strength.

The spacing of those ringframes vary from 0.70 m to 1.80 m, the dimensions are 0.30 x 0.25 m

Between the ringframes several tweenframes are placed 0.25 m x 0.25 m.

The dimensions of the upperdeck-beams are 0.25 m x 0.25 m, those of the lowerdeck are 0.35 m x 0.30 m.

The deckstringers are 0.45 m x 0.15 m.

There are two wales, the dimensions of the upperwale are 0.80 m x 0.15 m, those of the lowerwale 1.00 m x 0.15 m.

The hullplanking is 0.10 m thick, the ceiling 0.05 m.

The hullplanks are connected to the frames by galvanized bolts and nuts and where inevitable with barbed bolts.

The hullplanking has been caulked in the original way to obtain a watertight hull and a good friction between the planks, to improve the longitudinal stiffness of the ship.

The materials

The V.O.C. used for the constructionparts of the hull mainly oak and pine-wood for the decks.

It is difficult at present to obtain well seasoned oak timbers of big dimensions and specially oaken crooks are very scarce.

An important consideration in the choise of wood was that the ship, when ready, will always be moored in fresh water so that she will miss the preservating effect of seawater.

It was expected that oak for this purpose would have a too short duration and therefore a more durable kind of timber had to be chosen.

Iroko (*chlorophora excelsa*) is a kind of wood which is more durable than oak, the shrinkage is less, the strength and the weight is equal to oak, it has few knots, is well available in big dimensions and the price is reasonable.

These are the most important motives that the ship for the greater part has been made of iroko.

The disadvantage of pine-wood, if used for the decks, is that this kind of wood is rather soft and less proof against wear (ladies stiletto heels) and the fire-prevention authorities think it too inflammable to use it within the ship.

So the weatherdecks have been made of iroko as well.

The lowerdecks have been made of bangkirai (*shorea leavifolia*) because this kind of wood is very wearproof and little inflammable.

The keelson, the bilgegirders and the pillars have been made of azobé (*lophira procera*).

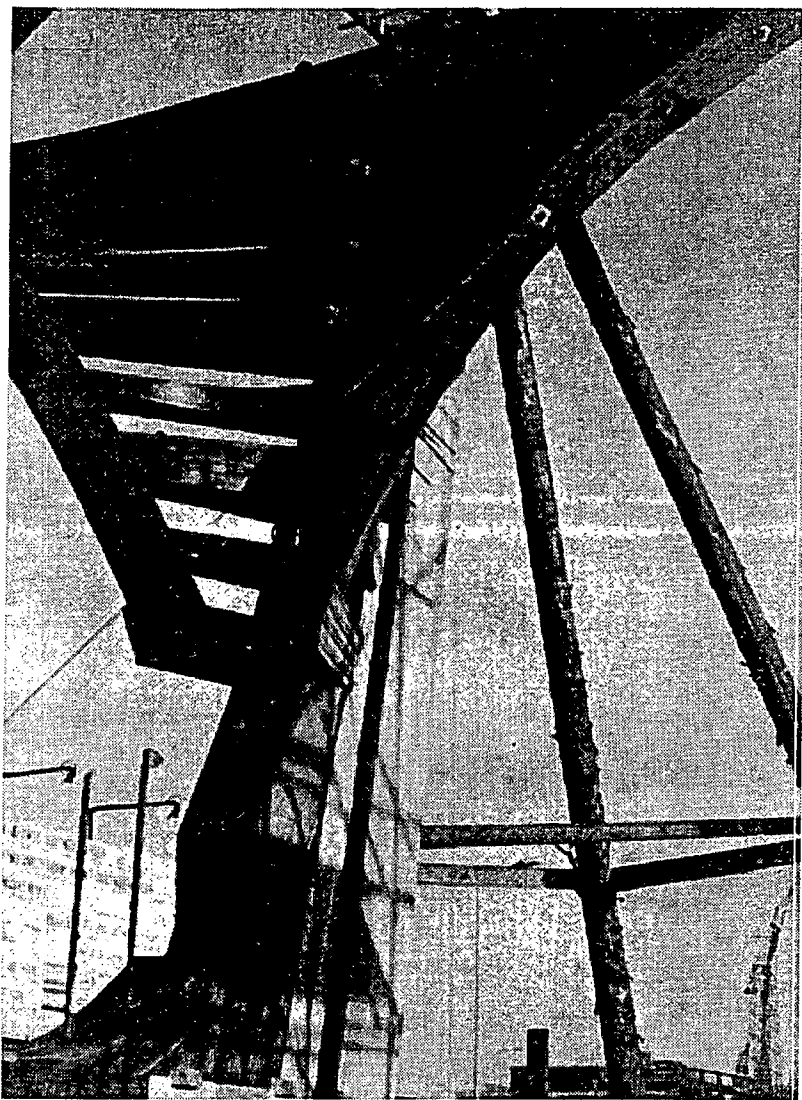


Photo 5 A part of the stern

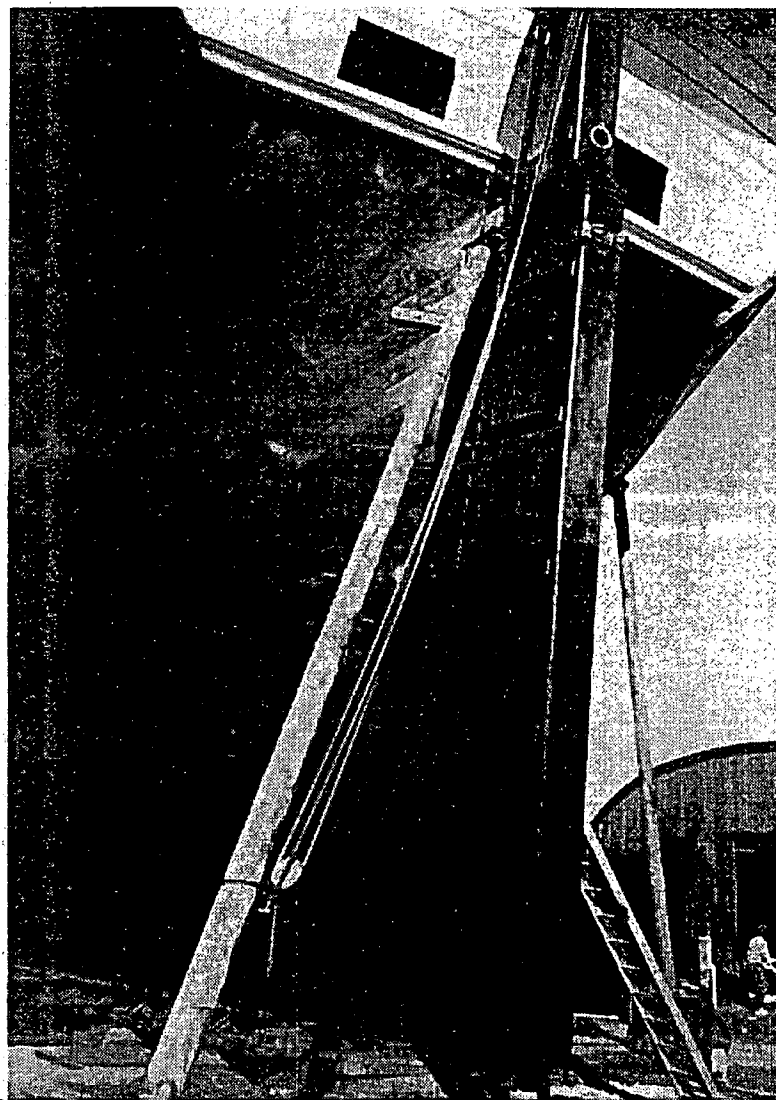


Photo 6

The construction of the hull

The drawings, belonging to the specifications, have been made by "Bureau voor Scheepsbouw", mentioned before.

The detail drawings were made in the drawingroom of the shipyard after which they were lofted on the moldloft-floor.

Originally the frames were composed of several curved pieces of wood but setting aside the problem to obtain these crooks, this composition gives a loss in strength and a considerable loss of wood.

For that reason the frames, deckbeams and other parts of the replica have been laminated and glued.

In this way a construction has been obtained which is stronger and more rigid than the original one and on the other hand one is sure that a component is thoroughly sound whilst the grain is parallel to the curve of the wooden part.

In the Norges Tekniske Høgskole in Trondheim in Norway full scale tests have been carried out with a glued laminated and a conventional wooden section of a fishing-vessel, wide 5.50 m.

The result was that the laminated construction was 22 % higher in strength and 30 - 50 % higher in stiffness than the conventional construction.

Another advantage is that the layers of glue will act as a barrier against decay.

The kind of glue that has been used is based on resorcinolphenol and is excellently suitable for this purpose.

Before gluing the wood has to be kiln-dried to about 14 % humidity.

The gluingwork has to be executed in a special workshop in which the air has the required temperature and humidity; gluing in the open air does not give reliable results.

The keel has been laminated too and as the workshop did not have sufficient length this work had to be done by a firm which is specialized in this work.

The length of the keel was about 40 m.

The ship has 75 frames and they are laminated in such a way that they have over the whole length the correct bevel for the hullplanking and the ceiling.

This has saved a considerable amount of work and wood.

In laminating the frames their strength and stiffness have increased so it was possible to reduce the number of frames compared with the original construction which saved work, material and improves the ventilation between the hullplanking and the ceiling.

Aside from laminating wooden parts, just mentioned, the ship has been built of solid wood and the construction is equal to that of the original "Amsterdam".

An exception is that the number of riders have been increased. In those days the ships of the V.O.C. were never docked in gravingdocks, because there were no docks in The Netherlands, but they were inclined so far that the keel came out of the water.

Calculations showed that when the ship will be put on dockblocks out of the water the stresses in the frames can be locally rather high.

As the replica has to be docked periodically in the future it has been decided to install more riders than was usual for merchantships.

Where wooden parts have to be bent, in most cases this can be done without heating.

When this will be impossible or too risky the timbers have to be bent by heating one side and wetting the other side.

Formerly this work was done above a fire of wood and reed but in this case it has been done by infra-red heating.

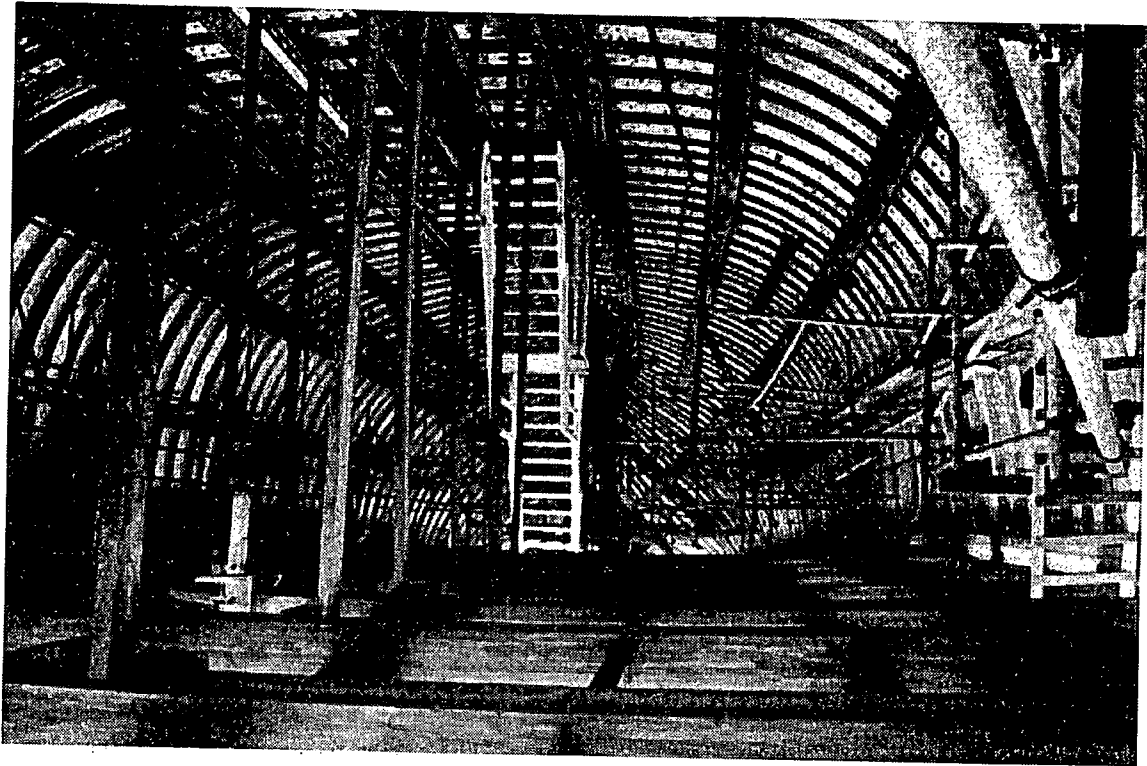


Photo 7 Frames without the ceiling

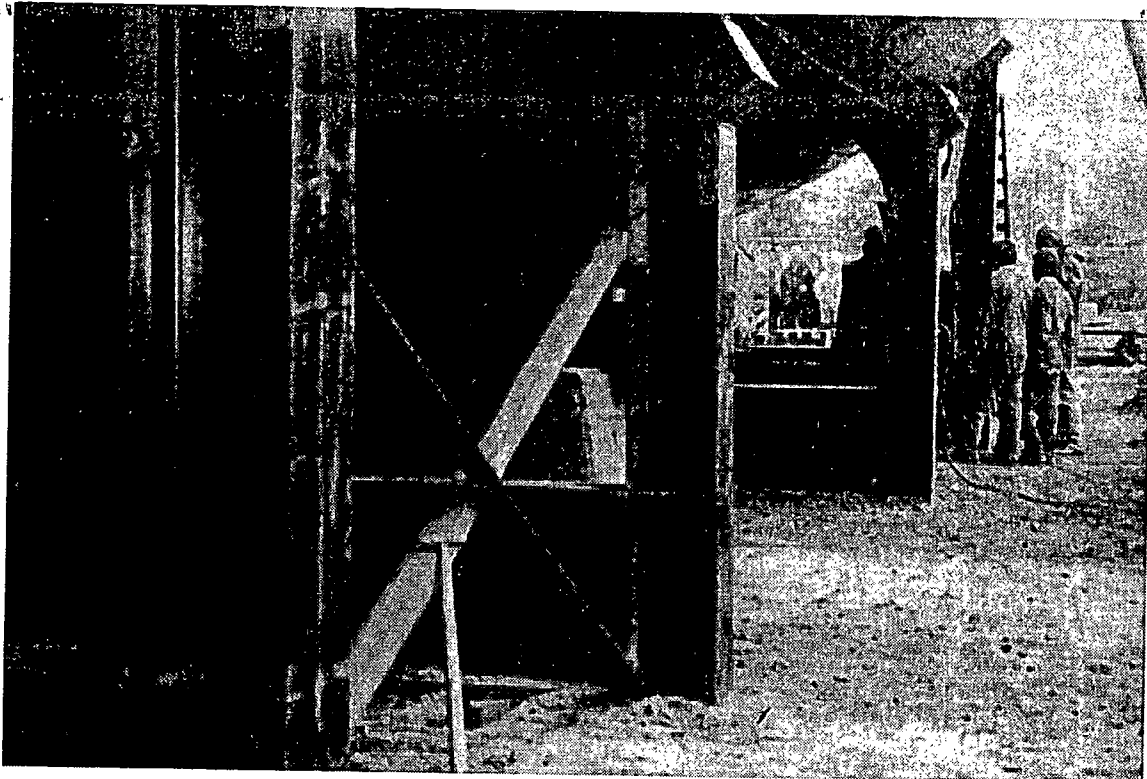


Photo 8 Steel construction for the launching

The launching

As the presence of pipelines and electrical cables excluded a normal slipway, the ship has been built in a horizontal position and the launching operation required a profound study. It has been decided that the ship, when her strength would be sufficient, had to be transported from the building-side on a pontoon.

The pontoon with the ship had to be towed to a floatingdock after which the ship could take the water.

For this transport two enormous "Mammoet" waggons were available, each waggon had 100 wheels which were supported by hydraulical cilinders in such a way that when the ground is uneven the platform on the top of the waggon will be straight.

First the ship had to be lifted.

During the building the wooden keel had been based on a heavy steel profile.

For lifting the ship six heavy steel bars have been welded with right angles to this profile.

On the ends of these bars vertical bars have been welded to prevent the ship from capsizing. Under each bar were four hydraulical jacks placed which were computer controlled so that during the lifting the keel did not bend.

After the ship had been lifted 1.40 m high the waggons could be rolled under the construction.

The platforms of the waggons were raised and the jacks could be removed.

In spite of the fact that the connection of the yard with the pontoon was far from flat, the transport of the ship progressed smoothly.

The transport to the floating dock and that of rolling the ship on the dock and after that the undocking have not given problems either.

The weight of the ship and the steel construction was about 450 tons. Some days after the launch the "Amsterdam" has been christened by H.R.H. Princess Margriet.

The rigging

After the ship had been launched the masts could be placed.

The masts and the bowsprit have been made of oregon-pine and built up of parts of several trees, glued to each other.

The lower masts and the bowsprit have rope-wouldings. The tops have been made of iroko, the mast-caps of oak. The yards and the mizzenyard have been made of oregon-pine and the blocks of elm. In selecting the ropematerial the durability was an important factor to cut down the exploitationcosts.

The original used ropes had a short duration and required much maintenance.

For the standing rigging Hercules-rope has been chosen, reinforced with steel core-threads.

The running rigging has been made of polyester, polypropene and nylon of a quality which is u.v.- and ozon-proof.

The foremast and the mainmast have been provided with lightning conductors.

The finishing touches

For the appearance of the ship the sculptures and the decorations are of importance.

However the V.O.C. spent in 1750 less money for adornments than the company used to do one century before, this decorations required a lot of work.

The most extensive ornaments are the figure-head, the Dutch lion, and the two statues on the transom, Neptune and Mercury. These sculptures are carved of iroko-wood and have a weight of more than one ton each.

After a scale-model 1:5 has been made the sculptures have been moulded on full scale roughly in layers of polystyrene, 5 cm thick.

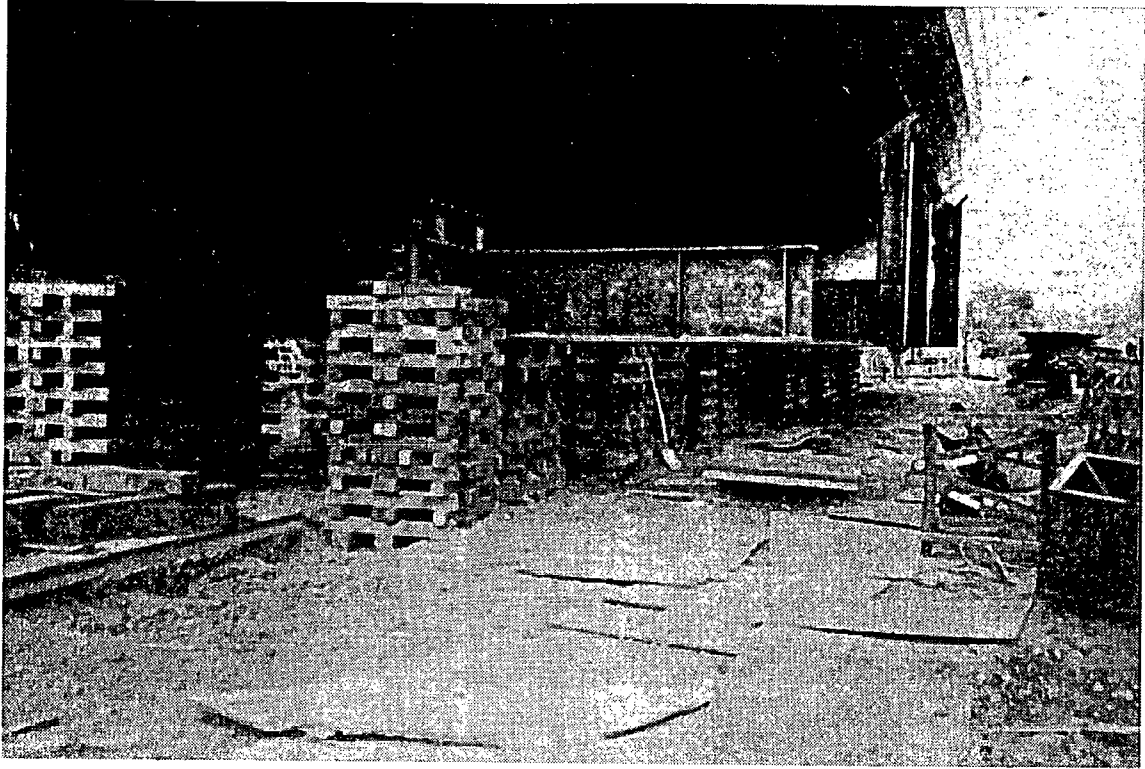


Photo 9 The hull in lifted condition

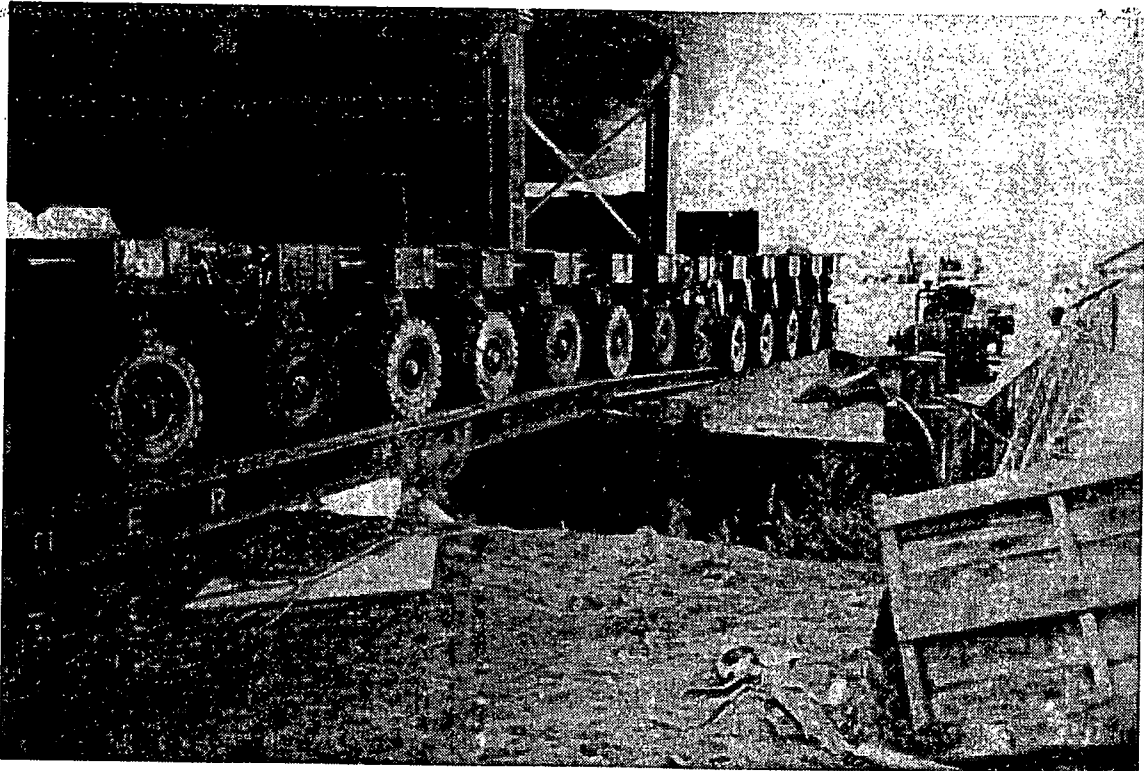


Photo 10 The transport from the building place to the pontoon

These layers were copied in layers of wood and glued together so that a rough form has been obtained with a minimum loss of wood.

After that the sculptures could be finished. All sculptures and decorations have been made by volunteers under the guidance of a skilled sculptor and the results are excellent.

The ship had to be ready for "Sail 90" in Amsterdam, that is to say the rigging must be complete.

After "Sail 90" the ship will be finished inside and completed with all kind of equipment which formerly had been on board, so that visitors can form a good impression how an indiaman in those times used to look.

The original "Amsterdam" was equipped during her voyage with 8 guns of 12-pounds, 16 guns of 8-pounds, 8 guns of 4-pounds and 10 swivelguns of 1-pound.

It has been decided to place on the replica 4 guns of each type.

The barrels have been casted of iron and the swivelguns have been made of nodulair castiron so that they can be used for firing salutes.

The destination

After the "Sail 90" festivals the "Amsterdam" will be moored to a pier along the Maritime Museum in Amsterdam where she will be finished. In the course of 1991 she will be opened for the public. It is not the intention that the ship will be used for sailing voyages but, if this will be wanted afterwards the ship can be made ready for sea without high costs.

However during "Sail 90" she will be equipped with four sails; two jibs, the fore-topsail and the mizzensail, which sails have been made of the original hemp.

It will be possible that in the case of a maritime festival in a foreign harbour the ship will be towed over sea to add lustre to that event.

But, as stated before, the principal destination of the ship is the City of Amsterdam to give people a good impression of a V.O.C.-ship of about 1750.

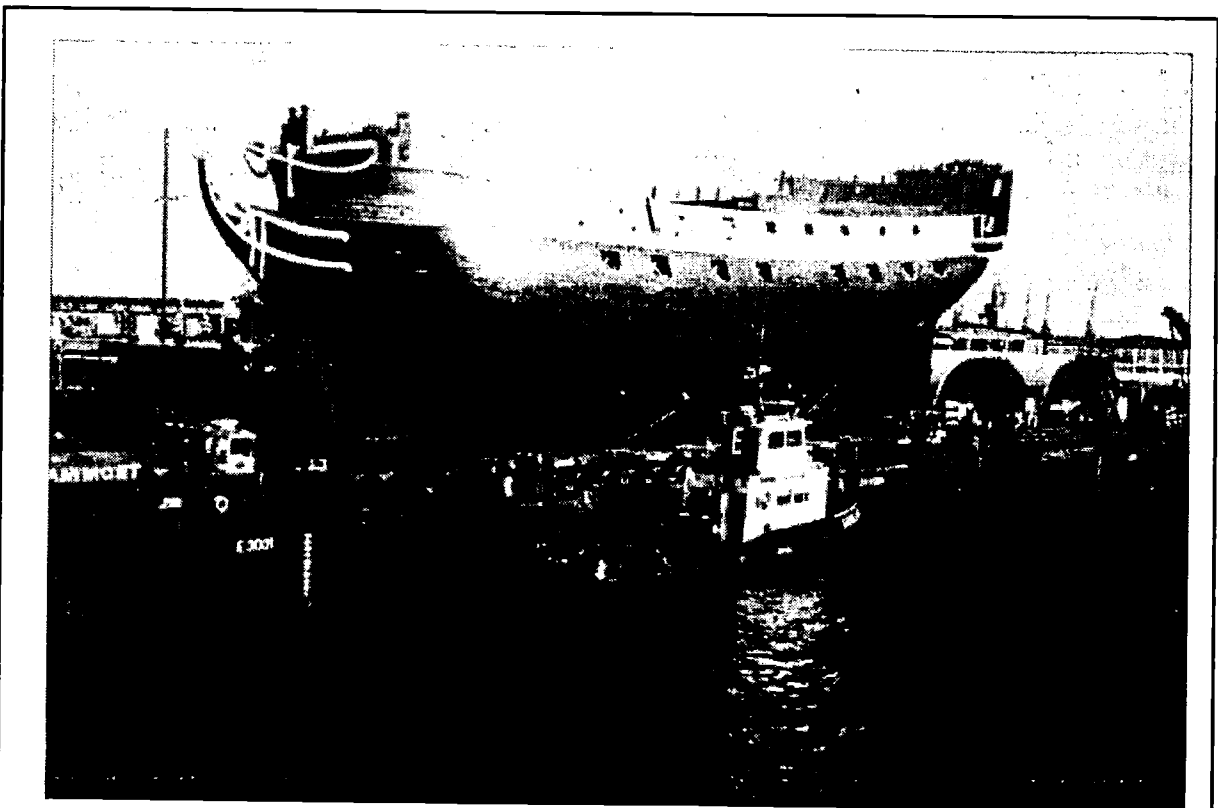


Photo 11 The hull on the pontoon

Photo 12
The ship is rigged

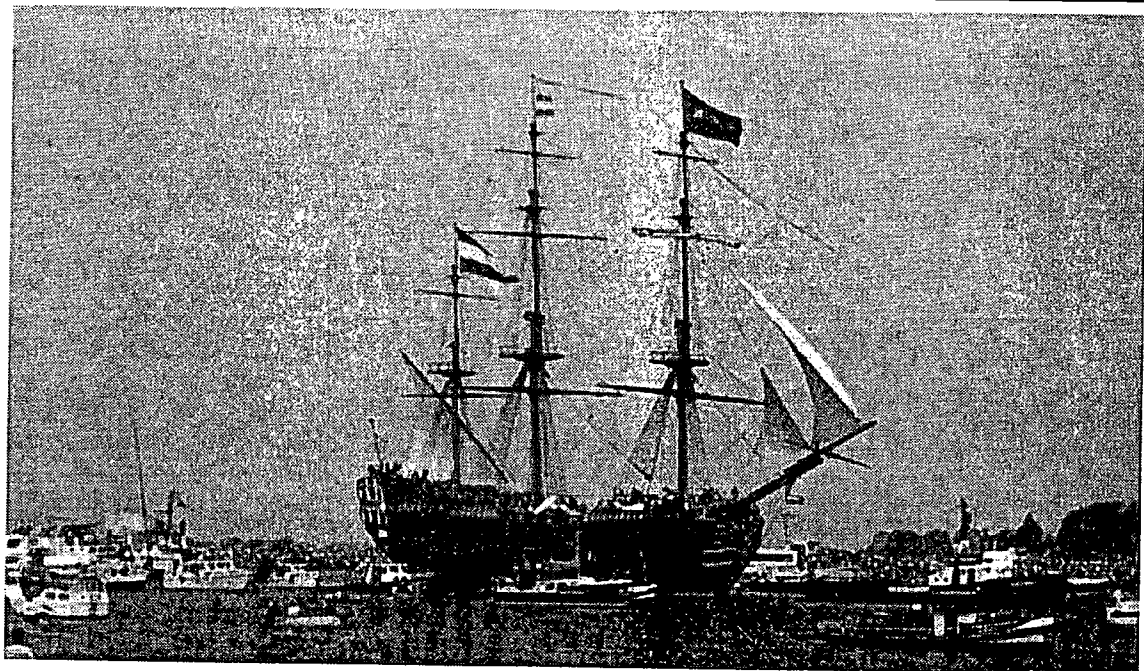
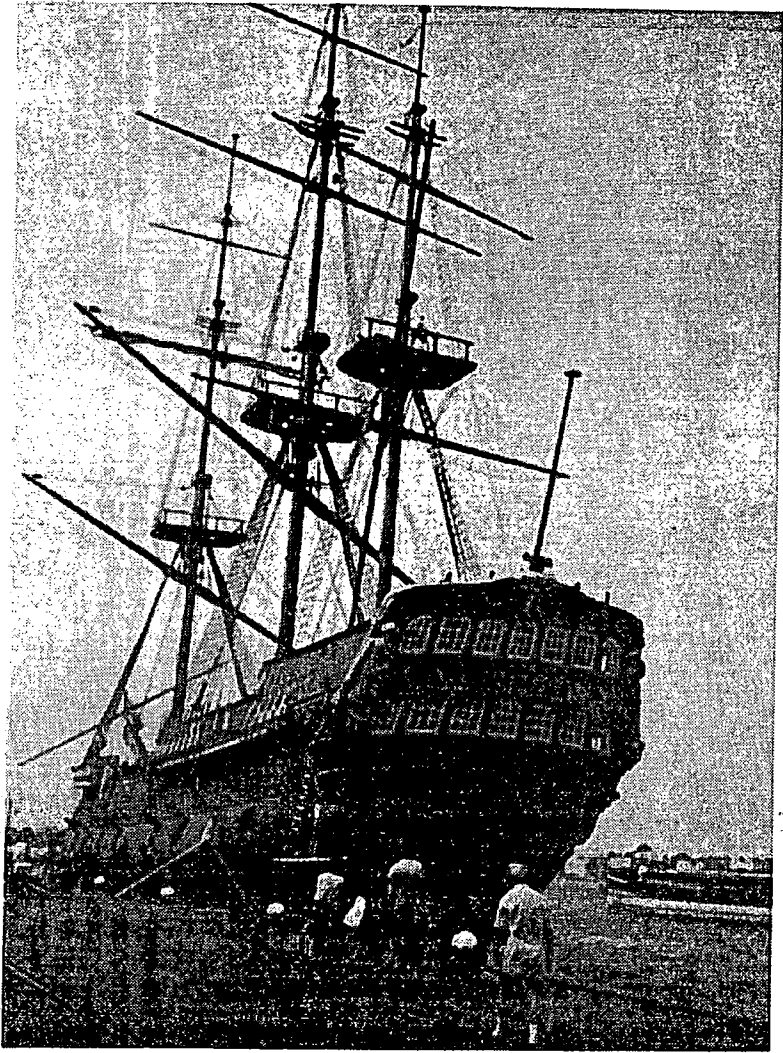


Photo 13 The "Amsterdam" during Sail '90

Carbon fibre reinforced spars and masts

by A.H.J. Nijhof

Delft University of Technology
Laboratory of Applied Mechanics

1 Introduction

On seaworthy sailing yachts mostly aluminium masts are used. These masts are loaded by a combination of an axial compressive force and a bending moment, Enlund et al. [4]. The dimensions of the cross sections of the mast are also determined by this load, preventing global buckling. The aim is to build a mast as light as possible, and to reduce the distance between the centre of gravity of the mast and the deck of the yacht. The flexural rigidity is proportional to the axial modulus of elasticity and under dimensional circumstances the mass is proportional to a specific modulus, i.e. the ratio of the axial modulus and the bulk density of the material. For this reason carbon fibre reinforced plastic (CFRP) is preferable to aluminium. However it will be necessary to critically evaluate the requirements in order to optimize the design.

2 Design requirements

The mast can be considered as a beam column, divided in panels by the rigging. (Figure 1). The compressive load is introduced step by step from top to bottom. The bending moment is introduced by a transverse force at the top (head stay and back stay) in a steady direction, and by lift and drag forces on the sails in variable direction. A computer programme calculates the needed area moments of inertia at different heights of the aluminium mast. Based on these values an appropriate section is chosen. Mostly a cylindrical section, but it is possible to take different sections for different panels or to taper a section.

In this context to compare a CFRP mast with an Al mast it will be sufficient to consider the mast as an axially loaded Euler column.

Due to shrouds and rigging one can expect two global buckling modes.

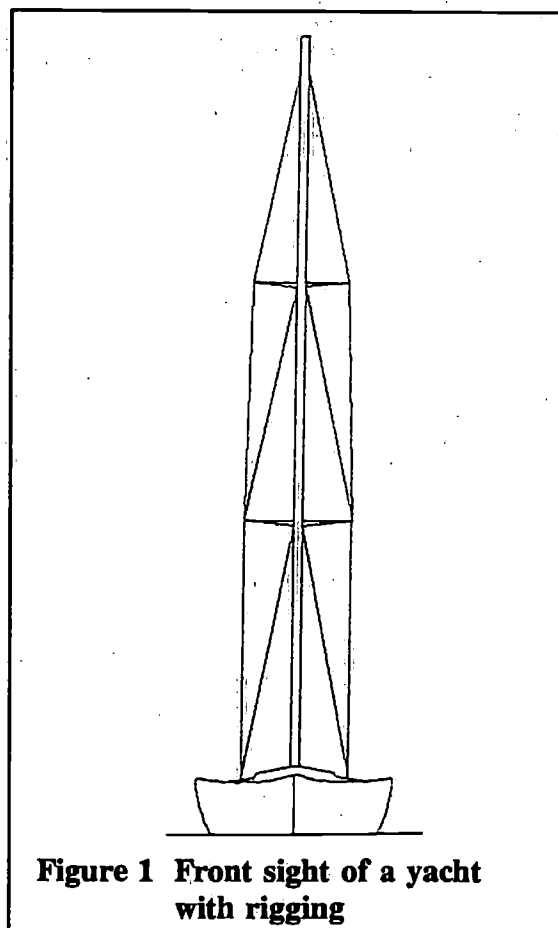


Figure 1 Front sight of a yacht with rigging

Firstly, buckling of the mast in cross direction with an S-shape (a panel in the form of a half wave).

Secondly, buckling in length direction of the yacht, the whole mast in the form of a quarter wave.

The values of rigidities and strengths of a FRP shell can be estimated. For that purpose manufacturer/supplier of the components of the material provide documentation. Predictions can be made with the help of a computer programme for laminates. But in reality it is necessary to test the design under laboratory conditions and in practice.

3 Optimizing a mast with respect to mass

3.1 A thin-walled isotropic cylinder

First of all we calculate the mast as a thin-walled cylinder of homogeneous, isotropic material, for instance, to take a concrete example, with an elliptic cross section. (Figure 2, left). The main axes of the section are the r_1 -axis and the r_2 -axis, the z -axis is in the axial direction of the cylinder. The measures of the median boundary are $2a$ in r_1 -direction and $2b$ in r_2 -direction, chosen so that $a \geq b$. Also the r_1 -axis points in the length direction of the yacht, and the r_2 -axis in the cross direction. The wall thickness, t , is constant. The length of the median boundary is s , the area of the wall section is A . The moment of inertia of the area with respect to the r_1 -axis is I_{11} , and with respect to the r_2 -axis I_{22} ($>I_{11}$), and the polar moment of inertia with respect to the z -axis is K . In Table 1 some formulas are arranged. The aim is to design the cylinder as light as possible. The dimensions of the mast are based on global or bending buckling. The buckling load depends on the fixing conditions at the ends of the mast.

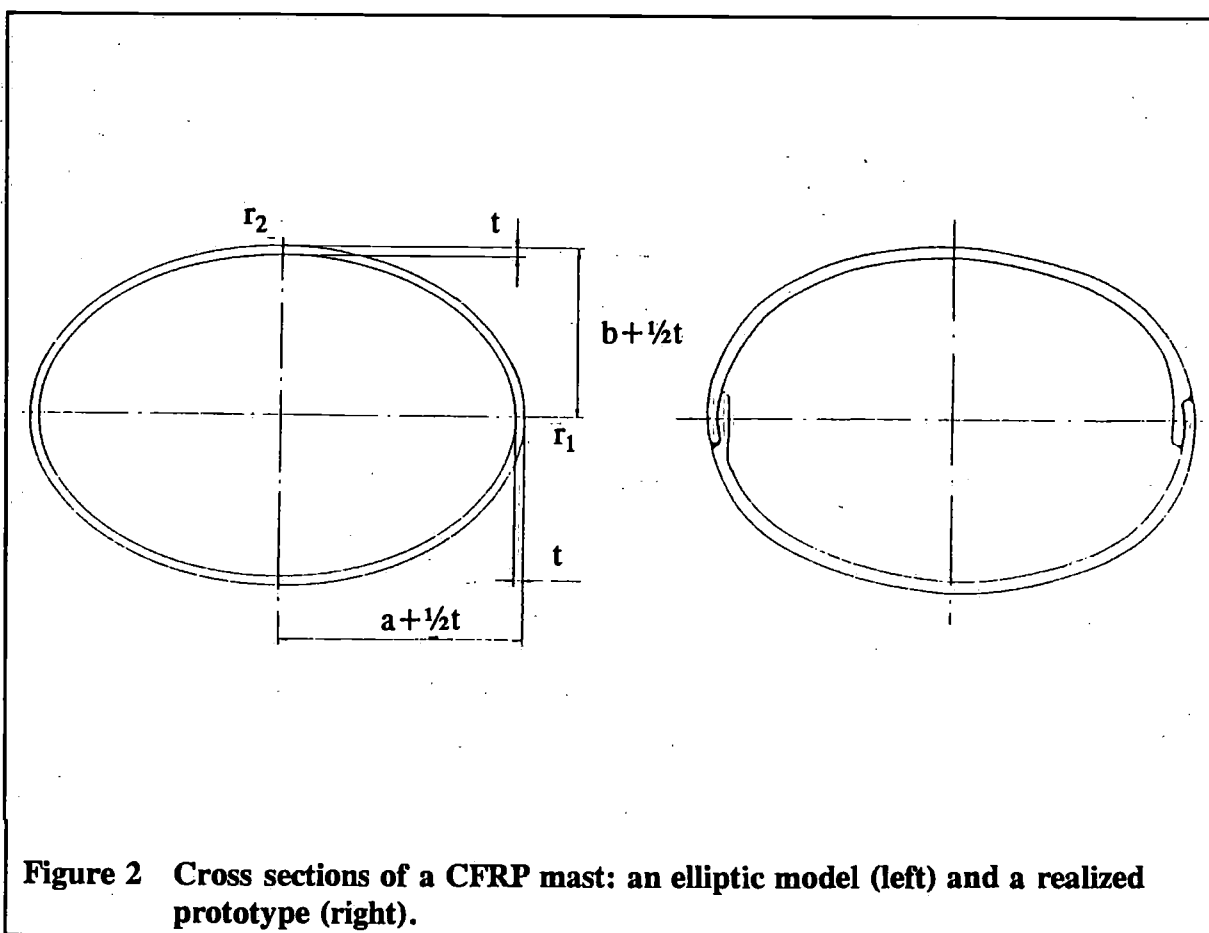


Figure 2 Cross sections of a CFRP mast: an elliptic model (left) and a realized prototype (right).

Table 1 Formulas for thin-walled cross sections with main axes of length $2a$ and $2b$ in r_1 - and r_2 -direction, respectively, and wall thickness t . (Dubbel [3]; Hütte [6], Young [11]). The factors f_s , f_A and f_K are dependent on the shape of the cross section.

shape of the cross section	length of the median boundary and area of the cross section	moment of inertia of an area	polar moment of inertia
in general	$s = f_s(a+b)$	$I_{11} = \int r_2^2 dA$	$K = \frac{4A_m^2}{s} t$
	$A = f_A(a+b)t \approx st$	$\approx f_1(3a+b)b^2t$	$\approx f_K \frac{a^2b^2}{a+b} t$

where A_m means the area surrounded by the median boundary.

shape of the cross section	length of the median boundary and area of the cross section	moment of inertia of an area	polar moment of inertia
elliptic	$s = k\pi(a+b)$	$I_{11} \approx \frac{\pi}{4}(3a+b)b^2t$	$K = \frac{4\pi^2a^2b^2}{S} t$
	$A = \pi(a+b)t$	$I_{22} \approx \frac{\pi}{4}(a+3b)a^2t$	$\approx \frac{4\pi a^2b^2}{k(a+b)} t$

$$\text{where } k = 1 + \frac{1}{4}\lambda^2 + \frac{1}{64}\lambda^4 + \frac{1}{256}\lambda^6 + \frac{25}{16384}\lambda^8 + \dots, \text{ with } \lambda = \frac{a-b}{a+b}$$

The formula of Euler indicates the axial buckling load F_{gb} of a column of length l and minimum moment of inertia of the cross section I_{\min} :

$$F_{gb} = - \frac{\pi^2 E I_{\min}}{l_b^2} \quad (1)$$

Here in the so-called buckling length l_b , depends on l and the fixing conditions (Young etc. [11]). E is the modulus of elasticity. A rough calculation gives the following result.

The chosen mast can be divided into three parts (Figure 1).

The mean part length is also $l_p \approx 1/3$. The buckling length in the cross direction of the yacht is $0.5 * 2l_p = l_p$, and in the length direction $2l = 6l_p$. In the case of equal buckling loads for both shapes of buckling, the relation between the main moments of inertia is:

$$\frac{I_{11}}{I_{22}} = \frac{l_{b,1}^2}{l_{b,2}^2} = \frac{l_p^2}{(6l_p)^2} = \frac{1}{36}$$

Mostly, for *Al* profiles is $I_{11} = 0.5... 0.8 I_{22}$. Also global buckling in cross direction is far more critical than in length direction. That means the minimum flexural rigidity EI_{11} dictates the buckling behaviour of the mast.

Supposing the ratio of the measures of the cross section in the main directions is prescribed. Due to the fact that the wall is thin the moment of inertia of the area of the cross section is a linear function of the wall thickness (see Table 1). With the help of Table 1 the quotient of the main moments of inertia is:

$$\frac{I_{11}}{I_{22}} = \frac{(3a + b)b^2}{(a + 3b)a^2} \quad (2)$$

The ratio b/a can be expressed in I_{11} and I_{22} .

$$\frac{b}{a} = 2 \sqrt{\frac{I_{11} + I_{22}}{I_{22}}} \cos\left[\frac{\pi}{3} - \frac{1}{3} \arccos \sqrt{\left(\frac{I_{22}}{I_{11} + I_{22}}\right)}\right] - 1 \quad (3)$$

Comparing the two cylinders of the same form of cross section but different measures (indicated by the respective subscripts α and β), the equality of the main moments of inertia results in:

$$(3a_\alpha + b_\alpha)b_\alpha^2 t_\alpha = (3a_\beta + b_\beta)b_\beta^2 t_\beta$$

$$(a_\alpha + 3b_\alpha)a_\alpha^2 t_\alpha = (a_\beta + 3b_\beta)a_\beta^2 t_\beta$$

Summation of both equations gives:

$$\frac{(a_\alpha + b_\alpha)^3}{(a_\beta + b_\beta)^3} = \frac{t_\beta}{t_\alpha} \quad (a)$$

The ratio of the areas of the cross sections, A_β and A_α , is:

$$\frac{A_\beta}{A_\alpha} = \frac{(a_\beta + b_\beta)t_\beta}{(a_\alpha + b_\alpha)t_\alpha} \quad (b)$$

This quotient equals the ratio of linear densities, μ_β and μ_α of the cylinders. Substitution of (a) in (b), results in:

$$\frac{\mu_\beta}{\mu_\alpha} = \left(\frac{t_\beta}{t_\alpha} \right)^{2/3} \quad (4)$$

That means that the thinner the wall is (and the diameter of the mast larger), the lighter the mast will be. There will be other technical reasons however to stop a further reduction of the wall thickness because there is a chance of inadmissible impact-sensitivity or an increasing wind load.

The torsional rigidity GK of the mast can be important in some cases. Here in G is the shear modulus and K is the polar moment of inertia of the area of the cross section. The polar moment of inertia of a thin-walled cross section is approximately:

$$K = f_K \frac{a^2 b^2}{a + b} t = f_K \frac{a^2 b^2}{(a + b)^4} (a + b)^3 t \quad (c)$$

f_K is a form factor. Comparing two cases of equal I_{11} and I_{22} , equation (3) leads to the conclusion that the ratio b/a is constant. From equations (a) and (c) one can conclude that under the circumstances also K is constant. Besides, twisting of the mast can be prevented by back stays.

Till now we are considering a cylindrical mast. By using Al profiles it is possible to design a lighter mast by taking parts of different profile, because the required moments of inertia decrease from bottom to top. Another step is to use a tapered part (the top).

An advantage of a FRP mast is the possibility to decrease the wall-thickness gradually, and/of to taper the mast.

3.2 A FRP mast in comparison with an Al mast

The buckling lengths being equal the flexural rigidities of two masts of different material should also be equal. The relevant modulus of elasticity is the axial one, E_α . Therefore:

$$E_\alpha I_{\min} = \text{constant} \rightarrow \frac{1}{I_{\min}} \sim E_\alpha \quad (5)$$

The linear density of the mast, μ , is the product of bulk density ρ and area A of the cross section:

$$\mu = \frac{1}{\rho A} \rightarrow \mu^{-1} = \rho A \quad (6)$$

The reciprocal of the linear density is a merit index with respect to the weight of the mast. Supposing the shapes of the cross sections are equal, only the wall thicknesses differ. The equality of flexural rigidities results in:

$$E_{\alpha,\alpha} t_\alpha = E_{\alpha,\beta} t_\beta \rightarrow \frac{A_\beta}{A_\alpha} = \frac{t_\beta}{t_\alpha} = \frac{E_{\alpha,\alpha}}{E_{\alpha,\beta}}$$

So the ratio of the linear densities will be:

$$\frac{\mu_{\beta}}{\mu_{\alpha}} = \frac{\rho_{\beta} A_{\beta}}{\rho_{\alpha} A_{\alpha}} = \frac{\rho_{\beta} E_{\alpha, \alpha}}{\rho_{\alpha} E_{\alpha, \beta}} = \frac{E_{\alpha, \alpha}}{E_{\alpha, \beta}} \frac{\rho_{\alpha}}{\rho_{\beta}} \quad (7)$$

One can use the specific modulus of elasticity - the quotient of (axial) modulus of elasticity and bulk density - as a merit index.

Theorizing about buckling problems one of the basic assumptions is that the columns will be ideal. In reality the ideal form and fixing conditions are more or less disturbed, the buckling load is smaller than the theoretical value, even for a homogeneous isotropic material as aluminium is.

FRP is a heterogeneous material, with flaws and misalignments of the fibres, one can expect that the gap between the values of the theoretical and the real buckling load is larger in the case of FRP than in the case of aluminium. The size of this gap depends on the manufacturing technique.

An advantage of a FRP wall is that the axial modulus, E_2 , is not a constant of material, but can be increased by orientating a greater part of the fibres in axial direction. Consequently the modulus of elasticity in tangential direction, E_t , decreases.

Theoretically local buckling of a cylinder with a circular cross section occurs at a stress.

$$\sigma' = \frac{E.t}{(3(1 - \nu^2))^{0.5} R}; \quad \text{conditions: } \frac{R}{t} > 10, \text{ both ends free} \quad (8)$$

R is the mean radius of the wall, ν is the Poisson's ratio of the material. In practice the local buckling load is 40...60% of the theoretical value (Young [11]).

For elliptical cross sections a similar formula is applicated, using the largest radius of curvature of the wall (Brush & Almroth [1]):

$$R_m = \frac{a^2}{b} \quad (9)$$

The value of F_{lb} compared to that of F_{gb} in the practical situation of an Al mast - almost 70 times larger - shows that local buckling shall not occur. Even in CFRP it is not expected.

4 Stiffnesses of FRP

A FRP spar or mast is a thin-walled shell built up of layers, called laminae. To calculate stiffnesses and strengths of these layered shells - laminates - the classic plate theory has been further developed into the laminate theory (e.g. Jones [7]).

4.1 A lamina

One of the hypotheses where the laminate theory is based upon is a plane stress in the laminae. We introduce a local coordinate system: the axes x_1 and x_2 in the plane of a lamina, and the x_3 -axis perpendicular to it.

Mostly FRP laminate give evidence of symmetry in two directions perpendicular to each other. Such a lamina is orthotropic. We take these main axes of material symmetry as x_1 - and

x_2 -axis. In the plane of the lamina the normal stresses σ_1 and σ_2 , and the shear stress σ_6 are working. Call the displacements in x_1 and x_2 -direction u_1 and u_2 , respectively. So the small deformations in the x_1x_2 -plane are the strains ϵ_1 and ϵ_2 and the (engineering) shear strain ϵ_6 :

$$\epsilon_1 = \frac{\partial u_1}{\partial x_1}; \quad \epsilon_2 = \frac{\partial u_2}{\partial x_2}; \quad \epsilon_6 = \frac{\partial u_1}{\partial x_2} + \frac{\partial u_2}{\partial x_1} \quad (10)$$

As far as the fibres dominate the stiffness behaviour of FRP's - also in fibre directions - linear elasticity can be assumed. The linear elastic behaviour of an orthotropic lamina in its plane can be described by four independent elastic constants, for instance, the moduli of elasticity E_1 and E_2 in the direction of the x_1 - resp. x_2 -axis, the shear modulus G_{12} between x_1 - and x_2 -axis, and Poisson's ratio ν_{12} to describe the contraction in x_2 -direction caused by uniaxial stress in x_1 -direction, the so-called engineering constants.

Conform Hooke's law involving the main material directions:

$$\begin{bmatrix} \sigma_1 \\ \sigma_2 \\ \sigma_6 \end{bmatrix} = \begin{bmatrix} Q_{11} & Q_{12} & 0 \\ & Q_{12} & 0 \\ \text{symm} & & Q_{66} \end{bmatrix} \begin{bmatrix} \epsilon_1 \\ \epsilon_2 \\ \epsilon_6 \end{bmatrix} \quad (11)$$

The proportional constants Q_{ij} ($= Q_{ji}$) are called the reduced stiffnesses of the appropriate plane stress. They can be expressed in the engineering constants:

$$Q_{11} = \frac{E_1}{1 - \nu_{12}\nu_{21}}; \quad Q_{22} = \frac{E_2}{1 - \nu_{12}\nu_{21}}; \quad (12)$$

$$Q_{12} = \frac{\nu_{21}E_1}{1 - \nu_{12}\nu_{21}} = Q_{21} = \frac{\nu_{12}E_2}{1 - \nu_{12}\nu_{21}}; \quad Q_{66} = G_{12}$$

To know the stresses in other directions in the x_1x_2 -plane, these stresses can be transformed to a $x_1'x_2'$ -coordinate system which is created by rotating the x_1x_2 -system over an angle ϕ around the x_3 -axis. The transformation formula is:

$$\begin{bmatrix} \sigma_1' \\ \sigma_2' \\ \sigma_6' \end{bmatrix} = \begin{bmatrix} m^2 & n^2 & 2mn \\ n^2 & m^2 & -2mn \\ -mn & mn & m^2 - n^2 \end{bmatrix} \begin{bmatrix} \sigma_1 \\ \sigma_2 \\ \sigma_6 \end{bmatrix} \quad (13a)$$

with $m = \cos \phi$; $n = \sin \phi$

The transformation matrix is indicated by $[T]$. It can then be written in short:

$$\{ \underline{\sigma}' \} = [T] \{ \underline{\sigma} \} \quad (13b)$$

If the stresses and the strains are related to the $x_1'x_2'$ - coordinate system their linear relation is:

$$\begin{bmatrix} \sigma'_1 \\ \sigma'_2 \\ \sigma'_6 \end{bmatrix} = \begin{bmatrix} Q'_{11} & Q'_{12} & Q'_{16} \\ & Q'_{22} & Q'_{26} \\ \text{symm} & & Q'_{66} \end{bmatrix} \begin{bmatrix} \epsilon'_1 \\ \epsilon'_2 \\ \epsilon'_6 \end{bmatrix}, \text{ in short: } \{\sigma'\} = [Q'] \{\epsilon'\} \quad (14)$$

the transformation formula of the reduced stiffnesses is:

$$[Q'] = [T] [Q] [T]^{-T} \quad (15)$$

Also transformation formulas of the engineering constants can be developed (e.g. Jones [7]).

4.2 The classic laminate theory

The Kirchhoff-Love hypothesis used in the laminate theory assumed that a material line perpendicular to the midplane of the laminate will stay perpendicular during deformation. The loads - forces in the plane, bending and twisting moments, also no force perpendicular to the plane - are involved to the midplane of the laminate. These loads are defined as resultants of the integration across the laminate thickness. The x - and y -axis of the global coordinate system are chosen in the midplane. The z -axis is perpendicular to the midplane, in the same direction as the x_3 -axis of the laminae.

The resultant normal forces N_x and N_y , and the resultant shear force N_{xy} are also defined as

$$N_x = \int_{-1/2h}^{1/2h} \sigma_x dz; \quad N_y = \int_{-1/2h}^{1/2h} \sigma_y dz; \quad N_{xy} = \int_{-1/2h}^{1/2h} \sigma_{xy} dz, \quad (16)$$

if h is the laminate thickness. (Figure 3, left.)

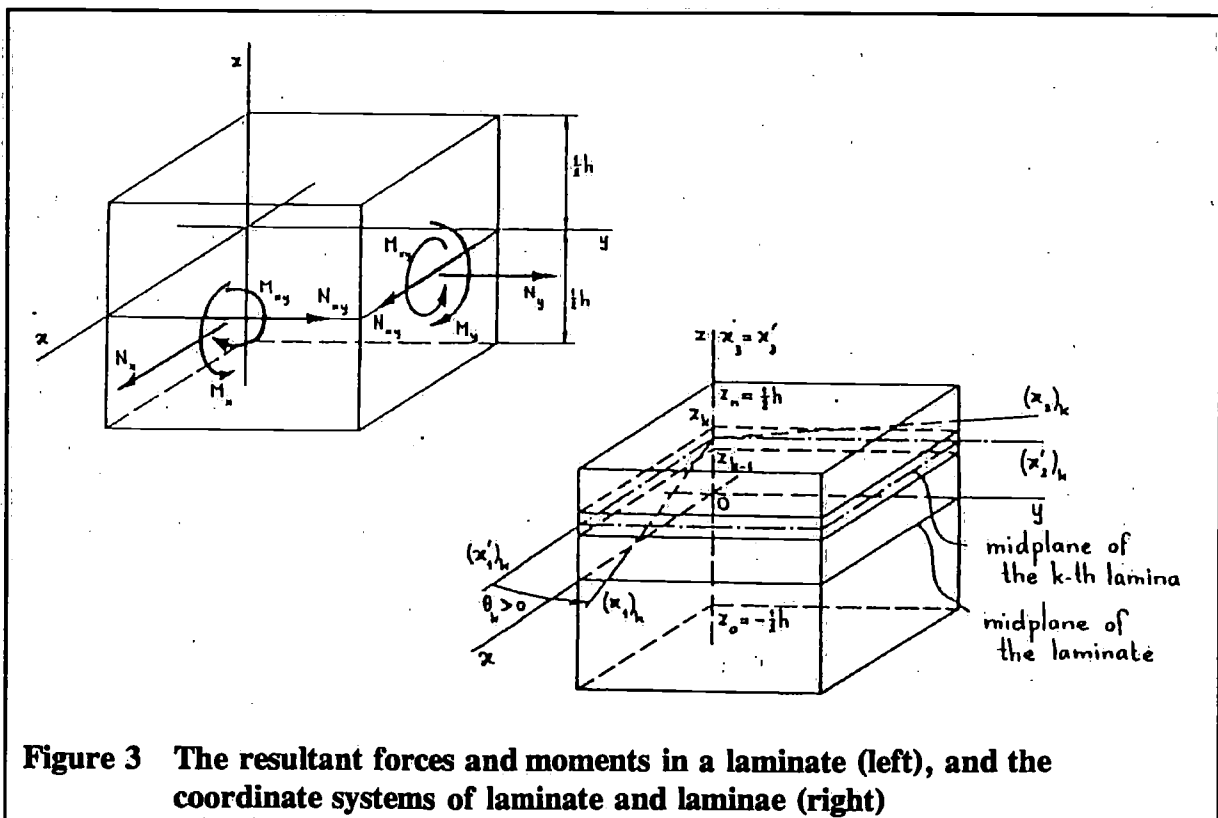


Figure 3 The resultant forces and moments in a laminate (left), and the coordinate systems of laminate and laminae (right)

And the resultant bending moments M_x and M_y and the resultant twisting moment M_{xy} are:

$$M_x = \int_{-1/2h}^{1/2h} \sigma_x z dz ; M_y = \int_{-1/2h}^{1/2h} \sigma_y z dz ; M_{xy} = \int_{-1/2h}^{1/2h} \sigma_{xy} z dz , \quad (17)$$

Introduce u , v and w as the displacements of a point anywhere in the laminate in resp. x -, y - and z -direction, and u^o , v^o and w^o those of a point in the midplane. The displacement u of a point on a distance z to the midplane can be expressed in the displacement u^o of the projection point in the midplane.

$$u = u^o - z \frac{\partial w^o}{\partial x} ,$$

The displacements out of the plane cause bending curvatures and a twisting curvature. The bending curvature is the reciprocal of the radius of curvature.

For instance, the bending curvature κ_x of the x -axis in the deformed situation - $w^o(x)$ - is:

$$\kappa_x = \frac{1}{R_x} = - \frac{\frac{\partial^2 w^o}{\partial x^2}}{\left\{ 1 + \left(\frac{\partial w^o}{\partial x} \right)^2 \right\}^{3/2}} = - \frac{\partial^2 w^o}{\partial x^2}$$

The minus sign is a matter of definition. In case of small inflections the strain in the direction of the x -axis is:

$$\epsilon_x = \frac{\partial u}{\partial x} = \frac{\partial u^o}{\partial x} - z \frac{\partial^2 w^o}{\partial x^2} = \epsilon_x^o + z \kappa_x$$

The strain ϵ_x^o is that of the midplane in the projection point.

The strain ϵ_y is expressed in an analogous way.

The shear strain with respect to x - and y -axis in a point on a distance z to the midplane is:

$$\begin{aligned} \epsilon_{xy} &= \frac{\partial u}{\partial y} + \frac{\partial v}{\partial x} = \frac{\partial}{\partial y} \left(u^o - z \frac{\partial w^o}{\partial x} \right) + \frac{\partial}{\partial x} \left(v^o - z \frac{\partial w^o}{\partial y} \right) = \\ &= \frac{\partial u^o}{\partial y} + \frac{\partial v^o}{\partial x} - 2z \frac{\partial^2 w^o}{\partial x \partial y} = \epsilon_{xy}^o + z \kappa_{xy} , \text{ where: } \kappa_{xy} = - 2 \frac{\partial^2 w^o}{\partial x \partial y} \end{aligned}$$

The deformations in a point on a distance z of the midplane can also be expressed in the deformations of the midplane and the bending curvatures κ_x and κ_y , and the twisting curvature κ_{xy} in the projection point:

$$\{\epsilon\} = \{\epsilon^o\} + z \{\kappa\} , \text{ with } \{\epsilon\}^T = \{\epsilon_x \ \epsilon_y \ \epsilon_{xy}\} , \{\kappa\}^T = \{\kappa_x \ \kappa_y \ \kappa_{xy}\} \quad (18)$$

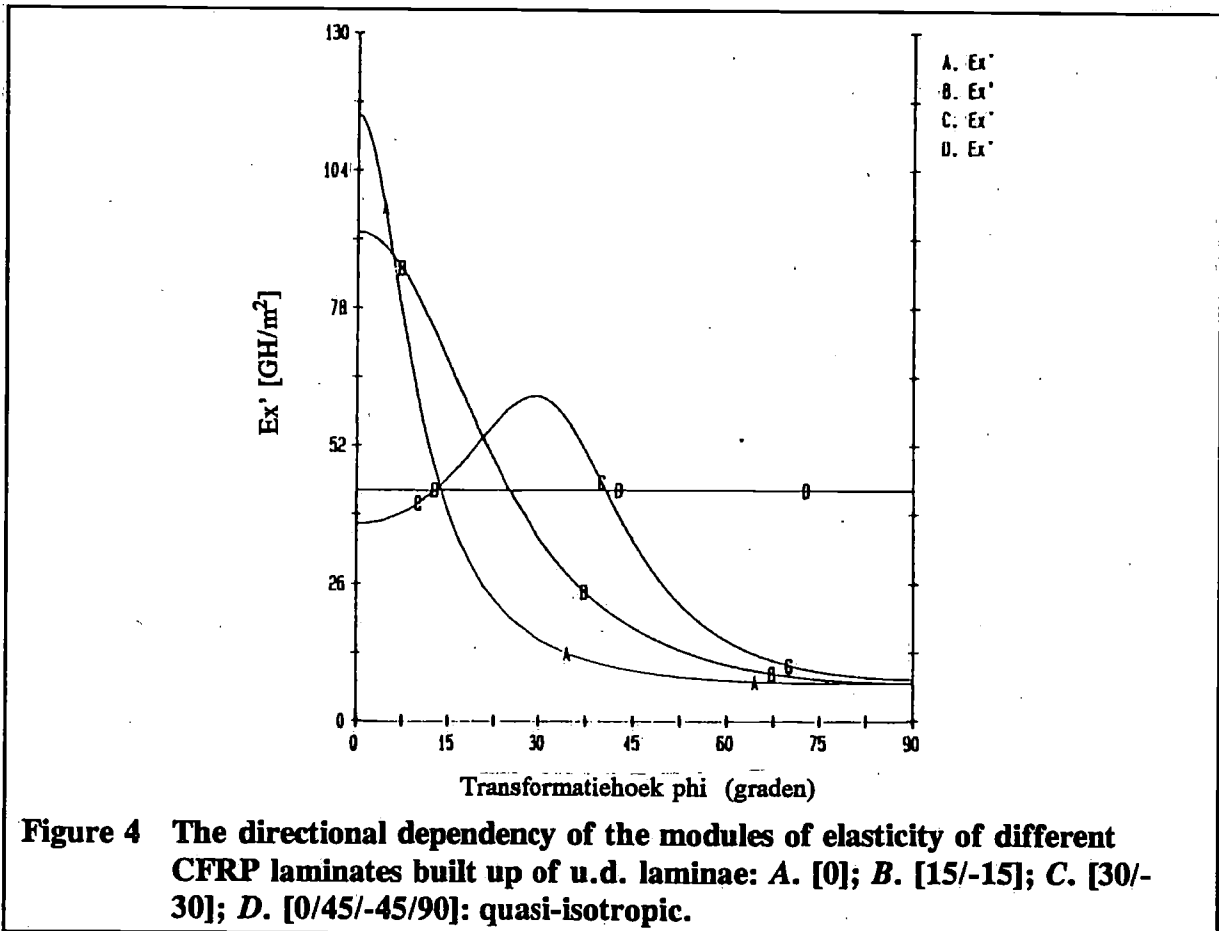
As a result of the laminate theory the linear relation between loads and deformations of the midplane is formulated as:

$$\begin{aligned}
 \begin{bmatrix} N_x \\ N_y \\ N_{xy} \\ \dots \\ M_x \\ M_y \\ \end{bmatrix} &= \begin{bmatrix} A_{11} & A_{12} & A_{16} & : & B_{11} & B_{12} & B_{16} \\ & A_{22} & A_{26} & : & & B_{22} & B_{26} \\ \text{symm} & & A_{66} & : & \text{symm} & & B_{66} \\ \dots & \dots & \dots & : & \dots & \dots & \dots \\ B_{11} & B_{12} & B_{16} & : & D_{11} & D_{12} & D_{16} \\ & B_{22} & B_{26} & : & & D_{22} & D_{26} \\ \text{symm} & & B_{66} & : & \text{symm} & & D_{66} \end{bmatrix} \begin{bmatrix} \epsilon_x^o \\ \epsilon_y^o \\ \epsilon_{xy}^o \\ \dots \\ \kappa_x \\ \kappa_y \\ \kappa_{xy} \end{bmatrix} \quad (19)
 \end{aligned}$$

The proportional constants, namely the extensional stiffnesses A_{ij} , the coupling stiffnesses B_{ij} , and the bending stiffnesses D_{ij} , can be expressed as functions of the stiffness properties of the n laminae of the laminate:

$$A_{ij} = \sum_{k=1}^n (Q'_{ij})_k (Z_k - Z_{k-1}) ; B_{ij} = \frac{1}{2} \sum_{k=1}^n (Q'_{ij})_k (Z_k^2 - Z_{k-1}^2) ;$$

$$D_{ij} = \frac{1}{3} \sum_{k=1}^n (Q'_{ij})_k (Z_k^3 - Z_{k-1}^3) ; ij \in \{1,2,6\} \quad (20)$$



In this formula z_{k-1} and z_k are the z -coordinates of the boundary planes of the k -th lamina. (Figure 3, right). The positive directions of transformation angle ϕ and lamina orientation angle θ are opposite: $\theta = -\phi$.

The transformation of the stiffnesses of the laminate - $[A]$, $[B]$ and $[D]$ - with respect to rotation in the plane goes in the same way as that of the reduced stiffnesses $[Q]$ of a lamina.

To illustrate the dependency of an engineering constant of a laminate on the direction, see Figure 4. The laminate code $[\theta_1/\theta_2/\theta_3]$, means that the laminate is built up of identical laminae, the bottom lamina makes an orientation angle θ , with the main axis of the laminate, and so on, and the laminate is symmetric with respect to the midplane, and has also 6 laminae.

5 Manufacturing methods

There are many different methods to fabricate a FRP spar of mast. Some of these methods shall be mentioned here.

5.1 Winding techniques

In winding processes the fibre construction is wound on a mandrel. The resin can be applied to the fibre construction before or after the winding operation. After curing the product must be removed off the mandrel or the mandrel out off the product. Postcuring in an oven is possible.

- Filament winding.

During several decades pipes are wound on a rotating mandrel in lathelike machines. Besides the advantages of the fabrication of an integral product and of winding under tension, which results in a higher fibre fraction, there are a number of disadvantages. Masts are long and a consequence of this length is bending of the mandrel, or the use of special supplies to prevent it.

The unmoulding operation also causes problems; maybe solvable by tapering the whole length of the mast, or by utilizing the difference in thermal coefficient of expansion between mandrel and CFRP mast.

If the cross section of the cylinder is not a circle, but e.g. an ellipse, the winding angle stays constant indeed (along a geodetic line, i.e. the shortest path between two points on a convex surface), but the momentaneous winding angle will vary. This variation causes sliding of the bundle of rovings across the surface, which results in fibre damage. To prevent this a NC winding machine is recommended.

A conical mast or mast top can be made with filament winding, but the winding angle increases towards the top and also the wall thickness. Moreover the mechanical properties will change along the mast.

To realize a specific varying wall thickness filament winding is not the appropriate method, because the number of layers is constant or there are belly turning points along the mast. When the torsional rigidity isn't important, filament winding has a disadvantage qua saving mass in comparison with fibres in mainly axial direction.

- Tape winding.

Apart from filament winding the winding of a woven tape with a small pitch is a possibility. That part of the fibres that lies in weft direction will make a small angle with the axial direction.

- Wrapping up.

The limit is wrapping up a woven fabric in tangential direction. The partition of warp and weft determines the ratio of the stiffnesses in axial and tangential direction.

- Combined methods.

It is possible to combine these manufacturing processes.

5.2 Resin Transfer Moulding

Characteristic for Resin Transfer Moulding (RTM) methods is the transfer of the resin in a closed mould filled with dry fibre material. After curing the mould will be opened and the product un moulded.

To get a high fibre percentage a rigid mould is less suitable. A choice can be made between a nonrigid mould part on the inner side (male) and a nonrigid mould part on the outer side (female) (Van Harten & Nijhof [5]). The use of a nonrigid part has consequences for size and surface quality.

- Vacuum film injection moulding (vacuum bag moulding).

One part of the mould is a film. Introducing vacuum in the product place underneath the film the atmosphere compresses the fibre package and the difference in pressure injects the resin into the mould through the fibre package. This method is suitable for shell-shaped products and can be used successfully for fabricating two halves of a mast which can be glued together in the next stage.

- RTM with an inflatable core.

It is difficult to make a long mast perfectly by RTM in a closed rigid mould. The way the resin has to go is long, the viscosity of the resin must be low and the pot life long. To shorten the way it is recommendable to inject along the whole length and to flow through the fibre package in tangential direction. A disadvantage is the presence of burrs. In order to get a high fibre percentage the fibre package needs a high density which slows down the flowing through.

5.3 Autoclave moulding

Autoclave moulding is comparable with vacuum injection moulding. Only the resin is applied in advance. And the autoclave is suitable for processing methods with increased temperature and pressure.

- Prepregs moulding.

Prepregs are preimpregnated layers of a fibre construction. There are u.d. prepregs and prepregs of a woven fabric. The layers can be wound or wrapped up, pressed on a mandrel or against the inner side of a mould.

When using prepregs in the autoclave temperature and pressure are being increased. Firstly the resin liquefies and the impregnation of all the layers improves. Excessive resin is pressed away, then starts curing.

- Wet lay-up autoclave moulding.

Unlike with prepregs moulding the resin is applied in a liquid state.

All these processing methods are suitable to make shell-shaped products, which can be combined to a complete mast.

6 Degrees of freedom in design

In contrast to an isotropic plate with one parameter, the thickness, there are many degrees of freedom in designing a laminate. Firstly the choice of the material components must be made and their proportions. Furthermore:

Type(s) of lamina(e).

The choice depends on the chosen manufacturing method.

- Unidirectional lamina as a prepreg (sheet or tape), using an autoclave, or as a tape of rovings in a filament winding process.
- Woven fabrics with two yarn systems perpendicular to each other: warp in production direction and weft in width direction. The ratio of amounts of fibre material in both directions is variable between wide boundaries.
- Combinations of different types of laminae.

Orientation of the laminae.

- With filament winding the orientation is given by the winding angle. In principle it is possible to change the winding angle every fully wound layer.
- The orientation of a woven fabric is defined by the angle between the warp direction and the main direction of the laminate. This angle can change from layer to layer.

The stacking sequence of the laminae.

- For a plane laminate this stacking sequence is essential. To reduce the coupling stiffness matrix $[B]$ to zero one of the most successful actions is to build the laminate symmetrically with respect to the midplane. And further, the bending stiffnesses D_{ij} are strongly determined by the stacking sequence, formula (20).
For a thin-walled cylinder the influence of the sequence on the mechanical properties is not so big. A good choice of the outer layer is important, because the behaviour against influences from outside, as impact, depends for the greater part on its properties.

To support the design process design graphics are made for different constructions (Figure 5).

As fibre material is chosen a HS Carbon fibre: modulus of elasticity $E_f = 226 \text{ GN/m}^2$, tensile strength $s_f = 3.04 \text{ GN/M}^2$ and density $\rho_f = 1740 \text{ kg/m}^3$. (Ten Cate Glas [9]).

By means of formulas based on micromechanical models the engineering constants of an unidirectional lamina can be predicted (Tsai & Hahn [10]). Using an epoxy resin with $E_m = 3.5 \text{ GN/m}^2$ a u.d. lamina with a fibre volume fraction $v_f = 0.5$ has approximately the following values of the engineering constants: $E_L = 114.8 \text{ GN/M}^2$; $E_r = 6.9 \text{ GN/m}^2$; $G_{Lr} = 3.6 \text{ GN/m}^2$; $\nu_{Lr} = 0.275$. The components are assumed to be isotropic: $\nu_f = 0.20$ and $\nu_m = 0.35$. Suppose the density of the epoxy resin is $\rho_m = 1200 \text{ kg/m}^3$. The density of the composite material is then: $\rho_c = 0.5 \rho_f + 0.5 \rho_m = 1470 \text{ kg/m}^3$.

Now calculations can be made to find out about the needed amounts of fibre material in different directions.

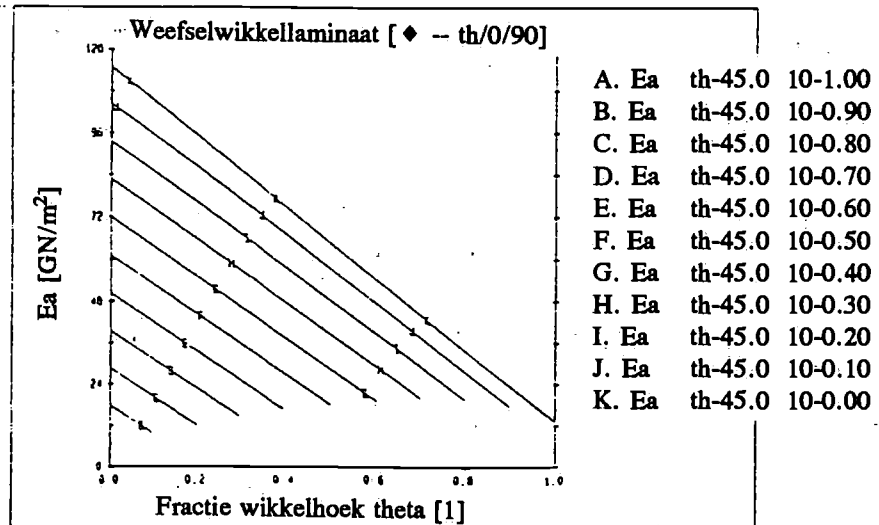
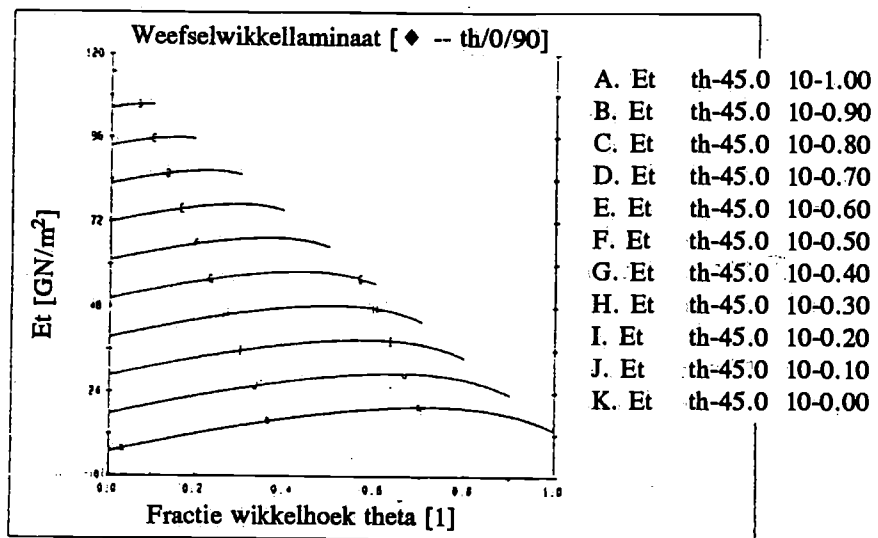
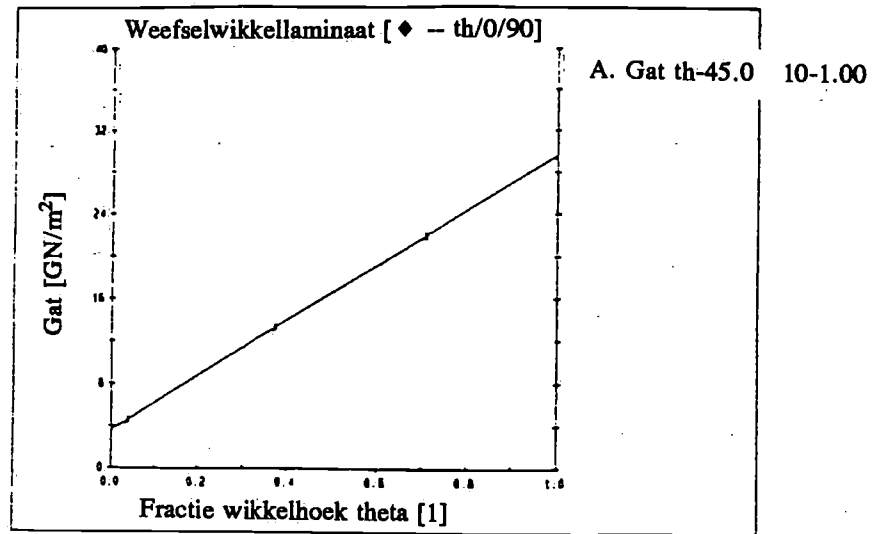


Figure 5 A set of design graphics of a CFRP laminate [$\pm 45/0/90$], with fractions $f_{\pm 45} + f_0 + f_{90}$, respectively: $f_{\pm 45} + f_0 + f_{90} = 1$. Engineering constants vs. $f_{\pm 45}$ as a function of parameters f_0 : (top) axial-tangential shear modulus, G_{ST} ; (middle) axial modulus of elasticity, E_a ; (bottom) tangential modulus of elasticity, E_t .

7 Compression tests on aluminium and CFRP mast section

To compare a CFRP mast with an aluminium mast compression tests are done on mast sections of both materials: aluminium cross section no. 6645 of Proctor Masts and a carbon/epoxy mast as a result of a cooperation of this company and Standfast Construction. The mast sections are axially compressed with prevention of rotation at both ends on a 600-tons testing machine of the Laboratory of Ship Structures (Buisman [2]). As free span length is taken twice the panel length, circa 6.8 m. The buckling length is the half of the span length.

7.1 Calculations for buckling

- Aluminium mast section.

Substituting the data of material and cross section the Euler formula delivers a buckling load of -128 kN, and a tensile/compressive stiffness $EA = 99 \text{ MNm}^2$. In a prebuckling state the calculated buckling load causes a strain of $-1293 \mu\text{m/m}$.

- CFRP mast section.

The CFRP mast section is built from two identical shells glued together with some overlap. (See Figure 2b).

The reinforcements of the wall are:

- 10 layers of carbon woven fabric with linen weave, type CD 220 of Ten Cate Glas [9], 220 g/m^2 , where is 68% in warp direction and 32% in weft direction; warp in axial direction of the mast;
- 2 layers of carbon woven fabric with 5H satin weave, type CD 282 of Ten Cate Glas [9], 280 g/m^2 , where the mass is equally divided between warp and weft, and with the orientation $\pm 45^\circ$.

The total mass of the carbon fabrics is $a_f = 2760 \text{ g/m}^2$. The fibre mass fraction is $m_f = 0.60$, corresponding to a fibre volume fraction $v_f \approx 0.5$. The whole wall also has a nominal mass per unit of area $a_c = 4600 \text{ g/m}^2$.

With the help of PLAMOR, a PC-programme developed by our group and based on the laminate theory, the engineering constants of the wall are calculated with respect to the axial and the tangential directions.

The results are:

$$E_a = 70.2 \text{ GN/m}^2; E_t = 39.5 \text{ GN/m}^2; G_{at} = 8.87 \text{ GN/m}^2; \nu_{at} = 0.178.$$

On the basis of the nominal measures the buckling load is calculated: -138 kN. And also the tensile/compressive stiffness $E_a A = 96 \text{ MNm}^2$.

The maximum strain before buckling will be $-1444 \mu\text{m/m}$.

7.2 The results of the compression tests

- Aluminium mast section.

The aluminium mast section is axially compressed with velocity 0.1 mm/s, till buckling occurred at a maximum load of -137 kN. The force-strain curve is linear, till a mean strain of $-1340 \mu\text{m/m}$.

The measured compressive stiffness is 102 MN/m^2 , being 3% higher than the predicted value. The measured buckling load is over 7% higher than predicted.

- CFRP mast section.

The CFRP mast section is compressed with the same velocity. At a load of -110 kN the first deviation of linearity is observed and the displacement of the clamping device is stopped. After that the specimen is relieved till the original length is reached.

The test is repeated. The third time the movement of the clamp is stopped when the mast is buckled (114 kN and $-1180 \mu\text{m/m}$), and this situation is maintained till next morning (Figure 6). No relaxation is ascertained.

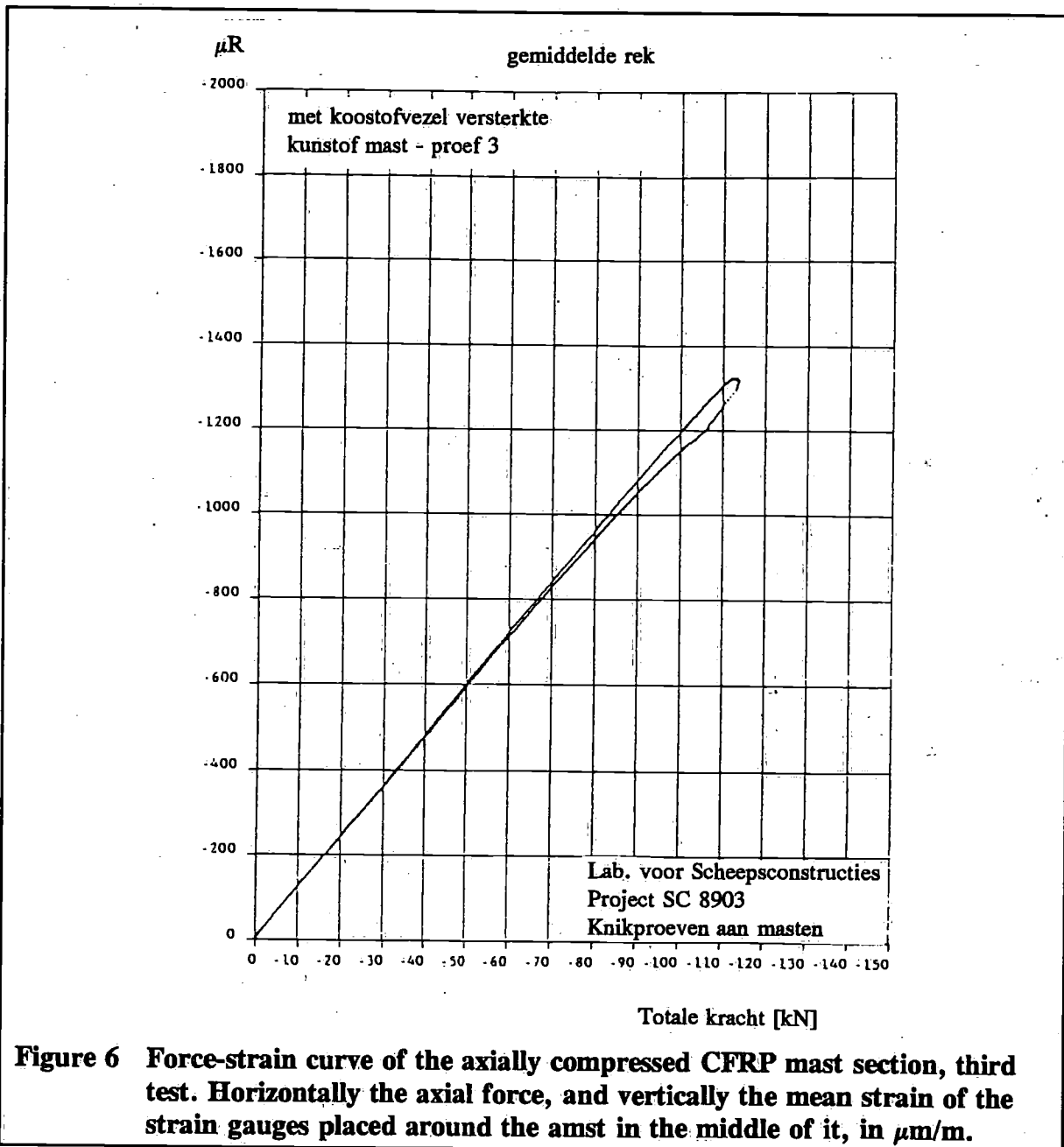


Figure 6 Force-strain curve of the axially compressed CFRP mast section, third test. Horizontally the axial force, and vertically the mean strain of the strain gauges placed around the mast in the middle of it, in $\mu\text{m/m}$.

The compression load decreased abruptly till -105 kN, because the glued joint of the two shells fractured somewhere. After relief and compressing the specimen again the buckling load remained -105 kN.

During the fifth test cycle the test is continued after buckling. The specimen is broken in a brittle manner near the middle of the specimen, by shearing along the circumference of the mast. The angle between shearing plane and the plane of the wall was roughly 45° .

The highest measured value of the compressive stiffness appears to be 7% lower than the predicted value, the highest value of the buckling load was measured 17.5% lower than the prediction.

The buckling load of a thin-walled cylinder is proportional to the thickness of the wall. To reach the same buckling load of the CFRP mast as of the aluminium mast, it is necessary to increase the wall thickness and also the amount of carbon fabrics with a factor $137/114 = 1.20$. That means an increase of the linear density with 20% to $1.20 * 2.43 = 2.92$ kg/m. That is $\frac{1}{3}$ lighter than the (nominal) linear density of the Al. mast. One must keep in mind that the torsional rigidity of the CFRP mast is still smaller than of the Al. mast.

8 Discussion

Assuming the validity of the laminate theory CFRP masts can be designed with the help of design graphics based on it. To optimize the mast with respect to mass it is necessary to know the critical requirements. In the discussed example it was assumed that the lowest flexural rigidity was normative. The lightness of the mast is promoted by the assumption of a low torsional rigidity. The question of the lowest limit can only be answered in practice.

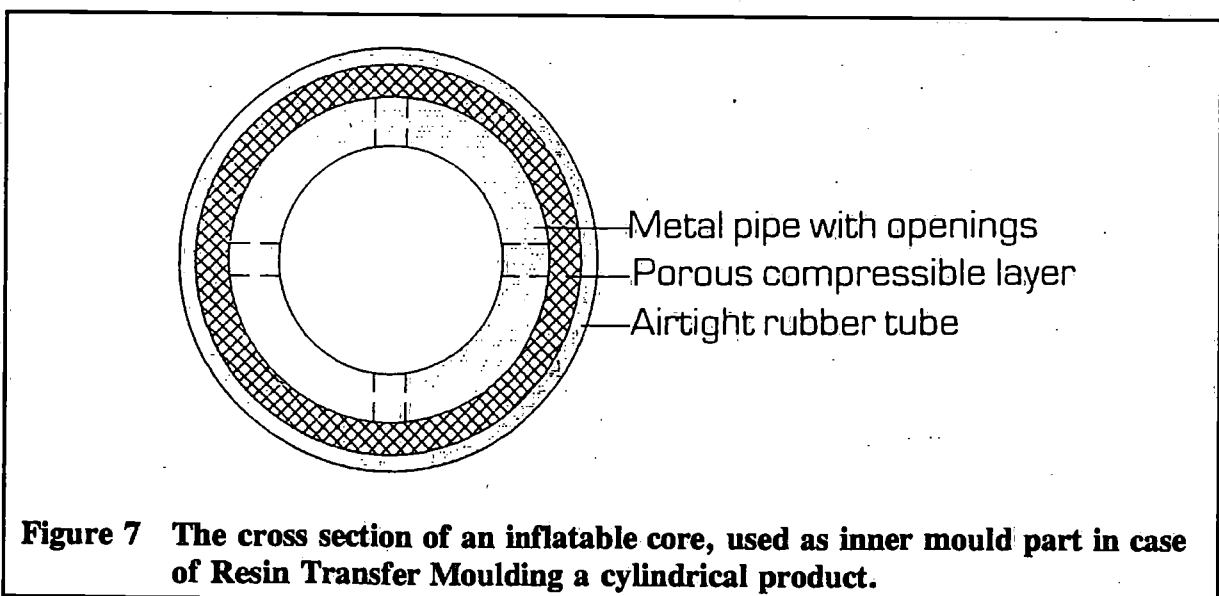
The tested CFRP mast sections consisted of two identical shells glued together. The shells were moulded in an open mould by vacuum film injection. This method is relatively simple and cheap.

The glued joint needs care and attention. The shells must have a non-twisted and non-bended form so that it is not necessary to force the shells when glueing together. As a device for the glueing process a closed mould with an inflatable bag as core can be used.

To avoid stress concentrations the edges of the shells must be tapered.

The best is to avoid openings in the wall of the mast. If there is an opening the moments of inertia of the removed area shall at least be compensated, for instance by a ring-shaped reinforcement around the opening on the inner side of the wall, in a radially tapered form to avoid peeling.

In our Laboratory a subject for final project is inspired by this issue, that is to make a device producing a cylinder in a closed mould by Resin Transfer Moulding, with the help of an inflatable core (Rouland [8]). This core is a rigid pipe, covered with a porous compressible layer and an airtight rubber tube outside (Figure 7). The fibre reinforcements can be wrapped up the core.



Compared to a built up of shells it is not so easy to make more complicated cross sections, for instance with a groove to store the rolled up sail, just like installing a reinforcing ring around an opening inside.

9 Conclusions

On the basis of a comparison of the measured values of compressive stiffness and buckling load of a CFRP mast section to the calculated ones, the following conclusions can be drawn:

- The CFRP mast behaves linear elastic till buckling.
- To correctly predict the compressive stiffness, one needs knowledge of the real properties of the components alone and in combination.
- The buckling load is considerably lower than the predicted value. Proportionally the difference between predicted and measured value is for the buckling load larger than for the compressive stiffness, perhaps due to inhomogeneity of the composite material.
- These conclusions are tentative: The FRP's show a relatively larger variation in properties than metals do.
For quantitative conclusions more tests are needed.
- The results of these investigations are encouraging regarding the technical feasibility of a CFRP mast and the sailing benefit of it due to lower weight.

References

- [1] Brush, D.O. & B.O. Almroth,
'Buckling of bars, plates and shells', New York, 1975.
- [2] Buisman, B.C.,
"Drukproeven op masten van met koolstofvezel gewapende kunststof en aluminium",
Technische Universiteit Delft, Lab. voor Scheepsconstructies, 1991.
- [3] Dubbel,
"Taschenbuch für den Maschinenbau", Berlin, 1981.
- [4] Enlund, H., A. Pramila & P.G. Johansson'
'Calculated and measured stress resultants in the mast and rigging of a Baltic 39 type yacht',
International Conference on Design Considerations for Small Craft, London, '84.
- [5] Harten, K. van, & A.H.J. Nijhof,
'Resin Transfer Moulding',
TU Delft, Faculteit WbMT, Vakgroep Vezeltechniek, 1991 (in Dutch).
- [6] Hütte,
"Des Ingenieurs Taschenbuch, 1. Theoretische Grundlagen", Berlin, 1955.
- [7] Jones, R.M.,
'Mechanics of composite materials', Tokyo, 1975.
- [8] Rouland, H.G.M.,
"Vervaardiging van een koolstofvezelversterkte mast d.m.v. vacuüm injectie met een opblaasbare kern",
TU Delft, Master's thesis, 1992.
- [9] Ten Cate Glas, Brochure "Carbon fibre", 88-5".
- [10] Tsai, S.W. & H.T. Hahn,
'Introduction to composite materials', Westport, 1980.
- [11] Young, W.C.,
'Roark's formulas for stress and strain', Singapore, 1989.

Design and Construction of the America's Cup Yacht "Challenge Australia"

by Dr. Peter van Oossanen

Van Oossanen & Associates.
Wageningen, The Netherlands.

Summary

This paper describes the design and construction of "Challenge Australia", the Australian yacht that challenged for the America's Cup in 1992. The races for this prestigious sailing trophy in 1992 were the first in the new International America's Cup Class, defined in 1988-1989. Special consideration in the paper is given to the mathematical model that was used for the investigation of optimum length, volume of displacement, sail area, and other design parameters. The model tests carried out for the enhancement and validation of this mathematical model are described and specific results given and discussed. The final design and construction of the canoe body and the chosen keel configuration, and the performance thereof, is dealt with in detail. An account is also given of the performance of the yacht in the actual races for the America's Cup, together with an explanation for not performing as well as expected.

1 Introduction

From May 1989 through to February 1992, the author was head of the design team for the Australian Challenge for the America's Cup (ACAC). Together with David Lugg (structural design) and Neil Loveland (design draughtsman), he was responsible for the design of "Challenge Australia", which participated in the races for the America's Cup, of San Diego, early in 1992. This was the first America's Cup in which the new International America's Cup Class (IACC) yacht was used.

The ACAC Syndicate had available a relatively small budget, allowing for the design and construction of only one yacht. This required that all of the research into the merits of different design configurations had to be carried out by mathematical modelling and model testing since comparative, side-by-side, full-scale experimentation requires two or more yachts. It was therefore decided to utilize 18 months of the available time for research and design-oriented work, and to start building the yacht no sooner than October 1990, leaving about 9 months for the building programme and about 6 months for sailing, performance evaluation, crew training, etc, before the races for the America's Cup began.

While it was realized that other teams competing for the 1992 America's Cup had significantly greater budgets and more technical resources, it was also realized that if a novel canoe body, keel or rudder configuration could be found, leading to superior performance, it would be possible to bridge any superiority in speed the other participants may have, caused by having better sails, by better crew work, etc, resulting from having more facilities and better crew training possibilities. It follows that the crux of the ACAC campaign plan lay in the

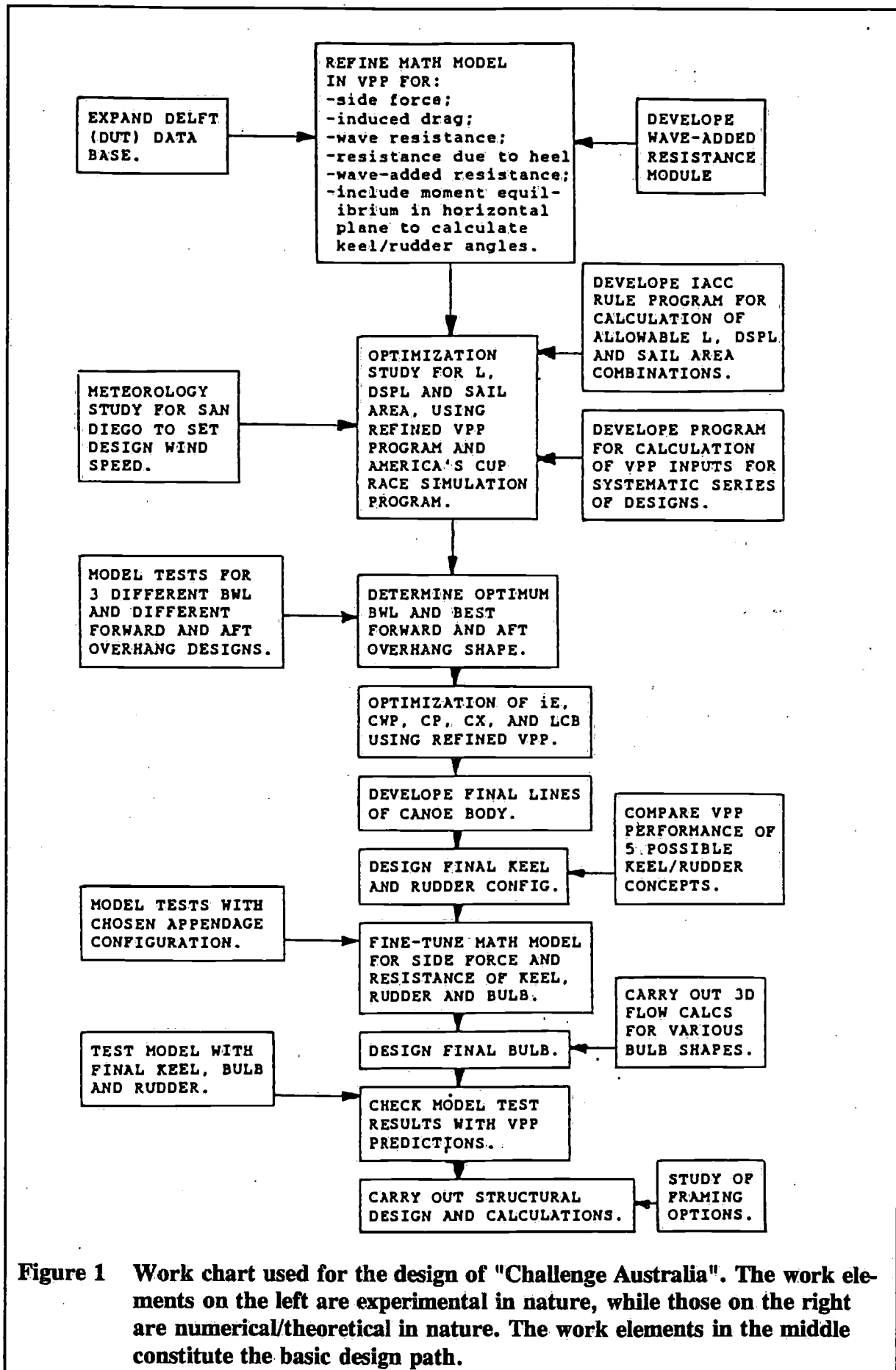


Figure 1 Work chart used for the design of "Challenge Australia". The work elements on the left are experimental in nature, while those on the right are numerical/theoretical in nature. The work elements in the middle constitute the basic design path.

research, development and design area, this being another reason to reserve more than half of the available 32 months for this part of the campaign.

This paper describes the research and design work carried out, starting with the initial model test programme to generate a side force and resistance data base (Paragraph 4), the work done to improve the author's VPP used for determining the optimum length, displacement and sail area (Paragraph 5), the optimization study itself (Paragraph 6), the meteorology study for San Diego (Paragraph 7), the second series of model tests to determine the optimum waterline beam and the best type of overhang forward and aft (Paragraph 8), the design of the final canoe body and appendages (Paragraph 9), the final series of model tests (Paragraph 10), and the structural design and construction of the yacht (Paragraph 11). Finally, in Paragraph 12, an explanation is given for the yacht's non-optimum performance in San Diego, followed by some final remarks and conclusions.

2 Adopted design methodology

An intricate plan was drawn up, composed of many mathematical modelling and model experimentation elements. This is shown in Figure 1, where the various work-elements are indicated in rectangular blocks.

An approach such as outlined in Figure 1 is essential in order to determine the canoe body and appendage configuration with the best performance. The central role herein of a mathematical model (VPP) for the calculation of the speed of a specific design is necessary in order to investigate the desired value of design variables such as length, displacement, sail area, waterline beam, canoe body draught, stability, longitudinal position of the centre of buoyancy, prismatic coefficient, size of keel and rudder, etc. It is not possible to investigate all of these design variables by model or full-scale testing, or a combination thereof, due to the sheer magnitude of the number of variables, while few, if any, yacht designers can make accurate judgements about the required value of a large number of these variables on the basis of experience alone, particularly as the IACC yacht constitutes a new class.

On taking the inevitable decision to use a mathematical model, i.e. a computer program for the investigation of the main design variables, it is important to possess a sound knowledge of the strong and weak points of this mathematical model. In the case at hand, the author's VPP was used which incorporates the results and experience of many previous projects. Although this VPP has been continuously updated and improved over the last years, it was considered to be not accurate enough in certain areas. A relatively large effort was made to improve the mathematical modelling in those areas. Even so, the final decision with respect to the required waterline beam, longitudinal position of the centre of buoyancy, and type of stem and stern overhang, were based on model testing rather than calculations. It was considered necessary, for the same reason, to validate the performance of the final design through a full series of model tests, before the building programme commenced.

3 The new America's Cup design and construction rule

The International America's Cup Class (IACC) Rule, according to which these yachts have to be designed and built, came into being in 1988-1989, after Dennis Conner and the catamaran "Stars and Stripes" defeated the 40 metre K-Class yacht "New Zealand" in an unfair match. All agreed that this should never happen again and it was decided to change the so-called "Deed of Gift" governing the America's Cup event, to no longer allow a challenger to challenge for the Cup under the original terms thereof with respect to the type of yacht,

but only in a special, America's Cup Class yacht. An account of this, for future America's Cup events very important development, has been given by Kirkman (see Reference 1), Chance (Reference 2) and Pedrick (Reference 3), amongst others.

In a number of meetings in 1988 and 1989, between would-be challengers and leading yacht designers, the overall parameters of the new class were defined to be as follows:

- An overall length of about 23 metres
- The length-displacement ratio to be in-between present-day IOR maxi yachts and so-called ultra-light displacement yachts (ULDB's), which was calculated to correspond to a mass between 16.000 and 25.000 kg, depending on measured length and sail area
- To disallow hiking wings and unusual canoe body shapes which, in practice, was interpreted to mean that the canoe body is not to have any hollows except in way of appendages
- A maximum beam of 5.5 metres
- A maximum draught to the bottom of the keel of 4.0 metres in the measurement condition
- A maximum of 2 rotatable appendages, the axis of rotation to be at a maximum of 45 degrees to the vertical
- A maximum height of the sloop rig of 32 metres, with the hoist of the genoa being 80% of that of the mainsail
- A maximum spinnaker area equal to 1.5 times the measured upwind sail area
- Construction of hull and deck to be based on commercial grade carbon epoxy composites over a Nomex honeycomb core, cured at up to 95 degrees Celsius at 1 atmosphere of pressure
- Construction of appendages and spars to be of higher grade carbon fibre, to be cured at up to 135 degrees Celsius in an autoclave at up to 5 atmospheres of pressure. Minimum skin thickness and weight of skins and core to be specified in 3 areas of the hull and deck.

The basic equation governing the value of measured length, measured sail area and displacement is based on the results of VPP predictions for about 500 designs. The formula derived by regression analysis, by the University of Southampton (see Reference 4) is:

$$(L + 1.25 \cdot S^{0.5} - 9.8 \cdot DSP^{1/5}) / 0.388 = 42$$

where:

L = Rated length in metres

S = Rated sail area in square metres

DSP = Rated displacement, equal to the mass in kg divided by 1025.

The rated length is given by the formula:

$$L = LM \cdot (1 + 0.01 \cdot (LM - 21.2)^8) + FP + DP + WP + BP$$

where: $LM = LBG + G$

Here,

LBG = Length of the hull between girth stations in metres. The girth stations are the vertical, transverse planes situated at the intersection of the waterplane 200 mm above the measurement flotation waterplane with the stem and stern of the hull, on the centre line

- G* = Function of the girth and slope of the topsides at the forward and aft girth stations, with a minimum value equal to 1.9 metres
- FP* = Freeboard penalty, defined as 4 times the sum of any freeboard deficiency at the forward, mid-length (i.e. 50% *LBG*), and aft girth stations, at which locations the minimum freeboards are 1.5, 1.25 and 1.2 metres in the measurement condition, respectively
- DP* = Draught penalty, defined as 4 times the excess draught
- WP* = Weight (i.e. mass) penalty, defined by formula for the case the mass is less than 16.000 kg or more than 25.000 kg
- BP* = Beam penalty, equal to 4 times the excess beam over the maximum value, in metres.

The rated sail area is given by:

$$S = SM \cdot (1 + 0.001 \cdot (SM^{0.5} - 16.9)^8)$$

where: $SM = MSA + I \cdot J/2$

in which:

- SM* = Measured sail area in square metres
- MSA* = Area of mainsail for which a formula is given based on the mainsail girths at 5 locations
- I* = Height of foretriangle in metres
- J* = Base of foretriangle in metres.

The original Rule document counts some 45 pages, while the interpretations issued since May 1989, covering all aspects of design and construction, count that much again (see Ref. 5).

4 First series of model tests: Generation of data base for side force and resistance

The length-displacement ratio of the IACC yacht is significantly greater than that of the 12-Metre Class yachts they replace, IOR yachts, and other displacement-type yachts, with the exception of ULDB'S. Typical values are given in Table 1.

Table 1 Typical values of the length-displacement ratio of different types of yacht

Type of yacht	Value of $LWL/VOLCB^{1/3}$
12-Metre Class	4.6
IOR max yacht	6.0
IACC yacht	7.0
ULDB yacht	8.0

LWL = Length of waterline in racing condition in metres
VOLCNCB = Volume of displacement of canoe body in m³

Since significant model testing has only been carried out for 12 Metre Class and IOR yachts, most designers of IACC yachts were suddenly confronted in 1989 with the problem of how to accurately determine the side force and resistance of these yachts without having to revert

to the towing tank for each design studied, specifically with respect to the prediction of wave resistance and its dependence on canoe body characteristics. Although existing VPP's will have provided a reasonable estimate for each design, an accurate determination of side force and resistance characteristics will generally not have been possible due to a lack of a suitable data base from which to derive formulae using regression analysis or appropriate relationships using some other method.

This was also the case when the design work for "Challenge Australia" was started.

To generate a data base on which to mathematically model the side force and resistance characteristics of IACC yachts accurately, a contract was entered into with the Delft University of Technology to expand their systematic series of yacht models, to cover the values of the length-displacement ratio, length-beam ratio, beam-draught-ratio, prismatic coefficient, and longitudinal position of the centre of buoyancy, of interest. Half of the costs of these tests were paid for by ACAC, subject to the condition that the results of these tests remain confidential till after the 1992 America's Cup. The values of the design variables of the 12 models added to the systematic series are given in Table 2.

Table 2 Values of design variables of the models added to the Delft Systematic Series of models, on behalf of the "Challenge Australia" project.

Model No	$LWL/VOLCB^{1/3}$	LWL/BWL	BWL/TC	CP	LCB
29	7.5	4.0	10.87	0.549	- 4.4
30	6.5	4.0	7.07	0.549	- 4.4
31	8.5	4.0	15.82	0.549	- 4.4
32	7.5	4.0	10.86	0.551	- 2.1
33	7.5	4.0	10.87	0.545	- 6.6
34	7.5	4.0	10.37	0.520	- 4.4
35	7.5	4.0	11.47	0.579	- 4.4
36	7.5	4.0	10.16	0.550	- 4.3
37	7.5	4.0	9.45	0.551	- 4.5
38	7.5	3.0	19.32	0.549	- 4.4
39	7.5	5.0	6.96	0.549	- 4.4

BWL = Maximum beam on the waterline
TC = Maximum draught of canoe body
CP = Prismatic coefficient
LCB = Longitudinal position of the centre of buoyancy in % of *LWL*, relative to the mid-length (50% *LWL*) location. A minus sign indicates that *LCB* is situated behind the mid-length location.

The standard keel and rudder of the Delft Systematic Series was used in these tests to render the results comparable to those of the earlier 28 models. Totally new polynomial expressions were derived for the residual resistance at discrete values of the Froude number, using all of the 39 models.

The results of the tests with these earlier models have been published by Gerritsma et al (see Ref. 6 and 7). The results of the added 12 models, called series III, will be published by the Delft University of Technology as well (see Reference 8).

5 Refinement of Velocity Prediction Program

One of two basically different methods can be adopted in a mathematical model for the calculation of the speed of a sailing craft. The first and most frequently adopted method is to determine the thrust and side force developed by the wind on the sails and then to calculate at what boat speed, heel and leeway angles these aerodynamic forces make equilibrium with the hydrodynamic forces. Here, 3 equations are available to find these 3 unknowns, viz: force equilibrium in the horizontal plane, in the direction of the boat speed vector and in the direction at 90 degrees thereto (the hydrodynamic lift direction), while the third equation involves the heel angle and moment equilibrium of all forces in the vertical, transverse plane.

The second method, less often adhered to, is to assume a specific value for the boat speed and the leeway angle, and to calculate the hydrodynamic side force and resistance in a straight-forward manner. Knowing the boat speed and the resultant hydrodynamic force, the calculation of the resultant aerodynamic force on the sails, for equilibrium, is a relatively simple matter. This, in turn, permits the calculation of the apparent and true wind speeds and angles. On performing these calculations for a series of leeway angles from 0 degrees to, say, 12 degrees, all the points-of-sail ranging from running square before the wind, to sailing high-on-the-wind, are covered. An interpolation method then yields boat speed, heel angle, leeway angle, etc, at any required value of the true or apparent wind speed and angle.

This second method has been adopted by the author in his VPP. Apart from the mathematically more simple process for finding the conditions for aerodynamic-hydrodynamic equilibrium, it places the hydrodynamic properties of the canoe body and its appendages in a more central role than does the first method. This results in a favourable situation with respect to mathematical modelling since much more is known about hull hydrodynamics than is known about rig and sail aerodynamics, by virtue of the fact that towing tank testing has yielded a wealth of information while, by comparison, little is known about the forces on the individual sails. The various modules in the program are as follows:

Input Part

- 1 Input of values for all geometric "design" parameters
- 2 Input of values for density of air and water, viscosity of air and water
- 3 Input of matrix of boat speed and leeway angles for which calculations have to be done
- 4 Input values for the rotation angle of rotatable appendages (such as trim tab and rudder) if these are not to be calculated by the program, which has the option of utilizing the condition that the moments of all forces in the horizontal plane must also be zero.

Hydrodynamic Part

- 5 Provide first estimate of heel angle
- 6 Calculate side force of canoe body and all appendages
- 7 Calculate induced drag of canoe body and all appendages
- 8 Calculate skin friction and pressure drag of canoe body and all appendages
- 9 Calculate wave resistance of canoe body and of any appendage piercing the water surface
- 10 Calculate resistance due to heel
- 11 Calculate stability (GZ curve)
- 12 Calculate centres of all hydrodynamic forces on canoe body and appendages and

- calculate resultant force and its point of application (in x , y and z coordinates)
- 13 Calculate or input the height of the vertical centre of the resultant force on the sails
 - 14 Calculate the heeling moment
 - 15 Calculate the effect of crew weight and position on GZ curve
 - 16 Calculate new heel angle by equating heeling moment to righting moment
 - 17 If heel angle is greater then the value at which sails are "reefed" then limit heel angle to this value and adjust the height of the vertical centre of the sail force or shorten foot length of sails
 - 18 Repeat steps 6 through 17 until heel angle value has converged.

Aerodynamic Part

- 19 Estimate a first value for the apparent wind angle and make a first estimate of what sails are being used
- 20 Calculate the lift and drag forces on each sail (CLs and CDs), based on the assumed apparent wind angle
- 21 Calculate the resultant aerodynamic force and associated drag angle equal to $ARCTAN(CDs/CLs)$
- 22 Calculate a new value for the apparent wind angle by equating the resultant aerodynamic force direction opposite to the resultant hydrodynamic force direction (the sum of the hydrodynamic and aerodynamic drag angles is equal to the apparent wind angle plus the leeway angle)
- 23 Determine which sails are being used, based on the calculated apparent wind angle value (spinnaker versus jib or genoa, for example)
- 24 Repeat steps 20 through 23 until the value of the apparent wind angle has converged
- 25 Calculate the apparent wind speed by equating the resultant aerodynamic force equal to the resultant hydrodynamic force
- 26 Calculate true wind speed and angle from the apparent wind speed and angle and the boat speed
- 27 Correct the calculated true wind speed and apparent wind speed and angle for a standard wind gradient, to derive the values valid for the top of the mast where the wind sensing gear is fitted.

Added Resistance due to Waves Part

- 28 If true wind is forward of abeam calculate added resistance due to waves on providing either inputs for wave height and period, or fetch and duration of wind over fetch.
- 29 Repeat steps 12 through 27 until wind direction and speed no longer change, that is until the calculated added resistance due to waves has converged.

Interpolation Part

- 30 Repeat steps 5 through 27 for all boat speeds and leeway angles prescribed (usually about 30 boat speeds and about 50 leeway angles per boat speed), filling a set of two dimensional arrays for such important quantities as boat speed, leeway angle, heel angle, total side force, total resistance, apparent wind speed and angle, true wind speed and angle, etc.

- 31 Interpolate to find the required performance for previously input values of true wind speed and angle.

Output Part

- 32 Output of performance in tables and graphs.

The author's VPP, has 3 modes of operation. The first of these is a detailed output mode, which gives the results of all of the hydrodynamic and aerodynamic calculations for each speed and leeway angle combination considered. This mode is utilized when detailed design problems need to be addressed and not the overall performance of the vessel. Because of the vast amount of output generated in this mode, only a few boat speed-leeway angle combinations can be addressed in one run of the program. The second mode of operation gives one line of output for each boat speed-leeway angle combination, printing the calculated values of the main parameters, such as heel angle, sail thrust and sail heel forces (equal to the total resistance and hydrodynamic side force respectively), apparent and true wind speeds and angles, and the speed-made-good to windward. The third mode of operation only outputs the results of the interpolated values for boat speed, speed-made-good to windward, and the true and apparent wind angles relative to the track of the yacht through the water, for the prescribed true wind speeds and angles, on which results the polar performance diagram is based. This program mode writes the polar performance data to an output file, which is read by the program that draws the polar diagram. To facilitate the editing of input files (over 100 variables have to be input for any configuration considered), special input and input file editing programs have been prepared.

6 Optimization study for length, displacement and sail area

6.1 Outline of Optimization Study

With the refined VPP, a systematic study was carried out to find that combination of length, displacement and sail area, allowed by the America's Cup rating formula, yielding the fastest time around the America's Cup race course. For this purpose a computer program was written, called "ACRULE", for the calculation of all of the variables stipulated by the IACC Rule once the length between girths (*LBG*) and the displacement mass (*W*) are input. These variables were treated as the main, independent variables.

With the Rule parameters calculated in this way for each design (described more fully in Paragraph 6.2.1), a weight and stability calculation was then carried out and the remaining VPP inputs determined, using another computer program, called "ACDESIGN", specially written for this task as well (see Paragraph 6.2.2).

For each design, the speeds calculated by the VPP on each of the legs of the America's Cup course were tabled in LOTUS 123 for different true wind speeds and a set of races were simulated in the computer in which the wind speed remained constant or was allowed to fluctuate according to specific, prepared scenarios (see Paragraph 6.3). Investigation of the results clearly revealed the sensitivity of length, displacement and sail area on the race results and it was relatively simple to determine the optimum values of these 3 main design variables, once the applicable wind speed scenario had been determined.

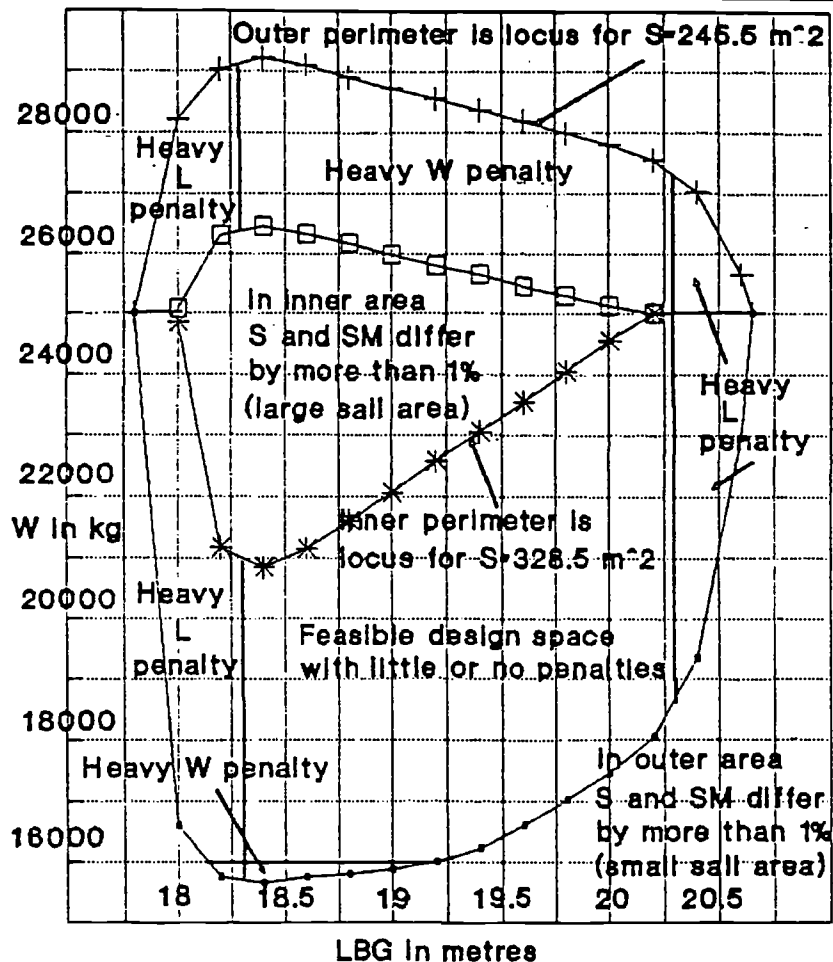


Figure 2 The design space allowed by the IACC Rule is considerably larger than area in which little or no penalties are incurred

6.2 Generation of Systematic Series of Designs

6.2.1 IACC Rule-Requirements for Each Design

The ACRULE program, specially prepared for this systematic study, requires inputs for the girths forward and aft, topside angles forward and aft, freeboards, and the maximum beam and maximum draught, in addition to *LBG* and *W*. The program then calculates all of the dependent design values, including the sail area of the mainsail, genoa and spinnaker, assuming maximum hoist values and using previously determined data on the required type of mainsail roach, in the form of (non-dimensional) mainsail girths, and the ratio of genoa area to total sail area. In the program, a maximum and minimum value of the upwind sail area is adhered to, to obtain practical designs. If the input values for *LBG* and *W* give rise to too large or small a sail area, the program allows modification of one or both of these inputs to obtain a design with a previously determined maximum or minimum sail area.

The initial matrix of designs and the associated selection of *LBG*, *W* and *S*, was based on wanting to cover the entire design space, not only the design space without penalties. The entire design space is shown in Figure 2, from which follows that heavy (length) penalties, leading to substantial reductions in sail area, arise when *LBG* is less than about 18.3 m and greater than about 20.3 m. Likewise, substantial reductions in sail area arise when *W* is less than 16.000 kg or greater than 25.000 kg. In this figure the adopted maximum and minimum rated sail area (*S*) is that value for which the corresponding measured sail area (*SM*) is no more than about 1% smaller than *S*. It was thought that larger or smaller values of *S* would

result in too much of a sail area penalty. It should be remarked, however, that during the America's Cup races it became apparent that in the light conditions prevailing off San Diego, a large sail area was extremely important and this, above all else, was being adhered to by most of the designers, often leading to a trade-off with length and displacement in such a way that the difference between S and SM was greater than 1% of S . The final values (prior to Round Robin 2), for "Challenge Australia", after her rated length was reduced by 0.73 m, was $S = 349.7 \text{ m}^2$ and $SM = 339.6 \text{ m}^2$, i.e. a difference of about 2.9%.

Table 3 Values of the length between girth stations (LBG) and displacement mass (W) used in the initial part of the optimization study.

Length between girths (LBG) in metres	Mass of displacement (W) in kg				
18.2	15748,	16000,	19802,	21171	and 26320
18.6	15741,	16000,	18564,	21126	and 26337
19.0	15888,	16000,	19028,	22055	and 25998
19.2	15964,	16000,	19255,	22544	and 25824
19.4		16214,	19627,	23040	and 25652
19.8		17019,	20538,	24057	and 25307
20.2		18049,	21524,	and 25000	
20.6		22986,	23993	and 25000	

The initial matrix of LBG and W values, for which the optimization study was carried out, is given in Table 3. For each length up to 5 displacement and (corresponding) sail area values were chosen, thereby covering a large part of the permissible W and S values for that length. A small value of the displacement W corresponds with a small value of S , while for a large mass a large value of S is possible. On increasing W to over 25,000 kg, however, the value of S decreases again because of the heavy W penalty that then comes into play. For the wind conditions prevailing off San Diego it was not considered worthwhile to investigate the performance of designs in this latter regime in detail.

Further combinations were studied in the region of best performance, after the associated LBG and W values thereof had been ascertained.

The program prints a complete formula calculation, with penalties and sail measurements, in the format adhered to in the IACC Rule documentation. An example of part of the output of this program is given in Table 4.

6.2.2 VPP Inputs for Each Design

For each design, the required inputs for the VPP calculations was generated in a systematic way using a program that was specially written for this task, called "ACDESIGN". This program uses the output values of ACRULE, in addition to predetermined values for the ratio of various design variables, the mass of the various components of the structure and equipment on board, the vertical centre of gravity thereof, etc.

The ACDESIGN program starts with the calculation of the design variables for the "racing" condition of the yacht as opposed to the variables valid for the "measurement" condition,

calculated by the ACRULE program. Inputs have to be provided concerning the mass and centre of mass of the crew, additional gear and sails, etc, that are on board during racing, and not included in the displacement W .

Table 4 Example of part of output of program for the calculation of IACC Rule parameters, for which values of LBG , W , freeboards, girths, topside angles, maximum draught, etc, have to be input.

-	Input value of overall length in metres;	24.123
-	Input value of length of aft overhang in metres;	2.033
-	Calculated length of forward overhang in metres;	1.890
-	Input value of forward topsides angle in degrees;	20.000
-	Input value of aft topsides angle in degrees;	45.000
-	Input value of forward girth (FG) in metres;	2.750
-	Input value of aft girth (AG) in metres;	3.933
-	Calculated value of forward beam correction (FBC);	-0.116
-	Calculated value of aft beam correction (ABC);	0.000
-	Calculated value of forward girth correction (FGC);	0.300
-	Calculated value of aft girth correction (AGC);	1.600
-	Calculated value of girth component of L in m (G);	1.900
-	Input value of freeboard at forward length mark in m;	1.500
-	Input value of freeboard at mid- LBG location in m;	1.250
-	Input value of freeboard at aft length mark in m;	1.200
-	Calculated value of freeboard penalty (FP);	0.000
-	Input value of draught to bottom of keel in m (D);	4.000
-	Calculated value of draught penalty (DP);	0.000
-	Input value of maximum beam in metres (B);	5.000
-	Calculated value of beam penalty (BP);	0.000
-	Input value of length between girth stations (LBG);	20.200
-	Input value of mass of displacement in kg (W);	25000.000
-	Calculated value of mass penalty (WP);	0.000
-	Calculated value of rated displacement in m^3 (DSP);	24.390
-	Calculated value of measured length in metres (LM);	22.100
-	Calculated value of rated length in metres (L);	22.195
-	Calculated value of rated sail area in m^2 (S);	324.615
-	Calculated value of measured sail area in m^2 (SM);	323.885
-	Assumed height of mast datum band above sheer;	0.500
-	Assumed height of boom above datum (BAD);	1.500
-	Assumed height of upper mast band above datum;	32.000
-	Input value of clew offset of mainsail in metres (CO);	0.000
-	Input value of ratio of genoa area to total sail area;	0.306
-	Calculated mainsail girth along boom in metres ($E5$);	10.253
-	Calculated value of E4 mainsail girth ($E4/E5=0.931$);	9.544
-	Calculated value of E3 mainsail girth ($E3/E5=0.813$);	8.332
-	Calculated value of E2 mainsail girth ($E2/E5=0.585$);	6.001
-	Calculated value of E1 mainsail girth ($E1/E5=0.082$);	0.837
-	Calculated value of measured mainsail area in m^2 ;	224.835
-	Calculated value of measured foretriangle area in m^2 ;	99.050
-	Assumed value of hoist of genoa in metres (I);	25.600
-	Calculated value of foretriangle foot in metres (J);	7.738
-	Calculated spinnaker pole length in metres;	10.447
-	Calculated value of spinnaker area in m^2 ;	485.828

Inputs then have to be provided for the beam on the racing-trim waterline, the prismatic coefficient, waterplane area coefficient, maximum transverse area coefficient, and the volume, in % of the total displacement volume, of the combined appendages.

With these inputs, together with the values for *LBG* and *W*, the calculation of the total volume of displacement and canoe body volume of displacement is carried out. The overall length and beam, waterline length, length of forward and aft overhang, etc, is then determined using a set of constants for the ratios *LOA/LBG*, *LWL/LBG*, *BMAX/BWL* (with *BMAX* limited to a maximum of 5.5 metres), etc. These were determined from a "parent" design on which all other designs considered in this optimization study were based. The value of the canoe body draught and the maximum draught in the racing condition follow directly from the inputs supplied after some mathematical manipulation.

The calculation of the mass and vertical centre of mass is carried out on the basis of formulae for each component of the structure, equipment and crew on board. These are based on a detailed study of the carbon structure of hull and deck, spars and rigging, sails, winches, etc. The amount of lead ballast is determined by simply subtracting the mass determined in this way from the total mass of displacement. A calculation is then carried out to determine the amount of ballast carried in the bulb at the bottom of the fin keel. The previously-supplied input specifying the total volume of the appendages is used for this purpose. If all of the ballast cannot be housed in the bulb, the vertical position of the centre of mass of the lead that has to be fitted elsewhere has to be input. The keel fin and rudder geometry are kept the same. Only the bulb size is varied in accordance with wanting to house most of the ballast therein. An example of the output of ACDESIGN is given in Table 5.

6.3 Some Typical Results

The results of the VPP calculations revealed that length and sail area are extremely important and that an increase in displacement, to gain more length and sail area, is worthwhile. In fact, it became clear that the maximum displacement without penalty needs to be adopted in order to maximize performance in every wind speed over 8 knots. This is revealed in Figure 3 where the time around the America's Cup race course in decimal hours is set out against the length between girth stations in metres for different true wind speeds at the mast-head. The curves shown, for different wind speeds, seem to be rather insensitive with *LBG* but in actual fact the opposite is true. The differences between the various designs add up to several minutes over the course, except for 8 knots of true wind speed, for which the overall performance is almost independent of *LBG* for the 4 designs here considered. The results of Figure 3 are for a maximum value of the displacement *W*, without penalty, and a constant waterline beam of 4 metres.

Many more results of this type were studied. All of these pointed to the same conclusion, viz; that in more than 8 knots of true wind the optimum performance is obtained for the maximum *LBG* length (around 20.2 metres) and the maximum displacement of 25.000 kg, without penalties. At 8 knots of true wind speed or less, however, optimum performance favours a smaller length and medium values of the displacement and sail area.

7 Meteorology study to determine design wind speed

To ascertain the wind conditions on the proposed race site off San Diego, one of Australia's leading marine meteorologists was requested to carry out a wind study. His report (see Reference 9) revealed that 90 percent of the measured wind speed values, between 12.00 and 17.00 hours, at Lindbergh Airport in San Diego and nearby Mission Bay, in March, April and May, were between 7 and 14 knots, with an average value between 10 and 11 knots.

Wind speeds on the actual race course were predicted to be between 6 and 13 knots. These values were at 10 metres above sea level and by allowing for a standard wind gradient with increasing height above sea level, these values were interpreted to be between 8 and 15 knots, with an average value in-between 11 and 12 knots, at the mast-head. With this result it was concluded that the "small boat" option was not a viable one.

Table 5 Example of part of output of the program used to generate a systematic series of designs for the (VPP) study of the optimum length, displacement and sail area.

-	Code number of design		20225	
-	<i>LBG</i> length in metres;		20.200	
-	Mass <i>W</i> in measurement condition in kg;		25000.000	
-	Length of waterline in racing trim flotation in m;		19.131	
-	Overall length in metres;		24.123	
-	Maximum beam of waterline in racing trim flotation;		4.000	
-	Overall, maximum beam in metres;		5.000	
-	Total volume of displacement in m ³ ;		26.349	
-	Volume of displacement of canoe body in m ³ ;		23.910	
-	Maximum draught to bottom of bulb in racing trim;		4.038	
-	Maximum draught of canoe body in racing trim in m;		0.907	
-	Average chord length of keel in m;		1.500	
-	Height of keel fin in metres;		2.431	
-	Average chord length of rudder in metres;		0.700	
-	Height of rudder in metres;		2.500	
-	Maximum height of bulb in metres;		0.700	
-	Maximum width of bulb in metres;		1.000	
-	Maximum length of bulb in metres;		5.946	
-	Volume of bulb in m ³ ;		1.847	
-	Mass of total yacht in racing trim in kg;		27056.207	
-	Vertical centre of mass of yacht above racing trim waterline in metres;		-2.13	
	Item	Weight in kg	VCG	
			Weight in %	
-	Hull and deck;	2074.09	0.45	7.67
-	Deck fittings;	928.04	1.40	3.43
-	Spars;	901.90	13.02	3.33
-	Keel fin;	342.13	-1.88	1.26
-	Rudder and steering;	59.25	-1.25	0.22
-	Sails;	303.11	8.34	1.12
-	Running rigging;	113.10	1.28	0.42
-	Batteries, elect.;	150.00	1.28	0.55
-	Crew;	1440.00	1.78	5.32
-	Sails, etc, below;	500.00	0.00	1.85
-	Ballast;	20244.59	-3.76	74.83
-	Other ballast;	0.00	0.00	0.00
-	Total, racing;	27056.21	-2.13	100.00

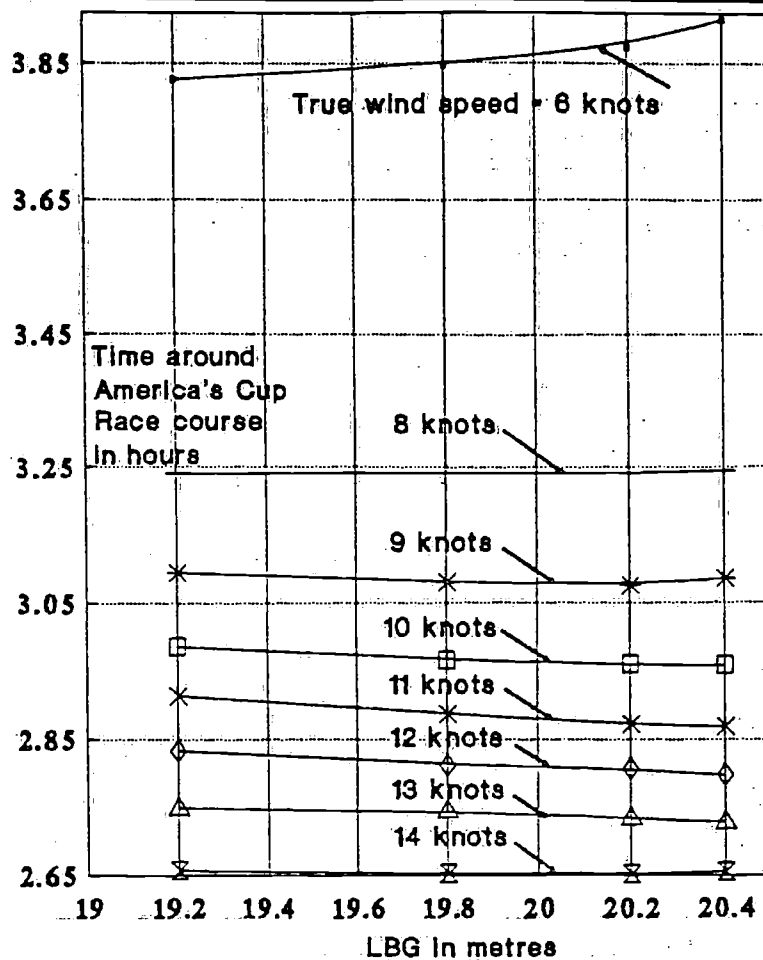


Figure 3 Calculated time around the initially-proposed America's Cup race course (21.9 nautical miles) for designs with maximum displacement (N), without penalty. The initial VPP study revealed that in over 8 knots of true wind the optimum LBG was 20.2 metres and the optimum W was 25.000 kg.

8 Second series of model tests: Determination of waterline beam, *LCB*, and type of forward and aft overhang

At this stage linesplans were designed for the manufacture and testing of 5 models at the Delft University of Technology. These tests were aimed at addressing 3 problem areas which could not be satisfactorily dealt with in the VPP study. These were: the determination of the optimum waterline beam (*BWL*), the determination of the optimum position of the longitudinal centre of buoyancy (*LCB*), and the type of forward and aft overhang. In each case the VPP was considered either not accurate enough to pin-point the desired value (in the case of *BWL* and *LCB*), or the VPP could not address the problem adequately at all (type of overhang). The design of these 5 models was kept as similar as possible in order to only vary the parameters that had to be studied. The first 3 models, models A, B and C, had varying waterline beam (3.5, 4.0 and 4.5 metres) and an *LCB* position corresponding to a distance of 3.5% of *LWL* behind the mid-*LWL* location. A modest 12-Metre type of bow overhang was adopted, similar to that of the mini-America's Cup day-sailers designed by the author's team early in the project. A drawing of this mini AC design, two of which were built for the purpose of evaluating mainsail and spinnaker shapes, the best ratio of genoa area to total sail area, etc,

is given in Figure 4. These yachts are 40% of a full size, "mid-Rule", America's Cup yacht. They were later used by the crew to gain more match-racing experience.

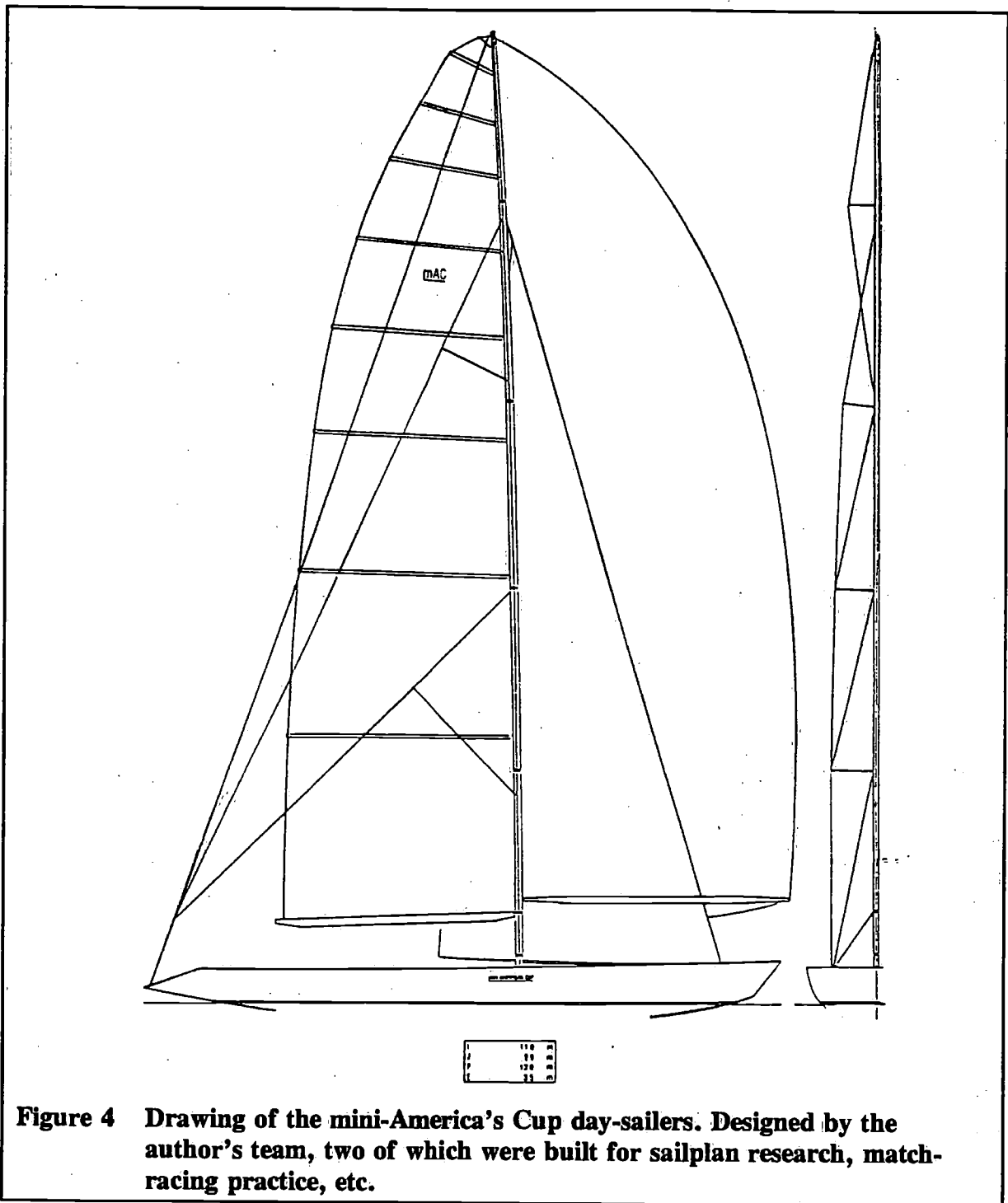


Figure 4 Drawing of the mini-America's Cup day-sailers. Designed by the author's team, two of which were built for sailplan research, match-racing practice, etc.

The fourth model, model D, was similar to model B except for a more aft position of the longitudinal centre of buoyancy (5.7% of *LWL* behind the mid-*LWL* location). Model E was similar to model B, except for the forward and aft overhang. A raked IOR type of stem was adopted while the overhang aft was eliminated and a skiff-type stern was adopted with a narrow waterline, somewhat similar to the design of the final New Zealand IACC yacht. A stern of this type is allowed by the IACC Rule and gives rise to an important increase in waterline length. The main particulars of these 5 models are given in Table 6.

Table 6 Main particulars of models A through E, used for determining the optimum waterline beam (models A, B, and C), to check the viability of positioning *LCB* further aft (model D), and to determine the effect of maximizing the length of the design waterline by adopting an IOR-type stem and a skiff-type stern.

Entity	Model A	Model B	Model C	Model D	Model E
- <i>LOA</i> (m)	24.619	24.398	24.430	23.996	22.246
- <i>BOA</i> (m)	4.501	4.977	5.500	4.830	4.746
- <i>LWL</i> (m)	18.974	18.798	18.660	18.860	19.892
- <i>BWL</i> (m)	3.500	4.000	4.500	4.000	4.000
- <i>TC</i> (m)	1.013	0.905	0.800	0.863	0.820
- <i>VOLCB</i> (m ³)	23.867	23.867	23.850	23.870	23.871
- <i>LCB</i> (% <i>LWL</i>)	-3.526	-3.681	-3.838	-5.669	-3.690
- <i>CP</i>	0.536	0.537	0.539	0.530	0.535
- <i>CB</i>	0.355	0.351	0.355	0.367	0.366
- <i>CWP</i>	0.672	0.670	0.674	0.676	0.661

- where	<i>LOA</i>	= Length over all
	<i>BOA</i>	= Beam over all
	<i>LWL</i>	= Length on the design waterline
	<i>BWL</i>	= Maximum beam on the design waterline
	<i>TC</i>	= Maximum draught of the canoe body
	<i>VOLCB</i>	= Displacement volume of the canoe body
	<i>LCB</i>	= Position of the longitudinal centre of buoyancy
	<i>CP</i>	= Prismatic coefficient of canoe body
	<i>CB</i>	= Block coefficient of canoe body
	<i>CWP</i>	= Area coefficient of design waterplane.

From the values presented in Table 6, it follows that these models did not constitute a true systematic series since variations occur in more than one variable at a time. Although the models A, B, C and D could have been derived from one parent model by transformation techniques, this was not done because of having to fulfil various IACC Rule requirements with respect to girths, slope of topsides, slope of the buttocks aft of the aft girth station, etc. This led to the decision to design each model separately (for which the hull design system "MACSURF" was used), leading to the variations identified.

One and the same keel and rudder configuration was used on each of the 5 models. A basic design was made for this purpose consisting of a fixed fin with an average chord length of 1.61 m and a height of 2.62 m. A simple axi-symmetric bulb with a length of 3.41 m and a maximum diameter of 0.7 m was fitted to the bottom of this fin. This bulb, filled with lead, was sufficient to obtain the stability of the fullsize yacht in the test tank.

The results of the upright resistance tests for the models A, B and C, as a function of Froude number, are given in Figure 5. Noticeable differences in the resistance values occur in the important speed range between the Froude number values of 0.35 and 0.45, and at relatively very high speeds, in excess of the Froude number value of 0.525. In the lower of these two speed ranges, model A is not much better than model B, but both are better than model C. In the higher speed range the differences are greater, favouring the more slender canoe body.

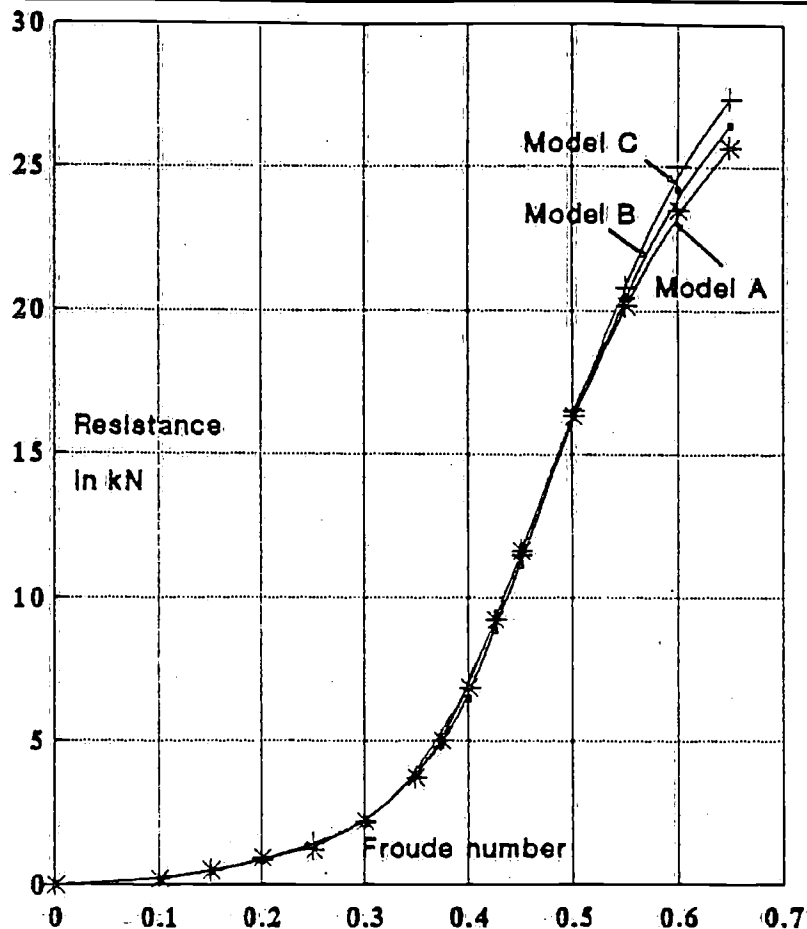


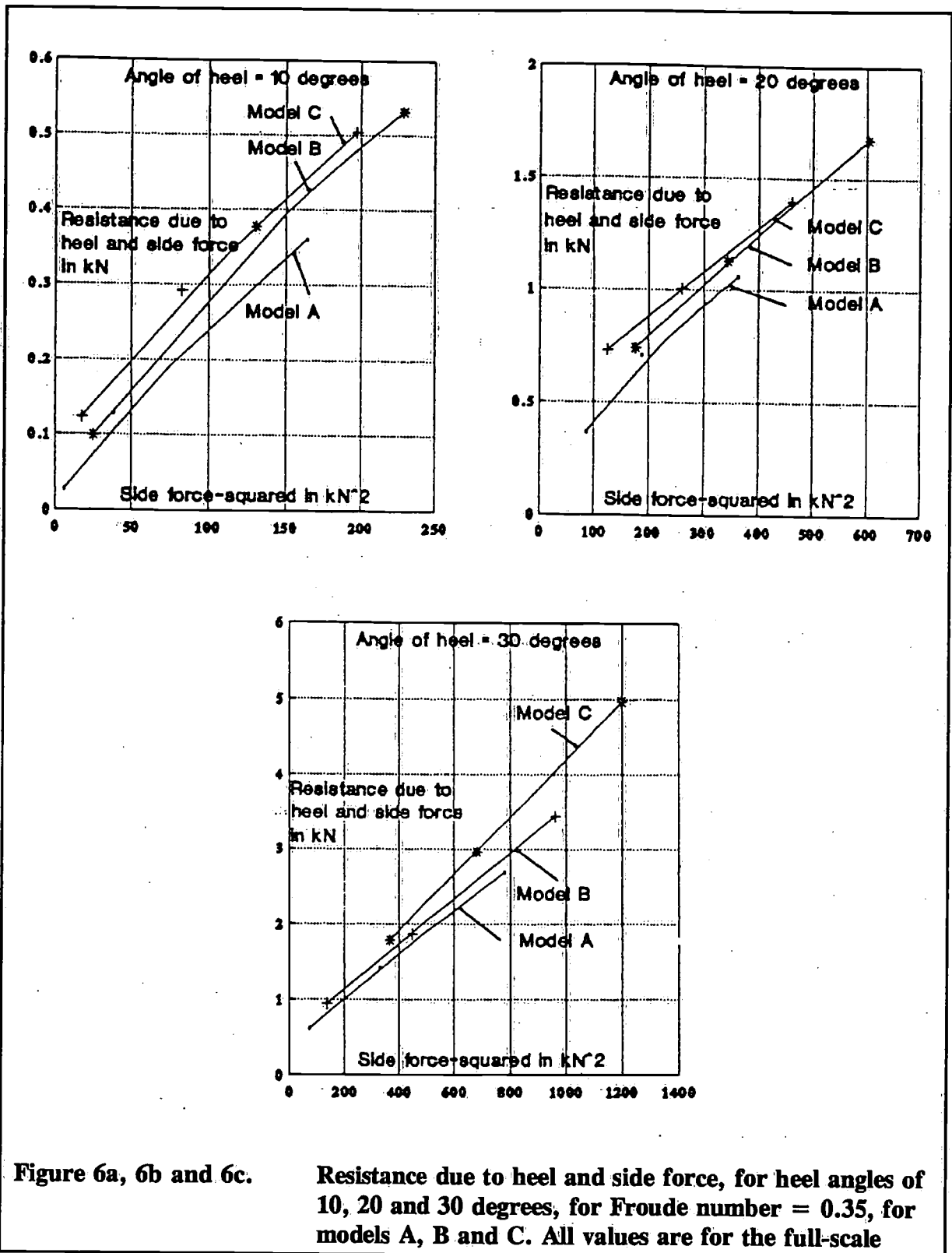
Figure 5 Comparison of the upright resistance of models A, B and C, each with a different waterline beam. The values are for the full-scale.

For the important Froude number value of 0.35, being approximately the maximum speed attainable on-the-wind, the resistance associated with heel and side force of Models A, B and C is shown in Figures 6a, 6b and 6c, for 10, 20 and 30 degrees of heel, respectively. This resistance increase is given as a function of the side force-squared. The fact that the lines shown are more or less straight, indicates that the resistance increase with increasing side force is mainly composed of induced resistance.

The resistance at zero side force is theoretically that due to heel alone. From these figures it follows that model A is better than model B, while model B is better than model C. The resistance due to heel for the 3 models, as can be deduced from these figures, is given in Table 7.

Table 7 Approximate full-scale values for the resistance due to heel alone for models A, B and C in kN, as determined from model tests.

Model identification	10 degrees of heel	20 degrees of heel	30 degrees of heel
A	0.01	0.22	0.40
B	0.04	0.45	0.53
C	0.08	0.50	0.46

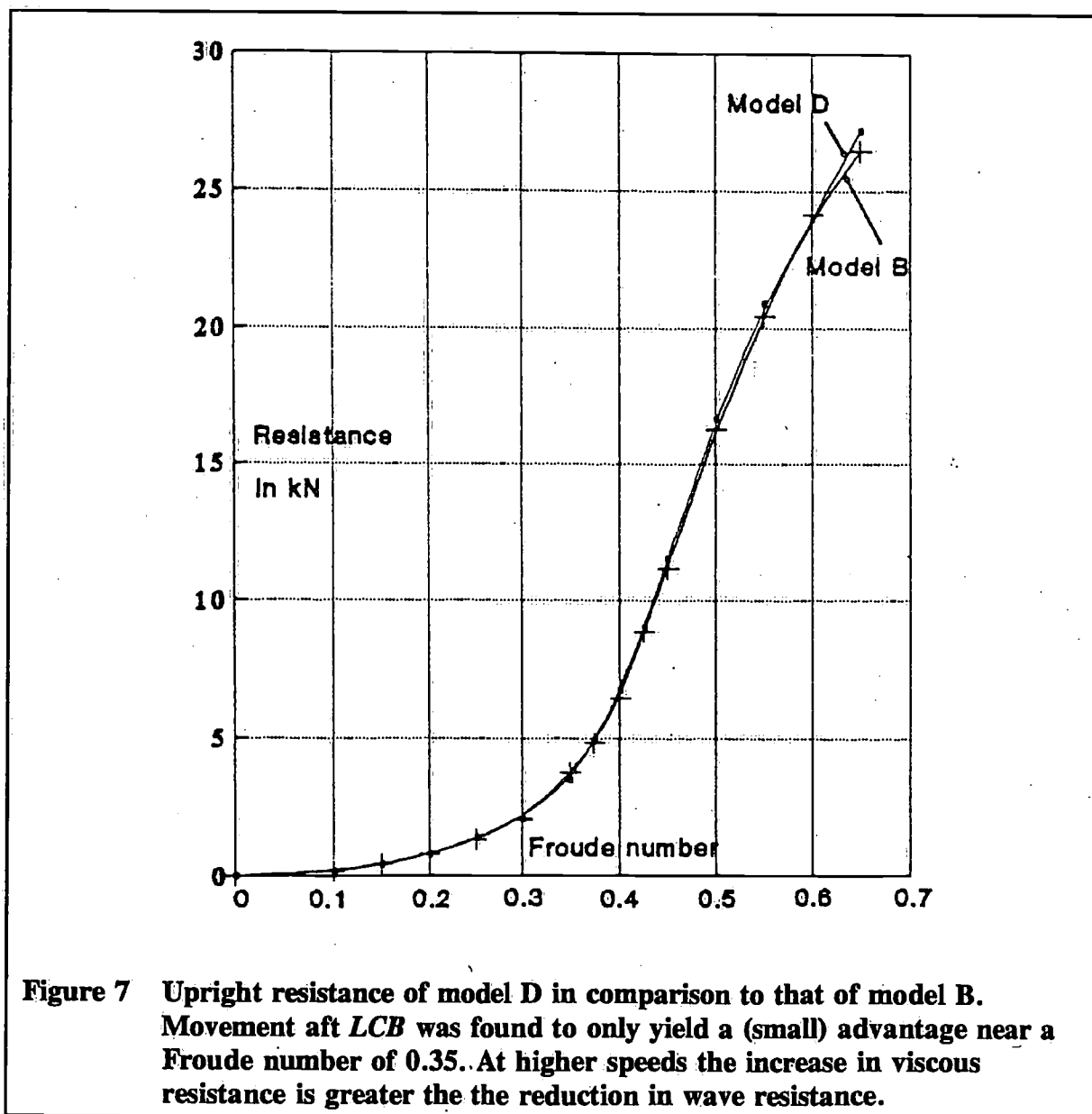


Although the keel and rudder of these 3 models are the same, the canoe body influence on the development of side force is different, primarily due to the differences in the BWL/TC ratio. The keel of model C has the smallest effective aspect ratio and hence the greatest induced resistance at equal side force values. This can be seen from the relatively steep slope of the resistance versus side force-squared line for model C in Figure 6c, valid for 30 degrees of heel (At other heel angles this is less noticeable). Model C has the largest BWL/TC ratio.

From analyses of this type for a range of speeds, and from additional VPP considerations involving the differences in (form) stability between the 3 designs, the conclusion was drawn that the *LWL/BWL* ratio should not be smaller than 4.5, from which the required *BWL* value was determined.

The upright resistance of model D, compared to model B, is shown in Figure 7. Although the scale of this figure is insufficient to properly determine the exact differences, it can be seen that in the Froude number range around 0.35, model D is marginally better. At higher speeds, however, this is not the case. The more slender forebody of model D, associated with the shift of *LCB* further aft, does not lead to sufficient reduction in wave resistance to offset the increase in viscous resistance caused by the fuller aft-body. Accordingly, a moderate *LCB* position was adhered to.

The results of the tests with the model possessing the long waterline (model E), realized by adopting an IOR-type stem and a skiff-type transom, was disappointing. The upright resistance was greater than for the otherwise equivalent model B over the entire speed range.



The analyses thereof revealed that the lack of overhang aft, and the associated lack of buoyancy due to the adopted narrow waterline aft, lead to appreciable trim down by the stern and greater wave resistance because of this, even though the waterline length was greater. The increased wetted area of this model was the cause of a greater resistance at low speeds.

Although the performance of model E could have been improved by adopting a greater water-plane area aft to reduce the encountered trim problem, this would have increased the wetted area and, thus, the resistance in the low-speed region. As demonstrated by the final New Zealand yacht, such a design is probably only feasible if moderate Rule dimensions are adhered to and not the maximum dimensions.

Further VPP analyses revealed that for the design wind speed of between 11 and 12 knots (see Paragraph 7), the average boat speed over the America's Cup course (as proposed in 1989) is approximately 10.2 knots. That is equivalent to a Froude number value of about 0.38. At this speed more than half of the resistance is associated with wave-making and the decision was therefore taken to maximize the design waterline length by adopting a raked IOR stem rather than a 12-Metre type overhang. The skiff-type stern was not adopted. As it turned out (see Paragraph 12), the wind conditions off San Diego were found to be significantly lighter than predicted, leading to importantly lower average boat speeds. If this had been realized during the design phase, a 12-Metre type of overhang would have been adopted leading to a lower wetted area and better performance in the lighter conditions.

9 Final design of canoe body and appendages

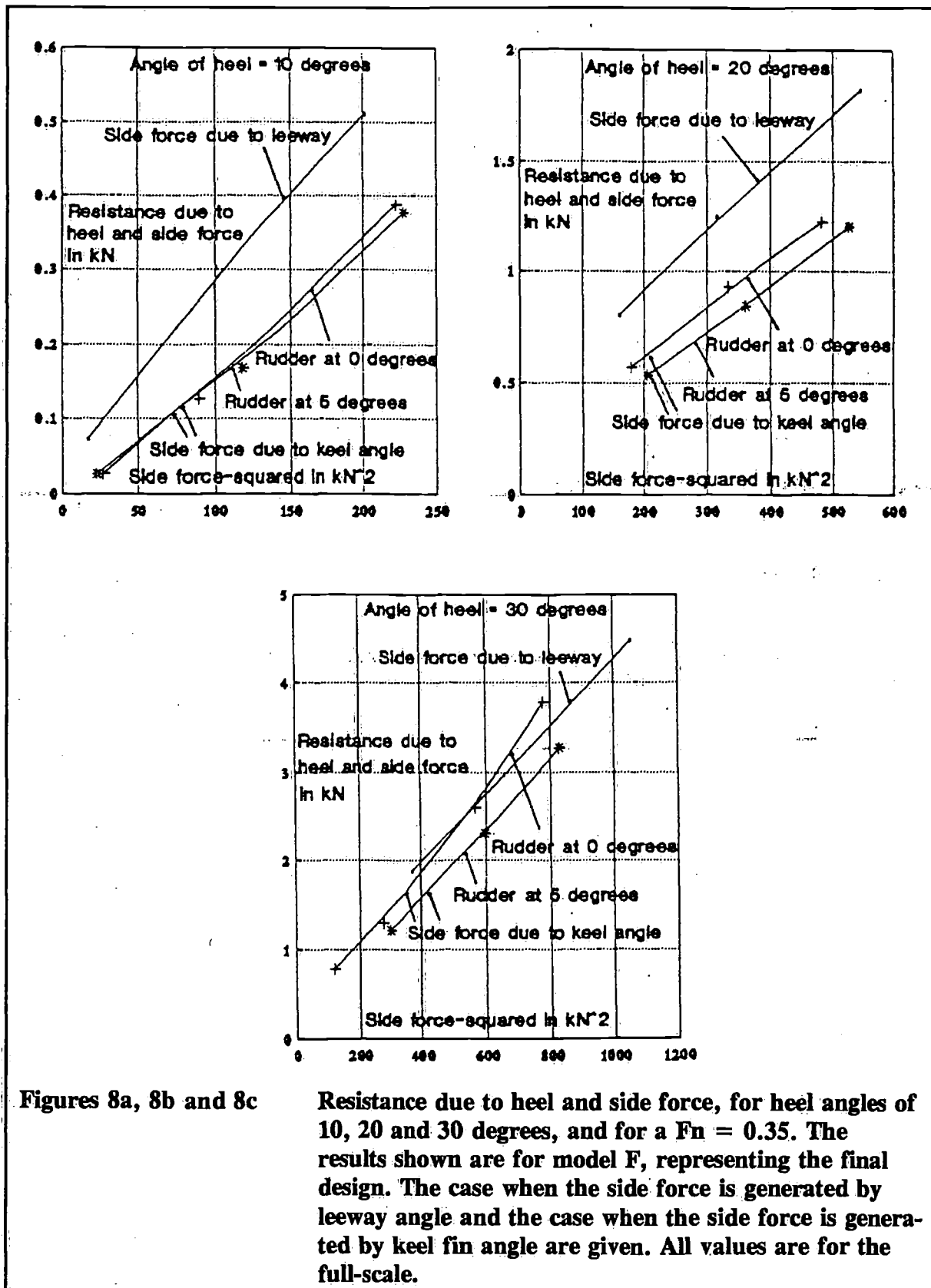
With the test results of models A, B, C, D and E, it was possible to finalize the design of the canoe body. Various sets of lines were developed and studied using MACSURF, all differing slightly within the bounds afforded by the fixed set of parameters that were deduced from the VPP and model test studies. Attention was paid to various details such as the free-to-trim characteristic with heel. Bow-down trim with increasing heel was minimized as much as possible, the final value being 0.7 degree of bow-down trim at 30 degrees of heel.

From the very beginning of the project design work on the appendages had been in progress. Five possible appendage configurations were defined as being potentially possible and interesting, within the confines of the IACC Rule. These were the following:

- A conventional keel fin with trim tab, connected to a bulb housing the ballast, and a conventional rudder
- A keel strut, connected to a bulb housing the ballast, a forward rudder and a conventional rudder
- A completely rotatable keel fin, around a fixed structural member connected to a bulb housing the ballast, and a conventional rudder
- A tandem keel with 2 struts, both connected to a bulb housing the ballast, one of the struts fitted with a trim tab, and a conventional rudder
- A tandem keel with 2 struts, both connected to a bulb housing the ballast, and both fitted with trim tabs, with no rudder.

In order to simulate the performance of each of these concepts in the VPP, the mathematical model therein was expanded to include a forward appendage. Either a free-hanging forward rudder or a fin/strut type appendage also fixed to the bulb, with or without a trim tab, was allowed for. The existing mathematical model was already capable to deal with a fully rotatable appendage. In order to be able to calculate the required (equilibrium) trim tab angle or

helm angle of forward or aft rudder, the VPP was further expanded to include the moment equilibrium equation for the horizontal plane, as explained in Paragraphs 2 and 5, requiring considerable study of the x , y and z coordinates of the centre of effort of all hydrodynamic and aerodynamic forces.



Figures 8a, 8b and 8c

Resistance due to heel and side force, for heel angles of 10, 20 and 30 degrees, and for a $F_n = 0.35$. The results shown are for model F, representing the final design. The case when the side force is generated by leeway angle and the case when the side force is generated by keel fin angle are given. All values are for the full-scale.

The VPP calculations for these 5 different appendage configurations revealed that considerable performance enhancement is possible on being able to reduce leeway to zero or almost zero. According to these results, the completely rotatable keel fin was particularly good in this respect. Although the structural arrangement thereof was not simple to achieve, it was superior to the other arrangements except for the tandem arrangement with twin trim tabs and no rudder. The seemingly insurmountable problems associated with balance and steering with this latter arrangement, particularly as the time on the water before the start of Round Robin No. 1 would be very limited, precluded further consideration thereof, however. Accordingly, it was decided to pursue the fully rotatable keel fin option.

The final design of the appendages was also based on considerable numerical work involving the "Doublet-Source Panel program, called "DSA", purchased from AeroHydro Inc., to determine the flow and induced drag-versus-lift characteristics of the various lifting surface options. The merits of fitting winglets on the bulb and lifting surfaces were also studied using DSA. Finally, a series of bulb shapes were developed using DSA and boundary-layer calculations. A particularly good design with low resistance and a low centre of volume was developed on the basis that the leeway angle would be very small. This bulb was subsequently cast and fitted, housing almost 20.000 kg of lead.

10 Third series of model tests: Validation of performance

A model of the final configuration was built and tested at the Delft University of Technology. The keel fin was made rotatable and a full matrix of keel fin angle and rudder angle values were investigated. The model test results compared very well with the numerical predictions and the design-performance was validated. Figures 8a, 8b and 8c show the resistance due to heel and side force at the Froude number value of 0.35, for the "conventional" case the keel is not rotated and the side force is realized by allowing the yacht to make leeway, and the case the keel is rotated and the yacht is sailed without leeway. The case for 10, 20 and 30 degrees of heel is considered.

It should be borne in mind that when, on-the-wind, the yacht is sailed at zero leeway, the case of zero helm yields virtually no side force on the rudder, while the conventional case of zero helm when making leeway yields an angle-of-attack of the flow into the rudder equal to about half of the leeway angle and, hence, appreciable side force on the rudder (see Reference 10 for example). The comparison of the resistance due to heel and side force of the yacht when sailed conventionally, to the case the rotatable keel is used, should be based on the situation that the rudder produces equal side force in both cases. Without straining the rudder, this is not possible however and, alternatively, rudder angles of 0, 5 and 8 degrees were investigated.

Figures 8a, 8b and 8c show the respective lines for 0 and 5 degrees of helm. At 10 degrees of heel, when the total side force is not large, the difference generated by 5 degrees of additional helm is small. The rotatable keel here leads to a modest resistance reduction of between 0.1 and 0.15 kN (about 3.1% of the upright resistance at that speed). At 20 degrees of heel the rotatable keel results in a major resistance reduction of between 0.4 and 0.55 kN, when 5 degrees of helm is used. This is about 11.9% of the upright resistance! At 30 degrees of heel the rotatable keel with zero load on the rudder is about equivalent to the conventional sailing situation. Again, when seeing this result, it should be borne in mind that zero helm in the conventional sailing case, when making leeway, results in a load on the rudder corresponding to an angle-of-attack of about half the leeway angle. At 30 degrees of heel the leeway angle is significant and the load on the rudder, at zero helm angle, also. Since the aspect

ratio of the rudder is greater than the effective aspect ratio of the keel, it follows that additional rudder side force, in leading to a reduction of the required keel (and canoe body) side force, reduces the overall level of the induced resistance.

Accordingly, when the rotatable keel is used at zero helm angle and the same induced resistance is obtained as is produced in the conventional situation, a performance improvement is inherently present. At 5 degrees of helm angle, the rotatable keel fin leads to a resistance reduction of about 0.4 kN. At 8 degrees of helm this increases to about 0.6 kN, again about 12% of the upright resistance.

At large keel fin angles, such as required for 30 degrees of heel for the greatest (unrealistic) stability the model was tested at, the resistance due to heel and side force increases to beyond the values that can be expected on the basis of a side force-squared relationship. This can be seen in Figure 8c, where the resistance curve for the rotatable keel, at zero helm angle, deviates from the straight line for values of the side force-squared greater than about 600. This was found to coincide with a pronounced disturbance of the water surface above the leading edge of the keel. The keel fin angles in these cases were all greater than about 8 degrees, at which a pronounced gap starts to occur between the top of the keel fin and the canoe body (The canoe body was designed to have a flat area in way of the keel to avoid such a gap up to fin angles of about 8 degrees).

Figures 8a, 8b and 8c, and similar results for other boat speeds, prove that the elimination of leeway through the introduction of asymmetrically-oriented lifting surfaces reduces the total induced resistance of a sailing yacht by not letting the canoe body develop side force. The canoe body is a very inefficient producer of side force, accompanying a relatively large resistance component.

11 Structural design and construction

11.1 Adopted Approach

Although the IACC Rule is very specific concerning the thickness and density of the skin and core of the carbon hull-shell and deck structure, very little specifications are given concerning internal framing. The design of the structure can range from minimum skin and core requirements, with extensive framing, to a monocoque structure with a thick sandwich hull-shell and deck, and no framing at all. It follows that considerable freedom is possible, warranting a careful study of the possibilities.

Initial weight studies revealed that a minimum weight solution is obtained when minimizing the skin and core weight and adopting extensive framing. Early in 1990 the High Modulus Company of New Zealand were sub-contracted to carry out a study of possible framing concepts with a view of determining the optimum structural concept, with respect to obtaining minimum weight together with sufficient strength. High Modulus, together with the SP Systems Company in England, had been instrumental in assisting the technical committee responsible for the IACC Rule in determining the specifications of the structural design.

In the High Modulus report all possible concepts are evaluated, as follows:

- Various monocoque structures (maximum, medium and minimum thickness variants, a tailored core thickness variant, and a variant with core ribs)
- A space-framed interior in a minimum thickness hull-shell and deck structure
- A space-frame variant with "adjustable" longitudinal stiffness

- A longitudinal, full depth bulkhead arrangement
- A longitudinal bulkhead arrangement in which the area of the bulkheads is reduced by angling them at half depth
- A variant with longitudinal stringers
- A conventionally, transverse-framed structure with few frames
- A diagonally-framed concept
- A variant adopting a large number of small, on-edge, single skin frames in close proximity.

Each of these concepts were evaluated with respect to Rule eligibility, strength, interior suitability with respect to sail stowage, weight, stiffness, cost, durability, adaptability with respect to moving the mast and keel, manufacture and aesthetics. The "winning" concepts on the basis of a chosen point-scoring system was, in order of preference, as described below.

11.2 A Space-Framed Structure, with Strip-Planked Core

This a radical, but very promising structure in which the minimum-weight shell is treated solely as a barrier to the water, capable of withstanding the water pressure. All primary loads (rig and keel) and overall bending loads are carried by a grid of carbon tubes. The exact arrangement of the carbon tubes is dependent on the location of load inputs to a finite element structural design program. Connection of the tubes to the hull is a complicated matter requiring research. The hull shell has to be strengthened locally for the propagation of the loads. This concept restricts the useful space in the hull, which fact does not matter much for IACC yachts, which have minimal internal space requirements. A sketch of this arrangement is shown in Figure 9a.

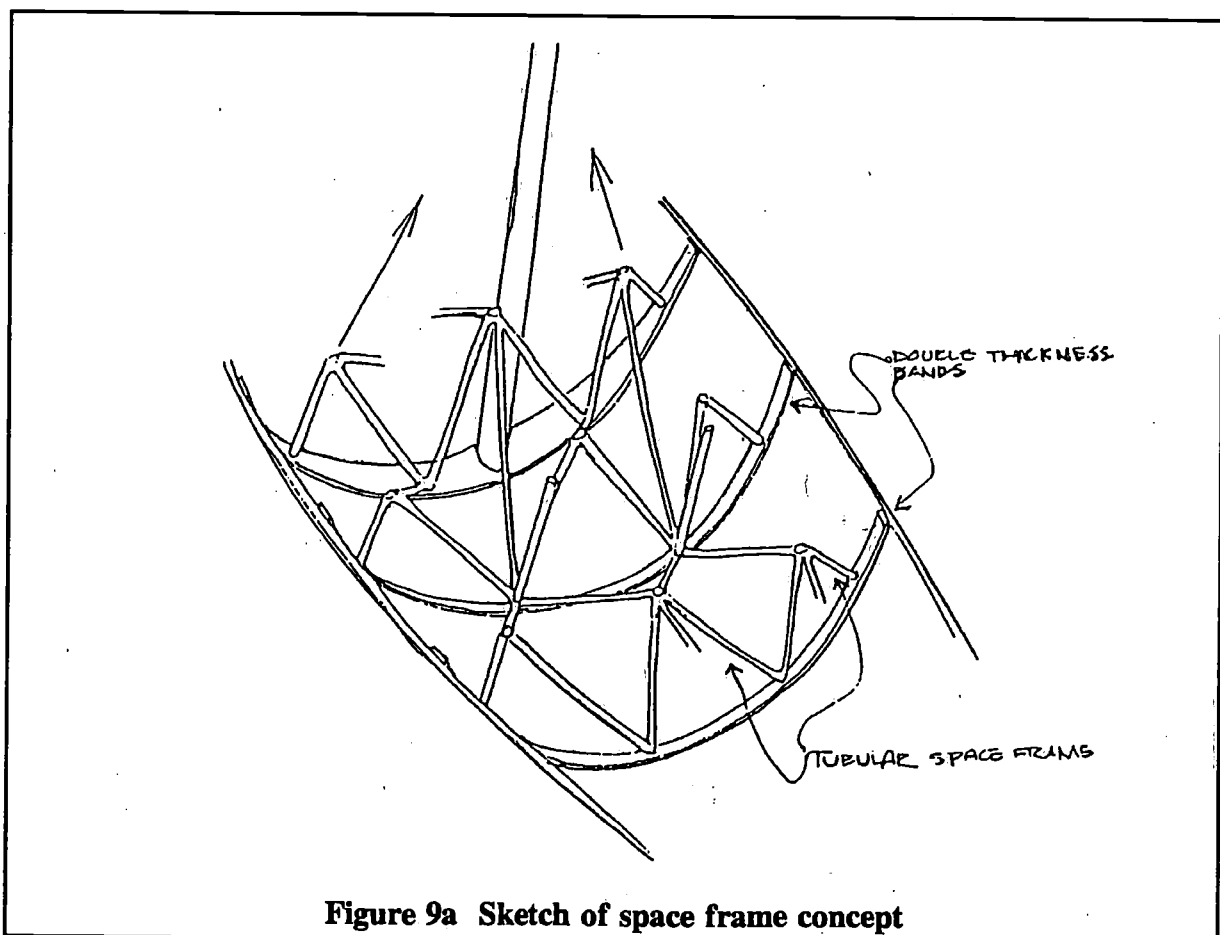


Figure 9a Sketch of space frame concept

The proposed construction is over a simple male framework by strip-planking with a premade sandwich of thin veneers of low density timber each side of a minimum allowable density foam core. The timber veneers in the skins enable a higher carbon content laminate, resulting in a stiffer shell. This leads to a light structure since much of the core-to-skin adhesive weight is eliminated. Once the outside is laminated and the shell removed from the mould the additional core in way of the attachment points for the space frame is added. The inside skin is then applied which then covers the shell. The internal tubes are all carbon glued and taped together to form rigid connections.

11.3 A Longitudinally (Web)-Framed Structure, Male Moulded

Here, the internal structure consists of a pair of longitudinal webs connecting the deck and hull-shell throughout the length of the yacht. Outboard of the webs is a horizontal "shelf" supporting the topsides. These strength members have cores with minimum density Nomex honeycomb, sheathed with 2 layers of very light carbon fabric. Connection to the hull, and each other, is by a tape join of a single layer of double bias carbon reinforcement. In addition to the longitudinal structure there are transverse knees connecting the underside of the deck with the webs in way of genoa tracks, winches and other deck hardware. Transverse webs or partial bulkheads are also positioned outboard of the two primary longitudinals in way of the mast. The keel and mast loads are distributed onto the webs with a series of bottom floors. Figure 9b gives a sketch of this concept.

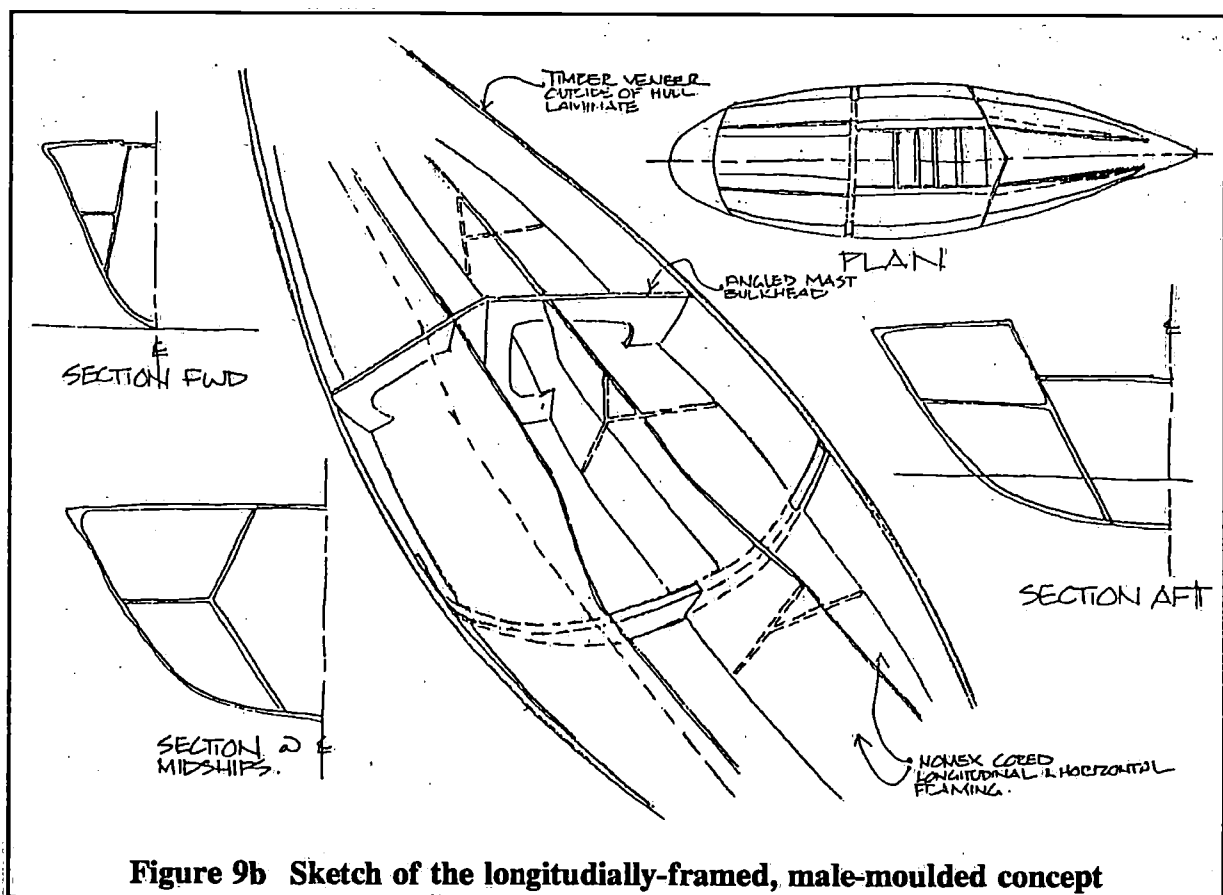


Figure 9b Sketch of the longitudinally-framed, male-moulded concept

The hull and deck shells are built over a full male mould in the conventional manner using either on-site wet prepregs or a dry prepreg system. The skin materials are a combination of carbon and Kevlar reinforcements, primarily uni-directionals but with a few layers of woven fabric where the special requirement of a bi-directional is needed. The outside skin is built

to less than the Rule minimum in composites, and then a thin veneer of timber is applied diagonally. This timber veneer is thick enough to be used as a fairing layer because, at a density of approximately 400 kg/m^3 , it is nearly half of the weight of a filled resin fairing compound. Once the hull is fair, it is carefully sheathed with glass cloth, leaving a clear timber finish. The core consists of minimum weight Nomex honeycomb throughout.

11.4 Transversely-Framed, Cold-Moulded Timber Concept

The internal arrangement consists of complete transverse ring frames spaced at 900 to 1200 mm intervals. The close spacing is not a requirement of the plating, but rather to minimise the size of the frames. The use of minimum thickness plating is therefore possible as the stress levels due to water pressure are particularly low. The frames themselves are rather novel. The web consists of a corrugated strip of laminate forming a lattice between the shell and the capping. This flexible strip is glued into the hull, across a radiused knee at the gunwhale, and over the deck. To the top of this a 4 to 6 mm thick capping of carbon unidirectional is glued. This results in extremely light frames which can be pre-fabricated and installed quickly, with a high degree of control over the weight. In the midships area the frames are increased in size and strength, and a bulkhead added to carry mast and chainplate loads. A sketch of this concept is given in Figure 9c.

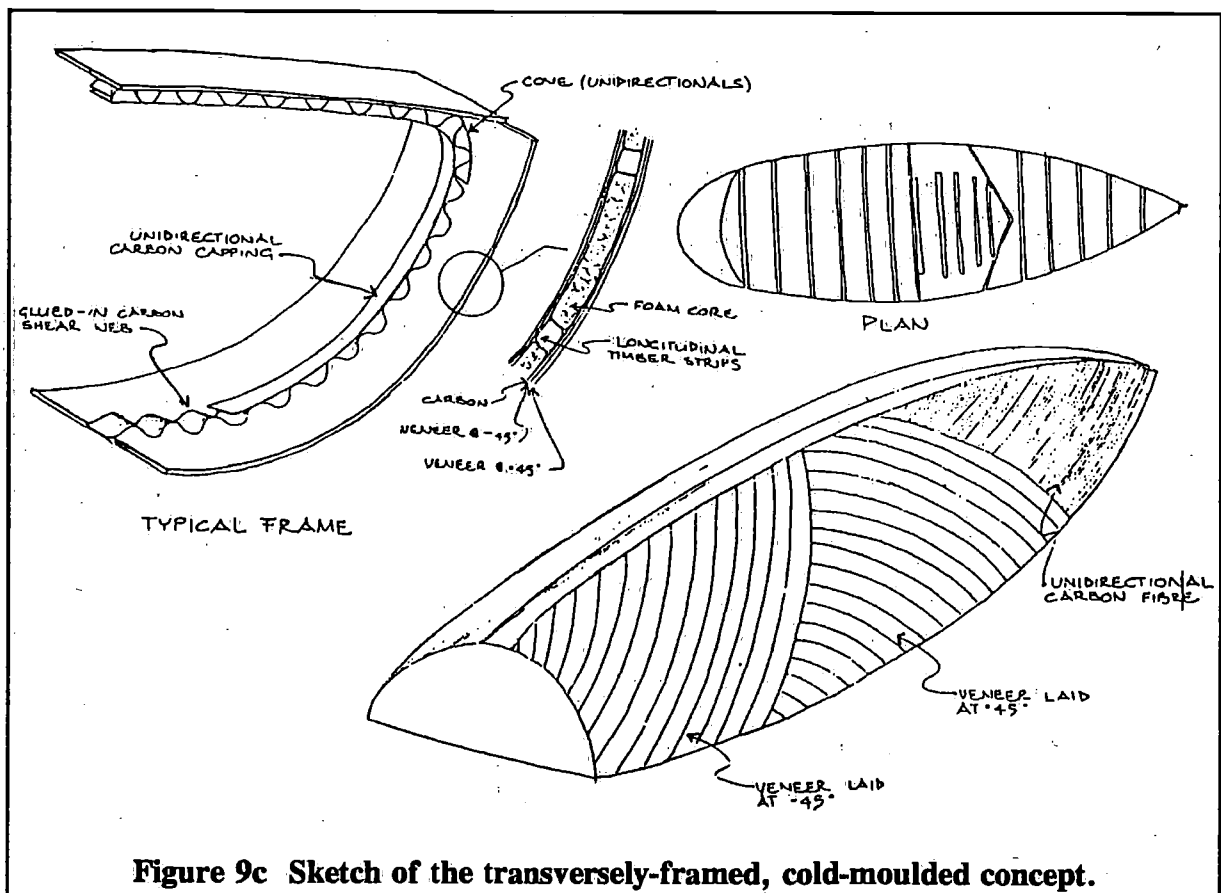


Figure 9c Sketch of the transversely-framed, cold-moulded concept.

The hull and deck shell are built over a male mould in a cold moulded timber sandwich. The inside skin consists of two veneers of 1.5 to 2.5 mm low density timber, with a longitudinally-orientated, carbon uni-directional between the layers. To this a core of minimum allowable density foam is glued between "stringers" of timber. The timber in the core does increase the weight, but compensates for the low strength of the minimum density foam, and facilitates the fixing of the outside skin. As with the inside skin the outside consists of two layers of

diagonally-orientated timber, and longitudinal uni-directional carbon. Total thickness is in the order of 5 to 6 mm, allowing the timber to act as a fairing material at a fraction of the weight of a filled resin mix. Final sheathing can be done with glass cloth.

11.5 A Transversely (Web)-Framed Carbon Structure, Female Moulded

This is the "conventional" concept. Over the last few years this has evolved to be the most popular solution. Most racing yachts, with the exception of a few semi-monocoque shells which are really just a deviation from this concept with fewer frames, are transversely framed. From this background this type of arrangement is an automatic choice for evaluation, as a basis for comparison if nothing else, see Figure 9d.

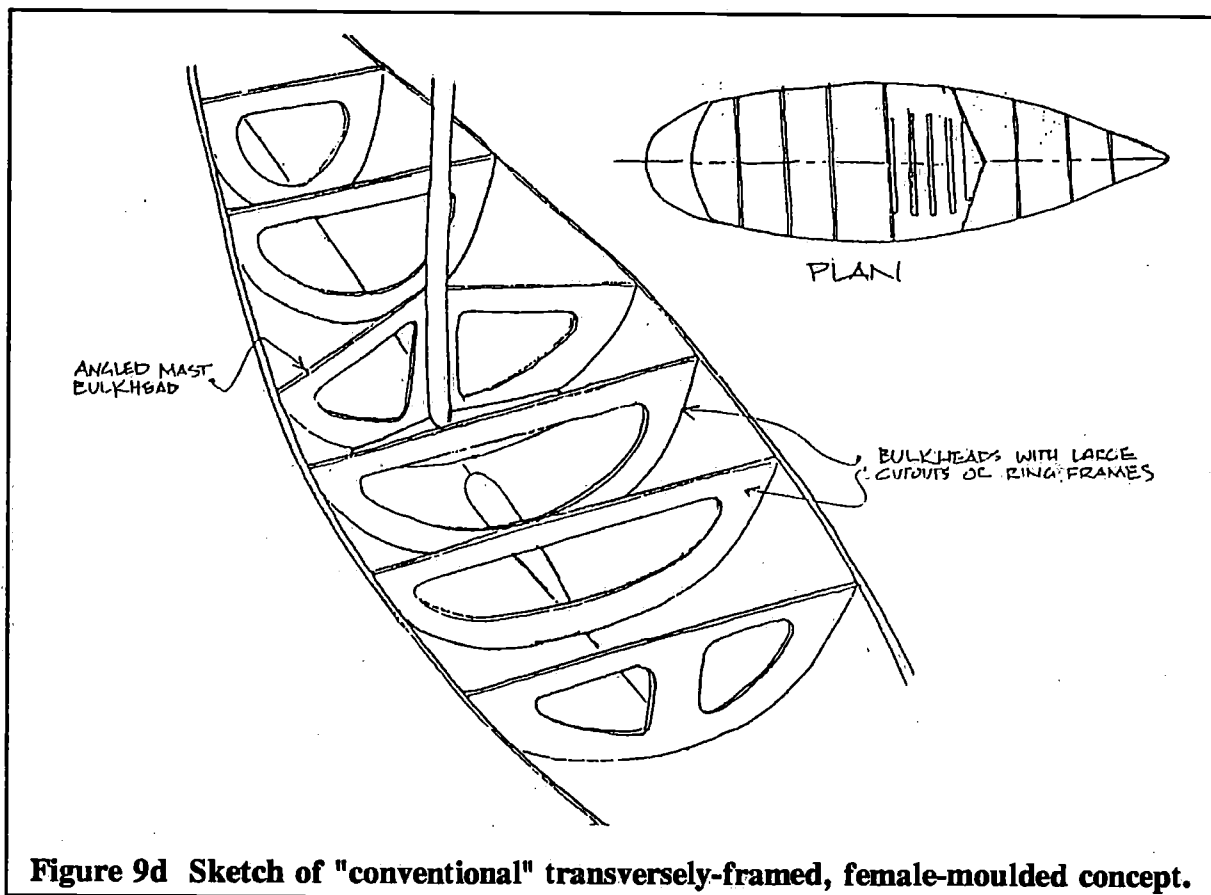


Figure 9d Sketch of "conventional" transversely-framed, female-moulded concept.

In keeping with the "conventional" nature of the framing the shells are laminated from the material anticipated in the Rule. The skin laminates are composed of carbon and/or either Kevlar or polyethelene fibres. Either a dry prepeg or a wet system based on an epoxy or a low density vinyl ester resin (allowing a significant gain in laminate modulus) would be used. Core material is Nomex honeycomb of minimum allowable thickness in all but the keel area where foam would be substituted. Laminating is into a full composite female mould to eliminate significant fairing.

11.6 A Variable-Thickness Monocoque Concept

The arrangement of this option is simple. Midships there is a major mast/chainplate bulkhead, behind which there are a number of short keel floors. At the rear of the keel a full frame extends up to the deck. This keel framing is covered by a sole to produce a clean sail

handling platform. The deck is supported by transverse beams amidships where there are thickened areas of the shell for the sail tracks and major fittings. This is a "full" monocoque, or a development of conventional, transverse framing to the point where more structure cannot be left out. The disadvantage of an over-weight core has been minimized by the tapering of the thickness along the length, see Figure 9e.

The materials and moulding method are the same as for the transversely-framed conventional carbon structure.

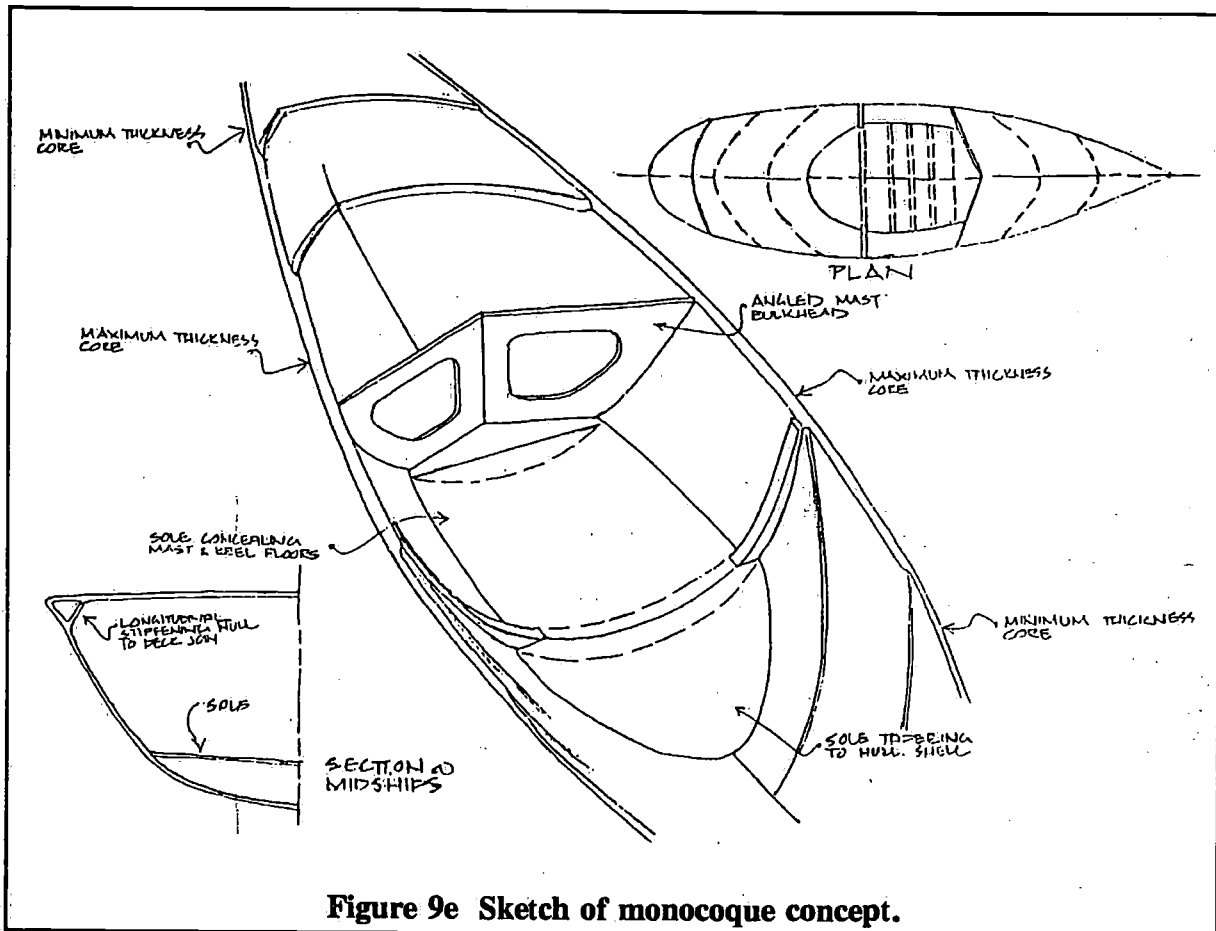


Figure 9e Sketch of monocoque concept.

11.7 Construction Details

On only utilizing a point-scoring system for weight and stiffness, the first 2 of these concepts were found to be superior while the remaining 3 concepts came in reasonably closely matched in second place. As implementation of the first 2 concepts would require considerable research and additional cost for tooling on the part of the builder, it was decided to adopt the "conventional", transversely-framed, all-carbon option. McConaghy Boats Pty Ltd in Sydney were awarded the building contract. Materials and engineering assistance was provided by SP Systems (Australia) Pty. Ltd.

Details of the structural design were then determined by the design team with assistance from H. Jackson, a composites expert from New Zealand, who was sub-contracted for the Purpose. The loads on the hull-shell, deck and cockpit, ring frames, longitudinal centre-line girder in way of the mast and keel, etc, were all diligently calculated by various methods. Specimen sandwich beams were built and tested to destruction, to verify the properties of the candidate laminates and materials, and to determine the deflections as a function of the load applied.

All materials and finished components were weighted before being bonded into the yacht. The final mass of the hull-shell, which was faired before being released from the mould, was 960 kg. The whole carbon structure, composed of hull-shell, deck and cockpit, all internal structure (frames, longitudinal girder, keel casing, etc) completely faired and painted, was less than 2.000 kg, within 50 kg of the calculated design value.

The attachment of the 20.000 kg bulb to the carbon structure was through a novel, high tensile steel girder arrangement passing snugly through a carbon casing and a gland arrangement. A bearing compound was poured into the casing to close the gap between the girder and the carbon structure. Control shafts were fitted in front and behind this girder, passing through the keel fin on the centre-line, to allow rotation of the keel fin, which was an all-carbon structure filled with foam. The fin itself rotated about the girder, utilizing a large number of teflon bearings fitted to the surface thereof. A steel pin passed horizontally through the top of the girder and the 2 transverse keel bulkheads to lock the keel structure securely in place. The yacht was also lifted from this pin, in what is basically a onepoint lift. An outline of the structural arrangement is shown in Figure 10. Most of the credit for designing the details of the ingenious keel structure goes to D. Lugg, the author's principal design associate during this project.

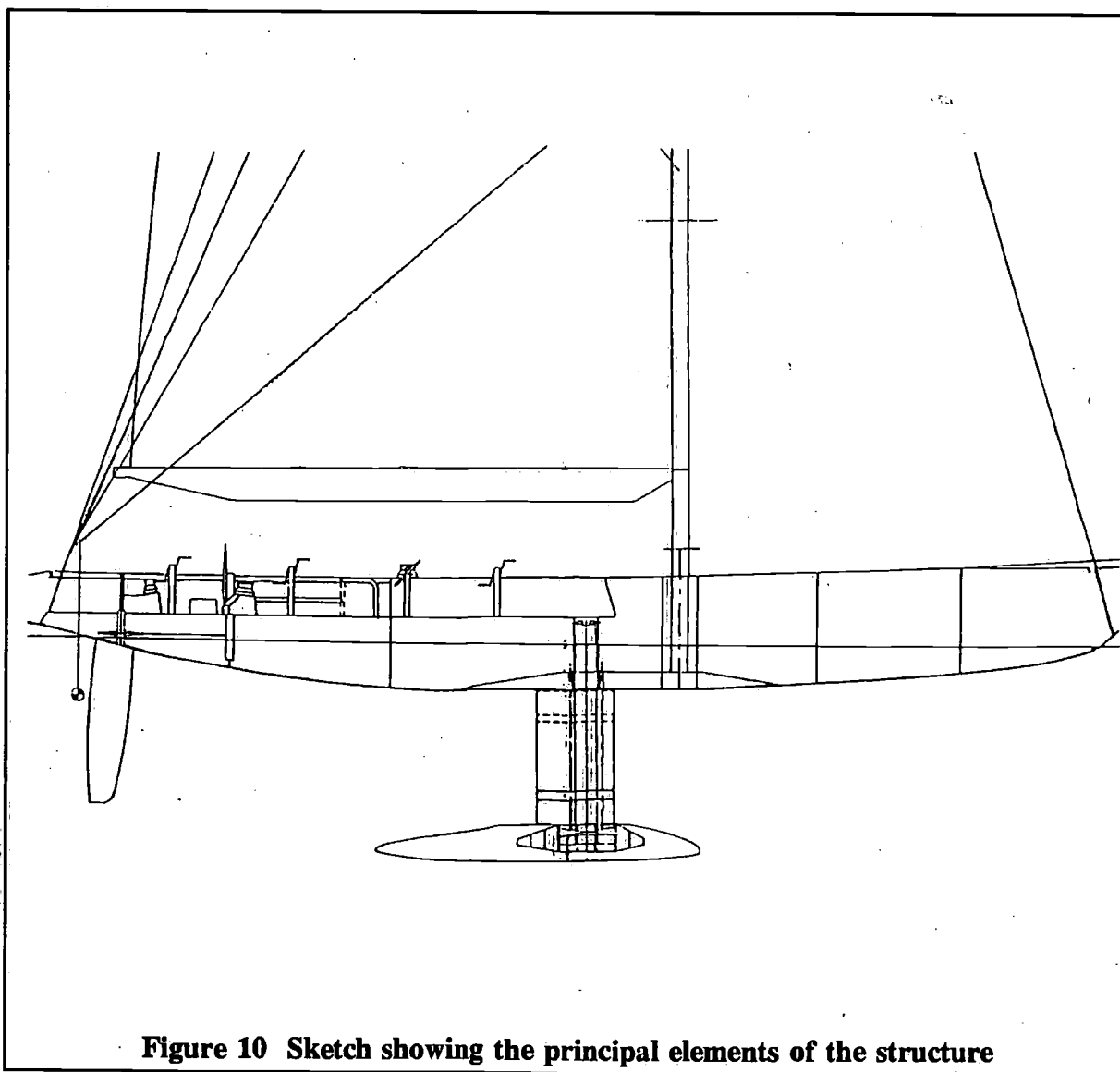


Figure 10 Sketch showing the principal elements of the structure

The carbon masts and booms, two of each were built by the Omohundro Company in California, were exactly according to the mass and centre of gravity requirements and were masterpieces of carbon structure. The carbon spinnaker poles were filament-wound in Australia. Barient winch systems, Harken deck gear and Navtec rigging was used.

Sails and sail design were provided by North Sails in Australia through a special arrangement in which the syndicate's own loft was set up in San Diego, and R. Hook, an Australian working for North's Inc., became the syndicate's sail designer. The relationship with North's, as always, was a fruitful one.

12 Final remarks

The research, development and design programme, described in this paper, constituted a thorough and rewarding project. The end result led the "Challenge Australia" team that were privy to the work carried out and the results obtained, to believe that the yacht would be competitive with realistic chances to do well. Although early practice races off San Diego against other participants resulted in favourable reports and analyses, the yacht did not fare well in the formal races, and was eliminated before the semi-finals. To understand why this happened it is necessary to look at how the project developed after June 1991.

First of all, it was impossible to adhere to the time-table that had been set. The intention was for the yacht to be finished and sailing in Sydney in June 1991, and building commenced in November 1990, more-or-less on time. By then the economic recession in Australia had reached its worst period and, apart from a lack of financial backing from would-be sponsors, the main sponsor was no longer willing to commit as much to the project as originally intended. The yacht was launched late in September 1991 because of this, leaving only three weeks of sailing in Sydney. This was barely enough time to select the crew and carry out some basic crew training. No time was spent on evaluating performance, on developing instruments (particularly the special leeway measurement device the design team had developed for the setting of the keel fin to the correct angle), on implementing computer systems, on developing target boat speeds, etc. The yacht was shipped to Los Angeles late in October 1991, where it arrived about 4 weeks later.

In a meeting in August 1991 with the Syndicate Chairman, it was decided that the keel was not to be "used", i.e. rotated, until racing commenced in January 1992. In the discussion during that meeting, arguments put forward about needing time to learn how to use the keel, time to develop target boat speeds for the zero leeway case, time to find out if the sails needed modification for this condition, etc, were not heeded. The syndicate management considered security to be more important and considered that it was better to disguise the fact that this novel feature was present on the yacht for as long as possible. To ensure that the yacht had sufficient ability to go to windward with the keel set amidships, the design of the fin had to be modified (enlarged) and it became necessary to build a second fin for the races in which the rotation mechanism was to be used. Due to lack of time, this second fin was never built and the keel was forever to be a compromise in this respect.

When the rotation mechanism was used for the first time late in January 1992, it was found that the approximate target boat speeds that had been developed up to then were no longer valid.

In setting the keel at angles approximately in accordance with obtaining zero leeway angle, the yacht was sailing higher and slower than before. A discussion ensued about the merits of the keel concept and whether or not the targets the crew had developed were too fast,

meaning that the yacht had been footing rather than pointing. For some it was impossible to accept the lower target boat speeds associated with using the keel. To make matters worse, the leeway sensor that had been fitted just prior to the first round robin was found to be leaking and failed to give any useful leeway measurement. This meant that it was impossible to determine the exact keel setting for zero leeway and values had to be used based on the model test results. There was too much doubt within the team about the keel concept and about the importance of leeway angle to enable an all-out effort to be launched to find out how to sail the yacht. Time, also, was no longer available for this purpose.

The major reason for the yacht not being competitive in most of the races, however, was the fact that the wind conditions were much lighter than those considered during the design process and those predicted by the consultant meteorologist. The mast-head wind speeds in San Diego on most race days would prove to be less than 9 knots. Particularly at the start of the races, around 12 noon, the wind was always extremely light. A study carried out by representatives of the the Bureau of Meteorology in Melbourne, members of the "Challenge Australia" team in San Diego, revealed that during the last 20 years, 90 percent of the wind speed readings at Lindbergh airport in San Diego at 12 noon, from the beginning of January through to May, were between 5 and 10 knots. They further found that the wind on the race course, based on the readings taken from the buoy positioned near the race site especially for the America's Cup competitors, was generally 2 to 3 knots lighter than the corresponding readings at Lindbergh Airport. This meant that the yacht should have been designed for mast-head true wind speed values of between 4 and 9 knots, with an average value of about 7 knots! This required a vastly different design concept to what was finally adopted, i.e. a shorter waterline length, possibly a smaller displacement, a 12-Metre type of bow, etc.

After 4 races in Round Robin 1, in which "Challenge Australia" lost by 2 minutes 15 seconds from Spain (wind 4 knots at the start and 10 knots at the finish), by 8 minutes 52 seconds from Japan (wind 7 knots at the start and 5 knots at the finish), by 5 minutes 3 seconds from New Zealand (wind 10 knots at the start and 14 knots at the finish), and 2 minutes 18 seconds from "Spirit of Australia" (wind 5 knots at the start and 7 knots at the finish), the syndicate management decided to withdraw from Round Robin 1 to start modifications to the yacht. In the only race in which wind speeds were approximately according to the design value (against New Zealand), the yacht showed good boat speeds. In that race nearly 5 minutes were lost on the first windward leg because of a wind shift. That day the Press Centre put out the following text:

"....After a pretty even start, it was obvious for all that New Zealand on the starboard tack was sailing higher and faster. She was certainly helped by the wind shift to the right, being the windward boat on starboard. Thanks to this shift, New Zealand was 4 minutes 46 seconds ahead at the windward mark. The distance (thereafter) remained the same with Challenge reducing the delta. Challenge was maybe quite fast today but she sailed to the wrong side of the shift right after the start."

On 27 January, the yacht was withdrawn from Round Robin 1 and modifications commenced. The rated length was reduced by cutting of the stem, removing a triangular piece of deck and hull, and bonding hull and deck together again. In this way a gain of about 15 square meters in upwind sail area was achieved. The mainsail was modified to allow for much more area in the roach in accordance with the belief that with more wind high up the rig, due to appreciable wind sheer, considerably more sail force could be obtained.

This work was completed just before the start of Round Robin 2. There was no opportunity

to test the new light weather mainsail until the morning of the first race. It then became obvious that the carbon battens that had been modified by some of the crew during the modification period to suit this big roach, were not stiff enough. There was no alternative but to venture into the first race, again against Spain, using a medium-air mainsail that did not have the increase in area for which the hull modifications were carried out. That first race was lost by 5 minutes 46 seconds, the wind being 4 knots at the start and 8 knots at the finish.

At that stage the syndicate management decided that further work on the yacht would be to no avail and the campaign was wounddown. The meteorologists and the design team were no longer required. The keel was locked into the neutral position, and the winglets and the leeway sensor (that by now was working perfectly) were removed. The author's last involvement was to design a modification to the bulb so as to derive a more forgiving shape when sailing with the keel locked, at normal leeway angles.

From a design perspective the latter part of the campaign suffered seriously because no middle technical management was present to supervise work and deal with the many daily technical problems. It was impossible to concentrate on performance assessments, etc, because of this. Important jobs, such as developing flaps or fillets at the top and bottom of the keel fin to close the small gaps there, were never addressed because of this fact and because of lack of time. There was also no in-house support to look after electronics, on-board computers, performance analysis and related work. This had to be allotted to non-specialists in the crew as much as possible. In many instances local US specialists had to be brought in to solve major problems. People were always unsure of their positions in both the crew and in the support group, leading to much aggravation and under-achievement. The task of ascertaining target boat speeds, on the basis of performance analysis, was addressed by different people at different times. No adequate targets were ever developed and the yacht was sailed by "feel" more than anything else.

13 List of references

- [1] Kirkman, K.L.,
"Gentlemen, Choose Your Weapons - The Race Conditions for the America's Cup",
Marine Technology, Vol. 27, No. 2, March 1990.
- [2] Chance, B.,
"The New America's Cup Class",
Proceedings of the Ninth Chesapeake Sailing Yacht Symposium, March 1989, Society
of Naval Architects and Marine Engineers.
- [3] Pedrick, D.,
"The New America's Cup Class",
Proceedings of the Ninth Chesapeake Sailing Yacht Symposium, March 1989, Society
of Naval Architects and Marine Engineers.
- [4] "Performance Prediction Calculations Relating to a New America's Cup Class Yacht",
Wolfson Unit Report No. 914, The University of Southampton, February 1989.
- [5] "International America's Cup Class Rule", May 1989 (and subsequent public and
confidential interpretations), office of the Technical director of the America's Cup
Class, Fremantle, Australia.
- [6] Gerritsma, J., Keuning, J. A. and Onnink, R.,
"Geometry, Resistance and Stability of the Delft Systematic Yacht Hull Series",
International Shipbuilding Progress, Vol. 28, No. 328, December 1981.

- [7] Gerritsma, J., Keuning, J. A. and Onnink, R.,
"Results and Analysis of the Delft Systematic Series II Yacht Hull Form Experiments",
Proceedings of the Tenth Chesapeake Sailing Yacht Symposium, February 1991, The
Society of Naval Architects and Marine Engineers.
- [8] Gerritsma, J., Keuning, J. A. and Onnink, R., "Sailing Yacht Performance in Calm
Water and in Waves",
Twelfth HISWA Symposium on Yacht Design and Construction, Amsterdam, Nov.
1992
- [9] Badham, R.,
"Wind and Wave Report - Auckland and San Diego America's Cup Sites", October
1989.
- [10] Scott, W. H.,
"Directional Stability and Control of Sailing Yachts",
Proceedings of the First Chesapeake Sailing Yacht Symposium, January 1974,
The Society of Naval Architects and Marine Engineers.

Another new approach to cruising sailboats-fast, safe, long-distance cruisers

Lars Bergstrom

B & R Designs

For many years the B & R Designs team of Sarasota, Florida have been working with single-handed 'Transatlantic' and 'Round the World' racing sailboats. Recently a new range of cruising sailboats have been developed. The first boat built using this new philosophy is 'Route 66' - a fast 68' sailboat that is safe and simple, at present the couple who own 'Route 66' are on an extended sail around Europe. Neither a large crew or strong muscles are required to manage the boat.

Most fully crewed racing boats and their cruising offspring are 'poisoned' by 'human-written' rules - rules that are created for the 'handicap' measuring systems where allowances are given for anything that slows the boat down and where designers try to create a 'slow' boat that is 'faster' than the speed allowance given - what if, for instance, before the 100m sprint in track and field competition, the athletes go to a doctor to get time allowances for personal deficiencies! For a knee injury perhaps a 2 second allowance; a sore foot, a 3 second allowance and so on. After the race the athletes time's would be adjusted for each persons' condition and then the winner would be announced!

The single-handed races (Transat, BOC, etc.) follow, more closely 'nature's rule' - these boats need to be strong enough to sail in severe conditions; easy enough for one person to handle and if the boat is fast enough it will do well. This type of boat can set a good standard for cruising sailboats and as there is no need to build to a rule, a cruising boat can be much faster and safer.

Some rules for short-handed racing sailboats have to be accepted to limit the size and costs of a boat and accordingly make competition a sporting challenge. However, as the boat size limitation is defined by the present rule in terms of maximum overall length, this rule contributes to a tendency for competitors to choose a plumb bow. A plumb bow can produce a wet boat and this together with a rounded blunt stem can cause, at high speed, a sudden deceleration when the bow goes down in the water. This type of bow is most undesirable for a cruising sailboat. The new designs feature a sharp, sloped bow shape which reduces resistance. 'Route 66' and the new cruising designs feature spray deflectors which are incorporated as part of the deck joint on the forward section of the hull and these divert the spray away from the hull. Diverting the spray helps to keep the boat dryer and also gives a lifting force that, at speed, helps prevent the bow from diving.

Racing rules generally ban the use of electrically or hydraulically assisted winches. Powered winches are great for cruising as they give the smallest and possibly least strong crew member an opportunity to manage the boat unassisted.

Water ballast is a good, safe and inexpensive way to achieve stability. The amount of water

ballast is calculated to be the primary contributor to stability when the angle of heel is between 0 - 20 degrees. Twenty degrees is the cross-over point where water ballast and the inherent stability produced by the keel and hull should be about equal and above twenty degrees the inherent stability should be the major contributor. Using water ballast adds greatly to the safety of the boat as the keel can be lighter and in the event of a 90 degree heel, there is less stress on all parts of the structure. With water ballast the point of gravity is unsymmetrical in relation to the center line. This means that the boat is incapable of remaining upside-down if it should be unfortunate enough to be rolled.

In extreme conditions the negative side of water ballast is if the boat experiences a 90 degree heel so part of the deck is underwater and if the wind is strong enough to push the boat sideways, the heeling moment created by the wind force on the hull that is above the water and the resistance from the water on the submerged part of the hull, means that it can take some time for the boat to self-right. If a sea anchor can be deployed off the bow, this will assist the bow to swing into the wind and then the boat will self-right.

After the successes of 'Tuesday's Child' and 'Thursday's Child', Warren Luhrs of Hunter Marine commissioned B & R Designs to conceive a new 60' single-hander. A hull was calculated for minimum resistance and a towing tank model was built from these calculations. At the same time a model of 'Thursday's Child' was built as she had known performance. The tank tests were done at the Royal Institute of Technology in Stockholm. The results showed that the new hull shape had about half the wave resistance as the hull shape of 'Thursday's Child'. 'Hunter's Child' was the first boat built using the new hull shape, she was built in the United Kingdom and has been sailing now for a number of years. 'Hunter's Child' has recently undergone changes in preparation for the 94-95 BOC Challenge.

During the tank testing the new hull shape was weighted down in increasing increments and the results showed that even with considerably higher weight there was a smooth transition from displacement speeds to more planing speeds and that performance was less affected than would have occurred with a conventional hull form.

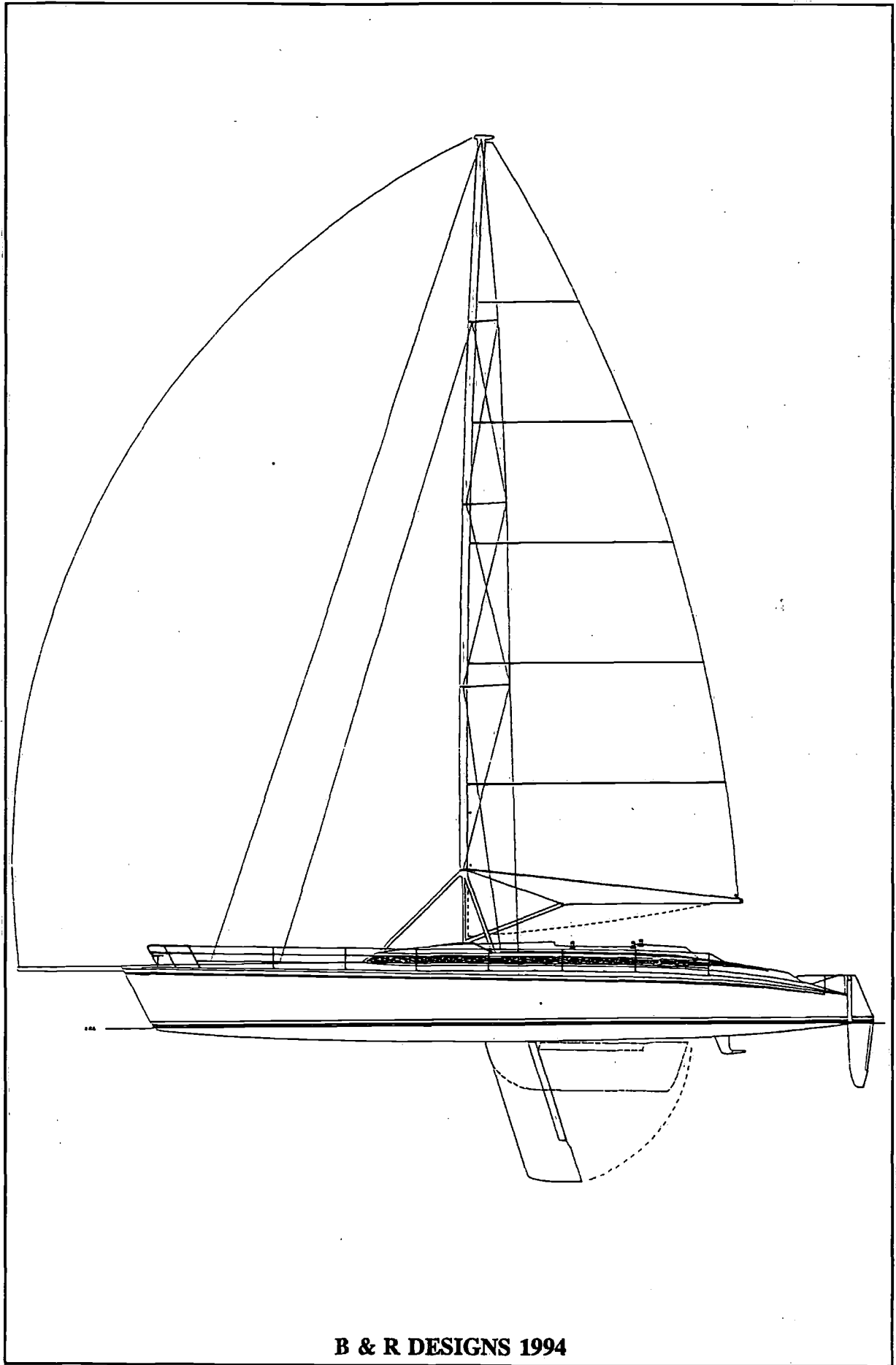
After 'Hunter's Child' B & R Designs' next project was a thirty foot sailboat to fit the Ultimate 30 rule using the same hull lines as 'Hunter's Child'. This boat with maximum crew weight corresponds, weightwise, to a sixty foot sailboat of 26,000 lbs., a good overall weight for a cruising sailboat. The thirty foot boat, 'Benz Express' has shown great speed potential - speeds in excess of 30 knots. 'Route 66' has the same hull lines as both 'Hunter's Child' and the 'Benz Express'. In relation to its size however, 'Route 66' is lighter than both of these boats and has, comparatively speaking, less sail area but potentially a higher top speed. One interesting aspect of the hull designs of 'Route 66' and 'Benz Express' is an air outlet slot which crosses the underbody about two thirds of the way along the waterline back from the bow. It is a groove across the hull approximately 4" wide covered with a plate that is flush with the hull on the forward end and angling down at the rear creating a slot of measuring about ¼" between the hull and the plate. It was found during the tank tests that the surface friction and wave resistance for this hull appear to be of the same magnitude. When sailing 'Benz Express' at around 10 knots an area of lower pressure is created on the hull at the location of the slot strong enough to suck air from inside the boat. As the air, together with the water, travels over the rear part of the hull the surface friction in this area seems to be greatly reduced. When hull resistance is reduced, boat speed is increased. The air outlet slot was adopted for 'Route 66' it also serves as a seachest dump for the water ballast system and the cockpit drains. One of the changes made to 'Hunter's Child' has been to retrofit an airtight slot.

Long-distance cruising sailboats are often on the same tack for extended periods. The transom of this type of hull is rather wide and would require a long rudder blade for good control when heeled. On 'Thursday's Child', 'Hunter's Child' and 'Route 66' a pivoting rudder is used that can be set vertically for most heel angles. This allows for a smaller rudder blade to be used which reduces resistance while maintaining control because when the boat is heeled with the rudder in a vertical position the sideforce from the rudder is horizontal. Along the trailing edge is a trim tab and an autopilot is connected to the trim tab for steering. There is less load on the autopilot when it is connected to the trim tab and the rudder is controlled by adjusting the trim tab. The connection between the autopilot and the trim tab is independent of the steering cables so if a cable should break the autopilot can be engaged and steering control maintained. Sailing 'Thursday's Child' from New York to San Francisco when she broke the Clipper Ship Record, a steering cable broke whilst sailing in strong winds with a spinnaker set, immediately the autopilot was engaged and there was no loss of control.

B & R are working on a new keel/rudder configuration for cruising boats, a shallow draft blade with a bulb to which the rudder is attached. This protects the rudder from damage that could occur if the boat runs aground. Over the years many repairs have been made to free standing rudders on shallow draft boats as the rudders are easily damaged if run aground. Extensive wind tunnel tests were carried out on this keel/bulb/rudder combination and the results showed that the performance was suitable for a cruising boat. On the trailing edge of the rudder blade a trim tab is fitted which is operated by an autopilot.

A problem often experienced by a sailboat fitted with a backstay or running backs when sailing on the same tack for extended periods is the leeward rigging slackens and as it is constantly moving, rigging fatigue can occur. In the late 60's the B & R rig was developed which triangulates the rigging in such a way that the shrouds remain fairly taut. This rig is safer and more suitable for cruising sailboat. Running backstays are not required as swept-backed spreaders are used to support the mast. The diagonals, (rigging wire or rod attached at the tip of one spreader and down to the base of the lower spreader or the base of the mast) eliminate the need for inner forestays. This type of rig was used on many IOR racing boats in the 70's and early 80's. IOR boats as well as most other sailboats use overlapping foresails and have a narrow base for staying the masts. Cruising boats with no rule restrictions can choose more efficient alternatives. A sail area based on foresails that only come to the spreaders means the base of the rig can utilize the whole beam of the boat. On 'Thursday's Child' and 'Route 66' this principle was used - a rig with no running backs or backstay. 'Hunter's Child' is now fitted with a B & R rig. This allows for the use of a fully battened mainsail with an increased roach. For light-wind conditions there is a masthead forestay on which a much larger foresail, in very light cloth, can be set. One criticism sometimes heard of the B & R rig is that it is difficult to sail downwind because of the swept-back spreaders. In fact when using a downwind spinnaker the wind is directed into the spinnaker by the angle of the main. With cruising spinnakers it is usual to 'tack' downwind and therefore not necessary to let the main all the way out. Another concern sometimes voiced about the rig is that the main cannot be let all the way out when the boat is close to broaching - broaching mostly occurs with racing boats that have proportionally more sail area to the size of the hull. As the new cruising boat hull shape has more inherent directional stability it does not have the same broaching tendencies. As an example 'Thursday's Child' has been sailing for over 150,000 miles with no sign of a tendency to broach.

On both 'Thursday's Child' and 'Hunter's Child' the masts are deck stepped and have struts that are attached to the mast about 7' above the deck and at the lower end to the chainplates.



B & R DESIGNS 1994

The struts support the mast so it is equivalent of a keel-stepped mast that is supported by the deck. This makes it possible to use a smaller mast section and gives a very rigid point for a spinnaker pole attachment. Using a smaller mast section creates less drag and minimizes disturbance on the mainsail. With 'Benz Express' and 'Route 66', B & R Designs has gone one step further and incorporated a third strut which angles forward, forming a tripod for the mast to be stepped on. All of the mast load is taken up by these three struts. The shrouds and forestay are attached to the lower ends of the struts. This method allows the major forces to be retained within the rig structure which greatly reduces the load on the hull. Using the tripod system means that only the heeling moments from the keel and the slamming loads from the water need to be considered when calculating the dimensions for the lay-up of the hull. Since the hull loads are considerably reduced the construction of the hull can be lighter without sacrificing safety.

An additional safety factor is the rigid boom system which has been used very successfully on 'Route 66' - this allows the boom to swing only from side to side. The 'barn-door' boom is calculated and dimensioned to take the entire load from the mainsail with no help from a mainsheet. The loosefooted mainsail is stretched along the boom with an outhaul and even when the boom is let out the mainsail retains a good shape. This system has similarities to a sailboard, where the sail is sheeted without using a mainsheet or traveller. On 'Route 66' the sheeting angle of the sail is controlled by a line running to the windward side. A fully battened mainsail is used and a single line reefing system; the same line controls the tack and clew of the mainsail. This makes reefing simple and easy to control even when running downwind (see illustration).

The philosophy behind 'Route 66' and the new long-distance cruisers is that the boat should be simple to sail, safe and fast. Managing a sailboat should be enjoyable and possible for any family member.

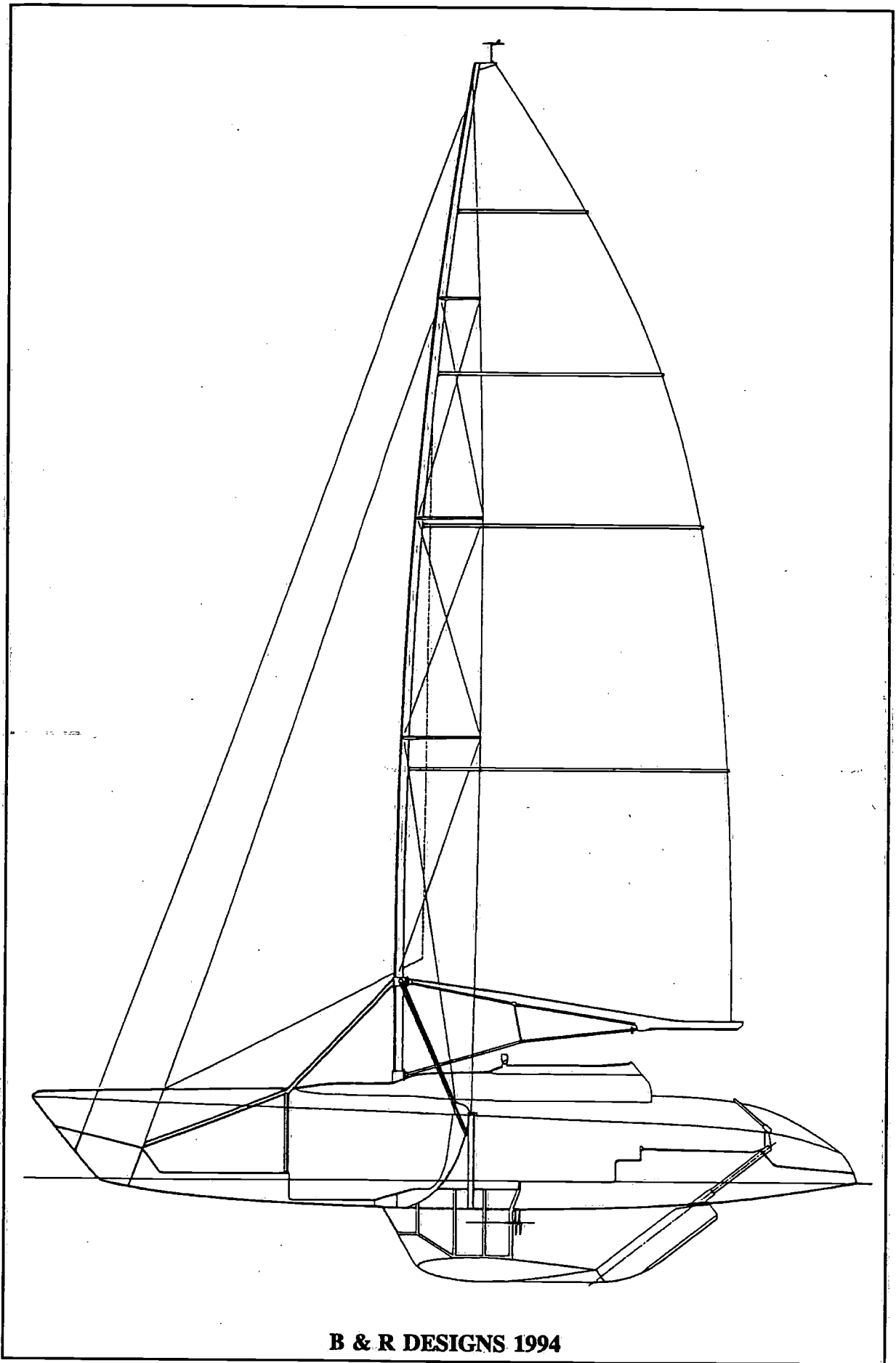
The cockpit of 'Route 66' is equipped with hydraulic and mechanical winches. All the lines lead aft to the cockpit area.

At present the possibility of using an electrical motor for auxiliary power is being investigated. A diesel generator will be used to charge the batteries and run the water maker. The fuel is used as tackable ballast.

The interior of 'Route 66' is laid out for comfort and good visibility. There is a fully equipped forward facing navigation/steering station and wrap around windows. The decor is simple and clean, all parts made from foam-cored fiberglass with a white gloss finish. Using the tripod mast support system allows the windows to be large as the loads on the deck are reduced and the mast base is eliminated from the interior.

Sheeting points for the foresails are led aft to the rear part of the cockpit and this gives a good shape to the sails for more open winds. For upwind sailing there is a line over a block on the mast at the top of the tripod. This line controls the angle of attack for the foresail and is operated from the cockpit.

The line flips over when tacking. No tracks are used on the deck for sail handling.

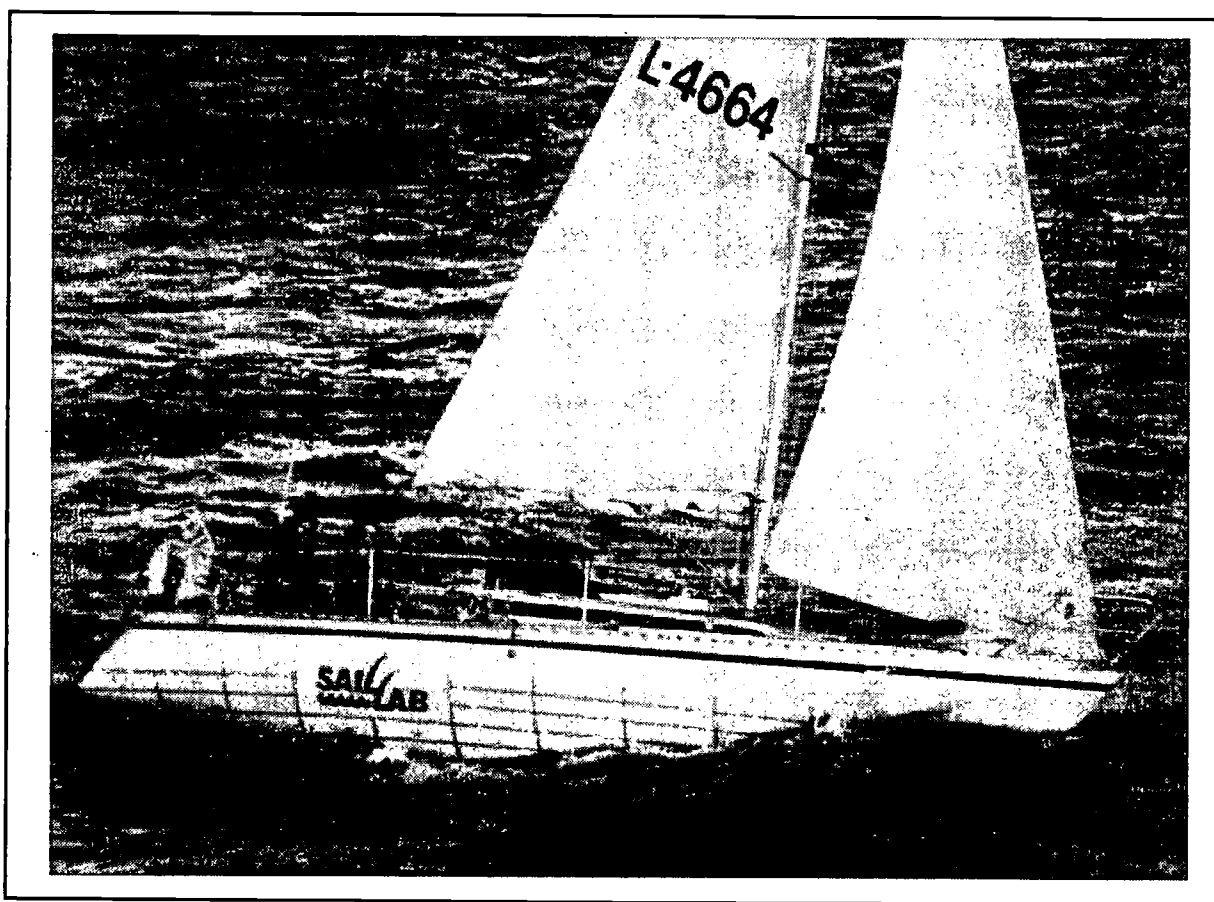


B & R DESIGNS 1994

Load measurements on the 9.4 m sailing yacht "SAIL LAB"

by Markku Hentinen & Gunnar Holm

VTT Maritime Technology
P.O. Box 1705, Espoo
FIN-02044 VTT - Finland



Preface

The SAIL LAB project was carried out as a joint project between the Finnish yachtbuilding boatyards, the insurance companies and some yacht designers during 1984-88. The laboratory yacht was built by NAUTOR and the installations, measurements and analysis were performed by the Ship Laboratory of VTT (Technical Research Centre of Finland).

The results were aimed at improving the background information needed for the product development process. The focus was on the actual loads acting on a sailing yacht, such as slamming, rudder, chainplate and grounding loads from the keel. These were issues that had only briefly been touched on before in literature. The Technology Development Center of Finland supported the project with additional financing.

In reply to the question "why not before?", one can state that, for one thing, when the interest to optimize structures was growing in the eighties, small size electronical equipment was also available during that time, for both measurements and analysis. It was, however, only through the interest and activity of all the involved parties the project was made possible. This is appreciated as research funding from SME-type boatbuilders was and is always going to be limited.

1 Introduction

The origin of this Project derives from the fact that very little information was available on the magnitude of the loads on sailing yachts. There was almost a total lack of published measurements of loads at that time and there were only a few articles, in which the loads were derived though an indirect procedure. This indirect way of assuming or measuring stress levels and calculating the load using linear plate theory was also initially used by us. The results showed tremendous differences between the different more or less established scantling determination methods. Our conclusion was that something was wrong and more information was needed.

During that time ICOMIA also performed a survey on the actual scantlings of serial produced boats. The result showed that most boats were way over the minimum level. So the question was: Is it possible to establish a load level for proper scantling determination? The Finnish yachtbuilding boatyards and designers were also interested in improving and optimizing the structures of their products. This made the project possible.

In the beginning of the eighties we made some load measurements on behalf of boatyards. This was for their own use on the yachts of their customers. The problem of making measurements on board someone else's yacht, often brand-new and just polished, with a lot of gauges, wires, instrument tape recorders, amplifiers (of the size they had at that time) and other measurement equipment became familiar to us. We therefore sought a solution where we could perform both long-term sailing measurements and laboratory-type tests entirely on our own terms.

We drafted the project so that it would include a yacht specially made for measurements - a SAILing LABoratory. This could accommodate enough battery capacity, proper protection for the electronics, through-hull pressure gauges, strain gauges in the laminates, frames, rig and on the rudder stock.

2 The measuring techniques and principles adopted

To attain the goals set for the project, several initial choices were made. Firstly the size of the yacht had to be such that a sufficient amount of measurement equipment could be safely installed on board. On the other hand, a small yacht was needed for obvious economic reasons, and these also supported a type with available moulds.

2.1 The "laboratory"

The choice was a boat of the Finn Flyer 31 type, at that time half tonner size. The main particulars are:

Length	9.38 m	Draught	1.76 m
Beam	3.21 m	Displacement	3284 kg
<i>Bwl</i>	2.51 m	<i>RSAT</i>	42.3 m ² (fractional 2-spreader rig with double runners)

The type represents a fairly typical cruising yacht at that time and still only the more extreme racers have main dimensions greatly differing from these.

The hull was built with the starboard side of sandwich construction and the port side of single-skin construction with two longitudinal stringers in addition to the bottom structure.

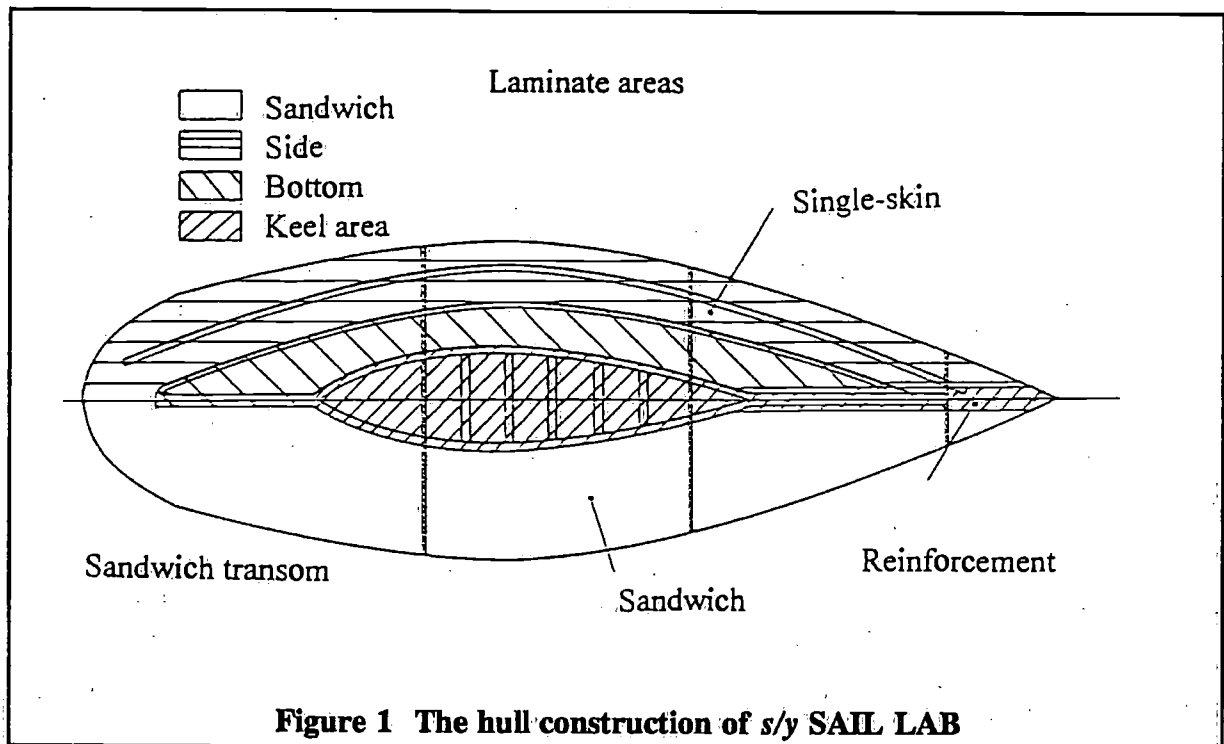


Figure 1 The hull construction of s/y SAIL LAB

The reason for an asymmetrical structure was that we wanted to study separately the strength and response behaviour of these two different structures. This has been done in later projects. As the objective of the project was to investigate the loads it can be stated that the external slamming loads are independent of the hull structure but dependent on the hull form.

The yacht was then equipped with two spraywatertight and separately ventilated lockers with transparent doors for the electronics, on each side of the yacht with a seat inbetween. The chart (and measurement log.) table was then on the centreline aft under the cockpit. This control centre worked well even for a tired scientist monitoring the system.

Racing-type accommodation and equipment for offshore racing facilitated self-sufficient sailing for several days. The boat was built in only 7 weeks to good standards by NAUTOR, and this high quality was necessary during the November trials on the Gulf of Finland!

2.2 The equipment

For long-term measurements a fast data logger was used. The frequency of this made it possible to take 100 readings/second from each channel. Each signal was then classified into ± 32 classes in the memory of the logger. A statistical distribution of the different numbers of counts in each class was then listed after each measurement period. The period was usually 12 hours but it could be shorter if desired.

The principle then for the analysis of the results was to use peak value analysis for the "daily maxima" values. A probability distribution curve (Gumbel asymptotic) was fitted to the results and an extrapolated maximum value was estimated from this curve.

Channel: 51		
Class	Counts	peaks
13	5251	1
12	92404	1
11	212369	0
10	77043	0
9	15329	3
8	67891	1
7	129747	0
6	19280	0
5	1425	2
4	1460	2
3	4978	6
2	2600	0
1	893	11
0	192	0

Figure 2 Example of classified data. Headstay; 0.672 kN/class, maximum 8.74 kN.

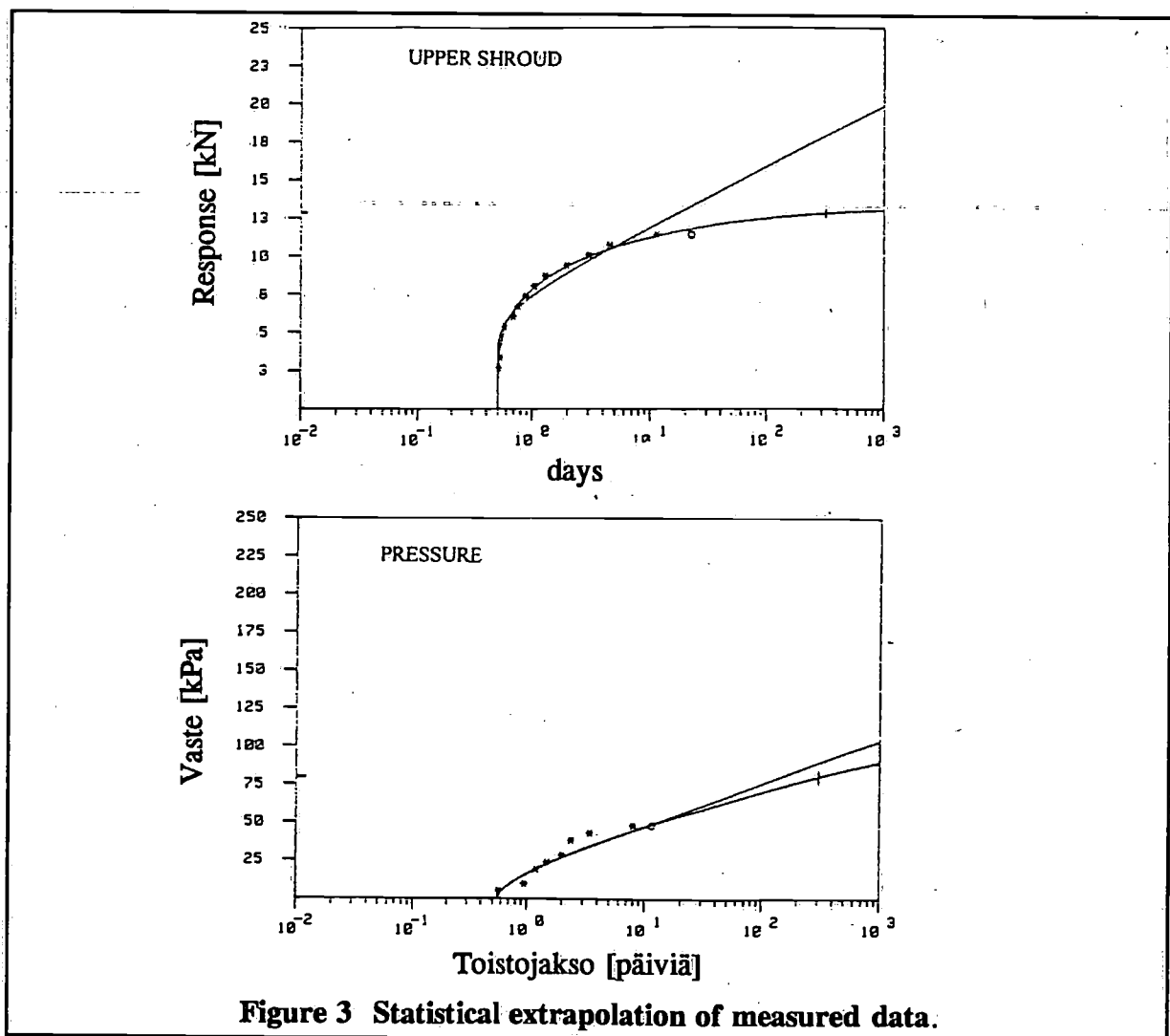


Figure 3 Statistical extrapolation of measured data.

The principle behind this is that during the tests it will not necessarily be the highest values that are experienced due to the comparatively short measurement time. However, a statistical pattern of the peak values (daily maxima) is obtained and the extrapolated value gives the maxima which would probably be measured if the measurement period was extended to the extrapolated time.

As can be seen from the results, some measured phenomena have a maximum value independent of how rough the conditions would grow during extended measurements. Others increase constantly with the extrapolated conditions. In the first case a very accurate result is obtained of the maximum loads in any conditions. In the later case, the results are more tied to the actual conditions during the measurements and the extrapolated conditions.

For time domain recordings of some of the loads, an instrument tape recorder was used. This enabled us, for example, to study the slamming pressure and the structural response in the time domain. This was also used during the grounding experiments and when studying the chainplate loads in certain specific sailing conditions such as gybes and broaches.

3 Sailing conditions during the tests

The statistical data were gathered during some 2700 nautical miles of sailing during which 300 hours was measuring time. The statistical data of the load distribution were measured over a period of 12 h. For the shorter test runs a shorter period was used.

The tests included the following events:

- Gotland Runt 1985 (an approx. 350 nm offshore race)
- Gotland Runt 1986 (fourth in IOR Class 5-6 with 23 participating boats in the class)
- Helsinki - Hanko - Sandhamn (Approach race and back from Gotland Runt)
- Some other races and sailing outside Helsinki in light, medium and fresh wind conditions.

During the tests, normal sailing procedures were applied. As maximum loads were also of interest no unnecessary saving of the boat were considered. A total crew of 4 to 5 persons was usually on board. As the measurement equipment operated automatically it could be left unattended for long periods. At certain intervals general control procedures or instrument tape-recording were performed by the respective research scientists.

The boat was built to good quality standards so no problems caused by water ingress or excessive damp occurred with the equipment. This was also thanks to the experience of the people responsible for the installation of the equipment. They had already been working with ship structures, icebreaker hulls and other field measurements in very severe conditions, in which protection of gauges and working electronics are of vital importance to successful measurements.

At this point it is also worth mentioning that at that time we also performed continuous automatic load measurements on board the Swan 651 s/y FAZER Finland, which took part in the 1985-86 Whitbread Round the World Race. These measurements were performed as contract research on behalf of NAUTOR.

A more accurate picture of the sailing conditions is shown in Figures 4 and 5, where the maximum wind speed and boat speed during the different measurement periods is shown.

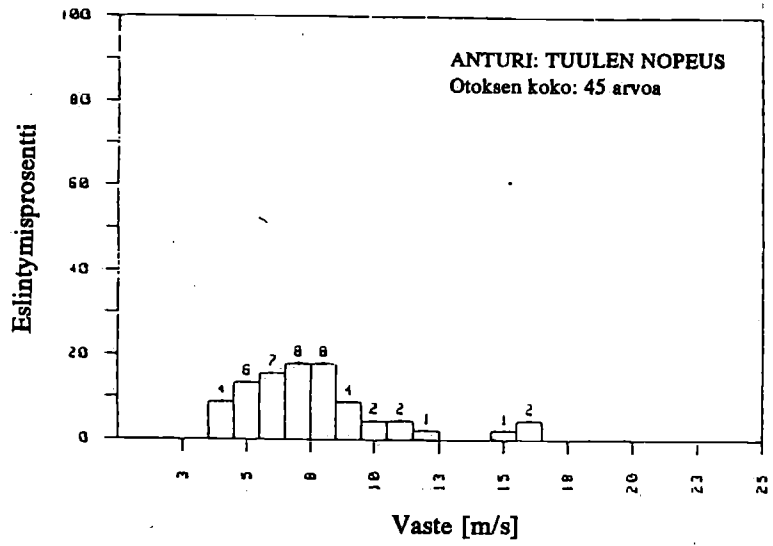
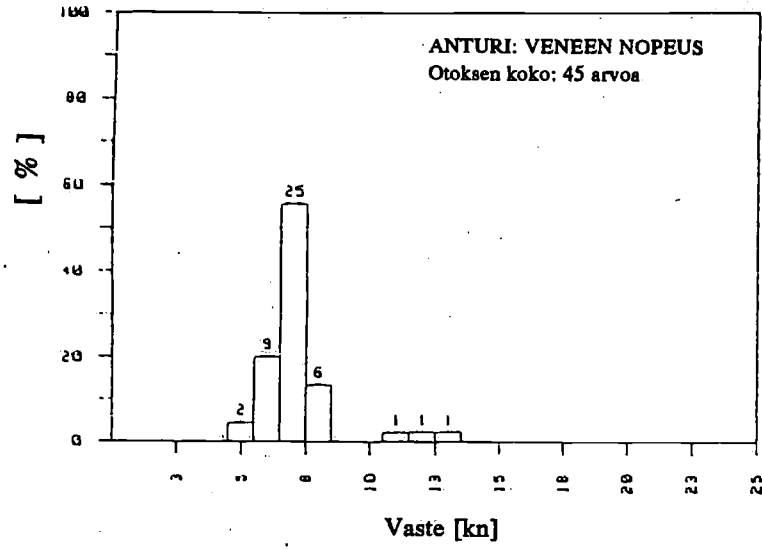


Figure 4 Daily maxima of boat speed and wind speed

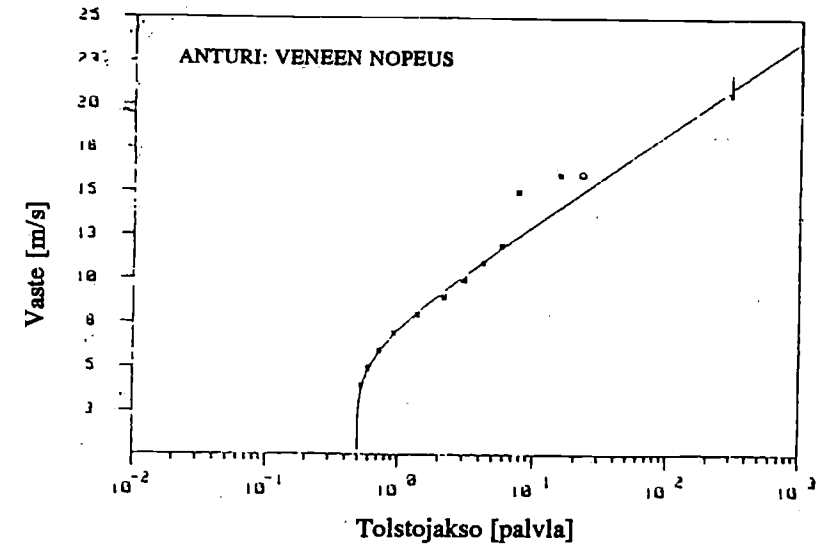
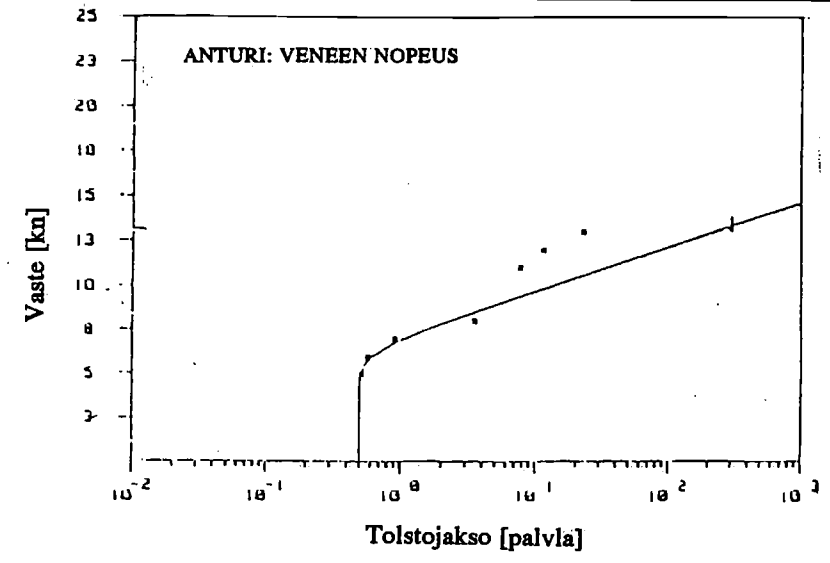


Figure 5 Extrapolated boat speed and wind speed

Executing the extrapolation procedure to these values yields the following values for the predicted 300 continuous sailing days which correspond to 20 - 30 years of ordinary use.

Maximum wind speed 21.5 m/s
Maximum boat speed 13.5 knots

It can immediately be noted that these values certainly can be exceeded with a typical racing yacht, but for ordinary cruising boats, active sailing starts to transform into haul-to conditions, where the load level decreases significantly. Capsizing, collision and other unexpected loads are dealt with separately.

4 Measured slamming loads

4.1 Applied measurement method

Two different methods were applied for the slamming pressure measurements. A direct method with five pressure gauges was used. The pressure values from all the gauges were recorded, and the mean value between two, three, four and five gauges were also recorded. In this way, results on the possible area reduction factor were obtained.

This factor, already widely applied in planing boat design and also included in the ABS offshore rules, takes into account the fact that the mean pressure decreases as the area under consideration increases. The reason for this is that the slamming pressure usually consists of a pressure front moving along the hull surface, diminishing in magnitude as it passes over a certain point.

In addition to pressure gauge measurements, the total force on the longitudinal stringer in the bow was measured by subtracting the shear forces at the ends. The shear strains were measured from the web laminates of the stringer. This method gives the total load on the stringer fairly accurately, especially when it is calibrated with a known force.

We also measured the strain both in the middle of the stringer and in the single skin and sandwich panels in the bow, but this was only for checking the strain level against the applied scantlings. As the bending moment in the middle of a panel is completely dependent on the pressure distribution and on the degree of fixation along the edges, no direct conclusions about the pressure can be drawn from such measurements.

4.2 Measured slamming loads

The pressure peaks and the moment in the middle of the bow stringer during one slamming event can be seen from Figure 6. The pressure peak is very steep and short, but as time passes by some 0.2 - 0.3 s, a sufficient area is under pressure to create a force and consequently a bending moment in the stringer.

Looking at the extrapolation of the pressure values of gauge 63, one will notice that even if the maximum measured value was 53 kPa, a maximum local pressure of around 70 - 90 kPa can be expected. The poor match with the Gumbel curve can be explained by the fact that there is a frequent hydrostatic component with many counts acting between approx. 0 to 12 kPa (0 - 1.2 water head) when no slamming occurs.

The rare slamming events and pressures represent then a new distribution higher up the scale at 30 - 50 kPa.

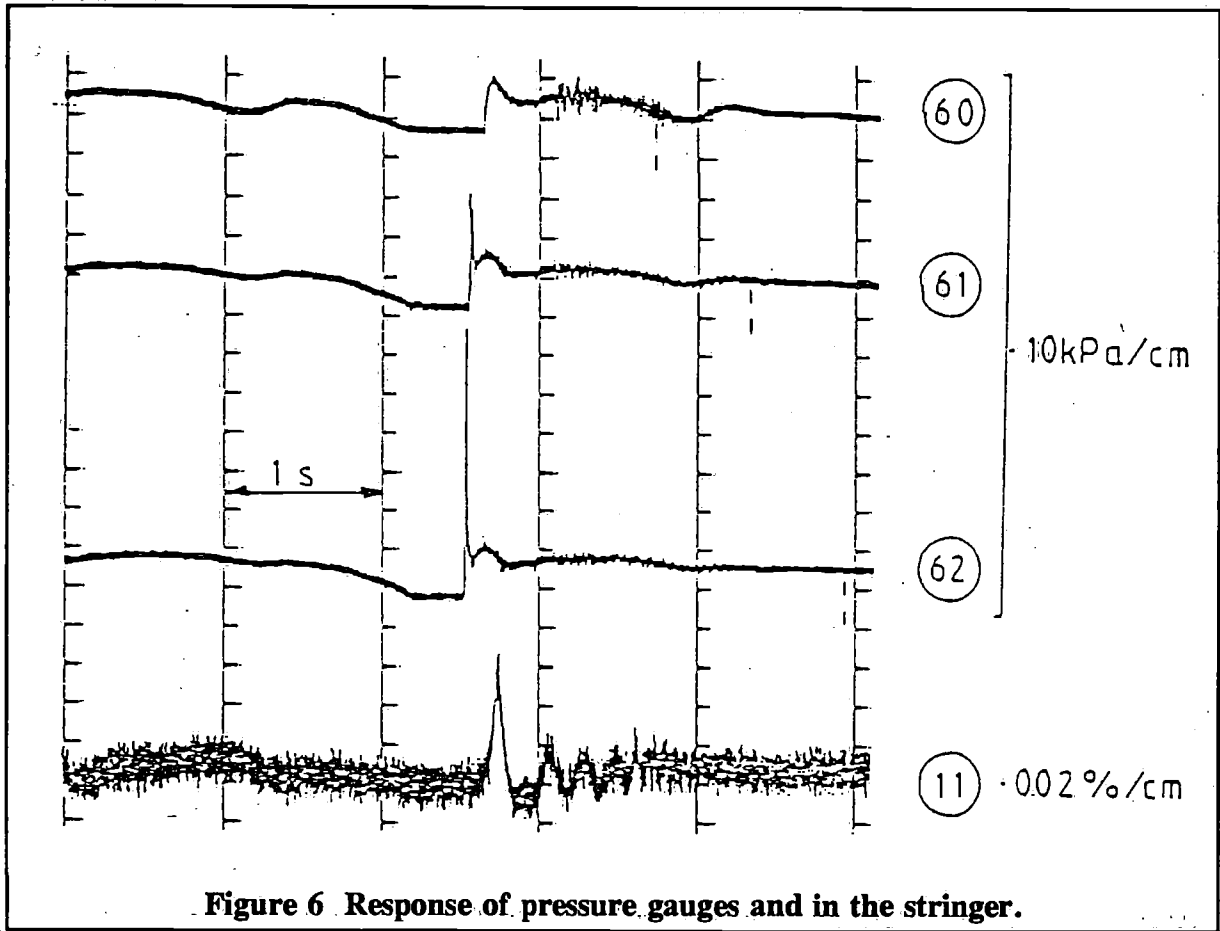


Figure 6 Response of pressure gauges and in the stringer.

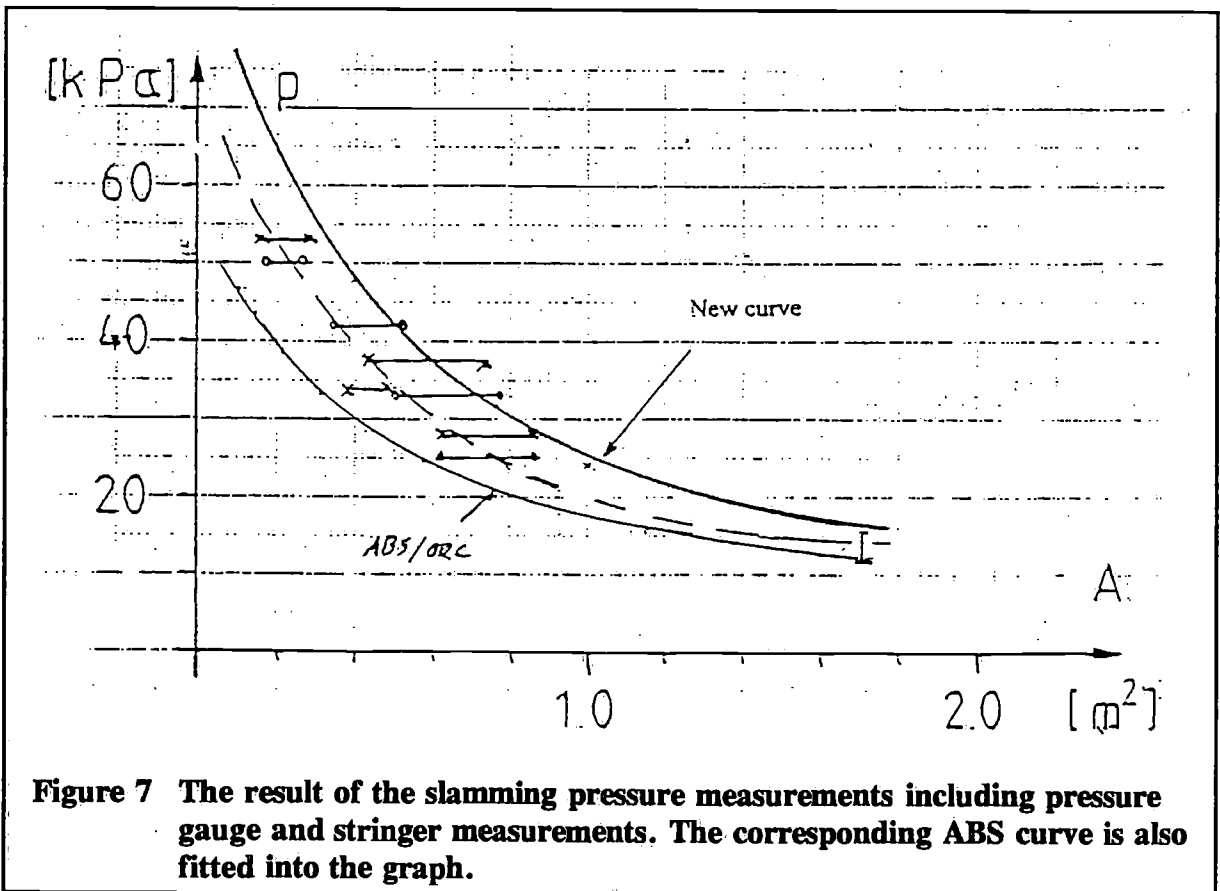


Figure 7 The result of the slamming pressure measurements including pressure gauge and stringer measurements. The corresponding ABS curve is also fitted into the graph.

Some of the poorly matching values higher up are certainly due to the fact that we actually waited for bad weather to perform "maximum value" measurements. Therefore long-time statistics did not fit in.

The results can be seen in Figure 7, in which the entire pressure reduction curve is drawn through the measured values. Both pressure gauge values and the stringer values are used. The maximum local values extend up to 70 - 90 kPa and one can notice that a 70 kPa pressure corresponds to an area of 0.075 m². This is the area of a 194 x 387 mm panel with a aspect ratio of 2, which can be seen on aluminum yachts!

At the 0.8 m² area level, one can notice that the measured values are 30 kPa when the ABS guide gives only 20. This is an alarmingly high difference, especially when the guide uses a safety factor of only 2 for FRP. We will return to the question of why so many yachts still sail around safely, later on in this paper.

4.3 Possibilities of theoretical methods

In order to extend the measured values of slamming pressures to other yacht types, some kind of calculation method is needed. Statistical methods and class rules are examples of these, but the problem can also be approached more theoretically by trying to model the physical phenomenon more accurately.

The determination of the maximum local pressure can be divided into two main problems: the relative velocity between a hull point and the wave surface, and a hull shape-dependent coefficient for pressure calculation. The former task includes the determination of design waves. The selection of relevant parameters can also be added to the task list. In parallel with the Sail Lab project, the above-mentioned problems were investigated [3] and a brief summary of the results is given in the following.

The vertical motion of a hull point was calculated with a method based on strip theory. Modifications were made to take into account some of the effects of three dimensionality as well as the keel and rudder. The maximum relative velocity was determined by assuming that the yacht meets a wave group that excites the harmonic motion of the yacht. The worst case was then searched for by simulating the encountering of different asymmetric waves in time domain (figure 8).

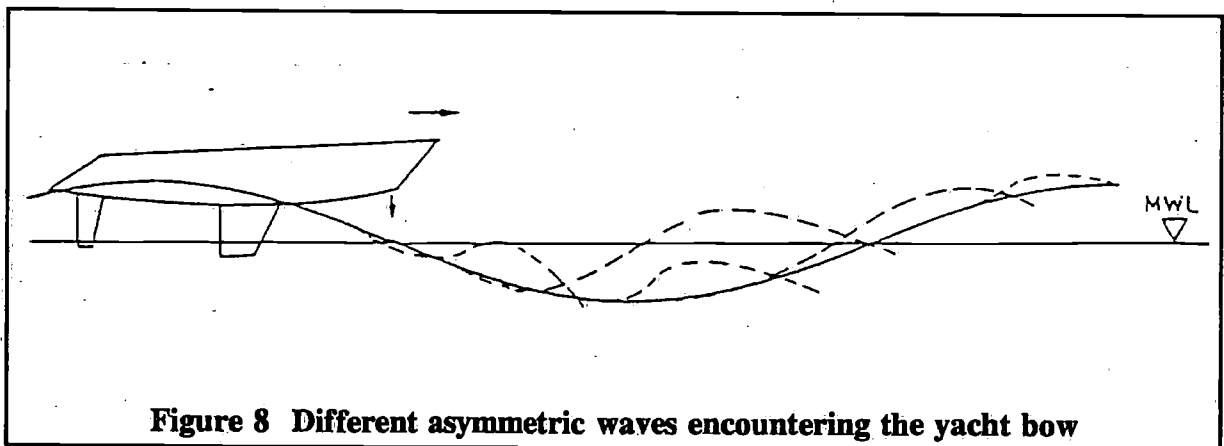


Figure 8 Different asymmetric waves encountering the yacht bow

The coefficient between the relative velocity and impact pressure was determined by measuring both quantities in full scale. The relationship between pressure p and relative velocity r is assumed to be:

$$p = \frac{1}{2} \rho k_1 r^2$$

where k_1 is a dimensionless coefficient which is dependent on the hull shape and the angle between the plating and the wave surface. The maximum measured value for the Sail Lab was $k_1 = 4.7$.

The threshold relative velocity, below which slamming does not occur, was 0.73 m/s.

The effects of the boat size and wave height on the maximum pressures were examined by applying a semi-empirical method that was developed in the work. An example of the results is shown in Figure 9.

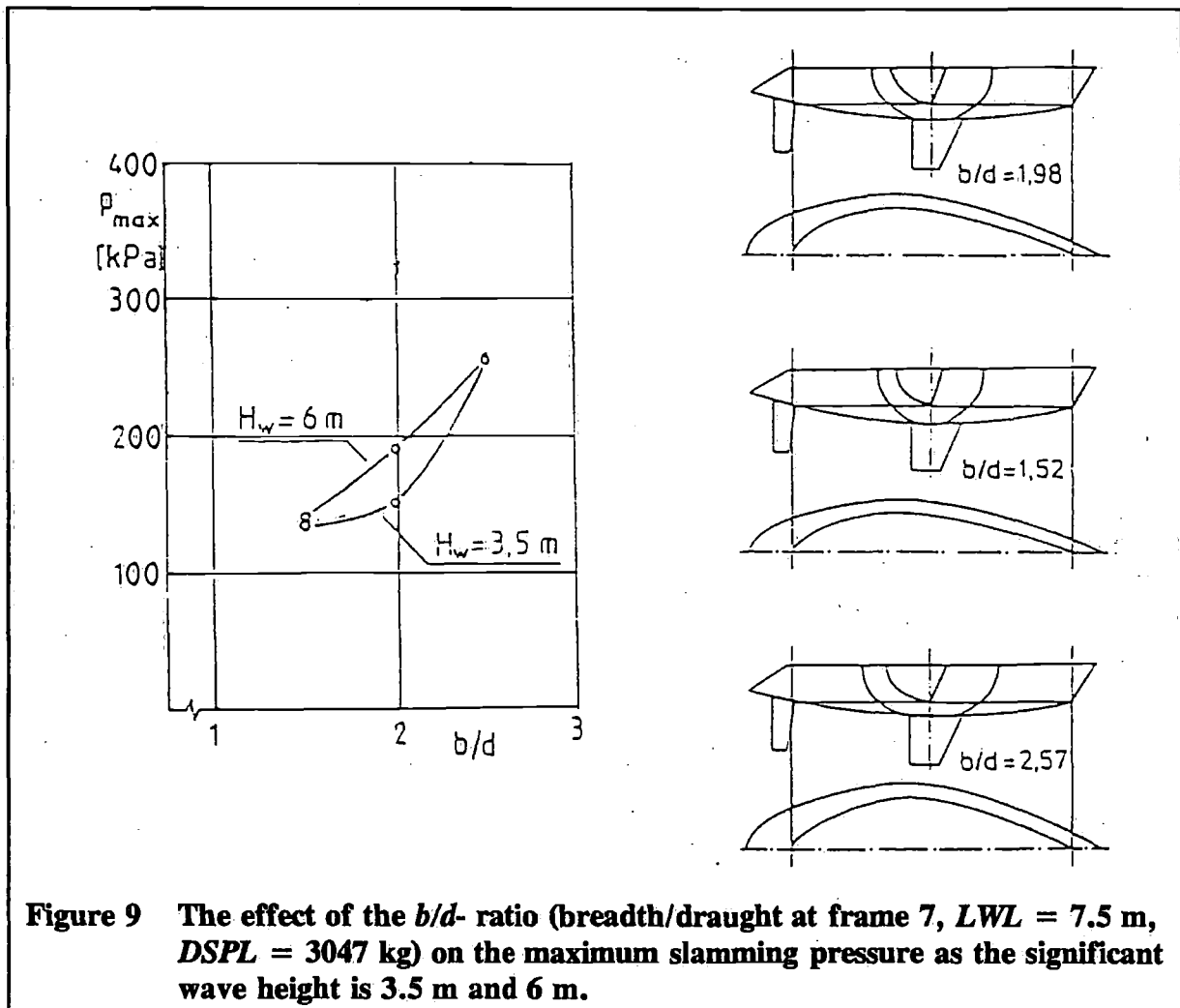


Figure 9 The effect of the b/d - ratio (breadth/draught at frame 7, $LWL = 7.5$ m, $DSPL = 3047$ kg) on the maximum slamming pressure as the significant wave height is 3.5 m and 6 m.

4.5 Nonlinear behaviour of large panels

As shown in the previous chapter, the slamming pressures clearly exceed the design pressures that are normally used. However, this does not seem to lead to damage in the majority of the existing structures. The reasons for this may be:

- built-in safety factors in the design methods as the response is calculated
- dynamic effects in the response of the plating as the pressure peak runs by
- nonlinear behaviour of the hull panels

The last item seems to have a significant effect on the response and is discussed briefly in the following:

The stresses and deflections of hull panels are usually calculated with linear theories. In fact, the bending behaviour of FRP hull panels is characterized by remarkable geometric nonlinearities due to the large panel size and relatively low stiffness of the material. The phenomenon becomes significant if the deflection exceeds half of the plate thickness. This is common in structures designed for the allowed stress rather than the maximum deflection. The analysis of the plate bending problem must then be extended to include membrane stresses.

To give an idea of the significance of membrane effects on typical yacht structures, the deflections and stresses of two panels are calculated using the method presented in reference [4]. The scantlings are based on NBS and Lloyd's rules (Table 1) and the results for simply supported and clamped panels (in-plane movement prevented in both cases) are shown in Figures 10 and 11.

Table 1 Two hull panels designed according to NBS and Lloyd's.

		NBS long span	Lloyd's short span
Bending strength	σ_B [MPa]	172	172
Bending modulus	E_B [MPa]	7554	7554
Span width	s_{free} [mm]	575	325
Thickness	t [mm]	6.85	6.69
Poisson's ratio	ν	0.3	0.3

As can be seen from Figure 10, all examples except the clamped short-span panel behave nonlinearly as the relevant lateral pressure is in the range 0 - 40 kPa. Figure 11 shows that the stresses in the different panels are very near each other when nonlinear theory is used. The difference between the values given by linear and nonlinear methods is very large (>200% in all cases except the clamped short-span panel) when the loading is 40 kPa. It should also be noted that the panels in the boat structures are very often convex, which means that the membrane stresses are compressive, not tensile. If the convexity is small, the panel snaps through to a concave shape.

This was demonstrated with the uppermost front panel (BB) of Sail Lab by applying an artificial four-point load to the structure. The mid-panel deflection shown in Figure 12 indicates that after the snap-through phenomenon the panel behaves like the examples shown in Fig. 10.

4.6 Slamming conclusions

The results from the slamming measurements showed higher pressure values than expected. The area reduction curve could be confirmed. Further theoretical analysis and parameter investigations showed that, after a certain wave height, the slamming loads do not increase substantially. The effect of boat size is clear, significant and almost linear.

As a result of these high loads, the actual load-bearing capacity of typical boat structures has been investigated showing pronounced nonlinear behaviour. This phenomenon gives a higher stiffness and strength to the structure than would be expected through linear plate theories. This linear theory is the base of almost all scantling determination methods developed so far.

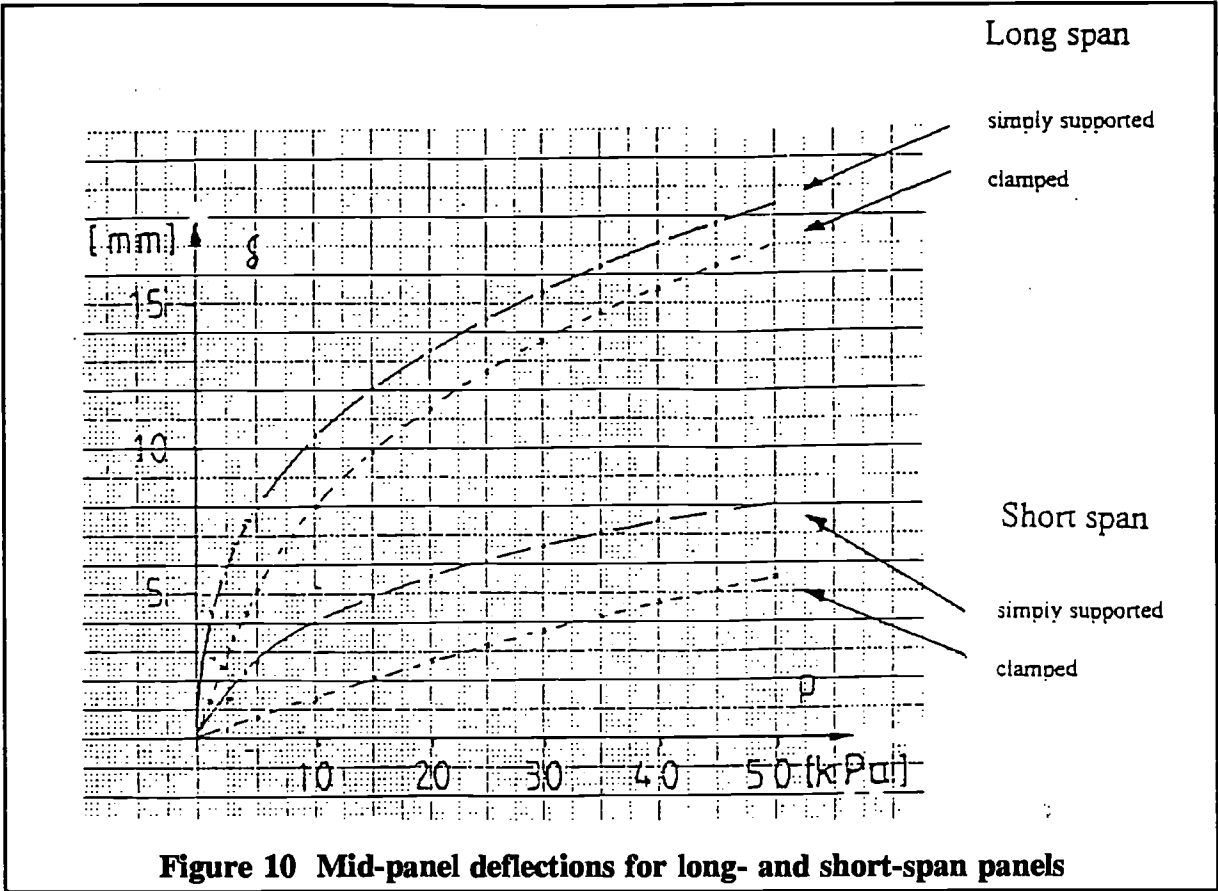


Figure 10 Mid-panel deflections for long- and short-span panels

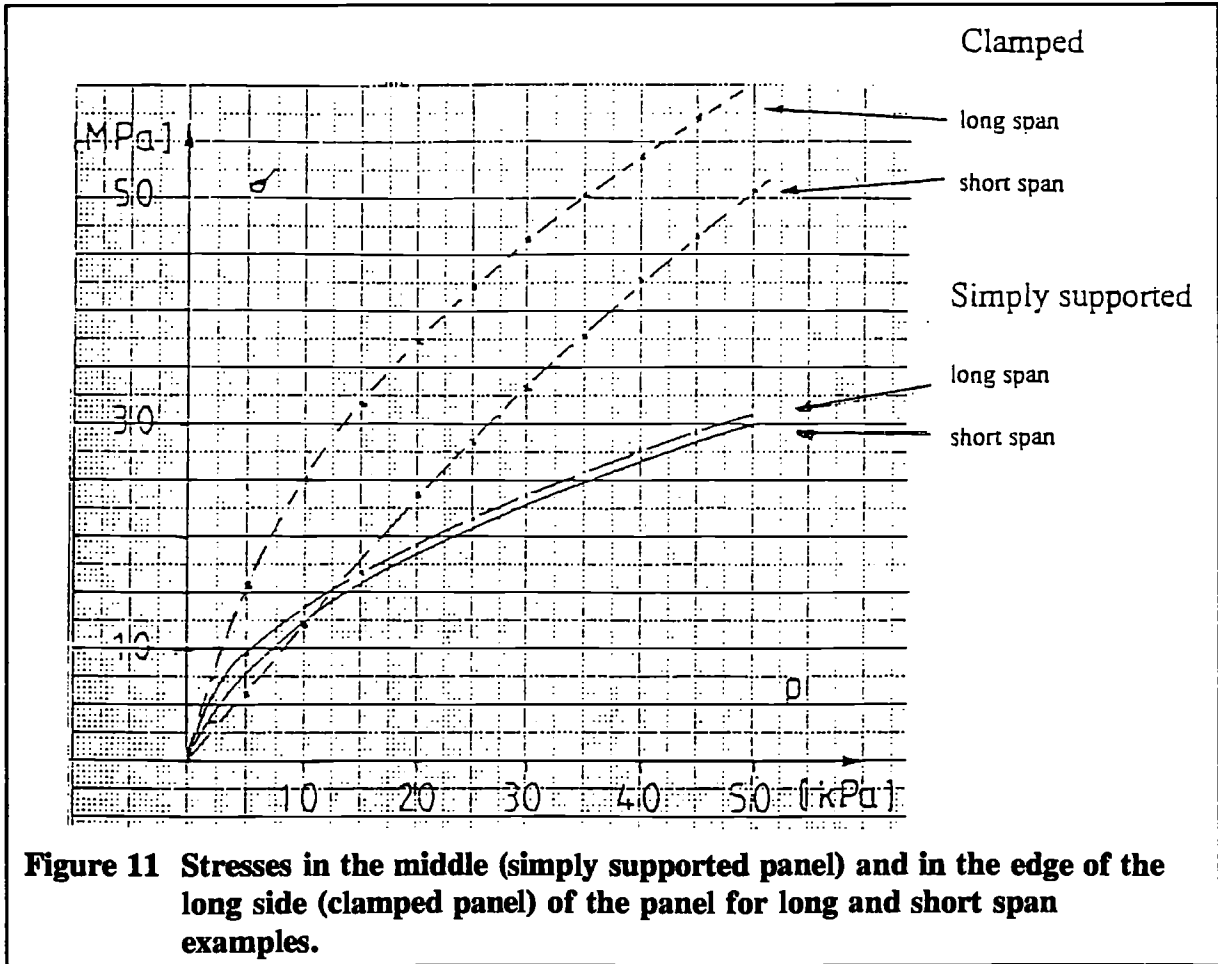


Figure 11 Stresses in the middle (simply supported panel) and in the edge of the long side (clamped panel) of the panel for long and short span examples.

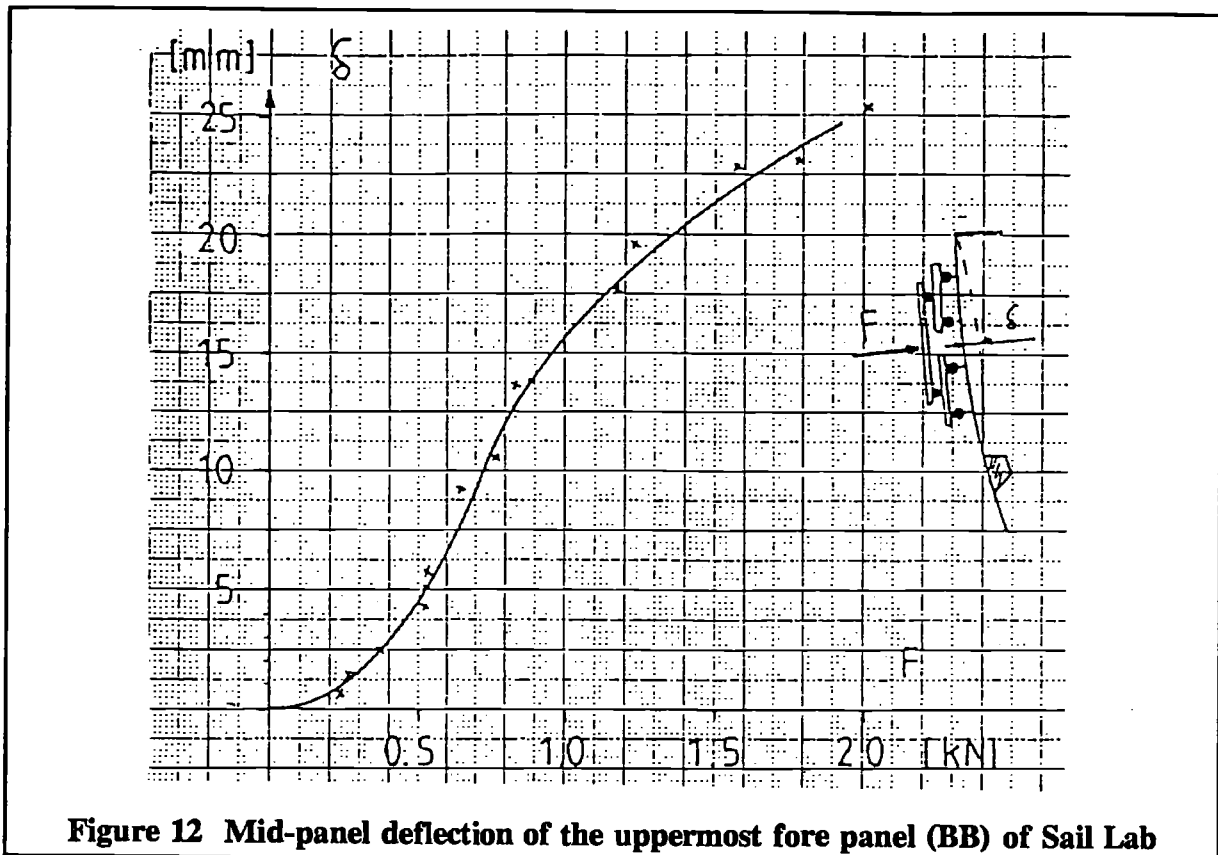


Figure 12 Mid-panel deflection of the uppermost fore panel (BB) of Sail Lab

We also believe that production boats in general, with a few exceptions, are still well above the required minimum strength level. Not all the strengthening effect problems and, on the other hand, buckling problems with curved structures have been touched on in this paper, but these may also provide additional margins for typical boat hull structures. Therefore the structural problems are relatively limited in spite of the high pressures.

It is clear that all these effects have to be mastered much more accurately in highly optimized racing yachts. Damage can be avoided with careful analysis and accurate load determination.

5 Measured rudder loads

Difficulties in steering may endanger the safety of the yacht, so the rudder is one of the most critical parts of a yacht's structure. The dimensioning of the rudder blade, stock and bearings is still a problem, as can be observed from the last Whitbread Round the World Race.

For the dimensioning of the spade rudder stock, the maximum lift and drag force and the distance between the centre of pressure and the bearings are needed. The loading history may also be critical because of fatigue aspects.

The well-known formula (1) for the lift force includes two difficult factors: the maximum lift coefficient C_L and the maximum boat speed V_s . These parameters are discussed in the following chapters.

$$L = 0.5 C_L \rho A V_s^2 \quad (1)$$

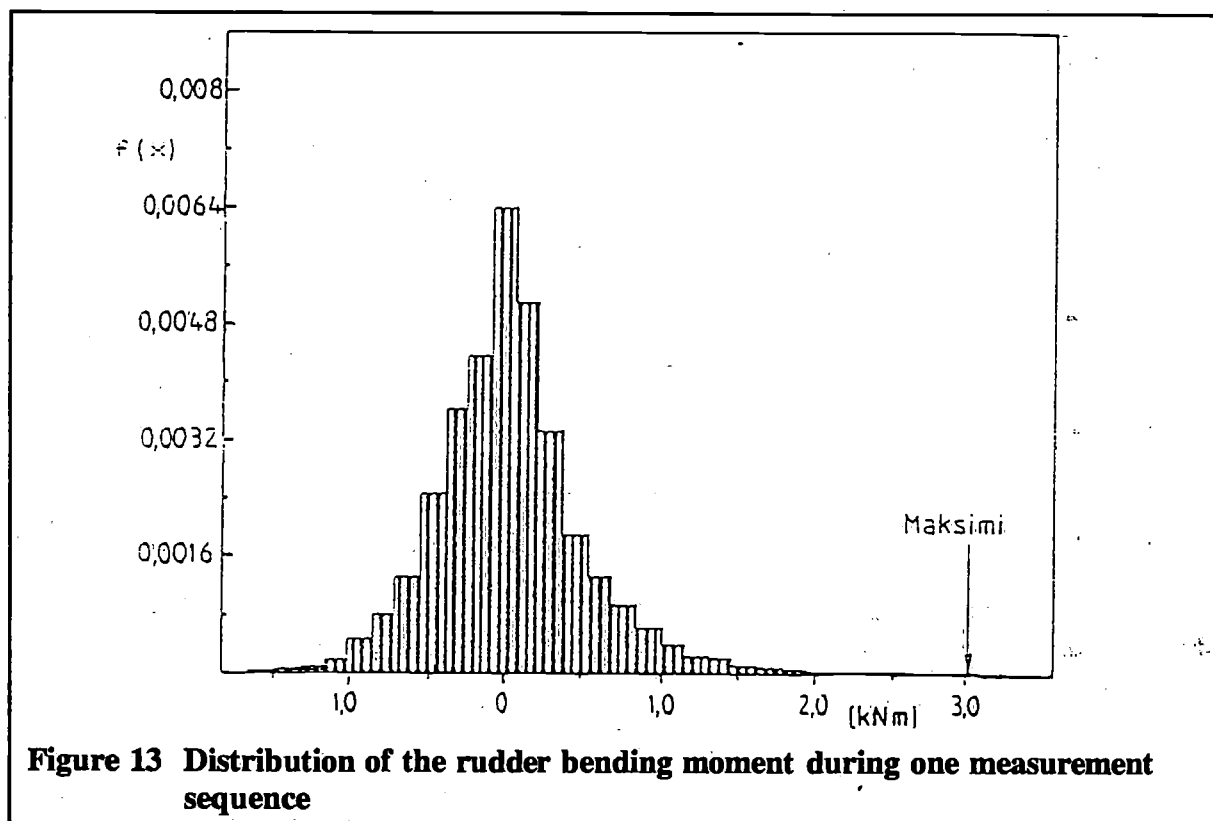
By using different rule scantlings, the stress levels for the measured bending moment are also presented.

5.1 The measured values compared to scantling rules

The torque and bending moment affecting the rudder stock were determined by measuring the strains just above the spherical lower bearing. The maximum bending moment was 4.48 kNm and the the maximum torque 0.54 kNm. An example of the distribution of the different loading levels is shown in Figure 13. The extrapolated values (see chapter 2.2) are 5.0 kNm for bending and 0.65 kNm for torque.

The requirements of some rule scantlings are compared with the measured values in the following way:

- The stress levels are calculated by using the previously mentioned bending moment and the section moduli given by different scantling rules.
- Factors of safety are calculated for the material that was used in Sail Lab.



The results for the Nordic Boat Standard, the American Bureau of Shipping and the installed rudder stock in Sail Lab are shown in Table 2.

Table 2 Stresses for the rudder stocks dimensioned by different scanning methods, as a bending moment of 5.0 kNm is applied. Factors of safety are given for a material having $\sigma_b = 580$ MPa and $\sigma_{0.2} = 250$ MPa

	W [mm ³]	M [kNm]	σ [MPa]	n (break)	n (0.2)
NBS-90	19422	5.0	257	2.26	0.97
ABS/ORC	15228	5.0	328	1.77	0.76
Sail Lab	16163	5.0	309	1.88	0.81

The proportionality limit is clearly exceeded with the installed and ABS/ORC rudder stocks. The magnitude of the resulting permanent deformation depends on the material properties. In the usual way of dimensioning, the material should operate at its elastic range.

5.2 The location of the centre of pressure

The maximum bending moment and the torque in the rudder stock are directly proportional to distances r and s as shown in Figure 14. The locations of the centres of pressure according to different dimensioning rules, are also plotted.

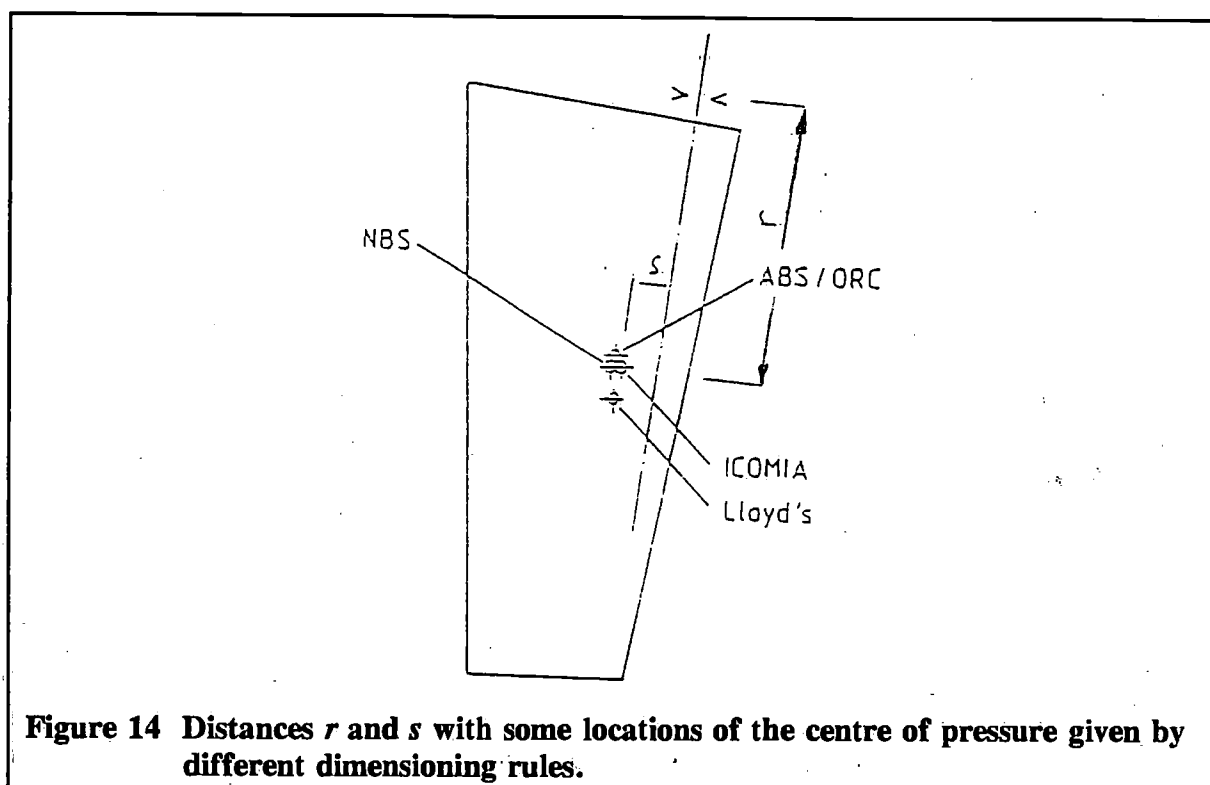


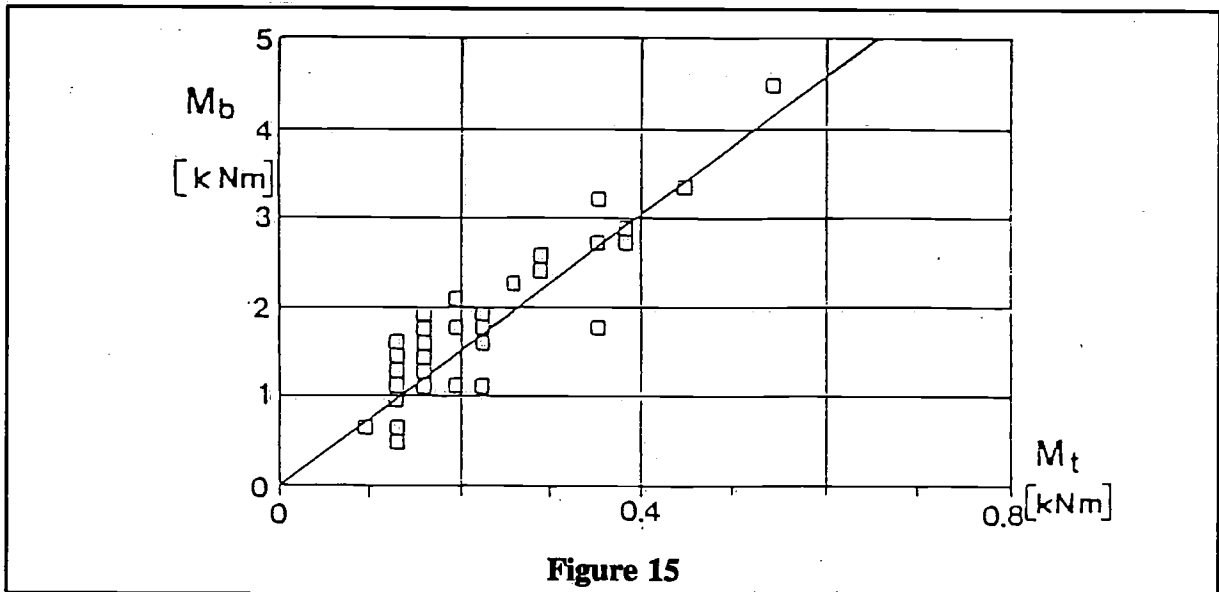
Figure 14 Distances r and s with some locations of the centre of pressure given by different dimensioning rules.

The location of the centre of pressure depends on the effective aspect ratio AR_E (taken as the geometric aspect ratio taper ratio) and sweep angle, and moves along the rudder blade depending on the angle of incidence [12]. Because the maximum values are sought, the stalling angle is usually the most relevant situation. Spanwise, the geometric centre of effort is usually a good approximation for the centre of pressure. Chordwise, the aftermost position of the centre of effort is $0.3 \cdot c$ from the leading edge ($c =$ chord length), if $AR_E > 1.2$ [12]. The maximum value for the bending moment arm r is thus $1.05 \cdot r_R + r_B$, as $AR_E \geq 2$ ($r_R =$ distance between the blade root and the geometric centre of effort, $r_B =$ distance between the lower bearing and the rudder root)

The measured ratio between the bending moment M_b and torque M_t supports the above-mentioned theoretical values. The average ratio between M_t and M_b is 0.13 while the ratio between s and r is 0.14. Figure 15 shows the maximum values of M_b and M_t during each measuring sequence.

5.3 The maximum attainable speed

Displacement-type hulls normally advance at Froude numbers ≤ 0.4 . However, new hull forms are designed to surf along the waves on downwind legs, and $Fn \approx 1$ can be achieved momentarily.

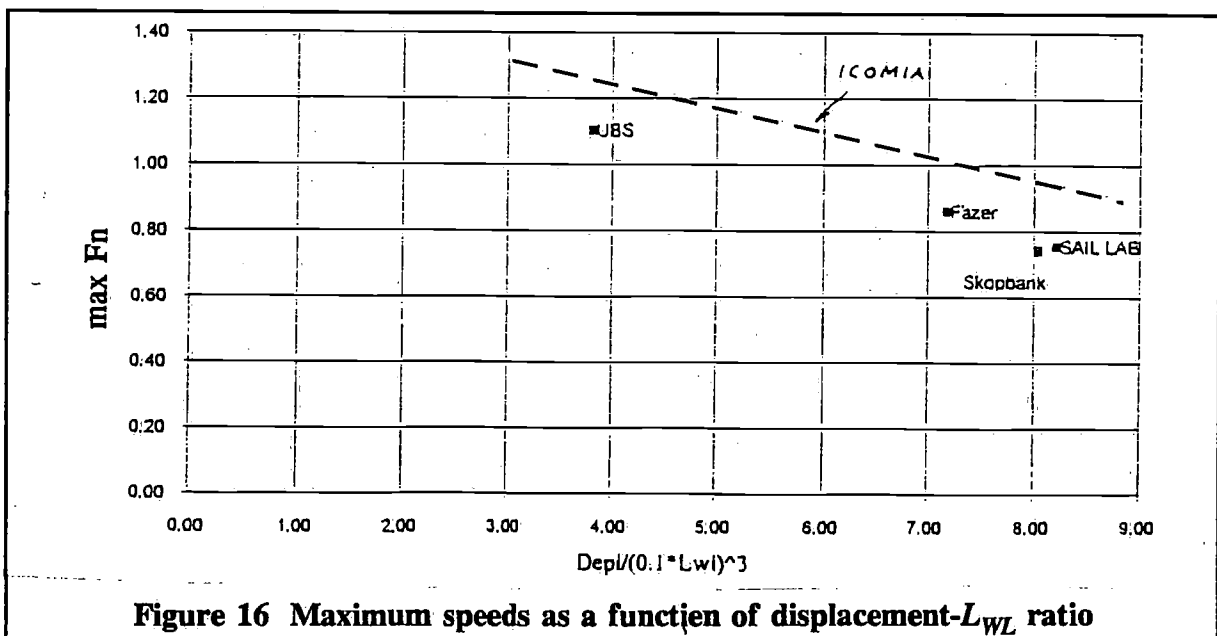


Some indications of maximum speeds can be found from the scantling rules, although the safety factors included in different terms makes direct use or comparison difficult:

- The Nordic Boat Standard: $V = 4\sqrt{L}$, which corresponds to $Fn \approx 0.65$ Lloyd's: "max. speed + 3 kn"
- ABS/ORC: not given directly, but can be derived from the given expression $C = 1.5$ to be $Fn \approx 0.45$.

The draft for an ICOMIA standard includes a speed coefficient k_1 , which is a function of displacement and L_{WL} . This gives some estimate of the surfing ability of the yacht. In Figure 16, the values of k_1 are transformed to Froude numbers.

Some registered maximum speeds are also plotted in Figure 16. Skopbank of Finland achieved 16 kn, Fazer Finland 21.5 kn and Union Bank of Switzerland ab. 30 kn during the Whitbread Round the World Races of 1982 and 1986. Sail Lab has surfed at 12.6 kn in 1986.



5.4 The maximum attainable lift coefficient

The hydrodynamic performance of a rudder blade can be obtained fairly reliably by combining analytical theory and scale model tests, see Table 3. However, in real conditions the maximum values of lift coefficient C_L fall well below the theoretical ones. This can be due to:

- disturbed stream around the rudder blade
- roughness and unevenness of the blade surface
- at surfing speeds, smaller rudder angles are used

Table 3 Maximum values of C_L for different NACA-profiles [13]

Foil	(L/D) max	Incidence degrees for (L/D) max	C_L at (L/D) max	C_{Lmax}	Incidence degrees for C_{Lmax}	C_D at (L/D) max
Flat plate	about 10	4-5	--	0.72	20-25	
NACA 0006	24	4	0.30	0.88	16	0.0125
0009	23	5	0.35	1.27	18	0.0152
0012	22	5	0.35	1.53	22	0.0159
0015	21	5	0.35	1.53	22	0.0167
0018	20	6	0.35	1.50	23	0.0175

Near the stalling angle, the drag force normally comprises 15 - 25% of the resultant force.

The measured bending moment of the rudder stock can be analysed further by assuming that the centre of pressure is located as suggested in chapter 5.2. The moment arm is then 0.622m and the area of the rudder blade is 0.558 M². The maximum values for the resultant force coefficient $C_R = \sqrt{C_L^2 + C_D^2}$ as a function of speed of advance can thus be determined:

$$C_R = \frac{M_b}{0.0464v^2}$$

As shown in Figure 17, the coefficient C_R seems to decline clearly below 1.0 as the Froude number increases over 0.6.

It can be concluded that a constant lift coefficient does not give satisfactory results for dimensioning. The measurements performed in the Sail Lab project give new information for the dimensioning of typical rudders. Further research is required to clarify the effects affecting the maximum lift coefficient vs. speed, the required steering force at surfing speeds, and the maximum force exerted on the rudder or wheel by the helmsman.

As a result of the Sail Lab project, a method taking into account the maximum attainable speed and the maximum lift coefficient was developed and programmed.

6 Chainplate load distribution

During the measurements all the stay and shroud loads were measured. At the transverse chainplates, the vertical chainplate load was measured by adding "electronically" the vertical component of the main, intermediate and lower shrouds. Here this vertical component is dealt with and it corresponds to a situation in which all the shrouds are attached to the same chainplate.

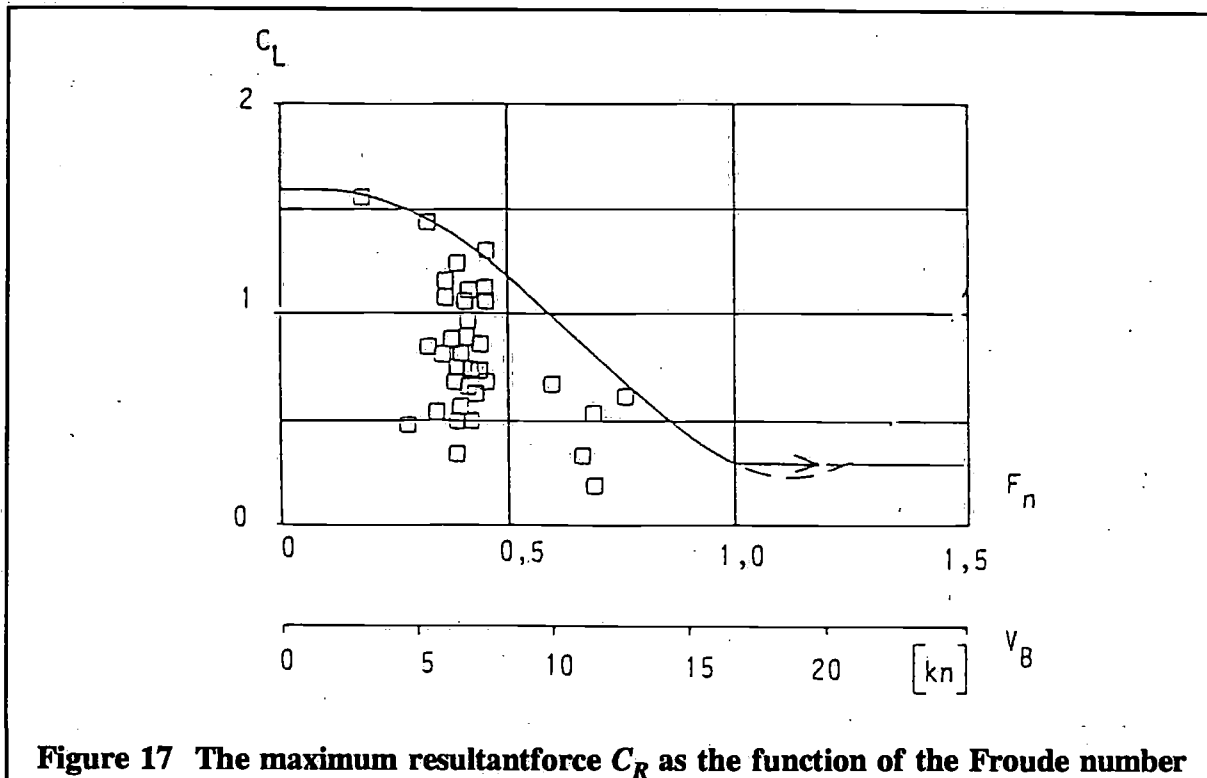


Figure 17 The maximum resultant force C_R as the function of the Froude number

From the extrapolation graph it can be concluded that the maximum value increases only marginally from the measured value when the measuring time is extended. This is due to the fact that the most important parameter influencing the load is, as is well known, the stability of the yacht. A yacht without stability has only transverse loads corresponding to the pretension of the shrouds.

The chainplate load histogram can be viewed in Figure 18. The pretension here is in the region of 8 - 9 kN and the sample is taken from typical sailing on both tacks in true wind conditions of 14 - 16 m/s.

From the histogram one can notice the slack at the opposite tack and the low number of really high recordings.

There have always been a debate over which values should be regarded as a proper way of establishing the stability of a yacht. For our purpose, we arrived at the following formula for maximum chainplate load calculations.

$$PT = \frac{45 \cdot RM \ 1^\circ \cdot Displ}{b \cdot G}$$

were	$RM \ 1 \ deg$	Righting moment at 1 degree of heel
	$Displ$	Actual displacement of the yacht (full load)
	b	Chainplate distance from centre line
	G	Displacement of yacht when deriving $RM \ 1 \ deg$.

This formula based on the measurements and the analysis procedure confirms more or less the established methods suggested by S&S 1970. From the measurements we also derived additional formulae for the calculation of headstay- and runnerloads. These are dependent on the pretension ratio of the runner system and the longitudinal geometry of the rig.

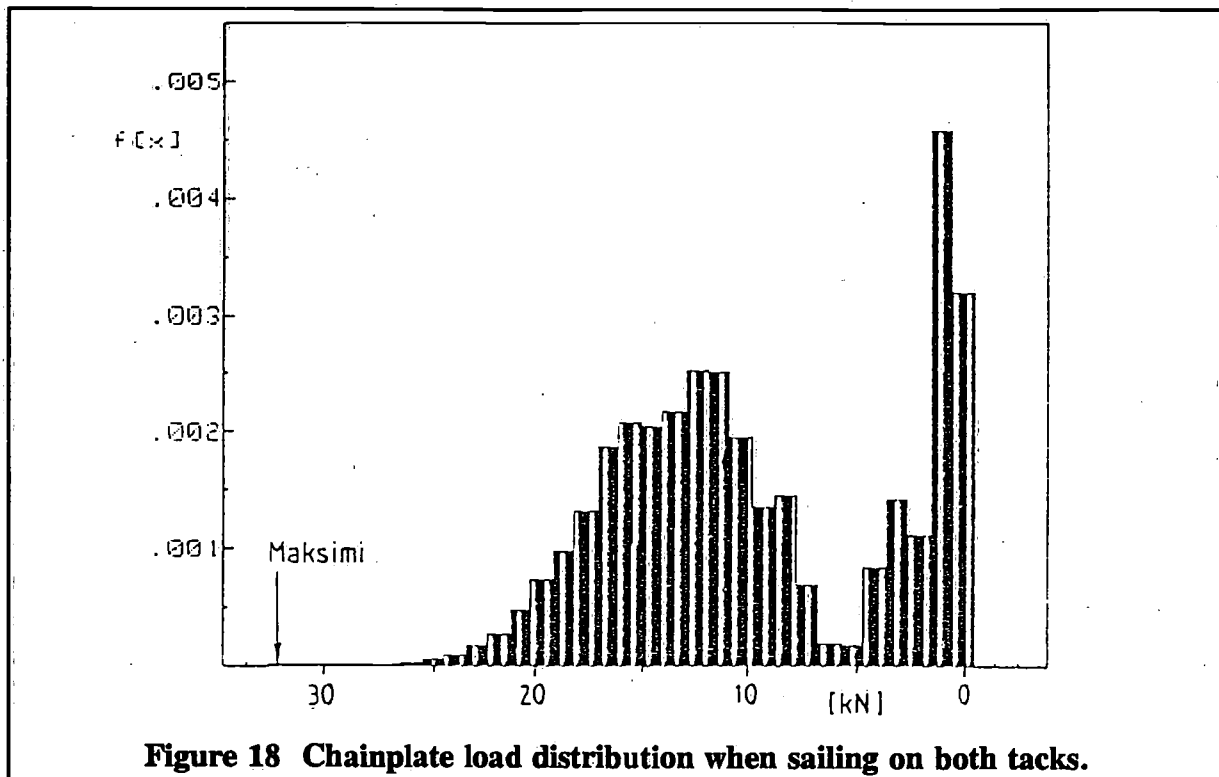


Figure 18 Chainplate load distribution when sailing on both tacks.

7 Principles for the grounding analysis

The bottom and keel structure of a yacht should withstand the stresses caused by running aground - at least at moderate speeds. This is especially true in the Scandinavian archipelago, where rocky waters demand very precise navigation.

7.1 Description of the problem

When running aground, the impact on the keel causes deformations of the structure and changes in the yacht's motion condition. These can be divided into three groups shown in Figure 19.

The bottom structure acts as a spring and damper between the keel and the hull. If the crash is not right-angled and/or there is some sideways, the yacht also heels during grounding.

Based on these phenomena, the parameters influencing the loads when running aground include:

- Boat speed
- Mass and radius of gyration of the keel
- Mass and radius of gyration of the yacht excluding the keel
- Stiffness of the bottom structure
- Stiffness of the ballast keel material in the elastic and plastic range (in compression, high strain rate)
- Contact angle (the angle between the keel tip and the ground)
- Profile shape and planform of the keel in proximity to the contact area
- Hull shape (moment to change trim, sinkage, added mass)

There are few published references dealing with the problem and thus new methods of analysis had to be found.

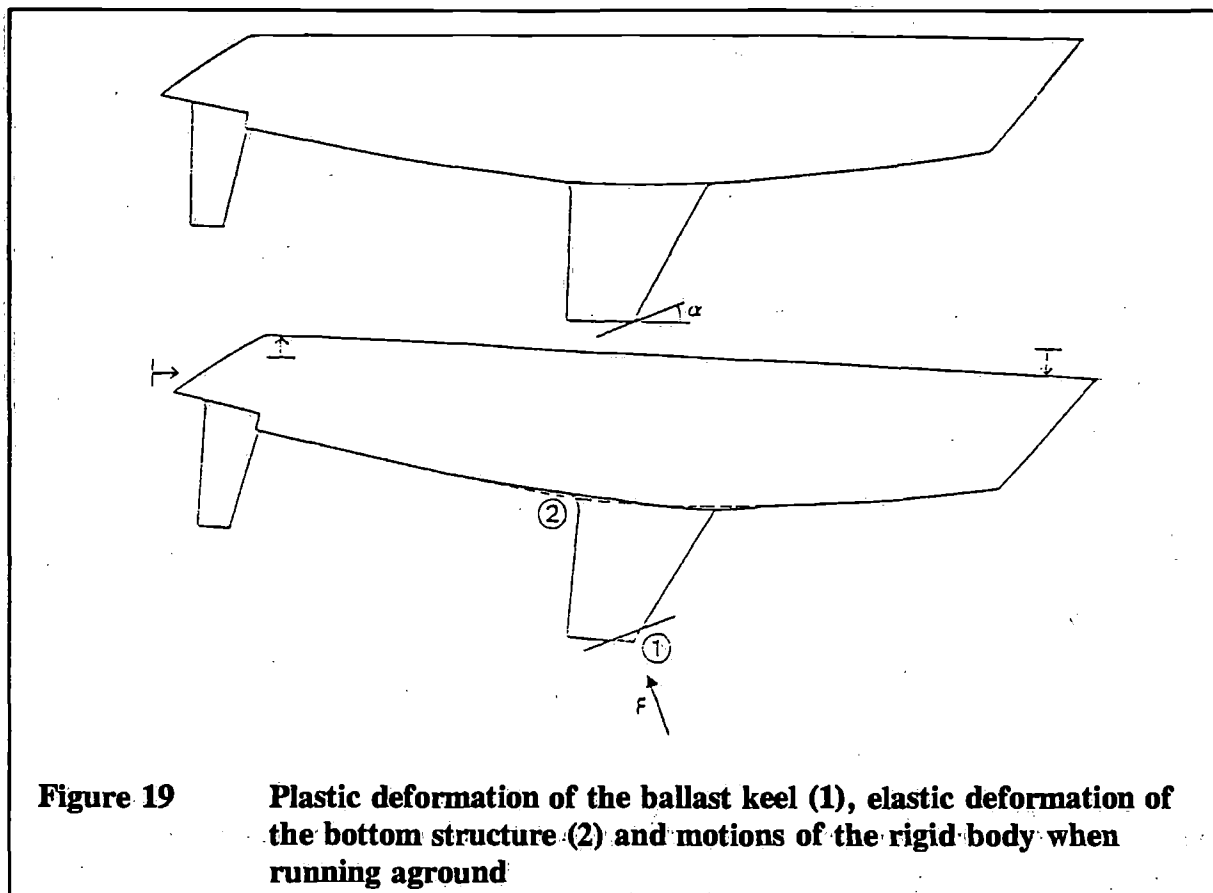


Figure 19 Plastic deformation of the ballast keel (1), elastic deformation of the bottom structure (2) and motions of the rigid body when running aground

7.2 Possible methods of analysis

Both theoretical and empirical methods can be used in the analysis. The following aspects should be taken into account when choosing a theoretical method:

- 1 Models based on the change of momentum. Simple, but because only the mean value of the affecting force can be determined, the time history of the load and the magnitudes of different local deformations remain unknown.
- 2 Models based on the energy principle. The original kinetic energy is converted to strain energy and new forms of kinetic energy during the grounding. The relative importance of the different parameters can therefore be examined, but the time history of the deformations still remains unknown.
- 3 Simulating the incident on a time scale gives information on the time history of the loading and the response of the structure. The equilibrium between the load and both local and global deformations is searched for by iteration at each timestep. In order to simulate the vibratory behaviour of the bottom structure, a dynamic model is required.

The empirical methods are based on a test series in model or full scale. The measured data can be used either

- 1 Autonomously, if the effects of all the main parameters can be determined
- 2 Together with a theoretical method for verification or completion.

The first alternative requires a large amount of data because of the many influential parameters (see chapter 7.1). The verification or completion of some theoretical method is thus more relevant.

In the Sail Lab project, a combination of full-scale tests and a simulation model was used. In this way, the simulation model could be verified and the test results extended to a wider range.

7.3 Calibration and measurements

The grounding tests were made on natural granite outside Helsinki. The shear strains were measured from the keel floors during running aground. The contact angle was 15° and rock was assumed to be infinitely stiff. The motions of the yacht were photographed. The signal given by the strain gauges was calibrated by pulling the keel in different directions with a known force (Figure 20). During the tests the signals were recorded without any filters.

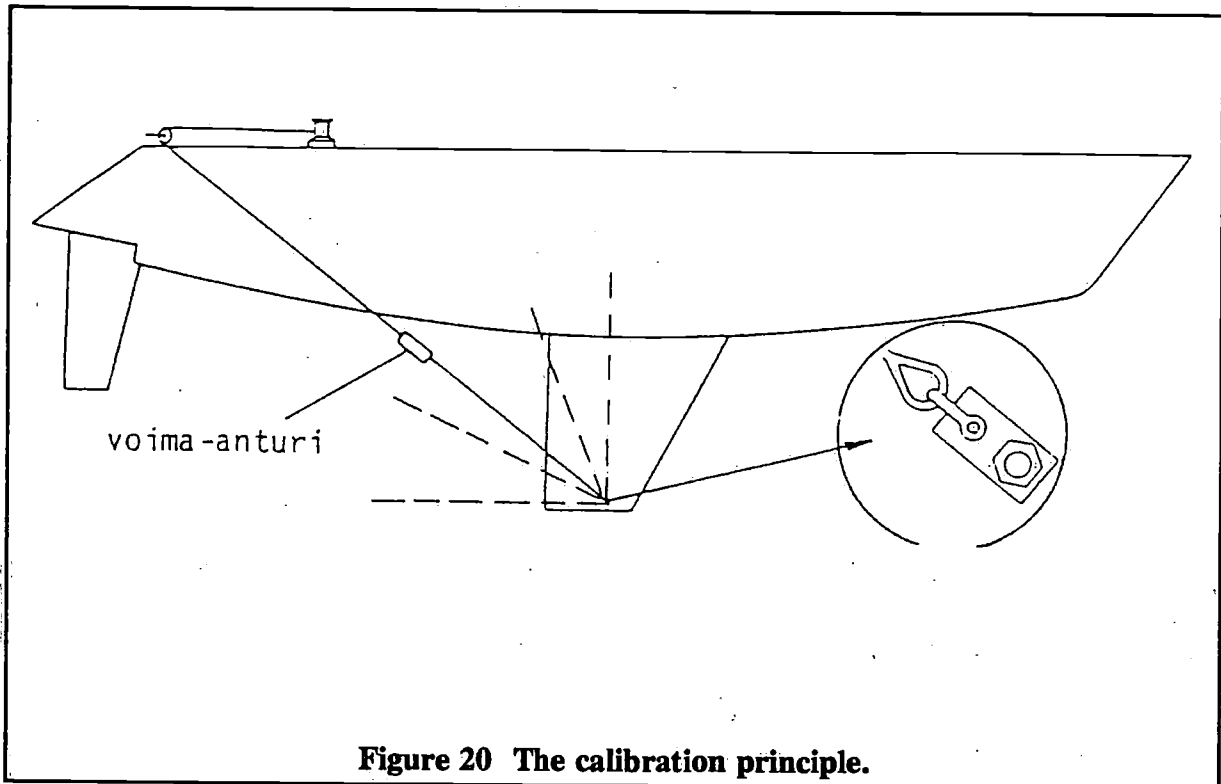


Figure 20 The calibration principle.

The parameters varied during the measurements were boat speed and keel material. The maximum speed was limited to approx. 3 kn, because even the smallest microcrack beneath the measuring points could have destroyed the gauges. The groundings were done by motoring, and the heeling and leeway angles were assumed to be zero.

The effect of the keel material was investigated, by replacing the fore corner of the keel with similarly formed pieces of other materials.

The signals measured from the keel floors include three interesting points:

- Several impacts can be clearly distinguished, although during the tests the boat seemed to stop immediately. The first impact is the hardest and is thus crucial to the dimensioning (see Figure 21)
- After the impact the bottom structure vibrates at a frequency of about 12 Hz and the amplitude is as much as a quarter of the maximum amplitude.
- The rising time of the response is about 0.05 s and the beginning of the rise is very sharp.

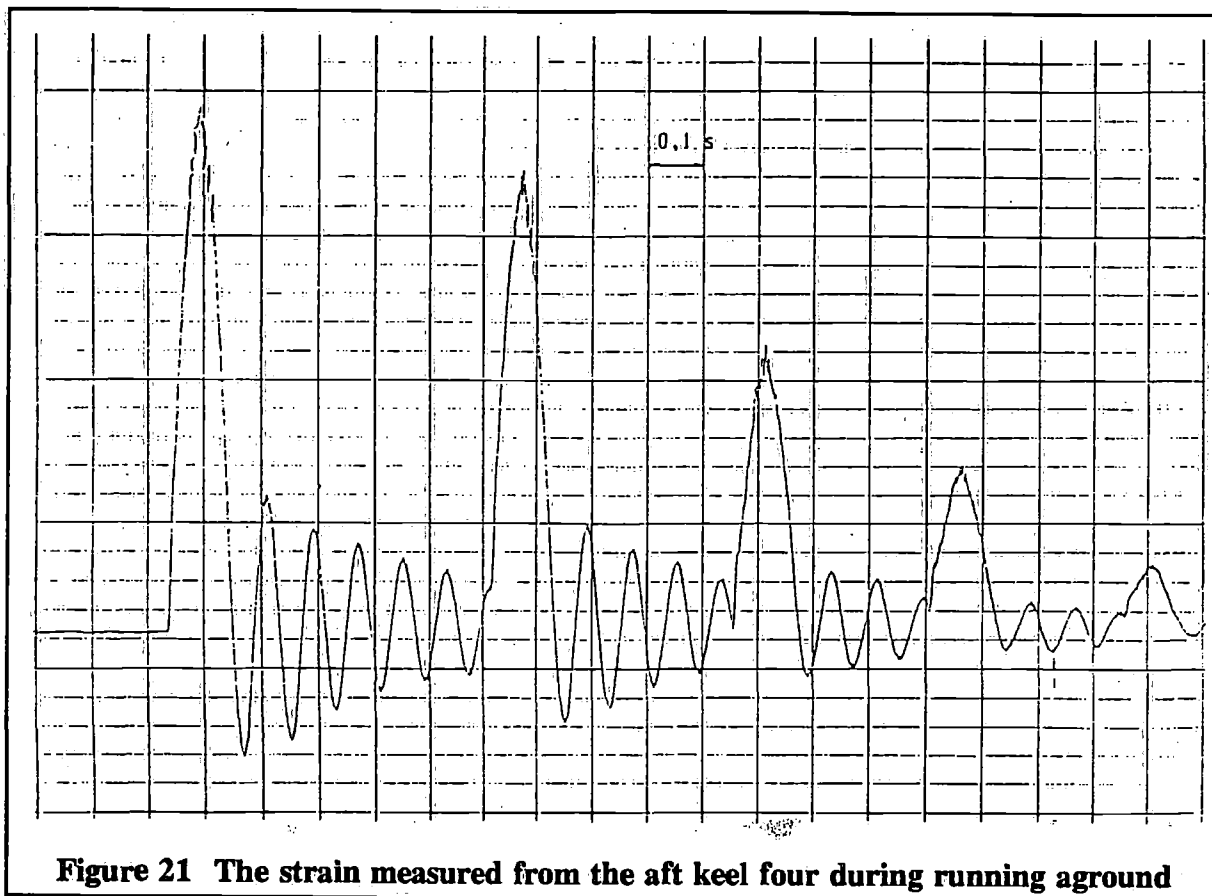


Figure 21 The strain measured from the aft keel four during running aground

7.4 Calculation model

The structure of the Sail Lab research yacht was designed to be simple and clear for easier analysis. However, the modelling of the dynamic behaviour of the keel-hull structure is difficult because of the material properties, the many different structural members, and the surrounding water.

The dynamic characteristics needed for the simulation model include both rigid body motions (heave, trim) and the displacements caused by the elasticity of the structure. The equation of motion can be expressed in a matrix form:

$$[M]\{y\} + [C]\{y\} + [K]\{y\} = \{F(t)\}$$

where

- [M] = matrix containing the yacht mass plus added mass of water
- [C] = damping matrix
- [K] = stiffness matrix
- {F} = vector of external forces (impact force)
- {y} = displacement vector

The solution of the eigenvalue problem gives both natural frequencies and natural modes. The displacements at different points of the structure can be calculated using these values. A simplified beam model of the hull and the keel was created and analysed with the HUVI program, which was developed by VTT for vibration analysis. The weight and stiffness distribution as well as the added mass distribution of the beam model are shown in Figure 22. The grounding force affects the node nr. 35.

The stiffness of the bottom structure was determined so that the lowest elastic natural mode of the model corresponds to the measured natural frequency (77.8 rad/s).

The time history of the grounding force has a significant effect on the response of the structure. By simulating the phenomenon, it was possible to identify an impulse shape that causes a similar response of the bottom structure to that measured during the tests.

The shape of the keel profile and the plastic behaviour of the material was also taken into account in the simulation procedure. The equilibrium between the contact area and the total impact force was searched for at each time step.

7.5 Parameter studies

The effect of different parameters on the magnitude of the vertical load affecting the bottom structure during grounding was investigated with the simulation model. The following parameters were studied:

- Boat speed (extended range)
- Displacement and radius of gyration of the yacht
- Draught and aspect ratio of the keel
- Stiffness of the bottom structure
- Contact angle (the angle between the keel tip and the ground)
- Friction between the ground and the keel

The importance of the boat speed and displacement is natural since they affect the available kinetic energy. By contrast, the significant effect of the contact angle was somewhat surprising. The vertical load acting on the bottom at the aft edge of the keel reaches its maximum as the contact angle is approx. 60° when the aspect ratio is 1.24.

In general, the loads acting on the bottom structure during running aground are very high. The dynamic nature of the incident makes simple calculations inaccurate and extensive calculations are needed to predict the maximum forces at a given grounding speed. The results of the Sail Lab project make it possible to get an estimate of the loads easily, if the type of hull-keel structure is not very far from the typical design of Sail Lab.

8 Conclusions

During the past year or so, several reports have been written in yachting magazines about hull failures of yachts. Leaving the keel problems aside, many writers conclude something like "... it wasn't really a strength problem - only delamination.....". They are then referring to material and manufacturing problems.

With the experience we obtained from the measurements, our impression is that there is a lot to learn about slamming loads, and the mechanisms of the structures are yet by no means fully understood.

The results show that the slamming loads are high and exceed the levels commonly expected. This is so even for a medium displacement type yacht. There is a significant load area reduction but this is not as steep as the ABS guide assumes. The fact that boats are not breaking down is, in our opinion, due to the general overdimensioning of boats and the additional strength of the nonlinear behaviour of both single-skin and the sandwich boat structures.

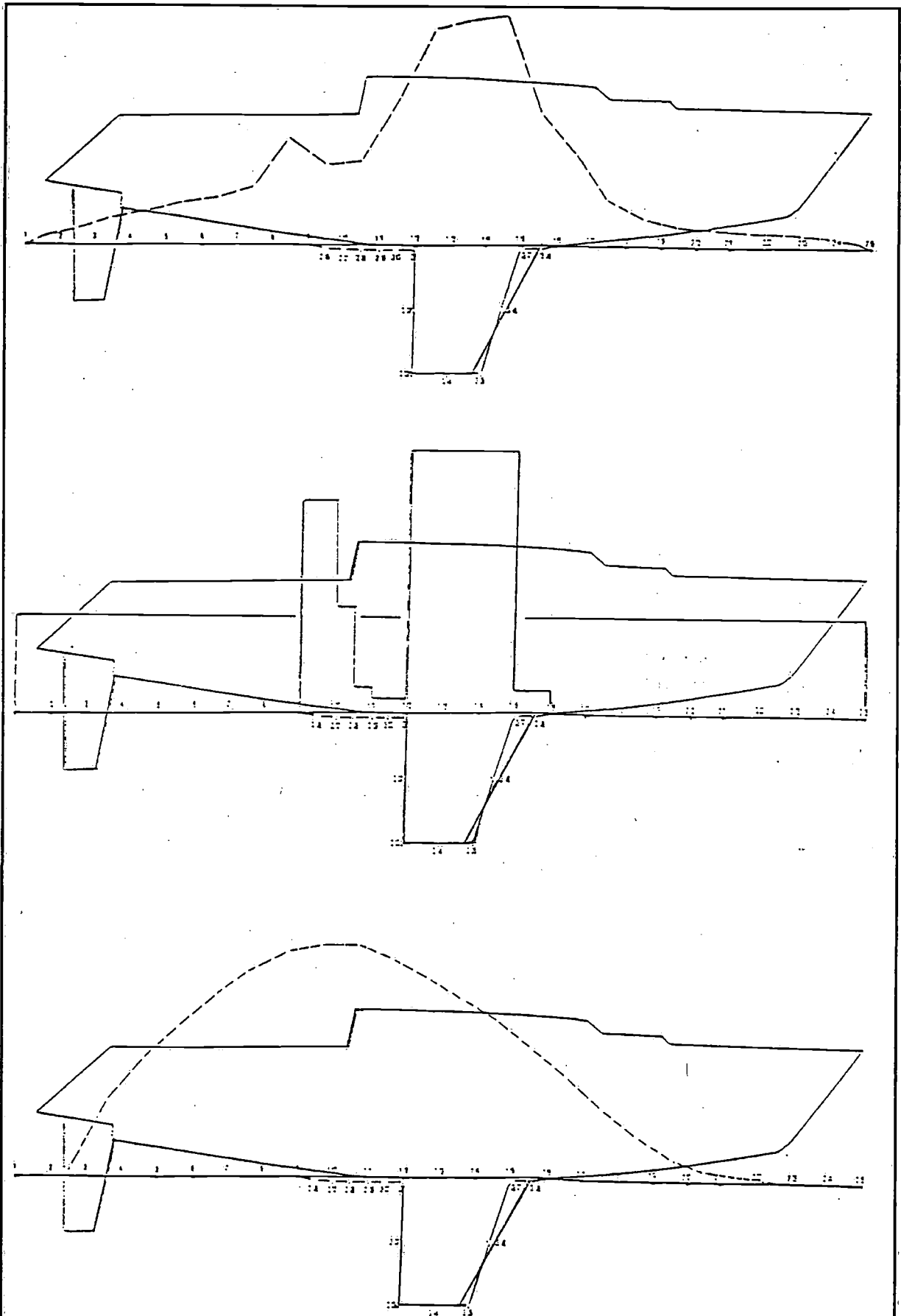


Figure 22 The beam model and its weight-, stiffness and added mass distribution

For the dimensioning of the spade rudder, the measurements gave new information of the phenomena affecting the maximum loads. An interesting lift coefficient reduction takes place in high speeds and this can at least partly be attributed to the actual steering force a helmsman is able to manage. Another source of this reduction is the force or moment the yacht needs to turn.

The rigging loads can often be predicted accurately enough with relatively simple calculation models. By contrast, the grounding loads have been difficult to predict and the results of the Sail Lab project give valuable information of this area.

References

- [1] Hentinen M., Holm G.,
"Aaltoiskut, rustirauta- ja perasinkuormat",
SAIL LAB -projekti, raportti 1, VTT, Laivatekniikan laboratorio, 1986. (SAIL LAB report 1, unpublished)
- [2] Hentinen M., Holm G.,
"Maksimikuonnat ja karilleaj on parametrit",
SAIL LAB -projekti, Raportti 2, VTT, Laivatekniikan laboratorio, 1988. (SAIL LAB report 2, unpublished)
- [3] Hentinen M.,
"Slamming pressures in sailing yachts",
VTT Research Notes 715, Espoo 1987 (in Finnish).
- [4] Heger, F.J., Chambers, R.E. & Dietz, A.G.H,
"Structural plastics design manual",
Vol 2. Simpson Gumbertz & Heger Inc. 1982.
- [5] Keuning P.J. and T.F. van der Werff,
"Rig load measurements and comparison with calculations",
11 th International Symposium on Yacht Design and Yacht Construction, HISWA, 1990, ss. 101 - 128
- [6] Elfström, C., Virstedt, P.,
"Mätning av deformationer och spanningar i på olika sätt förstärkt botten i en fenkölsbåt typ Shipman Accent",
Chalmers tekniska högskola, Inst. for skeppsbyggnad, 1976.
- [7] ABS "Guide for Building and Classing Offshore Racing Yachts",
ABS, 1982 and 1986 + amendments.
- [8] Joubert P.N.,
"Strength of bottom plating of yachts",
Journal of Ship Research, Vol 26, No 1, 1 march 1982.
- [9] Mull, G.W.,
"Strength requirements for sailing yachts",
Symposium Yacht Architecture, HISWA, 1981.
- [10] Weissman-Bennan D.,
"A fibreglass scantling design procedure",
Westlawn Yacht Design Symposium, 1984.
- [11] Silvia D.A.,
"Small craft design structures",
The University of Michigan Ottawa, 1971.
- [12] Molland A.F.,
"Rudder design data for small craft",
Ship Science Report No.1/1978.

- [13] Marchaj C.A.,
"Aero-hydrodynamics of sailing",
Adlar Coles Ltd, 1979.
- [14] Jacobs F.A.,
"Some applications of aeronautical engineering in the construction of yachts",
8th International HISWA Symposium on developments of interest to yacht architecture,
1983.
- [15] Enlund H. & al,
"Calculated and measured stress resultants in the mast and rigging of a Baltic 39 type
yacht",
International Conference on Design Considerations for Small Craft, London 1984, +
discussion part.

Recently published papers and articles

- Talvia J.,
"Messungen zur Segelyachtlasten",
12 th Symposium Yachtentwurf und Yachtbau 1991, Hamburg Messe, ss. 57 - 85.
- Keuning P. J., and van der Werff T.F.,
"Rig Load measurements and Comparison with Calculations",
11 th International Symposium on Yacht Design and Yacht Construction, HISWA,
Amsterdwn 1990.
- Belgrano G.,
"A structural overview of the 1993/94 Whitbread Boats",
Seahorse, issue 164, Oct 1993.
- Tamulaites M.,
"Imagine's bumpy ride", SAIL, February 1994.
- Lyons D.,
"W60 Slamming Pressures",
Seahorse magazine, issue 175, September 1994.
- Fogg R., Belgrano G.,
"Whitbred 60 Refinements", Seahorse magazine, issue 175.
- Hentinen, M. & Holm, G.,
"Geometrical nonlinearities of laterally loaded reinforced plastic plates",
VTT Research Reports 694, Espoo 1990 (in Finnish).
- Hentinen, M. & Hildebrand, M.,
"Nonlinear behaviour of single-skin and sandwich hull panels",
FAST'91, First International Conference Fast Sea Transportation, Trondheim 1991.
- Hildebrand, M.,
"On the bending and transverse shearing behaviour of curved sandwich panels",
VTT Research Notes 1249, Espoo 1991.